An Intelligent SIP Message Parser for Detecting and Mitigating DDoS Attacks

Abdullah Akbar
Research Scholar, Department of Computer Science and Engineering
Jawaharlal Nehru Technological University Hyderabad, Hyderabad, Telangana, India

Dr. S. Mahaboob Basha
Professor, Department of Computer Science and Engineering
Al Habeeb College of Engineering & Technology, Ranga Reddy District, Telangana, India

Dr. Syed Abdul Sattar
Professor, Department of Electronics and Communication Engineering
Royal Institute of Technology and Science, Ranga Reddy District, Telangana, India

Dr. Syed Raziuddin
Professor, Department of Computer Science and Engineering
Deccan College of Engineering & Technology, Hyderabad, Telangana, India

Abstract- Voice over Internet Protocol (VOIP) is widely used for multimedia and voice calls transmission through internet telephony. Session Initiation Protocol (SIP) is predominantly used in establishing multimedia session among the nodes deployed in VoIP services implementations. The increasing usage of SIP servers for multimedia transmissions has resulted in a high and frequent experience of Distributed Denial of Service (DDoS) attacks. In this paper, we propose a solution through SIP message parser intelligence to detect DDoS attacks in the VoIP networks. To identify the malformed messages, we have used Support Vector Machine (SVM) based classifier mechanism. Our parser reduces time complexity better as compared to other methods since our method uses kernel tree analysis which does not require the representation of the entire SIP message as a feature space. Our parser have achieved 99.89% detection accuracy while tested with several different types of malformed SIP messages.

Keywords – SIP (Session Initiation Protocol), DDoS (Distributed Denial of Service), VOIP (Voice over Internet Protocol), SVM (Support Vector Machine)

I. INTRODUCTION

SIP is known as application layer signaling protocol which is used widely in Next Generation Networks and 3G IP (Internet Protocol) multimedia subsystems. It is basically used for initiation, management and termination of the voice calls and video call sessions in a VoIP network. It is a simple, open and scalable signaling protocol working on the principle of IP-Packet network. SIP server has predominant functionalities to consume average CPU time - Rachid El Khavari [2008]. The first and foremost functionality is parsing. Parsing translates the SIP messages into an internal structure utilized for further processing methods. The second step is transaction maintenance. This is used to maintain transaction state as specified by the protocol. The third functionality is message sending where we set the SIP header fields and is used to construct the outgoing SIP messages. It is also used to resolves the next hop address and calculate the checksum. Then it adds packet headers and delivers the packet to the IP Layer. SIP message is used for a request or an acknowledgement to a corresponding request. The request and acknowledgement is written in the header and message body. SIP messages are known as text based like HTTP format. The following message is well formulated SIP Message - Raihana Ferdous et.al [2012].

T INVITE sip:me@myorg.gr SIP/2.0

To: Researcher abdullah <dgen@theirorg.gr>

From: Abdullah Akbar

<sip:akbar@myorg.gr>;tag=76341
CSeq: 2 INVITE
Authorization: Digest username="akbar",
realm="192.251.164.23", algorithm="md5",
uri="SIP:197.250.160.71",
nonce="41358a56632c7b3d382b39e0979ca5f98b9fa03b",
response="a6455dce70e7b098d127220584cd57"
Contact: <SIP:199.250.160.71:9380>;>

[SIP Headers]

Content-Type: application/sdp

v=0
o=Ayesha Jahan 2890844526 IN IP4 wife.high-drama.org
c=IN IP4 102.105.108.102
t=0 0

[Session Description]

m=audio 49570 RTP/AVP 0
a=rtpmap:0 PCMU/8050

[Body]

According to RFC 3261, the SIP stacks are capable of processing the messages used for REGISTER, INVITE, ACKNOWLEDGE, CANCEL, BYE and OPTIONS - Lukas Kramer et.al. [2015].

SIP based multimedia transmission can be established between two users or callers. User A can send a SIP INVITE message to the corresponding proxy and the proxy can forward the message to the user B. At this junction, the SIP proxy server will parse the incoming message and identify the incoming request. It transforms into essential understandable format through parsing and stores it in the server for next action to be taken. Then it will read the address where the message has to be sent and then it will send the message to the appropriate user B in the VoIP network.

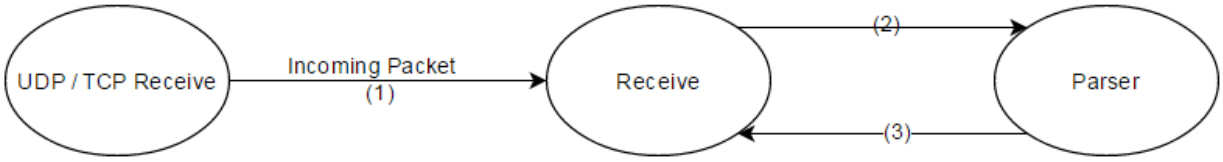

Figure 1. Processing / Parsing of a SIP message in SIP Proxy server

SIP servers are capable of performing the parsing process for well-formed SIP messages as depicted in Figure 1. A well formulated message will carry all the essential information in the header and body of the SIP message. Session Initiation Protocol is capable of initiating, terminating, managing the messages in the VoIP networks. During the session establishment time any attacker can send a malformed or a bogus message with various combinations. This kind of syntax is different from the well formulated SIP images. The SIP parser can't understand the syntax of the malformed messages and subsequently drops them. This type of messages may be invalid and can't be sent to the designated user or client system -Tasos Dagiuklas [2005].

II. RELATED WORK

SIP servers can perform different functionalities like parsing, transaction management, message transmission and dropping, withdrawing etc. SIP parsing predominantly perform the transformation of SIP message into a different format suitable for internal analysis used for further actions and functionalities. Transaction management keeps the message in a state suitable for transaction by the protocol - Jia Zou et.al [2015].

SIP parsers are predominantly utilized in SIP hierarchy IMS (IP Multimedia Subsystem) networks to perform input streaming to build specific and appropriate SIP messages. The headers of the SIP messages will be checked and compared with the standard syntax available in the SIP parser and approved messages will be sent it to the designated user or node of the network - Dimitris Geneiatakis et.al [2015].

SIP messages would be processed by the SIP parser and then sent to SIP server for further processing. The parser can read the header of SIP messages directly from the input stream. SIP parser can process the messages of both TCP and UDP transport protocols. The structured messages would be parsed and send to server for processing. The unstructured messages can be read and dropped by the SIP parser - Zifu Fan, Xiaoyu Wan [2009].

DDoS attacks are seemingly the more commonly observed attacks in the IMS networks. An example of such a DDoS attack is portrayed in Figure 2. The vulnerabilities in application and protocol stack are markedly observed and can influence the operating system performance. The attacker can instigate the DDoS attack from his system to the target machine in IMS networks. The result of DDoS attack can expose the vulnerabilities in application servers, network stacks and gives rise to more general operating system vulnerabilities. The impact of such vulnerabilities can't be predicted. They can influence the projects and system resources with more massive attacks and make them destroyed or eavesdropped. DDoS attacks from internal or external source prediction with normal mechanism are not impossible and unstoppable. The mounting of attack is generally performed with unpredictable and uncommon methods. There is no proper methodology used to launch a DDoS attack to destroy a target network. The attacker will have several different choices to enforce the Distributed Denial of Service Attacks - Md. Ruhul Islam et.al [2011].

SIP message is defined to be text based protocol session establishment and negotiation of session constraints. It is incorporated via transport layer transmission. SIP messages can exchange the signaling information according to the elementary client server principle. SIP messages predominantly classified as SIP requests and SIP responses. SIP messages are rich with header field and message body. This predominant quality has been used by the SIP parsing mechanism to identify the malformed messages and appropriate messages –Rachid El Khayari [2008].

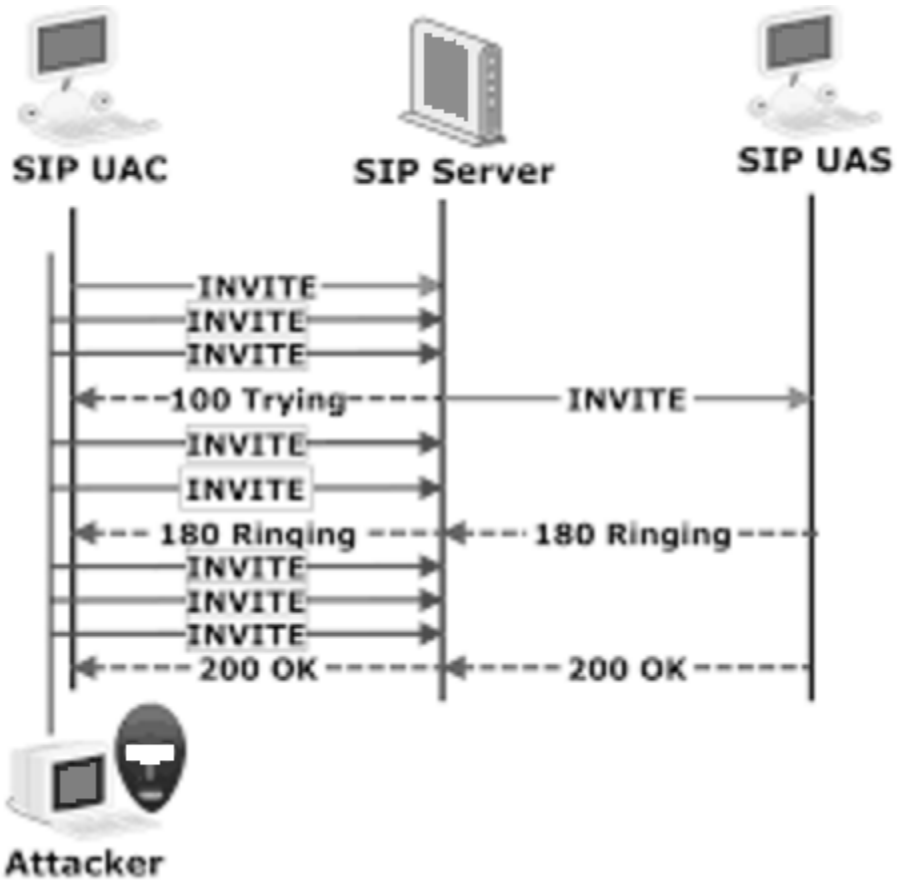

Figure 2. DDoS attack in IMS networks

SIP parsing model is very much possible in various IMS network entities to handle the potential vulnerabilities and malformed SIP messages generated through Distributed Denial of Service attacks. In this method the malformed SIP messages are generated through DDoS attacks - Lukas Kramer et.al. [2015]. The SIP server would be kept in SIP parsing mode with self-defined rules. SIP parsing mode is activated to protect the network from malformed messages with malformed values and structure. Once the malformed messages are generated and sent to the SIP server which is activated with SIP parsing, then the SIP parsing would read the messages and identify the malformed or DDoS attacks. The malformed SIP messages would be dropped by the SIP parsing server component - Yulong Wang [2013].

IMS network is rich with layered architecture consists of application plane, control plane and user plane. SIP is regarded as the most suitable application layer control protocol for IMS networks. If the Distributed Denial of Service attack generates any vulnerability during SIP processing, the malformed SIP message could enter into the IMS network and create abnormal state and affect the quality of services of the IMS network. As a result the attached assets and services of IMS would be damaged – Hongbin Li et.al. [2010]. Therefore to administer the situation SIP parsing mode is introduced. The SIP parsing mode parses the SIP messages received by the SIP server and manipulate the SIP fields after they are extracted by SIP entity. The SIP parsing can transform the messages into a separate format to perform storage, string segmentation, matching and dropping and sending to the designated node etc. - Dimitris Geneiatakis et.al [2008]. SIP parsing mode is specific to IMS network alone. When the DDoS attack generates the malformed SIP messages it can be parsed easily during the SIP parsing mode. The specific values of SIP fields available in SIP messages comply with fixed format. This format is different from the format generated by the DDoS attacks and malformed SIP messages - Ajay Kumar Shrestha et.al [2014]. The parsing mode can test match the syntax of the SIP messages generated by DDoS attacks with the standard format of SIP messages header and body syntax as specified in the introduction of this paper. Then the functionality of SIP parser can drop the message from transmission of network. This is the core functionality of the SIP parser to identify the DDoS attacks and its malformed SIP messages.

III. Proposed Architecture

The proposed malformed SIP message detector consists of a lexical analyzer and an intelligent SIP parser as shown in Figure 3. The lexical analyzer scans the incoming SIP message and breaks the message into lexemes and stores into a table according to their class. The lexical analyzer discards syntactically incorrect SIP messages. Syntactically correct SIP messages are passed to Support Vector Machine (SVM) based on intelligent SIP parsing. SIP messages are represented into a structured data structure like syntax parse tree in order to apply machine learning techniques. Basically the intelligent SIP parser is a classifier which classifies the incoming syntactically correct SIP messages as valid SIP message or invalid (malformed) using tree kernel method.

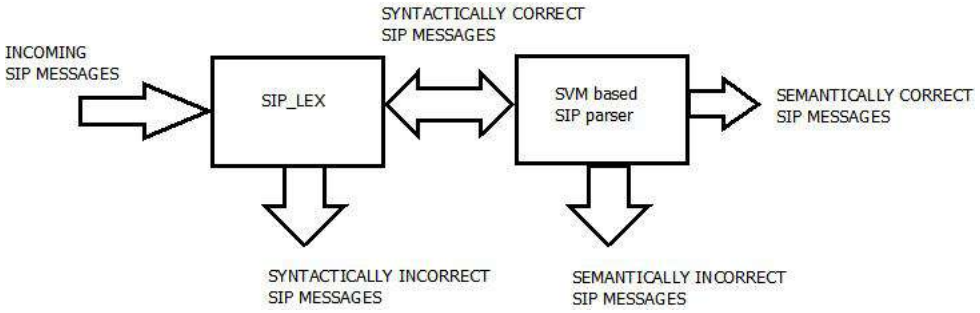

Figure 3. SIP Message Parsing Architecture

IV. Implementation Methology

The main aim over here is to illustrate the SIP parsing technique which is used to detect malformed SIP messages emanating from a network of bots. Existing SIP parsers use signature based technique to detect the malformed messages. The disadvantage of this technique is they cannot process large datasets. Some machine learning methods like multi class classifier approach suffer with the inability to represent the entire SIP message into a feature space. We have used SVM based technique to categorize incoming SIP messages as well-formed and malformed. We represent the incoming SIP message as a parse tree (T2). We will select one of the valid SIP parse tree (T1) from database and apply kernel tree method on both structures to calculate similarity between T1 and T2. Similarity score is a feature vector used for training the SVM. Training is carried out on subset of known valid messages and

malformed messages until we get reasonable detection rate specified in SIP standard. Once SVM classifier is successfully trained it is able to detect any new SIP message either as malformed or well-formed. This entire flow is described aptly in Figure 4.

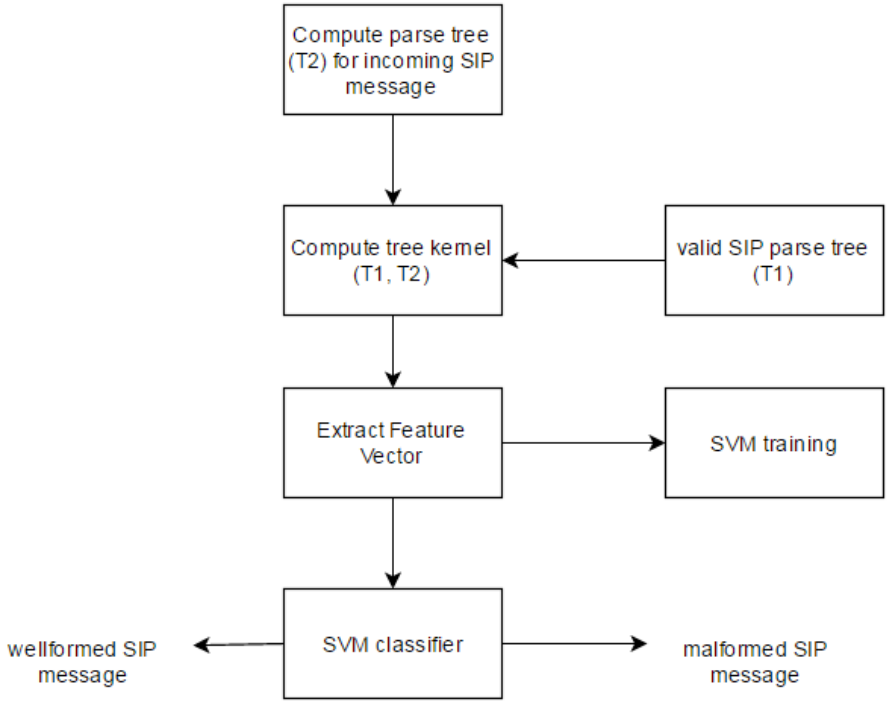

Figure 4. SIP Message Classification using Support Vector Machine

III. PERFORMANCE EVALUATION AND RESULTS

To evaluate the performance of SIP parser in terms of detection accuracy and time to detect we have used a large number of SIP traces consisting of several types of malformed message as described in Table I. Malformed SIP messages are in accordance to RFC 4475 which describes several SIP traces to trouble the SIP applications. Valid SIP messages given for parser are according to RFC 3261. A total of 5000 SIP message are generated by a message generator consisting of both malformed and valid messages. A total of 500 well-formed messages and 4500 malformed messages are categorized into several types as shown below in Table I.

TABLE I - TEST SCENARIOS USED FOR PERFORMANCE EVALUATON

Test Scenario	Description	No of messages
TS-1	Error in Request line	512
TS-2	Syntactic error in mandatory field	455
TS-3	Missing mandatory header	1125
TS-4	Duplicate entry in unique header	328
TS-5	Presence of invalid string in message	456
TS-6	Message with multiple Request method	236
TS-7	Message with unknown content	543
TS-8	Message with invalid method name	845

We can conclude from test results shown in Table II, that our intelligent SIP parser can better detect DDoS attack compared to both rule based and multiple classifier system based techniques.

TABLE II - DETECTION RATES FOR PROPOSED INTELLIGENT SIP PARSER

TEST SCENARIO	Detection Rate (%)		
	Rule based	Multiple classifier system	Proposed Method
TS-1	93.3	97.2	99.2
TS-2	91.2	96.1	98.6
TS-3	94.8	95.2	98.5
TS-4	95.3	97.3	99.4
TS-5	98.4	98.8	99.8
TS-6	97.5	98.4	99.5
TS-7	95.3	97.4	99.3
TS-8	94.5	96.5	98.5

We have achieved 99.1% detection rate for SIP malformed messages as detailed in Table II.

IV.CONCLUSION

This paper has analyzed the possible attacks to SIP networks and the simple mechanism of SIP server functionality. Based on the SIP messages construction with header and body, the SIP parser is distinguishing the malformed messages and well-formed messages with SVM based classifier. The paper has suggested a novel technique for SIP parsing mechanism to detect the malformed messages. This mechanism can effectively encounter the malformed messages generated by the DDoS attackers with faster detection time accuracy compared to conventional approaches.

REFERENCES

[1] Dimitris Geneiatakis, Georgios Kambourakis, Tasos Dagiuklas, Costas Lambrinoudakis and Stefanos Gritzalis [2004] Framework for Detecting Malformed Messages in SIP Networks published in the framework of the IST 2004-005892 project SNOCER, Funded By European Union.

[2] Jia Zou, Wei Xue, Zhiyong Liang, Yixin Zhao, Bo Yang, Ling Shao [2015] SIP Parsing Offload: Design and Performance

[3] Zifu Fan, Xiaoyu Wan [2009] The Design And Realization Of Sip Dos Attack Detection Plugin Based On Balanced Message Number Principle published in IEEE Proceedings of ICCTA2009

[4] Hongbin Li, Hu Lin, Xuehua Yang, Feng Liu [2010] A Rules-Based Intrusion Detection and Prevenetion Framework Against SIP Malformed Messages Attacks published in Proceedings of IC-BNMT2010 of IEEE

[5] Sohil Aziz, Mehroz Gul [2010] A Self Learning Model for Detecting SIP Malformed message attacks published in IEEE proceeding of IC-BNM 2010

[6] I. Skuliber, V. Jankovic, R. Zec, Ericsson Nikola Tesla d.d., Zagreb, Croatia [2011] Multicore SIP Parsing with Imperative and Declarative Implementations published in IEEE 2011

[7] Raihana Ferdous, Renato Lo Cigno, Alessandro Zorat [2012] On the Use of SVMs to Detect Anomalies in a Stream of SIP Messages Published in 2012 11th International Conference on Machine Learning and Applications978-0-7695-4913-2/12 $26.00 © 2012 IEEE

[8] Ajay Kumar Shrestha [2014] Security of SIP-Based Infrastructure against Malicious Message Attacks published in 978-1-4799-6399-7/14 ©2014 IEEE

[9] Lukas Kramer, Johannes Krupp, Daisuke Makita, Tomomi Nishizoe, Takashi Koide, Katsunari Yoshioka, Christian Rossow [2015] AmpPot: Monitoring and Defending Against Amplication DDoS Attacks published in springer 2015

[10] Yulong Wang, Dong Wang and Lei Wang [2013] A Parsing Mode based Method for Malformed SIP Messages Testing for IMS network published in Journal Of Networks, VOL. 8, NO. 4, APRIL 2013

[11] Md. Ruhul Islam, Smarajit Ghosh [2011] Secure SIP from DoS based Massage Flooding Attack International Journal of Computer Applications in Engineering Sciences [VOL I, ISSUE II, JUNE 2011]

[12] Tasos Dagiuklas, Dimitris Geneiatakis, George Kambourakis, Dorgham Sisalem, Sven Ehlert, Jens Fiedler, Jiří Markl, Michal Rokos, Olivier Botron, Jesus Rodriguez and Juntong Liu [2005] Low Cost Tools for Secure and Highly Available VoIP Communication Services

[13] Dimitris Geneiatakis, Tasos Dagiuklas, Costas Lambrinoudakis, Georgios Kambourakis and Stefanos Gritzalis [2008] Novel Protecting Mechanism for SIP-Based Infrastructure against Malformed Message Attacks:Performance Evaluation Study

[14] Rachid El Khavari [2008] SPAM over Internet Telephony and how to deal with it published in Technische Universitat Darmstadt

[15] Anil Mehta, Neda Hantehzadeh, Vijay K. Gurbani, Tin Kam Ho and Flavia Sancier [2012] On using multiple classifier systems for Session Initiation Protocol (SIP) anomaly detection published in IEEE ICC 2012 - Communication and Information Systems Security Symposium

[16] Nikos Vrakas, Costas Lambrinoudakis [2013] An intrusion detection and prevention system for IMS and VoIP services published in Int. J. Inf. Secur. (2013) 12:201–217 DOI 10.1007/s10207-012-0187-0 Regular Contribution

[17] Jin Tang, Yu Cheng and Yong Hao [2012] Detection and Prevention of SIP Flooding Attacks in Voice over IP Networks published in IEEE Infocom 2012 Proceedings

[18] A. Mehta, N. Hantehzadeh, V. K. Gurbani, T. K. Ho and F. Sander, "On using multiple classifier systems for Session Initiation Protocol (SIP) anomaly detection," Communications (ICC), 2012 IEEE International Conference on, Ottawa, ON, 2012, pp. 1101-1106.

ResearchGate

See discussions, stats, and author profiles for this publication at: https://www.researchgate.net/publication/322797577

Energy Aware On-Demand Multipath Routing Protocol in Mobile Ad Hoc Networks

Article · October 2016

CITATIONS
17

READS
281

1 author:

M.Bheema Lingaiah
Malineni Lakshamaih Women's Engineering College
3 PUBLICATIONS **38** CITATIONS

SEE PROFILE

Some of the authors of this publication are also working on these related projects:

Mobile Ad Hoc Networks View project

All content following this page was uploaded by M.Bheema Lingaiah on 07 February 2018.

The user has requested enhancement of the downloaded file.

Energy Aware On-Demand Multipath Routing Protocol in Mobile Ad Hoc Networks

M.Bheemalingaiah[1],
Research Scholar,
Dept. of CSE,
J.N.T.University, Anantapur
A.P, India.

saibheem2008@gmail.com

M. M. Naidu[2],
IEEE member,
Dept. of CSE, Retired Professor,
S.V. University College of Engineering,
Tirupati, India.

mmnaidu@yahoo.com

D. Sreenivasa Rao[3]
Professor,
Dept. of ECE,
J.N.T.Uniersity,
Hyderabad, India.
dsraoece@gmail.com

P.Vishvapathi[4]
Principal,
Ellenki College of Engineering & Technology,
Hyderabad, India.
.
vpujala@gmail.com

Abstract: Mobile Ad Hoc Networks are treated as the emerging filed in the wireless communication. They comprise only mobile nodes that use wireless transmission and can be set anywhere and anytime because they eliminate complexity of infrastructure and central admission. They are essentially suitable when infrastructure is not present or difficult or costly to setup or when network setup is to be done quickly within a short period. They are very attractive for tactical communication in the military, rescue missions, emergency situations and mobile communications. The routing is the major issue in the field of MANET due to the mobility nature and lack of infrastructure of the network. The different routing protocols have been proposed to address the routing issue. The nodes in the MANET are typically powered by batteries which have limited energy reservoir. Sometimes it becomes very difficult to recharge or replace the battery of nodes and in such situation energy conservations are essential. The lifetime of the nodes show strong dependence on the lifetime of the batteries. In the MANET nodes depend on each other to relay packets. The loss of some nodes may cause significant topological changes, undetermined the network operation, and affect the lifetime of the network. Hence the energy consumption becomes an important issue in MANET. We proposed an Energy-Aware On-demand Multipath Routing (EAOMR) protocol by modifying the standard multipath routing protocol Ad hoc On demand Multipath Routing (AOMDV) protocol. It selects energy aware node-disjoint multipath between source and destination pairs by using new two power aware metrics, minimize cost per packet and minimize the maximum node cost to increases the network of lifetime .Finally we compare the performance of EAOMR with AOMDV protocol by using Network Simulator 2(NS2) to prove better performance of proposed protocol by using different performance metrics, throughput, packet delivery ratio, routing overhead, average end-to-end delay, packet loss and energy consumption by varying network size, node's speed, pause time, data rate, number of source and destination pairs .

Index terms: MANET, EAOMR, AOMDV, Multipath Energy, Routing.

I. INTRODUCTION

MANETs are considered as autonomous, self-configured, multi-hop wireless networks. They don't rely on any stationary infrastructure; no centralized control and they are quickly deployable anywhere at any time. In the MANET, all nodes are mobile that cooperate in friendly manner, they are connected dynamically and they have the ability to leave existing nodes from the network and enter new nodes into the network at any time, due to this, the topology of the MANET is highly dynamic and it frequently changes. In the MANET, every node the route discovery and route maintenance phase. The MANEs are widely used in military, civilian and commercial applications [1][2]. The routing is the most active research field in the MANET. The routing protocols, which are developed for wired networks are not suitable for wireless networks, due to the mobility. The routing problem becomes more serious in MANET, due to following characteristics of MANET

- Highly dynamic topology due to node's mobility
- No infrastructure for centralized administration
- Bandwidth and Energy constrained

- Hidden and exposed problem
- Error prone wireless channel
- Poor wireless variable link capacity

The routing protocols in MANET can be classified as follows

- Pre-computed routing(table driven) vs. On-Demand Routing
- Link State Routing vs. Distance Vector Routing
- Periodical update vs. Event-Driven Up-Date
- Flat structure vs. Hierarchical Structure
- Decentralized Computation vs. Distributed Computation
- Source routing vs. Hop-by-Hop Routing
- Global Position Based Vs Global Position-Less Routing
- Single Path Routing Vs Multipath Routing
- Power aware routing Vs Power Unaware Routing
- Security routing Vs Non Security Routing
- Multicast routing Vs Uncast routing

Main categories namely table driven routing protocol and On-demand routing protocol. The table driven routing protocol also as called proactive routing protocols or pre-computed routing [2]. In Table-driven routing protocols each node computes route to all other nodes in network in advance, each node maintains one or more tables containing routing information to every other node in the network. All nodes update these tables so as to maintain a consistent and up-to-date view of the network. When network topology changes the nodes propagate and update messages throughout the network in order to maintain consistent and up-to-date routing information about the whole network. Some well known and standard table driven protocols are as follows

- Wireless Routing Protocol (WRP)
- Global State Routing (GSR)
- Fisheye State Routing (FSR)
- Hierarchical State Routing (HSR)
- Zone Based Hierarchical LSR Protocol (ZHLS)
- luster Switch Gateway Routing (CGSR)
- Destination Sequenced Distance-Vector Protocol (DSDV)

The on-demand routing protocols build routes only when a node needs to send the data packets to a destination by invoking the route discovery. Some of the well known and standard on demand routing protocols are as follows

- Dynamic Source Routing (DSR)
- Cluster Based Routing Protocol (CBRP)
- Ad-hoc On-demand Distance Vector Routing Protocol (AODV))
- Temporally Ordered Routing Algorithm (TORA)
- Associatively Based Routing (ABR)
- Signal Stability Based Adaptive Routing (SSR).

The on-demand routing is the most popular approach in the MANET compared to table-driven routing, instead of periodically exchanging route messages to maintain a permanent route table of the full topology, the maintenance of whole information about network topology in routing tables is eliminated and the dissemination of routing information throughout the network is also eliminated because that will consume a lot of the scarce bandwidth and power when the link state and network topology changes rapidly and it also works well when network size increases. Hence in this work, we considered on-demand routing.

II. RELATED WORK

The most of existing routing protocols are single path routing protocols. They find single route and utilize it for data transmission from source to destination. Due to dynamic topology, poor and variable wireless links, dynamic characteristics of radio channel, node failure, the currently using route becomes invalid. Due to this the overhead for finding new route from source to destination may be high and extra delay for new route discovery may be introduced and data transmission becomes late [3]. To overcome this drawback by using multipath routing, it is latest trend in the MANET; it finds multiple paths from any source to destination in a single route discovery.

Due to the introduction of multipath routing, the time for searching the route will be reduced drastically and also it helps to reduce the latency for searching the other route at the situation of path failure. In MANETs, multipath routing is considered as trusted approach for ad hoc networking. Due the mobile nature or weak signal strength, the node failure occurs frequently in the MANETs. At the condition of route failure, the multipath routing serves as the best approach for finding the alternate path. The applications of multipath routing are given below.

- Reliability
- Fault tolerance
- Balancing Of Load
- Bandwidth aggregation
- Reduced delay
- Energy consumption
- Reduction of routing overhead
- Provide the Quality of Service(QoS)
- Improve network security and secure communication

There are two types of multipath, Node-disjoint multipath and Link-disjoint multipath. The node-disjoint multipath does not have any nodes in common, except for the source and the destination. Whereas, link-disjoint multipath does not have any common links, but may have common nodes.

In the recent years, many researchers made the contribution to address the multipath routing. The several multipath on-demand routing protocols were proposed. Some well known standard Multipath path routing Protocols are

- Ad hoc On-demand Distance Vector Multipath Routing (AODVM)[4]
- Ad hoc On-demand Multipath Distance Vector (AOMDV)[5]
- Split Multipath Routing (SMR)[6]
- Multipath Source Routing (MSR)[7

The comparison of above on- demand Multipath Routing Protocol is shown in table1

Table.1 Comparison of On demand Multipath Routing Protocol

	AODVM	AOMDV	SMR	MSR
Loop-Free paths	No	No	No	No
Node Disjoint	Yes	Yes	No	Yes
Link-Disjoint	No	Yes	Yes	No
Routing Overhead control	No	No	No	No
Complete Routes Known at source	No	No	Yes	Yes
Multipath used Simultaneously	Yes	Yes	Yes	Yes
TTL limitation	Yes	Yes	Yes	Yes
QOS Support	No	No	No	No
Multicast Support	No	No	No	No
Power / Energy Management	No	No	No	No
Security Support	No	No	NO	No

The MANETs contains only mobile modes and they are originally operated with the battery power, so, the major constraint for mobile nodes are battery power. Therefore, the energy is consumed during the transmission of packets. The energy optimization is another important research challenge [1]. Optimizing the energy consumption is one of the designing issues for multipath routing.

New Power Aware Metrics: Suresh Singh, Mike Woo and C. S. Raghavendra[8] raised the power awareness issue in or the ad hoc routing and introduced new metrics for path selection. Minimizing the number of hops is no longer the objective of a routing algorithm, but rather the optimization of multiple parameters such as packet error rate, energy consumption, bandwidth, routing overhead, route setup, route repair speed and possibility of establishing parallel routes etc. A critical issue is power constrained. Developing routing protocols for MANETs has been an extensive research area during the past few years. In particular, energy efficient routing is the most important design criteria for MANETs since mobile nodes will be powered by batteries with limited capacity. The power failure of a mobile node not only affects the node itself but also its ability to forward packets on behalf of others and thus the overall network lifetime. For this reason, many research efforts have been devoted to developing energy aware routing protocols. Different routing protocols use one more metrics to determine optimal paths. Presently most common metric being used are:

- ***Shortest length***
- ***Shortest delay***
- ***Link quality***
- ***Location stability***

The limitation on availability of power for operation is significant bottleneck given the requirements of portability, weight and size of commercial hand held devices. Hence, the use of routing metrics that consider the capabilities of power sources of network nodes contributed to the efficient utilization of energy and increases the life time of the network. The authors present five power aware metrics that do result in energy-efficient routes. The five new metrics are as follows

- ***Minimize energy consumed per packet***: This metric will minimize the average energy consumed per packet.
- ***Maximize time to network partition***: This metric tries to increase the life of Network.
- ***Minimize variance in node power levels***: This metric ensures that all the nodes in the network remain up and running together for as long as possible.
- ***Minimize cost per packet***: This metric minimizes cost for sending a packet.
- ***Minimize the maximum node cost***: This metric minimizes the maximum cost of the node.

To serve this purpose, several energy aware multipath routing protocols were proposed [2]. Multipath Power Sensitive Routing (MPSR)[9],Energy-Aware Multipath Routing (EMRP)[10] protocol, Multipath Energy-Efficient Routing Protocol (MEER)[11],Lifetime-Aware Multipath Optimized Routing (LAMOR**[**12], Energy Aware Source Routing (EASR)[13], Grid-Based Energy Aware Node-Disjoint Multipath Routing Algorithm (GEANDMRA**)[**14], Ant-based Energy Aware Disjoint Multipath Routing Algorithm.(AEADMRA)[15], Energy-Aware Grid Multipath Routing(EAGMR) Protocol[16], Power-Aware Multi-Path Routing(PAMP)**[**17] Protocol , Energy Efficient On-Demand Multipath Routing(MMRE-AOMDV)[18]Protocol, Energy Aware Node-Disjoint Multipath(ENDMR)[19], Energy Aware Clustered Based Multipath Routing (EACMR)[20], Power-Aware Node-

Disjoint Multipath Source Routing (PNDMSR)[21],An optimized energy aware routing OEAR[22], The Link Stability with Energy Aware(LSEA) routing protocol[23], Energy Efficient Power Aware Multipath Dynamic Source Routing (DSR-SR)**[**24**],** Energy Efficient Multipath Routing(EEMR)[25], Energy Conservation for Ad Hoc On-Demand Distance Vector Multipath Routing Protocol**[**26], Energy Optimized Ad hoc on-Demand Multipath Routing Protocol[27] and Enhanced Power aware Multipath Routing [28]Protocol.

A) Problem statement: In table 1 shows that AOMDV [5] does not support energy management i.e the main drawback of AOMDV [5] is it does not find energy aware multipath from source to destination. It finds only unaware energy multipath between source to destination. To overcome the drawback, we proposed a novel energy aware node-disjoint multipath routing protocol by using following two new power metrics [8] to find optimal energy aware node node-disjoint multipath between source and destination.

- Minimize the maximum node cost
- Minimize cost per packet

This protocol is named as Energy Aware On-demand Multipath Routing (EAOMR) Protocol. Some protocols have been proposed based on AOMDV to find the energy aware multipath from source to destination, however these protocols failed in considering of the above two new power metrics to find energy aware node-disjoint multipath between source to destination.

III. Energy Aware On-demand Multipath Routing (EAOMR) Protocol.

The main aim of EAOMR is to find the energy aware node-disjoint multipath form source to destination by using by using node's cost and two power aware metrics, minimize the maximum node cost and minimize cost per packet. It consists of the following four main mechanisms

It consists of the following four main mechanisms

- Route selection
- Route Discovery
- Route Maintenance

A) Route selection using node's Cost function

The main objective of route selection is to select the optimal paths to prolong network's life time. It is based on cost function .The main objective of cost function is to give more weight (or) cost to node with less energy to prolong its life time [19]. Let c_i^t be the battery capacity (residual energy) of a node n_i at time t. Let $f_i(c_i^t)$ be the battery cost function of node n_i at time t. The cost of node n_i is equal to value of battery cost function, which in turn inversely propositional to residual energy of the node n_i i.e. $f_i(c_i^t) = 1/c_i^t$. We describe the following cost function

$$f_i(c_i^t) = \rho_i \times \left[\frac{F_i}{c_i^t} \right] \times w_i \qquad (1)$$

Where $f_i(c_i^t)$: Cost of node n_i at time t

ρ_i : Transmit power of node n_i

F_i : Full-charge capacity of node n_i

c_i^t :Residual energy (Remaining battery capacity) of a node n_i at time t.

w_i : weight factor which depends upon various factors, like battery's quality, battery's capacity, life time, battery's back up, and price.

Cost of the path

Let P_j be the path from source s to destination d via intermediate nodes n_1- n_2 ---- -----n_{k-1} -n_k at time t.

$$P_j^t = s - n_1 - n_2 - n_3 - n_4 - - - - n_{k-1} - n_k - d$$

We consider two different costs for each path. The first cost is chosen as maximum cost of any intermediate node on the path P_j at time t, it is also called as **primary cost ,** it is denoted by

$$C'(P_j^t) = \max\{ f_i(c_i^t) \quad / \quad \forall n_i \in P_j^t \ \} \qquad (2)$$

Note: Where max is function that selects the maximum cost of interrelate node on the path p_j at time t .The second cost is average cost it is sum of cost of all intermediate nodes on the path p_j at time t divided by total number of intermediate nodes, it is also called **secondary cost**, it is denoted by

$$C''(P_j^t) = \frac{\sum_{i=1}^{k} f_i(c_i^t)}{k} \qquad (3)$$

Where K equal to number of intermediate nodes on path p_j at time t, it is also equal to number of hops minus one or hop_count minus one on path p_j at time t.

B) Route Section Techniques in EAOMR

Optimization is the act of obtaining the best results under given circumstances [32]. In design, construction and any maintenance of any engineering system, engineers have to take many technological and managerial decisions at several stages. The ultimate goal of such decisions is to either minimize the effort required or maximize the desired benefit. Since the effort required or the benefit desired in any practical situation can be expressed as a function of certain decisions variables, optimization can be defined as the process of finding the conditions that give the maximum or minimum value of a function.

There two techniques have been proposed t for route selection

***1) First Technique**:*

In this technique, the first priority is given to primary cost and second priory is given to secondary cost. By using primary cost all set of feasible paths are selected and secondary cost is used to select the optimal paths. This technique as described as follows

Optimization problem is stated as follows

Let γ be threshold (cut-off) residual energy of battery of a node and it is considered that this threshold energy of battery is equal for all the nodes irrespective of their battery capacities. If node's energy reaches threshold, then node will die shortly. Let M be set of node-disjoint multipath that were found during route discovery technique from source s to destination d at time t, a feasible path is node-disjoint path that must minimize the equation subject to $\gamma < c_i^t \le F_i$, it is denoted by

$$P_f^t = \{P_j^t / C^{'}(P_j^t) = Min\{ C^{'}(P_j^t) / \ \forall P_j^t \in M\}\} \quad (4)$$

Where Min is a function that selects least cost. Let F be the set of all feasible paths based equation (4) .An optimal path is the feasible path with least average cost , it denoted by

$$P_o^t = \{P_j^t / C^{"}(P_f) = Min\{C^{"}(P_j^t)\}, \forall P_j^t \in F\} \quad (5)$$

2) Second Technique by using Resulting Cost of path

In some situations there may be more than one criterion to be satisfied simultaneously [33]. An optimization problem involving multiple objective functions is known as a multi-objective programming problem. With multiple objectives there arises possibility. In this technique, equal priority is given to both costs and the route is selected by combination of both costs primary cost and secondary cost and is called resulting cost. The resulting cost of path P_j^t at time t is denoted by

$$RC(P_j^t) = C^{'}(P_j^t) + C^{"}(P_j^t) \quad (6)$$

All these costs of node-disjoint multipath are stored in on-dimensional array and apply quick sort algorithm to sort these resulting costs in ascending order for selecting routes. During selection of routes, the routes are selected according to their ascending order of their resulting costs. The first priority is given to route whose resulting cost is least in sorted array and least priority is given to route whose resulting cost is highest in sorted array. In the simulation, we used this technique.

C) Route Discovery of EAOMR

The EAOMR is extension of AOMDV [5] to find energy aware node-disjoint paths by some modifications. The AOMDV protocol is the use of routing information already available in the underlying AODV [30] protocol as much as possible. For each destination, a node maintains the advertised _hopcount, which is defined as the maximum hop count for all the paths, which is used for sending route advertisements of the destination. Each duplicate route advertisement received by a node defines an alternate path to the destination. Loop freedom is assured for a node by accepting alternate paths to destination if it has a less hop count than the advertised_hop count for that destination. Because the maximum hop count is used, the advertised hop count therefore does not change for the same sequence number. When a route advertisement is received for a destination with a greater sequence number, the next-hop list and the advertised hop count are reinitialized. AOMDV [5] can be used to find node-disjoint or link-disjoint routes. To find node-disjoint routes, each node does not immediately reject duplicate RREQs. Each RREQs arriving via a different neighbor of the source defines a node-disjoint path. This is because nodes cannot be broadcast duplicate RREQs, so any two RREQs arriving at an intermediate node via a different neighbor of the source could not have traversed the same node. In an attempt to get multiple link-disjoint routes, the destination replies to duplicate RREQs, the destination only replies to RREQs arriving via unique neighbors. After the first hop, the RREPs follow the reverse paths, which are node disjoint and thus link disjoint. The

trajectories of each RREP may intersect at an intermediate node, but each takes a different reverse path to the source to ensure link disjointness. The advantage of using AOMDV is that it allows intermediate nodes to reply to RREQs, while still selecting disjoint paths. But, AOMDV has more message overheads during route discovery due to increased flooding and since it is a multipath routing protocol, the destination replies to the multiple RREQs those results are in longer overhead.

The proposed modifications are explained briefly as follows.

1) Modifications of Control Packets Format

There are three types of control packets used in the AOMDV

- RREQ packet
- RREP packet
- RERR packet

RREQ and RREP packets are used in route discovery technique, where RERR packet is used in the route maintenance technique and they are modified as follows

a) Modification of Route Request Packet (RREQ)

The Route Request Packet (RREQ) of AOMDV [5] is same as RREQ of AODV[30] .The RREQ of AOMDV is extended as RREQ of the EAOMR by adding one extra field at the end, is called first hop field . Several changes are needed in the AODV [30] route discovery procedure to enable computation of node-disjoint paths between source-destination pairs. Each RREQ now carries an additional field called ***firsthop*** to indicate the first hop (neighbor of the source) taken by it. Also, each node maintains ***firsthop_ list*** for each RREQ to keep track of the list of neighbors of the source through which copy of the RREQ has been received. The size of ***firsthop*** field is 4bytes as shown in fig.1

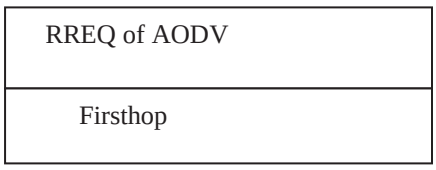

Fig .1. RREQ of EAOMR

b)Modification of Route Reply Packet (RREP)

The Route Reply Packet (RREP) of AOMDV[5] is same as RREP of AODV[30]. The RREP of AOMDV is extended as the RREP of the EAOMR by adding two extra fields at the end, first field is called as Max-Cost field and second field is called as Total-Cost field, it is also called as sum field. The size of each field is 4 bytes as shown in fig. 2.

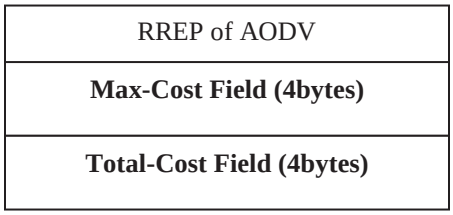

Fig.2**.** RREP packet format of EAOMR

Max_Cost field: When RREP packet passes through a node, it compares its cost with cost in Max_Cost field of RREP packet, if its cost is greater than cost in Max-Cost field of RREP packet, then this field is updated by the node by copying its cost; otherwise this field is not disturbed. Initially by default value of this field is set to zero value by destination during generation of RREP packet to source node. This field is not disturbed by source node.

Total_Cost field (Sum field): It carries the cumulative cost of all intermediate nodes of a path from destination to source**,** when the RREP packet passes through a node; its cost is added to this field. Initially, by default value of this field is set to zero by destination during generation of the RREP packet to source node and this field is not disturbed by source node.

c) Route Error (RERR) packet format:

There is no modification in the Route Error (RERR) packet of EAOMR, it is same as RERR of AOMDV [5] it is also same as RERR of AODV [30] .

2) Modifications of Routing Tables

The *advertised_hopcount* of a node i for a destination d represents the "maximum" hop-count of the multiple paths for d available at i. "Maximum" hopcount is considered, as then the advertised hop-count can never change for the same sequence number. The protocol only allows accepting alternate routes with lower hop-counts. In AOMDV [5], Advertised_hopcount replaces hopcount in AODV [30]. A route_ list replaces nexthop in AODV and essentially defines multiple next hops with respective hopcounts. However, all next hops still have the same sequence number. When route list is empty, by default initial value of advertised_ hopcount is infinity ∞ .

In EAOMR , the structure of routing table of each node is shown in fig3 , the structure of routing table of each node is extended by adding two extra fields to each entry of Route list of AOMDV [5], first field is Max_Cost and second filed Total _Cost and initially these fields are empty , the question is why should node i has store these two field values? In case If node i has to be reply to source

node. Then it constructs RREP reply packet in that case these values is required. That's why these field values are stored for future purpose in it routing table

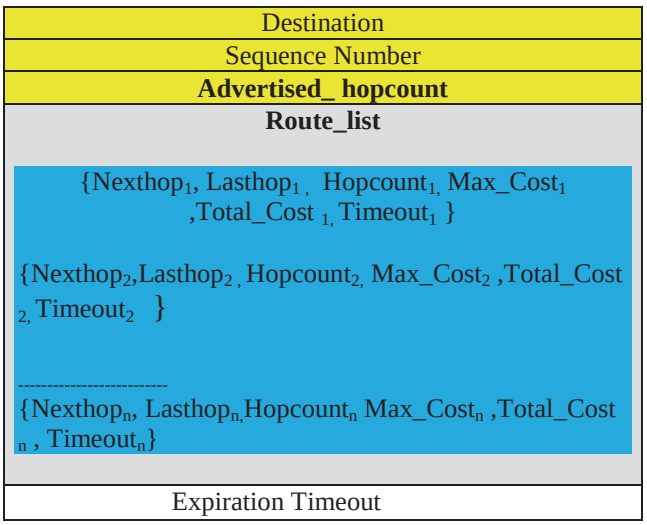

Fig. 3. Structure of Routing Table entries in EAOMR

3) Modification of Functions of Nodes:

a) Source Node: In AOMDV [5], when a source node wants to send data to a destination, it looks up its route cache to determine if it already contains a route to the destination. If it finds that an unexpired route to the destination exists, then it uses this route to send the data. If the source node does not have such a route, then it initiates the route discovery process by broadcasting a route request (RREQ) packet to neighbors and if destination is found, it replies by sending RREP to source. In the EAOMR, the functions of the source node similar, but source node maintains unexpired energy aware node- disjoint Multipath to a destination in its cache. They are selected according to route selection technique described in section 3.11.

***b) Intermediate Node*:** The main functions of an intermediate node in AOMDV [5] is as follows

- Preventing loops by using Route Update Rule
- Updating Routing Table for maintaining multiple paths
- Setting Reverse Path for sending RREQ packets
- Setting Forward Path for data transmission

Each node must follow the route update rule for prevention loops as well as to update its routing table for maintaining multiple paths when it receives RREQ Packet or RREP packet from its neighbor node. The modified route update in EAOMR is described section 4 in fig 5. Other two functions are **as** follows

Forwarding of RREQ and setting up reverse path to source node:

In AOMDV**,** while forwarding of RREQ, at the intermediate nodes, unlike in AODV, duplicate copies of RREQ are not immediately discarded. Each copy is examined to see if it provides a new node-disjoint path to the source. This is ascertained by examining the ***firsthop*** field in the RREQ copy and the ***first-list*** in the node for the RREQ. If it does provide a new path, the AOMDV [5] route update rule is invoked to check if a reverse path can be set up. If a reverse path is set up and a valid route to the destination is available at the intermediate node, it sends back a RREP to the source. Just as in AODV, only the first arriving RREQ copy is forwarded if a route to destination is unavailable. This technique is same as in EAOMR and while forwarding RREQ packets, route update rule of EAOMR is same as route update rule of AOMDV.

Forwarding RREP Packets and Setting up forward path to destination node:

Each RREP arriving at an intermediate node takes different reverse routes when multiple routes are already available. When node i receives a RREP packet from its neighbor node j for destination d then it uses route update rule is shown fig .5. It constructs or generates route reply by using following rule. It compares its cost with cost in Max_Cost field of RREP of node j, if its cost is greater than cost in Max_Cost field of RREP of node j, then this field is updated by the node i by copying its cost, otherwise this field is not disturbed by node i and adds its cost to Total-Cost field. Then node i set up the forward path from source to destination and sends its RREP to its neighbor node in its reverse path. The propagation of RREP packets from destination node to source node in EAOMR is in the following fig .4. Each RREP packet carries and provides the primary cost and secondary cost of a path to source node for selecting feasible and optimal energy aware node-disjoint paths for sending data to destination.

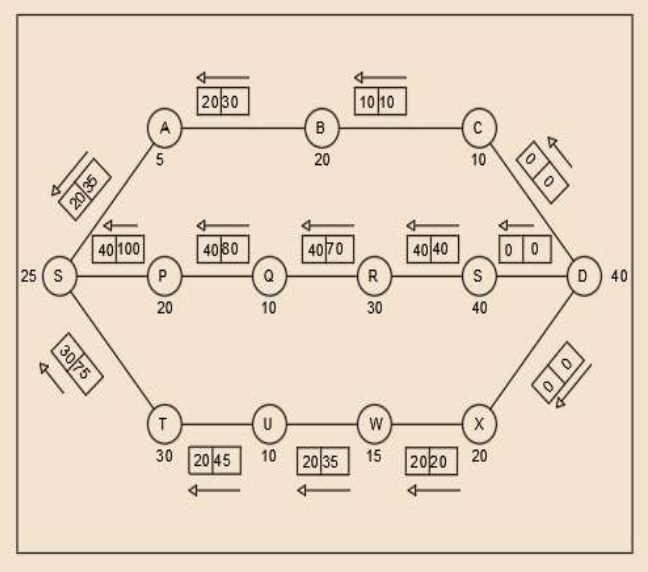

Fig.4. the Propagation of RREP packets

c) Destination node:

At the destination, reverse routes are set up just like in the case of intermediate nodes. However, in the hope of getting link-disjoint paths which would be more numerous than node-disjoint paths, the destination node adopts a "looser" reply policy. It replies up to copies of RREQ (arriving via *unique* neighbors), regardless of the ***firsthop***s taken by these RREQs. Unique neighbors guarantee link-disjointness in the first hop of the RREP. Beyond the first hop, the RREP follow the reverse routes that have been set up already which are node-disjoint (and hence link-disjoint). Each RREP arriving at an intermediate node takes a different reverse route when multiple routes are already available. Note that because of the "looser" reply policy it is possible for the trajectories of RREPs to cross at an intermediate node.

4) Modified Route update rule (Algorithm) in EAOMR

//This is used whenever a node i receives a route advertisement to a destination d from a neighbor node j,

// Variables seq_i^d , $advertised_hopcount_i^d$ and $route_list_i^d$ represent the sequence number, advertised_ hopcount and route_ list for destination d at node i respectively.

// $RREP_i$ and $RREP_j$ are route reply packets which are generated by node i and node j respectively.

// Update MAX-Cost and Total cost by node i for constructing RREP

$$If \ \ (f_i(c_i^t) > RREP_j[\text{Max_Cost}])$$

$$RREP_i[Max_\text{Cost}] = f_i(c_i^t)$$

Else

$$RREP_i[Max_\text{Cost}] = RREP_j[Max_\text{Cost}]$$

// Update Total -Cost by node i

$$RREP_i[Total_\text{Cost}] = RREP_j[Total_\text{Cost}] + RREP_i[Total_\text{Cost}]$$

$if\ (seq_i^d = seq_j^d)$ then

$$seq_i^d = seq_j^d$$

$$if\ (i \neq d)$$

{

$$route_list_i^d = Null$$

// update route list by creating new entry

$insert\ \ (j,\ advertised_hopcount_j^d + 1,\ RREP_i[Max_\text{Cost}],\ RREP_i[Total_\text{Cost}])$ in to $route_list_i^d$

}

Else

$$advertised_hopcount_i^d = 0$$

End if

Else if ($seq_i^d = seq_j^d$) and

$((advertised_hopcount_i^d, i) > (advertised_hopcount_j^d, j))$

// update route list by creating new entry

$insert\ \ (j,\ advertised_hopcount_j^d + 1,\ RREP_i[Max_\text{Cost}],\ RREP_i[Total_\text{Cost}])$ in to $route_list_i^d$

End if

Fig.5. Modified Route Update Rule in EAOMR

D) Route Maintenance

The EAOMR handles route maintenance in a manner similar to the AOMDV [5]. Whenever a link breakage

happens in a route due to a node moving away, the previous hop node of the moved away node is responsible for sending a Route Error (RERR) message back to the source to inform the breakage. It chooses alternative routes to maintain the connection. If there are no more redundant routes left, then it will start a new route discovery.

IV. PERFORMANCE ANALYSIS OF EAOMR BY USING NS2.

In this section, we describe the Performance Evaluation And Comparison of EAOMR and AOMDV by using Network Simulator 2 (NS2) [34] with simulation setup The NS2 is popular and standard simulation tool for implementing all types of network protocols. It was developed by the University of California at Berkeley and it is widely used by research scholars. The NS2 was developed by using two computer programming languages one is C++ another is OTcl (Object oriented Tool Command Language) interpreter as a command and configuration interface. The Network Animator (NAM) is an animation tool for inspecting network topology and data transmission shown in fig 5

Different performance metrics are employed to test the EAOMR against the AOMDV both are implemented using Network Simulator 2, in the new version of simulator is NS2.23, Ubuntu operating system was used. The area for network configuration is chosen as 1000m x 1000m and the nodes are deployed with in this region. . For the mobile scenarios, the random waypoint model is used for node mobility. In this model, the random waypoint model is used for node mobility. In this model, a node chooses a random destination point in the network and moves towards that destination point at a constant speed then the node reaches its destination, where it stays for a certain pause time, after which it chooses another random destination point and repeats the process.

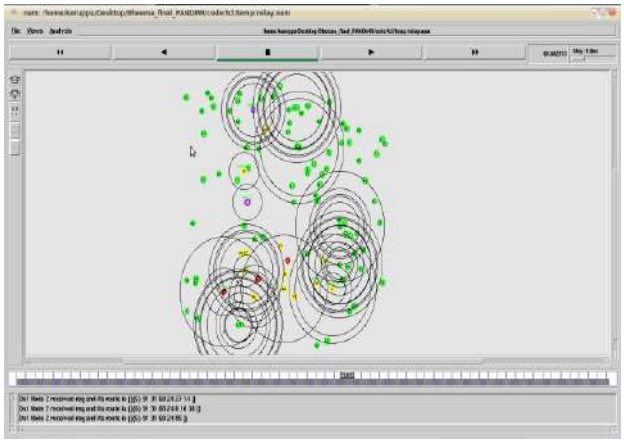

Fig. **5. Shown in Network Animator (NAM) with 50 nodes**

The channel bandwidth is 2Mbps, a free space radio propagation model is used in which the signal power attenuates is $1/r^2$, where r is the distance between the nodes. All the nodes have the same transmission range of 250 meters. The distributed coordination function of IEEE802.11 DCF is used as MAC layer. All nodes operate in promiscuous mode, so it can overhear packets destined for others. The simulation ends after 100sec. The data traffic is generated by Constant Bit Rate (CBR) sessions initiated between the source and destination. All the nodes are assumed to have the same amount of battery capacity with full residual energy at the beginning of the simulation and initial energy of each node is set to 50 Joules. The transmitting power and receiving power of each node are set to 0.079Watts and 0.066Watts respectively. The idle power of each node is set to 0.005Watts the following table 2 shows the simulation setup.

The following quantitative performance metrics are used to measure the performance of both protocols.

- Overhead
- Throughput
- Packet Delivery Ratio
- Packet loss Ratio
- End to End Delay of packets
- Energy Consumption

By varying the following parameter

Number of nodes (density) [25, 50, 75, 100]
Fixed {Speed=30m/S, Pause Time=4s, Data Rate=50Kbps and Load=4}

Mobility of node(speed) [10 m/s, 20m/s, 30m/s, 50m/s],

Fixed {Network Size=50, Pause Time=4s, Data Rate=50kbps and Load=4}

Data Rate [10Kbps, 20Kbps, 30Kbps, 50Kbps]

Fixed {Network Size=50, Speed= 2m/S, Pause Time=4s and Load=4}

Pause time [2sec, 4sec, 6sec, 8sec],

Fixed {Network Size=50, Speed= 30m/S, Data Rate =50kbps and load=4}

Number of source nodes and Destination pairs (increasing load) [1, 2, 3, 4]
Fixed {Network Size=50, Speed= 2m/S, Pause Time =4ms, Data Rate =50kbps}

Here we have derived some facts or relationships among performance metrics and parameters based on our previous work

Sno	Parameter and Values
1	Network size and Node's Placement 1000 x 1000 Sq meters (Size of NAM),
2	Number of Nodes: 25, 50, 75, 100
3	Total Simulation time : 100s
4	Node's Mobility : Random Way Point Mobility odel(RWPMM)
5	Node's Speed: 10 m/s, 20m/s, 30m/s, 50m/s
6	Node's Pause Time: 2s, 4s, 6s, 8s
7	Application Layer : Constant Bit Rate(CBR)
	Packet Payload size: 512 bytes
	Data rate :10Kbps, 20Kbps,30Kbps ,50Kbps
	Number of source and destination pairs : 1, 2, 4,8
8	Transport Layer: User Datagram Protocol(UDP) ,CBR
9	Network Layer: EAOMR and AOMDV Routing Protocols
10	Data Link Layer: Logical Link Control Layer (LLC)
	Medium Access Layer(MAC):IEEE 802.11 DCF
11	Physical Layer:
	Antenna Model : Omni Directional
	Wave Propagation Model: Two-way Ground Model
	Channel Type: Wireless Channel Physical layer Channel Bandwidth: 2Mbps Lucent Wave LAN card with frequency 915MHz Transmission range of node : 250 meters Interference range of node: 500 meters
	Interface Queue Type: CMU Priority Queue with size 50 packets
12	Energy Model:
	Initial energy of each node: 50Joules
	Transmission Power: 0.079 Watts
	Receiving Power:0.066 Watts
	Idle Power: 0 .035 Watts
	Sleep Power: 0.005 watts
	Transition Power :0.2 watts
	Transition Time: 0.005 sec

Table.2. Different Parameters and Values

Fact 1: The overhead

It is directly proportional to probability of collisions, packet loss, packet error rate, packet delay, bandwidth consumption and energy consumption. It is indirectly proportional to packet delivery ratio and throughput. Hence the overhead depends on overall performance of the routing protocol.

Fact 2: Network's size (density)

If size of network increases, distance between source and destination also increases, due to this number of hops increases between sources to destination. Hence overhead increases for route discovery and end to end packet delay also increases. Hence network size is directly proportional to overhead, end to end packet delay, congestion, bandwidth consumption, energy consumption, packet collision and loss. The network' size is indirectly proportional to throughput, packet delivery ratio**.**

Fact 3: Speed

It is directly proportional to path failure rate, overhead, congestion energy consumption, bandwidth consumption. packet delay, packet collision and packet loss. It is indirectly to throughput, Packet Delivery Ratio.

Fact 4: Pause Time

The increase pause time means increasing network stability. Hence it is indirectly proportional to path failure rate, overhead, energy consumption, Packet loss, bandwidth consumption and congestion, packet delay, packet collision packet loss. It is directly proportional to throughput, Packet Delivery Ratio.

Fact 5: Data Rate

It is directly proportional to congestion, energy consumption, packet loss and bandwidth consumption, packet delay. It is directly proportional to throughput, Packet delivery ratio until congestion occurs.

Fact 6: Number of source and destination pairs (load)

It is directly proportional to overhead, energy consumption, bandwidth consumption, congestion, packet delay, packet loss and packet collision. . It is directly proportional to throughput, Packet Delivery Ratio until congestion occurs

A) Analysis of Routing Overhead

The optimization of routing overhead is crucial part when designing new routing protocol because the overhead is

directly proportional to congestion, probability of collisions, packet loss, packet error rate, packet delay, bandwidth consumption and energy consumption. It is indirectly proportional to packet delivery ratio and throughput. Hence the overhead depends on overall performance of the routing protocol. The routing overhead is defined as the number of control packets as generated at the time of simulation. The overhead is the most important performance metric to compare the routing protocols.

Routing Overhead= Number of Control Packets (RREQ, RREP, REEP) generated by routing protocol during simulation.
The normalized routing overhead is calculated as follows

$$\text{Normalized Routing Overhead}=\frac{x}{y} \qquad (7)$$

Where x is total number of routing packets generated

and y is total number of packets received

The Link-disjoint and Node-disjoint Multipath variant of AOMDV protocol have been evaluated the performance between them [33]. These protocols investigated with varying node density and pause time. The various QoS matrices are computed to analyze the performance. It is evident from the results that node disjoint multipath performs better as compared to link disjoint multipath routing technique. Theoretically, it is noticed that node-disjoint is better compare to link-disjoint. It proved that simulation results also justified the same [33].

1) Overhead by Varying Number of nodes (Density):

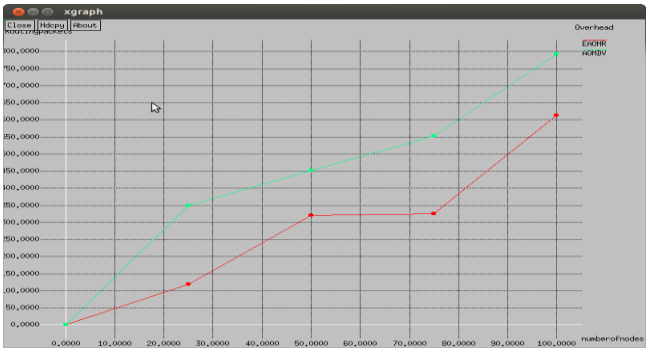

Fig. 4.1 Overhead Vs Network's Size (density)

Fig.4.1. shows, Overhead Vs Number of nodes by varying number of nodes (density) 25, 50, 75 and 100. The overheads of both protocols increased. In case of 50 and 75 nodes the overhead of EAOMR has not been changed but the overhead of AOMDV is increased drastically and exponential compared to the EAOMR. However in all above four cases EAOMR produces less overhead than AOMDV, because the EAOMR was designed to find node-disjoint multipath that are energy aware and AOMDV was designed to link-disjoint multipath that are energy unaware.

2) Overhead by varying node's speed

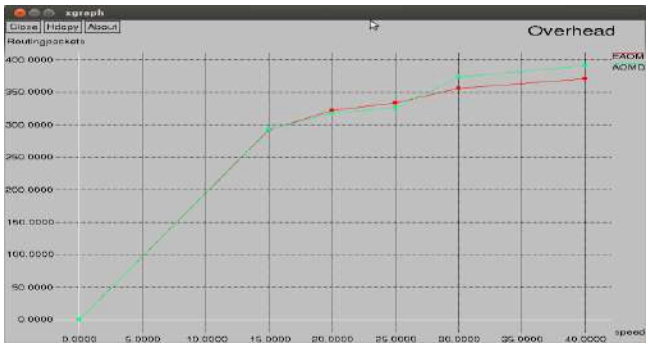

Fig.4.2 Overhead Vs Speed (m/s)

Fig 4.2 shows the Overhead Vs Speed of node , speed is varied as 10m/s, 20m/s, 30m/s, 50m/s, usually speed increases overhead are also increases because probability of path failure rate increases. At speed 10m/s, the overhead of both protocols is same. At speed 20m/s, the overhead of EAOMR is slightly increased than overhead of AOMDV and it is approximately equal. Later at high mobility, the EAOMR produces less overhead than AOMDV and it performs much better than AOMDV when speed increases.

3) Overhead Vs Varying pause time

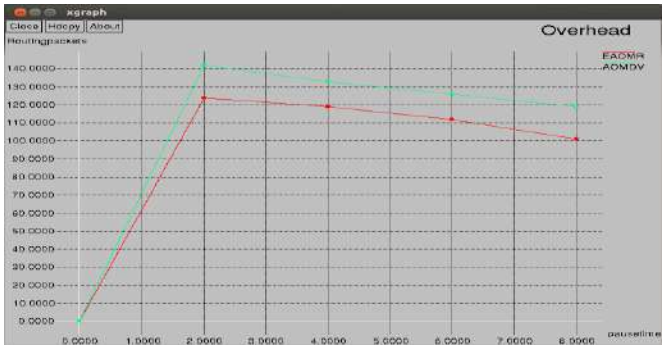

Fig. 4.3. Overhead Vs Pause Time

Fig.4.3 shows, Overhead Vs Pause Time, here pause time is varied as 2s, 4s, 6s and 8s. Usually, the pause time increases network stability also increases and path failure rate decreases. So pause time is indirectly proportional to overhead. Fig 4.3 shows the overheads of both protocols decreased when increasing the pause time and EAOMR yielded less overhead than overhead of AOMDV.

4) Overhead Vs Varying Data Rate

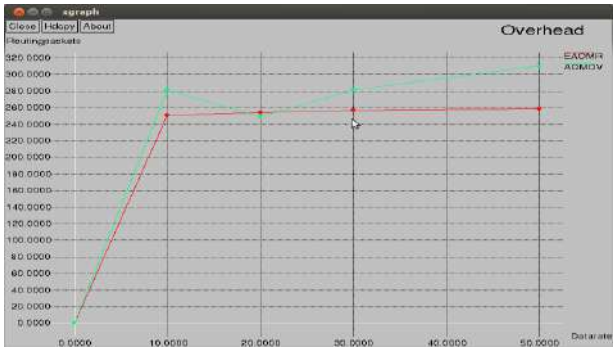

Fig . 4.4. Overhead Vs Data Rate (Kbps)

Fig. 4.4 shows overhead Vs Data rate, here data rate is varied as 10Kbps, 20Kbps, 30Kbps and 50Kbps and usually data rate is directly proportional to the overhead. In three cases 10Kbps, 30Kbps and 50Kbps, EAOMR yielded less overhead than overhead of AOMDV. At 20Kbps the overhead of the EAOMR is slightly increased than overhead of AOMDV, because the overheadoes not purely depend on the data rate.

The path failure rate is also depends on the dynamic characteristics of ad hoc network. i.e it depends on unpredictable in node mobility, poor wireless link quality, error-prone radio shared channel, hidden and exposed problems.

5) Overhead by varying Source and Destination pairs (connections)/load.

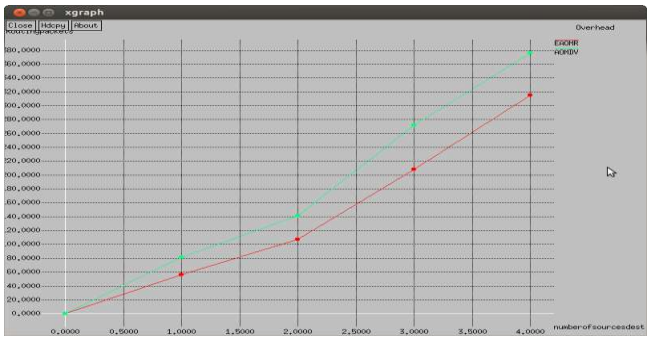

Fig.4.5. Overhead Vs Number of Source and Destination pairs (connections)

Fig.4.5 shows overhead Vs number of sources and destination pairs (load), here number of source and detonation pairs is varied as 1, 2, 3 and 4. The number of sources (load) is directly proportional to the overhead. When increasing load, the overheads of both protocols increased exponentially. However in all four cases the EAOMR yielded less than overhead of AOMDV and the overhead of the AOMDV drastically increases compared to the overhead of EAOMR, because the overhead of EAOMR was designed to find node-disjoint multipath that are energy aware and AOMDV was designed to find link-disjoint multipath that are energy unaware . Theoretically, it is noticed that node- disjoint is better compare to link-disjoint. It proved that simulation results also justified the same [33].

B) Analysis of Energy Efficiency

It is an important qualitative metric to measure the performance of different protocols. The energy efficiency is calculated as the ratio of total received data (bytes) to the total energy consumption using equation 8 [10]

$$\text{Energy Efficiency}=\frac{x}{y} \quad (8)$$

Where x is total received data in terms of bytes and y is total energy consumption in terms of joules

$$\text{Total energy consumption}=\sum_{i=1}^{n}(E_i - R_i) \quad (9)$$

Where E_i denotes the initial energy of i^{th} node , R_i denotes the residual energy of i^{th} node and n total number of nodes in the network. In Table 2, in energy model, we used the following new parameters

- Sleep Power is power consumption (Watt) in sleep state
- Transition Power is power consumption (Watt) in state transition from sleep to idle (active)
- Transition Time is time (second) used in state transition from sleep to idle (active)

The overhead is directly proportional to energy consumption. The following four scenarios shown that overall EAOMR has less energy consumption compared to the AOMDV because the EAOMR has yielded less overhead compared to the AOMDV.

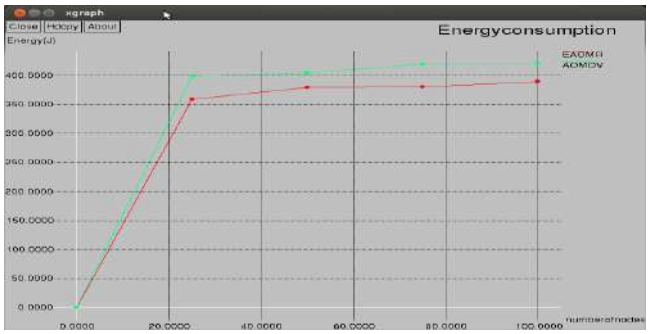

Fig.4.6. Energy Consumption Vs Number of Nodes

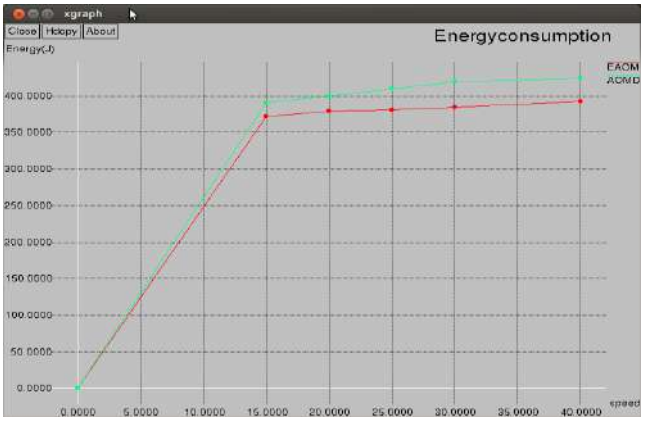

Fig.4.7. Energy Consumption Vs Speed

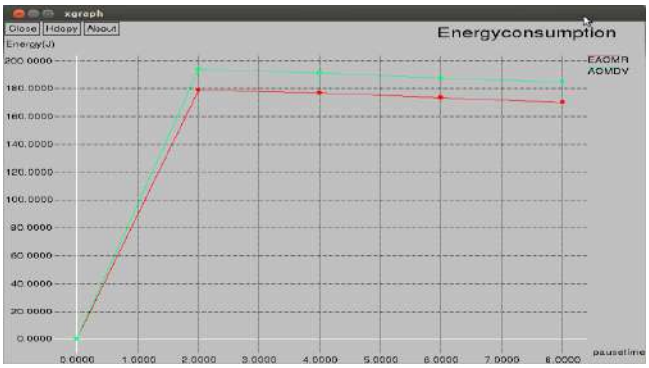

Fig.4.8. Energy Consumption Vs Pause time

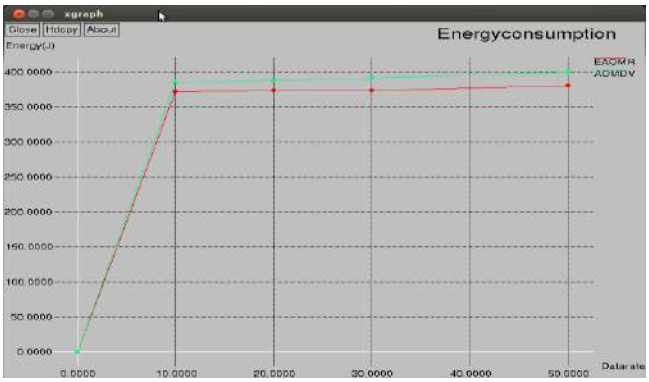

Fig..4.9. Energy Consumption Vs Data Rate

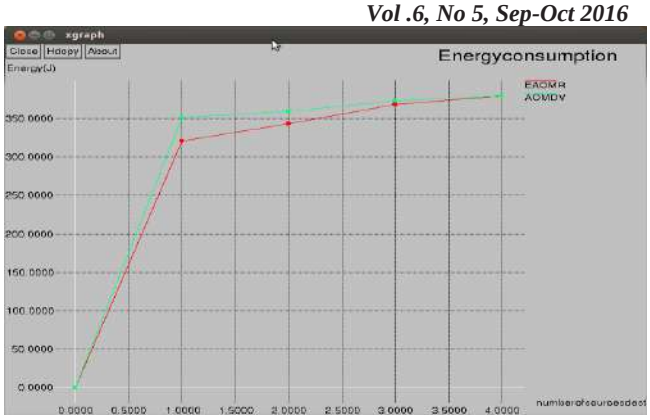

Fig.4.10. Energy Consumption Vs Number of Source and Destination Pairs

C) Throughput (Kbps) analysis:

To measure the protocol performance, throughput serves as the better parameter. The throughput is defined as the ratio of number of packets received to the number of packets transmitted [10] and it is indirectly proportional to the overhead.

The throughput is calculated by using the following equation. $$\text{Throughput}=\frac{x\times 8}{t\times 100}\,Kbps \quad (10)$$

Where x is number of bytes received and t is simulation time

The following five cases show that the overall EAOMR yielded higher throughput than the AOMDV because overhead of EAOMR is less than the overhead of AOMDV

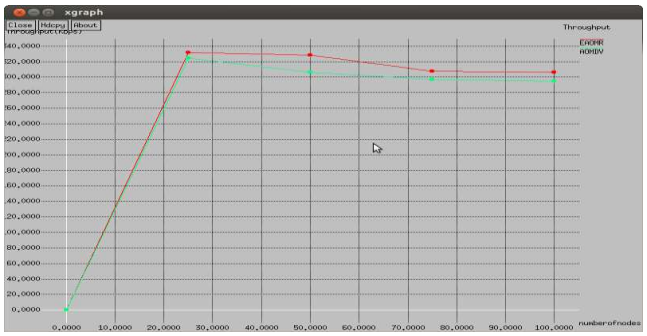

Fig. 4.11. Throughput Vs Number of Nodes (Network size)

Fig 4.12. Throughput Vs Speed

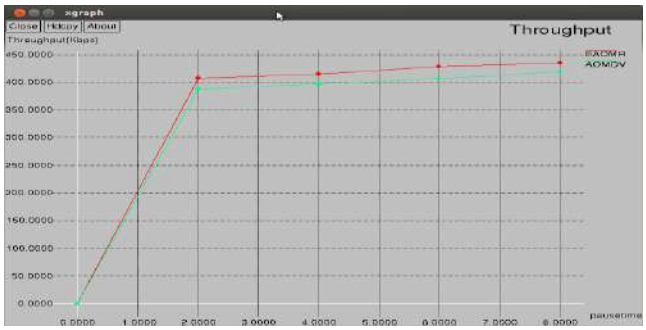

Fig 4.13.Throughput Vs Pause time

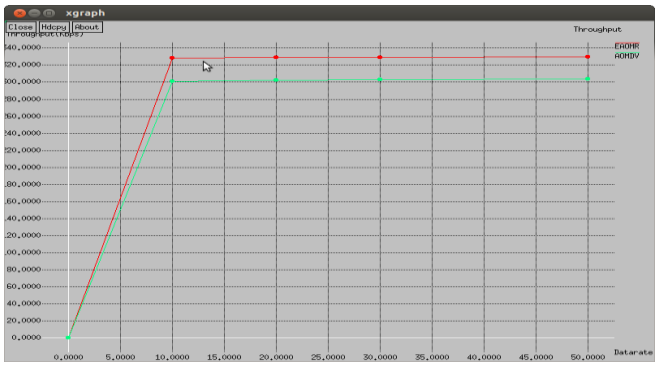

Fig . 4.14. Throughput Vs Data Rate (CBR)

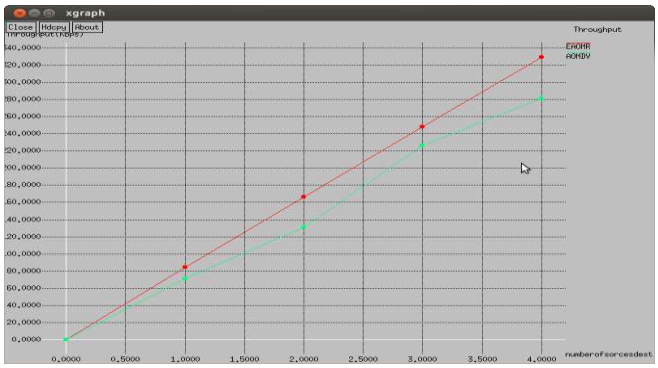

Fig. 4.15. Throughput Vs Number of Source and Destination pairs (connections)

D) Analysis of Packet Delivery Ratio (PDR):

To find the efficiency of the protocols, *PDR* is one of the important qualitative metrics. It is defined as the ratio of data packets received and packet sent [10], it is calculated as follows

$$\text{PDR}=\frac{x}{y}\times 100 \qquad (9)$$

Where x is the total number of packets received and y is the total number of packets sent at end of the simulation time.

The following all five cases show that overall the EAOMR yields higher PDR than the PDR of the AOMDV because overhead of EAOMR is less than the AOMDV

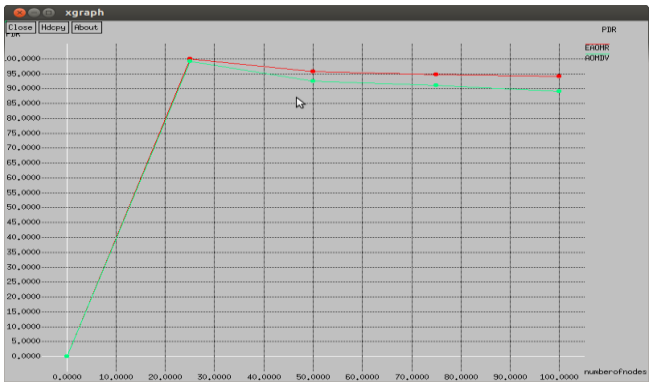

Fig. 4.16. PDR Vs Number of Nodes

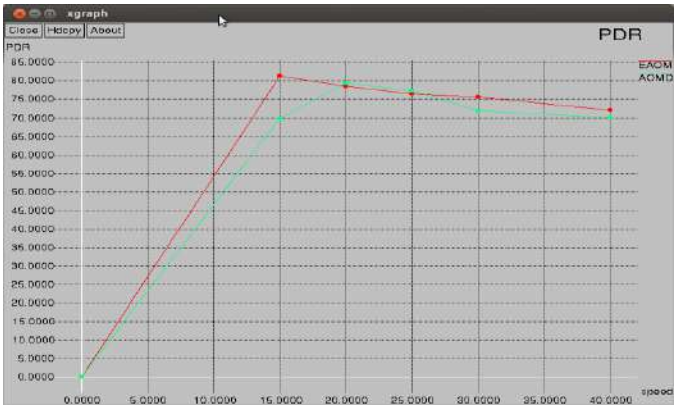

Fig. 4.17. PDR Vs Speed

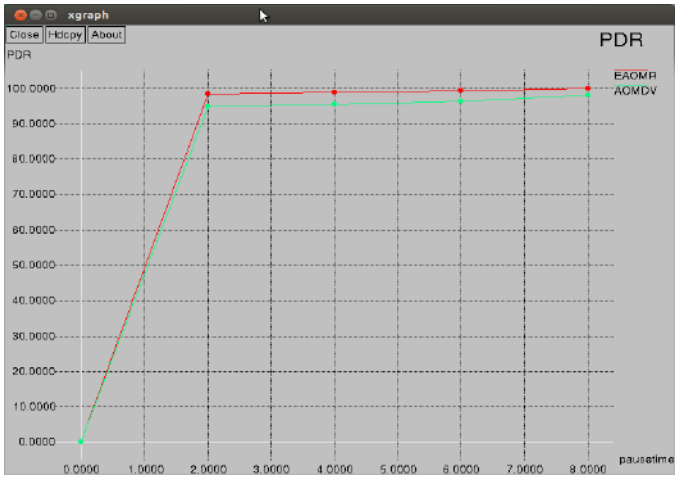

Fig..4.18. PDR Vs Pause time

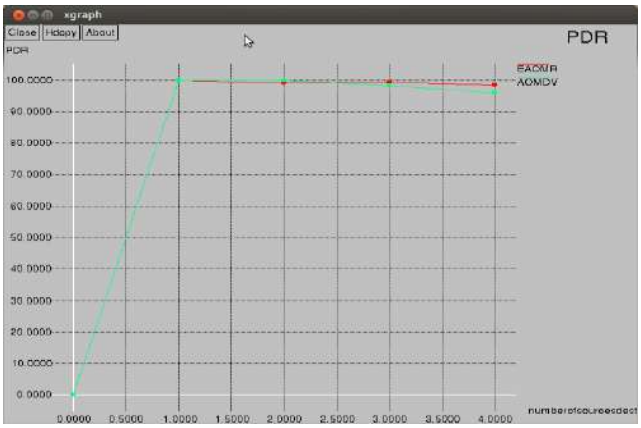

Fig.4.19. PDR Vs Data Rate (load)

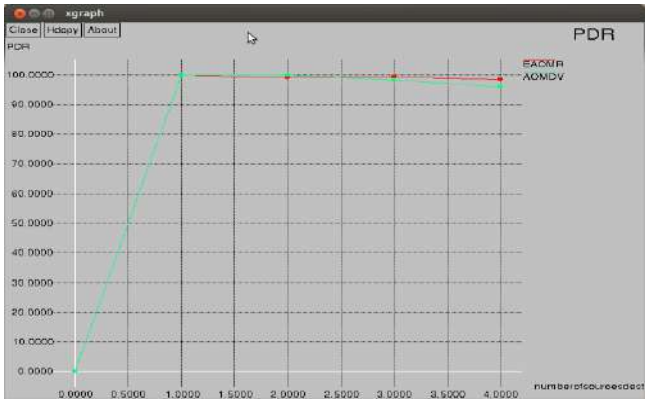

Fig.4.20. PDR Vs Number of Source to Destination Pairs

E) Analysis of Average End-to-End Data Packet Delay (ms)

To measure the performance of the proposed protocols end to end delay is the major performance factor which should be considered. The Average end to end delay is defined as the time taken to transmit the packet from source node to the destination node. The total end to end average delay of data packets includes queuing delay, buffering delay, propagation delay and retransmission delay. The average end to end delay of n received data packets [10] by using the following equation .

$$\text{delay} = \frac{\sum_{i=1}^{n}(R_i - S_i)}{n} \qquad (11)$$

Where R_I denotes the time at which the packet i is received and S_i denotes the time at which the packet i has been sent to the destination or it also defined as follows

$$\text{Average delay} = \frac{\text{Total delay of each data packets}}{\text{Total data packets received.}}$$

Following five cases show that overall, the EAOMR yielded low average end-to-end packet delay than the average end-to-end packet delay of AOMDV.

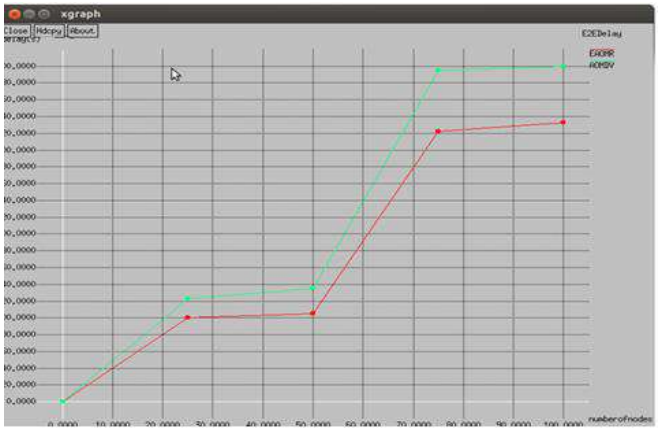

Fig 4.21. Delay Vs Number of Nodes

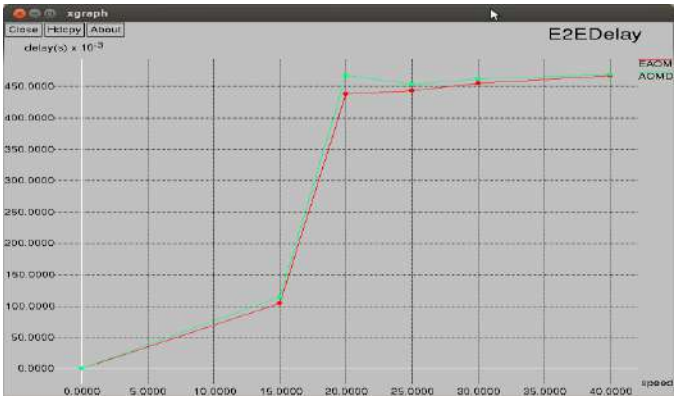

Fig. 4.22. Delay Vs Speed

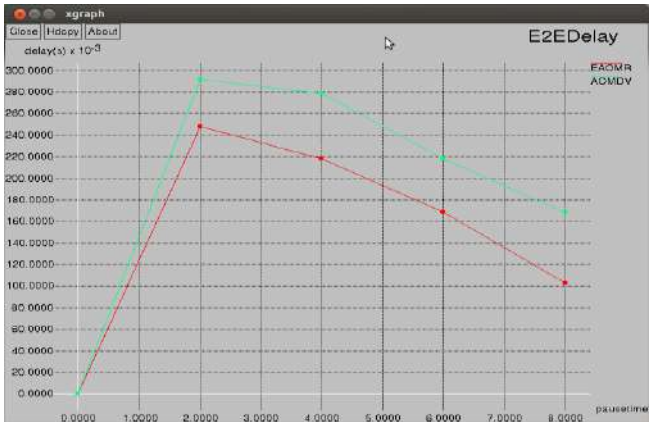

Fig. 4.23. Delay Vs Pause Time

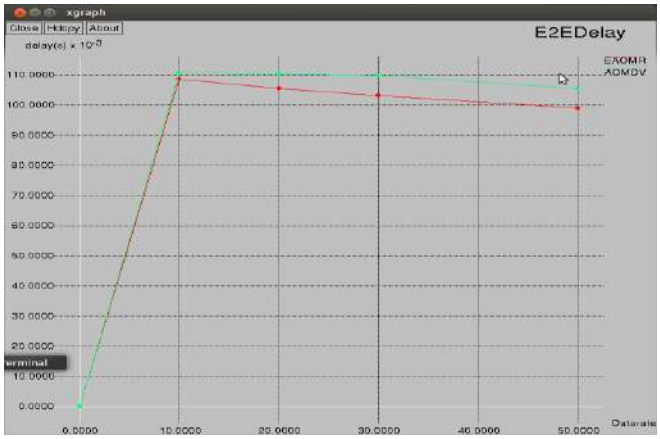

Fig .4.24. Delay Vs Data Rate (Kbps)

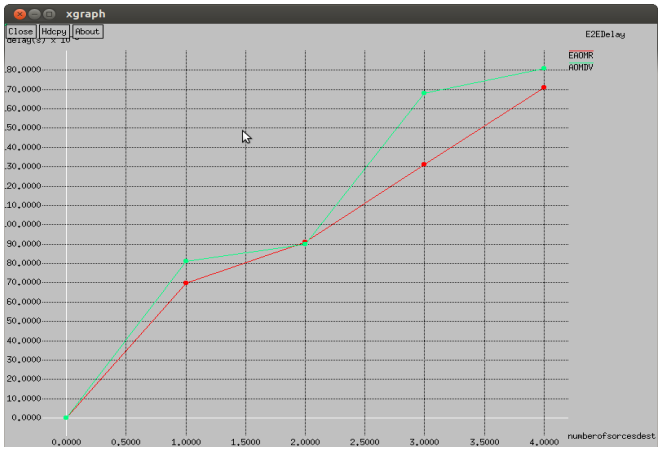

Fig. 4.25. Delay Vs Number of Source and Destination pairs

F) Packet Loss Ratio (PLR) (%):

The PLR is used to measure the performance of the routing protocols. The PLR is defined as the ratio of number of packets not delivered to the destination to the total number of packets sent [10]. The PLR is calculated by using the equation 5.

$$PLR = \frac{x - y}{x} \times 100 \quad (11)$$

Where x is total number of data packets sent and y is total number of data packets received.

Number of data packets lost=x- y.

Some data packets that are not reach the destination and they are lost during transmission to due to congestion and collision in the network.

The following five cases shown that overall the EAOMR has less packet loss compared to the AOMDV because the EAOMR has yielded less overhead compared to the AOMDV.

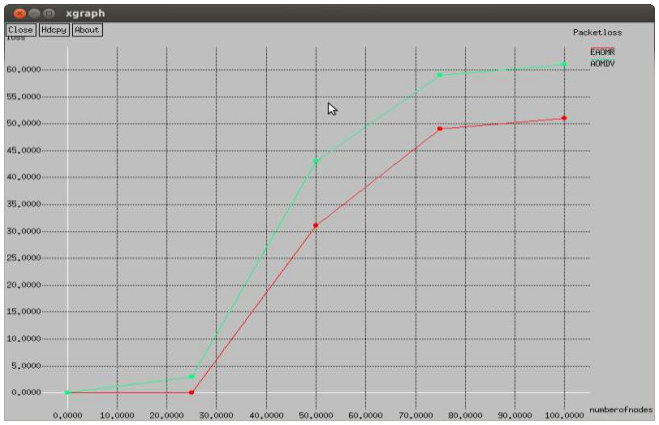

Fig .4.26. Packet loss Vs Number of nodes

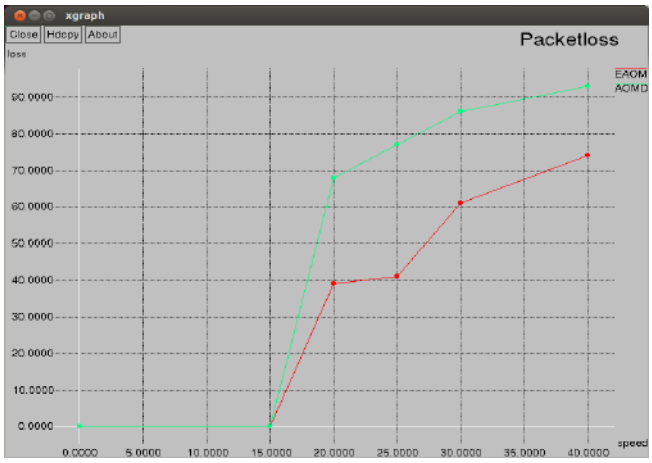

Fig. 4.27. Packet loss Vs Speed (m/s)

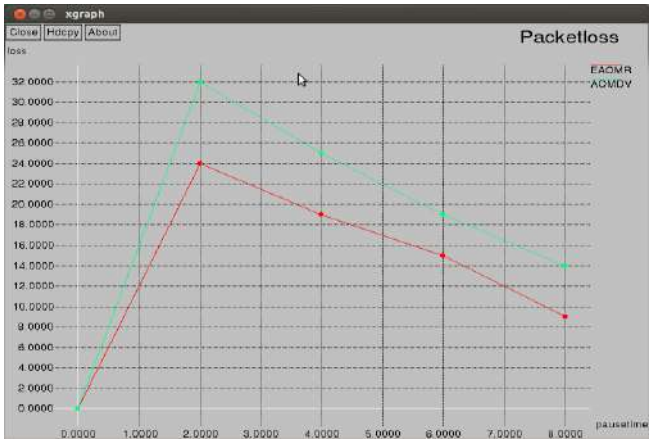

Fig .4.28. Packet loss Vs Pause Time (Sec)

Fig .4.29. Packet loss Vs Data Rate (Kbps)

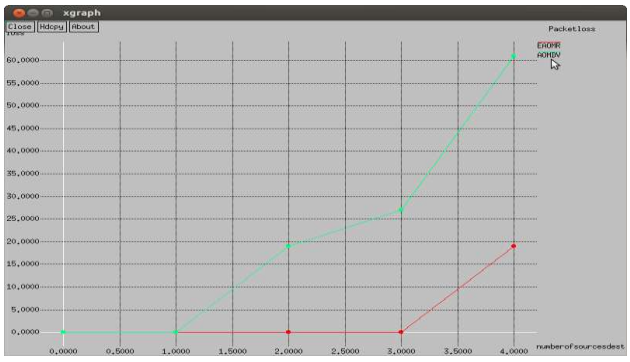

Fig .4.30. Packet loss Vs Number of Source and

V .CONCLUSIONS AND FUTURE WORK

In this paper, we proposed a novel energy aware node-disjoint multipath routing protocol , Energy Aware On-demand Multipath Routing (EAOMR) Protocol to find energy aware node-disjoint multipath between source and destination by using two new power aware metrics and based on AOMDV. We have derived some facts related to performance metrics and parameters. We also made a contribution to measure the performance of two different multi-path dynamic routing protocols such as EAOMR and AOMDV. The performance of the two protocols is tested with well-known simulator called as NS2 [34]. The performance of the EAOMR and AOMDV are tested by using various quantitative performance metrics like, end-to end delay of packets, throughput, routing control overhead, packet delivery ratio, energy efficiency, and packet loss rate and by varying various parameters like network's size, mobility of node, pause time, data rate and load .It is proved that EAOMR has better performance than AOMDV and it is concluded that the EAOMR is one of scalable, robust and energy efficient multipath routing protocol in MANET. In future work, we will propose new EAOMR by consider the selection of routes using first proposed technique.

REFERENCES

[1] C.S.R. Murthy and B.S.Manoj, "Ad hoc Wireless Networks: Architectures and Protocols", *Prentice Hall, 2004.*

[2]M. Bheemalingaiah, C. Venkataiah, K. Vinay Kumar, M. M. Naidu, D. SreenivasaRao, " Survey of Energy Aware On-demand Multipath Routing Protocols in Mobile Ad Hoc Networks", International Journal of Advanced Research in omputer Science and Software Engineering,Volume 6, Issue 4, April 2016.

[3] YibinLiang , thesis on Multipath "Fresnel Zone" Routing for Wireless Ad Hoc Networks", Virginia Polytechnic Instituteand State University, March, 2004.

[4] Zhenqiang Y, Krishnamurthy S. V and Tripathi S. K. "A Framework for Reliable Routing in Mobile Ad hoc Networks", *InProceedings of IEEE INFOCOM,* 2003, Vol. 1, pp. 270 -280.

[5]Mahesh K. M and Samir R. D, "On-demand Multipath Distance Vector Routing in Ad hoc Networks", *In Proceedings of IEEE International Conference on Network Protocols,* pp.14-23, 2001.

[6] S. J. Lee and M. Gerla, "Split Multipath Routing with Maximally Disjoint Paths in Ad hoc Networks", *InProceedings of IEEE ICC*, pp. 3201-3205, 2001.

[7]L. Wang, Y. Shu, Z. Zhao, L. Zhang and O. Yang, "Load Balancing of Multipath Source Routing in Ad hoc Networks", *InProceedings of IEEE ICCC*, 2002, Vol. 5, pp. 3197 – 3201.

[8] Suresh Singh, Mike Woo and C. S. Raghavendra, "Power-Aware Routing in Mobile Ad Hoc Networks", in *Proceedings of Mobicom 98 Conference*, Dallas, October, 1998.

[9]Anand P. S, Anto A. J, Janani V and Narayanasamy P, "Multipath Power Sensitive Routing Protocol for Mobile Ad

hoc Networks", *Proceedings of Wireless on Demand Network Systems, Springer,*Vol. 2928, pp. 84-89, 2004.
[10] Meng Li, Lin Zhang, Victor O. K. Li, Xiuming Shan and Yong Ren , "An Energy-Aware Multipath Routing Protocol for Mobile Ad Hoc Networks" , *Proceeding of ACM Sigcomm Asia'05, Apr. 10-12, Beijing, China, 2005.*
[11] Yuan P, Bai Y and Wang H, "A Multipath Energy-Efficient Routing Protocol for Ad hoc Networks", *Proceedings of International Conference on Communications, Circuits and Systems, Vol. 3,pp. 1462 - 1466 , 2006.*
[12] Liansheng T, Ling X, King T. K, M. Lei and Zukerman, "LAMOR: Lifetime-Aware Multipath Optimized Routing Algorithm for Video Transmission over Ad hoc Networks", *Proceedings of IEEE Vehicular Technology Conference, Vol. 2, pp: 623-627, 2006.*
[13] Do-Youn H, Eui-Hyeok K, and Jae-Sung L,"An Energy Aware Source Routing with Disjoint Multipath Selection for Energy-Efficient Multihop Wireless Ad hoc Networks", *in Proceedings of International Federation for Information Processing, pp: 41-50, 2006.*
[14] Zhengyu W, Xiangjun D and Lin C, "A Grid-Based Energy Aware Node-Disjoint Multipath Routing Algorithm for MANETs", *in Proceedings of International Conference on Natural Computation, ,Vol. 5, pp: 244-248, 2007.*
[15] Zhengyu W, Hantao S, Shaofeng J, and Xiaomei X, "Ant-based Energy Aware Disjoint Multipath Routing Algorithm in MANETs", *in Proceedings of International Conference on Multimedia and Ubiquitous Engineering, pp: 674-679, 2007.*
[16] Zhengyu Wu, Hantao Song, Shaofeng Jiang, Xiaomei Xu," Energy-Aware Grid Multipath Routing Protocol in MANET", *Proceedings of the First Asia International Conference on Modelling & Simulation (AMS'07), IEEE, 2007.*
[17] Jin S. Y, K. Kang, Y. J. Cho and S. Y. Chae,"Power-Aware Multi-Path Routing Protocol for Wireless Ad hoc Network", *Proceedings of IEEE Wireless Communications and Networking Conference, pp: 2247-2252 , 2008.* [18] Yumei Liu, Lili Guo, Huizhu Ma and Tao Jiang, "Energy Efficient On-Demand Multipath Routing Protocol for Multi-hop Ad Hoc Networks", *978-1-4244-2204-3/08/IEEE, 2008.*

[19] M. Bheemalingaiah, M. M. Naidu, D. Sreenivasa Rao and G. Varaprasad, " Energy Aware Node-Disjoint Routing in Mobile Ad Hoc Networks", *Journal of Theoretical and Applied Information Technology, pp: 416-431. 2009.*
[20] M. Bheemalingaiah, M. M. Naidu and D. Sreenivasa Rao, "Energy Aware Clustered Based Multipath Routing in Mobile Ad Hoc Networks", *Internal Journal of Communications, Network and System Sciences, Vol 2, pp: 91-168, 2009.*
[21] M. Bheemalingaiah, M. M. Naidu, D. Sreenivasa Rao and G. Varaprasad, "Power Aware Node-Disjoint Multipath Source Routing in Mobile Ad Hoc Networks", *International Journal of Mobile Network Design and Innovation, Vol. X, No. Y, 2010.*
[22] Seema Verma, Rekha Agarwal, and Pinki Nayak, "An Optimized Energy Aware Routing (OEAR)Scheme for Mobile Ad Hoc Networks using Variable Transmission Range" ,*International Journal of Computer Applications (0975-8887), Vol 45, No. 12, May 2012.*
[23] Senthil Murugan Tamilarasan and Kannan Eswariah, "The Link Stability with Energy Aware Ad hoc On Demand Multipath Routing Protocol in Mobile Ad Hoc Networks", *Proceeding of American Journal of Applied Sciences 10 (8): 844-848, ISSN: 1546-9239,2013.*
[24] Kavita Sharma and Vivek Sharma **,** " Energy Efficient Power Aware Multipath Dynamic Source Routing*", Proceeding of International Journal of Computer Science and Network Security, VOL.14 No.8, August, 2014*
[25] May Cho Aye and Aye Moe Aung, "Energy Efficient Multipath Routing for Mobile Ad Hoc Networks", *Proceeding of International Journal of Information Technology, Modeling and Computing (IJITMC) Vol. 2, No.3, August, 2014.*
[26] Omar Smail, Zoulikha Mekkakia, Belhadri Messabih and Rachida Mekki, " Energy Conservation for Ad Hoc On-Demand Distance Vector Multipath Routing Protocol", *International Journal of Computer Network and Information Security, ,VOL 6, 1-8. 2014.*
[27] P.Periyasamy and . E.Karthikeyan , "Energy Optimized Ad hoc on-Demand Multipath Routing Protocol for Mobile Ad hoc Networks*", International Journal of Intelligent Systems and Applications, vol 11, pp: 36-41, 2014.*
[28] Shimja.K.J and Joish George**, "**Enhanced Power aware Multipath Routing Protocol for MANETs*", International Journal of Research and Development organization, Vol 2, Issue 9, September, 2015*
[29] D. A. Maltz, J. Broch, J. Jetcheva, and D. B. Johnson," The Effects of On-Demand Behavior In Routing Protocols For Multihop Wireless Ad Hoc Networks",. *IEEE Journal on Selected Areas in Communications*, 17(8):1439–1453, August 1999.
[30] Charles E. P, E. M. Belding-Royer and I. Chakeres, "Ad hoc On-Demand Distance Vector Routing", IETF Internet draft, 2003.
[31] J. Broch, D. Johnson, and D. Maltz, "Dynamic Source Routing Protocol for Mobile Ad HocNetworks", *IETF* Internet draft, 2004.
[32] S.S.Rao, "Optimization theory and applications', Weley Eastern Limited, Second Edition.
[33] Indrani Das, D.K. Lobiyal and C.P.Katti **, "** An Analysis of Link Disjoint and Node Disjoint Multipath Routing for Mobile Ad Hoc Network", International Journal of Computer Network and Information Security, 3, 52-57, 2016.
[33]Network Simulation 2 official website: http://www.isi.edu/nsnam/ns/

View publication stats

ISSN: 2277-9655
Impact Factor: 4.116

IJESRT

INTERNATIONAL JOURNAL OF ENGINEERING SCIENCES & RESEARCH TECHNOLOGY

NON-LINEAR PUSHOVER ANALYSIS OF RCC BUILDING WITH BASE ISOLATION SYSTEM

Asst Prof. Noor Mohammed, Mohammed Huzaifa Yaman, Shaik Mohammed Siddiq
* Department of Civil Engineering NSAKCET, India

DOI: 10.5281/zenodo.59636

ABSTRACT

Buildings are designed as per the code regulations meeting all specific requirements of code and assuming a linear elastic behaviour for the structural members. Moreover, it is also necessary to know the behaviour of a building that were designed with older codes or which may not have been designed for earthquake forces. During the seismic excitation the building responds well beyond its elastic and linear capacity and enters into non-linear stage.

So, the present work is intended to provide a systematic procedure to assess the behaviour of a structure during the seismic excitation. For studying the behaviour a non-linear static analysis procedure known as pushover analysis is used. The literature pertaining to pushover analysis is reviewed.

A Nine storey residential building located in the Hyderabad city, which was designed and constructed for gravity loads alone, was considered for analysis. The present structure is studied using the evaluation procedures provided in ATC-40 and FEMA-273 documents. Under detailed evaluation a target displacement for Immediate Occupancy, Life Safety, Collapse Prevention was given and the performance is checked in accordance with IS 1893:2002

INTRODUCTION

Natural hazards bring many damages to man-made interventions such as habitat and infrastructural facilities causing loss to life and property. Earthquakes are one of those hazards with the sudden violent movement of earth's surface with the release of energy. According to the revised provisions of IS 1893 (Part 1): 2002, the seismic zones of India become more vulnerable and reduced to four zones. So it is important to design the structures with seismic resistance. Recent earthquakes in the Indian subcontinent, India-Pakistan earthquake on October 8, 2005 with a magnitude of 7.4 on Richter scale, Gujarat earthquake on January 26, 2001 with a magnitude of 7.6 on Richter scale have led to an increase in the seismic zoning factor over many parts of the country. Buildings are designed as per the building code regulations, aptly termed as prescriptive based design. It ismethodology based upon meeting all of the specific requirements of the code. In prescriptive based design, the normal engineering practice is to assume linear-elastic behaviour for structural members, which fails to account for redistribution of forces due to member non-linear behaviour and dissipation of energy due to material yielding.

The present work aims at the study of following objectives:

- How the seismic evaluation of a building should be carried out.
- To study the behavior of a building under the action of seismic loads with and without rubber base isolator.
- To find the performance of a building so as to suggest some retrofitting techniques, if required.

GENERAL

The seismic evaluation process consists of two phases, namely preliminary evaluation phase and detailed evaluation phase. After the building is preliminary evaluated using rapid visual screening, the detailed evaluation is carried out using pushover analysis. Performance based approach requires a non-linear lateral load verses deformation analysis. The pushover analysis is a static method of non-linear analysis. The pushover analysis is an elegant method to observe the successive damage states of a building both in the existing condition and under a proposed retrofit scheme. The

concept of protecting a building from the damaging effects of an earthquake by introducing some type of support that isolates it from the shaking ground is an attractive one, and many mechanisms to achieve this result have been proposed. Although the earlier proposals go back hundred years, it is only in recent years that base isolation has become a practical strategy for earthquake resistant design. It is a passive control device that is installed between the foundation and the base of the building. The base isolation system introduces a layer of low lateral stiffness between the structure and the foundation. With this isolation layer the structure has a natural period which is much longer than its fixed base natural period. This lengthening of the period can reduce the pseudo-acceleration and hence the earthquake induced forces in the structure

MODELLING PARAMETERS

Building Description:Reinforced Concrete Frame of 9 storeys, with plan size 21mx21m, with heights of 21m respectively are modeled.

S.No.	*Description*	*Information*	*Remarks*
1.	*Plan size*	*21 m x 20 m*	----
2.	*Building height*	*30m*	----
3.	*Number of storeys above ground*	*9*	----
4.	*Number of basements below ground*	*0*	----
5.	*Type of structure*	*RC frame*	----
6.	*Open ground storey*	*Yes*	----
7.	*Type of building*	*Regular frame with open ground storey*	*IS 1893:2002 Clause 7.1*
8.	*Grade of concrete and steel used*	*M25, Fe415*	----
9.	*Software used*	*SAP2000 V16*	----

S. No.	Specifications	G+9 storey
1.	Slab Thickness	150mm
2.	Beam dimensions	300x230mm
3.	Column dimensions	400x400mm,
4.	Unit weight of concrete	25kN/m^3
5.	Live loads	3kN/m^2
6.	(a) Sdl	1.5kN/m^2
7.	Importance factor	1
8.	Seismic zone	V
9.	Response reduction factor	5

TABLE 1: DATA OF RC FRAME CONSIDERED IN STUDY

ISSN: 2277-9655
Impact Factor: 4.116

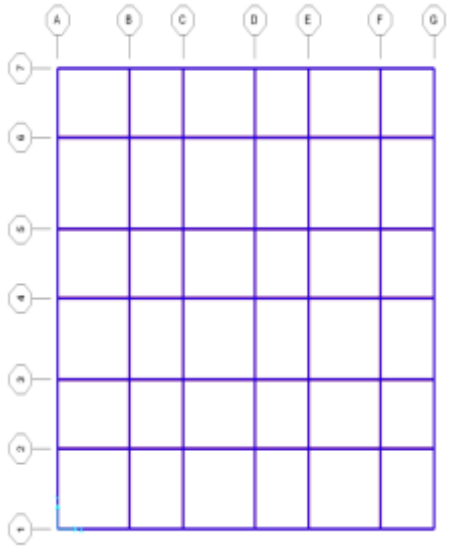

Fig 1: Plan Of Rcc Frame Model

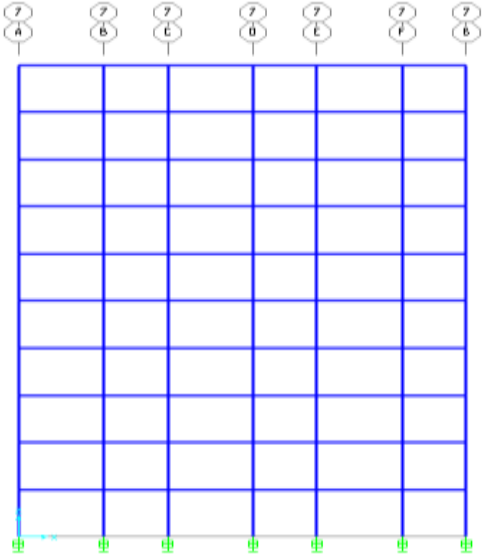

Fig 2: Elevation View Of Rcc Frame Model

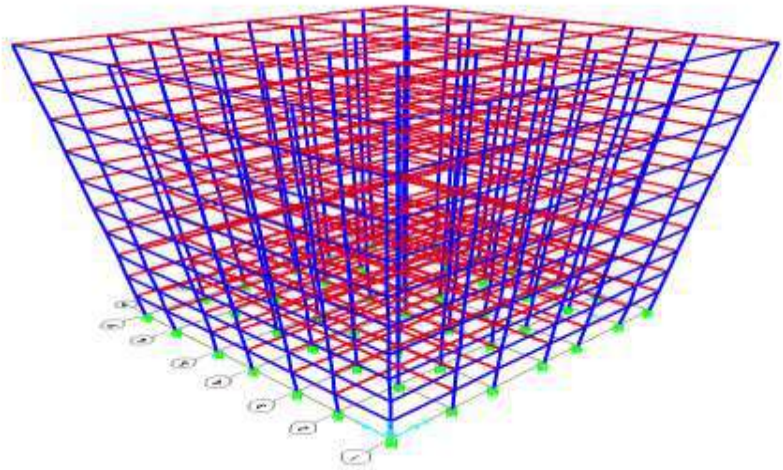

Fig 3: Isometric View Of Rcc Frame Model

BASE ISOLATION

The concept of protecting a building from the damaging effects of an earthquake by introducing some type of support that isolates it from the shaking ground is an attractive one, and many mechanisms to achieve this result have been proposed. As buildings with longer time periods attract less seismic force the isolation system deflects the seismic energy. In particular, high energy in the ground motions at higher mode frequencies are deflected .In buildings, the base isolator protects the structure from earthquake forces in two ways:

(i) By deflecting the seismic energy and

(ii) By absorbing the seismic energy. The seismic energy is deflected by making the base of the building flexible (instead of fixed) in lateral directions, thereby increasing the fundamental time period of the structure.

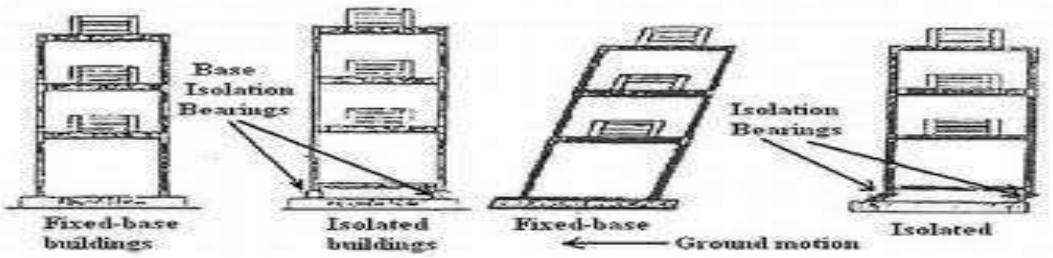

The effective stiffness of the isolator is calculated by, $K_{eff}=\frac{4\pi^2 R}{gT_b^2}$

The yield force is given by $F_y = K_u D_y$.

ANALYSIS RESULTS

The Results obtained are of different parameters such as Storey displacement, Modal Periods etc. The results obtained by carrying out Non-linear static analysis for Buildings as listed.

Result For Non-Linear Static Analysis Of 9 Stories Building

PUSHOVER FOR 9 STOREY			
STOREY LEVEL	LOAD CASE	STOREY DISPLACEMENT ISOLATOR WITHOUT IN mm	STOREY DISPLACEMENT WITH ISOLATOR IN mm
9	PUSH-X	431.9	604.7
8	PUSH-X	429.9	604.4
7	PUSH-X	426.9	603.7
6	PUSH-X	422.6	602.7
5	PUSH-X	414.2	601.3
4	PUSH-X	388.1	599.7
3	PUSH-X	332.1	597.7
2	PUSH-X	253.6	595.4
1	PUSH-X	166.5	592.8
BASE	PUSH-X	78	589.6

Table 2: Showing Displacement In X-Direction For 9 Storey Building

PUSHOVER FOR 9 STOREY			
STOREY LEVEL	LOAD CASE	STOREY DISPLACEMENT WITHOUT ISOLATOR IN MM	STOREY DISPLACEMENT WITH ISOLATOR IN mm
9	PUSH-Y	392.3	606.2
8	PUSH-Y	390	605.6
7	PUSH-Y	386.8	604.7
6	PUSH-Y	382.5	603.5
5	PUSH-Y	374.4	602
4	PUSH-Y	349.7	600.1
3	PUSH-Y	296.7	598
2	PUSH-Y	223.9	595.6
1	PUSH-Y	143.9	593
BASE	PUSH-Y	64.8	589.8

Table 3: Showing Displacement In Y-Direction For 9 Storey Building

ISSN: 2277-9655
Impact Factor: 4.116

Step	StepNum	time Period without isolator	Time period with isolator
		Sec	sec
Mode	1	0.955058	2.181772
Mode	2	0.951113	2.18072
Mode	3	0.861339	2.015096
Mode	4	0.316245	0.452162
Mode	5	0.314956	0.450839
Mode	6	0.286143	0.404495
Mode	7	0.185252	0.224906
Mode	8	0.184371	0.223754
Mode	9	0.169922	0.205859
Mode	10	0.131856	0.149702
Mode	11	0.131316	0.14898
Mode	12	0.121162	0.137592

Table 4: Showing Time Periods For 9 Storey Building

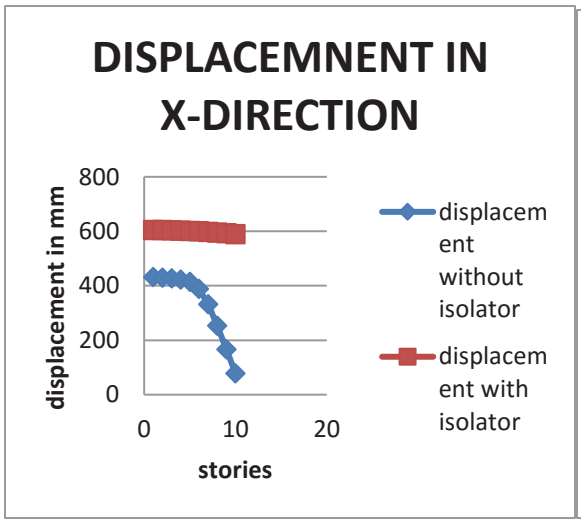

Fig 4: Displacement in x –direction

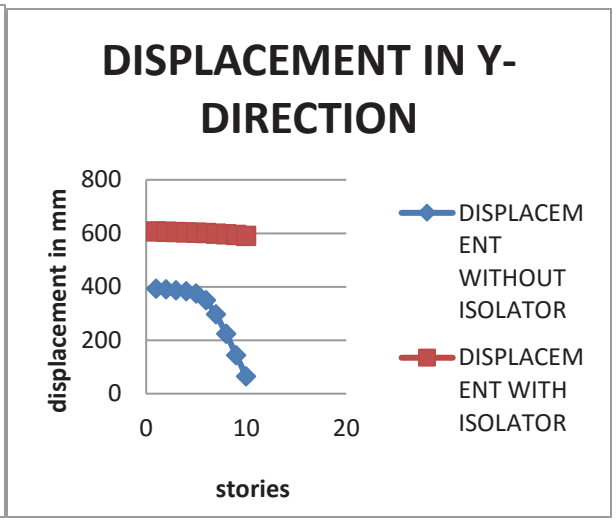

Fig 5: Displacement in y –direction

TABLE 5: SHOWING TIME PERIOD FOR 9 STORIES BUILDING

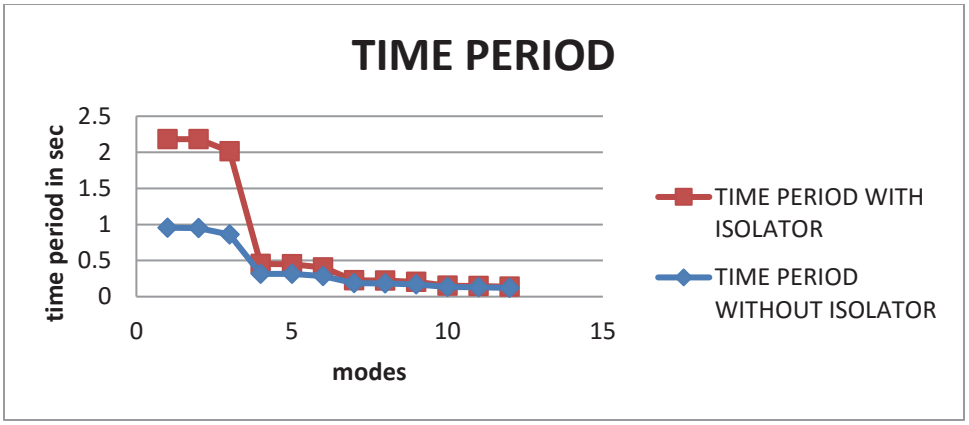

Fig 6: Time Period Of 9 Stories Building

CONCLUSIONS

The nonlinear static (Pushover) analysis as introduced byATC-40 has been utilized for the evaluation of an existing reinforced concrete building frame, in order to examine its applicability. Potential structural deficiency in RC frame, when subjected to a moderate seismic loading.

- The pushover analysis is a useful tool for accessing in elastic strength and deformation demands and for exposing design weakness. The pushover analysis is a relatively simple way to explore the nonlinear behavior of buildings.
- Sequence of formation of plastic hinges (yielding) in the frame members can be clearly seen in the beams only. The building clearly behaves like the strong column- weak beam mechanism.
- Looking at the deflected shape the highest inelastic roof displacement of 234 mm was observed as the structure is about to reach its ductile limit (Collapse Prevention), where significant strength loss begins.
- The storey drifts were decreased by 97% for nine storey symmetric building suggesting the effectiveness of Base Isolators for Buildings.
- Most of the present structural systems are highly advanced in terms of structural efficiency and aesthetic quality, but lacks the much needed geometric versatility. As we have seen, that base isolation has in addition to strength and aesthetics, that extra quality of geometric versatility, making it the most suited structural system to this respect. Thus the base isolation, with an optimal combination of qualities of aesthetic expression, structural efficiency and geometric versatility is indeed the language of the modern day builder.

SCOPE FOR FURTHER STUDY

- Further studies can be done to compare the accuracy of non-linear pushover analysis and non-linear time history analysis taking the displacement as a common parameter.
- Further studies on the effect of various lateral load patterns (such as uniform building code, Indian code, SRSS and FEMA-273) utilized in pushover analysis can be done.
- Soil structure interaction has always attracted many researchers as an interesting topic for static procedures. The same can also be done for non-linear time history analysis using soil structure interaction.

REFERENCES

[1] Ashraf Habibullah and Stephen Pyle “Practical three dimensional non-linear static pushover analysis” Structures Magazine, winter, 1998.
[2] A. Kadid and A. Boumrkik“Pushover analysis of reinforced concrete framed structures”Asian Journal of Civil Engineering, Building and Housing, Vol. 9, No.1 (2008), pp.75-83.
[3] Amarnath Chakrabarti, Devdas Menon, Amlan K. Sengupta, Handbook on Seismic Retrofit of Buildings, Narosa Publications, 2010.
[4] ATC 40, Seismic evaluation and retrofit of concrete buildings, Vol.1, Applied Technology Council, Redwood city, CA, 1996.
[5] C.V.R. Murty, Indian Institute of Technology Kanpur, Earthquake tips, IITK-BMTPC earthquake tips: Learning seismic design and construction, April 2007.
[6] C.V.R. Murthy and Andrew W. Charleson, Earthquake Design Concepts, Prepared under NPEEE, Published by NICEE – IITK, 2009.
[7] FEMA 356, NEHPR guidelines for pre standard and commentary for the seismic rehabilitation of buildings, prepared for Federal Emergency Management Agency, Washington DC.
[8] FEMA 273, NEHRP Guidelines for the Seismic Rehabilitation of Building, prepared for Federal Emergency Management Agency, Washington DC, 1997.

International Journal for Research in Applied Science & Engineering Technology (IJRASET)
ISSN: 2321-9653; IC Value: 45.98; SJ Impact Factor: 6.887
Volume 6 Issue XII, Dec 2018- Available at www.ijraset.com

HVAC Design of Air-Cooled Chiller by Revit Tool and Power Consumption Analysis when Different Compressors are used for an Office Building

Mohammad Sameer Uddin[1], Mohammad Abrar Hussain[2]
[1, 2]*Nawab Shah Alam Khan College of Engineering and Technology, India*

Abstract: ***Air-conditioning of mercantile building found to be important criteria; contemporarily efficient design and the reduced power consumption are also two of the major factors that has to be considered in to an account, for which chillers are found to be the best air- conditioning units so far like air-cooled and water-cooled chillers among which water- chillers found to be much efficient than the air-cooled chillers. But, what if there is no adequate availability of water at the desired place where water-cooled chiller has to be installed? And also, compressors are the major component of chiller systems if not selected appropriately would increases the energy crises and consumption drastically. This project mainly describe about the power consumption when different classified compressors are used for an air-cooled chiller also it describes about the design of (HVAC)Heating ventilation and air-conditioning using Revit tool- a BIM (Building Information Modelling software) which helps an individual to clearly visualize the model of building and various services that are installed such as HVAC, Electrical and Plumbing and also it helps a design engineer to outfit the MEP services within time that involves in designing the services by the other CAD designing tools like Auto CAD, duct designing softwares like Eductulator or McQuay-duct-sizer etc. High power consumption requirements are being demanded by the air-cooled chillers because they are the units which use the 25% of the electricity of a commercial building. Therefore, it is uttermost importance to analyse the different parameters such as energy consumption, performance coefficient in order of reducing power consumption for a mercantile buildings.. In air-cooled chiller we direct air across the condenser coils with the ease of a fan whereas in water-cooled vapor refrigerant is condensed by passing water over the condensing coils. Air-cooled chiller has specific power (input) consumption up to 1.51KW/Ton where as water-cooled chiller has 0.56-0.8KW/Ton. Operating cost is also as important as energy consumption, as air-cooled chiller is preferred because of its lower maintenance cost as it doesn't require a cooling tower, pumps, and condensing water by chemicals action as well. But water-cooled chiller has comparatively low condensing temperatures than the air-cooled chillers.***

I. INTRODUCTION

A. Centralised Air-Conditioning Systems

Whenever large space or volumes are wanted to be cooled, this is recommended to refer centralised air conditioning and chilling system in which only a sole outdoor compact generally called chiller and many indoor compacts are stationed for different space or volumes to be conditioned.

A centralised air conditioning and chilling system is used for cooling building space or volumes like hotels, airports, shopping malls etc, are wanted to be conditioned comprehensively.

B. Chilled Water Central Air-Conditioning System

When the no. of floors of a building is to be conditioned at the same time setup of chilled water system is recommended. There are two categories of cooled water systems are used they are:

1) *Air-cooled chiller system*
2) *Water-cooled chiller system.*

Here for this project we are going to discuss about air cooled systems only

The refrigeration cycle of an air-cooled chiller includes two activities:

a) The dissipation of the fluid refrigerant in the evaporator which retains warmth and brings down the temperature of the chilled water system.
b) The build-up of the refrigerant vapor realisable all around cooled condenser and dismissal of warmth to the environment.

©IJRASET: All Rights are Reserved

ISSN: 2321-9653; IC Value: 45.98; SJ Impact Factor: 6.887
Volume 6 Issue XII, Dec 2018- Available at www.ijraset.com

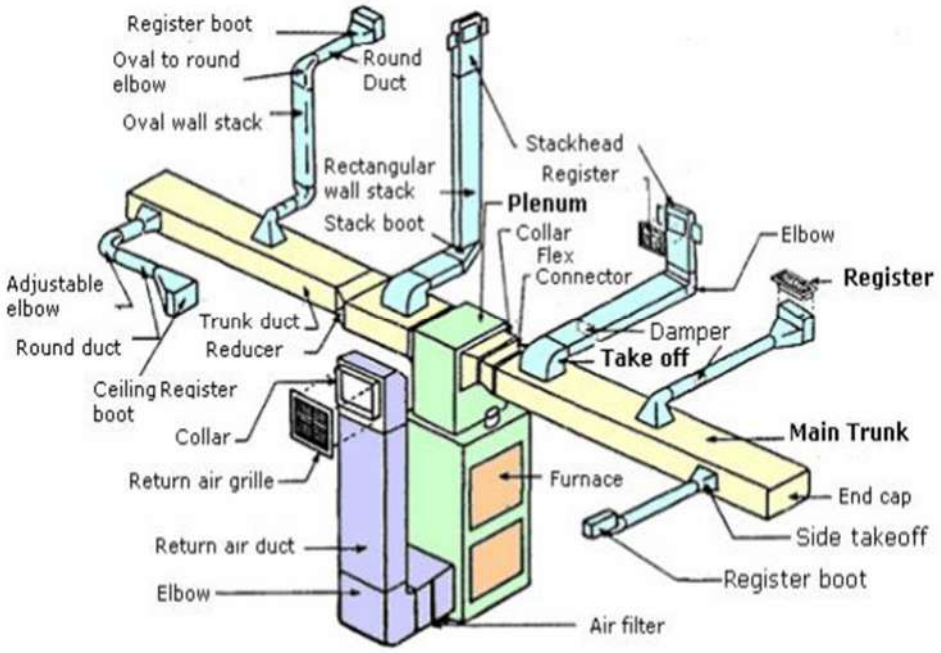

Figure1 simplified diagram of different hvac components

II. REVIT

Revit MEP is the Construction data demonstrating plan and documentation programming for MEP (Mechanical, Electrical and Plumbing).

To get over the tool Revit it is of uttermost importance to have clear idea about the Construction information modelling abbreviated as BIM.

A. BIM

The Construction Information is a gathering of information that is organized such that the data can be shared. The BIM is a digitalized model of a working in which information about the task is put away which can be 3D, 4D (time), 5D (cost)… … .nD (a term that covers some other related data). Subsequently, for the exhaustive data of the task BIM has an tentative adaptability and potential which is useful for a MEP and the other Engineer to find the thoughts however much and soon as could be expected.

B. Services offered by BIM

a) Revit architectural services.
b) Revit structural services.
c) Revit MEP services.
d) BIM 3D, 4D modelling, drafting, coordination, family creation, simulation services, cost estimation.
e) Revit BIM services, clash detection, quantity take off.

How the BIM has been used in this project is explained below with the help of revit software this below shown figures was made:

C. Engineering Design stages with BIM

1) LOD: 100 conceptual Geometry - simplified design.
2) LOD: 200 Approximate Geometry - Basic design.
3) LOD: 300 Precise geometry - Detailed design (bidding model).
4) LOD: 400 Fabrication - construction documents.
5) LOD: 500 AS-built - AS-built.

©IJRASET: All Rights are Reserved

ISSN: 2321-9653; IC Value: 45.98; SJ Impact Factor: 6.887
Volume 6 Issue XII, Dec 2018- Available at www.ijraset.com

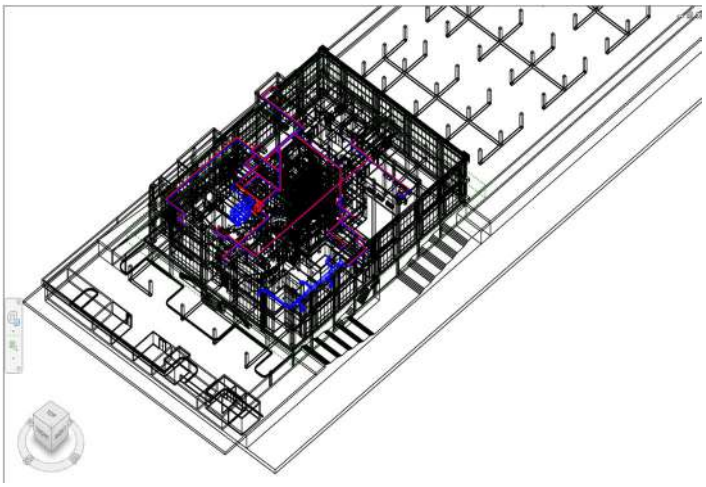

Figure 1- level-1 contains overall amount

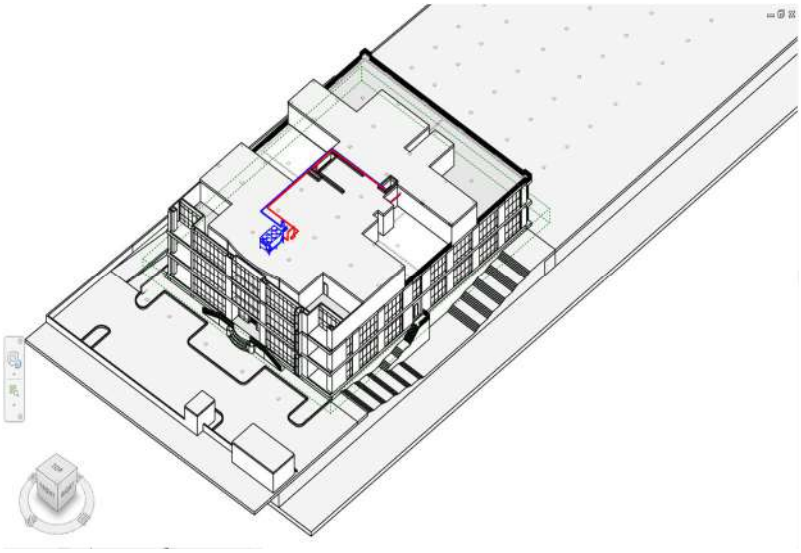

Figure 2- level-2 contains shell with openings

Figure 3- level-3 basic architectural details but no surface finish

©IJRASET: All Rights are Reserved

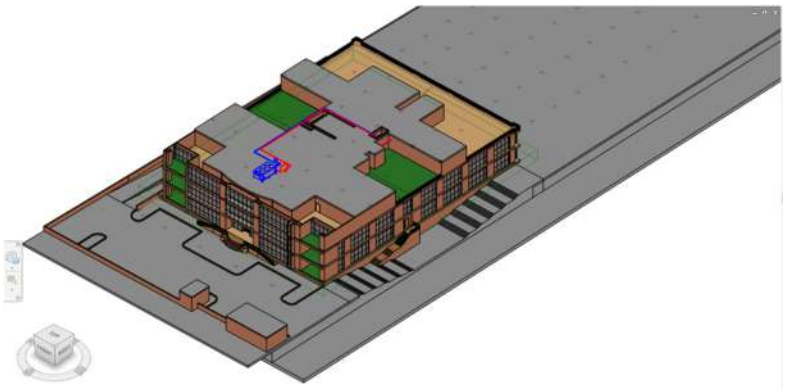

Figure 4- level-4 detailed architectural and structural details

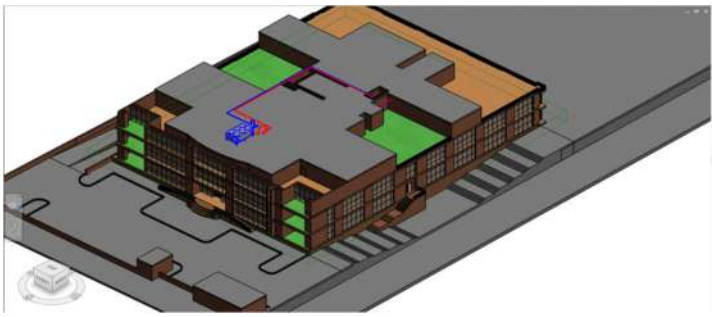

Figure 5- level-5 accurate architectural and structural details.

III. COMPRESSORS

A. Introduction to Refrigerant Compressors

A refrigerant compressor is a machine used to pack the refrigerant vapor to high weight refrigerant vapor keeping in mind the end goal to expand its weight and reaches to the immersion temperature with the end goal that the temperature is more than that of cooling medium. It is the main segment in flowing the refrigerant all through the cycle of refrigeration for which work must be finished amid the dissemination action. It requires a prime mover to work the cycle. Compressor is thought to be the most imperative segment and furthermore the greatest power consumer.

In this undertaking, we have consider distinctive sorts of compressors for the power utilization investigation for that it is vital to experience the investigation of various kinds of compressors.

B. Types Of Refrigerant Compressors Used In HVAC

1) Based On The Method Of Compression: Reciprocating compressors, Rotary compressors and Centrifugal compressors.

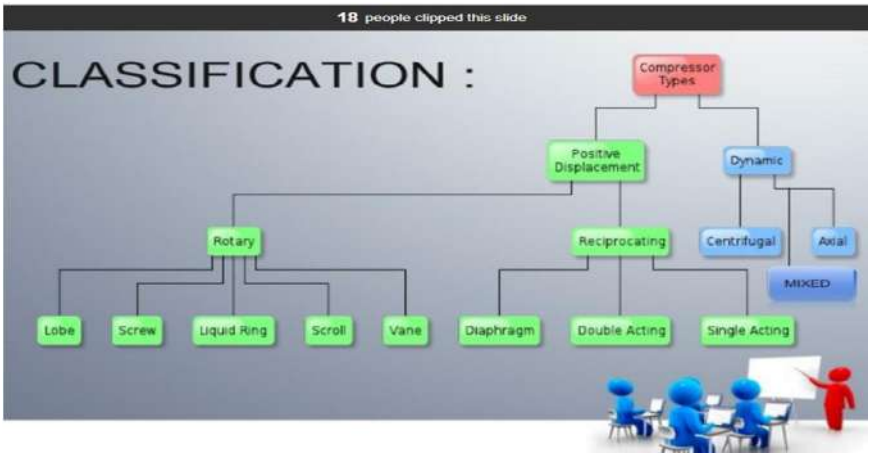

Figure-6 different compressor types

©IJRASET: All Rights are Reserved

ISSN: 2321-9653; IC Value: 45.98; SJ Impact Factor: 6.887
Volume 6 Issue XII, Dec 2018- Available at www.ijraset.com

Now we shall discuss each of the compressors in brief.

a) *Reciprocating Compressors:* On the off chance that the vapor refrigerant is compacted by the piston activity of Backward or forward i.e. reciprocating activity then the kind of compressor is called reciprocating compressors.

b) *Rotary Compressors:* In this kind of compressor rotary activity is performed on the working medium with in a limited chamber, the activity might be by screw or scroll, hence rotating compressors are of two sorts they are revolving screw and rotational scroll compressors.

IV. STATEMENT OF PROBLEM

Experimentation strategy was being utilized amid the ordinary outline of the system or past experience was being considered while planning structure, which was never been done professionally has lead for the experimental estimation and results.

In a refrigeration cycle compressor part is in charge of the power utilization and furthermore modify of COP for the better productivity of the structure. We are happy and regarded for such a superb chance to break down the power utilization on various compressors introduced in an air-cooled chiller.

In this task we have considered the plan of the ducting structure in BIM programming (Revit) for its better adaptability of investigation of load and other re-enactment highlights and examination of the power utilization is done on various compressors as this should be possible by intensive audit of various compressors indexes which was extremely useful for us to experience the particular power utilization at various load like ¼ stack, ½ stack, ¾ load and full load.

V. HEAT LOAD CALCULATION

A. Introduction to HAP

Hourly analysis program is a HVAC tool helps an engineer in designing the heat load and also helpful for the selection of an air-conditioning system based in the load obtained.

There are two major functions of HAP they are:

1) To calculate design load and

2) Energy simulation.

It is so flexible that an individual can put the input data and can get the output as quick and accurate as possible, as it follow the code and standards of ASHRAE 62.1.2007

B. Outside conditions

For summer

1)	Dry bulb temperature-	:	106^0F.
2)	Wet bulb temperature	:	76^0F.
3)	Daily range	:	14^0F.
4)	Latitude	:	17.86^0N.
5)	Longitude	:	-72.6^0E.
6)	Elevation	:	1788 ft.
7)	Maximum temperature- ranging months:		May to July.

C. Building Details

The locale of the site is at Hi-tech city, Hyderabad, Telengana. All the four sides are exposed to sunlight. The front face is facing towards north-east direction. Glass glazing is outfitted to the outer wall made of 8in. light weight concrete with 50mm as air gap is outfitted between glass glazing and 8in. Wall.

The office construction is consisting of basement, ground floor, first floor and the roof floor.

Area of basement is 68780 ft^2. Area of ground floor is 18565 ft^2. Area of first floor is 18585 ft^2. Area of roof floor is 18585 ft^2.

The details are required to input in the weather tab of HAP as shown below

©IJRASET: All Rights are Reserved

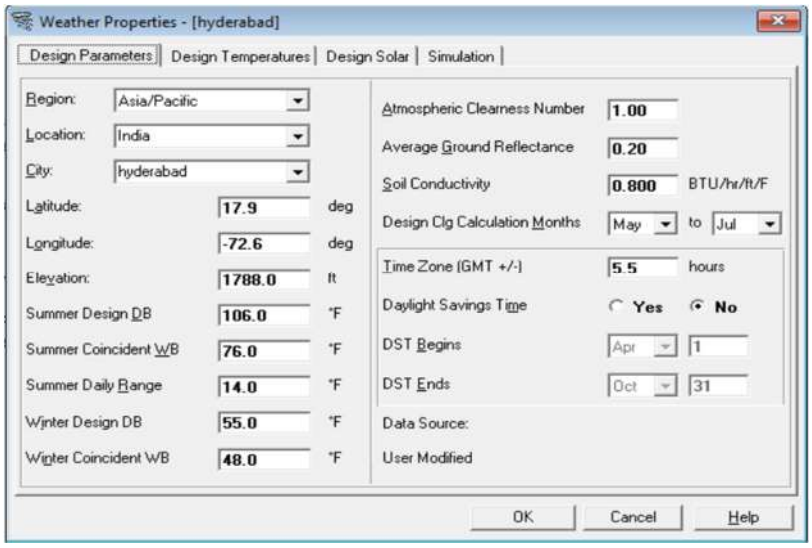

Figure 7- weather data in HAP

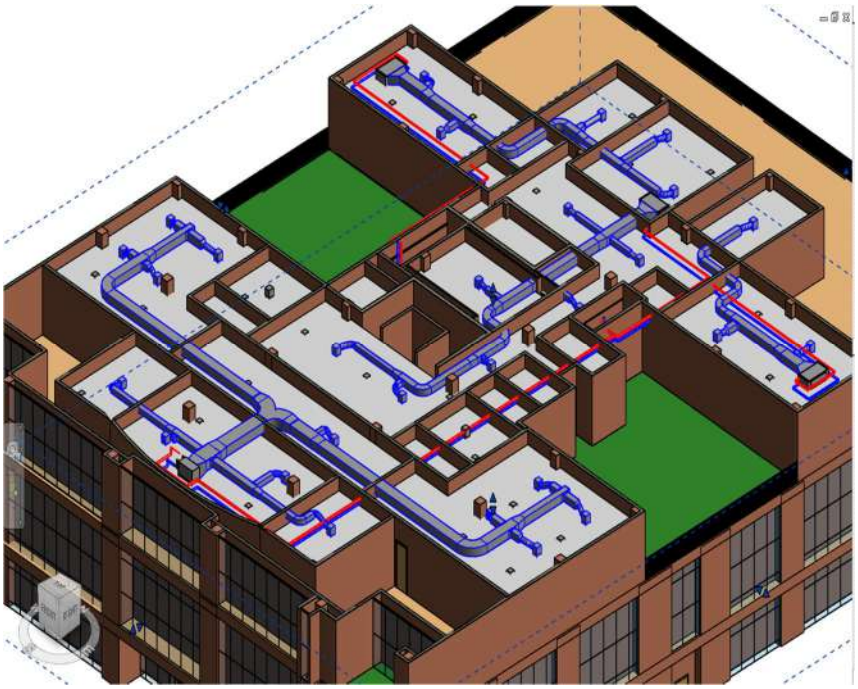
Figure 8- Sample of the Revit tool in 3D.

VI. RESULTS

After going through the various catalogues of Hitachi for different compressors the estimated, specific-power consumption for different compressors like screw, scroll and reciprocating air compressor when NH_3 (Ammonia) R717 as refrigerant the following results have been collected they are as follows:

If the compressor is operating at different loads such as quarter, half, three quarters and full load then specific-power consumption for different compressor are recorded from the catalogue outfits from Hitachi. From the graph shown in the figure outfits the characteristics curves of the different compressors at different loads are show.

By interpretation we can say that screw compressors are best for the load if it is operating at full load else scroll compressor would be preferred operation is for all the loads. When it comes to rotary compressor it is not nominated for its high specific- power consumption and vibrations and noise at full load operation.

Now total power consumption at different load of different compressors are shown below in the table

©IJRASET: All Rights are Reserved

Table-1 Results of total tonnage of various compressors at various loads

	Quarter ¼ load	Half ½ load	¾ load	Full load
Screw compressor	36.822 KW	57.038 KW	83.746 KW	87.640 KW
Scroll compressor	39.707 KW	59.922 KW	91.688 KW	101.79 KW
Reciprocating compressor	58.476 KW	70.025 KW	98.185 KW	135.009 KW

Note: Total tonnage obtained after the heat load estimation for the entire construction is

A. 72.2 TR.

The above obtained results are from HAP and this data is used for the modelling of the HVAC services in Revit.

After extracting the results of different specific-power consumption values of different compressors at different loads the following are nominated:

Better to choose Air-cooled-Screw chiller of capacity 75 TR for this project as the total load calculated to be 72.2 TR, because it operates with better performance at three quarter ¾ and full load and with very less noise whereas air-cooled-scroll chiller operates with better performance as close to the air-cooled screw chiller but it produces noise and vibrations during its operation.

VII. CONCLUSION

By observing the present market, there are lots of engineers would get bewildered at the selection of a compressor which would be cleared by putting the factor of space or volume i.e. for the small space or volume it would be a better idea to select reciprocating compressor and for the space or volumes it is preferred to select rotary compressors like screw and scroll and for the extremely large centrifugal compressor found to be the most suitable.

After going thoroughly through the study of different compressors we have the following conclusion points:

1) Design of HVAC system was so flexible by using the software of BIM (Construction information modelling) like Revit.
2) There was a feasibility to calculate the heat load through Revit as well as HAP but preferred HAP as it outfits accurate results.
3) Duct sizing and pipe sizing of chilled water piping was done by the Revit software itself and found to be user friendly than AutoCAD.
4) After extracting the results of different specific-power consumption values of non-identical compressors at different loads the following are nominated

A. Scopes

This project could be used as a referral for the student for their project in the future. It outfits information about the different compressors used and their power consumption for the student which would be helpful for them to get thought of moving on to creative ideas and their implementations, Thus, helping an individual in going through the various compressors behaviour. It outfits the information of power consumption when it is operating as at different part loads. It outfits an idea how flexible is it if one uses Construction information modelling software like Revit.

REFFERENCE

[1] Carrier handbook, mcgraw-hill publishing company 1965.
[2] Ashrae handbook, 2001 fundamentals applications.
[3] Hvac design manualby james e.brombaugh.
[4] Refrigeration and air-conditioning
[5] Smacna design manual
[6] Revit design city pural site

©IJRASET: All Rights are Reserved

ResearchGate

See discussions, stats, and author profiles for this publication at: https://www.researchgate.net/publication/343239324

Designing Geothermal Heating and Cooling System

Article *in* International Journal of Engineering and Technical Research · July 2020

DOI: 10.17577/IJERTV9IS070473

CITATIONS
0

READS
1,895

2 authors:

Prateek Mahapatra
Manav Rachna University, India, Faridabad
3 PUBLICATIONS **0** CITATIONS
SEE PROFILE

Shivam Kumar Singh
Manav Rachna University, India, Faridabad
3 PUBLICATIONS **0** CITATIONS
SEE PROFILE

All content following this page was uploaded by Prateek Mahapatra on 27 July 2020.

The user has requested enhancement of the downloaded file.

Published by :
http://www.ijert.org

International Journal of Engineering Research & Technology (IJERT)
ISSN: 2278-0181
Vol. 9 Issue 07, July-2020

Designing Geothermal Heating and Cooling System

Prateek Mahapatra
Department of Mechanical Engineering
Manav Rachna University
Faridabad, India

Shivam Singh
Department of Mechanical Engineering
Manav Rachna University
Faridabad, India

***Abstract*- The main objective of this study is to propose a simple design of geothermal heating and cooling system and test this design's feasibility. Findings: In this study, it was observed that this system was able to maintain a room temperature of 25°C. Novelty/Applications: The novelty lies in the use of the concept of constant ground temperatures of the earth in an air conditioning system that uses water as a refrigerant with no use of heat pump which can provide both heating and cooling. This system can be modified or upgraded according to the needs of a person. This system can be a replacement for air coolers in industries where air conditioners cannot be used.**

Keywords- Geothermal energy; Air conditioning system; Heat exchanger; HVAC systems.

I. INTRODUCTION

A ground-coupled heat exchanger is an underground heat exchanger that can capture heat from the ground and can also dissipate heat to the ground. They use the Earth's near-constant subterranean temperature to warm or cool air or other fluid for residential, agricultural, or industrial uses [1]. This paper deals in-depth with our demonstration of using Geothermal energy as a future alternative to traditional heating and air conditioning systems. Geothermal energy is the energy that is harnessed from the mother earth. A geothermal air conditioning system is considered to be the most efficient air conditioning system available to date on this planet [2]. A Ground Coupled Heat Exchanger is a cheaper and greener alternative of evaporative cooler and air conditioning system. It is a type of renewable energy system that usually exchanges heat with the ground or earth rather than the ambient air (Atmospheric air in the neutral state). As we all know that the temperature of the ambient air fluctuates throughout the year but in case of the ground the temperature of the ground at a certain depth stays relatively constant (nearly around 20º-25ºC) throughout the year all around the globe. The ground-coupled heat exchanger exchanges heat with the heat sink i.e. (ground) at nearly constant temperature rather than exchanging heat with heat sink i.e. (ambient air). The major advantage of exchanging heat with the ground at constant temperature rather than with ambient air at fluctuating temperature is it usually consumes the same amount of electricity throughout the year. While in the case of ambient air the electricity consumption varies according to the working load. For example in summer the working load is more as more amount of energy is required to pump heat from room to cooled and already hotter heat sink whereas in winter the temperature of the heat sink is low so directly the amount of workload as well as energy consumption is low. So, comparatively ground or earth as a heat-sink is an economical way than a conventional system having ambient air as heat-sink when electricity consumption is considered. As ground and water temperatures, 4-6 feet below the earth's surface, stay relatively constant throughout the year. This allows the system to provide extremely efficient heating or cooling all year long in virtually any climate. Systems based on geothermal energy cool in much the same way that they heat, moving hot air through a geothermal heat pump or air-to-liquid transfer. In the case of cooling, geothermal systems move heat from above ground to the cooler environment 20 feet under the earth's surface. Water circulated through a geothermal loop carries heat below the earth's surface, where it is absorbed into the ground; the cooled water is then carried back up to regulate the higher ambient temperature. Due to the mass of the earth below, geothermal systems can cool even intense sources of heat. Geothermal cooling is used in green data centers and various industrial environments with almost no power use, no carbon production, and no water used but that which exists within the closed system.

II. PRINCIPLE OF OPERATION

The Geothermal heating and cooling system work on the phenomena of the earth having constant temperature throughout the year around the globe below a certain depth beneath the earth's surface. Usually, it is 20-25°C but may vary according to certain geological and geographical conditions [1]. The heat transfer rate between the geothermal heating and cooling system and earth depends upon the conductivity of soil, the thermal inertia of soil along with many other parameters like water holding capacity of the soil, and the depth [2]. There is some efficiency advantage of geothermal heating and cooling system over evaporative air cooler and air conditioning system is Geothermal heating systems can extract up to six times the heat energy they use in electrical energy.

The system consists of the following parts i.e. air filter (4), water reservoir (2), water pump (3), cooling coils (5), fan (6), AC cooler motor (6), and HDPE pipes (1).

(This work is licensed under a Creative Commons Attribution 4.0 International License.)

International Journal of Engineering Research & Technology (IJERT)
ISSN: 2278-0181
Vol. 9 Issue 07, July-2020

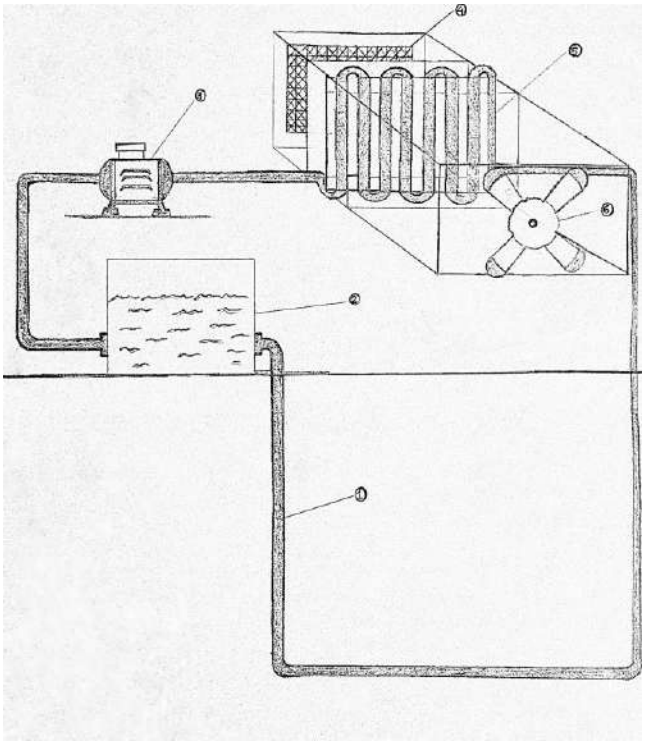

Figure 1: Diagram of Geothermal Heating and Cooling System

The system consists of the following parts i.e. air filter (4), water reservoir (2), water pump (3), cooling coils (5), fan (6), AC cooler motor (6), and HDPE pipes (1). First, the water stored inside the water reservoir (2) or tank is pumped out using a domestic water pump (3) and is transported to the cooling system where it will flow through the loops of copper tube or cooling coil (5) inside the cooling unit. Then hot air from the surrounding is extracted or sucked in by the cooling unit which consists of an external casing, air filters (4), copper tube loops or cooling coil (5), AC cooler motor (6), and fan (6). Now the hot air sucked in will give its heat to the copper tube by convection thus cold air will flow out of the cooling unit and then the hot copper tube will transfer its heat to the cold water flowing inside it by convection. Now the hot water will flow out of the cooling unit through HDPE pipes (1) into the ground. As we know that the temperatures 4-6 ft below earth surface remain constant throughout the year as the ground absorbs nearly half of the solar energy our planet receives and at even greater depths around 3-5 meters the temperatures are even lower. Deep below the earth's surface, we will be having a network of HDPE pipes (1) or ground loops which will transfer heat from hot water to the ground which will act as a heat sink due to which water will again become cold or regain its initial temperature. Then the cold water flows through the HDPE pipe (1) and gets collected in the water reservoir (2) and this cycle is continuously repeated thus cooling the room. Similarly in the winter season, the ground is hotter so it will work as an indoor heater.

III. EXPERIMENTAL PROCEDURE

The objective of this paper is to design a geothermal heating and cooling system and to test this system's feasibility. For testing this system we consider a standard bedroom of dimensions 12ft*10ft*10ft then the volume of the room will be 1200ft^3 and to calculate the value of CFM (Cubic feet per minute) we are using the formula i.e. (Room Volume)/(60 Minutes) × number of times the air in the room should be changed in one hour. According to the air exchange index, the typical air change per hour for a room is considered to be 6 so for the selected room size of 1200ft^3 the value of CFM will be 120. Now for the required room, we need to calculate the value of cooling coil load and size of cooling coil and to calculate these values we considered the following data i.e. the airflow as 120 CFM, the water pump pumps water at 0.23 Kilogram/second, outside air temperature as 45°C and required room air temperature as 25°C. Then from these data, we calculate the specific volume and specific humidity of air at the inlet and outlet of the system using Figure 1: Psychrometric Chart. After finding these values we calculate the enthalpy of air at the inlet and outlet of the system. From these obtained values we calculated the dry air mass volume flow rate and condensate water mass flow rate. Then after calculating all these values we calculate the cooling load of this system. Then for the sizing of the cooling coil, we calculate the surface area required for convective heat transfer.

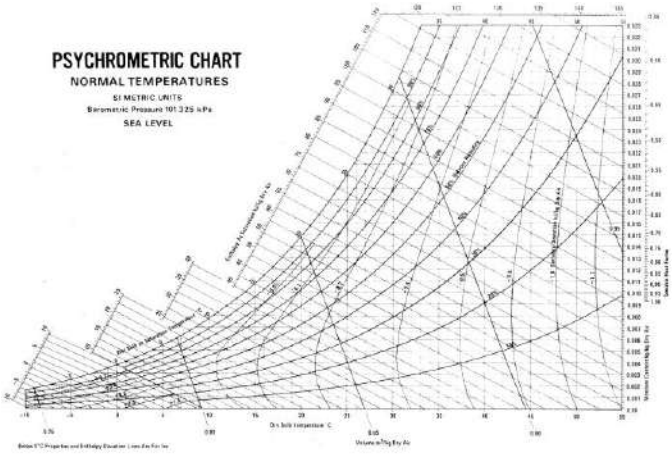

Figure 2: Psychrometric Chart

TABLE 1

Property	***Air In***	***Air Out***
Air Volume Flow Rate (V*)	0.056 m^3/s	-
Air Temperature (T)	45 °C	25 °C
Relative Humidity (RH)	50%	100%
Specific Volume (V_1)	0.9 m^3/s (Dry Air)	
Specific Humidity(W)	W_1 = 0.031	W_2 = 0.020
Enthalpy (h)	h_1 = (1.006 × 45) + 0.031 × [(1.84 × 45) + 2501] = 125.36 KJ/Kg	h_2 = (1.006 × 25) + 0.020 × [(1.84 × 25) + 2501] = 76.09 KJ/Kg

Dry air mass volume flow rate (M_a^*) = V^*/V_1
Ma^* = 0.056/0.9 = 0.062 Kg/s
Condensate water mass flow rate (Mw^*) = $M_a^* \times (W_1 - W_2)$
Mw^* = 0.062 × (0.031 – 0.020) = 0.0006 Kg/s

(This work is licensed under a Creative Commons Attribution 4.0 International License.)

International Journal of Engineering Research & Technology (IJERT)
ISSN: 2278-0181
Vol. 9 Issue 07, July-2020

TABLE 2

S.No.	Parameters	Values
1.	Cooling Water Mass Flow Rate (M*)	0.23 Kg/s
2.	Water Inlet Temperature	25 °C
3.	Water Specific Heat Capacity (Cp)	4.2 KJ/Kg K
4.	Water Out Condensate Water Temperature	45 °C
5.	Enthalpy ($h_w = h_f$ at 25^0C)	104.83 KJ/Kg

Cooling Load (Q^*) = $Ma^* \times (h_2 - h_1) + (M_w^* \times h_w)$
$Q^* = [0.062 \times (76.09 - 125.36)] + (0.0006 \times 104.83) = 2.9KW = 2.9KJ/s$
Cooling coil outlet temperature (T_{out}) = $T_{in} + Q^*/(M^* \times C_p)$
$Tout = 25 + 2.9/(0.23 \times 4.2) = 28^oC$

For the sizing of cooling coil, we will use the formula mentioned below for calculating heat for forced convection which will give us the surface area of the coil that should be in contact with the air for the required cooling load of the coil.

$$Q = h \times A_s \times (T_s - T_\infty)$$

Where
Q = Cooling load or heat generated
h = Overall heat transfer coefficient between air and water when copper acts as a medium
A_s = Surface area at which convective heat transfer occurs
T_s = Surface temperature of the A_s
T_∞ = Temperature of water

$$2900 = 13.1 \times A_s \times (45 - 25)$$
$$A_s = 2900/262 = 11.06\ m^2 = 119.04\ ft^2$$

If we are taking one cooling coil of an effective face area of 12 ft^2 then the cooling unit requires 9.92 or approx 10 coils of the same dimensions stacked together to provide an effective surface area of 119.04 ft^2.

IV. CONCLUSION

From the given results we concluded that for a cooling load of a room this system was able to maintain an optimal room temperature of 25°C with the use of water as a refrigerant. But there is also a significant increase in the use of copper for constructing cooling coils that makes the construction of this system expensive. Although this system is expensive but significantly uses less energy and is more durable than the conventional air cooler. In the future, additives like nanoparticles in water can further increase the efficiency of this system, and also this system can be used in industries where air conditioners and air coolers are not viable for installation.

ACKNOWLEDGEMENT

We are sincerely thankful to Manav Rachna University, Faridabad for providing us the opportunity to write a research paper on the topic "Designing Geothermal Heating and Cooling System".

REFERENCES

[1] M. Kumar, S. Kumbare, To Study Earth Tube Heat Exchanger Cooling of Air in Different Month of Bhopal MP, International Journal of Innovative Trends in Engineering (IJITE). 10 (2015) 27–29.
[2] G.G. Momin, Experimental Investigation Of Geothermal Air Conditioning, American Journal of Engineering Research (AJER). 2 (n.d.) 157–170.

AUTHOR'S PROFILE

Prateek Mahapatra: B.tech Mechanical Engineering, Department of Mechanical Engineering, Manav Rachna University (MRU), Faridabad. Research areas are Thermal Engineering, Automotive Designs, Internal Combustion Engines and Design Analysis. Published 1 article in Indian Journal of Science and Technology.

Shivam Singh: B.tech Mechanical Engineering, Department of Mechanical Engineering, Manav Rachna University (MRU), Faridabad. Research areas are Thermal Engineering, Automotive Designs, Internal Combustion Engines and Design Analysis. Published 1 article in Indian Journal of Science and Technology.

(This work is licensed under a Creative Commons Attribution 4.0 International License.)

View publication stats

ResearchGate

See discussions, stats, and author profiles for this publication at: https://www.researchgate.net/publication/329100558

EFFICIENT MULTICAST ROUTING PROTOCOL FOR MANETS

Article · November 2018

CITATIONS
0

READS
194

3 authors, including:

Vijaya Lakshmi M
G. Narayanamma Institute of Technology and Science
13 PUBLICATIONS **13** CITATIONS

SEE PROFILE

Some of the authors of this publication are also working on these related projects:

wireless networks View project

All content following this page was uploaded by Vijaya Lakshmi M on 18 February 2019.

The user has requested enhancement of the downloaded file.

EFFICIENT MULTICAST ROUTING PROTOCOL FOR MANETS

M.Vijayalakshmi, Assoc.Prof., ECE,GNITS,
Hyderabad, INDIA
Email: mvlakshmi_gnits@yahoo.co.in

Dr.D. Sreenivas Rao., Prof., ECE, JNTUCEH,
Hyderabad, INDIA
Email: dsraoece@gmail.com

Abstract: ***Mobile ad hoc networks (MANETs) have several prominent features because of which MANETs are visualized to support advanced applications. Multicast routing reduces the communication costs of applications. Several multicast routing protocols have been proposed for MANET. While previous MANET multicast protocols focused on the reductions of control overhead, the multicast protocol investigated in this research attempts to reduce the amount of bandwidth used by the network both in terms of control overhead and data rebroadcasts by. Unlike previously proposed MANET multicast algorithms, this new protocol will focus on reducing the amount of unnecessary data rebroadcast by considering QOS constraints like bandwidth, power and end to end delay considering though the creation of a more efficient multicast tree.***

Keywords: *Mobile ad hoc networks, Multicasting, EMCR, MAODV.*

I. INTRODUCTION

A mobile ad hoc network (MANET) is an interconnected system of mobile nodes without any centralized coordinator. Every mobile node in MANETs must be able to function as a router and a host to forward the data from one node to another node within the network. MANETs have several prominent features such as flexibility, robustness, rapid deployment, inherent mobility support and highly dynamic topology. Because of these special features, MANETs are visualized to support advanced applications such as military operations, civil applications, and audio, video conferencing and disaster situations. When applications want to send the same data to more than one destination, multicasting is used [1] - [3].Multicasting is a mechanism for data routing, and it allows the group communication in the network. So, Multicasting becomes one of the challenging issues in MANET applications, in which the source node is connected to set of destinations, reduces the communication costs of applications. Several multicast routing protocols have been proposed for MANET. Existing multicast routing protocol can be broadly classified into 2 categories: Mesh-based multicast routing protocols [4] and tree-based multicast routing protocols [5]. The study given in [6] - [11] discuss the complete survey of the current routing algorithms proposed for the wireless MANETs. In MANETs, bandwidth has become one of the most precious resources in the network and to utilize the bandwidth properly in the network, network coding (NC) can be used. NC is an efficient networking mechanism where the transferred data will be encoded and also decoded to maximize throughput of the network and record all the transmission. Decoding of the transmissions is performed at the destination node. So, for the delivery of data, lesser transmissions are sufficient but on the other hand, the large amount of processing has to be performed at the intermediate node and destination node [12].NC maximizes the network capacity and hence is considered as a reliable technique [13]. When NC is used, the data packets can be combined by the intermediate nodes prior forwarding the packets. Hence, NC minimizes the overall number of data transmission and is appropriate for broadcasting purposes [14].It should be note that the conservation of bandwidth is imperative to the success of any wireless network. While previous MANET multicast protocols focused on the reductions of control overhead, the multicast protocol investigated in this research attempts to reduce the amount of bandwidth used by the network both in terms of control overhead and data rebroadcasts by. It can usually be assumed that data transmission consumes more bandwidth than control overhead[15][16][18]. Even a small decrease in data retransmissions should substantially improve network performance. Unlike previously proposed MANET multicast algorithms, this new protocol will focus on reducing the amount of unnecessary data rebroadcast by considering QOS constraints like bandwidth, power and end to end delay considering though the creation of a more efficient multicast tree[17][19][21]. Paper is organized as follows: Section I is Introduction, Section II is about EMCRP, Section III is about simulation and results and conclusions are discussed in Section IV.

II. DESIGN OF PROPOSED EMCR PROTOCOL (EFFICIENT MULTI CAST ROUTING PROTOCOL)

In this work, proposed to design EMCR protocol has three schemes and the QoS constraints like available bandwidth, available power and end-to-end delay are considered to select the routes, that are the routes with sufficient bandwidth, power and delay minimized. The protocol involves three phases .1 Route selection algorithm 2.Link failure detection 3. Route optimization

2.1 Route selection algorithm

1: When a node S_N wants to send data packet to multiple D_N nodes, it defines the three QoS constraints like bandwidth, power and end to end delay

2: Then S_N includes the predefined QoS constraints in a route request message, and broadcasts it, to determine the path towards the D_N.

3: When the SN broadcasts the Req Routes, it predefines' T Limit;

4: When the neighboring nodes receive the Req Routes message, it checks the three constraints;

5: if The three constraints are satisfied then

6: the adjacent node accepts the request and enters the route information in the routing table and sets the route status as observed;

7: end if

8: The adjacent intermediate node sends the route reply, Rep routes to the S_N .

9: if The time taken by the Req routes to reach the neighboring node exceeds the T limit then

10: The request is ignored by the receiving node.

11: end if

12: if The time taken by the Rep routes to reach the neighboring node exceeds the T limit then

13: This reply is dropped by the SN, and the route entry in the routing table is deleted.

14: end if

15: All the Rep routes received within the T limits are accepted by the S_N.

16: Based on the reply received and its route information, paths are determined from the source to multiple D_N.

i. Available Bandwidth (BW) : Available bandwidth(BW) represents available link bandwidth in the path from source node to the destination node multicast tree. The available bandwidth is calculated by using Eqn. 1.

$$BW = \alpha BW_L + \frac{(1-\alpha)T_{idle}}{T_P} B_{Channel} \quad (1)$$

where

α: is the weight factor and its value lies 0 and 1,

BW_L is the available local bandwidth of the node in the preceding period,

T_{idle} is the channel idle time,

T_P is the time interval period and $B_{Channel}$ is the channel capacity in bits per second.

ii. Available Power (P) The available power of a node in multicast tree is denoted by

$$P = P_{Total} - P_{Consumed} \quad (2)$$

$$P_{consumed} = \frac{P_{Tresold}\, d^n}{K} \quad (3)$$

iii. Available Delay (D) : The delay (D) is the maximum value of delay in the path from source node to destination nodes. The delay of multicast tree is calculated as follows

$$D = N\left[d_{trans} + d_{proc} + d_{prop}\right] \quad (4)$$

where, N is the number of links, d_{proc} is the processing delay involved with each packet, d_{prop} is the propagation delay between two nodes and d_{trans} is the transmission delay. Dtrans is calculated by using the following equation,

$$d_{trans} = \frac{N}{T} \quad (5)$$

Where, N is the number of bits and T is the rate of transmission.

Route Request Message:

When a source node needs to communicate with another node, it broadcasts the route request message (Req routes) to its neighboring node.

ABW	E_r	D_y	T_{limit}	Reqroute

The format of the (Rep routes) is same as MAODV with an additional QOS constraints. Where, BW represents, the available bandwidth of a node, Er represents the available power of a node, D represents end to end delay, T limit represents the time limit to travel between one node to another and Req route represents the fields of MAODV route request message .

Route Reply Message: When a neighboring intermediate node receives Reqroutes message, it sends the route reply

ABW	E_r	D_y	T_{limit}	Reproutes

2.2 Link Failures

During second phase of algorithm Given a particular multicast session, a node can be a source, a receiver, an intermediate node, a source and a receiver, or a receiver and an intermediate node .

Frequent changes in network topology can cause links failures that disrupt communication between nodes. Because of the highly dynamic nature of the network link failures must be detected and fixed quickly.

1.If a router finds that a direct connection between it and its upstream node no longer exists, the host will initiate branch rediscovery.

1.1. Branch rediscovery proceeds in much the same way as does multicast route discovery, except in reverse. (steps from 1.1.1)

1.2 A node looking to rejoin the multicast tree floods the network with a JOIN packet. Each JOIN packet contains the [source, group] pair of the session of interest and the address of the node initiating the branch rediscovery.

1.3 As the JOIN message traverses the network, intermediate nodes mark an entry in their multicast routing tables, set their timers to HOLD_REFRESH_TIME, and store the address of the last hop of the JOIN.

1.4 Nodes that receive a new JOIN message and do not have a valid route to the source decrement the TTL

and forward the message if the TTL is greater than zero.

1.5 If the node has a valid route to the source it adds the last hop of the JOIN to its downstream list and unicasts a JOIN-ACK message to the last hop of the JOIN. Nodes forward the JOIN-ACK message until it reaches the lost node.

1.6 The initiator of the JOIN may receive many JOIN-ACK messages, each advertising a different path to the source.

1.7To enable one of these branches, the initiator send a JOIN-OPT message back up the tree.

1.8 The lost node unicasts this JOIN-OPT message to its new upstream node.

1.9 If a node receives a JOIN-OPT message and multicast routing has not been enabled, the node enables routing and forwards the JOIN-OPT message to its upstream node.

1.10. The JOIN-OPT message travels towards the multicast source, enabling forwarding, until it reaches the node that sent the original JOIN-ACK.

Else go to step 2

Branch rediscovery

1.1.1During branch rediscovery nodes MAY notify that they are performing branch rediscovery.

1.1.2 To do this, a node would send a JOIN-NOTIFY message to its downstream nodes. This message is sent just before a host sends a JOIN message and accomplishes two goals.

1.1.3 First, it informs nodes that an upstream node is attempting to rejoin the multicast tree and that they MUST NOT respond to a branch request for the multicast session or forward a JOIN from the originator of the JOIN-NOTIFY.

1.1.4 Secondly, it updates the timers of the downstream nodes. Failing to do this may cause nodes to time out before the link can be repaired. JOIN-NOTIFY messages have the same format as JOIN messages.

End if

2. The router directly transfers the data to upstreaming node

End

3. Link failures in a wireless network may prevent nodes from explicitly leaving a multicast group.

3.1 For this reason a node MUST keep track of which of its downstream nodes are also one-hop neighbors.

3.2Each downstream entry keeps a timer that is updated periodically if the node finds the address in its list of one-hop neighbors.

3.3 If the address cannot be found before the timer expires, the entry is removed.

3.4 If the downstream list is empty and the node does not want to receive multicast data, the node MUST send a PRUNE message to its upstream neighbors.

3.5The timer SHOULD be long enough to allow a JOIN message to reach the node if a link fails and the downstream node is still interested in the session

End

2.3 Route Optimization

1. A member of the multicast tree MAY perform a route optimization if it manages to overhear a TREE-REFRESH message broadcast by a source other than its upstream node.

1.1 If a node overhears such a message it can check the information stored in the message to determine whether, if by joining the new branch, inefficiencies in the network can be reduced

Else

1.2 If a node can determine that it is an only child, it MAY leave its upstream node and join the new node. This move would allow its original parent to prune itself from the multicast tree if it is non-receiver, or allow the node to stop forwarding multicast data if it is a multicast receiver.

2.If a node that is performing the route optimization has a hop count that is larger than or equal to the hop count of the new parent, it unicasts a JOIN-OPT message to the new upstream node and LEAVE -OPT message to its former parent.

2.1Nodes that receive a JOIN-OPT message add the last hop address to their downstream list.

2.2 Nodes that receive a LEAVE -OPT message remove the last hop address from their downstream lists. 2.1.1Before sending the JOIN-OPT message, the node sets its NON_RECEIVER value to zero to prevent the node from attempting a new route optimization before it receives a new TREE-REFRESH message from its new parent that accurately represents the status of the network.

2.1.2 A reduction of redundant control and data packets is possible by using the set of MPR nodes made available from the OLSR routing protocol.

2.1.3 By reducing the number of JOIN messages, routers are able to reduce overhead during link recovery and to eliminate advertisements for faulty routes.

III. Results and Discussions

The performance of the EMCR, and MAODV routing protocols are evaluated. The simulation results are carried out using the Network Simulator (NS 2. 34). The EMCR protocol is compared with existing MAODV protocol through the simulations. The simulation scenario table 1 used for simulation these routing protocols.

The Figure 1 to 4 simulation results acquired by changing number of nodes and traffic remains constant.

Table: 1. Simulation Scenario

S. No.	Network Parameters	Value
1.	Routing Protocols	EMCR, MAODV
2.	Simulation area	1000 X1000
3.	MAC	IEEE 802.11
4.	Number of Nodes	10,20,30,40,50
5.	Traffic Type	CBR
6.	Date Rate	1 Mbps
7.	Speed	20 m/s
8.	Initial Energy	5 Joules
10.	Simulation time	100 sec

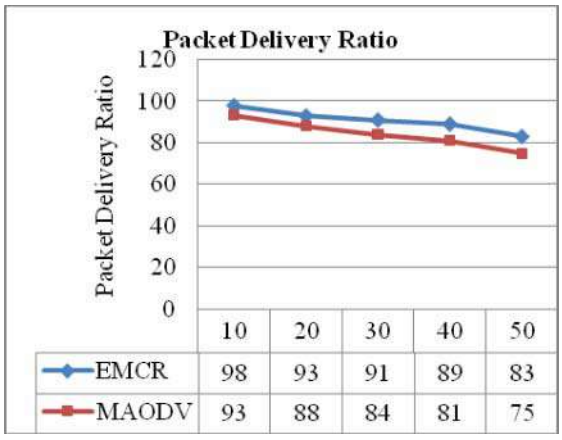

Figure 1. Packet Delivery Ratio Vs Number of Nodes

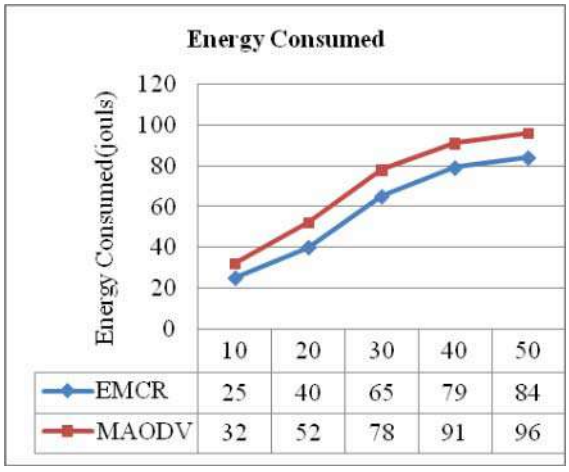

Figure 2. Energy Consumed Vs Number of Nodes

Figure. 1. Shows that the Packet Delivery Ratio of EMCR and MAODV protocol by varying number of nodes. From the simulation results EMCR protocol has higher packet delivery ratio than MAODV protocol.

Form the figure. 2, it shows that energy consumption of EMCR and MAODV protocols when number of nodes is varied. The EMCR is less energy consumption than MAODV protocol. The EMCR protocol is more energy efficient.

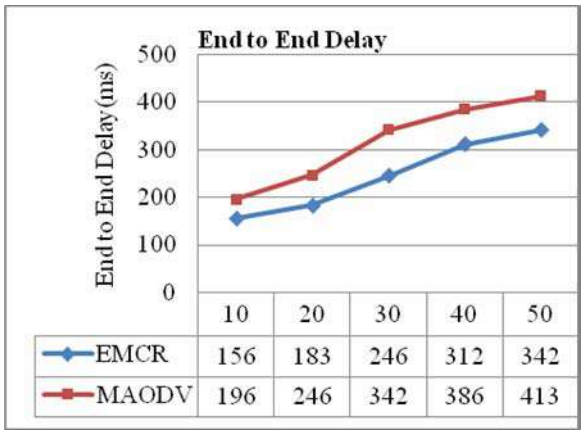

Figure 3.End to End Delay Vs Number of Nodes

The figure 3. shows that end delay is increasing with increasing nodes. The end to end delay of EMCR, protocols less when compare to MAODV by varying number. of nodes i.e. from 10 to 50 nodes and node speed remains constant.

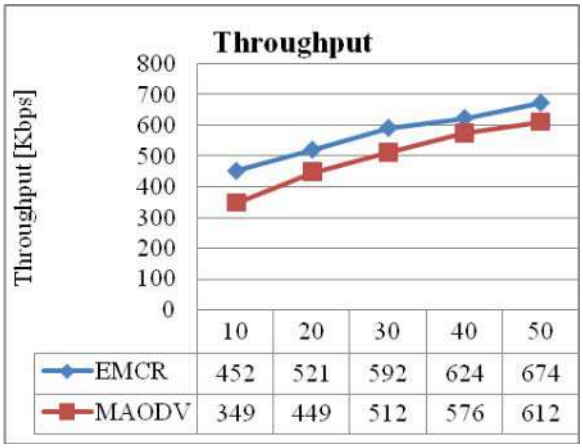

Figure 4. Throughput Vs Number of Nodes

IV. CONCLUSION

Form the figure.4. It shows that throughput is increasing with increasing nodes. Throughput for EMCR, MAODV protocols by varying number of nodes i.e. from 10 to 50 nodes and node speed constant. The EMCR protocol has good throughput when compare with MAODV protocol.

REFERENCES

[1] Siva Ram Murthy and B. S. Manoj."Chapter 3 Ad Hoc Wireless Networks, "in Ad Hoc Wireless Networks: Architectures and Protocols, pp. 213-245.

[2] Luo Junhai, Xue Lin and Ye Daniye, "Research on Multicast Routing protocols for Mobile Ad Hoc Networks, "in Elseveier Computer Networks, Vol. 52, pp. 988-997. 2008.

[3] Su W, Lee S and 1.Gerla M., "On-demand multicast routing protocol in multi hop wireless mobile networks(ODMRP), "in Springer Link Mobile Networks and Applications, Vol. 7, pp. 441-53, 2002.

[4] E.M Royer and C. E Perkins, "Multicast adhoc on demand distance vector (MAODV) Routing. "Internet Draft, draft-ietf-draft-MAODV-OO.txt 2000. 6

[5] S. Badarnch and M Kadich, "Multicast Routing protocols in Mobile Ad Hpc Networks: A comparative Survey and Taxonoly, "in EURASIP Journal of f'I1reless Communication and Networking. pp. 1-42. Vol. 2009.

[6] A Boukerche, B Turgut, N Aydin, M Z. Ahmad, Ladislau Bini and Damla Turgut, "Routing protocols in ad hoc networks: A survey, "in Elsevier Journal of Computer Networks. Vol. 55.pp. 3031-3080. 2011.

[7] R C Biradar and S S. Manavi, "Review of Multicast Routing protocols in Mobile Ad Hpc Networks. "in Elsevier Journal of networks and Computer Applications. Vol. 32, pp. 221-239.2012.

[8] Lue Junhai, Ye Danxia, Xue Lin and Fan Mingya, "Survey of Multicast Routing protocols for Mobile Ad Hpc Networks. "in IEEE Communications, Surveys and Tutorials, Vol. 11, No. I, pp. 78-91, First Quater 2009.

[9] J M Vella and S Zammit, "A Survey of Multicasting over Wireless Access networks, "in IEEE Communications, Surveys and Tutorials, Vol. 15, No. 2, pp. 78-91, Second Quater 2013.

[10] E Alolaibi and B Mukharjee, "A survey on routing algorithms for Wireless Ad Hoc Mesh Networks, "in Elsevier Computer Networks, Vol. 56. pp. 940-965. 2012.

[11] B. Nagalakshmi. D. Venkatesh and K Ramesh. "Probability Scheme With Network Coding Technique in Wireless Ad Hoc Networks: Reducing the Number of Transmissions with Enhanced Security, "in International Journal of Advanced Research in Electrical. Electronics and Instrumentation Engineering, Vol. 2, Iss. 6. pp. 2320-2325.June 2013.

[12] M Hay, B Saeed. Chung-Horng Lung. Thomas Kunz. and Anand Srinivasan. "Network Coding and Quality of Service for Mobile Ad Hoc Networks. "in Int.J Communications, Network and System Sciences, Vol. 7. pp. 409-422. 2014.

[13] S Yang. J Wu and M Cardei, "Efficient Broadcast in MANETs Using Network Coding and Directional Antennas. "in IEEE INFOCOM 2008, pp. 1-6. 2008.

[14] Li Xu. Liu Tianjian, Liu Ying and Tang Yan, "Optimized Multicast Routing Algorithm based on Tree Structure in MANETs, "in China Communications. pp. 90-99. Feb. 2014.

[15] Y S Yena, H C Chaoc. R S Changd and A Vasilakos. "Flooding-limited and multi-constrained QoS multicast routing based on the genetic algorithm for MANETs. "in Elsevier Mathematical and Computer Modelling, Vol. 53, pp. 2238-2250. 2011.

[16] K Chi , X Jiang and S Horiguchi, "Network coding-based reliable multicast in wireless networks. "in Elsevier Computer Networks. Vol. 54. pp 1823-183, 2010.

[17] N C Wang. "Power-aware dual-tree-based multicast routing in mobile ad hoc networks, "in lET Communications. Vol. 6, Iss. 7. pp. 724-732, 2012.

[18] J A Torkestani and M R Maybodi, "Mobility based multicast routing algorithm for wireless adhoc networks . A learing automata approach. "in Elsevier Computer Communication. Vol. 33. pp. 721-735. 2010.

[19] J A Torkestani and M R Maybodi. "A link stability based multicast routing protocol for wireless mobile adhoc networks, "in Elsevier Journal of network and computer applications. vol. 34. pp.1429-1440. 2011.

[20] Li Layuan and Li Chunlin. "A QoS multicast routing protocol for clustering mobile ad hoc networks. "in Elsevier Computer Communications, Vol. 30. pp. 1641-1654. 2007.

[21] Ozkasap, Z Genc and E Atsan. "Epidemic-based reliable and adaptive multicast for mobile ad hoc networks."in Elsevier Computer Networks. Vol. 53. pp. 1409-1430. 2009.

[22] R C Biradar. S S Manavi and M Reddy "Link stability based multicast routing in MANET. "in Elsevier computer Networks. Vol. 54, pp. 1183-1196. 2010.

[23] R C. Biradar. S S. Manvi. "Neighbour supported reliable Multipath multicast routing MANETs. "in Elsevier journal of Network and Computer Application, Vol. 35. pp. 221-229.2011.

[24] C Cheng, H Eric Hsiao-Kung Wu, Gen Huey chen. "Stable Backbone hosts and stable multicast routes in two tier mobile Ad hoc networks."in IEEE Transactions on vehicular Technology, Vol. 58, No. 9, Nov 2009.

[25] S Baolin and Li Layuan, "QoS-aware multicast routing protocol for Ad hoc networks. "in Journal of Systems Engineering and Electronics. Vol. 17. No. 2. pp. 417-422, 2006.

View publication stats

Secured Packet Level Authentication Scheme for Code Update in Multihop WSN

Md Aleemuddin Ghori, Syed Abdul Sattar

Abstract: ***Wireless sensor network is an imminent technology and is getting Popularity quickly and a lot of attention because of their low cost solutions and capable to implement in military as well as for civilians. This technology has many applications as well as several environmental monitoring target tracking scientific exploration patient monitoring and data acquisition in hazardous environments. In Wireless Sensor Networks These tiny sensor nodes are deployed randomly in a hostile environment to collect sensor data and hence they are susceptible to outsider attacks therefore security is an important issue. Several security schemes have been proposed to provide the authenticity and integrity for network programming applications but they are either lacks the data confidentiality or they are not energy inefficient as they are based on digital signature. So still there is a need to design a security Scheme to Enhanced the existing security mechanism for providing the authenticity and integrity of program updates in existing network programming protocols.***

Keywords: Wireless, Networks, imminent technology, program updates in existing

I. INTRODUCTION

Wireless Sensor Networks (WSNs) is an advanced and emerging technology which has its application across a wide range of industrial scientific and military as well as for the civilian sector example oil and gas-pipelines power distribution networks water distribution networks and nuclear power plants. In multi-hop wireless sensor networks the remote reprogramming is created by changing application necessities and software errors [1]. In this context resource-awareness time-efficiency and the combination of appropriate security solutions are the keys to success and acceptance of a code update mechanism. To satisfy this demand a dependable data dissemination protocol for time-efficient and secure code updates in wireless sensor networks is utmost required. A desirable feature is resistance to node capture and even if a node is compromised and its key material is exposed an adversary should not be able to gain control of the other parts of the network by using this material. Therefore, securing sensor networks against these threats becomes challenging [2] for the researchers and an authentication scheme for network programming is needed to ensure that the adversary should not be able to locate program image.

Revised Version Manuscript Received on August 28, 2016.

Dr. Md Aleemuddin Ghori, M. Tech, PhD, Professor, Department of Computer Science & Engineering, Royal Institute of Technology and Science, Chevella (Telangan) -501503, India.

Dr. Syed Abdul Sattar, BE, MTech, PhD (ECE), PhD (CS), Professor & Dean of Academics, Royal Institute of Technology and Science, Chevella (Telangan) -501503, India.

II. PROBLEM DEFINITION

The existing network programming protocols [3-7] focus on reliable efficient application image dissemination with the minimal end-to-end update latency with the prevalent appearances but provide no security mechanism. The absence of security mechanism on broadcast of application image imposes a vulnerability of installation with arbitrary application image in WSNs. Attacker could just capture one sensor node in WSNs and inject the malicious code image the same way as these network programming protocols operate. Without any appropriate security mechanism the entire WSN could be taken control by the attacker with slight effort by compromising only one sensor node[8].

A. Paper Contribution

Our main aim through this paper is to design a security scheme for network programming protocols by using one-way multiple key chains to secure code update in a multi-hop sensor networks. Our scheme does not involve any asymmetric cryptographic techniques resulting in energy efficient mechanism. In addition the selections of design parameters in the scheme are discussed to maximize the difficulties of different types of attacks against this scheme. This paper establishes the association between the network topology and security Mechanism.

III. DESIGN AND IMPLEMENTATION

This section describes the design of our secure network programming scheme where the Sensor nodes are grouped according to their hop distance to base station in one-way multiple key chains. The sensor nodes in different hop group share different one-way key chain with the base station for packet authentication and integrity check and hence prevent the malicious code update from the nodes in the upstream hop group. Our scheme works at the packet level and consists of two phases. First phase is initialization and key pre-distribution and the second is packet pre-processing and verification phase.

3.1. Initialization and key pre-distribution phase.

Our scheme employs one-way multiple key chains to secure the Deluge protocol. Key chains are based on a function H with the property that its computation is easy while its inverse H^{-1} is extremely difficult to compute. A hash chain with length L is generated by applying H to an initial element repeatedly for L times. (i.e. $\forall\ 0 \leq i \leq L, 1 \leq j \leq S, K_{i,j} = H(K_{i+1,j})$ shown in Fig . 3.1) The last value after H has been applied L times is called the committed value of the hash chain (Fig. 3.1). Before the sensor nodes are deployed the base station constructs S hash chains. It generates S distinct random seed numbers and computes a one-way hash chain with length of L+1 starting

Published By:
Blue Eyes Intelligence Engineering
& Sciences Publication Pvt. Ltd.

from each seed which is the $(L - i + 1)^{th}$ output of hash function derived from j^{th} random seed number and is denoted as $K_{i,j}$) Sensor nodes are divided into S groups according to their hop distance to the base station (see Fig. 3.2). The committed value of the i^{th} key chain ($K_{0,i}$) corresponding to the hop distance is pre- distributed to nodes in the i^{th} hop group before the keys are deployed.

Table 3.1: The notations in Section 3.3 and Section 3.4

Notation	Meaning
H(B)	H(B) Hash of B
A||B	A||B Message A concatenated with message B
Ka	Ka Shared key between node a and base station
EKa(M)	EKa(M) Encryption of message M with symmetric key Ka
DKa(M)	DKa(M) Decryption of M with symmetric key Ka
A :	A : The operation after : occurs in Node A
A ➔ B : P	A ➔ B : P Node A unicasts a packet P to node B
A ➔ ✸ : P	A ➔ ✸ : P Node A broadcasts a packet P
MA <= MB	MA <= MB Message MB is copied to message MA
R	R The transmission range of sensor nodes and base station
rA	rA The distance between node A and the base station
rAB	rAB The distance between node A and node B
rDi	rDi The radius of deployment circle for the ith group
S	S The number of hops in which a secure program image will propagate in our scheme
N	N The number of nodes in WSN
L	The maximum number of packets that the base station will need to broadcast

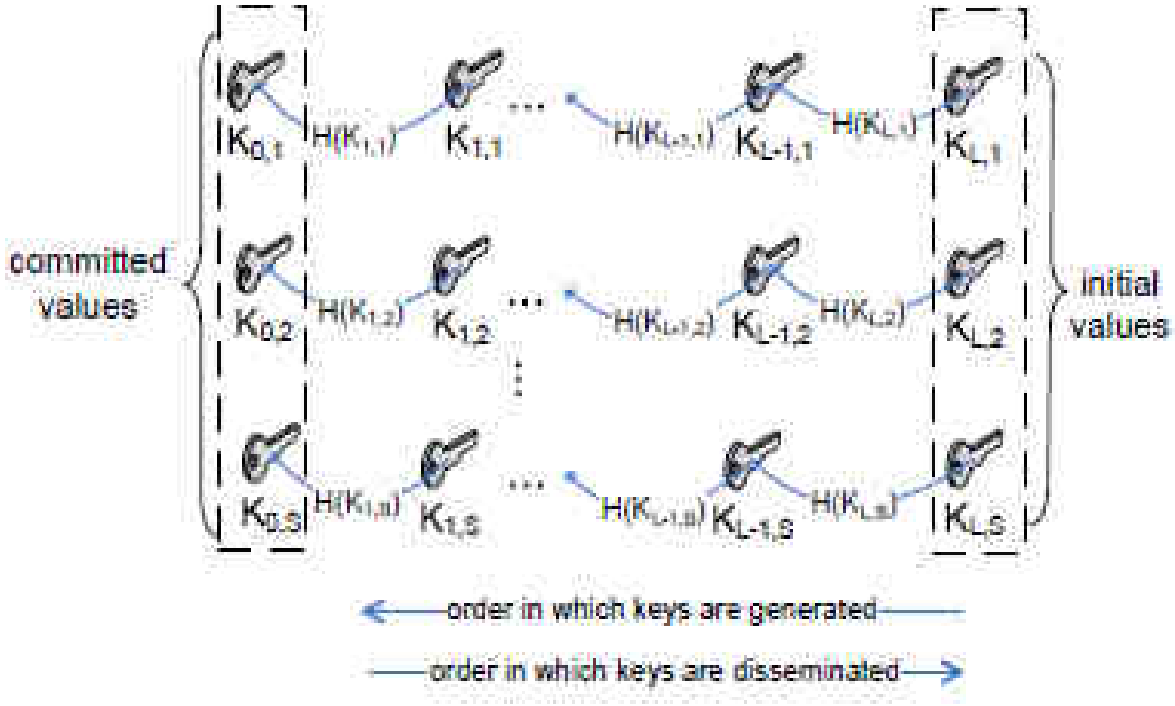

Figure 3.1: Establishment of multiple one-way key chains.

3.2. Phase 2: packet pre-processing and verification

After the node deployment once the base station has a program update to broadcast the program image is divided into fixed-size packets like P0, P1, ...P_{L-1} (shown in Fig. 3.4). The base station pre-processes these packets so that the sensor nodes can verify the packets accordingly.

3.3. Packet pre-processing

First we describe the packet pre-processing of the very first packet of program image (P0). The committed value of the first key chain ($K_{0,1}$ in Fig. 3.1) is used to encrypt the next key element in the order of key dissemination ($K_{1,1}$ in Fig. 3.1). The encrypted result ($E_{K_{0,1}}(K_{1,1})$) is the key update segment for the first hop group. Then $K_{1,1}$ is concatenated with P0 and the result is hashed yielding the packet authentication segment ($H(P_0 || K_{1,1})$). The key update segments and packet authentication segments the successive hop groups are generated in the same way using their corresponding key chains. Finally all these segments are concatenated with P0 as shown in Fig. 3.3, giving the first packet to be transmitted. The way in which the key update and packet authentication segments are concatenated with the data packet is used in a countermeasure against tunnel attack and this packet pre-processing procedure is repeated for successive packets in the image to be broadcast.

Published By:
Blue Eyes Intelligence Engineering
& Sciences Publication Pvt. Ltd.

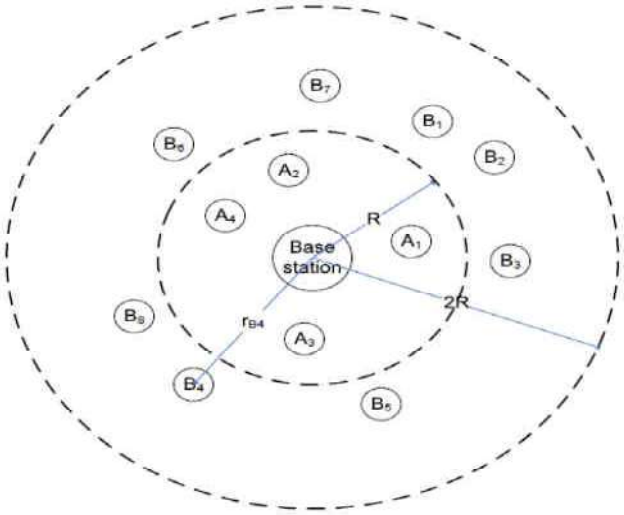

Figure 3.2: Grouping of nodes when S = 2, A $_{1, 2...}$ are nodes in the one-hop group while B $_{1, 2...}$ are nodes in the two-hop group.

The packet pre-processing result (P'$_i$) for the Ith (∀ i, 0 ≤ i < L) packet (P$_i$) propagated to S hops is

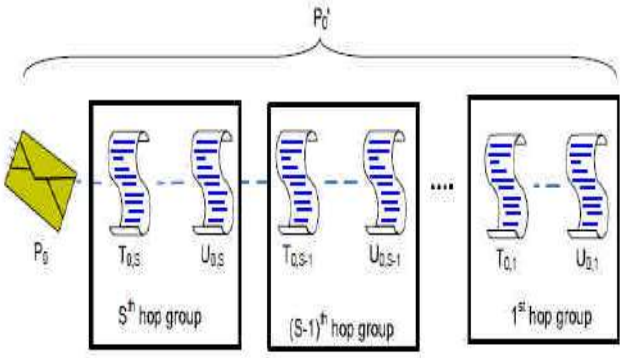

Figure 3.3: The packet pre-processing for the first data packet: P'$_i$ = P $_0$ ||T$_{0, s}$ ||U$_{0, s}$ ||….||T$_{0, 1}$ ||U $_{0, 1}$,, where T$_{0, j}$ = H P $_0$ ||K $_{1, j}$, U $_{0, j}$ = E $_{K 0, j}$ (K $_1$, j), ∀ 0 ≤ j ≤ S

$$P'_i = P_i \| T_{i,s} \| U_{i,s} \| \ldots \| T_{i,1} \| U_{i,1},$$

Where

$$T_{i,j} = H\,MAC\,(K_{i+1,j}, Pi) \qquad (3.1)$$

And

$$U_{I,j} = E_{K\,i,j}\,(K_{i+1}, j) \qquad (3.2)$$

The complete mechanism of packet pre-processing is illustrated in Fig.3.4, while the complete verification of i th packet in node A (A ε G$_j$) is shown in Algorithm

3.2.2. Packet verification

The packet verification for the first data packet destined to the first hop group will be described. The verification of subsequent packets in the other hop groups use the same procedure with keys corresponding to those that were used in the packet pre-processing. After the pre-processing of a packet and the respective concatenation (i.e., P'$_0$ = P $_0$ ||T $_{0, 1}$ || U $_{0, 1}$), P'$_0$ is transmitted to nodes in the first hop group. After retrieving the correct group information from P'$_0$ (i.e., the sensor node parses the right fields T$_{0,1}$ and U$_{0,1}$), the sensor nodes verify the key update segment (U $_{0,1}$) and packet authentication (T $_{0, 1}$) segments as follows.

3.4. Key update segment

The sensor node decrypts U $_{0, 1}$ with K $_{0, 1}$. i.e., D$_{K 0, 1}$(U $_{0, 1}$). The sensor node checks if H (D $_{K 0, 1}$(U $_{0,1}$)) is the same as K $_{0,1}$ (line 7 in Algorithm). If it is, the authenticity of U $_{0, 1}$ is ensured and K $_{0,1}$ is replaced by K $_{1,1}$ for the next packet verification (line 8 in Algorithm). Otherwise, this packet is discarded (line 17 in Algorithm).

3.3.1. Packet authentication segment

After the sensor node retrieves the authenticated packet K $_{1, 1}$ from U $_{0, 1}$, it performs the HMAC operations with K $_{1, 1}$ as the key over P0 to see if it matches T $_{0,1}$ since a simple hash function has been found problematic in integrity verification (line 10 in Algorithm). If it does then the integrity of packet is assured (line 12 in Algorithm). Otherwise this packet is discarded (line 14 in Algorithm).

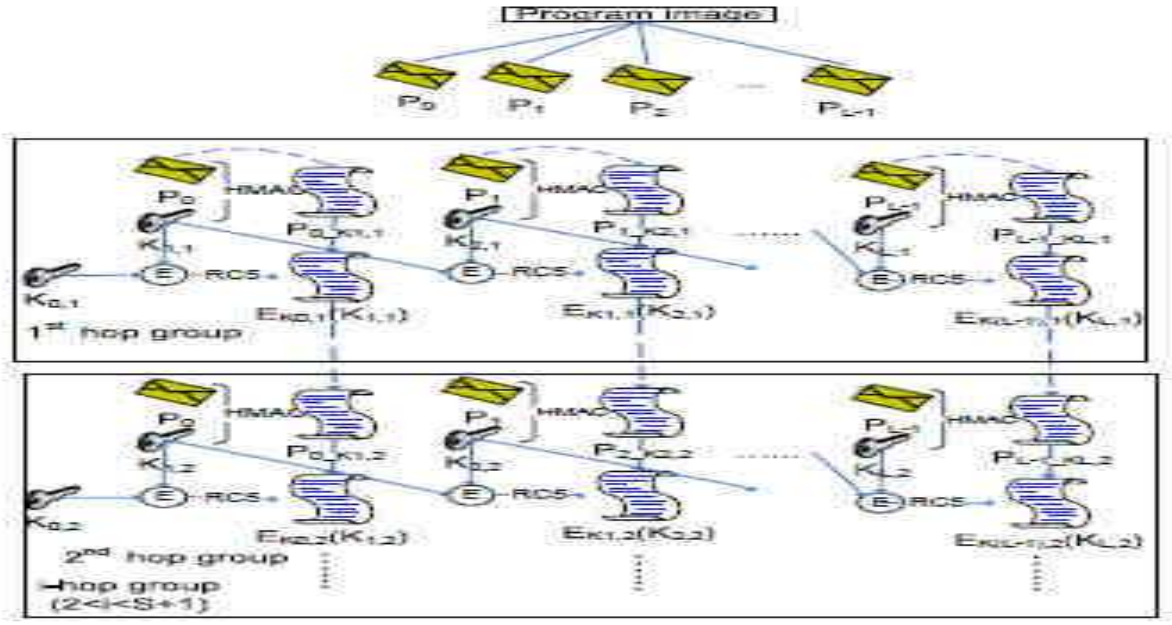

Figure 3.4: Packet pre-processing in the base station U $_{i, j}$ = E $_{K i, j}$ (K $_{i+1, j}$), T $_{i, j}$ = HMAC (K $_{i+1, j}$, P $_i$). Algorithm

Published By:
Blue Eyes Intelligence Engineering
& Sciences Publication Pvt. Ltd.

The i^{th} $(1 \le i \le L)$ packet (P_i) verification in node (A) where A ε G_j $(1 \le j \le S)$

1 base station: Key_ Section_ i j <== $E_{K\,i-1,\,j}$ $(K_{i,\,j})$
2 base station: $P_{i_K\ i,\,j}$ <== $H(P_I \| K_{I,\,j})$
3 base station: P'_i <== $P_i \| P_{i_K\,i,\,j} \| Key_ Section_ i\ j$
4 base station → * : P'_i
5 P'_i has been propagated by j - 1 nodes
6 A : receive P'_i ∀ A ε G_j group
7 if $H(D_{K\,i,\,j}(Key_ Section_ i\ j\ )) = K_{i,\,j}$ then
8 A : $K_{i+1,\,j}$ <== $D\,K_{i,\,j}$ (Key_ Section_ i j)
9 A : remove Key_ Section_ i j from P'_i
10 if HMAC ($K_{i+1,j}$, P_i) = $P_{i_K\,i,\,j}$ then
11 A : remove $P_{i_K\,i,\,j}$ from P'_i
12 A : accept P_i
13 A : advertise P_i
14 else
15 A : drop P'_i
16 end if
17 else
18 A :drop P'_i
19 end if
20 if P_i is requested then
21 A → * : P'_i
22 end if

3.5. Implementation and performance evaluation

We implemented our scheme as an extension to the Deluge network programming protocol that is distributed with Tiny OS [8, 9]. In Deluge the base station programs are written in Java and run on a PC. These Java programs are used to construct and broadcast the new code dissemination packets into the WSN [10]. The programs for the sensor nodes are nesC programs. They are used to receive the packets of broadcast program images and update the appropriate node program image slots. On the base station side we used the JCE provider in the Bouncy Castle Crypto Application Program Interface (API) for hash function (SHA-1) key generation and packet encryption (RC5). On the sensor node side we employed the hashing operation from Tiny ECC and packet decryption from Tiny sec. The committed values of the key chains are generated in the base station and pre-distributed on the nodes in the corresponding hop group before deployment. The operations of packet pre-processing are implemented in ImageInjector.java while the operations of packet verification are implemented in delugePageTransferM.nc. The reference codes for the base stations and sensor nodes are available in and respectively. Our evaluation consists of two parts. We first evaluated our scheme using the TOSSIM Then we tested our scheme in a network of Tmotes. We compare our scheme with the original Deluge and Sluice in terms of end-to-end latency

IV. CONCLUSION

Current network programming protocols can propagate and disseminate the application image in sensor networks reliably and efficiently. However security issues did not play an important role in design of these systems in early stages. As a result an attacker could simply propagate and disseminate its own malicious code image in sensor network pretending to be a genuine entity. Although some security schemes have been proposed to defend against the malicious code distribution they are either not power efficient or lack the consideration on code confidentiality and integrity and hence exploiting on the security design itself. Our future work will include the design of security models for network programming to improved security and scalability in multihop wireless sensor networks.

REFERENCES

1. Sangwon Hyun, Peng Ning, An Liu, and Wenliang Du. Seluge: Secure and dos-resistant code dissemination in wireless sensor networks. In IPS08:Proceedings of the 7th international conference on Information processing in sensor networks, pages 445–456, 2008.
2. Cynthia Kuo, Mark Luk, Rohit Negi, and Adrian Perrig. Message-in-a-bottle: User-friendly and secure key deployment for sensor nodes. In SenSys ’07: Proceedings of the 5th international conference on Embedded networked sensor Systems. ACM Press, 2007.
3. Wenyuan Xu, Wade Trappe, and Yanyong Zhang. Channel surfing: defending wireless sensor networks from interference. In IPSN ’07: Proceedings of the 6th international conference on Information processing in sensor networks, pages 499–508, New York, NY, USA, 2007. ACM Press.
4. Prabal K. Dutta, Jonathan W. Hui, David C. Chu, and David E. Culler. Securing the deluge network programming system. In IPSN ’06: Proceedings of the 5th international conference on Information processing in sensor networks, pages 326–333. ACM Press, 2006.
5. Yong Wang, G. Attebury, and B. Ramamurthy. A survey of security issues in wireless sensor networks. Communications Surveys & Tutorials, IEEE, 8(2):2– 23, 2006.
6. Carl Hartung,James Balasalle, and Richard Han. Node compromise in sensor networks: The need for secure systems. Technical report, University of Colorado at Boulder, January 2005.
7. Karlof and D. Wagner. Secure routing in wireless sensor networks: attacks and countermeasures. In Sensor Network Protocols and Applications, 2003. Proceedings of the First IEEE. 2003 IEEE International Workshop on, pages 113–127, 2003.
8. Limin Wang. Mnp: multihop network reprogramming service for sensor networks In SenSys ’04: Proceedings of the 2nd international conference on Embedded networked sensor systems, pages 285–286. ACM Press, 2004.
9. Chris Karlof, Naveen Sastry, and David Wagner. Tinysec: a link layer security architecture for wireless sensor networks. In SenSys ’04: Proceedings of the 2ndinternational conference on Embedded networked sensor systems, pages 162– 175. ACM Press, 2004.
10. Jing Deng, Richard Han, and Shivakant Mishra. Secure code distribution in dynamically programmable wireless sensor networks. In IPSN ’06: Proceedings of the 5th international conference on Information processing in sensor networks, pages 292–300. ACM Press, 2006.

Published By:
Blue Eyes Intelligence Engineering
& Sciences Publication Pvt. Ltd.

Trusted and Secured Clustered Protocol in MANET

Syeda Kausar Fatima
Research Scholar,
JNTUH

Syed Abdul Sattar, PhD
Prof & Dean
SAKCET

D. Srinivasa Rao, PhD
Prof. ECE Dept.
JNTUH

ABSTRACT
Mobile Ad hoc Networks (MANETs) are subject to various kinds of attacks. Deploying security mechanisms is difficult due to inherent properties of ad hoc networks, such as the high dynamics of their topology, restricted bandwidth, and limited resources in end device. With such dynamicity in connectivity and limited resources it is not possible to deploy centralized security solution. Like many distributed systems, security in ad hoc networks widely relies on the use of key management mechanisms. However, traditional key management systems are not appropriate for them. This work aims at providing a secure and distributed authentication service in ad hoc networks. A trusted and secured clustered protocol in MANET, where clusters are formed based on **highly-trusted nodes having sufficient energy is proposed. Secured communication** with public key authentication service based on trust model and network model to prevent nodes from obtaining false public keys of the others when there are malicious nodes in the network is organised. Efforts to present energy efficient, secure and trusted clustering to enhance the security assurance and significant adaptation of trustworthy communication is presented. Simulation results demonstrate that proposed routing protocols can improve the energy efficiency, packet delivery ratio and route stability.

Keywords
MANET, Trust, Key management, Cluster

1. INTRODUCTION
A mobile ad hoc network is a collection of nodes with no infrastructure while its nodes are connected with wireless links. Nodes in the network are able to sense and discover nearby nodes. They communicate with each other by forwarding packets hop by hop in the network. Also, the topology of the ad hoc network is dynamically changing and the nodes of the ad hoc network are often mobile. A major challenge in the design of the mobile ad hoc network is to protect its vulnerability from security attacks. As in many distributed systems, security in ad hoc networks is based on the use of a key management system for authentication. Specific key management systems have to be developed to suit the characteristics of mobile ad hoc networks.

Cluster-based data transmission in MANETs has been investigated by researchers to achieve the network scalability and management, which maximizes node lifetime and reduce bandwidth consumption by using local collaboration among mobile nodes [1]. Clustering schemes [2] organized the network into one hop disjoint clusters then elect the most qualified and trustworthy nodes which play the role of cluster heads. Cluster heads are responsible for monitoring all the routing activities within the cluster itself. Thus need for secure clustering solutions which are resilient to the various security problems of MANET and provide secure and reliable clustering even in the presence of malicious nodes and attackers. Some cryptography-based clustering schemes such as [3- 6] have been designed for MANETs which are able to operate in hostile environment and use PKI or symmetric encryption techniques, but they do not offer sufficient protection against insider attackers and compromised nodes.

2. BACKGROUND AND MOTIVATION
Several trust models [8–11] have been proposed for self organizing networks in distributed paradigm. Jiang and Baras [12] examined the efficiency of trust based reactive routing protocols in the presence of attacks in the networks. This method is considered first-hand information to evaluate other node's trust values to make trustworthiness. Yan et al. [13] proposed a secure AODV based routing protocol for an ad hoc network which is established a secure end-to-end route. The trust values are calculated based on direct observation which is transitive.

Pirzada and McDonald [14] enhanced the trust management by considering the confidence level of trust of each node. They have used confidence level as a weight to compute trust value. Ghosh et al. [15] developed a trust model to strengthen the security of MANETs and they dealt with the issues associated with recommendations. Their model was utilized only trusted routes for making effective communication and isolates the malicious nodes based on the evidence obtained from direct interactions and recommendations. Ghosh et al. [16] proposed a mechanism for distinguishing selfish peers from cooperative nodes that is based on local monitoring. In order to distinguish between selfish and cooperative peers, a series of well-known statistical tests are applied for obtaining features from the observed AODV actions. The objective of mechanism design [10] is to address problem of designing incentives for nodes to provide truthful information and computing optimal system wide solution for finding the optimal cost efficient leaders. Vickrey, Clarke, and Groves (VCG) model is applied for node incentives to ensure truth telling to be the dominant strategy for any node. They have proposed local election algorithms, namely, cluster-dependent leader election and cluster independent leader election which provided globally optimal election solutions with a low cost. The Nodes with the most remaining energy are elected as the cluster head. This approach makes storage overhead because the cluster head kept an extra service table and each node maintains a reputation table and neighboring nodes list.

Milan et al. proposed a scheme [17], where a game theoretic model is applied to study the impact of collisions on a hop-by-hop reputation based mechanism for regular networks with uniform random traffic. The nodes in MANETs are equipped with different resources and provide discrete services. It did not deal with irregular topologies and non-uniform routing. It also discussed the perception and interaction asymmetries that could impair cooperation between nodes. Safa et al. presented a cluster based trust aware routing protocol (CBTRP) [18] to ensure secure routing path and established the trust based environment. This mechanism is used to distinguish the trusted nodes from malicious nodes. CBTRP makes use of the weighted clustering algorithm (WCA) [19] to elect cluster heads.

The weighted degrees are taken into consideration such as battery power, number of neighbors, transmission power, and mobility of the nodes to form optimal cluster head. CBTRP has also taken security into account to form trusted clusters. It organized the network into 1-hop clusters in which every node is able to elect the most qualified and trustworthy node to be its cluster head. Cluster members forward the packets through the trusted cluster heads. Malicious nodes do not forward the packets to them. In CBTRP model, the trust value is computed based on the information that one node can gather about the other node's vital information including analyzing the received, forwarded, and overheard packets. Analyzing the node's behaviour, the node is selfish, acting like a black hole, and carrying out a modification attack, fabrication attack and latency delays. This approach provides improved connectivity in MANETs in the presence of malicious nodes and also it ensured the passage of packets through trusted routes only by behavior of each node. Once a malicious node is discovered, it is isolated from the network such that no packet is forwarded from it.

Chatterjee et al. [20] proposed a secure trusted auction oriented clustering based routing protocol (STACRP) to provide trusted structured framework for MANETs. Two auction mechanisms, namely, Procurement and Dutch, determine the forward cost of one hop. STACRP organized the network as one hop clusters and elects the trusted nodes as cluster head (CH) by using a secret voting scheme. Each node maintains information of itself and its neighboring nodes for cluster maintenance. The trust model is analyzed using Markov chain which guarantees to selfish node to revoke its status from warned status to normal status by proper forwarding of others packets. This achieved a secure reliable routing solution. STACRP detected selfish nodes and enforces cooperation between nodes to achieve better throughput and packet delivery ratio with less routing overhead

Main contribution of the proposed approach is to obtain a practicable degree of tradeoffs between trust and security. Network trust metric parameters intimacy, integrity, mobility, and reliability identified and combined to evaluate the cumulative trust to provide ground level of security for human centric application with human notions. Unlike discussed trust management systems in order to growing years wise advanced technology [2, 12, 16], efforts are put forward to combine best of existing trust management models for soft security concerns while dynamically observing the impetus behavior of a node in open and dynamic pervasive environment. Exiting models are based on one or more trust or security parameters for WSN or MANETS, while our trust metric consists of five crucial trust parameters for direct and indirect communication in pervasive environment. To reduce the overheads and dependency, clustering is used for group based communication.

3. MODEL OF THE SECURE CLUSTER BASED SCHEME

The contribution of the proposed trusted secure clustering based routing protocol, TSCP are organized in two different phases such as trust management and clustering phase. In trust management phase, the protocol evaluates the node trust level in trust table with different trust factors. The trust factors present the node trust level in different states to determine trust calculation. The cluster management phase evaluates the clustering phase based on trust values and organize secure cluster communication with secured key sharing. The below sections present the detailed description of proposed protocol.

3.1 Trust Computation

We assume that each node maintains a trust table to keep trust factors with respective of communication as per node dynamic behaviour its social and QoS trust factors. Dynamic behaviour between two communicating nodes as X and Y over time t will autonomously update when it interacts with other node on demand or expiry to save resources.

Trust calculation consists of two processes, first evaluate the communicating node table credentials about trust factors and second calculates the mean of trust value based on each parameter as per predefined threshold. Consider following trust parameters for evaluating the node information.

Intimacy ($\mathrm{Tr}_{xy}^{\mathrm{intimacy}}$ (t)): it measures the interaction experiences following the maturity model [21]. It is computed by finding the ratio of positive number of interactions between nodes x and y over the maximum number of interactions over the time period [0, t] as

$$Tr_{xy}^{intimacy}\ (t) = It_x = (\frac{Pve_x}{T_x}) \quad (1)$$

Where It_x is the interaction ratio considering only positive Interaction Pve_x over total no of Interaction T_x through node x.

Integrity: this refers to the confidence of node x that node y is truthful based on node x's direct observations toward node y. Node x calculate approximately (t) by observing a count of suspicious untruthful experiences of node y that node x has observed. If the count exceeds a system-defined threshold, node y is considered totally dishonestat time t, i.e., (t) = 0. Otherwise, (t) is computed by 1 minus the ratio of the count to the threshold. It can be measured as

$$Tr_{xy}^{intigrity}\ (t) = n \times \alpha \times S \quad (2)$$

where n is normalized interaction value, α is over time t experience and S is security level of recommending Service Interface.

Mobility: Node mobility is a significant parameter to estimate the battery life where average distance between nodes required with limited energy provided. Thus average movement can measured by two factors, first the mobility incidences of the mobile nodes in a given time (t) bounded by a battery life threshold where high mobility with limited battery life will be punished that makes it highly unaffordable to achieve cooperative and second Uncertainty measures misbehaviour of nodes during failure to stabilize themselves in competitive forces where nodes are penalized for irregular haziness. Thus the node mobility misbehaviour impact can be measured for given time t as.

$$\mathrm{Tr}_{xy}^{\mathrm{mobility}}\ (\mathrm{t}) = ((1 - \mathrm{Mo_x(E, D)} + (1 - \mathrm{Pen_x(t)}))/2 \quad (3)$$

Where $\mathrm{Pen_x(t)}$ is the x mobile node's penalty measure for visit the similar position for t times ($0 \le \mathrm{Pen_x(t)} \le 1$), and $\mathrm{Mo_x}$ () is the node x punishment credentials with $0 \le \mathrm{Mo_x(E, D)} \le 1$.

Reliability: the reliability of nodes may be evaluated in different ways, but, in general, it may be defined as the capability of nodes to respect a service agreement. This is a particular procedure that lies behind the identity certification or the encryption process. In the remaining part of this section, the word trust is used to identify the reliability of nodes also

that may be evaluated in different ways, but, in general, it can be considered as the capability of nodes to respect a service agreement. Trust based reliability over a time t can be computed as probability of packets being lost, inserted and multiplied as

$$\mathrm{Tr}_{xy}^{\text{reliability}}(t) = (|S_{pkt} - R_{pkt}|)/S_{pkt} \quad (4)$$

where S_{pkt} = Total no. of packets sent by Y to X and R_{pkt} = Total no. of packets received by Y sent from X.

3.1.1 Trust Calculation

The trust calculation is conducted, particularly between two neighbor nodes in a cluster. When a node X evaluates trust on another node Y at time t. We assume five trust components as described above like intimacy, integrity, energy, selfishness and reliability. The trust value that node X evaluates towards node Y at time t, $\mathrm{Tr}_{xy}(t)$, is represented as a real number in the range of [0, 1] where 0 indicates distrust and 1 complete trust.

$$Tr_{xy}(t) = TC1 \times Tr_{xy}^{intimacy} + TC2 \times Tr_{xy}^{integrity} + TC3 \times Tr_{xy}^{mobility} + TC4 \times Tr_{xy}^{reliability} \quad (5)$$

Where $TC1, TC2, TC3,$ and $TC4$ are total costs associated with these four trust factors with equal threshold of 0.25 for each trust factor and computation of all these four factors gives as a results as $TC1 + TC2 + TC3 + TC4 = 1$. Based on the higher probobability values of $TC1, TC2, TC3,$ and $TC4$ the best trust formation value will consider for formation of node trust.

Algorithm 1: Trust Evaluation

Step1 To calculate node trust based on node interaction and analyze node X and Y data.

Step 2 Calculate trust value for all four parameters

$(\mathrm{Tr}_{xy}^{\text{intimacy}}, \mathrm{Tr}_{xy}^{\text{integrity}}, \mathrm{Tr}_{xy}^{\text{mobility}}, \mathrm{Tr}_{xy}^{\text{reliability}})$

Step 3 Identify each trust parameter with corresponding trust value as per pre-defined threshold [0.0–0.2]

Step 4 Estimate the overall trust value Tr_{xy} over a specified time t

$$Tr_{xy}(t) = TC1 \times Tr_{xy}^{intimacy} + TC2 \times Tr_{xy}^{integrity} + TC3 \times Tr_{xy}^{mobility} + TC4 \times Tr_{xy}^{reliability}$$

Step 5 Finally aggregate the trust value according to weighted cost.

3.2 Cluster Formation

Clustering is a standard energy efficient technique used in mobile networks to provide locality of communication through organizing the several nodes in different virtual groups known as clusters that saves energy and reduces network contention. Here several nodes are physically neighbouring and helps to organize the pervasive ad hoc networks hierarchically. An essential operation with clustering technique is to select cluster head shown in Fig. 1. The base station or mobile base stations are satellite based setups or machines capable of analyzing the data collected from the cluster heads and displaying a global view of actions being monitored.

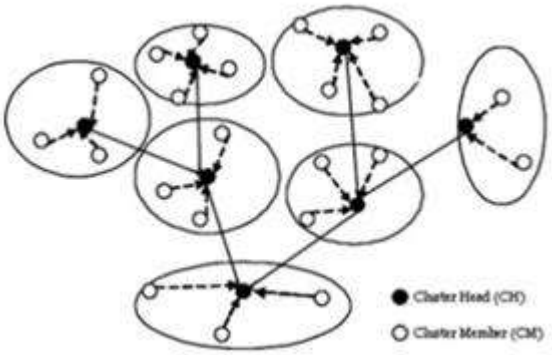

Fig 1: MANET Clustering

Inspired by Multi-objective optimization [22, 23], where multiple optimal solutions using multiple fitness functions used at same time to find optimal solution. Here fitness function is a function used to measure the optimality of a solution in evolutionary algorithm. In multi-objective optimization multiple optimal solutions using more than one objective function is used at same time.

Thus inspired by a multi-objective optimization, we use two objective functions $1(), and f2()$. The cluster head selection algorithm is based on proposed trust calculation metric as defined in Eq. (5). The algorithm initially assumes that each mobile node in the network may become a cluster head with probability 1 or 0 where nodes make autonomous decisions without any centralized control to measure the trustworthiness of the node, life time and extended security.

The fitness function in the proposed work, the fitness is evaluated based on two objective functions $f1(), and f2()$ where $f1()$ computes the trustworthiness Tr_{xy} Eq. (5) of the node, $f2()$ is used to estimate the remaining lifetime or residual energy for to elect the cluster head with a probability p which is proportional to the residual energy of the node. Thus a mobile node with higher remaining lifetime has higher possibility to become head.

Let assume NL_t is the predicted life time of the node before set up the nodes and TC_c be the time consumed to set up of the n mobile nodes as cluster, then total residual energy RE_n of all mobile nodes can be estimated as

$$RE_n = \frac{nE_{ini}(NL_t - TC_c)}{NL_t}$$

where E_{ini} is the initial energy of each node and n is the total number of nodes.

Further the probability p proportional to the residual energy can be defined to the as if NL_t number of candidates is c % of the total number of nodes with leftout energy E_l then

$$P = n \times \frac{E_l}{RE_n} \times \frac{c}{100}$$

3.2.1 Secure Cluster Communication

Assume that a MANET consist of set of clusters C where $C = \{C_1, C_2, C_3 \ldots . C_n\}$each cluster contains n number of nodes, and the public parameters in the clusters are $(H_1, H_2, H_3, P_1, P_2, \varphi, P_{pub}, n, g, h, p, \alpha, q, G_1, G_2)$. Where H_1, H_2, H_3 are cyclic groups whose orders are all q, where q

is large primer number. φ represents an isomorphic function which maps from H_2 to H_1, where α is an asymmetric function where it maps from $H_1 \times H_2 \rightarrow H_3$, non-zero generators $P_2 \in H_2^*, P_1 = \varphi(P_2) \in H_1^*$. The messages between different clusters will be forwarded by the cluster heads, due to the existence of the session keys between the cluster heads, the cluster head chooses a random number s which is belongs to Z_q, and then calculate the public key as $P_{pub} = s\,P_1$, and p and q are large primary numbers, g is a generator with q order which belongs to Z_q. Hash functions are G_1, G_2 where the messages can transmitted in the common channel. The generation of public keys across clusters and secure communication describe in next section.

3.3 Nodes Secret Shares and Key Generation

In a cluster T, the cluster head defines polynomial of degree function as

$$k-1 : f(x) = a_0 + a_1 x + a_2 x^2 + \cdots . + a_{k-1} x^{k-1} \bmod q$$

To compute the authentication key by deriving the authentication parameter as

$$\varepsilon_j = g^{a_j} \bmod p, (j = 0 \ldots . k-1)$$

This authentication key is generated at the same time to validate the authentication of node

The cluster head calculates secrete shares for the normal nodes as

$$U_i^T = f(ID_i) \bmod q$$

Then the cluster head generate the authentication parameter as a node verification where $Ver_{node} = \frac{1}{s + H_1(U_i^T || T || ID)} P_2$

The verification key is encrypted and the encrypted verification key is transferred to node

$$Enc_i\{U_i^T, \varepsilon_j, Ver_{node}\}$$

3.3.1 Key Generation

Step 1: The cluster head chooses two large primer numbers as p1 and p2 and $N = p1\ p2$

Step 2: Define a cluster key as $K = \{(N, p1, p2, c, d) : cd = 1 (\bmod \Phi(N))\}$

Step 3: Compute cluster encryption key and decryption key as follows

$$enc_k(x) = x^d \ mod\ N$$

And

$$dec_k(y) = y^c \ mod\ N$$

N and d forms a cluster public key and p1 , p2 and c forms a cluster private key

Step 4: Encrypt the message with cluster public key so that the key computation processing is reduced with the help of this and as well as reduces traffic overhead with the help of cluster key formation.

4. PERIODIC UPDATES

In this section, the key updates on different cycles to ensure the keys efficiency by updating the keys on different cycles are presented. This section describes the updates of secrete shares, node keys and cluster keys. According to the security limitations in MANET, the networks needs to get regulate key updates to ensure of security.

There are deadlines for all the circles, if this circle is over, then, the cluster will reselect the cluster head, a new service group will be formed consequently. After all the work has been done, the new cluster head will broadcast the update news to the cluster members, if the node receives the news, it needs to send its authentication parameter to the cluster head, and its qualification of update will be checked by the service group. When receive the authentication parameter from the node, the service group will judge whether $\hat{e}(H_1(U_i^T || T || ID)P_1 + P_{pub}, V_{er})$, if this statement presents true results, the service group will update the keys to the nodes.

If the authentication details failure $\hat{e}(H_1(U_i^T || T || ID)P_1 + Ppub, Ver \neq e(P1, P2)$, the node will get refused for update.

Step1 : Secret Share update : Reselection of clusterhead is based on trust value and energy level, After selection of new cluster head the new cluster head will choose a polynomial expression such as

$$S(x) = a_0 + a_1 x + a_2 x^2 + \cdots . + a_{k-1} x^{k-1} \bmod q$$

The cluster head will generate new ID's to cluster members

Step 2: Update of nodes keys : After successful node data transaction, when a node needs to send new transaction the system need to update new nodes new public key by computing the public key P_n as

$$P_n = \frac{H_1(U_i^T || T || ID)P_1 + P_{pub}}{x'}$$

Step 3: Update cluster keys: Two new large prime numbers P_1, P_2' should be chosen after the cluster head has been selected, the new cluster key will be generated as the method mentioned above, the new cluster key will be sent to all the nodes in the cluster, the broadcast will be encrypted by the new cluster key in the circle T+1.

5. SECURITY ANALYSIS

According to the MANET characteristics and security limitations there are some possibilities of potential attacks exist in the MANET. A trusted and secured clustered protocol is designed by analyzing the characteristic of the Mobile Ad Hoc Network and the potential attacks exist in the MANET, we propose a security protocol with perfect forward secrecy and backward secrecy. Even though the malicious nodes eavesdrop the traffic which is broadcasted in the network, it is impossible for them to get any useful information due to all the broadcasts are encrypted by the cluster key, only the nodes which know the key can decrypt the message. By this way, all the broadcasts can be protected well, at same time as a result of introduction of cluster key can greatly save the network resources such as bandwidth, node computational power and so on. The communications between the nodes are greatly protected as well because all of them are encrypted before transmitted by the nodes' private keys. The node without the key will never know them. In maintaining the privacy of the information, it is impossible for the node to deny the message which had been sent from it. The periodic update of keys

which is brought up in the end of protocol can resolve the problem of key leakage or loss. According to the protocol, the group network can work in a secure and more efficient manner.

6. PERFORMANCE ANALYSIS

Firstly, this section provides the computation cost and network scenario parameters for the implementation of the TSCP protocol. Then analyze the routing performance and effectiveness of the TSCP protocol in providing complete anonymity with the existing schemes through simulation results.

6.1 Simulation Setup

The proposed TSCP protocol is for MANET is implemented on ns2 simulator version 2.35. The network scenario parameters used for simulation are listed in Table II.

Table 1: Simulation Parameters

No. of Nodes	50,100,150 and 200.
Area Size	1000 X 1000
Mac	802.11
Radio Range	250m
Simulation Time	10 sec
Traffic Source	CBR
Packet Size	512
Receiving Power	0.395
Sending power	0.660
Idle Power	0.035
Initial Energy	10.0 J
Rate	5,10,15,20 and 25Kbps

In the simulation scenario an ad hoc network of size 1000m × 1000m consists of 50,100,150 and 200 mobile nodes. The mobile nodes are moving in the field according to the random waypoint model, and their average speeds range from 2 to 7 m/s. The bidirectional Constant Bit Rate (CBR) traffic is generated and the radio range of mobile node is 250m.

The proposed protocol maintains the each node trust in different trust factors, for validating each node authentication. The protocol configures trust factors to maintain node trust update parameters. During the process the TSCP protocol computes the trust based on different trust factors and determine trust evolution based on different trust parameters. The networks are organized into multiple clusters by considering each node trust value, based on the trust value and node energy level the proposed model elects a cluster head. The TSCP organizes key generation algorithms for ensuring node authentication and secured data distortion. We determine the performance by considering different key size and different network size.

6.2 Simulation Results

The performance of TSCP protocol is analyzed and the observations are made with respect to the parameters of packet delivery ratio, end to end delay, throughput and energy consumption represented in Fig 6. Fig 6 demonstrated the comparison performance of TSCP, and STACRP by varying node speeds

According to Fig. 6 (a), TSCP has the better packet delivery ratio than STACRP [20] under different mobile speed such as 5, 10, 15, 20 and 25 m/s. The packet delivery ratio of TSCP protocol is around 93.5% and for STACRP is about 92% when there is a node mobility of 2m/s. In case of STACRP, as the mobility increases the packet delivery ratio is decreased significantly about 87% to 85% when the mobile speed is 7 m/s. On the other hand, under the same scenario and mobile speed the packet delivery ratio of TSCP protocol is about 89.5%. The difference between TSCP protocol and STACRP on packet delivery ratio is less than 5%.

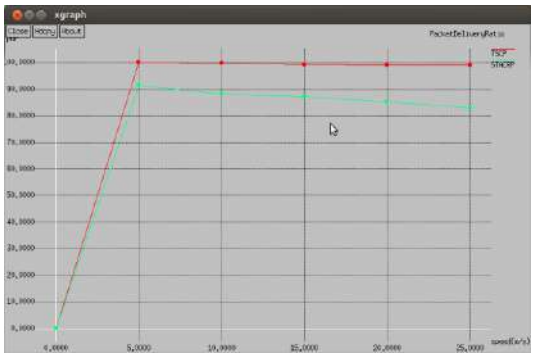

Fig 6(a) Packet Delivery Ratio vs Speed

Fig. 6 (b) shows that the comparison of TSCP, and STACRP end to end delay performance where the STACRP protocol end to end delay is increased, while mobile speed increases. TSCP performance is far better while compare to STACRP, it has less end-to-end delay.

Fig 6(b) End to End delay vs Speed

Fig 6(c) Throughput vs Speed

Fig. 6 (c), TSCP performs slightly better throughput than STACRP. The throughput of STACRP decreases as the node speed increases.

Fig. 6 (d), shows the Energy consumption, energy consumption of TSCP slightly increased while node speed increased but while compare to STACRP the energy

consumption ratio is less than STACRP. TSCP protocol energy consumption rate is almost 8 % less than STACRP.

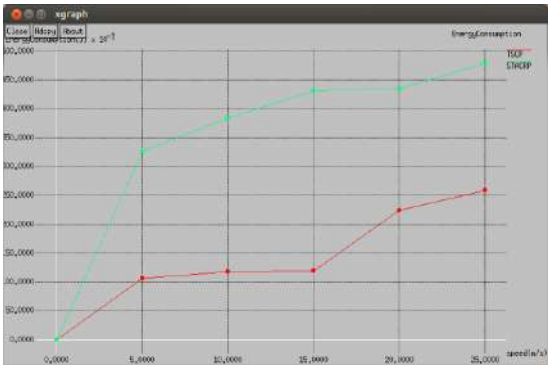

Fig 6(d) Energy Consumption vs Nodes

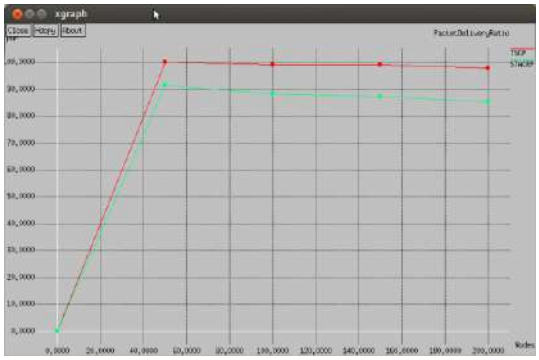

Fig 6(e) PDR vs Nodes

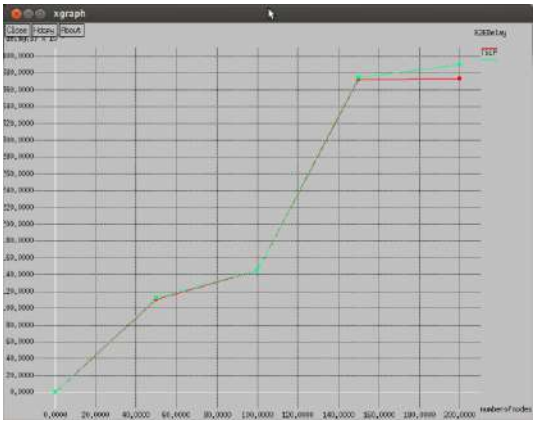

Fig 6(f) Delay vs Nodes

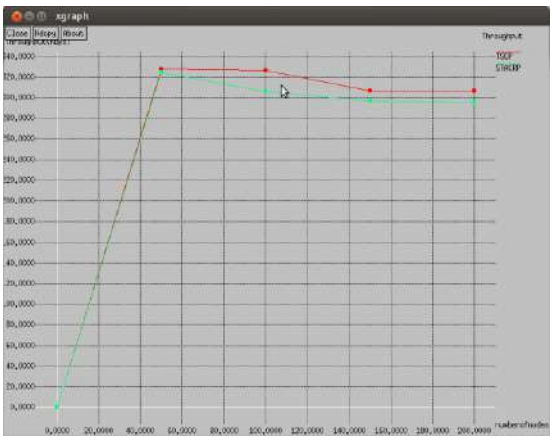

Fig 6(g) Throughput vs Nodes

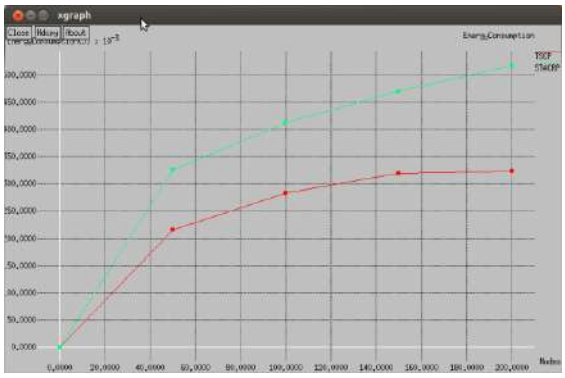

Fig 6(h) energy consumption vs Nodes

7 CONCLUSION

In this project a trusted and secured clustered protocol in MANET to organize secured and trusted communication in mobile pervasive environment is proposed. The proposed protocol organize individual node trust and reliability based on different node characteristics. Fitness functions to find out multi- dimension clustering with extended security consideration to improve energy efficient trusted clustering is formulated. A lightweight key management techniques for node authentication and secured communication with low resource computations. Based on the simulation results the proposed model perform energy efficient and robust.

8 REFERENCES

[1] A.A. Abbasi and M. Younis, "A Survey on Clustering Algorithms for Wireless Sensor Networks," Computer Comm., vol. 30, nos. 14/ 15, pp. 2826-2841, 2007.

[2] C. Tselikis, S. Mitropoulos, N. Komninos, and C. Douligeris, "Degree-based clustering algorithms for wireless Ad Hoc networks under attack," IEEE Communications Letters, vol. 16, no. 5, pp. 619–621, 2012.

[3] Y. Zeng, J. Cao, S. Guo, K. Yang and L. Xie, "SWCA: A Secure Weighted Clustering Algorithm in Wireless Ad Hoc Networks", IEEE Wireless Communications and Networking Conference WCNC, (2009).

[4] I. Nishimura, T. Nagase, Y. Takehana and Y. Yoshioka, "Secure Clustering for Building Certificate Management Nodes in Ad-Hoc Network", International Conference on Network-Based Information Systems, (2011), pp. 685-689.

[5] H. Rifà-Pous and J. Herrera-Joancomartí, "A Fair and Secure Cluster Formation Process for Ad Hoc Networks", Journal Wireless Personal Communications: An International Journal archive, vol. 56, no. 3, (2011) February.

[6] V. Sivaranjani and D. Rajalakshmi, "Secure Cluster Head Election for Intrusion Detection in MANET", Journal of Computer Applications, vol. 5, Issue EICA2012-4, (2012) February 10.

[7] M. Bechler, H. Hof, D. Kraft, F. Pahlke, and L. Wolf, "A ¨ cluster-based security architecture for Ad Hoc networks," in Proceedings of the 23rd AnnualJoint Conference of the IEEE Computer and Communications Societies (INFOCOM '04), vol. 4, pp. 2393–2403, March 2004.

[8] W. J. Adams and N. J. Davis, "Toward a decentralized trustbased access control system for dynamic collaboration," in Proceedings of the 6th Annual IEEE System, Man and Cybernetics Information Assurance Workshop (SMC '05), pp. 317–324, June 2005.

[9] A. Boukerche and Y. Ren, "A security management scheme using a novel computational reputation model for wireless and mobile Ad Hoc networks," in Proceedings of the 5th ACM International Symposium on Performance Evaluation of Wireless Ad-Hoc, Sensor, and Ubiquitous Networks (PE-WASUN '08), pp. 88–95, October 2008.

[10] R. Li, J. Li, P. Liu, and H. Chen, "An objective trust management framework for mobile Ad Hoc networks," in Proceedings of the IEEE 65th Vehicular Technology Conference (VTC '07), pp. 56– 60, April 2007.

[11] G. Theodorakopoulos and J. S. Baras, "Trust evaluation in adhoc networks," in Proceedings of the ACM Workshop on Wireless Security (WiSe '04), pp. 1–10, October 2004.

[12] T. Jiang and J. S. Baras, "Ant-based adaptive trust evidence distribution in MANET," in Proceedings of the 24th International Conference on Distributed Computing Systems Workshops, pp. 588–593, March 2004.

[13] Z. Yan, P. Zhang, and T. Virtan, "Trust evaluation based security solution in Ad Hoc networks," in Proceedings of 7th Nordic Workshop on Secure IT Systems, 2003.

[14] A. A. Pirzada and C. McDonald, "Establishing trust in pure ad-hoc networks," in Proceedings of the 27th Australasian Conference on Computer Science (ACSC '04), vol. 26, pp. 47–54, 2004.

[15] T. Ghosh, N. Pissinou, and K. Makki, "Collaborative trustbased secure routing in multihop Ad Hoc networks," in NETWORKING 2004. Networking Technologies, Services, and Protocols; Performance of Computer and Communication Networks; Mobile and Wireless Communications: Proceedings of the 3rd International IFIP-TC6 Networking Conference, Athens, Greece, May 9–14, 2004, vol. 3042 of Lecture Notes in Computer Science, pp. 1446–1451, 2004.

[16] T. Ghosh, N. Pissinou, and K. Makki, "Towards designing a trusted routing solution in mobile Ad Hoc networks," Mobile Networks and Applications, vol. 10, no. 6, pp. 985–995, 2005.

[17] F. Milan, J. J. Jaramillo, and R. Srikant, "Achieving cooperation in multihop wireless networks of selfish nodes," in Proceedings of the Workshop on Game Theory for Communications and Networks (GameNets '06), October 2006.

[18] H. Safa, H. Artail, and D. Tabet, "A cluster-based trust-aware routing protocol for mobile Ad Hoc networks," Wireless Networks, vol. 16, no. 4, pp. 969–984, 2010.

[19] M. Chatterjee, S. K. Das, and D. Turgut, "WCA: a weighted clusrering algorithm for mobile Ad Hoc networks," Journal of Cluster Computing, vol. 5, no. 2, pp. 193–204, 2002.

[20] P. Chatterjee, I. Sengupta, and S. K. Ghosh, "STACRP: a secure trusted auction oriented clustering based routing protocol for MANET," Cluster Computing, vol. 15, pp. 303–320, 2012.

[21] Velloso PB et al (2010) Trust management in mobile ad hoc networks using a scalable maturity-based model. In: IEEE Trans. Netw. Service Management, vol. 7, no. 3, pp 172–185

[22] Ali H, Shahzad W, Khan FA (2012) Energy-efficient clustering in mobile ad-hoc networks using multi-objective particle swarm optimization. Applied Soft Computing 1913–1928

[23] Marmol FG, Perez GM (2010) Towards pre-standardization of trust and reputation models for distributed and heterogeneous systems. Compute Stand Interfaces 32:185–196

Discovery of web usage patterns using fuzzy mountain clustering

Zahid Ahmed Ansari*

Department of Computer Science Engineering,
P.A. College of Engineering,
Mangalore, India
Email: zahid_cs@pace.edu.in
*Corresponding author

Abdul Sattar Syed

Department of Computer Science Engineering,
Royal Institute of Technology and Science,
Hyderabad, India
Email: syedabdulsattar1965@gmail.com

Abstract: Analysis of web server logs of e-business organisations is critical to provide insight into users' web usage behaviour which can assist in designing most attractive websites. In this article, a mountain density function (MDF)-based fuzzy clustering framework to discover user session clusters from web logs is proposed. Major steps in this framework include web log preprocessing, MDF-based discovery of user session clusters and their validation. To deal with high dimensionality of user sessions, a fuzzy approach for assigning weights to user sessions has been proposed. For the discovery of user session clusters, fuzzy c-means (FCM) and fuzzy c-medoids (FCMed) algorithms are explored. Since the selection of suitable initial cluster centres is a big challenge, MDF-based fuzzy c-means (MDFCM) and fuzzy c-medoids (MDFCMed) algorithms are proposed to overcome this problem. Our results show that quality of clusters formed using MDFCM/MDFCMed is much better than FCM and FCMed.

Keywords: fuzzy clustering; mountain density function; MDF; fuzzy cluster validation; user session clustering.

Reference to this paper should be made as follows: Ansari, Z.A. and Syed, A.S. (2016) 'Discovery of web usage patterns using fuzzy mountain clustering', *Int. J. Business Intelligence and Data Mining*, Vol. 11, No. 1, pp.1–18.

Biographical notes: Zahid Ahmed Ansari is working as a Professor in the Department of Computer Science Engineering, P.A. College of Engineering, Mangalore, India. He received his ME degree from Birla Institute of Technology, Pilani, India and PhD degree from Jawaharlal Nehru Technological University, Kakinada, India. He has 40 research papers to his credit, published in various international journals and conferences. His areas of research include data mining, soft computing, high performance computing and model driven software development. He is a life member of CSI and also a member of ACM.

Copyright © 2016 Inderscience Enterprises Ltd.

Abdul Sattar Syed is working as a Professor in Computer Science Engineering and Dean Academics, Royal Institute of Technology, Hyderabad, India. He received his ME and PhD degrees from Jawaharlal Nehru Technological University, Hyderabad, India. He has 150 research papers to his credit, published in various national and international journals and conferences. His areas of research include wireless local area networks, data mining and soft computing. He is a member of various professional bodies such as CSI, IETE, IE, ISTE and NESA.

1 Introduction

The World Wide Web as a huge source of information is a fertile land for applying the data mining principles. Web usage mining is described as the automatic discovery of usage patterns from the data collected as a result of user interactions with web resources from the websites (Mobasher, 2007). The discovered patterns are usually represented as collections of web resources that are frequently accessed by groups of users having common interests (Carmona et al., 2012). Clustering algorithms have been widely applied to discover the user session clusters representing similar URL access patterns. These extracted clusters represent users' access patterns based on their common navigational behaviour. Ansari et al. (2011a, 2011c) have presented a framework for web session data clustering using hard clustering algorithms.

Due to the human interactions and non-deterministic browsing patterns of various web users, user session data may be incomplete or may involve noise and outliers. Such data, which suffers from ambiguity and vagueness do not have the crisp boundaries and often have overlapping clusters (Chau et al., 2006). Fuzzy clustering of user session data categorises each user session into clusters, where each user session can belong to several clusters with different degrees of membership. This enables the clusters to grow into their natural shapes.

One of the most popularly used fuzzy clustering technique fuzzy c-means (FCM) (Bezdek, 1981) performs the fuzzy clustering in such away that a given object may belong to several clusters with the degree of belongingness specified by membership grades. Another category of fuzzy clustering algorithm known as fuzzy c-medoids (FCMed) algorithm (Krishnapuram et al., 2001) extends the hard c-medoid algorithm by incorporating the fuzzy set concepts to produce fuzzy clusters (Mei and Chen, 2011). Each cluster is represented by a representative object as the medoid of that cluster.

One of the major problems associated with the FCM and FCMed methods is that they are sensitive to the initial selection of cluster centres. Therefore, estimation of suitable values for the initial cluster centres is a big challenge associated with these methods. This article proposes a mountain density function (MDF)-based initialisation strategy to find the suitable set of initial cluster centres. A user session clustering framework is presented that integrates the MDF cluster centre initialisation to the FCM and the FCMed algorithms. Figure 1 depicts a broader picture of the proposed framework. Three main steps involved in this framework are:

1 web log data preprocessing and fuzzy weight assignment to the user sessions

2 discovery of user session clusters using MDF-based fuzzy clustering techniques

3 validation of the discover clusters.

The remainder of this paper is organised as follows. In Section 2, we briefly discuss about web log preprocessing, user session representation and methodology to assign fuzzy weights to the user sessions. Section 3 provides detailed description of the proposed MDF-based fuzzy user session clustering framework and its underlying mathematical model. In Section 4, we discuss the validity indexes utilised for accessing the quality of the discovered fuzzy clusters. Section 5 portrays the experimental results and the related discussions. Finally, conclusions are presented in Section 6.

Figure 1 MDF-based fuzzy user session clustering framework (see online version for colours)

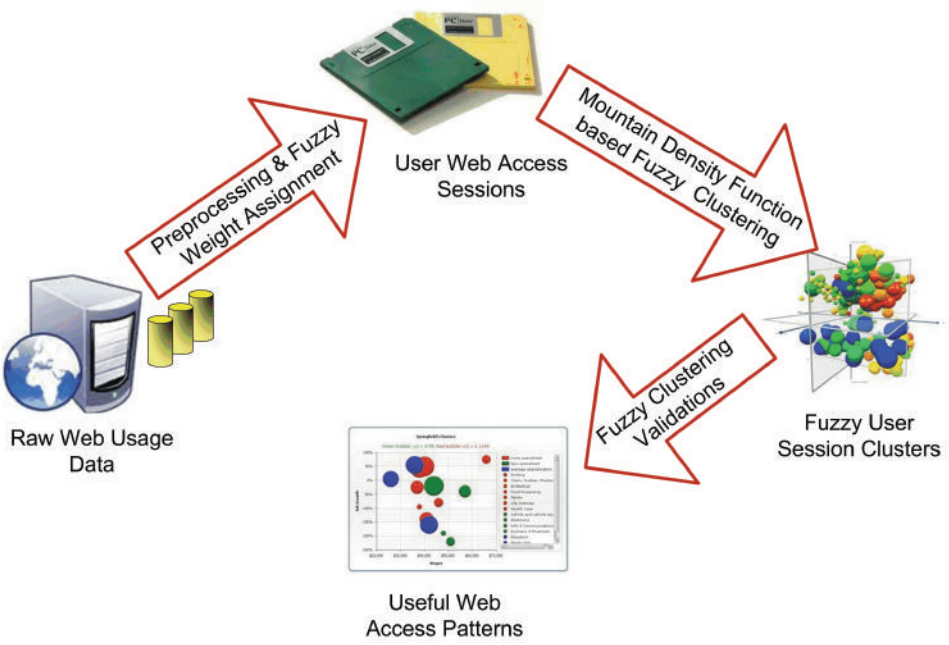

2 User session extraction and fuzzy weight assignment

In order to transform the unlabelled, semi-structured textual raw web log data into a set of numeric user session vectors, preprocessing of web logs is mandatory. Preprocessing utilises a variety of algorithms and heuristic techniques to perform various tasks such as data cleaning, user identification and session identification, etc. Ansari et al. (2011b, 2011d) have provided the details of the various techniques utilised for preprocessing the web log data. Each of the extracted user session vector captures a set of URLs accessed during that user session as described in Subsection 2.1. Subsection 2.2 briefly describes the fuzzy set theoretic approach to assign weights to user sessions and page URLs accessed in those sessions based on a linear and standard *S* fuzzy membership functions.

2.1 Representation of user sessions

Let $\mathscr{S} \leftarrow \{s_1, s_2, \cdots, s_m\}$ be the set of user sessions discovered as a result of preprocessing the web logs. Let $\mathscr{U} \leftarrow \{u_1, u_2, \cdots, u_n\}$ be the set of all the URLs appearing in the preprocessed log. Here, m and n are the number of user sessions discovered and the total number of URLs appearing in the preprocessed web log respectively. Each user session is a vector of URL values in an n-dimensional space. A user session s_i is represented as given in (1)

$$s_i = \left\{ s_i^1, s_i^2, \cdots, s_i^n \right\} = \left\{ \mathscr{A}_i^{u_1}, \mathscr{A}_i^{u_2}, \cdots, \mathscr{A}_i^{u_n} \right\} \tag{1}$$

where each $s_k^i \leftarrow \mathscr{A}_i^{u_k}$ represents the frequency of occurrence of the URL u_k within the session s_i. The set of the extracted user sessions $\mathscr{S}$ are represented in the following matrix form:

$$\mathscr{S}\{m, n\} \leftarrow \begin{pmatrix} \mathscr{A}_1^{u_1} & \mathscr{A}_1^{u_2} & \cdots & \mathscr{A}_1^{u_n} \\ \mathscr{A}_2^{u_1} & \mathscr{A}_2^{u_2} & \cdots & \mathscr{A}_2^{u_n} \\ \vdots & \vdots & \ddots & \vdots \\ \mathscr{A}_m^{u_1} & \mathscr{A}_m^{u_2} & \cdots & \mathscr{A}_m^{u_n} \end{pmatrix} \tag{2}$$

2.2 Fuzzy approach for URL and session weight assignment

Filtering the web access logs by removing references to low support URLs (i.e., those which are not supported by a specified number of user sessions), can provide an effective dimensionality reduction method while improving clustering results. For this purpose, fuzzy weights are assigned to all the URLs using membership function based on their user sessions support count (i.e., the number of user sessions accessing a particular URL). All URLs with session support count lower than a lower bound α_1 are assigned the weight 0. On the other hand, all the URLs with session support count higher than an upper bound α_2 are assigned the weight 1. The remaining URLs with session support count between α_1 and α_2 are assigned the weight between 0 and 1 using a fuzzy membership function. We utilise linear fuzzy membership function (LFMF) and standard S fuzzy membership function (SFMF) to assign the weights to various URL items. Let x be the be the session support count for the URL u_k, then ω_{u_k}, the LFMF-based weight assigned to the URL u_k is computed using:

$$\omega_{u_k} = \begin{cases} 0, & \text{if } x \le \alpha_1 \\ 1, & \text{if } x \ge \alpha_2 \\ (x - \alpha_1)/(\alpha_2 - \alpha_1), & \text{if } \alpha_1 < x < \alpha_2 \end{cases} \tag{3}$$

The SFMF-based weight assigned to the URL u_k is computed using:

$$\omega_{u_k} \leftarrow \begin{cases} 0, & \text{if } x \le \alpha_1 \\ 2\left((x-\alpha_1)/(\alpha_2-\alpha_1)\right)^2, & \text{if } \alpha_1 \le x \le x_0 \\ 1-2\left((x-\alpha_2)/(\alpha_2-\alpha_1)\right)^2, & \text{if } x_0 \le x \le \alpha_2 \\ 1, & \text{if } x \ge \alpha_2 \end{cases} \tag{4}$$

where $x_0 \leftarrow (\alpha_1 + \alpha_2) / 2$ is the crossover point.

Since very small sized sessions may represent the noise present in the data, weights are assigned to all the sessions using a fuzzy membership function based on the number of URLs accessed by those sessions. Let β_1 and β_1 be the lower and upper threshold for the session URL count and $y = |s_i|$ be the number of URLs accessed in the user session s_i, the LFMF and SFMF-based weights ω_{s_i} assigned to the user session s_i are computed using the modified versions of equations (3) and (4) respectively by replacing ω_{u_k} with ω_{s_i}, α_1 with β_1, α_2 with β_2, x with y and x_0 with y_0, where $y_0 = (\beta_1 + \beta_2) / 2$ is the crossover point.

3 Discovery of fuzzy user session clusters

Let $\mathcal{V} = \{v_j \mid j = 1 \cdots c\}$ represent a set of n-dimensional vectors representing the cluster centre corresponding to each of the c clusters in $\mathcal{G} = \{g_j \mid j = 1 \cdots c\}$.

$$v_j = \left\{v_j^1, v_j^2, \cdots, v_j^n\right\}, \forall j = 1 \cdots c.$$

where v_j^k represents the k^{th} URL attribute value of the j^{th} cluster centre. Let μ_{ij} represents the grade of membership of the user session s_i in the cluster g_j where

$$\mu_{ij} \in [0, 1], \forall i = 1 \cdots m \text{ and } \forall j = 1 \cdots c \tag{5}$$

The $m \times c$ fuzzy partition matrix $\mathcal{P}[\mu_{ij}]$ describes the allocation of the user session vectors to various clusters satisfies the following constraints:

$$\sum_{j=1}^{c} \mu_{ij} = 1, \forall i = 1 \cdots m \qquad 0 < \sum_{i=1}^{m} \mu_{ij} < m, \forall j = 1 \cdots c \tag{6}$$

The following subsections describe the algorithmic details of FCM, FCMed and the proposed MDF-based fuzzy user session clustering techniques.

3.1 FCM-based user session clustering

FCM algorithm incorporates the fuzzy set theoretic concept of partial membership and enables the formation of overlapping clusters. The objective function $\mathcal{J}_{FCM}$ of the FCM-based user session clustering, is the weighted sum of distances between the user sessions and their cluster centres as described in (7)

$$\mathcal{J}_{FCM} \leftarrow \sum_{j=1}^{c}\sum_{i=1}^{m}\mu_{ij}^{q}\mathcal{E}^2\left(s_i, v_j\right) \tag{7}$$

where $\mathcal{E}^2(s_i, v_j)$ is the Euclidean distance between the user session s_i and the cluster centre v_j. The Euclidean distance $\mathcal{E}^2(s_i, v_j)$ for the case when no weights are assigned to user sessions and URLs is computed using:

$$\mathcal{E}^2(s_i, v_j) \leftarrow \sum_{k=1}^{n}\left|s_i^k - v_j^k\right|^2 \tag{8}$$

If fuzzy weights are assigned to the user sessions as well as the URLs, $\mathcal{E}^2(s_i, v_j)$ is computed using:

$$\mathcal{E}^2(s_i, v_j) \leftarrow w_{s_i}\sum_{k=1}^{n} w_{u_k}\left|s_i^k - v_j^k\right|^2 \tag{9}$$

where w_{s_i} is the fuzzy weight assigned to the user session s_i and w_{u_k} is the fuzzy weight assigned to the k^{th} URL of s_i. Minimisation of the value of the objective function $\mathcal{J}_{FCM}$ is achieved by updating the grade of the memberships of user sessions to various clusters and recalculating the cluster centres in an alternating fashion until convergence occurs. During each iteration, the cluster centres are updated using (10)

$$v_j \leftarrow \frac{\sum_{i=1}^{m}\mu_{ij}^{q}s_i}{\sum_{i=1}^{m}\mu_{ij}^{q}} \tag{10}$$

Fuzzy partition matrix $\mathcal{P}$ is updated using (11)

$$\mu_{ij} \leftarrow \frac{\left(\frac{1}{\mathcal{E}^2\left(s_i, v_j\right)}\right)^{1/(q-1)}}{\sum_{j=1}^{c}\left(\frac{1}{\mathcal{E}^2\left(s_i, v_j\right)}\right)^{1/(q-1)}} \tag{11}$$

Algorithm 1 describes the steps involved in FCM-based user session clustering.

3.2 FCMed-based user session clustering

In FCMed clustering method, each cluster is represented by a representative user session object known as the medoid of that cluster (Joshi and Krishnapuram, 2000). Let $\mathcal{D} = \{d_j \mid d_j \in \mathcal{S}$ and $j = 1 \cdots c\}$ be a set of n-dimensional vectors representing the cluster medoids corresponding to each of the c clusters in $\mathcal{G} = \{g_j \mid j = 1 \cdots c\}$. Here, $\mathcal{D}$ is a subset of the set of user sessions $\mathcal{S}$.

$$d_j = \left\{ d_j^1, d_j^2, \cdots, d_j^n \right\}, \forall j = 1 \cdots c.$$

where d_j^k represents the k^{th} URL attribute value of the j^{th} cluster medoid. The $m \times c$ fuzzy partition matrix $\mathscr{P} = [\mu_{ij}]$ can be populated in the similar way as defined for the FCM algorithm:

$$\mu_{ij} \leftarrow \frac{\left(\frac{1}{\mathscr{E}^2 \left(s_i, d_j \right)} \right)^{1/(q-1)}}{\sum_{j=1}^{c} \left(\frac{1}{\mathscr{E}^2 \left(s_i, d_j \right)} \right)^{1/(q-1)}} \tag{12}$$

The new cluster medoids can be computed using

$$p \leftarrow \arg\min_{1 \le k \le m} \sum_{i=1}^{m} \mu_{ij}^q \mathscr{E}^2 \left(s_i, s_k \right); \quad d_j \leftarrow s_p \tag{13}$$

Algorithm 2 describes the steps involved in the FCMed-based user session clustering algorithm.

Algorithm 1 FCM-based user session clustering

Input: c, error threshold ϵ, maximum iterations η and set of user sessions $\mathscr{S} = \{s_1, \cdots, s_m\}$

Output: Set of c cluster centres $\mathscr{V} = \{v_1, \cdots, v_c\}$ and the fuzzy partition matrix $\mathscr{P}$

Initialise the set of cluster centres $\mathscr{V}(0)$, by randomly selecting the c user sessions from $\mathscr{S}$
$t \leftarrow 1$
repeat
  Compute the entries of the partition matrix $\mathscr{P}(t)$:
  for $i \leftarrow 1, m$ **do**
    for $j \leftarrow 1, c$ **do**
      Compute $\mu_{ij}(t)$ using (11)
    end for
  end for
  Compute the set of new cluster centres $\mathscr{V}(t)$:
  for $j \leftarrow 1, c$ **do**
    Compute v_j(t) using (10)
  end for
  Compute the objective function $\mathscr{J}_{FCM}(t)$ using (7)
  $t \leftarrow t + 1$
until $\left| \mathscr{J}_{FCM}(t) - \mathscr{J}_{FCM}(t-1) \right| < \epsilon \,||\, t = \eta$

Algorithm 2 FCMed-based user session clustering

Input: c, maximum iterations η and set of user sessions $\mathscr{S} = \{s_1, \cdots, s_m\}$

Output: Set of c cluster medoids $\mathscr{D} = \{d_1, \cdots, d_c\}$ and fuzzy partition matrix $\mathscr{P}$

Initialise the set of medoids $\mathscr{D}(0)$, by randomly selecting c user sessions from $\mathscr{S}$
$t \leftarrow 1$
repeat
  Compute the partition matrixP(t) entries:
  for $i \leftarrow 1, m$ **do**
    for $j \leftarrow 1, c$ **do**
      Compute $\mu_{ij}(t)$ using (12)
    end for
  end for
  Compute the set of new medoids $\mathscr{D}(t)$:
  for $j \leftarrow 1, c$ **do**
    Compute $d_j(t)$ using (13)
  end for
  $t \leftarrow t + 1$
until $\mathscr{D}(t) = \mathscr{D}(t-1) \,||\, t = \eta$

3.3 MDFCM and MDFCMed-based user session clustering

In the proposed MDFCM and MDFCMed algorithms, initial cluster centres are selected by computing MDF values for every user session. The user session with the highest MDF value is selected as the first initial cluster centre. The subsequent initial cluster centres are generated by the iterative destruction of the effects of previously selected cluster centre by revising the MDF. Let $\mathscr{S} = \{s_1, s_2, ..., s_m\}$ be the set of m user sessions in an n-dimensional Euclidean space. In order to identify the first initial cluster centre, each user session s_i is considered as a potential candidate and the first MDF value at the user session s_i, denoted as $\mathscr{M}_1(s_i)$ is computed using:

$$\mathscr{M}_1(s_i) \leftarrow \sum_{k=1}^{m} \exp\left(-\frac{\mathscr{E}^2(s_i, s_k)}{\mathscr{R}^2}\right), \forall i = 1, ..., m \tag{14}$$

where $\mathscr{R}$ is a positive constant defining the neighbourhood of the user session s_i. The MDF value of the user session s_i is an approximation of the density of all user sessions in the vicinity of s_i. User sessions outside the radial distance have little influence on its MDF value. The user session with the highest MDF value is chosen as the first cluster centre v_1 as given below:

$$i_1 \leftarrow \arg\max_{i=1}^{m} \left\{\mathscr{M}_1(s_i)\right\}; \quad v_1 \leftarrow s_{i_1} \tag{15}$$

Algorithm 3 MDFCM-based user session clustering

Input: c, neighbourhood radius $\mathscr{R}$, error threshold ϵ, maximum iterations η and set of user sessions $\mathscr{S} = \{s_1, \cdots, s_m\}$

Output: Set of c cluster centres $\mathscr{V} = \{v_1, \cdots, v_c\}$ and partition matrix $\mathscr{P}$

Initialise the set of cluster centres $\mathscr{V}(0)$

for $i \leftarrow 1, m$ **do**
  Compute mountain values $\mathscr{M}_1(s_i)$ using (14)
end for
Compute the first cluster centre $v_1(0)$ using (15)
for $j \leftarrow 2, c$ **do**
  for $i \leftarrow 1, m$ **do**
    Compute revised mountain values $\mathscr{M}_j(s_i)$ using (18)
  end for
  Compute the j^{th} cluster centre $v_j(0)$ using (19)
end for
$t \leftarrow 1$
repeat
  Compute the partition matrix $\mathscr{P}(t)$ entries:
  for $i \leftarrow 1, m$ **do**
    for $j \leftarrow 1, c$ **do**
      Compute $\mu_{ij}(t)$ using (11)
    end for
  end for
  Compute the set of new cluster centres $\mathscr{V}(t)$:
  for $j \leftarrow 1, c$ **do**
    Compute v_j(t) using (10)
  end for
  Compute the objective function $\mathscr{J}_{FCM}(t)$ using (7)
  $t \leftarrow t + 1$
until $\left|\mathscr{J}_{FCM}(t) - \mathscr{J}_{FCM}(t-1)\right| < \epsilon \,||\, t = \eta$

While selecting the second cluster centre, the MDF value of each user session is revised in order to reduce the effect of the MDF around the first cluster centre v_1 as given below:

$$\mathscr{M}_2(s_i) \leftarrow \mathscr{M}_1(s_i) - \mathscr{M}_1(v_1)\exp\left(-\frac{\mathscr{E}^2(s_i, v_1)}{\mathscr{R}^2}\right), \quad \forall i = 1, ..., m \tag{16}$$

After revising the MDF values of all the user session, the second cluster centre is chosen with the highest MDF value as given below:

$$i_2 \leftarrow \arg\max_{i=1}^{m} \left\{ \mathscr{M}_2 \left(s_i \right) \right\}; \quad v_2 \leftarrow s_{i_2} \tag{17}$$

Similarly, for the selection of j^{th} cluster centre, revision of the MDF value for each user session is performed as given below:

$$\mathscr{M}_j \left(s_i \right) \leftarrow \mathscr{M}_{j-1} \left(s_i \right) - \mathscr{M}_{j-1} \left(v_{j-1} \right) \exp\left(-\frac{\mathscr{E}^2 \left(s_i, v_{j-1} \right)}{\mathscr{R}^2} \right), \quad \forall i = 1, ..., m \tag{18}$$

and the j^{th} cluster centre v_j is selected as given below:

$$i_j \leftarrow \arg\max_{i=1}^{m} \left\{ \mathscr{M}_j \left(s_i \right) \right\}; \quad v_j \leftarrow s_{i_j} \tag{19}$$

Algorithm 3 describes the steps involved in MDFCM-based user session clustering. Similarly, algorithm for MDFCMed-based user session clustering may be obtained by replacing the Step 1 of Algorithm 1 by Steps 1 to 10 of Algorithm 3.

4 Assessment of fuzzy cluster validity

This section describes the quality measures utilised in this research for evaluating the quality of the discovered fuzzy clusters.

4.1 Xie Beni (XB) index

Xie Beni (*XB*) validity index (Xie and Beni, 1987) is defined as below:

$$XB = \frac{\sum_{j=1}^{c} \sum_{i=1}^{m} \mu_{ij}^{q} \mathscr{E}^2 \left(s_i, v_j \right)}{m \cdot \delta_{\min}^2} \tag{20}$$

where $\delta_{\min}^2$ is the square of minimum Euclidean distance between the cluster centres as given below:

$$\delta_{\min}^2 = \min_{l,k=1 \cdots c \wedge l \neq k} \mathscr{E}^2 \left(v_l, v_k \right) \tag{21}$$

A small value of *XB* index indicates a compact and well separated cluster.

4.2 Fukuyama Sugeno (FS) index

Fukuyama Sugeno (*FS*) index (Fukuyama, 1989) is defined as:

$$FS = \sum_{i=1}^{m} \sum_{j=1}^{c} \mu_{ij}^{q} \mathscr{E}^2 \left(s_i, v_j \right) - \sum_{i=1}^{m} \sum_{j=1}^{c} \mu_{ij}^{q} \mathscr{E}^2 \left(v_j, v \right) \tag{22}$$

where v is the mean of all the cluster centre vectors

$$v = \sum_{j=1}^{c} \frac{v_j}{c} \tag{23}$$

For compact and well-separated clusters smaller values for *FS* are expected.

4.3 Zahid separation (SC) compaction validity index

SC index (Limouri et al., 1999) is defined as:

$$SC = \mathcal{T}_1 - \mathcal{T}_2 \tag{24}$$

where

$$\mathcal{T}_1 = \frac{\sum_{j=1}^{c} \mathcal{E}^2\left(v_j, v\right)/c}{\sum_{j=1}^{c}\left(\sum_{i=1}^{m} \mu_{ij}^q \mathcal{E}^2\left(s_i, v_j\right) \Big/ \sum_{i=1}^{m} \mu_{ij}\right)} \tag{25}$$

and

$$\mathcal{T}_2 = \frac{\sum_{j=1}^{c-1}\sum_{k=j+1}^{c}\left(\sum_{i=1}^{m}\left(\min\left(\mu_{ij}, \mu_{ik}\right)\right)^2 \Big/ \sum_{i=1}^{m}\min\left(\mu_{ij}, \mu_{ik}\right)\right)}{\sum_{i=1}^{m}\left(\max_{1\le j\le x} \mu_{ij}\right)^2 \Big/ \sum_{i=1}^{m}\max_{1\le j\le c}\mu_{ij}} \tag{26}$$

A large value of *SC* index indicates a good intra cluster cohesion and small inter cluster overlap.

4.4 Error index

Error index represents the objective function of the fuzzy user session clustering as defined as below:

$$\mathcal{J} \leftarrow \sum_{j=1}^{c}\sum_{i=1}^{m} \mu_{ij}^q \mathcal{E}^2\left(s_i, v_j\right) \tag{27}$$

A lower value of error index represents the better clustering result.

5 Experimental results and discussion

Input web access logs were taken from the proxy servers of a university campus. The web access logs covered a period of one week, from June 1, 2008 to June 8, 2008. There were 723,263 web log requests in total. We used the Perl scripts to separate out the requests pertaining to Google website. Number of the web log requests extracted for Google resources are 12,744.

5.1 Results of preprocessing the web log data

Table 1 shows the preprocessing results. After performing the cleaning, the web logs contain 11,567 entries. Total no. of users identified in the log files are 30. User sessions are identified using time-oriented heuristics.

Table 1 Preprocessing results

Items	*Google*
Initial no of log entries	12,744
Log entries after cleaning	11,567
No of users identified	30
No. of URLs accessed	116
User sessions Identified	319

In order to assign the fuzzy weights to user sessions, a lower bound β_1 of the session URL count is set to 1 and upper bound β_2 of the session URL count is set to 4. Table 2 shows the result of assigning fuzzy weights to the user sessions.

Table 2 Results of user session weight assignment

URL count	*No. of sessions*	*Session weight*	
		LFMF	*SFMF*
4+	91	1	1
4	4	0.75	0.875
3	32	0.5	0.5
2	54	0.25	0.125
1	212	0	0

5.2 Fuzzy user session clustering results

Details of the experimental process are given below:

- multiple runs of FCM, FCMed, MDFCM and MDFCMed-based user session clustering algorithms are conducted
- for each run of the above algorithms XB, FS, SC and error cluster validity indexes are computed
- for each run of the above algorithms following kinds of input user sessions are used
  1. user sessions with no weights
  2. user sessions with LFMF-based weights
  3. user sessions with SFMF-based weights
- following parameter settings are used:
  1. number of clusters c, is varied from 2 to 50

2 fuzziness index q is set to 2

3 error threshold ϵ is set to 0.01

4 maximum iterations η is set to 100

5 neighbourhood radius $\mathscr{R}$ is set to $\sqrt{n}$.

5.3 FCM vs. MDFCM

Figure 2 depicts the values of various fuzzy validity indexes for user session clusters discovered by applying FCM and MDFCM-based user session clustering. Figure 2(a) shows the XB index scores as a function of number of clusters. A smaller value of this index represents better quality of the clusters with more intra-cluster compaction and inter cluster separation. From the figure, it is very clear that the quality of the fuzzy clusters formed by MDFCM algorithm is much better than that of those discovered by FCM algorithm for different values of number of clusters. Figure 2(b) describes the FS index scores as a function of number of clusters. Since FS index represents the difference of the within cluster compaction and inter cluster separation, a lower value of this index represents better cluster quality. From the figure, it is obvious that MDFCM-based user sessions clustering results in clusters of improved quality in terms of FS index as compared with those discovered by FCM algorithm for different values of number of clusters. Figure 2(c) provides values of SC index as a function of number of clusters. A higher value of this index represents better fuzzy cluster quality.

Figure 2 FCM vs. MDFCM, (a) XB index vs. no. of clusters (b) FS index vs. no. of clusters (b) FS index vs. no. of clusters (d) error index vs. no. of clusters (see online version for colours)

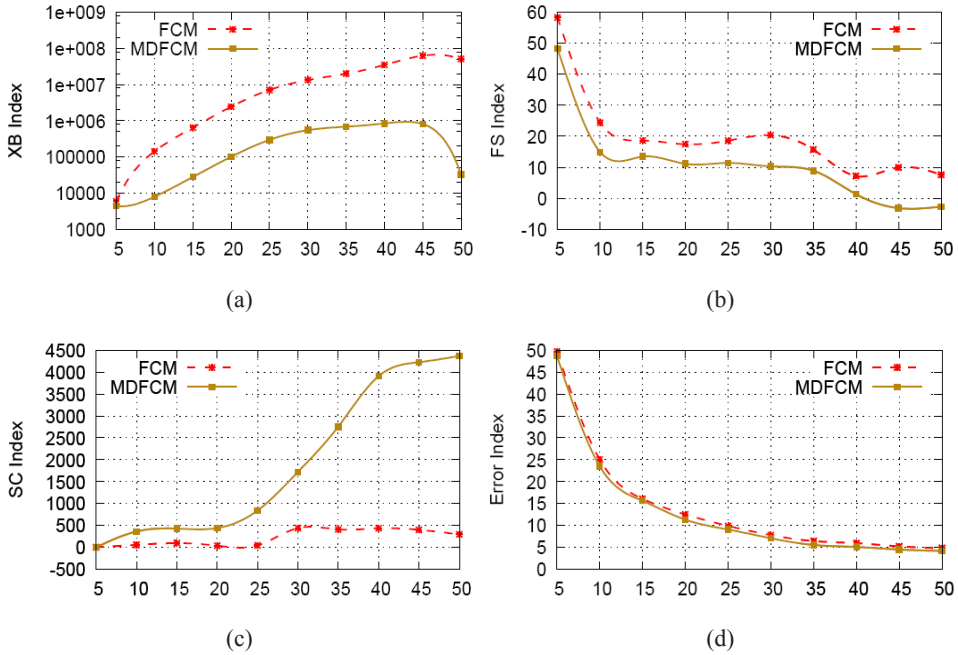

Figure clearly indicates that MDFCM-based user sessions clustering results in high quality of clusters in terms of SC index as compared with those discovered by FCM algorithm for different values of number of clusters. Figure 2(d) shows the fuzzy clustering error index scores as a function of number of clusters. A smaller value of this index represents less fuzzy clustering error and better quality of the clusters. The figure clearly indicates that the fuzzy clustering error by using MDFCM-based user sessions clustering is less as compared with that with FCM algorithm. The main reason for the improved quality of cluster is due to the more appropriate selection of initial cluster centres by making use of the MDF-based initialisation strategy.

5.4 FCMed vs. MDFCMed

Figure 3 provides various validity index values for user session clusters discovered by applying MDFCMed and FCMed algorithms. Figures 3(a), 3(b), 3(c) and 3(d) clearly indicate (based on the same reasons as explained for Figure 2) that the quality of the fuzzy clusters discovered using the proposed MDFCMed algorithm is much better than MDFCMed algorithm in terms of XB, FS, SC and Error validity Indexes.

Figure 3 FCMed vs. MDFCMed, (a) XB index vs. no. of clusters (b) FS index vs. no. of clusters (c) SC index vs. no. of clusters (d) error index vs. no. of clusters (see online version for colours)

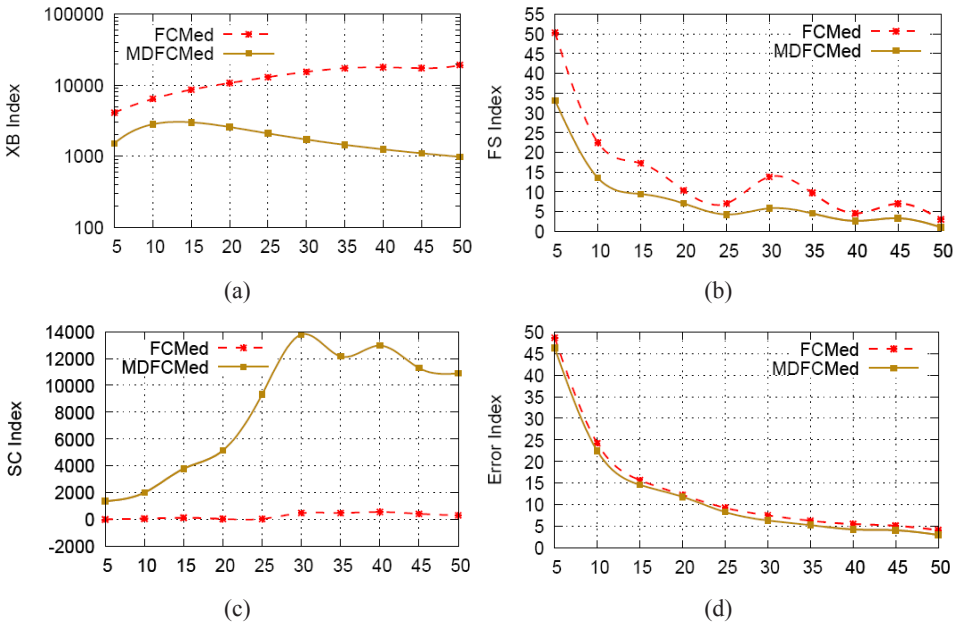

5.5 Comparison of the time performance

Figures 4(a) and (b) depict the graphs of execution time versus the number of clusters for FCM and MDFCM clustering of user sessions without and with LFNF-based weight

assigned to them respectively. From these figures, it is clear that execution timings of the proposed MDFCM algorithm is slightly better than that of FCM algorithm. Figures 4(c) and 4(d) depict the graphs of execution time versus the number of clusters for FCMed and MDFCMed clustering of the user sessions without and with LFNF-based weight assigned to them. From these figures, it is clear that execution timings of the proposed MDFCMed is slightly better than that of FCMed algorithm.

Figure 4 Execution time (ms) of FCM, FCMed, MDFCM and MDFCMed, (a) time vs. no. of clusters (no session weight) (b) TIME VS. NO. OF CLUSTERS (LFMF weight) (c) time vs. no. of clusters (no session weight) (d) time vs. no. of clusters (LFMF weight) (see online version for colours)

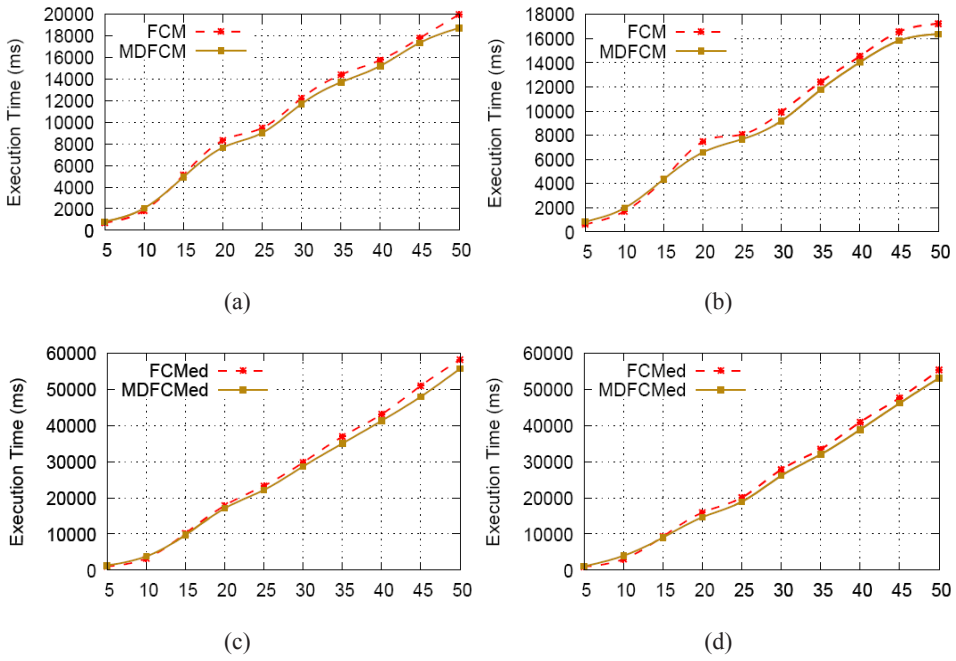

5.6 MDFCM with and without session weights

Figure 5 provides the values of various fuzzy cluster validity indexes for user session clusters discovered by applying the proposed MDFCM algorithm as a function of the number of clusters. Figures 5(a), 5(b), 5(c) and 5(d) clearly indicate that the quality of the fuzzy clusters formed by using fuzzy weighted user sessions is better than that of those with without user session weights in terms of XB, FS, SC and error validity indexes. Also, the quality of the clusters using user sessions with LFMF and SFMS-based weights are comparable to each other.

Figure 5 MDFCM with and without session weights, (a) XB index vs. no. of clusters (b) FS index vs. no. of clusters (c) SC index vs. no. of clusters (d) error index vs. no. of clusters (see online version for colours)

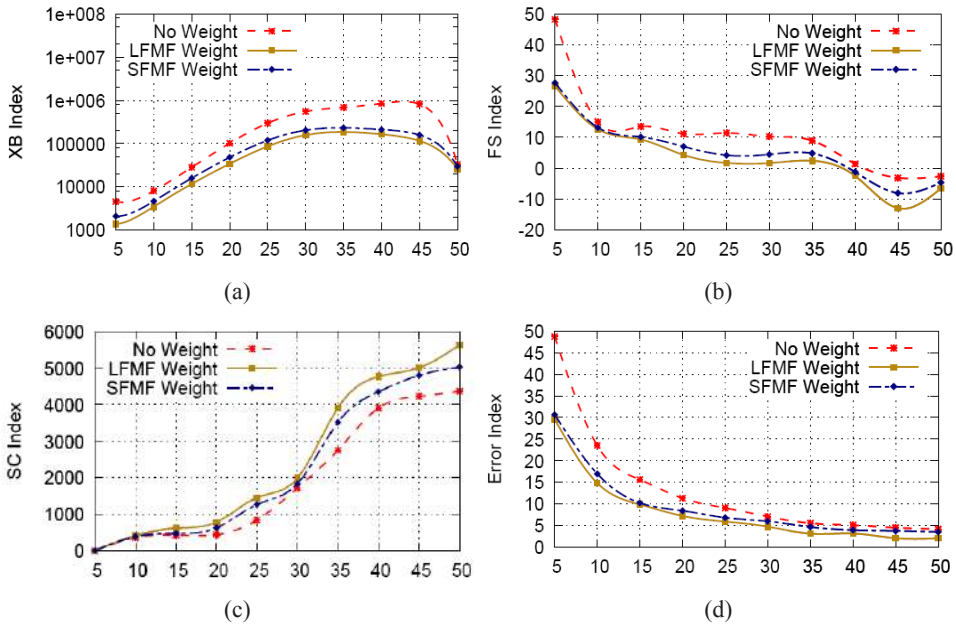

6 Conclusions

In this article, a MDF-based fuzzy clustering framework is proposed to discover the web user session clusters from the web usage data with the objective of improving the quality of the extracted clusters. The contribution of this work in the discovery of web usage clusters is:

- For the effective discovery of user session clusters, FCM and FCMed clustering techniques are explored and the mathematical formulation of user session clustering using these algorithms are presented.
- In order to deal with the problem of the selection of appropriate initial cluster centre, which plays a vital role in the formation of high quality clusters, a MDF-based MDFCM and MDFCMed algorithms are proposed and their mathematical and algorithmic details are presented.
- A fuzzy set theoretic approach for assigning fuzzy weights to the user sessions and associated URLs is proposed to deal with the high dimensional user session data mixed with noise and outliers in the form of insignificant sessions and URLs. Fuzzy weight assignment is performed using LFMF and SFMF fuzzy membership functions.
- The above mentioned algorithms are implemented and several experiments are carried out to evaluate their validity and performance using various fuzzy clustering validity indexes such as XB, FS, SC and error indexes.

Following conclusions may be drawn from the results obtained from the various experiments carried out in this research:

1 Experimental results clearly indicate that MDFCM and MDFCMed algorithms perform the identification of appropriate initial cluster centres resulting in the formation of fuzzy clusters of much better quality in terms of various fuzzy clustering indexes such as XB, FS, SC and the error indexes.

2 The time performance of the proposed MDFCM and MDFCMed algorithms are slightly better or comparable to those of FCM and FCMed algorithms respectively. The main reason behind the improvement in the time performance, in spite of the extra computational cost for MDF values, is that MDF-based selection of the initial cluster centres, results in the faster convergence of these algorithms especially when the number of clusters are high, thus reducing the overall time clustering time.

3 The fuzzy weight assignments to user sessions and URL items have been found to improve the MDFCM and MDFCMed-based user session clustering performance and quality in terms of XB, FS, SC and error indexes. This indicates that the fuzzy weight assignment very well served the purpose of reducing adverse effect of insignificant user sessions and URLs resulting in the formation of the improved quality clusters.

References

Ansari, Z.A., Ahmed, W., Azeem, M.F. and Babu, A.V. (2011a) 'Discovery of web usage profiles using various clustering techniques', *International Journal of Computer Information Systems*, July, Vol. 1, No. 3, pp.18–27.

Ansari, Z.A., Azeem, M.F., Babu, A.V. and Ahmed, W. (2011b) 'Preprocessing users web page navigational data to discover usage patterns', in *The Seventh International Conference on Computing and Information Technology*, Bangkok, Thailand, May.

Ansari, Z.A., Babu, A.V., Ahmed, W. and Azeem, M.F. (2011c) 'A comparative study of mining web usage patterns using variants of k-means clustering algorithm', *International Journal of Computer Science and Information Technologies (IJCSIT)*, July, Vol. 2, No. 4, pp.1407–1413.

Ansari, Z.A., Babu, A.V., Ahmed, W. and Azeem, M.F. (2011d) 'A fuzzy set theoretic approach to discover user sessions from web navigational data', in *IEEE Recent Advances in Intelligent Computational Systems (RAICS) 2011*, September, pp.879–884.

Bezdek, J.C. (1981) *Pattern Recognition with Fuzzy Objective Function Algorithms*, Kluwer Academic Publishers, Norwell, MA, USA.

Carmona, C.J., RamArez-Gallego, S., Torres, F., Bernal, E., del Jesus, M.J. and GarcAa, S. (2012) 'Web usage mining to improve the design of an e-commerce website', *Elsevier Expert Systems with Applications*, Vol. 39, No. 12, pp.11243–11249.

Chau, M., Cheng, R., Kao, B. and Ng, J. (2006) 'Uncertain data mining: an example in clustering location data', in *Advances in Knowledge Discovery and Data Mining, Lecture Notes in Computer Science*, Vol. 3918, pp.199–204, Springer.

Fukuyama, S.M.Y. (1989) 'A new method of choosing the number of clusters for the fuzzy c-means method', in *Proceeding of Fifth Fuzzy Syst. Symp*., pp.247–250.

Joshi, A. and Krishnapuram, R. (2000) 'On mining web access logs', in *Proceedings of the ACM SIGMOD Workshop on Research Issues in Data Mining and Knowledge Discovery (DMKD 2000)*, May.

Krishnapuram, R., Joshi, A., Nasraoui, O. and Yi, L. (2001) 'Low complexity fuzzy relational clustering algorithms for web mining', *IEEE transactions on Fuzzy Systems*, Vol. 9, No. 4, pp.595–607.

Limouri, M., Essaid, A. and Zahid, N. (1999) 'A new cluster validity for fuzzy clustering', *Pattern Recognition*, Vol. 32, No. 7, pp.1089–1097.

Mei, J-P. and Chen, L. (2011) 'Fuzzy relational clustering around medoids: a unified view', *Elsevier Fuzzy Sets and Systems*, Vol. 183, No. 1, pp.44–56.

Mobasher, B. (2007) 'Data mining for web personalization', in *The Adaptive Web*, pp.90–135, Springer, Berlin Heidelberg.

Xie, X.L. and Beni, G. (1987) 'A validity measure for fuzzy clustering', *IEEE Trans. Pattern Analysis and Machine Intelligence*, Vol. 13, No. 8, pp.841–847.

IJIREEICE

ISSN (Online) 2321 – 2004
ISSN (Print) 2321 – 5526

International Journal of Innovative Research in
Electrical, Electronics, Instrumentation and Control Engineering
ISO 3297:2007 Certified
Vol. 4, Issue 11, November 2016

Design & Implementation of Secure Provenance Transmission for Streaming Data

Mohd Abdul Sattar[1], Mohd Anas Ali[2]

Associate Professor& Head, Dept of ECE, Nawab Shah Alam Khan College of Engineering & Technology, Hyderabad, India[1]

Assistant Professor, Dept of ECE, Nawab Shah Alam Khan College of Engineering & Technology, Hyderabad, India[2]

Abstract: In this paper, a solution about secure provenance transmission for streaming data which is introduced based on Raspberry Pi processor, is presented. The embedded system, video capture, and video monitor are introduced. Video 4 Linux is used to get the camera video data, which is transferred to the Web Server, and the data is displayed on the client browser. The main aim of this paper is to design a system that has a USB camera, which continuously captures videos of the people then processes the captured videos via USB host to the Raspberry Pi to display it on the display device unit, and the parallel connection of Ethernet module, web page is created on the remote PC using HTTP protocol because HTTP protocol provides secure data transmission. And for more security we are creating some IP address to view the live streaming data on remote PC and when the person appears in front of camera the processor collects the information and stores temporarily in the database to check or recognize, is this person the right person to use or not. Compared with video capture system based on digital signal processor(DSP), this system has the advantage of fewer modules, lower cost, higher intelligence, higher system stability, and higher security. The design of system presented in this paper will integrate ARM11, USB cam, Remote PC, Display Monitoring unit, and Ethernet. The entire process proves continuous, and a surveillance secured system.

Keywords: Security, Raspberry Pi (ARM11), Ethernet, HTTP.

I. INTRODUCTION

The word provenance is used synonymously with the word lineage in the database community. It is also sometimes referred to as source attribution or source tagging. Provenance means origin or source. The rapid growth of the Internet, embedded systems and sensor networks technology has greatly contributed to the wide development of streaming applications. Examples include real-time financial analysis, location-based services, control of automated systems, stock market. This diversity of data sources accelerates the importance of data provenance to ensure secure and predictable operation of the streaming applications. Data provenance is considered as an effective tool for evaluating data trustworthiness, since it summarizes the history of the ownership and the actions performed on this data. As an example considered, a battlefield surveillance system gathers enemy locations from various sensors deployed in vehicles, air-crafts, satellites etc., and manages queries over these data. Now a days research peoples mostly prefer data mining applications that are used in so many areas such as web service, communication and security in surveillance systems. In this paper, we use high performance Raspberry Pi processor. Video data is captured from a USB camera, the captured data is sent to Raspberry Pi board via USB cable which consists of ARM processor and transferred over Internet through Ethernet and then the monitor client will receive the compressed data frame to restructure, and recompose video images by using HTTP protocol.

II. PROPOSED METHOD

The proposed method is used to overcome the drawback present in existing method. The design for the video encoding system involves various aspects such as the selection of the hardware platform and the embedded operating system (Raspbian). The development board with ARM architecture is selected as the hardware platform. Start-up codes, OS kernel and user's application programs are together stored in a NAND FLASH (a Memory Card). Application programs run in 64MB SDRAM, which can also be used as the room of various data and the stack. A CMOS camera capturing videos is connected to a USB interface in the board.

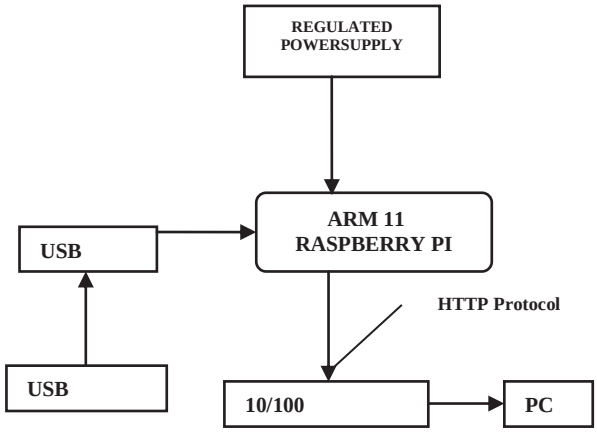

Copyright to IJIREEICE

IJIREEICE

ISSN (Online) 2321 – 2004
ISSN (Print) 2321 – 5526

International Journal of Innovative Research in
Electrical, Electronics, Instrumentation and Control Engineering
ISO 3297:2007 Certified
Vol. 4, Issue 11, November 2016

This system is used to design capturing &continuous streaming of videos like live cricket matches etc. capturing these live data and videos are stored inside internet by using HTTP protocol.

III. HARDWARE DESIGN OF PORTABLE DEVICE

1. USBCAMERA:
A webcam or USB camera is a video camera that feeds its image in real time to a computer or computer network. Unlike an IP camera which uses a direct communication using Ethernet or Wi-Fi, a USB camera is generally connected by USB cable, FireWire cable, or similar cable.

2. RASPBERRY PI:
The Raspberry Pi is a low cost, credit-card sized computer that plugs into a computer monitor or TV, and uses a standard keyboard and mouse. It is a capable little device that enables people of all ages to explore computing, and to learn how to program in languages like Scratch and Python. It's capable of doing everything you'd expect a desktop computer to do, from browsing the internet and playing high-definition video, to making spreadsheets, word-processing, and playing games.
In the proposed system, secure provenance transmission for streaming data system we, used the Raspberry Pi. It is a credit-card sized single board computer developed in the UK by the Raspberry Pi foundation. The Raspberry Pi has Broadcom BCM2835 system on chip (SoC), which includes an ARM1176JZF-S 700 MHz processor. Video Core IV GPU, and was originally with 256 megabytes of RAM, later upgraded to 512 MB. It does not include a built in hard disk or solid state drive, but uses an SD Card for booting and long term storage.

The Raspberry Pi has the ability to interact with the outside world, and has been used in a wide array of digital maker projects, from music machines and parent detectors to weather stations and tweeting birdhouses with infra-red cameras. We want to see the Raspberry Pi being used by kids all over the world to learn to program and understand how computers work.

The Raspberry Pi has the ability to interact with the outside world, and has been used in a wide array of digital maker projects, from music machines and parent detectors to weather stations and tweeting birdhouses with infra-red cameras. We want to see the Raspberry Pi being used by kids all over the world to learn to program and understand how computers work.

3. Processor / SoC (System on Chip):
The Raspberry Pi has a Broadcom BCM2835 System on Chip module. It has an ARM1176JZF-S processor.
The Broadcom SoC used in the Raspberry Pi is equivalent to a chip used in an old smartphone (Android or iPhone).While operating at 700 MHz by default, the Raspberry Pi provides a real world performance roughly equivalent to the 0.041 GFLOPS. On the CPU level the performance is similar to a 300 MHz Pentium II of 1997-1999, but the GPU, however, provides 1 GPixels/s, 1.5 GTexel/s or 24 GFLOPS of general purpose compute and the graphics capabilities of the Raspberry Pi are roughly equivalent to the level of performance of the Xbox of 2001. The Raspberry Pi chip operating at 700 MHz by default, will not become hot enough to need a heat-sink or special cooling.

4. Power source:
The Raspberry Pi is a device which consumes 700mA or 3W of power. It is powered by a MicroUSB charger or the GPIO header. Any good smartphone charger will do the work of powering the Pi.

5. SD Card:
The Raspberry Pi does not have any onboard storage available. The operating system is loaded on a SD card which is inserted on the SD card slot on the Raspberry Pi. The operating system can be loaded on the card using a card reader on any computer.

6. GPIO:
GPIO – General Purpose Input Output
General-purpose input/output (GPIO) is a generic pin on an integrated circuit whose behaviour, including whether it is an input or output pin, can be controlled by the user at run time.
GPIO pins have no special purpose defined, and go unused by default. The idea is that sometimes the system designer building a full system that uses the chip might find it useful to have a handful of additional digital control lines, and having these available from the chip can save the hassle of having to arrange additional circuitry to provide them.

GPIO capabilities may include:
• GPIO pins can be configured to be input or output
• GPIO pins can be enabled/disabled
•Input values are readable (typically high=1, low=0)
•Output values are writable/readable
•Input values can often be used as IRQs (typically for wakeup events)

The production Raspberry Pi board has a 26-pin 2.54 mm (100 mills) expansion header, marked as P1, arranged in a 2x13 strip. They provide 8 GPIO pins plus access to I²C, SPI, UART, as well as +3.3 V, +5 V and GND supply lines. Pin one is the pin in the first column and on the bottom row.

7. DSI Connector:
The Display Serial Interface (DSI) is a specification by the Mobile Industry Processor Interface (MIPI) Alliance aimed at reducing the cost of display controllers in a mobile device. It is commonly targeted at LCD and similar display technologies. It defines a serial bus and a communication protocol between the host (source of the image data) and the device (destination of the image data).

IJIREEICE

ISSN (Online) 2321 – 2004
ISSN (Print) 2321 – 5526

International Journal of Innovative Research in
Electrical, Electronics, Instrumentation and Control Engineering
ISO 3297:2007 Certified
Vol. 4, Issue 11, November 2016

A DSI compatible LCD screen can be connected through the DSI connector, although it may require additional drivers to drive the display.

8. RCA Video:
RCA Video outputs (PAL and NTSC) are available on all models of Raspberry Pi. Any television or screen with a RCA jack can be connected with the Raspberry Pi.

9. Audio Jack:
A standard 3.5 mm TRS connector is available on the Raspberry Pi for stereo audio output. Any headphone or 3.5mm audio cable can be connected directly. Although this jack cannot be used for taking audio input, USB mics or USB sound cards can be used.

10. Status LEDs:
There are 5 status LEDs on the Raspberry Pi that show the status of various activities as follows:
"OK" - SD Card Access (via GPIO16) - labelled as "OK" on Model B Rev1.0 boards and "ACT" on Model B Rev2.0 and Model A boards
"POWER" - 3.3 V Power - labelled as "PWR" on all boards
"FDX" - Full Duplex (LAN) (Model B) - labelled as "FDX" on all boards
"LNK" - Link/Activity (LAN) (Model B) - labelled as "LNK" on all boards
"10M/100" - 10/100Mbit (LAN) (Model B) - labelled (incorrectly) as "10M" on Model B Rev1.0 boards and "100" on Model B Rev2.0 and Model A boards

11. USB 2.0 Port:
USB 2.0 ports are the means to connect accessories such as mouse or keyboard to the Raspberry Pi. There is 1 port on Model A, 2 on Model B and 4 on Model B+. The number of ports can be increased by using an external powered USB hub which is available as a standard Pi accessory.

12. Ethernet:
Ethernet port is available on Model B and B+. It can be connected to a network or internet using a standard LAN cable on the Ethernet port. The Ethernet ports are controlled by Microchip LAN9512 LAN controller chip.

13. CSI connector:
CSI – Camera Serial Interface is a serial interface designed by MIPI alliance aimed at interfacing digital cameras with a mobile processor.
The Raspberry Pi foundation provides a camera specially made for the Pi which can be connected with the Pi using the CSI connector.

14. JTAG headers:
JTAG is an acronym for 'Joint Test Action Group', an organization that started back in the mid 1980's to address test point access issues on PCB with surface mount devices. The organization devised a method of access to device pins via a serial port that became known as the TAP (Test Access Port). In 1990 the method became a recognized international standard (IEEE Standard 1149.1). Many thousands of devices now include this standardized port as a feature to allow test and design engineers to access pins.

15. HDMI:
HDMI – High Definition Multimedia Interface.
HDMI 1.3 a type A port is provided on the Raspberry Pi to connect with HDMI screens.

IV. SOFTWARE DESIGN

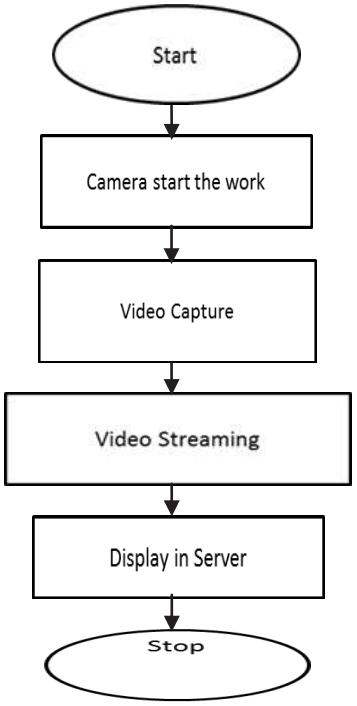

Fig 2: Flow Chart of Software System

V. EXPERIMENTAL RESULTS

Secure provenance transmission for streaming data using Raspberry Pi ARM1176JJZF-S 700 MHz processor was implemented successfully. We can see the results of the project as shown in figures. Figure 3 shows snap shot of the overall project secure provenance transmission for streaming data.

Fig 3: Snapshot of hardware kit

After switch on the power supply, USB camera continuously capturing the video and it is stored in

IJIREEICE

ISSN (Online) 2321 – 2004
ISSN (Print) 2321 – 5526

International Journal of Innovative Research in
Electrical, Electronics, Instrumentation and Control Engineering
ISO 3297:2007 Certified
Vol. 4, Issue 11, November 2016

Raspberry Pi and the raspberry pi acts as a server and the video displayed in remote PC by using HTTP protocol. The processed stream data packets are uploaded into server using HTTP protocol and transmitted through Ethernet cable, so that user inputs the corresponding IP address http://192.168.1.105/.html which is specific to router and then webpage is opened and the login page created with user name and password. If you entered correct login details it will open and video displayed. Otherwise incorrect login details message displayed.

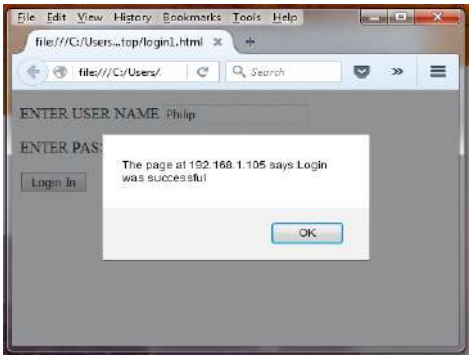

Fig 4: Login details on the webpage

After entering login details correctly then the webpage is opened and the output of video is streaming as shown in below figure 5.

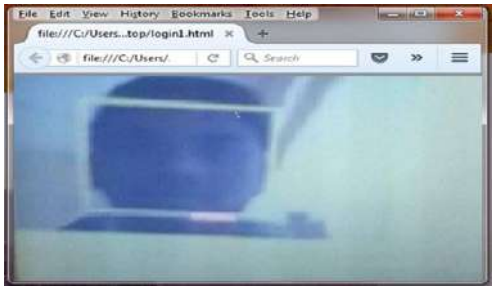

Fig 5: The output video streaming

VI. CONCLUSION

The system "Secure provenance transmission for streaming data system" has been successfully designed, developed and tested. It has been developed by integrating features of all the hardware components and software used. Presence of every module has been reasoned out and placed carefully thus contributing to the best working of the unit. Secondly, using highly advanced ARM board and with the help of growing technology, the system has been successfully implemented.

ACKNOWLEDGMENT

We express our sincere gratitude to **Prof. Mohd. Muzaffar Ahmad**, Electronics & Communication Engineering Department, Nawab Shah Alam Khan College of Engineering& Technology, Hyderabad, for extending his valuable insight for completion this work.

REFERENCES

[1] ChenRongfang, Wang Haibin, Hu Zhenhua, Zheng Pin. Remote Monitor System of Power Network Based on Embedded Internet Technology. Microcomputer Information. vol. 24, no. 7-2, pp. 78-80,2008S3C6410MicrocontrollerUser'sManalRevsion1,http://www.samsungsemi.com/

[2] Siyi.Zou, "Design and Application of Embedded Linux". Beijing: Tsinghua University Press, pp:90-93,2002.

[3] ZhangYuJie, HuaiWeihua, TianZe. Design of Industrial Temperature Monitoring Equipment Based on Embedded Linux Operating System.ComputerEngineering and Design, vol. 30, no. 17, pp. 3940-3942, 2009.

[4] Video4Linux User's Manual, http://www.v4l.com.cn. [5] Craig Zacker. "TCP/ IP Administration". China Water Power Press. Beijing ,vol 8,pp:12- 18.1998.

[5] Institute for Informatics– University Karlsruhe. Http://www.irf.uka.de/seminaret/redundant/vortrag15/(3.Feb. 2006)

[6] MANNING, C. The digital video site. Http://www.new mediarepublic.com/video/compression/adv08.html (3. Feb. 2006)

[7] HUFFMAN, D. A. (1951). A method for the construction of minimum redundancy codes. In the Proceedings of the Institute of Radio Engineers 40, pp. 1098-1101.

[8] CAPON, J. (1959). A probabilistic model for run-length coding of pictures.IRE Trans. On Information Theory, IT-5, (4), pp. 157-163.

[9] Yoshiro Imai, Yukio Hori :A Mobile Phone-Enhanced Remote Surveillance System with Electric Power Appliance Control and Network Camera Homing, IEEE Computer(Third International Conference on Autonomic and Autonomous Systems ICAS 2007).

BIOGRAPHIES

MOHD ABDUL SATTAR, received B.Tech. Degree in Electronics and Communication Engineering from NIT, Warangal and M.Tech. in Embedded Systems from JNTU Hyderabad. He is an Associate Professor& Head of the Dept. of ECE in Nawab Shah Alam Khan College of Engineering & Technology, Malakpet, Hyderabad.

MOHD ANAS ALI, received B.Tech degree in Electronics and Communication Engineering from Pujya Shri Madhavanji College of Engineering & Technology affiliated to JNTU Hyderabad in 2013. He is Assistant Professor at Nawab Shah Alam Khan College of Engineering & Technology, Malakpet, Hyderabad.

Indoor Air Quality Considerations for HVAC Systems Design in India

Raza Ahmed Khan, Dr. Kavita Daryani Rao, Dr. M. Manzoor Hussain, Dr. S. Kumar

Abstract— The performance and design of Heating, Ventilation, and Air-Conditioning (HVAC) Systems decides the soundness of Indoor Air Quality (IAQ) to a large extent. Almost all modern buildings are air-conditioned and a huge number of occupants spend considerable time inside these buildings. Hence, the goodness of indoor air is vital to their health and productivity. In this study, a research questionnaire survey is carried out for the HVAC designers to obtain information regarding their design practices in India. A large number of HVAC designers and offices were contacted and explained about the study. However, 52 HVAC designers / offices participated from across the country. Their responses were recorded and analyzed to build up a picture of the prevalent HVAC design practices in India.

Index Terms— Heating, Ventilation, & Air-Conditioning (HVAC); HVAC Designers; HVAC Systems; Indoor Air Quality (IAQ); Questionnaire Survey; Standards.

1 Introduction

THE economic liberalization policy and subsequent entry of multi-national companies in Indian market resulted in sprouting of many advanced air-tight glazed buildings .throughout major cities of the country. All these modern buildings employ air-conditioners to control their indoor environments.

Now people spend most of their time indoors, where the concentration of pollutants are often much higher than those outside. Hundreds of chemical and biological pollutants are found indoors, many of which are known to have significant health impacts. Many research findings have highlighted the indoor environmental pollution as the greatest risks to human health [1].

The Heating, Ventilation, and Air-Conditioning (HVAC) design offices are the places where decisions on the performance of the buildings are first taken, either good or bad. It is therefore essential to know the design criteria that these designers take into account for Indoor Air Quality (IAQ) issues.

2 Methodology

The research methodology adopted for the investigation of IAQ problems that are related to HVAC systems is through gathering the required information from the feedback of HVAC designers. Self-administered questionnaire surveys (see Appendix) and personal interviews with the designers were carried out which provided useful information.

An extensive literature review was done to acquire the in-depth understanding of the issues related to IAQ and HVAC systems, which was helpful in formulating the questionnaire in particular.

- *Raza Ahmed Khan is currently pursuing Doctoral Research Program from Jawaharlal Nehru Architecture & Fine Arts University (JNAFAU), India, PH-09848058830. E-mail: raza_a_khan@hotmail.com*
- *Dr. Kavita Daryani Rao is Professor in Architecture, JNAFAU, India.*
- *Dr. M. Manzoor Hussain is Professor in Mechanical Engineering, Jawaharlal Nehru Technological University Hyderabad (JNTUH), India.*
- *Dr. S. Kumar is Professor in Architecture, JNAFAU, India.*

The questionnaire is developed seeking information regarding the experience and design practices of HVAC design professionals in India. The designers were introduced to the objectives of the study, its scope and the usefulness of its results. Several aspects of design and compliance with guidelines and standards were also discussed during personal meetings. The architectural and engineering plans of some of the sample buildings were reviewed wherever possible, to have an insight into the design practices.

Various manufacturers and suppliers of HVAC systems were contacted, and information obtained about the range of HVAC products in the Indian market. Useful information and product information brochures were downloaded from the manufacturer's website

The information thus gathered from the HVAC designer's feedback, manufacturers and suppliers was useful in identifying the design criteria, standards followed, most common types of HVAC systems and products that are employed in commercial and office buildings.

It was encouraging to observe that many designers appreciated the objectives of the study and actively participated. However, some designers could not respond due to their job engagements. More than 100 designers were contacted personally and over e-mail throughout the country for the questionnaire survey. They were requested to either fill it on-line on "google forms" or on paper sheets [2]. A total of 58 HVAC designers responded by filling the questionnaire both on-line and on papers.

3 Questionnaire Analysis

The questionnaire for HVAC designers was developed and administered with the aim of obtaining information on the following aspects of design practice:

(a) General information like the years of experience, types of HVAC systems designed, their manufacturers, etc.
(b) The criteria for design and selection of HVAC products and their manufacturers
(c) The range of temperature and relative humidity for designing commercial and office buildings in India

(d) The rates of ventilation and fresh air intakes
(e) Common choices of filters, location and types of duct insulation

The response to this questionnaire was used to build up a picture of the prevalent design practices in India. Data analysis and discussion of this questionnaire are discussed in the subsequent sections.

3.1 Background Information

Most of the HVAC designers, who were contacted, were senior professionals having sound experience in designing HVAC systems in different building types. Out of the 58 HVAC designers who responded, around 41% of respondents possess more than 10 years of experience, 19% possess between 5-10 years of experience, another 19% has 2-5 years of experience, and 21% are relatively freshers with less than 2 years of designing experience. It is interesting to note that 60% of respondents have more than 5 years of working experience and about 59% have less than 10 years of field experience. It indicates that the respondents are well experienced and that the HVAC field has emerged in the past 10 years in India.

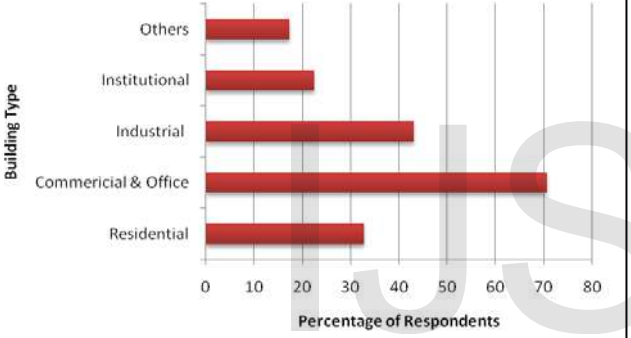

Fig.1. Types of buildings designed by surveyed designers

As per the feedback received from the designers, about 71% of them deal with the design of HVAC systems in commercial and office buildings as shown in Fig.1. Other building types that they design include industrial buildings (about 43%), residential buildings (about 33%) and institutional buildings (about 22%). 17% of the designers also deal with the design of other buildings like hotels and hospitals.

3.2 HVAC Systems Design and Selection

A large variety of HVAC systems are available for commercial and office buildings in India. These systems differ according to the size of the building, occupant activities, building age, climatic conditions, geographic location and so on.

According to the Indian designers, the most frequently used HVAC system for commercial and office buildings is the chilled water system with Air Handling Units (AHUs) as shown in Fig.2. 77% of respondents prefer to use chilled water system with 74% using AHUs and 53% opting for Fan Coil Units (FCUs). It is however, interesting to note that about 60% of HVAC designers are utilizing the Varible Refrigerant Flow (VRF) systems. The split systems are used by 46% of respondents where as 44% employ rooftop packaged units, followed by Variable Air Volume (VAV) systems at 37%. The split systems are available in the variants of ducted and non-ducted.

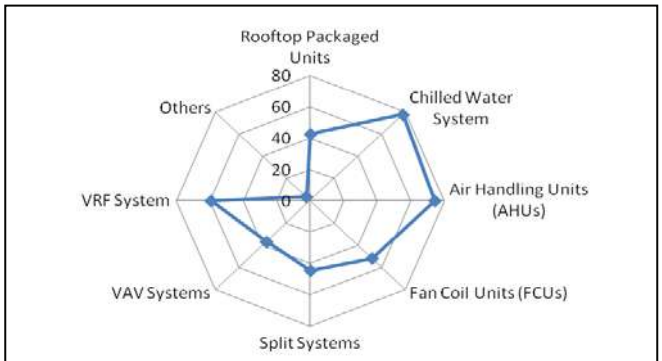

Fig.2. Most common HVAC systems used in commercial and office buildings in India.

There are more than a dozen HVAC system manufacturers available in the Indian market which caters to the commercial and office building sector. The popular manufacturers among the HVAC designers are Carrier (70%), Blue Star (52%), Daikin (44%), Voltas (39%) and Trane (30%) as shown in Fig.3. The other manufacturers like Kirloskar (17%) and LG (15%) are popular in other sectors like industrial and residential buildings. There are few other trade names that are recommended by about 11% of respondents.

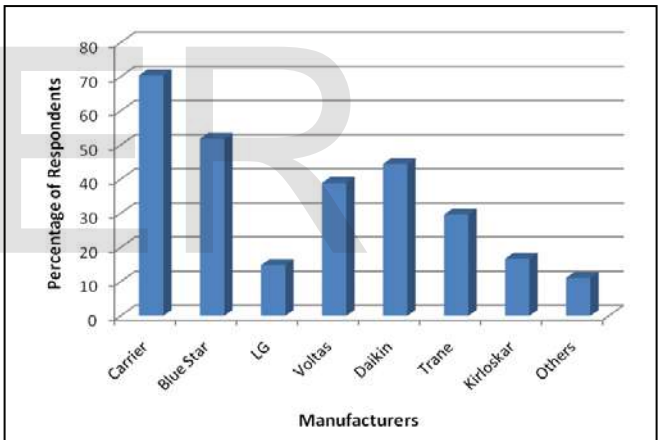

Fig.3. Most common manufacturers of HVAC systems in commercial and office buildings in India.

According to the HVAC designers, the most important criteria for the selection of these manufacturers is their good experience with the product, with about 72% of the respondents indicating this aspect. 40% of the designers have pointed out that the manufacturers are usually specified by the building owners. About 28% respondents have expressed that local weather conditions dictate the choice of manufacturers, where as 19% designers say that availability of product in the market is crucial to this decision.

The main criterion for designing and selecting the HVAC system in commercial and office building is to provide good IAQ to building occupants. This was indicated by about 78% of respondents. 72% designers also expressed that the next important criterion is the energy conservation, and 67% have marked that providing the thermal comfort in office spaces is crucial to productivity.

3.3 Indoor Conditions and Ventilation Design

ASHRAE Standard 55-2013: Thermal Environmental Conditions for Human Occupancy specifies the combinations of indoor thermal environmental factors and personal factors that will produce thermal environmental conditions acceptable to a majority of the occupants within the space [3]. The standard addresses the four primary environmental factors (temperature, thermal radiation, humidity, and air speed) and two personal factors (activity and clothing) that affect thermal comfort.

The HVAC designer anticipates based on owner's feedback, the occupant activity and equipment, which may reject heat into the space prior to calculating the heating loads.

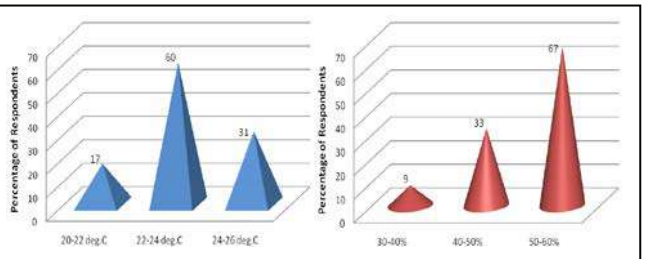

Fig.4. Design range practices for indoor temperature and relative humidity

The most common range of indoor temperature that the HVAC designers normally design for commercial and office buildings in India is 22^{0}C to 24^{0}C as shown in Fig.4. About 60% of designers normally design in this range, whereas 31% design in the range of 24^{0}C to 26^{0}C and 17% in the range of 20^{0}C to 22^{0}C. These values are within the acceptable range as ASHRAE Standard 55 recommends that the temperature in occupied spaces be maintained between 21^{0}C to 26^{0}C (70^{0}F to 78^{0}F).

Most designers (about 67%) specify relative humidity in the range of 50 to 60% as shown in Fig.4. 33% of respondents design in the range of 40 to 50% and only 9% desing between 30 to 40% relative humidity. These values too are within the acceptable range as ASHRAE Standard 55 recommends that the relative humidity in occupied spaces be maintained between 30 to 60 percent.

ASHRAE Standard 62.1-2013: Ventilation for Acceptable Indoor Air Quality specifies that any one of the Ventilation Rate Procedure, the IAQ Procedure, and the Natural Ventilation Procedure can be used to meet the requirements of ventilation [4].

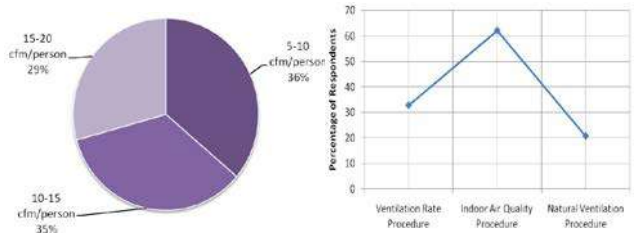

Fig.5. Design ventilation rate practices and the procedures adopted for ventilation

Ventilation air or the fresh outdoor air is a crucial aspect of HVAC designs as it controls the indoor air contamination through dilution [5]. The ventilation rates that are incorporated by different designers are as follows: 5-10 cfm/person by 36%, 10-15 cfm/person by 34%, and 15-20 cfm/person by 29% as shown in Fig.5.

All the three procedures specified by ASHRAE are practised by the Indian designers. IAQ procedure is used by about 62% of respondents, 33% refer to the Ventilation Rate procedure, and about 21% opt for the Natural Ventilation procedure as shown in Fig.5. It has to be noted that the intake airflow determined using each of these approaches may differ significantly because of assumptions about the design, any of these approaches is a valid basis for design.

3.4 HVAC System's Components Design

Proper filter selection plays an important role in the control of IAQ issues. Efficiency, resistance to air flow, and dust holding capacity are the main characteristics that distinguish different types of air filters [6]. As shown in Fig.6, about 53% of designers generally recommend bag filters for commercial and office buildings in India. About 45% specify the High Efficiency Particulate Air (HEPA) filters, 29% respondents recommend rigid aluminum filters, 28% suggest media filters, and only 7% opt for Electrostatic Air Cleaners (EAC).

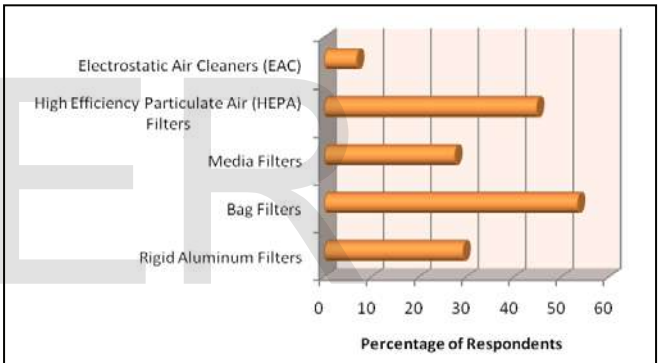

Fig.6. Most common air filters specified by HVAC designers

It is important for the HVAC designers to know the types of contaminants that are or could be present in the building environment so as to prescribe proper filter efficiency. The air filtration efficiency normally specified by designers is as follows: 48% respondents prescribe more than 90% filtration efficiency, 43% specify between 70 to 90% filtration efficiency, 12% designers recommend 60 to 70% filtration efficiency, and only 5% design for 50 to 60% filtration efficiency. It is a healthy trend to recommend high efficiency filters as they provide cleaner air and cleaner HVAC system coils, duct works, and diffusers.

In order to have better control over IAQ issues, HVAC designers must take into account the minimum maintenance requirements, equipment access and servicieability, and overall equipment reliability [7].

In response to the question on the design of coil condensation pan to ensure complete condensate drain and prevent blockage, about 93% designers indicated that they recommend U-trap connections and 17% specify P-trap connections to the condensate drain lines.

The ductwork system is one of the most important compo-

nent of the HVAC system that affects the air quality. It becomes pathway for pollutants and transports it form one place to areas throughout the building [8].

The ductworks made of Galvanized Iron (GI) sheets are popular among surveyed designers with about 93% recommending it. 14% respondents also specify aluminum duct and a minor 3% even recommends PVC ducts.

Regarding the duct insulation, fiberglass is very popular among designers with about 53% recommending it as shown in Fig.7. About 36% respondents specify EPS / styrofoam / thermocol insulation, 19% respondents recommend rockwook insulation, 17% designers specify cellulose fiber insulation, and 17% designers recommend nitrile rubber insulation.

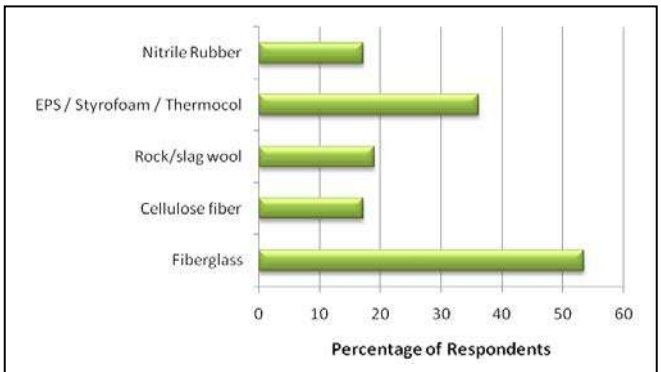

Fig.7. Types of thermal insulation used in HVAC systems

Almost 93% of designers highly recommend external insulation to duct. However, about 24% respondents specify internal insulation as acoustical lining for sound absorption. However care must be exercised for internal insulation as there is a potential for biological and mold growth in it when subjected to humid air [9].

3.5 IAQ Strategies in HVAC Design

In response to a question on separate smoking zones inside commercial and office buildings, about 60% respondents agreed that they provide such tobacco smoking zones in buildings with local exhaust. 29% designers provide such zones as per the requirements, and about 12% designers have never provided such zones in their buildings. ASHRAE recommends that 100% air in smoking lounges should be exhausted [4].

About 78% of the designers allocate local exhaust with localized contaminant generation like toilets, kitchen, labs, printers, etc. Almost 19% indicated that they design it based on the requirements or specifications of the building owners.

To compensate for the exhausted air from the building, fresh outside air is introduced into the building. It also acts as a dilution strategy for the building contaminants [10]. The surveyed HVAC designers emphasized that various considerations have to be taken into account while designing the fresh air intakes. 69% designers feel that the location of air intake is crucial, about 64% respondents are of the opinion that outdoor air quality is important, and 41% specifies proper bird screen and mesh to prevent the unwanted entry.

The HVAC designers were asked about the special components that they normally use in their designs. About 64% designers use energy recovery wheels, 36% use dehumidifiers and electric heater, 33% use humidifiers, and 9% use underfloor ducting as shown in Fig.8.

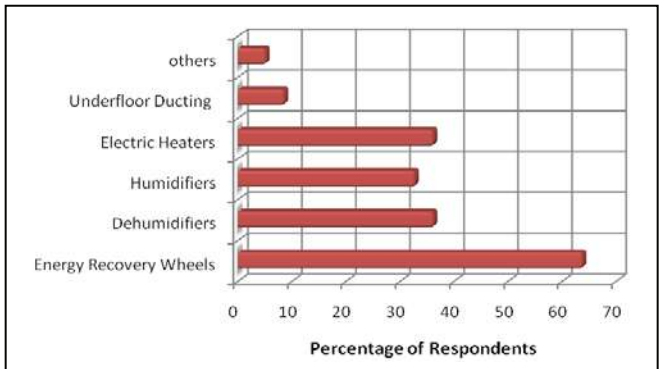

Fig.8. Special components used in HVAC designs

In response to a question on the standards that are referred while designing the HVAC systems, the designers listed out some of them. About 60% refer to the ASHRAE Standard 62 for IAQ and ISHRAE Standards, 53% refer to SMACNA Standards for ductworks, 45% refer to ASHRAE Standard 90 for Energy Conservation, 36% refer to ASHRAE Standard 55 for Thermal Comfort, 40% refer to IGBC / LEED-NC Standards for Green Buildings, and 33% refer the NFPA Standards for Fire Safety.

The HVAC designers were asked about the strategy they employ for better IAQ in commercial and office buildings. 59% designers suggested that fresh air intake is a sound strategy to improve IAQ. About 53% respondents feel that Fresh Air Handling Units (FAHUs) is a better idea for good IAQ. 34% participants opined that using high efficiency filters can enhance IAQ, while 17% believe that providing local exhaust at the source of pollutant generation is the best solution.

4 Conclusion

The responses to questionnaire represent the general HVAC design practice for commercial and office buildings in India. The chilled water system, AHUs and VRFs are the most popular HVAC systems. Providing good IAQ is the main criterion for designing and selecting these systems. All design professionals design the indoor conditions and ventilation rates as per the relevant standards. Bag filters and HEPA filters are most commonly used filters. More than 80% designers recommend use of more than 70% filtration efficiency. 93% of respondents use GI sheets for ductworks with external insulation. Fiberglass and thermocol are popular thermal insulations. 78% participants design local exhaust for local pollution sources. Fresh outside air is introduced to compensate for the exhaust air. Energy recovery wheels are being recommended by many professionals. Standards are being referred by designers, including the green building codes. The HVAC industry is expanding in India, new products are being introduced and young professionals are choosing HVAC as their careers.

APPENDIX – HVAC DESIGNER'S QUESTIONNAIRE

11. What kind of **air filters** do you generally recommend for HVAC systems (C&O Bldgs)?
☐ Rigid Aluminum Filters ☐ High Efficiency Particulate Air Filters (HEPA)
☐ Bag Filters ☐ Electrostatic Air Cleaners (EAC)
☐ Media Filters ☐ Others (specify) _____

12. What is the **air filtration efficiency** that you normally specify?
☐ >90% ☐ 70-80% ☐ 60-70% ☐ 50-60% ☐ Others (specify) _____

13. Do you take any measure during the design of **coil condensation/drain pan** to ensure complete condensate drain and prevent blockage?
☐ P-trap ☐ U-trap ☐ T-trap ☐ Others (specify) _____

14. What is the **ducting material** that you generally prescribe for air distribution system?
☐ PVC Duct ☐ GI Duct ☐ Aluminum Duct ☐ Others (specify) _____

15. What kind of **thermal insulation** you specify for the ducting system?
☐ Fiberglass ☐ EPS / Styrofoam / Thermocol
☐ Cellulose fiber ☐ Others (specify) _____
☐ Rock/slag wool

16. Which type of **insulation** you generally specify for ducts?
☐ Internal to the duct ☐ External to the duct

17. Do you normally allocate **separate areas for smoking** with local exhaust (C&O Bldgs)?
☐ Always ☐ Sometimes ☐ Never

18. Do you provide **local exhaust system** for spaces with localized contaminant generation (like kitchen, laboratories, copy machines, etc.) in C&O Bldgs?
☐ Always ☐ Sometimes ☐ Never

19. What are the considerations you take into account while designing for **fresh air intake**?
☐ Outdoor air quality ☐ Bird screens and mesh
☐ Location of air intake ☐ Others (specify) _____

20. What are the **special components** that you normally use in HVAC designs?
☐ Energy Recovery Wheels ☐ Electric Heaters
☐ Dehumidifiers ☐ Underfloor Ducting
☐ Humidifiers ☐ Others (specify) _____

21. Which **standards** you refer to while designing the HVAC Systems for C&O Bldgs?
☐ ASHRAE Standard 55 *version* _____ ☐ SMACNA
☐ ASHRAE Standard 62 *version* _____ ☐ NFPA
☐ ASHRAE Standard 90 *version* _____ ☐ USGBC / IGBC / LEED-NC
☐ ISHRAE Standards ☐ Others (specify) _____

22. What **strategies** do you employ for **better Indoor Air Quality** (C&O Bldgs)?
☐ Fresh Air Intake ☐ Fresh Air Handling Units (FAHU)
☐ Local Exhaust at Source of Generation ☐ Others (specify) _____
☐ High Efficiency Filters

Additional Comments: _____

Thank you for participating in this study. We appreciate your efforts and time spent to make this research more meaningful. We strongly encourage you to kindly provide the following details (optional):

HVAC Designer's Name: _____ Designation: _____

Design Office (Name & Address): _____

E-mail: _____ Phone (Mobile): _____

Research Questionnaire for HVAC Design Professionals

Dear HVAC Designer,

The following information is required for an academic research project to study the existing Heating, Ventilating and Air-Conditioning (HVAC) design practices in Commercial & Office buildings in India.

We request you to kindly participate in this study by providing valuable information in this questionnaire. We assure you that the confidentiality of your inputs will be maintained and used for research purpose only. Should you have any queries regarding this study, please feel free to contact the undersigned.

Raza A. Khan
Research Scholar, JNAFAU
Ph: 9848058830

Dr. Kavita Daryani Rao
Research Supervisor
JNAFA University, Hyderabad

1. How long have you been involved in designing the HVAC systems in buildings?
☐ <2 years ☐ 2-5 years ☐ 5-10 years ☐ 10-15 years ☐ _____

2. What **kind of buildings** have you designed the HVAC systems so far?
☐ Residential
☐ Commercial & Office
☐ Industrial
☐ Institutional
☐ Others (specify) _____

The following questions refer to HVAC design in Commercial & Office Buildings (C&O Bldgs).
You may choose more than one options, wherever required. Write your comments in blank spaces.

3. What **type of HVAC system** is mostly used in commercial & office buildings in India?
☐ Rooftop Packaged Units ☐ Split Systems
☐ Chilled Water System ☐ VAV Systems
☐ Air Handling Units (AHUs) ☐ VRF System
☐ Fan Coil Units (FCUs) ☐ Others (specify) _____

4. Which **manufacturer / brand name** of HVAC systems do you normally use in your projects?
☐ Carrier ☐ Daikin
☐ Blue Star ☐ Trane
☐ LG ☐ Kirloskar
☐ Voltas ☐ Others (specify) _____

5. What is the **criteria for selection** of a particular manufacturer?
☐ Specified by the building owner
☐ Suitable for local weather conditions
☐ Availability in the market
☐ Good experience with the product
☐ Others (specify) _____

6. What is your **main criterion** for designing and selecting the HVAC system? (You may give ranking)
☐ Energy conservation
☐ Thermal comfort
☐ Indoor air quality
☐ Others (specify) _____

7. What is the range of **indoor temperature** that you normally design (C&O Bldgs)?
☐ 20°-22°C ☐ 22°-24°C ☐ 24°-26°C ☐ Others (specify) _____

8. What is the range of **indoor relative humidity** that you normally design (C&O Bldgs)?
☐ 30-40% ☐ 40-50% ☐ 50-60% ☐ Others (specify) _____

9. What is the **ventilation rate** (outside fresh air) that you incorporate to design the HVAC system?
☐ 5-10 cfm/person ☐ 10-15 cfm/person ☐ 15-20 cfm/person ☐ Others (specify) _____

10. Which procedure is followed to determine the required **ventilation rate**?
☐ Ventilation Rate Procedure ☐ Natural Ventilation Procedure
☐ Indoor Air Quality Procedure ☐ Others (specify) _____

ACKNOWLEDGMENT

The authors wish to thank Jawaharlal Nehru Architecture & Fine Arts Unviersity and NSAK College of Engineering & Technology of JNTUH for facilitating this research work. The authors also wish to thank the HVAC designers who participated in this study. Thanks is also due to the Indian Society for Refrigerating and Air-Conditioning Engineers (ISHRAE) for encouragement.

REFERENCES

[1] EPA, "Healthy Buildings, Healthy People: A Vision for the 21st Century", United States Environment Protection Agency, EPA 402-K-01-003, October 2001.

[2] Google Forms: http://www.google.com/forms/

[3] ASHRAE (2013). "Thermal Environmental Conditions for Human Occupancy", ANSI/ASHRAE Standard 55-2013, American Society of Heating, Refrigerating and Air-Conditioning Engineers, Inc., Atlanta, Georgia.

[4] ASHRAE (2016). "Ventilation for Acceptable Indoor Air Quality", ANSI/ASHRAE Standard 62.1-2016, American Society of Heating, Refrigerating and Air-Conditioning Engineers, Inc., Atlanta, Georgia.

[5] F.C. McQuiston and J.D. Parker, "Heating, Ventilating, and Air Conditioning: Analysis and Design", John Wiley & Sons, 2004.

[6] H.E. Burroughs, "Filtration: An Investment in IAQ", HPAC Journal, August, Vol.69, No.8, pp,55-65, 1997.

[7] S.M. Hays, R.V. Gobbell, and N.R. Ganick, "Indoor Air Quality: Solutions and Strategies", McGraw-Hill Inc., New York, 1995.

[8] L. Zhijian, Z. Zunqiang, Z. Yexuan, X. Wei, L. Hao, "Investigation of dust loading and culturable microorganisms of HVAC systems in 24 office buildings in Beijing", Energy and Buildings, Vol.103, pp-166-174, September 2015.

[9] M. Meckler, "Improving Indoor Air Quality through Design, Operation and Maintenance", The Fairmont Press, Inc., Lilburn, 1996.

[10] I.M. Budaiwi, "Impact of Combined Dilution and Pressurisation Effects of Ventilation Air on Indoor Contaminant Concentration", Indoor Built Environment,Vol.7, No.5-6, pp.289-299, 1998.

IOSR Journal of Computer Engineering (IOSR-JCE)
e-ISSN: 2278-0661,p-ISSN: 2278-8727, Volume 18, Issue 2, Ver. III (Mar-Apr. 2016), PP 77-81
www.iosrjournals.org

An Efficient Resource Allocation with Adaptive Rate Scheduling For WCDMA Networks

Vandana Khare[1], Dr. Y. Madhavee Latha[2], Dr. D. Sreenivasa Rao[3]
[1]*Associate Prof. –ECE department, CMR College of Engineering & Technology, Hyderabad, India*
[2]*Principal, Malla Reddy Engineering College for Women, Hyderabad, India*
[3]*Professor in ECE Department, JNTUH, Hyderabad, India*

Abstract: *WCDMA is a spread spectrum technique that uses a unique spreading code to spread the data before transmission based on its orthogonal property. WCDMA is mainly used for 3rd generation cellular and mobile networks. In Centralized Call Admission Control (CCAC) technique, when a new call arrives into the system, it checks whether the call should be admitted or not on the basis of signal to interference ratio (SIR) and transmission power in the network. If the call is accepted, it will create some interference to the new arrivals during data transmission and reception. This new interference would degrade the performance of new arrival users. Hence, proper Resource Allocation in the network is very essential to regulate the Real Time traffic with guaranteed quality of service (QoS). At the same time, Scheduling also plays an important role to monitor the Real Time traffic. This paper proposes a novel approach to Resource Allocation with Connection Admission Control (RA-CAC) and Adaptive Rate Scheduling (ARS) scheme to minimize delay by maximum resource utilization for Real time traffic with better QoS. The simulation results show that the proposed scheme can significantly increase packet delivery ratio, throughput & reduce delay.*

Keywords: *ARS, CCAC, QoS, RA-CAC, SIR, WCDMA*

I. Introduction

Wide band Code Division Multiple Access technique uses channels with bandwidth much greater than that of the data to be transferred. Wideband CDMA can support services with higher rate when it is compared with the narrow-band CDMA and it is much more adaptable to distribute multimedia traffic. On the other hand, a new Medium Access Control protocol (MAC) is required to manage packet access efficiently in Wideband CDMA wireless networks [2]. Efficient Call Admission Control (CAC) and Medium Access Control (MAC) protocols are necessary for the QoS provisioning in WCDMA environment. But due to the bursty nature of packet traffic, CAC alone is not enough to provide most optimal resource utilizations [6]. In an integrated multiclass packetized network, efficient utility based CAC is required for providing better quality of service in WCDMA Network for Third Generation (3G) cellular and mobile communication. Radio resources for CDMA networks are mainly related to transmission power, channel rates and the spreading of bandwidth.

In this paper, a Resource Allocation with Connection Admission Control Scheme (RACAC) and an Adaptive Rate Scheduling (ARS) scheme are designed for Real time traffic like voice, video and data. RACAC determines the optimum number of admitted users with marginal utility; so as to minimize the call rejection rate. At the same time, ARS adjusts the rate of the incoming session based on feedback obtained from already admitted sessions.

The rest of the paper is organized as follows: Section II gives the details about the related work. The complete detail about proposed methodology is illustrated in Section III. Next, Section IV gives the result evaluation for the proposed approach. Finally, conclusions are provided in Section V.

II. Related Work

Juan Liu, Wen Chen [1] has presented the major problem for maximizing utility for fair and efficient multicasting in cellular networks. The optimal multicast scheme is developed for two scenarios: Users experiencing nearly equal path losses and different path losses. Especially it has been found that the pure multicast scheme is optimal in the equal path loss. On the other hand, when the users that attempt to receive the same messages are uniformly distributed in a cell, the group multicast scheme should be applied. This result is of group multicast scheme that adapts data transmission rate to the worst case users among a group and it cannot satisfy throughput maximization for all the users distributed in a cell for improving the quality of services. However, the number users should be controlled for better QoS performance.

Bijan Golkar [2] has proposed Resource Allocation in Autonomous cellular Networks and developed a Network Clustering scheme in which scheduling cell is defined by a set of coordinating Base Stations (BS). Proposed approach is that each terminal communicates with only one BS and alternatively each terminal can communicate with more than one BS in the scheduling cell. Resource Allocation across the scheduling cell is

distributed. This means that each scheduling cell is performed without knowledge from previous work. However, Power control is still an area to work thoroughly in case of autonomous cellular networks.

Mohamed Khadim Karry and Yasir khan [3] have proposed Evaluation and Comparison of Resource Allocation strategies for new streaming services in wireless cellular networks. There are two categories of services in wireless cellular networks. In first category, there are variable bit rate (VBR) and constant bit rate (CBR) and in the other category, streaming call (video, voice, broadcast) is given that is used in current generation based on QoS and demand of user. However, there is delay in the scheme.

N. Mohan and T. Ravichandran [4] have proposed to design a new CAC algorithm with power control for multiple services like voice, video and data for multiclass users. It determines the optimum set of admissible users with optimum transmitting power level, so as to minimize the interference level and call rejection rate. In addition to this, an adaptive scheduling scheme to allocate optimum rate for each traffic queue is proposed to minimize the scheduling delay. The proposed algorithms achieve reduced call blocking probability, and optimum rate with reduced delay. However, there is a delay in the scheme.

Rekha Patil and Dr.A.Damodaram [5] have developed a cross-layer based joint algorithm for power control and scheduling. The multiple access problems are solved via two alternating phases, namely scheduling and power control. They introduced the notion of power control as part of a contention-based multiple access protocol that characterizes successful transmissions depending on a set of signal-to-interference-and-noise ratio (SINR) constraints (which directly translates to quality of service (QoS) constraints on the bit-error rate (BER) at individual receivers). The scheduling algorithm is essential to admit the transmission of static as well as mobile users of multi service classes, in order to eliminate strong levels of interference that cannot be overcome by power control. By simulation experiments, they evaluate the performance of their algorithm in a set of admissible and non-admissible users and show that power control algorithm converges for a set of admissible users. However, there is a decrease in the power.

Young-Long Chen et al [6] have proposed a novel approach which combines the CAC and power control mechanisms and operates in a centralized control manner. The essence of the proposed centralized call admission control scheme is to combine the two mechanisms and to treat the call admission decision as an eigen-decomposition problem. In order to reduce the computational complexity of the eigen-decomposition problem, the paper proposes an additional scheme, which uses a norm operation rather than direct computation. The proposed scheme, even with the norm approximation, outperforms conventional call admission methods in terms of both its blocking rate and its outage rate. Consequently, the actual SIR of each link in a neighboring base station may not be guaranteed, with the result that outage may occur.

Tajje-eddine Rachidi et al [7] have presented QaPC and QaHO mechanisms as enabling QoS parameters, which are based on the class of service, the bit rate, and the Service Degradation Descriptor (SDD). They have used bit rate, service class and Service Degradation Descriptor for enabling QoS parameters. The proposed QoS aware mechanism significantly improves QoS contract upholding for premium mobile users, as well as increases resource utilization, while improving SHO acceptance. However, there is overload in the system.

Leonardo Badia et al [8] have proposed a novel optimization technique based on the Logarithmic Barrier Method, which is shown to exhibit a good trade-off between computational complexity and accuracy of the solution. This simple strategy has proven to be fast and efficient. However, for very low SIR, the optimization is very low.

III. Proposed Resource Allocation With Connection Admission Control Algorithm

Consider a WCDMA network with a single downlink and a Base Station (BS). The BS transmits radio signals to a number of member nodes of the network. For the network operation, the time t is indexed by frames of equal length. New incoming sessions representing connections are indexed in the incoming sequence. As the session arrives, record the arrival and calculate the throughput achievement ratio with the help of target throughput and achieved throughput. The CAC considers the session that arrived at time t and represents its utility function but since the utility function is dependent on achievement ratio which is a future function, we have to calculate predicted achievement ratio and allot the resource based on conditions.

3.1 RACAC Algorithm

Step 1: When a new session i arrives, record the $Arrival_i$.

Step 2: Initialize power P_i to get a target throughput $(_TP_i\ _)$ and achieved throughput of session i $(achieved_TP_i)$ is computed.

Step 3: Calculate Achievement ratio Ach_Ratio_i of session i.

Step 4: Based on utility function, calculate predicted Achievement Ratio, $\widetilde{Ach_Ratio_t}$ by Future Target throughput FTP_i.

Step 5: calculate predicted Achievement Ratio $\widehat{Ach_Ratio_t}$ of both the session and consider cumulative.
Step 6: check the following conditions.

If $\widehat{Ach_Ratio_t} \geq 1$, Go to step 1 and assign a rate increment including new session.
Else if
$\widehat{Ach_Ratio_t} < 1$, then
Assign a power increment for both the sessions.

Step 7: If $TP_i = FTP_i$ or ≥ 0, Go to step 1 and admit the new sessions .
Else if
new arrival is blocked and Go to step 3.

3.2 Adaptive Rate Scheduling (ARS)

A heuristic based feedback control unit (FCU) is present in the network, which records all the information related to the session rate of every session. On the basis of the rate of the operating sessions, the rate of the incoming sessions is adjusted.

3.2.1 ARS algorithm

1. The average scheduling delay of the session *i* is estimated from the first session admitted into the network.
2. The FCU determines the sessions whose average delay is greater than or lesser than the threshold delay.
3. If $D_{avg}(i) > D_{threshold}(i)$, then it indicates that an error has occurred during session operation with greater probability and session i has degraded as a result of the improper assignment
4. If $D_{avg}(j) < D_{threshold}(j)$, then FCU preempts all the sessions with $i \neq j$.
5. Preemption is conducted by sending the rate information as a feedback to the CAC so that the rate allocation can be performed according to the new incoming session.

IV. Simulation Results

In this section, proposed Resource Allocation with Connection Admission Control (RACAC) scheme and Adaptive Rate Scheduling scheme (ARS) are simulated for Real-time Traffic in WCDMA networks using an NS-2 simulator.

4.1 Based on Number of Users

In our first experiment, we vary the ratio of the number of users 1, 2, 3…6 to the packet delivery ratio from 0 to 1.2. From Figure 1, it can be observed that the proposed RACAC scheme has 34% more delivery ratio, when compared to the CCAC scheme.

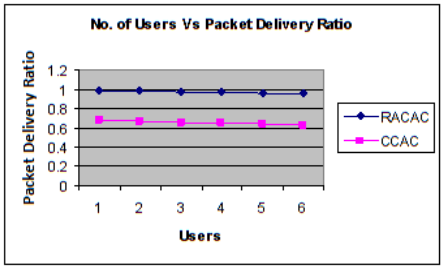

Fig.1. No. of users vs. Packet delivery ratio

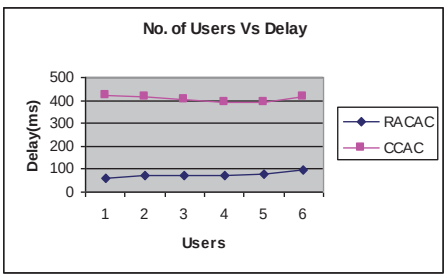

Fig.2. No of users vs. Delay

With the help of Figure 2, it is clear that the proposed RACAC Scheme attains 80% less delay, when compared to the CCAC scheme.

4.2 Results of RACAC-ARS scheme

The RACAC-ARS technique is compared to the Centralized Call Admission Control and Fixed rate Scheduling (CCAC-FS) scheme. By having a look at Figure 3, it is clear that RACAC-ARS scheme attains a higher delivery ratio, when compared to the CCAC-FS scheme.

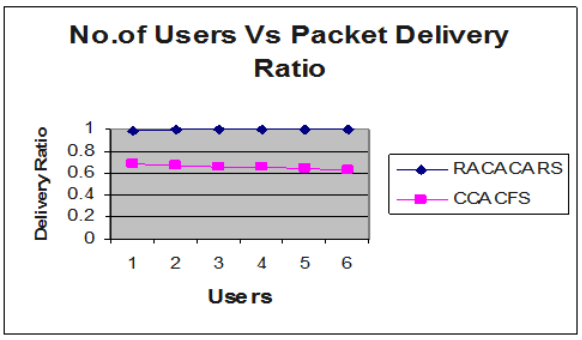

Fig.3. Users vs. Packet delivery ratio

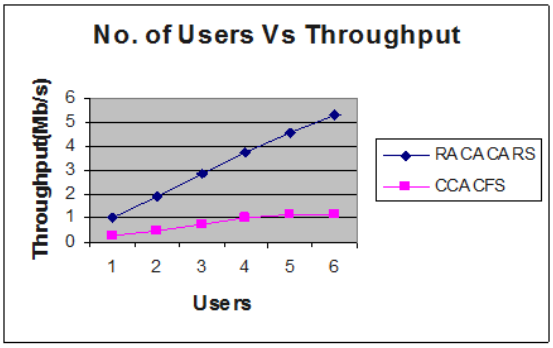

Fig.4. No of users vs. Throughput

Similarly, the average throughput shown in Figure 4 can help us observe that the RACAC-ARS scheme attains a higher throughput than CCAC-FS, when the number of users is increased.

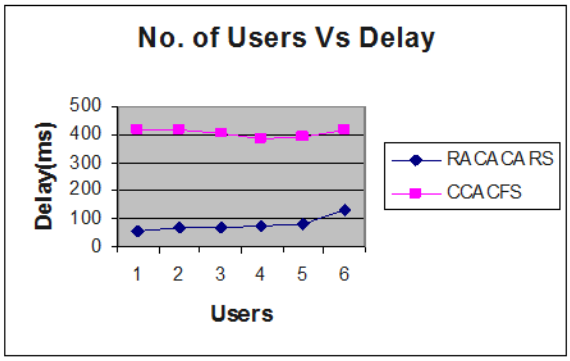

Fig.5. Users vs. Delay

Similarly, the average delay shown in Figure 5 tells us that the RACAC-ARS scheme attains a lesser delay than the CCAC-FS scheme.

V. Conclusion

In this work, the Resource Allocation with Connection Admission Control Scheme maximizes the throughput by proper resource allocation in the WCDMA networks and the Adaptive Rate Scheduling scheme dynamically adapts rates based on the feedback obtained from existing sessions. The proposed scheme keeps the call dropping probability below the threshold level while maintaining higher system reliability. We observed that during simulation, Resource Allocation with CAC and Adaptive Rate Scheduling provide an efficient throughput & a lesser delay in the network. A power control part that manages interference is still remaining out of this research work, and a hand off in WCDMA network will definitely be worked out in future.

References

[1]. Juan Liu, Wei Chen,Member, Ieee, Yingjun Zhang, Seniormember, Ieee, And Zhigang Cao, Senior Member, Ieee, A Utility Maximization Framework For Fair And Efficient Multicasting In Multicarrier Wireless Cellular Network**,** Ieee/Acm Transactions On Networking, Vol. 21, No. 1, February 2013.

[2]. Bijan Golkar,Student Member, Ieee And Elvino S.Sousa,Fello,Ieee ,Resource Allocation In Autonomous Cellular Networks**,** Ieee Transactions On Wireless Communication,Accepted For Publication In 2013.

[3]. Mohamed Kadhem Karray,Yasir Khan(2012) "Evaluation And Comparison Of Resource Allocation Strategies For New Streaming Services In Wireless Cellular Networks", Ieee Transaction On Communications Vol12,No.3 January 2012.

[4]. N. Mohan And T. Ravichandran, "An Efficient Multiclass Call Admission Control And Adaptive Scheduling For Wcdma Wireless Network", European Journal Of Scientific Research 33.4 (2009).

[5]. Rekha Patil And Dr.A.Damodaram, "Joint Scheduling And Power Control For Multiclass Users In Cdma Wireless Ad Hoc Networks", Wseas Transactions On Communications (2008).

[6]. Young-Long Chen, Jyu-Wei Wang, Jyh-Liang Chen And Jyh-Horng Wen, "Performance Of Call Admission Control With Power Control In Multimedia Cellular Systems", International Journal Of Applied Science And Engineering 5.1 (2007).

[7]. Tajje-Eddine Rachidi, Amal Yasmine Elbatji, Mehdi Sebbane And Hicham Bouzekri, "Qos-Aware Power Control And Handoff Prioritization In 3g Wcdma Networks", Wireless Communications And Networking Conference, 2004. Wcnc. 2004 Ieee. Vol. 2. Ieee, 2004.

[8]. Leonardo Badia, Adriana Telesca And Michele Zorzi, "On The Network Utility Optimal Allocation Of Radio Resources In Wcdma Systems", Ieee Communications Letters, Vol. 10, No. 5, May 2006.

Mrs. Vandana Khare is pursuing PhD in Communication Engineering from JNTU, Hyderabad (T.S). She completed M.E (Digital techniques) in 1999 from SGSITS, INDORE (M.P), India and B.E in ECE in the year 1994 from GEC Rewa (M.P). She is working as Associate Professor in ECE at CMR College of Engineering, Secunderabad (TS) since 2014. She has 17 years of teaching experience. She has published 13 research papers in International journals & presented 05 papers in National & International conferences. She is a life member of ISTE & IETE Technical societies. Her research interests include computer networks, mobile computing and Bio-medical imaging.

Dr .Y. Madhavee Latha is presently working as Principal at MRECW, Secunderabad. She received PhD (Signal Processing) from JNTU, Hyderabad. She has more than 15 years of experience in the field of teaching. She contributed various research papers in journals & Conferences of national as well as international repute. Her areas of interest include multimedia systems, communication & signal processing. She is a senior member of ISTE, IETE & IEEE technical societies.

Dr. D. Sreenivasa Rao received the B Tech degree (ECE) from Nagarjuna University in 1986, M.E (Digital Systems) from Osmania University in 1994 and PhD (Computer Communication Networks) from University Of Hyderabad In 2004. His Research Interest I The Area Of Communication And Computer Networks. Presently, 12 Research Students Are Working Under His Guidance. He Has 22 Publications In Various National, International Conferences And Generals. He Has 23 Of Teaching Experience and Had Worked At CBIT As A Lecturer In The ECE Department for 6 Years During 1988 – 1994. He Worked At ECE Department Of JNTU Ananthpur In Various Capacities For 11 Years During 1994-2005 Presently, He Is Working As A Professor In The ECE Department If JNTUCE, Hyderabad. He Has Chaired A Sessions At Various National Conferences. He Is An Advisory Comity Member For GNIT, Hyderabad. He Is Also A Governing Body Member For Syed Hashim College Of Science And Technology, Member Of JNTY Forum For Science And Society And A Co-Ordinator For Campus Networking At JNTUCE, Hyderabad.

Volume 6, Issue 10, October 2016 ISSN: 2277 128X

International Journal of Advanced Research in Computer Science and Software Engineering

Research Paper

Available online at: www.ijarcsse.com

Performance Analysis of QOS Aware Fault Tolerant Multipath Routing Protocol in Mobile Ad Hoc Networks

[1]M. Bheemalingaiah, [2]M. M. Naidu, [3]D. Sreenivasa Rao, [4]P.Vishvapathi

[1] Research Scholar, Department of CSE, J.N.T. University, Anantapur, Andhra Pradesh, India

[2] Senior IEEE Member, Retired Professor, Department of CSE, S.V. University, Tirupati, Andhra Pradesh, India

[3] Professor, Department of ECE, J·N.T University, Hyderabad, Telagana, India

[4] Principal, Ellenki College of Engineering & Technology, Hyderabad, Telagana, India

Abstract: ***With the advance of wireless communication technologies, small-size and high-performance computing and communication devices like commercial laptops and personal digital assistants are increasingly used in daily life. After the success of second generation mobile systems, more interest was started in wireless communications. This interest has led to two types of wireless networks: infrastructure wireless network and infrastructure less wireless network, it is also called Mobile Ad hoc Network (MANET). The Mobile Ad Hoc Networks are essentially suitable when infrastructure is not present or difficult or costly to setup or when network setup is to be done quickly within a short period. They are very attractive for tactical communication in the military and rescue missions. The Mobile Ad Hoc Networks (MANETs) are also expected to play an important role in the civilian fora as convention centers, conferences and electronic classrooms. Many such applications require Quality of Service (QoS) guarantees. These applications are extremely delay-sensitive and need high packet delivery ratio. However, certain factors limit the ability of the Mobile Ad Hoc Network to achieve the desired goals. These factors include the delay caused by network congestion, limited bandwidth, limited energy of the nodes, packet loss due to collisions and link failure. Multipath routing can be used in On-demand routing to achieve faster and efficient recovery from route failures in highly dynamic Mobile Ad Hoc Network. In this we have chosen QOS Aware Fault Tolerant Multipath Routing (QOS FTMR) protocol to analyze its performance w.r.t performance of the AOMDV protocol by using various quantitative performance metrics like throughput, packet delivery ratio, end-to-end delay, overhead, packet loss and energy consumption by varying various parameters like network's size, node's speed, node's pause time, data rate and number of source and destination pairs.***

Key words: MANET, QOS FTMR, AOMDV, Bandwidth.

I. INTRODUCTION

Mobile Ad hoc Network (MANET) is a wireless network without any fixed infrastructure or centralized control. Mobile Ad Hoc Networks are considered as autonomous, self-configured, multi-hop wireless networks. They don't rely on any stationary infrastructure; no centralized control and they are quickly deployable anywhere at any time. In the MANET, all nodes are mobile that cooperate in friendly manner and they are connected dynamically in an arbitrary manner. Each node behaves as a router, it takes part in discovery and route maintenance and mobile nodes have the ability to leave existing nodes from the network and enter new nodes into the network at any time and due to this the topology of the MANET is highly dynamic and it frequently changes.

They are very attractive for tactical communication in the military and natural disasters like earthquake, flood, tsunami, fire and emergency services. The main characteristics of the MANET are dynamic topology, bandwidth constrained, variable capacity links, energy constrained operation [1].

A) Advantages and Applications of Mobile Ad Hoc Networks

1) *Low cost of deployment:* Mobile Ad-Hoc Networks can be deployed on the fly; they don't require any expensive infrastructure such as copper wires, data cables, etc or not any central administration to support the network.
2) *Fast deployment:* They are very convenient and easy to deploy, when it compared to WLANs, because it requires less manual intervention.
3) *Dynamic Configuration*: Configuration of Mobile Ad-Hoc Networks changes dynamically with time.

The Mobile Ad Hoc Networks has various potential applications in various fields. The following are some well-known applications [1][2] of MANET.

Military

- Automated battlefield
- Special operations
- Homeland defense

© 2016, IJARCSSE All Rights Reserved

Civilian

- Disaster Recovery(flood, fire, earthquakes etc)
- Law enforcement (crowd control)
- emergency operation it includes search and rescue in remote areas
- Environment monitoring (sensors)
- Space/planet exploration

Commercial

- Sport events, festivals, conventions
- Patient monitoring
- Ad hoc collaborative computing (Bluetooth)
- Sensors on cars (car navigation safety)
- Vehicle to Vehicle communications
- video games at amusement parks, etc

B) QOS AND Routing in MANET

Quality of service (QoS)[1][2] is the performance level of a service offered by the network to the user. The goal of QoS provisioning is to achieve a more deterministic network behavior, so that information carried by the network can be better delivered and network resources can be better utilized. A network or a service provider can offer different kinds of services to the users. Here, a service can be characterized by a set of measurable prespecified service requirements such as minimum bandwidth, maximum delay, maximum delay variance (jitter), and maximum packet loss rate. After accepting a service request from the user, the network has to ensure that service requirements of the user's flow are met, as per the agreement, throughout the duration of the flow (a packet stream from the source to the destination). In other words, the network has to provide a set of service guarantees while transporting a flow.

The routing is the most active research field in the MANET. The routing protocols designed for wired networks are not suitable for wireless networks due to the node mobility issues in wireless networks. The different protocols are proposed to deal with routing problem in the MANET. These routing protocols can be classified into two main categories: Table driven routing protocols and on demand routing protocols [3]. Minimizing the number of hops is no longer the objective of a routing algorithm, but rather the optimization of multiple parameters such as packet error rate, energy consumption, bandwidth, routing overhead, route setup, route repair speed and possibility of establishing parallel routes etc. Developing routing protocols for MANETs has been an extensive research area during the past few years. In particular, QOS routing is the most important design criteria for MANETs [1][3]. Most existing ad hoc routing protocols build and utilize only one single route for each pair of source and destination nodes. Due to node mobility, node failures, and the dynamic characteristics of the radio channel, links in a route may become temporarily unavailable, making the route invalid. The overhead of finding alternative routes may be high and extra delay in packet delivery may be introduced. Multipath routing addresses this problem by providing more than one route to a destination node. Source and intermediate nodes can use these routes as primary and backup routes. Alternatively, the traffic can be distributed among multiple routes to enhance transmission reliability, provide load balancing and secure data transmission [3]. Multipath routing effectively reduces the frequency of route discovery therefore the latency for discovering another route is reduced when currently used route is broken. Multipath routing appears to be a promising technique for ad hoc routing protocols. Providing multiple routes is beneficial in communications, particularly in the MANETs where routes become obsolete frequently because of mobility and poor wireless link quality. Multiple paths can be useful in improving the effective bandwidth of communication, responding to congestion and heavy traffic, and increasing delivery reliability [2].

In the wired networks, source-destination pair remains fixed during a transmission session and thus a virtual circuit can be created. Hence the resources are strictly reserved. The packet delay and packet delivery ratio are guaranteed during a session holding time, providing what is called **Hard QoS** [3][4]**.** However, the hard QoS cannot be applied to the MANETs, because resources cannot be guaranteed during a data transmission session due to the unstable links, unreliable wireless channel and unguaranteed resources

C) Issues and challenges in providing QoS in Mobile Ad Hoc Networks

Providing QoS support in MANETS is an active research area. MANEs have certain unique characteristics that pose several difficulties in provisioning QoS[1][2]. A detailed discussion on how the characteristics of MANETs affect QoS provisioning is given below:

1) Dynamically varying network topology: Since the nodes in an ad hoc wireless network do not have any restriction on mobility, the network topology changes dynamically. Hence the admitted QoS sessions may suffer due to frequent path breaks, thereby requiring such sessions to be re-established over new paths. The delay incurred in re-establishing a QoS session may cause some of the packets belonging to that session to miss their delay targets/deadlines, which is not acceptable for applications that have stringent QoS requirements.

2) Imprecise state information: In most cases, the nodes in an ad hoc wireless network maintain both the link-specific state information and flow-specific state information. The link-specific state information includes bandwidth, delay, delay jitter, loss rate, error rate, stability, cost, and distance values for each link. The flow specific information

© 2016, IJARCSSE All Rights Reserved

includes session ID, source address, destination address, and QoS requirements of the flow (such as maximum bandwidth requirement, minimum bandwidth requirement, maximum delay, and maximum delay jitter). The state information is inherently imprecise due to dynamic changes in network topology and channel characteristics. Hence routing decisions may not be accurate, resulting in some of the real-time packets missing their deadlines.

3) Lack of central coordination*:* Unlike wireless LANs and cellular networks, MANETs do not have central controllers to coordinate the activity of nodes. This further complicates QoS provisioning in MANETs do not have central controllers to coordinate the activity of nodes. This further complicates QoS provisioning in MANETs.

4) ***Error prone shared radio channel:*** The radio channel is a broadcast medium by nature. During propagation through the wireless medium the radio waves suffer from several impairments such as attenuation, multi-path propagation, and interference (from other wireless devices operating in the vicinity). The wireless channel is error-prone due to multi-path fading, shadow fading, path loss and other factors, this resulting in unreliable communication.

5) Hidden terminal problem: The hidden terminal problem is inherent in MANETs. This problem occurs when packets originating from two or more sender nodes, which are not within the direct transmission range of each other, collide at a common receiver node. It necessitates retransmission of packets, which may not be acceptable for flows that have stringent QoS requirements.

6) Limited resource availability*:* Resources such as bandwidth, battery life, storage space, and processing capability are limited in MANETs. Out of these, bandwidth and battery life are very critical resources, the availability of which significantly affects the performance of the QoS provisioning mechanism. Hence efficient resource management mechanisms are required for optimal utilization of these scarce resources.

7) Unguaranteed resources: The channel resources are shared among nodes in the MANETs. No centralized resource allocation is used in the MANETs and thus resource sharing is based on competition and coordination among hosts. Therefore, resources cannot be strictly guaranteed. Hence it is another challenging issue for resource reservation in MANETs

8) Insecure medium**:** Due to the broadcast nature of the wireless medium, communication through a wireless channel is highly insecure. Hence security is an important issue in MANETs, especially for military and tactical applications. MANETs are susceptible to attacks such as eavesdropping, spoofing, denial of service, message distortion, and impersonation. Without sophisticated security mechanisms, it is very difficult to provide secure communication guarantees.

Hence the ***Soft QoS*** or better than best effort is proposed to meet the characteristics of the MANETs[1][3]. The Soft QoS is defined such that a transient time when QoS is not met is allowed during network partitions or when routing failures occur. To support the Soft QoS, any bandwidth reservation scheme should be designed to meet the Soft QoS requirements. The applications requiring QoS support are mostly real-time applications. The minimum bandwidth is used to deliver the video and audio packets. Both admission control and adaptive feedback service are required in the QoS support design.

D) The following are the basic design issues for QoS-aware routing protocols

1) Bandwidth Estimation: To offer a bandwidth-guaranteed route, the key idea is to obtain information about the available bandwidth from lower layers. This bandwidth information helps in performing call admission and QoS adaptation [2] [3]. In the MANET nodes share the bandwidth with their neighbor nodes, and thus the bandwidth available to a node is a dynamic value that is affected by its neighbors' traffic. Therefore, the two key problems in bandwidth estimation are how exactly to estimate the available bandwidth and how frequently to do the estimations. Also, the trade-off between the benefit from using bandwidth estimation and the cost in terms of packet overhead and computing resources used for bandwidth estimation is another key issue[2][3].

2) Route discovery: There are two main approaches to routing in the MANET: reactive routing and proactive routing. The reactive routing reduces overhead at the expense of delay in finding a suitable route, whereas the reverse is true for proactive routing. For QoS-aware routing, another issue is determining what combination of reduced latency and reduced overhead is best for supporting QoS[2][3].

3) Resource reservation: The bandwidth resources are shared by neighboring hosts in the MANET. Therefore, another challenging issue is how to allocate this shared resource and what type of resource reservation scheme should be used for setting up and maintaining the QoS-aware route[[2][3].

4) Route maintenance: The mobility of nodes in MANETs causes frequent topology changes in the network, making it difficult to meet the QoS constraints. Incorporating a fast route maintenance scheme into QoS-aware routing is the design consideration. The typical approach to route maintenance, which entails waiting for the host to discover a route break, significantly affects the routing performance. Therefore, some prediction scheme or redundant routing is necessary to assist in route maintenance [2] [3].

5) Route selection: QoS-aware routing has more stringent requirements on route stability, since frequent route failures will adversely affect the end-to-end QoS. Thus, in some sense the path with the largest available bandwidth is not only the consideration but also path reliability should also be considered when selecting a suitable path for a QoS-aware routing protocol [2l[3].

E) QoS parameters

QoS parameters differ from application to application [1][2]. For example, for multimedia applications, the data rate and delay are the key factors, whereas, in military use, security and reliability become more important. If considering

© 2016, IJARCSSE All Rights Reserved

QoS required by emergency cases such as rescue, the key factor should be the availability. In sensor networks, battery life and energy conservation would be the prime QoS parameters [1][2]. The QoS parameter considered here is aimed to real time applications. In real time applications, QoS requests can be expressed in term of many metrics in routing protocols. The most popular metrics are data rate and delay. To satisfy QoS requirements, the corresponding available data rate and delay that could be provided by the network of each route should be calculated in order to see which route could be used with satisfying QoS. As a result, we will see how available data rate and delay are calculated.

F) Classification of generally used QOS metrics

The QoS metrics can be classified into three categories [1][2]. They are additive metrics, concave metrics, and multiplicative metrics. Additive metrics is defined as sum of the value of the metric on all links along the path. Delay and jitter are additive metrics. Delay along the path is the sum of the delay at every link along the path. A concave metric means the minimum metric value over a path. Metric value on every link along the path is taken into account. The minimum metric value stands for the metric value of the whole path. Data rate is a concave metric. The minimum data rate of all the links along the path should be the data rate of this route. A multiplicative metric represents the product of the metric values on all links over a path. The criteria of reliability or availability of one link, e.g. link outage probability is a multiplicative metric. The generally used metrics for real time applications are data rate, delay, delay variance (jitter), and packet loss. Two of the most important ones are data rate and delay. They will be discussed in detail in the following sections. The QoS is an agreement to provide guaranteed services, such as bandwidth, delay, jitter and packet delivery rate to users[3][4]. Supporting more than one QoS constraint makes the QoS routing problem NP-complete.

II. RELATED WORK

Ongoing research activities in the area of QOS have targeted different layers of the network protocol stack. However, most such research has been targeted at the MAC layer, network layer and transport layer. Developing core protocols at different layers is an area of extensive research in the past few years. Here, we discuss the related work at network layer.

The several proactive routing protocols were developed. These protocols use table-driven algorithms (link state or distance vector) to compute multiple routes. But these protocols generate excessive routing overhead and perform poorly in mobile networks because of their proactive nature. The on-demand routing is the most popular approach in the MANET. Instead of periodically exchanging route messages to maintain a permanent route table of the full topology, the on-demand routing protocols build routes only when a node needs to send the data packets to a destination. The standard protocols of this type are the Dynamic Source Routing (DSR)[6] and the Ad hoc On-demand Distance Vector (AODV)[7]routing protocol.

The much work has been done on single path on-demand protocols that offer QoS at network layer, some of them are the Ticket-based QoS Routing is a distributed protocol that uses tickets to find delay-constrained or bandwidth-constrained routes [8]. The OLSR-based QoS Routing integrated QoS features into the Optimized Link State Routing (OLSR) protocol to find a path with larger bandwidth [9]. The Ad Hoc QoS On-demand Routing **(**AQOR)[10] has the features like available bandwidth estimation, end-to-end delay measurement, bandwidth reservation and adaptive route recovery. QoS Routing protocol tries to provide soft QoS or better than best-effort service for a bandwidth constraint, rather than guaranteed hard QoS[11].

The several multipath on-demand routing protocols were proposed. The extension explores alternate, disjoint routes that can be useful in case the primary route breaks. Some of the standard protocols are Ad hoc On-demand Multipath Distance Vector (AOMDV)[12] is an extension to the AODV[7] protocol for computing multiple loop-free and link-disjoint paths. The Split Multipath Routing (SMR)[13] is an on-demand Multipath source routing protocol that builds multiple routes using a request/reply cycle, it can find an alternative route that is maximally disjoint from the source to the destination. The Multipath Source Routing (MSR) [14] is an extension of the on-demand DSR [6] protocol to distribute traffic among multiple routes in a network. The Ad hoc On-demand Distance Vector Multipath Routing (AODVM)[15] is an extension to AODV [7] for finding multiple node disjoint paths. These protocols build multiple routes based on demand but they did not consider the QOS metrics.

Recently, several On-demand multipath routing protocol have been developed to support QOS, Split Multipath Routing with Maximally Disjoint Path Protocol [16] establishes and utilizes multiple routes of maximally disjoint paths. Providing multiple routes helps minimizing route recovery process and control message overhead. The protocol uses a per-packet allocation scheme to distribute data packets into multiple paths of active sessions. This traffic distribution efficiently utilizes available network resources and prevents nodes of the route from being congested in heavily loaded traffic situations. A QoS-aware Multi-path Dynamic Source Routing Protocol (MP-DSR)[17] focusing on a new QoS metric, end-to-end reliability. End-to-end reliability is used to reflect the probability of sending data successfully from the source node to the destination node within a time window. MPDSR does not provide strict end-to-end reliability guarantees, rather it provides soft QoS guarantees with respect to end-to-end reliability by discovering a set of multiple disjoint paths and transmitting data along these paths. MP-DSR is based on the existing Dynamic Source Routing protocol (DSR) [5] and takes advantage of its distributed on-demand nature. Multi-Path QoS Routing Protocol[18] is an on-demand protocol for a multi-path QoS route from a source host to a destination host in a MANET, where a multi-path is a network with a source and a sink satisfying certain bandwidth requirement. The basic idea is to distribute a number of tickets from the source, which can be further partitioned into sub tickets to search for a satisfactory multi-path. So no global information will be collected in advance before a QoS route is required. A mobile host only knows the available

© 2016, IJARCSSE All Rights Reserved

bandwidth to each of its neighbors. When a source node S needs a route to a destination D of bandwidth B, it will send out some probe packets each carrying some tickets. Each ticket is responsible of searching for a multi-path from the source to the destination with an aggregated bandwidth equal to B.

An Adaptive QoS Routing Protocol with Dispersity for Ad-hoc Networks (ADQR)[19]which is a bandwidth constrained multiple path on-demand routing protocol for ad-hoc networks to support end-to-end Quality of Service. ADQR is a source- initiated on-demand routing protocol consisting of two phases namely the route discovery phase and the route maintenance phase. The protocol uses signal strength for route discovery. The route discovery mechanism is based on request-reply operations. In the route discovery phase, ADQR finds multiple disjoint paths with network resource information using retransmission scheme. On Demand Link State Multipath QoS Routing Protocol [20] reactively collects link-state information from source to destination, and aims to dynamically construct a partial network topology which is only sketched from source to destination. Therefore the protocol finds multi-path routes at the destination under the CDMA-over-TDMA channel model which satisfies a given bandwidth requirement. A unipath is found from source to the destination and then the destination accurately determines a QoS multipath routing and replies to the source host. This greatly improves the success rate by means of searching the QoS multi-path routing.The Interference-aware multipath routing protocol (IMRP)[21] was designed for real-time or multimedia applications in ad hoc wireless networks. IMRP is a source-initialized, on-demand multipath routing protocol. With available bandwidth pre- evaluation and Interference susceptibility, IMRP reduces the call dropping rate and improves the QoS stability. A Novel QoS in Node-Disjoint Routing [22] which provides QoS support for MANETs. NDMR has two novel aspects: it reduces routing overhead and achieves multiple node-disjoint routing paths. It is an extension of AODV[7] protocol. It includes the path accumulation feature of DSR [6] in route request packets. It can efficiently discover multiple paths between source and destination nodes with low broadcast redundancy and minimal routing latency. The QoS Supporting Multipath Routing Protocol (Q-AOMDV)[23] is ad hoc on-demand multipath routing protocol which provides quality of service (QoS) supports in terms of bandwidth, hop count and end-to-end delay in mobile ad hoc networks(MANET). The protocol uses path preference probability that is calculated by delays, bandwidth, and hop-count to select the path to transmit the packet. The Multi-path Failure-tolerant Security-aware QoS Routing (MuSeQoR) [24] tackles the twin issues of reliability (protection against failures of multiple paths) and security, while ensuring minimum data redundancy.

The Delay Aware AODV-Multi-path routing [25] is based on AODVM[15] routing protocol to find node disjoint multipath and uses end-to-end delay, instead of hop count, as metric for route selection. Multiple paths, together with the end-to-end delay provided by each path, are stored in routing tables. Upon route failure, the route table is first searched for an alternative route to the destination before a new route discovery process is initiated. This reduces both routing overhead and end-to-end packet delay. None of the above existing QOS-On demand multipath routing protocol considers efficient bandwidth estimation method to select optimal paths to support QOS. To overcome come this drawback, QOS Aware FTMR protocol [26] was designed that uses novel approach that focuses on exploring different way to estimate the available bandwidth and incorporating a QoS-aware scheme into AOMDV [12] protocol by using two important QOS metrics bandwidth and load. It selects the QOS aware link-disjoint multipath from source to destination based on application QOS requirement.

III. QUALITY OF SERVICE AWARE FAULT TOLERANT MULTIPATH ROUTING (QOS FTMR) PROTOCOL

In this section we describe QOS FTMR [26] by default it means that QoS aware FTMR. The Ad hoc On-demand Multipath Distance Vector (AOMDV[12] is one of the standard protocol multipath routing protocol and it an extension to the AODV[7] protocol for computing multiple loop-free and link-disjoint paths. But it is not suitable for proving QOS. The QOS FTMR [26] is extension of AOMDV [12] to find bandwidth and load aware link disjoint paths from source to destination by doing some modifications. There are mainly two types of disjoint paths: node-disjoint and link-disjoint. The Node-disjoint paths do not have any nodes in common. Link-disjoint paths usually guarantee links fail independently except the case when multiple links connect to a node fail together as this node moves out of transmission range.

The following are the main functions of QOS FTMR

- Estimation load of node
- Bandwidth Estimation using Hello Messages
- Route Discovery and Bandwidth Reservation
- Route Selection
- Route Maintenance

A) Node's load

In order to calculate the high throughput path among the existing paths from source to destination, we considered load and delays of total path. If the distance increases delay also increases [29].

1) Delay on Transmission: Nodal processing involves four types of delays namely processing delay, propagation delay, queuing delay, and delay for transmission:

a) Processing Delay (DP): When a packet arrives (with all its bits), processing delay is the time consumed to determine the packet header and examine where it should be directed. After processing, the router directs the packets to the queue. This delay is usually in microseconds (μs).

© 2016, IJARCSSE All Rights Reserved

b) Queuing Delay (DQ): Queuing delay is the waiting time in the queue for a packet before it transmits onto a link. The queuing delay of a specific packet will depend on the number of earlier-arriving packets that are queued and waiting for transmission across the link. It is usually of the order milliseconds (ms). In the present work, we consider average queuing delay in our computations

c) Transmission Delay (DT): The amount of time required to push (i.e., transmit) all of the packet's bits onto the link is called as transmission delay. This includes the addition of current router information apart from sending acknowledgement signal from current router to the parent router/ downstream router on successful transmission.

d) Propagation Delay (DG): The time required to propagate from the end of the downstream router to the upstream router is called as propagation delay. It is usually of the order milliseconds. So, the total nodal delay is given by:

$$TND = DP+DQ+DT+DG$$

Each of the above delay has a considerable impact on packet transmission. A large processing delay keeps the buffer empty for most of the time; and a large transmission delay fills the queue and subsequently the packets (upcoming) may be lost due to unavailability of bandwidth. Queuing delay is maximum for a proper path selected and minimized for the best path selected. In this work, our focus is more on queuing delay as other delays are mostly hardware dependent.

2. Load: The QOS FTMR [26], each node estimates its current load it is used in the routed discovery and route selection. If the node heavily loaded, it is called congested node. Since congestive phenomena can cause data loss, large delays in data transmission, and a large variance in these delays, controlling or avoiding congestion is a critical problem in networks management and design. Hence traffic management in computer networks becomes essential. It can be done with the help of queue management schemes to provide the congestion control, congestion avoidance and fair bandwidth allocation at the router [27].In the MANET, each node maintains an interface queue of packets. If packets are waiting in interface queue more than 30 sec, then they will be dropped. All packets from the routing layer are queued at the *interface queue* waiting for MAC layer to transfer. The interface queue is FIFO with simple priority, i.e., control packets have higher priority and will be put in the front of the queue. The size of the queue is usually 50 packets. The priority scheduling gives high priority to control packets. In this work node's load is considered as follows the, the queue status of node n_i at time t is shown in fig. 1.

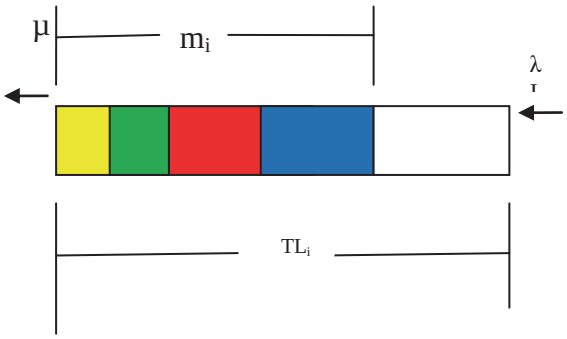

Fig.1. Queue Q_i of node n_i

Where λ is the packet arrival rate, μ is the service rate; T_i is the total size of queue Q_i in terms of bytes. m_i is the total size of all packets present in queue Q_i at time t in terms of bytes. The load of node n_i at time t is equal to

$$L^t(n_i) = m_i \qquad (1)$$

To find load of path there is need to find number of packet is in queue for every node who are participating in route selection algorithm. When RREP packet is forwarded to source node during route discovery process this packet keep record of every node load and add to its path load. When this RREP packet reaches to source, it read this value and select path having low load for route establishment as sending data packet to lightly loaded path.

B) Bandwidth Estimation Using HELLO Messages

The QoS-aware routing protocol that either provides feedback about the available bandwidth to the application (feedback scheme), or admits a flow with the requested bandwidth (admission scheme). Both the feedback scheme and the admission scheme require knowledge of the end-to-end bandwidth available along the route from the source to the destination. Thus, bandwidth estimation is the key to supporting QoS[4][5]. In QOS FMTR [26] each node estimates its current available bandwidth [26]. It is used in the route discovery and route selection. The bandwidth estimation is most important to provide QoS in MANET, the nodes share the bandwidth with their neighbors and thus the bandwidth available to a node is a dynamic value that is affected by its neighbors' traffic. Therefore, the two key problems in bandwidth estimation are how exactly to estimate the available bandwidth and how frequently to do the estimations. Also, the trade-off between the benefit from using bandwidth estimation and the cost in terms of packet overhead and computing resources used for the bandwidth estimation is another key issue. A node's available bandwidth is not only decided by the raw channel bandwidth, but also by its neighbor's bandwidth usage and interference caused by other sources, each of which reduces a node's available bandwidth for transmitting data. However, the bandwidth estimation is extremely difficult, because each node has imprecise knowledge of the network status and links change dynamically.

© 2016, IJARCSSE All Rights Reserved

Therefore, an effective bandwidth estimation scheme is highly desirable. The bandwidth estimation can be done using various methods, in this work the following efficient technique was used for estimation of bandwidth, which in turn induces only little bit overhead and does not take any extra time

To know the frequency reuse pattern, we first study the underlying IEEE 802.11 MAC. As defined in the IEEE 802.11 MAC, the nodes are allowed to access the wireless channel when the media is free. The media can be free if no nodes are transmitting packets within the interference range. Normally, the interference range is twice the transmission range, based on the settings of the Lucent WaveLAN card. Therefore, the frequency can be reused outside of the second neighboring node's range. The actual upper bound of the bandwidth in the two-hop circle varies with the topology and the traffic status, but the raw channel bandwidth is the soft upper bound of total bandwidth[4][5]. It uses soft upper bound bandwidth in the estimation to approximate the bandwidth usage. With the above frequency reuse pattern, it can simplify the bandwidth calculation problem for determining the residual bandwidth within the two-hop neighborhood range. Therefore, each node can approximate its residual bandwidth information based on the information from nodes within two-a hop (the interference range) is shown in fig.2.

Let λ be the total raw bandwidth of wireless channel c, Let BW(η^t_i) be the total available (residual) bandwidth of n_i at time *t*. Let $D^{'}_t(n_i)$ be the set of all one hop (first) neighbors of n_i, its first degree is denoted by $|D^{'}_t(n_i)|$. Let $D^{''}_t(n_i)$ be the set of all two hop neighbors of n_i, its second degree is denoted by$|D^{''}_t(n_i)|$. The n_i and its one hop and two hop neighbors will share the wireless channel *c*. so the total of $|D^{'}_t(n_i)|+|D^{''}_t(n_i)|+1$ nodes will share the bandwidth of wireless channel c.For example in Fig.2. one hop neighbors of *A* are *B*, *C* and *D* so $D^{'}_t(A)=\{B,C,D\}$, Two hop neighbors of *A* are *E* and *F* so $D^{''}_t(A)=\{E,F\}$, Once a node knows the bandwidth consumption of its first neighbors and second neighbors, the available bandwidth estimation becomes simple. The residual bandwidth is simply the raw channel bandwidth minus the overall consumed bandwidth, divided by a weight factor F. It needs to divide the residual bandwidth by a weight factor due to the IEEE 802.11 MAC nature and some overhead required by the routing protocol. So bandwidth of n_i is denoted by

$$Bw(n_i^t) = \left(\lambda - \left(\eta_i^t + \sum_{j \in D_t^{'}(n_i)} \eta_j^t + \sum_{k \in D_t^{''}(n_i)} \eta_k^t \right) \right) \quad (2)$$

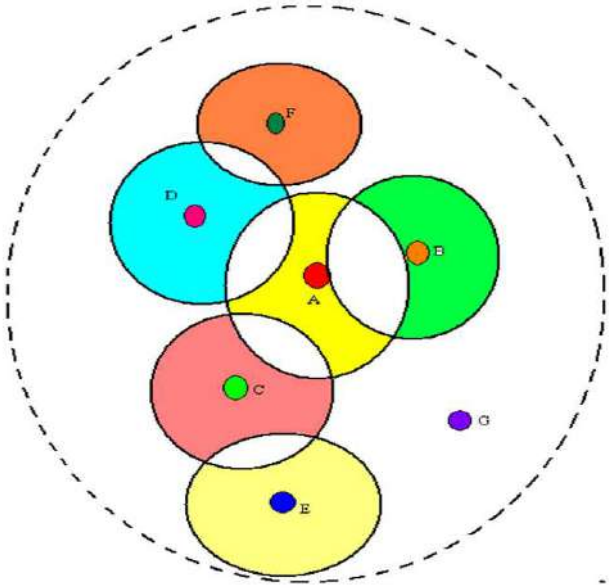

Fig.2. The outside big dotted circle indicates node A's interference range and the other small-size circles indicate node A and its neighbors' transmission ranges

On demand routing protocols try to eliminate the conventional routing tables and consequently reduce the need for updating these tables to track changes in the network topology [4][5]. In contrast to table-driven routing protocols all up-to-date routes are not maintained at every node, instead the routes are created when required. Each node maintains only the status of its neighbors. Periodically, each node broadcasts a hello message to all its neighbors to indicate its active status. Each node receives the hello messages from its neighbors and updates its neighbor information table. The hello messages are already in usage in on demand routing, the QOS FTMR[26][is based on on-demand routing, to estimate the available bandwidth in addition to active node's status, its consumed bandwidth status and its neighbor consumed bandwidth are also included into hello message . This result in little bit overhead and no extra time. This technique is called as hello message method. Every node to disseminate information about the bandwidth it is currently using in hello messages and for a node to estimate its available bandwidth based on the bandwidth consumption indicated in the hello messages from its two-hop neighbors. In the hello bandwidth estimation method, the node's current bandwidth usage as well as current bandwidth usage of its one usage hop neighbors is piggybacked onto the standard hello message is shown in table 1

© 2016, IJARCSSE All Rights Reserved

Table 1. Hello message structure

Node ID	Consumed Bandwidth	Time Stamp
Neighbor ID1	Consumed Bandwidth	Time Stamp
Neighbor ID2	Consumed Bandwidth	Time Stamp
•	•	•
Neighbor ID n	Consumed Bandwidth	Time Stamp

Table 2. Neighbor cache structure

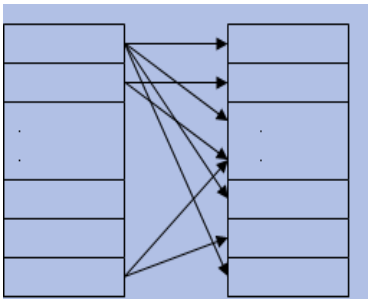

First neighbor table Second neighbor

The bold item of the first row is the node's own information. The following rows are the neighbors' information. Each node determines its consumed bandwidth by monitoring the packets it feeds into the network [4][5]. This value is recorded in a bandwidth consumption register at the node and is updated periodically. Each node estimates its available bandwidth based on the information provided in the hello messages and knowledge of the frequency reuse pattern. The nodes are located beyond the transmission range but within the interference range, we call them second neighboring nodes.

The bandwidth information about first neighboring nodes is obtained directly but there is no way to get the bandwidth information about second neighboring nodes directly. There are several ways to get the bandwidth information about second neighbors such as disseminating the bandwidth information using higher transmission power to reach the two-hop neighborhood, and setting up a separate signaling channel to broadcast the bandwidth information. However, using higher power to disseminate information not only consumes much more power, it also destroys the frequency reuse pattern and causes much more interference. Using a separate channel to disseminate the bandwidth information requires additional control that is a heavy burden for the MANETs in terms of bandwidth consumption and hardware support. Therefore, hop relay to disseminate the bandwidth information about second neighboring nodes[4][5] .

Once a node receives a hello message from its neighbors, it determines whether it is an updated one by examining the message's timestamp. We use the cache structure shown in Table 2. This includes a first neighbor table and a second neighbor table. The second neighbors are linked with their corresponding first neighbors in the cache. Once a node knows the bandwidth consumption of its first neighbors and its second neighbors. Using this approach to gather the first and second neighboring nodes' information is imprecise. Fig.2. shows an example topology that will result in imprecise information. The outside big circle indicates node A's interference range and the other small-size circles indicate the transmission range of node A and transmission ranges of its neighbors'. In addition, G does not fall into any of transmission ranges of A's neighbor. In this situation, A will never know G's status. If G transmits data, A's knowledge of available bandwidth is imprecise. However, this hidden node problem does not happen frequently since it has to meet. The bold item of the first row is the node's own information. The following rows are the node's strict requirements to "hide" the node. This kind of inaccuracy is tolerable because of wireless channel, the ultimate aim is better than best-effort, and the possibility of hidden nodes is low in a well connected network. Even if this situation occurs, it can be overcome by using a conservative bandwidth estimation, which leaves some extra bandwidth to conceal this hidden node effect.

C) Incorporating QoS in Route Discovery:

In the QOS FTMR [26], the route selection is based on the route discovery. In order to facilitate the computation of multiple link disjoint paths from the source to destination, an Ad hoc On-Demand Multipath Distance Vector AOMDV [12] protocol was chosen as a candidate protocol and made some modifications to enable the discovery of such paths to support QoS. The AOMDV [12] is the extension of AODV [7] to provide multiple link-disjoint or node-disjoint paths. For each destination, a node maintains the advertised hop count, which is defined as the maximum hop count for all the paths, which is used for sending route advertisements of the destination. Each duplicate route advertisement received by a node defines an alternate path to the destination. Loop freedom is assured for a node by accepting alternate paths to destination if it has a less hop count than the advertised hop count for that destination. Because the maximum hop count is used, the advertised hop count therefore does not change for the same sequence number. When a route advertisement is received for a destination with a greater sequence number, the next-hop list and the advertised hop count are reinitialized. AOMDV[12] can be used to find node-disjoint or link-disjoint routes. To find node-disjoint routes, each node does not immediately reject duplicate RREQs. Each RREQs arriving via a different neighbor of the source defines a node-disjoint path. This is because nodes cannot be broadcast duplicate RREQs, so any two RREQs arriving at an intermediate node via a different neighbor of the source could not have traversed the same node. In an attempt to get multiple link-disjoint routes, the destination replies to duplicate RREQs, the destination only replies to RREQs arriving via unique neighbors. After the first hop, the RREPs follow the reverse paths, which are node disjoint and thus link disjoint. The trajectories of each RREP may intersect at an intermediate node, but each takes a different reverse path to the source to ensure link disjointness. The advantage of using AOMDV [12] is that it allows intermediate nodes to reply to RREQs, while still selecting disjoint paths. But, AOMDV [12] has more message overheads during route discovery due to increased flooding and since it is a multipath routing protocol, the destination replies to the multiple RREQs those results are in longer overhead.

© 2016, IJARCSSE All Rights Reserved

Proposed modifications

1) Modifications at control packets: The Route Request (RREQ) packet of the AOMDV [12] is extended as RREQ packet of QOS FTMR[26] adding the one extra field is called the **Bandwidth specification field.** This field is used to specify the requested bandwidth by source during the route request. The Route Reply (RREP) packet the AOMDV [12] is extended as RREP packet of the QOS FTMR[26] adding with one extra field is called **load field** to carry the cumulative load**.** This is also called Interface queue Occupancy (IFQO) field, an intermediate node adds its load to this field during the processing of the RREP when setting up the forward path to destination.

2) Modifications at Data structure (Table): In the AOMDV [12], each node maintains routing table is used to keep the track record of received RREQs and set up reverse path to source. The AOMDV[12] routing table extended as routing table of QOS FTMR[26] by adding three extra fields IFQO , Bandwidth Requested field and bandwidth reservation field. In the QOS FTMR [26]. In AOMDV the route list of each entry has two fields nexthop and hopcount, In QOS FTMR the IFQO subfield is introduced to each entry of route list, the Bandwidth Request field and Bandwidth reservation field are introduced to routing table is shown in fig 2

Table 3: Structure of Routing Table (RT) in QOS FTMR OR Table 3: Structure of Routing Table (RT) in QOS FTMR

Destination Address(DA)
Sequence Number(SN)
Advertised_ Hopcount(HP)
Route List(RL)
{ Nexthop$_1$, Hopcount$_1$, , IFQO$_1$ } **{ Nexthop$_2$, Hopcount$_2$, , IFQO$_2$, },** ……... ..... **{ Nexthop , Hopcount$_k$ IFQO$_K$, }**
Bandwidth Requested(BRQ)
Bandwidth Reservation (BR)
Expiration Timeout(ET)

			Route List(RL)					
DA	**SN**	**HP**	**Next hop**	**Hop count**	**IFQO**	**BRQ**	**BR**	**ET**

3) Modifications at Source node: In the AOMDV [12], when the source node wants to send a packet to a destination, it looks up its route cache to determine if it already contains a route to the destination. If it finds that an unexpired route to the destination exists, then it uses this route to send the packet. But if the node does not have such a route, then it initiates the route discovery process by broadcasting a Route Request (RREQ) packet. In the QOS FTMR [26], when the source node wants to send a packet to a destination, it looks up its route cache to determine if it already contains a route to the destination. If it finds that an unexpired route to the destination exists and it satisfies the current application bandwidth requirement, then it uses this route to send the packet. But if the node does not have such a route, then it initiates the route discovery process by broadcasting a RREQ packet by specifying the bandwidth requirement in the RREQ packet and it computes the optimal paths after getting route replies .

4) Modifications at Intermediate node: In the AOMDV [12] the propagation of RREQ packet follows the same rule as in the AODV [7] except that duplicate RREQ packets received at an intermediate node are processed for possible alternate path back to the source. Every node maintains a reverse path table which keeps track of all the neighbors from which a RREQ packet is received and the corresponding hop-count back to the source. The intermediate node is allowed to sending route reply (RREP) if it has fresh route to destination and it supports the requested bandwidth of source otherwise it process the RREQ.

Again QOS routing protocols are classified in two types

- Admission Scheme
- Adaptive Feedback Scheme.

In an admission scheme, the node compares its residual bandwidth with the requested bandwidth. If its residual bandwidth is greater than the requested bandwidth, it forwards this RREQ Otherwise, it discards this RREQ. In an Adaptive Feedback Scheme node compares its residual bandwidth with the min-bandwidth field in the RREQ. If its residual bandwidth is greater than the min-bandwidth, it forwards the RREQ. Otherwise, it updates the min-bandwidth value using its residual bandwidth.

In the QOS FTMR [26] uses admission scheme, the propagation of RREQ packet follows the same rule as the AOMDV [12] in addition to that it eliminates the some paths if they do not support QoS this result in an increased packet delivery ratio, decreasing end-to-end delays for data packets, lower control overhead, and fewer collisions of packets. In this approach, RREQ packet arrives at intermediate node, it is inspected the requested bandwidth field. If its current available bandwidth is greater or equal to requested bandwidth then by using AOMDV [12] update rule is shown fig 3, it forwards the RREQ by recording the information about destination address, Seq_num, hop count and its previous node address (next hop address in reverse path) from which RREQ was received into reverse path table, requested bandwidth and reserved bandwidth in to its routing table show in table 3 .

If its current available bandwidth is less than requested bandwidth then it discards arrived RREQ packet.

© 2016, IJARCSSE All Rights Reserved

Modified Route update rule (Algorithm)

//This is used whenever a node i receives a route advertisement to a destination d from a neighbor node j,

// Variables seq_i^d , $advertised_hopcount_i^d$ and $route_list_i^d$, represent the sequence number, advertised_ hopcount and route_ list for destination d at node i respectively.

// When node i receives RREQ or RREP from its neighbor node j its routing table by using route update rule

Compare requested bandwidth with node's bandwidth

$Bw(n_i^t) < RREQ_j[\text{Re}\,questedBandwidth]$

Discard the $RREQ_j$

Else

{

$if\,(seq_i^d = seq_j^d)$ then

$seq_i^d = seq_j^d$

$if\,(i \neq d)$

{

$route_list_i^d = Null$

// update route list by creating new entry

$insert\ \ (j,\ advertised_hopcount_j^d + 1,\ \text{IFQO}_i,$

$)\ \text{in to}\ route_list_i^d$

// Enter the Requested bandwidth in to bandwidth field and Enter Reversed bandwidth in reserved bandwidth field

$RT[Requested\ \ bandwidth] = RREQ[Requested\ \ bandwidth]$

$\text{RT}[Reversed\ \ bandwidth] = RREQ[Requested\ \ bandwidth]$

}

Else

$advertised_hopcount_i^d = 0$

End if

Else if ($seq_i^d = seq_j^d$) and $((advertised_hopcount_i^d, i) > (advertised_hopcount_j^d, j))$

//update route list by creating new entry

$insert\ \ (j,\ advertised_hopcount_j^d + 1,\ \text{IFQO}_i,$

$)\ \text{in to}\ route_list_i^d$

// Enter the Requested bandwidth in to bandwidth field and Enter Reversed bandwidth in reserved bandwidth field $RT[Requested\ \ bandwidth] = RREQ[Requested\ \ bandwidth]$

$\text{RT}[Reversed\ \ bandwidth] = RREQ[Requested\ \ bandwidth]$

End if

End if

}

Fig.3. Modified Route Update Rule for QOS FTMR

5) Modifications at Destination node : When RREQ arrives at destination, records the information of previous node address (next hop) from which RREQ was received. Then generates the RREP, sets load field of RREP is zero and it is sent to node from which RREQ was received. After receiving RREP, Intermediate node, adds the its load (IFQO value) to load field of RREP and records information about destination address, sequence number, hop count and next hop node address (from which RREP was received) and cumulative load from destination node to itself into its routing table is shown table 3, finally the RREP is forwarded to a node from which the RREQ was received by seeing its reverse path table by using AOMDV [12] update rule. Finally several RREP packets are received by the source. It sorts the of RREP packet based on IFQO and record this information into its cache which contains the following fields destination address, destination sequence number, neighbor (next hop) address, valid, hop, IFQO. The path with least load is selected as an optimal path (primary path) for the data transmission. If more than one path has least load then an optimal path is selected based on hop count.

6) Bandwidth Reservation: The bandwidth resources are shared by neighboring nodes in the MANETs. Therefore, another challenging issue is how to allocate this shared resource and what type of resource reservation scheme should be used for setting up and maintaining the QoS-aware route. QOS FTMR [26] uses following scheme to reserve the bandwidth. After forwarding first RREQ the node temporary reserves requested bandwidth by recording requested bandwidth in to requested bandwidth field and reserved bandwidth in into reserved bandwidth field in to its routing table show in table 3. Then it should disseminate the update information immediately to their neighbors by placing the

© 2016, IJARCSSE All Rights Reserved

it's consumed bandwidth plus reserved bandwidth into consumed bandwidth field of hello message. Here node reserves the requested bandwidth in advance by adding it to consumed bandwidth field of its Hello message. The bandwidth is reserved only one time for each source when it forwards the first RREQ and the bandwidth is not reserved when forwarding the latter duplicate RREQs.

Where the bandwidth is only reserved for a certain interval and if no data packet is received by node from the source for a while, the reservation is automatically released and allocated to other requests if any, otherwise it is given to other nodes. No bandwidth is reserved when duplicated RREQs are forwarded by the node and if the node didn't get corresponding reply within time, the reservation is automatically concealed.

D) Route selection

Let P_j be the path from source node s to destination node d via intermediate nodes n_1, n_2--------n_k at time *t*.

$$P_j = s - n_1 - n_2 - n_3 - n_4 - - - - n_{k-1} - n_k - d$$

Let $L^t(P_j)$ be the total load on the path P_j from the s to d at time t, it is the sum of the individual loads of all the intermediate nodes on P_j at time t, it is denoted by

$$L^t(P_j) = \sum_{i=1}^{k} L^t(n_i) \qquad (3)$$

The delay is directly proportional to load; the main objective of route selection is to choose an optimal path (primary path). It is least load (delay) and every intermediate node of this path supports the requested bandwidth.

E) Route Maintenance

The QOS FTMR [26] handles route maintenance in a manner similar to the AOMDV [12]. The AODV uses a timer-based technique to remove stale routes promptly. Each routing entry is associated with a soft state timer called route expiration time out. This timer is refreshed whenever a route is used. Periodically, new expired routes are invalidated. Whenever a link breakage happens in a route due to a node moving away, the previous hop node of the moved away node is responsible for sending a Route Error (RERR) message back to the source to inform the breakage. It chooses alternative routes to maintain the connection. If there are no more redundant routes left, then it will start a new route discovery.

The Route maintenance in AOMDV is similar to AODV except that a destination is declared unreachable only when all routes to it break. Also it is necessary to keep track of the maximum sequence number heard from Route Error (RERR) packet through multiple downstream neighbors so that when all paths break, the destination sequence number is updated to this maximum value.

IV. SIMULATION OF QOS FMTR

In this section, we describe the Performance Evaluation and Comparison of QOS FTMR [26] and AOMDV [12] by using Network Simulator 2 (NS2) [30] with simulation setup. The NS2 is popular and standard simulation tool for implementing all types of network protocols. It was developed by the University of California at Berkeley and it is widely used by research scholars. The NS2 was developed by using two computer programming languages one is C++ another is OTcl (Object oriented Tool Command Language) interpreter as a command and configuration interface. The Network Animator (NAM) is an animation tool for inspecting network topology and data transmission shown in fig 4

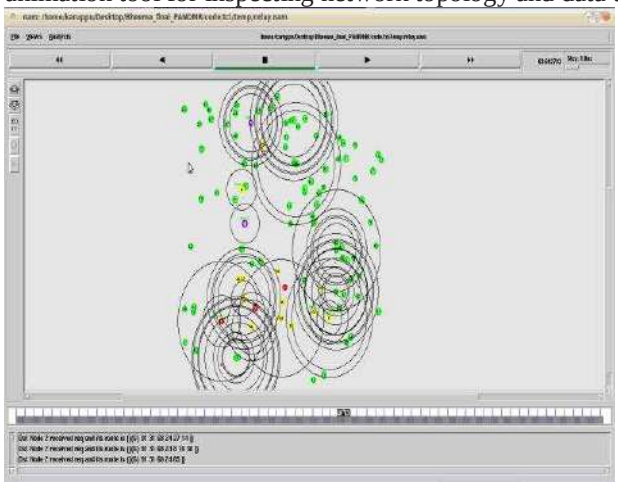

Fig.4. Shown in Network Animator (NAM) with 50 nodes

Different performance metrics are employed to test the QOS FTMR against the AOMDV both are implemented using Network Simulator 2, in the new version of simulator is NS2.23, Ubuntu operating system was used. The area for network configuration is chosen as 1000m x 1000m and the nodes are deployed with in this region. . For the mobile scenarios, the random waypoint model is used for node mobility. In this model, the random waypoint model is used for

© 2016, IJARCSSE All Rights Reserved

node mobility. In this model, a node chooses a random destination point in the network and moves towards that destination point at a constant speed then the node reaches its destination, where it stays for a certain pause time, after which it chooses another random destination point and repeats the process.

The channel bandwidth is 2 Mbps, a free space radio propagation model is used in which the signal power attenuates is $1/r^2$, where r is the distance between the nodes. All the nodes have the same transmission range of 250 meters. The distributed coordination function of IEEE802.11 DCF is used as MAC layer. All nodes operate in promiscuous mode, so it can overhear packets destined for others. The simulation ends after 100sec. The data traffic is generated by Constant Bit Rate (CBR) sessions initiated between the source and destination. All the nodes are assumed to have the same amount of battery capacity with full residual energy at the beginning of the simulation and initial energy of each node is set to 50 Joules. The transmitting power and receiving power of each node are set to 0.079Watts and 0.066Watts respectively. The idle power of each node is set to 0.005Watts the following table 2 shows the simulation setup.

The following quantitative performance metrics are used to measure the performance of both protocols.

- Overhead
- Throughput
- Packet Delivery Ratio
- Packet loss Ratio

Table.4. Parameters and Values

Sno	Parameter and Values
1	Network size and Node's Placement 1000 x 1000 Sq meters (Size of NAM),
2	Number of Nodes: 25, 50, 75, 100
3	Total Simulation time : 100s
4	Node's Mobility : Random Way Point Mobility odel(RWPMM)
5	Node's Speed: 10 m/s, 20m/s, 30m/s, 50m/s
6	Node's Pause Time: 2s, 4s, 6s, 8s
7	Application Layer : Constant Bit Rate(CBR)
	Packet Payload size: 512 bytes
	Data rate :10Kbps, 20Kbps,30Kbps ,50Kbps
	Number of source and destination pairs : 1, 2, 4,8
8	Transport Layer: User Datagram Protocol(UDP), CBR
9	Network Layer: QOS FTMR and AOMDV Routing Protocols
10	Data Link Layer: Logical Link Control Layer (LLC)
	Medium Access Layer(MAC):IEEE 802.11 DCF
11	Physical Layer:
	Antenna Model : Omni Directional
	Wave Propagation Model: Two-way Ground Model
	Channel Type: Wireless Channel Physical layer Channel Bandwidth: 2Mbps Lucent Wave LAN card with frequency 915MHz Transmission range of node : 250 meters Interference range of node: 500 meters
	Interface Queue Type: CMU Priority Queue with size 50 packets
12	Energy Model:
	Initial energy of each node: 50Joules
	Transmission Power: 0.079 Watts
	Receiving Power:0.066 Watts
	Idle Power: 0 .035 Watts
	Sleep Power: 0.005 watts
	Transition Power :0.2 watts
	Transition Time: 0.005 sec

- End to End Delay of packets
- Energy Consumption

By varying the following parameter

Number of nodes (density) [25, 50, 75, 100]
Fixed {Speed=30m/S, Pause Time=4s, Data Rate=50Kbps and Load=4}
Mobility of node(speed) [10 m/s, 20m/s, 30m/s, 50m/s],
Fixed {Network Size=50, Pause Time=4s, Data Rate=50kbps and Load=4}
Data Rate [10Kbps, 20Kbps, 30Kbps, 50Kbps]

© 2016, IJARCSSE All Rights Reserved

Fixed {Network Size=50, Speed= 2m/S, Pause Time=4s and Load=4}
Pause time [2sec, 4sec, 6sec, 8sec],
Fixed {Network Size=50, Speed= 30m/S, Data Rate =50kbps and load=4}
Number of source nodes and Destination pairs (increasing load) [1, 2, 3, 4]
Fixed {Network Size=50, Speed= 2m/S, Pause Time =4ms, Data Rate =50kbps}

Here we have derived some facts or relationships among performance metrics and parameters based on our previous work

Fact 1: The overhead

It is directly proportional to probability of collisions, packet loss, packet error rate, packet delay, bandwidth consumption and energy consumption. It is indirectly proportional to packet delivery ratio and throughput. Hence the overhead depends on overall performance of the routing protocol.

Fact 2: Network's size (density)

If size of network increases, distance between source and destination also increases, due to this number of hops increases between sources to destination. Hence overhead increases for route discovery and end to end packet delay also increases. Hence network size is directly proportional to overhead, end to end packet delay, congestion, bandwidth consumption, energy consumption, packet collision and loss. The network' size is indirectly proportional to throughput, packet delivery ratio

Fact 3: Speed

It is directly proportional to path failure rate, overhead, congestion energy consumption, bandwidth consumption, Packet delay, packet collision and packet loss. It is indirectly to throughput, Packet Delivery Ratio.

Fact 4: Pause Time

The increase pause time means increasing network stability. Hence it is indirectly proportional to path failure rate, overhead, energy consumption, Packet loss, bandwidth consumption and congestion, packet delay, packet collision packet loss. It is directly proportional to throughput, Packet Delivery Ratio.

Fact 5: Data Rate

It is directly proportional to congestion, energy consumption, packet loss and bandwidth consumption, packet delay. It is directly proportional to throughput, Packet delivery ratio until congestion occurs.

Fact 6: Number of source and destination pairs (load)

It is directly proportional to overhead, energy consumption, bandwidth consumption, congestion, packet delay, packet loss and packet collision. . It is directly proportional to throughput, Packet Delivery Ratio until congestion occurs

A) Analysis of Routing Overhead

The optimization of routing overhead is crucial part when designing new routing protocol because the overhead is directly proportional to congestion, probability of collisions, packet loss, packet error rate, packet delay, bandwidth consumption and energy consumption. It is indirectly proportional to packet delivery ratio and throughput. Hence the overhead depends on overall performance of the routing protocol. The routing overhead is defined as the number of control packets as generated at the time of simulation. The overhead is the most important performance metric to compare the routing protocols [28].

Routing Overhead= Number of Control Packets (RREQ, RREP, REEP) generated by routing protocol during simulation.

The normalized routing overhead is calculated as follows

$$\text{Normalized Routing Overhead}=\frac{x}{y} \qquad (3)$$

Where x is total number of routing packets generated and y is total number of packets received

1) Overhead by Varying Number of nodes (Density): Actually, QOS FTMR[26] is an extension of AOMDV[12] to provide to better quality of service (QOS) as per requirement of user's applications, usually real time traffic such audio, video, multimedia. QoS mechanisms are badly needed to ensure the required quality of the connection. While designing QOS FTMR [26], the overhead is increased in following cases

Case 1: The hello messages are already in usage in on demand routing protocols. Each node maintains only the status of its neighbors. Periodically, each node broadcasts a hello message to all its neighbors to indicate its active status. Each node receives the hello messages from its neighbors and updates its neighbor information table. The AOMDV [12] is On-demand routing protocol. In QOS FTMR, each node estimates the available bandwidth in addition to active node's status; its consumed bandwidth status and its neighbor consumed bandwidth are also included into hello message. This result in little bit overhead and no extra time.

Case 2: Only two new extra fields are introduced in QOS FTMT, The Route Request (RREQ) packet of the AOMDV is extended as RREQ packet of QOS FTMR adding the one extra field is called the **Bandwidth specification field.** This field is used to specify the requested bandwidth by source during the route request. The size of this field is only four bytes.

The Route Reply (RREP) packet of AOMDV is extended as RREP packet of the QOS FTMR adding with one extra field is called **load field** to carry the cumulative load**.** This is also called Interface queue Occupancy (IFQO) field. The size of this field is also four bytes. Hence in both cases only little bit overhead is increased and there is no complexity.

© 2016, IJARCSSE All Rights Reserved

While designing QOS FTMR, the overhead is decreased in following case

Case 3: The AOMDV is designed to simply find link-disjoint multipath between source and destination those paths don't aware of bandwidth requirement of application. But QOS FTMR is designed to find QOS aware link-disjoint multipath between source and destination that satisfy bandwidth requirement of application. Hence it eliminates several paths if they don't satisfy the bandwidth requirement of application during route discovery from source node to destination node. Due to this less number of QOS aware link-disjoint multipath is yielded compared to number link-disjoint multipath between any source node to destination node. This resultant in overhead of QOS FTMR decreases drastically compare to overhead of AOMDV

Let A be the set of all link-disjoint multipath from source to destination and let B be the set of all OQS aware link-disjoint multipath from source to destination. Then B must be proper subset of A , Mathematically, it is denoted by $B \subset A$ or A must be super set of B, it is denoted $n(B) < n(A)$ by $A \supseteq B$. For example A is set of all English alphabets, B is set of vowels.

$$A = \{a, b, c, d, e, f .....x, y, z\},\ n(A) = 26$$

$$B = \{a, e, i, o, u\},\ n(B) = 5$$

Hence $n(B) < n(A)$ (4)

Overhead of AOMDV in case 3 overtakes combined overhead of OOS FTMR in case 1 and case2. Hence QOS FTMR always yields less overhead compare to overhead of AOMDV.

In all graphs, instead of QOS FTMR, we use the FTMR for shortcut and simplicity.

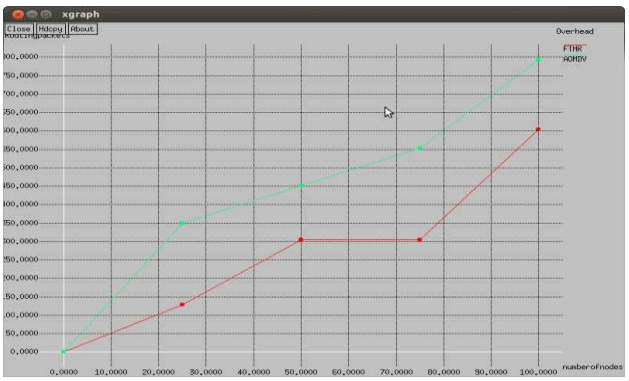

Fig.4.1. Overhead Vs Number of Nodes

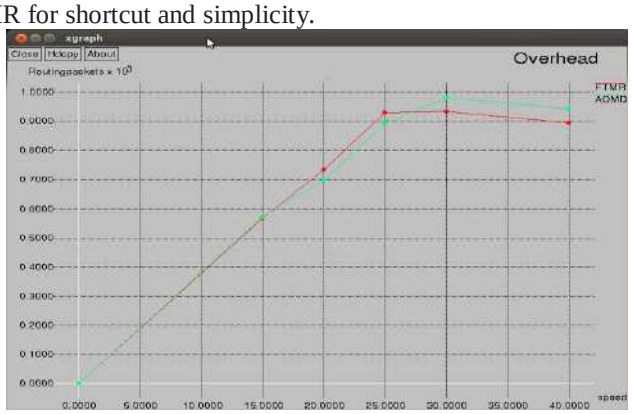

Fig.4.2. Overhead Vs Speed

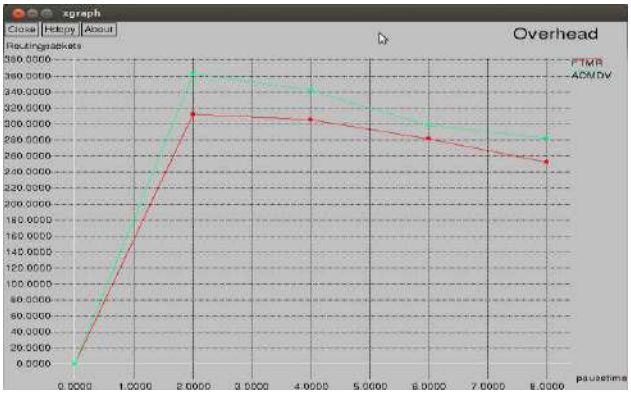

Fig.4.3. Overhead Vs Pause time

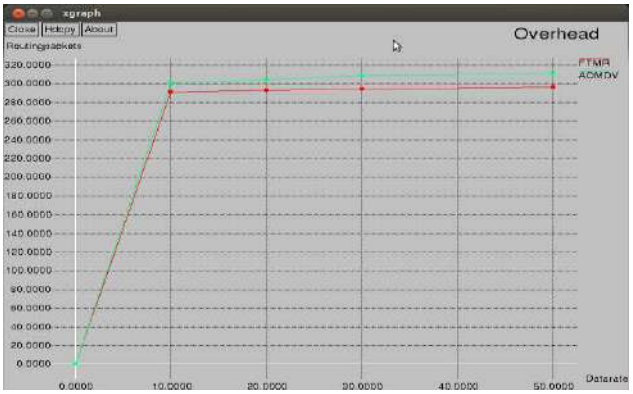

Fig.4.4. Overhead Vs Data Rate

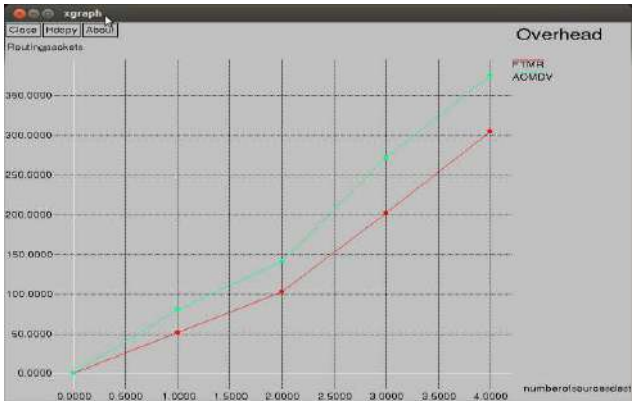

Fig.4.5. Overhead Vs Number of Source and Destination Pairs

© 2016, IJARCSSE All Rights Reserved

Fig.4.1. shows, Overhead Vs Number of nodes by varying number of nodes (density) 25, 50, 75 and 100, as per fact2, if size of network increases, distance between source and destination also increases, due to this number of hops increases between sources to destination. Hence overhead increases for route discovery and end to end packet delay also increases. In both protocols overhead is increased when network's size increases. But QOS FTMR has yielded less overhead compared to overhead of AOMDV, because QOS FTMR eliminates the several link-disjoint multipath that don't satisfy QOS requirements of application. It selects only link-disjoint multipath that satisfy QOS requirements of application.

2) Overhead by varying node's speed: Fig 4.2 shows the Overhead Vs Speed of node , speed is varied as 10m/s, 20m/s, 30m/s, 50m/s, usually speed increases overhead also increases because probability of path failure rate increases. At speed 10m/s, the overheads of both protocols are same. At speed 20m/s, the overhead of QOS FTMR is slightly increased than overhead of AOMDV and it is approximately equal. Later at high mobility, the QOS FTMR produces less overhead than AOMDV and it performs much better than AOMDV when speed increases

3) Overhead Vs Varying pause time: Fig.4.3 shows, Overhead Vs Pause Time, here pause time is varied as 2s, 4s, 6s and 8s. Usually, the pause time increases network stability also increases and path failure rate decreases. So pause time is indirectly proportional to overhead. Fig 4.3 shows the overheads of both protocols decreased when increasing the pause time and QOS FTMR yielded less overhead than overhead of AOMDV, because QOS FTMR eliminates the several link-disjoint multipath that don't satisfy QOS requirements of application. It selects only link-disjoint multipath that satisfy QOS requirement of application.

4) Overhead Vs Varying Data Rate: Fig. 4.4 shows overhead Vs Data rate, here data rate is varied as 10Kbps, 20Kbps, 30Kbps and 50Kbps and usually data rate is directly proportional to the overhead. The QOS FTMR yielded less overhead than overhead of AOMDV because QOS FTMR eliminates the several link-disjoint multipath that don't satisfy QOS requirements of application. It selects only link-disjoint multipath that satisfy QOS requirement of application.

5) Overhead by varying Source and Destination pairs (connections)/load: Fig.4.5 shows overhead Vs number of sources and destination pairs (load), here number of source and detonation pairs is varied as 1, 2, 3 and 4. The number of sources (load) is directly proportional to the overhead. When increasing load, the overheads of both protocols increased exponentially. However in all four cases the QOS FTMR[26] yielded less than overhead of AOMDV and the overhead of the AOMDV drastically increases compared to the overhead of QOS FTMR, because QOS FTMR eliminates the several link-disjoint multipath that don't satisfy QOS requirements of application. It selects only link-disjoint multipath that satisfy QOS requirements of application.

B) Throughput (Kbps) analysis:

To measure the protocol performance, throughput serves as the better parameter. The throughput is defined as the ratio of number of packets received to the number of packets transmitted [28] and it is indirectly proportional to the overhead.

The throughput is calculated by using the following equation. $$\text{Throughput} = \frac{x \times 8}{t \times 100} Kbps \quad (5)$$

Where x is number of bytes received and t is simulation time the following five cases show that the overall QOS FTMR yielded higher throughput than the AOMDV because overhead of QOS FTMR is less than the overhead of AOMDV.

The following figures shows that the QOS FTMR has yielded better throughput compared to the throughput of AOMDV, because QOS FTMR selects link-disjoint multipath that satisfy QOS requirement in advance and it forwards the data packets through selected link-disjoint multipath from source to destination.

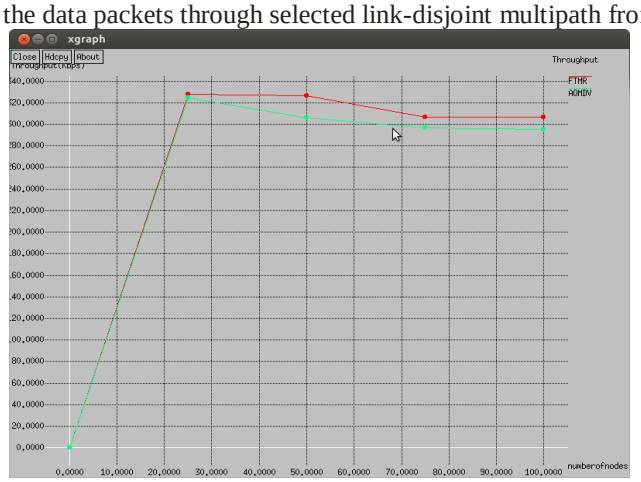

Fig. 4.6. Throughput Vs Number of nodes

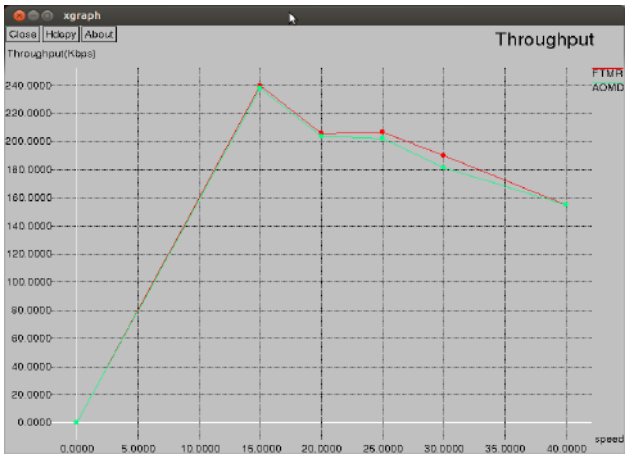

Fig. 4.7. Throughput Vs Speed

© 2016, IJARCSSE All Rights Reserved

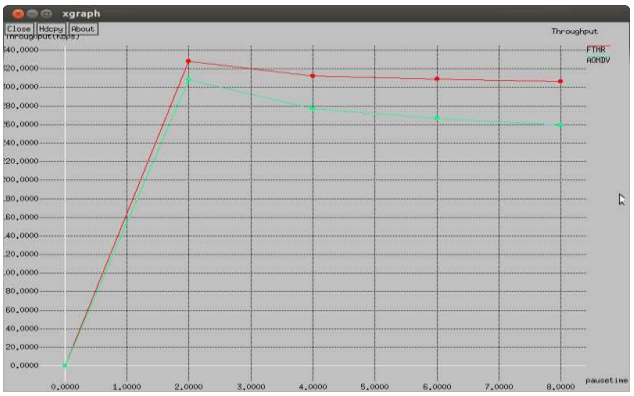

Fig. 4.8. Throughput Vs Pause Time

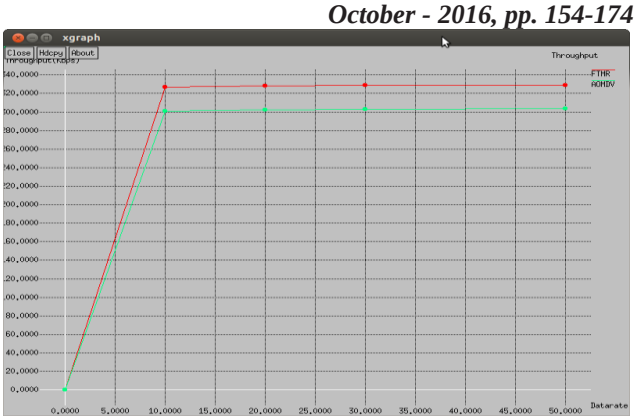

Fig. 4.9. Throughput Vs Data Rate

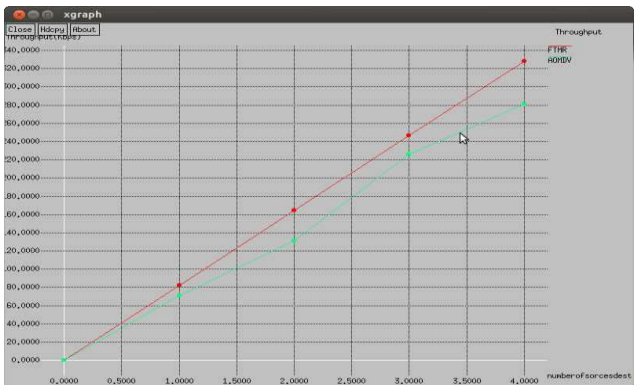

Fig. 4.10. Throughput Vs Number of source and Destination Pairs

C) Analysis of Packet Delivery Ratio (PDR):

To find the efficiency of the protocols, *PDR* is one of the important qualitative metrics. It is defined as the ratio of data packets received and packet sent [28], it is calculated as follows

$$\text{PDR}=\frac{x}{y}\times 100 \quad (6)$$

Where x is the total number of packets received and y is the total number of packets sent at end of the simulation time.

The following all five cases show that overall the QOS FTMR yields higher PDR than the PDR of the AOMDV because overhead of QOS FTMR is less than the AOMDV

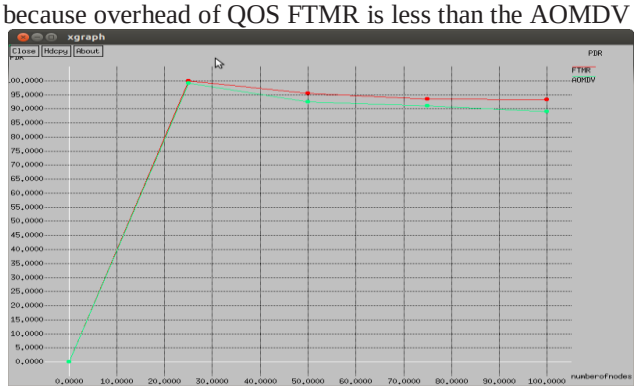

Fig.4.11.Packet Delivery Ratio Vs Number of Nodes

Fig.4.12.Packet Delivery Ratio Vs Speed

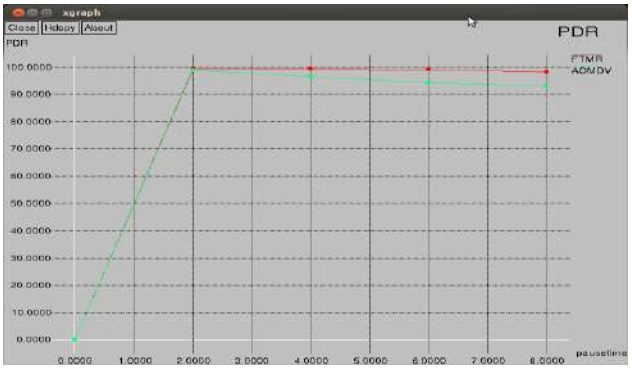

Fig.4.13.Packet Delivery Ratio Vs Pause Time

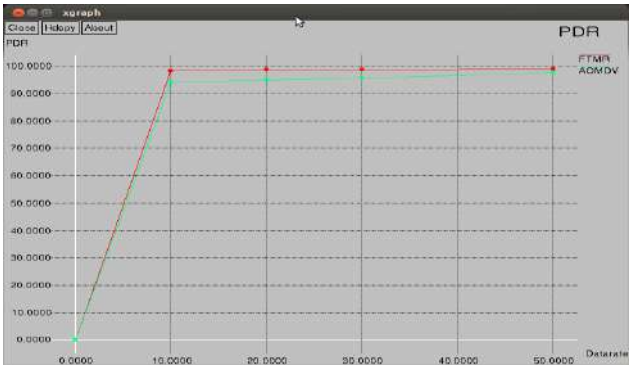

Fig.4.14.Packet Delivery Ratio Vs Data Rate

© 2016, IJARCSSE All Rights Reserved

Fig.4.15.Packet Delivery Ratio Vs Number of Source Destination Pairs

D) Analysis of Average End-to-End Data Packet (ms)

To measure the performance of the proposed protocols end to end delay is the major performance factor which should be considered. The Average end to end delay is defined as the time taken to transmit the packet from source node to the destination node. The total end to end average delay of data packets includes queuing delay, buffering delay, propagation delay and retransmission delay. The average end to end delay of n received data packets [28] by using the following equation .

$$\text{Average End To End delay of Received packets} = \frac{\sum_{i=1}^{n}(R_i - S_i)}{n} \quad (7)$$

Where R_i denotes the time at which the packet i is received and S_i denotes the time at which the packet i has been sent to the destination or it also defined as follows

$$\text{Average End to End delay of Received Packets} = \frac{\text{Total delay of each data packets}}{\text{Total data packets received.}} \quad (8)$$

Following five cases show that overall, the QOS FTMR yielded low average end-to-end packet delay than the average end-to-end packet delay of AOMDV, because OQS FTMR selects link-disjoint multipath that not only satisfy bandwidth requirement of application but also it selects that have less load.

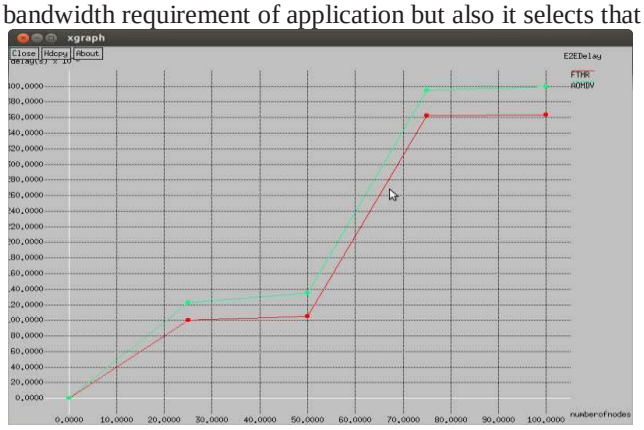

Fig. 4.16. Aveage End-to- End Packet Delay Vs Number of Nodes

Fig. 4.17. Aveage End-to- End Packet Delay Vs Speed

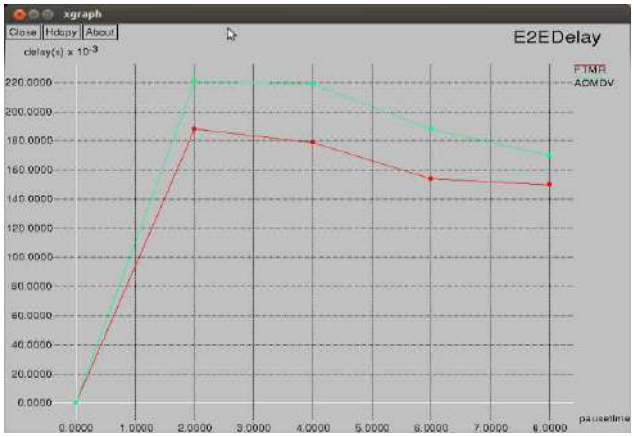

Fig. 4.18. Aveage End-to- End Packet Delay Vs Pause Time

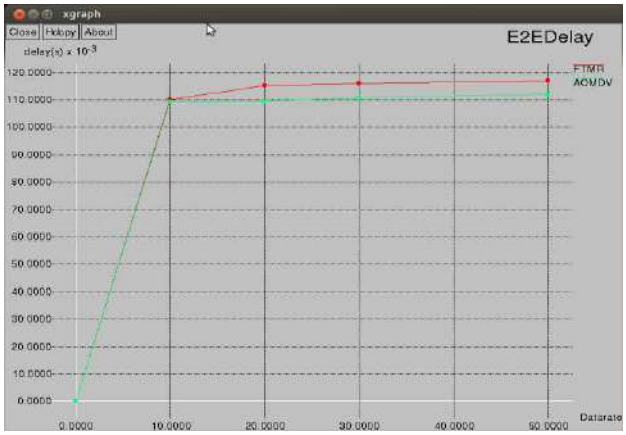

Fig. .4.19. Aveage End-to- End Packet Delay Vs Data Rate

© 2016, IJARCSSE All Rights Reserved

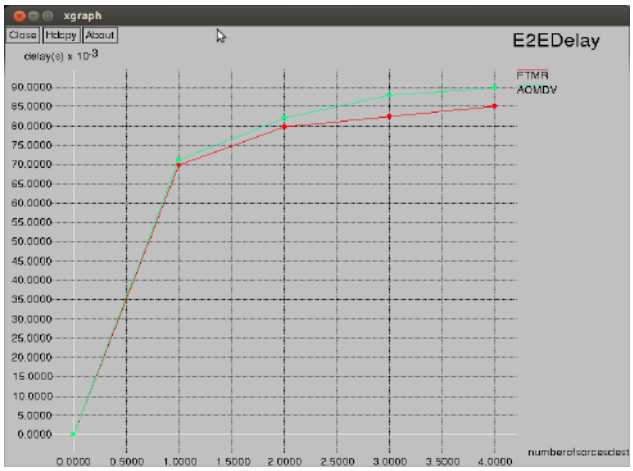

Fig. 4.20. Aveage End-to- End Packet Delay Vs Number of Source and Destination Pairs

E) Packet Loss Ratio (PLR) (%):

The PLR is used to measure the performance of the routing protocols. The PLR is defined as the ratio of number of packets not delivered to the destination to the total number of packets sent [28] .The PLR is calculated by using the following equation.

$$\text{PLR} = \frac{x - y}{x} \times 100 \quad (9)$$

Where x is total number of data packets sent and y is total number of data packets received.
Number of data packets lost=x- y.

Some data packets that are not reach the destination and they are lost during transmission to due to congestion and collision in the network.

Following five cases show that overall, the QOS FTMR has yielded less packet loss than the packet loss of AOMDV, because OQS FTMR selects link-disjoint multipath that not only satisfy bandwidth requirement of application but also it selects that have less load.

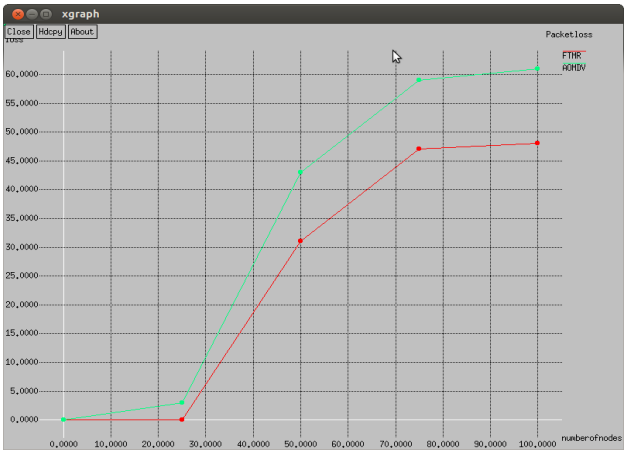

Fig.4.21. Packet Loss Vs Number of Nodes

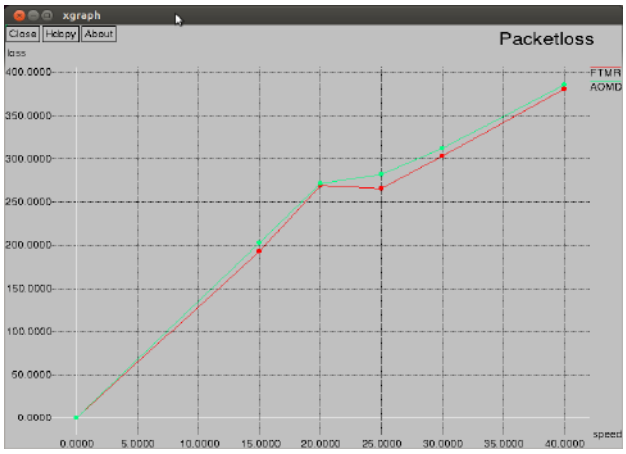

Fig.4.22. Packet Loss Vs Speed

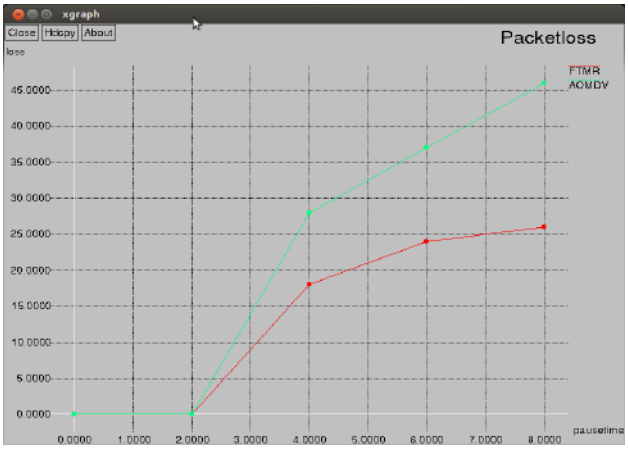

Fig.4.23. Packet Loss Vs Pause time

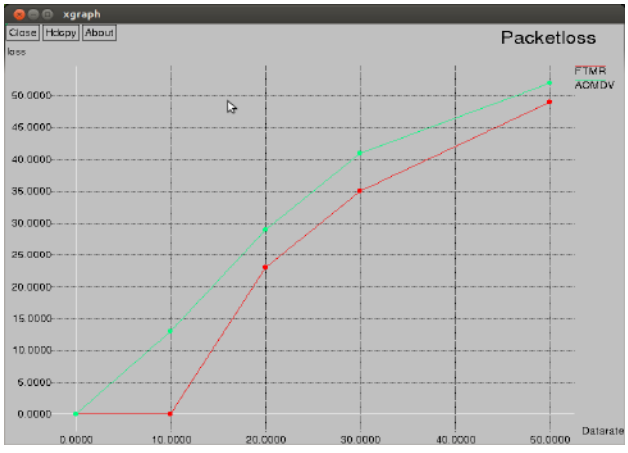

Fig.4.24. Packet Loss Vs Data Rate

© 2016, IJARCSSE All Rights Reserved

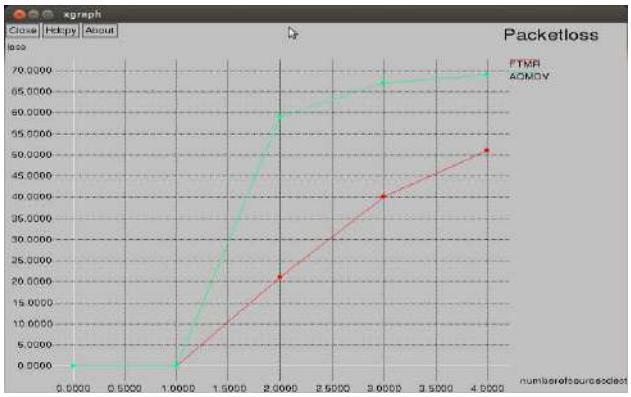

Fig.4.25. Packet Loss Vs Number of Source and Destiantion Pairs

F) Analysis of Energy Efficiency

It is an important qualitative metric to measure the performance of different protocols. The energy efficiency is calculated as the ratio of total received data (bytes) to the total energy consumption using following equation [28]

$$\text{Energy Efficiency} = \frac{x}{y} \quad (10)$$

,

Where x is total received data in terms of bytes and y is total energy consumption in terms of joules

$$\text{Total energy consumption} = \sum_{i=1}^{n} (E_i - R_i) \quad (11)$$

Where E_i denotes the initial energy of i^{th} node , R_i denotes the residual energy of i^{th} node and n total number of nodes in the network. In Table 4 in energy model, we used the following new parameters

- Sleep Power is power consumption (Watt) in sleep state.
- Transition Power is power consumption (Watt) in state transition from sleep to idle (active).
- Transition Time is time (second) used in state transition from sleep to idle (active).

The overhead is directly proportional to energy consumption. The following five scenarios shows that overall QOS FTMR has less energy consumption compared to enegy consumption of the AOMDV because the QOS FTMR has yielded less overhead compared to the AOMDV. Following five cases show that overall, the QOS FTMR yielded energy consumption than the energy consumption of AOMDV, because OQS FTMR selects eliminates many path that don't satisfy bandwidth requirement of application in the route discovery itself.

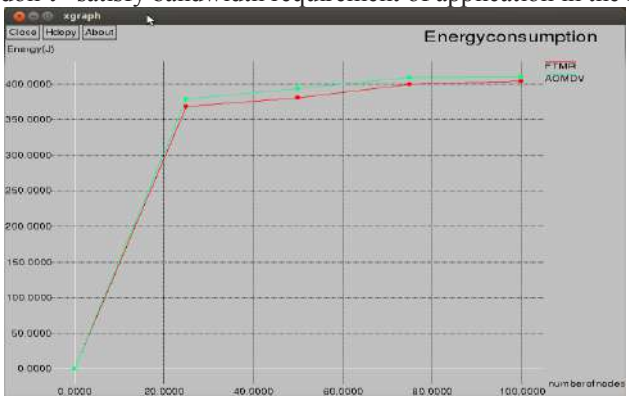

Fig. 4.26.Energy Cnsumption Vs Number of Nodes

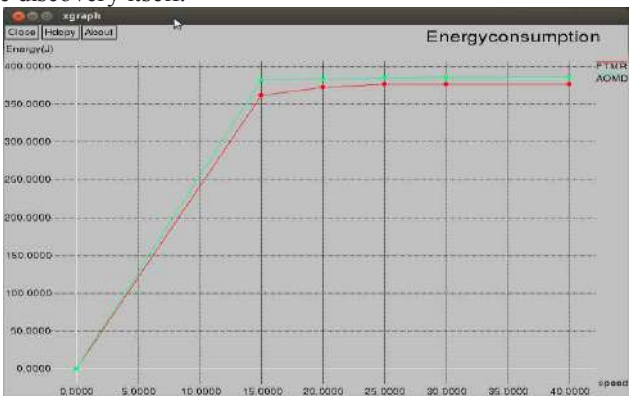

Fig. 4.27.Energy Cnsumption Vs Speed

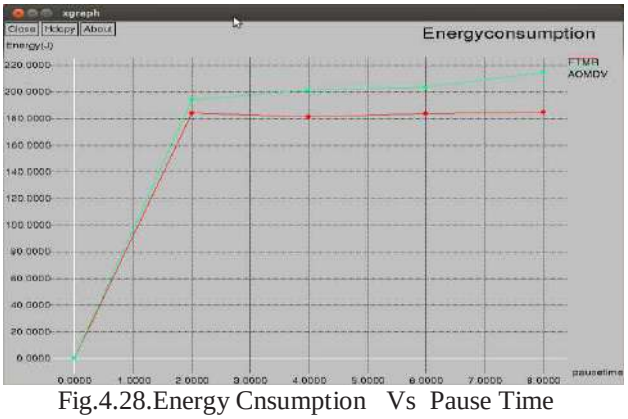

Fig.4.28.Energy Cnsumption Vs Pause Time

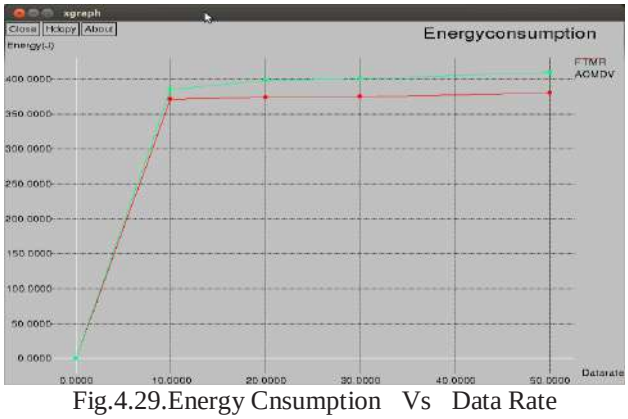

Fig.4.29.Energy Cnsumption Vs Data Rate

© 2016, IJARCSSE All Rights Reserved

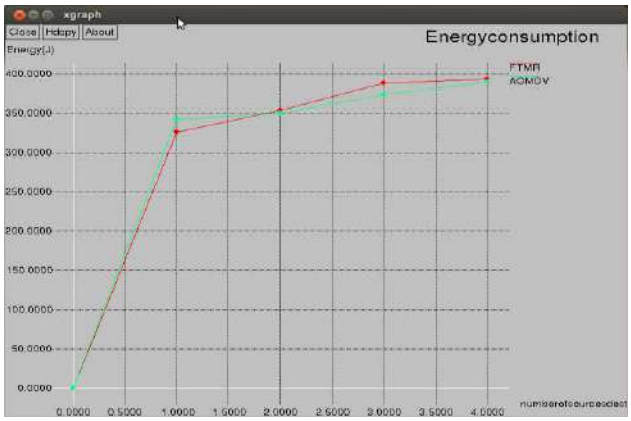

Fig. 4.30.Energy Cnsumption Vs Number of Souce and Destanation Pairs

VI. CONCLUSIONS AND FUTURE WORK

In this paper, we have chosen QOS FTMR protocol and it has been discussed elaborately all section of this paper . We also made a contribution to measure the performance of two different multi-path dynamic routing protocols such as QOS FTMR and AOMDV. The performance of the two protocols is tested with well-known simulator called as NS2. The performance of the QOS FTM and AOMDV are tested by using various quantitative performance metrics like, throughput, packet delivery ratio, end-to end delay of packets, routing control overhead, , energy efficiency, and packet loss rate and by varying various parameters like network's size, mobility of node, pause time, data rate and load .It is proved that QOS FTMR has better performance than AOMDV and it is concluded that the QOS FTMR is one of scalable, robust and QOS efficient multipath routing protocol in MANET. The QOS FTMR was designed by using IEEE 802.11 standard at MAC layer in NS2 .23. The IEEE 802.11 is widely adopted in the WLAN community, and many devices have been commercialized with IEEE 802.11that provides better than best-effort service for real-time video and audio applications.

The IEEE 802.11e standard is advanced of IEEE 802.11, the QoS features of the IEEE802.11e will be beneficial to prioritize for example voice and video traffic over more elastic data traffic [26]. The IEEE 802.11e supports quality of service by introducing priority mechanism. All types of data traffic are not treated equally as it is done in the original standard, instead, the 802.11e supports service differentiation by assigning data traffic with different priorities based on their QoS requirements. Furthermore, four different access categories have been defined each for data traffic of a different priority. In future work the QOS FTMR will be implemented by using IEEE 802.11e standard at MAC layer to provide best quality of services to applications of future generation.

REFERENCES

[1] S. R. Murthy, C. and Manoj, B. S., "Ad hoc Wireless Networks: Architectures and Protocols", *Prentice Hall,* 2004.

[2] T. Bheemarjuna Reddy, I. Karthigeyan, B.S. Manoj, C. Siva Ram Murthy, "Quality of service provisioning in ad hoc wireless networks a survey of issues and solutions", *Journal of Ad Hoc Networks, Elsevier, 4, pp: 83–124, 2006.*

[3] Adibi. S and Erfani. S, "A multipath routing survey for mobile ad-hoc networks**",** *3rd IEEE Consumer Communications and Networking Conference, Volume 2, Issue , 8-10, Page(s): 984 – 988. Jan. 2006.*

[4] Lei Chen, "Protocols for Supporting Quality of Service in Mobile Ad hoc Networks", *Ph.D thesis, University of Rochester, New York, 2006.*

[5] Chen Lei and Heinzelman Wendi, "QoS-aware Routing Based on Bandwidth Estimation for Mobile Ad Hoc Networks", *in IEEE Journal on Selected Areas in Communications, issue 3, pp 561-572, 2005.*

[6] Johnson,D. and Maltz,D.," Dynamic Source Routing Protocol for Mobile Ad Hoc Networks", *IETF Internet draft. 2004.*

[7] Charles, E. P., Belding-Royer, E. M. and Chakeres, I., "Ad hoc On-Demand Distance Vector Routing", *IETF Internet draft, 2003.*

[8] Chen,S. and Nahrstedt, K., "Distributed Quality-of-Service Routing in Ad-Hoc Networks", *IEEE Journal on Selected Areas in Communications, vol. 17, 1999.*

[9] Ge,Y ., Kunz ,T. and Lamont ,L. "Quality of Service Routing in Ad-Hoc Networks Using OLSR", *in Proceeding of the 36th Hawii International Conference on System Science, 2003.*

[10] Xue, Q. and Ganz ,A.,"Ad hoc QoS On-demand Routing (AQOR) in Mobile Ad hoc Networks", *Journal of Parallel and Distributed Computing, 2003.*

[11] Lin,C. and Liu,J., "QoS Routing in Ad Hoc Wireless," in *IEEE Journal on Selected Areas in Communications, August, pp. 1426–1438, 1999.*

[12] Mahesh K. M and Samir R. D, "On-demand Multipath Distance Vector Routing in Ad hoc Networks", *In Proceedings of IEEE International Conference on Network Protocols, pp.14-23, 2001.*

[13] S. J. Lee and M. Gerla, "Split Multipath Routing with Maximally Disjoint Paths in Adhoc Networks", *In Proceedings of IEEE ICC, pp. 3201-3205, 2001.*

© 2016, IJARCSSE All Rights Reserved

[14] L. Wang, Y. Shu, Z. Zhao, L. Zhang and O. Yang, "Load Balancing of Multipath Source Routing in Ad hoc Networks", *In Proceedings of IEEE ICCC, 2002, Vol. 5, pp. 3197 - 3201.*

[15] Zhenqiang Y, Krishnamurthy S. V and Tripathi S. K. "A Framework for Reliable Routing in Mobile Ad hoc Networks", *In Proceedings of IEEE INFOCOM, 2003, Vol. 1, pp. 270 -280.*

[16] S. J. Lee and M. Gerla, "Split Multipath Routing with Maximally Disjoint Paths in Ad hoc Networks," *in Proceedings of the IEEE International Conference on Communications (ICC), Vol. 10, pp. 3201-3205, 2001.*

[17] R. Leung, J. Liu, E. Poon, A.L.C. Chan, and B. Li, "MP-DSR: A QoS aware Multipath Dynamic Source Routing Protocol for Wireless Ad-hoc Networks," *in Proceedings of the 26 th IEEE Annual Conference on Local Computer Networks (LCN 2001), pp.132-141, 2001.*

[18] W. H. Liao, Y.C. Tseng, S. L. Wang, and J. P. Sheu, "A Multi-Path QoS Routing Protocol in a Wireless Mobile Ad Hoc Network," *Telecommunication Systems, vol.19, no. 3-4, pp. 329-347, 2002.*

[19] Y. Hwang, and P. Varshney, "An Adaptive QoS Routing Protocol with Dispersity for Ad-hoc Networks," *in Proceedings of the 36th Hawaii International Conference on System Sciences (HICSS_03), pp. 302-11, 2003.*

[20] Y. S. Chen, Y. C. Tseng, J. P. Sheu, and P. H. Kou, "An On-Demand, Link-State,Multi-Path QoS Routing," *Journal of Computer Communication, Vol. 27, pp. 27-40, 2004.*

[21] Y. H. Wang and H. Z. Lin , " Multipath QoS Routing with Interference Provision in Ad Hoc Wireless Network," *Journal of Information Science and Engineering, Vol. 22, pp.1325-1338, 2006.*

[22] L. Liu and L.Cuthbert, "A Novel QoS in Node-Disjoint Routing for Ad Hoc Networks," *in IEEE International Conference on Communications Workshop, Beijing pp.202 – 206, 2008.*

[23] X. Li and L. Cuthbert, "On-demand Node-Disjoint Multipath Routing inWireless Ad hoc Networks," *in Proceedings of the 29th Annual IEEE Conference on Local Computer Networks, LCN 2004, Tampa, Florida, U.S.A., November 16-18, 2004.*

[24] T. Bheemarjuna Reddy , S. Sriram , B. S. Manoj and C. S. R. Murthy "Multi-path Failure-tolerant Security-aware QoS Routing in Ad hoc Wireless Networks", *In Proceeding of Computer Networks, 2006, pp. 1389-1286.*

[25] Boshoff, J.N, Helberg A.S.J. , "Improving QoS for real-time multimedia traffic in Ad-hoc Networks with delay aware multi-path routing", *Wireless Telecommunications Symposium, 2008. 24-26, April 2008 Page(s):1 – 8.*

[26] M. Bheemalingaiah, M. M. Naidu, D. Sreenivasa Rao and G.varaprasad," QOS Fault Tolerant Multipath Routing for Mobile Ad Hoc Network", *International Journal of Computer Sciences and Engineering Systems, Vol. 4, No. 1, ISSN 0973-4406 , January 2010.*

[27] Byung-Gon Chun and Mary Baker, "Evaluation of Packet Scheduling Algorithms in Mobile Ad Hoc Networks**",** *Mobile Computing and Communications Review, 6, 2002,PP: 36-49.*

[28] M.Bheemalingaiah,M.M.Naidu,D.Sreenivasa Rao, P. Vishavapathi " Energy Aware On-demand Multipath Routing Protocol in Mobile Ad Hoc Networks", *International Journal of Computer Networks and Wireless Communications, Vol.6, No.5, pp: 14-33, sep-oct 2016.*

[29] Shital Umredkar , Sitendra Tamrakar and Umesh Kumar Lilhore, "Improved AODV based on Load and Delay for Route Discovery in MANE", *IOSR Journal of Computer Engineering (IOSR-JCE),Volume 14, Issue 2,), PP 32-40, Sep. - Oct. 2013.*

[30] Network Simulation 2 official website: *http://www.isi.edu/nsnam/ns/*

© 2016, IJARCSSE All Rights Reserved

Global Journal of Computer Science and Technology: E
Network, Web & Security
Volume 17 Issue 2 Version 1.0 Year 2017
Type: Double Blind Peer Reviewed International Research Journal
Publisher: Global Journals Inc. (USA)
Online ISSN: 0975-4172 & Print ISSN: 0975-4350

Cluster based Multicast Adhoc on Demand Routing Protocol for Increasing Link Stability in Manets

By M. Vijayalakshmi & Dr. D. Sreenivasa Rao
G.Narayanamma Institute of Technology and Science

Abstract- The critical issues faced in the MANET energy consumption, QoS (Quality of Services), exposure to attacks, link stability. Link stability is much essential to be discussed for improving communication. 'Link Stability' is significant because radio links are generally varied due to node mobility. This instability leads to increased rerouting which further escalates routing overhead. One way of reducing routing overhead is to use multicasting instead of unicast routing. Multicast Routing Protocol transmits data concurrently to a group of destination nodes to achieve better resource utilization. This paper present a multicasting routing protocol Link Stability based Multicast Adhoc on demand routing protocol (LSMAODV) that uses received signal strength as a metric to estimate link stability and node stability. The comparison between AODV, MAODV and LSMAODV is measured for link and node stability. In this paper, three clusters are created and one node from each cluster is selected as cluster head based on the packet priority. This paper aims to find the link with high probability of longer lifetime between the nodes.

Keywords: link stability, node stability; multicast routing; mobile adhoc network.

GJCST-E Classification: F.2.2, C.2.2

Strictly as per the compliance and regulations of:

© 2017. M. Vijayalakshmi & Dr. D. Sreenivasa Rao. This is a research/review paper, distributed under the terms of the Creative Commons Attribution-Noncommercial 3.0 Unported License http://creativecommons.org/licenses/by-nc/3.0/), permitting all non-commercial use, distribution, and reproduction inany medium, provided the original work is properly cited.

Cluster based Multicast Adhoc on Demand Routing Protocol for Increasing Link Stability in Manets

M. Vijayalakshmi [α] & Dr. D. Sreenivasa Rao [σ]

Abstract- The critical issues faced in the MANET energy consumption, QoS (Quality of Services), exposure to attacks, link stability. Link stability is much essential to be discussed for improving communication. 'Link Stability' is significant because radio links are generally varied due to node mobility. This instability leads to increased rerouting which further escalates routing overhead. One way of reducing routing overhead is to use multicasting instead of unicast routing. Multicast Routing Protocol transmits data concurrently to a group of destination nodes to achieve better resource utilization. This paper present a multicasting routing protocol Link Stability based Multicast Adhoc on demand routing protocol (LSMAODV) that uses received signal strength as a metric to estimate link stability and node stability. The comparison between AODV, MAODV and LSMAODV is measured for link and node stability. In this paper, three clusters are created and one node from each cluster is selected as cluster head based on the packet priority. This paper aims to find the link with high probability of longer lifetime between the nodes. The simulation are carried out and compared the result of the proposed routing protocol (LSMAODV) based on minimum hop count. Analysis of simulation results show improvement of various routing performance metrics such as routing overhead and packet drop ratio.

Keywords: link stability, node stability; multicast routing; mobile adhoc network.

I. Introduction

Mobile Adhoc networks (MANET) are collections of wireless mobile devices, which can communicate with each other without any infrastructure support. It is denoted as self-configured and self-maintained network. Every node in MANET acts as both the host and a router and it communicate with each other without the support of any fixed centralized control. In MANET, the mobile nodes are interconnected by multi-hop wireless links in a dispersed manner [1]. The design of MANET routing protocol vary from wired network routing protocol; since a MANET is categorized by node mobility, node link unreliability, limited energy, limited bandwidth, high error rates, and security risk. The essential characteristics needed to design a routing protocol are dynamic topology, limited bandwidth, battery, CPU resources and multi-hop communication. There are many routing protocols projected for MANET. Based on the principles of routing, the protocols can be classified either proactive or reactive. Proactive routing protocols use to communicate regularly and update routes for every pair of nodes at every time of period. Every mobile node will operate as a sender, receiver or an intermediate node of the data in the system. Thus system will create the awareness towards the findings to deliver an outstanding merits and flexibility related to bandwidth spatial reuse, intrinsic fault tolerance and low-cost fast distribution [2]. In the network, the each node receives the information from the packet and updates their interpretation by applying a shortest-path algorithm to find the next hop node to reach the endpoint.

The main principle of a MANET routing protocol develop a competent route between the communicating nodes to reach the end point. Thus, the message will deliver on time with less number of packets drops providing stable connectivity with less routing overheads. MANET routing protocol is generally classified into two types. They are table-driven and source-initiated [3]. Table-driven routing protocol sustain with one or more tables at each node to save routing information. This protocol is used when there is a change in network topology in order to propagate the updates throughout the network to maintain a reliable network. Existing table-driven routing protocols include the following routing methods such as DSDV (Destination Sequenced Distance Vector) [4], CGSR (Cluster head Gateway Switch Routing) [5], and WRP (Wireless Routing Protocol) [6]. Source-initiated routing protocols are used when a source node requests for a route. This protocol process is inspected with only the possible routes. For example, source-initiated protocols contain AODV (Ad Hoc on Demand Distance Vector) [7], DSR (Dynamic Source Routing) [8], TORA (Temporally Ordered Routing Algorithm) [9], ABR (Associativity Based Routing) and SSR (Signal Stability Routing) [10], etc.

Link stability rely on wireless link features such as link failures, packet loss rate, channel sensing rate, channel fading rate, bit error rate, band width fluctuations and environmental effects. The wireless channel variation due to the packet loss resulting in link failures and reduces link reliability. Thus, the failure in channel sensing and channel fading increase the errors that

Author α: GNITS, JNTUCEH, Hyderabad, India.
e-mail: mvlakshmi_ gnits@yahoo.co.in
Author σ: Professor, JNTUCEH, Hyderabad, India.
e-mail: dsraoece@gmail.com

© 2017 Global Journals Inc. (US)

trigger large dissimilarity in the existing bandwidth. The existing communication systems use checksum and sequence numbering for controlling the errors and some of them use positive recovery of packet retransmission. If checksum technique is not performed in the system then it affects the system performance. Similarly, Route stability relies on the performance of source, destination and intermediate nodes and the wireless channel connecting end-to-end route. When the lifespan of a route decreases, then the probability of end-to-end delivery can be improved with alternate routes between source and destination. Finally, to develop the route stability, there is a necessity to improve the constructed mesh based and multipath routing techniques.

The stability based routing protocols are intended to choose the stable route for passing through the stable links. These link stability and route stability protocols increases the lifetime of routing and the packet delivery. These protocols are compared with the shortest path routing protocols. Since mobile networks are very unstable links and the stability of routes becomes a main objective in the development of a mobile routing protocol. Communication links in Adhoc network are fundamentally unreliable because of their medium characteristics and varying internode distances due to node mobility. This leads to disconnection and result in reconfiguration of communication links. Each reconfiguration needs initiation of route discovery process and is expensive. Reconfiguration also expose to resource-constrained network as mobile devices that constitute MANET have limited resources in terms of computing power, memory, transmission power, and battery life.

A major challenge of MANET is to implement QoS to prevention of attacks, reduction in energy consumption, incorporating fault-tolerance and delay of nodes [12]. The primary objective of this paper is to improve QoS by improving the Priority based Adhoc on Demand Routing Protocol (PAODV) and thus increase the route stability through proper selection of links that are likely to be more stable. Some of the applications of MANET are rescue operations in military battlefield, disaster relief efforts, and audio and video conferencing. This applications needs support of survivable, reliable and efficient communication. Hence, this paper focus on developing a clustering based Priority Adhoc on demand routing protocol for increasing link stability and node stability in MANET.

II. Literature Survey

Currently, there are several new multicast routing protocols are estimate to achieve efficient multicasting in MANET. Some of the routing protocols are Multicast Adhoc On-Demand Vector (MAODV), Adhoc Multicast Routing protocol Utilizing Increasing ID Numbers (AMRIS), Core Assisted Mesh Protocol (CAMP), Location Guided Tree (LGT), Lightweight Adaptive Multicast (LAM), and Differential Destination Multicast (DDM). The above protocols are mainly based on the features of distance vector routing or link-state routing with some benefits to help the routing process in definite ways [13]. Many multicast routing protocols reviewed in [2] which were scheduled to enhance QoS broadly and their behavior were assessed in terms of latency, packet loss ratio, jitter etc. Similarly, the performance in Ad-hoc networks was reviewed in [14]. Collision is a major problem since it results in packet drops, extensive delay of data and queuing of packets. So, the performance of Ad-hoc networks also reduces adversely. Hence, this paper proposed the model framework with the Enhanced Cluster head Gateway Switch Routing Protocol (ECGSR) with the origin of Ad-hoc On-demand Distance Vector Routing (AODV) based technique collision evading. A new AODV routing protocol was presented in [15], to enhance the stable link. In this paper the parameters are used for the establishment of Quality of Service (QoS) by node stability, load stability and least residual distance in order to select the link to the endpoint. The result showed that the proposed protocol enhanced the performance. Thus, the proposed work did not measure the power of the received signal at the endpoint though moving over the route.

Similarly, [16] examined an innovative Enhanced Adhoc On-demand Distance Vector (E-AODV) protocol which is related to AODV. AODV can be modified with reduced end to end delay with enriched packet distribution ratio. The ad hoc networks mainly select AODV protocols as it can deliver low routing overhead with high performance. His study proved that QoS in the MANET has no universally predefined parameters. But it was commonly a well-defined group of service quality which has the necessity to be achieved by the network while transferring a packet stream from a transmitter to its receiver end. The researchers also described that QoS is associated with certain parameters such as throughput, delay, and drop of packets. This would be established and approved by the mark of end user. QoS model also described an architecture that delivered the possible best facility.

Cluster Based Routing Protocol is intended to use in mobile ad hoc network (MANET). In this study, the mobile nodes of the Adhoc network is separated into a number of overlying or disjoints 2-hop distance clusters by the protocol in a dispersed manner [17]. Among the clusters, a cluster head is selected to maintain the information of all the cluster members. By this cluster participation, the information from Inter-cluster routes are projected dynamically and kept at each cluster head. Thus, by using this clustering technique, the flooding traffic between the data communication and the route discovery is competently minimized by the protocol and speeds up this process as well. The MANET network has two main protocols that are Tree-based protocols and mesh based protocols. MAODV and ODMRP (On-Demand Multicast Routing Protocol) are two popular

© 2017 Global Journals Inc. (US)

multicast routing protocols for tree-based and mesh based protocols, respectively.

The performance comparison and study of multicast protocols was reported by [18] which affords a vision into the functionality and presentation. Similarly, [3] justified MAODV as an on-demand routing protocol that determined the route only when a node has something to send. It is a hard state usage of protocol. This study revealed that if a member node of a multicast group needs to terminate its group membership, it must give a request for termination but, when a mobile node wants to join a multicast group or send a message but not having a route to the group, a Route Request (RREQ) was originated. All the nodes that are members of a multicast group and the non-member nodes that are not members of the group but their position are very critical for forwarding the multicast information that compose the tree structure. Every multicast group is recognized by a unique address and group sequence numbers for tracing the newness of the group situation.

In other study [19] examined an ant metaphor in dynamic routing for MANET, where ants spread the gathered data to nearest sources. Thus the dispersed routing system for motor vehicles that direct them through the city using the shortest way in time and the account of load is described. Similarly, a routing protocol based on swarm intelligence by using ants was reported by [20] where ants use heuristics to find the routes in multi-hop ad hoc networks. The other efficient hybrid multicast routing protocol suitable for high mobility applications was presented by [21] that addresses the scalability issue of ODMRP protocol. The data forwarding path and join query forwarding path were separate in this protocol. A routing protocol for MANET named as terminates routing, which has the purpose for keeping the assistance of scalability by considering the location-based routing, irregular topology and node mobility. A Mobility Prediction Aided Dynamic Multicast Routing (MPADMR) algorithm was proposed by [22]. Hence, this algorithm contains two steps, the construction of link lifetime constrained minimum hop count multicast tree and the dynamic multicast tree maintenance procedure.

The other study proved by [23] described multicast protocols performance characterization over a wide range of MANET situations. The performance of mesh and tree-based multicast routing schemes which related to flooding are evaluated and recommend by the protocols which is suitable for specific MANET situations. New algorithm for online multicast routing in ad hoc networks was proposed in [24]. A two level management approach for efficient constructing and maintaining a QoS routing path in ad hoc wireless networks was proposed in [25]. This scheme considerably reduced the quantity of control packets. So, for implementing real-time multicast services, degree constrained QoS aware routing algorithm was given by [26]. This scheme increased the overall performance of application-layer multicast services. Hence, this study proposed the new algorithm to find the clustering based Priority Adhoc on demand routing protocol for increasing link stability and node stability in MANET.

Similarly, the researches [29] established a Quality of Service (QoS) involved multi-cast routing protocol to select reliable neighbor nodes, which is named as QMRPRNS. Compared to other protocols this protocol have better reliability pair factor, hence it is preferable for reliable data transmission. QMRPRNS protocols select the route to transfer the data with more stability, reduced transmission delay. Further, it requires less time to data transmission, and the node failure probability is less due to QMRPRNS reliability pair factoring scheme. Moreover, these nodes have high reliability pair factor and associated with threshold reliability pair factor were designated for data transmission.

III. Existing Protocols

To increase the performance of the MANET, many researchers mainly suggest their view on the route discovery. In MANET the AODV routing protocol is mostly used for path discovery. The AODV routing protocol which creates less reactive routing protocol is used to determine the route after accepting the route request (RREQ) and the communication from the sender node. In this protocol, the route failure in the network was projected by sending the Route Error (RERR) indication message to the source node and it is achieved by the AODV protocol. Then the AODV resends the information's to the receiving node. In MANET system, MAODV is used to multicast the data packets. This multicast protocol creates the multicast group by developing the multicast tree. MAODV is the most effective protocol used for multicasting to provide service quality. The main drawbacks of MAODV and the chief principle of the group is it continuously send the multiple messages even if there is no transmitter, because of which the next sender will get delay and the controversy will be large in MAODV [27]. Metric based enhancement to AODV protocol [12] suggested reducing the link failure by picking the best link. Hence, this protocol accepts the route constancy to reach the endpoints. In order to avoid the overload of the messages due to traffic, the EM-AODV routing protocol supported various links as well as path to the endpoint. When compared with the AODV this protocol provides enhanced performance [28]. The major drawback of reactive routing protocol is the respective route detection methods were not considered with loss of route reply message during data communication which indicates the drop of network efficiency. Hence, [29] QMRPRNS: QoS based multicast routing protocol scheme only used to select reliable neighboring nodes for data transmission.

© 2017 Global Journals Inc. (US)

IV. Proposed Methodology

In this section, Link Stability Based Priority Multicast Adhoc on Demand Routing Protocol (LS PMAODV) using reliable neighboring nodes selection scheme has been proposed.

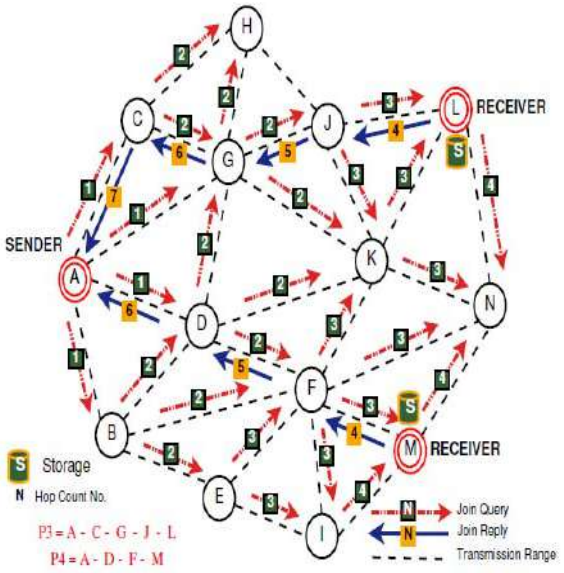

Figure 1: Flow diagram of LS PMAODV

The study deployed few mobile nodes randomly in a specific region which are associated with some initial energy. Here a reliability pair factor (F th RP) = 2.8 is taken as a threshold value. However, in general the value of (F th RP) is application dependent and fixed by the system administrator. Since multicast routing in MANET for a group communication is needed to establish a reliable communication links among the neighbouring nodes.

So in order to overcome the limitations of the MAODV multicast routing protocol, this paper presents a Link Stability based Priority Multicast Adhoc on demand routing protocol. The proposed protocol is processed in several phases such as basic idea formulation, route discovery mechanism, route reply process and route maintenance process.

a) *Proposed Link Stability Based Priority Multicast Adhoc On Demand Routing Protocol*

The flow of LS PMAODV protocol is illustrated in Figure 1. In this topology there is one sender, two receivers M and L (denoted by double ring). In LS PMAODV, forwarding nodes use the shortest path between multicast group members. Red arrow indicates 'JOIN Query' and blue arrow indicates 'JOIN Reply'. Weight on an arrow indicates hop count value for respective link. A link marked with both red and blue arrow is part of a path which returns back to source. Information about other possible paths is not discarded and is used to establish links in event of disconnections induced by mobility. For example, in Figure 1, route (P3) A → C → G → J→ L is established as soon as (P4) A → D → F → M is disrupted because of movement of J. As a result, this mesh structure is more resilient to tree-like topology as there is no requirement to reconfigure the entire route in change of node position.

According to LS PMAODV protocol, minimum hop count is utilized to determine the paths between source and destination nodes. Figure 1 shows paths between source A and destinations L and M is P3 and P4 that obtained from LS PMAODV protocol using minimum hop count while P3 and P4 are shown in Figure 1 using signal strength of nodes. Path P3 has changed from path P4 due to less signal strength of node A as compare to C. But in Path P4 doesn't change to P3 because it's already getting best signal strength.

b) *Link Stability*

Fluctuating link stability induced by mobility and/or medium characteristics in wireless network impacts network performance. Efficiency of a dynamic routing protocol can be characterized by its ability to deal with link unreliability and routing overhead in terms of computation and reconfiguration/ rerouting (Torkestani, 2011).

Using link stability as a basis for routing decision can lead to protocol being,

- *Energy Efficient:* low communication and computation overhead as less number of link breaks reduces number of re-routings.
- *Resilient to Mobility:* links are selected to resist connectivity breaks for longer periods in events of node movements
- *Stable:* same path is sustained for longer duration reducing overhead on routing tables. Link stability can be estimated using parameters such as (1) Signal to interference plus noise ratio, (2) Energy, (3) Link Delay and (4) Bit Error Rate. If node has more energy, it is likely to remain alive for a longer duration and its transmission range is higher.

Less the link delay, smaller is the distance and hence more probability of link remaining intact. Smaller BER means higher bandwidth and better quality of link.

c) *Mathematical modeling of the proposed system*

Link Stability is given by,

$$LS_{i,j} = \frac{v_2 - DSS_{i,j}}{v_2 - v_1} \quad (1)$$

Where, DSS is the differential signal strength. It is computed as follows.

$$DSS_{i,j} = SScur_{i,j} - SSnew_{i,j} \quad (2)$$

Where, SS represents Signal Strength at nodes in the interval i and j.

A path between source and destination is given as

© 2017 Global Journa ls Inc. (US)

$$P(s,d) = (s, e(s,x), x, e(x,y), y, ..., e(z,d), d) \quad (3)$$

The feasible path is represented by,

$$P(s,d) = P0, P1, ...Pn \quad (4)$$

Here, P is define as the path stability, by the product of link stability of its edges as follows,

$$Stability(P) = \prod_{e \in P} LS(e) \quad (5)$$

Where, LS is the Link Stability.

d) Algorithm of proposed protocol

In this section the algorithms for link stability discovery process and Link stability maintained process are provided.

i. *Algorithm 1 (Link stability discovery process)*

Link stability is estimated for every link routing from source to destination. For the selection of the next hop in establishing a route, link stability is estimated by computing Proposed Link Stability based Priority Multicast Adhoc on demand routing protocol in shortest path process.

1. Begin
2. Initialize $F^{th}_{RP} = 2.8,\ RQ = \{S_{addr}, MC_{addr}, ...\}$ and other fields of the request packet at S.
3. S broadcast the (RQ) packet to its adjacent nodes those are coming in its transmission range.
4. For every packet request (RQ) packet attained at its neighboring node do
5. If there is no neighbor of a particular node which broadcast the packet
6. Go to step 17.
7. Else
8. If F_{RP} (Rec node) $< F^{th}_{RP}$ value then
9. Discard the packet
10. Else
11. Store the request (RQ) packet at received node header and broadcast further across the network.
12. Repeat step 3-13 until destination nodes received the request (RQ) packets.
13. End if
14. End for
15. End

ii. *Algorithm 2 (Link stability maintained process)*

1. Begin
2. If a node N_i send a request (RQ) packet to the node N_j however, the node N_j go out from the transmission range of the node N_i (i.e.) there is no channel exist between the these two nodes then
3. At this stage the node N_i saves the current data packet in its multicast routing information table (MRIT)
4. After channel break down node N_i-1 to repair the path.
5. If the node N_i received the route repair reply (RR_REP) packet return from node N_i-1 within a fixed timeout ($T_{timeout}$). Then
6. The node N_i is ready to send a request packet (RQ) to node N_j.
7. Else
8. The node N_i send a route error (RE) packet to source node S to restart the routing discovery process
9. End if
10. End if
11. End

V. Results and Discussion

The parameters used in stimulation, are shown in Table I.

Table 1: Simulation Senario

Parameters	Values
No of nodes	60
Number of clusters	3
Network size	1000 × 1000 m^2
Node placement	Random
Node mobility	Mobility
MAC layer protocol	IEEE 802.11
Simulation time	100sec
Initial energy	100j

The proposed LS PMAODV protocol and the technique is implemented using Network Simulator 2 (NS-2) software. Generally, NS-2 is the most standard nonspecific network simulator which supports a wide range of protocols in all layers. It uses OTcl as configuration and script interface. NS-2 is the paradigm of reusability. The network size of the proposed simulation model in terrain area is 100 m x 100 m using Adhoc On-Demand Distance Vector (AODV) routing protocol for monitoring the important parameters like Packet Delivery Ratio (PDR), end-to-end Delay, energy consumption, network life time, computation overhead, connectivity, link stability and throughput. The parameters used in stimulation, which are shown in Table 1.

a) Packet delivery ratio

Packet Delivery Ratio is defined as the ratio of aggregate number of data packet that is successfully delivered to the aggregate number of data packet sent. Fig.2 shows the packet delivery ratio for different number of nodes. It is clearly evident the proposed approach achieves high packet delivery ratio than other protocols. Fig.3 shows the packet delivery ratio for varied speed. The proposed protocol LS PMAODV has high packet delivery ratio when compared to other protocols.

© 2017 Global Journals Inc. (US)

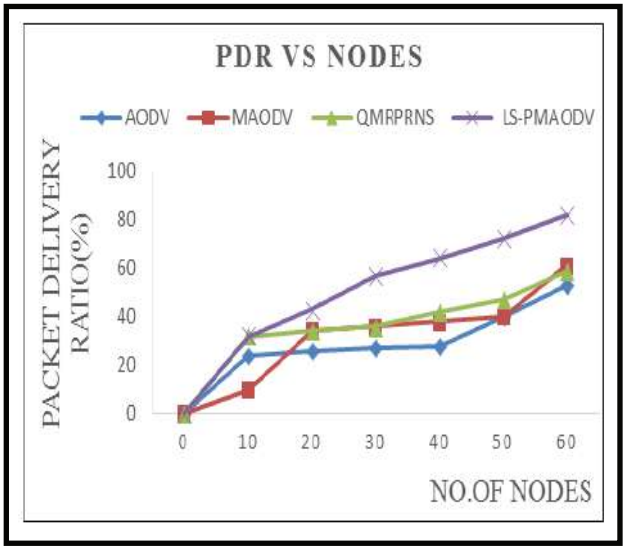

Figure 2: Packet Delivery Ratio Vs Node

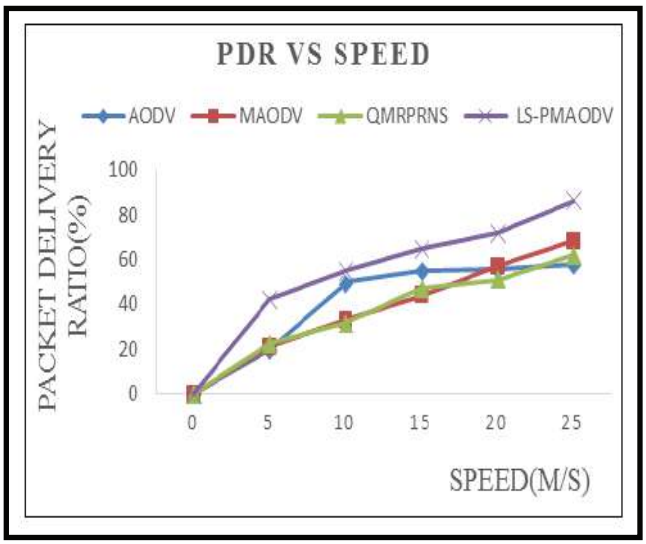

Figure 3: Packet Delivery Ratio Vs Speed

b) End-to-End Delay

End-to-End Delay of data packets is calculated as the time it takes to transmit data packets from the source to the destination. Low end-to-end delay is preferred for better application execution. Fig.4 shows the end-to-end delay for different number of nodes. It is clearly evident the proposed approach provides less end-to-end delay than other protocols. From Fig 5, it is obvious that the LS PMAODV has lower end-to-end delay for different node speed. Furthermore, LS PMAODV achieves lower end-to-end delay than AODV, MAODV and QMRPRNS.

© 2017 Global Journa ls Inc. (US)

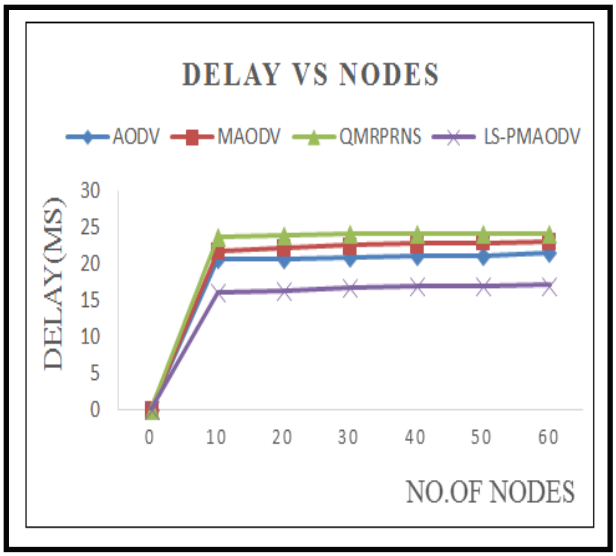

Figure 4: End-to-End Delay Vs Node

c) Energy Consumption

The energy consumption is the total of utilized energy of the considerable number of nodes in the system, where the energy is utilized due to transmitting (P_t), reception (P_r), and initialization (Pi). Accepting every transmission expends a vitality unit, the aggregate energy utilization is proportional to the aggregate number of parcels sent in the system.

Fig.6 shows the energy consumption for different number of nodes. It is clearly evident the proposed approach has less energy consumption than other protocols. From Fig 7, it is obvious that the LS PMAODV has less energy consumption for different speed when compared to other existing protocols.

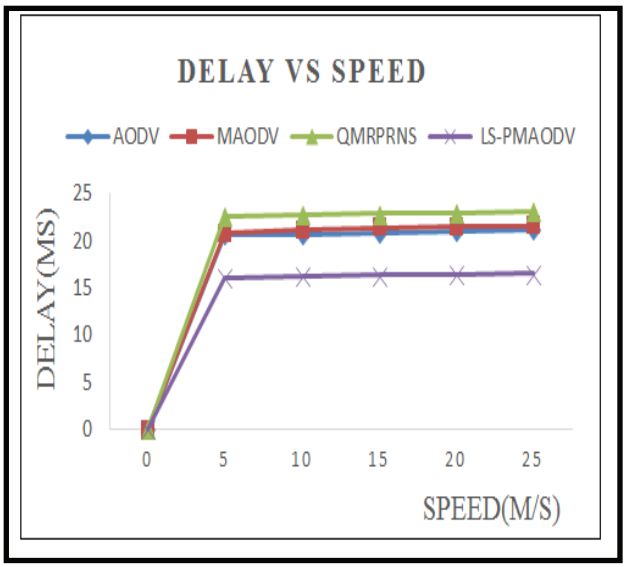

Figure 5: End-to-End Delay Vs Speed

© 2017 Global Journals Inc. (US)

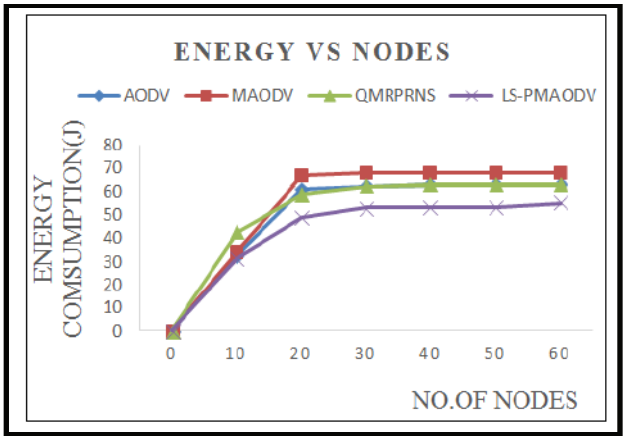

Figure 6: Energy Consumption Vs Node

d) Network lifetime

Network lifetimes determine the interval between the start of a packet transmission of the network till the first node fails due to battery depletion. Fig. 8 depicts the lifetime of nodes for different number of nodes It is obvious that the proposed method results in longer node life time when compare to other existing methods. Fig. 9 depicts lifetime of nodes for different speed. It reveals that LS PMAODV increases the node lifetime than other methods.

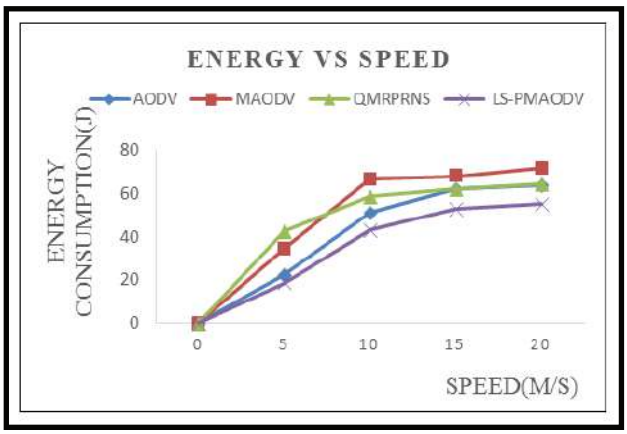

Figure 7: Energy Consumption Vs Speed

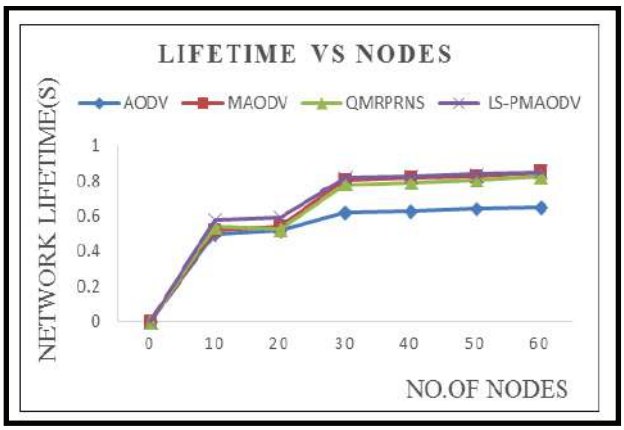

Figure 8: Network Lifetime Vs Node

© 2017 Global Journals Inc. (US)

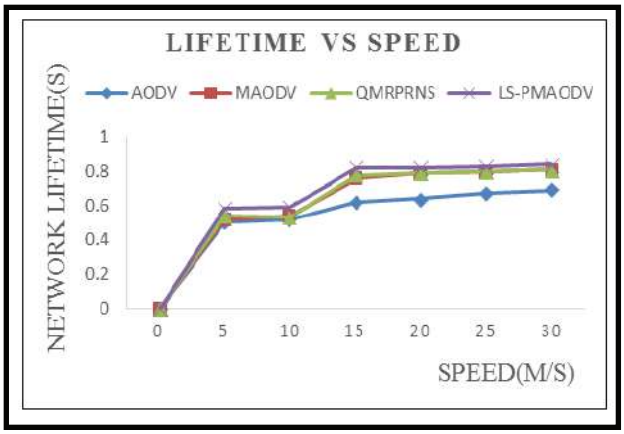

Figure 9: Network Lifetime Vs Speed

e) Computation overhead

Computation Overhead is the combination of excess or indirect computation time, memory and bandwidth. The main problem of wireless network is reliability and traffic overhead. Overhead is also the combination of excess or indirect computation time, memory, and bandwidth.

Fig. 10 shows the computation overhead for different number of nodes. It is clearly evident the proposed approach has less computation overhead than other protocols. From Fig 11, it is clear that the LS PMAODV has less computation overhead for different node speed when compared to other existing protocols.

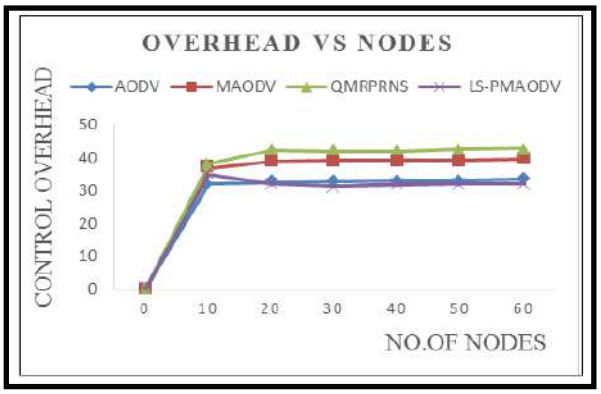

Figure 10: Computation Overhead Vs Node

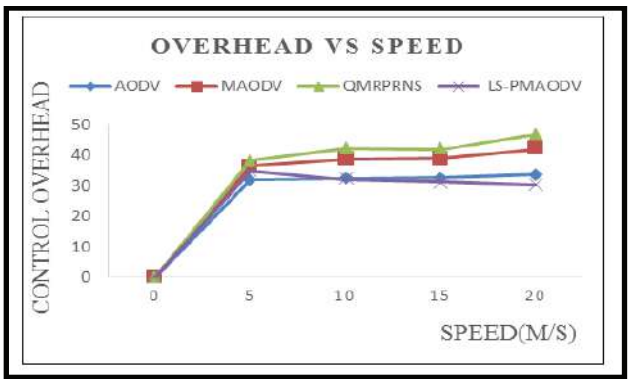

Figure 11: Computation Overhead Vs Speed

f) Connectivity

Connectivity plays the main role, which have the ability to report information to the fusion center, even though it has the critical for sensing the coverage. A wireless sensor network (WSN) is a network comprises of enough space for distributing the autonomous devices using sensors to screen the physical or environmental conditions. A WSN framework combines to form a portal that gives remote network which acts a backbone to the wired world and conveyed hubs.

© 2017 Global Journals Inc. (US)

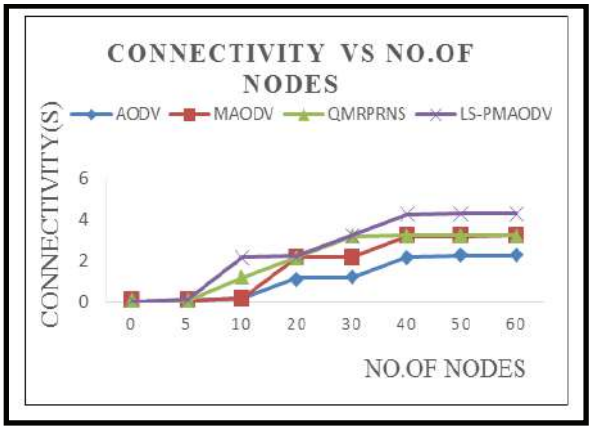

Figure 12: Connectivity Vs Node

Fig. 12 shows the connectivity for different number of nodes. It is evident the proposed approach provide high connectivity than other protocols. From Fig 13, it is clear that the LS PMAODV has high connectivity for different node speed when compared to other existing protocols.

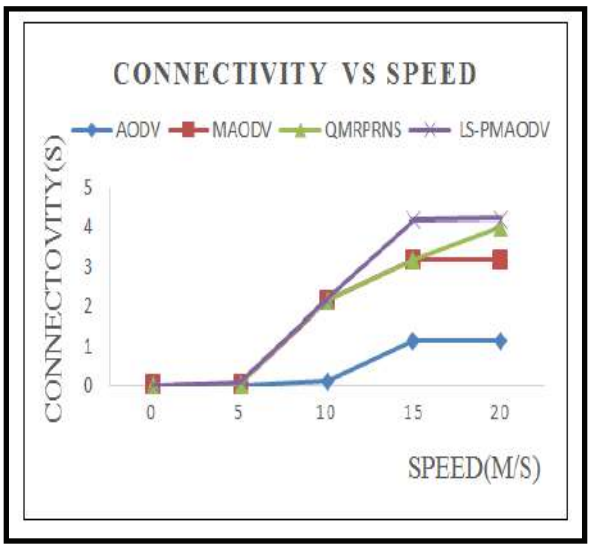

Figure 13: Connectivity Vs Speed

g) Link Stability

Link Stability is a statistical-based approach has been adopted in order to discriminate among several links which are more stable for some periods of time without exactly predicting the residual link lifetime of each link. Thus, to enable mobile devices to make smart decisions in connection to the stability, a practical method is used, based exclusively on observations related to the link, in previous time instants. As a result, this analysis produces an evaluation of the link residual lifetime of the link, since the stability of a link is given by its probability of persisting for a certain time span. Fig 14 and 15 shows the number of nodes vs. link stability and speed vs. link stability respectively.

© 2017 Global Journals Inc. (US)

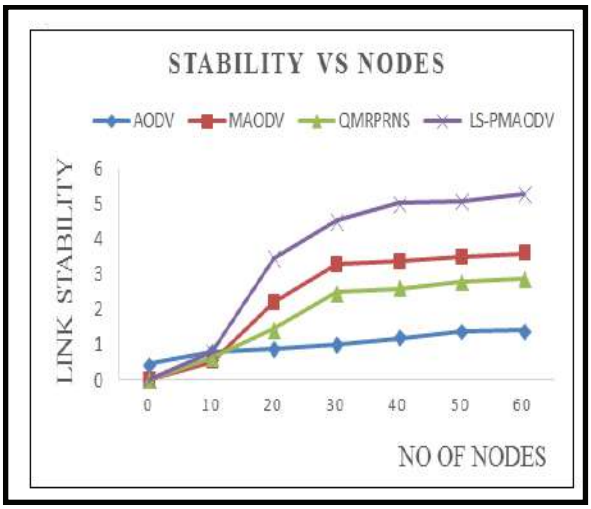

Figure 14: Link stability Vs Node

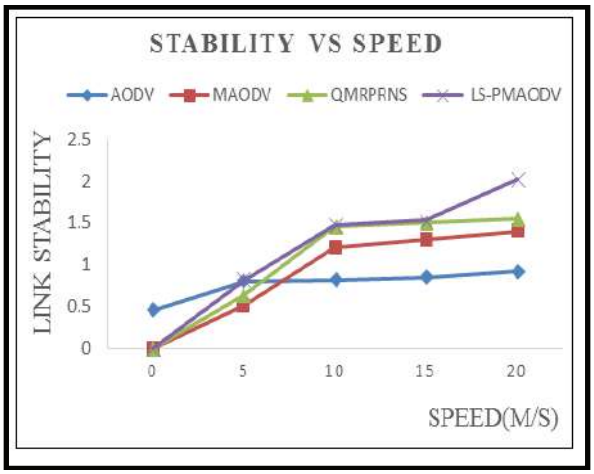

Figure 15: Link stability Vs.Speed

It is clearly evident that LS PMAODV provides high link stability than AODV, MAODV and QMRPRNS.

h) Throughput

In data transmission, network throughput is the amount of data transmitted successfully from sender node to receiver node in a given time period and typically measured in bits per second (bps), megabits per second (Mbps) or Gigabits per second (Gbps). Fig 16 and 17 shows the throughput achieved for different number of nodes and different speed respectively. From Fig 17 and 18, the throughput for LS PMAODV is greater than other protocols.

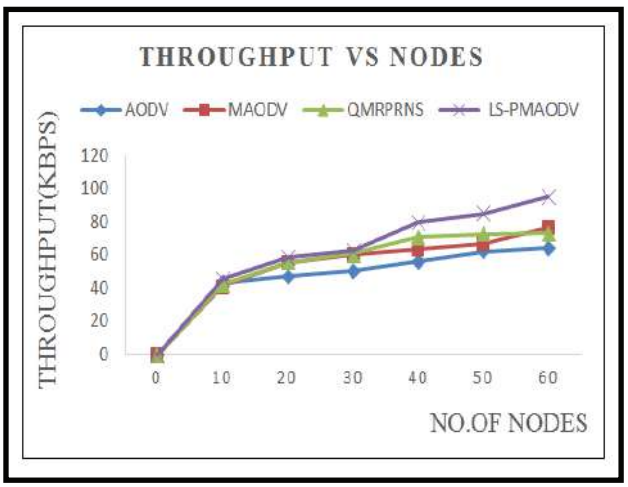

*Figure 16:*Throughput Vs Node

© 2017 Global Journals Inc. (US)

Figure 17: Throughput Vs Speed

VI. Conclusions

This research paper describes the link stability based priority multicast Adhoc and demand distance vector routing protocol to enhance the route discovery of nodes which is stable of MANET .The proposed LSMAODV protocol is implemented using Network Simulator 2 (NS-2). The support level of predictable performance for network system is decreased the delay and to enhance the efficiency. The QoS metrics such as delay, energy consumption, an end to end latency, loss, overhead are minimized and PDR, throughput are enhanced using the proposed protocol compared to the existing AODV and MAODV routing protocols. The clustering arrangement stores the energy of the cluster member nodes. Hence, the proposed method is enormously energy efficient which is linked to the AODV and MAODV algorithm in achieving high QoS in MANET.

References Références Referencias

1. Layuan, L., Chunlin, L., A QoS multicast routing protocol for clustering mobile ad hoc networks, Computer Commu-nications, (2007), 30(7), 1641-1654.
2. Sutariya, D., Kamboj, P., A Survey of QOS Multicast Routing Protocol for MANET, (2013), 73(10), 3589-3599.
3. Royer, E.M and Chai-Keong Toh. A Review of Current Routing Protocols for Ad Hoc Mobile Wireless Networks. IEEE Personal Communications, pp. 46–55, April 1999.
4. Perkins, C.E., Bhagwat, P., Highly dynamic Destination Sequenced Distance-Vector routing (DSDV) for mobile computers, in: T. Imielinski, H. Korth (Eds.), Proceedings of SIGCOMM'94 Conference on Communications Architectures, Protocol and Applications, ACM, London, UK, 1994, pp. 234–244.
5. Chiang, C.C., Routing in clustered multihop mobile wireless networks with fading channel, in: T.S. Chua, H.K. Pung, T.L. Kunii (Eds.), Proceedings of the IEEE Singapore International Conference on Networks, Springer, Singapore, 1997, pp. 197–211.
6. Shree, M., Garcia-Luna-Aceves, J.J., An efficient routing protocol for wireless networks, ACM Mobile Networks and Application Journal 1 (1996) 183–197.
7. Perkins, C., Ad hoc On-Demand Distance Vector (AODV) routing, RFC3561[S], 2003, <http://www.ietf.org/rfc/rfc3561.txt>.
8. Johnson, D.B., Maltz, D.A., Hu, Y.C., The dynamic source routing protocol for mobile ad hoc networks, Internet Draft, draft-ietfmanet- dsr-10.txt, 2004.
9. Park, V.D., Corson, M.S., Temporally ordered routing algorithm (TORA) version 1: functional specification, Internet Draft, draft-ietfmanet-tora-spec- 00.txt, November 1997.
10. Dube, R., Rais, C.D., Wang, K., Tripathi, S.K., Signal stability based adaptive routing for ad hoc mobile networks, IEEE Personal Communications 4 (1997) 36–45.
11. Charles. Wireless access technology - WiFi and WiMAX. Available at: http://network.chinabyte. com/222/12223722.shtml (Accessed: 5 July 2014) 2011.
12. Huang, Z.C., Shen, C.C., A comparison study of omnidirectional and directional MAC protocol for ad-hoc networks, IEEE Global Telecommunications Conference (2002) 57–61.
13. Chen, X., Wu, J., Multicasting techniques in mobile ad-hoc networks, The Handbook of Ad-hoc Wireless Networks (2003) 25–40.
14. Devarajan, K., Padmathilagam, V, An Enhanced Cluster Gateway Switch Routing Protocol (ECGSR) for Congestion Control using AODV Algorithm in MANET, International Journal of Computer Applications, (2015), 123(3).
15. De, M.C.C., Gossain, H., Agrawal, D.P., Multicast over wireless mobile ad-hoc networks: present and future direc-tions, IEEE Network, (2003), 5259.
16. Vinay., P. Viradia, Improved AODV Routing Protocol for MANET, Journal of Engineering Research and Applica-tions, (2014), ISSN: 2248-9622, Vol. 4, Issue 1 (Version 3), pp .368-374.

© 2017 Global Journa ls Inc. (US)

17. Phate, N., Saxena, M., Rizvi, M. A., High temperature fiber optic laser-induced breakdown spectroscopy sensor for analysis of molten alloy constituents, Minimizing conges-tion and improved QoS of AODV using clustering in mobile ad hoc network, (2014), (pp. 1-5).
18. Rango, F. De.; Fazio, P.; (2012); Link Stability and Energy Aware Routing Protocol in Distributed Wireless Networks, IEEE Trans. on Parallel and Distributed systems, 23: 713-726.
19. Rajashekhar Biradar, Sunilkumar Manvi, and Mylara Reddy. Link stability based multicast routing scheme in MANET. Computer Networks. 54(7): 1183-1196, 2010.
20. Geunes, M., U. Sorges, U., I. Bouazizi, I., Ara–the ant-colony based routing algorithm for manets, in: ICPP workshop on Ad Hoc Networks (IWAHN 2002), August 2002, pp. 79–85.
21. Biswas, J., Barai, M., Nandy, S.K., Efficient hybrid multicast routing protocol for ad-hoc wireless networks, local computer networks, in: 29th Annual IEEE International Conference on November 2004, pp. 180–187.
22. Rong B, Amoussou G, Dziong Z, Kadoch M, Ahmed KE. Mobility prediction aided dynamic multicast routing in MANET. In: Proceedings of the IEEE/ Sarnoff symposium on advances in wired and wireless communication, Princeton, NJ, 2005. p. 21–4.
23. Viswanath K, Obraczka K, Tsudik G. Exploring mesh and tree-based multicast routing protocols for MANETs. IEEE Transactions on Mobile Computing 2006;5(1): 28–42.
24. Jiang, S., He, D., Rao, J., A prediction-based link availability estimation for routing metrics in MANETs, IEEE/ACM Transactions on Networking 13 (2005) 1302–1312.
25. Cheng H, Cao J, Wang X. A fast and efficient multicast algorithm for QoS group communications in heterogeneous network. Elsevier, Computer Communications 2007; 30: 2225–35.
26. Ramanathan, R., Hain, R., An ad hoc wireless testbed for scalable, adaptive QoS support, Wire-less Communications and Networking Conference, (2000), (Vol. 3, pp. 998-1002).
27. Sedrati, M., Bilami, A., Benmohamed, M., M-AODV: AODV variant to Improve Quality of Service in MANETs, arXiv preprint arXiv, (2011), 1104.1186.
28. Lakshmi, S. M., Sikamani, K. T., Energy-aware multicast opportunistic routing protocol (Eamor) to optimize lifetime of MANET, In Current Trends in Engineering and Tech-nology (ICCTET), Interna-tional Conference , (2013), (pp. 210-212).
29. Yadav, A. K., & Tripathi, S. (2016). Qmrprns: Design of qos multicast routing protocol using reliable node selection scheme for manets. Peer-to-Peer Networking and Applications, 1-13.

© 2017 Global Journals Inc. (US)

DYNAMIC RESOURCE ALLOCATION WITH POWER CONSTRAINT IN WCDMA WIRELESS NETWORKS

By

VANDANA KHARE * Y. MADHAVEE LATHA ** D. SRINIVASA RAO ***

* Research Scholar, JNT University, Hyderabad, India.
** Principal, Malla Reddy Engineering College for Women, Hyderabad, India.
*** Professor, Department of Electronics and Communication Engineering, JNTUH, Hyderabad, India.

Date Received: 21/03/2017 Date Revised: 13/04/2017 Date Accepted: 15/04/2017

ABSTRACT

WCDMA is a Wideband Code Division Multiple Access technique. Because of high data rate, it is mainly used in the 3rd generation mobile networks. In Centralized Call Admission Control (CCAC) technique, when a new call arrives, the system checks whether the call should be admitted or not on the basis of Signal to Interference Ratio (SIR), transmission power, and the network load. If the call is accepted, it will increase some interference to the ongoing calls. This new interference would degrade the performance of ongoing calls, increase the outage rate, and ultimately affects the Quality of Service of the network. Hence, to reduce the interference while improving Quality of Service in the WCDMA network, an efficient Resource Allocation with Power Constraint (PC) in the network is required for achieving a higher throughput with appropriate handoff, improved battery life as well as network performance. This paper proposes an algorithm for Resource Allocation with Power Constraint (PC) for real time traffic in WCDMA Network. The simulation result shows that the proposed scheme can significantly reduce power consumption and increase throughput with less delay.

Keywords: SIR, CAC, RA, QoS, WCDMA.

INTRODUCTION

WCDMA is a spread-spectrum modulation technique which uses channels with bandwidth much greater than that of the data to be transferred. Wideband CDMA can support services with higher rate when it measured up with the narrow-band CDMA. It is adaptable to distribute multimedia traffic. On the other hand, a new Medium Access Control protocol (MAC) is required to manage the packet access efficiently in wideband CDMA wireless networks [1] in order to make use of such instruments. Efficient Call Admission Control (CAC) and Medium Access Control (MAC) protocols are necessary for the QoS provisioning in WCDMA environment [2]. But CAC alone is not enough to provide most optimal resource utilizations [7] due to the bursty nature of packet traffic [11]. In an integrated multiclass packetized network, Resource Allocation with power constrained is required for minimizing the interference and improve network performance to maintain better quality of service in WCDMA wireless network [3].

In this paper, the authors have proposed a new Resource Allocation based Connection Admission Control (RACAC) algorithm for multiple services like voice, video, and data for multiclass users [6]. It determines the optimum set of admissible users with optimum rate, so as to minimize the interference level and call blocking probability and adaptive rate scheduling algorithm to adjust the rate for every session.

The rest of the paper is organized as follows, Section 1 gives the details about the related work. The complete details about proposed methodology is given in section 2. Next, section 3 gives the results evaluation for the proposed approach, finally conclusions are provided in the last section.

1. Related Work

Jraifi Abdelouahed [1] has presented the major problem that contributes in limiting the performance of cellular

ISSN: 2277-9655
(I2OR), Publication Impact Factor: 3.785

IJESRT

INTERNATIONAL JOURNAL OF ENGINEERING SCIENCES & RESEARCH TECHNOLOGY

OPTIMIZATION OF LATERAL FORCE RESISTING SYSTEM IN TALL BUILDINGS UNDER SESMIC LOADS IN DIFFERENT SEISMIC ZONES

Prof. Syed Farrukh Anwar*, Asst. Prof. Noor Mohammed, MD. Ishtiyaq Ahmed
* Department of Civil Engineering.
Department of Civil Engineering.
Department of Civil Engineering.

ABSTRACT

The evolution of tall building structural systems based on new structural concepts with newly adopted high strength materials and construction methods have been towards "stiffness" and "lightness". Structural systems are become "lighter" and "stiffer". It is common knowledge that rather than directly standing the forces, it is better to reduce them and dissipate the magnitude of vibrations. Structure design of high rise buildings is governed by lateral loads due to wind or earthquake. Lateral load resistance of structure is provided by interior structural system or exterior structural system. The selected structural system should be such that it should be effectively utilized for structural requirements. Efficient lateral systems, decreases the lateral deformations caused by the seismic forces in the buildings. The distribution of the mass symmetrically reduces the torsional effect in the building.

In this work, it is proposed to carry out an analytical study, on multi-storeys buildings of 10, 20 and 30 stories, was carried out accounting for different seismic zones. The suitability and efficiency of different lateral systems that are commonly used as conventional frame, concrete infill, diagrid and shear wall were investigated. These buildinq1g models are analysed, using ETABS 2015 software, to the action of lateral forces employing linear static and linear dynamic approaches as per IS 1893 (Part I): 2002. The results of the analyses, in terms of lateral deformations, base shear, modal time period respective storey drifts.

KEYWORDS:.

INTRODUCTION

Mankind has always had a fascination for height and throughout our history; we have constantly sought to metaphorically reach for the stars. From the ancient pyramids to today's modern skyscraper, a civilization's power and wealth has been repeatedly expressed through spectacular and monumental structures. Today, the symbol of economic power and leadership is the skyscraper. There has been a demonstrated competitiveness that exists in mankind to proclaim to have the tallest building in the world. The design of sky scrapers is usually governed by the lateral loads imposed on the structure. As buildings have taller and narrower, the structural engineer has been increasingly challenged to meet the imposed drift requirements while minimizing the architectural impact of the structure. In response to this challenge, the profession has proposed a multitude of lateral schemes that are now spoken in tall buildings across the globe. For this purpose, 10, 20 and 30 storied building is considered in which diagrid system, conventional frame, shear wall frame and infill wall frame are provided with four seismic zones. Linear static analysis is also known as time seismic coefficient method. It is an important and accurate technique for structural seismic analysis especially when the evaluated structural response is linear. Linear static and dynamic analysis was carried out with four seismic zones (II, III, IV and V) for 10, 20 and 30 storied building.

MODELLING PARAMETERS

Building Description: Reinforced Concrete Frames of 10 storeys, 20 storeys and 30 storeys with plan size 18mx18m, with heights of 30m, 60m and 90m respectively are modelled.

S. No.	Specifications	10,20&30 storey
1	Slab Thickness	150mm
2	Beam dimensions	
	10 STORIES	450x230mm
	20,30 STORIES	500X230mm
3	Column dimensions	450x600mm,
		750x500mm
4	Grade of concrete	M30
5	Grade of steel	Fe-500
6	Unit weight of concrete	25kN/m^3
7	Live loads	3kN/m^2
	(a) Floor load	1.5kN/m^2
8	Diagrid	500x500 mm
9	Type of structure	Diagrid two story module
10	Importance factor	1
11	Seismic zone	II,III,IV&V
12	Response reduction factor	5

Table 1 Data of RC Frames considered in study

unit weight of masonry	20kn/m3
modulus of elasticity E	3285.9Mpa
poisons ratio U	0.15
SHEAR MODULUS G	1428.65 MPa
thickness of wall	230mm

Table 2 Data of infill Frames considered in study

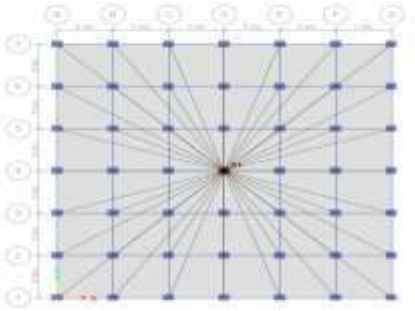

Fig 1: plan of Rcc frame model

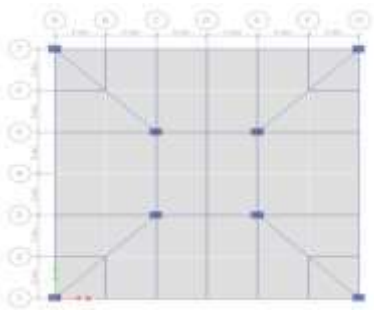

Fig 2: plan of Diagrid frame model

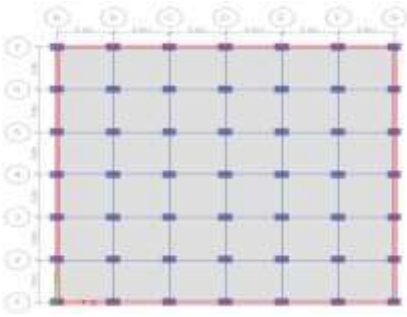

Fig 3: plan of infill frame model

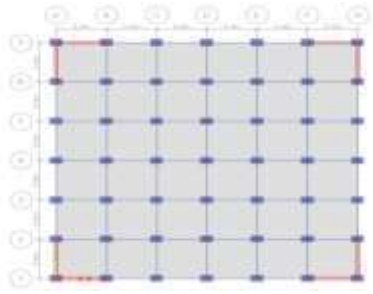

Fig 4: plan of shear wall frame model

ANALYSIS RESULTS

The Results obtained are of different parameters such as Storey drifts, Base shear, Modal Periods etc. The results obtained by carrying out linear static and linear dynamic analysis for Buildings as listed.

RESULT FOR LINEAR DYNAMIC ANALYSIS OF 10 STORIES BUILDING

RESPONSE SPECTRUM						
	BARE FRAME	DRIFT	infill	DRIFT	diagrid	DRIFT
STORY 1	3.4	3.4	1.5	1.5	0.6	0.6
STORY 2	9.4	2.0	3.4	0.6	1.7	0.4
STORY 3	16	2.2	5.4	0.7	2.9	0.4
STORY 4	22.3	2.1	7.3	0.6	3.6	0.2
STORY 5	28.2	2.0	9.2	0.6	4.9	0.4
STORY 6	33.3	1.7	11	0.6	5.5	0.2
STORY 7	37.7	1.5	12.6	0.5	6.8	0.4
STORY 8	41.2	1.2	14	0.5	7	0.1
STORY 9	43.7	0.8	15.1	0.4	8.1	0.4
STORY 10	45.3	0.5	15.9	0.3	8.6	0.2

TABLE 3: showing displacement and story drift with response spectrum for 10 storie

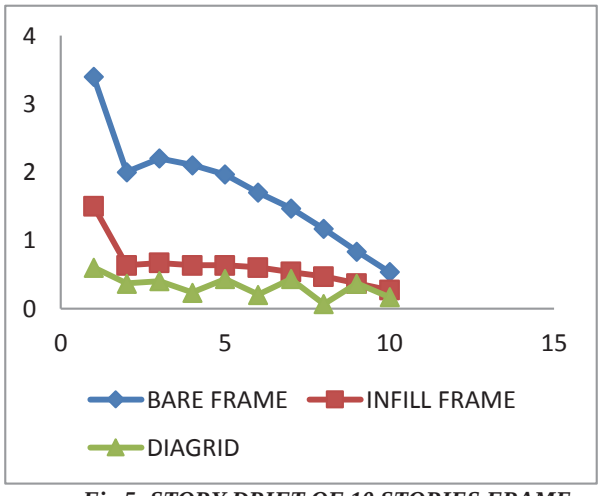

Fig 5: STORY DRIFT OF 10 STORIES FRAME

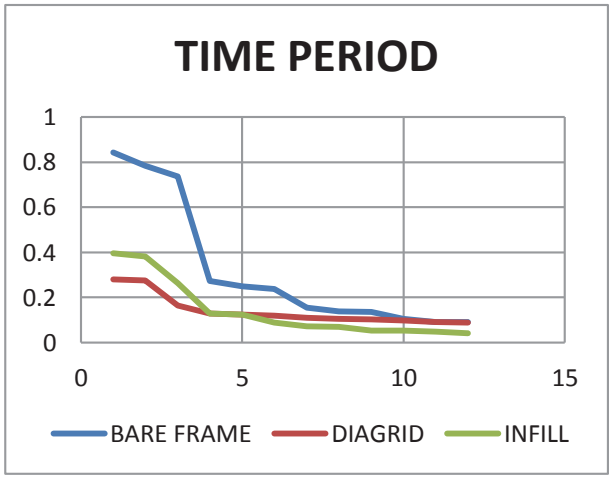

Fig 6: STORY DISPLACEMENT OF 10 STORIES FRAME

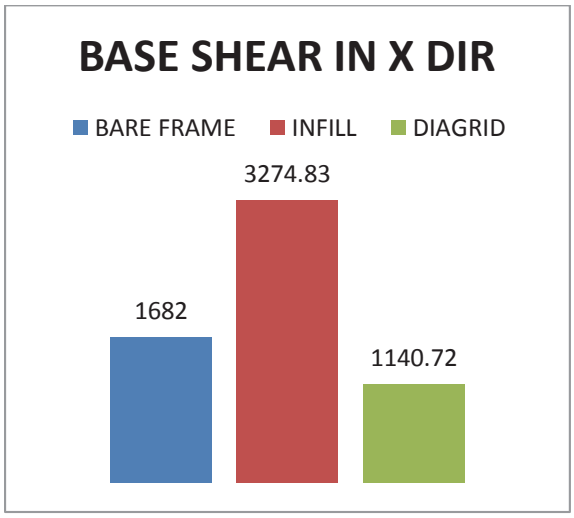

Fig 7: TIME PERIOD OF 10 STORIES FRAME

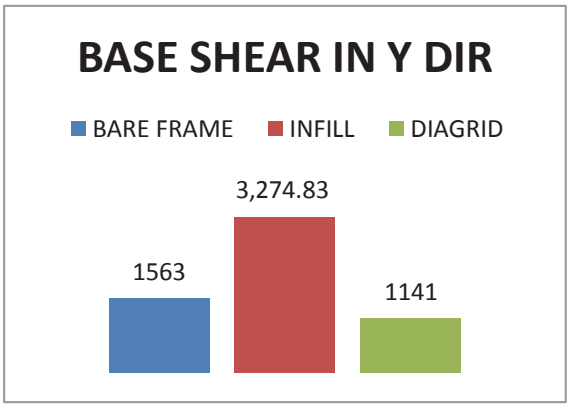

Fig 8: BASE SHEAR OF 10 STORIES FRAME

RESULTS FOR LINEAR DYNAMIC ANALYSIS OF 20 STORIES BUILDING

RESPONSE SPECTRUM						
	BARE FRAME	DRIFT	DIAGRID	DRIFT	INFILL	DRIFT
STORY 1	2.6	2.6	1.2	1.2	1.6	1.6
STORY 2	7.7	1.7	3.1	0.6	4	0.8
STORY 3	13.7	2.0	5	0.6	6.6	0.9
STORY 4	19.8	2.0	6.9	0.6	9.5	1.0
STORY 5	26	2.1	9.2	0.8	12.5	1.0
STORY 6	32	2.0	11.5	0.8	15.6	1.0
STORY 7	37.8	1.9	14.1	0.9	18.8	1.1
STORY 8	43.5	1.9	16.5	0.8	22.1	1.1
STORY 9	48.9	1.8	19.3	0.9	25.3	1.1
STORY 10	54	1.7	21.8	0.8	28.6	1.1
STORY 11	58.9	1.6	24.7	1.0	31.8	1.1
STORY 12	63.6	1.6	27.3	0.9	35	1.1
STORY 13	67.9	1.4	30.3	1.0	38.1	1.0
STORY 14	72	1.4	32.8	0.8	41.1	1.0
STORY 15	75.7	1.2	35.7	1.0	44	1.0
STORY 16	79	1.1	38.1	0.8	46.8	0.9
STORY 17	81.9	1.0	40.9	0.9	49.4	0.9
STORY 18	84.4	0.8	43.1	0.7	51.9	0.8
STORY 19	86.5	0.7	45.9	0.9	54.1	0.7
STORY 20	89.1	0.9	47.7	0.6	56.2	0.7

TABLE 4: showing displacement and story drift with response spectrum for 20 stories

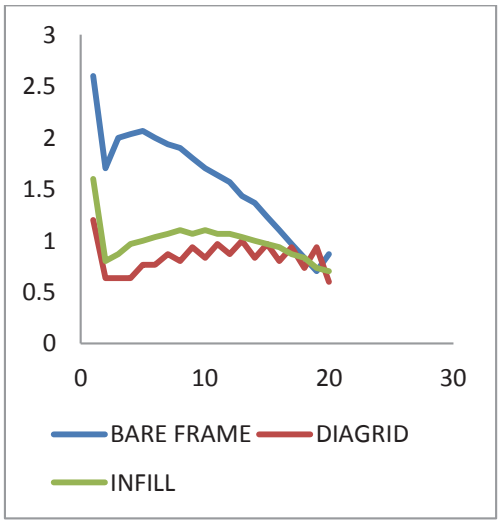

Fig 10: STORY DRIFT OF 20 STORIES FRAME

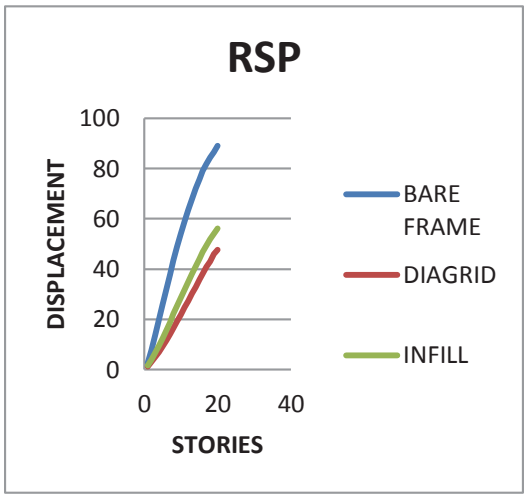

Fig 11: STORY DISPLACEMENT OF 20 STORIES FRAME

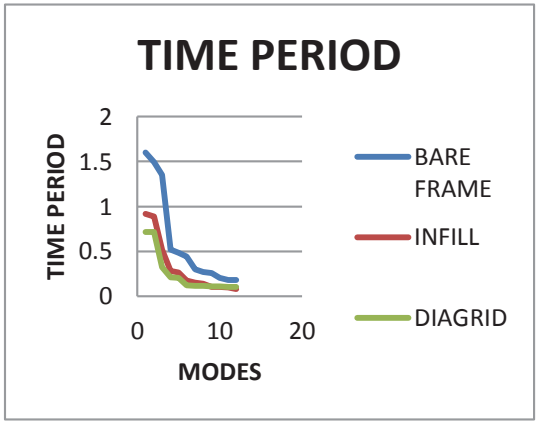

Fig 12: TIME PERIOD OF 20 STORIES FRAME

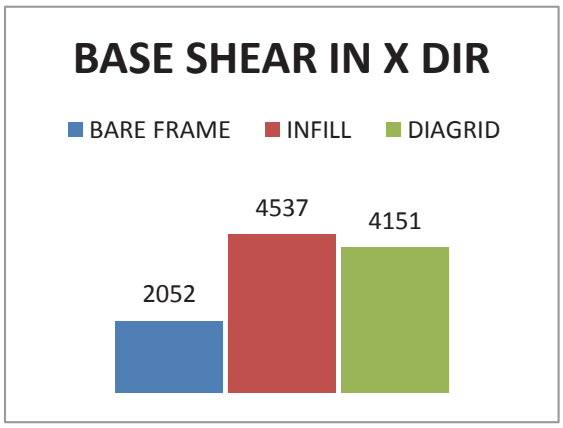

Fig 13: BASE SHEAR OF 20 STORIES FRAME

RESULTS FOR LINEAR DYNAMIC ANALYSIS OF 30 STORIES BUILDING

RESPONSE SPECTRUM								
	BARE FRAME	DRIFT	infill	DRIFT	diagrid	DRIFT	shear wall	DRIFT
STORY 1	2.6	2.6	1.5	1.5	0.9	0.9	1.2	1.2
STORY 2	7.6	1.7	3.8	0.8	2.7	0.6	3.9	0.9
STORY 3	13.6	2.0	6.4	0.9	4.5	0.6	7.5	1.2
STORY 4	19.9	2.1	9.2	0.9	6.3	0.6	11.8	1.4
STORY 5	26.2	2.1	12.2	1.0	8.5	0.7	16.7	1.6
STORY 6	32.6	2.1	15.3	1.0	10.7	0.7	21.9	1.7
STORY 7	38.8	2.1	18.6	1.1	13.3	0.9	27.4	1.8
STORY 8	45	2.1	22.1	1.2	15.8	0.8	33	1.9
STORY 9	51.1	2.0	25.6	1.2	18.7	1.0	38.7	1.9
STORY 10	57.1	2.0	29.2	1.2	21.5	0.9	44.5	1.9
STORY 11	63.1	2.0	32.9	1.2	24.6	1.0	50.2	1.9
STORY 12	68.9	1.9	36.6	1.2	27.7	1.0	55.8	1.9
STORY 13	74.6	1.9	40.4	1.3	31	1.1	61.4	1.9
STORY 14	80.1	1.8	44.3	1.3	34.3	1.1	66.9	1.8
STORY 15	85.6	1.8	48.1	1.3	37.8	1.2	72.3	1.8
STORY 16	91	1.8	52.1	1.3	41.3	1.2	77.6	1.8
STORY 17	96.2	1.7	56	1.3	44.9	1.2	82.7	1.7
STORY 18	101.3	1.7	60	1.3	48.5	1.2	87.7	1.7
STORY 19	106.2	1.6	63.9	1.3	52.3	1.3	92.6	1.6

STORY 20	111.1	1.6	67.9	1.3	55.9	1.2	97.3	1.6
STORY 21	115.7	1.5	71.9	1.3	59.7	1.3	101.9	1.5
STORY 22	120.2	1.5	75.8	1.3	63.4	1.2	106.3	1.5
STORY 23	124.4	1.4	79.7	1.3	67.2	1.3	110.5	1.4
STORY 24	128.5	1.4	83.5	1.3	70.9	1.2	114.5	1.3
STORY 25	132.3	1.3	87.3	1.3	74.7	1.3	118.4	1.3
STORY 26	135.9	1.2	91	1.2	78.3	1.2	122	1.2
STORY 27	139.2	1.1	94.7	1.2	82.1	1.3	125.5	1.2
STORY 28	142.1	1.0	98.2	1.2	85.6	1.2	128.8	1.1
STORY 29	144.8	0.9	101.6	1.1	89.4	1.3	131.9	1.0
STORY 30	149.3	1.5	103	0.5	92.7	1.1	134.9	1.0

TABLE 5: showing displacement and story drift with response spectrum for 30 stories

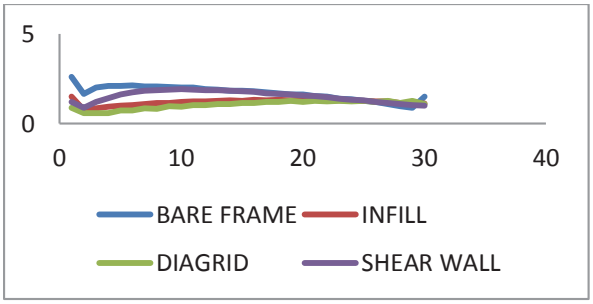

Fig 15: STORY DRIFT OF 30 STORIES FRAME

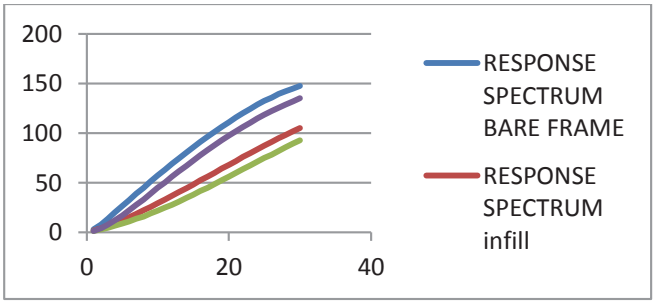

Fig 16: STORY DISPLACEMENT OF 30 STORIES FRAME

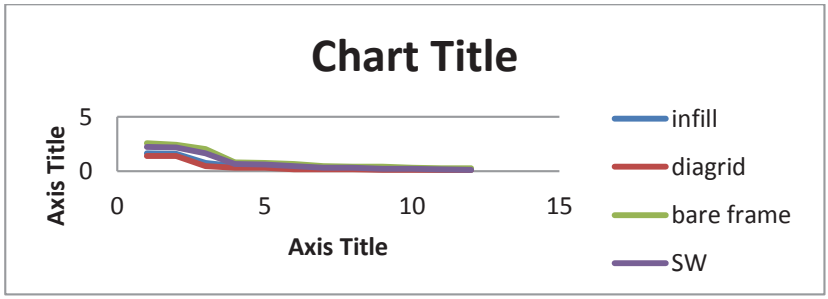

Fig 17: TIME PERIOD OF 30 STORIES FRAME

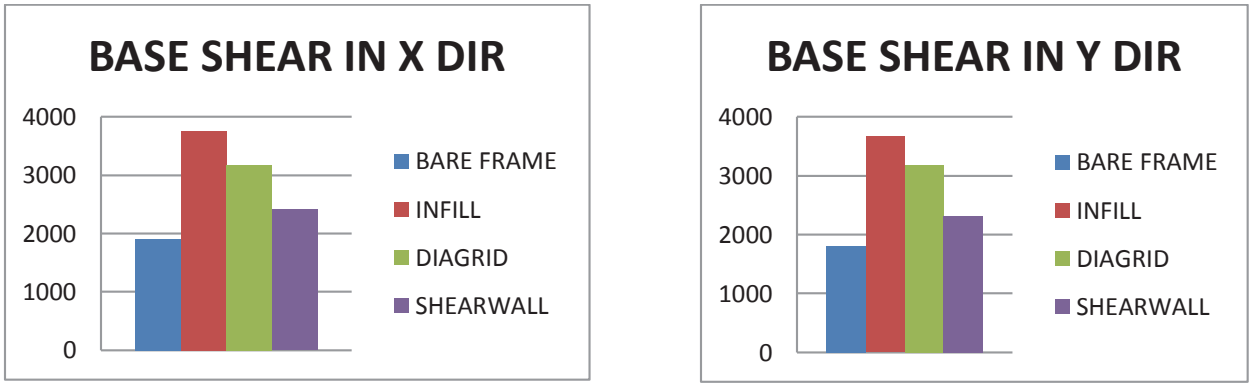

Fig 18: BASE SHEAR OF 30 STORIES FRAME IN X AND Y DIRECTION.

CONCLUSIONS

Today's complex-shaped tall buildings require more complicated system design, analysis and construction. Not only architectural but also structural and other related performance issues should be considered holistically to produce higher quality built environments. Well-organized coordination between architects and engineers is essential.

- For ten story buildings, In order to control the seismic response diagrid were modeled and the results showed that there is a drastic decrease in storey displacements by 81% and 46% compared to 10 stories bare frame and infill frame and storey drifts by 60% and 33% compared to other symmetric building.
- In present work, due to using infill wall it gives good ductility and increase in strength carrying capacity and initial stiffness of Rcc frame .the reduction of story drift by 40% compared to 10 stories normal Rcc framed structure.
- For twenty story buildings, In order to control the seismic response diagrid were modeled and the results showed that there is a drastic decrease in storey displacements by 47% and 16% compared to 20 stories bare frame and infill frame.
- For thirty story buildings, In order to control the seismic response diagrid were modeled and the results showed that there is a drastic decrease in storey displacements by 37% ,31% and 12% compared to 30 stories bare frame, shear wall frame and infill frame.
- As the lateral loads are resisted by diagonal columns, the top storey displacement is very much less in diagrid structure as compared to the other frame building.
- As time period is less, lesser is mass of structure and more is the stiffness, the time period is observed less in diagrid frame structure which reflects more stiffness of the structure and lesser mass of structure.
- The overall results suggested that diagrid structure is excellent seismic control for high-rise symmetric Bu

SCOPE FOR FURTHER STUDY

1. To study the shear lag effect on tall structure exhibit a considerable degree of shear-lag with consequential reduction in structural efficiency.
2. To study the Wind effects on tall building frames-influence of dynamic parameters.
3. In the present study, openings were not considered in infills. Presence of opening in infills significantly reduces the stiffness and strength of the infilled frames. Suitability of the proposed strengthening schemes must be verified for Masonry-infilled frames with openings with walls.

REFERENCES

[1] Smith, B. S. and Coull, A.Tall Building Structures: Analysis and Design“, John Wiley & Sons, Inc., 1991
[2] A. Coull & E.stafford Smith, „Tall Buildings, with particular reference to shear wall structures“, Pergamon Press, 1967
[3] Mir M. Ali,Performance characteristics of tall framed tube buildings in seismic zones“, Elsevier Science Ltd,1996
[4] Journal of Structural Engineering vol. 120 Nos. 1-4, 1994, P 1221- „ Simple Method for Approximate Analysis of framed tube structures“
[5] S.M.A. Kazini, R. Chandra, “Analysis of Shear-walled Buildings “
[6] Chen, Genda, and Jingning Wu. 2001. “Optimal Placement of Multiple Tune Mass Dampers for Seismic Structures.” Journal of Structural Engineering 127 (9): 1054–1062.
[7] Moon, Kyoung Sun. 2008. “Optimal Grid Geometry of Diagrid Structures for Tall Buildings.” Architectural Science Review 51 (3): 239–251.
[8] Pankaj Agarwal and manish shrikhande, (2006), "earthquake resistant design of structures", eastern economy edition publisher of engineering books.
[9] R. Clough, and J. Penzien (1993), “Dynamics of Structures”, Second Edition, McGraw-Hill, Inc., ISBN 0-07-011394 .

INTL JOURNAL OF ELECTRONICS AND TELECOMMUNICATIONS, 2017, VOL. 63, NO. 3, PP. 269-277
Manuscript received December 20 , 2016; revised June, 2017. DOI: 10.1515/eletel-2017-0036

Optimal Spectrum Utilization and Flow Controlling In Heterogeneous Network with Reconfigurable Devices

Syed Shakeel Hashmi, Syed Abdul Sattar, and K. Soundararajan

Abstract*—Fairness provisioning in heterogeneous networks is a prime issue for high-rate data flow, wherein the inter-connectivity property among different communication devices provides higher throughput. In Hetnet, optimal resource utilization is required for efficient resource usage. Proper resource allocation in such a network led to higher data flow performance for real-time applications. In view of optimal resource allocation, a resource utilization approach for a reconfigurable cognitive device with spectrum sensing capability is proposed in this paper. The allocation of the data flow rate at device level is proposed for optimization of network fairness in a heterogeneous network. A dynamic approach of rate-inference optimization is proposed to provide fairness in dynamic data traffic conditions. The simulation results validate the improvement in offered quality in comparison to multi-attribute optimization.

***Keywords*—rate-inference optimization, heterogeneous network, flow control, spectrum utilization**

I. INTRODUCTION

WITH regard to emerging trends in wireless communication, heterogeneous networks represent an evolving area. A heterogeneous network (HetNet) is acquired as a cluster of distinct subnetworks, which are grouped together to maintain long-range communication with different wireless communication architectures. The integrated mode approach of communication has resulted in efficient communication, with higher throughput performance for wireless communication. The architecture is in development to suite the upcoming requirements of demanded services for next-generation wireless communication. Such networks are evolving towards a new mode of communication; various wireless-enabled networks are integrated together to support long-range communication, and the optimality issues with respect to resource utilization and usage are under investigation. Referring to the changed format of wireless networks integrated together, the resources are to be properly controlled to achieve the objective of fairness among the distributed networks with user compatibility. For optimal resource allocation, various methods have been developed in the past, e.g., spectrum allocation, routing optimization, and power efficiency.

For the development of optimal resource allocation in heterogeneous networks, an approach for the optimal allocation of resources in terms of spectrum efficiency, fairness and battery power during communication is outlined in [1]. A multi-attribute scheduling algorithm approach is proposed, where these parameters are used for resource scheduling. This multi-attribute approach is significant because it controls the allocated data rate based on an optimized utility function in the HetNet. This optimization is proved wrt. optimal rate allocation over maximization of the spectrum efficiency and fairness factor. In order to be fair to the user, an interference alignment (IA) scheme for resource allocation was presented in [2]. A spectral coexistence mechanism to mitigate the interference in heterogeneous networks was presented. The resource allocation in terms of optimal interference management was advised. In [3], the optimality issue of resource allocation with respect to traffic density was outlined. The offered capacity for transmission was governed by the solution of a continuous linear programming (LP) approach, where a solution is derived by a scheduler unit based on the number of mobiles in the network. A weighted distribution scheme for all the available weights in the network is presented in [4]. The approach of resource allocation based on an existing wireless network for user preference and mobile terminal power is presented. A cost optimization approach was derived for different networks of macro-, pico-, femto- and relay-based communication approaches towards service uniformity in these networks. In [5], a topology-governed inference management for enhancing the performance of a heterogeneous network is outlined. To obtain the objective of optimal resource allocation in heterogeneous networks, an adaptive interference coordination in inter-cellular interference for smart resource allocation is presented. An intracellular fairness objective was suggested. In [6],[7], a new dynamic scheduling over a heterogeneous network, following packet scheduling, was presented. A media-independent handover concept has been realized to offer efficient transmission of multimedia services using a heterogeneous network. For provisioning of the spectral efficiency in a heterogeneous network, a cell range expansion (CRE) problem was addressed in [8],9] by setting a positive bias factor in the short-range communication network. The objective was derived as the average area weighted load per cell, defined as the weighted spectrum efficiency and energy efficiency approach. With a similar objective for the spectral efficiency in [10],11], the spectrum efficiency (SE) and energy efficiency (EE) derived over a realistic network were presented. An operation relation and quality governance for efficient coding was suggested. In [12], SE and EE objectives were analysed using a biased inter- and intra-radio access technologies (RAT) offloading technique. The analysis yields a multi-objective optimization problem, maximizing the SE and EE subjected to the bounding quality of services. Most of the approaches are developed for resource optimization, and the offering quality of services is an observable parameter. To offer

S. S. Hashmi is with the ECE Department, Icfai Tech School, IFHE University and Research Scholar at JNTU Anantapur, India (e-mail: hashmi@ifheindia.org)

S. A. Sattar is with ECE Department, NSAKCET, Hyderabad, India (e-mail: syedabdulsattar1965@gmail.com).

K. Soundararaj is with ECE Department, NSACET, Hyderabad, India (e-mail: soundararajan.tkr@gmail.com).

QoS in heterogeneous networks, a quality objective with regard to an interference constraint across the cell coverage is presented in [13] . The QoS parameters are defined as a function of link bandwidth, node buffer and queuing service and are employed at the router level in a heterogeneous network. In [14], an end-to-end QoS framework for heterogeneous networks is focused on. The objective of QoS provisioning was made over multiple autonomous systems. In [15],16], a routing algorithm based on proactive coding was suggested, and a QoS-driven control selection was outlined. A general backward utility formation was introduced to observe the dynamic QoS variation in the network. With respect to the resource variation issue and governing of QoS, multi-hop communication with regard to homogeneous and heterogeneous networks was presented in [17]. The variant parameter of a micro-site with regard to a traffic load condition was analysed. In [18],19], IP-oriented QoS signalling as a function of end-to-end QoS offering and seamless mobility for joint resource management was presented. The approach of node automaticity and quality monitoring was presented with mobility concerns for QoS offering. The method derived from supporting various services in different architectures of heterogeneous networks. In providing QoS, spectrum allocation based on the device level is presented in [20]. An energy-efficient cooperative spectrum sensing strategy for immune noise uncertainty was presented. Coarse and fine sensing schemes are employed to achieve energy efficiency in HetNets. A relation property of noise immunity over power consumption was derived. To offer resource utilization via sharing, a device-to-device-level coding is presented in [21] based on a spectrum partitioning approach, and an improved spectrum efficiency for D2D and cellular networks was derived. Under quality-of-service governance, the spectrum is divided into several subfrequencies, and each band is allocated a D2D pair for transmission. Optimality was observed for maximization of D2D transmission power. The approach was developed under the constraint of offering QoS to the cellular transmission conformation. In [22], a device-level coding using cognitive radio units (CRNs) is presented. An active resource allocation problem for heterogeneous networks under imperfect channel conditions was presented The optimality issue was resolved by applying an optimal power allocation problem under a known channel condition. In the suggested approach under network abstraction, the node operating as a router was controlled via different approaches to achieve the objective of higher performance in a heterogeneous network. In [23], a bandwidth buffering mechanism addressing the allocation issue and different queuing services to provide end-to-end QoS provision in heterogeneous networks was suggested. isA self-clocked fair queuing mechanism for providing QoS governance was presented, and the issues of the end-to-end requirement and user connectivity were addressed. While the provision of optimal quality of service and fairness was solved in different aspects, multi-objective control for HetNets is still to be developed to achieve optimal equilibrium in resource utilization with offered QoS and network operation.

In this paper, a new approach for quality-governed data flow operation is outlined to achieve efficient operational performance in heterogeneous networks. An integration approach for device performance and network control is proposed to reach the target of higher performance in a heterogeneous network. The remainder of this paper is organized as follows. Section II outlines the system model used for the developed approach. The conventional model of the multi-attribute optimization approach, based on spectral efficiency and fairness as outlined in [1], is presented in section III. Section IV outlines the proposed spectrum sense optimization approach and rate flow control for heterogeneous networks. Section V illustrates the experimental results derived from the proposed approach in comparison to conventional modelling.

II. System Model

For the communication of data, a cluster of subnetworks capable of wireless transmission is used. An instance of the network model following the heterogeneous network representation is shown in Fig. 1.

Fig. 1. Heterogeneous Architecture

The network is defined with a set of communication terminals, defined as cognitive user units (CuEs), where each device has the property of cognitive operation. In this network, the communication terminals are linked with access points (AP_i), where each of these access points is set with different communication standards. The access network is defined with a Wi-Fi terminal, a cellular terminal and a WiMAX link point. In the process of communication, a communication terminal requests access. Based on the available access terminal, an access link is selected to offer maximum resources. The selected access terminal is then linked with the communication terminal via a GRCU (global resource control unit). To perform the resource allocation, the communication terminal registers the selected access terminal to the GRCU, and then a handshake process is carried out between the GRCU and the communication terminal, confirming the allocation. Once the allocation is confirmed, communication is established from the communication terminal to the destination terminal via the selected access point, controlled by the GRCU. The flow control of the heterogeneous network is illustrated in Fig. 2.

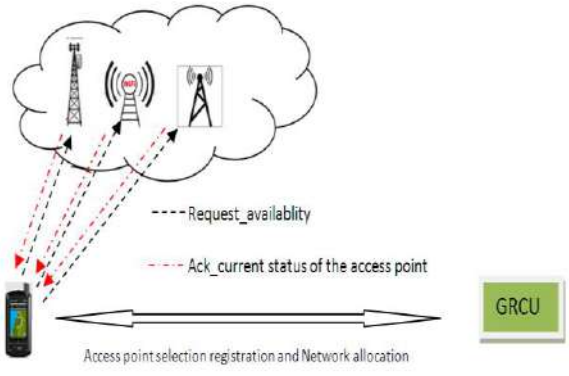

Fig. 2. Control flow diagram of the considered Heterogeneous Network

During the process of communication, a terminal access was granted by the GRCU, registering the sensed access point with the highest available resource. The resource allocations take place in the GRCU unit, and an optimal data rate is allocated based on the current state of the registered access units. For resource allocation, the GRCU unit operates with a multi-attribute optimization approach as outlined in [1]. The conventional approach of multi-attribute optimization is outlined in the next section.

III. Multi-Attribute Optimization Approach [1]

To provide efficient coding for resource allocation in heterogeneous networks considering Wi-Fi, 4G (LTE/WiMAX), and 3G (HSPA/EVDO) architectures, a multi-attribute optimization approach is suggested in [1]. In the process of the multi-attribute optimization approach, 3 factors were considered: 1) Spectral efficiency, 2) Fairness and 3) Battery life. Spectral efficiency is calculated as the utility function of the allocated rate over the total spectrum k available at time t for u users belonging to a set of users U, i.e.,

$$\gamma^t = \frac{\sum_{u\in U} r_u^t}{k} \tag{1}$$

where the allocated rate r_u^t is defined by

$$r_u^t = \sum_{a\in A} x_{ua}^t * r_{ua}^t \tag{2}$$

where A is the set of BS/APs registered and $a \in A$ is the radio offered to A at time t.

The optimal spectral allocation is obtained by optimizing the allocation rate, defined by the maximum sum rate (MSR) optimization problem. However, the MSR has a limitation for the global user resource allocation problem, which yields an unfairness in spectrum allocation. To optimize the spectrum allocation, a utility factor γ_{util}^t is used, which is defined by [1] as

$$\gamma_{util}^t = \frac{\gamma^t - \gamma_{min}^t}{\gamma_{max}^t - \gamma_{min}^t} \tag{3}$$

where γ_{max}^t is the maximum achievable spectral efficiency utility function and γ_{min}^t is the minimum spectral utility function. When the network achieves γ_{max}^t efficiency, the utility function is given a value of 1, while the value is 0 when the achieved spectral efficiency is γ_{min}^t. To provide a fair platform, the allocated rate is controlled by a fairness utility function θ_{util}^t. This utility function θ_{util}^t is defined by [1] as,

$$\theta_{util}^t = 1 - \frac{|BU^t|}{|U|} \tag{4}$$

The fairness utility function is defined as a function of user blockage, where it takes a value of 1 when the number of blocked users (BUs) = 0 and takes a value of 0 when the total blockage is maximal. For long-term fairness, the utility function is defined by [1] as

$$\phi_{util} = \frac{(\sum_{u\in U}\sum_t r_u^t)^2}{|U| * \sum_{u\in U}(\sum_t r_u^t)^2} \tag{5}$$

where the long-term fairness is derived by the aggregated observation of long-term small rate allocations. As a third attribute, battery life is considered for optimal resource allocation. The utility factor under this objective is defined by [1] as

$$\omega_{util}^t = 1 - \frac{\sum_{u\in U} \omega_u^t - \omega_{min}^t}{\omega_{max}^t - \omega_{min}^t} \tag{6}$$

where ω_u^t is the utility function for the battery life of each user. These multiple attributes are controlled, to obtain an efficient coding for spectral efficiency, fairness and long life of nodes in a heterogeneous network. However, the concerns of device efficiency and service quality have not been focused on. The optimization is derived based on the utility factors of these attributes, and the control is made wrt. the allocated rate at time t. To achieve higher efficiency in resource utilization with a quality concern in such Heterogeneous Networks, a quality-governed approach with device reconfiguration is proposed.

IV. Proposed Optimization Attribute

A. Spectrum sense optimization

In the present approach, during the initialization process, the cognitive user equipment (CuE) performs a search operation in Connectivity Access Networks (CANs) based on the order of network preference. In this approach, the order of preference is set as Wi-Fi, WiMAX and Cellular networks. For each of these networks, a utility factor is calculated, and the network offering the higher fairness factor is chosen. The selected CAN is registered with the GRC, and communication is then formed over the registered CAN. In the process of communication, the GRC allocates the spectrum for communication under the limitation of $\gamma_{util} \in [0,1]$. The rate allocation is based on the demanded spectrum to the GRC, where the GRC performs multi-attribute resource allocation to allocate resources to the requested unit. However, with the communication process, the spectrum is dynamically engaged and released based on the demanded service. The vacant spectrum can be utilised for current active users towards extra spectrum allocation to improve service quality. As the devices are cognitive in nature, the cognitive property of resource allocation can be used for these spectrum allocations. The initial spectrum allocation for user u € U is given by the utility value γ_U^t. On the release of a primary allocation rate r_i^t, the available spectrum is defined by

$$\gamma_{av1}^t = \sum_{u\in U} \gamma_u^t - r_i^t \tag{7}$$

This available spectrum is called the secondary spectrum and can be utilised by the active primary users (p_u). On the request for this secondary spectrum, the GRCU computes the spectral interference energy, E, for n active user as defined by [20] as

$$E = \sum_{i=1}^{n} (\frac{y_i}{\sigma})^P \tag{8}$$

where y_i is the received information and σ is the observed channel variance. Parameter 'P' is varied over a range of 1-10 to derive the energy variation wrt. the interference variation in the channel. To allocate the available secondary spectrum, the obtained energy 'E' is used as the allocation parameter. In the data flow process, the optimal encoding mode can be determined by reaching the best trade-off between the amount of coding bits and the obtained service quality. This problem can be modelled as a maximum sum rate optimization problem [1]. This MSR optimization is developed to achieve the objective of fairness of resource utilization in a heterogeneous network. The MSR optimization is governed for allocation of the maximum rate of data flow achieving maximum spectral efficiency. To achieve better service quality for the spectrum allocation, a distribution optimization is proposed. To govern

quality, a cost function with distortion and rate allocation is defined, subjected to minimization of distortion (D), subjected to an allocation free secondary spectrum 'R' constraint to the allocation rate R_c, which is given by γ_{av1}^t. The optimization operation of the spectrum is defined as

$$\min_{\{m\}}\{D\} \text{ subject to } R \le R_c \tag{9}$$

which indicates that the encoder should satisfy the minimum distortion 'D.'

The allocation of spectrum to a user with the data rate satisfying the instantaneous fairness utility function $\theta^t{}_{util}$ was developed [1]. However, in real-time data traffic, such as video streaming or VoIP services, the fairness is defined by the offered BER, controlled by the allocation of data rate. In practical usage, in the network abstraction layer (NAL), the network operates at a different level to provide proper allocation of resources under different data traffic conditions. In wireless communication, the transmission channel is time-varying and distortive in nature. For minimization of error during signal propagation, an independent channel model is used, deriving the bit error rate (BER) of the transmission channel. The packet loss probability 'ρ' during the transmission of 'L' bits for a given BER is defined by

$$\rho = 1 - (1 - ber)^L \tag{10}$$

The quality utility function γ_{int}^t is then defined by

$$\gamma_{util_\varphi}^t = \frac{\gamma_\varphi^t - \gamma_{min}^t}{\gamma_{max}^t - \gamma_{min}^t} \tag{11}$$

where,
$$\gamma_\varphi^t = \frac{\sum_{u\in U} \gamma_{u\varphi}^t}{k} \tag{12}$$

$$\gamma_{u\varphi}^t = (\gamma_{ua}^t + L) \tag{13}$$

where $\gamma_{u\varphi}^t$ is the allocated rate with the primary data rate γ_{ua}^t and secondary spectrum of L bits. During the transmission process, the packet stream is divided into L-bit slices represented as $s_{n,m}$. For the Tx of the m[th] slice in the n[th] frame, the BER is defined by $ber_{n,m}$, which is the channel BER for the transmission, and $\rho_{n,m}$ is the packet loss rate for a slice $s_{n,m}$. To find the optimal bits of length 'L,' minimizing the packet loss ρ, the optimization was subjected to min (ρ) and max(L).

$$\min(\rho) \Rightarrow \max(L) \tag{14}$$

To generate the data transmitting bits 'L' for demand service quality, given by required BER. An optimal value of L is derived, obtaining minimal packet loss. In the operation of rate allocation, the fairness utility function is governed by two levels of maximum or minimum spectral utility functions. The utility component in this case is normalized to two levels, [0, 1]. While this is developed with the concern of maximum or minimum spectrum utilization, the traffic flow per node is not considered. Data traffic on a heterogeneous node is dynamic in nature, and the two-level normalization process is only for spectrum utilization, wherein this is limited at the device level. The issue arises when the nodes are highly congested due to variable data traffic from different sources, flowing in at different data rates. Though the optimal spectrum utilization is used, if the nodes are blocked at the node level, the network will fail to deliver the demanded service rate. Hence, in addition to spectrum utility function, a device-level optimization is required. To achieve this objective, a rate interference approach is proposed in consideration of the data flow per node for the allocated spectrum. This update in rate allocation results in higher spectrum efficiency in consideration of the cognitive property of the CuE. In addition to spectrum efficiency, a fairness optimization is applied to achieve a higher service level in Heterogeneous Networks.

B. Rate-inference optimization

While the suggested approach of rate allocation for the fairness approach is observed to be very effective in data flow, when applied to the data flow over a wireless channel with multiple sources, it is observed that the rate of transmission and the offered quality need to be optimized. In the approach of data traffic data flow, due to remote capturing, the allocated resources of power and spectrum will be limited. In such a case, the proper utilization of resources and intermediate node support is highly required to achieve greater performance. The approach of observing for error allocation coding is simpler,and effective for service data flow, but without control of the flow, this allocation may not result in effective service quality at receiving units due to the incurred latency issue. Hence, the access control is also needed with spectrum allocation; with this objective, a buffer-based management scheme to control the rate of allocation was proposed. As in the proposed work, each intermediate node is considered to be a router, and each node encounters multiple data traffic at this node and observes heavy congestion. To overcome this issue, buffer management is applied. The cross-layer optimization of service stream data traffic at the router level was proposed in [14]. The approach of coding was introduced at the network abstraction layer (NAL), where the buffer-based congestion control follows buffer management and the relative quality of service (QoS) is mapped to schedule the rate of data traffic flow. The cross-layer approach processes the measured buffer length and derives the packet En buffer or doping probability based on receiving data traffic. At the Service coding layer, the communication data are blocked into slices and passed to NAL for rate allocation. The method computes the utility function '$\gamma^t{}_{util}$' as

$$\gamma^t{}_{util} = \begin{cases} 0; & \theta_{util}^t < \gamma^t{}_{min} \\ 1; & \theta_{util}^t > \gamma^t{}_{max} \\ max_p \times \frac{\gamma^t{}_{util} - \gamma^t{}_{min}}{\gamma^t{}_{max} - \gamma^t{}_{min}}; & otherwise \end{cases} \tag{15}$$

where max_p is defined as the maximum number of packets exchanged over a node. In the approach of cross-layer modelling, θ_{util}^t is updated by $1 - \phi^t$, where ϕ^t is the update applied in period t and ϕ is the constant value 1.001 defined as the random exponential marking.

The update factor is occasionally updated according to the average buffer length and the input rate and output rate of the buffer. This approach controls the flow of data traffic by accepting or dropping service packets based on the probability index ϕ^t and the importance of the packet. The factor is incremented if the input rate exceeds the output rate and decremented otherwise. The approach of traffic flow control at node level is defined by the following algorithm.

Algorithm: Flow control Rate Allocation

Calculate the average buffer length $q_1(t)$ in period t;
Receive packetσ;
Calculate the utility function $\gamma^t{}_{util}$;
Randomize a number μ;
if ($\gamma^t{}_{util} < \mu$)
En buffer packet σ;
else
re-traffic the packet σ with $U = arg_{i\epsilon[I,L]} minU(i)$;
buffer packetσ;
End if
Where,
$U_i(t)$ The important index of the i packet in the buffer in period t

The rate allocation is defined by,

$$R_{alloc}(t) = \begin{cases} R(t) + \Delta t, & if\ \theta^t{}_{util} < \gamma^t{}_{min} \\ R(t) + (\Delta t - d(t)), & if\ \theta^t{}_{util} > \gamma^t{}_{max} \\ R(t) - \dfrac{R(t)}{d(t)}, & otherwise. \end{cases}$$

where
$R_{alloc}(t)$= allocated data rate
$R(t)$ = full rate
Δt = incremental data rate
$\gamma^t{}_{min}$ = minimum limit of the buffer
$\gamma^t{}_{max}$ = maximum limit of the buffer

In the above equation, the allocated data rate is varying with respect to the node congestion level. If the current buffer length is at the minimum level, the data will be allocated with an increment of 'Δt.' If the current buffer length in a node is in between the minimum and maximum utility level, the allocated data rate is governed by the traffic flow. Similarly, if the current buffer length exceeds the maximum limit, which represents a traffic flow, the allocated data rate will vary according to the offered traffic utility function θ^t_{util}.

V. Experimental Results

To evaluate the operational performance of the proposed approach, a MATLAB simulation model is developed, where a distributed wireless Heterogeneous network is simulated with the proposed optimization attribute of the rate flow control approach and compared with the conventional approach of multi-attribute optimization [1] and QoS-based buffer management [14]. For the simulation, a network is defined in Table I with the following network parameters:

For the analysis of the proposed rate flow attribute-based coding approach over the conventional multi-attribute control approach, different networks with varying node distributions are used. Node densities of 30 and 40 terminals are simulated, and the obtained observations are illustrated below.

With the network under consideration, a network with randomly distributed terminals is modelled. The randomly distributed network architecture used for the simulation is illustrated in Fig. 3. The terminals are defined in a random manner with the topology of N terminals scattered at randomly distributed X and Y coordinates. The terminals are defined with random resources of node powers and available spectrum.

The coverage region for each node is illustrated in Fig. 4. The bounded region for each node is computed by the possible range coverage of each node. The communication range of each terminal is defined by its protocol defined for each node, and the terminal in this coverage range is used for the computation of an access link possibility.

TABLE I
SIMULATION NETWORK PARAMETERS

Network parameter	*Values*
Node distribution in the network	*Random*
Power allocation	*Random*
Communication protocol	*IEEE 802.11, LTE (4G)*
Network area	*200 x 200*
Number of communication terminals	*1-5*
Memory size / node (M)	*3M*
γ_{min}	*0.15xM*
γ_{max}	*0.75xM*
Initial blockage probability	*0.1*

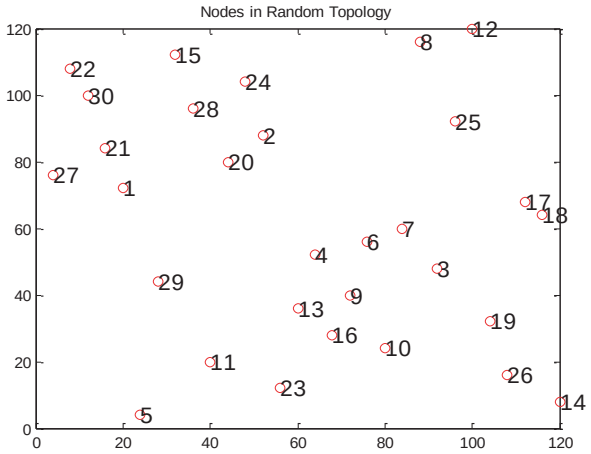

Fig. 3. Randomly distributed access points for a terminal density of 30

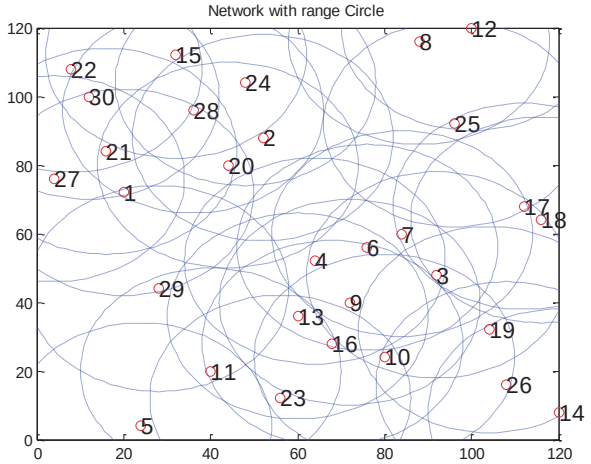

Fig. 4. Network with coverage regions marked

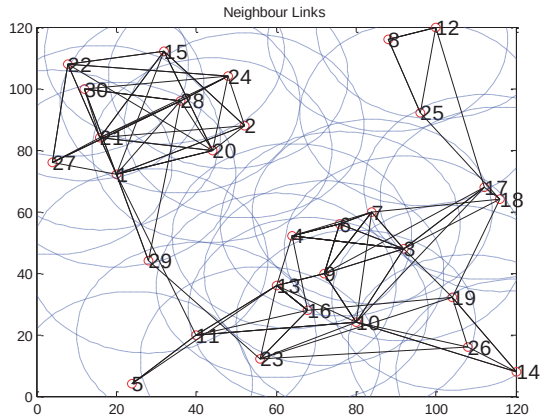

Fig. 5. Network with 1-Hop neighbours

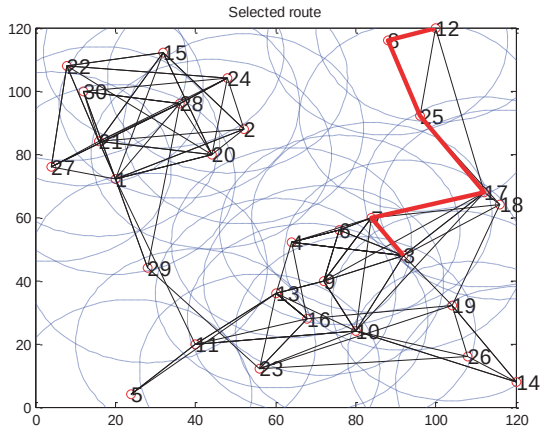

Fig. 6. Network with a selected path for communication

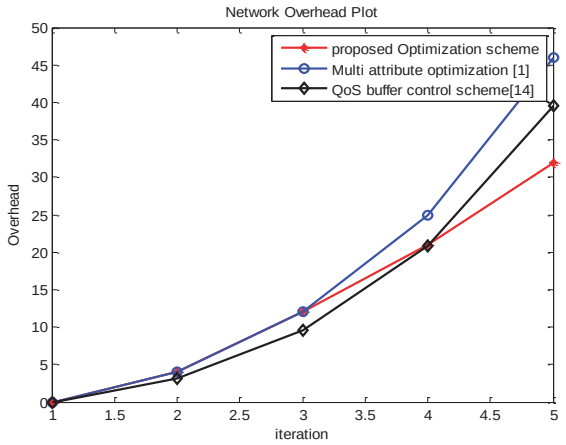

Fig. 7. Network overhead with packet forwarding

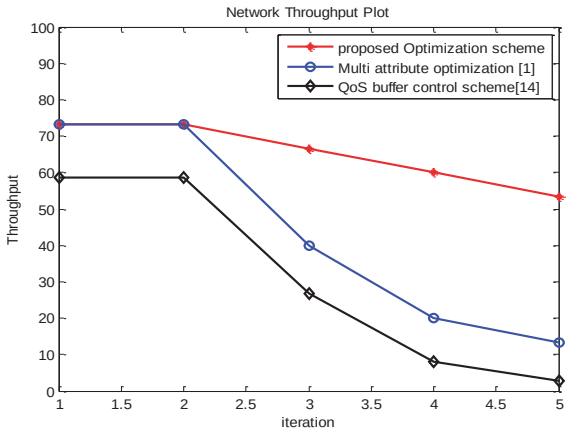

Fig. 8. Network throughput with the forwarding of packets

The network with 1-hop neighbours is illustrated in Fig. 5. Each node computes the distance of nodes with all other terminals, and the distance below the communication range is defined as a 1-hop neighbour for the refereeing node. In the process of neighbour discovery, the Terminal distances falling below the communication range are declared as direct neighbours, and each node exchanges their one-hop neighbour details to formulate a link network.

With the one-hop neighbour list, an AODV routing protocol is developed to evaluate the route from a given source to the destination. The routes are generated via the data exchange from source to destination in a broadcasting manner. A forward and backward tracing method is applied to obtain the route parameters used for forwarding packets. Among the generated routes, a path with minimum hops (i.e., the shortest path) is selected for communication. The selected path for the developed network is as illustrated in Fig. 6.

In the process of communication, data are forwarded along the path selected from source to destination via intermediate terminals. During the process of data exchange, the packets are buffered, and based on the computed congestion level, packets are forwarded. To transfer the packets, the per node forwarding data rate is computed based on the congestion level, and allocated data rate packets are released or queued in the node. The queued packets internally build an overhead in the network. This overhead is defined as the number of packets queued for processing at each node. With the forwarding of packets from source to destination at each intermediate node, packets are buffered; the overhead observed is hence presented in Fig. 7.

Due to the rate flow attribute coding, the congestion is controlled over a limit of buffering in contrast to buffering to a higher level of buffer queue. Due to early control and rate flow attribute estimation, the overhead for such a network is observed to be minimized with the forwarding of packets.

The network throughput for the developed network is illustrated in Fig. 8. Due to the higher data rate of packet forwarding in the proposed approach, it is observed that more packets are received, hence resulting in higher throughout in the network. The throughput of these simulated systems is defined as the number of packets generated over packets received for an observed communication time period. The throughput is observed to be the same for the first 1-hop forwarding, and in such a case, the buffering is observed to be minimized; hence, the allocated data rate is improved. However, as the amount of packet forwarding increases, the congestion level increases, resulting in the decrement of throughput, which is maintained to be higher and linear in the case of rate flow attribute coding.

The observed end-to-end delay factor for the developed system is presented in Fig. 9. The delay for the rate control approach is higher than that of the rate flow attribute coding, as the buffering of data at each node is minimized at the node level and the packets are released faster. The congestion level in such coding is developed in a rate flow attribute manner, wherein packets are buffered in the queue based on the rate control approach, which builds the forwarding delay for each node.

The buffered Q length for such a system is presented in Fig. 10. The Q lengths are measured as the volumes of data packets buffered with an increase in forwarding of data packets. It is

observed that the Q length of buffering is reduced for rate flow attribute coding due to the increment in the data rate. The queuing is, however, observed to be equal in the initial communication phase and gradually increases with the forwarding of packets.

The allocated data rate for the developed method over the simulation network is as outlined in Fig. 11. The terminal is communicated for the given data packet, and each level of buffering of these terminals computes the allocable data rate for forwarding. This forwarding results in proper control of congestion and hence results in efficient network performance.

To evaluate the impact of node density, a similar observation is made for the node density of 40 terminals. The obtained observation for such a network is illustrated in the following observation.

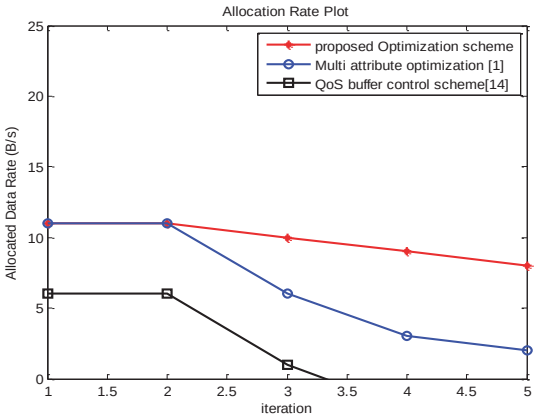

Fig. 11. Allocated data rate with forwarding of packet

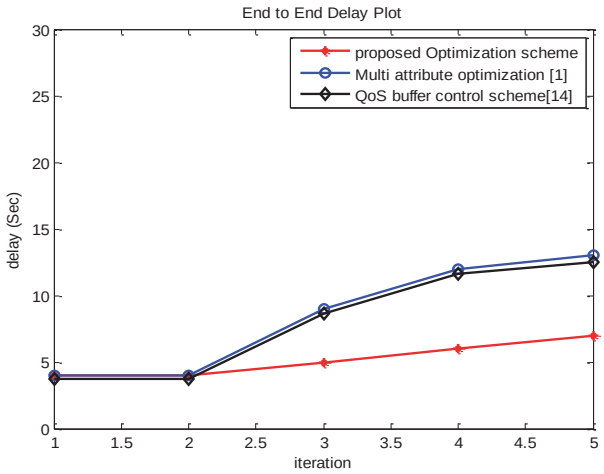

Fig. 9. Observed delay for the simulated network with a node density of 30

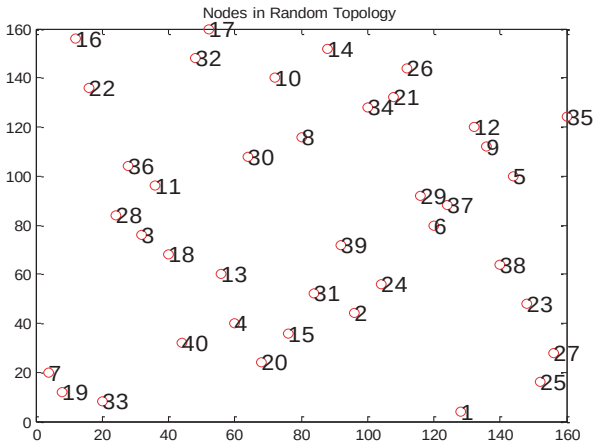

Fig. 12. Network topology for randomly distributed terminals with a node density of 40

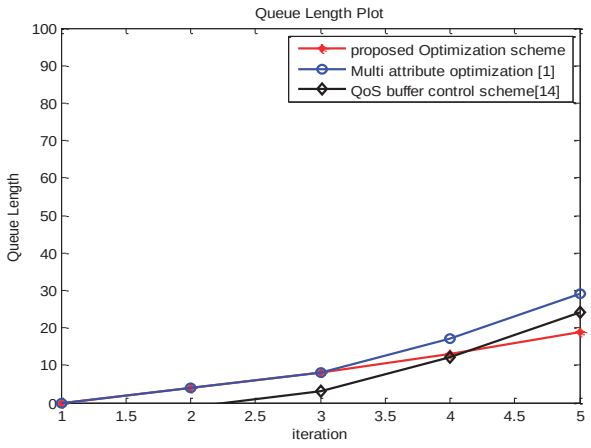

Fig. 10. Buffered Q_length with an increase in forwarded packets

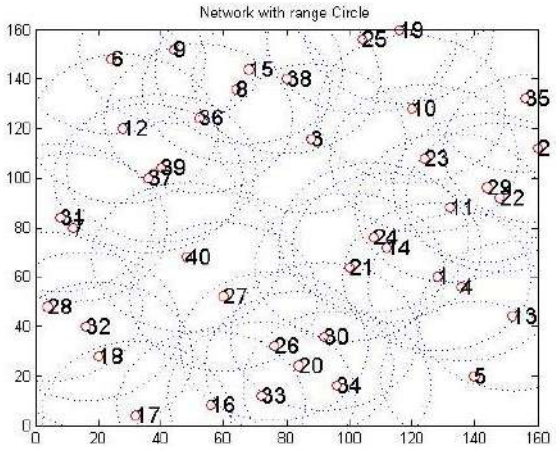

Fig. 13. Marked coverage regions for each node in the network

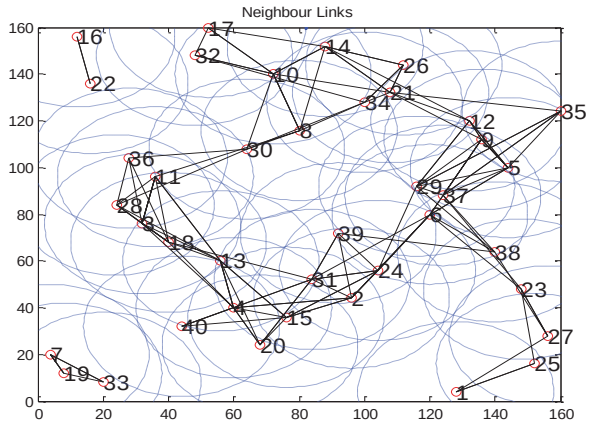

Fig. 14. Network with 1-hop neighbour links

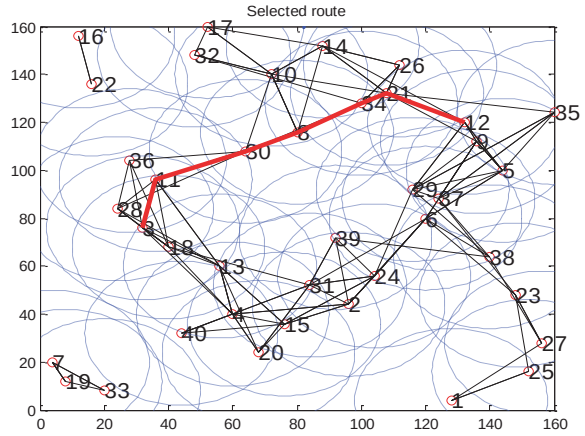

Fig. 15. Network with a selected route for communication

The node distribution, coverage range, neighbour links and selected path for communication are as illustrated in Figures 12-15, respectively.

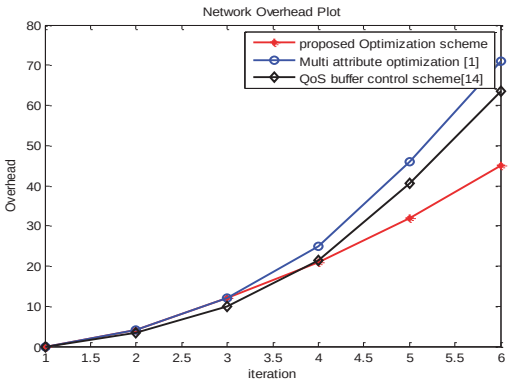

Fig. 16. Network overhead with an increase in the forwarding of packets

The network overhead in such a case is observed to be reduced from 122 to 71. The overhead is minimized due to the existence of more terminals to exchange the data, which results in faster data exchange. However, due to the non-optimal rate control approach, the overhead is observed to be higher in the rate control approach in comparison to the rate flow attribute approach.

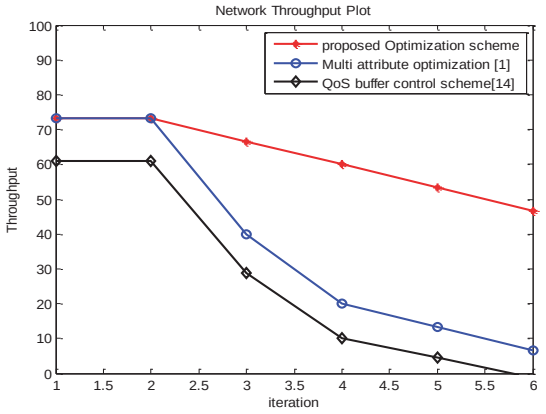

Fig. 17. Network throughput for the developed network for a node density of 40

The network throughput for this developed network is observed to be improved from 30 to 52 in the case of the rate flow attribute-based control approach. This is observed to be minimized in the case of the rate control method due to the higher data buffering per node.

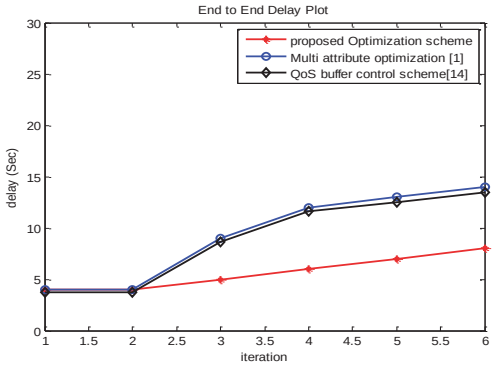

Fig. 18. End-to-end delay for the developed network

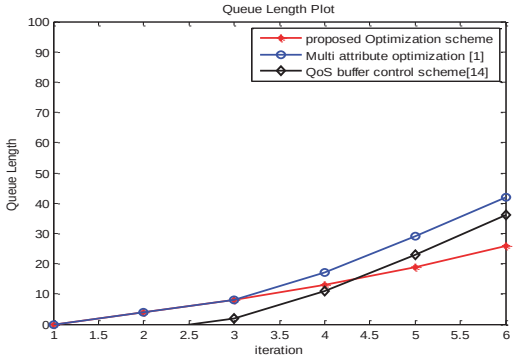

Fig. 19. Observed Q-Length at the terminal for the developed network

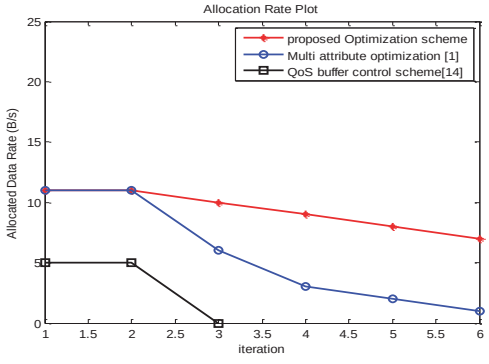

Fig. 20. Allocation of data rate for the developed methods

The observed delay factor is minimized from 10 to 7 for higher node density, the Q_length is decreased from 42 to 25, and the allocable data rate is increased from 5 to 7 for the developed rate flow attribute method. The obtained observations for the delay, Q_length and allocated data rate is presented in Figures 18-20. The observation made for a node density of 40 terminals is presented in Table II. The allocated data rate could be observed to be improvised in rate flow attribute-based coding as presented in Table II. The average queue length is hence reduced from 29 to 19 in this case. The network throughput is observed to be increased from 13.34 to 53.36 in such case. The delay is minimized from 13 to 7 for the rate flow attribute-based control approach in comparison to the rate control approach.

TABLE II
COMPARATIVE OBSERVATION OF THE THREE DEVELOPED METHODS AT A NODE DENSITY OF 40

Method	Allocated DR	Average Q_Length	Throughput	Delay
Multi-attribute optimization [1]	[11 11 6 3 2]	[0 4 8 17 29]	[73 73 40 20 13]	[4 4 9 12 13]
QoS Buffer optimization [14]	[11 11 8 5 5]	[0 4 8 15 22]	[73 73 47 32 27]	[4 4 7 10 11]
Proposed approach optimization	[11 11 10 9 8]	[0 4 8 13 19]	[73.33 73.33 66 60 53.6]	[4 4 5 6 7]

CONCLUSION

In the suggested approach, the cognitive property of devices is utilised for a secondary spectrum sensing operation to achieve a higher data rate allocation under ideal spectrum availability. In the flow control approach, the buffer control mechanism is improved for the given quality of service, where the traffic monitoring is introduced based on the allocated data rate and buffer status. An improvement in the network operation metric of throughput is observed.

REFERENCES

[1] R. Amin, J. Martin, J. Deaton, L. A. DaSilva, A. Hussien, A. Eltawil, “Balancing spectral efficiency, energy consumption, and fairness in future heterogeneous wireless systems with reconfigurable devices,” *IEEE Journal on Selected Areas in Communications*, vol. *31*(5), pp. 969-980, 2013. DOI: 10.1109/JSAC.2013.130515

[2] S. K. Sharma, S. Chatzinotas, B. Ottersten. "Interference alignment for spectral coexistence of heterogeneous networks," *EURASIP Journal on Wireless Communications and Networking* , vol. 201(1), pp. 1-14, 2013. DOI: 10.1186/1687-1499-2013-46

[3] S.V. Hanly, C. Liu, P. Whiting, "Capacity and stable scheduling in heterogeneous wireless networks." *IEEE Journal on Selected Areas in Communications* vol. 33(6), pp. 1266-1279, 2015. DOI: 10.1109/JSAC.2015.2416971

[4] H. M. Tahir, A. H. Al-Ghushami, Z. R. Yahya, "Selection of access network using cost function method in heterogeneous wireless network." *Multimedia Computing and Systems (ICMCS), 2014 International Conference on*. IEEE, 2014.

[5] A. Khandekar, N. Bhushan, J. Tingfang, V. Vanghi, “LTE-advanced: Heterogeneous networks”, In *Wireless Conference (EW), 2010 European* (pp. 978-982), IEEE, 2010.

[6] W. Mansouri, K. Mnif, F. Zarai, M. S. Obaidat, “A new multi-rat scheduling algorithm for Heterogeneous wireless networks”, Journal of Systems and Software, Elsevier, 2015.

[7] F. W. Karam, T. Jensen, "On schemes for supporting QoS and mobility in heterogeneous networks." *Proceedings of the 7th International Conference on Frontiers of Information Technology*. ACM, 2009.

[8] M. Liu, Y. Teng, M. Song. "Tradeoff Analysis between Spectrum Efficiency and Energy Efficiency in Heterogeneous Networks (HetNets) Using Bias Factor." *Journal of Communications* 10.10, 2015.

[9] K. Son, E. Oh, B. Krishnamachari. "Energy-efficient design of heterogeneous cellular networks from deployment to operation."*Computer Networks* vol. 78, pp. 95-106, 2015.

[10] G. He, S. Zhang,, Y. Chen, S. Xu, “Spectrum efficiency and energy efficiency tradeoff for heterogeneous wireless networks”, In *2013 IEEE Wireless Communications and Networking Conference (WCNC)*, pp. 2570-2574, IEEE, 2013.

[11] R. Q. Hu, Y. Qian, "An energy efficient and spectrum efficient wireless heterogeneous network framework for 5G systems." *IEEE Communications Magazine* vol. 52.5 (2014), pp. 94-101, 2014.

[12] J. B. Rao, A. O. Fapojuwo, "Analysis of Spectrum Efficiency and Energy Efficiency of Heterogeneous Wireless Networks With Intra-/Inter-RAT Offloading," *IEEE Transactions on Vehicular Technology* 64.7 (2015), pp. 3120-3139, 2015.

[13] H. Shi, J. Li, Z. Li, H. Ju. "Dynamic spectrum allocation in heterogeneous wireless networks under interference constraints across the cell coverage." *Wireless Communications and Mobile Computing*15, no. 7 (2015), pp. 1188-1197, 2015.

[14] B. Iancu, D. Vasile, A. Peculea. "A novel end-to-end QoS framework over heterogeneous networks-an architectural approach."*Acta Technica Napocensis* 51.2 (2010): 42, 2010.

[15] L. Badia, M. Miozzo, M. Rossi, M. Zorzi, „Routing schemes in heterogeneous wireless networks based on access advertisement and backward utilities for QoS support [Quality of Service based Routing Algorithms for Heterogeneous Networks],“ . *IEEE Communications Magazine*,*45*(2), pp. 67-73, 2007.

[16] K. Yang, Y. Wu, H. H. Chen. "QoS-aware routing in emerging heterogeneous wireless networks [Quality-of-Service-Based Routing Algorithms for Heterogeneous Networks]." *IEEE Communications Magazine* 45.2 (2007), pp. 74-80, 2007.

[17] F. Richter, A.. J. Fehske, P. Marsch, G.P. Fettweis, (2010, May). Traffic demand and energy efficiency in heterogeneous cellular mobile radio networks. In *Vehicular Technology Conference (VTC 2010-Spring), 2010 IEEE 71*st, pp. 1-6. IEEE.

[18] G. Fodor, E. Anders, A. Tuoriniemi. "Providing quality of service in always best connected networks." *IEEE Communications Magazine* 41.7 (2003), pp. 154-163, 2003.

[19] G. Aristomenopoulos, T. Kastrinogiannis, Z. Li, S. Papavassiliou, (2011), “An autonomic qos-centric architecture for integrated heterogeneous wireless networks”, *Mobile Networks and Applications*, *16*(4),pp. 490-504, 2011.

[20] J. C. Clement, B. B. Reddy, D. S. Emmanuel, "An Energy-Efficient Cooperative Spectrum Sensing Strategy with Robustness Against Noise Uncertainty for Cognitive Radio Networks." *Arabian Journal for Science and Engineering* (2015), pp. 1-7, 2015.

[21] Z. Dai, J. Liu, C. Wang. "QoS-based device-to-device communication schemes in heterogeneous wireless networks." *IET Communications* 9.3 (2015), pp. 335-341, 2015.

[22] R. Xie, F. R. Yu, H. Ji. "Dynamic resource allocation for heterogeneous services in cognitive radio networks with imperfect channel sensing." *IEEE Transactions on Vehicular Technology* 61.2 (2012): 770-780, 2012.

[23] W. Sheikh, A. Ghafoor, “Quality-of-service routing in heterogeneous networks with optimal buffer and bandwidth allocation”, In*2007 IEEE International Conference on Communications* (pp. 480-485) IEEE, 2007.

Journal of Engineering and Applied Sciences 12 (Special Issue 1): 5814-5820, 2017
ISSN: 1816-949X
© Medwell Journals, 2017

Energy Aware on Demand Routing for MANETs based on Intermediate Node Residual Status

[1]Mahabubul Haq Atif and [2]Syed Abdul Sattar
[1]Department of CSE, Rayalaseema University, Kurnool, Andhra Pradesh (AP), India
[2]Department of CSE, Nawab Shah Alam College of Engineering, Hyderabad, Telangana (TS), India

Abstract: MANETs (Mobile Ad-hoc Networks) are self-configuring network that comprised of mobile nodes having no fixed infrastructure. These devices are dynamic and move freely so that they form varying network topology. The challenge for successful communication is to form an appropriate route to maintain connectivity consistently between mobile nodes having limited battery power. Therefore, MANETs need to have improved network lifetime to perform a streamlined and dynamic routes between multiple mobile nodes. This research focuses on designing a protocol for MANETs which is energy efficient and congestion avoidance between mobile nodes. In this mechanism, two important attributes, i.e., link stability and network lifetime are addressed. We used NS-2 Network Simulator to analyze the performance. The outcome of this simulated demonstration that developed energy aware mechanism is better than the existing EDDSR, MDR and LEAR routing protocols.

Key words: MANETs, node, network lifetime, link stability, routing, LEAR

INTRODUCTION

MANETs (Muhammad *et al*., 2015) (Mobile Ad-hoc Networks) are self-configuring and infrastructure less networks that comprises of a set of mobile nodes forming peer-to-peer communications. The network topology of MANETs is autonomous, dynamic and consisting of number of intermediate mobile nodes between communicating peer nodes. Each node in a network has to act as a source, receiver and router to forward the packets. MANETs have many applications such as environment monitoring, wireless sensor network, military and law enforcement. These applications need to be cost and/or time effective. Communicating nodes in MANETs depends upon intermediate nodes for communication when they are not in radio range of each other. Moreover, forwarding packets by other nodes consume resources of node particularly energy. The primary issue in MANETs is availability of limited power as they are powered by batteries that have limited lifetime.

Mobile nodes are equipped with batteries that have a limited amount of power and lifetime. These batteries cannot be recharged or replaced during the mission and hence, energy management is considered as a necessary factor. The nodes consume the energy during data reception, data processing and data transmission. MANETs consist of single and multiple communicating entities have peer-to-peer connectivity and are required to route the traffic properly. To improve the performance of communication and lifetime of network, we need to design a routing mechanism in such a way that the packets are routed with minimum energy consumption and based on energy awareness of nodes. One of the important goal of routing in MANETs is to create a cost optimum as well as energy efficient path. Hence, we chose energy aware routing as the best procedure of managing the energy in Mobile Ad-hoc Networks. However, properties and resources of MANETs make this task more challenging. To solve the issues of energy management, in literature many routing protocols have been put forwarded. These protocols were broadly classified into three categories:

- Energy efficient routing path
- Reliable routing path and
- Routing path with higher energy nodes

The protocol designed based on energy efficient routing path concentrates on reduction of energy usage during transmission and reception to minimize the amount of energy required for communications by the mobile nodes present in a network. This goal is achieved either by reducing the energy consumption when the nodes are in idle state or by minimizing the amount of energy required for packet delivery. A routing path with higher energy nodes has the protocol that uses higher energy nodes to find the routes whereas a reliable routing path has the protocol that detects the route according to

Corresponding Author: Mahabubul Haq Atif, Department of CSE, Rayalaseema University, Kurnool, Andhra Pradesh (AP), India

anticipated energy count. To recover from packet loss, this type of link routing used a concept of minimum amount of retransmission. Each protocol has its own merits and demerits and accordingly it is judged which protocol is suitable for a specified network condition.

In order to deep analyze the routing protocols performance, network condition is divided into categories and then the performance of different routing protocols is analyzed and compared. Researchers can have an effective use of the results produced in our project for their experimentations. Though in literature various researchers carried out a lot of analyses and research to contrast the routing protocols for energy management, this project has a new technical performance system such as forwarding packets from various sources through conversion of node into bottleneck intermediate node, which is one of the best procedure in assessing the multi-hop environment routing protocols for energy management. This system of performance analysis is an innovative feature of this study.

In the first part of our study, the state of the art analysis of proactive and reactive routing protocol performances such as DSDV (Moravejosharieh *et al*., 2013), AODV (Chaubey *et al*., 2015) and DSR are defined. For a particular network condition, it is difficult to judge which mechanism is suitable for routing protocols. Thus, we divided the network condition into broader categories and then compared the different performance systems by analyzing routing protocol performances with various network conditions with mobility considerations such as variable radio area, variable packet size and variable hop-count. The outcome of this analysis can be used by the researchers in their experiments. Ultimately, we considered DSR to be the best suited to develop a routing protocol in MANETs energy efficiency. Due to heterogeneous mobile nodes batteries with limited power, energy efficiency is a necessary issue in designing of MANETs. It is essential to have reduced amount of energy consumed during wireless communications. If the routing protocol does not consider the power required and relies upon shortest path, then the affect is caused on the lifetime of network by power failure of a node. The goal of energy efficient routing protocol is to find the route that consumes minimum amount of energy during end to end packet travelling as well as to make residual energy of a node and have reliable routing through links. This improves the network lifetime as well as the overall performance. Therefore, a routing protocol is still required to address these issues in MANETs.

In second part of our study, we designed "Energy aware routing for MANETs based on a current processing state of Node". In this protocol, we make use of DSR to achieve energy efficiency. DSR (Dynamic Source Routing) is a protocol that stores all nodes from source to destination. It is a source initiated protocol similar to "AODV" protocol. Proposed work enhances DSR protocol to improve network lifetime and to reduce routing cost upon mobile networks. Though the researchers carried out a lot of experiments and thesis for the development of energy efficient routing protocols with different performance analyses, our research has a new technical performance system which makes nodes possible to become a "Bottleneck node". It is the mediator condition for forwarding the traffic through intermediate node. Hence, we create a routing process to avoid the node to become "Bottleneck node" which results in improvement of performance and lifetime of a network.

Routing in manets: According to literature review of routing in MANETs, it seems more challenging over infra-structured networks. The literature shows a lot of routing protocols that were developed with extra attempts to manage the attributes of MANETs environment. The work of routing in MANETs is more taxing by the limiting factors such as mobility, heterogeneity and dynamic network topology. In most of the existing protocols, there are different patterns of designs that are followed by MANETs according to reactive and proactive approaches. In proactive routing protocols, the nodes are allowed to have a clear vision over the network topology. Therefore, all nodes in traffic can be routed quickly and properly. An extra overhead is made by periodic messages. DSDV, ABR and OSLR are the few examples of proactive routing (Mohammad *et al*., 2015; Varshney *et al*., 2016; Chaubey *et al*., 2015; Moravejosharieh *et al*., 2013; Dulman *et al*., 2003).

The reactive or source initiative routing follows on-demand approach and is an alternative to proactive routing mechanism. The establishment of route occurs only when there is a transmission or communication between a source and a destination. The route request function of source node follows a route reply function of a destination node to initiate the route. The route maintenance function maintains the initiated route till it is required. AODV and DSR are the examples of reactive source initiative routing protocol.

The DSR protocol is similar to AODV protocol which forms a route when it is requested by a transmitting node but instead of depending upon a routing table, DSR protocol uses source routing. In DSR protocol, the complete path is discovered by the sender of the packet through which the packets are forwarded. This route is listed in the packets by the sender which takes the address of next node to identify each hop to be forwarded

through which the packets are transferred to the destination host. The performance of DSR routing protocol is better than that of AODV and DSDV protocol. Unlike table driven approach, DSR uses a reactive approach to avoid the need to flood the network periodically through the table update messages.

Need of energy awareness in MANETs: The battery power of mobile nodes is finite in MANETs. MANET's properties are highly suitable for various applications like disaster recovery and battlefield but recharging and changing of batteries looks very difficult. After losing the power completely, nodes cannot be used further for communication as they are removed from the network. In MANETs, it is necessary to manage the energy because it is difficult to change or substitute the battery, shortage of central coordination, peer to peer characteristics network and finite energy storage. The utilization of active energy in MANETs occurs through packet communication such as packet reception and packet transmission. Inactive utilization of energy occurs through rest state of node but as they are listening medium they can respond to any feasible communication requests by other nodes and it utilized the energy when the node is at rest. Most of the researchers developed the routing protocols such as correct path between source and destination, simply based on energy efficient beside this they are also developed the energy management as they can provide the network functions for a longer time.

Literature review: In the first stage of our research, we have done the analysis of performance of DSDV, AODV and DSR concerning radio area, traffic mobility and hop count regarding variable packet size. Performance of this routing protocol is analyzed based on reactive and proactive approach. The simulator used for calculating the performance of DSR, AODV and DSDV is NS-2 Network Simulator in terms of throughput, packet loss and end to end delay. The outcome of this simulation shows that DSR performance is slightly better than AODV and DSDV, which is shown in Fig. 1-5.

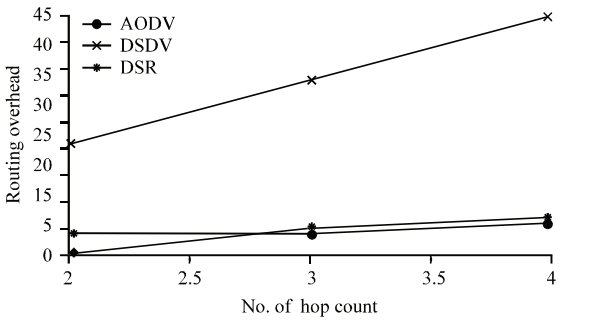

Fig. 1: Routing overhead comparison of routing protocols (AODV, DSDV, DSR)

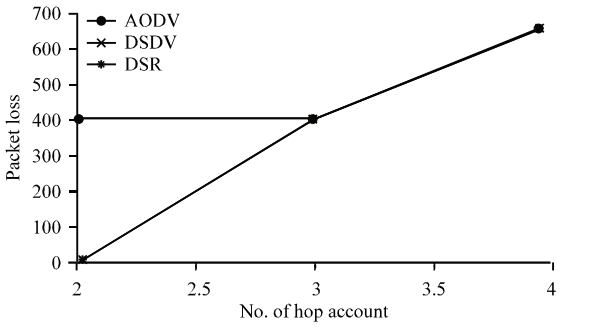

Fig. 2: Packet loss comparison of routing protocols (AODV, DSDV, DSR)

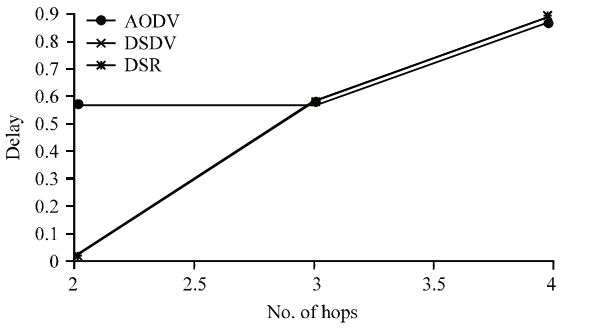

Fig. 3: End to end delay comparison of routing protocols (AODV, DSDV, DSR)

DSR based energy efficient routing: We have done literature review on DSR based energy management routing protocols as its performance is better than other routing protocols such as AODV and DSDV. In Dynamic Source Routing (DSR), the complete system of nodes is carried by each data packet which needs to be passed to reach the destination. DSR is based upon the process route discovery and route maintenance. A Route Request (RREQ) is broadcast by a node in the process of route discovery. After reaching the destination or intermediate node, RREQ process is terminated and Route Reply (RREP) is sent back to the source. The source node uses the route from RREP to transmit the packets towards the destination. A broken link or a link in disconnection is detected by route maintenance process which sends the Route Error packet (RERR) to the source. The source discovers a new route towards the destination and deletes the broken link from its cache.

To estimate the lifetime of a node, a new cost function is described by the Minimum Drain Rate (MDR)

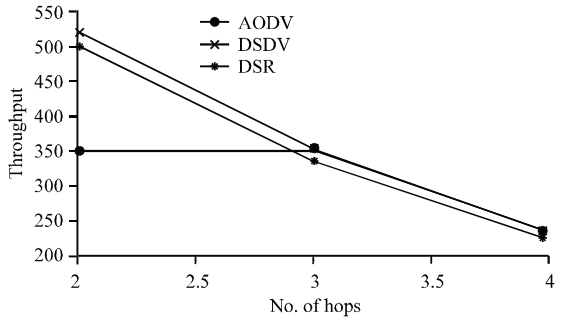

Fig. 4: Throughput comparison of routing protocols (AODV, DSDV, DSR)

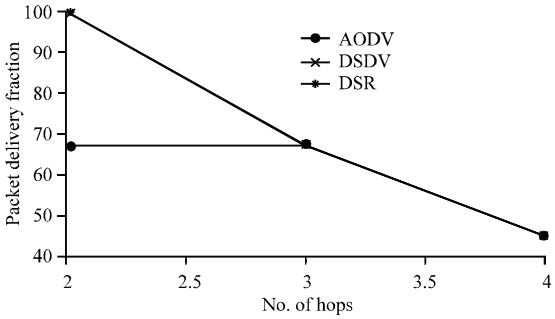

Fig. 5: Packet delivery fraction comparison of routing protocols (AODV, DSDV, DSR)

mechanism. The cost function is based upon the conditions of traffic load and battery power (Woo *et al*., 2001; Vazifehdan *et al*., 2014). MDR is fully based upon source-destination based mechanism. Only the source or destination makes decision during transmission and intermediate nodes can piggyback their current costs through the messages in routing.

To distribute the packets to all energy-rich nodes, the "Local Energy-Aware Routing" (LEAR) is introduced. A node discovers a node only when its current amount of energy exceeds a specific threshold. Otherwise, it creates a message known as Drop Route Request (DR- REQ) and drops Route Request (RREQ). RREQ reaches the destination node only when it passes through all intermediate nodes with sufficient amount of energy. If RREQ does not reach the destination, then the source does not receive RREP from the destination. It then starts a second attempt to discover a route towards destination.

A route cache is used in this protocol where an intermediate node generates a message known as Route Cache (RCAC) and sends towards a destination. The destination node responds either to first route request or to route cache and ignores all the other messages. Route cache will be replied only when power is above specific threshold. Otherwise Drop Route Cache (DR-CAC) or

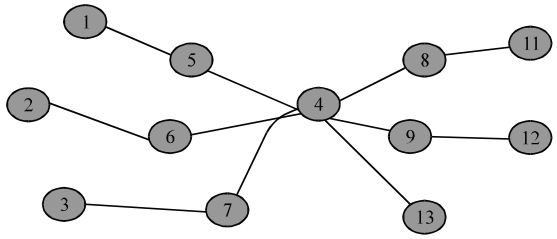

Fig. 6: Scenario of node to become bottleneck

Cancel Route Cache (CR-CAC) is replied to the node which sends route cache. The node then attempts to discover the other paths after getting next route request.

However, all the above discussed protocol does not concentrate the issue of node to become bottleneck. It is a situation in the network where multiple source node forwarding the packets through an identical intermediate node. If node receives the packets greater than its resource capacity of handling packets, then packets get drop from intermediate node and if this situation continue for some extend may cause complete network to congestion (Mohammad *et al*., 2016a, b). Bottleneck intermediate node is shown in Fig. 6.

MATERIALS AND METHODS

Proposed energy aware routing protocol: The Energy Dependent DSR (EDDSR) mechanism is proposed which can be used in the route discovery process of DSR. We devised a new mechanism whose aim is to increase the lifetime of node with low amount of energy stored. In this mechanism, each node shows its readiness to forward packets according to its current energy level. Each node in the medium calculates its Residual Battery Power known as "RBP_i". If RBP_i is lower than the specific threshold, then the rebroadcasting of RREQ by a node is delayed. If residual power of a node is enough, then it behaves as a DSR nodes and proceeds its network activities.

A predicted node lifetime n_i is described by the ratio RBP_i, DR_i in which RBP_i represents residual battery power and Dr_i represents drain rate which described the amount of energy consumed per second.

In EDDSR mechanism, the nodes with shorter lifetime are prevented from route discovery process to increase their lifetime. Therefore, the route requests sent by a node having small lifetime will be cancelled by the nodes closer to destination. RERR packets are sent to the sourc to inform the source when the energy of a node is below critical levels. EDDSR mechanism finally uses RCAC as suggested by Local Energy-Aware Routing (LEAR) protocol. Hence, the behavior of intermediate nodes with RRCAC message is similar to RREQ.

We proposed a new mechanism called as "Energy Aware Proactive Routing for MANETs based on intermediate node current condition" to find the energy aware route from source to destination. We named it as EDDSR as it is extension of existing DSR routing protocol with energy awareness. In proposed algorithm, a route is selected according to "Contemporary Processing State" of an intermediate node to achieve extended network lifetime and link reliability in terms of node's input buffer and residual energy. A major handout over the work proposed is classified as follows:

- Energy required to process K Kilobytes of packets through an intermediate node
- Current Processing State (CPS) of node in terms of energy and its input buffer traffic
- Priority of node by describing value of threshold
- Selecting path of route according to priority of a node

When threshold condition is satisfied by a node in terms of energy, then it can participate in routing. The information processing capability optimizes the metric node based on residual energy and current traffic to prevent the node from becoming a bottleneck. In DSR protocol, it uses first priority message of a node to discover an optimistic route.

To calculate the CPS (Contemporary Processing State) of a node in terms of input buffer traffic and energy consumed, consider a node N_x having energy E_x in joules and B as buffer in kilobytes which must process the x kilobytes of packets in a present state.

Consider a packet termed as K_x which requires energy e_x joules of energy and buffer space b kilobytes to process from an intermediate node. To calculate the contemporary processing state, we need to calculate subset of packets so that firstly, all communication packets are combined with size in bytes at the most of energy E_x in joules. Secondly, a sufficient amount of packets must be processed by an intermediate node in a contemporary state and also, part of the packets must not be processed. To successfully process packet K_x, a node need to consume the energy $e(K_x)$ within multi-hop mobile ad-hoc network environment and it is computed by the equation given:

$$e(K_x) = T(K_x) + R(K_x) + D(K_x)$$

Where, $T(K_x)$, $R(K_x)$ and $D(K_x)$ send, receive and process node energy which needs to be sent, received and processed in K_x Kilobytes of packets through an intermediate node.

For calculation of the Contemporary Processing State (CPS) of a node according to energy and input buffer traffic, the data packets need to be processed through an intermediate node N_x in kilobytes (where x = 1, 2, 3, ...). The packets need to be processed completely because partial processing of packets impossible. N-Topples with positive values are considered as given below: number of packets for processing N_x from a given node is in K_x (Kilobytes where x = 1, 2, 3). E (K_x) is the energy required by a node for processing of packet K_x.

Now, we use Knapsack algorithm design in two-dimensional arrays to get optimal results. The equation is as follows:

$$S[0,..., n, 0...e_x]1 \le x \le n \forall \text{ and } 0 \le e(K_x) \le e$$

Where, $SS[T(K_x), e_x]$ processes maximum number of packets with "K_x" Kilobits of data (where x = 1, 2, 3, ...,) (Algorithm 1).

Algorithm 1; the algorithm calculates contemporary processing state of a node:

$S[0, e(kx)] = 0$ $\quad 0 \le e(kx) \le ex$

no packet process through the node

$S[x, e(kx)] = \forall -\infty e(kx) < 0$, illegal condition

Optimization as:

$S[i,e(kx)] = \max(S[x-1,e(kx)], \quad Sx+S[x-1,e(k)-e(kx)]) \quad \forall \quad 1 \le I \le x$ and $0 \le e(kx) \le ex$

We designed an algorithm for calculation of contemporary processing state of a node. Our protocol is based upon DSR but we use CPS as route selection metric instead of hop count. Each node has to calculate the value of CPS in a network and the rest of mechanism follows DSR protocol (Algorithm 2).

Algorithm 2; for proposed protocol:

Step 1.: (loop, initialization)
for $e(k_y) \leftarrow 0$ to e_y till node energy
set $S[0,e(k_y)] \leftarrow 0$
Step 2.: (loop)
for $y \leftarrow 1$ to m (set number of packets)
set $S[y,0] \leftarrow 0$
Step 3.: (loop inspecting the packet to process or not)
for $i \leftarrow 1$ to m
for $e(k_y) \leftarrow 0$ to e_y
if$(e(k_y)) \leftarrow 0$ to e_y(then packets can be processed by a node)
if $(k_y + S[Y-1,e(k_y)-e_y] > S[Y-1,e_y])$ then
set $S[Y, e_y] \leftarrow k_y + s[Y-1, e_y] - e_y$
else
set $S[Y,e_y] \leftarrow s[Y-1,e_y] + (e(k_y) > e_y)$
Step 4.: (finish)
Exit

RESULTS AND DISCUSSION

Performance evaluation of proposed protocol (MDDSR): After calculating the EDDSR mechanism, we have compared this with LEAR, MDR and pure DSR in a

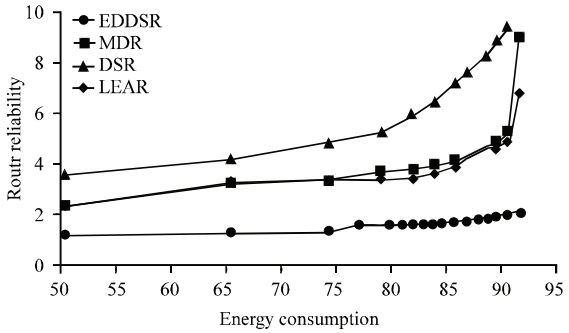

Fig. 7: Routing reliability comparison between proposed and existing mechanisms

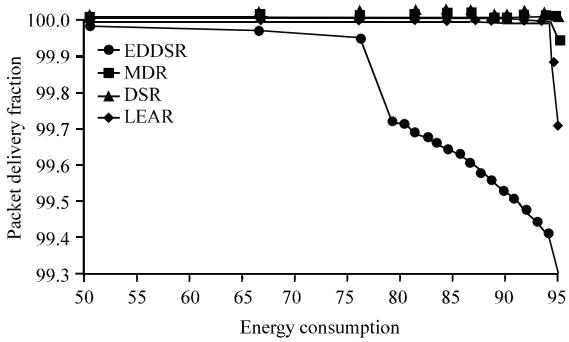

Fig. 8: Packet delivery fraction comparison between proposed and existing

Table 1: Simulation parameters

Parameters of network	Values
Time for simulation	300 (sec)
Total number of nodes	10-100
Type of link layer	Logical link
Type of MAC layer	802.11
Type of radio propagation	Two-ray ground
Type of queue	Drop tail
Node's initial enargy	15 Joules
Range of transmission	250 m
Antenna	OMNI antenna
Receiving and transmission power	350 and 650 MW
Routing protocol	DSR
Traffic	FTP, CBR
Network area	500×500 m
Type of mobility	Random wave propogation

scenario of sparse and dense network; we compared four mechanisms with respect to energy parameter. Moreover, our main focus is to compute node life time, i.e., due to lack of battery capacity it takes some time for a node to stop working. The network parameters consider in our simulation shown in Table 1. To investigate the overheating effects, we consider the energy cost and repeat all the simulations because of overheating activities.

Figure 7-9 compares number of nodes died over time after the capacity of a battery expires in a static network

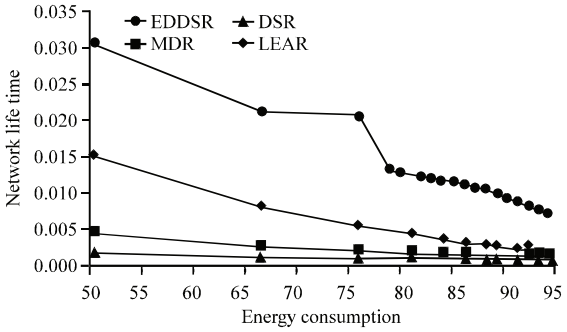

Fig. 9: Network lifetime comparison between proposed and existing mechanisms

environment. All protocols have a similar behavior but there is a slight amount of improvement found in EDDSR when simulation ends. This attitude is because of use of EDDSR rerouting techniques which helps us to avoid using a node with a weak battery.

When we consider overheating activity, balancing of energy consumption by the power aware algorithm fails because of large amount of energy consumed during overhearing activities.

In dynamic network scenario (Siddiqua *et al*., 2015), EDDSR and MDR outperform DSR. In addition, DSR consumes large amount of energy because of routing activities and the LEAR mechanism induces a large amount of energy consumption. This effect occurs due to frequent use of process of route discovery which uses DDREQ packets sent by broadcasting.

The perspective of MDR and EDDSR seems to have a better outcome from the mobility of a node which allows new routes after breakage of route. Therefore, EDDSR and MDR are able to balance the utilization of node and energy consumption accordingly. MDR is independent of the route cache and it has the capability to acquire fresh routes through periodical initiation of route discovery procedure. These routes reflect the node's residual power as well as the actual topology which removes the overhead caused due to route discovery. EDDSR does not allow an intermediate node to send RREP consisting an invalid route towards the source. In a manner of this appreciation, we also observed a small amount of expenditure of routing energy for both mechanisms.

CONCLUSION

In this research, we proposed a Energy Dependent DSR (EDDSR) method to improve energy efficiency in MANETs. Initially we compared the basic routing algorithms of MANETs designed based on hop count routing metric, through simulation we conclude that DSR is best suited protocol for achieving energy efficiency

as it is designed based on demand source initiative mechanism. Thus, we developed a on demand reactive energy dependent routing based on DSR. Through simulation, we conclude that our proposed work out perform with respect to energy efficiency parameters.

LIMITATION

The proposed on-demand routing protocol considers only few parameters in routing like energy, congestion control and neglects other parameters of QOS.

SUGGESTION

In future another on-demand routing protocol can be designed which considers other parameters of QOS also.

REFERENCES

Chaubey, N., A. Aggarwal, S. Gandhi and K.A. Jani, 2015. Performance analysis of TSDRP and AODV routing protocol under black hole attacks in MANETs by varying network size. Proceedings of the 5th International Conference on Advanced Computing and Communication Technologies, February 21-22, 2015, Rohtak, India, pp: 320-324.

Dulman, S., J. Wu and P. Havinga, 2003. An energy efficient multipath routing algorithm for wireless sensor networks. Proceedings of the IEEE International Symposium on Autonomous Decentralized Systems, April 9-11, 2003, Pisa, Italy.

Mohammad, A.A.K., A. Mirza and M.A. Razzak, 2015. Reactive Energy Aware Routing Selection Based on Knapsack Algorithm (RER-SK). In: Emerging ICT for Bridging the Future-Proceedings of the 49th Annual Convention of the Computer Society of India CSI, Satapathy, S., A. Govardhan, K. Raju and J. Mandal (Eds.). Springer, Berlin, Germany, ISBN: 978-3-319-13730-8, pp: 289-298.

Mohammad, A.A.K., A. Mirza and S. Vemuru, 2016a. Analytical model for evaluating the bottleneck node in MANETs. Indian J. Sci. Technol., 9: 1-6.

Mohammad, A.A.K., A. Mirza and S. Vemuru, 2016b. Cluster based mutual authenticated key agreement based on chaotic maps for mobile ad hoc networks. Indian J. Sci. Technol., 9: 1-11.

Moravejosharieh, A., H. Modares, R. Salleh and E. Mostajeran, 2013. Performance analysis of AODV, AOMDV, DSR, DSDV routing protocols in vehicular ad hoc network. Res. J. Recent Sci., 2: 66-73.

Siddiqua, A., K. Sridevi and A.A.K. Mohammed, 2015. Preventing black hole attacks in MANETs using secure knowledge algorithm. Proceedings of the 2015 International Conference on Signal Processing and Communication Engineering Systems (SPACES), January 2-3, 2015, IEEE, Guntur, India, pp: 421-425.

Varshney, P.K., G.S. Agrawal and S.K. Sharma, 2016. Relative performance analysis of proactive routing protocols in wireless ad hoc networks using varying node density. Invertis J. Sci. Technol., 9: 161-169.

Vazifehdan, J., R.V. Prasad and I. Niemegeers, 2014. Energy-efficient reliable routing considering residual energy in wireless ad hoc networks. Mobile Comput. IEEE. Trans., 13: 434-447.

Woo, K., C. Yu, H.Y. Youn and B. Lee, 2001. Non-blocking, localized routing algorithm for balanced energy consumption in mobile ad hoc networks. Proceedings of 9th International Symposium on Modeling, Analysis and Simulation of Computer and Telecommunication Systems, August 15-18, 2001, Cincinnati, OH., USA., pp: 117-124.

QUALITY OF SERVICE STABILITY BASED MULTICAST ROUTING PROTOCOL FOR MANETS

M.Vijayalakshmi[1] and D.SreenivasaRao[2]

[1]Department of Electronics and Communication Engineering, GNITS, India

[2]Department of Electronics and Communication Engineering, JNTUH, India

ABSTRACT

Mobile Ad Hoc Networking Does Not Own Any Fixed Infrastructure And Hence, Stable Routing Is The Major Problem. The Mobility Nature Of Manet's Node Facilitates Rediscovery Of A New Path To Organizing A Routing. In Order To Intensify The Quality Of Service And Routing Stability In Manet, We Propose A Dynamic Quality Of Service Stability Based Multicast Routing Protocol By Modifying The Cuckoo Search Algorithm Through A Modernizing Mechanism Which Is Derived From The Differential Evolution Algorithm. Tuned Csa Is A Combined Feature Of Csa And De Algorithms. Periodically, Each Node In The Network Creates Neighbour Stability And Qos Database At Every Node By Calculating The Parameters Like Node And Link Stability Factor, Bandwidth Availability, And Delays. Finally, Multicast Path Constructs Route Request And Route Reply Packets, Stability Information And Performing Route Maintenance.

KEYWORDS: *MANETS, QOS, TUNED CSA, DQSMRP*

1. INTRODUCTION

Mobile Ad hoc Networks (MANETs) are foremost in class kind of wireless communication networks in which mobile nodes link on an on-demand basis. MANETs are having the ability to configure on their own and easing peer-level communications among mobile nodes independent by having no fixed infrastructure. When the route traffic occurs, constructing a MANET with each node's to continuously retain the information remains a major challenge. Normally, MANETs are used for group communications where multicast protocols are efficiently compared to unicast protocols since they improve the efficiency of the wireless links in MANETs. The multicast protocols are also used as application demands for transmitting copies from either single or multiple sources to the receivers.

Multicasting reduces the communication costs by sending the single copy of the data to multiple recipients through which it minimizes link bandwidth, processing and transmission delay. Previous researchers have developed different algorithms to improvise the ability for selecting the routing path(s) and thereby, effectively met the desired Quality of Service (QoS) [1]. This infrastructure consequences in a highly dynamic topology causing a challenging task for QoS Routing.

When compared with well-established networks such as Wi-Fi, Global System for Mobile communication (GSM) and Code Division Multiple Access (CDMA), MANET was not reliable to meet QoS performances. The MANET performance is determined by the QoS through the basic parameters like bandwidth or delay or loss. QoS routing addresses both the issues of deciding a path from source to destination and fulfilling the QoS constraints like bandwidth, delay

DOI:10.5121/cseij.2017.7101

and loss. Route selection method is used to fulfill QoS requirements. The goal of QoS routing strategy is to maximize the network resources in order to reduce the constraints in MANET's mobile nodes.

In real time applications, QoS routing protocol works based on multi-hop mobile networks [3, 4]. Particularly, QoS requirement depends on constraints such as link constraints, path constraints and tree constraints. End to End delay is usually affected by path constraint whereas, delay-jitter [5] by tree constraint. In order to meet all the constraints, robust techniques are required to solve the QoS requirements. Heuristic techniques are better to solve these constraints rather than deterministic methods. Researchers have studied various improvements based on heuristic methods [5, 6] and at the same time devised various solutions to solve QoS routing problems using heuristic methods[7].

Ad hoc mobile routing (AM Routing) was studied through which a specific unicast routing protocol was identified as more feasible than other unicast routing protocols (8). In QoS routing, network topology was constructed in which bandwidth link works in destination point [9]. A new protocol was proposed for ad hoc networks which are used to establish and maintain a shared mesh for each multicast group called Policy-based Unified Multi-radio, Architecture for Agile Mesh *Networking (*PUMA) [10]. A new single mixed metrics have been delineated for multi-constraint QoS routing [11]. Previous literaturehas found that Agent Based Multicast Routing Scheme (ABMRS) on MANET's could be used as a set of static and mobile agents for QoS routing [12, 13]. Optimized link state routing protocol was launched and scrutinized in different research papers [14].

Besides that, several heuristic methods are examined to study the multi-constraint QoS routing. In [15], Simulated Annealing (SA) was introduced to solve the QoS routing problems. Reference [16]] discussed Bees Life Algorithm (BLA) to solve the QoS multicast routing problem and constraints such as delay, allowed jitter, and requested bandwidth have been studied. Similarly, a Tabu search [17] based method concentrates on two important constraints in QoS such as bandwidth and end-to-end delay. Ant algorithm optimization was globally accepted for the effective and systematic handling of QoS routing [18][19] Harmony search (HS) algorithm, a unique algorithm was used to find the path of the MANET and it was discussed based on bandwidth-delay-constraints in multicast routing problem [20].

Hybrid methods have been proposed to address the delay of premature convergence [21]. A PSO-GA algorithm was evolved using a combination of both particle swarm optimization (PSO) method and genetic algorithm (GA) which provides an effective and efficient search for the solution. In [22], the new fuzzy genetic algorithm is also introduced for QoS multicast routing is also discussed.

Thus in this paper, we propose Dynamic Quality of Service Stability based multicast routing protocol (DQSMRP) for the multi-constraint QoS routing problem. Recently, Cuckoo Search (CS) is derived from reproduction strategies [23] which are widely used in heuristic based algorithms. [24, 25].It is more exhaustive and provides quick search to obtain better solutions to routing in more reliable and robust manner.

2. PROBLEM DEFINITION, RESEARCH METHODOLOGY

The optimization problem is used to solve the QoS routing problem which is the primary objective to find a multicast tree constraints based on the cost function in order to reduce the practical constraints. Four different constraints are considered for formulating the current study

such as delay, packet loss, bandwidth and jitter. The following equation provides formulation data for computation [5] QoS routing function is formulated as below

$$MinC(H(x,s)) = C_c + \delta_1 C_b + \delta_2 C_d + \delta_3 C_{dj} + \delta_4 C_{pl} \quad \text{.....(1)}$$

Reasons to merge both cost optimization and multi-constrained routing are as follows

- Formulations are based on multiple constraints and the multicast structure in order to spot an attainable path for each node having source and destination.
- To shrink the network resource utilization by users.

In progressively,

$$C(H(x,s)) = \sum_{e \in H(x,S)}^{\cdot} c(y) \quad \text{..... (2)}$$

The Delay Constraint is defined as the allowed delay limit that exists in any branch of the network. When there is no link provided between any two nodes, a penalty occurs.

$$Delay(R(x,y)) = \sum_{e \in R(x,y)}^{\cdot} dl(x) + \sum_{n \in R(x,y)}^{\cdot} dl(y) \quad \text{.....(3)}$$

The Bandwidth Constraint is the requirement of average bandwidth among all tree branches in the network.

$$Bandwidth(R(x,y)) = min(bw(x)), x \in R(x,y) \quad \text{.....(4)}$$

Specifically $\delta_1, \delta_2, \delta_3, \delta_4$, are the bandwidth, delay, delay-jitter and packet-loss for the corresponding penalty constants. The objective of the initiated solution is to solve the multicast QoS routing problem as described by numerical experiments in the coming section.

2.1 TUNED CUCKOO SEARCH MULTICAST ROUTING PROTOCOL

A technique that produces simple implementation and quality solutions is the best solution provider. This paper provides better results over the existing algorithms such as meta-heuristic techniques. Before analyzing the proposed method, the cuckoo algorithm is discussed as follows.

2.1.1. AN OVERVIEW OF CUCKOO SEARCH ALGORITHM

By analogy of reproduction strategy, CS algorithm is a well known prominent heuristic search algorithms which follow the principle of cuckoos (chosen nests of other birds for laying eggs) [26, 27]. Generally, the host bird would not permit the cuckoo eggs to easily differentiate and vice-versa. The important optimization procedure is as follows:

- **Initial Solution:** Cuckoo egg symbolizes a set of solutions and its value of dimensions was extracted from various nests randomly;
- **Next Generation:** The best eggs with common solutions only able to proceed to the next generation.
- **Acceptance Rule:** New egg will succeed in the nest if eggs are unknown. Important step of CS are explained as follows:

- Step 1: Randomly set "Pop" host nests, a group of the population. (e.g.,$P = x\sum_{i=1}^{pop} P_i$)
- Step 2: Evaluate the fitness of all nests$F = x\sum_{i=1}^{pop} f(P_i)$
- Step 3: Do Iterations <Max. Iterations.
- Step 4: Produce a cuckoo egg P^i by applying a Lévy flight from a random nest
- Step 5: Compute the fitness of $f(P_i)$
- Step 6: Check for existence: choose again a random nest J
- Step 7: if $f(p_i^1) < f(P_i)$ then
- Step 8: $P_{j=x}p_i^1$
- Step 9: end if
- Step 10: Remove a fraction of the worst nests at the rate of $R_c^{\square}$
- Step 11: Randomly, Building new nests at new locations using Levy flights replacements
- Step 12:End While

The benefit of this heuristics is its simplicity. The single parameter of CS algorithm should be considered enough when compared with PSO and Ant colony algorithms.

2.1.2 NODE STABILITY

For efficient better packet delivery services in forwarding group, the mobile node is to be very stable .The way of providing stability is that moving node around its current position. Node stability metric have been used in previous work of authors is given in [28]. It is studied that stable path nodes have been found from packets from the source to the multicast group. Self-stability and neighbor nodes stability are two metrics to represent node stability.
Following steps to find stability of a node:

- In MANET's nodes, it establishes self-stability, i.e., node movement is relative to its previous position.
- MANET's node gives the node stability factor from self-stability and neighbor stability. Actually, stability is based on the distance between the movements of nodes positioning within transmission range. Stable node is created when movement within transmission range.

2.1.3 NEIGHBOR NODE STABILITY

It can be defined as how the node is being connected to its neighbour to obtain self-stability. Whenever nodes are in transmission range, it can exchange messages with each other. Each node consists of connectivity information, the signal stability of one-hop neighbors, and also maintains a neighbor list. The degree of a node n is denoted as number of links (or nodes) which connected to it and denoted as ND.

$$N_s(t) = \propto \times \frac{1}{ND} \sum_{i=1}^{ND} S_s^i(t) + (1-\propto) \times N_s(t-1) \quad \ldots\ldots\ldots\ldots\ldots\ldots (5)$$

Where, α is the weighting factor (lies between 0 and 1) and is distributed between 0.6 and 0.7 since they yield better results in simulation.

2.1.4 LINK STABILITY

Link stability between the nodes defines quality and existence of the connection. It is reckoned based on two parameters:

- Received Signal Strength and
- A lifetime of the Link.
- The algorithm represents a pseudocode for updating link stability status between the nodes.

  The different parameters used in the algorithm are as follows:
  - Lifetime – Duration of continuous connectivity between the nodes
  - Lifetime threshold – Indicates the maximum limit of link lifetime that decides link stability
  - Link stability status – It is a Boolean variable that defines link stability between the nodes.
  - Recent – Indicates most recent response received for a Hello packet from a neighbor
  - P – Represents Total Number of Hello packets
  - Received signal strength – Represents the strength of the signal received from a neighbor
  - Signal threshold – Is acceptable signal strength to be received from neighbors

2.1.5 ALGORITHM: LINK STABILITY STATUS BETWEEN THE NODES

- Step 1: P = No of Hello Packets;
- Step 2: Lifetime = 0;
- Step 3: Link stability status = 0;
- Step 4: Recent = 0;
- Step 5: Lifetime threshold = P × Hello Packet Interval;
- Step 6: While P > 0 do
- Step 7: If received signal strength ≥ signal threshold then
- Step 8: Lifetime = lifetime + 1;
- Step 9: Recent = 1;
- Step 10: P = P−1;
- Step 11: else
- Step 12: Recent = 0;
- Step 13: P = P−1;
- Step 14: end if
- Step 15: end while
- Step 16: lifetime sec = lifetime × Hello Packet Interval;
- Step 17: if (lifetime sec > lifetime threshold) and (Recent)
- Then
- Step 18: link stability status = 1;
- Step 19: else
- Step 20: link stability status = 0;
- Step 21: end if

2.1.6 DELAY ESTIMATION

For delay estimation, an arbitrary node that contributes to traffic forwarding using the M/M/1 queuing system is modeled. This queue represents a single queuing station with a single server [29]. The authors assume that the contributing nodes are served by a single server with first come first serve queuing policy. Packets arrive according to a Poisson distribution rate (λ), and the probability distribution of the service rate is exponential, denoted by μ. The maximum size of the queue in every node is represented by K.

To satisfy delay requirements in multimedia real-time applications, packets must be received by multicast receivers which satisfy the application delay constraints. When a packet is to be sent either by a source node or forwarding group of nodes, it experiences three types of delays: queuing, contention and transmission delay. The total delay considered over a link between two nodes is given by

$$d_{Total} = d_q + d_c + d_t \quad \text{……(6)}$$

The queuing delay denoted by d_q is the delay between the time the packet is assigned to a queue and the time it starts transmission. The packet waits and gives other packets in transmission queue are transmitted at this particular time. This is the amount of time a packet is spent in the interfacing queue (T).

2.1.7 BANDWIDTH ESTIMATION

Bandwidth is one of the key principles for assessing Quality of service (QoS). The authors considered their previous work presented in [30], to calculate the available bandwidth based on their channel status of the radio link to calculate the idle and busy periods of the shared wireless media. Bandwidth is measured by the node activities and its surrounding neighbors using the channel utility.

In IEEE 802.11 MANETs, once it is achieved to gain the channel access, a node can be able to transmitting data packets. Hence, a node senses the channel and estimates bandwidth by using the idle and busy times in a predefined interval. This is expressed by the following equation.

$$BW = \frac{T_{idle}}{T_{interval}} \times C \quad \text{……..(7)}$$

2.1.8 ROUTE DISCOVERY PROCESS USING TUNED CUCKOO PROCESS

Multicast stable QoS path creation involves two phases: a request and a reply phase. Request phase invokes route discovery process to find routes having a group of receivers using stable and QoS intermediate nodes. It helps to reply phase for updating of RIC and also performs confirmation process. It acts as intermediate nodes that help to create a multicast mesh to the group of receivers.

RR packets are used in source node to find the route to its group of receivers. The sequences of operations that occur are as follows:

- Source node prepares an RR packet with an application of bandwidth and delay requirements.

- Selective transmission of RR packet to neighbors once satisfies stability criteria, i.e., SFBN greater than SFTH, and bandwidth requirement, i.e., estimated bandwidth greater than twice the application requirements.
- Once received, node discards RR packet (both sequence number and source address).
- If RR packet is not a duplicate, check if the availability of Routing Information Cache (RIC); if available, RP packet create and start reply propagation to the source.
- If RR packet is a duplicate, then discard it and stop transmission of RR packet.
- If not duplicate and no route available in RIC, transmit the RR packet by updating its fields (route record, Stability Factor Between Nodes (SFBN) record, bandwidth record, delay record, time to live, and nexthop address) to its neighbors as in step 2.
- Perform steps 3 to 6 (Till destination reached).
- If the receiver is not reached within certain hops, send RE packet to the source node.

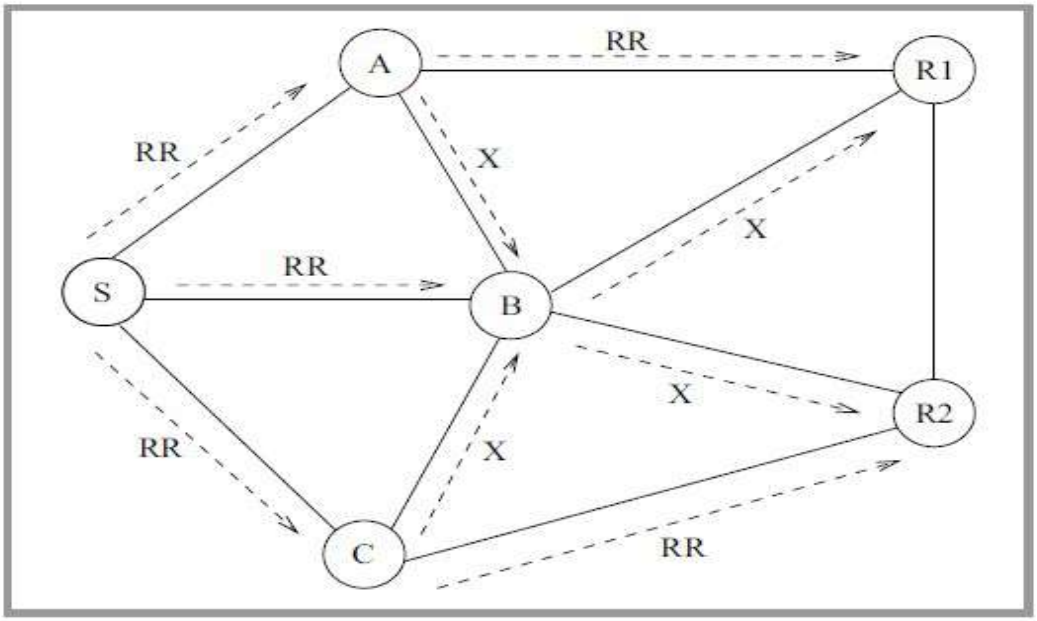

Figure 1: Route request paths from S to R1 and R2

3. RESULTS AND DISCUSSION

3.1 SIMULATIONS AND PERFORMANCE EVALUATION

In this section, the performance of proposed protocol with DQSMRP and Fully Distributed Multicast Routing Protocol (FDMRP) [31] is compared, through a considerable set of simulations. These etiquettes have been taken for comparison because both are mesh based. These protocols are collated in terms of packet delivery ratio, control overhead and average end-to-end delay. Simulations considering the values of the production parameters are taken for several iterations, and these are computing the mean. The values lying within 95% of the confidence interval of the mean are used for computing the mean value, which is shown in the graphs in result analysis section. The various network scenarios have been simulated. Simulation environment consists of four models: Network, Channel, Mobility and Traffic. An ad hoc network is created at an area of l × b square meters as network model; it is having N number of mobile nodes spaced randomly. Limited bandwidths in coverage area around each node have shared to its

neighbors. It is assumed that the operating range of transmitted power and communication range are constant.

3.1.1 PERFORMANCE PARAMETERS

Following metrics have been used to scrutinize the performance:

- **Packet Delivery Ratio (PDR)** : The ratio of a number of average data packets received at the multicast receivers to the number of data packets sent by the source.
- **Packet Over Head** : The ratio of control packets sent to the network to the total number of average data packets delivered to the receivers.
- **Average End-to-End Delay**: The average delay experienced by the successfully delivered packets in reaching their receiver.

No. of Nodes	50,100,150 and 200.
Routing Protocol	DQSMRP
Area Size	1000 X 1000
Mac	802.11
Radio Range	250m
Simulation Time	10 sec
Traffic Source	CBR
Packet Size	512
Receiving Power	0.395
Sending power	0.660
Idle Power	0.035
Initial Energy	10.0 J
Node Speed	5,10,10 and,20 ms
No of destinations	2,4,6 and 8

Table 1: Simulation scenario

3.2 RESULT ANALYSIS

The simulation results of DQSMRP and FDMRP present the comparison results by varying number of multiple destinations and node speed. According to the simulation results in Fig 2 to Fig 7, the performance of TCSMRP is more reliable than FDMRP. The execution of DQSMRP packet delivery ratio is gathered more than 14.2% compare to FDMRP. Moreover, the rendering of DQSMRP starts to end delay is less than FDMRP. The performance rate is almost 18% less and the delay ratio is varied with respective of node speed and number of destinations. According to the overhead performance scenario, the overhead rate is 22% less than FDMRP.

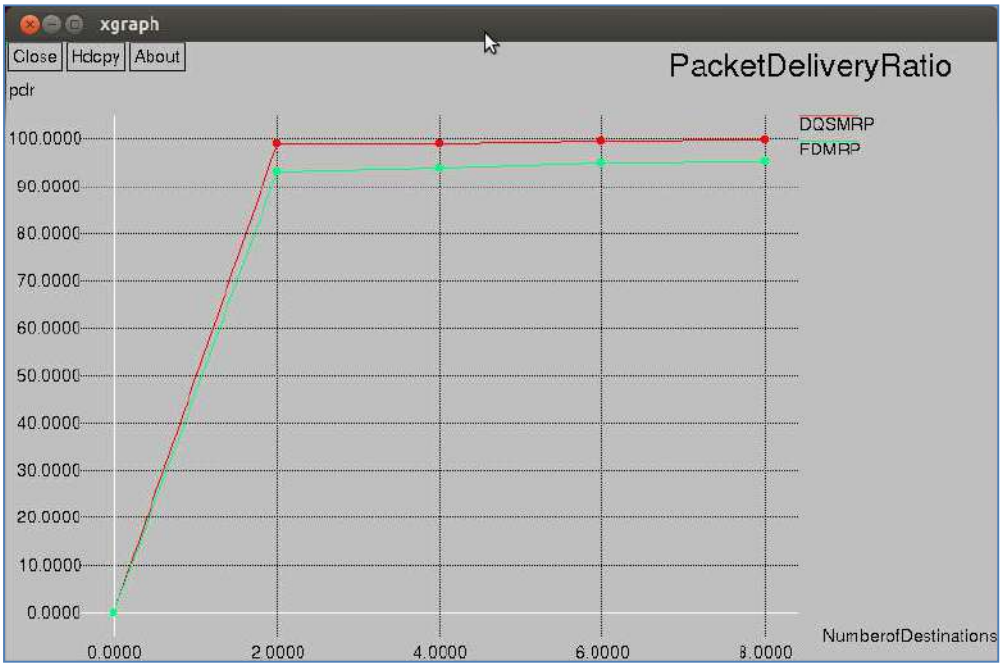

Figure 2: PDR vs Number of Destinations

Figure 3: PDR vs Node Speed

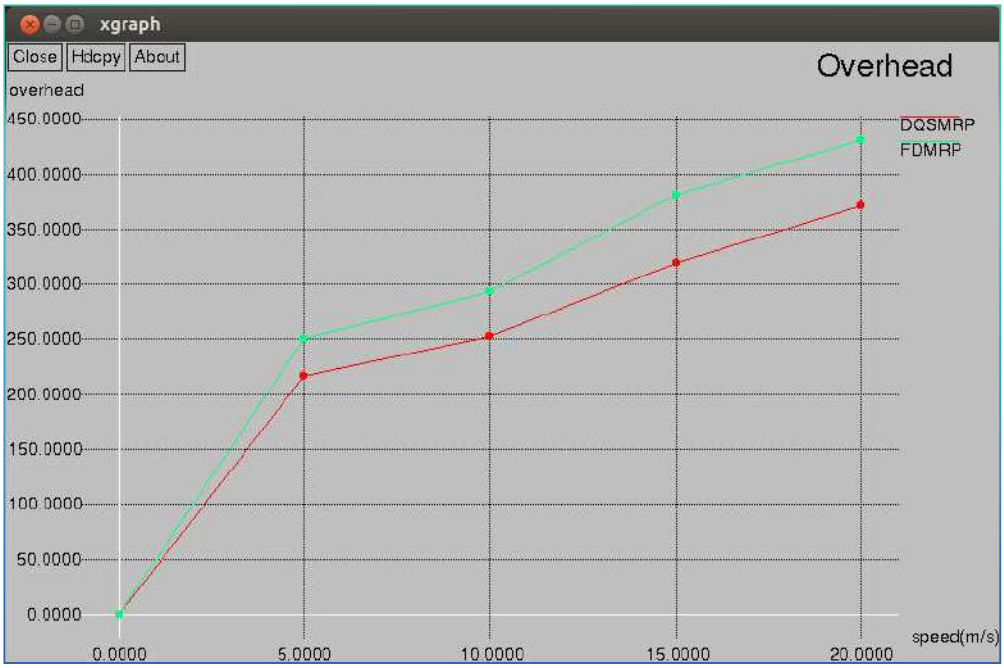

Figure 4: Overhead vs Node Speed

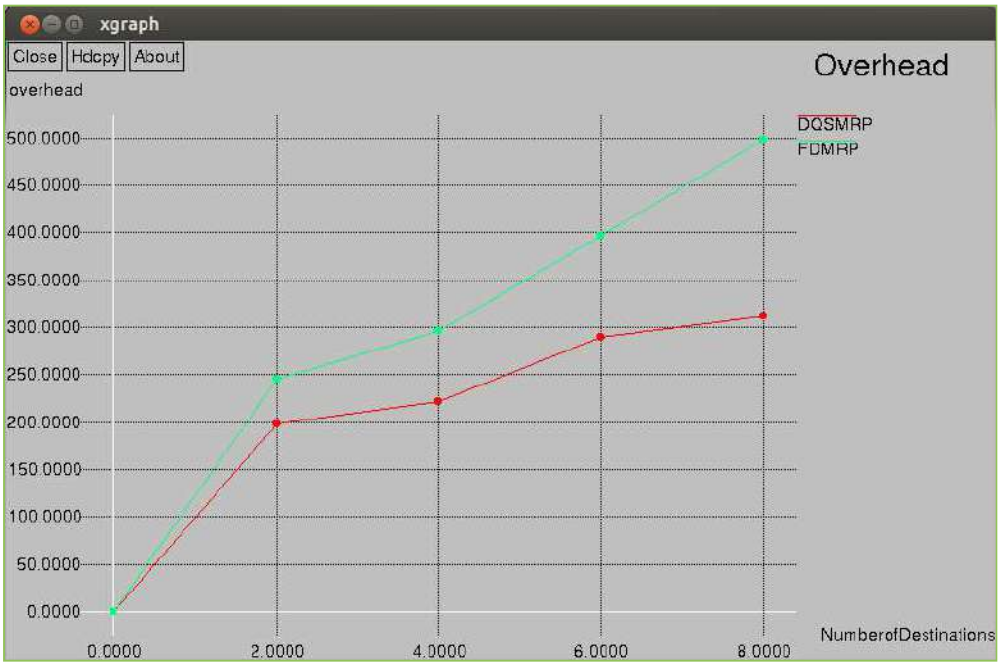

Figure 5: Overhead vs Number of destinations

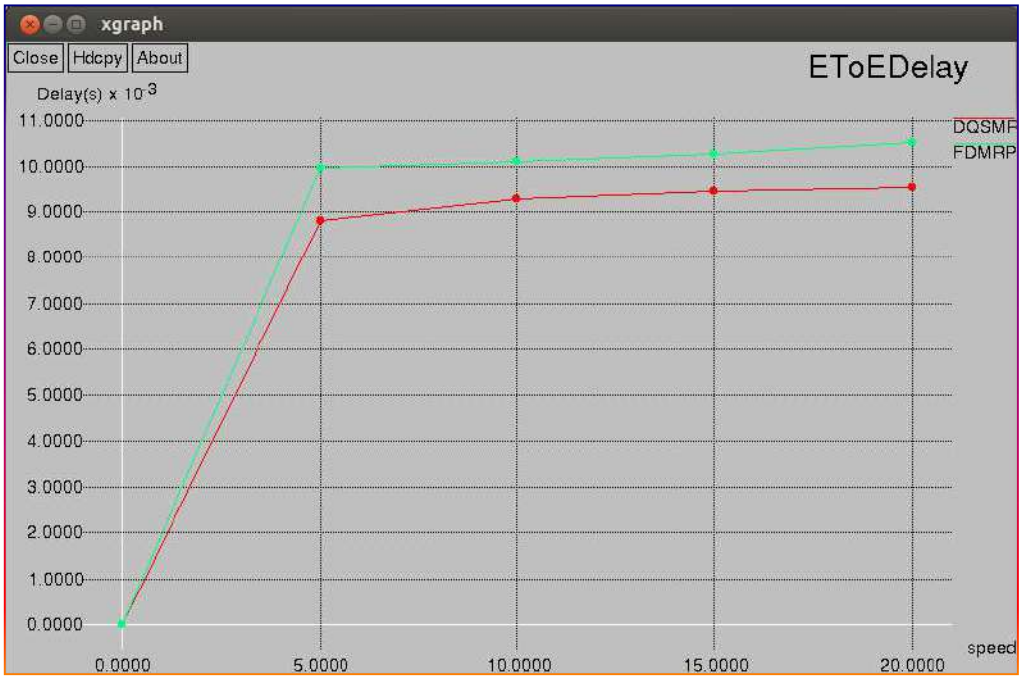

Figure 6: End - End Delays vs Speed

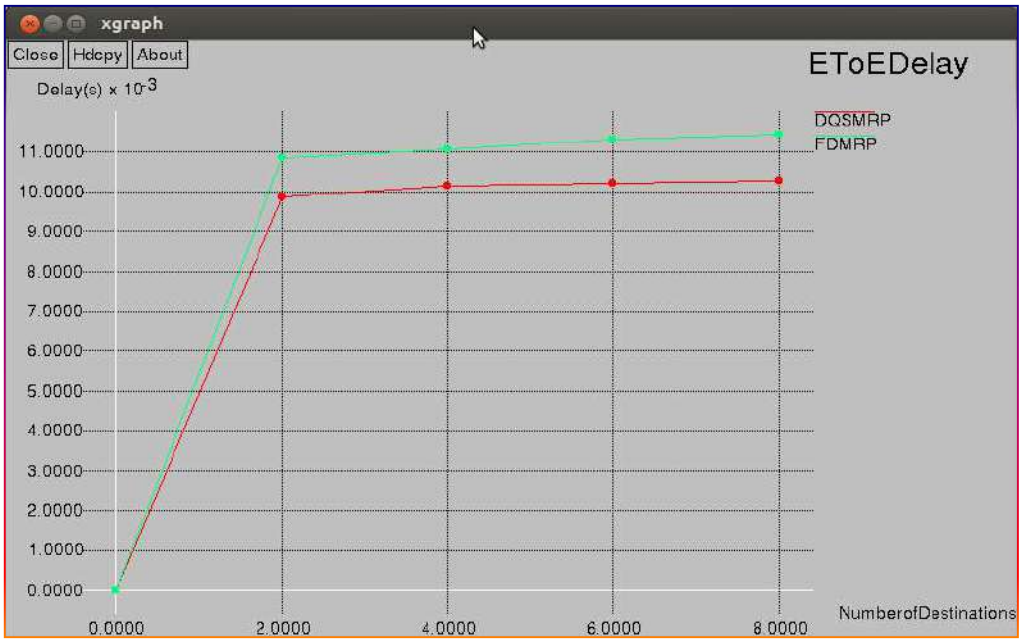

Figure 7: End - End Delays vs Number of Destinations

4. CONCLUSIONS

This paper clarifies about a hybrid computational intellectual algorithm i.e., Tuned Cuckoo Search Algorithm (TCSA), that includes the dominant characteristic of two different heuristic techniques have been used to solve QoS multicast routing. The QoS routing in a MANET is a

intricate to determine a prime routing. The general conclusion from presented simulation experiments reveals that proposed routing protocol performs better than FDMRP in terms of packet delivery ratio, packet overhead and average delay from start to end as a function of varying number of receivers, sources and node speeds. In future works, the author's aims to study further by comparing our Tuned Cuckoo Search Multicast Routing Protocol with some more QoS based routing protocols in MANETs. Numerical experiments have shown that the propounded hybrid TCSA algorithm provides advanced search multicast trees, particularly in both swift convergence and robustness, when compared to other algorithms. This proposed algorithm shall be the escort for real-time networks with suitable sophistication based on when and where it utilized.

REFERENCES

[1] R. A. Guérin and A. Orda, "QoS routing in networks with inaccurate information: theory and algorithms," IEEE/ACM Transactions on Networking, vol. 7, no. 3, pp. 350–364, 1999.

[2] D. H. Lorenz and A. Orda, "QoS routing in networks with uncertain parameters," IEEE/ACM Transactions on Networking, vol. 6, no. 6, pp. 768–778, 1998.

[3] L. Hanzo II and R. Tafazolli, "A survey of QoS routing solutions for mobile ad hoc networks" IEEE Communications Surveys & Tutorials, vol. 9, no. 2, pp. 50–70, 2007.

[4] C. R. Lin and J.-S. Liu, "QoS routing in ad hoc wireless networks," IEEE Journal on Selected Areas in Communications, vol. 17, no. 8, pp. 1426–1438, 1999.

[5] L. Zhang, L. B. Cai, M. Li, and F. H. Wang, "A method for least-cost QoS multicast routing based on genetic simulated annealing algorithm," Computer Communications, vol. 32, no. 1, pp. 105–110, 2009.

[6] X. Yuan and X. Liu, "Heuristic algorithms for themulti-constrained quality of service routing," inProceedings of the 20th Annual Joint Conference of the IEEE Computer and Communications Societies (INFOCOM '01), vol. 2, pp. 844–853, IEEE, 2001.

[7] M. Abolhasan, T. Wysocki, and E. Dutkiewicz, "A review of routing protocols for mobile ad hoc networks," Ad Hoc Networks, vol. 2, no. 1, pp. 1–22, 2004.

[8] J. Xie, R. R. Talpade, A. Mcauley, and M. Liu, "AMRoute: ad hoc multicast routing protocol," Mobile Networks and Applications, vol. 7, no. 6, pp. 429–439, 2002.

[9] Y. S. Chen, Y. C. Tseng, J. P. Sheu, and P. H. Kuo, "An on-demand, link-state, multi-path QoS routing in a wireless mobile ad-hoc network," Computer Communications, vol. 27, no. 1, pp. 27–40, 2004.

[10] R. Vaishampayan and J. J. Garcia-Luna-Aceves, "Efficient and robust multicast routing in mobile ad hoc networks" in Proceedings of the IEEE International Conference on "Mobile Ad-hoc and Sensor Systems", pp. 304–313, IEEE, October 2004.

[11] P. Khadivi, S. Samavi, and T. D. Todd, "Multi-constraint QoS routing using a new single mixed metrics,"Journal of Network and Computer Applications, vol. 31, no. 4, pp. 656–676, 2008.

[12] S. S. Manvi and M. S. Kakkasageri, "Multicast routing in mobile ad hoc networks by using a multi-agent system" Information Sciences, vol. 178, no. 6, pp. 1611–1628, 2008.

[13] F. Kuipers, P. Van Mieghem, T. Korkmaz, and M. Krunz, "An overview of constraint-based path selection algorithms for QoS routing," IEEE Communications Magazine, vol. 40, no. 12, 2002.

[14] K. Kunavut and T. Sanguankotchakorn, "Multi-Constrained Path (MCP) QoS routing in OLSR based on multiple additive QoS metrics," in Proceedings of the International Symposium on Communications and Information Technologies (ISCIT '10), pp. 226–231, IEEE, Tokyo, Japan, October 2010.

[15] L. Liu and G. Feng, "Simulated annealing based multi-constrained QoS routing in mobile ad hoc networks," Wireless Personal Communications, vol. 41, no. 3, pp. 393–405, 2007.

[16] S. Bitam and A. Mellouk, "Bee life-based multi-constraints multicast routing optimization for vehicular ad hoc networks," Journal of Network and Computer Applications, vol. 36, no. 3, pp. 981–991, 2013.

[17] N. Ghaboosi and A. T. Haghighat, "Tabu search based algorithms for bandwidth-delay-constrained least-cost multicast routing," Telecommunication Systems, vol. 34, no. 3-4, pp. 147–166, 2007.

[18] Z. Subing and L. Zemin, "A QoS routing algorithm based on ant algorithm," in Proceedings of the IEEE International Conference on Communications (ICC '01), vol. 5, pp. 1581–1585, IEEE, 2001.

[19] C.-H. Chu, J. Gu, X. D. Hou, and Q. Gu, "A heuristic ant algorithm for solving QoS multicast routing problem," in Proceedings of the IEEE Congress on Evolutionary Computation (CEC '02), vol. 2, pp. 1630–1635, IEEE, Honolulu, Hawaii, USA, May 2002.

[20] R. Forsati, A. T. Haghighat, and M. Mahdavi, "Harmony search based algorithms for bandwidth-delay-constrained least-cost multicast routing" Computer Communications, vol. 31, no. 10, pp. 2505–2519, 2008.

[21] R. F. Abdel-Kader, "Hybrid discrete PSO with GA operators for efficient QoS-multicast routing," Ain Shams Engineering Journal, vol. 2, no. 1, pp. 21–31, 2011.

[22] P. Chen and T. L. Dong "A fuzzy genetic algorithm for QoS multicast routing" Computer Communications, vol. 26, no. 6, pp. 506–512, 2003.

[23] X. S. Yang and S. Deb, "Engineering optimization by cuckoo search," International Journal of Mathematical Modelling and Numerical Optimisation, vol. 1, no. 4, pp. 330–343, 2010.

[24] S. Walton, O. Hassan, K. Morgan, and M. R. Brown, "Modified cuckoo search: a new gradient-freeoptimization algorithm," Chaos, Solitons & Fractals, vol. 44, no. 9, pp. 710–718, 2011.

[25] X. S. Yang and S. Deb, "Cuckoo search: recent advances and applications," Neural Computing and Applications, vol. 24, no. 1, pp. 169–174, 2014.

[26] O. Baskan, "Determining optimal link capacity expansions in road networks using cuckoo search algorithm with levy flights," Journal of Applied Mathematics, vol. 2013, Article ID 718015, 11 pages, 2013.

[27] P. Civicioglu and E. Besdok, "A conceptual comparison of the Cuckoo-search, particle swarm optimization, differential evolution and artificial bee colony algorithms" Artificial Intelligence Review, vol. 39, no. 4, pp. 315–346, 2013.

[28] P. I. Basarkod, S. S. Manvi, and D. S. Albur, "Mobility-based estimation of node stability in MANETs", in Proc. Int. Conf. Emerg. Trends in Comput., Commun. and Nanotechnol. ICE-CCN 2013, Tuticorin, India, 2013, pp. 126–130.

[29] K. S. Trivedi, Probability and Statistics with Reliability, Queuing, and Computer Science Applications, 2 ed. Wiley Interscience, 2005

[30] P. I. Basarkod and S. S. Manvi, "Multiple parameters based approach to estimate bandwidth in mobile ad hoc networks", Int. J. Comp. Sci. Issues, Special Issue (IJCSI), vol. 1, no. 1, pp. 37–43, 2011.

[31] Woongsoo Na, Yunseong Lee, Jongha Yoon, Junho Park, and Sungrae Cho, "Fully Distributed Multicast Routing Protocol for IEEE 802.15.8 Peer-Aware Communication", International Journal of Distributed Sensor Networks Volume 2015.

International Journal of Engineering Technology Science and Research
IJETSR
www.ijetsr.com
ISSN 2394 – 3386
Volume 4, Issue 10
October 2017

Design of Improved Remote Data Transfer Using Concurrent Multipath through Mobile Device

Rajeshwari M Goudar[1]
Research Scholar, UniversityCollege of Engg, JNTU, Kakinada[1]
Syed Abdul Sattar[2]
Nawab Shah Alam Khan, College of Engg& Technology, Hyderabad[2],
Ch Satyanarayana[3]
University College of Engg, JNTU,Kakinada[3]

ABSTRACT

With faster growth of mobile technology and internet more and more technical features are provided through mobile devices which made the ease of day to day activities of the users of mobile devices. Millions of users are making use of mobile devices for making faster communication, sending and receiving of data or information seamlessly from remote places. Today's mobile devices are having the features of personal computers (pcs) and hence the integration of the devices between mobile and pcs can be monitored and better interaction can be accomplished.

Due to the widespread use of wireless technologies convergence of wired and wireless networks made easy to perform tasks on mobile devices. Today's corporate world is handling most of the work through remote place by controlling the activities over different networks. Administrator of the network will handle all the activities of network through mobile device without his presence in a server room of the network. Research activities are being carried out that allow remote control of devices.

An effort is made to explore multipath aggregation problem in order to get solutions which will improve throughput by making effective use of multiple paths of heterogeneous wireless networks concurrently. This work is mainly tested at application layer by forwarding single data transport connection over the multiple paths. The purpose of logical segmentation of a file streaming is made by using multi-homed clients is to be developed at application layer. The new approach uses CMT-SCTP protocol with existing server infrastructure client based manner.

KEYWORDS

Concurrent Multi-path, Bandwidth Aggregation, Interface

I INTRODUCTION

The first computer communication network started since the birth of Internet which covered area more than laboratory among three American universities and Stanford Research Institute by using 50 Kbit/s links [1]. The packet switched network was used for the first datagram in the world is sent for long distance and their onwards technology of communication journey started its progress. The fast growing wired and wireless technology of communication enabled, use of mobile devices, smartphones by millions of people to access the data of huge size by using Internet. The increasing data access demands for high speed of data transfer at the end hosts. This can be achieved by aggregating multiple network interfaces (paths) and using multiple paths simultaneously. The aggregation of bandwidth is useful when media of data is accessible by using slow wireless networks. The single wireless network path is, unable to provide the required data rate of transmission.

Today's wireless devices like smartphones and laptops are equipped with multiple number of interface which will be enabled to communicate with wireless local area networks. These devices are located in the coverage areas of wireless networks. Operating systems use single interface only for data transmission and other

International Journal of Engineering Technology Science and Research
IJETSR
www.ijetsr.com
ISSN 2394 – 3386
Volume 4, Issue 10
October 2017

interfaces will be idle in spite of available multiple interfaces. TCP and UDP transport protocols are used for majority of data transfer. However TCP and UDP protocols are not supporting for multiple number of IP addresses. By using multiple paths, packet reordering is essential and it can affect the performance.

Main goal of this proposed work is to improve data transfer speed by using multiple-paths i.e. interfaces available in the network at user's end host. This can be achieved by aggregating multiple network interfaces(paths) and using multiple paths simultaneously. This will be very much useful when the media of data access is possible through several slow networks. The single wireless network path is, unable to provide the required data rate of transmission like high quality multimedia streaming.

Smartphones and laptops devices equipped with multiple interfaces are commonly used for communicating different wireless technologies such as 3G, Wi-Fi, cellular networks and wireless local area networks. These mobile devices are present in the coverage areas of networks. Whenever the device is in the range of access networks then the device which executes the application can send the data simultaneously by using multiple paths as shown in fig. 1.

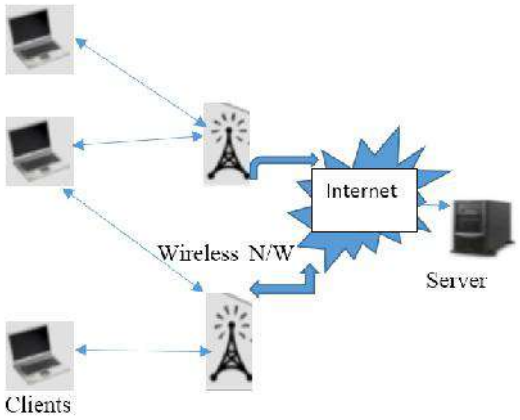

Fig. 1: Multipath network for data transmission

Remainder of the paper is organized as below. Section II briefs about the related work of bandwidth aggregation at different layers of standard protocol stack. Section III presents CMT-SCTP protocol which is followed by architecture of system in section IV and conclusion is given in Section V.

II Related work:

The main aim of aggregation of multiple paths is to improve the throughput. Solution of aggregation of multipath should attain at least average throughput, equivalent to the total addition of throughput of each individual paths.Continuous research work is carried out by researchers in order to provide the bandwidth aggregation on different layers of the protocol stack which use multi-homed devices.

Link layer

Multipath aggregation at link layer is also called as bonding or bundling at link layer as more number of physical channels are bundled into one logical channel [2]. Ethernet channel allows many of the hosts to be connected in order to obtain improved throughputby using multiple cables of Ethernet. Ethernet bundling prevents reordering of frames by making use of same port of Ethernet for the data flow. Ethernet speed is always more than the requirement of single application. Multilink Point to Point Protocol (PPP) also uses aggregation of the links[3]. At link layer, bandwidth aggregation works for two systems only. It is not useful for connecting multiple systems. Generic link layer (GLL) approach for bandwidth aggregation for link layer is proposed by Koudouridis[14]. Multiple radio access networks are used for communication with destination node.

International Journal of Engineering Technology Science and Research
IJETSR
www.ijetsr.com
ISSN 2394 – 3386
Volume 4, Issue 10
October 2017

Network layer

Multipath routing in network layer uses different paths(end to end) between the source and thedestination. Forwarding of IP traffic data over the multiple paths require the host to be multi-homed. The multi-homed system is one which has multiple providers of IP address ranges.

Aggregation of multiple paths at network layers use tunneling mechanism for transfer of packets from server to all IP addresses at client side. Bandwidth aggregation with infrastructure for network layer was proposed by Chebrolu et al. [4,5].Knowing the addresses of multi-homed clients, server calculates the packet delivery time to send the packetsintelligently with the aim of reducing reordering of packets at receiver. Earliest Delivery Path First (EDPF) is used for bandwidth aggregation at network layer is used by the author Kameshwari Chebrolu [5] at Network Layer, where minimal changes are made for existing infrastructure. EDPF works mainly based on the principle of ensuring packets which meet playback deadlines. Here scheduling of packets is based on estimation of transmission time ofthe packets. EDPF well performs similar to the Aggregated Single Link (ASL), where single interface will replace multiple interfaces which are having same kind of aggregated bandwidth.

Transport layer:

Single path transport protocols are not able to support for multimedia and other business applications which demand for reliability and fault tolerance. Multipath techniques can solve deficiencies of single path protocols by using inverse multiplexing of resources to send packets over multiple paths which provide fault tolerance, better reliability and enhanced throughput. Use of multipath transport layer is suitable for the devices which provide heterogeneous access technologies like Wi-Fi, 3G,Wi-max etc. Mobile devices by using multiple paths provide improved reliability and the ability to shift from one technology to other. It is also possible for the mobile nodes to pool their low bandwidth which can support for high bandwidth demanding applications. CMT-SCTP protocol is useful for multiple paths aggregation at transport layer for failover of multiple IP addresses and not for use of simultaneous data transfer. Iyengar etal.[7,8] developed concurrent multipath transfer protocol, the extension of SCTP supports for data transfer forone end to other end paths. Different capacity of the paths and delay will cause packet reordering and faster transmission. Authors propose for virtual queues to be used at the sender side to know the packet reordering and packet losses.

Many of researchers continued the work in order to strengthen idea of CMT, by developing CMT-SCTP, load sharing SCTP(LS-SCTP). Fiore et al. [9] and Perotto et al. [10] suggested to use Westwood's bandwidth estimation in order to send the chunks over available paths efficiently.

Dreibholz and Adhari etal. [11, 12] proposed SCTP-based multipath aggregation solution over the asymmetric paths.Distributed Stream Control Transmission Protocol (DSCTP) makes use of [15] multi-streaming and multi-homing for the aggregation of the bandwidths of interfaces. It makes use theavailable active streams simultaneously.

Application layer:

The application which wants to transfer the data on multiple paths will establish several transport connections and binding them to IP addresses. Data to be transferred is distributed as per the available capacity of the path. The data file to be sent is split into number of logical segments and transmitted concurrently over different paths.

Application Layer Protocol based Aggregation (ALPA) is a protocol used at the application layer for bandwidth aggregation is proposed in the paper[16] by considering the dynamics of wireless links. The objective this work is mainly to minimize energy consumption and guaranteed quality of service by dynamically scheduling of data transmission for both network interfaces.

IIICMT SCTP Protocol

Stream control transmission protocol (SCTP) is a standard transport layer protocol developed by Internet Engineering Task Force (IETF). CMT SCTP is an extension of SCTP protocol. It provides services

International Journal of Engineering Technology Science and Research
IJETSR
www.ijetsr.com
ISSN 2394 – 3386
Volume 4, Issue 10
October 2017

equivalent to TCP and UDP apart from multi-homing and multi-streaming. SCTP is one of the reliable protocol. It supports for multiple IP addresses. It is useful for addressing interfaces which are connected to different networks. It uses one single identified path for data transmission and other are used for the purpose of backup and retransmissions. Today's mobile devices like laptops and smart phones are having multiple interfaces. The multi-homing service allow these devices for establishment of connection with more number of networks similar to smart phone with 4G and Wi-Fi connections.

In an SCTP association, one of the path is usedfor transmission of data and others are used for retransmissions or backup whenever path failure occurs.The multi-streaming service is used for concurrent transmission of streams.SCTP supports forthe transfer of simultaneous data over multiple paths by using CMTSCTP so as to updatethroughput of aggregated transmission [13]. CMT-SCTP protocol allows for utilization of multi paths simultaneously. It facilitates for higher data transmission among the hosts, having multiple interface devices so as to maximize aggregated transmission throughput.

CMT-SCTP allows for the payload data to be distributed across all of available paths at the same time. An example for association of two paths SCTP and CMT-SCTP is as shown in the fig 2 a) and Figure 2 b). Apart from increase in the performance by using CMT SCTP but there are some issues related to reordering of the data at the receiver end. However main issues related are fast retransmission and selective acknowledgement traffic. In order to avoid these issues, algorithms for CMT-SCTP are proposed [13].

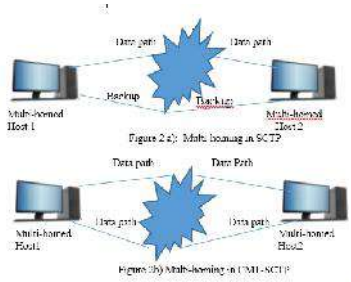

Fig. 2b) Multi-homing in CMT-SCTP

Association buffer is used to keep data chunks irrespective of the path on which these data chunks were transmitted. It supports for multi-buffer structure. CMT-SCTP association is as shown in the fig.3.

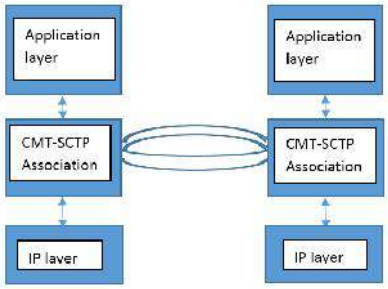

Fig. 3: CMT-SCTP Association

IV Architecture of system

The general architecture for multipath data transfer consists of multiple clients and server from which data is to be fetched are connected in a wired/wireless network. Let the client C makes request for required file transfer from server S. The server S transmits the requested file using multiple paths where concurrent transmission takes place in the form of data chunks. Each path connected through an intermediate node which forwards the incoming packets from first path P_1 towards the client on second path P_2 based on the optimum selection of path based on estimation of path selection for communication which is as shown in figure 4. Client can be smartphone, mobile device or laptop and nodes can be access point, base station, Wi-Fi, Wi-

International Journal of Engineering Technology Science and Research
IJETSR
www.ijetsr.com
ISSN 2394 – 3386
Volume 4, Issue 10
October 2017

max, wireless routers or personal computers used as clients. Server is connected through buffer interfaces in the form of FIFO queue. The paths between server and client are of variable bandwidth. Variable bandwidth is the rate at which the paths send the data from server buffers as a function of time. Intermediate nodes just forward the data packets received as it is to the client.

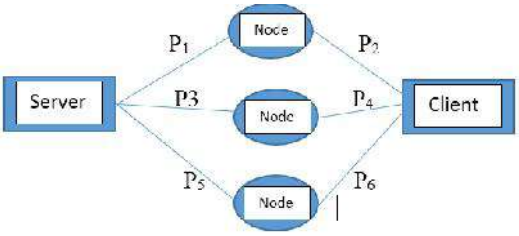

Fig. 4: Bandwidth aggregation architecture

The overall architecture of system mainly consists of following modules.

A Creation of Network:

A simulation environment is created by connecting multiple machines in wireless network including a server. Some of the nodes will work as transportation media of Wi- fi /wi-max. Each of these nodes have their own unique speed of transmission and others will act as clients. Database is maintained for both the files to be transmitted at the server side and database for keeping the received files at client side. Receiving buffers are used at the client side to receive incoming packets. Clients will make request for the required data for the server and server will check for the requested file in its database and responds by sending the file requested using multi-paths of the network available using optimal paths for communication using bandwidth aggregation. CMT-SCTP association is created between client and server and socket is used for the process of transportation. Compressed data to be sent is received by data splitter and there by divided into number of data chunks and these chunks are sent on different paths based on the selection of paths of communication using path estimation and selection of paths as shown in system architecture diagram represented in the fig. 5.

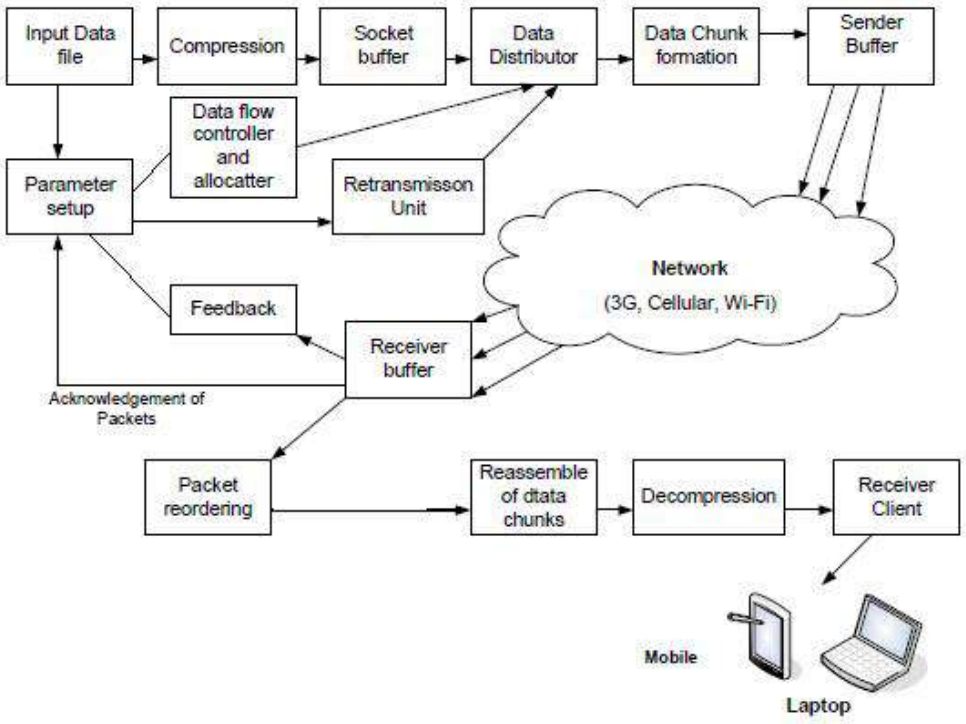

Fig. 5: System architecture

International Journal of Engineering Technology Science and Research
IJETSR
www.ijetsr.com
ISSN 2394 – 3386
Volume 4, Issue 10
October 2017

B. Server activity:

Server activity module starts first to collect list of clients activated/started in the network. It is ready to provide the following information/services.

1. List of clients connected in the network
2. List out the processes which are being executed at the selected client
3. Facility to kill a particular process, shutdown or termination of client machine
4. Sending and receiving of messages from server to the clients
5. Transfer of requested file by the client from server using bandwidth aggregation

Various operations will be executed remotely for controlling of process, file operations, sending a message, capturing of screenshots. All these operations are controlled by mobile device. Mobile device can be connected either through internet connection or through Wi-Fi connection. The server module performs operations such as control of processes, and killing of the running process of the client node. One has to select the process which is to be terminated from the list of the processes. In order to read a particular file one has to enter the path of the file and can have the access to the file. Other operations like broadcasting of message and sending notification to particular client is also possible.

C. Client activity:

Client gets started and have the facilities for requesting a file required from server end, Sending and receiving of messages. Activities of client are controlled by server.

D. Data flow rate controller and allocator:

Data flow rate controller and allocator is mainly concerned with choosing of best paths from the subset of communication paths and assign the transmission or bandwidth allocation rates to each of the path. Bandwidth allocation vector R =(r_0,r_1,r_2,r_3 … r_{n-1}) is maintained to keep track of number of transmission paths and bandwidth allocation values(n) along each of the path and is arranged in ascending order so that a path with maximum available bandwidth value is selected. r_i is thebandwidth allocated to the source i so that there is no congestion in the network and it is always less than the capacity of the link. If the available bandwidth is allocated with equal amount of bandwidth among all the connections and there is no proper utilization of bandwidth as each of the application is not utilizing the bandwidth. So there is a need of utility maximization algorithm for maximizing bandwidth allocation to each of the application.

E. Packets forwarding: Server is connected to the clients with multiple paths in the network. Each of path in the network is independent of each other path and has its own transmission speed. Each of these communication paths are having the properties as listed below.

a) Bandwidth available (B_a): It is measured in terms of bits transferred in the given unit amount of time.

b) Round trip time (RTT_p): It is total time taken for sending of data packet and receiving of acknowledgement for the data packet.

c) Path loss rate(L_p): It is the rate of loss of packets for that path of communication.

Each of the communication path is assigned with transmission capacity. Optimal throughput is obtained by using flow rate controller and allocator using utility maximization algorithm.

F. Reordering of packets:

The end to end delay of each path differs in the network. During the transfer of packets using concurrent multipath, there are chances of receiving the packets out of order. So packet scheduling [11] [12] [13] [15] is used to arrange transmission sequence in order to minimize the delay caused due to the reordering of packets at receiver end. The desired output at the receiver is generated by reordering of packets received through concurrent multi-paths.

V Conclusion:

Bandwidth aggregation for improving the throughput is proposed for accessing remotely required data by the clients connected in a network using mobile device. It is useful for remote monitoring and sharing of data. A terminal equipped with multiple network interfaces can access data through concurrent multi-paths. By using services of bandwidth aggregation, significant enhancement in the performance is achieved in terms of throughput, reliability and resource sharing over the use of single interface. A virtual bigger logical link with high bandwidth can be created by using multiple links of lower bandwidth in order to meet demands of applications which require higher bandwidth. Here a dynamic bandwidth aggregation is used at transport layer of the network. Compression and decompression of data is implemented in order to enhance the transmission throughput and better quality of service. Bandwidth aggregation is attained by using lower bandwidth channels and thereby achieving increase in transmission throughput.

In future, mobile and wireless communication systems will support for the increase in volume of data and thereby increase in the range of application domains which demand for high speed of transmission of data. The popularity of multi-homed mobile terminals facilitate for bandwidth aggregation to provide improved data transmission, throughput and reliability. In this work, the design of system is addressed to get aggregate bandwidth when a mobile device has several interfaces for communication and transfer of data. The extension of this research work can be useful for high streaming of video where dynamic availability of access networks with multiple interfaces of mobile device.

REFERENCES

[1] Zakon, R. H. Hobbes' Internet Timeline. IETF RFC 2235, November 1997.

[2] Association, I. S. Link aggregation for local and metropolitan area networks. IEEE Standard 802.1AX-2008, November 2008.

[3]Simpson, W. A. The Point-to-Point Protocol (PPP). IETF RFC 1661, July 1994.

[4] Chebrolu, K., Raman, B., and Rao, R. R. A network layer approach toenable TCP over multiple interfaces. Wireless Networks 11, 5 (2005), 637–650.

[5] Chebrolu, K., and Rao, R. R. Bandwidth aggregation for real-time applicationsin heterogeneous wireless networks. IEEE Transactions on Mobile Computing 5, 4(2006), 388–403.

[6] C. Paasch, G. Detal, F. Duchene, C. Raiciu, and O. Bonaventure, "Exploringmobile/WiFi handover with multi-path TCP," in Proceedings ofthe 2012 ACM SIGCOMM workshop on Cellular networks: operations,challenges, and future design. ACM, 2012, pp. 31–36.

[7] Allman, M., Balakrishnan, H., and Floyd, S. Enhancing TCP's Loss RecoveryUsing Limited Transmit. IETF RFC 3042, January 2001.

[8] Allman, M., Kruse, H., and Ostermann, S. An Application-Level Solutionto TCP's Satellite Inefficiencies. In Proceedings of the First International Workshopon Satellite-based Information Services (WOSBIS) (Rye, New York, USA, 1996).

[9] Fiore, M., Casetti, C., and Galante, G. Concurrent multipath communicationfor real-time traffic. Comput. Commun. 30, 17 (2007), 3307–3320.

[10] Perotto, F., Casetti, C., and Galante, G. SCTP-based Transport Protocolsfor Concurrent Multipath Transfer. WCNC (2007).

[11] Dreibholz, T., Becke, M., Rathgeb, E. P., and Tuxen, M. On the Useof Concurrent Multipath Transfer over Asymmetric Paths. In Proceedings of theIEEE Global Communications Conference (GLOBECOM), ISBN 978-1-4244-5637-6 (December 2010).

[12] Adhari, H., Dreibholz, T., Becke, M., Rathgeb, E. P., and Tuxen, M.Evaluation of Concurrent Multipath Transfer over Dissimilar Paths. In Proceedingsof the 1st International Workshop on Protocols and Applications with Multi-HomingSupport (PAMS), Singapore (March 2011).

[13]J. R. Iyengar, P. D. Amer, and R. Stewart, "Concurrent multipath transferusing SCTP multi-homing over independent end-to-end paths," Networking,IEEE/ACM Transactions on, vol. 14, no. 5, pp. 951–964, 2006.

[14]Koudouridis GP,Aguero R, AlexandriE, ChoqueJ, DimouK,KarimiHR, LedererH, Sachs J, Sigle , "Generic link layer functionality for multiradio access networks". In Proceedings of mobile summit, 2005.

[15] Mohammad Mamun Elahi, Shahin Khan, "A DistributedSCTP Scheme for Bandwidth aggregation", 16th International Conference of Computer and Information Technology, 8-10 March 2014.

[16] Zaiyang Tang, Zirui Wang, Peng Li, Song Guo, Xiaofei Liao, and Hai Jin "An Application Layer Protocol for Energy-Efficient Bandwidth Aggregation with Guaranteed Quality-of-Experience", IEEE Transactions on Parallel and Distributed Systems2014.

An Efficient and Scalable Mechanism for Managing the RDF Data in the Cloud

Tahera Abid[1], Sumera Jabeen[2]
[1]Assistant Professor, Dept of IT, Nawab Shah Alam Khan College of Engineering & Technology
[2]Assistant Professor, Dept of IT, Nawab Shah Alam Khan College of Engineering & Technology

Abstract: Despite late advances in scattered Resource Description Frame work (RDF) data organization, setting up a ton of RDF data in the cloud is still to a great degree troublesome. Slighting its evidently essential data illustrate, RDF truly encodes rich and complex graphs mixing both case and development level data. Sharing such data using set up strategies or partitioning the graph using standard min cut estimations prompts outstandingly inefficient appropriated operations and to a high number of joins. In this paper, we delineate Diplo Cloud, a gainful and adaptable scattered RDF data organization structure for the cloud. Contrary to past procedures, Diplo Cloud runs a physiological examination of both illustration and graph information going before allocating the data. In this paper, we portray the building of Diplo Cloud, its essential data structures, and moreover the new figurings we use to distribute pass on data. We in like manner show an expansive evaluation of Diplo Cloud exhibiting that our system is every now and again two solicitations of size snappier than best in class structures on standard workloads.

Keywords: RDF, triple stores, cloud computing, Big data

1.INTRODUCTION

The presence of circulated figuring enables to adequately and proficiently plan enrolling resources, for example to test another application or to scale a present programming foundation adaptably. The multifaceted idea of scaling out an application in the cloud (i.e., adding new enrolling centers to suit the advancement of some system) particularly depends upon the technique to be scaled. Every now and again, the occupation waiting be done can be viably part into a huge course of action of subtasks to be run independently and at the same time. Such operations are generally called embarrassingly parallel. Embarrassingly parallel issues can be reasonably adequately scaled out in the cloud by pushing new strategies on new product machines. There are however numerous methods that are essentially more difficult to parallelize, generally in light of the fact that they involve progressive systems (e.g., shapes in perspective of numerical procedures, for instance, Newton's technique). Such systems are called unavoidably progressive as their running time can't be quickened through and through paying little personality to the amount of processors or machines used. A couple of issues, finally, are not intrinsically progressive in that capacity but instead are difficult to parallelize before long in perspective of the plenitude of between process action they create.

Scaling out sorted out data taking care of routinely falls in the third arrangement. Generally, social data planning is scaled out by allocating the relations and redoing the inquiry means to reorder operations and use spread variations of the overseers engaging intra administrator parallelism. While a couple of operations are definitely not hard to parallelize (e.g., gigantic scale, spread counts), various operations, for instance, flowed joins, are more complicated to parallelize in light of the resulting movement they possibly deliver. While essentially more later than social data organization, RDF data organization has gotten various social techniques; Many RDF structures rely upon hash-isolating (on triple or property tables) and on appropriated judgments, projections, and joins. Our own Grid-Vine system was one of the key structures to do in that capacity concerning large scale decentralized RDF organization.

Hash partitioning has many purposes of enthusiasm, including straightforwardness and effective load-changing. Regardless, it in like manner makes much between process development, given that related triples (e.g., that must be picked and after that joined) end up being scattered on all machines. In this article, we propose DiploCloud, a capable, scattered and versatile RDF data get ready structure for flowed and cloud circumstances. Notwithstanding many appropriated

structures, DiploCloud uses an unflinchingly non-social amassing plan, where semantically related data outlines are mined both from the event level and the graph level data and get co-arranged to restrict between center point operations.

The fundamental commitments of this article are:

- a new creamer amassing model that capably and sufficiently divides RDF graph and physically co-finds related case data; another structure outline for dealing with fine-grained RDF fragments in immense scale;
- novel data circumstance strategies to co-discover semantically related bits of data; new data stacking and request execution procedures misusing our structure's data portions and records;
- an expansive exploratory evaluation exhibiting that our system is regularly two solicitations of enormity speedier than best in class structures on standard workloads. DiploCloud develops our past approach diplodocus ½RDF, a powerful single center point triple store. The system was also extended in TripleProv to help securing, following, and addressing provenance in RDF request taking care of.

2. RELATED WORK

Numerous procedures have been proposed to streamline RDF storing and SPARQL question dealing with; we list underneath two or three the most surely understood approachs and structures. We suggest the per user to late investigations of the field for a more total degree. Techniques for securing RDF data can be extensively arranged in three subcategories: triple-table strategies, property table systems, and diagram based approachs.

Since RDF data can be seen as sets of subject predicate-challenge triples, various early approachs used a creature triple table to store all data. Hexa store proposes to record RDF data using six possible records, one for each change of the plan of sections in the triple table. RDF-3X and YARS adopt after a practically identical strategy. BitMat keeps up a three-dimensional piece 3D shape where each cell addresses an intriguing triple and the cell regard implies closeness or nonattendance of the triple. Diverse methods propose to quicken RDF question get ready by considering structures bundling RDF data in light of their properties. Wilkinson et al. propose the usage of two sorts of property tables: one containing clusters of characteristics for properties that are much of the time co-got to together, and one abusing the sort property of subjects to aggregate relative game plans of subjects together in a comparative table.

Owens et al. propose to store data in three B+-tree records. They use SPO, POS, and OSP changes, where each document contains all parts of all triples. They isolate a request to major outline plans which are then planned to the set away RDF data. Different further techniques propose to store RDF data by misusing its graph structure. Yan et al. propose to disengage the RDF chart into subgraphs and to gather discretionary records (e.g., Bloom channels) to quickly recognize whether a few information can be found inside a RDF subgraph or not.

Ding et al. prescribe to part RDF data into subgraphs (iotas) to more adequately track provenance data by looking into clear center points and misusing an establishment power and down to earth properties .Das et al. in their structure called gStore orchestrate data in continuity list tables. Each vertex is addressed as a section in the table with an once-over of its dynamic edges and neighbors. To document vertices, they amass a S-tree in their continuity list table to decrease the chase space.

Brocheler et al. propose a balanced twofold tree where each center point containing a sub outline is arranged on one plate page.

Appropriated RDF question taking care of is a dynamic field of research. Past SPARQL organizations together methodologies (which are outside of the degree of this paper), we allude to a few conspicuous strategies underneath. Like a growing number recently systems, The Hadoop Distributed RDF Store (HDRS) uses Map Reduce to process coursed RDF data. RAPID+ widens Apache Pig and engages more powerful SPARQL question dealing with on Map Reduce using a choice request polynomial math. Their ability show is a settled hash-layout. Data is accumulated around a subject which is a first level key in the guide i.e. the data is co-arranged for a common subject which is a hash a

motivation in the guide. The settled segment is a hash depict predicate as a key and question as a regard.

Sempala extends over Impala stores data in a wide united property tables keeping one star-like shape per push. The scholars split SPARQL inquiries to Basic Graph Patterns and revise them to SQL, following they process a trademark join if essential. Jena HBase2 uses the HBase standard wide-table structure to realize both triple-table and property-table scattered accumulating. Its data exhibit is a portion arranged, deficient, multi-dimensional orchestrated guide. Areas are accumulated into section families and timestamps add an additional estimation to each cell. Cumulus RDF3 uses Cassandra and hash-distributing pass on the RDF tiples.

It stores data as four records (SPO, PSO, OSP, CSPO) to help a whole rundown on triples and questions on named diagrams (settings). We starting late tackled a correct evaluation to choose how much such noSQL systems can be used to direct RDF data in the cloud4 . Our past Grid Vine structure uses a triple-table accumulating approach and hash-allocating pass on RDF data over decentralized P2P frameworks. YARS2,5 Virtuoso6 , 4store , and SHARD hash divide over various machines and parallelize the inquiry get ready. Virtuoso by Erlin et al. stores data as RDF quads containing the going with segments: outline, subject, predicate, and challenge. Each one of the quads are hung on in one table and the data is distributed perspective of the subject. Virtuoso executes two records. The default record (set as a fundamental key) is GSPO (Graph, Subject, Predicate, Object) and a partner bitmap document (OPGS). A practically identical approach is proposed by Harris et al., where they apply a clear accumulating model securing quads of (appear, subject, predicate, question). Data is distributed as non covering sets of records among parts of comparable subjects; segments are then spread among center points with a round-robin figuring.

They keep up a hash table of outlines where each entry centers to an once-over of triples in the graph. Also, for each predicate, two radix tries are used where the key is either subject or question, and independently dissent or subject and graph are secured as areas (they in this way can be seen as customary P:OS and P:SO documents). Literals are recorded in an alternate hash table and they are addressed as (S,P, O/Literal). SHARD keeps data on HDFS as star-like shape spinning around a subject and all edges from this center. It exhibits a condition accentuation estimation the guideline thought of which is to rehash over all announcements and incrementally tie factors and satisfy obliges.

3. STORAGE MODEL

Our ability system in DiploCloud can be seen as a crossbreed structure growing a couple of the considerations from above. Our system depends on three rule structures: RDF molecule gatherings (which can be seen as hybrid structures gaining both from property tables and RDF subgraphs), format records (securing literals in limited records as in an area arranged database structure) and a successful key rundown requesting URIs and literals in light of the groups they have a place with. Rather than the property-table and segment organized approachs, our structure in perspective of organizations and iotas is more adaptable, as in each format can be changed logically, for example following the consideration of new data or a move in the workload, without requiring to adjust exchange designs or particles.

Similarly, we introduce a stand-out blend of physical structures to manage RDF data both on a level plane (to adaptably co-discover components or qualities related to a given case) and also vertically (to colocate course of action of components or qualities joined to practically identical cases). Iota bundles are used as a piece of two courses in our structure: to insightfully collect arrangements of related URIs and literals in the hash table (along these lines, pre-preparing joins), and to physically co-discover information relating to a given inquiry on plate and on a fundamental level memory to diminish circle and CPU save latencies. Design records are for the most part used for examination and aggregate inquiries, as they allow to process not inconsequential courses of action of literals profitably.

Key Index

The Key Index is the central record in DiploCloud; it uses a lexicographical tree to parse each moving toward URI or strict and dole out it a unique numeric key regard. It by then stores, for each key and every design

ID, an asked for once-over of the significant number of clusters IDs containing the key (e.g., key 10011, identifying with a Course question [template ID], appears in bunches 1011, 1100 and 1101‖. This may appear like a truly difficult to miss strategy for requesting regards, yet we show up underneath this truly empowers us to execute numerous request profitably just by scrutinizing or intersection such records in the hash table direct. The key document is responsible for encoding all URIs and literals appearing in the triples into a stand-out system id (key), and back. We use a tweaked lexicographic tree to parse URI sand literals and dole out them a stand-out numeric ID.

The lexicographic tree we use is basically a prefix tree part the URIs or literals in perspective of their fundamental prefixes (since various URIs share the same prefixes) with the true objective that each substring prefix is secured once and only once in the tree. A key ID is secured at each leaf, which is made out of a sort prefix (encoding the sort of the part, e.g., Student or xsd: date) and of an auto augmented case identifier. This prefix trees empower us to absolutely keep up a vital separation from potential effects (caused for instance while applying hash deals with gigantic datasets), and also let us insignificantly co-find both sort and case ids into one limited key. A minute structure makes an elucidation of the keys at the end of the day into their one of a kind casing. It is made out of a game plan of revamped records (one for each sort), each relating a case ID to its contrasting URI/strict in the lexicographic tree with a particular ultimate objective to engage compelling key look-ups.

Formats

One of the key improvements of DiploCloud turns around the usage of illustrative amassing plans [36] to viably gather tremendous aggregations of related regards on plate and in essential memory. When setting up another database, the database official may give DiploCloud two or three signs as for how to store the data on plate: the head can give a summary of triple cases to decide the root center points, both for the configuration records and the molecule clusters (see for instance Fig. 1, where Student‖ is the root center of the iota, and Student ID‖ is the root center point for the design list). Gathering appends are used to make sense of which packs to make: another gathering is made for each event of a root center point in the database. The clusters contain all triples pulling back from the root center point while exploring the chart, until the point when the moment that another case of a root center is crossed (thusly, one can join bunches in light of their root centers).

Arrangement joins are used to make sense of which literals to store in design records. In light of the limit plans, the structure handles two standard operations in our system: i) it keeps up a mapping of triple designs in primary memory and ii) it manages organize records. At whatever point another triples enters the structure, it accomplices design IDs identifying with the triple by considering the kind of the subject, the predicate, and the sort of the challenge. Each unmistakable summary of (subject-sort, predicate, question sort) describes another triple design. The triple organizations expect the piece of a case based RDF outline in our system. We don't rely upon the unequivocal RDF arrangement to describe the designs, since a broad degrees of necessities (e.g., spaces, ranges) are frequently disposed of in the layout (as it is for example the case for the data we consider in our examinations).

In case another design is perceived (e.g., another predicate is used), by then the arrangement boss updates its in-memory triple format graph and implants new design IDs to reflect the new case it found. On the off chance that there ought to be an event of amazingly inhomogeneous instructive files containing countless triple designs, trump cards can be used to regroup similar arrangements (e.g., ―Student - likes - *‖). Note this is amazingly exceptional eventually, since all the datasets we encountered as of recently (even those in the LOD cloud) regularly consider two or three thousands triple organizations at most. From that point, the system inserts the triple in one or a couple of particles. In case the triple's challenge identifies with a root. An arrangement list, the inquiry is moreover inserted into the design list contrasting with its format ID. Designs records store strict regards nearby the key of their looking at bundle root. They are secured moderately and separated in sub records, both on plate and on a basic level memory. Design records are regularly orchestrated

by considering a lexical demand on their strict regards—however unique solicitations can be shown by the database chief when he broadcasts the configuration roots. In that sense, format records are reminiscent of parts in a fragment arranged database structure.

4. SYSTEM OVERVIEW

Diplo-Cloud is a neighborhood, RDF database structure. It was planned to continue running on gatherings of item machines with a particular true objective to scale out easily when dealing with more prominent RDF datasets. Our structure setup takes after the outline of various propelled cloud based passed on systems (e.g., Google's Big Table), where one (Master) center point is accountable for collaborating with the clients and orchestrating the operations performed by the other (Worker) centers.

Master Node

The Master center point is made out of three essential sub sections: a key document (c.f.), responsible for encoding URIs and literals into limited system identifiers and of deciphering them back, a portion chief (c.f.), accountable for partitioning the RDF data into rehashing subgraphs, and an appropriated request operator (c.f.), responsible for parsing the moving toward question, reconsidering the request suspects the Workers, assembling ultimately reestablishing the results to the client. Note that the Master center can be reproduced at whatever guide vital toward ensure suitable inquiry stack changing and adjustment to non-basic disappointment. The Master can moreover be duplicated to scale out the key rundown for to an incredible degree generous datasets, or to replicate the dataset on the Workers using assorted separating plans (everything considered, each new event of the Master is responsible for one allotting plan).

Worker Nodes

The Worker center points hold the allotted data and its relating adjacent records, and are accountable for running sub inquiries and sending comes to fruition back to the Master center. Hypothetically, the Workers are impressively less troublesome than the Master center point and depend on three essential data structures: i) a sort list, gathering all keys in perspective of their sorts ii) a movement of RDF molecules, securing RDF data as to a great degree negligible sub outlines, and iii) a molecule document, securing for each key the once-over of atoms where the key can be found.

5. DATA PARTITIONING AND ALLOCATION

Triple-table and property-table hash-allocating starting at now the most surely understood separating plans for dispersed RDF structures. While clear, such hash parceling methodicallly surmises some passed on coordination overhead (e.g., to execute joins/path traversals on the RDF diagram), in this way making it uncivilized for most broad scale gatherings and circulated registering conditions showing high framework latencies. The other two standard social allotting frameworks, (tuple) round-robin and range separating, are relatively defective for the data and setting we consider, since they would portion triples either unpredictably or in light of the subject URI/sort, from this time forward truly compelling the parallelism of most managers (e.g., since numerous events having a comparable sort would end up on a comparative center point). Allocating RDF data in light of standard outline partitioning methodology is in like manner from our perspective despicable in a cloud setting, for three rule reasons: Loss of semantics: standard graph dividing consider unlabeled outlines by and large, and therefore are totally freethinker to the indulgence of a RDF diagram including classes of center points and edges. Loss of parallelism: dividing RDF graph based, for instance, on a min-cut computation will provoke outstandingly coarse fragments where a high number of related events (for instance associated with a comparable sort or sharing interfaces with comparative articles) will be help establish, along these lines drastically confining the level of parallelism of various chairmen (e.g., projections or decisions on particular sorts of instances).Limited versatility: finally, trying to portion immense RDF outlines is fantastical in cloud circumstances, given that bleeding edge diagram allotting methodology are unavoidably united and data/CPU genuine (as an account affirmation, we expected to get an extreme server and let it continue running for a couple of hours to section the greatest dataset we use in METIS). DiploCloud has been viewed

as beginning from the most punctual stage to help dispersed data isolating and co-region plots in a compelling and versatile way. DiploCloud grasps a widely appealing game plan between tuple-distributing graph allotting by choosing a rehashing, fine-grained outline isolating procedure abusing molecule formats. Diplo Cloud's molecule formats discover rehashing plans occurring in the RDF data regularly, by evaluating both the event level (physical) and the framework level (sensible) data, in this manner the explanation physiological9 partitioning.

Physiological Data Partitioning:

We now portray the three basic iota based data distributing procedures supported by our system: Scope-k particles. The minimum troublesome system is to physically describe different configuration sorts (as per normal procedure the structure considers various types) filling in as root center points for the particles, and a short time later to co-locate each and every further center that are direct or round aboutly related with the roots, up to given degree k.Scope-1 molecules, for example, co-arrange in the particles all root center points with their prompt neighbors (cases or literals) as portrayed by the formats. Degree 2 or 3 particles interface great arrangements from the root center (e.g., understudy; takes; course and course; hasid; xsd : whole number) recursively up to significance k to show up the joins around each root, to the disadvantage of rapidly growing limit costs since much data is ordinarily repeated everything considered. The degree of the particles is portrayed for this circumstance physically and incorporates data duplication. All data above Scope-1 is replicated; this is the cost to pay with a particular ultimate objective to benefit by precomputed joins inside the iotas, which on a very basic level extends request execution as we show up in the going with. Manual allocating. Root center points and the best way to deal with interface the distinctive organizations can similarly be demonstrated by hand by the database official, who just needs to make a setup record deciding the roots and the way formats should be associated with portray the nonexclusive condition of each particle sort. Using this system, the chief basically decides, in perspective of advantage sorts, the right way following which particles should be physically extended.

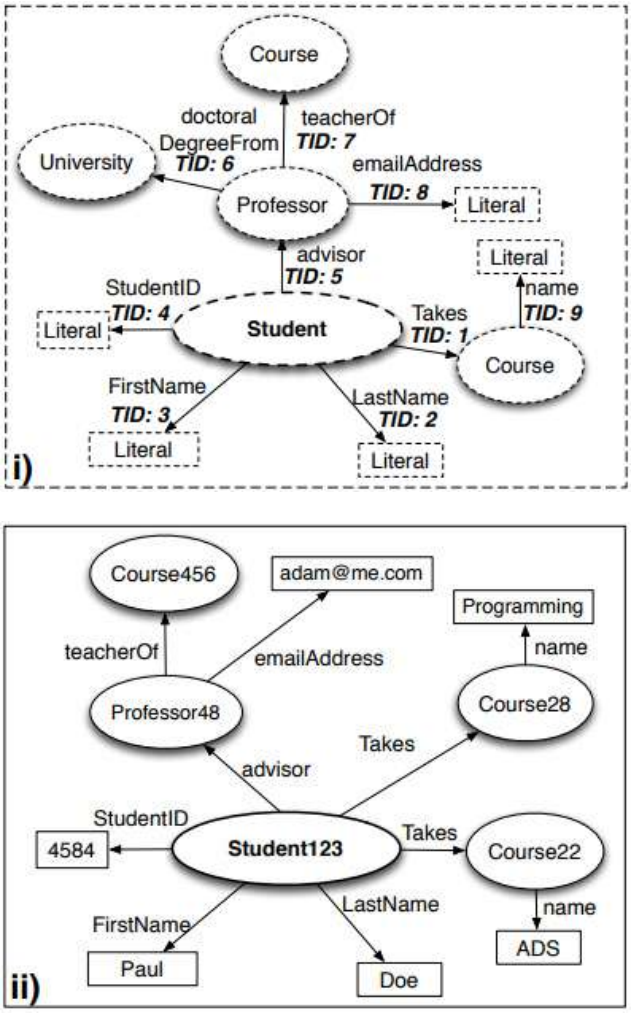

Fig. A molecule template (i) along with one of its RDF molecules (ii).

The structure by then therefore duplicates data following the supervisor's detail and precomputes all joins inside the particles. This is frequently the best response for decently stable datasets and workloads whose essential components are striking. Adaptable allotting. Finally, Diplo Cloud's most versatile allotting figuring starts by portraying degree 1 particles obviously, and a short time later alters the organizations following the inquiry workload. The structure keeps up a sliding-window w following the present history of the workload, and moreover related bits of knowledge about the amount of joins that must be performed and the ensnaring edges (e.g., missing co-zone among understudies and courses causing endless). By then at each time age , the system: i) grows one molecule format by particularly connecting

the edges (oversees) that are responsible for the most joins to a given point of confinement for their maximal significance and ii) decreases (up to scope-1) each extended iota whose developments were not addressed in the midst of the last age.

In that way, our structure slowly acclimates to the workload and rises visit routes in the RDF chart while keeping the general size of the particles little. Similarly to the two past techniques, when the degree of a molecule is expanded, the structure duplicates the critical bits of data and pre-registers the joins. The advantage of this system is that it begins with respectably clear and insignificant data structures and after that therefore acclimates to the dynamic workload by growing and reducing the degree of specific molecules, i.e., by including and ousting pre-enlisted routes in perspective of design subtle elements. By virtue of an incredibly one of a kind workload, the system won't modify the structures remembering the ultimate objective to avoid visit reexamining costs that would not by viably amortized by the adjustment being referred to get ready.

6. CONCLUSION

DiploCloud is a capable and flexible system for administering RDF data in the cloud. From our perspective, it strikes a perfect agreement between intra director parallelism and data co-region by considering rehashing, fine-grained physiological RDF distributes scattered data task designs, driving however to possibly more noteworthy data (reiteration introduced by higher degrees or flexible molecules) and to more erratic installs and updates. DiploCloud is particularly suited to gatherings of thing machines and cloud conditions where compose latencies can be high, since it intentionally tries to keep up a key separation from all complicated and scattered operations for question execution. Our test appraisal showed that it decidedly takes a gander at to state of-theart systems in such circumstances. We plan to continue making DiploCloud in a couple of headings: First, we expect to join some further weight parts (e.g., HDT). We mean to wear down a modified designs exposure in light of progressive cases and untyped segments. Furthermore, we plan to wear down planning a gathering engine into DiploCloud to help a greater game plan of semantic confinements and request locally. Finally, we are at the present time testing and growing our structure with a couple of associates in order to manage significantly enormous scale, passed on RDF datasets as to bioinformatics applications.

7. FUTURE ENHANCEMENT

Various RDF structures rely upon hash-distributing on coursed decisions, projections, and joins. Our own particular Grid Vine system was one of the principle structures to do all things considered concerning gigantic scale decentralized RDF organization.

REFERENCES

[1] K. Aberer, P. Cudre Mauroux, M. Hauswirth, and T. van Pelt, GridVine: Building Internet-scale semantic overlay networks,‖ in Proc. Int. Semantic Web Conf., 2004, pp. 107–121.

[2] P. Cudre Mauroux, S. Agarwal, and K. Aberer, GridVine: An infrastructure for peer information management, IEEE Internet Comput., vol. 11, no. 5, pp. 36–44, Sep./Oct. 2007.

[3] M. Wylot, J. Pont, M. Wisniewski, and P. Cudre Mauroux. (2011). diplodocus [RDF]: Short and longtail RDF analytics for massive webs of data. Proc. 10th Int. Conf. Semantic Web - Vol. Part I, pp. 778–793 [Online]. Available: http://dl.acm.org/citation.cfm?id=2063016.2063066

[4] M. Wylot, P. Cudre Mauroux, and P. Groth, TripleProv: Efficient processing of lineage queries in a native RDF store,‖ in Proc. 23rd Int. Conf. World Wide Web, 2014, pp. 455–466.

[5] M. Wylot, P. Cudre Mauroux, and P. Groth, Executing provenance- enabled queries over web data,‖ in Proc. 24th Int. Conf. World Wide Web, 2015, pp. 1275–1285.

[6] B. Haslhofer, E. M. Roochi, B. Schandl, and S. Zander. (2011). Europeana RDF store report. Univ. Vienna, Wien, Austria, Tech. Rep. [Online]. Available: http://eprints.cs.univie.ac.at/2833/1/europeana_ts_report.pdf

[7] Y. Guo, Z. Pan, and J. Heflin, An evaluation of knowledge base systems for large OWL datasets,‖ in Proc. Int. Semantic Web Conf., 2004, pp. 274–288.

[8] Faye, O. Cure, and Blin, A survey of RDF storage approaches,‖ ARIMA J., vol. 15, pp. 11–35, 2012.

[9] B. Liu and B. Hu, An Evaluation of RDF Storage Systems for Large Data Applications,‖ in Proc. 1st Int. Conf. Semantics, Knowl. Grid, Nov. 2005, p. 59.

[10] Z. Kaoudi and I. Manolescu, RDF in the clouds: A survey,‖ VLDB J. Int. J. Very Large Data Bases, vol. 24, no. 1, pp. 67–91, 2015.

[11] C. Weiss, P. Karras, and A. Bernstein, Hexastore: sextuple indexing for semantic web data management,‖ Proc. VLDB Endowment, vol. 1, no. 1, pp. 1008–1019, 2008.

[12] T. Neumann and G. Weikum, RDF-3X: A RISC style engine for RDF, Proc. VLDB Endowment, vol. 1, no. 1, pp. 647–659, 2008.

[13] A. Harth and S. Decker, Optimized index structures for querying RDF from the web, in Proc. IEEE 3rd Latin Am. Web Congr., 2005, pp. 71–80.

[14] M. Atre and J. A. Hendler, BitMat: A main memory bit-matrix of RDF triples,‖ in Proc. 5th Int. Workshop Scalable Semantic Web Knowl. Base Syst., 2009, p. 33.

[15] K. Wilkinson, C. Sayers, H. A. Kuno, and D. Reynolds, Efficient RDF Storage and Retrieval in Jena2,‖ in Proc. 1st Int. Workshop Semantic Web Databases, 2003, pp. 131–150.

Communications on Applied Electronics (CAE) – ISSN : 2394-4714
Foundation of Computer Science FCS, New York, USA
Volume 7 – No.3, June 2017 – www.caeaccess.org

Attack Resistance Dynamic Detection and Data Trust Routing in MANET

Syeda Kausar Fatima
Research Scholar, JNTUH, India

Syed Abdul Sattar, PhD
Prof & Dean SAKCET, TS, India

D. Srinivasa Rao, PhD
Prof. ECE Dept. JNTUH, India

ABSTRACT
Organizing trust in Ad Hoc network is a challenging task when environment cooperation is critical to achieving system goals such as reliability and scalability. Ad Hoc networks are easily accessible due to its dynamic nature. The main issue is to assure secure network services. In order to achieve this, a secure organizing trust aware routing is always research challenge in Mobile Adhoc Networks. This paper organizes the trust level to improve trust organization system in MANET by achieving attack resistance. To achieve attack resistance level, we contribute our research by understanding trust factors in MANET. This paper has been prepared keeping in mind that it needs to prove itself to be a valued resource dealing with both the important core and the focused security issues in this area.

Keywords
MANET, Security, Trust Management in MANET

1. INTRODUCTION
MANETs are self-sufficient systems consisting of mobile nodes that are linked by multi-hop wireless links. Trust Model which are established for wired network cannot be used in wireless network. MANETs are highly susceptible to various security attacks. Providing secure Communication in MANET is proved to be a important challenge. Common validation schemes are not applicable in Ad hoc network since public key infrastructure is hard to deploy [1] [2].

In mobile ad hoc networks (MANETs), the scattered decision making should take into account trust in the elements: the sources of evidence, the processors of information, the fundamentals of the communications network across which the evidence is communicated, etc.[3] This trust must often be derived under time-critical conditions, and in a distributed way. In MANETs, reputation-based trust management systems are shown to be an actual way to cope with adversary. [4] By launching trust with the nodes it has or has not directly related, a node in the network diagnoses other nodes and predicts their future behaviour in the network. Hence, trust plays a key role for a node in selecting with which nodes it should cooperate, refining data availability in the network. Further, scrutinizing trust values has been shown to lead to the detection of malicious nodes in MANETs. Despite all the growth for securing MANETs, leads to added challenges. Trust organization mechanism is considered to be an effective dimension to solve these problems [4]. In the situation of MANET, there are several trust management models that have been proposed in the realm of network [5], where trust can be considered as the reliance of a network node on the ability to forward packets or offer services timely, integrally and reliably. In the existing models, decision factors are often incomplete in the trust derivation, which are not fully integrated with the inherent characteristics of MANET. When the factors of decision-making are given, though we know that different factors have different weights, the precise weights are difficult to determine. Existing methods in these models for weight determination are lack of rationality and practicability. As a result, they cannot calculate an accurate trust value for each node. Hence, these models are ineffective in MANET trust management, and their applications are very simple [5].

1.1 Motivation for Trust Management in MANETs
The concept of "Trust" initially derives from social sciences and is well-defined as the degree of particular certainty about the behaviours of a specific entity [7]. Blaze et al. [8] first introduced the term "Trust Management" and recognised it as a discrete factor of security service area in networks and explained that "Trust organization provides a unified approach for specifying and understanding security policies, credentials, and relationships." Trust management in MANETs is needed when participating nodes, without any previous connections, desire to found a network with an satisfactory level of trust relationships among themselves. Examples would be in building initial trust bootstrapping [9], combination operations without predefined trust, and validation of certificates generated by another party when links are down or ensuring safety before entering a new zone [10]. In addition, trust management has varied applicability in many decision making circumstances including intrusion detection, authentication, access control, key management, segregating misbehaving nodes for effective routing, and other purposes. Trust management, including trust establishment, trust update, and trust revocation, in MANETs is also much more challenging than in traditional centralized environments. For example, collecting trust information or suggestion to evaluate trustworthiness is difficult due to changes in topology induced by node mobility or node failure. Further, resource constraints often restrict only the trust assessment process.

2. RELATED WORK
Govindan and Prasant et al [8] considered trust propagation, aggregation and prediction as the main trust dynamics which can help in trust computations. According to them the trust computation is based on following metrics Trust propagation • Trust aggregation • Trust prediction • Trust applications. The trust values will be propagated in the network so that the trust can be established between nodes which are not in immediate contact. While propagating the trust, trust values from multiple paths will be aggregated to get a combined trust value which can be stored in the history. The stored trust value will be used in the trust predictions and this predicted trust

value will be further used in the applications that need security. The stored trust value can also be used in the trust computation block in the form of feedback knowledge. Therefore, trust computations, trust propagation, trust aggregation and trust prediction blocks are closely interconnected in our envisioned trust system but the system computes extract computational resources to organize trust in MANET and the trust prediction is not accurate.

In the ATM scheme [9] there are two major functional modules: behavior data collection and trust management. The trustworthiness of each node is then assessed in the trust management module. In the ATM scheme, we train and then use a SVM classifier to evaluate the trustworthiness of the nodes. The trust management module supports the following two modes for the SVM classifier: training mode and testing mode. In the training mode, several known adversaries exhibiting known misbehaviours are deployed in the network to generate the training dataset so that a SVM classifier can be learned from this dataset.

In [10], proposes a fully distributed trust-based public key management approach for MANETs using a soft security mechanism based on the concept of trust. Instead of using hard security approaches, as in traditional security techniques, to eliminate security vulnerabilities, our work aims to maximize performance by trading off risk (i.e., security vulnerability) for trust. In this work, we propose a composite trust-based public key management (CTPKM) with no centralized trust entity with the goal of maximizing performance (e.g., service availability or efficiency) while mitigating security vulnerability. Each node employs a trust threshold to determine whether or not to trust another node. Each node's decision making using the given trust threshold affects performance and security of CTPKM

In [11], classify the clustering scheme for trust-based clustering schemes and illustrate how reputations are integrated in these schemes. Trust-based clustering algorithms integrate the trust management systems with clustering algorithms to decrease the overheads of reputation management. The growing interest in the reputation-based systems inspired numerous trust-based clustering schemes for MANETs. But there is a lack of solution to operate in both secure and hostile environments.

Raihana Ferdous et al [12] have proposed a Cluster head(s) selection algorithm based on an efficient trust model. This algorithm aims to elect trustworthy stable cluster head(s) that can provide secure communication via cooperative nodes. However the way the messages passed through may overload the Cluster head, creating a bottleneck due to additional message exchanges. Another possible limitation is the way that the message authentication between intermediate Cluster heads are treated, where there can be a delay in identifying a malicious neighboring node.

Li et al. [13] classify trust management as reputation-based framework and trust establishment framework. A reputation based framework uses direct observation and second-hand information distributed among a network to evaluate other nodes. A trust establishment framework evaluates neighbouring nodes based on direct observations while trust relations between two nodes with no prior direct interactions are built through a combination of opinions from intermediate nodes.

Yuxin Liu et al. [14] proposed active trust that avoids black holes through active creation of number of detection rotes to quickly detect and obtain nodal trust and improve data route security. This scheme detects the misbehavior but it does not isolate it. Therefore, in our system, we are considering only those nodes which are isolated by rating their trust value as low as 0 for non-cooperation.

3. PROBLEM DEFNITION

In this section, the research problem that is addressed will be defined in more detail, comprising the network model as well as the adversary model.

A. Network Model

A Mobile Adhoc Network generally refers to a wireless network of heterogeneous nodes or other computing devicesresponsible for dynamically discovering other nodes for forwarding packets to their destination.This type of network enables continuous monitoring of mobile nodes and secure data transmission. All of the nodes in MANETs are equipped with the same wireless communication interface, such as IEEE 802.11g. The nodes are limited in energy as well as computational and storage capabilities.

B. Adversary Model

First of all, the nodes are assumed to be trustworthy since they are usually better protected. The connected mobile nodes, are generally more susceptible to various attacks, and they can be compromised at any time after the MANET is formed. The adversary can be an outsider located in the wireless range of the mobile nodes, or the adversary can first compromise one or more nodes and behave as an insider later. The adversary is able to eavesdrop, jam, modify, forge, or drop the wireless communication between any devices in range. The goals of the adversary may include intercepting the normal data transmission, forging or modifying data, framing the benign devices by deliberately submitting fake recommendations. More specifically, malicious attacks are considered in this paper.

C. Cluster Formation

After deployment of nodes into network, the nodes broadcast packet P_i which it represents initial trust value (T_i), node id (N_i) , and node coordinates (N_{x_i}, N_{y_i}). Cluster formation function represents all these values $f(C_i) = \{N_i, P_i, T_i\}$. The network area is divided into different zones $(x) = \begin{cases} \log_x X, \\ \log_x Y, \ x \geq 1 \end{cases}$, where x represent number of zones. Each zone again sub-portioned into horizontal level. The nodes are divided with corresponding zone function, based on the cluster function the nodes are initialized into the cluster. A circle is formed with a fixed radius by selecting (either randomly or with highest cooperating neighbor density within 1 hop distance) a node as center and an arbitrary small length as radius. Center of the new circle is computed as the mean of the points within the circle while the radius in increased by the distance of two successive centers. The nodes reply back and in this way clusters are formed in the network.

4. PROPOSED MODEL

The main goal is to convince the adversary to launch an attack where the system can identify the attack behavior and then isolate the attacker. Thus, the proposed system can lower the trust of suspicious nodes and increases the node trust in network routing. In attack resistance detection routing, nodal trust can be easily identified and it can easily identify the

trusted routes by choosing trusted nodes by resisting the route against black holes.

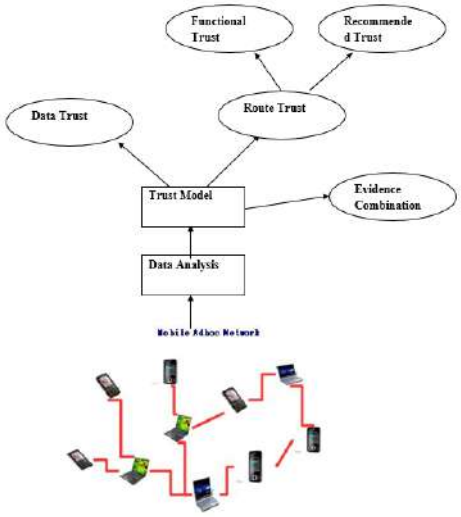

Fig 1: Proposed Model Block Diagram

4.1 Classification of Trust Types

There are three different trust types such as Route trust, Data trust and Evidence Combination trust are considered in proposed model.

Route Trust or Path Trust

The route trust expresses the credibility for the set of nodes on a routing path, and its value is defined as the minimum of one-hop trust values. The source nodes determine service level basing on the assessment of route trust value. The route trust value can be defined as a constraint in the trusted routing decision making.

$$\text{Route Trust: } RT_{sd} = \min_{\substack{s \le n \le d-1 \\ k = n+1}} \{TV_{nk}\} \quad (1)$$

To calculate route trust, the RREQ and RREP packets are modified so that they contain the trust value of the node from which the packet is received. Both packets are changed because during route discovery a node transmits the RREQ packet by broadcasting [5]. A node knows only the node from which the packet is received, not the node to which it is to be transmitted. Therefore, the RREQ packet is modified to incorporate the previous node's trust value and the RREP packet is modified to incorporate the next node's trust value.

Algorithm 1: Attack Resistance Dynamic Detection Routing:

1: Initiate Route Request $RREQ$

2: For :

3 Discover neighbour node for each node N_i:

4 Let N_i.accesTime=Current_time

5 End for

6: For: each node which produces a detection packet P, such as node N , Do

7: Create packet p, and do value assignment for α and α'

8: Choose node M as the next hop which node M meets access time is the minimum and nearer the sink

9: Send packet p to node M

10: End for

11: For each node that receives a detection packet, such as node M, Do

12: let P. α =P. α -1, P. α' =P. α' -1

13: If P. α' =0 then

14: Build opinion packet q, and make value assignment for each part

15 : Send opinion packet q to the source

16 : End if

17: If 0 then P. $\alpha \neq$ 17: detection routing continue

18: End if

19: End for

20: For each node that receives opinion packet q, such as node L, Do

21: If q.destination is not itself then

22: send q to the source node

23: End if

24: End for

The attack resistance dynamic detection routing protocol packet structure represented into six different parts. (1) packet head (2) packet type (3) Source node ID (4) Max detection route length (5) Source node sends packet acknowledge for every hops (6) Packet ID

Table1: Detection Routes Packet Structure

Phead	Ptype	SID	α	α'	PID

According to the figure, the source node selects neighbour node to launch the detection route. When the node receives a detection packet from source node the route length α is decreased by 1. Then after that the max detection route length α become a 0, to generate a route trace packet and produce a route trace to the source and the restores α to the initial value. If the α is 0 then selects next route o hop to in similar manner. The structure of reverse trace packet is composed of following parameters 1) packet head (2) packet type (3) Source node ID (4) destination id (5) detection packet id (6) Packet ID

Table2: Reverse Trace Packet

Phead	Ptype	SID	DID	τ	PID

The route trace packet routed backed to the source node with destination node information. The route track packet process is clearly presented in Algorithm-1.

4.2 Route Trust Calculation

While detection routing and data routing, each node performs a nodal trust calculation to assist in routing level attack avoidance. If node A performs a routing for node B at time t, if the data detection are successfully routed, then consider the trust of node from A to B to be $\Delta_A^B(t)$ otherwise consider trust value as $\Lambda_A^B(t)$

Let consider node A interacts with node B within a time span of t, the detection value of the node A is determined as follows

$$\{\Delta_A^B(t_1)\big|\Lambda_A^B(t_1), \Delta_A^B(t_2)\big|\Lambda_A^B(t_2), \ldots . \Delta_A^B(t_{n-1})|\Lambda_A^B(t_{n-1})\} \quad (2)$$

$\Delta_A^B(t_i)|\Lambda_A^B(t_i)$ represents a trust value between node A to B at time $t_i$is a trust. The detection routing scheme estimates the trust value at following levels i.e direct trust, recommended trust and compressive trust. The direct trust value between node A to B is measured as

Let consider the trust set of node A to B at time span t_i. The direct trust of node A to B as

$$DT_A^B = \sum_{i=1}^{n}\{\big(\Delta_A^B(t_{n-1})\big|\wedge_A^B(t_{n-1})\big).af(i)\}/w \quad (3)$$

Where $af(i)$ is an attenuation function to weight direction trusts at different times [0,1]. In this scheme, the trust calculation should meet the following condition. If the node is found to be malicious in the latest detection, then its trust should be below the threshold, and the node will not be chosen for later routing. If the malicious node returns to the normal node, it needs several detections to take it into routing consideration.

In recommended trust, the Node A is the trust evaluator, node E is the target of evaluation, and node B is a recommender of A. Consider E_A^B to be the direction trust of A to B andE_B^C to be the direction trust of B to C; then, the recommendation trust of A to C is

$$RT_A^C = E_A^B + E_B^C \quad (4)$$

Comprehensive trust is the total trust, which merges the recommendation trust and direction trust:

$$CT_{A,B}^T = \alpha E_A^B + (1-\alpha)E_B^C \quad (5)$$

Once the node initiates a detection route, it estimates the direction trust according to direct trust Eq. (3) for received feedback packet. Through interactions, the node obtains the recommendation trust from its neighbors according to recommended trust Eq. (4). Finally, it calculates the comprehensive trust according to Eq. (5).

4.3 Data Trust

The main idea of this trust type is to determine trustworthiness of traffic data (data trust) is evaluated based on the data sensed and collected from multiple mobile nodes. We propose the use of the semantics of the data, and correlate it with observations from neighbour [3] nodes. The data transmission is occurred based on trust values and discovers shortest path distance. If source and destination are presented within same region, checks teh trust value of each other and invokes direct communication. If it is indirect communication, a forwarder node discovers nearest node to the sink node from set of candidates whose trust is greater than preset threshold as the next hop. If the forwarder node cannot locate any such suitable next hop node, it will send an opinion failure to the sender node, and the sender node will re-calculate the unselected node set and select the node with the largest trust as the next hop; similarly, if it cannot find any such appropriate next hop, it sends a feedback failure to its sender node. This process should repeat until it identifies an appropriate next hop node. Once sender nodes obtains secured connection the secured data transmission takes place, which is presented in next section.

Algorithm 2: Data Trust Calculation:

1 For each node that produces or receives a data packet, such as node N, Do
2: select a next hop node M where the node M has higher trust, near to destination D and never been selected in this data routing process
4: **If** N discovers such node M, for that instance,
5: Encrypt the data packet P sent to node M
6: **If** node M is the destination then
7: check the trust level D_{tl} where $D_{tl} == DT_A^B$, then encrypt the data send to the destination 8: End if
9 : Else
10: Send failure opinion to the upper node, such as node L
11: End if
12: End for
13: **For** each node that receives failure opinion, such as node M, Do
14: Repeat step 2 to step 11
15: End for

4.4 Evidence Combination Trust

In AdHoc networks, nodes produces different amount of data, ensuring of the data is trusted or not is more critical factor. Generally data is collected as a pieces, it is essential to identity that whether the data is from the trusted source, and trust route. In order to ensure the trust combinations, the proposed scheme uses Dempster–Shafer Theory of Evidence (DST) [38] is used to combine together various piece of evidences even if some of them might not be accurate. In DST, probability is replaced by an uncertainty interval bounded by belief (*bel*) and plausibility (*pls*). Belief is the lower bound of this interval and represents supporting evidence. Plausibility is the upper bound of the interval and represents non-refuting evidence.

Let assume if a node N_a examines that one of its neighbour $N_b$packets with probability k, then the actual node N_a has $k$degree of belief for that particular packet droping of that nodeN_b and 0 degree of belief when that node N_b is absence. The belief value is measured with respective of event e_i at which is observer by node $N_a$is computed as

$$bel_{N_a}(e_i) = \sum_{j:e_j \in e_i} d_{N_a} e_j$$

Where $e_j$are all basic events, these basic events composes a main event as e_i. $d_{N_a}e_j$ is a view of the event e_j by a node N_a. According to the above formula, the node N_a gets a single event report e_j of node N_b . We can future derive the belief and Plausibility for the packet dropping level of node N_b by the following: $bel_{N_a}N_b = d_{N_a}(N_b) = k$ and plausibility $pls_{N_a} = 1 - bel_{N_a}N_b = 1 - k$. we define the combined packet dropping level of node $N_b$as the following

$$pd\ N_b = bel\ (N_b) = m(N_b) = \sum_{p=1}^{K} d_{N_a}(N_b)$$

Here $d_{N_a}(N_b)$ indicates the view of node N_a on another node N_b . We can combine reports from different nodes by applying the Dempster's rule, which is defined as following

$$m_1 N_b \oplus m_2 N_b = \frac{\sum_{q,r:e_q \cap e_r = N_b} m_1(e_q) m_2(e_r)}{1 - \sum_{q,r:e_q \cap e_r = \Phi} m_1(e_q) m_2(e_r)}$$

Here we use DST to combine the local evidence collected by a node N_a itself and external evidence shared by other nodes.

5. TRUST EVALUATION

There are different assumptions considered to determine node trust. The active detection routing initiates detection route, initially each node initiates single detection route packet with certain route length (i.e The route length is number of hops and route length should vary with respective of network size). If the detection route length is α hops and one detection opinion packet is returned to the detection source every α ($\alpha \leq \bar{\alpha}$) hops, then the total number of detection hops in this route is

$$hop_{\bar{\alpha},\alpha} = \sum_{j=1}^{n} j\alpha + 2\bar{\alpha}$$

Active trust scheme can quickly detect malicious nodes based on successful routing probability, first ART calculates the success rate of any node in 1-hop transmission, if a failure node transmission means that sender node identifies that all of the detected nodes whose hops lesser than itself are black holes; the detected nodes cannot be selected, and sender node must select from the undetected nodes. If the selected undetected node is a black hole, the transmission fails. There are 3 states for sender node, that is, nodes whose hops are larger than, the same as and smaller than sender node's. For the nodal degree d, the number of nodes whose hops are smaller than sender node's is$d/3$, if direct trust node $m_d \geq d$, then all of the neighbours of sender node can be detected; then, only if all of the next hop nodes are black hole nodes the data transmission fail, the sender node broadcast this information to other nodes to avoid blackhole nodes for future communication. Then the sender node selects trusted nodes with average route length and distribute a data to destination.

6. SECURED COMMUNICATION AND DATA DISTRIBUTION

This section presents a secured data communication across mobile nodes, with dynamic detection routing and data trust management. Based on Attack Resistance Dynamic Detection Routing and Data trust routing algorithms, the source node S_i broadcast detection packet. The detection packet of source node contains the different route hops, where the detection packet interacts with group of mobile nodes, to obtain the detection status. In next stage the route trace packet, obtains the node route information with opinion of different hop nodes with help of opinion packets, which determines the node trust, once the data trust determines the node trust. The following process determines secured data communication.

Step 1: The sender generates a cluster key (C_{gk}) for group of nodes in a cluster C_i, after collecting the opinion of D_{tl} through detection hops $hop_{\bar{\alpha},\alpha}$. It generates a cluster key for different clusters C_i where $i = \{1,2, \dots \dots n\}$

Step 2: Then, the Source nodes multicast cluster key value in an encrypted form as $N_{ck} = C_{gk} \times hop_{\bar{\alpha},\alpha}$. The cluster members can find their cluster key using their secret key values as used $N_{ck} \bmod S_{ck} = C_{gk}$. The sender encrypts destination key and broadcast encrypted destination node key to the group of members in a discovered hops.

Step 3: Sender encrypts the data with encrypted cluster key N_{ck} to the next hop member, before broadcasting data to the next hop, the sender broadcast detection packet, where the opinion packet obtains node trust, based on node data trust condition the broadcast will exchange, if not it will not allow the node in the current hop, it will discover new hop where it can obtains suitable trusted nodes.

Step 4: After receiving the data from sender node, the forwarder node in a hop verifies the group key and cluster key to ensure source node.

Step 5: The forwarder node verifies the authentication of other hop nodes by processing group member key, $N_{chk} = C_{gk} \times hop_{\bar{\alpha},\alpha}$.

Step 6: Once the receiver receives a data from group of nodes, the receiver node decrypts the data which was forwarded by the nearest hop node using group key and verifies the authenticity of forwarder node.

$$D_R = (E_{ck} \&\& | N_{chk} | \&\& N_{ck}) == True$$

Step 7: The forwarder nodes can in turn forward the received data packet to other forwarder nodes by encrypting it using over a N_{chk} long range using multihop communication.

Step 8. After receiving the packets, the forward users can decrypt the packet using the D_R and process the messages.

7. EXPERIMENTAL STUDY

In this section, the performance of the proposed ARDDT approach is compared with the existing trust based routing mechanism of TEDR in MANET. The metrics used for the performance evaluation of the proposed ARDDT approach and existing approaches are PDR, throughput, average delay and detection rates. The proposed system is simulated with the network simulator-2 (NS-2) with the simulation parameters of Table 1.

Table 3: Simulation Parameters

No. of Nodes	50,100,150 and 200.
Area Size	1000 X 1000
Mac	802.11
Radio Range	250m
Simulation Time	20 sec
Traffic Source	CBR
Packet Size	512
Receiving Power	0.395
Sending power	0.660
Idle Power	0.035
Initial Energy	10.0 J
Attacks	Blackhole, Flooding Attacks
Data rate	2 Mbps

Packet delivery ratio – data packets successfully delivered to the destination / data packets generated by the source.

End-to-End Delay – the total time consumed that the data packet takes to reach from the source to destination vice versa.

Energy Consumption - It is the amount of energy consumed by the nodes for the data transmission.

Throughput – the average number of data packets transmitted per unit of time.

7.1. Simulation Results

The performance of ARDDT protocol is analyzed and the observations are made with respect to the parameters of packet delivery ratio, End-to-End Delay, routing packet overhead and throughput. Below figures demonstrate the performance of ARDDT protocol and TEDR at different attacks.

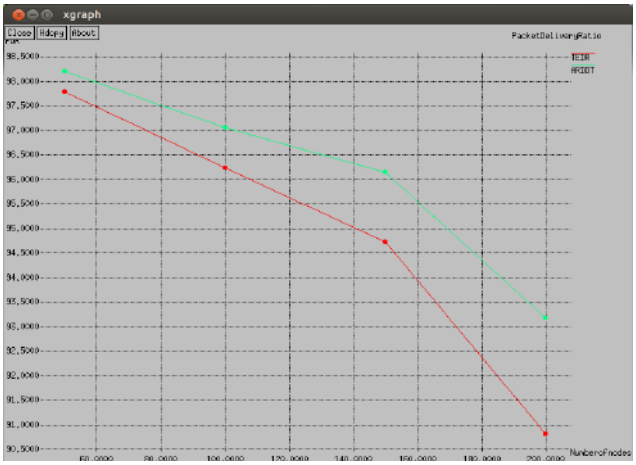

Fig 7.1 (a) Packet Delivery Ratio vs Nodes

According to Fig. 7.1 (a), ARDDT has the better packet delivery ratio than TEDR under different attacks. The packet delivery ratio of ARDDT protocol is around 97% and for TEDR is about 95% when there is no mobility. In case of TEDR, as the number of nodes increases the packet delivery ratio is decreased significantly about 7%. The biggest difference between ARDDT protocol and TEDR on packet delivery ratio is less than 8%.

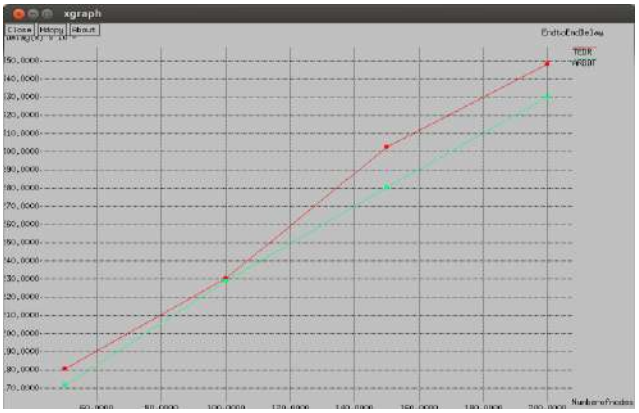

Fig 7.1 (b) End to End delay vs Speed

Fig. 7.1 (b) illustrates the end-to-end delay against different malicious nodes. According to the result, the delay rate increased with respective of number of nodes.

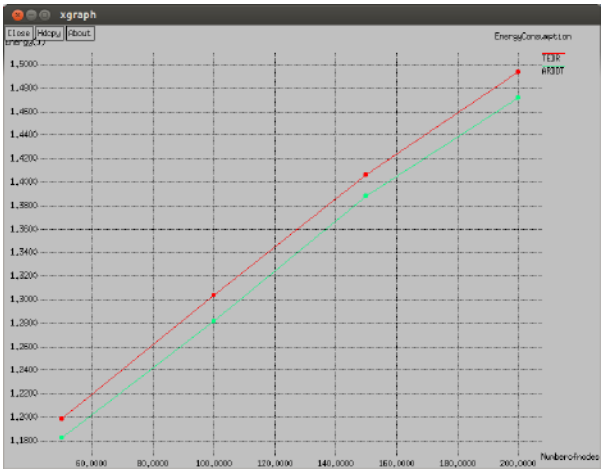

Fig 7.1 (c) Energy consumption vs Nodes

Fig. 7.1 (c) shows that the proposed ARDDT protocol and TEDR energy consumption performance with respective of number of nodes, where energy consumption rate increased with respective of attack level. Based on the results the energy consumption rate of ARDDT is lesser than TEDR.

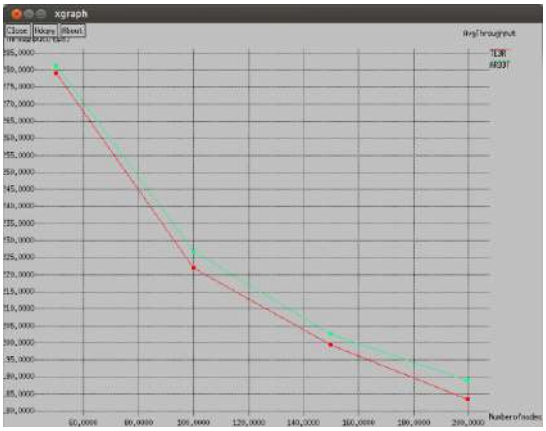

Fig 7.1 (d) Throughput vs Nodes

Fig. 7.1 (d) the average throughput rate of ARDDT is varied with respective of number of attacker nodes, where we estimated throughput rate by varying different malicious rate. The proposed model, ARDDT improved the reliability which it results to the better throughput compare to TEDR.

8. CONCLUSION

In this paper, Attack Resistance Dynamic Detection Routing and Data trust routing in MANET for resisting MANET against DoS attacks is carried. The proposed scheme determines the trust level at routing level, data level and evidence level. The trustworthiness of data and nodes are modelled and evaluated as two separate metrics, namely *data trust* and *node trust*, respectively. In particular, *data trust* is used to determine the node trust level before delivering data to the next hop node. This scheme predicts malicious on a traditional MANET by producing detection routing and data packets. In the next stage, secured data distribution is carried across different group of nodes in a cluster. The simulation results determines the efficiency of proposed routing protocol in comparison of existing TEDR protocol. According to the simulation results the ARDDT protocol manages attack nodes efficiently and produced better secured efficiency.

9. REFERENCES

[1] Heenavarshney and Pradeep Kumar, "Secure Communication Architecture Based On "BBCMS" Clustering Algorithm for Mobile Adhoc Network (MANET)", International Journal of Innovative Technology and Exploring Engineering (IJITEE), ISSN: 2278-3075, Volume-3, Issue-2, July 2013.

[2] Sandeep Kr. Agarwal, Amit Garg and K. V. Arya, "Security Issues & Clustering Based Solutions in Mobile Ad-hoc Networks - A Survey", Journal of International Academy of Physical Sciences, Vol. 16 No.3 (2012).

[3] Jin-Hee Cho, Ananthram Swami and Ing-Ray Chen. "A Survey on Trust Management for MobileAd Hoc Networks", IEEE COMMUNICATIONS SURVEYS & TUTORIALS, 2016.

[4] ErmanAyday and FaramarzFekri. "An Iterative Algorithm for Trust Management and Adversary Detection for Delay Tolerant Networks", Georgia Institute of Technology, Atlanta, GA, 30332.

[5] Hui Xia1, Zhiping Jia1, Lei Ju1, Xin Li1, Youqin Zhu2. "A Subjective Trust Management Model with Multiple Decision Factors for MANET based on AHP and Fuzzy Logic Rules", IEEE/ACM International Conference on Green Computing and Communications, 2011.

[6] SînzianaMazilu*, MihaelaTeler*, CiprianDobre. "Securing Vehicular Networks based on Data-Trust Computation", Communications, 31(18), pp. 4343-4351, 2008.

[7] Poonam Gera, KumkumGarg, and Manoj Misra. "Trust-based Multi-Path Routing for Enhancing Data Security in MANETs", International Journal of Network Security, Vol.16, No.2, PP.102-111, Mar. 2014.

[8] Kannan Govindan and PrasantMohapatra. "Trust Computations and Trust Dynamics inMobile Adhoc Networks: A Survey", IEEE, 14(2), 279-298.

[9] Wenjia Li, Anupam Joshi and Tim Finin. "ATM: Automated Trust Management for Mobile Ad-hoc Networks Using Support Vector Machine", Baltimore, MD 21250.

[10] Jin-Hee Cho, Kevin S. Chan and Ing-Ray Chen. "Composite Trust-based Public Key Management in Mobile Ad Hoc Networks",IEEE 2014.

[11] MoazamBidaki and Mohammad Masdari. "Reputation-Based Clustering Algorithms in Mobile Ad Hoc Networks", International Journal of Advanced Science and Technology Vol. 54, May, 2013

[12] RaihanaFerdous, Vallipuram Muthukkumarasamy, Elankayer Sithirasenan, "Trust-based Cluster head Selection Algorithm for Mobile Ad hoc Networks", I Proceedings of IEEE INFOCOM, vol 4, Mar 2014, pp 2393-2403.

[13] J. Li, R. Li and J. Kato, Future Trust Management Framework for Mobile Ad Hoc Networks: Security in Mobile Ad Hoc Networks, IEEE Communications Magazine, vol. 46, no. 4, Apr. 2008, pp. 108-114.

[14] Yuxin Liu, Mianxiong Dong, Member, IEEE, Kaoru Ota, Member, IEEE, Anfeng Liu, "Secure and Trustable Routing in Wireless Sensor Networks", IEEE Transactions 1556-6013 (c) 2016, pp. 1-14.

[15] Syeda Kausar Fatima, Dr.Syed Abdul Sattar, Dr. D. Srinivasa Rao and Syeda Gauhar Fatima " Trust Enhanced Dynamic Routing for MANET", International Journal of Advanced Research in Engineering and Technology Volume 8, Issue 3, May - June 2017, pp. 25–36.

International Journal of Innovations & Advancement in Computer Science
IJIACS
ISSN 2347 – 8616
Volume 6, Issue 9
September 2017

Literature Survey on Secure Energy Aware Routing Protocols in MANETs

Mr Mahabubul Haq Atif
Research Scholar, Rayalaseema University, Kurnool, Telangana State, India
Dr. Syed Abdul Sattar
Principal and Professor, Computer Science Engineering, NSAKCET, Hyderabad, T.S. India.

ABSTRACT

MANET is a self-configurable network that consists of set of communicating devices termed as nodes which are mobile and capable to communicate with each other through wireless links without pre-established infrastructure. The nodes behaves as hosts and also as routers capable of receiving and forwarding incoming packets to neighbor nodes paving path to reach the destination node. Primarily Nodes in the MANETS are driven by non-chargeable batteries having limited power. Due to consistent usage of energy in listening, receiving, forwarding of incoming packets, the nodes decrease their residual energy and reduce their lifetime. Secondarily nodes in MANETs are very much exposed to open environment making immune to different types of attacks. Thus design of Secure-energy aware routing protocols is utmost important requirement in MANETs. Many algorithms are been proposed considering parameters like security, minimum energy consumption in routing in MANETs. In this paper we specify some routing protocols that consider these parameters.

KEYWORDS: Routing, Energy aware routing, Security, MANETs, Nodes

I INTRODUCTION

In wireless communications, Mobile Ad Hoc Networks (MANETs) is one of the major emerging networks. MANET is a network of self-organization, self-configuration and self-administration of devices (nodes) capable of communicating with each other without any centralized management or pre-established infrastructure. In MANETs nodes, which are mobile, develop connectivity in the form of links with other nodes on ad-hoc basis. Applications of MANETs are in natural disaster recoveries, defense, mining, war-fields etc.

Generally available networks are comprised of fixed pre-organized infrastructure. Access of networks is based on relationship between a network operator and a network subscriber. The subscriber requires making an agreement with the network operator for the mobile network access, and also with any ISP for the access of Internet. For having commercial network, a pre-configured fixed network is desired. Due to today's growing communication demands, fixed infrastructure is replacing wireless technology. These wireless network setups also come down in worst environments of natural disasters like earth quakes, cyclones, war fields etc. Research works are carried on to target such conditions and provide a new communication network, capable of supporting wireless ad-hoc network establishment with self configuration of network communicating devices. MANET is solution for such worse conditions where we don't require any pre-established infrastructure. Each device comes up with its own configuration and do not depend on manual configurations. Research has been initiated to target these reasons that should provide a new communication technology which is capable of supporting wireless ad-hoc network establishment and auto configuration of network communication devices.

International Journal of Innovations & Advancement in Computer Science
IJIACS
ISSN 2347 – 8616
Volume 6, Issue 9
September 2017

II ROUTING IN MANETs

Routing protocol defines standard set of rules for selection of paths from source node to destination node via intermediate nodes in a network that can be used to send packets from source to destination. Design of efficient Routing protocol is the key task in the design of MANETs as the performance of the MANETs system generally based on approach of routing methodology.

In MANETs routing protocols are basically classified into two categories: Proactive Routing protocols or Table-Driven routing protocols and Reactive Routing protocols or On-Demand routing protocols.

a. PROACTIVE ROUTING PROTOCOLS

In proactive type routing protocols each host or node discovers and maintains information of routes to all destinations in the form of routing table irrespective of their requirement. The advantage is, when any node is ready to transmit data-packet there will be no delay as routes are ready which can be used.

Common drawbacks of proactive routing protocol are:

i. Discovery of routes which are not in use.

ii. Maintaining all routes which involves frequent discovery of new routes for link failures due mobility of nodes.

iii. Waste of bandwidth due to more control packets for periodic updates intimating other nodes about changes in routes. Some of the well known of reactive type are DSDV, WRP, OLSR, TBRPF etc

b. REACTIVE ROUTING PROTOCOLS

In MANETs, nodes have limited energy source i.e. battery, that cannot be charged or replaced. so better approach is to use nodal energy only when needed and thus keep the nodes inactive when not in use. This is considered in Reactive routing protocols in which routes are discovered, maintained only when source is ready to transmit data. It reduces the network overheads by optimum utilization of the bandwidth and by avoidance of unnecessary discovery and maintenance of routes. Advantages of Reactive routing protocols are:

i. Reducing overheads by reducing limited control packets as needed route discoveries are only done.
ii. Saves energy of nodes to some extent.

iii. Bandwidth utilization is optimum due to minimum flow control packets.

iv Stale routes are generally avoided.

III CHALLENGES IN MANETs

The major challenging features in MANETs:

Mobility of nodes:

Due to mobility of nodes in MANETs there will be frequent changes in the topology leading to multiple link failures and re-construction of routes which increases overhead.

Absence of Centralized Management:

There is no fixed infrastructure in MANETs which opposes centralized management. Thus each node is participates in configuring and managing the network.

Bandwidth Limitation

Wireless links have less data-transmission capability when compared with the wired link. This leads to low bandwidths in MANETs.

Routing Overheads

Due to consistent change topology behavior, routing of the packets between nodes in the network is one of the challenging tasks. Nodes may join or leave network any time causing to route failures leading to route discoveries more frequently which increases network overheads.

International Journal of Innovations & Advancement in Computer Science
IJIACS
ISSN 2347 – 8616
Volume 6, Issue 9
September 2017

Limited power source:

Nodes in MANETs rely on limited power supply from batteries which cannot be replaced or recharged. This results in loss of nodes if their complete energy is consumed in communication.

Lack of Security:

In MANETs nodes are exposed to attack-prone environment as any node can be hijacked or compromised due to its mobility and any packet can be dropped leading to loss of data.

IV ENERGY CONSUMPTION IN MANETs

The main advantage of MANETs is its infrastructure –less feature, MANETs can be deployed in rescue and emergency applications. Every node in MANETs is associated with limited battery power as there is no chance of recharge or replacement of batteries due to node's remote location. The nodes which are dead cannot be further utilized in communications in the network that leads to the instability in topology.

In MANETs, consumption of energy is in following stages.

Stage of Transmission:

Every node, when want to send packets to another node in the network, requires energy for transmission of the packet which is termed as transmission energy. The energy required depends on the data-packet size and some network conditions. If size of the data-packet increases, there will be more consumption of transmission power.

Stage of Receiving:

Every intermediate node behaves as a router by receiving incoming packets from one node and transmitting them to another node. Energy required for receiving an incoming data packet is called Receiving energy. Reception energy required is the ratio of Receiving energy and Time required for receiving the packet.

Stage of Idle:

In MANETs, every node by default will be in the idle stage which consistently listens to the channel for presence of packets and looses unnecessary energy. Node, when finds any incoming packet in the channel it will transit out of the idle state.

Stage of Overhearing:

In this stage receiving energy of nodes are consumed as packets are forwarded to these nodes to which actually packets are not intended, but need to be sent as per the routing protocol procedure and unnecessary decrease in energy.

Figure 1 consumption of Energy in MANETs at different stages

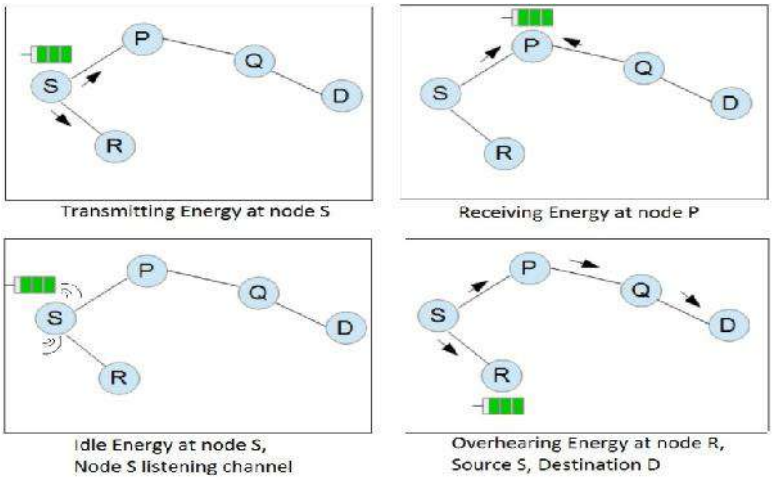

International Journal of Innovations & Advancement in Computer Science
IJIACS
ISSN 2347 – 8616
Volume 6, Issue 9
September 2017

V LITERATURE SURVEY

There are innumerous researches that have been carried out by different authors in the area of energy consumption and security issues in mobile ad hoc network as these two parameters plays very important roles for improving QoS of MANETs. Without energy awareness lifetime of network comes down and without security, nodes and data packets gets compromised. Following are various proposed works which considers energy or security in routing protocols.

Saleh A. Alghamdi (2015), have proposed load balancing maximal minimal nodal residual energy ad-hoc on-demand multipath distance vector routing protocol (AOMDV). The working of the protocol is that it generates link disjoint paths and evaluates these paths by considering maximal nodal residual energy. Path with higher nodal residual energy is taken into consideration first for packet transmission. It then calculates the maximum and an exact number of packets each path can transmit and deliver the packets on the basis of the capacity of the path without destroying the energy of nodes. Distribution of packet among multiple paths minimizes the energy utilization of a single path. Network with 200 nodes, existing AOMDV protocol consumes about 0.49 J of energy where proposed protocol consumes only 0.35 J. The main drawback of this protocol is a higher end to end delay as it concentrates on a maximum number of packets transmitted to the destination.

K.Raja proposed " Trust Based and Energy-Aware Routing Protocol for Heterogeneous Multihop Wireless Networks". He presented multi-hop wireless E-STAR network that integrates the trust and payment systems along with the routing protocol so as to enhance route stability and reliability. Payment system charges the nodes which send the packets and assign trust values to these forwarded packets. Trust system important role in evaluating the nodes' reliability and trustworthiness' and then forward packets in form of multi-dimensional trust values. For every node Trust values are calculated. Two routing protocols are proposed which are used for traversal of packets through trusted nodes with sufficient energy so as to minimize route failures. For strengthening the trust-evaluation, recommendations from every node is considered for trust calculation by Trusted Party.

Malathy proposed "Secure and Reliable E-star with ALERT protocols for heterogeneous multi-hop wireless network ".She proposed E-STAR for constructing reliable and stable routes along with ALERT concept in

heterogeneous multi-hop wireless networks. E-STAR network, which integrates the trust and payment systems along with the routing protocol, enhances route stability and reliability. Payment system charges the nodes which send the packets and assign trust values to these forwarded packets. Trust system important role in evaluating the nodes' reliability and trustworthiness' and then forward packets in form of multi-dimensional trust values. For every node Trust values are calculated. In this way, E-STAR can make the nodes not only to relay packets, but also to maintain route stability and report correct battery energy capabilities. For anonymity ALERT hides mainly source and destination identity using pseudonym that changes frequently. And ALERT also hide route between source and destination. ALERT also have strategy against intersection-attacks.

Ramanna Havinal(2016),proposed Minimal Energy Consumption with Optimized Routing protocol(MECOR) which utilizes mathematical and signaling attributes of a node to handle energy and routing problems. The energy model is designed based on MAC methods i.e. distributed coordination function in which network allocation vector is checked by the source node and if it is greater than zero node has to wait until it drops to zero which saves energy transmission of a node. Probability theory and energy model are used to estimate cumulative energy for data transmission and to obtain a route from source to a destination it uses shortest path technique and chooses the path which has less energy wastage. He has also taken into account hidden node problem which may cause a collision by transferring unnecessary data packets. To stop this, the protocol uses two extra control messages CM_{RTS} and CM_{CTS} that utilizes lesser energy when compared to data packets generated by hidden nodes. According to the analysis, proposed protocol saves upto 58.82% of energy in various mobility environments. Due to additional control messages, network overhead is increased in this protocol.

Senthilnathan Palaniappan(2015), have proposed Energy efficient stable routing using Quality of Service(QoS) monitoring agents[3]. He has contributed in establishing stable and energy efficient paths using

various link reliability metrics. These are probabilistic link reliable time(PLRT), link expiration time(LET), link received signal strength(LRSS), link packet error rate(LPER), and residual battery power. During route discovery, to choose an energy efficient stable path, the fuzzy logic technique is used which inputs all metrics and based on fuzzy rules route selection is calculated. The residual battery power of the node is calculated and used by the fuzzy system as major standard in obtaining energy efficient path. Protocol conserves 8% of residual energy compared to Cross-Layer Metric-Based Location Aided Routing protocol. The drawback of this protocol is when number of nodes increases in network, frequent route breakage occurs which caused decrease in the packet delivery ratio.

Jipeng Zhou(2016), proposed Ant colony-based energy control routing protocol under various node mobility models[4]. It uses an ant colony optimization algorithm to select best path. Path selection is based on hop count and energy of node as well as minimum and the average energy of paths. To obtain a path from source node to destination node, source node creates Fant(forward ant) packet and transmit it to all its neighbor nodes. When Fant packet is received, each neighbor node verifies if it has already received the same packet and if yes it removes the packet. When the packet reaches to a destination it will send Bant (backward ant)packet in reverse path. Each intermediate node calculates a number of hop count, minimum residual energy E_{min}, total residual energy E_{sum}, and average residual energy E_{avg}. Once the packet returns back to a source node, it will generate pheromone on the path. Based on factors such as its number of hop count, nodes energy, and an amount of delay, a value of pheromone is decided. The value is used to select path while sending the data packet. Proposed protocol is evaluated in Random walk, Random waypoint, and Reference point group. The number of dead nodes increases when nodes speed is higher, because node changes its position frequently and makes topology unstable which causes route rediscovery and consumes more nodes energy.

X. Wang(2015), presented Improving the Network Lifetime of MANETs through Cooperative Medium Access Control(MAC) Protocol[5]. Here distributed energy efficient location- based protocol(DEL-CMAC) is proposed to increase network lifetime. Proposed energy model considers the energy utilization at transceiver and amplifier level and chooses best relay for data transmission based on residual energy and location information. After the route is obtained, hop by hop cooperative relay terminals are chosen. Dynamic transmitting power and relaying operations are managed by control messages i.e. Eager to Help(ETH) and Interference indicator(II). ETH packet selects the best relay based on minimum transmitting power and maximum residual energy. II is used to convey source terminal that amount of interference available in the path. Control packets Request To Send, Clear To Send, Acknowledgement, and Eager To Help are transmitted with fixed transmission power whereas transmitting power for Data packets and Interference Indicator packets are dynamically assigned. Network with low node density increases power utilization as sometimes same node needs to act as both source and cooperative relay which consumes more power.

Gu, Chao (2014), proposed Energy-Aware Routing Protocol for Mobile Ad Hoc Networks Based on Route Energy Comprehensive Index [6]. A new routing metric Route Energy Comprehensive Index(RECI), selecting the path with maximum RECI value and minimum hop count. This Protocol creates a Utility Function (UF) for nodes energy consumption based on residual energy and energy drain rate at time t. Node value of RECI is calculated which is a ratio of UF value and sum of all nodes UF value. Prior to sending RREQ to an intermediate node, source calculates energy consumption UF and adds it as part of RREQ. Intermediate node rectifies if the packet is already received then calculates RECI value and forward duplicate RREQ to next node. Destination node gets multiple RREQ packets, choose the best route which has larger RECI value and sends RREP packet to the source node in reverse path. This protocol will not discard duplicate packets coming from the same source because it may possible that packet could come from the path which is more energy efficient. Limitation of this protocol, single route gets flooded and resulting decreased packet delivery ratio.

Li (2015), have proposed An Energy Level Based Routing Protocol [7]. This Proposed is based on residual energy and delay characteristics. Based on the energy level of each node, packet forward decision is taken. After the packet reaches to an intermediate node and if the route to the destination is missing from the routing table, for certain amount of time it will hold the packet (which decreases with the increase in current available

energy). Making shorter delay for nodes with higher energy level. Neighbor nodes receive back the packets from nodes as the time expires. Each intermediate node will accept packet received first and discard all other packets came from nodes with low energy. As a consequence, destination node will receive a request from the path having nodes with higher level energy. The Delay function of this protocol designate energy of nodes into four different states. They are safety, sub safety, danger and very danger. Nodes which are in danger and very danger state uses Delay function and puts the node in sleep mode, unlike the nodes with safety, sub safety states will follow same request delay forwarding technique to reach the destination node. As each node will hold packet for time inversely proportional to its energy level causes a longer delay for nodes with less energy. As a result, some RREQ needs to retransmit which makes hefty congestion and colossal routing load.

Shadi S (2014), proposed Energy efficient zone based routing protocol [8]. The amount of energy and bandwidth wasted in route rediscovery process is considered. To reduce unnecessary broadcasting, this protocol uses zone based parallel collision guided (ZCG) system. Clustering algorithm which divides a network into zones and selects one node as zone leader according to low and high battery power. All nodes are idle at first, while generating network they will broadcast Hello message with each other to form a zone and decides zone leader among the list of idle nodes. Zone leader initiates path discovery. Based on the energy cost of each packet the energy model is designed and compute as an incremental cost. Each node wants to communicate with a node of another zone, it sends a request to its zone leader. Zone leader calculates time and sends path discovery message to both nodes to start route discovery in parallel. When any intermediate node receives two packets from both nodes with same broadcast id, it will save it into its routing table and sends an RREP packet to both nodes to form the bi- directional route. Redundant rebroadcasting is shunned by member nodes based on the value of Zone to Live (ZTL). Because of dynamic behavior of mobile nodes, each member node within zone changes its position frequently which causes a number of packet flows between zone leader and sometimes creates unwanted traffic.

Muthusamy (2015), have proposed Enhancement of accuracy metrics for energy levels [9]. The existing OLSR protocol's hello interval (that generates hello message to inform neighbor about nodes existence) and TC interval matrix (generates TC message to update topological changes) are improved to improve network lifetime. MPR selection and route discovery algorithm are modified. Route selection is performed via MPR node, protocol selects a number of MPR nodes based on higher residual energy (ignoring the node which has low residual energy) and number of two hop neighbor covered by the node. Limitation of this protocol is that the overall inaccuracy is directly proportional to the traffic rate.

G Ravi (2015), proposed protocol for energy efficient mobile applications [10] in ad hoc network Adaptive Fidelity Energy Conservation Algorithm(AFECA) and SPAN, the two energy saving mechanisms together form this protocol. AFECA is integrated with ZRP to form EAZRP (Energy Aware Zone Routing Protocol). This allows a way to select idle nodes and can switch their state to active, sleep or listen states. This repeated change in states conserves energy. Every single request goes through the coordinator node and puts to sleep mode by SPAN, when the node is idle. Furthermore, energy consumption is optimized by hardware circuit which switches the sleep mode. EAZRP protocol's packet delivery ratio is inversely proportional to the network size.

Nidhi Choudhary et. Al (2015) presented solution for avoidance of black hole attack by identifying of the malicious attacker by using timer based detection method. In this method a trust value is defined by each node for its neighbor node and with each data packet a timer is inserted, if the trust value for a node decreases below a threshold value then all other nodes put that node in their blacklist table.

Ali Dorri et. al. (2015) proposed a way out for identification and removal of cooperative Black hole Attack, when the source node wants to send data packets to the destination, at first it uses AODV (Ad hoc On-Demand Distance Vector)routing protocol to find a recent new path. The best path is selected and the source node checks the Next_Hop_Node and Previous_Hop_Node of the RREP (Route Reply) in order to check the safety of the path. By using a Data Routing Information table (that contain Node Id, From and Through column; Indicates receive data from the specific node and the node sent packet data through the specific node in the network respectively,) the source node can identify malicious nodes and remove them from the network.TCP connections is used in this proposed method in order to decrease false positive detection. By

Simulation results we can notice that it has decreased the packet overhead and processing time in malicious nodes detection.

Pooja et. al. (2015) proposed a solution for Black hole attack detection. To detect Black hole nodes Hint-based Probabilistic routing protocol is used. Each node hint value is calculated and the value is stored at each node's buffer. In this method to compute the hint value of all neighbor nodes of sender and to check the value with trusted authority (Hint Value <= Trusted Authority) if yes then set the node as Black hole node otherwise Fair node.

Ashish Kumar Jain et. Al (2015) proposed a solution for Black hole Attack detection using RREP caching Mechanism. In this method the AODV routing protocol is modified by ignoring the first RREP packet reaching the source node. Simulation shows that this method modified AODV protocol works very well under no. of black hole nodes.

Table 1 Analysis of Energy Aware Routing Protocols

Name of the protocol	Abbreviation	Type	Energy Aware	Pros	Cons
Load balancing maximal minimal nodal residual energy AOMDV	AOMDV	Multipath	High	Uses multiple energy efficient link disjoint paths Network load is distributed	High end-to-end delay
Minimal Energy consumption with Optimized Routing Protocol	AODV	Single Path	High	Energy consumption per request is linear Packet error rate is less	increases network overhead
Energy-efficient stable routing using QoS	AOMDV	Multipath	Medium	Stable routes are selected Reduce number of route reconstruction	Packet delivery ratio is less
Ant colony-based routing protocol	AOMDV	Multipath	Low	Energy efficient route selection Network throughput is higher	Communication overhead
Improving the Network Life-time through Cooperative MAC protocol	IEEE 802.11 DCF	Multipath	High	Finds energy efficient paths	Number of dead node increases
Energy-Aware Routing Protocol based on RECI	AODV	Single Path	Low	Network lifetime is longer	Choosing of threshold value is major issue
Energy Level Based Routing	AODV	Single Path	Medium	Request delay mechanism is used Lower energy consumption	Lower the node energy longer the delay
Energy efficient Zone Based Protocol	ZRP	Single Path	Medium	Route discovery happen in parallel Zone leader takes all routing decisions	Packet collision at intermediate node consumes highest energy
Enhancement of accuracy metrics for energy levels in OLSR	OLSR	Single Path	Medium	Performs better in high mobility speeds Saves more residual energy compared to original OLSR protocol	Overall throughput is less
Protocol for energy efficient mobile applications	AFECA / SPAN	Single Path	Low	Produce better throughput	EAZRP increases overhead when network size grows

Raushan Kumar et. al. (2015) proposed a solution for black hole attack detection to modify the AODV at source and destination node. In this approach secure route discovery the sequence numbers of the receiver node and the sender node are verified in the RREP and RREQ messages respectively. Whenever RREP and RREQ message comes to respective node the packets sequence no. compares with the threshold value for prevention and detection of Black hole Attack in a network. Here threshold value is defined for three different environments (Small, Medium and Large)and compare with respective threshold value.

Ayesha Siddiqua et. Al (2015) proposed a way to detect and prevent Black hole attack utilizing secure knowledge algorithm. It uses promiscuous mode to ensure data delivery to receiver node, also tracks the packet loss reasons before claiming node as a black hole node. In the proposed technique, AODV protocol is improved in a way that every node in a network listens to its neighboring nodes promiscuously and nodes compares the neighbor node information stores in its fm and rm table entries: fm table hold the detail about recent packet forwarded. rm table hold the detail about neighboring node detail like destination address, TTL value, and Node Energy. Entries in the table which has fm ≠ rm and threshold value is crossed then modification attack or else it is trusted node. If rm and threshold value is reached then it is declared as Black hole attack.

Miss Bhandare A.S. et. Al (2015) proposed a method against Co-operative Black hole attack in which it used detection and defense mechanism, it is deigned to eject the intruder that bring out black hole attack by taking decision about safe route on basis of Normal V/S Abnormal activity. Various Fake RREP Parameter like Destination Sequence Number, Hop Count, Destination IP Address, Time Stamp are considered are make them decision to identify the attack is called Malicious Node Detection System (MDS). The PDR is improved by 76 to 99 %. There is no further overhead needed because in this method the decision about less secured route is taken autonomously by source.

VI CONCLUSION

In this paper we have discussed various routing protocols for MANETs which considers energy or security. We find that these two parameters play very important role for improving QoS of MANETs. Without energy awareness lifetime of network comes down and without security, nodes and data packets gets compromised. Beside other considerations these parameters are to be utmost considered while designing routing protocol for MANETs.

REFERENCES

[1] Saleh A Alghamdi,., "Load balancing maximal minimal nodal residual energy ad hoc on-demand multipath distance vector routing protocol", Journal of Wireless Network (2016), 22: 1355
[2] Attimarad, Girish and V. and Giri Prasad, M. N., and Havinal, Ramanna "MECOR: Minimal Energy Consumption with Optimized Routing in MANET", Journal of Wireless Personal Communications (2016),88:963
[3] Chellan, Kalaiarasan and Palaniappan, Senthilnathan, "Energy-efficient stable routing using QoS monitoring agents in MANET", EURASIP Journal on Wireless Communications and Networking (2015),13
[4] Deng, Yuhui and Cui, Lin and Liu ,Zhou, Jipeng and Tan, Haisheng and, Deng Deng, "Ant colony-based energy control routing protocol for mobile ad hoc networks under different node mobility models", EURASIP Journal on Wireless Communications and Networking(2016), 105
[5] J. Li and X. Wang, "Improving the Network Lifetime of MANETs through Cooperative MAC Protocol Design", IEEE Transactions on Parallel and Distributed Systems(2015), vol. 26, no. 4, pp. 1010-1020
[6] Zhu, Qi and Gu, Chao "An Energy-Aware Routing Protocol for Mobile Ad Hoc Networks Based on Route Energy Comprehensive Index", Journal of Wireless Personal Communications(2014), vol. 79, no. 2, pp. 1557-1570
[7] Peiyan Yuan, and Li, Layuan and Li, Chunlin and, "An Energy Level Based Routing Protocol in Ad Hoc Networks", Journal of Wireless Personal Communications(2015), 81: 981
[8] Marina De Vos, Tim Lewis and Simon Armour ,Julian Padget, Yusheng Ji, ,Shadi S. Basurra, "Energy efficient zone based routing protocol for MANETs", Ad Hoc Networks (2015), Volume 25, Part A, February 2015, Pages 16-37,ISSN 1570-8705
[9] Veerappa Gounder Palanisamy, Sakthivel Muthusamy, "Enhancement of accuracy metrics for energy levels in MANETs", Journal of Computers and Electrical Engineering(2015), Pages 100-108, ISSN 0045-7906

[10] Kashwan K.R., Ravi G, "A new routing protocol for energy efficient mobile applications for ad hoc networks", Journal of Computers and Electrical Engineering(2015),Pages 77-85, ISSN 0045-7906
[11] Pratapa A, Reddy and N. Satyanarayana,, "Energy- efficient stable multipath routing in MANET", Journal of Wireless Networks (2016), P1-9
[12] J. Kim , J. Shin, G. H. Kim, and D. Yang, "OPEED: Optimal energy efficient neighbor discovery scheme in opportunistic networks", Journal of Communications and Networks, vol. 17, no. 1, pp. 34-39, Feb. 2015.
[13] Xin Wang and Jinhua Zhu, "Model and Protocol for Energy-Efficient Routing over Mobile Ad Hoc Networks", IEEE Transaction on Mobile Computing, Vol. 10, no. 11, 2011
[14] Heinzelman Wendi B. and Tavli Bulent, "Energy- Efficient Real-Time Multicast Routing in Mobile Ad Hoc Networks", IEEE Transaction on Mobile Computing, Vol. 60, no. 5, 2011
[15] Fidel Thachil, K.C. Shet, "A Trust Based Approach for AODV protocol to Mitigate Black hole attack in MANET ," 2012 International conference in Computing Science.,IEEE 2012.
[16] Durgesh Kshirsagar, Ashwini Patil, "Black hole AttackDetection and Prevention by Real Time Monitoring", 4th ICCCNT 2013, July 4-6, 2013, Tiruchengode, India.
[17] TamilSelvan, L.; Sankaranarayanan, V., "Prevention of Black hole Attack in MANET," Wireless Broadband and Ultra Wideband Communications, 2007. AusWireless 2007. The 2nd International Conference on , vol., no.,pp.21,21, 27-30 Aug. 2007.
[18] Satoshi Kurosawal, Hidehisa, Nakayama, Nei Kato, Abbas Jamalipour and Yoshiaki Nemoto. "Detecting Black hole Attack on AODV-based Mobile Ad Hoc Networks by Dynamic Learning Method." In: International Journal of Network Security, Vol. 5, No.3, pp.338–346, Nov. 2007.
[19] Sukla Banerjee, "Detection/Removal of Cooperative Black and Gray Hole Attack in Mobile Ad-Hoc Networks", World Congress on Engineering and Computer Science , October 2008, pp. 337-342.
[20] K. Raja, Dr. R. Saminathan, S. Abarna , " Trust Based and Energy-Aware Routing Protocol for Heterogeneous Multihop Wireless Networks", International Journal of Engineering and Innovative Technology (IJEIT) Volume 3, Issue 8, February 2014.
[21] Malathy, S.Rosy Robilda, "Secure and Reliable E-star With Alert Protocols for heterogeneous Multihop Wirelesss Network" International Conference on Emerging Engineering Trends and Science (ICEETS – 2016) Page 376

Trusted and Secured Clustered Protocol in MANET

Syeda Kausar Fatima
Research Scholar,
JNTUH

Syed Abdul Sattar, PhD
Prof & Dean
SAKCET

D. Srinivasa Rao, PhD
Prof. ECE Dept.
JNTUH

ABSTRACT
Mobile Ad hoc Networks (MANETs) are subject to various kinds of attacks. Deploying security mechanisms is difficult due to inherent properties of ad hoc networks, such as the high dynamics of their topology, restricted bandwidth, and limited resources in end device. With such dynamicity in connectivity and limited resources it is not possible to deploy centralized security solution. Like many distributed systems, security in ad hoc networks widely relies on the use of key management mechanisms. However, traditional key management systems are not appropriate for them. This work aims at providing a secure and distributed authentication service in ad hoc networks. A trusted and secured clustered protocol in MANET, where clusters are formed based on **highly-trusted nodes having sufficient energy is proposed. Secured communication** with public key authentication service based on trust model and network model to prevent nodes from obtaining false public keys of the others when there are malicious nodes in the network is organised. Efforts to present energy efficient, secure and trusted clustering to enhance the security assurance and significant adaptation of trustworthy communication is presented. Simulation results demonstrate that proposed routing protocols can improve the energy efficiency, packet delivery ratio and route stability.

Keywords
MANET, Trust, Key management, Cluster

1. INTRODUCTION
A mobile ad hoc network is a collection of nodes with no infrastructure while its nodes are connected with wireless links. Nodes in the network are able to sense and discover nearby nodes. They communicate with each other by forwarding packets hop by hop in the network. Also, the topology of the ad hoc network is dynamically changing and the nodes of the ad hoc network are often mobile. A major challenge in the design of the mobile ad hoc network is to protect its vulnerability from security attacks. As in many distributed systems, security in ad hoc networks is based on the use of a key management system for authentication. Specific key management systems have to be developed to suit the characteristics of mobile ad hoc networks.

Cluster-based data transmission in MANETs has been investigated by researchers to achieve the network scalability and management, which maximizes node lifetime and reduce bandwidth consumption by using local collaboration among mobile nodes [1]. Clustering schemes [2] organized the network into one hop disjoint clusters then elect the most qualified and trustworthy nodes which play the role of cluster heads. Cluster heads are responsible for monitoring all the routing activities within the cluster itself. Thus need for secure clustering solutions which are resilient to the various security problems of MANET and provide secure and reliable clustering even in the presence of malicious nodes and attackers. Some cryptography-based clustering schemes such as [3- 6] have been designed for MANETs which are able to operate in hostile environment and use PKI or symmetric encryption techniques, but they do not offer sufficient protection against insider attackers and compromised nodes.

2. BACKGROUND AND MOTIVATION
Several trust models [8–11] have been proposed for self organizing networks in distributed paradigm. Jiang and Baras [12] examined the efficiency of trust based reactive routing protocols in the presence of attacks in the networks. This method is considered first-hand information to evaluate other node's trust values to make trustworthiness. Yan et al. [13] proposed a secure AODV based routing protocol for an ad hoc network which is established a secure end-to-end route. The trust values are calculated based on direct observation which is transitive.

Pirzada and McDonald [14] enhanced the trust management by considering the confidence level of trust of each node. They have used confidence level as a weight to compute trust value. Ghosh et al. [15] developed a trust model to strengthen the security of MANETs and they dealt with the issues associated with recommendations. Their model was utilized only trusted routes for making effective communication and isolates the malicious nodes based on the evidence obtained from direct interactions and recommendations. Ghosh et al. [16] proposed a mechanism for distinguishing selfish peers from cooperative nodes that is based on local monitoring. In order to distinguish between selfish and cooperative peers, a series of well-known statistical tests are applied for obtaining features from the observed AODV actions. The objective of mechanism design [10] is to address problem of designing incentives for nodes to provide truthful information and computing optimal system wide solution for finding the optimal cost efficient leaders. Vickrey, Clarke, and Groves (VCG) model is applied for node incentives to ensure truth telling to be the dominant strategy for any node. They have proposed local election algorithms, namely, cluster-dependent leader election and cluster independent leader election which provided globally optimal election solutions with a low cost. The Nodes with the most remaining energy are elected as the cluster head. This approach makes storage overhead because the cluster head kept an extra service table and each node maintains a reputation table and neighboring nodes list.

Milan et al. proposed a scheme [17], where a game theoretic model is applied to study the impact of collisions on a hop-by-hop reputation based mechanism for regular networks with uniform random traffic. The nodes in MANETs are equipped with different resources and provide discrete services. It did not deal with irregular topologies and non-uniform routing. It also discussed the perception and interaction asymmetries that could impair cooperation between nodes. Safa et al. presented a cluster based trust aware routing protocol (CBTRP) [18] to ensure secure routing path and established the trust based environment. This mechanism is used to distinguish the trusted nodes from malicious nodes. CBTRP makes use of the weighted clustering algorithm (WCA) [19] to elect cluster heads.

The weighted degrees are taken into consideration such as battery power, number of neighbors, transmission power, and mobility of the nodes to form optimal cluster head. CBTRP has also taken security into account to form trusted clusters. It organized the network into 1-hop clusters in which every node is able to elect the most qualified and trustworthy node to be its cluster head. Cluster members forward the packets through the trusted cluster heads. Malicious nodes do not forward the packets to them. In CBTRP model, the trust value is computed based on the information that one node can gather about the other node's vital information including analyzing the received, forwarded, and overheard packets. Analyzing the node's behaviour, the node is selfish, acting like a black hole, and carrying out a modification attack, fabrication attack and latency delays. This approach provides improved connectivity in MANETs in the presence of malicious nodes and also it ensured the passage of packets through trusted routes only by behavior of each node. Once a malicious node is discovered, it is isolated from the network such that no packet is forwarded from it.

Chatterjee et al. [20] proposed a secure trusted auction oriented clustering based routing protocol (STACRP) to provide trusted structured framework for MANETs. Two auction mechanisms, namely, Procurement and Dutch, determine the forward cost of one hop. STACRP organized the network as one hop clusters and elects the trusted nodes as cluster head (CH) by using a secret voting scheme. Each node maintains information of itself and its neighboring nodes for cluster maintenance. The trust model is analyzed using Markov chain which guarantees to selfish node to revoke its status from warned status to normal status by proper forwarding of others packets. This achieved a secure reliable routing solution. STACRP detected selfish nodes and enforces cooperation between nodes to achieve better throughput and packet delivery ratio with less routing overhead

Main contribution of the proposed approach is to obtain a practicable degree of tradeoffs between trust and security. Network trust metric parameters intimacy, integrity, mobility, and reliability identified and combined to evaluate the cumulative trust to provide ground level of security for human centric application with human notions. Unlike discussed trust management systems in order to growing years wise advanced technology [2, 12, 16], efforts are put forward to combine best of existing trust management models for soft security concerns while dynamically observing the impetus behavior of a node in open and dynamic pervasive environment. Exiting models are based on one or more trust or security parameters for WSN or MANETS, while our trust metric consists of five crucial trust parameters for direct and indirect communication in pervasive environment. To reduce the overheads and dependency, clustering is used for group based communication.

3. MODEL OF THE SECURE CLUSTER BASED SCHEME

The contribution of the proposed trusted secure clustering based routing protocol, TSCP are organized in two different phases such as trust management and clustering phase. In trust management phase, the protocol evaluates the node trust level in trust table with different trust factors. The trust factors present the node trust level in different states to determine trust calculation. The cluster management phase evaluates the clustering phase based on trust values and organize secure cluster communication with secured key sharing. The below sections present the detailed description of proposed protocol.

3.1 Trust Computation

We assume that each node maintains a trust table to keep trust factors with respective of communication as per node dynamic behaviour its social and QoS trust factors. Dynamic behaviour between two communicating nodes as X and Y over time t will autonomously update when it interacts with other node on demand or expiry to save resources.

Trust calculation consists of two processes, first evaluate the communicating node table credentials about trust factors and second calculates the mean of trust value based on each parameter as per predefined threshold. Consider following trust parameters for evaluating the node information.

Intimacy ($\mathrm{Tr}_{xy}^{\mathrm{intimacy}}$ (t)): it measures the interaction experiences following the maturity model [21]. It is computed by finding the ratio of positive number of interactions between nodes x and y over the maximum number of interactions over the time period [0, t] as

$$Tr_{xy}^{intimacy}\ (t) = It_x = (\frac{Pve_x}{T_x}) \quad (1)$$

Where It_x is the interaction ratio considering only positive Interaction Pve_x over total no of Interaction T_x through node x.

Integrity: this refers to the confidence of node x that node y is truthful based on node x's direct observations toward node y. Node x calculate approximately (t) by observing a count of suspicious untruthful experiences of node y that node x has observed. If the count exceeds a system-defined threshold, node y is considered totally dishonestat time t, i.e., (t) = 0. Otherwise, (t) is computed by 1 minus the ratio of the count to the threshold. It can be measured as

$$Tr_{xy}^{intigrity}\ (t) = n \times \alpha \times S \quad (2)$$

where n is normalized interaction value, α is over time t experience and S is security level of recommending Service Interface.

Mobility: Node mobility is a significant parameter to estimate the battery life where average distance between nodes required with limited energy provided. Thus average movement can measured by two factors, first the mobility incidences of the mobile nodes in a given time (t) bounded by a battery life threshold where high mobility with limited battery life will be punished that makes it highly unaffordable to achieve cooperative and second Uncertainty measures misbehaviour of nodes during failure to stabilize themselves in competitive forces where nodes are penalized for irregular haziness. Thus the node mobility misbehaviour impact can be measured for given time t as.

$$\mathrm{Tr}_{xy}^{\mathrm{mobility}}\ (\mathrm{t}) = ((1 - \mathrm{Mo_x(E, D)} + (1 - \mathrm{Pen_x(t)}))/2 \quad (3)$$

Where $\mathrm{Pen_x(t)}$ is the x mobile node's penalty measure for visit the similar position for t times ($0 \le \mathrm{Pen_x(t)} \le 1$), and $\mathrm{Mo_x}$ () is the node x punishment credentials with $0 \le \mathrm{Mo_x(E, D)} \le 1$.

Reliability: the reliability of nodes may be evaluated in different ways, but, in general, it may be defined as the capability of nodes to respect a service agreement. This is a particular procedure that lies behind the identity certification or the encryption process. In the remaining part of this section, the word trust is used to identify the reliability of nodes also

that may be evaluated in different ways, but, in general, it can be considered as the capability of nodes to respect a service agreement. Trust based reliability over a time t can be computed as probability of packets being lost, inserted and multiplied as

$$\mathrm{Tr}_{xy}^{\text{reliability}}(t) = (|S_{pkt} - R_{pkt}|)/S_{pkt} \quad (4)$$

where S_{pkt} = Total no. of packets sent by Y to X and R_{pkt} = Total no. of packets received by Y sent from X.

3.1.1 Trust Calculation

The trust calculation is conducted, particularly between two neighbor nodes in a cluster. When a node X evaluates trust on another node Y at time t. We assume five trust components as described above like intimacy, integrity, energy, selfishness and reliability. The trust value that node X evaluates towards node Y at time t, $\mathrm{Tr}_{xy}(t)$, is represented as a real number in the range of [0, 1] where 0 indicates distrust and 1 complete trust.

$$Tr_{xy}(t) = TC1 \times Tr_{xy}^{intimacy} + TC2 \times Tr_{xy}^{integrity} + TC3 \times Tr_{xy}^{mobility} + TC4 \times Tr_{xy}^{reliability} \quad (5)$$

Where $TC1, TC2, TC3,$ and $TC4$ are total costs associated with these four trust factors with equal threshold of 0.25 for each trust factor and computation of all these four factors gives as a results as $TC1 + TC2 + TC3 + TC4 = 1$. Based on the higher probobability values of $TC1, TC2, TC3,$ and $TC4$ the best trust formation value will consider for formation of node trust.

Algorithm 1: Trust Evaluation

Step1 To calculate node trust based on node interaction and analyze node X and Y data.

Step 2 Calculate trust value for all four parameters

$(\mathrm{Tr}_{xy}^{\text{intimacy}}, \mathrm{Tr}_{xy}^{\text{integrity}}, \mathrm{Tr}_{xy}^{\text{mobility}}, \mathrm{Tr}_{xy}^{\text{reliability}})$

Step 3 Identify each trust parameter with corresponding trust value as per pre-defined threshold [0.0–0.2]

Step 4 Estimate the overall trust value Tr_{xy} over a specified time t

$$Tr_{xy}(t) = TC1 \times Tr_{xy}^{intimacy} + TC2 \times Tr_{xy}^{integrity} + TC3 \times Tr_{xy}^{mobility} + TC4 \times Tr_{xy}^{reliability}$$

Step 5 Finally aggregate the trust value according to weighted cost.

3.2 Cluster Formation

Clustering is a standard energy efficient technique used in mobile networks to provide locality of communication through organizing the several nodes in different virtual groups known as clusters that saves energy and reduces network contention. Here several nodes are physically neighbouring and helps to organize the pervasive ad hoc networks hierarchically. An essential operation with clustering technique is to select cluster head shown in Fig. 1. The base station or mobile base stations are satellite based setups or machines capable of analyzing the data collected from the cluster heads and displaying a global view of actions being monitored.

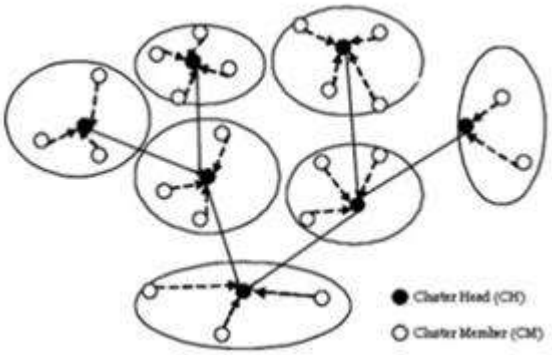

Fig 1: MANET Clustering

Inspired by Multi-objective optimization [22, 23], where multiple optimal solutions using multiple fitness functions used at same time to find optimal solution. Here fitness function is a function used to measure the optimality of a solution in evolutionary algorithm. In multi-objective optimization multiple optimal solutions using more than one objective function is used at same time.

Thus inspired by a multi-objective optimization, we use two objective functions $1(), and f2()$. The cluster head selection algorithm is based on proposed trust calculation metric as defined in Eq. (5). The algorithm initially assumes that each mobile node in the network may become a cluster head with probability 1 or 0 where nodes make autonomous decisions without any centralized control to measure the trustworthiness of the node, life time and extended security.

The fitness function in the proposed work, the fitness is evaluated based on two objective functions $f1(), and f2()$ where $f1()$ computes the trustworthiness Tr_{xy} Eq. (5) of the node, $f2()$ is used to estimate the remaining lifetime or residual energy for to elect the cluster head with a probability p which is proportional to the residual energy of the node. Thus a mobile node with higher remaining lifetime has higher possibility to become head.

Let assume NL_t is the predicted life time of the node before set up the nodes and TC_c be the time consumed to set up of the n mobile nodes as cluster, then total residual energy RE_n of all mobile nodes can be estimated as

$$RE_n = \frac{nE_{ini}(NL_t - TC_c)}{NL_t}$$

where E_{ini} is the initial energy of each node and n is the total number of nodes.

Further the probability p proportional to the residual energy can be defined to the as if NL_t number of candidates is c % of the total number of nodes with leftout energy E_l then

$$P = n \times \frac{E_l}{RE_n} \times \frac{c}{100}$$

3.2.1 Secure Cluster Communication

Assume that a MANET consist of set of clusters C where $C = \{C_1, C_2, C_3 \ldots . C_n\}$each cluster contains n number of nodes, and the public parameters in the clusters are $(H_1, H_2, H_3, P_1, P_2, \varphi, P_{pub}, n, g, h, p, \alpha, q, G_1, G_2)$. Where H_1, H_2, H_3 are cyclic groups whose orders are all q, where q

is large primer number. φ represents an isomorphic function which maps from H_2 to H_1, where α is an asymmetric function where it maps from $H_1 \times H_2 \rightarrow H_3$, non-zero generators $P_2 \in H_2^*, P_1 = \varphi(P_2) \in H_1^*$. The messages between different clusters will be forwarded by the cluster heads, due to the existence of the session keys between the cluster heads, the cluster head chooses a random number s which is belongs to Z_q, and then calculate the public key as $P_{pub} = s\,P_1$, and p and q are large primary numbers, g is a generator with q order which belongs to Z_q. Hash functions are G_1, G_2 where the messages can transmitted in the common channel. The generation of public keys across clusters and secure communication describe in next section.

3.3 Nodes Secret Shares and Key Generation

In a cluster T, the cluster head defines polynomial of degree function as

$$k-1 : f(x) = a_0 + a_1 x + a_2 x^2 + \cdots . + a_{k-1} x^{k-1} \bmod q$$

To compute the authentication key by deriving the authentication parameter as

$$\varepsilon_j = g^{a_j} \bmod p, (j = 0 \ldots . k-1)$$

This authentication key is generated at the same time to validate the authentication of node

The cluster head calculates secrete shares for the normal nodes as

$$U_i^T = f(ID_i) \bmod q$$

Then the cluster head generate the authentication parameter as a node verification where $Ver_{node} = \frac{1}{s + H_1(U_i^T || T || ID)} P_2$

The verification key is encrypted and the encrypted verification key is transferred to node

$$Enc_i\{U_i^T, \varepsilon_j, Ver_{node}\}$$

3.3.1 Key Generation

Step 1: The cluster head chooses two large primer numbers as p1 and p2 and $N = p1\ p2$

Step 2: Define a cluster key as $K = \{(N, p1, p2, c, d) : cd = 1 (\bmod \Phi(N))\}$

Step 3: Compute cluster encryption key and decryption key as follows

$$enc_k(x) = x^d \ mod\ N$$

And

$$dec_k(y) = y^c \ mod\ N$$

N and d forms a cluster public key and p1 , p2 and c forms a cluster private key

Step 4: Encrypt the message with cluster public key so that the key computation processing is reduced with the help of this and as well as reduces traffic overhead with the help of cluster key formation.

4. PERIODIC UPDATES

In this section, the key updates on different cycles to ensure the keys efficiency by updating the keys on different cycles are presented. This section describes the updates of secrete shares, node keys and cluster keys. According to the security limitations in MANET, the networks needs to get regulate key updates to ensure of security.

There are deadlines for all the circles, if this circle is over, then, the cluster will reselect the cluster head, a new service group will be formed consequently. After all the work has been done, the new cluster head will broadcast the update news to the cluster members, if the node receives the news, it needs to send its authentication parameter to the cluster head, and its qualification of update will be checked by the service group. When receive the authentication parameter from the node, the service group will judge whether $\hat{e}(H_1(U_i^T || T || ID)P_1 + P_{pub}, V_{er})$, if this statement presents true results, the service group will update the keys to the nodes.

If the authentication details failure $\hat{e}(H_1(U_i^T || T || ID)P_1 + Ppub, Ver \neq e(P1, P2)$, the node will get refused for update.

Step1 : Secret Share update : Reselection of clusterhead is based on trust value and energy level, After selection of new cluster head the new cluster head will choose a polynomial expression such as

$$S(x) = a_0 + a_1 x + a_2 x^2 + \cdots . + a_{k-1} x^{k-1} \bmod q$$

The cluster head will generate new ID's to cluster members

Step 2: Update of nodes keys : After successful node data transaction, when a node needs to send new transaction the system need to update new nodes new public key by computing the public key P_n as

$$P_n = \frac{H_1(U_i^T || T || ID)P_1 + P_{pub}}{x'}$$

Step 3: Update cluster keys: Two new large prime numbers P_1, P_2' should be chosen after the cluster head has been selected, the new cluster key will be generated as the method mentioned above, the new cluster key will be sent to all the nodes in the cluster, the broadcast will be encrypted by the new cluster key in the circle T+1.

5. SECURITY ANALYSIS

According to the MANET characteristics and security limitations there are some possibilities of potential attacks exist in the MANET. A trusted and secured clustered protocol is designed by analyzing the characteristic of the Mobile Ad Hoc Network and the potential attacks exist in the MANET, we propose a security protocol with perfect forward secrecy and backward secrecy. Even though the malicious nodes eavesdrop the traffic which is broadcasted in the network, it is impossible for them to get any useful information due to all the broadcasts are encrypted by the cluster key, only the nodes which know the key can decrypt the message. By this way, all the broadcasts can be protected well, at same time as a result of introduction of cluster key can greatly save the network resources such as bandwidth, node computational power and so on. The communications between the nodes are greatly protected as well because all of them are encrypted before transmitted by the nodes' private keys. The node without the key will never know them. In maintaining the privacy of the information, it is impossible for the node to deny the message which had been sent from it. The periodic update of keys

which is brought up in the end of protocol can resolve the problem of key leakage or loss. According to the protocol, the group network can work in a secure and more efficient manner.

6. PERFORMANCE ANALYSIS

Firstly, this section provides the computation cost and network scenario parameters for the implementation of the TSCP protocol. Then analyze the routing performance and effectiveness of the TSCP protocol in providing complete anonymity with the existing schemes through simulation results.

6.1 Simulation Setup

The proposed TSCP protocol is for MANET is implemented on ns2 simulator version 2.35. The network scenario parameters used for simulation are listed in Table II.

Table 1: Simulation Parameters

No. of Nodes	50,100,150 and 200.
Area Size	1000 X 1000
Mac	802.11
Radio Range	250m
Simulation Time	10 sec
Traffic Source	CBR
Packet Size	512
Receiving Power	0.395
Sending power	0.660
Idle Power	0.035
Initial Energy	10.0 J
Rate	5,10,15,20 and 25Kbps

In the simulation scenario an ad hoc network of size 1000m × 1000m consists of 50,100,150 and 200 mobile nodes. The mobile nodes are moving in the field according to the random waypoint model, and their average speeds range from 2 to 7 m/s. The bidirectional Constant Bit Rate (CBR) traffic is generated and the radio range of mobile node is 250m.

The proposed protocol maintains the each node trust in different trust factors, for validating each node authentication. The protocol configures trust factors to maintain node trust update parameters. During the process the TSCP protocol computes the trust based on different trust factors and determine trust evolution based on different trust parameters. The networks are organized into multiple clusters by considering each node trust value, based on the trust value and node energy level the proposed model elects a cluster head. The TSCP organizes key generation algorithms for ensuring node authentication and secured data distortion. We determine the performance by considering different key size and different network size.

6.2 Simulation Results

The performance of TSCP protocol is analyzed and the observations are made with respect to the parameters of packet delivery ratio, end to end delay, throughput and energy consumption represented in Fig 6. Fig 6 demonstrated the comparison performance of TSCP, and STACRP by varying node speeds

According to Fig. 6 (a), TSCP has the better packet delivery ratio than STACRP [20] under different mobile speed such as 5, 10, 15, 20 and 25 m/s. The packet delivery ratio of TSCP protocol is around 93.5% and for STACRP is about 92% when there is a node mobility of 2m/s. In case of STACRP, as the mobility increases the packet delivery ratio is decreased significantly about 87% to 85% when the mobile speed is 7 m/s. On the other hand, under the same scenario and mobile speed the packet delivery ratio of TSCP protocol is about 89.5%. The difference between TSCP protocol and STACRP on packet delivery ratio is less than 5%.

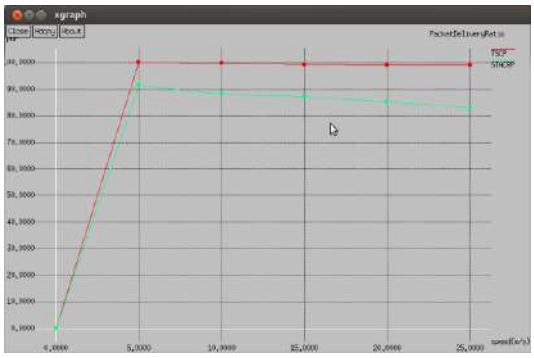

Fig 6(a) Packet Delivery Ratio vs Speed

Fig. 6 (b) shows that the comparison of TSCP, and STACRP end to end delay performance where the STACRP protocol end to end delay is increased, while mobile speed increases. TSCP performance is far better while compare to STACRP, it has less end-to-end delay.

Fig 6(b) End to End delay vs Speed

Fig 6(c) Throughput vs Speed

Fig. 6 (c), TSCP performs slightly better throughput than STACRP. The throughput of STACRP decreases as the node speed increases.

Fig. 6 (d), shows the Energy consumption, energy consumption of TSCP slightly increased while node speed increased but while compare to STACRP the energy

consumption ratio is less than STACRP. TSCP protocol energy consumption rate is almost 8 % less than STACRP.

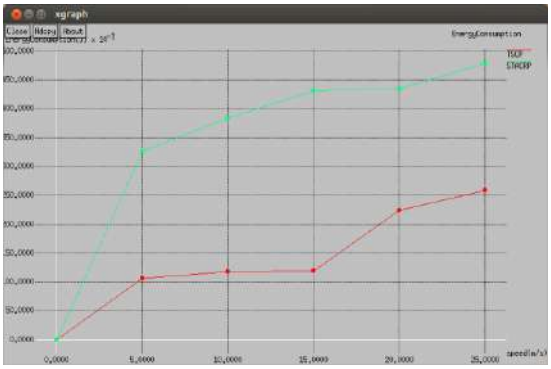

Fig 6(d) Energy Consumption vs Nodes

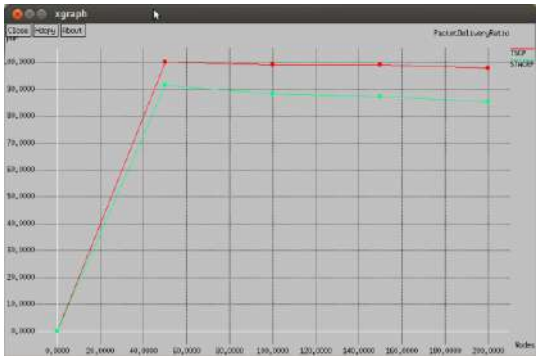

Fig 6(e) PDR vs Nodes

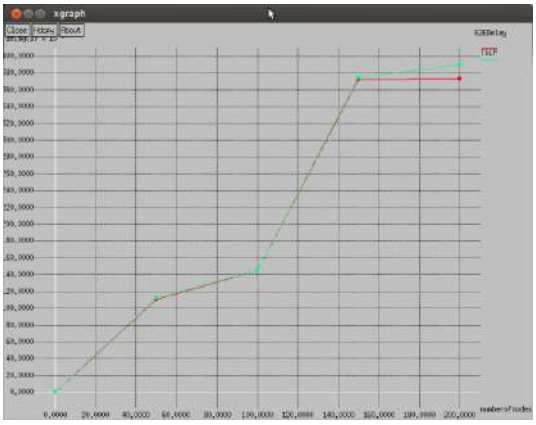

Fig 6(f) Delay vs Nodes

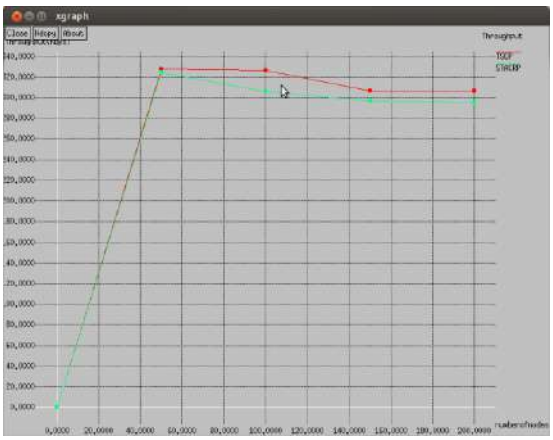

Fig 6(g) Throughput vs Nodes

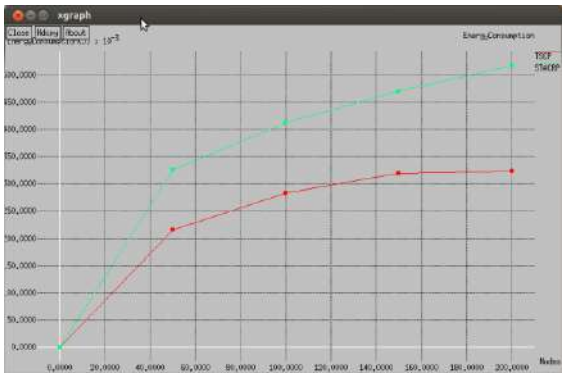

Fig 6(h) energy consumption vs Nodes

7 CONCLUSION

In this project a trusted and secured clustered protocol in MANET to organize secured and trusted communication in mobile pervasive environment is proposed. The proposed protocol organize individual node trust and reliability based on different node characteristics. Fitness functions to find out multi- dimension clustering with extended security consideration to improve energy efficient trusted clustering is formulated. A lightweight key management techniques for node authentication and secured communication with low resource computations. Based on the simulation results the proposed model perform energy efficient and robust.

8 REFERENCES

[1] A.A. Abbasi and M. Younis, "A Survey on Clustering Algorithms for Wireless Sensor Networks," Computer Comm., vol. 30, nos. 14/ 15, pp. 2826-2841, 2007.

[2] C. Tselikis, S. Mitropoulos, N. Komninos, and C. Douligeris, "Degree-based clustering algorithms for wireless Ad Hoc networks under attack," IEEE Communications Letters, vol. 16, no. 5, pp. 619–621, 2012.

[3] Y. Zeng, J. Cao, S. Guo, K. Yang and L. Xie, "SWCA: A Secure Weighted Clustering Algorithm in Wireless Ad Hoc Networks", IEEE Wireless Communications and Networking Conference WCNC, (2009).

[4] I. Nishimura, T. Nagase, Y. Takehana and Y. Yoshioka, "Secure Clustering for Building Certificate Management Nodes in Ad-Hoc Network", International Conference on Network-Based Information Systems, (2011), pp. 685-689.

[5] H. Rifà-Pous and J. Herrera-Joancomartí, "A Fair and Secure Cluster Formation Process for Ad Hoc Networks", Journal Wireless Personal Communications: An International Journal archive, vol. 56, no. 3, (2011) February.

[6] V. Sivaranjani and D. Rajalakshmi, "Secure Cluster Head Election for Intrusion Detection in MANET", Journal of Computer Applications, vol. 5, Issue EICA2012-4, (2012) February 10.

[7] M. Bechler, H. Hof, D. Kraft, F. Pahlke, and L. Wolf, "A ¨ cluster-based security architecture for Ad Hoc networks," in Proceedings of the 23rd AnnualJoint Conference of the IEEE Computer and Communications Societies (INFOCOM '04), vol. 4, pp. 2393–2403, March 2004.

[8] W. J. Adams and N. J. Davis, "Toward a decentralized trustbased access control system for dynamic collaboration," in Proceedings of the 6th Annual IEEE System, Man and Cybernetics Information Assurance Workshop (SMC '05), pp. 317–324, June 2005.

[9] A. Boukerche and Y. Ren, "A security management scheme using a novel computational reputation model for wireless and mobile Ad Hoc networks," in Proceedings of the 5th ACM International Symposium on Performance Evaluation of Wireless Ad-Hoc, Sensor, and Ubiquitous Networks (PE-WASUN '08), pp. 88–95, October 2008.

[10] R. Li, J. Li, P. Liu, and H. Chen, "An objective trust management framework for mobile Ad Hoc networks," in Proceedings of the IEEE 65th Vehicular Technology Conference (VTC '07), pp. 56– 60, April 2007.

[11] G. Theodorakopoulos and J. S. Baras, "Trust evaluation in adhoc networks," in Proceedings of the ACM Workshop on Wireless Security (WiSe '04), pp. 1–10, October 2004.

[12] T. Jiang and J. S. Baras, "Ant-based adaptive trust evidence distribution in MANET," in Proceedings of the 24th International Conference on Distributed Computing Systems Workshops, pp. 588–593, March 2004.

[13] Z. Yan, P. Zhang, and T. Virtan, "Trust evaluation based security solution in Ad Hoc networks," in Proceedings of 7th Nordic Workshop on Secure IT Systems, 2003.

[14] A. A. Pirzada and C. McDonald, "Establishing trust in pure ad-hoc networks," in Proceedings of the 27th Australasian Conference on Computer Science (ACSC '04), vol. 26, pp. 47–54, 2004.

[15] T. Ghosh, N. Pissinou, and K. Makki, "Collaborative trustbased secure routing in multihop Ad Hoc networks," in NETWORKING 2004. Networking Technologies, Services, and Protocols; Performance of Computer and Communication Networks; Mobile and Wireless Communications: Proceedings of the 3rd International IFIP-TC6 Networking Conference, Athens, Greece, May 9–14, 2004, vol. 3042 of Lecture Notes in Computer Science, pp. 1446–1451, 2004.

[16] T. Ghosh, N. Pissinou, and K. Makki, "Towards designing a trusted routing solution in mobile Ad Hoc networks," Mobile Networks and Applications, vol. 10, no. 6, pp. 985–995, 2005.

[17] F. Milan, J. J. Jaramillo, and R. Srikant, "Achieving cooperation in multihop wireless networks of selfish nodes," in Proceedings of the Workshop on Game Theory for Communications and Networks (GameNets '06), October 2006.

[18] H. Safa, H. Artail, and D. Tabet, "A cluster-based trust-aware routing protocol for mobile Ad Hoc networks," Wireless Networks, vol. 16, no. 4, pp. 969–984, 2010.

[19] M. Chatterjee, S. K. Das, and D. Turgut, "WCA: a weighted clusrering algorithm for mobile Ad Hoc networks," Journal of Cluster Computing, vol. 5, no. 2, pp. 193–204, 2002.

[20] P. Chatterjee, I. Sengupta, and S. K. Ghosh, "STACRP: a secure trusted auction oriented clustering based routing protocol for MANET," Cluster Computing, vol. 15, pp. 303–320, 2012.

[21] Velloso PB et al (2010) Trust management in mobile ad hoc networks using a scalable maturity-based model. In: IEEE Trans. Netw. Service Management, vol. 7, no. 3, pp 172–185

[22] Ali H, Shahzad W, Khan FA (2012) Energy-efficient clustering in mobile ad-hoc networks using multi-objective particle swarm optimization. Applied Soft Computing 1913–1928

[23] Marmol FG, Perez GM (2010) Towards pre-standardization of trust and reputation models for distributed and heterogeneous systems. Compute Stand Interfaces 32:185–196

International Journal of Applied Engineering Research ISSN 0973-4562 Volume 12, Number 8 (2017) pp. 1779-1783
© Research India Publications. http://www.ripublication.com

Adaptive Power Control for Quality of Service Improvement in WCDMA Wireless Networks

Vandana Khare
Associate Prof. –ECE department, CMR College of Engineering & Technology, Hyderabad, India.
& Research scholar, JNT University, Hyderabad, India

Dr. Y. Madhavee Latha
Principal, Malla Reddy Engineering College for Women, Hyderabad, India.
& Research supervisor, JNT University, Hyderabad, India.

Dr. D. Sreenivasa Rao
Professor in ECE Department, JNTUH, Hyderabad, India.
& Research supervisor, JNT University, Hyderabad, India.

Abstract

In third generation (3G) cellular networks, WCDMA is a widely used technique for Quality of Service (QoS) improvement because of its high data transmission rate. Power control scheme is also very essential to reduce interference and improve network performance. Existing techniques are rarely considered for the power controlling scheme along with Resource Allocation for different traffic classes. This paper proposes a Resource Allocation with Connection Admission Control (RA-CAC) scheme, along with a power control scheme for improving Signal strength as well as providing a handoff in WCDMA Wireless networks. According to the proposed scheme, the transmitted power during the session entry is controlled using a constrained Power Control (PC). The simulation results show that the proposed scheme can significantly increase throughput, residual energy & reduce call blocking probability as well as delay.

Keywords: 3G, RA-CAC, QoS, WCDMA & PC

INTRODUCTION

In 3G devices, the WCDMA technique is heavily used for creating a wireless connection. WCDMA technologies support a data rate ranging from 144Kbps to 2Mbps. WCDMA technologies provide multimedia services such as the wired and wireless broadband networks. When compared with the narrow band CDMA technique, WCDMA is capable of handling services with greater data rate and is also capable of allocating multimedia traffic.

Issues in WCDMA networks:

- ✓ Pilot pollution
- ✓ HO problem
- ✓ SHO parameter
- ✓ Hierarchical cells

QoS for WCDMA networks :

In a network, QoS is a method of ensuring the service level that will be delivered in an application. Based on the application needs, the QoS factors are taken into account. In communication networks, most of the multimedia traffic needs guaranteed Quality of Service (QoS). Delay jitter, bandwidth, delay, etc., are some of the QoS factors [2] [3].The nature of the WCDMA network is a soft type of capacity nature. As a result, the cell coverage range relies on QoS factors like reliable interference points, spatial mobile user distribution as well as the subsequent time-dependent user traffic intensity [4].

In this paper, we propose a Resource Allocation with Connection Admission Control (RACAC) Scheme along with Power Control scheme for Real time traffic. RACAC allocates resources for existing and new arrival users based on utility function and maximizes throughput with the help of throughput achievement ratio and the Power Control scheme controls transmitted power with the help of a PC constraint for admitted sessions. The rest of the paper is organized as follows: **Section II** gives the details about the related work. The complete detail about proposed methodology is illustrated in **Section III**. Next, **Section IV** gives the results evaluation for the proposed approach and finally, conclusions are provided in **Section V**.

RELATED WORK

Juan Liu, Wen Chen [1] has presented the major problem for maximizing utility for fair and efficient multicasting in cellular networks. The optimal multicast scheme is developed for two scenarios: Users experiencing nearly equal path losses and different path losses. Especially, it has been found that the pure multicast scheme is optimal in the equal path loss. On the other hand, when the users that attempt to receive the same messages are uniformly distributed in a cell, the group multicast scheme should be applied. This result is of group multicast scheme that adapts data transmission rate to the worst case users among a group and it cannot satisfy

throughput maximization for all the users distributed in a cell for improving the quality of services. However, the number users should be controlled for better QoS performance.

Bijan Golkar [2] has proposed Resource Allocation in Autonomous Cellular Networks and developed a Network Clustering scheme in which the scheduling cell is defined by a set of coordinating Base Stations (BS). Proposed approach is that each terminal communicates with only one BS and alternatively each terminal can communicate with more than one BS in the scheduling cell. Resource Allocation across the scheduling cell is distributed. This means that each scheduling cell is performed without knowledge from previous work. However, Power Control is still an area to work thoroughly, in case of Autonomous Cellular Networks.

Mohamed Khadim Karry and Yasir khan [3] have proposed Evaluation and Comparison of Resource Allocation strategies for new streaming services in wireless cellular networks. There are two categories of services in wireless cellular networks. In first category, there are variable bit rate (VBR) and constant bit rate (CBR) and in the other category, streaming call (video, voice, broadcast) is given that is used in current generation based on QoS and demand of the user. However, there is delay in the scheme.

N. Mohan and T. Ravichandran [4] have proposed to design a new CAC algorithm with Power Control for multiple services like voice, video and data for multiclass users. It determines the optimum set of admissible users with optimum transmitting power level, so as to minimize the interference level and call rejection rate. In addition to this, an Adaptive Scheduling scheme to allocate optimum rate for each traffic queue is proposed to minimize the scheduling delay. The proposed algorithms achieve reduced call blocking probability, and optimum rate with reduced delay. However, there is a delay in the scheme.

Rekha Patil and Dr.A.Damodaram [5] have developed a cross-layer based joint algorithm for Power Control and Scheduling. The multiple access problems are solved via two alternating phases, namely, Scheduling and Power Control. They introduced the notion of power control as part of a contention-based multiple access protocol that characterizes successful transmissions depending on a set of Signal-to-Interference-and-Noise Ratio (SINR) constraints (which directly translates to quality of service (QoS) constraints on the bit-error rate (BER) at individual receivers). The Scheduling algorithm is essential to admit the transmission of static as well as mobile users of multi service classes, in order to eliminate strong levels of interference that cannot be overcome by power control. By simulation experiments, they evaluate the performance of their algorithm in a set of admissible and non-admissible users and show that Power Control algorithm converges for a set of admissible users. However, there is a decrease in the power.

Young-Long Chen et al [6] have proposed a novel approach which combines the CAC and Power Control mechanisms and operates in a centralized control manner. The essence of the proposed Centralized Call Admission Control scheme is to combine the two mechanisms and to treat the call admission decision as an eigen-decomposition problem. In order to reduce the computational complexity of the eigen-decomposition problem, the paper proposes an additional scheme, which uses a norm operation rather than direct computation. The proposed scheme, even with the norm approximation, outperforms conventional call admission methods in terms of both its blocking rate and its outage rate. Consequently, the actual SIR of each link in a neighboring base station may not be guaranteed, with the result that outage may occur.

Tajje-eddine Rachidi et al [7] have presented QaPC and QaHO mechanisms as enabling QoS parameters, which are based on the class of service, the bit rate, and the Service Degradation Descriptor (SDD). They have used bit rate, service class and Service Degradation Descriptor for enabling QoS parameters. The proposed QoS aware mechanism significantly improves QoS contract upholding for premium mobile users, as well as increases resource utilization, while improving SHO acceptance. However, there is overload in the system. **Leonardo Badia et al** [8] have proposed a novel optimization technique based on the Logarithmic Barrier Method, which is shown to exhibit a good trade-off between computational complexity and accuracy of the solution. This simple strategy has proven to be fast and efficient. However, for very low SIR, the optimization is very low.

PROPSED RESOURCE ALLOCATION WITH CONNECTION ADMISSION CONTROL ALGORITHM

Consider a WCDMA network with a single downlink and a Base Station (BS). The BS transmits radio signals to a number of member nodes of the network. For the network operation, the time t is indexed by frames of equal length. New incoming sessions representing connections are indexed in the incoming sequence. As the session arrives, the arrival is recorded and the throughput achievement ratio is calculated with the help of target throughput and achieved throughput. The CAC considers the session that arrived at time t and represents its utility function but since the utility function is dependent on achievement ratio which is a future function, we have to calculate predicted achievement ratio and allot the resource based on conditions.

RACAC Algorithm-

Step 1: When a new session i arrives, record the $Arrival_i$.

Step 2: Initialize power P_i to get a target throughput $(_TP_i_)$ and achieved throughput of session i $(achieved_TP_i)$ is computed.

Step 3: Calculate Achievement ratio Ach_Ratio_i of session i.

Step 4: Based on utility function, calculate predicted Achievement Ratio, $\widehat{Ach_Ratio_i}$ by Future Target throughput FTP_i.

Step 5: calculate predicted Achievement Ratio $\widehat{Ach_Ratio_i}$ of both the session and consider cumulative.

Step 6: check the following conditions.

If $\widehat{Ach_Ratio}_t \geq 1$, Go to step 1 and assign a rate increment including new session.

Else if

$\widehat{Ach_Ratio}_t < 1$, then

Assign a power increment for both the sessions.

Step 7: If $TP_i = FTP_i$ or ≥ 0, Go to step 1 and admit the new sessions .

Else if

new arrival is blocked and Go to step 3.

POWER CONTROL SCHEME

The transmitted power during the session entry is controlled using the Power Control (PC) constraint. The PC constraint is developed on the basis of the Signal-to-Interference Ratio (SIR) obtained from the inner closed loop.

Power Control algorithm-

1. The network maintains a SIR_{target} value which is pre defined.
2. After the session i is admitted into the network, SIR_{est} is calculated.
3. The SIR_{est} is compared with the SIR_{target}.
4. If $SIR_{est} > SIR_{target}$ then

   PC sends REQ_POW_RED to transmitter
5. Else If $SIR_{est} < SIR_{target}$ then the

   PC sends REQ_POW_INC to transmitter

   End

SIMULATION RESULTS

In this section, proposed Quality of service based Resource Allocation with Connection Admission Control (RACAC) along with Power Control scheme are simulated for Real-time Traffic in WCDMA networks using an NS-2 simulator.

Based on Number of Users-

In our first experiment, we vary the number of users as 18, 36, 54…..108 and throughput from 0 to 200. It is observed that the proposed QRAAS scheme has a higher throughput when compared to the CCACFS scheme.

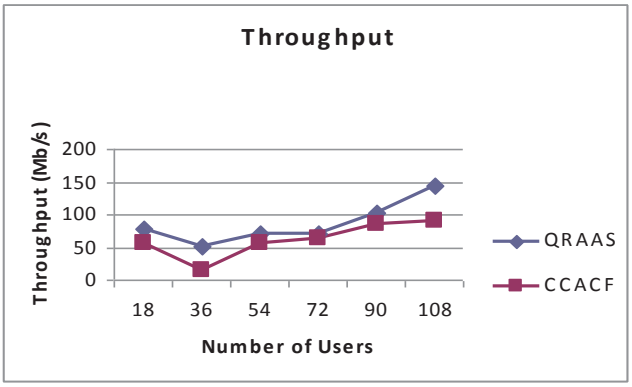

Figure 1: Users vs. Throughput

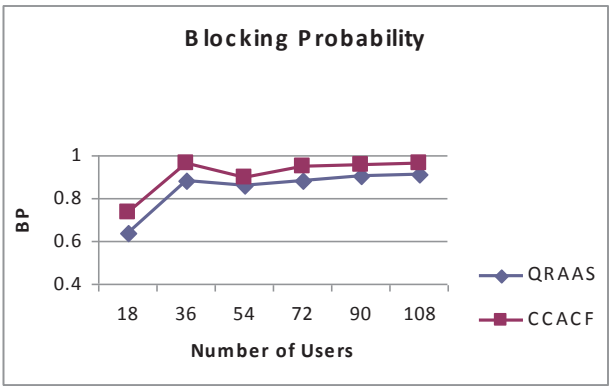

Figure 2: Users vs. Blocking Probability

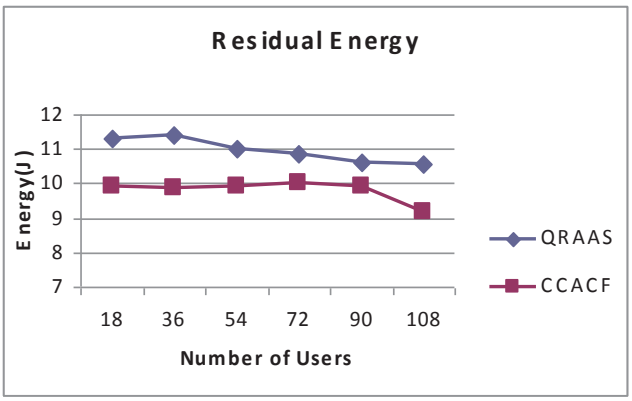

Figure 3: Users vs. Residual Energy

Figure 4: Users vs. Delay

Figures 1 to 4 show the results of throughput, blocking probability, residual energy and delay, respectively, by varying the number of users from 18 to 108 for the VBR traffic in QRAAS and CCACFS scheme. When comparing the performance of the two schemes, we find that QRAAS outperforms CCAC by 41% in terms of throughput, 7% in terms of blocking probability, 9% in terms of residual energy and 7% in terms of delay.

CONCLUSION

In this paper, we have proposed a Resource Allocation with Connection Admission Control (RACAC) along with adaptive Power Control (PC) constraint for minimizing interference and providing handoff in 3G-WCDMA Wireless networks. The algorithm is proposed for RACAC scheme based on the predicted throughput achievement ratio and depending upon the target throughput and future target throughput of every session. In case of Power Control scheme, when the estimated Signal to Interference Ratio is greater than the target Signal to Interference ratio, then, PC command requests to reduce the transmitted power. If it is less than the target Signal to Interference ratio, then, PC command requests to increase the transmitted power. Estimated Signal to Interference ratio is calculated with the help of spreading factor, received power, thermal noise and inter as well as intra cellular noise. Whenever an existing or new arrival hits the Power Control (PC) Constraint, the transmitted power is incremented or decremented with the help of PC command. From our simulation results, we have proven that the Resource Allocation with Adaptive Power Control scheme provides efficient handoff in WCDMA Wireless network by improving the throughput and reducing the delay for existing and new arrival users.

REFERENCES

[1] Juan Liu, Wei Chen,*Member, IEEE*, YingJun Zhang, *SeniorMember, IEEE*, and Zhigang Cao, *Senior Member, IEEE* ,A Utility Maximization Framework for Fair and Efficient Multicasting in Multicarrier Wireless Cellular Network**,** IEEE/ACM TRANSACTIONS ON NETWORKING, VOL. 21, NO. 1, FEBRUARY 2013.

[2] Bijan Golka,student *Member, IEEE* and Elvino S.Sousa,Fello,*IEEE* ,Resource Allocation in Autonomous Cellular Networks**,** IEEE TRANSACTIONS ON WIRELESS COMMUNICATION,ACCEPTED FOR PUBLICATION in 2013.

[3] Mohamed kadhem karray,yasir khan(2012) "Evaluation and comparison of resource Allocation strategies for new streaming services in wireless cellular networks", IEEE TRANSACTION ON COMMUNICATIONS VOL12,NO.3 JANUARY 2012.

[4] N. Mohan and T. Ravichandran, "An Efficient Multiclass Call Admission Control and Adaptive Scheduling For WCDMA Wireless Network", European Journal of Scientific Research 33.4 (2009).

[5] Rekha Patil and Dr.A.Damodaram, "Joint Scheduling and Power Control for Multiclass Users in CDMA Wireless Ad Hoc Networks", Wseas Transactions on Communications (2008).

[6] Young-Long Chen, Jyu-Wei Wang, Jyh-Liang Chen and Jyh-Horng Wen, "Performance of Call Admission Control with Power Control in Multimedia Cellular Systems", International Journal of Applied Science and Engineering 5.1 (2007).

[7] Tajje-eddine Rachidi, Amal Yasmine Elbatji, Mehdi Sebbane and Hicham Bouzekri, "QoS-Aware Power Control and Handoff Prioritization In 3g WCDMA Networks", Wireless Communications and Networking Conference, 2004. WCNC. 2004 IEEE. Vol. 2. IEEE, 2004.

[8] Leonardo Badia, Adriana Telesca and Michele Zorzi, "On the Network Utility Optimal Allocation of Radio Resources in WCDMA Systems", IEEE Communications Letters, Vol. 10, No. 5, May 2006.

ABOUT THE AUTHORS :

Mrs. Vandana Khare is pursuing PhD in Communication Engineering from JNTU, Hyderabad (T.S). She completed M.E (Digital techniques) in 1999 from SGSITS, INDORE (M.P), India and B.E in ECE in the year 1994 from GEC Rewa (M.P). She is working as Associate Professor in ECE at CMR College of Engineering, Secunderabad (TS) since 2014. She has 17 years of teaching experience. She has published 13 research papers in International journals & presented 5 papers in National & International conferences. She is a life member of ISTE & IETE Technical societies. Her research interests include computer networks, mobile computing and Bio-medical imaging.

Dr .Y. Madhavee Latha is presently working as Principal at MRECW, Secunderabad. She received PhD (Signal Processing) from JNTU, Hyderabad. She has more than 15 years of experience in the field of teaching. She contributed various research papers in journals & Conferences of national as well as international repute. Her areas of interest include multimedia systems, communication & signal processing. She is a senior member of ISTE, IETE & IEEE technical societies.

Dr. D. Sreenivasa Rao received the B Tech degree (ECE) from Nagarjuna University in 1986, M.E (Digital Systems) from Osmania University in 1994 and PhD (Computer Communication Networks) from University Of Hyderabad in 2004. His Research Interest I The Area Of Communication And Computer Networks. Presently, 12 Research Students Are Working Under His Guidance. He Has 22 Publications In Various National, International Conferences And Generals. He Has 23 Of Teaching Experience and Had Worked At CBIT As A Lecturer In The ECE Department for 6 Years During 1988 – 1994. He Worked At ECE Department Of JNTU Ananthpur In Various Capacities For 11 Years During 1994-2005 Presently, He Is Working As A Professor In The ECE Department If JNTUCE, Hyderabad. He Has Chaired A Sessions At Various National Conferences. He Is An Advisory Comity Member For GNIT, Hyderabad. He Is Also A Governing Body Member For Syed Hashim College Of Science And Technology, Member Of JNTY Forum For Science And Society And A Co-Ordinator For Campus Networking At JNTUCE, Hyderabad.

IJARCCE

ISSN (Online) 2278-1021
ISSN (Print) 2319 5940

International Journal of Advanced Research in Computer and Communication Engineering
ISO 3297:2007 Certified
Vol. 6, Issue 1, January 2017

Challenges in Integration of Microelectronics & Photonics with Nano-chemistry

Mohd. Muzaffar Ahmad[1], Mohd. Abdul Sattar[2], Mohd. Anas Ali[3]

Professor, Dept of ECE, Nawab Shah Alam Khan College of Engineering & Technology, Hyderabad, India[1]

Associate Professor & Head, Dept of ECE, Nawab Shah Alam Khan College of Engineering & Technology, Hyderabad, India[2]

Low Voltage/Low Current Electronics Security System Engineer, Techno I Electronics Security System, Hyderabad, India[3]

Abstract: Electronics, in particular VLSI technology, has made possible design of sophisticated, complex and powerful systems for user. Although silicon technology is evolving continuously to produce smaller, faster and reliable systems with low power, eventually the integration of Microelectronics and Photonics with Nano-chemistry as the driving force is the new area of research that spans from environmental management , smart health-care, smart energy management to new innovations in communications, processing and man-machine interfaces. This has created tremendous opportunities for realization of new systems. The co-existence of silicon technology with these emerging technologies, photonics and nano-chemistry has created new design opportunities for the designer, bringing new challenges to be solved. In this paper, some of the important challenges have been discussed.

Keywords: Photonics, nano-chemistry, VLSI Photonics, deep-submicron VLSI.

I. INTRODUCTION

Although silicon technology is in the process of continuous evolution of producing smaller, faster & reliable systems with low power, eventually the integration of microelectronics with photonics and other emerging technologies is the driving force which has created tremendous opportunities for realization of new systems. Photonics, specifically silicon photonics, is an alternative to electronics systems to transmit, distribute and process high volumes of digital information at a very fast speed. Other than its communication properties, the way light interacts/interfaces with other materials, makes it an ideal tool for intelligent medical diagnosis and instrumentation of high precision and accuracy. The integration of microelectronics with photon-based sciences, nano-chemistry and biotechnology brings into forefront the future soc technology resulting into intelligent Systems-on-Chip (isoc) products. These isocs will result in development of newer circuits and systems with exra-ordinary new properties, almost in every segment of the economy. This integration lays down the foundation for a future in which sensing, imaging, information processing and communication can be integrated. Emerging concept of isoc in medical sciences will become the building block of an important tool kit for aging population. This evolution is the result of novel concepts that integrate microelectronics, photonics, nano-chemistry and biotechnology. CMOS photonics is aimed at harnessing the massive bandwidth & reach benefits of photonic technology, while enabling cost effective mass manufacturing through use of established CMOS processing techniques. Today, the telecommunication community aims at Tera bits per second (Tbps) system with a reach of 40 km routine.

Before, we talk of challenges arising because of integration of technologies, let us talk of the challenges to be faced in deep-submicron VLSI.

The first challenge is interconnect. The delays through the interconnect can easily be longer than the gate driving it. Crosstalk between signals on wires can cause major problems as well. Proper design methodologies and careful analysis are keys to taming the problem introduced by the interconnect.

Another challenge is power consumption. Power consumption is a concern on every large chip because of large amount of heat generated by so many transistors. Excessive power consumption can make a chip so hot that it becomes unreliable and even non-functional. Careful analysis of the power consumption is the remedy for keeping the power consumption within the specified limits.

Another challenge is reliability. As we move into nanometer-scale VLSI, the transistors become less reliable. We must apply reliability techniques at all levels of abstraction – circuit, logic and architecture – if we are to cost effectively manage the transistors to nano-meter scale technology.

If we want to create complete systems-on-chip (socs), we have to face the challenge of design complexity. Over the long run, the VLSI designers will have to become even more skilled at programming, in addition to designing

IJARCCE
ISSN (Online) 2278-1021
ISSN (Print) 2319 5940
International Journal of Advanced Research in Computer and Communication Engineering
ISO 3297:2007 Certified
Vol. 6, Issue 1, January 2017

layout, circuit and architecture, as some fraction of the system is implemented as on-chip software. A multiprocessor system-on-chip (mpsoc), has been reported, which is a System-on-Chip with multiple processing elements. Some of these mpsocs have regular architecture, while other mpsocs are heterogeneous.

II. SILICON PHOTONICS

Silicon Photonics can be defined as the utilization of silicon based materials for the generation, guidance, control and detection of light to communicate over distance. Optical technology suffered from a reputation as an expensive solution, based on high cost of hardware components, as they are typically fabricated using exotic materials that are expensive for manufacturing. These limitations prompted to research the construction of fiber-optic components from other materials such as silicon. Silicon photonics has attained much attention in recent years owing to the maturity of silicon in the electronics industry and its possibility of monolithic integration of both photonic and electronic devices on chip. It develops high volume low cost optical components using standard CMOS process – the IC manufacturing process used today.

Silicon photonics is an evolving technology in which data is transferred among computer chips by optical rays. Optical rays can carry far more data is less time than electrical conductors. Its overarching goal is to develop high volume, low cost optical components using standard CMOS processing the same manufacturing process used for microprocessors and semiconductor devices.

The components of silicon photonics are silicon light source, silicon wave of waveguide, silicon modulator, silicon based photo detector.

The work toward a silicon based light source is going on but still far from completion. Until an efficient reliable silicon based light source is available, a photonic integrated system will need to use a conventional III – V material light emitter. The basic silicon waveguide is a rib waveguide where as silicon rib is raised above a silicon base resting on an insulating layer; these waveguides are commonly referred to as SOI rib waveguides.

The silicon modulator is an external modulator, based on, based on the design of a Mach-Zender interferometer where an incoming beam of light is split in half and the two resulting beams travel through two different arms of the interferometer and then the two beams recombine at other end. The current design for a silicon based photo detector is to have a layer of Si-Ge between a P-type and an N-type layer.

In the field of silicon photonics, there have been challenges in fabricating optical devices such as laser source, modulators, detectors etc. on silicon for high speed switching speeds that provide high data rates for communication links. Tbps data rate has already been achieved in optics with Dense wavelength Division Multiplexing (DWDM) technology. With further developments in Silicon Photonics, it is expected to bring an optical revolution in Electronics & Communication industry with the realization of the above said Tbps data links using micro-electronic silicon chips.

III. O-PCBS & VLSI PHOTONICS

The development of optical printed circuit boards (O-PCBs) & VLSI photonic circuits has been reported recently [1][2]. Micro/nano-photonic wires and devices are interconnected and integrated on a chip to form micro/nano circuits of various functions that are compact, high speed, intelligent, light weight, low energy and environment friendly, low cost and high volume applications. Photonic devices include micro/nano-scale lasers, switches, couplers, detectors, sensors, actuators, modulators and related devices to perform the functions of sensing, storing, transporting, processing, switching, routing and distributing optical signals on flat modulator boards or substrates for diverse applications. The O-PCBs are designed to overcome the limitations of the electrical PCBs and the VLSI photonic systems are designed to overcome the limitations of the VLSI electrical systems. The scientific & technological challenges & issues of interconnection and integration include diverse compatibility issues between micro/nano-devices of diverse nature, such as materials mismatch, size mismatch, shape mismatch, optical mismatch and mechanical/thermal mismatches. Coupling of the light from nano-wires CdS light emitting devices (LEDs) or nano-wire GaN LEDs into the photonic crystal nano-wave guides has been reported in the said & related papers.

IV. SILICON PHOTONICS AND VLSI ELECTRONICS FOR COMPUTING SYSTEMS

The work on computer systems based on silicon photonic interconnects has been reported [3]. The ever growing complexity, computation and communication requirements of military & commercial applications continue to drive the need for scaling high performance computer systems. The architects have faced these challenges by not only increasing the clock speed, but also expanding the complexity of processor architectures, and devising chips with several multi-thread cores.

Processors with up to 8 cores & 64 threads are now commercially available and commercial processors with much larger number of cores are in the offing. Designers have affectingly translated this increase in transistors into increase performance. Optical interconnected enables large collection of chips, giving high system performance, using optical proximity communication, allows, chips to communicate without a soldered connection and enables seamless re-workability for high system yield. WDM optics also offers unmatched bandwidth density. A microsystem architecture has been reported that takes advantage of new silicon photo interconnect technologies to create a collection of tightly connected chips that

IJARCCE
ISSN (Online) 2278-1021
ISSN (Print) 2319 5940
International Journal of Advanced Research in Computer and Communication Engineering
ISO 3297:2007 Certified
Vol. 6, Issue 1, January 2017

exhibit large bandwidths, balance communication and computation, and scalable improvement in performance.

A fundamental issue/challenge facing optical technology in the past has been the interface between the optical fiber & the die. This is exacerbated in the case of SOI waveguides since the silicon wave guide is extremely small, with a core only 0.1 um2 in cross sectional area. By comparison, an optical fiber has a core with a cross sectional area 85 nm2, 3 orders of magnitude larger. Thus coupling light from an optical fiber into a silicon waveguide will result into spillage and loss of the most of light around the edges.
Thus, it is important to focus the light from fiber down to the spot size of the silicon waveguide. this can be done efficiently by using a holographic lens. while it is quite obvious that low coupling loss is important in the performance of optical systems, the holographic lens also allows wafer scale test, both after the wafers are complete and during processing.

V. VLSI AND NANO-CHEMISTRY / NANO TECHNOLOGY

In early 1980's, scaling of the MOS transistors beyond 140 nm appeared as an impossible task. However, in subsequent years, manipulation of materials by nano-chemists and material engineers, emergence of novel and copper technology and new techniques in lithography pave the way for realization of feature sizes of the order of 20 nm–30nm. Parallel with such development, new nanochemistry is trying to shape the new materials for the future. Better understanding of the unique properties of atoms and molecules, will result into progress of novel technologies that, in turn, will result into further development of VLSI circuits and system.

In a related development, there has been emergence of Carbon Nano Tubes (CNTs) which will revolutionize the development of electronic circuits and systems. Carbon Nano Tubes are hollow, cylindrical Nano – structures composed of single sheet of carbon atoms. They have exceptional electrical, physical and thermal properties. They are stronger than steel and 200 times lighter than steel. They are 1000 times thinner than human hair. Single Walled Carbon Nano Tubes (SWNT) have been used for building carbon nano tube computers. The structure of a SWNT can be visualized as a layer of graphite, a single atom thick called graphene, which is rolled into a seamless cylinder. Carbon Nano Tubes can exhibit both metal and semiconductor properties. Carbon Nano Tube Field effect transistors are promising candidate as an alternative of silicon CMOS. The CMOS VLSI, as we know it today, has certain limitations. There is huge amount of energy leakage. Also, we can't have feature size below 20 nm. Quantum effect comes into action below 20 nm, and therefore, we can't make transistors smaller than this. Digital circuits based on transistors fabricated from CNTs have the potential to outperform silicon by improving the energy delay product a metric of energy efficiency by more than an order of magnitude. Hence, CNTs are an exciting complement to existing semiconductor technologies.

At present, the processor speed is limited to 4 GHZ per core. A group of scientists of Stanford university have created world's first carbon tube processor. This processor is basically free from energy leakage and is, thus, highly energy efficient. By using CNTs, we can create 10-15 GHZ. Processor in a single core. It can be implemented in present computer architectures like MIPS. The CNT computer runs an operating system that is capable of multi tasking. The future of carbon Nano Tube Computer lies in continuous improvement of computational power at low energy losses. Low metal usage helps to build environment friend processor.

VI. CONCLUSION

In this paper we discussed some of the important challenges which arise due to integration of microelectronics and photonics, specifically VLSI photonics with nanochemistry. Some of these challenges have been solved while others are yet to be solved. For the challenges yet to be solved, some possible solutions have been suggested by us for a few of them.

ACKNOWLEDGMENT

We express our sincere gratitude to Prof. Mohd. Muzaffar Ahmad, Electronics & Communication Engineering Department, Nawab Shah Alam Khan College of Engineering & Technology, Hyderabad, for extending his valuable insight for completion this work.

REFERENCES

[1] E. H. Lee "Optical Circuit Board (O-PCB) as a platform for VLSI Photonics", IEEE/LEDs, Summer Topical Meeting. San Diego, CA, USA, June 29-34, 2004.
[2] E. H. Lee "Micro/Nano-Photonic Integration on Optical Printed Circuit Board (O-PCB) " SPIE- Europe, Strasbourg, France, April 3-7, 2006.
[3] Manish, S Barreh, J., Brooks, J., Golla, R., Grohski, G, Gura, Bikram, S., Sheam, D., Sparcklen, L., Wynn, A. "Ultra SPARC T2: A highly threaded, power-efficient, SPARC SOC, IEEE asian solid State Circuits Conference (ASSCC' 07), 12-14 Nov 2007, pp 22-25, 2007.
[4] A. V. Krishnamoorthy and D.A.B. Miller "firehose architectures for free space optically interconnected VLSI circuits", J. Parallel and Distributed Computing, vol 41, pp 109-114, 1997.
[5] A. V. Krishnamoorthy and D.A.B. Miller "Scaling optoelectronic VLSI circuits into the 21st century: A technology roadmap", IEEEJ Select Topics Quantum Electron, vol 2, pp 55-76, Apr 1996.
[6] D. Zhon, F. P. Preparata, and S.M. Kaug, "Interconnection delay in very speed VLSI", IEEE Trans. Circuits Syst. Vol 38, pp 779-789 July 1991.
[7] R. A. Soref and BR Bennet, "Electro optical effects in Silicon" IEEEJ of quantum Electron, vol QE – 23, No. 1, Jan 1987, pp 123-9.
[8] R. Chemberlain, M. Franklin, R. Krchnavek and B. Baysal, "Design of an optically-interconnected multicomputer" Proc. Of 5th Int'l conf. on Massively Parallel Processing using Optical interconnects, pp 114-122, June 1998.

IJARCCE

ISSN (Online) 2278-1021
ISSN (Print) 2319 5940

International Journal of Advanced Research in Computer and Communication Engineering
ISO 3297:2007 Certified
Vol. 6, Issue 1, January 2017

[9] R. G. Beausoleil, "Large scale integrated photonics for high performance interconnects", J. Emerg. Technol. Comput. Syst. 7, 1-54 (2011).
[10] K. Dhira, K. Kobayashi, N. Iizuka, Hyoshida, M. Ezaki, H. Uemura, A Kojima, K. Nakamura, H. Furuyama, H. Shibata " On-chip optical interconnection by using integrated III-IV Laser diode and photodetector with silicon waveguide", Opt. Express 18, 15440-15447 (2010).

BIOGRAPHIES

Mohammad Muzaffar Ahmad, received B. Tech. Degree in Electrical Engineering from Indian Institute of Technology (IIT), Kanpur and M.Tech. in Digital & Computing Systems from Indian Institute of Technology(IIT), Kanpur . He was a Professor & Head of the Dept. of ECE in Nawab Shah Alam Khan College of Engineering & Technology, Malakpet, Hyderabad. He is also a retired scientist of DRDO

Mohd Abdul Sattar, received B.Tech. Degree in Electronics and Communication Engineering from National Institute of Technology(NIT), Warangal and M.Tech. in Embedded Systems from JNTUH. He is an Associate Professor & Head of the Dept. of ECE in Nawab Shah Alam Khan College of Engineering & Technology, Malakpet, Hyderabad. He is also a member of IEEE.

Mohd Anas Ali received B.Tech. Degree in Electronics and Communication Engineering from Pujya Shri Madhavanji College of Engineering & Technology affiliated to JNTU Hyderabad in 2013 & M.Tech. degree in Embedded System from Nawab Shah Alam Khan College of Engineering & Technology. He is presently working at Techno I Security Systems, Abids, Hyderabad.

IJARCCE

ISSN (Online) 2278-1021
ISSN (Print) 2319 5940

International Journal of Advanced Research in Computer and Communication Engineering
ISO 3297:2007 Certified
Vol. 6, Issue 3, March 2017

A Review on IoT - Technology, Application, Architecture, Services

Mohammed Anwaruddin[1], Mohd. Abdul Sattar[2], Mohd. Anas Ali[3]

Assistant Professor, Dept. of ECE, Nawab Shah Alam Khan College of Engineering & Technology, Hyderabad, India[1,3]

Associate Professor, Dept. of ECE, Nawab Shah Alam Khan College of Engineering & Technology, Hyderabad, India[2]

Abstract: The "internet of things" (IoT) concept is used to define or reference systems that rely on the autonomous communication of a group of physical objects. The applications areas of the IoT are numerous, including: smart homes, smart cities and industrial automation. IoT systems often provide great benefits to numerous industries and society as a whole. Many of the IoT systems and technologies are relatively novel. The aim of this paper is to provide the last and most innovative contributions concerning the Protocol, Technology, Application, Architecture & Issues of interest in IoT solutions that involve interconnected smart things that interoperate with the objective of solving problems, provide functionality or optimize tasks. Topics of interest include (but are not limited to):

- Smart things network and communication: architectures, services and protocols.
- Smart things: privacy, security and identification.
- Internet of Things systems and applications.
- User-centric solutions to define IoT collaborative process.
- Innovative IoT Solutions for handicapped persons.
- Smart things and RFID/NFC communications.
- Intelligent systems based on connected vehicles.
- Smart things networks for real world data management.
- Practical experiences in Smart cities, large-scale IoT systems.
- Opportunistic IoT, based on opportunistic networking techniques.

Keywords: RFID, IoT, NFC,M2M

I. INTRODUCTION

The Internet of Things (IoT) becomes an attractive research topic, in which the real entity in physical world becomes virtual entity in cyber world, and both physical and digital entities are enhanced with sensing, processing, and self- adapting capabilities to perform interaction through special addressing scheme. Along with the combination of Internet and modern sensor technologies such as Radio Frequency Identification (RFID), Near Field Communication (NFC), and Wireless Sensor and Actuator Networks (WSAN), IoT itself is suffering from more rigorous security challenges. Several issues in terms of system architecture, standard, and human involvement are subsequently raised. The following security problems seem to be intense speculations, such as how to design appropriate security framework for things' intelligent applications? What is advanced security technology applied into mass data processing? How to maintain a balance between things' high security requirements and supporting infrastructures' hardware limitation? And how human society securely participates in both cyber and physical worlds with inter- connection?

Such significant obstacles influence the development of the future IoT, along with the exposure of mass data which causes various potential vulnerabilities from robust adversaries. Besides, resource restrictions including

heterogeneous networks and sensor nodes, communication channels/interfaces, bandwidth, storage, and energy, may also induce unique model design. Towards the general IoT, studies on its architecture model, standard, communication protocol, and network management have been researched. Towards the particular IoT security, there are several open issues such as cryptographic algorithms, authentication protocols, access control, trust/privacy, and governance frameworks. Several researches mainly focus on specific communication techniques (e.g., WLAN, RFID), detailed cryptographic mechanisms (e.g., key management), and practical applications (e.g., supply chain management, multimedia traffic).Meanwhile, the security frameworks in traditional networks can also provide merits for IoT security protection. However, security issue towards the future IoT is not a simple technically tough problem, but a multidimensional topic which combines the information security, network security, infrastructure security, and management security. Most existent schemes provide solutions for special communication techniques or applications, which may lack universality for the complicated system. Thus, we will establish an integrated security architecture to promote universal security consideration for the future IoT. In the paper, we focus on a typical future IoT architecture (short for U2IoT), Protocol, Technologies, Application, Issues, Security, Services which comprises two subsystems that Unit IoT and Ubiquitous IoT. In the U2IoT model, conceptions of mankind neural system and social organization framework are introduced for the future IoT. Thereafter, we propose a systematic security architecture (named IPM) by integrating the awareness and interactivity of cyber world, physical world, and human social into the U2IoT model. Meanwhile, the proposed IPM is presented with embedded interactions among information, physical, and management. Specifically, 1) information security model with the considerations for basic and advanced security requirements that are mapped into the security layer to deal with sensing, networking, application, and social attribution; 2) physical

Copyright to IJARCCE

IJARCCE

ISSN (Online) 2278-1021
ISSN (Print) 2319 5940

International Journal of Advanced Research in Computer and Communication Engineering
ISO 3297:2007 Certified
Vol. 6, Issue 3, March 2017

security including external con-text and inherent infrastructure are inspired by artificial immune, and it ensures that the things should be adapt-able to dynamic semantic contexts with innate and adaptive immunities against malicious attacks; 3) management security provides recommended strategies for hierarchical classified scenes with rationality and compatibility. IPM realizes the unison of cyber world, physical world and human social to guarantee security and privacy for U2IoT.

The remainder of the paper is organized as follows. In Section 2, we illustrate the existent U2IoT model, and pro-pose the security architecture (IPM). The main features of IPM referring to information security, physical security, and management security are given in Section 3. Finally, Section 4 draws a conclusion.

The Internet can be described as a ubiquitous infrastructure that has evolved from being a technology for connecting people and places to a technology connecting things. The future is the Internet of Things (IoT), which aims to unify everything in our world under a common infrastructure, giving us not only control of the things around us, but also keeping us informed of the state of the things around us. One of the main problems with IoT is that it is so vast and such a broad concept that there is no proposed, uniform architecture. In order for the idea of IoT to work, it must consist of an assortment of sensor, network, communications and computing technologies, amongst others. But when you start putting together different types of technologies, the problem of interoperability arises. One proposed solution is to adopt the standards of the services-oriented architecture (SOA) deployed in business software systems. Another takes a similar approach, suggesting the integration of Web Services into sensor network with the use of IoT optimized gateways, which would bridge the gap between the network and the terminal. In general, it may be beneficial to incorporate a number of the technologies of IoT with the use of ser-vices that can act as the bridge between each of these technologies and the applications that developers wish to implement in IoT. This paper breaks down four main categories of services according to technical features, as proposed and described by [3]. In categorizing IoT services, we aim to provide application developers a starting point, giving them something to build upon so that they know the types of services that are available. This will allow them to focus more on the application instead of designing the services and architectures required to sup-port their IoT application. The IoT envisions hundreds or thousands of end-devices with sensing, actuating, processing and communication capabilities able to be connected to the Internet. These devices can be directly connected using cellular technologies such as 2G/3G/Long Term Evolution and beyond (5G) or they can be connected through a gateway, forming a local area network, to get connection to the Internet. The latter is the case where the end-devices usually form Machine to Machine (M2M) networks using various radio technologies, such as Zigbee (based on the IEEE 802.15.4 Standard), Wi-Fi (based on the IEEE 802.11 Standard), 6LowPAN over Zigbee (IPv6 over Low Power Personal Area Networks), or Bluetooth (based on the IEEE 802.15.1).Regardless the specific wireless technology used to deploy the M2M network, all the end-devices should make their data available to the Internet. This can be achieved either by sending the information to a proprietary web server accessible from the Internet or by employing the cloud. Online platforms such as "ThingSpeak.com" or Open.Sense, among any other alternatives, are virtual clouds able to receive, store, and process data. Besides acting as remote data bases, M2M clouds also offer the following key services:

1. They offer Application Programming Interfaces (API) with built-in functions for end-users, thus providing the option to monitor and control end-devices remotely
from a client device.

2. They act as asynchronous intermediate nodes between the end-devices and final applications running on devices such as smart phones, tablets or desktops. Our paper focuses on the protocols that handle the communication between the gateways, the public Internet, and the final applications. They are application layer protocols that are used to update online servers with the latest end-device values but also to carry commands from applications to the end-device actuators.

The rest of the paper is organized as follows. Section 2 describes our research motivation whereas each of the other sections is dedicated to a specific application layer protocol. At the first part of each section we introduce each application layer protocol, we present its usage, we discuss the reliability and security features it offers and we then compare its suitability for the IoT with other application layer protocols. Finally, in Section 9, we present overall conclusions based on the previous sections and we provide further research areas.

2 Research Motivation:
The IoT is a term used for a huge wave of innovation originated in industries, but currently heading to urban centers, in-home environments, and individuals.

II. TECHNOLOGIES INVOLVED

There are several technologies that can be used to implement the concept of Internet of Things. In this section, we discussed the following technologies:

-Radio Frequency Identification (RFID)
- Near Field Communication (NFC)
- Machine-to-Machine Communication (M2M)
-Vehicle-to-Vehicle Communication (V2V)

2.1 Radio frequency identification (RFID):

RFID system is composed of one or more reader(s) and several RFID tags. Tags are characterized by a specific address and are applied to objects. Tags uses radio frequency electromagnetic fields to transfer data attached to an object. The tags contained electronically stored information which can be read by the RFID reader when the object came in the proximity of the reader (WIKIPEDIA, 2013). RFID allows to monitor objects in real-time, without the need of being in line-of-sight. From the physical point of view RFID tag or label is a tiny microchip combined with an antenna in a compact package. The tag's antenna picks up signals from an RFID reader and then returns the signal, usually with some additional information. Hitachi has developed a tag with dimensions 0.4*0.4*0.15 mm (ATZORI; IERA; MORABITO, 2010).The RFID tags comes in three configurations, the first one is Passive Reader Active Tag(PRAT) in which the reader is passive and receives the signal from the battery operated active tags. The transmission range of the RFID tag and the reader is from 1-2000 feet depending upon the architecture. The second one is Active Reader Passive Tag (ARPT), which is most commonly used. This tag does not have onboard power supplies, so it harvests the energy required to send data from the query signal sent by the RFID reader. The last one is an Active Reader Active Tag (ARAT). In this both the

IJARCCE

ISSN (Online) 2278-1021
ISSN (Print) 2319 5940

International Journal of Advanced Research in Computer and Communication Engineering
ISO 3297:2007 Certified
Vol. 6, Issue 3, March 2017

reader and the tags are active, but tags are only awoken by the reader when it comes in the proximity of the reader. Transmission may appear in various frequency bands spanning low frequencies (LF) at 124-135 KHz up to ultra-high frequencies (UHF) at 860-960 MHz (WIKIPEDIA, 2013).An Electronic Product Code (EPC) is one common set of data stored in a tag. EPC's are coded on RFID tags because of which objects can be tracked and identified uniquely. The tag contains a 96-bit string of data. The first eight bits are a header which identifies the version of the protocol. The next 28 bits identify the organization that manages the data for this tag, the organization number is assigned by the EPC Global consortium (EPCGLOBAL, 2013). The next 24 bits are an object class, identifying the kind of product; the last 36 bits are a unique serial number for a particular tag. These last two fields are set by the organization that distributed the tag (WIKIPEDIA, 2013). Rather like a URL, the entire electronic product code number can be used as a key into a global database to exclusively identify a particular product (BURLINGTON, 2009). The RFID tags are used in many applications like Monitoring the life cycle of a product, manage the inventory in the warehouse, tracking of goods, tracking of animals, airport baggage tracking logistics (HARRISON, 2009), mobile payment, etc. We can combine the RFID technology with the other technologies like sensing technology to open a new horizon for new applications.

2.2 Near field communication (NFC):

NFC is quite similar to RFID, or it can be looked as an integration of RFID reader into a mobile phone, which makes NFC customer-oriented as mobile phone is the most popular personal device worldwide (VILMOS; MEDAGLIA; MORONI, 2011). NFC can also be seen as a type of radio communication between NFC enabled mobile devices by touching them together or bring close in the proximity of the other phone. From the technical point of view, NFC operates within the unlicensed Radio Frequency band of 13.56 MHz (MEDAGLIA, 2011); the typical operating range of NFC device is 20 cm. The operating range is directly depended on the size of the antenna in the device. NFC is a short range, low power wireless link evolved from RFID that can transfer small amounts of data between two devices held in proximity. Unlike Bluetooth, no paring is required before the actual transfer of data (TECHRADAR, 2013). NFC enabled communication between the smart objects is safe as this cannot be done from a remote location, so one with his/her NFC enabled device should be present there for the application like payment. The NFC technology will significantly contribute to the future development of IoT. It will provide the necessary tool to be wirelessly connected to any smart objects. Mobile NFC also has the potential to transform the mobile headsets into different types of smart objects like when we need to pay the bills and then our mobile can be used as our credit card.

2.3 Machine-to-Machine Communication (M2M)

Machine-to-Machine (M2M) refers to the communications between computers, embedded processors, smart sensors, actuators and mobile devices (DYE, 2008). The use of M2M communication is increasing in the scenario at a fast pace. For instance, researchers predicted that, by 2014, there will be 1.5 billion wirelessly connected devices excluding mobile phones. There are four components of M2M which are sensing, heterogeneous access, information processing, application and services (CHEN; WAN; LI, 2012).From the technical point of view, M2M is a five-part structure (ETSI, 2013) shown in Figure 2. The structure is defined as follows:

M2M Device: A device capable of replying to request for data contained within that device.

M2M Area Network (Device Domain): Provide connectivity between M2M Devices and M2M Gateways.

M2M Gateway: Use M2M capabilities to ensure M2M Devices inter-working and interconnection to the communication network.

M2M Communication Networks (Network Domain): Communications between the M2M Gateway(s) and M2M application.

M2M Applications: Contains the middleware layer where data goes through various application services and is used by the specific business-processing engines.

M2M has several applications in various fields like healthcare, smart robots, cyber transportation systems (CTS), manufacturing systems, smart home technologies, and smart grids (LAWTON, 2004). Example of M2M area network typically includes personal area network technologies, such as Ultra-wideband and Bluetooth or local networks.

2.4 Vehicle-to-vehicle (V2V) communication:

V2V Communication is a new concept in which lots of research has to be done. In this, vehicles act as a node in a network and communicate with each other with the use of sensors connected in an ad-hoc network. The infrastructure of V2V network is a bit complicated as there is no fixed topology to be followed as vehicles are moving from one place to another all the time. Applications for vehicular networks can be divided into four broad categories, namely safety and collision avoidance, traffic infrastructure management, vehicle telematics, and entertainment services and Internet connectivity (BOOYSEN; ZEADALLY; ROOYEN, 2011).Vehicles communicate with each other within a range of 1000 m. Two types of communication are possible; first one is vehicle-to-vehicle and the other one is the vehicle with the road-side infrastructure. Vehicular communication system is developed as a part of Intelligent Transport System (ITS). From a network architecture point of view, focus is initially placed on routing protocols; Physical layer (PHY), Medium Access Control (MAC) layer, and broadcasting (BOOYSEN; ZEADALLY; ROOYEN, 2011).

III.APPLICATION

Ample of application is there where Internet of Things is playing a vital role. In the near future, there will be even more applications using Internet of Things. As the world is going through a technological revolution, more and more objects will use the technology of RFID,NFC, M2M communication and V2V communication for automation as shown in Figure 3.

3.1 Transportation and logistic domain

3.1.1 Smart parking:

The new Smart Parking sensor's to be buried in parking spaces to detect the arrival and departure of vehicles. The Smart parking provides extensive parking management solutions which helps

IJARCCE

ISSN (Online) 2278-1021
ISSN (Print) 2319 5940

International Journal of Advanced Research in Computer and Communication Engineering
ISO 3297:2007 Certified
Vol. 6, Issue 3, March 2017

motorists save time and fuel (LIBELIUM, 2013). A significant contribution to congestion arises from motorists searching for accessible parking spaces. Providing accurate information about parking spaces helps traffic flow better, and this will also allow the deployment of application to book parking spaces directly from the vehicle. This will help to reduce CO_2 emissions and to minimize traffic jams.

3.1.2 3D Assisted driving:

Vehicles like cars, buses and trains along with the roads and rails equipped with sensors may provide valuable information to the driver to provide better navigation and safety. With the use of assisted driving, we will be able to find the right track with prior information about traffic jams and incidents. In an Enterprise context, information about the vehicle transporting goods together with information about the type and status of the goods can integrate to provide valuable information about the delivery time, delivery delays and faults.

3.1.3 Augmented maps:

Tourist augmented maps with tags allow NFC-equipped phones to browse the information about the places and quickly connect it to the web services providing information about hotels, restaurants, monuments, theatre and the local attractions. This can be done by hovering your mobile phone over the tag within its reading range so that the additional information about the marker can be displayed on the screen.

Logistics:

Implementing the Internet of Things in Retail chain monitoring has many advantages: RFID and NFC can be used to monitor almost every link of supply chain, ranging from commodity details, raw material purchasing, production, transportation, storage, sale of product and after sales services. With the help of IoT, we will track the inventory in the warehouse so that stock can be refilled at the appropriate time for continuous sale and this will reduce the waiting time of customer which result in customer satisfaction, which further results in increased sales.

3.2 Healthcare domain

3.2.1 Health tracking:

We can track health of a person with the help of combination of RFID and NFC technology together. With the use of sensors and the technology stated above we can track the person's body temperature, heart beat rate, blood pressure, etc. In case of emergency, the individual and their personal doctor will be notified with all the data collected by the sensors.

3.2.2 Pharmaceutical products:

Safety of pharmaceutical product is of utmost importance to prevent the health of patients. Attaching smart labels to drugs, tracking them through the supply chain and monitoring their status with sensors has benefits like items require specific storing conditions so they can be monitored whether their requirements are fulfilled or not. We can also track the expiry of drugs with the use of sensors; this will prevent the transferring of expired drugs to the patient.

3.2.3 Data collection:

Automatic data collection and transfer of that data to the doctor will help in reducing in the processing time, reducing the data collection errors, automated care and routine auditing. This will also forward all the previous health record related to the patient which helps in accuracy of the medication given by the doctor.

3.3 Smart environments domain

3.3.1 Smart water supply

Smart cities must monitor water supply to ensure that there is adequate access for resident and business need. Wireless Sensor Networks provide the technology for cities to monitor their water piping systems more accurately and discover their greatest water loss risks. Cities that are addressing water leakage problem with sensor technology are producing high savings from their investment. Tokyo, for example, has calculated they save $170 million each year by detecting water leakage problems early (LIBELIUM, 2013). The system can report pipe flow measurement data regularly, as well as send automatic alerts if water use is outside of an estimated normal range. This allows a smart city to determine the location of leaking pipes and prioritize repairs based on the amount of water loss that could be prevented.

3.3.2 Smart homes and offices:

We are surrounded by various electronic gadgets around us such as microwave ovens, refrigerators, heaters, air conditioners, fan and lights. Actuators and sensors can be installed in these devices in order to utilize the energy sufficiently and also to add more comfort in life. These sensors can measure the outside temperature and even can determine the occupants inside the rooms and thereby control the amount of heating, cooling and flow of light etc. Doing all these can help us to minimize the cost and increase energy saving.

3.3.3 Improved gyms:

The gymnasium experience can be enhanced by involving new technologies like a separate exercise profile which can be installed on machines and each person can be identified from his identification id alone and thereby, concerned profile will get activated.

3.3.4 Food sustainability:

Food that we eat has to go through various stages before they arrive in the refrigerators. They are bound in a strict food cycle: production, harvesting, transportation and distribution. With the use of appropriate sensors, we can prevent the food from climatic damages by keeping a good eye on temperature, humidity, light, health etc. Sensors can measure these variations precisely and notify the concerned person. Monitoring helps in prevention of possible plant.

3.4 M2M and V2V communication domain

3.4.1 Industrial Maintenance:

The sensors fit in the machinery are used to monitor the temperature and vibration in industrial motors, and also warn when irregular operation is detected. Industrial maintenance is the term for the task of keeping the equipment running at peak

Copyright to IJARCCE

IJARCCE

ISSN (Online) 2278-1021
ISSN (Print) 2319 5940

International Journal of Advanced Research in Computer and Communication Engineering
ISO 3297:2007 Certified
Vol. 6, Issue 3, March 2017

efficiency in a factory. It includes scheduled cleaning, parts replacement and lubrication and repairs. The field of industrial maintenance does not involve just the repair of already existing malfunctions (LIBELIUM, 2013), but preventive maintenance typically is also a vital part of the field. Companies waste billions due to inefficient maintenance management. This will help Companies to save money and time.

3.4.2 Smart Cars:

Machine to machine (M2M) communications, and especially Smart Cars, could help to improve accident prevention. A pilot to operate remote control car in order to minimize car accident and reduce human error was developed by McGill University (SANTORELLI; MORAWSKI;LE-NGOC, 2011). These driverless cars will provide functioning more than just safety such as they can save valuable time, reduce stress of driving etc. Some studies carried out by the Institute of Electrical and Electronics Engineers (IEEE) reveal that, by 2040, driverless cars will account for up to 75 per cent of cars on the road worldwide (LIBELIUM, 2013).

3.4.3 Smart Grid:

Smart Grid is defined as an electrical grid which is designed to improve the efficiency of power transmission, and quality of service to the end user. In Smart Grid, all the devices in the network are connected with the sensors which regularly send the data related to power consumption to the central server. Central server determines the pattern of consumption and the amount of power consumption. This allows companies to increase their production to meet the transient power requirement (BOOYSEN et al., 2012).

3.5 NFC application domain

3.5.1 Travelling:

NFC can enhance the travelling experience to a greater extent: it can help us to minimize the check in time during the stay in hotels. When the room is booked in a hotel, a secure digital key is sent to the traveller. One can use that digital ticket, with the NFC enabled locks, and directly enter into the room without wasting any time in check-in lounges.

3.5.2 Health:

NFC can be useful in monitoring personal health. It can gather information about health and send the collective data to health monitoring center. These centers can, therefore, analyse health and provide the valuable report and information to the individual.

3.5.3 Payment:

With the help of NFC technology, a user can leave his credit cards at home and can make a copy of credit cards on the mobile device. In case he needs to make any payment, he can electronically make the payment by using the clone of credit cards on the mobile phone, and NFC activated devices.

In scenario, the effect of IoT can be seen in all technical areas. It helps in smart communication between objects but several issues are there to be addressed before the worldwide implementation of IoT. In this section, we identify some important issues related to addressing, routing protocol, security and privacy, standardization issue and congestion and overload issue.

3.5.4 Addressing and networking issue:

Each and every device connected in the network has a unique address by which it can be identified. As the IoT is gaining grounds in scenario, the demand for these unique address increases at a very fast rate. There are very limited number of address available in IPv4 addressing and will soon reach zero as it identifies each node through a 4-byte address. To handle the ever increasing demand of unique address, one require IPv6 addressing scheme to fulfil the requirement. IPv6 addresses are expressed by means of 128 bits and, therefore, it is possible to define 1038 addresses, which should be enough to identify any object. Another important issue is regarding networking i.e. which protocol is to be used to send the data from source to destination. In traditional internet, the protocol utilized at the transport layer for reliable communications is the Transmission Control Protocol (TCP) (CERF;DALAL; SUNSHINE, 1974). It is clear that TCP is insufficient for the IoT because we need to set-up a connection first in case of TCP, but most of communication in IoT is a very short communication. So, considerable time will be wasted in the connection setup. One more issue with TCP is congestion control, TCP is responsible for end-to-end congestion control, but in case of IoT the amount of data transfer is very small, so TCP congestion control is useless. As a consequence, TCP cannot be used efficiently for the end-to-end transmission control in the IoT. Till now, no solutions have been proposed and, therefore, research is required in this area.

3.5.5 Routing protocol issue in V2V communication:

Routing is a very important aspect in the field of V2V communication as it is a type of distributed processing with a great number of nodes and a constrained and highly variable network topology. There are two basic ways by which one can route the data from source to destination. The first one is source routing: in this all the information like how to get from source to destination is collected on the source and then stored in the packets to be send, and the job of the intermediate node is to read this information and route the packet according to it towards the destination. Second one is hop-to-hop routing: in this routing technique, node has information only about the next node; the work of intermediate node is a bit complex as they know the destination address only, not the whole route to get towards the destination (KUMAR;KUMAR; KADIAN, 2011). This hop-to-hop is more efficient as in this we can choose the best next hop according to the topology. The architecture of routing in V2V communication is the same as the architecture of routing in other connectionless networks. Routing is the backbone of the network. There are lots of protocols present there like Geographical Source Routing (JERBI et al., 2009) which is hop-to-hop routing. This routing is based on the topology information given by global positioning system; frequently changes in topology causes route oscillation and path instability. In On-Demand Routing protocol (DAS; PERKINS; ROYER, 2000) node attempts to discover a route to the destination when it has a packet to send. In this protocol, flooding method is used to discover the route which creates the congestion in the network as it sends the packet to all the nodes for route discovery. There are various other routing technique like Greedy Perimeter Stateless Routing (GPSR)(KARP; KUNG, 2000), Dynamic MANET on Demand (DYMO) (CHAKERES; PERKINS, 2006),etc., but each one has its shortcoming. The key challenge is to design a protocol which will improve reliability of protocols and reduce

IJARCCE

ISSN (Online) 2278-1021
ISSN (Print) 2319 5940

International Journal of Advanced Research in Computer and Communication Engineering
ISO 3297:2007 Certified
Vol. 6, Issue 3, March 2017

delivery delay time and number of packet transmission. To make VANET a reality, lots of research is needed as each one of the existing protocol has some drawbacks as explained above. The driver behaviour should also be concerned in designing the routing protocols.

3.5.6 Privacy and security issue:

The IoT is extremely vulnerable to attacks as its components spend most of the time unattended, so it became very easy to attack them. Apart from this, one more thing is that, most of the communication is wireless which makes snooping very easy. This is probably one of the biggest concerns for consumers when it comes to IoT. For instance, in NFC enabled devices, the device not only works as a credit card but also the key to your house, it will also contain the personal information of the owner. If a smartphone is stolen, the thief move's the phone over a card reader at a store to make a purchase (NFC, 2013). To avoid this, smartphone owners must protect their phone with strict password protection, so hacker is not able to come out with the correct password. More specifically, the major problems related to security concern authentication and data integrity. Authentication is required before making a connection between the two devices to prevent data theft. The infrastructure is required for the authentication as we generally have to exchange some public and private keys through the node. Solutions like cryptography and key management have been proposed in the recent past (e.g., (KAVITHA; SRIDHARAN, 2010),(ESCHENAUER; GLIGOR, 2002a)), but none of them will prevent from the man-in-the-middle attack and proxy attack problem.

Data integrity prevents any modification in the data by middle man; it ensures that the data received at the receiver node is in the unaltered form as send by the sender. Solutions have been proposed like Keyed-Hash Message Authentication Code (HMAC) scheme (ESCHENAUER;GLIGOR, 2002b), to protect the data against the attack but still new research is required in the field of security and privacy.

3.6 Standardization issue:

Standards are required to allow global interoperability. As the term Internet of Things is gaining popularity, the more and more number of devices is activated daily. To ensure the proper functionality of these devices, there should be certain standards we have to follow to provide proper service to the client. As the platform on which these IoT devices works is not the same in all cases, so it became more necessary to define certain standards to make those devices compatible with the others. EPCglobal (Electronic Product Code) (EPCGLOBAL, 2013),as well as ISO (International Organization for Standardization), offers a family of standards, and they are gaining popularity in the wireless sensor area.

3.7 Congestion and overload issue:

Congestion is occurred due to simultaneous messages from several devices that can lead to peak load situation and may have a tremendous impact on the network (3GPP, 2010). This affects the performance of the network, and may lead to failure of the network if the network is overloaded. This situation is mainly seen in M2M and V2V communication, and it can be solved with the help of emerging technologies like LTE-advanced or existing technologies like LTE high bandwidth networks (TALEB; KUNZ, 2012). The congestion situation also occurred because of malfunction of server or application; so to avoid this one has to design an application in such a way that can handle maximum load with minimum failure. Overload issue can be solved with the help of time controlled features, i.e., allow connection to the network only at a certain time periods, defined by the network operator. Only in this time period, the devices are allowed to connect, devices are not able to connect to the network in the forbidden time period. The other solution is by rejecting the connection request by specific network nodes, particularly from those that are causing congestion and shall have no impact on the traffic (TALEB; KUNZ, 2012). This will help in managing the overall load of the network by rejecting the nodes which are creating the congestion.

IV ARCHITECTURE

4.1 Proposed Security Architecture for U2IoT:

The U2IoT model is shown in Figure 1(a), which is essentially a heterogeneous system including Unit IoT and Ubiquitous IoT. Thereinto, Unit IoT resembling human neural network, refers to the basic cell providing solutions for special applications. Ubiquitous IoT includes the industrial IoT, local IoT, national IoT, and global IoT which is integration of multiple Unit IoTs with ubiquitous features, and it is similar to the social organization framework.

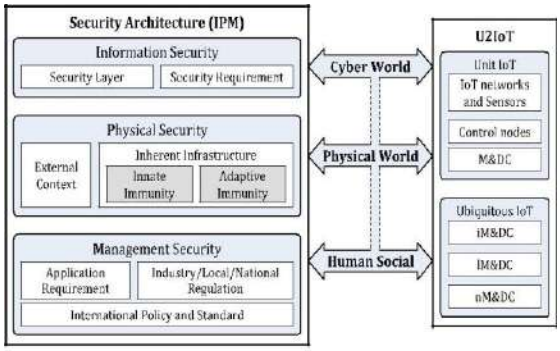

FIGURE 1. U2IOT MODEL AND ITS SECURITY ARCHITECTURE (IPM). (A) THE U2IOT (UNIT IOT AND UBIQUITOUS IOT) MODEL; (B) THE PROPOSED SECURITY ARCHITECTURE (IPM) BASED ON U2IOT.

I: Information security includes two perspectives (*i.e*., security layer and security requirement). Awareness of information data is captured, interpreted, and rep-resented by things' capability, along with aggregation algorithms, protocols, and functions are included for intelligent information interactions.

P: Physical security relates to environmental monitoring, motion detection, localization, tracking, perimeter control, and consumption supervision. The concept of artificial immunity is applied to detect passive and active defenses for maintaining homeostasis.

M: Management security provides the recommended application requirement, industry/local/national regulation, and international policy and standard to guide activities and events in the human social. In IPM, human social activities occurring in physical world are identified and mapped into the unique cyber world, which realizes harmonious unification of human, network and things. Such triple relationships of entity in U2IoT, makes entity identification and service discovery are effectively

IJARCCE
ISSN (Online) 2278-1021
ISSN (Print) 2319 5940
International Journal of Advanced Research in Computer and Communication Engineering
ISO 3297:2007 Certified
Vol. 6, Issue 3, March 2017

performed in current cyber-physical world, and are easily to extend to human social and its social networks. The security aspects underline main characteristics of U2IoT entities.

4.2 Information Security

Information security protects both raw data and contextualized information, and an information security model that comprises U2IoT, security layer, and security requirement is established in **Figure 2**.

1) *Considering Social Factor for Security Layer*: U2IoT is generally divided into four layers as follows.

Sensor layer: it comprises generalized sensors and gateways to perform entity identification and service discovery. The function of sensor layer is to perceive the entities, to extract information, and to realize se-mantic resource discovery. The sensor techniques are applied to realize effective integration and interaction adaptation of the collected uncertain information.

Network layer: it includes network interfaces, communication channels, network management, information maintenance, and intelligent processing. The centralized, distributed, and hybrid network topologies are involved to assist monitoring and maintaining the real-time network configuration. The network layer ensures reliable information transmission by adopting data coding, extraction, fusion, restructuring, mining, and aggregation algorithms. The main function is to transfer and process the information obtained by sensor layer, and to realize data exchange among large-scale heterogeneous networks.

Application layer: it exports functionalities for specific applications, and provides embedded interfaces for infrastructures to perform testing, monitoring, or auditing applications. The standard protocols and service composition technologies are applied to realize the integration between heterogeneous distributed networks and its applications, such as logistics monitoring, smart grid scheduling, intelligent search, and cloud computing. Such applications should adapt in dynamic environments.

Particularly, an additional social layer on the top of the architecture considers the social attribution in U2IoT. The social layer is mainly devoted to communicate among objects and other supporting networks to perform correlation between the cyber individual and the corresponding profile in social networks. Correlative social attributions are granted to each entity, and hierarchical management and data centers operate overall security considerations. In social layer, diverse interfaces are accessed by a real entity which acts on its corresponding cyber entity to control its behaviors. Meanwhile, other social compositions are also considered, such as ownership control management, social relationship modeling, and entity behavior formalization. In the perspective of information security, the sensor and network layers specify multiple networks and sensor nodes, which are used to capture data streams, to detect activities and events with identification algorithms, and to realize specific application functions. Core of data acquiring is sensor technology (e.g., RFID, WSN, femtocell) and Global Sensor Network (GSN) middleware, whose security is challenged by constrained resources. Note that distributed control nodes provide the capabilities to survive under formidable conditions, and by information security controls such as error detection and correction, random access control, and fault tolerance are recommended.

2) *Adding Intelligence and Compatibility for Security Requirement*: Elements of security requirements include CIA Triad, authority, non-repudiation, and privacy. Additional requirements that intelligence and compatibility are added into advanced security considerations, which provide reliable security and privacy protection. **Table 2** presents the comparison of security requirements among the traditional network, general IoT, and U2IoT. *Intelligence* represents that an entity should own abstract capabilities including self-learning, self- *Compatibility* requires that an entity has appropriate interconnection and interoperability to adjust to heterogeneous data formats, interfaces, channels, and networks in U2IoT model. The supplemental requirements address advanced criterions for information interaction. Meanwhile, compatibility can be promoted to scalability, expansibility and modularity among heterogeneous entities and the multi-context environments.

The both requirements operate together to promote the security and privacy preservation: 1) ensure diverse entities own artificial intelligence and autonomous security control against the strong attackers; 2) ensure heterogeneous entities, networks and applications establishing re-liable interconnection without compromising any communication data and individual privacy.

Physical security is denoted in external context and inherent infrastructure, in which human-like security immune safeguard is achieved.

1) *External Context*: Simple context and complex con-text are specified in [16], in which the former determines the basic identity, location, and entity status by a single parameter; the latter refers to geographical structures, traceability information, and real world conditions. Above both contexts are refined to support creating, debugging and integrating applications of Ubiquitous IoT, and provide interface interconnection and restriction for Unit IoTs. In U2IoT model, the borders of each entity's external con-text merge even vanish, and the obscure contexts spanning from an individual, an object, or an environment to social relationships, should support the hierarchical IoT subsystem. Particularly, intrusion detection algorithm is significant to acquire context information for monitoring sensors behavior, discover control node breaches, and other potential vulnerabilities.

2) *Inherent Infrastructure*: Artificial immune security system as computational intelligence is applied to analyze inherent infrastructure, which belongs sensorial sys-tem inspired by principles and processes of the natural immune system. Typical algorithms (e.g., clonal selection, negative selection, and immune network) exploit the immune system's features of detection, learning and memory to constitute innate immunity and adaptive immunity. Physical security issues such as intrusion detection, adaptive disposition, context-driven feedback, and error recovery can be addressed as follows.

3) Innate immunity: It provides basic barriers against foreign invasions in real-time environment, and it is triggered upon sensors identifying abnormal or malevolent attacks by the intelligent pattern recognition mechanisms. Co-stimulation signals are transmitted to distributed control nodes via Unit IoT networks, and then rejection reactions are performed by management centers. During defense operations, activation thresh-olds are defined to ensure the detection optimization, and fuzzy diagnosis can also applied for imperfect detection. Note that the innate immune defense is non-specific, meaning that U2IoT model responds to the various attacks in a general scheme. Such system can-not afford long-lasting immunity

Copyright to IJARCCE
DOI 10.17148/IJARCCE.2017.6326

IJARCCE
ISSN (Online) 2278-1021
ISSN (Print) 2319 5940
International Journal of Advanced Research in Computer and Communication Engineering
ISO 3297:2007 Certified
Vol. 6, Issue 3, March 2017

against a certain at-tack. The innate immune system is dominant to con-front the dynamic contexts and continuously refreshing threats.

4) Adaptive immunity: It refers to acquired resistance, where an attack is marked as a specific signature. Selective response requires recognizing non-self element during attack prototype presentation. If U2IoT has been infected by the same or similar invasion, specific memory module would be aroused to eliminate damaging effects by generating improved response to return the system into secure state. Adaptive immunity executes fuzzy diagnosis to variations of the same former attack, and optimal stimulation such as subsidiary vaccination is available by updating M&DCs' profile databases. According to both innate and adaptive immunities, three main features should be achieved in U2IoT model.

***5. Multithreaded and Hybrid Configuration*:** The U2IoT model may apply multithreaded security algorithms for the massively parallel network architecture that comprises a diverse set of components. The components are organized in hybrid mode, in which both centralized and distributed configurations are included. Towards Unit IoT, the allocation of the sensing and query processing is performed by the central M&DC. Towards Ubiquitous IoT, the industry IoTs and local IoTs are relatively independent, which commonly construct national IoT. In U2IoT model, such multithreaded and hybrid configuration are through-out all the networks, sensor and control nodes, and management and data centers.

***6. Multilayered and Autonomous Organization*:** There is no single security mechanism that offers complete immunity. Therefore, multilayered protection should independently operate for all-round safeguards. During the layered organization, U2IoT model autonomously makes its decisions by detecting potential attacks and proposing feasible solutions based on artificial immune algorithms.

***7. Heterogeneity*:** U2IoT model should be accessible by a large number of heterogeneous communication technologies with different networks, channels, interfaces, and hard-ware/software capabilities. Such heterogeneity of entities adds complexity to its security situations, which makes that a certain attack may simultaneously act on multiple entities in different IoTs, but the attack cannot act on all the involved IoTs. The immune protection ensures that the entire heterogeneous components cannot be corrupted due to the same attacker.

4.3. Management Security

Towards the future IoT, it is scarcely possible to establish a uniform security protocol as Internet, just like different nations and/or regions cannot adopt an identical safety precaution. Hence, distinctive management mechanisms are significant for both security and interconnection requirements. Due to the limitations of technological approaches, appropriate management should couple with the implementation of information security and physical security. Security strategies working on human behaviors should be considered to ensure that virtual cyber data is adapted to the real physical contexts.

4.3.1Application requirement for distributed sensor and control nodes provides generic/specific protection. IPM is of benefit to practical application security, such as historical query, project management, risk assessment, software de-sign, and system certification. For a specific scenario, customized requirements are assigned to describe the authorized/-unauthorized usage in a particular organization or individual. Additionally, application requirement should also be consistent with privacy prevention which realizes that the sensitive data is exchanged, stored, and shared with-out revealing any user privacy.

4.3.2Industry/Local/National regulation mainly serves for iM&DC/lM&DC/nM&DC to provide rules and guidance for U2IoT. It takes legal or disciplinary actions to resist the offensive individuals or institutions which do not com-ply with the regulations. There into, industry regulation describes approaches to achieve high-level security objective for a special industrial authority organization, such as agriculture, energy, and military. For instance, in the chemical hazards medical management, the regulations require certain parameters (e.g., temperature, vibrations, and relative proximity), caution the users for violation thresholds, and guarantee system security by warning abnormal implement and configuration. Thereinto, local regulation should coincide with local customs and practices to adopt humanistic perspectives for designing, implementing, and maintaining the local IoTs. National regulation governs guide-lines to realize nation-to-nation compatibility, and formal memorandum of agreements needs to be shared across national boundaries. Additionally, customized roles and responsibilities can be codified among different nations.

4.3.3International policy: considers the global IoT consociation during connectivity and consistency of nM&DC and global IoT. Moreover, international standards should be addressed by governments to promote security confidence and ensure interoperability. It indicates that a general international governance framework with reasonable enforcement policies will provide permanent mechanism towards security protection.

V.SERVICES

5.1 Types of Services:

There are an exceptional number of applications that can make use of the Internet of Things, from home and office automation to production line and retail product tracking. The number of applications is endless. For each application, a particular IoT service can be applied in order to optimize application development and speed up application implementation. Note that the categorizations that follow come from.

5.1.1 Identity-Related Services

Identity-related services can be divided into two categories, active and passive, and can serve either individuals or enterprise, which can lead to a number of different kinds of applications. The general identity-related service consists of two major components: 1) the things, all of which are equipped with some kind of identification identifier, such as an RFID tag; and 2) the read device(s), which read the identity of the thing based on its label, in this case reading the information encoded into the RFID tag.

5.2 Information Aggregation Services

Information aggregation services refer to the process of acquiring data from various sensors, processing the data, and transmitting and reporting that data via IoT to the application. These types of services can be thought of, more or less, as one way: information is collected and sent via the network to the application for processing.

IJARCCE

ISSN (Online) 2278-1021
ISSN (Print) 2319 5940

International Journal of Advanced Research in Computer and Communication Engineering
ISO 3297:2007 Certified
Vol. 6, Issue 3, March 2017

Information aggregation services do not have to implement a single type of communication channel in order to work together. With the use of access gateways (**Figure 1**), an information aggregation service could make use of different types of sensors and network devices and share their data via a common service to the application. For example, an application could make use of RFID tags to be aware of the identity of some devices, while also using a ZigBee network to collect data from sensors, then use a gateway device to relay this information to the application under the same service, say a Web Service such as JSON or XML. Not only would this allow a developer of an application to incorporate a number of different technologies into the application, but it could also allow the application to access various IT and enterprise services that may already be in place.

5.3. Collaborative-Aware Services

Collaborative aware services are services that use aggregated data to make decisions, and based on those decisions perform an action. As IoT takes shape, it should bring about the development of complicated services that make use of all of the data that can be retrieved from the extensive network of sensors. This will require not only being able to retrieve information, but to relay back responses to the collected information to perform actions. These services will thus require "terminal-to-terminal" as well as "terminal-to-person" communication. By providing collaborative aware services, the IoT infrastructure naturally requires greater reliability and speed, and will require the terminals to either have more processing power or be linked with some other device that does.

5.4. Ubiquitous Services

Ubiquitous services are the epitome of the Internet of Things. A ubiquitous service would not only be a collaborative aware service, but it would be a collaborative aware service for everyone, everything, at all times. In order for IoT to reach the level of providing ubiquitous services, it would have to overcome the barrier of protocol distinctions amongst technologies and unify every aspect of the network. There is no particular system architecture for the Internet of Things, but there have been numerous papers written about the use of Web Services or REST (representational state transfer) APIs (application programming interfaces) to unite loosely coupled things on the Internet under a single application so that they can be reused and shared. IPv6 is also a protocol that could greatly benefit the increase in ubiquitous services. Reference [4] proposes such an architecture that, if implemented, would be considered a ubiquitous service.

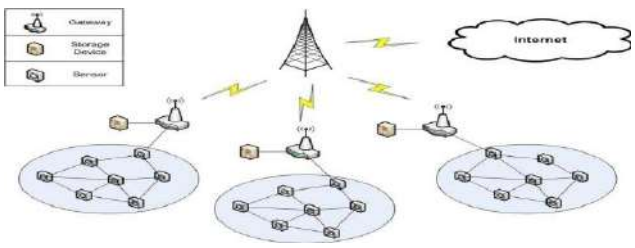

FIGURE 2. RFID NETWORK EXAMPLE.

Moving past what each of the categories means, the following subsections provide examples of each type of ser-vice in an attempt to offer developers a starting point when developing their own application. The idea is to provide a series of examples for each service type that use a common technology so as to provide a basic frame-work to build an application upon a specific type of ser-vice.

V. APPLICATIONS OF IOT SERVICES

6.1. Identity-Related Services

Identity-related services are the most simple, yet maybe one of the most important, services to be provided to an application of the Internet of Things. Applying an identity-related service to an application provides the developer with vital information about every device, or every*thing*, in their application.

The most prominent technology used in identity-related services is RFID. RFID is a technology that enables data to be transmitted by a tiny portable device, called a tag, which is read by an RFID reader and is processed ac-cording to the needs of that particular application. RFID provides an upgrade from the traditional form of device identification: barcode scanning. RFID is more versatile because it does not require line of sight transmission, and, in the case of active RFID tags, can transmit its data as opposed to simply just being read by a reader device.

Most IoT applications that are aimed at providing an identity-related service make use of RFID technology. As described, the RFID tag stores an identification code unique to that device. The RFID reader reads that code, and looks up the device in the RFID server, which then returns the detail information require by the application.

Production and shipping are two common applications that would benefit greatly from the use of an identity ser-vice. Another application that uses an identity-related service describes a model that can solve the information asymmetry problem in supply chain management and supply chain information transmission. Every IoT application will either be based on, or at least incorporate some instance of, an identity-related service. This is because for the IoT to incorporate every-thing in the physical world to the digital world, the application will need to be able to identify all of the devices that are connected.

6.2. Information Aggregation Services

Information aggregation services incorporate identity related services, along with other components such as WSNs, and access gateways to collect information and forward it to the application for processing. The information aggregation service is just responsible for providing the application with all of the information that is collected, and potentially processed along the way, from the terminals of the system (sensors, RFID tags, etc.). In this regard, the WSN can be a powerful tool for collecting and communicating data between terminals and the platform (host of application), as long as the platform is within range of the WSN. But this would not be an IoT application on its own; an IoT application would consist of multiple WSNs all configured to work together to provide information about the world around them. The link between these networks is an access gateway. The general structure of this network is shown in **Figure 2**. Each access gateway in the IoT network will have access to the database server, thus every device would be connected and information from the entire network aggregated at the database server. There are a number of applications out there that make use of information aggregation services and access gate-ways. In [7], the importance of extending the information aggregation service to beyond the WSN is proposed by using a cellular network (CN) to extend the range of the WSN. The idea is that if a terminal is outside of the WSN of interest, it uses CN resources

to access that information through the use of an "IoT gateway," which essentially implements both WSN and CN resources.

Information aggregation services are useful in monitoring situations, such as energy monitoring in the house and in the enterprise, or, if the Internet of Things has been realized, monitoring of anything, anywhere. For example, introduces a monitoring and control system for use in an agriculture greenhouse production environment. The system measures and records critical temperature, humidity and soil signals which is then trans-mitted through the network to the platform for processing. Another application uses a ZigBee WSN to monitor physiological data of patients that automatically generates electronic medical records.

6.3. Collaborative-Aware Services

The key difference between information aggregation ser-vices and collaborative-aware services are the use of the data collected to make decisions and perform actions. As mentioned before, the keys to creating a collaborative-aware service are network security, speed, and terminal processing power. Terminals can no longer be just simple sensors that collect information, or if there are simple sensors in the network, there must be separate embedded devices within the network that can make use of the data.

There are fewer applications published in terms of IoT and collaborative-aware services. We can, however, at-tempt to apply new technologies to a collaborative-aware service. An example of a new technology that will help shape the way the Internet of Things grows is IPv6. IPv6 is a new version of the Internet Protocol (IP) that allows for a significantly greater number of addressable devices to be connected to the internet. Although the use of IPv6 has had a slow start, it is definitely the internet protocol of the future due to the lack of available IP addresses. Moving forward, one of the most important factors in IoT be-coming reality is being able to address each of the embedded devices in the world, which converting to IPv6 would allow. Reference offers a number of applications for IoT, many of which could be considered collaborative-aware services, or which could at least provide a baseline for such a service. They propose integrating every object into the IP infrastructure using both IPv6 and 6LoWPAN, which is the use of IPv6 over low power wireless personal area networks. They propose a network with three types of nodes, all of which can be reprogrammed to function as any of the three types. The three types essentially are a base station node (IPv6 router), a mobile node (wireless dongle that allows WSN connectivity to a standard laptop) and specialized nodes, which are used for specialized tasks. This becomes a collaborative-aware service because it incorporates terminal-terminal and terminal-person communication, which is accomplished due to the use of the IPv6 protocol.

6.4. Ubiquitous Services

Ubiquitous services are the ultimate goal of the Internet of Things, taking collaborative-aware services to the next level by providing complete access and control of every-thing around us, whether it is through a computer or a mobile phone or something else. Ubiquitous services have yet to be realized in the world today, but most research in IoT is ultimately aimed at providing some piece to the puzzle that will ultimately be ubiquitous services. Reference first talks about why the Internet of Things is so difficult to realize. One of the biggest hurdles for IoT is having a single architecture that allows the many different application layer standards to communicate and interoperate. Reference proposes an architecture, based on RESTful services, in which a universal API would be created so that everyone who creates devices to be used in the Internet of Things has an architecture to adopt in order to be interoperable with the rest of the world's devices

REFERENCES

[1] Tasos Kaukalias and Periklis Chatzimisios, Internet of Things (IoT) C Enabling technologies, applications and open issues, Encyclopaedia of Information Science and Technology(3rd Ed.), IGI Global Press, 2014.
[2] Periklis Chatzimisios, Industry Forum & Exhibition Panel on Internet of Humans and Machines, IEEE Global Communications Conference (Globecom 2013), Atlanta, USA, December 2013.
[3] Angelo P. Castellani, Mattia Gheda, Nicola Bui, Michele Rossi, Michele Zorzi, Web Services for the Internet of Things through CoAP and EXI, IEEE International Conference on Communications Workshops (ICC), 5-9 June 2011, pp. 1-6.
[4] Sye Loong Keoh, Sandeep S. Kumar, Hannes Tschofenig, Securing the Internet of Things: A Standardization Perspective, Internet of Things Journal IEEE (Volume:1,Issue: 3), June 2014, pp. 265-275.
[5] Maria Rita Palattella, Nicola Accettura, Xavier Vilajosana, Thomas Watteyne, Luigi Alfredo Grieco, Gennaro Boggia, Mischa Dohler, Standardized Protocol Stack for the 8Internet of (Important) Things, Communications Surveys & Tutorials IEEE 15(3),2013, pp. 1389-1406.
[6] Thamer A. Alghamdi, Aboubaker Lasebae, Mahdi Aiash, Security Analysis of the Constrained Application Protocol in the Internet of Things, Second International Conference on Future Generation Communication Technology (FGCT), 12-14 Nov.2013, pp. 163-168.
[7] Shahid Raza, Hossein Shafagh, Kasun Hewage, Ren Hummen, Thiemo Voigt, Lithe: Lightweight Secure CoAP for the Internet of Things, Sensors Journal, IEEE 13(10),Oct. 2013, pp. 3711-3720.
[8] Shinho Lee, Hyeonwoo Kim, Dong-kweon Hong, Hongtaek Ju, Correlation Analysis of MQTT Loss and Delay According to QoS Level, International Conference on Information Networking (ICOIN), 28-30 Jan. 2013, pp. 714-717.
[9]http://mqtt.org/2011/08/mqtt-used-by-facebook-messenger, cited 28 Jul 2014.
[10] Dinesh Thangavel, Xiaoping Ma, Alvin Valera, Hwee-Xian Tan, Colin Keng-Yan Tan, Performance Evaluation of MQTT and CoAP via a Common Middleware, IEEE Ninth International Conference on Intelligent Sensors, Sensor Networks and Information Processing (ISSNIP), 21-24 April 2014, pp. 1-6.
[11] http://www.zdnet.com/google-moves-away-from-the-xmpp-open messagingstandard-7000015918/, cited 28 Jul 2014.
[12] Sven Bendel, Thomas Pringer, Daniel Schuster, Alexander Schill, Ralf Ackermann, Michael Ameling, A Service Infrastructure for the Internet of Things based on XMPP,IEEE International Conference on Pervasive Computing and Communications Workshops(PERCOM Workshops), 18-22 March 2013, pp. 385-388.
[13] Michael Kirsche, Ronny Klauck, Unify to Bridge Gaps: Bringing XMPP into the Internet of Things, IEEE International Conference on Pervasive Computing and Communications Workshops (PERCOM Workshops), 19-23 March 2012, pp. 455-458.
[14] Roy Thomas Fielding, Architectural Styles and the Design of Network-based Software Architectures, PhD thesis, University of California, Irvine, USA, 2000.
[15] Bipin Upadhyaya, Ying Zou, Hua Xiao, Joanna Ng, Alex Lau, Migration of SOAP based Services to RESTful Services, 13th IEEE International Symposium on Web Systems Evolution (WSE), 30 Sept. 2011, pp. 105-114.
[16] http://en.wikipedia.org/wiki/Advanced Message Queuing Protocol, cited 28 Jul 2014.
[17] Frank T. Johnson, Trude H. Bloebaum, Morten Avlesen, Skage Spjelkavik, Bjørn Vik, Evaluation of Transport Protocols for Web Services, Military Communications and Information Systems Conference (MCC), 7-9 Oct. 2013, pp. 1-6.
[18] Joel L. Fernandes, Ivo C. Lopes, Joel J. P. C. Rodrigues, Sana Ullah, Performance Evaluation of RESTful Web Services and AMQP Protocol, Fifth International Conference on Ubiquitous and Future Networks (ICUFN), 2-5 July 2013, pp. 810-815.9
[19] http://www.amqp.org/about/examples, cited 28 Jul 2014.
[20] http://en.wikipedia.org/wiki/WebSocket, cited 28 Jul 2014.
[21] Victoria Pimentel, Bradford G. Nickerson, Communicating and Displaying Real-Time Data with WebSocket, Internet Computing IEEE 16(4), July-Aug. 2012, pp. 45-53.

IJARCCE

ISSN (Online) 2278-1021
ISSN (Print) 2319 5940

International Journal of Advanced Research in Computer and Communication Engineering
ISO 3297:2007 Certified
Vol. 6, Issue 3, March 2017

BIOGRAPHIES

MOHD ANWARUDDIN, received B.Tech. Degree in Electronics and Communication Engineering from JSN College of Engineering & Technology, Adilabad and M.Tech. in DECS from JNTUA College of Engineering, Anantapur. He is an Assistant Professor of the Dept. of ECE in Nawab Shah Alam Khan College of Engineering & Technology, Malakpet, Hyderabad.

MOHD ABDUL SATTAR, received B.Tech. Degree in Electronics and Communication Engineering from National Institute of Technology(NIT), Warangal and M.Tech. in Embedded Systems from JNTUH. He is an Associate Professor & Head of the Dept. of ECE in Nawab Shah Alam Khan College of Engineering & Technology, Malakpet, Hyderabad. He is also a member of IEEE.

MOHD ANAS ALI, received B.Tech. Degree in Electronics and Communication Engineering from Pujya Shri Madhavanji College of Engineering & Technology affiliated to JNTU Hyderabad in 2013 & M.Tech. degree in Embedded System from Nawab Shah Alam Khan College of Engineering & Technology. He is presently working at Techno I Security Systems, Abids, Hyderabad.

International Journal of Advanced Research in Engineering and Technology (IJARET)
Volume 8, Issue 3, May - June 2017, pp. 25–36, Article ID: IJARET_08_03_004
Available online at http://iaeme.com/Home/issue/IJARET?Volume=8&Issue=3
ISSN Print: 0976-6480 and ISSN Online: 0976-6499
© IAEME Publication

TRUST ENHANCED DYNAMIC ROUTING FOR MANET

Syeda Kausar Fatima
Research Scholar, ECE Department,
Jawaharlal Nehru Technological University (JNTUH), Hyderabad, Telangana India

Dr. Syed Abdul Sattar
Professor and Dean, Nawab Shah Alam Khan College of Engineering & Technology (NSAKCET), Hyderabad, Telangana India

Dr. D. Srinivasa Rao
Professor, ECE Department, Jawaharlal Nehru Technological University, Hyderabad, Telangana India

Syeda Gauhar Fatima
Associate Professor, ECE Department,
Deccan College of Engineering and Technology (DCET), Telangana, India

ABSTRACT

Nowadays Mobile Adhoc Network (MANET) is becoming more popular due to its mobile and ease of deployment nature. However due to wireless and dynamic nature of network topology, it make them more exposed to various types of attacks. The main issue is to assure secure network services. In order to overcome this issue, a Trust Enhanced Dynamic Routing for MANET with Threshold Signature and Randomization process is proposed. In this technique, a secure cluster is formed based on the trust probability value where each node monitors trust value to determine the node trust level and minimum trust level of neighbor node. The node with high trust value is considered as the Cluster Head. In order to overcome the eavesdropping attacks during routing process randomization process is employed which monitors the each node to block malicious and increases node security level. The simulation results determines the comparative study results with the combination of attacks and without attacks.

Key words: MANET, security, trust, attacks.

Cite this Article: SyedaKausar Fatima, Dr. Syed Abdul Sattar, Dr. D. Srinivasa Rao and Syeda Gauhar Fatima. Trust Enhanced Dynamic Routing for MANET. *International Journal of Advanced Research in Engineering and Technology,* 8(3), 2017, pp 25–36.
http://iaeme.com/Home/issue/IJARET?Volume=8&Issue=3

1. INTRODUCTION

1.1. MANET

MANETs are highly vulnerable to various security attacks. Providing secure communication in MANET is proved to be a significant challenge. Authentication and trust model which are developed for wired network cannot be used in wireless network. Common authentication schemes are not applicable in Ad hoc network since public key infrastructure is hard to deploy [1] [2].Security supports are a significant factor in the design of security system in ad hoc networks. It is particularly important to protect the identities of individual nodes to avoid personal privacy concerns. For this a security system for ID-based anonymous cluster-based MANETs and a threshold signature [9] is proposed to protect the privacy of nodes. Here the basic operations consist of generating pairing parameters, private keys, and secret sharing.

Each node is having the ability to build a network by finding the node to communicate and share the data via radio waves. MANETs have several significant characteristics and challenges [4] for e.g. dynamic topology, distributed operation, light weighted terminal etc. Mobile ad hoc networks are vulnerable to security problems than the wired networks, different types of security solutions are used like cryptography and IDS etc. to avoid the security attacks but the malicious attackers block or modify the data traffic traversing them by refusing the cooperation and violates authenticity and confidentiality of network so these type of nodes are difficult to identify as they act as a validate user, so we use a concept of trust to solve such problems, trust is calculated on the basis of reputation, direct, indirect trust (recommendation). In which we calculate the degree of dependence on other nodes by which we then decide whether to communicate with that node or not.

2. LITERATURE REVIEW

Peng Zhou, Siwei Jiang, Athirai Irissappane, Jie Zhang, Jianying Zhou, and Joseph Chee Ming Teo et al [1]propose a suite of optimization methods to minimize the energy cost of watchdog usage, while keeping the system's securityin a sufficient level. Watchdog optimization algorithms have demonstrated excellent performance in saving energy and maintaining security, they are still subject to some challenges, which may need further investigation.

Bijon, Khalid Zaman, Md Munirul Haque and Ragib Hasanet al [2] proposes model that provides a feature of multi-hop recommendation where every valid recommendation comes only from DTNs. This model also reduces traffic in a great volume by updating multiple trust fields of intermediate nodes. It also introduces the concept of path reliability based aging. It also successfully reflects uncertainty while combining multiple recommendations.

N. Bhalaji, A. Shanmugam et al [4] proposed the trust model and analysed each node calculates trust value and association status for all its neighboring nodes through monitoring its behavior in the network. Then this trust model is integrated into the Dynamic Source Routing (DSR) protocol which is the most common on demand routing protocol used in MANET. In the proposed scheme the route is not selected on the basis of first arrival of RREP and waits till it gets the RREP from all neighboring nodes and decides the path to be routed based on the nature of association between them.

Abderrezak Rachedi and Abderrahim Benslimane [6] have proposed an anonymous protocol to secure nodes which have important roles in the network. Also they presented an Anonymous Dynamic Demilitarized Zone (ADDMZ) to protect the CA node identity and to avoid the single point of failure in the cluster. ADDMZ is formed by a set of confident nodes which have a high trust level between them and their goal is to filter the communication between the cluster member node and the CA node. They present protocol to realize these

mechanisms by using the identity based cryptographic from bilinear maps. However, it is possible to attack RA nodes by selecting randomly nodes at the attacker's neighborhood, but the risk to detect the attacker is high.

Yo Han Park et al [7] have proposed a security system for ID-based anonymous cluster-based MANETs to protect the privacy of nodes. Moreover, they propose a threshold signature scheme without pairing computations, which diminishes the computation load on each node. Their proposal satisfies most properties for an anonymous security system and effectively copes with dynamic environments with greater efficiency by using secret sharing schemes. As long as the CH does not reveal the respective polynomials, anonymity of each node is guaranteed.

Raihana Ferdous et al [8] have proposed a Cluster head(s) selection algorithm based on an efficient trust model. This algorithm aims to elect trustworthy stable cluster head(s) that can provide secure communication via cooperative nodes. However the way the messages passed through may overload the Cluster head, creating a bottleneck due to additional message exchanges. Another possible limitation is the way that the message authentication between intermediate Cluster heads are treated, where there can be adelay in identifying a malicious neighboring node.

Yao Yu and Lincong Zhang et al [9] have proposed a secure clustering algorithm based on reputation in defense of threats in clustering. In the algorithm, the nodes reputation is used to improve security, which is evaluated by combining the experience of the node in the routing process. In addition, they consider degree and relative mobility in the clustering to guarantee the stability of clusters. Moreover, it is efficient in the cluster rebuilding and healing. The proposed algorithm can effectively improve the security and stability of network. However there occurs overhead in the system.

Noman Mohammed et al [10] have proposed a solution for balancing the resource consumption of IDSs among all nodes while preventing nodes from behaving selfishly. To address the selfish behavior, they design incentives in the form of reputation to encourage nodes to honestly participate in the election scheme by revealing their cost of analysis. To address the optimal election issue, they propose a series of local election algorithms that can lead to globally optimal election results with a low cost. However the percentage of leaders is less in this model.

Hard security, designed to protect data and system integrity, may not be enough to protect nodes from misbehavior by other malicious nodes. At the present time, soft security threats are most effectively countered using trust and reputation management (TRM) systems.

3. TRUST DYNAMICVECTORROUTING PROTOCOL (TEDR)

A Trusted Dynamic Vector routing organize trusted dynamic routing which is rely on existing distance information exchanged among neighboring nodes for seeking a routing paths. The nodes maintains a routing table (Table -1) with corresponding tuple $(d, W_{N_{i,d}})$, where $d$denotes new destination node and $W_{N_{i,d}}$ minimum estimated path cost to send a packet from node i to node d.

Corresponding routing table (Table -1) extended with node trust representation. The corresponding routing table (Table -2) determines the extended trusted routing table $(d, W_{N_{i,d}}, C_t^{N_i}, H_t^{N_i}, T_{N_{i,d}})$, with node candidate, interactivity history, trust count. Here each tuple associated with a set of node candidates $C_t^{N_i}$for the next hop with minimal cost is marked.$H_t^{N_i}$, represents a interactive history from node t to node i, and each tuple (N_j, H_{N_j}) in $H_t^{N_i}$, is used to represent that N_i previously used the node H_{N_j}as the next hop to forward the

packet from the source node N_j to the destination node d. $T_{(N_{i,h}),(N_{h,d})}$, a set of trust count values from node to next hop node and next hop node to destination node. Each tuple $\left(N_j, h_{N_j}\right)$in $H_t^{N_i}$, is used to represent that $N_i$previously used the node h_{N_j}as the nexthop to forward the packet from the source node N_j to the destination node d.

Assume that a node n has m number of neighbor nodes at particular instance. Each neighbor monitors independently with probability p. The probability at node n is monitored at trust level l. Let assume each node monitors the neighbor nodes with minimum probability of P_i^{min}, where neighbor nodes are monitored with desired trust level. According to the figure -1 node – 5 represents three neighbor nodes (1,4,6). Assume trust level l =1, the node 5 monitors the neighbor nodes (0.81, 0.94 and 0.98) respectively, with the trust level probability of$P_5^{min} = \max(0.81, 0.94, 0.98) = 0.96$

$$P(l/m) = \sum_{i=1}^{m} \binom{m}{i} p^i (1-p)^{m-1}$$

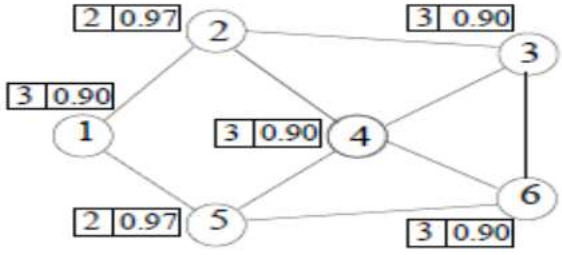

Figure 1 Calculation of Minimum Monitoring Probability

To determine node corresponding neighbors trust level probability by exchanging node degree, we define a degree as a number of neighbor nodes at instance of time. Based on that let r will be the minimum degree of node i. For the time instance t, let 5 will be the node degree of node i, to obtain the optimal trust level of node with minimum probability will be measured as

$$P_i^{min} = \sum_{j=1}^{m_i} \binom{m_i}{j} p^j (1-p) \geq T$$

The term T, as explained earlier denotes a threshold value, which is the minimum probability with which the desired trust level l. Each node in the network is monitored with the desired trust level (l) when $P_i^{min}$of each node i iscalculated using minimum degree of its neighbors (m_i)

Table 1 The routing table for the original distance-vector-based routing.

Destination Node (t)	Cost ($W_{Ni,t}$)	Nexthop
N_1	7	N_6
N_2	8	N_{21}
N_3	9	N_9

Table 2 The routing table for the security-enhanced routing algorithm

Destination Node (t)	Cost ($W_{Ni,t}$)	Nexthop Candidates (C_t^{Ni})	History Record for Packet Deliveries to the Destination Node t(H_t^{Ni})
N_1	7	{ $\hat{}N_6, N_{20}, N_{21}$}	{(N_2, N_{21}), (N_3, N_6),..(N_{31}, N_{20})}
N_2	8	{N_9 , $\hat{}N_{21}$}	{(N_1 , N_9), (N_3, N_9),..(N_{31}, N_{21})}
N_3	9	{ $\hat{}N_9$}	{(N_1, N_9), (N_2, N_9),..(N_{31}, N_9)}

The Mechanism employed by each node in the network o determine the minimum monitoring probability , which is derived in Minimum Degree for k. Fig -2 described more pictorially about *MDK* algorithm. According to the fig -3, each node intitiates this algorithm to know the probability which are the nodes it has to monitor its neighborhood. Once this algorithm derived the node neighbourhood monitoring probability, then the node (M) broadcast the message (Send Degree) to one hop neighbours, once the 1-hop neighbour of node M reply back with their respective degree. The minimum of these degree is assigned to k, and the minimum monitoring probability of node M is calculated.

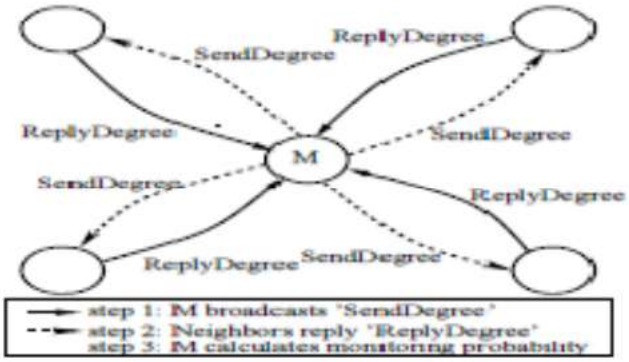

Figure 2 Description of MDK

Algorithm 1: MDK

Input : Node M, send degree, reply degree

Output : Minimum degree of k and minimum probability

1. Node Mbroadcast a message of send degree to neighbours

$$M \rightarrow brodcast : (Senddegree)$$

2. On receiving of the Send Degree message from node M, each neighbour node, $S$of M replies a Reply Degree message.

$$S \rightarrow M : (Replydegree)$$

3. On receiving of each reply degree messages of neighbour node S of M, Node M performs following operations :

- For each message dodegree = ReplyDegree;
- ii. k = Minimum(degree);
- If l > k then P_{min}M = 1.
- Otherwise, pmin M is assigned the minimum value of p (where *l*is the desired trust level of the neighbor, T +ϙ=1, ϙ is a very small positive number)such that

$$\sum_{i=1}^{k} \binom{k}{l} p^i (1-p)^{k-i} \geq T$$

3.1. Cluster Head Selection Based on TEDR

This section describes about the selection of Cluster Head (CH) in a MANET based on node fitness, node degree, node mobility, residual energy level and trust-value. For this purpose, initialize the initial trust rate value as (1), energy rate (10J), and mobility rate. Compute node fitness, the node fitness function derives based on sum of node energy level and node trust leve. The node degree represents how many number of neighbor nodes for each node in a network. The following procedure determines the election of efficient and trusted CH.

Step 1: Calculate the percentile of node degree as PN_d

$PN_d \leftarrow \left\{Numberof\ 1-hopnodesinsidethe\frac{cluster}{N}\right\} * 100$ where N is number of nodes

Step 2: Calculate the percentile of node energy level.

$$PN_E = \left\{\frac{RE_n}{T}\right\} * 100$$

Step 3: Calculate the percentile of node mobility

$$P_m = \{Avg(MS)/T \times 100\}$$

Step 4: Compute the percentile of node trust

$$P_{TV} = w1.PN_d + w2.PN_E + w3.P_m$$

where w1, w2, and w3 are weight factors given to different parameters such as node degree, energy, and mobility.

$$w1 + w2 + w3 = 1$$

Based on section 3.1 and Table 1 and 2, the Cost (WN_i, t) and history record for Packet Deliveries to the Destination Node $t(H_t, N_i)$. The node TV is determined as

$$TV_{i,j} = \sum_{\substack{0 \le i \le m \\ 0<j<n}} \frac{P_{TV}(i,j)}{cost(WN_i, t)}$$

Where $i, j \in nodes$, TVi, j represents node i's TRUST_VALUE for node j.

The CH selection technique can be explained as below:

Step 1: First, Initialize the parameters to 0 or null.

CHcur ⟵ 0

CHprev ⟵ 0

Timeprev ⟵ 0

Curr () ⟵ 0

Step 2: Calculate the TV of each node from the equation ()

$TV_{i,j} = \sum_{\substack{0 \le i \le m \\ 0<j<n}} \frac{P_{TV}(i,j)}{cost(WN_i t)}$

Step 3: Compare the given condition to select CH

While (Timeprev_Curr () or TRUST_VALUE (CHprev) ≤ 1 =true) do

CHprevremains as Cluster Head

End while

Step 4: Compare Trust Value of previous and current Cluster Head

If Trust_Value(CHprev)=Trust_Value(CHcur) and Cost(CHprev)=Cost(CHcur) then

bothCHprev and CHcurremains as cluster heads

Else

select new Cluster Head
Select new cluster head(s)
end if

4. AUTHENTICATION TECHNIQUE USING THRESHOLD SIGNATURE

4.1. Generation of Pseudonyms

The CH generates pseudonyms for all the node inside the cluster by using corresponding polynomial.

For this it performs (S1, n1)-KK of km. Also each CH calculate $id_R = H_0(ID_R)$ and secret sharing $f^{CH_j}_m(x) : PK_R = f^{CH_j}_m(x)(id_A)\ where(1 \le R \le n_1)$

4.1.2. Authentication Technique

The authentication process starts with the generation of threshold signature.

The network consist of the following parameters:

Cluster Head (CH)

A set of Member Node X = {N1……N_{S2}) where N_{S2} represents identity of the ith ($1 \le i \le S1$) member.

A set of signer $Y = \{K1,.....K_{S2}\}$ where K is a subset of N and K_{S2} represents the identity of the jth ($1 \le i \le S2$) member

Verifier V

4.2 Generation of Threshold Signature

In order to generate a threshold signature for message N, a number of S2 (b_1, b_2, b_3, b_4, b_5) nodes including the members of N perform the following steps as shown in Fig (3):

Step 1: In the first step, all the member node request for threshold signature. This is started by one of the signers by sending a threshold generation request to selected CH along with list of signers as(TK1… TK_{S2}).

Step 2: In the next step they sends tokens. For this CH selects a random token $T_R \in Z*_q$ where $(1 \le R \le S_2)$ and sends them to the corresponding signers very securely.

Step 3: After that each signer creates a signature: $Sig_{PK_R} = H_0(N).K_{PK_R}$ and calculates with a corresponding token: $T \cdot Sig_{PK_R} = TA \cdot Sig_{PK_R}$

Step 4: After that start sending signature along with pseudonym public key. Here, each node sends the message tuple to the verifier V and CH_j.

$$((N, Q_{PK_R}, Q_{PK_V}, T \cdot Sig_{PK_R}, HMAC_{PK_R}(M, Q_{PK_V}, T.Sig_{PK_A})) \quad (2)$$

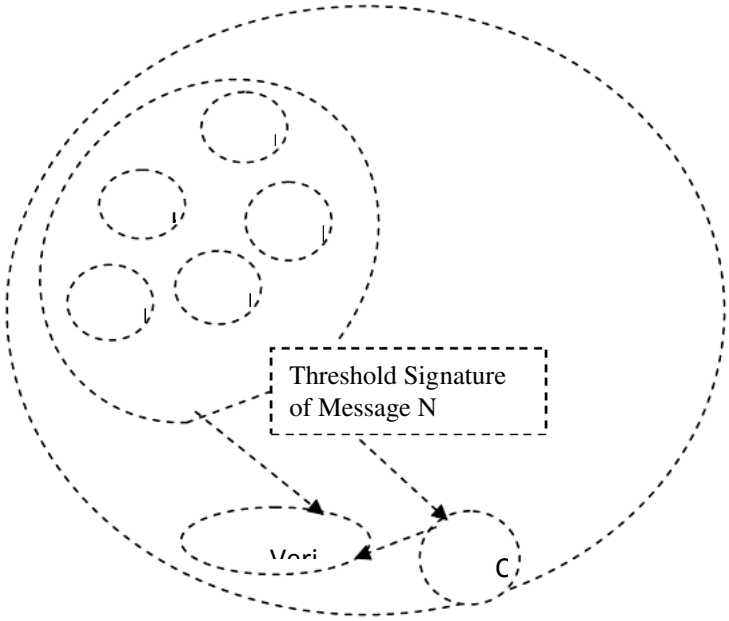

Figure 3 Representation of Authentication Technique Using Threshold

5. RANDOMIZATION PROCESS

Consider the delivery of a packet with the destination t at a node N_i. In order to minimize the probability that packets are eavesdropped over a specific link, a randomization process for packet deliveries shown in Procedure 1 is adopted. In this process, the previous nexthop h_s (defined in H_t^{Ni} of Table 2) for the source node s is identified in the first step of the process (line 1). Then, the process randomly picks up a neighboring node in C_t^{Ni} excluding h_s as the nexthop for the current packet transmission. The exclusion of h_s for the nexthop selection avoids transmitting two consecutive packets in the same link, and the randomized pickup prevents attackers from easily predicting routing paths for the coming transmitted packets.

Procedure 1

RANDOMIZEDSELECTOR (s, t, pkt)

1: Let h_s be the used nexthop for the previous packet delivery for the source node *s*.
2: if $h_s \in C_t^{Ni}$ then
3:if $| C_t^{Ni} | > 1$ then
4: Randomly choose a node *x* from $\{ C_t^{Ni} - h_s \}$ as anexthop, and send the packet pkt to the node *x*
5: $h_s \leftarrow x$, and update the routing table of N_i.
6: else
7: Send the packet *pkt* to h_s.
8: end if
9: else
10: Randomly choose a node *y* from C_t^{Ni} as nexthop, and send the packet *pkt* to the node *y*.
11:$h_s \leftarrow y$, and update the routing table of N_i.
12: end if.

5.1. Trust Table Maintenance

Let every node in the network be given a routing table and a link table. We assume that the link table of each node is constructed by an existing link discovery protocol, such as the Hello protocol. On the other hand, the construction and maintenance of routing tables are revised based on the well-known Bellman-Ford algorithm and described as follows:

Initially, the routing table of each node (e.g., the node N_i) consists of entries {(Nj, W_{Ni}, C_t^{Ni}= {N_j}, H_t^{Ni} = 0) }, where $N_j \in Nbr_i$ and $W_{Ni, Nj} = w_{Ni, Nj}$. By exchanging distance vectors between neighboring nodes, the routing table of N_i is accordingly updated. The exchanging for distance vectors among neighboring nodes can be based on a predefined interval. The exchanging can also be triggered by the change of link cost or the failure of the link/node. TEDR considers cases when N_i receives a distance vector from a neighboring node N_j. Each element of a distance vector received from a neighboring node N_j includes a destination node t and a delivery cost

$W_{Nj,t}$from the node N_j to the destination node t. The algorithm for the maintenance of the routing table of N_i is shown in Procedure 2, and will be described below.

Procedure 2

DVPROCESS (t,$W_{Ni,t}$)
1: if the destination node t is not in the routing table then
2: Add the entry (t, ($w_{Ni,Nj}$+ $W_{Nj, t}$), C_t^{Ni} = { N_j }, H_t^{Ni} = 0)
3: else if ($w_{Ni,Nj}$+ $W_{Nj, t}$) < $W_{Ni, t}$ then
4: $C_t^{Ni} \leftarrow$ { N_j} and N_j is marked as the minimal-cost nexthop.
5: $W_{Ni, t} \leftarrow (w_{Ni,Nj}+ W_{Nj, t})$
6: for each node $N_k \in Nbr_i$ except N_j do
7: if $W_{Nk, t} < W_{Ni, t}$ then
8: $C_t^{Ni} \leftarrow C_t^{Ni} \cup \{ N_K \}$
9: end if
10: end for
11: Send (t, $W_{Ni, t}$) to each neighboring node $N_k \in Nbr_i$
12: else if ($w_{Ni,Nj}$ + $W_{Nj, t}$) > $W_{Ni, t}$ then
13: if ($N_j \in C_t^{Ni}$) then
14: if N_j was marked as the minimal-cost nexthop then
15: $W_{Ni, t} \leftarrow MIN_{Nk \in Nbri}$ ($w_{Ni,Nk}$ + $W_{Nk, t}$)
16: $C_t^{Ni} \leftarrow 0$
17: for each node $N_k \in Nbr_i$ do
18: if $W_{Nk,t} < W_{Ni,t}$ then
19: $C_t^{Ni} \leftarrow C_t^{Ni} \cup \{ N_j \}$
20: end if
21: end for
22: Send (t, $W_{Ni, t}$) to each neighboring node $N_k \in Nbr_i$.
23: else if $W_{Nj,t} < W_{Ni,t}$ then
24: $C_t^{Ni} \leftarrow C_t^{Ni} - \{ N_j \}$
25: end if
26: else if ($N_j \in C_t^{Ni}$) $\wedge$ ($W_{Nj,t} < W_{Ni,t}$) then
27: $C_t^{Ni} \leftarrow C_t^{Ni} \cup \{ N_j \}$
28: end if
29: end if

Initially for the elements that do not exist in the routing table, new entries for the corresponding destination nodes will be inserted. Otherwise, $w_{Ni,Nj} + W_{Nj,,t}$ is compared with $W_{Ni,t}$ saved in the routing table of N_i, and the following four cases are considered:

$w_{Ni,Nj} + W_{Nj,\ t} < W_{Ni,\ t}$ (lines 3-11). The corresponding minimal cost is updated in the routing table, and N_j is marked as the minimal-cost nexthop. Any neighboring node N_k which has an estimated packet delivery cost from N_k to t (i.e., $W_{Nk,t}$) no more than $(w_{Ni,Nj} + W_{Nj,\ t})$ joins the candidate set C_t^{Ni} .It is to aggressively include more candidates for the nexthop to t with reasonable packet delivery cost (i.e., $W_{Nk,t} < W_{Ni,t}$). Compared to the Bellman-Ford algorithm, more one neighboring node can be selected as the nexthop candidates in this step (lines 6-10) to accommodate multiple packet-delivery paths to the destination node t. Also, the selection policy described above can prevent the algorithm from generating the routing loops.

$w_{Ni,Nj} + W_{Nj,\ t} > W_{Ni,\ t}$ and N_j is in the set C_t^{Ni} of nexthop candidates (lines 13-25). Based on whether N_j is marked as the minimal-cost nexthop in the routing table of Ni, the following two cases are further considered.

N_j was marked as the minimal-cost nexthop (lines 14-22). For all neighboring nodes of N_i, the minimal cost to the destination node t is recomputed according to the distance vectors received from the neighboring nodes. Also, the nexthop candidates for the destination node t are reselected, and the selection policy is the same as lines 7-9 for Case 1.

N_j was not marked as the minimal-cost nexthop (lines 23 and 24). If $W_{Nj,t} > W_{Ni,t}$, N_j is removed

from C_t^{Ni}.

$(w_{Ni,Nj} + W_{Nj,\ t}) > W_{Ni,\ t}$ and N_j is not in the set C_t^{Ni} of nexthop candidates (lines 26 and 27). If $W_{Nj,t} > W_{Ni,t}$, N_j is inserted into C_t^{Ni}.

Otherwise, nothing is done.

When a node N_i receives a distance vector from a neighboring node, Procedure 2 is used to maintain the nexthop candidates for each entry in the routing table of N_i. Based on Procedures 1 and 2, our security-enhanced dynamic routing can be achieved without modifying the existing distance-vector-based routing protocols

6. SIMULATION RESULTS

Table 3 Simulation Parameters

No. of Nodes	50,100,150,200
Area Size	1000 X 1000
Mac	802.11
Routing protocol	TEDR
Simulation Time	40 sec
Traffic Source	CBR
Packet Size	512
Attacker	1,2,3,4 and 5
Antenna	OmniAntenna
Speed	5,10,15,20,25

6.1. Performance Metrics

The performance of TEDR Trust Enhanced Dynamic Routing for MANET with Threshold Signature and Randomization process technique is compared with TSCP Trust Based Routing

Protocol. The performance is evaluated mainly, according to the following metrics: .Average Packet Delivery Ratio,PDR ratio measured with respective of attack and without attacks**.**

6.2. Results

Based on Attackers

In our initial experiment, number of attackers are varied as 1, 2, 3,4and 5.

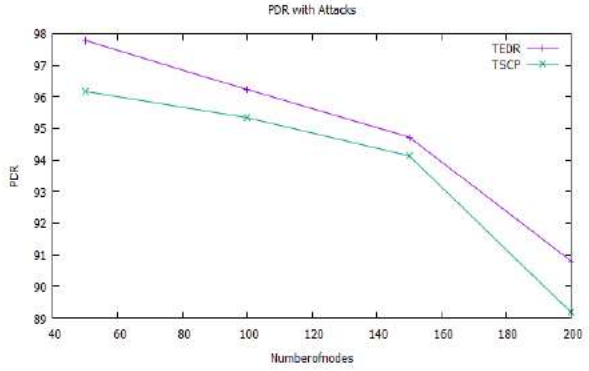

Figure 6 (a) NodesVs Delivery Ratio…

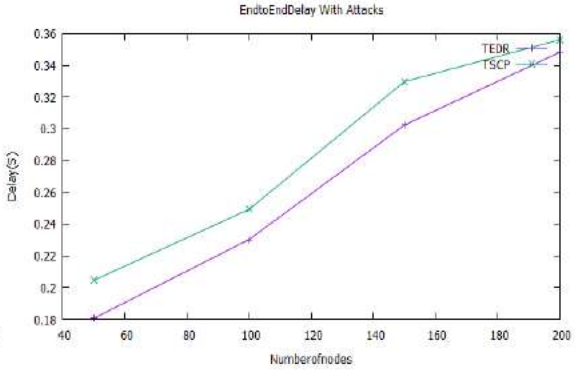

Figure 6(b) 2: Nodes Vs End2End Delay

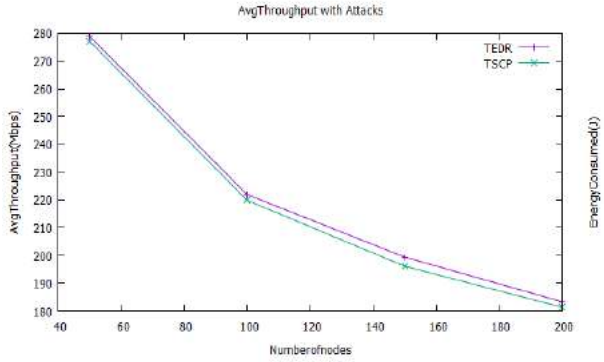

Figure 6 (c) Nodes VsAvg Throughput

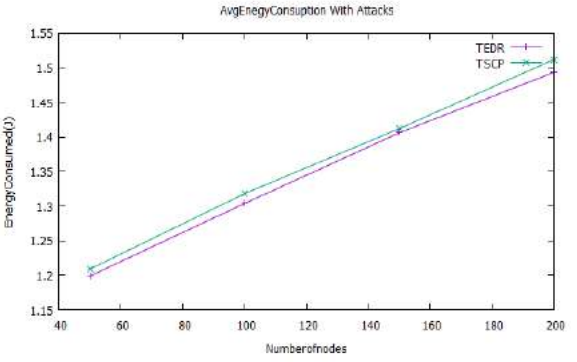

Figure 6 (d) NodesVs Avg Energy Consumption

From above figures we can see that the delivery ratio of our proposed TEDR is 5.2% higher than the existing TSCP technique. End to end delay of our proposed TEDR is 11% less than the existing TSCP technique. Average throughput of our proposed TEDR is 9.1% higer than the existing TSCP technique and energy consumption of our proposed TEDR is 11.2% less than the existing TSCP technique.

7. CONCLUSION

A trust enhanced dynamic routing protocol is proposed for MANET. In this technique, a secure cluster is formed based on the trust value. For each node participating in the cluster formation trust value is calculated. The node with high trust value is considered as the Cluster Head. In order to increase the security, the selected cluster head is further verified by using Threshold Signature. In order to overcome the eavesdropping attacks during routing process, randomization process is employed which monitor each node to block malicious and increases node security level.

REFERENCES

[1] Peng Zhou, Siwei Jiang, Athirai Irissappane, Jie Zhang, Jianying Zhou, and Joseph Chee Ming Teo Toward Energy-Efficient Trust System Through Watchdog Optimization for WSNs IEEE Transactions on InformationForensics and Security, VOL. 10, NO. 3, March 2015.

[2] Bijon, Khalid Zaman, Md Munirul Haque and Ragib Hasan. "A trust based Information sharing model (TRUISM) in MANET in the presence of uncertainty." Privacy, Security and Trust (PST), 2014 Twelfth Annual International Conference on. IEEE, 2014.

[3] Balakrishnan, Venkatesan and et al. "Team: Trust enhanced security architecture for mobile ad-hoc networks." Networks, 2007. ICON 2007. 15th IEEE International Conference on. IEEE, 2007.

[4] N.Bhalaji, A.Shanmugam Association between nodes to Combat Blackhole attack in DSR based MANET in Proceedings of the Sixth IFIP-IEEE WOCN, April 28-30 Procedia Engineering, 2012 - Elsevier

[5] Hajami, Abdelmajid, Kamal Oudidi, and Mohammed ElKoutbi. "An enhanced algorithm for MANET clustering based on multi hops and network density", New Technologies of Distributed Systems (NOTERE), 2010 10th Annual International Conference on. IEEE, 2010.

[6] Abderrezak Rachedi and Abderrahim Benslimane, "Security and Pseudo-Anonymity with a Cluster-based approach for MANET", Global Telecommunications Conference, 2008, IEEE GLOBECOM 2008, IEEE, 2008.

[7] YoHan Park, YoungHo Park and SangJae Moon, "Anonymous Cluster-Based MANETs with Threshold Signature", Hindawi Publishing Corporation International Journal of Distributed Sensor Networks Volume 2013, Article ID 374713.

[8] Raihana Ferdous, Vallipuram Muthukkumarasamy and Elankayer Sithirasenan, "Trust-based Cluster head Selection Algorithm for Mobile Ad hoc Networks", Trust, Security and Privacy in Computing and Communications (TrustCom), 2011 IEEE 10th International Conference on. IEEE, 2011.

[9] Yao Yu and Lincong Zhang, "A Secure Clustering Algorithm in Mobile Ad Hoc Networks", IPCSIT vol. 29 (2012).

[10] Noman Mohammed, Hadi Otrok, Lingyu Wang, Mourad Debbabi and Prabir Bhattacharya, "Mechanism Design-Based Secure Leader Election Model for Intrusion Detection in MANET", Dependable and Secure Computing, IEEE Transactions on 8.1 (2011).

[11] Syeda Kausar Fatima, Syed Abdul Sattar, D. Sreenivasa Rao, "Trusted and Secured Clustered Protocol in MANET", International Journal of Computer Applications (0975-8887) Volume 153-N04, November (2016) pp14-20 ©IJCA.

[12] S. Radha Rammohan. Anomaly Detection in Mobile Adhoc Networks (MANET) using C4.5 Clustering Algorithm. International Journal of Information Technology & Management Information System (IJITMIS), 7 (1), 2015, pp. 01-10.

[13] Aniket Deshpande and Dr. Ashok Kaushal, Identification of Important Sampling Parameters in Extrapolating the Performance of TCP in MANETs. International Journal of Computer Engineering and Technology, 7(6), 2016, pp. 01–08.

ISSN: 0976-9102 (ONLINE)
DOI: 10.21917/ijivp.2017.0230

FRACTAL COMPRESSION TECHNIQUE FOR COLOR IMAGES USING VARIABLE BLOCK

Nisar Ahmed[1] and Syed Abdul Sattar[2]

[1]Department of Electronics and Communication Engineering, Mewar University, India
[2]Department of Electronics and Communication Engineering, Nawab Shah Alam Khan College of Engineering and Technology, India

Abstract

The main intention of Fractal Image Compression is to reduce the size of image and maintain good level of their reconstructed image. A major issue in Fractal Image Compression is decrease in image quality, compression ratio and PSNR. To overcome these issues we employ Fractal transformation with entropy coding. There are two phases in the proposed approach. In the first phase color images are separated into three RGB planes using variable range block size. In second phase by applying the inverse transform and iterative functions the image is restored. It is observed that the results are improving in fractal compression for both gray images as well as color images. In this work high CR and PSNR is observed compared to fixed block range and other existing methods. The proposed work yields better CR of 20 and high PSNR.

Keywords:

Fractal Image Compression, Variable Block Size, CR, PSNR

1. INTRODUCTION

Images are interpreted as accumulation of bits (a bit is a binary unit of information) and stored in digital media storages in the computer. These bits are denoted as pixels or points that form the picture elements. A human eye progresses large amount of information of approximately 8 million bits to create a single image. Profuse pixels constitute the formation of a reasonable quality image which, the eye arbitrates the 8 million bits from 'yes' and 'no' answers to develop the image progression. Redundancy of the pixels enriches the absorption capability of the eye to interpret the images into prominence, thus making them more apprehensible. This redundancy can be manipulated and reduced through algorithms for optimum storage and restored for recovery. An image can be alternated in many ways that are either not noticed by the human eye or do not contribute to the decay of the image. The current most famous method of image compression depend on elimination of high frequency wavelengths of the signal and storing only the low frequency components.

Fractal based image compression (FIC) technique exploit redundancy due to self-similarity properties in images to achieve compression [1]. A domain optimization technique in fractal image compression [2] deals with reducing complexity and increasing accuracy that is range and domain block alignment and matching. Fractal Image Compression is a separated image that can be a part of parts; the main motto of the fractal image compression is to reduce the redundancy or the image as well as image irrelevance to store [3]. Moreover image compression is a transformation called relative transformation. Fractal image compression is proposed in [4] based on Lossy compression principle which provides a very high compression ratio by completely eliminating the redundant information. The drawback of this technique is the degradation during reproduction of the image because of insufficient pixels for the filler sections comprising the redundant pixels. The image which is reconstructed contains degradation relative to the original image because the compression scheme completely neglects the redundant information and is more capable for achieving higher compression [5]. Fractal image compression (FIC) is based on the theory of Iterated Function System (IFS) which is used to represent the self-similarities of the images and is represented as a finite set of contraction mapping for each image that has the fixed point which is identical to the image itself [6]-[8]. Fractal image compression (FIC) seems to be one of the favorable methods of lossy image compression due to its advantages like resolution independence, high compression ratio, and fast decompression [9]. This technique was initially proposed by Jacquin and is based on the method of lossy compression. Here the images are considered to be fractals rather than pixels, which will be mainly suitable for natural images for encoding, analyzing with other image compression methods [10], [11] Suggested another system focused In the current scenario, fractal image compression plays a major role in research areas, it is one of the kind of modern image compression technique coefficients. Gohar and Habib [12] suggested in image compression two different processes is carried out namely encoding and decoding. In encoding section the original image takes as an input and after processing the compressed image will be its output but in decoding section the process is carried out in reversible order. In the event that the neighborhood heights are not fulfilled, the second phase of the calculation is completed keeping in mind the end goal to investigate further likenesses from the complete picture. Kharate and Patil [13] proposed fractal compression process through the self-similar properties in various fractions of images which relies on the fact that the image parts are often resembles other parts of the same image. Sekhar and Aruna [14] proposed a fractal is a rough or fragmented geometric shape that can be subdivided into parts, each of which is reduced/size copy of the whole. Khalil [15] found a major drawback in Fractal image compression (FIC), where encoding of fractals is very complex, compressing time is very high due to its complexity and consumption of time to search for the best matching block and more powerful. Anson [16] has recommended the IFIC using range block size. Barnsley and Hurd [17] have recommended applying the transformation iteratively on the random initial image and the result will be re-arranged as the original image. Banu [18] has proposed an efficient search of the domain pools for color image compression using Genetic Algorithm (GA). The proposed method reduces the coding process time and intensive computation tasks. Image quality factor, compression ratio and coding time are analyzed in this approach and comparative results are obtained but this method is suitable for only limited categories like facial, building and vegetable images.

2. FRACTAL COMPRESSION

Fractal Image compression is one of the popular demanding research field in the current trend, mainly it deals with the images, video sequences, graphics, animations etc. Fractal compression is one of the kind of lossy image compression technique, here it will partition the images into blocks then perform some transformations and then compress it. Normally based on lossy compression, the compression ratio will be high but the quality of the images will not attain the expected results and there will be a loss of information's too. There are many technologies developed in different research areas to improve the image quality while compressing the images. In image compression consumption of time is more in encoding and decoding. There are some limitations existing too. This has motivated us to develop an efficient compression technique for color images to enhance high compression ratio and PSNR.

Various compression algorithms are used to reduce the size of the images without reducing the quality of images [19]. Algorithms like embedded zero wavelet algorithm, convergent algorithm, Fuzzy vector quantization algorithm etc. are used previously to compress the images with high quality [20].

3. PROPOSED ALGORITHM

The main objective of this research is to compress the image with high ratio and increase the PSNR of the encoding phase

Step 1: Divide color image into sub windows. Each sub window block is called R- block.

Step 2: For each R-block, find a Domain block, which most likely represents current R-block after a certain transform.

Step 3: For every R-block, find D-block from D-pool which is most likely parallel to it.

Crop the D-block size to the size of R-block by Shrink operation and, mark the D-block as D′-block after Shrink operation is applied.

Transpose the D′- block by using the following eight relative transformation equation matrices proposed by Jacquin. The eight relative transformations matrices are represented in the equations as follows,

Consider $T = [a_{ij}]_n$ with $n = 2$ where $1 \le (i,j) \le 2$, $\begin{bmatrix} a_{11} & a_{12} \\ a_{21} & a_{22} \end{bmatrix}$.

Relative transformations matrices can be represented with the following Eq.(1) to Eq.(8),

$$T_0 \text{ is } a_{ij} = \begin{cases} 1 & \text{if } i = j \\ 0 & else \end{cases} \tag{1}$$

$$T_1 \text{ is } a_{ij} = \begin{cases} (-1)^{2^i + j} & \text{if } i \neq j \\ 0 & else \end{cases} \tag{2}$$

$$T_2 \text{ is } a_{ij} = \begin{cases} -1 & \text{if } i = j \\ 0 & else \end{cases} \tag{3}$$

$$T_3 \text{ is } a_{ij} = \begin{cases} (-1)^{i+2^j} & \text{if } i \neq j \\ 0 & else \end{cases} \tag{4}$$

$$T_4 \text{ is } a_{ij} = \begin{cases} (-1)^{ij} & \text{if } i = j \\ 0 & else \end{cases} \tag{5}$$

$$T_5 \text{ is } a_{ij} = \begin{cases} (-1)^{ii+1} & \text{if } i = j \\ 0 & else \end{cases} \tag{6}$$

$$T_6 \text{ is } a_{ij} = \begin{cases} (-1)^{i+j} & \text{if } i \neq j \\ 0 & else \end{cases} \tag{7}$$

$$T_7 \text{ is } a_{ij} = \begin{cases} 1 & \text{if } i \pm j \\ 0 & else \end{cases} \tag{8}$$

Above eight relative transformation blocks are generated for each D′-block and these blocks are composite new D-pool.

Compare each R-block with the blocks which are in D′- pool and obtain nearly all like block. The parallelism can be measured with normal conflict MSE using the Eq.(9).

$$MSE = \left\| X_k D_k + Y_k I - R_k \right\| \tag{9}$$

where X and Y are the coefficients and should have the values for making the MSE minimum. The X_k and Y_k are represented in Eq.(10) and Eq.(11) respectively,

$$X_k = \frac{B^2 \langle D_k, R_k \rangle - \langle D_k, I \rangle \langle R_k, I \rangle}{B^2 \langle D_k, R_k \rangle - \langle D_k, I \rangle^2} \tag{10}$$

$$Y_k = \frac{\langle R_k, I \rangle - \langle D_k, I \rangle}{B^2} \tag{11}$$

$$W = \{D_k(x,y),\ T_k,\ X_k,\ Y_k\} \tag{12}$$

where R_k represents the relative transformation W for each R-block.

Fractal image coding, the original image is segmented into non-collaborating regions called range blocks and collaborating regions called domains blocks. For each range block affine transformations given in the Eq.(13) is used to match as best domain block.

$$W_i \begin{bmatrix} x \\ y \\ z \end{bmatrix} = \begin{bmatrix} a_i & b_i & 0 \\ c_i & d_i & 0 \\ 0 & 0 & s_i \end{bmatrix} \begin{bmatrix} x \\ y \\ z \end{bmatrix} + \begin{bmatrix} e_i \\ f_i \\ o_i \end{bmatrix} \tag{13}$$

where S_i controls the contrast and 0_i controls the brightness and a_i, b_i, c_i, d_i, e_i, f_i denote the eight symmetries such as identity, reflection about mid-vertical and horizontal axis, first and second diagonal.

The Fig.1 is the proposed fractal image compression.

1. Partition each plane image into non-overlapping blocks, called Range or R-block.
2. Select the maximum Range block of size (R_{max}) as 16 or 8 and minimum block of size (R_{min}) of 4 or 8. R-blocks are compared with domains from the domain pool, which are double the range size.
3. A window size of $\alpha \times \alpha$ is slided on 3 images in $\alpha/2$ or $\alpha/4$. The pixels are averaged in groups to reduce to the size.
4. After partitioning and transformation, fractal encoding finds suitable candidate from all blocks to encode any particular R block.

5. To increase encoding speed classification of sub-image into upper right, upper left, lower right and lower left quadrants is done as shown in Fig.2. It is shown that in any one of the three ways as canonical ordering [21].

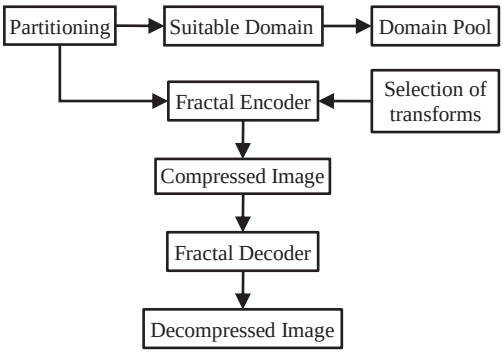

Fig.1. Proposed Fractal Compression Technique

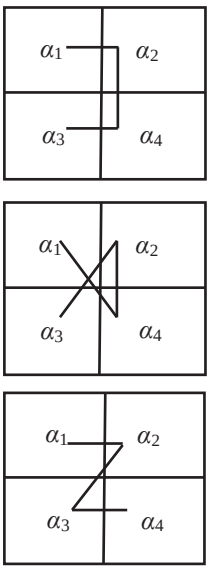

Fig.2. Arrangement of Sub Blocks Images

Classification Schemes are

- Major Class 1: $\alpha_1 > \alpha_2 > \alpha_3 > \alpha_4$
- Major Class 1: $\alpha_1 > \alpha_4 > \alpha_2 > \alpha_3$
- Major Class 1: $\alpha_1 > \alpha_2 > \alpha_4 > \alpha_3$

Entropy of coding is used to achieve fractal compression for mapping the range block to the domain block in the coding process.

4. RESULTS AND DISCUSSION

To find the effectiveness of the proposed method by means of the experimental results. The Satellite urban and rural images are reduced to standard size 256×256. The standard Lena images of size 512×512 has been used for fractal compression analysis. The first phase consists of applying color and gray images to a set of five images. We have used five different test images in our experiment. In the final phase we have calculated the CR and PSNR with the resultant images. The imageries are subjected to fractal compression scheme by using the variable range block size for three cases namely,

a) R_{max} = 16 and R_{min} = 4
b) R_{max} = 16 and R_{min} = 8
c) R_{max} = 8 and R_{min} = 4,

Three different variable range methods are displayed in Table.1 and Table.2, respectively. The novelty is, the proposed method is applied on both grey level and color images. The proposed method gives the comparable results when applied on both color and grey images. It is seen from Table.1 that the CR and PSNR values derived from Lena, Satellite Rural, Rose, Satellite Urban and Bird imageries do not show significant difference between the CR and PSNR values. However, Table.1 clearly demonstrates that CR and PSNR values derived for the Lena and other imageries show maximum values for case (b) where the variable range block size R_{max} = 16 and R_{min} = 8. It is clearly seen from Table.1 and Table.2 shows for Color and Grey images values for CR and PSNR for all the types of imageries. The variable range block sizes shows higher CR and PSNR compared to fixed and other methods. This comparison is shown in Table.3, Table.4, Table.5, and Table.6, respectively.

Table.1. CR and PSNR of Test Color Images

Test Images	**R_{max} =16 and R_{min} = 4**		**R_{max} =16 and R_{min} = 8**		**R_{max} = 8 and R_{min} = 4**	
	CR	**PSNR**	**CR**	**PSNR**	**CR**	**PSNR**
Lena Image	2.99	27.88	15.45	20.16	3.16	30.15
Satellite Rural Image	3.87	19.75	18.08	17.88	3.33	35.65
Rose Image	4.44	27.01	17.85	20.11	4.02	35.66
Satellite Urban Image	3.55	24.55	18.90	22.89	3.37	32.59
Bird Image	3.68	18.88	17.45	24.95	3.11	31.79

Table.2. CR and PSNR of Test Gray Images

Test Images	**R_{max}=16 and R_{min} = 4**		**R_{max}=16 and R_{min} = 8**		**R_{max}=8 and R_{min} = 4**	
	CR	**PSNR**	**CR**	**PSNR**	**CR**	**PSNR**
Lena Image	2.99	27.88	15.45	20.16	3.16	30.15
Satellite Rural Image	3.87	19.75	18.08	17.88	3.33	35.65
Rose Image	4.44	27.01	17.85	20.11	4.02	35.66
Satellite Urban Image	3.55	24.55	18.90	22.89	3.37	32.59
Bird Image	3.68	18.88	17.45	24.95	3.11	31.79

Variable range block size R_{max} = 16 and R_{min} = 8 are shown in Fig.3(a)-(b), Fig.4(a)-(b), Fig.5(a)-(b), Fig.6(a)-(b), Fig.7(a)-(b) and Fig.8(a)-(b). These are the reconstructed images for Color and Grey Lena, Rose, urban satellite, bird and rural satellite imageries. As seen in the figure and tables that the proposed IFIC method for the images of Lena, Bird, Satellite Rural, Rose and urban satellite gives significantly large CR values exhibits a very good quality of the reconstructed imageries.

(a) (b)

Fig.3. Results of Lena color image (a) Lena Image (b) reconstructed Lena image

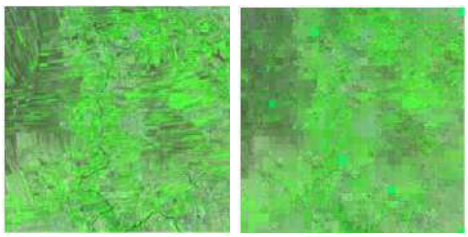

(a) (b)

Fig.4. Results of Satellite Urban color image (a) original satellite urban Image (b) re-constructed satellite image

(a) (b)

Fig.5. Results of Lena gray image (a) original lena gray Image (b) reconstructed lena image

(a) (b)

Fig.6. Results of Rose gray image (a) original rose gray Image (b) reconstructed rose image

(a) (b)

Fig.7. Results of Bird gray image (a) original gray bird Image (b) reconstructed bird image

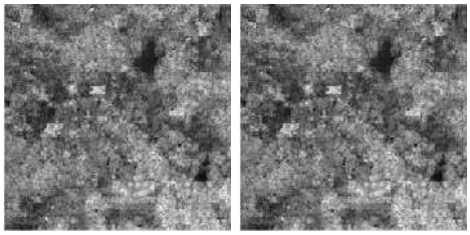

(a) (b)

Fig.8. Results of satellite rural gray image (a) original gray satellite Image (b) reconstructed satellite image

4.1 COMPARISON WITH OTHER EXISTING METHODS

The present Fractal Image Compression [FIC] is compared with the other existing methods, like standard algorithm of quadtree technique [22], fractal with quadtree and DCT technique [23], and Fractal image compressions based on variable size range block method [24]. The CR and PSNR values obtained from the present method of variable range block size for test imageries are compared with the results of existing methods [22], [23], [24]. Standard algorithm of quadtree technique (SAQT), fractal with quadtree and DST technique (FQandDST), FIC based on variable size range block method (FICVRB), Proposed FIC in both color and gray level image with range block size R_{max} = 16 and R_{min} = 8 are comparatively shown in the Table.3 to Table.6.

Table.3. Comparison of CR with other available methods for color images

Test Images	SAQT	FQ and DST	FIC VRB	FIC
Lena Image	10.01	14.44	13.0	17.53
Satellite Rural Image	8.68	13.35	15.5	18.99
Rose Image	8.32	12.56	15.4	18.13
Satellite Urban Image	10.66	13.87	13.87	17.78
Bird Image	9.99	14.98	16.56	16.55

The comparison chart of CR and PSNR values for the proposed method and other existing methods in both case i.e. color and grey image when applied on test images i.e. Lena, Satellite rural image, Satellite urban image, Bird and Rose images are shown in Fig.9 to Fig.12.

Table.4. Comparison of CR with other available methods for grey images

Test Images	SAQT	FQ and DST	FIC VRB	FIC
Lena Image	8.78	13.55	16.87	19.99
Satellite Rural Image	9.77	13.33	15.75	18.89
Rose Image	9.85	12.15	15.75	19.9

Satellite Urban Image	9.15	13.03	17.71	18.53
Bird Image	8.98	13.01	15.99	19.54

Table.5. PSNR of the proposed method and other available methods of color images.

Test Images	SAQT	FQ and DST	FIC VRB	FIC
Lena Image	24.89	29.45	18.55	30.33
Satellite Rural Image	26.33	30.98	23.01	33.55
Rose Image	26.08	32.01	21.50	35.55
Satellite Urban Image	25	30	16	32
Bird Image	26.45	31.67	23.80	33.11

Table.6. PSNR of the proposed method and other available methods of gray level images

Test Images	SAQT	FQ and DST	FIC VRB	FIC
Lena Image	23.13	29.88	26.5	32.25
Satellite Rural Image	25.15	31.19	24.55	31.15
Rose Image	24.33	29.10	18.55	32.01
Satellite Urban Image	25.36	31.87	25.55	31.95
Bird Image	25.15	30.48	23.76	32.78

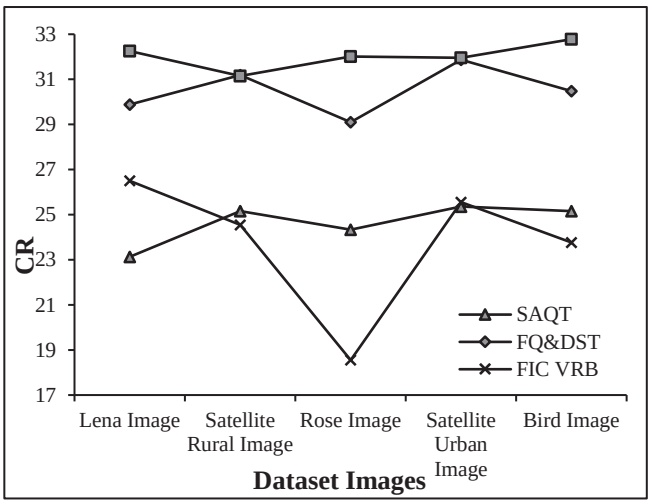

Fig.9. Comparison chart of CR of the proposed method with other existing methods when applied on color test images

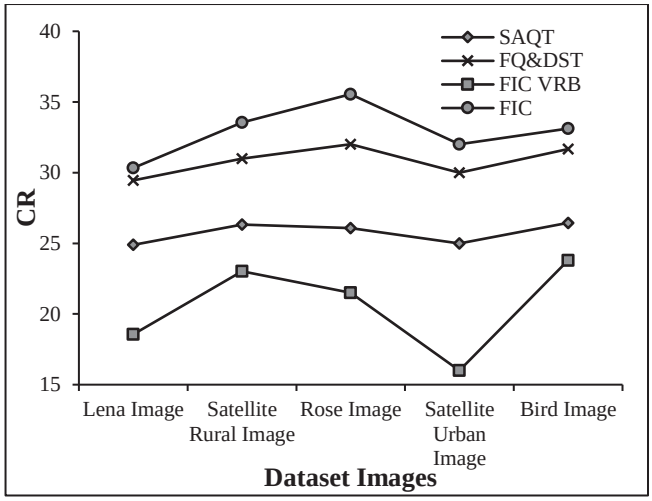

Fig.10. Existing methods when applied on gray test images Comparison chart of CR of the proposed method with other

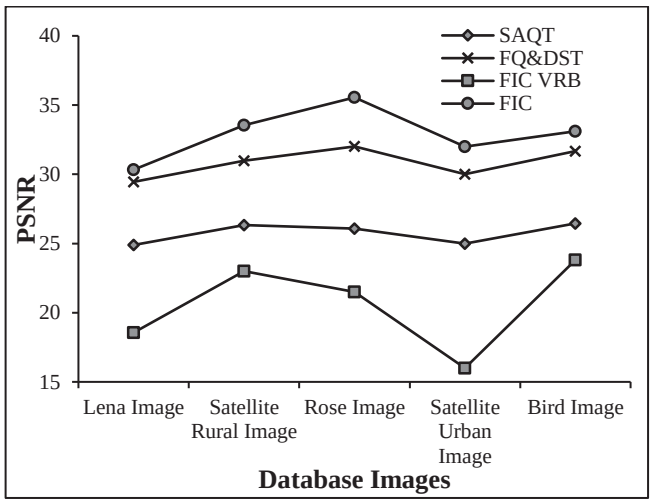

Fig.11. Comparison chart of PSNR of the proposed method with other existing methods when applied on color test images

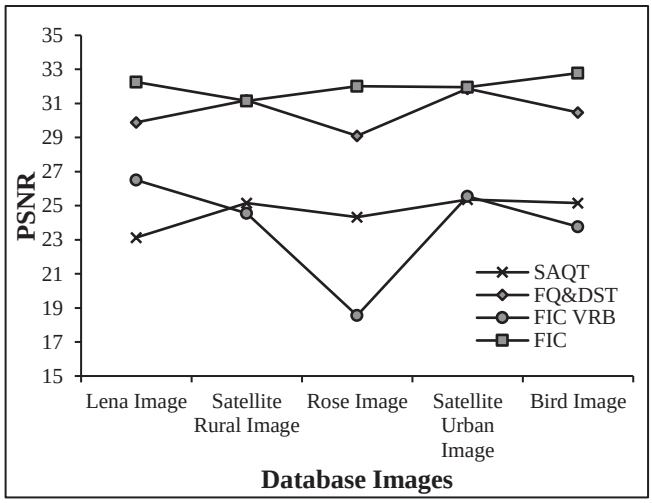

Fig.12. PSNR of the proposed method and other available methods of gray level images

5. CONCLUSION

In the present paper, an experimental work is done to get an improved fractal image compression. The experimental results clearly depict that for the variable range block size of R_{max} = 16 and R_{min} = 8 a better result is yielded with good image quality and low computational cost. The uniqueness of the proposed method is, the RGB image is divided into three planes and using range block fractal concept it is compressed with reduced computational cost. When compare with the fixed block size method of fractal compression schemes, the present method exhibits higher compression ratio and PSNR values for all types of imageries. When the proposed method is applied on both color and gray scale images it gives approximately same CR and PSNR values. The proposed method when applied on different types of images like satellite image, standard color images and natural image, gives comparatively good results. The PSNR values obtained in this approach is always nearer to 30.

REFERENCES

[1] Gagnpreet Kaur, Hitashi Hitashi and Gurdev Singh, "Performance Evaluation of Image Quality based on Fractal Image Compression", *International Journal of Computers and Technology*, Vol. 2, No.1, pp. 20-27, 2012.

[2] Zhuang Wu and Bixi Yan, "An Effective Fractal Image Compression Algorithm", *Proceedings of IEEE International Conference on Computer Application and System Modeling*, pp. 139-143, 2010.

[3] Sumathi Poobal and G.Ravindran, "Analysis on the Effect of Tolerance Criteria in Fractal Image Compression", *Proceedings of IEEE International Workshop on Imaging Systems and Techniques*, pp. 119-124, 2005.

[4] A. Selim, M.M. Hadhoud, M.I. Dessouky and F.E. Abd El-Samie, "A Simplified Fractal Image Compression Algorithm", *Proceedings of IEEE International Conference on Computer Engineering and Systems*, pp. 53-58, 2008.

[5] Dietmar Saupe, "Accelerating Fractal Image Compression by Multi-Dimensional Nearest Neighbor Search", *Proceedings of IEEE Data Compression*, pp. 222-231, 1995.

[6] Arnaud E. Jacquin, "Image Coding based on a Fractal Theory of Iterated Contractive Image Transformations", *IEEE Transaction on Image Processing*, Vol. 1, No. 1, pp. 18-30, 1992.

[7] M. Barnsley, "*Fractals Everywhere*", 2nd Edition, San Diego Academic Press, 1993.

[8] Y. Fisher, "*Fractal Image Compression*: *Theory and Application*", Springer, 1995.

[9] Brendt Wohlberg and Gerhard De Jager, "A Review of the Fractal Image Coding Literature", *IEEE Transactions on Image Processing*, Vol. 8, No. 12, pp. 1716-1729, 1999.

[10] Guojun Lu and Toon Lin Yew, "Applications of Partitioned Iterated Function Systems in Image and Video Compression", *Journal of Visual Communication and Image Representation*, Vol. 7, No. 2, pp. 144-154, 1996.

[11] Douda Sofia, Bagri Abdallah, Abdel Hakim and Amer Elimrani, "A Reduced Domain Pool based on DCT for a Fast Fractal Image Encoding", *Electronic Letters on Computer Vision and Image Analysis*, Vol. 10, No. 1, pp. 11-23, 2011

[12] Vahdati Gohar, Khodadadi Habib, Yaghoobi Mahdi and Akbarzadeh-T Mohammad, "Fractal Image Compression Based on Spatial Correlation and Hybrid Particle Swarm Optimization with Genetic Algorithm", *Proceedings of 22nd International Conference on Software Technology and Engineering*, pp. 134-138, 2010.

[13] G.K. Kharate and V.H. Patil, "Color Image Compression Based on Wavelet Packet Best Tree", *International Journal of Computer Science Issues*, Vol. 7, No. 2, pp. 31-35, 2010.

[14] D. Venkatasekhar and P. Aruna, "A Fast Fractal Image Compression using Huffman Coding", *Asian Journal of Computer Science and Information Technology*, Vol. 2, No. 9, pp. 272-275, 2012.

[15] M. Khalil, "Image Compression using New Entropy Coder", *International Journal of Computer Theory and Engineering*, Vol. 2, No. 1, pp. 39-42, 2010.

[16] Fractal Image Compression, Available at: http://www.math.psu.edu/tseng/class/Fractals.html.

[17] Michael Barnsley and Lyman Hurd, "*Fractal Image Compression*", AK Peters Limited, 1992.

[18] A.R. Nadira Banu Kamal and P. Priyanga, "Iteration Free Fractal Compression using Genetic Algorithm for Still Colour Images", *ICTACT Journal on Image and Video Processing*, Vol. 4, No. 3, pp. 785-790, 2014.

[19] Mohammed Ismail and S.M. Basha, "Improved Fractal Image Compression using Range Block Size", *Proceedings of IEEE International Conference on Computer Graphics, Vision and Information Security*, pp. 284-289, 2015.

[20] S.V. Veena Devi, A.G. Ananth, "Fractal Image Compression of Satellite Imageries using Variable Size of Range Block", *Proceedings of IEEE International Conference on Signal and Image Processing Applications*, pp. 172-175, 2013.

[21] Mario Polvere and Nappi Michele, "Speed-Up in Fractal Image Coding: Comparison of Methods", *IEEE Transaction on Image Processing*, Vol. 9, No. 6, pp. 1002-1009, 2000.

[22] A.H. Husseen, S.Sh. Mahmud and R.J. Mohammed, "Image Compression using Proposed Enhanced Run Length Encoding Algorithm", *Ibn AL- Haitham Journal for Pure and Applied Science*, Vol. 24, No. 1, pp. 18-25, 2011.

[23] K. Sharmila and K. Kuppusamy, "A New Color Image Compression Based on Fractal and Discrete Cosine Transform", *International Journal of Engineering and Computer Science*, Vol. 3, No. 7, pp. 7054-7057, 2014.

[24] S.V. Veenadevi and A.G. Ananth, "Fractal Image Compression of Satellite Color Imageries using Variable Size of Range Block", *International Journal of Image Processing*, Vol. 8, No. 1, pp. 1-8, 2014.

International Journal of Research and Review
www.ijrrjournal.com E-ISSN: 2349-9788; P-ISSN: 2454-2237

Short Communication

A Structural Study on Bubble Deck Slab and Its Properties

Mir Shahed Ali[1], Dr. S. Amaresh Babu[2]

[1]M.Tech Structural Engineering, Department of Civil Engineering, Nawab Shah Alam Khan College of Engineering and Technology, Hyderabad-24, TS.
[2]Head of Department, Department of Civil Engineering, Nawab Shah Alam Khan College of Engineering and Technology, Hyderabad-24, TS.

Corresponding Author: Mir Shahed Ali

ABSTRACT

Housing all over the world majorly comprises of concrete structures. They provide isolation and thermal comfort to the occupants. Majority of the concrete structures have flooring/roofing of thick concrete to bear the design loads. Due to his, the complete volume (eliminating the negligible volume of the reinforcement) of the roof slab comprises of concrete. Due to this, production of concrete has increased. Concrete production is not environment friendly. It is the primary producer of Carbon dioxide. In addition to this, the problem of concrete waste is at rise. Concrete waste can be reduced by two ways: recycling and using efficient volumes. Recycling is using the concrete waste in concrete generation which is of course of lower quality. Efficient volume is the way of using concrete in the most efficient way possible by substituting materials. In this paper, polyethylene balls are used in the slab to reduce concrete volume while maintaining the structural properties of the concrete. A comparison of strength of slab with the polyethylene balls and without them has been done to show the effectiveness of the new method. Various other strength tests were carried out and have been tabulated. At the end, cost effectiveness of the proposed slab has also been given.

Index terms: Bubble deck slab, Polyethylene balls, recycling concrete, concrete slabs systems.

1. INTRODUCTION

Concrete is strong in compression and weak when under tension. While considering a reinforced concrete slab, all the concrete above the neutral axis is subject to compressive forces and all the concrete below the neutral axis is subject to tensile forces. This supports the fact that concrete is the tension zone is of little use and contributes to making the slab heavier and reducing its overall efficiency. Upon having more slabs, it shall contribute to increased dead load of the structure. This dead load which is additional in nature and does not serve any positive purpose can be removed. This is done by introducing voids in the slab. Since voids cannot be made to form on their own, hollow balls or low weight balls are placed in the concrete to reduce the overall weight of the concrete. This concept bubble deck slab has hollow spheres made from recycled plastic placed between two layers or meshes of reinforcement. In this paper, we are going to study two-way slabs and design two ways slabs (both conventional and bubble deck and its types).

If weight of slab is reduced, then dimensions of other supporting structural members (such as beams and columns) shall also decrease. Since there is decrease in both the slab and supporting member volumes, reduction in total load of the structure and the volume of concrete used is evident.

A bubble deck slab reduces volume of concrete up to 33% in the slab itself and up to 18% reduction in the supporting structural members. This reduction is done by removing the volume of concrete in the center portion where there is no need of concrete structurally. Such a practice of removal of concrete from regions where there is little or no structural requirement is a very old practice, but in this case the approach is different due to use of recyclable plastic (polyethylene) balls. It also provides greater insulation due to air trapped inside since air is a bad conductor of heat. The structure shall retain the heat inside for a long period of time. This causes efficiency in energy utilization to heat up the room or cool down the room depending on the region of construction.

Time is also saved in laying a bubble deck slab as the amount of concrete needed to be handled is far less than a conventional slab. The number of manual labors involved in the task can also be reduced for the same area of the slab. It was observed that a bubble deck slab is developed 20% fast that a conventional slab of same area. All the previous statements show the savings done in terms of concrete volume, time, manual effort and transport timings.

2. Objectives

- To use hollow polyethylene balls in a slab.
- To show the procedure of the experiment and a comparison of all parameters between a bubble deck slab and a conventional slab.
- To estimate concrete volume saved
- To study and compare the self-weights of the slabs
- from the Universal Testing Machine.
- To study failure or cracking patterns on both the slab types
- To analyze the results of M20 and M25 grades of concrete on the slabs

3. Properties of materials used

3.1 Polyethylene bubbles

Bubbles are made of high-density polyethylene. It is a non-porous material which does not react chemically with concrete or the reinforcement. The bubbles usually have high stiffness and strength to support the concrete in conjunction with the reinforcement provided safely during both placing the concrete and after.

Diameter of bubbles ranges from 90mm to 120mm. Due to this, the depth of slab varies from 140mm to 170mm.

Bubble spacing should be more than $1/9^{th}$ of bubble diameter.

3.1.1 Chemical properties:

Table 1: Chemical properties

Property	Description
Marketing name of product	HDPE (High Density Poly-Ethene)
Chemical name	Polyethylene
Chemical designation	$(-CH_2-CH_2-)_n$
Genus	Polyolefin
Hazardous substance	NO
Color	desired color can be obtained
Odor	feebly of paraffin
Relative Density	950 kg/m^3
Melting point	135˚C
Softening point	123˚C
Solubility	Insoluble in water

3.2 Concrete

Concrete used for filling the slab should be more than M30. It is an added advantage if a self-compacting concrete variant is used. This way, there will be proper compaction ensured in every unreachable region inside the slab. Aggregate used in this concrete should be less than 15mm.

For the experiment,

Table 2: Properties of concrete

Material	Description
Concrete	M30 Concrete mix design as pe IS 10262: 2009 Slump Value: 74mm
Cement	Ordinary Portland Cement (OPC) 53 Grade Testing done as per IS 456: 2000 Fineness: 9.2% Specific gravity: 3.14 Consistency: 31.06%
Coarse aggregate	10mm Conforming to IS 383 Specific Gravity: 2.8
Fine aggregate	River sand 4.75mm to 150 microns Conforming to IS 383 Specific Gravity: 2.59 Sieve Analysis: C_c = 0.863, C_u = 9.702, D_{10} = 0.17
Water	Potable water used for curing and mixing Conforming to IS 456: 2000

3.3 Reinforcing bars:

This is an integral part of the whole assembly. The top and bottom slab of concrete have one mesh each, which can be either tied or welded. Transverse ribs are used to keep these meshes intact after the bubbles are placed in the allocated positions between the meshes. Height difference between the bars is related to the bubble diameter. If the bubble diameter is greater, the height difference is greater and vice versa.

For the experiment,

F_y = 500 N/mm^2 were used.

Diameter of the bars used is as per the design.

4. Advantages

Following are the advantages of bubble deck slabs that have been justly outlined.

1) Structure
   a) Less weight than a conventional slab
   b) Depth of foundation is less
   c) More strength for same volume of slab
   d) Use of beams can be nullified if the span allows
   e) Columns used are of less thickness
   f) Has similar stiffness and bending strength of that of a conventional slab
2) Fabrication
   a) Light weight
   b) Less equipment or cheap lifting equipment
   c) Less work for manual labors
3) Engineering properties
   a) Less time required to cure the slab due to less volume of concrete
   b) Lower creep due to less concrete in the center and less heat generation
   c) High explosion resistance due to bi-axial design of the slab
   d) High earth-quake resistance due to less weight and rigid design
4) Environment
   a) Less CO_2 emissions
   b) Less concrete used
   c) Recycling of plastic possible
   d) Less efforts for transporting
5) Safety
   a) Fire proofing design
   b) Moisture or condensation proof design
   c) Earthquake resistance to an extent due to reduced weight
6) Cost
   a) Savings in concrete costs
   b) Savings in manual labor costs
   c) Decrease in construction and/or fabrication time
   d) Savings in transportation costs due to low weight handling
   e)

5. Experiment

5.1 Design of concrete specimen

Design of concrete mix was carried out as per the IS 10262: 2009. Size of the specimen is taken as 0.5m×0.5×0.1m for calculation purposes. Material required for the said dimensions is given below in table

Table 3: Experiment material specification

Material	Weight in kg and volume in liter
Cement	438 kg
Fine aggregate (Sand)	583 kg
Coarse aggregate	920 kg
Water (from water: cement ratio taken as 0.45)	198 liters

5.2 Design of the reinforcement specimen

Dimension of the specimen is 0.5m×0.5m×0.1m

Cover for the specimen is 20mm in both directions

5 bars of 8mm diameter have been used

Figure 1: Cover and specimen Reinforcement

5.3 Compressive strength of Conventional Concrete Slab:

Testing was done on the UTM after curing for 28 days. Dimensions of the block for testing was 0.5m×0.5m×0.1m. Its weight when measured was 22.76Kg.Maximum load on the slab was observed as 640 KN.

Equation 1: Calculation of compressive strength

$$\text{Compressive strength of the block} = \frac{\text{Ultimate Load}}{\text{Area of Slab}}$$

From the above equation, the compressive strength of the concrete slab is 25.6 N/mm^2.

5.4 Compressive strength of Bubble Deck Slab:

Testing was done on the UTM after curing for 28 days. Dimensions of the block for testing was 0.5m×0.5m×0.1m. Its weight when measured was 20.43 Kg. It can be noted that the weight of the bubble deck slab is lighter in weight than the conventional slab. Maximum load on the slab was observed as 655 KN.

Equation 2: Calculation of compressive strength of the bubble deck

$$\text{Compressive strength of the block} = \frac{\text{Ultimate Load}}{\text{Area of Slab}}$$

From the above equation, the compressive strength of the concrete slab is 26.2 N/mm^2.

6. Testing procedure

1. This testing is done at 28-day age as described. The test slabs are simply supported and load at a single point.
2. To ensure uniformity, the cover distances from the either sides of the loading frame are checked and ensured that the load is acting at the center.
3. These specimens were placed on the Universal Testing Machine and load was made to act at the centerline.
4. All gauges were kept in appropriate locations and initial readings were noted.
5. After every load increment made, the values on gauges were recorded for both middle span deflection and cracks developed along with their propagation.
6. All deflections were measured at their middle-span. When the loading was advanced, the increment of load was made smaller till failure was reached.
7. At failure, the load indicator stopped working and deflection increased very fast without any increase in the load application.
8. All the values of load and deflection were noted for every 5KN interval.

Cracking patterns on the slab can be seen in the figure below.

Figure 2: Crack patterns while testing the slabs

7. Observation

The first observation is that the behavior of the bubble deck slab is very much dependent on the ratio of bubble diameter to the thickness of the slab.

For M20 concrete

Table 4: M20 concrete slab load and deflections

Load in KN	Conventional Slab	Bubble Deck Slab 1	Bubble Deck Slab 2
30	0.29	0.89	0.84
60	0.89	1.23	1.42
90	1.07	1.91	1.99
120	1.85	2.89	3.42
150	2.01	4.23	4.82
180	3.49	6.19	6.79
210	4.25	8.09	9.01

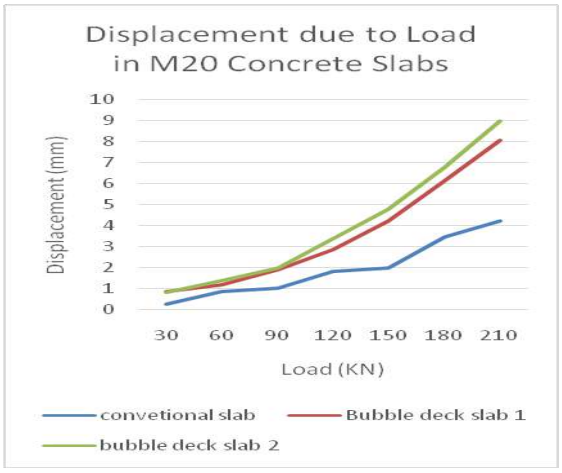

Graph 1: Displacement due to load in M20 Concrete slabs

For M25 Concrete used in the slab

Table 5: M25 concrete load and deflections

Load in KN	Conventional Slab	Bubble Deck Slab 1	Bubble Deck Slab 2
30	0.069	0.91	0.91
60	0.091	1.11	0.67
90	0.121	1.21	1.12
120	0.29	2.01	1.31
150	0.44	2.41	2.49
180	1.03	2.9	3.31
210	1.35	3.5	3.52
240	2.39	4.07	4.21
270	3.02	5.7	4.71
300	3.39	6.98	5.81
330	4.19	7.59	6.84

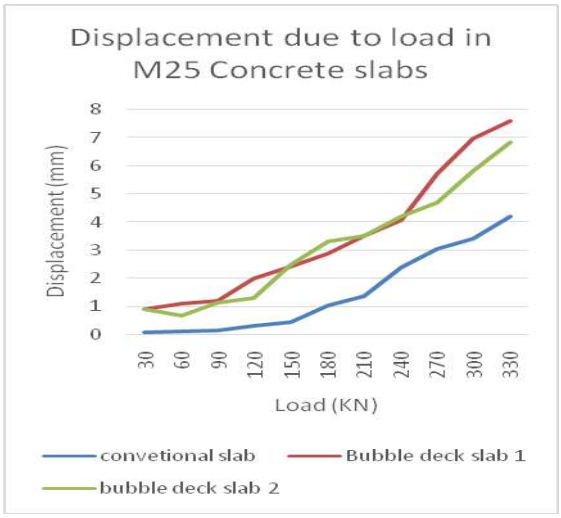

Graph 2: Displacement due to load in M25 concrete slabs

8. DISCUSSION

From this experiment, we can say that the bubble deck slab has a reduced volume of concrete which ultimately decreases the dead load on the slab. Parallelly, the load bearing capacity also increases with respect to a conventional concrete slab.

Type of arrangement of bubbles also plays a major role on the load carrying capacity of the slab. In alternative arrangement of the bubbles, there is an increase in the load bearing capacity than the convention slab but less than that of a continuous bubble deck slab. There is also a considerable change in the deflections shown by the bubble deck slabs which are nearer in deflection the conventional slabs.

Bubbles in the bubble deck slab improved the elasticity of the slab. A conventional slab deflects less than a bubble deck slab before failure. Based on the deflection, the failure can be estimated, and other preventive measures can be taken. Quantity of bubbles in the slab affects the elasticity property.

For a given volume, the compressive strength of a bubble deck slab is higher than the compressive strength of the conventional slab.

Comparison between the two slabs:

In a conventional slab, with dimensions 500mm×500mm×180mm, the maximum shear load taken by the slab was 160 KN. Crack propagation occurred at 75 KN.

In a bubble deck slab, with dimensions 500mm×500mm×180mm, the maximum shear load taken by the slab was 156 KN. Crack propagation occurred at 59 KN.

9. CONCLUSION

Bubble deck slabs give greater flexural strength, stiffness and shear force capacity. It was observed that when same quantity of concrete and reinforcement were used, the said structural properties of the slab increased by at least 60% than that of a conventional slab. The economy of construction increased by 40% when compared to a conventional slab.

For various experimental cases, the bubble deck slab had had deflections equal to that of conventional slabs under same loading conditions. Similarly, moments were 7-10% reduced to that of a conventional slab. The base shear of the structure also reduced (12-14%) due to decrease in loads by the concrete.

Economy in the corresponding structural members (such as beams and columns) was also obtained. It is due to the decrease in dead load and achievability of longer spans without increasing any dimension of the beams or columns.

There is an increased load bearing capacity in the bubble deck slab when compared to a conventional slab of same volume.

Usage of concrete is drastically decreased since 1kg of plastic replaced 100kg of concrete. This makes the bubble

deck a green initiative due to decrease in cement production and its CO_2 production.

Foundation sizes decrease for buildings as overall concrete weight decreases (in slabs, beams and columns).

Since concrete weight is decreased, the concrete handling time is also greatly reduced making the time to lay a slab lesser than that of a conventional slab. Time saving practice leads to money saving as the project will require less time and less labor to be completed.

If spacing between the balls increase the flexural strength also increases without any relation to the thickness of the slab.

Voids present in the slab due to the balls give it great thermal insulation compared to a conventional slab.

10. REFERENCES

- AarathiShethkar, Nagesh Bhanche. (2015). An Experimental Study on Bubble Deck Slab System with Elliptical Balls. Volume 12. Issue 1. Pages 21 -27.
- Annamiya, Anup Willson, Khadeehga, Mithoon, Mohammed Sheebili, Nincy C.K. (2018). Bubble deck slab. International Journal of Advance Engineering and Research Development (IJAERD). Volume 5. Issue 4. April 2018. Pages 2012-2015.
- Aron Maake, MeenaksiKhadao. (2018). Experimental study on bubble deck slab by using HDPE balls. International Journal of Advanced Innovative Technology in Engineering (IJAITE). Volume 3. Issue 2. March 2018. Pages 96-100.
- Bhagyasree Bade, Barelikhar. (2016). An Experimental Study on Two Way Bubble Deck Slab with Spherical Hollow Balls. International Journal of Recent Scientific Research (IJRSR). Volume 7. Issue 6. June 2016. Pages 11621-11626.
- Bhagyasree Bade, Suryavanshi. (2017). Structural Behavior on Two Way Bubble Deck Slab Using Hollow Spherical Balls. Vishwakarma Journal of Engineering Research (VJER). Volume 1. Issue 2. June 2017. Pages 116-124.
- Cobaix Engineering Manual. (2010). Retrieved from https://www.scribd.com/doc/200144278/Cobiax-Engineering-Manual-2010
- Deepan K., Sai Sharanya, Sai Ashwini. (2017). Experimental Study on Bubble Deck Slab using Polypropylene Balls. International Journal of Engineering Development and Research (IJEDR). Volume 5. Issue 4. Pages 716-721.
- Harshith Vanshrey, NithishJhauhari, Himansu Batt. (2017). A Review study on Bubble Deck Slab. International Journal for Research in Applied Science and Engineering Technology (IJRASET). Voume 5. Issue X. October 2017. Pages 2136-2139.
- Mohammed ShafeeqMushfeeq, ShikaShaini, Nishanth Raj. (2017). Experimental Study on Bubble Deck Slab. International Research Journal of Engineering and Technology (IRJET). Volume 4. Issue 5. May 2017. Pages 1000-1004.
- Najma Fathima, Vinay Singh. (2018). To Study Comparison Between Conventional Slab and Bubble Deck Slab. International Advanced Research Journal in Science Engineering and Technology. Volume 5. Issue 1. January 2018. Pages 70-76.
- Niraj Tewari, SaniaZaffar. (2016). Structural Behavior of Bubble Deck Slabs and Its Application. International Journal for Scientific Research and Development (IJSRD). Volume 4. Issue 2. Pages 433-437.
- Sonaal Nayak, DineyshJosi. (2017). A Voided Slab and Conventional Flat Slab- A Comparative Study. International Journal of Science Technology and Engineering (IJSTE). Volume 4. Issue 1. July 2017. Pages 44-50.
- Surendhar, Ranjitam. (2016. Numerical and Experimental Study in Bubble Deck Slab. International Journal of Engineering Science and Computing (IJESC). Volume 6. Issue 5. Pages 5959-5962.

How to cite this article: Ali MS, Babu SA. A structural study on bubble deck slab and its properties. International Journal of Research and Review. 2019; 6(10):352-357.

******

© 2017 IJSRST | Volume 3 | Issue 7 | Print ISSN: 2395-6011 | Online ISSN: 2395-602X
Themed Section: Science and Technology

Optimal Path Calculation for Route Leveraging APIs Using Location Based Service

Zahoora Abid[1], Tahera Abid[2],Khutaija Abid[3]
[1,2]Assistant Professor, Nawab Shah Alam Khan College of Engineering and Technology, Hyderabad, Telangana, India
[3]Assistant Professor, Al-Habeeb College of Engineering and Technology, Hyderabad, Telangana, India

ABSTRACT

A location based service (LBS) is an application for user's mobile device that requires necessary information about where the mobile device is located. Location-based services shall be query-based and provide the end user with valuable information, for e.g LBS enable mobile users to query points-of-interest (e.g.,ATM, restaurants) on various features (e.g., category, price, quality, and variety). They manage points-of-interest (POIs) specific to their applications, and enable mobile users to query for POIs that match with their preferences and time constraints and also it secures a user identity and locality within basic mobile communication services. For this approach this paper provides the survey about various techniques for providing the accurate and efficient query for the mobile users.
Keywords: Location Based Services (LSB), POIs, Query Processing

I. INTRODUCTION

There is growing need for useful approaches involving use of global positioning systems (GPS) information fromGPS trackers for traffic analysis. In recent years, activity-based evaluation using GPS equipment's as informationcollectors has been a principal challenge. All these forms of research focus on data from wearable GPS recorders considering of effortless specified undertaking logging and interactive validation with users. As data have improved,more sophisticated approaches of data assortment have been developed, represented at first by the shift from travel toactivity diaries, and continuing on to the progress of GPS enabled activity surveying. Traffic evaluation is a componentof key points in developing international locations that require better and efficient monitoring.

In order to compensate for uncertainties in journey time due to accidents, bad weather, traffic congestion, and so on, vehicles hauling time-sensitive freight build "buffer time" into their routes in order to help ensure that deliveries willprobably be made on time. Building buffer time into routes tends to increase the likelihood of on-time delivery, animportant measure of service. However, buffer time also tends to reduce measures of productivity associated with cost, such as driver and equipment idle time and the number of miles travelled per hour. An LBS requires 5 basiccomponents: the service provider's software applications, a mobile network to transmit information and requests forservice, a content provider to supply the end user with geo-specific information, a positioning component (see GPS) andthe end user's cellular device. There is an escalating demand to accurately and quickly determine the locationof a mobile at low cost. Location-based applications areflattering popular and available and provide the user withinformation based on their location. Computing the shortest path is foremost challenge within the spatial databases. The path computed by making use of the pre-stored information is not accurate. Thus, there is necessity for the live traffic data. There are a number of online service traffic providers like NAVTEQ [4],Tom tom[5],Google maps[6].However these traffic vendors do not furnish.

They always were growing popularity of online mapapplications and their wide deployment in mobile devicesand car navigation systems, increase number of clientsearch for point to point fastest paths and the corresponding travel times. On static road networks whereedge costs are constant, this problem has been

extensivelystudied and many efficient speedup techniques have beendeveloped to compute the fastest path in a matter ofmilliseconds. At the present time, a few online services provide live traffic information (by using examining accrued informationfrom road sensors, traffic cameras, and crowd sourcing approaches), These systems can calculate the image shortest pathqueries based on present traffic information; nevertheless, they don't record routes to drivers constantly because of high operating costs. Answering the shortest paths on the live traffic data can be considered as a continuous monitoringdifficulty in spatial databases, which is termed as online shortest paths computation in this work. Short-time periodtraffic forecasting objectives to furnish more reliable travel information service, to be able to support people in makingmore reasonable traffic decisions. With the growing availability of traffic data along with the progress of conversationscience, both the capacity and accuracy of travel time forecasting were enormously enhanced in real-time conditions anda great quantity of forecasting methods have been applied throughout recent years. Nonetheless, they're insufficient whenconfronted with the act world traffic issues, considering the real-time traffic condition can be affected conveniently andchanged continuously.

In most cases, the shortest path is computed by using offline information pre-stored within the navigation techniquesand the weight (travel time) of the road map is estimated by way of the avenue distance or old data. Unluckily, roadtraffic circumstances change over time. Without live traffic instances, the route returned through the navigation system isnow not guaranteed a correct result. Those historical navigation techniques would endorse a route based on the prestoreddistance information. Note that this route passes through four street upkeep operations (Indicated by way ofpreservation icons) and one traffic congested street (indicated by means of a redline). These days, several on-lineofferings furnish reside visitors knowledge (through analysing collected information from road sensors, traffic cameras,and crowd sourcing strategies),These systems can calculate the photograph shortest path queries based on currentreside
visitors information; nonetheless, they don't record routes to users regularly due to high working charges. Answering theshortest paths on the live traffic data may also be considered as a steady monitoring problem in spatial databases.

II. EXISTING SYSTEM

The shortest direction influence is computedbased on the live traffic circumstances [1]. They carefully analysed the prevailing work and speak about their inapplicability to the problem. To deal with the difficulty, they suggested a promising architecture that proclaims the index on the air. They first determined a predominant characteristic of the hierarchical index structure which permits us to compute shortest path on a small component of index. This major feature is utilized in their resolution, Live Traffic Index (LTI). Their experiments verified that LTI is a Pareto optimal answer in terms of four performance factors for online shortest path computation.

Shortest path computation is an principal function in present day auto navigation methods[2]. This function helps adriver to figure out the excellent route from his current place to destination place. In most cases, the shortest path iscomputed by using offline information pre-stored within the navigation techniques and the weight (travel time) of theroad map is estimated by way of the avenue distance or old data. The online shortest route computation; the shortestroute result is computed based on the traffic situations. Analyse the prevailing work and speak about their inapplicabilityto the situation (because of their prohibitive protection time and massive transmission overhead). To address the concern,advocate a promising structure that publicizes the index on the air. First determine a foremost characteristic of thehierarchical index constitution which enables us to compute shortest path on a small section of index.

III. PROPOSED SYSTEM:

When person desire to know destination information based on consumer’s requirement say for illustration user needsto reach nearest ATM or hospital. He can get ATM or hospital information using internet service provider. However hewishes effective result with respect to travel time and fee (i.e. nearest route). Consequently person needs application thatsupplies all of the expertise he desires.Figure 1 shows the architecture of proposed

process. The proposed procedure entails almost always threepredominant modules, user module, LBS module and Route-Saver module. In user module user receives a location mapincludes locations, user location and route map from user place (source) and possible destination.
In our proposed work, the users require accurate results that are computed with appreciate to live traffic information. The entire works require the LBS to know the weights (travel times) of all road segments. Considering that the LBS lackthe infrastructure for monitoring road traffic, the above works are inapplicable to our problem. Some works try andmodel the travel occasions of street segments as time-various features, which may also be extracted from historicaltraffic patterns. These services may just capture the consequences of periodic events(e.g. rush hours, weekdays).Nevertheless; they nonetheless cannot reflect traffic information, which can be effected by sudden events, e.g. Congestions, accidents and road maintenance. The LBS module is responsible for accumulating the specified data from consumer and LBS generate optimizedinformation which includes consumer's present area and route log to the destinations. Then this information istransferred to the Route-saver. Route-saver utilizes the contemporary traffic understanding bought from traffic providerand calculates the journey time and most beneficial path to source and destinations by using Nearest Neighbor queries.

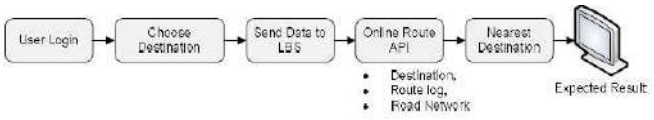

Figure 1: Framework for Proposed Work

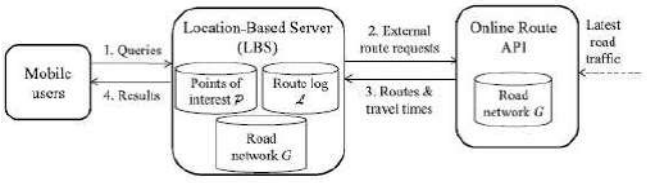

Figure 2. Maintenance of Structures at LBS

Conservative travel time bounds. Given an edge e(v, v-), we define $cw^-(e)$ and $cw^+(e)$ as conservative lower boundand upper-bound of travel time one, observe that the lower bound $cw^-(e)$ is limited by the Euclidian distance of eand maximum driving speed Vmax,
$cw^-(e) = dist(e)/ Vmax$

To reduce the number of route requests while providing efficient results, we combine information throughout a couple of routes within the log to derive tight lessen/higher bounding journey times. We also propose effective strategies.

to compute such bounds efficiently. Additionally, we compare the influence of exclusive orderings for issuing routerequests on saving route requests. And we learn the best way to parallelize route requests in order to reduce the queryresponse time additional.

Above figures show the screen shots our proposed work, the user has an access to router via an internet. Based on hispresent location he has to choose the destination point, and then LBS will communicate with server and shows you thenearest places of his choice.

Figure (a)and(b) shown window where you can choose the destination you need to go, onceyou selected point server will give you the nearest requested destination with shortest path. We can see the nearest destination point in the figure 3, here user wants to visit to a hospital, and using an applicationhe will enter the hospital as destination point. For the requested information server will revert back with all hospitalswhich is located around the user's current location. As we see in the figure 3, all the hospitals are marked in red colorand the nearest hospital is marked in a purple color, here user location is marked as source and is in green color.

Figure 3. Types of location based services

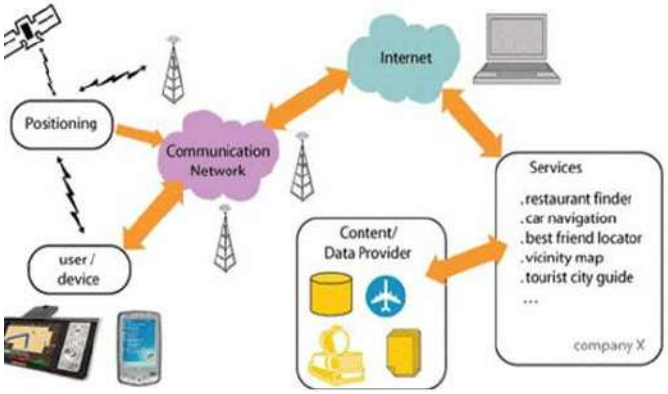

Figure 4: Location based services network architecture

(a)

(b)

Destination point request

Nearest Destination Point

Query processing

Algorithm 1: Location Point based Tree (LPT with Inverted Index):

The location point tree saves the location points along with the service details. The service identifies the service by using the spatial POI which will be stored on the LPT_II. To speed up itinerary process in this indexes all the objects' subspace spatial scopes by an LPT tree where the subspace spatial scopes are stored in the leaf nodes as data entries. Additionally, to support service recommendation, this follows mapping module and KNN search [7]. In the diagram p1, p2, p3, p4, p5…p7 are the service points. In the proposed system every service point will be stored with an mapping key for fast service search. The proposed system stores the above service point in the tree style.

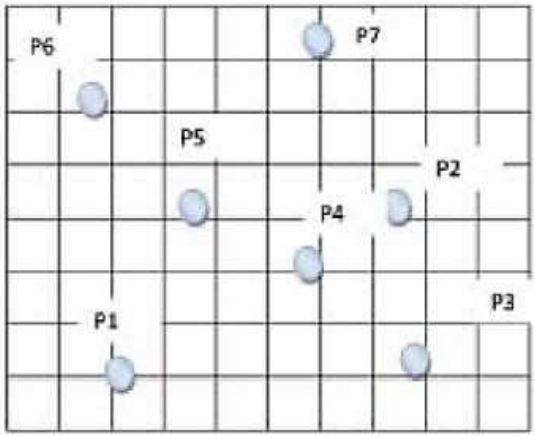

Algorithm 2: LPT_II maintenance tree Steps

The following table represents the location point and available service details in the location. The service can able provide appropriate services for the user interest based on the location point based service list. This helps in two ways. One is the retrieval time has reduced. And the next is fast search in the LPT helps to avoid the unavailable services [8].

POI	Services (S)
P1	S1,S3
P2	S4,S6
P3	S5,S4
P4	S4,S7
P5	S2,S8

Figure 3. LPT_II maintenance tree Steps

1. Initial location source with respect point p1,p2..pn
2. For every point in the source P do
   a. Initialize service S1…Sn for respective points.
   b. Set service and code for every service
3. Get rank for each service and store into the ascending order.
4. Store the node in the top level based on the rank
5. Prune the other items from the LPT.

USE CASE DIAGRAM:

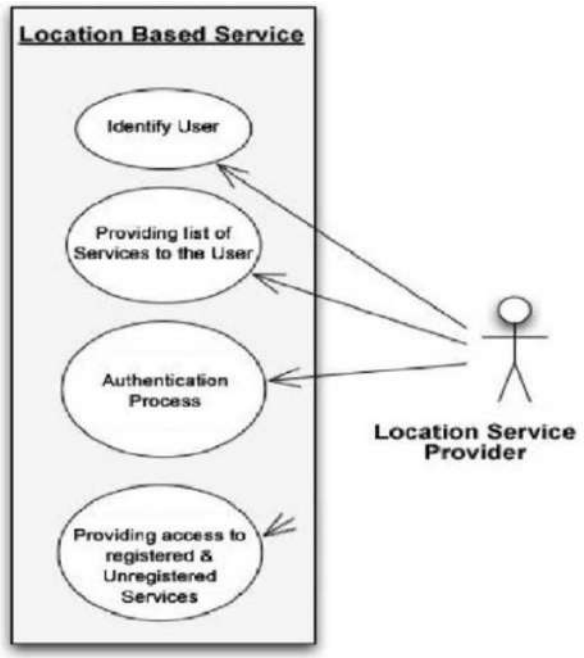

Figure 5 : Use case diagram for LBS

IV. CONCLUSION

In this paper, we propose a solution for the LBS to process range/KNN queries such that the query results haveaccurate travel times and the LBS incurs few number of route requests. Our solution Route-Saver collects recent routesobtained from an online route API (within d minutes). During query processing, it exploits those routes to deriveeffective lower-upper bounds for saving route requests, and examines the candidates for queries in an effective order.We have also studied the parallelization of route requests to further reduce query response time.

REFERENCES

[1] M. Argon and K. Sirisha, "Live Activity List Based Shortest Path Calculation", Issue 09, 2015.

[2] R.Subashini and A.Jeya Christy, "Online Shortest Path based on Live Traffic Circumstances" Volume 3, Issue. 11, 2014.

[3] DekondaSindhuja, R Vasavi and A KousarNikhath, "Online Shortest Path Computation using Live Traffic Index",Volume 25, Issue 3, 2015.

[4] "NAVTEQ Maps and Traffic," http://www.navteq.com, 2014.

[5] "TomTom NV," http://www.tomtom.com, 2015.

[6] "Google Maps," http://maps.google.com, 2015.

[7] D. Zhang , CY. Chow, Q. Li, X. Zhang, Y. Xu, ―Efficient Evaluation of k-NN Queries Using Spatial Mashups‖, Advances in Spatial and Temporal Databases (Lecture Notes in Computer Science), Vol. 6849, pp.348-366, 2011.

[8] D. Zhang, CY. Chow, Q Li, X Zhang, Y Xu, SMashQ: Spatial mashup framework for k-NN queries in timedependentroad networks", Distributed. Parallel Databases, Vol. 31, pp. 259–287, 2012.

Performance Analysis of the HVAC System in a Hospital Building in Hyderabad

Mohammed Ishaq, Raza Ahmed Khan, Mohammed Abdul Majeed

Abstract— Indoor air quality (IAQ) is a term which refers to the air quality within a building, especially as it relates to the health and comfort of building occupants. The hospital is a high risk indoor place which has airborne infection from patients. The complex hospital environment requires special attention to ensure healthy IAQ to protect patients and healthcare workers against hospital-acquired infections and occupational diseases. The aim of this study is to recommend effective guidelines for the control and management of hospital IAQ. A one week survey was carried out in the Continental Hospital and Research Centre situated at Gachi Bowli, Hyderabad. It is a massive eighteen storied structure, competently managed by senior professionals. In the experimental analysis for indoor air quality, measurements were recorded on four floors for Temperature, Relative Humidity and Carbon Dioxide. In the observation analysis the operation and maintenance of the HVAC system and the well-being of the occupants were observed.

Index Terms— CO_2, HVAC Systems, Indoor Air Quality, Occupant Comfort, Pollutants, Relative Humidity, Temperature

1 Introduction

Hospital buildings and health care facilities are among the most complex indoor spaces. In particular, the most demanding indoor zones are hospital operating theatres (suites) that comprise operating rooms (ORs) or surgical theatres, their interconnecting hallways and ancillary work areas. The indoor environmental quality (IEQ) in ORs, including thermal, visual and acoustical comfort and indoor air quality, affects the working conditions, well-being, safety and health of patient and the medical personnel who work in these environments. About 50% of the total number of doctors works in the ORs, as surgeons or with other responsibilities (e.g. anesthesiologist), while about 10% of the total medical staff also work in the OR. Heating, Ventilating and Air-Conditioning (HVAC) installations control indoor air quality and aseptic conditions, and secure health, safety and suitable indoor thermal (i.e. temperature, humidity, air quality and airflow) conditions for surgeons and medical staff, and of course, the patients. The air in an OR must be aseptic, at a reasonably constant temperature and humidity and have relatively low air velocity in order to avoid drafts and swirls that promote the recirculation of microbes and may disrupt the procedures during an operation. The ventilation rate is expressed as the volumetric air flow through the space divided by the volume of the space, e.g. number of air changes per hour (ACH). The desirable conditions can be met by proper design, installation, operation and maintenance of the electromechanical equipment, such as the HVAC equipment and lighting systems of the space. Due to their demanding indoor conditions, operating theatres constitute the most expensive sector of the healthcare establishment mandating an efficient management. Indoor air quality (IAQ) can be affected by gases (including carbon monoxide, radon, volatile organic compounds), particulates, microbial contaminants (mold, bacteria), or any mass or energy stressor that can induce adverse health conditions. Source control, filteration are the primary methods for improving indoor air quality in most health care facilities.

- *Mohammed Ishaq is M.Tech (HVAC) Student from NSAK College of Engineering & Technology, JNTUH, India, PH-00918978174590. E-mail: mishaq68@rediffmail.com*
- *Raza Ahmed Khan, Associate Professor, Mechanical Engineering, NSAK College of Engineering & Technology, JNTUH, India, PH-00919848058830. E-mail: raza_a_khan@hotmail.com*
- *Mohammed Abdul Majeed, Assistant Professor, Mechanical Engineering, NSAK College of Engineering & Technology, JNTUH, India, PH-00919052280350. E-mail: mamajeed79@gmail.com*

2. HVAC System Investigation

The preliminary HVAC investigation involved the discussions with property owners and building management, walk through investigation of building and surrounding areas, interviewing HVAC operation & maintenance personnel, study of as-built drawings, review of maintenance schedule and preventative maintenance program.

Preliminary observation/review of the HVAC system was carried out. Direct instrument measurements of carbon dioxide, relative humidity, and temperature were recorded to know the status of IAQ and comfort of building occupants.

3. Hospital Occupant Survey

A hospital occupant's questionnaire was developed to get the demographic background and socio-economic status of the respondents such as personal information, health status, symptoms of sickness, and level of comfort inside the hospital. The questionnaire include the occupant's health status and symptoms of Sick building syndrome (SBS) such as chronic cough, cough with phlegm, chest tightness, and shortness of breath. Questionnaires also contain questions on the previous workplace, working history, and location of current workstation (near the entrance door, near to photocopied area, etc), and also working background such as overtime, shift work

schedule, duration of work per day, duration of work per week and the employment years at the office. Zoning of each worker's workstation then categorized accordingly with the reference of floor plan. Reported sick building syndrome (SBS) symptoms were recorded from the respective respondents on each day of IAQ assessment conducted and the score given in the analysis of data as shown in Fig. 1.

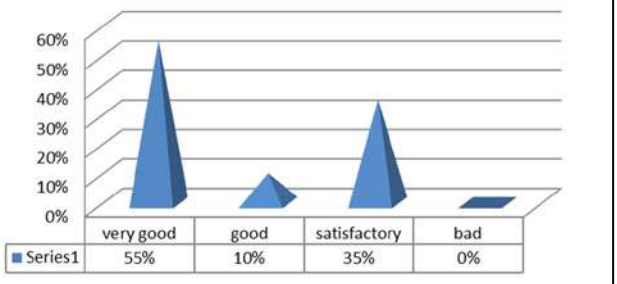

Fig. 1. Hospital occupant's perception of Indoor Air Quality

4. Hospital Building Infrastructure

The questionnaire was done in the Hospital Building in Hyderabad which is fully Air Conditioned controlled by Building Management Sysytem. A continuous data log of carbon dioxide, temperature, and relative humidity for approximately one week. Indoor air quality analysis was carried of the Hospital having buildup area of 1,20,000 sq mtrs with 18 floors of capcity 750 beds controlled and maintained by HVAC system of capacity 4000 Ton.The hospital requires close coordination among Medical staff, Support staff and patients along with the maintenance of diagnostic equipment along with disinfection and sterlization techniques in order to improve health of patients, avoid infections among patients and hazards for hospital occupants.

5. Parametric Measurement

The parametric measurement of carbondioxide, Relative humidity and Temperature are major factors in health care facilities indoor air quality (IAQ). The interiors are deemed to be the most important indicators that the quality of the indoor air is good enough, when people themselves are the main source of emissions. Poor indoor air quality leads to tiredness, lack of concentration and can even bring about illnesses.

5.1 Carbon dioxide

Carbon dioxide (CO_2) level is considered to be an indicator for purpose of evaluation of indoor air quality (IAQ). Hospital occupants asre the main sourse of Carbon dioxise levels variation and air borne infections along with the concentration of body odour. Carbon dioxide is relatively varies with respect to seasons and even within a day, human traffic, occupants living habits. The useful approach is to measure surrogate for indoor pollutants emitted by humans, and correlates with human metabolic activity. Carbon dioxide at levels that are unusually high indoors may cause occupants to grow drowsy, to get headaches, breathing and pulse rate increase, nausea, unconscious, further exposure 100,000 ppm leads to death. Humans are the main indoor source of carbon dioxide in most buildings. Indoor levels are an indicator of the adequacy of outdoor air ventilation relative to indoor occupant density and metabolic activity.

To eliminate most complaints, total indoor carbon dioxide should be reduced to a difference of less than 600 ppm above outdoor levels. NIOSH considers that indoor air concentrations of carbon dioxide that exceed 1,000 ppm are a marker suggesting inadequate ventilation.These higher limits are concerned with avoiding loss of consciousness (fainting), and do not address impaired cognitive performance and energy, which begin to occur at lower concentrations of carbon dioxide.

Carbon dioxide concentrations increase as a result of human occupancy, but lag in time behind cumulative occupancy and intake of fresh air. The lower the air exchange rate, the slower the buildup of carbon dioxide to quasi "steady state" concentrations on which the NIOSH are based. Therefore, measurements of carbon dioxide for purposes of assessing the adequacy of ventilation need to be made after an extended period of steady occupancy as recorded in figure no 2. Portable instruments used to measure carbon dioxide should be calibrated frequently and outdoor measurements used for calculations should be made close in time to indoor measurements.

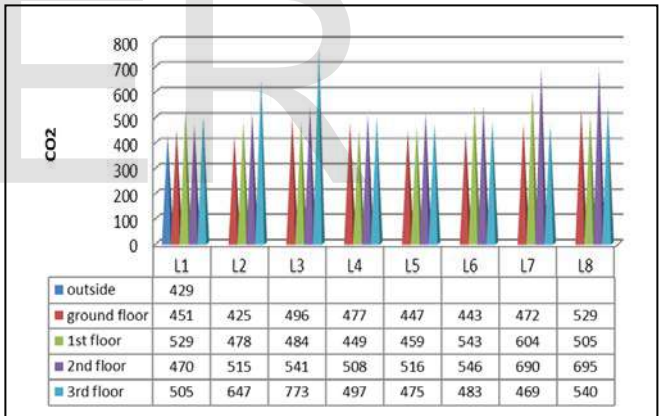

	L1	L2	L3	L4	L5	L6	L7	L8
outside	429							
ground floor	451	425	496	477	447	443	472	529
1st floor	529	478	484	449	459	543	604	505
2nd floor	470	515	541	508	516	546	690	695
3rd floor	505	647	773	497	475	483	469	540

Fig. 2. Carbon Dioxide values recorded at different floors

5. .2 Relative Humidity

Hospital buildings having high humidity levels can cause damage to sensitive hospital equipment and products used during surgery apart from discomfort to occupants. Sources of biological contaminants are major source of risk to patients health. Relative humidity also affects the shelf life and product integrity results unexpected malfunction. Air humidity must be maintained at acceptable levels because it is closely related to the space hygiene and thermal comfort conditions. Humidity control is most often accomplished by treating the ventilated air for lowering (dehumidification) or increasing (humidification) its water content, using proper equipment and controls. HVAC system configurations can achieve humidity targets for delivering the required supply air conditions, without energy wastage. High humidity levels favor the growth and transfer of bacteria that can be easily become airborne on wa-

ter molecules high humidity levels cause thermal discomfort. During low humidity level electro-medical equipment is effected by electrostatic discharge. The ventilation requirements influence humidity control. Depending on climatic conditions, additional ventilation may increase the dehumidification load more than the sensible cooling, imposing a disproportionate demand on the HVAC equipment. Low humidity levels (dry air) favor blood coagulation, which is undesirable during a surgery. In addition, moisture can be absorbed into the duct lining and building materials where it may support microbial growth. With the heavy use of electric equipment, low humidity levels may cause problems associated with static electricity on medical equipment and surfaces. In addition, this may even pose a fire hazard, as there may be flammable gases present in the environment. The recommended levels of indoor relative humidity are 30–60%, according to international regulations and standards. Most regulations establish where the use of in-flammable anaesthetic gases is possible, volatile liquids are used frequently, and in order to prevent the accumulation of static electricity should maintain a humidity of about 60%. Humidification may be necessary to increase low humidity levels, commonly encountered during winter. Special care must be exercised with humidification to assure that there is no potential for transferring bacteria through the ventilation system, since humidifiers may provide favorable environment for bacteria growth. Proper maintenance and cleaning practices will minimize this kind of risks. Humidification is best accomplished by supplying dry steam. Cold-water humidifiers in HVAC systems must be connected to a domestic water source and provided with a drain line to remove the water. Stand-alone, console-type humidifiers that re-circulate water for humidification should not be used because the water in these systems becomes contaminated with microorganisms rapidly and have been linked to outbreaks of Legionnaires' disease. Study recorded as shown in Figure no. 3.

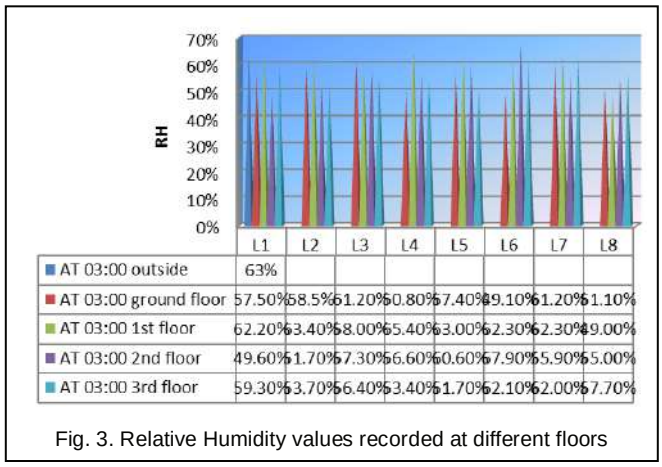

	L1	L2	L3	L4	L5	L6	L7	L8
AT 03:00 outside	63%							
AT 03:00 ground floor	57.50%	58.5%	61.20%	60.80%	67.40%	69.10%	61.20%	61.10%
AT 03:00 1st floor	62.20%	63.40%	68.00%	65.40%	63.00%	62.30%	62.30%	69.00%
AT 03:00 2nd floor	49.60%	51.70%	57.30%	56.60%	60.60%	57.90%	55.90%	55.00%
AT 03:00 3rd floor	59.30%	63.70%	66.40%	63.40%	61.70%	62.10%	62.00%	67.70%

Fig. 3. Relative Humidity values recorded at different floors

5.3 Temperature

The indoor air temperature must be maintained within the recommended ranges to ensure acceptable conditions. The Indoor air temperature must be uniform within the space. Special care must be taken to operation theater account for the different internal loads (e.g. surgical lamp) by proper design of the air conditioned supply and exhaust vents and temperature of the air supply stream. The desirable indoor air temperature is usually 20–24°C, according to international regulations and standards. Use of lower or higher temperature is acceptable when patients' comfort and/or medical conditions require those conditions. For example, for specialized procedures, such as cardiac surgery, the indoor air temperature may be set as low as 17°C, on the other hand paediatric surgeries usually demand a higher indoor air temperature because children are more sensitive to lower temperatures. In any event, a high indoor air temperature may cause discomfort and offers more favorable growing conditions for bacteria or their mitigation from and to the patient. Practically, it is not possible to provide all occupants with 100% acceptable indoor thermal conditions. Similarly, the medical staff working in an Operation Room may have a different perception of prevailing indoor conditions due to different levels of activity and even working positions within the OR. In general, surgeons tend to feel from ''slightly warm'' to ''warm''. Regulatory sweating is also present very often. Anaesthetists and nurses, by Contrast, experience from ''slightly cool to cold'' thermal sensation. This is especially true for temperatures below 21°C. These are in agreement with other studies where preferable thermal comfort conditions were reported for aesthetics (23–24°C), for nurses (22–24.5°C) and for surgeons (18–19°C). For patient's, the recommended air temperature ranges between 24 and 26°C. Medical clothing will have a direct impact on personnel's thermal comfort conditions. Surgical scrub garments are typically worn by OR personnel to control airborne contamination, although there is no scientific data to support this practice as a means for preventing transmission of infection. Heavier gown requirements used by the surgical team for protective reasons during an operation (i.e. because of AIDS) may require an indoor temperature down to 18°C or even lower. The field measurement was conducted at various floors present in figure-4 at various locations.

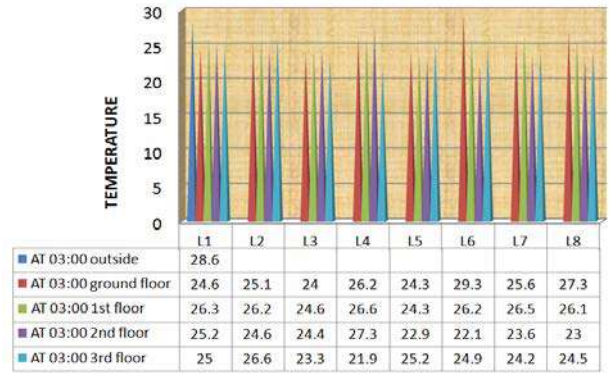

	L1	L2	L3	L4	L5	L6	L7	L8
AT 03:00 outside	28.6							
AT 03:00 ground floor	24.6	25.1	24	26.2	24.3	29.3	25.6	27.3
AT 03:00 1st floor	26.3	26.2	24.6	26.6	24.3	26.2	26.5	26.1
AT 03:00 2nd floor	25.2	24.6	24.4	27.3	22.9	22.1	23.6	23
AT 03:00 3rd floor	25	26.6	23.3	21.9	25.2	24.9	24.2	24.5

Fig. 4. Temperature values recorded at different floors

Finally, asymmetric thermal radiation from surgical lights on the surgical staff is a potential source of thermal discomfort. Thermal radiation emitted from surgical lights regardless of the indoor air temperature.

6. BUILDING HVAC SYSTEM

The procedures used to calibrate indoor air quality of health

care facilities are as follows:

- Determine the effective volume of the hospital.
- Record the temperature and humidity conditions, the method of distribution of air (ceiling outlets, side wall, floor outlets, etc.) and the operation hours of the system.
- Collect the specifications of the airside system (type, capacity of supply air, fresh air and return air flow rate, control method, etc.) and the accessories such as fresh air damper, type of diffuser, etc.

To calculate the air change rate when the air-conditioning system was operating, the hospital was pressurized and infiltration is reduced.

The Outdoor air requirement is significant important for IAQ. The outdoor air requirement is related with the number of occupants and net available occupancy.

HVAC system should provide sufficient fresh air to avoid concentration of contaminated indoor air pollution. Supply air velocity for each supply air grill was measured by using anemometer. Airflow rate was designed and measured of supply air flow rate for fan coil units and Air Handling Unit.

7. Conclusion

The measurements were carried out to check the values Carbon dioxide (CO_2), Relative Humidity (R.H %) & Temperature (T). It was observed that throughout the week the values of CO_2, relative humidity and temperature were in acceptable range. It indicates that the overall performance of HVAC systems is good in this hospital building.

Since the feedback gathered from the occupants of the building also indicate that a majority of them feel comfortable inside the building and do not report of any severe complaints, it can be concluded that the HVAC systems is providing sufficient amount of fresh air along with maintaining the temperature and relative humidity.

The above measurements were recorded for a period of one week only. However, a long term field measurements have to be recorded to analyze the performance of HVAC systems and IAQ issues on a minute scale.

Acknowledgment

The authors wish to thank Nawab Shah Alam Khan College of Engineering and Technology, Hyderabad for facilitating this research study.

8. References

[1] R.W. Marans. Evaluation Research in Architecture. In: J. Snyder, ed. Architectural Research. New York, 1984. Van Nostrand Reinhold.

[2] Akimenko VV, Anderson I, Lebowitz MD, Lindvall T. 1984. The "Sick" Building Syndrome

[3] Proceedings of the Third International Conference on Indoor Air Quality and Climate. Swedish Council for Building Research. Stockholm. 6:87-97

[4] American Society of Heating, Refrigerating and Air-Conditioning Engineers, Inc. 1990

[5] ANSI/ASHRAE Standard 62-1989. Ventilation for Acceptable Indoor Air Quality. Atlanta, USA.

[6] American Society of Heating, Refrigerating and Air-Conditioning Engineers, Inc. 1992.

[7] ANSI/ASHRAE Standard 55-1992. Thermal Environmental Conditions for Human Occupancy.Atlanta, USA.

[8] American Society of Heating, Refrigerating and Air-Conditioning Engineers, Inc. 1993.

[9] ANSI/ASHRAE Guideline 4-1993: Preparation of Operating and Maintenance Documentation forBuilding Systems. Atlanta, USA.

[10] Armstrong CW, Sherertz PC, Llewellyn GC. 1989. Sick Building Syndrome Traced to ExcessiveTotal Suspended Particulates. Proceedings of IAQ 89. 3-7

[11] E. Marcon, S. Kharraja, G. Simonnet, The operating theatre planning by

[12] the follow-up of the risk of no realization, International Journal of Production Economics 85 (1) (2003) 83–90.

[13] Macario, T.S. Vitez, B. Dunn, T. McDonald, Where are the costs in perioperative care? Analysis of hospital costs and charges for inpatient surgical care, Anesthesiology 83 (1995) 1138–1144.

IJSER

World Academy of Science, Engineering and Technology
International Journal of Chemical and Molecular Engineering
Vol:11, No:1, 2017

Polyvinyl Alcohol Processed Templated Polyaniline Films: Preparation, Characterization and Assessment of Tensile Strength

J. Subbalakshmi, G. Dhruvasamhith, S. M. Hussain

Open Science Index, Chemical and Molecular Engineering Vol:11, No:1, 2017 publications.waset.org/10006352/pdf

Abstract**—**Polyaniline (PANI) is one of the most extensively studied material among the conducting polymers due to its simple synthesis by chemical and electrochemical routes. PANIs have advantages of chemical stability and high conductivity making their commercial applications quite attractive. However, to our knowledge, very little work has been reported on the tensile strength properties of templated PANIs processed with polyvinyl alcohol and also, detailed study has not been carried out. We have investigated the effect of small molecule and polymers as templates on PANI. Stable aqueous colloidal suspensions of trisodium citrate (TSC), poly(ethylenedioxythiophene)-polystyrene sulfonate (PEDOT-PSS), and polyethylene glycol (PEG) templated PANIs were prepared through chemical synthesis, processed with polyvinyl alcohol (PVA) and were fabricated into films by solution casting. Absorption and infra-red spectra were studied to gain insight into the possible molecular interactions. Surface morphology was studied through scanning electron microscope and optical microscope. Interestingly, tensile testing studies revealed least strain for pure PVA when compared to the blends of templated PANI. Furthermore, among the blends, TSC templated PANI possessed maximum elasticity. The ultimate tensile strength for PVA processed, PEG-templated PANI was found to be five times more than other blends considered in this study. We establish structure–property correlation with morphology, spectral characterization and tensile testing studies.

Keywords**—**Processed films, polyvinyl alcohol, spectroscopy, surface morphology, templated polyanilines, tensile test.

I. Introduction

PANI is a well-known and most enormously considered amid conducting polymers. It has always been attractive due to its synthesis, strength, low price and good environmental stability [1]-[4]. PANIs also possess unique optical characteristics and conductivity which lead them towards superior industrial applications. At a recent time, extent development has been made on the process of PANI [5]-[7]. With the focus on environmental safety and processing methodologies, aqueous solution processed PANIs, turned out to be attractively important. Composites/blends of PANIs have excellent adhesion and anticorrosive properties [8]. By blending with other polymers [9]-[11] or by substitution and copolymerization, exploration has been made to enhance the poor mechanical properties and the processability of PANI [12]. Polyvinylidene fluoride, (PVDF)/PANI blends were synthesized using chemical polymerization of aniline and their thermal and mechanical properties were studied as a function of PANI doping levels. It was observed that presence of PANI led to the increase in the tensile strength and Young's modulus due to the reinforcement of PANI over PVDF matrix, thereby constraining the chain movements of PVDF [13]. Study on the effect of feeding ratio of aniline in PANI/PVA blend on the mechanical and electrical properties of the composites was reported by [14]. The tensile strength of the blend films has been attributed to the hydrogen bonding between PANI and PVA. Electromechanical response of the solution blended and HCl doped PANI/PVA blends subjected to static, dynamic and time–dependent strains was reported by [15]. Though recently, polyethylene terephthalate/PANI [16], polyurethane/PANI [17], PANI/polybenzimidazole [18] blends were characterized using IR and NMR spectra. The tensile strength was found to be diminished and permeability, diffusion, sorption capacities of all measured gases are observed to be decreased with increased content of PANI. Recently, enhancement of mechanical property by strategic inclusion of graphene oxide nano-filler in chitosan/gelatin polyelectrolyte complex [19] has been reported. However, we have limited our search on PANI/PVA blends only, relevant to the work presented in this paper.

We have prepared stable aqueous colloidal suspensions of templated PANIs, through modified procedure (along the similar lines reported in [20] and processed with PVA by solution casting into free standing films. We have characterized the films using various spectroscopy techniques and studied mechanical properties. For the TSC-templated PANI processed film, the ultimate tensile strength was found to be considerable, this could be due to the strong intermolecular interactions between the TSC-PANI and PVA, leading to the restricted orientations of TSC-PANI chains. Also, PVA being a good stabilizer leads to the rigidification of the polymer chains.

II. Materials and Methodology

A. Synthesis

TSC, ammonium persulfate (AP) and HCl (12 N) were

J. Subbalakshmi is an Associate Professor in the Department of Chemistry, in the Birla Institute of Technology and Science Pilani, Hyderabad Campus, Shameerpet, Hyderabad-500078 (phone: +91-040-66303561; fax: +91-040-66303998; e-mail: jslakshmi@hyderabad.bits-pilani.ac.in).

G. Dhruvasamhith is at Apoorva IT Solutions Private Ltd., as a Business Development Executive, Hyderabad (e-mail: dhruvasamhith108@gmail.com).

S. M. Hussain is at the Mechanical Engineering Department, Professor and Head, NSAKCET, Hyderabad-500036 (e-mail: smh.bits@gmail.com).

S. J. thanks financial support from the Department of Science and Technology, New Delhi, India, under FIST grant.

Open Science Index, Chemical and Molecular Engineering Vol:11, No:1, 2017 publications.waset.org/10006352/pdf

obtained from SD fine chemicals. Aniline (analytical grade), PEDOT-PSS and PEG were obtained from Sigma Aldrich. All colloidal suspensions were prepared in Milli-Q water. To a 0.84 mL (4.6 mmol) of aniline in round bottomed flask, 30 mL of 3M HCl was added slowly and the solution was kept for stirring for 15 min. 1.67 gm of PEG dissolved in 10 mL water was added to anilinium hydrochloride solution while stirring. 2.04 gm (4.4 mmol) of AP dissolved in 5 mL water was added dropwise for at least 30 mins. The solution was stirred for 2.5 hours more, to complete the polymerization (Fig. 1). Dark green colloidal solution was centrifuged and subjected to sonication. This solution was further processed into free standing films. 1 gm of PVA was dissolved in about 10 mL of water and left for about 3 days for dissolution. The templated PANIs and PVA solution were mixed in 1:1 volume ratios due to better film formation and subjected to solution casting. Similar methodology was followed for the preparation and fabrication of other templated PANI blends too.

B. Characterization

1. FT-IR and UV-Vis Spectroscopy

FT-IR spectra were recorded on Jasco FTIR-4200 spectrophotometer. Samples of blends in the form of KBr pellets were made from vacuum drying. Absorption spectra were recorded on the Jasco V-650 make of model Jasco-ISV-727.

2. Fabrication of Films

Glass plates were cleaned thoroughly with detergent, high purity water, acetone and were dried in hot air oven at 110 °C, prior to solution casting.

3. Differential Scanning Calorimetry

Shimadzu DSC-60 in the range of temperature 30-800 °C with heating and cooling rate of 10 °C min^{-1} for the differential scanning calorimetry study (DSC). Data were obtained using alumina pan containing 4 mg of sample under nitrogen atmosphere and at the rate of 100 mL min^{-1}. Empty alumina pan was used as reference.

4. Scanning Electron Microscopy

Morphology of solution casted films was studied under Philips XL 30ESEM scanning electron microscope. Gold sputtering was provided before examination of the micro features. Micrographs presented are at the same magnification for the films coated on glass substrates. An acceleration voltage of 5-10 kV and an emission current of 10 μA was supplied. To confirm that the features observed are due to processed templated PANIs, EDXS was used.

5. Optical Microscopy

Optical microscope images were obtained from MEIJI, IM 7200 model with viewing head MA 816, stage size 150×200 mm, polarizing filter 20 mm diameter.

6. Tensile Testing

Tensile strength, of the materials (~35 mm × 11 mm × 1.7 mm) have been found by performing tensile tests on the specimens as per ASTM standards on stable microsystems, TA.XT plus texture analyzer. In these tests, specimen was gripped between two supports and applied force by gradually increasing it. We measured elongation of specimen under these continually increased forces, calculated the stress developed in the specimens and measured the strain. The system was switched on and the polymer film was kept in between the grips. Tensile testing was conducted with strain rate as 1 mm/sec, till the time there was a failure in polymer film. The obtained data were later converted to stress vs strain.

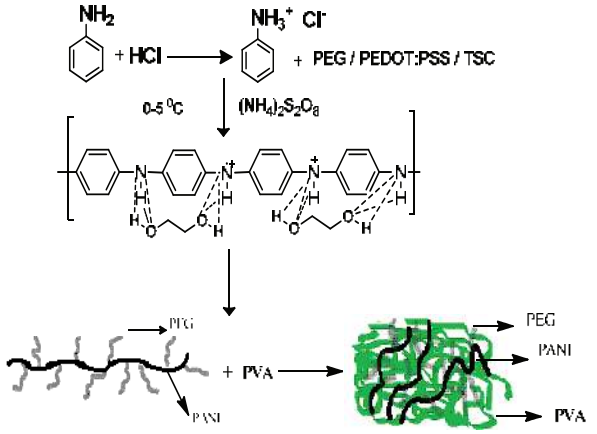

Fig. 1 Schematic representation of the plausible reaction and intermolecular interactions in (PANI-TSC/PVA) blend as an example

III. Results and Discussion

Fig. 2 shows the FT-IR spectra of blends considered in our study. Pure PVA possess broad band at 3400-3100 cm^{-1} due to O-H and C-H stretching vibrations [21]. Absorption at 1573, 1452, 2911 and 2838 cm^{-1} for PANI-PEG; 1541, 1406, 3047 and 2932 cm^{-1} for PANI-PEDOTPSS and 1543, 1473, 2853 and 2911 cm^{-1} observed for PANI-TSC correspond to C=C stretch of quinonoid and benzenoid rings and to the asymmetric and symmetric aliphatic C-H stretches respectively. The backbone of emeraldine salt has positive charges. Our investigations [22] on PANI-PEDOTPSS and PANI-TSC revealed that these form stable colloidal suspensions through electrostatic interactions as PEDOTPSS and TSC are ionic, while PEG behaves more like a surfactant and stabilizer. All samples exhibit absorption of O-H (H-bonded) stretching frequency with strong and broad feature; which also overlap with N-H and aromatic C-H stretch, extending from 3000-3600 cm^{-1}. Characteristic peaks of S=O, S-O and S-C at 1050, 668 and 595 cm^{-1} were observed in PANI-PEDOTPSS. N-H stretch (2352-2368 cm^{-1}) [23] was observed in all samples. Imine and secondary amine peaks were observed at 1300 and 1225 cm^{-1}. These typical vibrational frequencies show that templates have strong interaction with PANI and PVA. In the wavelength region of 400 to 1400 nm, PVA is almost found to be transparent [21]. The UV-Vis spectra (Fig. 3) showed polaronic band at 840 nm in addition to the hump at ~420 nm, a characteristic for the emeraldine salt. This feature is found to be more prominent in PANI-PEG/PVA and PANI-TSC/PVA. Broader polaronic

band feature is likely to be due to the exciton transitions of the quinonoid rings [24].

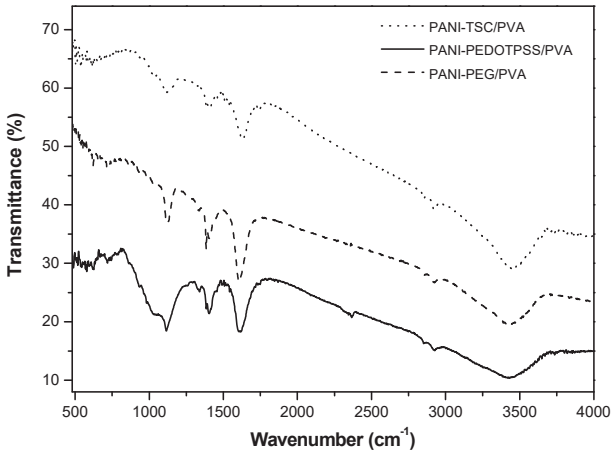

Fig. 2 FT-IR spectra of (……, PANI-TSC/PVA), (___, PANI-PEDOTPSS/PVA) and (- - -, PANI-PEG, PVA)

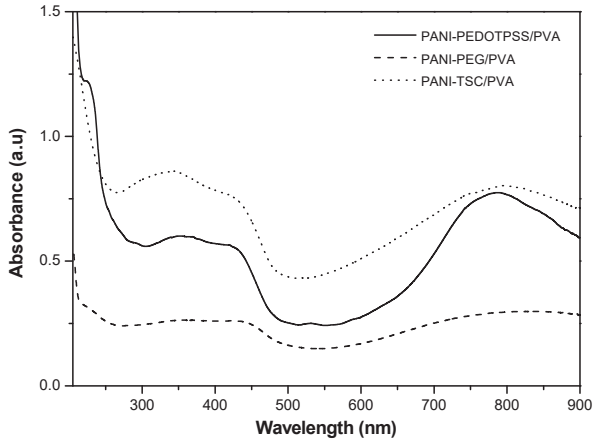

Fig. 3 UV-Vis spectra of (……, PANI-TSC/PVA), (___, PANI-PEDOTPSS/PVA) and (- - -, PANI-PEG, PVA)

The disappearance of 620 nm peak in all the blends indicates that imine nitrogen is protonated. Also, a broad band at 380 nm to 420 nm reveals the interactions in the components through hydrogen bonding [25]. PVA possess many hydroxyl groups that can strongly interact with templated PANI amine groups, this forces molecules to align along with it, also evident by the presence of a band elongated in the near infra-red region extending up to 1000 cm^{-1}.

The glass transition temperature (T_g) of PVA appears around 70-80 °C. The T_g of blends was observed to be higher than homo polymers, probably due to various intermolecular interactions. T_g of PANI-PEG/PVA and PANI-TSC/PVA was observed at ~100-106 °C (Fig. 4), broad exothermic peak ~ 230 °C in PANI-PEG/PVA corresponds to the crystallization of polymer. T_g of PANI-PEDOTPSS/PVA was found at 126 °C, small and broad exothermic peaks (Fig. 4) at 220 and 270 °C were also observed due to partial crystallization. T_g of PANI-PEDOTPSS/PVA was found to be higher than PANI-PEG/PVA, indicating some crosslinking and a complex molecular structure. PANI-TSC/PVA showed a single sharp exothermic peak leading to the only phenomenon of crystallization. However, endothermic peaks were not noticed.

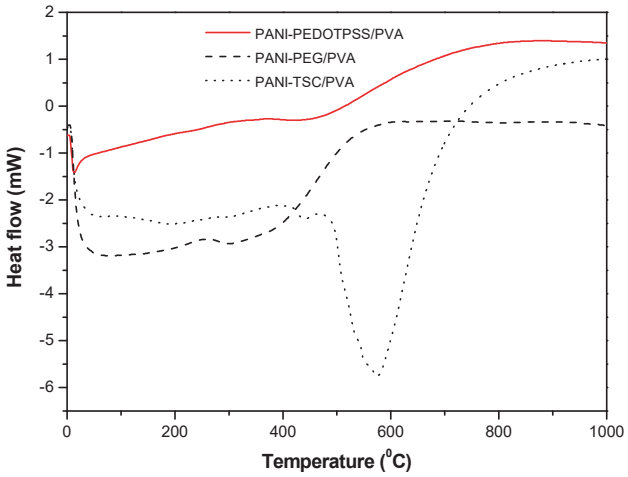

Fig. 4 DSC plots of the blends (……, PANI-TSC/PVA), (___, PANI-PEDOTPSS/PVA) and (- - -, PANI-PEG, PVA)

In our earlier investigations, SEM images on powders of templated PANI's [22] interestingly, revealed block like features with different particle sizes. Poly(4-styrenesulfonic acid sodium salt, NaPSS) when templated with small molecule such as TTF in different compositions, the SEM images [26] have shown flake and crystalline morphologies exhibiting various packing density. Carboxymethyl cellulose templated PANI film revealed uniform fibers of diameter 100-120 nm under scanning electron microscopy and showed semiconducting behavior [27]. Nevertheless, PSS templated PANI-carboxymethyl cellulose blend formed stable aqueous colloidal suspensions and their spin coated films prepared from different concentrations of colloidal suspensions under atomic force microscopy showed regular network-like structures for the films prepared at dilute/lower concentrations, indicating the efficacy of dilution as a new design element for network structures [28]. With such interesting morphological features observed in our previous PANI's, we extended our study on PVA processed template PANI's presented in this work.

SEM images (Figs. 5 (a)-(c)) showed that the blends were homogeneous without any holes or cracks. Aggregates or agglomerates like features in PANI-PEG/PVA, porous honeycomb network in PANI-TSC/PVA and homogeneity with spherical features in PANI-PEDOTPSS/PVA were observed. However, uniformity and good dispersion in the prepared blends leads to the significant retain in the mechanical property. As the strength of the blends is found to be less than PVA, probably, templated PANI could be acting as plasticizers. Optical microscope study (Figs. 5 (d)-(f)) also, exhibit the formation of homogenous blends. PVA is likely to be involved in some interactions at the surface level due to very little quantity considered.

Open Science Index, Chemical and Molecular Engineering Vol:11, No:1, 2017 publications.waset.org/10006352/pdf

Open Science Index, Chemical and Molecular Engineering Vol:11, No:1, 2017 publications.waset.org/10006352/pdf

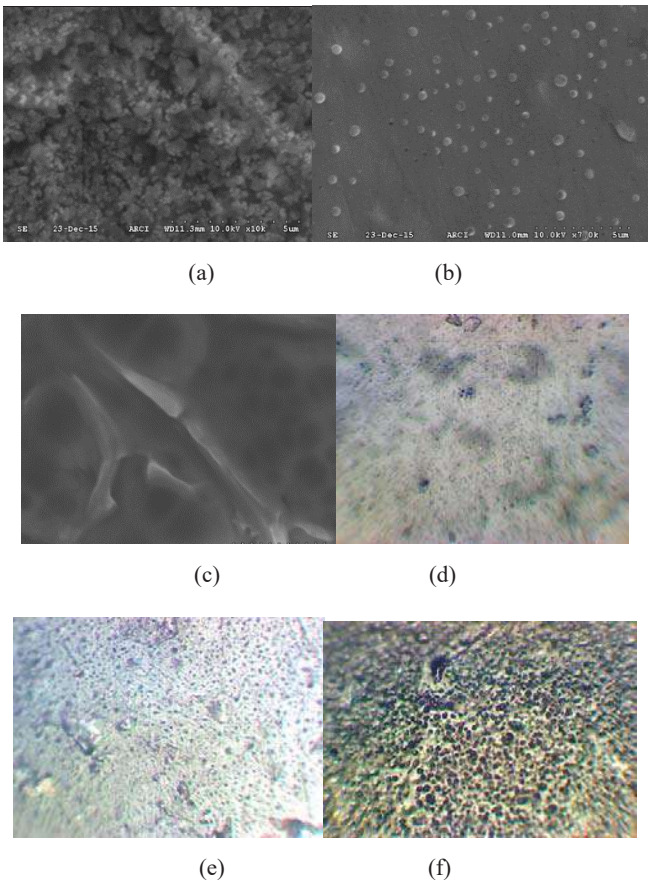

Fig. 5 Scanning electron microscopy images of (a) PANI-PEG/PVA (b) PANI-PEDOTPSS/PVA (c) PANI-TSC/PVA; Optical microscopy images of (d) PANI-PEG/PVA (e) PANI-PEDOTPSS/PVA and (f) PANI-TSC/PV

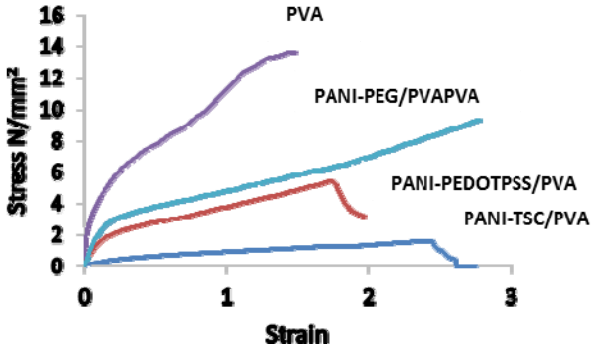

Fig. 6 Stress- strain curves of the studied polymer blends

PVA can form itself, very good quality films with appreciable strength and elongation. When it is blended with PANI templates, interesting mechanical properties were observed. In this paper, we try to investigate the strength of different polymer compositions and their combinations. The material when subjected to high-strain, it deforms permanently (plastic deformation) and at last fracture the specimen. At low stresses and strains, the polymeric material behaves as an elastic material. The point where the behavior starts to be non-linear is called the proportional limit. The local maximum in the stress-strain linear curve is called the yield point and indicates the starting of permanent deformation. Beyond the yield point the material stretches considerably and beyond this region is called the plastic region. Further elongation leads to strain hardening and rupture of the material at the end. At the rupture point the corresponding stress and strain are called the ultimate strength and the maximum strain at break. The stress-strain behavior of a polymeric material depends on combination and composition of the polymer. Stress-strain studies (Fig. 6) were performed on all the polymer blends prepared. PANI-PEG/PVA possess highest strain, PANI-TSC/PVA also has high strain and good elasticity. All the blends studied are very good elastic materials. However, strength is less than 10 N/mm^2.

PVA has highest mechanical strength 13.5 N/ mm^2, with moderate elasticity of 1.5 strain. PANI-PEG/PVA has highest strain of 2.8 but strength of 9.5 N/mm^2. PANI-TSC/PVA has high strain of 2.5 with good elasticity, but its strength was very less only 1.8 N/mm^2. The strength and strain of PANI-PEDOTPSS/PVA was found to be 5.2 N/mm^2 and 1.75. Strength of PVA could be due to extensive hydrogen bonding within the molecules. However, when it is blended with templated PANIs, PANI-PEG/PVA is found to have more strength when compared to PANI-PEDOTPSS/PVA and PANI-TSC/PVA. PEG being a stabilizer, when PANI is templated with PEG, we observed good uniform blend, moreover, when this is further blended with PVA, could lead to more stabilization due to several intermolecular interactions such as hydrogen bonding, weak Van der Waals interactions etc. Though, PANI-TSC/PVA has good elasticity, TSC being small molecule unlike PEG or PEDOT-PSS may not promote more extended polymer chains, thus decreasing the strength. However, the large strain exhibited by PANI-TSC/PVA could be due to several surface lever interactions. From our earlier reported work [22] we observed that PANI-PEDOTPSS and PANI-TSC form stable colloidal suspensions through electrostatic interactions as PEDOT-PSS and TSC are ionic. On the other hand, PEG behaves is more like a surfactant. Hence, PANI-PEG could more probably form via steric repulsions.

The synthesis and fabrication protocol we have developed allows the preparation of stable aqueous colloidal suspension of PANI in an environmentally friendly aqueous route and also the extension of this in the development of free standing elastic polymeric materials with appreciable strength and strain. FT-IR and UV-Vis spectra reveal possible intermolecular interactions between the templated PANI and PVA, which is correlated to their strength and strain. Effect of small molecule (TSC) and polymer (PEDOT-PSS and PEG) as templates on PANI and blend with PVA has been investigated. DSC suggests crystalline transformation in PANI-PEDOTPSS and PANI-PEG. SEM and optical microscopy reveals uniform features. Detailed characterization and tensile tests of all samples suggests organization and mutual interactions between templated polymers and PVA leading to an improved polymer blend leading for the fabrication of elastic materials. Presence of templated PANI's in the film helps in retaining

the tensile strength. Such blends might find their applications as optical, semiconducting materials and as organic vapor sensors.

REFERENCES

[1] D. C. Trivedi and H. S. Nalwa, "*Handbook of Organic Conductive Molecules and Polymers,*" vol. 2, pp. 509-511, London: John Wiley, 1997.

[2] J. Huang, S. Virji, B. H. Weiller and R. B. Kaner, "Polyaniline nanofibers: facile synthesis and chemical sensors," *J. Am. Chem. Soc.* vol. 125, pp. 314-315, Jan. 2003.

[3] H. S. Abdulla and A. I. Abbo, "Optical and electrical properties of thin films of polyaniline and polypyrrole," *Int. J. Electrochem. Sci.*, vol. 7, pp. 10666-10678, Nov. 2012.

[4] J. C. Michaelson, A. J. McEvoy and N. Kuramoto, "Morphology and growth rate of polyaniline films modified by surfactants and polyelectrolytes," *React. Polym*., vol. 17, no. 2, pp. 197-206, May 1992.

[5] C. W. Wang, Z. Wang, M. K. Li and H. L. Li, "Well-aligned polyaniline nano-fibril array membrane and its field emission property," *Chem. Phys. Lett*., vol. 341, pp. 431-434, Jun. 2001.

[6] H. Karami, M. F. Mousavi and M. Shamsipur, "A novel dry dipolar rechargeable battery based on polyaniline,"*J. Power Sourc.*, vol. 124, pp. 303-308, May 2003.

[7] H. Qui and M. Wan, "Synthesis, characterization, and electrical properties of nanostructural polyaniline doped with novel sulfonic acids (4-{*n*-[4(4-nitrophenylazo) phenyloxy]alkyl}aminobenzene sulfonic acid," *J. Polym. Sci. Part A: Poly. Chem.*, vol. 39, pp. 3485-3497, Aug. 2001.

[8] Z. Tian, H. Lu, L. Wang, M. Saleem, F. Ren, P. Ren, Y. Chen, R. Sun, Y. Sun and L. Huang, "Recent progress in the preparation of polyaniline nanostructures and their applications in anticorrosive coatings," *RSC Advances.*, vol 4, pp. 28195-28208, Jun. 2014.

[9] J. Laska, "Conformations of polyaniline in polymer blends", *J. Mol. Struc.*, vol. 701, pp. 13-18, May 2004.

[10] W. J. Bae, W. H. Jo and Y. H Park, "Preparation of polystyrene/polyaniline blends by in situ polymerization technique and their morphology and electrical property" *Syn. Metals*, vol. 132, pp. 239-244, Sep. 2002.

[11] C. Chen, J. C. La Rue, R. D. Nelson, L. Kulinsky and M. J. Madou, "Electrical conductivity of polymer blends of poly(3,4-ethylenedioxythiophene): Poly(styrenesulfonate):N-methyl-2-pyrrolidinone and polyvinyl alcohol," *J. Appl. Poly. Sci*., vol. 125, pp. 3134-3141, Aug. 2012.

[12] D. Li and R. B. Kaner, "Processable stabilizer-free polyaniline nanofiber aqueous colloids," *Chem. Commn.,* pp. 3286-3288, May 2005.

[13] L. F. Malmonge, S. C. Langiano, J. M. M. Cordeiro, L. H. C. Mattoso and J. A. Malmonge, "Thermal and mechanical properties of PVDF/PANI Blends," *Mat. Res.*, vol. 13, no. 4, pp. 465-470, Oct. 2010.

[14] J. Bhadra, N. J. Al-Thani, N. K. Madi and M. A. Al-Madeed, "Effects of aniline concentrations on the electrical and mechanical properties of polyaniline polyvinyl alcohol blends," *Arb. J. Chem..,* http://dx.doi.org/10.1016/j.arabjc.2015.04.017, Apr. 2015.

[15] S. Akhilesan, C. Lakshmana Rao and S. Varughese, "Electromechanical behavior of Polyaniline/Poly(Vinyl alcohol) blend films under static, dynamic and time dependent strains," *Smart Mater. Struct*., vol. 23, No. 7, pp. 1-11, Jun. 2014.

[16] A. V. Nand, S. Ray, J. Travas-Sejdic and P. A. Kilmartin, "Characterization of polyethylene terephthalate/polyaniline blends as potential antioxidant materials," *Materials Chemistry and Physics*, vol.134, pp. 443-450, Sep. 2012.

[17] D. Jaaoh, C. Putson and N. Muensit, "Deformation on segment-structure of electrostrictive Polyurethane/Polyaniline blends," *Polymer*, vol. 61, pp. 123-130, Mar. 2015.

[18] V. Giel, J. Kredatusova, M. Trchova, J. Brus, J. Jitka and J. Peter, "Polyaniline/Polybenzimidazole blends: Characterization of its physico-chemical properties and gas separation behavior," *European Polymer Journal.,* vol. 77, pp. 98-113, Apr. 2016.

[19] N. Cai, D. Hou, X. Luo, C. Han, J. Fu, H. Zeng and F. Yu, "Enhancing mechanical properties of polyelectrolyte complex nanofibers with graphene oxide nanofillers pretreated by polycation," *Composites Science and Technology*, vol. 135, pp. 128-136, Oct. 2016.

[20] L. Sun and S. C. Yang, "Solution processable conducting polymer polyaniline-polyelectrolyte complexes," *Mat Res. Soc. Symp Proc.,* vol 328, pp. 209-214, 1994.

[21] Z. Zhang and M. Wan, "Composite Films of Nanostructured Polyaniline with Poly(vinyl alcohol)," *Synth. Metals*, vol. 128, pp. 83-89, Apr. 2002.

[22] A. Jyothi Lakshmi, K. Shantanu and S. Jayanty, "Synthesis and Characterization of Templated polyanilines: A new class of polymeric materials," Chapter 14, Functionalized Engineering Materials and Their Applications, Apple Academic Press, CRC, Taylor and Francis Group, Nov. 2016. *(In publication)*

[23] R. Saxena, V. Shaktawat, N. Jain, N. S. Saxena, V. Sharma and T. P. Sharma, "Structural and thermal characterization of metal halide doped polypyrrole," *Ind. J. Pure App. Chem.,* vol. 46, pp.414-416, Jun. 2008.

[24] A. J. Epstein, J. M. Ginder, F. Zuo, R. W. Bigelow, H. S. Woo, D. B. Tanner, A. F. Ritcher, W. S. Huang and A. G. MacDiarmid, "Insulator-to-metal transition in polyaniline," *Synth. Met.,* vol. 18, pp. 303-309, Feb. 1987.

[25] G. Rupali, D. Amitabha and G. Goutam, "Polyaniline-Poly(vinyl alcohol) Conducting Composite: Material with Easy Processability and Novel Application Potential," *Synth. Metals,* vol. 123, pp. 21-31. Aug. 2001.

[26] S. Jayanty, "Synthesis, conductivity and morphology study of polystyrenesulfonate templated tetrathiafulvalene polyionic polymers," *Applied Science and Advanced Materials International*, vol. 1, no.2, pp. 56-59, Nov. 2014.

[27] S. Jayanty, "Carboxymethyl cellulose templated polyaniline: film morphology and conductivity," *International Journal of Energy, Sustainability and Environmental Engineering*, vol.1 (4-5), pp. 123-127, May 2015.

[28] T. Nakamura and S. Jayanty, "Poly(4-styrenesulfonate) templated polyaniline-carboxymethyl cellulose blend: morphology and surface resistivity of the spin coated films," *Soft Materials*, vol. 1, no. 4-5, pp. 309-315, Jul. 2016.

Open Science Index, Chemical and Molecular Engineering Vol:11, No:1, 2017 publications.waset.org/10006352/pdf

IJRECS @ July-Aug 2017, V-10, I-8
ISSN-2321-5485(Online) ISSN-2321-5784 (Print)

Scalable and Secure Method for Location based Query Processing with kNN Queries

Ishrath Nousheen[1], Waseema Masood[2]
[1]Assistant Professor, Dept of CSE, Nawab Shah Alam Khan College of Engineering & Technology
[2]Assistant Professor, Dept of CSE, Nawab Shah Alam Khan College of Engineering & Technology

Abstract: The huge development of the Internet has altogether decreased the cost of getting and sharing data about people, raising many worries about client protection. Spatial inquiries represent an extra danger to protection on the grounds that the area of an inquiry might be adequate to uncover delicate data about the querier. In this paper we concentrate on k closest neighbor (kNN) questions and characterize the thought of solid area security, which renders an inquiry indistinct from any area in the information space. We contend that past work neglects to help this property for discretionary kNN seek. Towards this end, we present techniques that offer solid area protection, by coordinating private data recovery (PIR) usefulness. In particular, we utilize secure equipment helped PIR, which has been demonstrated exceptionally effective and is right now considered as a handy component for PIR. At first, we devise a benchmark arrangement expanding upon a current PIR-based system. In this way, we recognize its disadvantages and present a novel plan called AHG to handle them. At last, we show the execution prevalence of AHG over our rival, and its reasonability in applications requesting the most abnormal amount of security.

1. INTRODUCTION

The installing of situating capacities (e.g., GPS) in cell phones encourages the development of area based administrations (LBS), which is considered as the following "executioner application" in the remote information showcase. Area based administrations enable customers to inquiry a specialist co-op, (for example, Google or Bing Maps) in an omnipresent way, keeping in mind the end goal to recover itemized data about purposes of intrigue (POIs) in their region (e.g., eateries, clinics, and so on.). Be that as it may, like web seeks or online buys, area subordinate inquiries may unveil delicate data around a person's wellbeing, money related status, political affiliations, and so forth.

Accept, for instance, that a client wishes to discover the closest night clubs to his/her area. To cover this data, the client may transmit the inquiry through an anonymizing system (e.g., Tor [1]) that shrouds his/her genuine IP address. All things considered, basically expelling the IP deliver is not adequate to secure the client's personality, which can be deduced from the directions of the question and foundation learning (e.g., the client's place of residence). Subsequently, really private administrations require area protection, i.e., the LBS ought to be careless of the question area. Furthermore, area protection is attractive freely of the camouflage of the client personality. For example, consider a versatile client who requests the closest night clubs, however wishes to conceal that he/she has gone to the particular zone. For this situation, the client requires area security regardless of the possibility that the supplier can induce his/her character.

The installing of situating capacities (e.g., GPS) in cell phones encourages the development of area based administrations (LBS), which is considered as the following "executioner application" in the remote information showcase. Area based administrations enable customers to inquiry a specialist co-op, (for example, Google or Bing Maps) in an omnipresent way, keeping in mind the end goal to recover itemized data about purposes of intrigue (POIs) in their region (e.g., eateries, clinics, and so on.). Be that as it may, like web seeks or online buys, area subordinate inquiries may unveil delicate data around a person's wellbeing, money related status, political affiliations, and so forth.

Accept, for instance, that a client wishes to discover the closest night clubs to his/her area. To cover this data, the client may transmit the inquiry through an anonymizing system (e.g., Tor [1]) that shrouds his/her genuine IP address. All things considered, basically expelling the IP deliver is not adequate to secure the client's personality, which can be deduced from the directions of the

question and foundation learning (e.g., the client's place of residence). Subsequently, really private administrations require area protection, i.e., the LBS ought to be careless of the question area. Furthermore, area protection is attractive freely of the camouflage of the client personality. For example, consider a versatile client who requests the closest night clubs, however wishes to conceal that he/she has gone to the particular zone. For this situation, the client requires area security regardless of the possibility that the supplier can induce his/her character.

At last, PIR-based methodologies use a PIR convention (e.g., [19]) actualizing a basic inquiry primitive, which recovers a particular database hinder from the LBS without the last finding which square was recovered. This primitive is impervious to get to design assaults. The customer diminishes a spatial inquiry to an arrangement of such private recoveries. To the best of our insight, there exist just two PIR-based techniques [17, 11]. [17] manages kNN seek, proposing calculations that may include a variable number of PIR square recoveries per spatial inquiry. Albeit every recovery is totally private, the cardinality of the PIR asks for per kNN question may uncover data, like that in get to design assaults for information change methods. Subsequently, these techniques damage solid area security. Then again, [11] involves a solitary PIR recovery for every inquiry. In this manner, it renders all questions vague, fulfilling solid area protection. In any case, it can just deal with single NN inquiries. Moreover, it prompts a restrictive computational and correspondence cost notwithstanding for little POI databases ($\simeq$ 1MB), on the grounds that it depends on a costly PIR convention ([19]).

This is the principal work to propose strategies for discretionary kNN look with solid area protection. There are two fundamental parts in our plans: (i) the PIR usefulness, and (ii) the inquiry design. The previous guarantees that the LBS is unmindful of each square recovered by the calculations. We utilize secure equipment PIR [24], which is at present the main down to earth decision for PIR in databases of non-immaterial size. Specifically, this system offers private piece recoveries with consistent correspondence cost and amortized polylogarithmic computational cost. The last means handling times near one moment notwithstanding for Gigabyte databases, while different plans (e.g., [19]) involve hours.

The question design guarantees that each inquiry recovers a similar number of squares amid its execution. A unimportant arrangement would uphold each question to recover a settled and self-assertively huge number of squares. In any case, such an answer may gravely affect the execution of our plans. Subsequently, we propose calculations that register a tight upper destined for the piece gets to that any question in the information space must perform, to such an extent that every one of its outcomes are recovered.

At first, we build a benchmark strategy, called BNC, by enhancing [17] and creating a question design keeping in mind the end goal to authorize solid area security. In this way, we bring up its disadvantages and propose a novel arrangement, called AHG, to handle them. We tentatively contrast AHG and BNC utilizing thorough secure equipment recreations, and demonstrate that AHG beats BNC in all settings. We additionally show that AHG highlights reaction times in the request of a couple of moments when testing with direct POI databases ($\simeq$ 130 MB), and scales great under Gigabyte databases. Subsequently, AHG constitutes the primary feasible answer for applications where solid area security is basic.

II. RELATED WORK

Section 2.1 reviews location obfuscation methods, Section 2.2 describes schemes that employ data transformation to protect location privacy, and Section 2.3 presents PIR-based location privacy techniques.

2.1 Location Obfuscation

This classification incorporates each technique that grows the LBS's supposition about the real question area to a more extensive sub space of the spatial area, called jumbling district. In [18, 7, 8], with the exception of its genuine question, the customer sends to the LBS an extra arrangement of "sham" inquiries. The muddling locale comprises of the particular areas incorporated into the question set sent to the LBS. Cheng et al. [4] accept that the customers issue run questions, and the POIs are other customers' areas. All areas must be secured. In this

manner, every area is muddled into a round locale. The LBS forms the question and returns a probabilistic answer, which is demonstrated by the cover of the roundabout districts with the inquiry go. Space Twist [26] is an incremental NN calculation executed at the LBS, which begins from an irregular area produced by the customer and ends when the customer gets all its real NNs. The confusion locale is a subset of the information space secured by the calculation.

In the Spatial K-namelessness [20, 15, 9, 12] worldview, the customer sends its question to a put stock in anonymizer, which builds an anonymizing spatial district (ASR) that contains the querier's area alongside another K − 1 customer areas. The anonymizer at that point sends the ASR to the LBS. The last executes the inquiry as for the ASR, and returns a superset of the outcomes to the anonymizer, which sift through the false positives. The jumbling locale is the arrangement of the K areas in the ASR.

All area obscurity approaches ensure powerless area protection in light of the fact that the jumbling district is normally a little sub space of the aggregate 2D space. By the by, they regularly highlight low inquiry handling cost, because of the economical operations they involve.

2.2 Data Transformation

In this setting the information proprietor is not quite the same as the LBS. The proprietor changes the database (utilizing some encoding philosophy) before transmitting it to the LBS. An approved customer that has the mystery change keys issues an encoded inquiry to the LBS. Both the database and the questions are mixed up by the LBS and, therefore, area security is ensured. The objective is to give the LBS seeking abilities over the encoded information.

OPES [2] encodes the information in a way with the end goal that their numeric request is saved, in this manner permitting straightforward separation correlation operations. Wong et al. [25] propose a safe point change, which safeguards the relative separations of all the database POIs to any inquiry point. This property renders kNN preparing attainable. Another arrangement [16] changes the focuses utilizing the Hilbert mapping [21], and the parameters of the change (arrange, scale, introduction, and so on.) are looked after mystery. This method permits rough NN seek specifically on the changed focuses.

Information change strategies give a more grounded idea of area protection than obscurity. In any case, they are all the more computationally serious because of the encoding/interpreting operations. Also, they are inclined to get to design assaults [24] on the grounds that a similar inquiry dependably restores the same encoded comes about. For instance, the LBS may watch the frequencies of the returned ciphertexts. Knowing about the setting of the database, it can coordinate the most well known plaintext POI with the most regularly returned ciphertext and, along these lines, disentangle data about the question.

2.3 PIR-based Location Privacy

Assume that a server keeps up a database comprising of N consecutive squares. PIR conventions empower a customer to recover the i th hinder from the server, without the server finding which piece was asked for (i.e., record i). These conventions protect against get to design assaults. They can be gathered into: (i) data theoretic [5, 3], (ii) computational [19, 10], and (iii) secure equipment [14, 23, 24]. The previous are secure against even a computationally unbounded foe. By the by, they expect the presence of a settled number of non-plotting servers. Computational PIR techniques are relevant notwithstanding for a solitary server, and they depend on the computational immovability of understood issues (e.g., the φ-concealing hardness suspicion in [10]). Notwithstanding, they involve costly operations straight in the database estimate, which prompt restrictive preparing costs (in the request of thousands of seconds notwithstanding for direct database sizes).

Secure equipment PIR is at present the main handy PIR component. It depends on an alter safe CPU that is situated at the server and is trusted by the customers. This CPU gets a customer piece ask for, which is incomprehensible by the server. It absently extricates the asked for obstruct from the server's circle, and returns it to the customer in an encoded shape understandable exclusively by the customer. This worldview prompts consistent correspondence cost, and amortized

polylogarithmic computational cost. The last means preparing times near a moment notwithstanding for Gigabyte databases.

There exist two PIR-based arrangements. [17] proposes kNN calculations that lessen the inquiry to an arrangement of PIR square recoveries performed through secure equipment PIR. A vital detail administered is that two distinct inquiries may involve a variable number of PIR asks. In this manner, albeit each PIR recovery is totally private as expressed over, the cardinality of these recoveries may reveal area data like that in get to design assaults in information change. Thus, [17] does not give solid area security. Then again, [11] fulfills this property in light of the fact that each question includes a solitary PIR ask for and, subsequently, all inquiries are undefined. By and by, this plan concentrates just on single NN preparing. In addition, it depends on the computational PIR convention of [19] and, in this way, acquires its inordinate correspondence and computational expenses.

In Section 4 we devise a contender by upgrading [17] and building an inquiry design with a specific end goal to fulfill solid area security. Besides, take note of that [17] expect that the kNN calculation keeps running inside the protected equipment. Considering that coding on the safe equipment is awkward, this usage decision makes application improvement troublesome. Despite what might be expected, we consider that the protected equipment underpins private piece recovery as an interface that can be utilized by any outside calculation, in this way upgrading the utility of the safe equipment.

R. Agrawal et al [2] concentrates on the innovation Encryption is utilized for ensuring delicate information. Be that as it may, once scrambled likewise effortlessly got to from the correct matches. In a specific order protecting plans can permit any examination administrator that can be utilized as a part of scrambled information. A portion of the total capacity are utilized as a part of examination administrator and comparably GROUPBY and ORDER BY can likewise be utilized. In these plan it protects the request and the handling over information encryption are likewise inexact. This will contain neither false positive nor miss any tuples. This ell precisely separates it other plan. This plan handles refreshes effortlessly. The OPES will decrease the helplessness to the assaults. However the programmer can access the data recovery yet he can't ready to see the information. The overhead on question handling will be decreased yet encryption key is vast and it involves more space.

Zhengli Huang et al [3] portrays that Randomization has the advantageous technique for information putting away. The information social occasion and information seeking have increments both in space and trouble. The randomization procedure does not give protection. Be that as it may, it needs to give clear reason which causing security issue, what are the purposes behind causing such security issue and how to offer assurance to security issues, and which information needs higher security. It is cleared in this approach by anatomization. The exploration of this strategy (ppdm) [3] went for filling the space consolidated information putting away and information protection. It seeks on numerous conceivable courses in social issues when all is said in done. They have investigated and taken numerous trial examination on the association between information joining and the measure of secure data that can be giving security situated in this proposed information strategies. To enhance security, the proposed an adjusted anatomization conspire, in which we let the blend of irregular commotions like the real information.

W. K. K et al [4] depicts that the specialist co-ops change over their foundations into open cloud condition. A portion of the conventional encryption strategy concentrate on giving unbreakable insurance despite the fact that they don't holds up the inquiries structures on the inculpation information. It concentrates on the data recovery on inculpation and they build up a different new inculpation technique which gives secure scalar item. The reason for the plans is to secure the information assaults in various level, at an alternate overhanging cost. This technique changing over the plain content to figure content utilizing encryption and decoding strategy just approved gatherings can perform unscrambling.

III. ACCURATE AND EFFICIENT QUERY PROCESSING

a. Hierarchical Routing Algorithm

This calculation is utilized for a proficient steering calculation which retaining two conceivable circumstance, i.e., inside group directing (WICR) and between-group steering (BCR), contingent upon whether the source and goal hubs have a place with a similar group or not. These calculations were proposed to play out some precomputation on the info information to lessen the inquiry intricacy. This chains of command approach depends on its inalienable various leveled topologies (e.g., street classifications, street lengths, and speed limits) [13]. This progressive group calculation is connected in street systems; and here the creators built up a group based various leveled chart show that backings productive way calculation on substantial street systems. At that point additionally another various leveled steering calculation that can altogether lessen the inquiry space over the customary calculations with adequate loss of precision. In view of the recognized groups, a progressive diagram display is produced for organizing the street systems, and a heuristic various leveled steering calculation is then used to decrease look and give close ideal arrangements.

b. Predictive Tree

Prescient questions on moving articles offer an essential classification of area mindful administrations in light of the items' normal future areas. This is utilized to prescient questions against moving articles on street systems. This approach gives a non specific foundation to noting the basic sorts of prescient questions including prescient point, range, KNN, and total inquiries, refreshes the probabilistic expectation of the protest's future areas progressively and incrementally as the protest moves around out and about system. It offer a central sort of area construct administrations based with respect to clients' future areas [14]. Regular sorts of prescient spatial inquiries incorporate prescient range inquiry, e.g., "discover all lodgings that are situated inside two miles from a client's foreseen area following 30 minutes", prescient KNN question, e.g., "locate the three cabs that are nearest to a client's area inside the following 10 minutes", and prescient total inquiry, e.g., "locate the quantity of autos anticipated that would be around the stadium amid the following 20 minutes. Indeed, Predictive inquiries are advantageous in different sorts of genuine applications, for example, (1) movement administration, to foresee regions with high activity in the following half hour, so proper choices are taken before blockage shows up, (2) area mindful publicizing, to appropriate coupons and deals advancements to clients more inclined to appear around a specific store amid the deal time in the following hour, (3) directing administrations, to think about the anticipated movement on every street section to locate the most brief way of a client's trek beginning following 15 minutes from the present time, (4) ride sharing frameworks, to coordinate the drivers that will go by a rider's area inside couple of minutes, and (5) store discoverers, to prescribe the nearest eateries to a client's anticipated goal in 15 minutes. The prescient tree prunes the space around each moving article with a specific end goal to decrease calculation, and increment framework productivity.

c. kNN Queries for Moving Objects on Road Networks

kNN seek is profoundly not quite the same as single-combine most limited way arrangement. In spite of the fact that kNN seek includes most limited way calculation, the key purpose of kNN look is to rapidly locate those promising best k questions as opposed to ascertain the briefest way from the inquiry area to all applicant protests at that point positions them. In this manner, it is not plausible to apply them to deal with the kNN look on street organizes adequately [15]. There are a significant number of concentrates on kNN inquiries for moving articles observing. These works considered the issue of finding closest moving items (e.g., navigates) to an area and concentrated on managing continuous updates of moving articles. For our situation, they underline on the effectiveness of the kNN inquiries on the static items (e.g., corner stores), of which the thoughts and usage are entirely unexpected. The kNN seek comprises of two sections. The first is the neighborhood Dijkstra seek inside Min Dist Inside Leaf. The time intricacy is $O(\tau \log \tau)$. The second one is MinDist-Outside-Leaf.

d. Road hierarchy-based partitioning

This technique is the normal chain of importance introduce in street systems to board the system into semantically significant regions. We develop abnormal

state regions by partitioning the diagram utilizing the biggest conceivable streets: Each range at this level is encased by huge interstates and will presumably contain countless and edges. We recursively subdivide ranges by logically diminishing the street scale [16]. A productive calculation is created that consequently segments a self-assertive street system and develops a characteristic order of ranges. These zones are fundamental to the calculation as they will be utilized to direct the driving example mining and versatile quickest way precomputation.

IV. OUTCOME OF THE SURVEY

- In this overview we have contemplated the exactness and effective information getting to issues in remote versatile innovation and break down the issue of different research articles.
- Wireless interchanges is one of the upgrowing advances to give better correspondence among individuals.
- Most of the specialists focus just on information transmission however neglected to focus on client precision.
- They were exactness issue while giving the information through the systems. Most remote exchanges are done through open climate so they were happened precision issue.
- They were issue under precision as a result of high computational and correspondence costs.
- LBS bolster area security control by the client. It underpins client control and adaptability.
- It gives Instant Messaging administration to server and customers

V. CONCLUSION

In this review, we have exhibited a diagram of precise and proficient inquiry preparing in versatile systems. With the progression of versatile advances, remote systems have turned out to be generally accessible and interconnected together. While in the meantime give an exact and required outcome will accommodating for the versatile client through LBS framework is most fundamental one. In this overview we have considered the skill of different methodologies and displayed the rundown about LBS procedures. This demonstrates the need of productive inquiry preparing in LBS space. With the constrained data through LBS is not an agreeable thing, to advance the fulfillment here we give many approach of their benefits and negative marks gave in this article.

REFERENCES

[1] Tor: anonymity online. http://www.torproject.org/.

[2] R. Agrawal, J. Kiernan, R. Srikant, and Y. Xu. Order preserving encryption for numeric data. In SIGMOD, 2004.

[3] A. Beimel, Y. Ishai, E. Kushilevitz, and J. E. Raymond. Breaking the O(n 1/(2k−1)) barrier for information-theoretic private information retrieval. In FOCS, 2002.

[4] R. Cheng, Y. Zhang, E. Bertino, and S. Prabhakar. Preserving user location privacy in mobile data management infrastructures. In Privacy Enhancing Technologies, 2006.

[5] B. Chor, O. Goldreich, E. Kushilevitz, and M. Sudan. Private information retrieval. In FOCS, 1995.

[6] M. de Berg, M. van Kreveld, M. Overmars, and O. Schwarzkopf. Computational Geometry: Algorithms and Applications. Springer-Verlag, 2nd edition, 2000.

[7] M. Duckham and L. Kulik. A formal model of obfuscation and negotiation for location privacy. In PERVASIVE, 2005.

[8] M. Duckham and L. Kulik. Simulation of obfuscation and negotiation for location privacy. In COSIT, 2005.

[9] B. Gedik and L. Liu. Location privacy in mobile systems: A personalized anonymization model. In ICDCS, 2005.

[10] C. Gentry and Z. Ramzan. Single database private information retrieval with constant communication rate. In ICALP, 2005.

[11] G. Ghinita, P. Kalnis, A. Khoshgozaran, C. Shahabi, and K. L. Tan. Private queries in location based

services: Anonymizers are not necessary. In SIGMOD, 2008.

[12] G. Ghinita, P. Kalnis, and S. Skiadopoulos. PRIVE: Anonymous location-based queries in distributed mobile systems. In WWW, 2007.

[13] H. Hu and D. L. Lee. Range nearest-neighbor query. TKDE, 18(1):7891, 2006.

[14] A. Iliev and S. Smith. Private information storage with logarithmic space secure hardware. In i-NetSec, 2004.

[15] P. Kalnis, G. Ghinita, K. Mouratidis, and D. Papadias. Preventing location based identity inference in anonymous spatial queries. TKDE, 19(12):1719–1733, 2007.

[16] A. Khoshgozaran and C. Shahabi. Blind evaluation of nearest neighbor queries using space transformation to preserve location privacy. In SSTD, 2007.

[17] A. Khoshgozaran, C. Shahabi, and H. Shirani Mehr. Location privacy; moving beyond k-anonymity, cloaking and anonymizers. KAIS, 2010 (to appear).

[18] H. Kido, Y. Yanagisawa, and T. Satoh. An anonymous communication technique using dummies for location based services. In ICPS, 2005.

[19] E. Kushilevitz and R. Ostrovsky. Replication is not needed: Single database, computationally-private information retrieval. In FOCS, 1997.

[20] M. F. Mokbel, C. Y. Chow, and W. G. Aref. The New Casper: Query processing for location services without compromising privacy. In VLDB, 2006.

[21] B. Moon, H. V. Jagadish, C. Faloutsos, and J. H. Saltz. Analysis of the clustering properties of the hilbert space-filling curve. TKDE, 13(1):124–141, 1996.

[22] K. Mouratidis, M. Hadjieleftheriou, and D. Papadias. Conceptual partitioning: An efficient method for continuous nearest neighbor monitoring. In SIGMOD, 2005.

[23] S. Wang, X. Ding, R. H. Deng, and F. Bao. Private information retrieval using trusted hardware. In ESORICS, 2006.

[24] P. Williams and R. Sion. Usable PIR. In NDSS, 2008.

[25] W. K. Wong, D. Q. Cheung, B. Kao, and N. Mamoulis. Secure kNN computation on encrypted databases. In SIGMOD, 2009.

[26] M. L. Yiu, C. Jensen, X. Huang, and H. Lu. Space Twist: Managing the trade-offs among location privacy, query performance, and query accuracy in mobile systems. In ICDE, 2008.

Impact Factor Value: 4.029 ISSN: 2349-7084
International Journal of Computer Engineering In Research Trends
Volume 4, Issue 10, October -2017, pp. 378-382 www.ijcert.org

Associating Social Media to e-Merchandise - A Cold Start Commodity Recommendation

[1]Ms. Habeebunissa Begum, [2]Dr. G.S.S Rao
[1]Pursuing M.Tech(CSE), [2]Professor & HOD
[1,2]Nawab ShahAlam khan College of Engineering and Technology, Hyd
Email:habeebunissabegum27@gmail.com ,profgssrao@gmail.com

Abstract: In recent years, the boundaries between e-commerce and social networking became increasingly blurred. Many e-commerce websites support the mechanism of social login where users can sign up the websites victimization their social network identities like their Facebook or Twitter accounts. Users can also post their contemporary purchased product on microblogs with links to the e-commerce product websites. Throughout this paper, we incline to propose a novel declare a cross-site cold-start product recommendation that aims to advocate product from e-commerce websites to users at social networking sites in "cold start" things, a retardant that has rarely been explored before. A massive challenge may be thanks to leverage knowledge extracted from social networking sites for a cross-site cold-start product recommendation. We tend to propose to use the coupled users across social networking sites and e-commerce websites (user's global organization agency have social networking accounts and have created purchases on e-commerce websites) as a bridge to map users' social networking choices to a clear feature illustration for a product recommendation. In specific, we incline to propose learning every users' and merchandises' feature representations (called user embedding and merchandise embedding, respectively) from info collected from e-commerce websites victimization continual neural networks, therefore, apply a modified gradient boosting trees methodology to rework users' social networking choices into user embedding. We incline to develop a feature-based matrix then resolving approach which could leverage the learned user embedding for a cold-start product recommendation. Experimental results on associate degree outsized dataset made of the most important Chinese microblogging service SINA WEIBO and conjointly the biggest Chinese B2C e-commerce website JINGDONG have shown the effectiveness of our planned framework.

Keywords: e-commerce, product recommender, product demographic, microblogs, recurrent neural networks.

1.Introduction:

Nowadays, Recommender Systems, aiming at serving to users understand relevant and attention-grabbing things from the information era, square measure wide studied and applied in varied fields ranging from e-commerce to medication prediction. Besides the countless studies on rising the recommendation performance the thanks to appropriately justify their commendation results associate degreed ultimately persuade users to settle for them easily is, also, an awe-inspiring challenge in every analysis and engineering fields. Though many novel algorithms have proved that they have to be achieved good, even extraordinary performance in varied matrices

© 2017, IJCERT All Rights Reserved

on offline datasets, feedbacks from on-line applications show that users would not invariably trust and follow the machine-produced results, that in extra hinders its wider development in real society Recently, the acquisition intention of users has attracted abounding attention from scientific community. utterly totally different from ancient recommender systems, they specialize in finding the factors which could verify one's temperament to shop for merchandise online. In fact, the $64000 online things one will face would be way more refined. Suppose one user arrives at a tee shirt channel, in spite of what she has purchased any merchandise, whether or not or not she is intensively motivated to buy for one issue this time can very have a sway on the $64000 recommendation result. Below this circumstance, the user's temperament, significantly her purchase intention would playanassociate degree associate primarily important role in decisive her judgment too easily settle for the items or not. Throughout this paper, we tend to tend to propose a scenario-based approach to examine the results of users' purchase intention on a real recommender system, Tmall.com. Firstly, we tend to tend to statistically analyze the dependence of 19 typical users' choices on their online activity sequence. Secondly, we tend to tend to propose a scenario-based approach to severally distinguish users into two groups: one with obvious purchase intention, and another whereas no such motivation.

2. Literature Survey

1] Opportunity model for e-commerce recommendation: Right product; right time

Author: -J. Wang and Y. Zhang

Description: Most of existing e-commerce conceiver systems aim to advocate the right product to a user, supported whether or not or not the user is maybe progressing to get or style of a product. On the alternative hand, the effectiveness of recommendations together depends on the time of the recommendation. permit the United States of America to require a user World Health Organization merely purchased a laptop computer as associate degree example. She would possibly purchase a replacement battery for a try of years (assuming that the portable computer's original battery usually fails to work around that time) and obtain a new portable computer in another a try of years. Throughout this case, it isn't an honest commit to recommend a fresh laptop computer or a replacement battery right once the user purchased the new laptop computer. it's going to hurt the user's satisfaction of the recommender system if she receives a likely right product recommendation at the wrong time. We incline to argue that a system mustn't exclusively recommend the first relevant item but together recommend at the right time.

2] Retail sales prediction and item recommendations using customer demographics at store level

Author: -M. Giering

Description: This paper outlines a retail sales prediction and merchandise recommendation system that was implemented for a sequence of retail stores. The relative importance of consumer demographic characteristics for accurately modeling the sales of each consumer kind area unit derived and implemented the model. information consisted of daily sales knowledge for 600 products at the look level, broken out by a group of non-overlapping consumer varieties. A recommender system was designed supported a fast online skinny Singular Price Decomposition. It's shown that modeling information at a finer level of detail by clump across consumer varieties and demographics yields improved performance compared to at least one mixture model designed for the entire dataset. Details of the system implementation area unit drawn and smart issues that arise in such real-world applications area unit mentioned.

3] Amazon.com recommendations: Item-to-item collaborative filtering

Author: -G. Linden, B. Smith, and J. York

Description: Recommendation algorithms square measure best superb for his or her use on e-commerce websites, where they use to input a handful of customer's interests to come back up with a list of prompt things. many applications use exclusively the items that customers purchase and expressly rate to represent their interests, however, they're going to in addition use different attributes, at the side of things viewed, demographic info, subject interests, and favorite artists. At Amazon.com, we have a tendency to tend to use recommendation algorithms to vary the net store for each consumer. the look radically changes supported consumer interests, showing programming titles to

© 2017, IJCERT All Rights Reserved

associate degree engineer and baby toys to a replacement mother. There square measure three common approaches to resolving the recommendation problem: ancient cooperative filtering, cluster models, and search-based ways. Here, we have a tendency to tend to check these ways with our algorithmic rule, that we have a tendency to tend to call item-to-item cooperative filtering.

4] The new demographics and market fragmentation

Author: -V. A. Zeithaml

Description: The underlying premise of this text is that dynamic demographics may end up in an exceeding breakage of the mass markets for grocery product and supermarkets. A field study investigated the relationships between 5 demographic factors-sex, female operative standing, age, income, and marital status status-and an outsized style of variables associated with preparation for and execution of market wanting. Results indicate that the demographic groups dissent in vital ways in which from the quality market shopper. Discussion centers on the ways in which during which dynamic demographics and family roles might need a sway on retailers and manufacturers of grocery product.

5. We know what you want to buy: a demographic-based system for product recommendation on microblogs

Author: - W. X. Zhao, Y. Guo, Y. He, H. Jiang, Y. Wu, and X. Li

Description: Product recommender systems area unit typically deployed by e-commerce websites to spice up the user experience and increase sales. However, the advice is prescribed by the merchandise knowledge hosted on those e-commerce sites and is barely triggered once user's area unit taking part in e-commerce activities. Throughout this paper, we have a tendency to tend to develop a totally distinctive product recommender system called breed, a bourgeois Intelligence Recommender System, that detects users' purchase intents from their microblogs in near period of time and makes product recommendation supported matching the users' demographic knowledge extracted from their public profiles with product demographics learned from microblogs and online reviews. Breed distinguishes itself from ancient product recommender systems inside the subsequent aspects: 1) breed was developed supported a microblogging service platform. As such, it isn't restricted by the information procurable in any specific e-commerce electronic computer. in addition, the breed is in an exceedingly position to trace users' purchase intents in near the period of time and build recommendations consequently. 2) Inbreed, product recommendation is framed as a learning to rank downside. Users' characteristics extracted from their public profiles in microblogs and products' demographics learned from every online product reviews and microblogs area unit fed into learning to rank algorithms for a product recommendation.

3. Proposed System

We propose to use the coupled users across social networking sites and e-commerce websites (user's global organization agency have social networking accounts and have created purchases on e-commerce websites) as a bridge to map users' social networking choices to latent choices for a product recommendation. In specific, we have an inclination to propose learning every users' and merchandises' feature representations (called user embedding and product embedding, respectively) from information collected from e-commerce websites exploitation continual neural networks then apply a modified gradient boosting trees methodology to remodel users' social networking choices into user embedding. We have an inclination to then develop a feature based mostly matrix resolving approach which could leverage the learned user embedding for a cold-start product recommendation. It targets text attribute, network attribute, and temporal attribute

© 2017, IJCERT All Rights Reserved

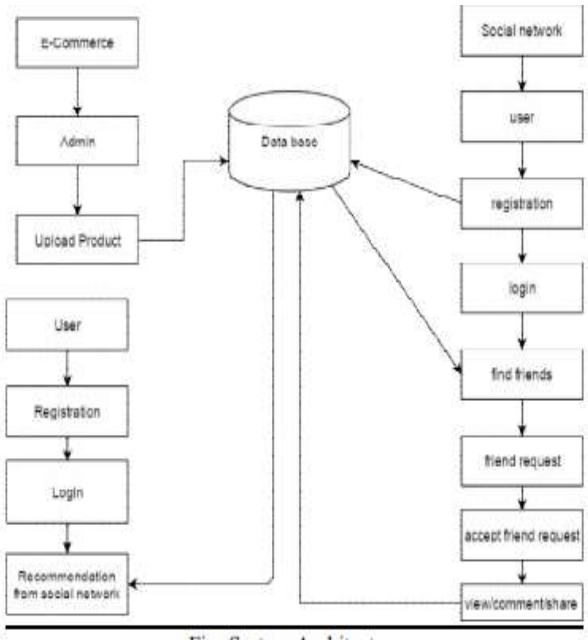

Fig: System Architecture

Advantages of Proposed System:

1. we have an inclination to propose a modified gradient boosting trees methodology to remodel users' microblogging attributes to latent feature illustration which can be merely incorporated for a product recommendation.

2. we have an inclination to propose and instantiate a feature-based matrix breakdown approach by incorporating user and product choices for a cold-start product recommendation.

3. The results show that our projected framework is therefore effective in addressing the cross-site cold-start product recommendation downside

4. Mathematical Model

INPUT:

Let S is that the Whole System include S=, I = Input, I =, U = User, U =, alphabetic character = question Entered by user, Q =, D = Dataset, P = Process:

Step1: Admin can transfer the merchandise in E-commerce web site.

Step2: That uploaded product are seen on Social sites wherever users will read, share and provides comments thereon product. The user will send and receive a lover request.

Step3: All the reviews ought to be seen in E-commerce website once user login to associate degree E-commerce site.

Output: User can get recommendation relating to of that product on associate degree e-commerce web site.

5.Scope Of Project

1)Easy to advertise a product exploitation social networking website.

2)Increase the interaction between the user and social networking website.

3)We believe that our study will have a profound impact on every analysis and business communities.

4)We propose a modified gradient is boosting trees technique to remodel users' microblogging attributes to latent feature illustration which can be merely incorporated for a product recommendation.

5) We tend to tend to propose and instantiate a feature-based matrix breakdown approach by incorporating user and merchandise choices for a cold-start product recommendation.

6. Conclusion

In this paper, we've to target a unique issue, cross-site cool begin item suggestion, i.e., prescribing things from e-trade sites to micro-blogging purchasers while not authentic get records. Our primary thought is that on the e-trade sites, purchasers and things are often spoken to within the same dormant component house through component learning with the repetitive neural systems. Utilizing an appointment of connected purchasers crosswise over each e-trade sites associate degreed long vary social communication destinations as an extension, we can learn to incorporate mapping capacities utilizing a modified angle boosting trees technique, that maps clients' qualities free from long very informal communication locales onto highlight representations gained from e-business sites. The mapped consumer parts are often adequately joined into associate degree embody based mostly network resolving approach for

© 2017, IJCERT All Rights Reserved

cold begin item proposal. we've designed a huge dataset from WEIBO and JINGDONG. The outcomes demonstrate that our planned system is while not a doubt compelling in tending to the cross-site icy begin item suggestion issue. we tend to trust that our study can have a major impact on each analysis and business teams.

References

1] F. Cheng, C. Liu, J. Jiang, W. Lu, W. Li, G. Liu, W. Zhou, J. Huang, and Y. Tang. Prediction of drug-target interactions and drug repositioning via network-based inference.PLoS Computational Biology, 8:e1002503, 2012.

2] E. Constantinides. Influencing the online consumer's behavior: the web experience.Internet research, 14:111–126, 2011.

3] J. L. Herlocker, J. A. Konstan, and J. Riedl.Explaining collaborative filtering recommendations. In Proceedings of the 2011 ACM conference on Computer supported cooperative work, pages 241–250. ACM,2011.

4] C. Jayawardhena, L. T. Wright, and C. Dennis. Consumers online: intentions, orientations and segmentation. International Journal of Retail &Distribution Management, 35:515–526, 2011.

5] A. Karatzoglou. Collaborative temporal order modeling. In Proceedings of the _fth ACM conferenceon Recommender systems, pages 313–316, 2009.

6] I. Konstas, V. Stathopoulos, and J. Jose. On social networks and collaborative recommendation.InProceedings of the 32nd International ACM SIGIR Conference on Research and Development in Information Retrieval, pages 195–202. ACM, 2007.

7] A. Liaw and M. Wiener.Classification and regression by randomforest.R news, 2:18–22, 2003.

8] C.-H. Park and Y.-G. Kim. Identifying key factors affecting consumer purchase behavior in an online shopping context.International Journal of Retail & Distribution Management, 31:16–29, 2002.

9] P. Resnick, N. Iacovou, M. Suchak, P. Bergstrom, and J. Riedl. Grouplens: an open architecture for collaborative filtering of netnews. In Proceedings of the 1994 ACM Conference on Computer Supported Cooperative Work, pages 175–186. ACM, 2001.

10] B. Sarwar, G. Karypis, J. Konstan, and J. Reidl.Item-based collaborative filtering recommendation algorithms. In Proceedings of the 10th InternationalConference on World Wide Web, pages 285–295. ACM, 2001.

11] J. B. Schafer, J. A. Konstan, and J. Riedl.E-commerce recommendation applications. In Applications of Data Mining to Electronic Commerce, pages 115–153. Springer, 2001.

12] E. Shen, H. Lieberman, and F. Lam. What am I gonna wear?: scenario-oriented recommendation. In Proceedings of the 12th international conference on intelligent user interfaces, pages 365–368. ACM, 2000.

13] K. H. Tso-Sutter, L. B. Marinho, and L. Schmidt-Thieme.Tag-aware recommender systems by fusion of collaborative filtering algorithms. In Proceedings of the 2008 ACM symposium on Applied computing, pages 1995–1999. ACM, 2008.

14] R. Verheijden. Predicting purchasing behavior throughout the clickstream.Master's thesis, Eindhoven University of Technology, May 1994.

15] F. Wu and B. A. Huberman.Novelty and collective attention.Proceedings of the National Academy of Sciences, USA, 104:17599–17601.

16].K.Arun ,A.SrinageshandM.Ramesh,"Twitter Sentiment Analysis on Demonetization tweets in India Using R language."International Journal of Computer Engineering in Research Trends., vol.4, no.6, pp. 252-258, 2017.

17] TekurVijetha, M.SriLakshmi and Dr.S.PremKumar," Survey on Collaborative Filtering and content-Based Recommending." International Journal of Computer Engineering in Research Trends., vol.2, no.9, pp. 594-599, 2015.

18] N.Satish Kumar, SujanBabuVadde," Typicality Based Content-BoostedCollaborative Filtering Recommendation Framework." International Journal of Computer Engineering in Research Trends., vol.2, no.11, pp. 809-813, 2015.

19] D.Ramanjaneyulu, U.Usha Rani," In Service-Oriented MSN ProvidingTrustworthy Service Evaluation."International Journal of Computer Engineering in Research Trends., vol.2, no.12, pp. 1192-1197, 2015.

20]B.Kundan,N.Poorna Chandra Rao and DrS.PremKumar," Investigation on Privacy and Secure content of location based Queries." International Journal of Computer Engineering in Research Trends., vol.2, no.9, pp. 543-546, 2015.

© 2017, IJCERT All Rights Reserved

Impact Factor Value: 4.029 ISSN: 2349-7084
International Journal of Computer Engineering In Research Trends
Volume 4, Issue 10, October -2017, pp. 413-418 www.ijcert.org

Energy and Memory Clone Detection in Wireless Sensor Network

[1] Mr. Amatul Mateen Shamsiya, [2]Dr. G.S.S Rao
[1]Pursuing M.Tech(CSE), [2]Professor & HOD
[1,2]Nawab ShahAlam khan College of Engineering and Technology, Hyd
Email: amatulmateen.shamsiya@gmail.com ,profgssrao@gmail.com

Abstract: An associate degree energy-efficient location-aware clone detection protocol is planned in densely deployed WSNs, which may guarantee productive clone attack detection and maintain satisfactory network life. Specifically, the situation info of sensors is employed and every which way choose witnesses situated in an exceedingly ring space to verify the legitimacy of sensors and to report detected clone attacks. The ring structure facilitates energy-efficient information forwarding on the trail towards the witnesses and also the sink. Planned protocol are able to do one hundred clone detection likelihood with unsuspicious witnesses. Moreover, in most existing clone detection protocols with random witness choice theme, the desired buffer of sensors is typically keen about the node density, whereas, in the planned protocol, the desired buffer of sensors is freelance of hop length of the network radius. Planned protocol are able to do long network life by effectively distributing the traffic load across the network.

Keywords: wireless sensor networks, clone detection protocol, energy efficiency, and network lifetime

---

1. Introduction

Wireless sensors are widely deployed for a spread of applications, starting from environmental observance to telemedicine and objects chase, etc.. For efficient sensing element placement, sensors are sometimes not tamperproof devices and are deployed in places while not observance and protection, that makes them liable to completely different attacks. for instance, a malicious user could compromise some sensors and acquire their personal info. Then, it will duplicate the sensing elements and deploy clones in an exceedingly wireless sensor network (WSN) to launch a spread of attacks that is spoken because of the clone attack. because the duplicated sensors have constant info, e.g., code and scientific discipline info, captured from legitimate sensors, they'll simply participate in network operations and launch attacks. owing to the low value for sensing element duplication and preparation, clone attacks became one in all the foremost vital security problems in WSNs. Thus, it's essential to effectively discover clone attacks so as to confirm healthy operation of WSNs. to permit economical clone detection, usually, a collection of nodes arewaschosen, that is known as witnesses, to assist certify the legitimacy of the nodes within the network. The personal info of the supply node, i.e., identity and also the location info ar shared with witnesses at the stage of witness choice. once any of the nodes within the network desires to transmit information, it initial sends the request to the witnesses for legitimacy verification, and witnesses can report a detected attack if the node fails the certification. to attain productive clone detection, witness choice and legitimacy verification ought to fulfill 2 requirements: 1) witnesses ought to be every which way chosen, and 2) a minimum of one in all the witnesses will with

© 2017, IJCERT All Rights Reserved

success receive all the verification message(s) for clone detection. The primary demand is to form it tough for malicious users listen in the communication between this supply node and its witnesses in order that the malicious users cannot generate duplicate verification messages. The second demand is to form certain that a minimum of one in all the witnesses will check the identity of the sensing element nodes to work out whether or not there's a clone attack or not. to ensure a high clone detection likelihood, i.e., the likelihood that clone attacks are with success detected, it's vital and difficult to meet these necessities in clone detection protocol style. completely different from wireless terminal devices, wireless sensors are sometimes of smaller size and cheaper price, and have restricted battery and memory capability. Therefore, the planning criteria of clone detection protocols for sensing element networks shouldn't solely guarantee the high performance of clone detection likelihood however additionally contemplate the energy and memory potency of sensors. within the literature, some distributed clone detection protocols are planned, like irregular economical and Distributed protocol (RED) and line chooses Multi-cast protocol (LSM). However, most approaches in the main specialize in rising clone detection likelihood while not considering potency and balance of energy consumption in WSNs. With such reasonably approaches, some sensors could assign their batteries owing to the unbalanced energy consumption, and dead sensors could cause network partition, which can more have an effect on the conventional operation of WSNs. Christo Ananth et al. mentioned a system, during this proposal, a neural network approach is planned for energy conservation routing in an exceedingly wireless sensing element network. Our designed neural network system has been with success applied to our theme of energy conservation. The neural network is applied to predict most vital Node and choosing the cluster Head amongst the association of sensing element nodes within the network. once having a definite prediction regarding most vital Node, we'd wish to expand our approach in future to completely different WSN power management techniques and observe the results. during this proposal, we have a tendency to used discretional information for our experiment purpose; it's additionally expected to get a period information for the experiment in future and additionally by exploitation ad-hoc networks the energy state of the node is maximized. The choice of cluster Head is planned exploitation the neural network with feedforward learning methodology. and also the neural network found able to choose a node amongst competitive nodes as Cluster Head. Most existing approaches will improve the productive clone detection at the expense of energy consumption and memory storage, which cannot be appropriate for a few sensing element networks with restricted energy resource and memory storage.

2. Problem Statement

Different from wireless terminal devices, wireless sensors are sometimes of smaller size and cheaper price, and have restricted battery and memory capability. Therefore, the planning criteria of clone detection protocols for sensing element networks shouldn't solely guarantee the high performance of clone detection likelihood however additionally contemplate the energy and memory potency of sensors. To prolong the network life, i.e., the time period from the beginning of the network till the primary incidence of a sensing element that runs out of energy, it's vital to not solely minimize the energy consumption of every node however additionally balance the energy consumption among sensors distributive situated in numerous areas of WSNs.

3. Existing System

1.Some distributed clone detection protocols are planned, like irregular economical and Distributed protocol (RED) and Line-Select Multicast protocol (LSM).

2.In most existing clone detection protocols, the desired buffer size depends on the network node density, i.e., sensors want an oversized buffer to record the changed info among sensors in an exceedingly high-density WSN, and so the desired buffer size scales with the network node density.

3.Such demand makes the present protocols not thus appropriate for densely deployed WSNs. A wireless ad-hoc network, additionally referred to as IBSS freelance Basic Service Set, may be a electronic network during which the communication links are wireless. The network is ad-hoc as a result of every node is willing to

© 2017, IJCERT All Rights Reserved

forward information for different nodes, then the determination of that nodes forward information is created dynamically supported the network property. this can be in distinction to older network technologies during which some selected nodes, sometimes with custom hardware and diversely referred to as routers, switches, hubs, and firewalls, perform the task of forwarding the info. stripped-down configuration and fast preparation create unintended networks appropriate for emergency things like natural or human-induced disasters, military conflicts. a significant limitation with mobile nodes is that they need high quality, inflicting links to be oftentimes broken and re-established. Moreover, the information measure of a wireless channel is additionally restricted, and nodes operate restricted battery power, which is able to eventually be exhausted. Therefore, the planning of a mobile unintended network is very difficult, however this technology has high prospects to be able to manage communication protocols of the longer term. The cross-layer style deviates from the normal network style approach during which every layer of the stack would be created to work severally. The changed transmission power can facilitate that node to dynamically vary its propagation vary at the physical layer. this can be as a result of the propagation distance is usually directionally proportional to transmission power. This info is passed from the physical layer to the network layer in order that it will take optimum choices in routing protocols. a significant advantage of this protocol is that it permits access to info between the physical layer and high layers (MAC and network layer). However, these tools focus totally on the simulation of the whole protocol stack of the system. Though this will be vital within the proof-of-concept implementations of systems, the requirement for a lot of advanced simulation methodology is usually there. Agent-based modeling and simulation provide such a paradigm. To not be confused with multi-agent systems and intelligent agents, agent-based modeling originated from social sciences, wherever the goal was to gauge and think about largescale systems with various interacting "AGENT" or parts in an exceedingly wide selection of random things to watch international phenomena. in contrast to ancient AI systems with intelligent agents, agent-based modeling is analogous to the important world. Agent-based models are so effective in modeling bio-inspired and nature-inspired systems. In these systems, the fundamental interactions of the parts of the system, additionally known as a fancy adaptive system, are easy however lead to advanced international phenomena like emergence the trail Discovery method is initiated whenever a supply node must communicate with another node that it's no routing info in its table. each node maintains 2 separate counters: a node sequence range and a broadcast id. The supply node initiates path discovery by broadcasting a route request (RREQ) packet to its neighbors. once associate degree intermediate node receives a RREQ, if it's already received a RREQ with constant broadcast id and supply address, it drops the redundant RREQ and doesn't air it. If a node cannot satisfy the RREQ, it keeps track of the subsequent info so as to implement the reverse path setup.

3.1 Disadvantages

1.Most approaches in the main specialize in rising clone detection likelihood while not considering potency and balance of energy consumption in WSNs. 2.Some sensors could assign their batteries owing to the unbalanced energy consumption, and dead sensors could cause network partition, which can more have an effect on the conventional operation of WSNs. 3.Most existing approaches will improve the productive clone detection at the expense of energy consumption and memory storage, which cannot be appropriate for a few sensing element networks with restricted energy resource and memory storage.

4. Proposed System

1.Besides the clone detection likelihood, we have a tendency to additionally contemplate energy consumption and memory storage within the style of clone detection protocol, i.e., associate degree energy- and memory-efficient distributed clone detection protocol with random witness choice theme in WSNs.

2.Proposed protocol is applicable to general densely deployed multi-hop WSNs, wherever adversaries could compromise and clone sensing element nodes to launch attacks.

3.An energy-efficient ring based mostly clone detection (ERCD) protocol to attain high clone detection likelihood with random witness choice, whereas

© 2017, IJCERT All Rights Reserved

guaranteeing traditional network operations with satisfactory network life of WSNs.

4.1 Advantages

1.Energy efficient

2.Memory efficient

3.High network lifetime can be achieved

5. System Architecture

5.1 ERCD PROTOCOL

In this section, we have a tendency to introduce our distributed clone detection protocol, particularly ERCD protocol, which may succeed a high clone detection likelihood with very little negative impact on network life and restricted demand of buffer capability. The ERCD protocol consists of 2 stages: witness choice and legitimacy verification. In witness choice, a random mapping operates is used to assist every supply node every which way choose its witnesses. within the legitimacy verification, a verification request is distributed from the supply node to its witnesses, that contains the personal info of the supply node. If witnesses receive the verification messages, all the messages are going to be forwarded to the witness header for legitimacy verification, wherever witness headers are nodes liable for deciding whether or not the supply node is legitimacy or not, by comparison, the messages collected from all witnesses. If the received messages are completely different from existing record or the messages are terminated, the witness header can report a clone attack to the sink to trigger a revocation procedure. Initially, the network region is just about divided into h adjacent rings, wherever every ring includes a sufficiently sizable amount of sensing element nodes to forward on the ring and also the breadth of every ring is r. To modify the outline we have a tendency to use hop length to represent the stripped-down range of hops within the paper. Since we have a tendency to contemplate a densely deployed WSN, hop length of the network is that the quotient of the gap from the sink to the sensing element at the border of network region over the transmission vary of every sensing element, i.e., the gap of every hop refers to the transmission vary of sensing element nodes. TABLE I shows the mathematical symbols used during this section. The ERCD protocol starts with a breadth-first search by the sink node to initiate the ring index, and every one neighboring sensor sporadically exchange the relative location and ID info [23], [24]. After that, whenever a sensing element node establishes an information transmission to others, it's to run the ERCD protocol, i.e., witness choice and legitimacy verification, to verify its legitimacy.

In witness choice, a hoop index is every which way chosen by the mapping operate because the witness ring of node a. to assist relieve the traffic load in an exceedingly hot spot, the realm around the sink cannot be chosen by the mapping operation. After that, node a sends its personal info to the node situated in witness ring, then the node forwards the knowledge on the witness ring to make a hoop structure. within the legitimacy verification, a verification message from the supply node is forwarded to its witnesses. The ring index of node a denoted Oa, is compared with its witness ring index Oa w to work out consequent forwarding node. If Oa w > Oa, the message are going to be forwarded to any node situated in ring Oa + 1; otherwise, the message is going to be forwarded to any node in ring Oa one. This step will forward the message toward the witness ring of node a. The ERCD protocol repeats higher than operations till a node, denoted b, situated within the witness ring Oa w is reached. Node b stores the personal info of node a and forwards the message to any node situated in ring Oa w among its transmission vary denoted as c. Then, node c stores the knowledge and forwards the message to the node d, wherever the link (c,d) has the longest projection on the extension line of the directional link from b to c. The procedure is going to be recurrent till node b reappears within the transmission vary. Therefore, the witnesses of node a have a hoop structure, consisting of b, c, b as 1. Fig.1 Ring structure of witness

© 2017, IJCERT All Rights Reserved

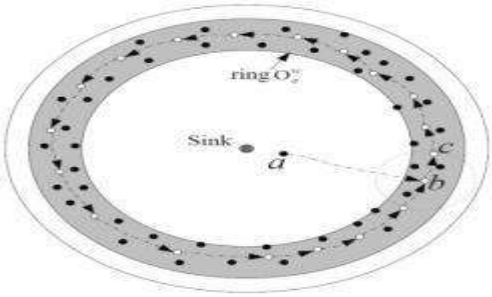

1.

Fig.5.1.1 Ring structure of witness

In the legitimacy verification, node a sends a verification message as well as its personal info following theconstant path towards the witness ring as in witness choice. to boost the likelihood that witnesses will with success receive the verification message for clone detection, the message are going to be broadcast once it's terribly near the witness ring, particularly three-ring broadcasts, i.e., the message is going to be broadcast in Oa w one, Oa w and Oa w +1 as shown in figure 1,2.

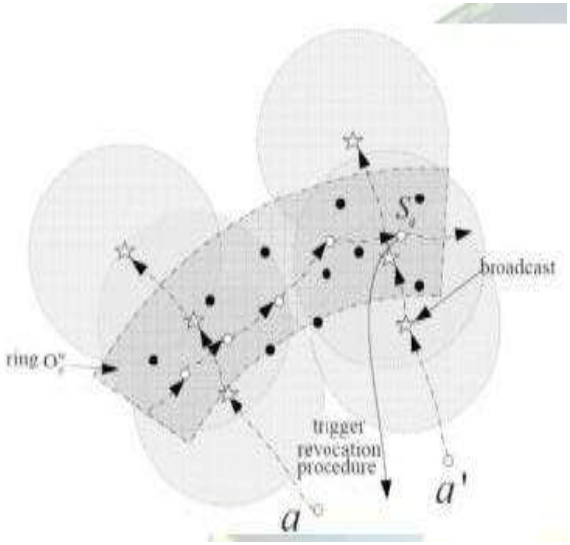

Fig.5.2.2 Legitimacy verification

In Theorem one, we have a tendency to prove that the three-ring broadcasts will make sure the network security, i.e., the clone detection likelihood is one, beneath the idea that each one witnessare unsuspicious. to work out whether or not there exists a lone attack or not, all the verification messages received by witnesses are forwarded to the witness header on theconstant route in witness choice. The sensing element nodes within the transmission route however not situated within the witness ring are known as the transmitters. The witness header of the supply node a, denoted by reserves, may be a sensing element situated in witness ring Oa w, meanwhile, it's additionally within the communication vary of the transmitter situated in ring index Oa w one or Oa w + one. The witness header Sais every which way was chosen by the transmitter within the neighboring witness ring, i.e., the ring of Oa w one or Oa w + one. If quite one copy or incorrect copies or terminated copies are received by the witness header, the ERCD protocol can trigger a revocation procedure; if no copy is received from the supply node owing to packet loss or silent cloned thenode, transmissions from the supply node won't be allowable.

6. Conclusion

In this paper, we've planned distributed energy economical clone detection protocol with random witness choice. Specifically, we've planned the ERCD protocol, which has the witness choice and legitimacy verification stages. Each of our theoretical analysis and simulation results hasincontestable that our protocol will discover the clone attack with nearly likelihood one since the witnesses of every sensing element node are distributed in an exceedingly ring structure that makes it simple be achieved by verification message. Additionally, our protocol is able to do higher network life and total energy consumption with an affordable storage capability of the info buffer. This can be as a result of we have a tendency to cash in of the situation info by distributing the traffic load everywhere WSNs, such the energy consumption and memory storage of the sensing element nodes around the sink node is mitigated and also the network life is extended. In our future work, we'll contemplate completely different quality patterns beneath varied network eventualities. sensing element networks are liable to node replication attacks. During this paper, we have a tendency to propose four distributed protocols for detecting these malicious attacks. The new protocols improve the state of the art by considerably reducing the number of memory area required, by equalization the memory and energy consumption across the network, and by raising the detection likelihood to almost 100also have some of thelimitations. they can't discover the replication attacks in an exceedingly mobile sensing element atmosphere.

© 2017, IJCERT All Rights Reserved

They believe the comparatively pricey public key cryptography. Our future work is to style replication detection protocols that use the key key cryptography and work for each static and mobile sensors.

References

[1] Z. Zheng, A. Liu, L. X. Cai, Z. Chen, and X. Shen, "ERCD: An energy-efficient clone detection protocol in wasns," in Proc. IEEE INFOCOM, Turin, IT, Apr. 14-19 2015, pp. 2436–2444.

[2] R. Lu, X. Li, X. Liang, X. Shen, and X. Lin, "GRS: The green, reliability, and security of emerging machine to machine communications," IEEE Communications Magazine, vol. 49, no. 4, pp. 28–35, Apr. 2013.

[3] Christo Ananth, A.NasrinBanu, M.Manju, S.Nilofer, S.Mageshwari, A.PeratchiSelvi, "Efficient Energy Management Routing in WSN", International Journal of Advanced Research in Management, Architecture, Technology and Engineering (IJARMATE), Volume 1, Issue 1, August 2012,pp:16-19

[4] Liu, J. Ren, X. Li, Z. Chen, and X. Shen, "Design principles and improvement of cost function based energy aware routing algorithms for wireless sensor networks," Computer Networks, vol. 56, no. 7, pp. 1951–1967, May. 2011.

[5] T. Shu, M. Krunz, and S. Liu, "Secure data collection in wireless sen-sor networks using randomized dispersive routes," IEEE Transactions on Mobile Computing, vol. 9, no. 7, pp. 941–954, Jul. 2010.

[6] Uma Vasala and Dr. G. R. Sakthidharan," Effective Key Management In Dynamic Wireless Sensor Networks"..”International Journal of Computer Engineering in Research Trends., vol.4, no.7, pp. 308-312, 2017.

[7] K.MANIMALA and .RANJITH," Mobile Transmission Using Rigorous Data for Wireless Sensor Networks"..”International Journal of Computer Engineering in Research Trends., vol.1, no.6, pp. 436-446, 2014.

[8] P. G. V. SURESH KUMAR1 , SEELAM SOWJANYA," Developing An Enterprise Environment by Using Wireless Sensor Network System Architecture"..”International Journal of Computer Engineering in Research Trends., vol.2, no.10, pp. 902-908, 2015.

[9] JALAGAM NAGAMANI, K.SUMALATHA," EAACK: Secure IDS for Wireless Sensor Networks"..”International Journal of Computer Engineering in Research Trends., vol.1, no.6, pp. 461-469, 2014.

[10] G V N LAKSHMI PRIYANKA, TELUGU KAVITHA, B SWATHI and P.SUMAN PRAKASH," Significance of DSSD towards Cut Detection in Wireless Sensor Network"..”International Journal of Computer Engineering in Research Trends., vol.2, no.1, pp. 8-12, 2015.

[11] Kumara Swamy,E Ramya," A Contemplate on Vampire Attacks in Wireless Ad-Hoc Sensor Networks"..”International Journal of Computer Engineering in Research Trends., vol.2, no.12, pp. 834-836, 2015.

[12] Shital Patil , Vishaka Patil , Rupali Warke , Priyanka Patil," Prevention of Packet Hiding Methods In Selective Jamming Attack"..”International Journal of Computer Engineering in Research Trends., vol.3, no.4, pp. 194-196, 2016.

© 2017, IJCERT All Rights Reserved

AIP Conference Proceedings

Failure prediction of CFRP composites using Weibull analysis

Cite as: AIP Conference Proceedings **2057**, 020014 (2019); https://doi.org/10.1063/1.5085585
Published Online: 11 January 2019

A. Vishnu Vardhan, V. Sai Sri Charan, Sai Raj, S. M. Hussaini, and G. V. Rao

View Online

Export Citation

ARTICLES YOU MAY BE INTERESTED IN

Effect of CNTs addition on the fracture behaviour of neat epoxy and epoxy-carbon fiber-reinforced composites
AIP Conference Proceedings **2057**, 020043 (2019); https://doi.org/10.1063/1.5085614

Experimental investigation on modal characteristics of plain woven glass/carbon hybrid composite beams with fixed-free end condition
AIP Conference Proceedings **2057**, 020011 (2019); https://doi.org/10.1063/1.5085582

Development of an in-house MATLAB code for finite element analysis of composite beam under static load
AIP Conference Proceedings **2057**, 020015 (2019); https://doi.org/10.1063/1.5085586

AIP Publishing

© 2018 Author(s).

Failure Prediction of CFRP Composites Using Weibull Analysis

A Vishnu Vardhan[1)] V Sai Sri Charan[1)] Sai Raj[1)] SM Hussaini[1,2,a)] and GV Rao[1,3)]

[1]Dept. of Mech. Engg, *Vignan Institute of Tech & Sci-Hyderabad, Pochampally, Nalgonda, TS-508284, India.*
[2]*Former Scientist, ISRO, Sriharikota, AP- 524124, India.*
[3]*Former Director, CPDC, DRDO, Hyderabad, India.*
[a)] Corresponding author: drsmh.prof@gmail.com

Abstract. Composite materials are extensively used in aerospace applications due to their higher specific strength. These materials are judged by its properties and behavior under different loading conditions. In this paper developed a mathematical relation to predict the failure of composite material under tensile load by using Weibull distribution. Tensile hoop stress and failure stresses of composite specimens were found by NOL ring test. Characteristics of Weibull distribution were found by the tensile test data and develop the distribution curves. Probability of failure of the composite materials can be effectively predicted by these curves.

INTRODUCTION

Composites are consists of two or more constituents that are combined at a macroscopic level without soluble in each other. They contain high performance reinforcements usually fiber form in thin diameter, mix with matrix material such as epoxy or soft metals like aluminum. Carbon fiber reinforced polymer (CFRP) composites are extensively used in various structural applications in aerospace, automobile, transportation etc. Carbon fibers are commercially available with a variety of tensile modulus values in different ranges [1, 2]. These are have exceptionally high tensile strength to weight ratios as well as tensile modulus, very low coefficient of linear thermal expansion (which provides dimensional stability in such applications as space antennas), high fatigue strengths. Carbon fibers have been extensively used in composites in the form of woven textiles, pre-pegs, continuous fiber, and chopped fiber. The composite parts can be produced through filament winding, tape winding, pultrusion, compression molding, vacuum bagging, liquid molding, and injection molding. Composites materials properties are completely different than its fibers and matrix [3, 4]. The performance of an engineering material is judged by its properties and behavior under different loading conditions in both normal and adverse test environments. This information is essential for selecting the proper material in a given application as well as designing a structure with the selected material [5]. In this research investigate the performance of CFRP composites with an emphasis on the general trends observed in their properties and behavior. Material properties are usually determined by conducting mechanical and physical tests under controlled laboratory conditions. The orthotropic nature of fiber-reinforced composites has led to the development of standard test methods that are often different from those used for traditional isotropic materials [6, 7]. Weibull analysis is the leading method in the world for fitting and analyzing data and predict material behavior. Waloddi Weibull invented the Weibull distribution in 1937 and delivered his hallmark American paper in 1951. He claimed that his distribution applied to a wide range of problems. He illustrated this point with various applications such as the strength of steels or any other materials. Leonard Johnson at General Motors improved on Weibull's plotting methods. He also proved that if a part has multiple failure modes, the time to first failure is best modeled by the Weibull distribution. It is found that the Weibull method works with extremely small samples, even two or three failures for engineering analysis. This characteristic is important with aerospace safety problems and in development testing with small samples. Pratt & Whitney Aircraft used Weibull analysis very effectively [8, 9].

The primary advantage of Weibull analysis is the ability to provide reasonably accurate failure analysis and failure forecasts with extremely small samples. Solutions are possible at the earliest indications of a problem without having to fail a few more. Small samples also allow cost effective component testing. Weibull tests are completed when the first failure occurs in each group of components. If all the components need to be tested for failure, the cost and time required is much greater. Another advantage of Weibull analysis is that it provides a simple and useful graphical plot of the failure data. The data plot is extremely important to the engineer and to the designers. In Weibull plot horizontal scale is a measure of failure strength or ultimate strength. The vertical scale is the cumulative percentage failed. In this paper develop Weibull distribution curve by the experimental data of tensile test. Find the characteristics of the curve and fit in the equation which can predict the failure of the materials before it actually happened.

Advances in Polymer Composites: Mechanics, Characterization and Applications
AIP Conf. Proc. 2057, 020014-1–020014-7; https://doi.org/10.1063/1.5085585
Published by AIP Publishing. 978-0-7354-1785-4/$30.00

THEORY OF WEIBULL ANALYSIS

Weibull distribution is being used to model extreme values such as failure times and fracture stress. The probability density function (PDF) of two-parameter distribution has been indicated in the following Eq. (1). This PDF Equation is the most known definition of two-parameter Weibull distribution [10].

$$f(x) = \frac{\beta}{\alpha} \times \left(\frac{x}{\alpha}\right)^{\beta-1} \times e^{-\left(\frac{x}{\alpha}\right)^{\beta}} \quad (1)$$

Where, α and β is the scale, shape parameter.

If PDF is integrated, cumulative density function (CDF) is obtained. Eq. (3)

$$F_f(x) = 1 - e^{-\left(\frac{x}{\alpha}\right)^{\beta}} \quad (2)$$

$$1\text{-}F_f(x) = e^{-\left(\frac{x}{\alpha}\right)^{\beta}} \quad (3)$$

$$F_s(x) = 1\text{-}F_f(x) \quad (4)$$

$$R_x = 1 - P_x \quad (5)$$

In the above equations;

x: Variable (usually life). Failure cycles in this study (Nf),

β: Shape parameter or Weibull slope,

α: scale parameter,

$F_f(x)$: Probability of failure (P_x),

$F_s(x)$: Probability of survival or reliability (R_x).

If the natural logarithm of both sides of the Eq. (3) is taken, the following Eq. (6) can be written as,

$$ln\left(ln\left(\frac{1}{1-F_f(x)}\right)\right) = \beta ln(x) - \alpha ln(x) \quad (6)$$

When the Eq. (6) is rearranged as linear equation,

Y= $ln\left(ln\left(\frac{1}{1-F_f(x)}\right)\right)$, X= ln(x), m= β and c= -β

$$Y = mX + C \quad (7)$$

$$\alpha = e^{-\left(\frac{c}{\beta}\right)} \quad (8)$$

According to Eq. (8) characteristic life (a) is the time or the number of cycles at which the population is expected to fail.

EXPERIMENTATION

Specimen of the composite material prepared by filament winding process available in the lab. Most common properties reported for fiber-reinforced polymers are those obtained from tensile testing of specimen. In the tensile test, the specimen was subjected to increasing tensile force while simultaneous observations were made on the elongation of the specimen. In this research tensile tests were carried by National Ordnance laboratories (NOL) ring test [11, 12]. NOL ring test was performed on specimen samples to measure tensile test in different orientation. NOL ring specimens were prepared using drum winding technique on a CNC filament winding machine. Physical evaluation of the composite test specimens was carried out to ensure the suitability for mechanical property evaluation. NOL-ring test on samples were carried out at room temperature using universal testing machine with load cell of 100kN and loading speed of 2mm/min. Width and thickness of each NOL-ring specimen was measured with help of micrometer. In this prepared specimens were elongated till rupture with help of test fixture, made according to ASTM D2290. NOL-ring test fixture setup is shown in FIGURE 1.

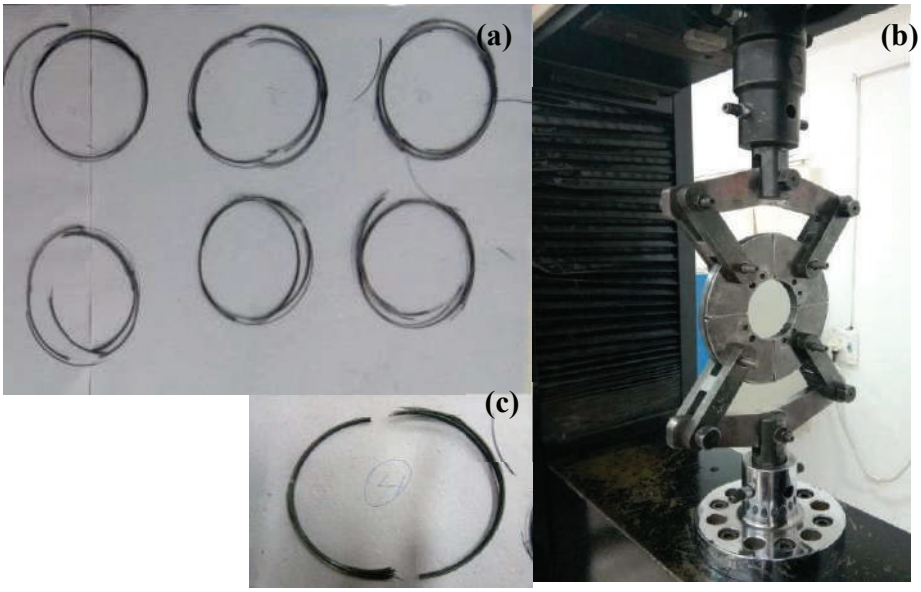

FIGURE 1. NOL Ring Test (a) Sample (b) Experimental set up (c) Fractured Sample

Composite specimen NOL-Ring test can be perform on Universal Testing Machine Instron 4505 available in the lab. The system is made up of a load frame, in which a specimen of the test material is mounted as shown in FIGURE 1. Applies a tension load to the specimen, and a control console that provides the calibration, test setup, and test operating controls. The crosshead control network allows programmable crosshead speeds and provides digital control of the crosshead position. The operating mode of the console data entry and readout functions can be SI units, as selected by a switch. A CPU-controlled sensor conditioner in the load weighing system allows calibration and balance procedures to be performed automatically. The sensor conditioner provides both an unranged analog and an automatically ranged digital load signal output suitable for several types of optional readout devices. Loading continues up to fracture of ring specimen.

RESULTS AND DISCUSSION

NOL Ring test simulate hoop conditions and measure hoop stress of the ring. It should be noted that the tensile strength, σ can be determined with help of equation 9.

$$\sigma=\frac{Fd}{2t} \qquad (9)$$

In equation (9) F is the ultimate burst force recorded in Newton (N), whereas t and d are the thickness and diameter of the NOL-ring sample in millimeter (mm), respectively according to ASTM D2290 standard. FIGURE 2 shows a typical force-displacement diagram at ambient temperature for one typical sample. The tensile strength of composite rings were determined for each experiment according to equation (9). The average values for each experiment are shown in TABLE 1. Displacements of all samples were around 6.5-8.8 mm of the tensile tests. From the results shown in the table can be observed that NOL-ring specimen No2 with tensile strength of 1962.4 MPa had shown the best results. Control system in filament winding technology is important factor in better winding patterns which is the main reason of high strength. Winding parameters during manufacturing of full section composite parts is influenced the strength [13].

Constructed histogram of fracture strength of the composite as shown in FIGURE. 3. From the histogram it is observed that the maximum frequency of repetition of failure stress is between 1675-1725 MPA with good frequency. Use the test data to construct Weibull distribution curve for analysis. Weibull distribution calculated probability of failure as per equation (2). Using this data construct a Weibull distribution curve in a software develop in house. Failure Censored was given at 2000 MPA, Total experimental values are 23. Probability plot for failure was drawn by least squares method. Plot shown in FIGURE. 4. Characteristics of Weibull distribution was calculated and tabulated in TABLE. 2.

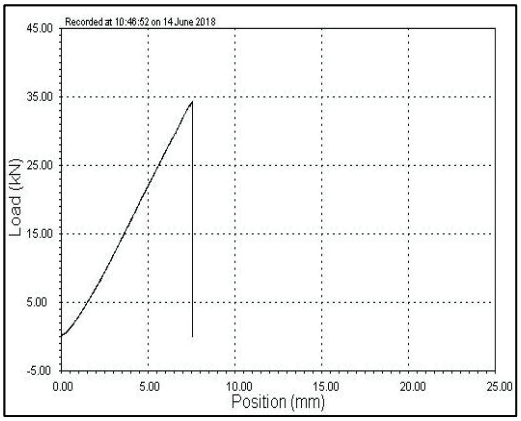

FIGURE 2. Load Vs Displacement of NOL ring test

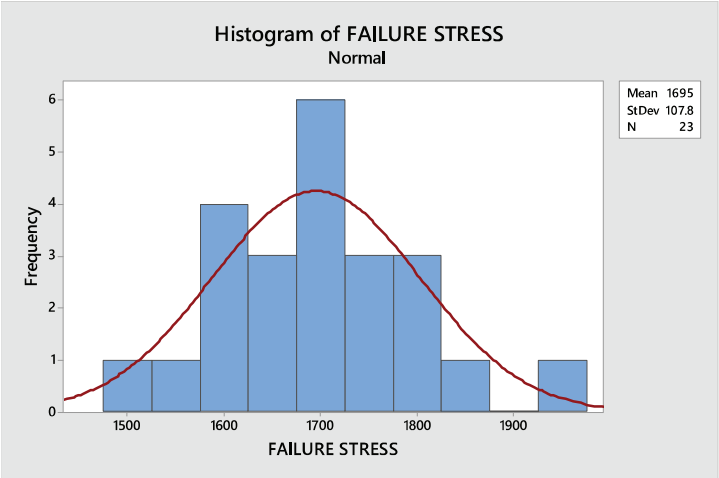

FIGURE 3. Histogram for fractured strength

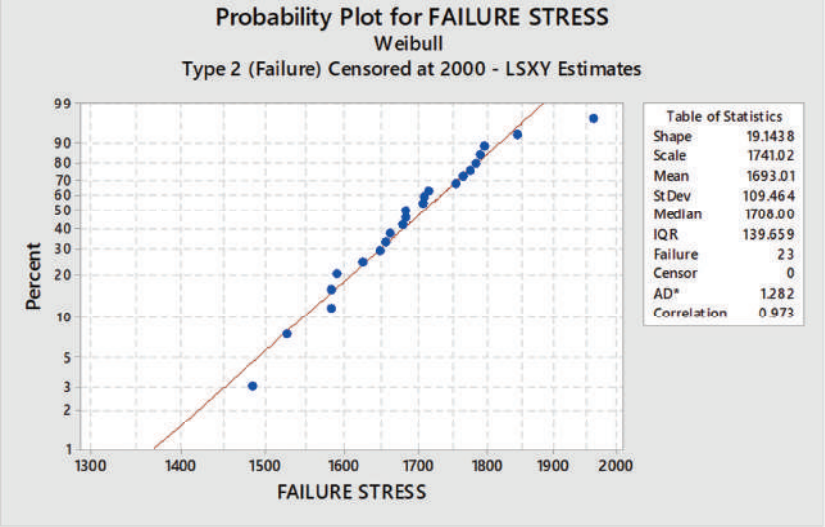

FIGURE 4. Weibull distribution Curve

TABLE 1: NOL ring test output data

S.NO.	SPECIMEN DIMENSION (mm)	MAXIMUM DISPLACEMENT (mm)	MAX. LOAD (KN)	NOL (MPa)
1.	6.46 x 1.58	7.589	34.257	1678
2.	6.57 x 1.55	8.842	39.963	1962
3.	6.60 x 1.55	7.488	32.367	1582
4.	6.50 x 1.57	8.091	36.204	1774
5.	6.58 x 1.59	7.986	35.889	1715
6.	6.45 x 1.56	7.909	35.486	1764
7.	6.48 x 1.58	8.345	36.726	1794
8.	6.54 x 1.60	8.263	36.708	1754
9.	6.49 x 1.61	8.152	37.248	1783
10.	6.47 x 1.60	7.644	34.848	1683
11.	6.60 x 1.60	8.269	38.117	1845
12.	6.60 x 1.62	7.779	36.499	1707
13.	6.33 x 1.63	7.219	33.513	1624
14.	6.56 x 1.65	7.780	36.420	1682
15.	6.64 x 1.66	8.227	39.437	1789
16.	6.49 x 1.49	6.393	29.507	1526
17.	6.52 x 1.52	6.168	29.400	1483
18.	6.38 x 1.54	6.618	31.092	1583
19.	6.52 x 1.54	7.176	34.289	1708
20.	6.48 x 1.53	7.068	32.919	1660
21.	6.59 x 1.60	7.082	34.737	1648
22.	6.72 x 1.60	7.151	34.211	1591
23.	6.56 x 1.53	7.059	33.211	1654

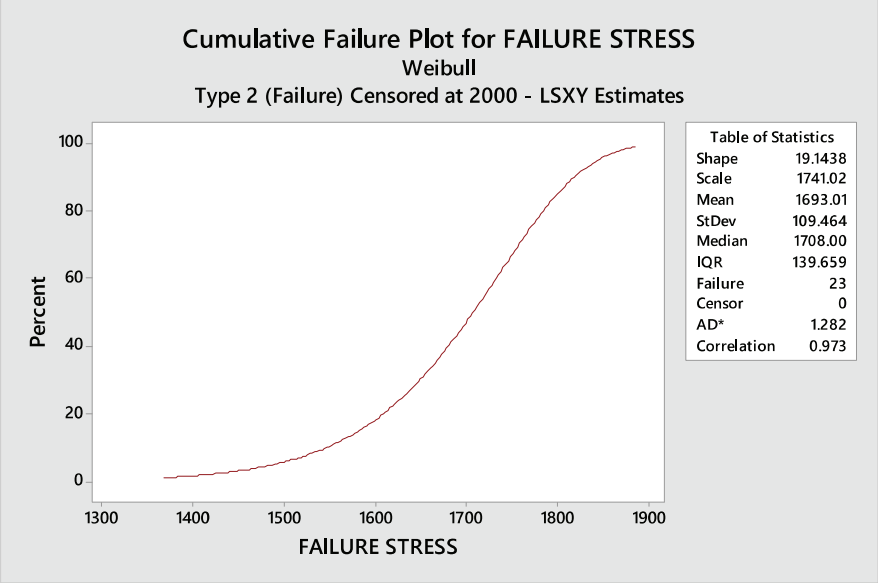

FIGURE 5. Cumulative Failure curve

Weibull distribution curve has set with calculated characteristics. Constructed cumulative failure plot shown in FIGURE.5. Calculated probability of failure stress from the curve and tabulated in TABLE. 3. It shows the probability

of failure (Px) at different stress (σ). Similarly constructed survival plot which shows the safety criteria for allowable stress in FIGURE. 6. Probability of Survival or Reliability (Rx) at different stresses are given in TABLE 4.

TABLE 2. Characteristics of distribution curve

	Estimated
Mean(MTTF)	1693.01
Standard Deviation	109.464
Median	1708.00
First Quartile(Q1)	1631.32
Third Quartile(Q3)	1770.98
Interquartile Range(IQR)	139.659

TABLE 3. Probability of Failure stresses

P_x	σ	P_x	σ	P_x	σ
1	1369.13	10	1547.93	91	1822.80
2	1419.99	20	1609.81	92	1827.35
3	1450.77	30	1649.74	93	1832.28
4	1473.13	40	1680.99	94	1837.68
5	1490.81	50	1708.00	95	1843.71
6	1505.48	60	1733.08	96	1850.65
7	1518.08	70	1757.98	97	1858.94
8	1529.13	80	1784.84	98	1869.60
9	1539.00	90	1818.54	99	1885.60

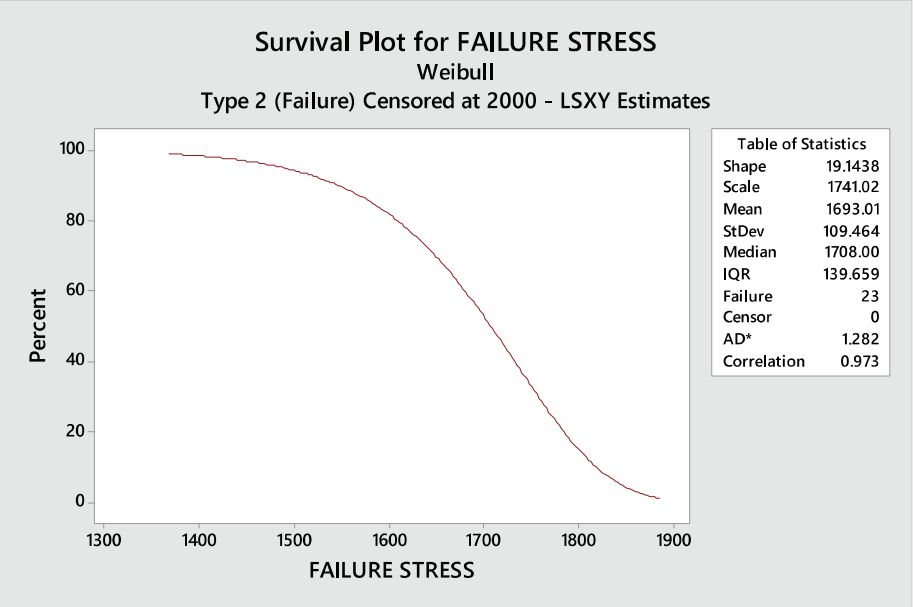

FIGURE 6. Probability of survival curve

TABLE 4. Parametric survival stresses

STRESS (MPA)	PROBABILITY OF SURVIVAL (%)	STRESS (MPA)	PROBABILITY OF SURVIVAL (%)
1380	99.0375	1590	83.8581
1380	98.8375	1620	77.7412
1410	98.2505	1650	69.9245
1410	98.2505	1680	60.3435
1440	97.3935	1710	49.2216
1440	97.3935	1740	37.1994
1470	96.1565	1770	25.367
1470	96.1565	1800	15.0718
1500	94.3934	1830	7.45171
1530	91.9158	1860	2.88685
1560	88.4926	1890	0.810291

CONCLUSION

Based on the experimental and analytical study it was found that the material could bear a stress of 1380 MPA without getting deformation with less than 1% failure chances. Failure stresses and reliability of any material can be predicted using Weibull Analysis. Maximum frequency of repetition of failure stress is between 1675-1725 MPA. The reliability stress data was forecasted that up to 1530 MPA probability of survival or reliability of the composite is more than 90%. Stress more than 1800 MPA reliability of the material was very less found to be less than 15%. This observations can be effectively utilize in designing of the CFRP for any applications.

REFERENCES

1. W. Chen, Y. Yu, P. Li, C. Wang and X. Yang. Effect of new epoxy matrix for T800 carbon fiber / proxy filament wound composites. Composites Science and Technology 67 2261–2270, (2007)
2. Miyagawa H, Rich MJ, Drzal LT. Thermo-physical properties of epoxy Nanocomposites reinforced by carbon nanotubes and vapor grown carbon fibers.Thermochimica Acta 442: 67-73. (2006)
3. D. Cohen. Influence of filament winding parameters on composite vessel quality and strength. Elsevier Science Limited, Composites Port A 28A 1035-1037, (1997)
4. Choi YK, Sugimoto K, Song S, Gotoh Y, Ohkoshi Y, Endo M. Mechanical and physical properties of epoxy composites reinforced by vapor grown carbon nanofibers. Carbon 43: 2199-2208. (2005)
5. Thostenson ET, Zhifeng R, Chou-Tsu W. Advances in the Science and Technology of Carbon Nanotubes and their Composites: a Review. Composites Science and Technology 61(13): 1899–1912, (2001)
6. Xu LR, Bhamidipati V, Zhong WH, Li J, Lukehart CM, Lara-Curzio E, Liu KC, Lance MJ. Mechanical property characterization of a polymeric nanocomposite reinforced by graphitic nanofibers with reactive linkers. Journal of Composite Materials 38(18): 1563-1582, (2004)
7. Vasiliev Valery V. and Morozov Evgeny V., Mechanics and Analysis of Composite Materials, Elsevier (2001)
8. Jiang, R.; Murthy, D.N.P. "A study of Weibull shape parameter: Properties and significance". Reliability Engineering & System Safety. 96 (12): 1619–26, (2011)
9. Sharif, M.Nawaz; Islam, M.Nazrul "The Weibull distribution as a general model for forecasting technological change". Technological Forecasting and Social Change. 18 (3): 247–56, (1980)
10. Chatfield, C.; Goodhardt, G.J. "A Consumer Purchasing Model with Erlang Interpurchase Times". Journal of the American Statistical Association. 68 (344): *828–835,* (1973)
11. M. A. Kinna. NOL-ring Test Methods. United States naval ordnance laboratory, with oak, Maryland, NOLTR: 64-156, (1964)
12. M. Plockl, M. G. R. Sauze, J. Scharringhausen and S. Horn. Failure Analysis of NOL-Ring Specimens by Acoustic Emission. 30th European Conference on Acoustic Emission Testing & 7th International Conference on Acoustic Emission University of Granada, (2012)
13. W. Polini and L. Sorrentino. Influence of winding speed and winding trajectory on tension in robotized filament winding of full section parts. Composites Science and Technology, 1574-1581, (2011)

Journal of Analysis and Computation (JAC)
(An International Peer Reviewed Journal), www.ijaconline.com, ISSN 0973-2861
Volume XI, Issue I, Jan- December 2018

A NEOTERIC HYBRID FIREFLY ALGORITHM AND COMBINED TREE DATA STRUCTURE FOR THE PURSUIT OF ACCURATE IMAGE COMPRESSION

Ruhiat Sultana [1], Syed Abdul Sattar [2]

[1]*Resaerch Scholar Rayalaseema University Kurnool Andhra Pradesh, India*

[2]*Principal Nawab Shah Alam Khan Engineering College Hyderabad Telangana, India*

ABSTRACT:

This paper proposed a hybrid firefly clustering algorithm, with dual tree DS to solve the problem of low image quality, low compression ratio and high time that occurs during lossless image compression. There are three phases in our proposed approach which is done before the process of compression. They are segmentation, feature extraction and classification. The segmentation of image is done by utilizing firefly clustering algorithm whereas the feature extraction is done by texture based techniques and these features are classified by the utilization of Decision-tree classifier. After that compression and encoding is performed by making use of quad-tree. In this paper the exact feature values are extracted, classified and compressed. Therefore it provides effective compression result than previous approaches. Our proposed technique is implemented in MATLAB and therefore the experimental results proved the effectiveness of proposed image compression technique in terms of high compression ratio and low noise ratio when compared with existing techniques.

Keywords: medical imaging, information system, firefly clustering, quad-tree.

[1] INTRODUCTION

Nowadays, by considering the important advances in multimedia and networks including telemedicine applications, the amount of information to store and transmit has dramatically increased over the last decade. To overcome the bandwidth limitations of transmission channels or storage systems, data compression is considered as a useful tool [1]. Image compression may be lossy or lossless. Lossy compression is the class of data encoding methods that uses inexact approximations and partial data discarding to represent the content. These techniques are used to reduce data size for storage, handling, and transmitting content. Lossy compression is most commonly used to compress multimedia data (audio, video, and images), especially in applications such as streaming media and internet telephony [2]. By contrast, lossless compression is typically required for text and data files, such as bank records and text articles. Lossless compression is a class of data compression algorithms that allows the original data to

be perfectly reconstructed from the compressed data. Lossless compression is used in cases where it is important that the original and the decompressed data be identical [3]. Compression is preferred for archival purposes and often for medical imaging, technical drawings, clip art or comics. The best image quality is based on better compression ratio and low noise ration. Enhanced image quality is the main goal of image compression, however, there are other important properties of image compression schemes: Scalability, Region of interest coding, Meta information and processing power [4].

Images compression becomes a vital practical issue because image-based representations are typically image intensive. The rendering techniques are classified into three major categories. They are rendering with no geometry, rendering with implicit geometry and rendering with explicit geometry [5]. Image compression is a critical tool that reduces the burden of storage and transmission. The drawbacks of image compression includes the reduction of compression rate and down grade computation time significantly. Compression work has been traditionally carried out in the image and video communities, and many algorithms and techniques have been proposed in the existing to achieve high compression ratios [6]. LOCO-I (LOW Complexity Lossless Compression for Images) is an efficient compression algorithm for continuous-tone lossless images which integrates the ease of Huffman coding with potential compression of context models. The algorithm relied on uncomplicated static context model, which approaches the capability of the complex universal context modeling techniques for obtaining high-order dependencies [7]. Selective encryption and modified entropy coders with multiple statistical models is used for doing both encryption and compression. Another approach which makes use of multiple statistical Models is employed to transform the entropy coders into encoded format. It is shown that security is obtained without the give up of compression performance and the computational speed [8].

For the compression of lossless images, an effective information hiding technique was presented. Here the information is secretly hided by the employment of index-modifying and side-match Vector-Quantization techniques. The information which is encoded is extracted in the decoder side [9]. A new coding scheme for transmitting the image data based on the circumstances of cloud Gaming is designed. Results shows that this approach leads to increased life time of the mobile battery while preserving an acceptable quality of the transmitted image [10]. A novel lossless color image compression scheme is presented. This scheme was based on reversible color transform (RCT) and Burrows–Wheeler compression algorithm (BWCA). The method makes use of RCT with bi-level BWT as a result it leads in better compression by taking advantage of the redundancy in the grey levels brought by the YUV color space [11]. Another lossless compression technique is presented to solve the drawbacks in the real-time transmission of aurora spectral images. This method decor relates the spatial and spectral domains bi-

dimensionally and eliminates the side information of recursively computed coefficients effectively to obtain high quality rapid compression [12].

Due to the advent of technology, the presence of various image formats strength is provided to image data. Due to this change in technology and the existence of different formats, high resolution images are produced and it requires more memory for the purpose of storage. To solve this problem a lossless technique of Image processing is introduced by taking Haar wavelet and Vector transform techniques into consideration [13]. An innovative lossless compression scheme has been discussed for 3D medical images. After the process of pre-processing, the image is encoded by the utilization of embedded zero tree wavelet technique [14]. Huge capacity and high image quality plays as prominent research contents of data hiding/ compression. An adaptive image steganography which utilizes absolute moment block truncation coding compression (AMBTC compression) and interpolation technique (ASAI), is presented to improve the performance of knowledge hiding scheme. As a result of this scheme a high embedding capacity with low computational complexity and better image quality can be achieved [15]. Another new algorithm is developed for the purpose of obtaining large capacity image steganography. In this approach, halftoning algorithm is employed to transform the gray-scale scanned document to binary image, which is a sparse matrix. In the next step, an algorithm is introduced to read the halftone image, and to convert each bit-stream of the sparse matrix into some meaningful decimal numbers, which are then to be embedded in 3-LSB bits of concealable pixels. Concealable pixels of stego image is filtered and the quality of hidden image is preserved by the utilization of standard deviation [16]

[2] RELATED WORK

This section provides an overview of the lossless image compression techniques available in the literature. Several algorithms and techniques have been proposed in the last decade, but there are considerable differences in, each with respect to the datasets used, segmentation objectives and validation. A summary of the different approaches and their features of lossless image compression is presented below

Nanrun zhou etal. [17] discussed about an image compression–encryption scheme to overcome these weaknesses and reduce the possible transmission burden. This scheme was an efficient image compression–encryption scheme which was based on hyper-chaotic system and 2D compressive sensing. Most of the existing image encryption algorithms based on low-dimensional chaos systems bear security risks and suffer encryption data expansion when adopting nonlinear transformation directly. To overwhelm this issue here the original image was measured by the measurement matrices in two directions to achieve compression and encryption simultaneously, and then the resulting image was re-encrypted by the cycle shift operation controlled by a hyper-chaotic system. Cycle shift operation can change the values of

the pixels efficiently. The presented cryptosystem decreases the volume of data to be transmitted and simplifies the keys distribution simultaneously as a nonlinear encryption system. Simulation results verify the validity and the reliability of the proposed algorithm with acceptable compression and security performance.

Venugopal etal. [18] presented a block based lossless image compression algorithm using Hadamard transform and Huffman encoding which was a simple algorithm with less complexity. Medical images play a significant role in diagnosis of diseases and require a simple and efficient compression technique. In this algorithm initially input image was decomposed by Integer wavelet transform (IWT) and LL sub-band was transformed by lossless Hadamard transformation (LHT) to eliminate the correlation inside the block. Further DC prediction (DCP) was used to remove correlation between adjacent blocks. The non-LL sub-bands were validated for Non-transformed block (NTB) based on threshold. The main significance of this method was it proposes simple DCP, effective NTB validation and truncation. Based on the result of NTB, encoding was done either directly or after trans- formation by LHT and truncated. Finally all coefficients were encoded using Huffman encoder to compress. From the simulation results, it was observed that the proposed algorithm yields better results in terms of compression ratio when compared with existing lossless compression algorithms such as JPEG2000. Most importantly the algorithm was tested with standard non-medical images and set of medical images and provides optimum values of compression ratio and was quite efficient.

Jinlei Zhang etal. [19] discussed about a novel distributed coding technique for hyperspectral images. The important needs of hyperspectral images are lossless compression, progressive transmission and low complexity onboard processing. Here the decoder produces efficient spectral image because every individual image is compressed in slices. An adaptive region-based prediction algorithm is designed here to eliminate spatial and spectral redundancies of images. This technique obtained accurate compression performance and less encoding complexity by utilizing spatial and spectral correlation simultaneously at the decoder side.

Seyun Kim and Nam Ik Cho [20] developed a novel image compression algorithm for lossless color images. This algorithm is based on hierarchical prediction which makes use of upper, lower and left pixels for pixel prediction and context-adaptive arithmetic coding in which the error was predicted using the context model and in this predicted error signal arithmetic coding is applied. Before the process of image compression the given RGB image is transformed to YCC image. After that grayscale image compression method is applied for the process of encoding. This algorithm diminishes the bit rates when compared with conventional JPEG images.

Atef masmoudi etal. [21] designed a new geometric finite mixture model-based adaptive arithmetic coding (AAC) for lossless image compression. Applying AAC for image compression, large compression gains can be achieved only through the use of sophisticated models that provide more accurate probabilistic descriptions of the image. In this work, we proposed to divide the residual image into non-overlapping blocks, and then we model the statistics of each block by a mixture of geometric distributions of parameters estimated through the maximum likelihood estimation using the expectation–maximization algorithm. Moreover, a histogram tail truncation method within each predicted error block was used in order to

reduce the number of symbols in the arithmetic coding and therefore to reduce the effect of the zero-occurrence symbols. Experimentally, we showed that using convenient block size and number of mixture components in conjunction with the prediction technique median edge detector, the proposed method outperforms the well-known lossless image compressors.

[3] FIREFLY-CLUSTERING WITH BI-FOLD TREE DS

The purpose of image compression is to minimize the size of image and maintain good level of their corresponding reconstructed images. Some of the major issues occurs in image compression is the decrease in image quality, compression ratio and increased time. To overcome these issues hybrid firefly clustering algorithm, with dual tree DS is proposed. There are three phases in our proposed approach. In the first phase image segmentation is done by utilizing firefly clustering algorithm. The second phase is feature extraction, which is done by texture based techniques and these features are classified by the utilization of Decision-tree classifier. The third phase is the compression process which is performed by making use of quad-tree. In the compression process encoding is performed. Encoding is used to protect important images prior to their transmission to the recipients. Encoding and decoding is done based on Huffman technique which makes the compression more secure.

[3.1] OPTIMAL IMAGE SEGMENTATION VIA FIREFLY CLUSTERING ALGORITHM

The important phase in image processing is segmentation. Here the images are segmented into several parts which contain some important information for the user. It is used to extract information from the image. Here clustering is used to segment the image. It contains various types of similarity pixels and consistent characteristics. It is the part of data mining algorithm that groups the data into various number of given clusters.

In this paper we utilized a new hybrid firefly algorithm with k-means clustering for segmentation. This firefly algorithm having two phases that is light intensity variation and calculating the attractiveness. Here attractiveness depends on the brightness of the firefly and the brightness in turn is defined by the objective function.

The light intensity is I(r) varies with distance ‘r’ monotonically and exponentially, is given by

$$I = I_0 e^{-\gamma r} \tag{1}$$

Where I_0= initial light intensity, γ= light absorptiType equation here.on coefficient

Attractiveness is $\beta = \beta_0 e^{-\gamma r^2}$

(2)

Where β = attractiveness

The Cartesian distance between two fireflies is given by

$$r_{ab} = \|x_a - x_b\|_2 = \sqrt{\sum_{k=1}^{d}(x_{a,k} - x_{b,k})^2}$$

(3)

Where x_a , x_b is the position of A, B firefly In this firefly process the less bright firefly a, is moving in the direction of the brighter firefly b. The movement is represented by

$$x_a = x_a + \beta_0 e^{-\gamma r^2}(x_b - x_a) + \alpha\varepsilon_a$$

(4)

The first step of firefly algorithm is initialization of the firefly population. The size of the firefly determines the number of solution so each firefly's light intensity is used to calculate its size. The distance between the fireflies is said to be Cartesian distance. The attractiveness function is defined from the light intensity and absorption coefficient.

K-mean is used to partition the data into k clusters. Initially the centroids is selected randomly. Then each data point is assigned to the cluster from which data point has minimum distance. Then the data point is grouped with another nearest centroid. Then the centroid is calculated again until convergence. In segmentation similar pixels are grouped together into cluster. The initial centroid determines the majority of efficiency and performance of the k-mean algorithm. When the algorithm is executed each time, the centroids are arbitrarily generated.

This algorithm having three steps:

1. Initialization
2. Cluster assignment
3. Exploration and evaluation

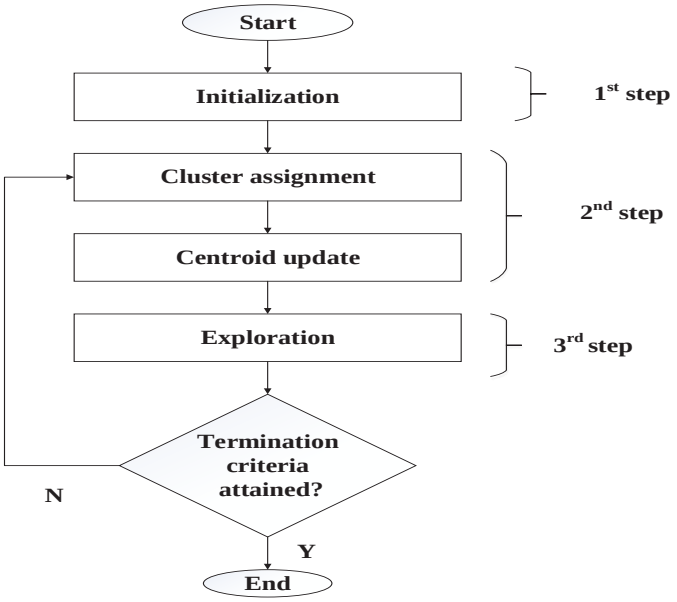

Figure: 1 hybrid firefly clustering algorithm

Let the solution space be S which contain determinate number of fireflies$x_a (a = 1 \dots N)$, where N is the number of fireflies. K is the number of clusters. The search space contains various attributes and its dimension is denoted by D. Then the centroids are computed incrementally from start to end of execution to achieve efficient centroid at each iteration. Therefore, to get the best configuration of centroids, with given b^{th} cluster with v^{th} attribute have centroid denoted by cen_{bv} therefore the weight matrix w_{ab} is defined as,

$$w_{ab} = \begin{cases} 1, x_a \in \text{cluster}_b \\ 0, x_a \notin \text{cluster}_b \end{cases} \quad (5)$$

The formula to estimate centroid is

$$cen_{b,v} = \frac{\sum_{a=1}^{S} w_{a,b} x_{a,v}}{\sum_{a=1}^{S} w_{a,b}}, b = 1 \dots K, v = 1 \dots . K * D \quad (6)$$

The objective function is the Euclidean which is minimized. The objective function for the firefly clustering is

$$F(cen) = \sum_{b=1}^{K} \sum_{a=1}^{S} w_{a,b} \sum_{v=1}^{K*D} \left(x_{a,v} - cen_{b,v}\right)^2 \quad (7)$$

The clustering matrix is defined by

$$clmat_{a,b} = min_{k \in K} (\|x_a - cen_k\|) \quad (8)$$

When clustering matrix is enhanced, then every data point is at minimum distance from its centroid.

[3.2] FEATURE EXTRACTION BY TEXTURE BASED TECHNIQUES

The segmented image from the above step is processed by feature based technique for the extraction of feature. Here Gabor wavelet filter is employed to extract the feature [23]. This texture based technique is used to extract the feature vector from segment region of interest. This system is similar to human visual system specifically in terms of representation of the frequency and orientation. It is divided into many filtered image which limited frequency and trends in intensity will change. It is considered to be suitable to distinguish the texture. The conversion is considered as wavelet transform in which the main wavelet is Gabor function. The segmented is given as the input to the Gaussian filter for further extraction. After that the transformed virtual and real parts are combined. In order to improve the size of transformed image, the texture features characterizing the image were removed. This concept can be applied to both query image and database image. The output of the Gabor filter is the accurately extracted features. The equation for Gabor filter is given by

$$g(x,y) = Exp\left[-\left[\frac{(x_\theta)^2}{2*(bw)^2} + (\gamma)^2 * \frac{(y_\theta)^2}{2*(bw)^2} \right] \right] * \frac{\cos(2\pi)}{\lambda x_\theta + p}$$

Where, x_θ and y_θ are the gray image of x and y, bw is the bandwidth value, p is the phase value.

[3.3] FEATURECLASSIFICATION USING DECISION TREE CLASSIFIER

The extracted feature is given as the input to the decision tree classifier for further classification of the feature values. The main advantage of using decision tree is that it runs faster to reduce time. Decision tree is a set of simple rulesand it is non-parametric because they do not need any assumptions about the allocation of the variables in each group. In the first step, feature is partitioned into two parts, the feature value with the highest importance is taken into consideration. This process is continual for each subset until no more splitting is possible. After this decision, the next feature is found then it splits the data optimally into two parts. All non-terminal nodes contain splits. If it is followed from root to leaf node then decision tree is the rule-based classifier. An advantage of decision tree classifiers is their simple structure which allows for interpretation and visualization. By using the training set, decision tree is built using objects, set of attributes and a group label. Attributes are a collection of properties containing all the information about one object. Unlike classes, each attribute have either ordered or unordered values, here the class is associated with the leaf and the output is obtained from the tree. A tree misclassifies the image if the class is labelled. The proportion of images correctly partitioned by the tree is called accuracy and the proportion of images incorrectly partitioned by the tree is called error. Here the features extracted from the above phase are classified for finding the optimal feature set [24].The output from the decision tree is the optimal feature value.

[3.4] ACCURATE IMAGE COMPRESSION & ENCODING USING QUAD-TREE AND HUFFMAN ENCODING

The optimal feature value is finally compressed in this phase. Here both compression and encoding process is done by using Huffman technique after the process of quad-tree decomposition. The optimal feature value found by the decision tree is given as the input for quad-tree. The output from the quad-tree is the compressed image. Encoding is also performed here by means of Huffman technique which is very secured than the existing encoding techniques. Encoding is an effective method for protecting important images before the transmission and reception. The image is always secure no matter whether the image is stored in the secondary storage or transmitted in networks. The quad-tree data structure is used to represent an image.The motivation of this scheme is to have both image encoding and compression process. The flow of the compression process is shown below.

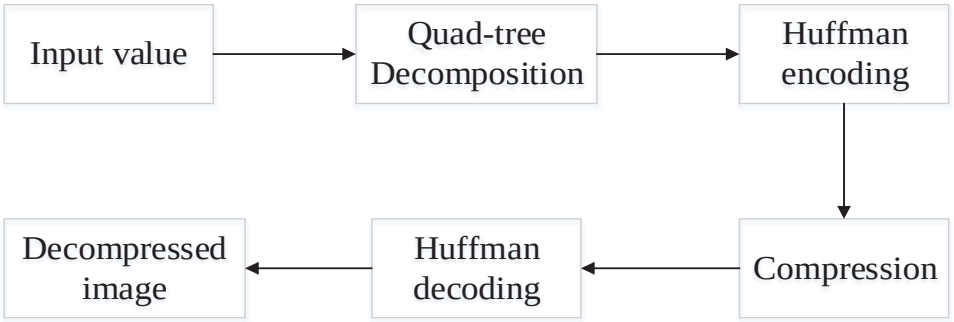

Figure: 2 Compression process

The Quad-tree approach divides the optimal feature value into four equal sized blocks, and then various tests are contained to check that i fit meets some criterion of homogeneity. If a block meets the criterion it is not divided any more, and the test criterion is applied to those blocks. This process repeats iteratively until each block meets the criterion. The result may have blocks of several different values.

The Huffman encoding algorithm begins by designing a list of all the alphabet symbols in drizzling order of their chances. At that time it builds from the lowest up, a binary tree with a symbol at each leaf. This is processed in steps, where two symbols with the least chances is selected at every step, added to the top of the partial tree, deleted from the list, and replaced with an auxiliary symbol representing the two original symbols. Once the list is reduced to simply one auxiliary symbol (representing the entire alphabet), the tree is complete. The tree is then traversed to recognize the code words of the symbols. Prior to the compression process begins, the encoder needs to recognize the codes. This is done in view of the chances of frequencies of incidence of the images. The chances or frequencies must be composed, as side data on the output, so that any Huffman decoder can have the capacity to decompress the data. This is basic, in such a way that the frequencies are integers and the chances can be composed as scaled integers. It consistently adds just a couple of hundred bytes to the output. It is also conceivable to compose the variable-length codes themselves on the output, however this may be uncomfortable, because the codes have different sizes. It is also conceivable to compose the Huffman tree on the output; however this may require more space than essentially the frequencies. In any case, the decoder must comprehend what is toward the begin of the

compressed document, read it, and construct the Huffman tree for the letters in order. Begin at the root and read the principle piece of the input (the compressed document). If it is 0, take after the base edge of the tree; if it is 1, take after the top edge. Read the accompanying piece and push another edge toward the leaves of the tree. Exactly when the decoder touches base at a leaf, it finds there the main, uncompressed image, and that code is discharged by the decoder.

Steps for encoding and compression
Step 1: The value of the image is decomposed into minimum and maximum value based on the threshold value.
Step 2: The values of x and y, mean values and block size from quad-tree decomposition is recorded.
Step 3: Find the mean value.
Step 4: Encode the image value using Huffman technique.
Step 5: Record the coding information.
Step 6: Compress the encoded value.
Step 7: Calculate compression ratio and PSNR values.

[4].RESULTS

This section shows the performance of proposed optimization clustering algorithm with dual tree data structure and the results obtained by them. In our proposed system the main objective is to accurately compress the given medical image and overcome the problems that occur during image compression.

Segmentation

During the segmentation process the given input image is segmented here using the combination of firefly and clustering algorithm. Our medical input image is shown below.

Figure: 2 Input medical image

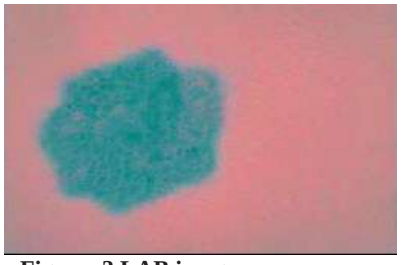

Figure: 3 LAB image

Before the process of segmentation, there are some initial steps to be carried out. When the input image is fetched it is transformed into Lab images whereas L represents the lightness and a and b are the color opponents green-red and blue-yellow. The Lab color space enhances the gamuts of RGB and CMYK color models. The input image which is transformed to Lab model

is shown below. After the color transformation of the input image, label is assigned before carrying out the segmentation process. The labelled image is shown below.

Figure: 4 Label assumed image segmented image

Figure: 5 Edge image

Figure: 6 Edge

Segmentation

The image shown below shows the computational efficiency of the firefly clustering algorithm. At first segmentation is done using the concept of clustering technique and here due to the occurrence of local optima problem firefly is integrates. Firefly algorithm constantly selects the efficient centroids throughout the search space using fireflies. It also shows that algorithm successfully overcome the local optima and achieve the global optima. The image segment evaluation index like the standard measure of correlation coefficient is very much effective to assess the quality of the image segmentation results. A higher value of correlation coefficient signifies better segmentation. To quantify the conformity level between the images after the segmentation the correlation coefficient can be used. The segmented image using firefly-clustering is shown below.

After the process of segmentation, the next step is the feature extraction. Here texture based features are extracted by the employment of gabor filter. The image after the process of feature extraction classified is shown below.

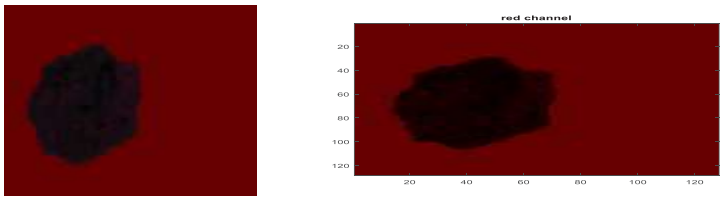

Figure: 8 LAB image

COMPRESSION

During the process of compression, there are some initial steps to be carried out. At first color transformation is to be done for the classified image obtained from the decision tree. The transformed RGB color image is shown below. After the color transformation down sampling should be done. Down sampling is the process of transforming the high resolution image into

small image with all the major information contained in it. Down-sampling should be done to the blue channeled image.

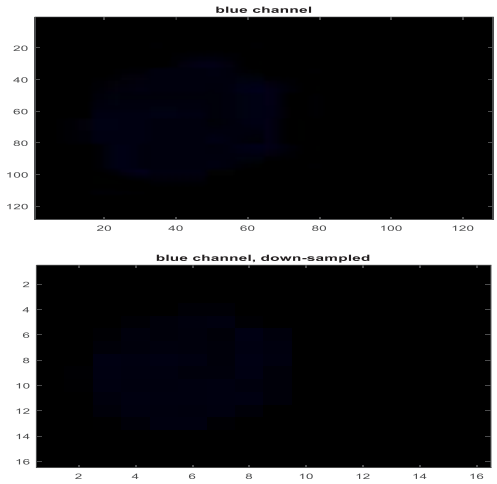

Figure: 9 RGB channel

The down-sampled image is shown below.

Figure: 10 Down-sampled image

Figure: 11 DCT image

Next to this the down-sampled image is organized into groups and Discrete cosine transform is applied. Here the image is partitioned into block of pixels. After that DCT is applied to each block. The image after applying DCT is shown below.

Finally the image is compressed by the employment of quad-tree and it is encrypted before broadcasting. The compressed medical image is shown below which our output for the proposed system is.

Figure: 12 Output image

[4.1] COMPARISON RESULT

To evaluate the compression result two measures are commonly applied. The first one is the PSNR (peak signal to noise ratio) and the next is the CR (compression ratio).

PSNR is the process of measuring the quality of reconstructed image. PSNR value for accurate compressed image must be always low. The PSNR value for our proposed system compared with the existing FIC approach and survey is shown below.

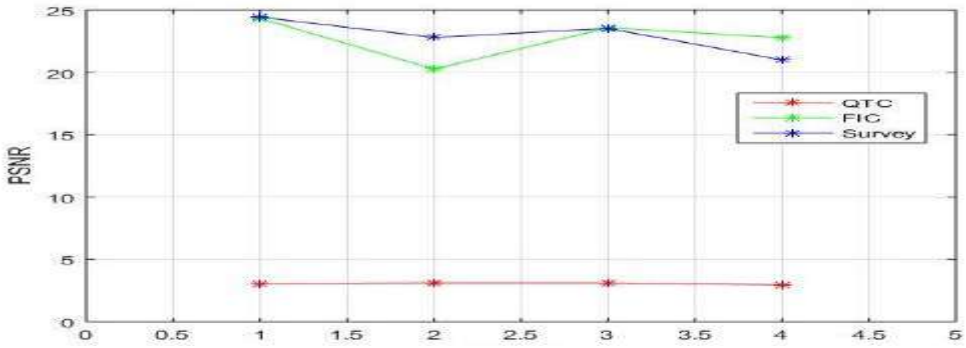

Figure: 13 Comparison of PSNR with existing

The compression ratio for the compressed image must be always high in order to obtain good quality image. Compression is nothing but it eliminates unwanted information in order to gain high compression ratio. The compression ratio for our proposed system compared with the existing FIC approach and survey is shown below.

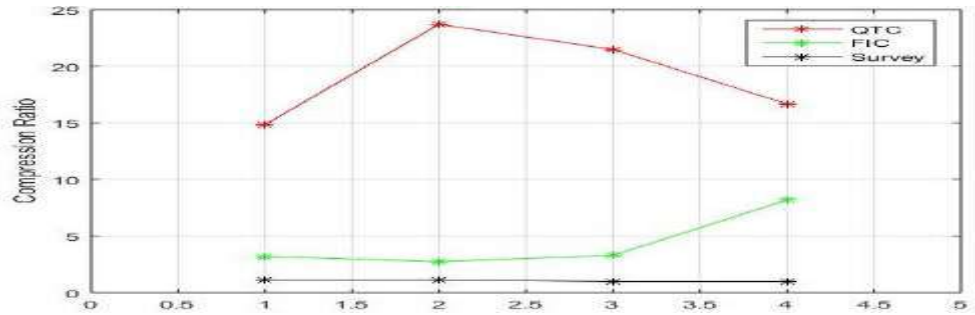

Figure: 14 Comparison of Compression ratio with existing

[5].CONCLUSION

Our proposed scheme is used to compress the image. The objective of image compression is to reduce irrelevance and redundancy of the image data in order to be able to store or transmit data in an efficient form. Lossless compression is a class of data compression algorithms that allows the original data to be perfectly reconstructed from the compressed data. . Some of the major issues occurs in image compression is the decrease in image quality, compression ratio and increased time. To overcome these issues hybrid firefly clustering algorithm, with dual tree DS is proposed. In the first phase the image is segmented by utilizing firefly clustering algorithm. In the second phase features are extracted by using texture based techniques and these features are classified by the utilization of Decision-tree classifier. In the third phase the quad-tree data structure is used to represent an image. In the compression process encryption is performed. The proposed image encryption scheme is based on the principle of lossless compression. The

proposed approach overcomes the issues that occur during the process of image compression. Results of our proposed technique showed that it out performed when compared to the previous work in terms of decreased PSNR value and increased compression ratio.

REFERENCES

[1] Brahimi T, Boubchir L, Fournier R and Naït-Ali A, "An improved multimodal signal-image compression scheme with application to natural images and biomedical data", Multimedia Tools and Applications, Springer, pp. 1-23, 2016.

[2] Pradhan A, Pati N, Rup S and Panda AS, "A modified framework for Image compression using Burrows-Wheeler Transform", In Computational Intelligence and Networks (CINE), In 2nd International Conference on IEEE, pp. 150-153, 2016.

[3] Conoscenti M, Coppola R and Magli E, "Constant SNR, rate control, and entropy coding for predictive lossy hyperspectral image compression", IEEE Transactions on Geoscience and Remote Sensing, vol. 54, No. 12, pp. 7431-41, 2016.

[4] Qureshi MA and Deriche M, "A new wavelet based efficient image compression algorithm using compressive sensing", Multimedia Tools and Applications, Springer, vol. 75, No. 12, pp. 6737-54, 2016.

[5] Shum HY, Kang SB and Chan SC, "Survey of image-based representations and compression techniques", IEEE transactions on circuits and systems for video technology, vol. 13, No. 11, pp. 1020-37, 2003.

[6] Karimi N, Samavi S, Soroushmehr SR, Shirani S and Najarian K, "Toward practical guideline for design of image compression algorithms for biomedical applications", Expert Systems with Applications. Vol. 56, pp. 360-7, 2016.

[7] Weinberger MJ, Seroussi G and Sapiro G, "LOCO-I: A low complexity, context-based, lossless image compression algorithm", In Data Compression Conference Proceedings, IEEE, pp. 140-149, 1996.

[8] Wu CP and Kuo CC, "Design of integrated multimedia compression and encryption systems", IEEE Transactions on Multimedia, vol. 7, No. 5, pp. 828-39, 2005.

[9] Aishwarya KM, Ramesh R, Sobarad PM and Singh V, "Lossy image compression using SVD coding algorithm", In Wireless Communications, Signal Processing and Networking (WiSPNET), International Conference on IEEE, pp. 1384-1389, 2016.

[10] Gharsallaoui R, Hamdi M and Kim TH, "Image compression with optimal traversal using wavelet and percolation theories", In Software, Telecommunications and Computer Networks (SoftCOM), 24th International Conference on IEEE, pp. 1-6, 2016.

[11] Khan A and Khan A, "Lossless colour image compression using RCT for bi-level BWCA", Signal, Image and Video Processing. Vol. 10, No. 3, pp. 601-7, 2016.

[12] Kong W, Wu J, Hu Z, Anisetti M, Damiani E and Jeon G, "Lossless compression for aurora spectral images using fast online bi-dimensional decorrelation method", Information Sciences, vol. 381, pp. 33-45, 2017.

[13] Sikka N, Singla S and Singh GP, "Lossless image compression technique using Haar wavelet and vector transform", In Research Advances in Integrated Navigation Systems (RAINS), International Conference on IEEE, pp. 1-5, 2016.

[14] Rajakumar K and Arivoli T, "Lossy Image Compression Using Multiwavelet Transform for Wireless Transmission", Wireless Personal Communications, vol. 87, No. 2, pp. 315-33, 2016.

[15] Tang M, Zeng S, Chen X, Hu J and Du Y, "An adaptive image steganography using AMBTC compression and interpolation technique", Optik-International Journal for Light and Electron Optics, vol. 127, No. 1, pp. 471-7, 2016.

[16] Soleymani SH and Taherinia AH, "High capacity image steganography on sparse message of scanned document image (SMSDI)", Multimedia Tools and Applications, pp. 1-21, 2016.

[17] Zhou N, Pan S, Cheng S and Zhou Z, "Image compression–encryption scheme based on hyper-chaotic system and 2D compressive sensing", Optics & Laser Technology, Elsevier, vol. 82, pp. 121-33, 2016.

[18] Venugopal D, Mohan S and Raja S, "An efficient block based lossless compression of medical images", Optik-International Journal for Light and Electron Optics, vol. 127, No. 2, pp. 754-8, 2016.

[19] Chaurasia V and Chaurasia V, "Statistical feature extraction based technique for fast fractal image compression", Journal of Visual Communication and Image Representation, vol. 41, pp. 87-95, 2016.

[20] Zhao D, Zhu S and Wang F, "Lossy hyperspectral image compression based on intra-band prediction and inter-band fractal encoding", Computers & Electrical Engineering, Elsevier, Vol. 54, pp. 494-505, 2016.

[21] Masmoudi A, Chaoui S and Masmoudi A, "A finite mixture model of geometric distributions for lossless image compression", Signal, Image and Video Processing. Vol. 10, No. 4, pp. 671-8, 2016.

[22] Chang HK and Liu JL, "A linear quadtree compression scheme for image encryption", Signal Processing Image Communication. Vol. 10, No. 4, pp. 279-90, Sep 1, 1997.

[23] Tallapragada VS, Reddy DM, Kiran PS and Reddy DV, "A Novel Medical Image Segmentation and Classification using Combined Feature Set and Decision Tree Classifier", International Journal of Research in Engineering and Technology.Vol. 4, No. 9, pp. 83-6, 2016.

[24] Sharma A and Sehgal S, "Image segmentation using firefly algorithm", InInformation Technology (InCITe)-The Next Generation IT Summit on the Theme-Internet of Things: Connect your Worlds, International Conference. IEEE. pp. 99-102, Oct 6, 2016

[25] Sundararaj GK and Balamurugan V, "An expert system based on texture features and decision tree classifier for diagnosis of tumor in brain MR images", InContemporary Computing and Informatics (IC3I, International Conference. IEEE. pp. 1340-1344, Nov 27, 2014.

[26] Ergen B and Baykara M, "Texture based feature extraction methods for content based medical image retrieval systems", Bio-medical materials and engineering. Vol.24, No. 6, pp. 3055-62, Jan 1, 2014.

COMPARATIVE STUDY OF R.C. TALL BUILDINGS BETWEEN SYMMENTRICAL AND UNSYMMENTRICAL SHAPES IN CONSIDERATION OF NON DUCTILE USING WITH AND WITHOUT OUTRIGGER AND BELT TRUSS SYSTEM

Mohd Parvez Affani[1], Shaik Mohd Javeed[2] Mohd Farrukh Anwar[3]

[1] Pg Student, M.tech in Structural engineering, Department of Civil Engineering, Nawab Shah Alam Khan College of Engineering and Technology, Hyderabad, Telangana

[2] Assistant Professor, M.tech in Structural engineering, Department of Civil Engineering, Nawab Shah Alam Khan College of Engineering and Technology, Hyderabad, Telangana

[3]Head of the Department (PHD) , Vice Principal ,M.tech in Structural engineering, Department of Civil Engineering, Nawab Shah Alam Khan College of Engineering and Technology, , Hyderabad, Telangana

ABSTRACT: Should be met through engineering judgment. In Metro cities like Mumbai, Delhi, Chennai, Bangalore, Kolkata, Hyderabad etc multi-storied buildings are common and disregarding that individuals are willing to remain in elevated structure (36 storeys').The analysis and outline of tall building structural system require more concentration than that of regular multi-storied building. The lateral stability of tall building assumes an important role in safe analysis and plan. demonstrate is generated in ETABS, the state of building like a rectangular(symmetrical) Y-formed and C molded buildings i.e. (Non symmetrical) The building is strengthened in lateral direction by providing Outrigger and Belt non truss system at every 9 to 10 ,18 to 19, 27 to 28 story levels Two strategies for analysis have been considered for lateral stability analysis viz linear static and linear dynamic for both seismic and wind. The various parameters like (1) Lateral displacement story.

I. INTRODUCTION

Tall building is need of developing scenario. Rapid improvement of tall building in the world has been creating impact on innovative advancement of structural system for tall building, result of which buildings are growing taller. There is no specific definition of tall building however Council on Tall Building and Urban Habitat (CTBUH) gives a few measures to define tall building. Tall building phenomenon will continue in a greater scale to address the issues of the growing populace in future large cities. The advancement in concrete technology over the twentieth century covering materials, structural systems, analysis and construction techniques, made it conceivable to manufacture concrete tall buildings. Structural system like minute resisting frame and shear divider and bracing system fulfill primary need of building . As building increases in stature there is effect of lateral load i.e. wind and earthquake on building structure. The

impact of wind and seismic forces acting on tall building becomes an important aspect of the outline. Improving the structural systems of tall buildings can control their dynamic response Wind and earthquake stack plays major impact on building deflection. To overcome lateral load because of earthquake and wind, concrete core has been provided at center of building. Concrete core is a very effective and practical structural system which supportive in reducing the deflection because of seismic and wind forces. During recent years, the frame-concrete core divider hybrid structure has been rapidly created and profoundly concerned by owners with its performance and economic favorable circumstances. The outrigger and belt truss system is commonly utilized as one of the structural system to effectively control the excessive drift because of lateral load, so that, during little or medium lateral load due to either wind or earthquake stack, the risk of structural and non-structural harm can be minimized. For elevated structures, particularly in seismic active zone or wind stack dominant, this system can be chosen as an appropriate structure. Outriggers have been utilized in the sailing ship industry for some years. They are utilized to resist wind. The slender pole provides the utilization of outriggers. As a comparison the core can be related to the pole, the outriggers resemble the spreaders and the exterior columns resemble the shrouds or remains. Innovative structural schemes are continuously being looked for in the field. Structural Design of High Rise Structures with the intention of limiting the Drift because of Lateral Loads as far as possible without paying a high premium in steel tonnage.

OUTRIGGER AND BELT TRUSS SYSTEM

Outriggers are rigid horizontal structure i.e. truss or shaft which connect core divider and outer column of building to improve building strength and overturning stiffness. Outriggers have been utilized in tall building for nearly 50 years, however innovative plan principle has been improving its efficiency. Outrigger system is one sort of structural system which is formed from a cantilever molded horizontal member connected to structures inner core and outer columns. Through the connection, the minute arm of the core will be increased which prompt higher lateral stiffness of the system. Central core in a building act as cantilever, outriggers are provided to reduce overturning minute in core and to transfer minute from core to outer column by connecting the core and column. Divider frame outrigger trusses is a standout amongst the most efficient and economical structures in tall building, at outer end they connected to the establishment through exterior columns. At the point when the structure is subjected to horizontal loading, the divider and outrigger trusses will rotate, causing compression in the downwind column and strain in column on the upwind side, these hub forces will resist the rotation in the divider. The outrigger systems can be produced in any combination of steel, concrete and composite construction. Normally in steel structure outrigger are in the form of trusses and in the form of divider or profound bar in concrete structure. Outrigger might be stretched out to both side of central core or core might be located at one side of building with outrigger extending to other side columns. Belt truss connects outer perimeter column of a building and offer a wider perimeter to resist lateral deflection of building. This efficient structural form consists of a central core, comprising either Braced Frames or Shear Walls, with horizontal cantilever trusses or girders known as outrigger Trusses, connecting the core to the outer columns.

The core might be centrally located with outriggers extending on both.

TYPES OF OUTRIGGER TRUSS SYSTEM

Conventional Outrigger Concept

In the conventional outrigger concept, the outrigger trusses or girders are connected directly to shear dividers or braced frames at the core and to columns located outboard of the core. Typically (however not necessarily), the columns are at the outer edges of the building. Figure 1 is a romanticized section through a tall building with two arrangements of outrigger trusses, including one at the best. The outrigger trusses configuration. Shallower and deeper trusses have been utilized, with diagonals of various configurations.

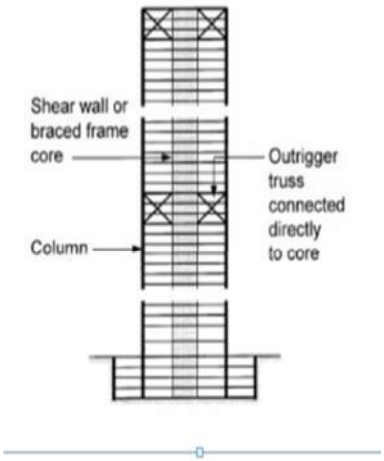

Tall building with conventional outriggers

Virtual Outrigger Concept

In the "virtual" outrigger, a similar transfer of overturning from the core to components outboard of the core is achieved, yet without a direct connection between the outrigger trusses and the core. The basic thought behind the virtual outrigger concept is to utilize floor diaphragms, which are typically very solid and strong in their own plane.

Belt Trusses As Virtual Outriggers

The utilization of belt trusses as virtual outriggers keeps away from a considerable lot of the problems associated with the utilization of conventional outriggers. The principle is the same as when belt trusses are utilized as virtual outriggers. Some fraction existing apart from everything else in the core is converted into a horizontal couple in the floors at the best and the base of the storm cellar.

NEED OF THE PROJECT

Accumulation of growing populace especially in developing countries has resulted in an increased tallness of buildings, this need creating impact on structural improvement of tall building. As building increases in tallness there is effect of wind and earthquake forces, to increase stiffness of building against lateral load extra structural system such as belt truss and outriggers is required. The reviewed approach for the outline and improvement of tall building using outrigger and belt truss is helpful to provide a potential arrangement. The study in turn is helpful for various research persons involved in outline the tall buildings by using outrigger and belt truss system

OBJECTIVE OF THE STUDY

To study the effect of introduction of Outriggers in tall structure subjected to dynamic wind loading. To study the influence of core divider and braced core divider with X braced outriggers C. To stud influence of concrete outrigger. To study the effect of Outriggers with Peripheral Belt Truss. To study the different configuration of the building under different

arrangement molded building i.e symmetrical and Unsymmetrical Buildings (Rectangular and Y formed building , C formed Building

II. METHODOLOGY

ANALYSIS OF A 36 STOREY BUILDING

The model considered for this study is 111.5 m skyscraper reinforced concrete building frame. The building represents a 36 storied office building. The stature of each story is 3m and every one of the floors are considered as Typical Floors. The location of the building is thought to be at Bhuj (Gujarat) . All divider piers are identical with a uniform divider thickness of 230mm over the entire stature. The Bracing bars (outriggers) and every other bar are 600mm wide and 600mm profound, Grade 40 concrete is considered (Compressive strength 40 N/mm²) throughout the tallness of the building. And number of stories considered for every one of the cases is 36 stories, and roof tallness is considered as 111.5 m. And story to story tallness is 3.0 m. And the outer columns sizes are considered as 800X800 mm and Inner columns measure are consider as 550X600 mm. shear divider thickness is considered as 230 mm.The technique for analysis of the previously mentioned system is construct up in light of the presumptions that the outriggers are rigidly attached to the core; The core is rigidly attached to the establishment; The sectional properties of the core, shafts and columns are uniform throughout the stature; Tensional effects are not considered; Material behavior is in linear elastic range; The Outrigger Beams are flexural rigid and induce just pivotal forces in the columns; The lateral resistance is provided just by the bending resistance of the core and the secure action of the exterior columns connected to the outrigger; The rotation of the core because of the shear deformation is immaterial.

STRUCTURAL MODELLNG

SL No	Structural details	Type of location
1	Utility of Buildings	Office Building
2	No of Storey	G+36
3	Area	2308 sq mts
4	Height of Building	111.5 mts
5	Shape of the Building	Rectangle, Y shaped, C shaped building
6	Types of Walls	SHEAR Wall -230 mm thickness Masonry wall – 230 mm thickness
7	**Geometric Details** Ground Floor	3.5 mts
	Story to story height	3.0 mts
	Beam	0.60X0.60 mts
	Columns (outer)	0.80X0.80 mts
	Columns (Inner)	0.55X0.60 mts
	Slab	0.150 mts
8	**Material Details** Concrete Grade All Steel Grades	M40 (All structural elements) FE 415 (All structural elements)
9	Type Of Construction	R.C.C FRAMED STRUCTURE
10	Place of construction	Bhuj - Gujarat
11	Loads considered in Buildings	Dead load, Live load, Earthquake ,Wind load
12	Wind Speed	50 m/s (Bhuj wind speed)
13	Seismic Zone	Zone – V (Bhuj)
14	Method of Analysis	RESPONSE SPECTRUM ANALYSIS EQUIVALENT STATIC ANALYSIS
15	NON Ductile properties	5 (Response reduction factor)
16	STATIC COMBINATION USED	1.2(Dead load+ Live load+ Earthquake in X direction)
17	IS codes used	IS456 :2000,IS1893:2002,IS 16700:2017,IS 875:1987 (Part 1, Part 2, Part 3)

Rectangle Building

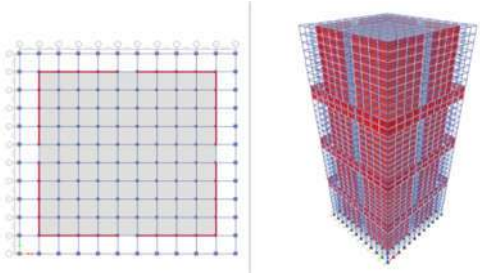

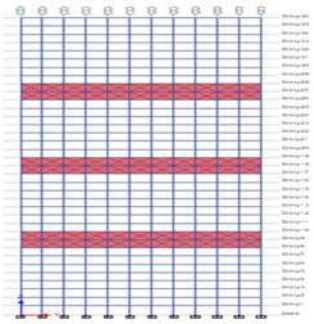

Y shaped building

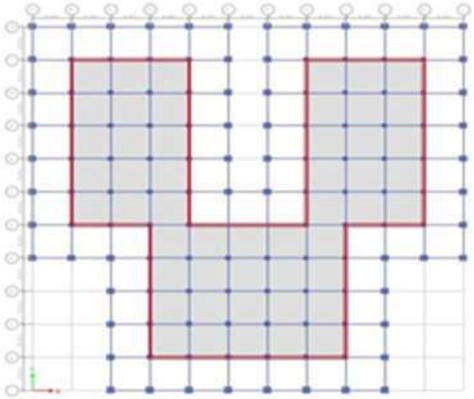

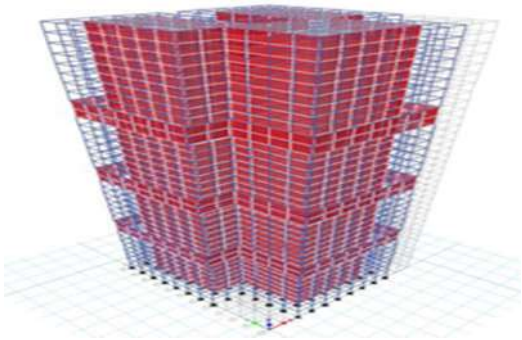

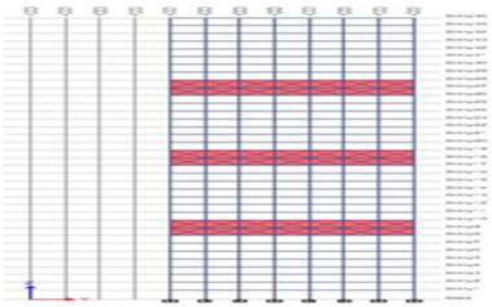

C shaped building

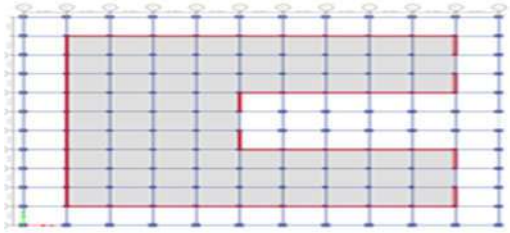

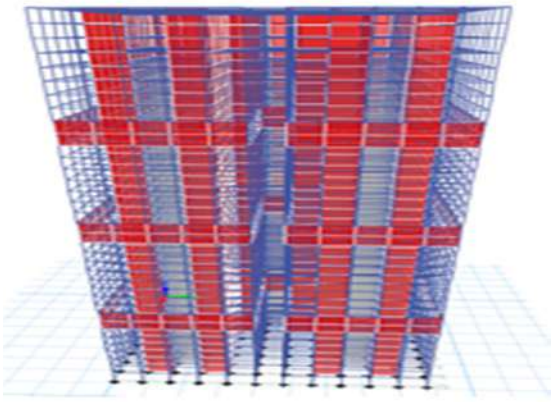

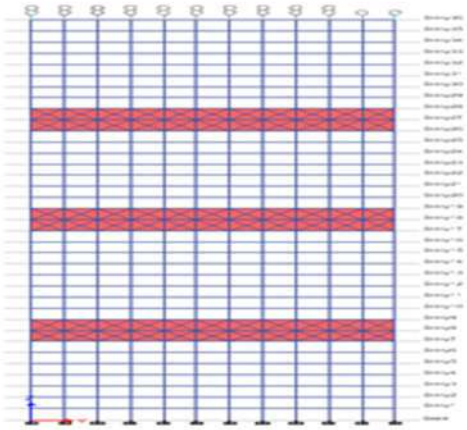

COMPARASTION OF EQUIVALENT STATIC ANALYSIS AND RESPONSE STRECTRUM ANALYSIS.

A.STOREY DRIFT

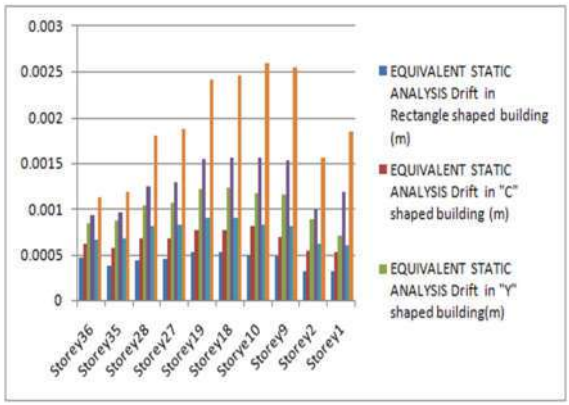

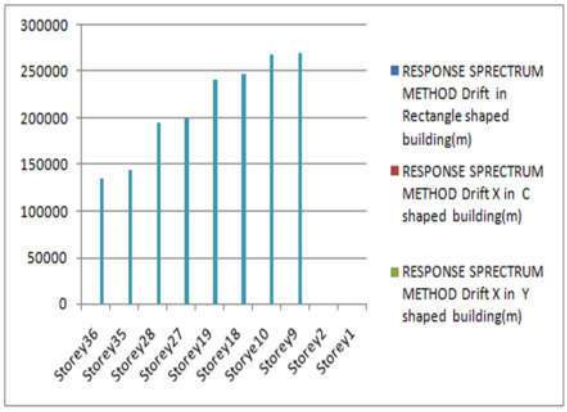

B.STOREY SHEAR FORCE

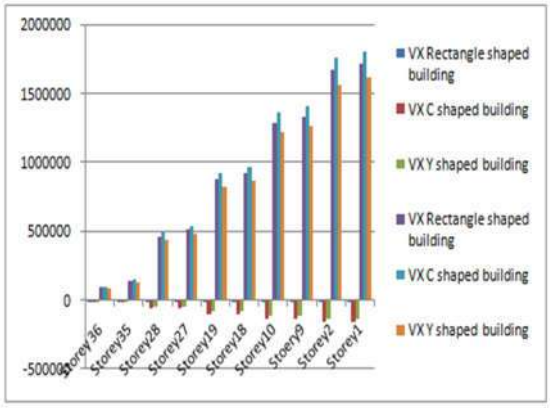

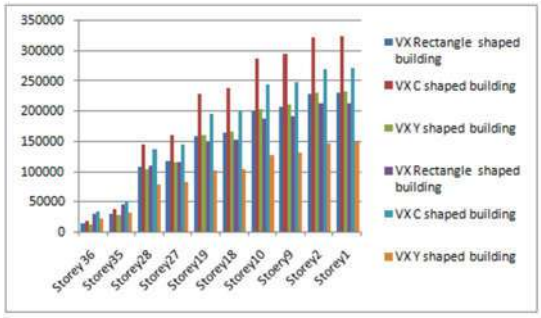

C.MOMENT FORCE

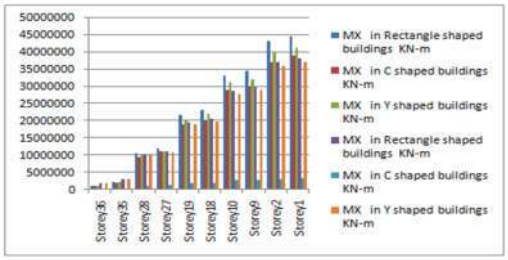

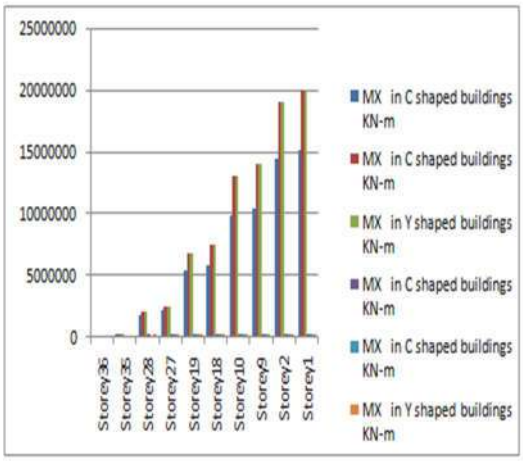

III. .CONCLUSIONS

After performing analysis and studying the results we can come to the below conclusion's:

1) The behavior of a structure under earthquake load is different from earthquake to earthquake. This well known phenomenon is well presented in the lateral displacement results obtained for both of the options. The location of the outrigger beam has a critical influence on the lateral behavior of the structure under earthquake load and the optimum outrigger locations of the building have to be carefully selected in the building design.
2) Comparison drift values both in the equivalent static analysis and response spectrum analysis the drift values show the less values in Rectangle shaped building(symmetrical) in static analysis. The response spectrum analysis shows much higher values due to the combination of all forces including static and dynamic loadings.
3) Considering the shear force in the both static and response spectrum analysis the

static analysis is having the least values in negative as compared to the response spectrum analysis.

4) The building minute demonstrates that the minute in response spectrum having less qualities as compared to the static analysis.
5) Considering all the above results and graphs the best reasonable structure is C formed building for the unsymmetrical shapes as compared to other building Y molded building both in static and response spectrum technique.
6) The utilization of outrigger and belt truss system in elevated structures increase the stiffness and make the structural form efficient under lateral burdens. Outrigger system is observed to be efficient in controlling the lateral loads and has proved to be Economical.

IV. REFERENCES

1.S. Fawzia, A. Nasir, T. Fatima (2011) Study of effectiveness of outrigger system for high rise composite buildings for cyclonic region, World Academy of Science Engineering and Technology, volume 5, 12-29.

2. J. Kim, Y. Jun and J. Park (2010) Performance of building structures with outrigger trusses subjected to loss of a column, 2nd Specialty Conference on Disaster Mitigation, Winnipeg, Manitoba.

3. Jaehong Lee, Minsik Bang, Jae-Yeol Kim (2008) an Analytical model for high-rise wall-frame structures with outriggers, The Structural Design of Tall and Special Buildings, 17, 839–851.

4. Pramod kumar Sharma, Vinay kumar singh chandrakar, Dr. P. D. Purey (2017)-"Lateral Stability analysis of High Rise building with the help of STAAD PRO"

5. Abbas Haghollahi, Mohsen Besharat Ferdous. Mehdi kastriet (2012). "Optimization of outrigger location in steel tall buildings subjected to Earthquake loads"

COMPARATIVE STUDY OF R.C. TALL BUILDINGS BETWEEN SYMMENTRICAL AND UNSYMMENTRICAL SHAPES IN CONSIDERATION OF NON DUCTILE USING WITH AND WITHOUT OUTRIGGER AND BELT TRUSS SYSTEM

Mohd Parvez Affani[1], Shaik Mohd Javeed[2] Mohd Farrukh Anwar[3]

[1] Pg Student, M.tech in Structural engineering, Department of Civil Engineering, Nawab Shah Alam Khan College of Engineering and Technology, Hyderabad, Telangana

[2] Assistant Professor, M.tech in Structural engineering, Department of Civil Engineering, Nawab Shah Alam Khan College of Engineering and Technology, Hyderabad, Telangana

[3]Head of the Department (PHD) , Vice Principal ,M.tech in Structural engineering, Department of Civil Engineering, Nawab Shah Alam Khan College of Engineering and Technology, , Hyderabad, Telangana

ABSTRACT: Should be met through engineering judgment. In Metro cities like Mumbai, Delhi, Chennai, Bangalore, Kolkata, Hyderabad etc multi-storied buildings are common and disregarding that individuals are willing to remain in elevated structure (36 storeys').The analysis and outline of tall building structural system require more concentration than that of regular multi-storied building. The lateral stability of tall building assumes an important role in safe analysis and plan. demonstrate is generated in ETABS, the state of building like a rectangular(symmetrical) Y-formed and C molded buildings i.e. (Non symmetrical) The building is strengthened in lateral direction by providing Outrigger and Belt non truss system at every 9 to 10 ,18 to 19, 27 to 28 story levels Two strategies for analysis have been considered for lateral stability analysis viz linear static and linear dynamic for both seismic and wind. The various parameters like (1) Lateral displacement story.

I. INTRODUCTION

Tall building is need of developing scenario. Rapid improvement of tall building in the world has been creating impact on innovative advancement of structural system for tall building, result of which buildings are growing taller. There is no specific definition of tall building however Council on Tall Building and Urban Habitat (CTBUH) gives a few measures to define tall building. Tall building phenomenon will continue in a greater scale to address the issues of the growing populace in future large cities. The advancement in concrete technology over the twentieth century covering materials, structural systems, analysis and construction techniques, made it conceivable to manufacture concrete tall buildings. Structural system like minute resisting frame and shear divider and bracing system fulfill primary need of building . As building increases in stature there is effect of lateral load i.e. wind and earthquake on building structure. The

impact of wind and seismic forces acting on tall building becomes an important aspect of the outline. Improving the structural systems of tall buildings can control their dynamic response Wind and earthquake stack plays major impact on building deflection. To overcome lateral load because of earthquake and wind, concrete core has been provided at center of building. Concrete core is a very effective and practical structural system which supportive in reducing the deflection because of seismic and wind forces. During recent years, the frame-concrete core divider hybrid structure has been rapidly created and profoundly concerned by owners with its performance and economic favorable circumstances. The outrigger and belt truss system is commonly utilized as one of the structural system to effectively control the excessive drift because of lateral load, so that, during little or medium lateral load due to either wind or earthquake stack, the risk of structural and non-structural harm can be minimized. For elevated structures, particularly in seismic active zone or wind stack dominant, this system can be chosen as an appropriate structure. Outriggers have been utilized in the sailing ship industry for some years. They are utilized to resist wind. The slender pole provides the utilization of outriggers. As a comparison the core can be related to the pole, the outriggers resemble the spreaders and the exterior columns resemble the shrouds or remains. Innovative structural schemes are continuously being looked for in the field. Structural Design of High Rise Structures with the intention of limiting the Drift because of Lateral Loads as far as possible without paying a high premium in steel tonnage.

OUTRIGGER AND BELT TRUSS SYSTEM

Outriggers are rigid horizontal structure i.e. truss or shaft which connect core divider and outer column of building to improve building strength and overturning stiffness. Outriggers have been utilized in tall building for nearly 50 years, however innovative plan principle has been improving its efficiency. Outrigger system is one sort of structural system which is formed from a cantilever molded horizontal member connected to structures inner core and outer columns. Through the connection, the minute arm of the core will be increased which prompt higher lateral stiffness of the system. Central core in a building act as cantilever, outriggers are provided to reduce overturning minute in core and to transfer minute from core to outer column by connecting the core and column. Divider frame outrigger trusses is a standout amongst the most efficient and economical structures in tall building, at outer end they connected to the establishment through exterior columns. At the point when the structure is subjected to horizontal loading, the divider and outrigger trusses will rotate, causing compression in the downwind column and strain in column on the upwind side, these hub forces will resist the rotation in the divider. The outrigger systems can be produced in any combination of steel, concrete and composite construction. Normally in steel structure outrigger are in the form of trusses and in the form of divider or profound bar in concrete structure. Outrigger might be stretched out to both side of central core or core might be located at one side of building with outrigger extending to other side columns. Belt truss connects outer perimeter column of a building and offer a wider perimeter to resist lateral deflection of building. This efficient structural form consists of a central core, comprising either Braced Frames or Shear Walls, with horizontal cantilever trusses or girders known as outrigger Trusses, connecting the core to the outer columns.

The core might be centrally located with outriggers extending on both.

TYPES OF OUTRIGGER TRUSS SYSTEM

Conventional Outrigger Concept

In the conventional outrigger concept, the outrigger trusses or girders are connected directly to shear dividers or braced frames at the core and to columns located outboard of the core. Typically (however not necessarily), the columns are at the outer edges of the building. Figure 1 is a romanticized section through a tall building with two arrangements of outrigger trusses, including one at the best. The outrigger trusses configuration. Shallower and deeper trusses have been utilized, with diagonals of various configurations.

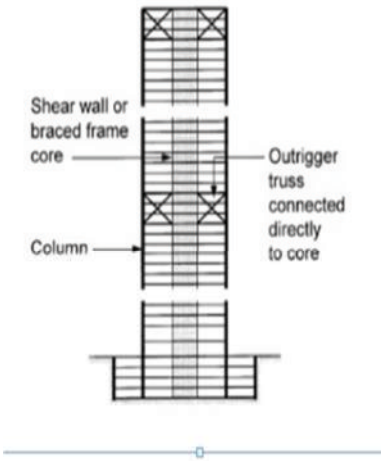

Tall building with conventional outriggers

Virtual Outrigger Concept

In the "virtual" outrigger, a similar transfer of overturning from the core to components outboard of the core is achieved, yet without a direct connection between the outrigger trusses and the core. The basic thought behind the virtual outrigger concept is to utilize floor diaphragms, which are typically very solid and strong in their own plane.

Belt Trusses As Virtual Outriggers

The utilization of belt trusses as virtual outriggers keeps away from a considerable lot of the problems associated with the utilization of conventional outriggers. The principle is the same as when belt trusses are utilized as virtual outriggers. Some fraction existing apart from everything else in the core is converted into a horizontal couple in the floors at the best and the base of the storm cellar.

NEED OF THE PROJECT

Accumulation of growing populace especially in developing countries has resulted in an increased tallness of buildings, this need creating impact on structural improvement of tall building. As building increases in tallness there is effect of wind and earthquake forces, to increase stiffness of building against lateral load extra structural system such as belt truss and outriggers is required. The reviewed approach for the outline and improvement of tall building using outrigger and belt truss is helpful to provide a potential arrangement. The study in turn is helpful for various research persons involved in outline the tall buildings by using outrigger and belt truss system

OBJECTIVE OF THE STUDY

To study the effect of introduction of Outriggers in tall structure subjected to dynamic wind loading. To study the influence of core divider and braced core divider with X braced outriggers C. To stud influence of concrete outrigger. To study the effect of Outriggers with Peripheral Belt Truss. To study the different configuration of the building under different

arrangement molded building i.e symmetrical and Unsymmetrical Buildings (Rectangular and Y formed building , C formed Building

II. METHODOLOGY

ANALYSIS OF A 36 STOREY BUILDING

The model considered for this study is 111.5 m skyscraper reinforced concrete building frame. The building represents a 36 storied office building. The stature of each story is 3m and every one of the floors are considered as Typical Floors. The location of the building is thought to be at Bhuj (Gujarat) . All divider piers are identical with a uniform divider thickness of 230mm over the entire stature. The Bracing bars (outriggers) and every other bar are 600mm wide and 600mm profound, Grade 40 concrete is considered (Compressive strength 40 N/mm²) throughout the tallness of the building. And number of stories considered for every one of the cases is 36 stories, and roof tallness is considered as 111.5 m. And story to story tallness is 3.0 m. And the outer columns sizes are considered as 800X800 mm and Inner columns measure are consider as 550X600 mm. shear divider thickness is considered as 230 mm.The technique for analysis of the previously mentioned system is construct up in light of the presumptions that the outriggers are rigidly attached to the core; The core is rigidly attached to the establishment; The sectional properties of the core, shafts and columns are uniform throughout the stature; Tensional effects are not considered; Material behavior is in linear elastic range; The Outrigger Beams are flexural rigid and induce just pivotal forces in the columns; The lateral resistance is provided just by the bending resistance of the core and the secure action of the exterior columns connected to the outrigger; The rotation of the core because of the shear deformation is immaterial.

STRUCTURAL MODELLNG

SL No	Structural details	Type of location
1	Utility of Buildings	Office Building
2	No of Storey	G+36
3	Area	2308 sq mts
4	Height of Building	111.5 mts
5	Shape of the Building	Rectangle, Y shaped, C shaped building
6	Types of Walls	SHEAR Wall -230 mm thickness Masonry wall – 230 mm thickness
7	**Geometric Details** Ground Floor	3.5 mts
	Story to story height	3.0 mts
	Beam	0.60X0.60 mts
	Columns (outer)	0.80X0.80 mts
	Columns (Inner)	0.55X0.60 mts
	Slab	0.150 mts
8	**Material Details** Concrete Grade All Steel Grades	M40 (All structural elements) FE 415 (All structural elements)
9	Type Of Construction	R.C.C FRAMED STRUCTURE
10	Place of construction	Bhuj - Gujarat
11	Loads considered in Buildings	Dead load, Live load, Earthquake ,Wind load
12	Wind Speed	50 m/s (Bhuj wind speed)
13	Seismic Zone	Zone – V (Bhuj)
14	Method of Analysis	RESPONSE SPECTRUM ANALYSIS EQUIVALENT STATIC ANALYSIS
15	NON Ductile properties	5 (Response reduction factor)
16	STATIC COMBINATION USED	1.2(Dead load+ Live load+ Earthquake in X direction)
17	IS codes used	IS456 :2000,IS1893:2002,IS 16700:2017,IS 875:1987 (Part 1, Part 2, Part 3)

Rectangle Building

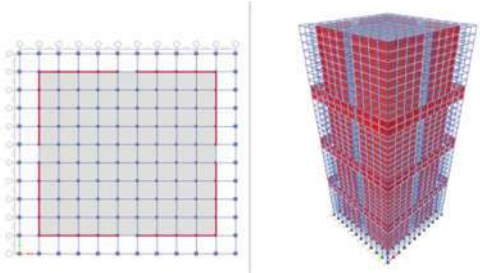

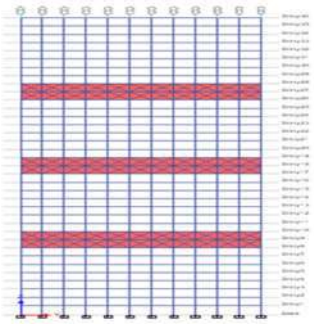

Y shaped building

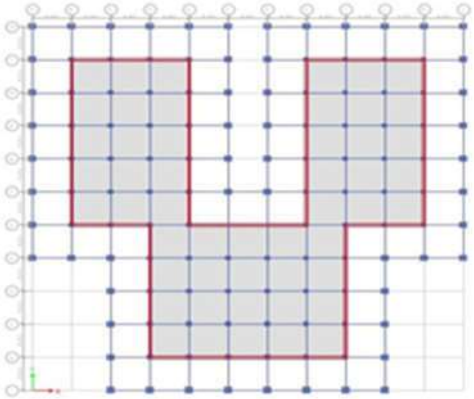

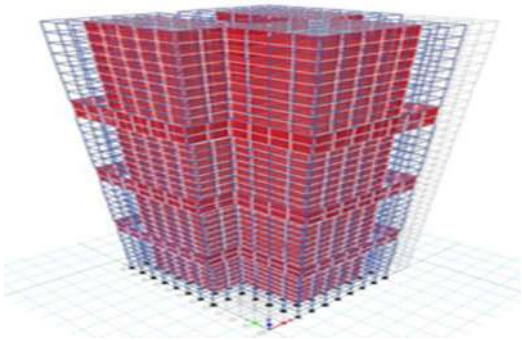

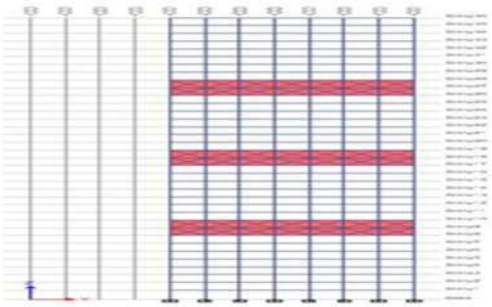

C shaped building

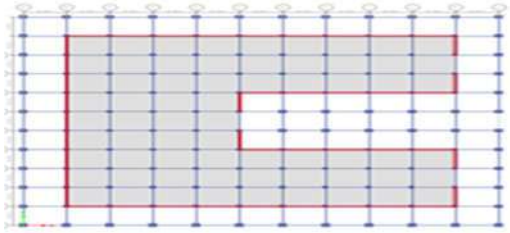

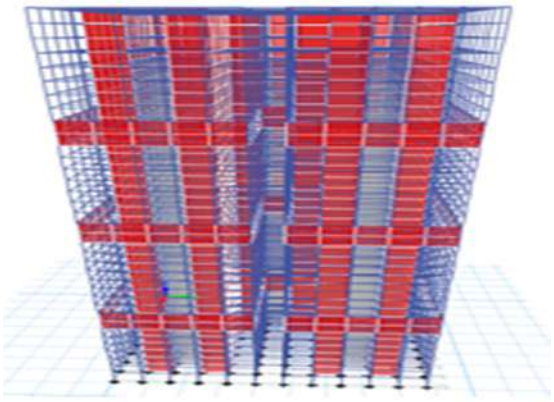

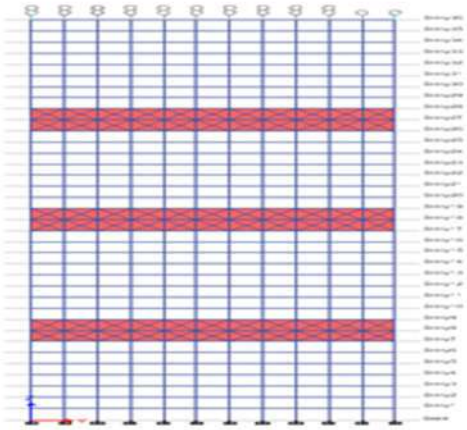

COMPARASTION OF EQUIVALENT STATIC ANALYSIS AND RESPONSE STRECTRUM ANALYSIS.

A.STOREY DRIFT

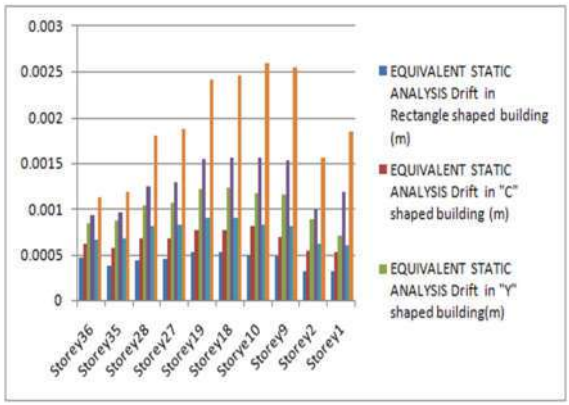

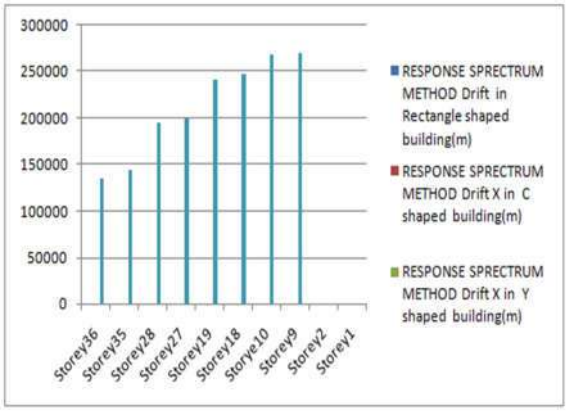

B.STOREY SHEAR FORCE

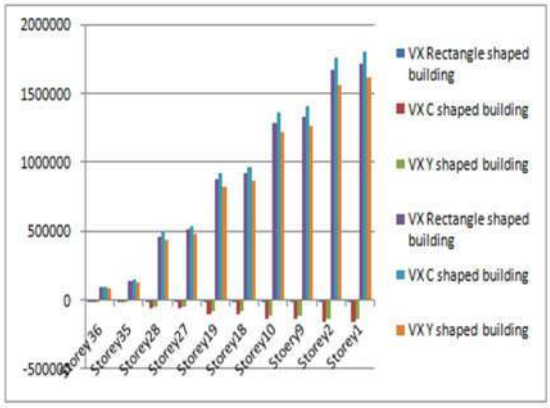

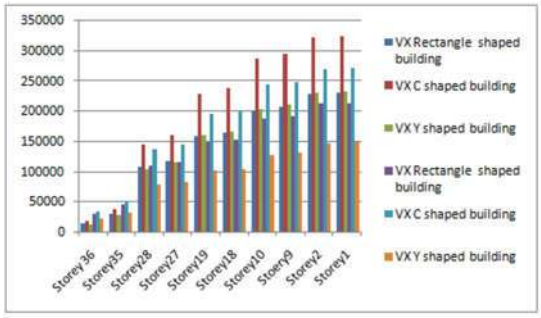

C.MOMENT FORCE

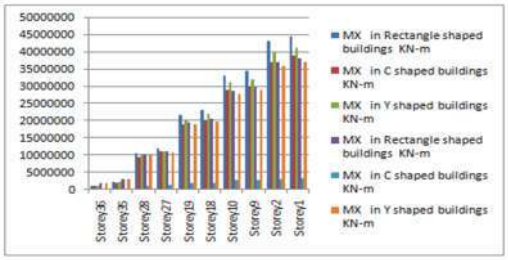

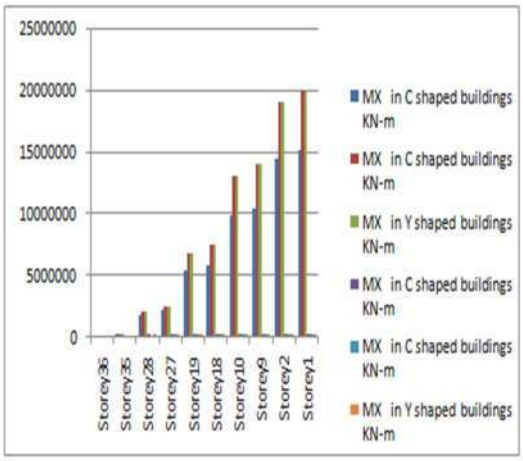

III. .CONCLUSIONS

After performing analysis and studying the results we can come to the below conclusion's:

1) The behavior of a structure under earthquake load is different from earthquake to earthquake. This well known phenomenon is well presented in the lateral displacement results obtained for both of the options. The location of the outrigger beam has a critical influence on the lateral behavior of the structure under earthquake load and the optimum outrigger locations of the building have to be carefully selected in the building design.
2) Comparison drift values both in the equivalent static analysis and response spectrum analysis the drift values show the less values in Rectangle shaped building(symmetrical) in static analysis. The response spectrum analysis shows much higher values due to the combination of all forces including static and dynamic loadings.
3) Considering the shear force in the both static and response spectrum analysis the

static analysis is having the least values in negative as compared to the response spectrum analysis.

4) The building minute demonstrates that the minute in response spectrum having less qualities as compared to the static analysis.
5) Considering all the above results and graphs the best reasonable structure is C formed building for the unsymmetrical shapes as compared to other building Y molded building both in static and response spectrum technique.
6) The utilization of outrigger and belt truss system in elevated structures increase the stiffness and make the structural form efficient under lateral burdens. Outrigger system is observed to be efficient in controlling the lateral loads and has proved to be Economical.

IV. REFERENCES

1.S. Fawzia, A. Nasir, T. Fatima (2011) Study of effectiveness of outrigger system for high rise composite buildings for cyclonic region, World Academy of Science Engineering and Technology, volume 5, 12-29.

2. J. Kim, Y. Jun and J. Park (2010) Performance of building structures with outrigger trusses subjected to loss of a column, 2nd Specialty Conference on Disaster Mitigation, Winnipeg, Manitoba.

3. Jaehong Lee, Minsik Bang, Jae-Yeol Kim (2008) an Analytical model for high-rise wall-frame structures with outriggers, The Structural Design of Tall and Special Buildings, 17, 839–851.

4. Pramod kumar Sharma, Vinay kumar singh chandrakar, Dr. P. D. Purey (2017)-"Lateral Stability analysis of High Rise building with the help of STAAD PRO"

5. Abbas Haghollahi, Mohsen Besharat Ferdous. Mehdi kastriet (2012). "Optimization of outrigger location in steel tall buildings subjected to Earthquake loads"

ANALYSIS AND DESIGN OF TRANSMISSION LINE TOWERS IN COMPARSION WITH WIND ANALYSIS

Mohd Abdul Quddus[1], Mohd Riyan[2] Dr.Mohd farrukh Anwar[3]

[1] Pg Student, M.tech in Structural engineering, Department of Civil Engineering, Nawab Shah Alam Khan College of Engineering and Technology, Hyderabad, Telangana 500024

[2] Assistant Professor, M.tech in Structural engineering, Department of Civil Engineering, Nawab Shah Alam Khan College of Engineering and Technology, Hyderabad, Telangana 500024

[3]Head of the Department ,(PHD) , M.tech in Structural engineering, Department of Civil Engineering, Nawab Shah Alam Khan College of Engineering and Technology, Hyderabad, Telangana 500024

Abstract: ***Transmission line towers carry heavy transmission conductors at a sufficient and safe height from ground. In addition to their self-weight they have to withstand all forces of nature like a strong wind, earthquake and snow load. Therefore, transmission line towers should be designed considering both structural and electrical requirements for a safe and economical design. Now-a-days Government of India is planning for Electrification of Semi-Urban and Rural areas. In fact designing of Huge Transmission Tower is the key interest for Power Transmission from Source to utility point. Steel Structures and their behavior are not same as of RCC. All the Transmission Tower is like Skeleton Structures and they have been made in the form of 3-D Truss. Analysis of Space Trusses is not an Easy task when they are subjected to large Wind and Seismic forces. Keeping in view the importance of Wind Forces and Seismic Forces a 3-D Model has been generated in SAP2000. All the Necessary checks has been Performed for safe and stable Design. Parameters such as Lateral***

I. INTRODUCTION

India has a large population residing all over the country and the electricity supply need of this population creates requirement of a large transmission and distribution system. Also, the disposition of the primary resources for electrical power generation viz., coal, hydro potential is quite uneven, thus again adding to the transmission requirements. Transmission line is an integrated system consisting of conductor subsystem, ground wire subsystem and one subsystem for each category of support structure. Mechanical supports of transmission line represent a significant portion of the cost of the line and they play an important role in the reliable power transmission. They are designed and constructed in wide variety of shapes, types, sizes, configurations and materials. The supporting structure types used in transmission lines generally fall into one of the three categories: lattice, pole and guyed.

Fastest growing telecommunication market has increased the demand of steel towers. The major loads considered for design of these towers are self-weight, wind load, seismic load, antenna load, platform load, steel ladder load etc. Failure of towers is generally due to high intensity winds. Several studies have been carried out by considering wind and earthquake loads. This study is performed as per the requirement and recommendation of the management for the validation of the results according to the IS codes to check whether the same structure can be safe for both the places without any change in structural configuration and for the different loading conditions for both the places. From the study of literature review, it is reported that the predominant external loads which act on these towers are wind and earthquake loads. For the economical purpose and uniformity in power system, it is an important study to save the cost of designing and maintenance as it is easy and beneficial to have uniform towers. Analysis and design is carried as per the recommendations given in IS: 800-2007(LSM).

OBJECTIVE OF THE STUDY

- The design and analysis transmission tower by using sap 2000 analysis.
- Non- linear dynamic analysis and design of transmission towers.
- The earthquake analysis with comparison of two different zones i.e. zone IV and zone V
- To determine wind analysis and comparison of the wind terrain categories i.e. terrain category III, and terrain category IV.
- Finding the best optimum tower design according to seismic conditions and terrain categories.

SCOPE OF PRESENT WORK

- Continuous demand due to increasing population in all sectors viz. residential, commercial and industrial leads to requirement of efficient, consistent and adequate amount of electric power supply which can only fulfilled by using the Conventional Guyed Transmission Towers.
- It can be substituted between the transmission lines of wide based tower where narrow width is required for certain specified distance.
- Effective static loading on transmission line structure, conductor and ground wire can be replaced with the actual dynamic loading and the results can be compared.
- Attempt in changing the shape of cross arm can lead to wonderful results.
- Rapid urbanization and increasing demand for electric, availability of land leads to involve use of tubular shape pole structure.
- lso restricted area (due to non-availability of land), more supply of electric energy with available resources and for continuous supply without any interruption in the transmission line, will demand the use of high altitude narrow based steel lattice transmission tower

II. STRCUTRAL MOLDELLING

Transmission Tower Dimensions: MODEL 1: SQUARE BASE TOWER

Description	Lengths
Total Height (H)	30 mts
Ground clearance (h1)	7.01 mts
Maximum sag of the lower most conductors wire (h2)	7.66 mts
Vertical distance between conductor wires (h3)	7.66 mts
Vertical distance between conductor and ground wire (h4)	7.66 mts
Length of cross arm from edge of hamper	4 mts
Span between the towers	200 mts
Length of wire between two suspension towers	230 mts
Basic wind pressure in kg/m2	50
Maximum Temperature of conductor	75°
Maximum Temperature of Ground wire	53°
Every day temperature	33°
Minimum Temperature	12°
Terrain Type	plain
Return Period	50 years
Tower Geometry	Square base
Peak type	Square
Tower type	Suspension tower
Angle of line deviation	0 ° -2 °
No. of circuits	Double circuit
Basic wind speed in m/sec	44
Minimum Width at Base	4.5 m Square Tower

Transmission Tower Dimensions: MODEL 2: trapezoidal Base Tower

Description	Lengths
Total Height (H)	30
Ground clearance (h1)	7.01 mts
Maximum sag of the lower most conductors wire (h2)	7.66
Vertical distance between conductor wires (h3)	7.66
Vertical distance between conductor and ground wire (h4)	7.66
Length of cross arm from edge of hamper	5 mts
Span between the towers	200 mts
Length of wire between two suspension towers	230 mts
Basic wind pressure in kg/m2	50
Maximum Temperature of conductor	75°
Maximum Temperature of Ground wire	53°
Every day temperature	33°
Minimum Temperature	12°
Terrain Type	plain
Return Period	50 years
Tower Geometry	Square base
Peak type	Square
Tower type	Suspension tower
Angle of line deviation	0 ° -2 °
No. of circuits	Double circuit
Basic wind speed in m/sec	50
Minimum Width at Base	4.5 m Trapezoidal Tower

Transmission Tower Dimensions: MODEL 3: Trapezoidal Base Tower:

Description	Lengths
Total Height (H)	30
Ground clearance (h1)	7.01 mts
Maximum sag of the lower most conductors wire (h2)	7.66
Vertical distance between conductor wires (h3)	7.66
Vertical distance between conductor and ground wire (h4)	7.66
Square base width	6.0 mts
Length of cross arm from edge of hamper	3 mts
Span between the towers	200 mts
Length of wire between two suspension towers	230 mts
Basic wind pressure in kg/m2	50
Maximum Temperature of conductor	75°
Maximum Temperature of Ground wire	53°
Every day temperature	33°
Minimum Temperature	12°
Terrain Type	plain
Return Period	50 years
Tower Geometry	Trapezoidal base
Peak type	Triangle
Tower type	Suspension tower
Angle of line deviation	0 ° -2 °
No. of circuits	Double circuit
Basic wind speed in m/sec	50
Minimum Width at Base	6 m Trapezoidal Tower

TOWER MODEL 1

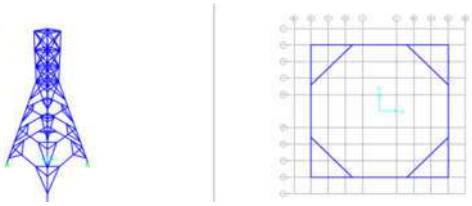

TOWER MODEL 2 :

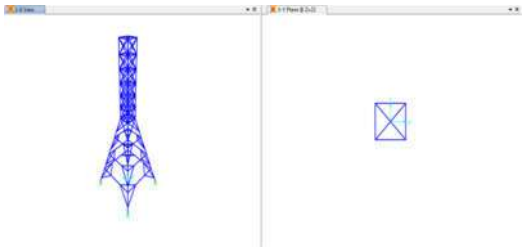

TOWER MODEL 3:

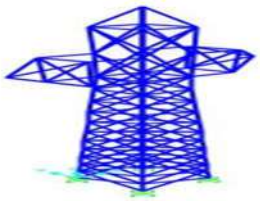

III. RESULTS AND ANALYSIS

1. RESULTS OF TRAMISSION TOWER COMPARASION OF THE RESULTS (U 1 displacement)

Joint	Output Case	U1 Transmission Tower MODEL1	U1 Transmission Tower MODEL 2	U1 Transmission Tower MODEL3
Text	Text	meters	meters	Meters
1	RSA	0	0	0
2	RSA	0.001012	0.000036	0
3	RSA	0.000671	0.000036	0
4	RSA	0.00116	0.000036	0
5	RSA	0.00101	0	0.002718
6	RSA	0	0.000036	0.002718
7	RSA	0.000934	0	0.002718
8	RSA	0.00045	0	0.002718
9	RSA	0.000996	0.000133	0.002289
10	RSA	0.000932	0.000133	0.001885
11	RSA	0	0.000133	0.001512
12	RSA	0.001012	0.000133	0.001174
13	RSA	0.000442	0.000309	0.000875
14	RSA	0.001251	0.000309	0.000616
15	RSA	0.00101	0.000309	0.000401
16	RSA	0	0.000309	0.000232
17	RSA	0.000934	0.000579	0.000108
18	RSA	0.000783	0.000579	0.000036
19	RSA	0.001023	0.000579	0.002289
20	RSA	0.000932	0.000579	0.001886

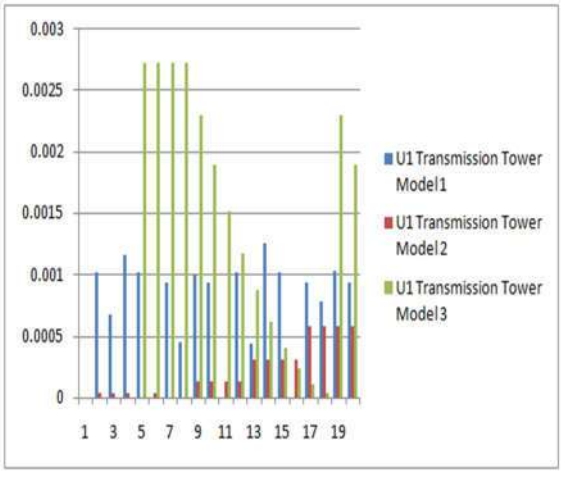

U 2 Displacements

Joint	Output Case	U2 Transmission Tower Model 1	U2 Transmission Tower Model 2	U2 Transmission Tower Model 3
Text	Text	meters	meters	Meters
1	RSA	0	0	0
2	RSA	0.000932	0.000036	0
3	RSA	0.000452	0.000036	0
4	RSA	0.00093	0.000036	0
5	RSA	0.000877	0	0.002724
6	RSA	0	0.000036	0.002721
7	RSA	0.000932	0	0.002724
8	RSA	0.000783	0	0.002721
9	RSA	0.00093	0.000133	0.002298
10	RSA	0.001115	0.000133	0.001896
11	RSA	0	0.000133	0.001523
12	RSA	0.001013	0.000133	0.001185
13	RSA	0.000675	0.000309	0.000884
14	RSA	0.001011	0.000309	0.000624
15	RSA	0.001189	0.000309	0.000408
16	RSA	0	0.000309	0.000236
17	RSA	0.001013	0.000579	0.00011
18	RSA	0.000438	0.000579	0.000036
19	RSA	0.001011	0.000579	0.002298
20	RSA	0.001249	0.000579	0.001896

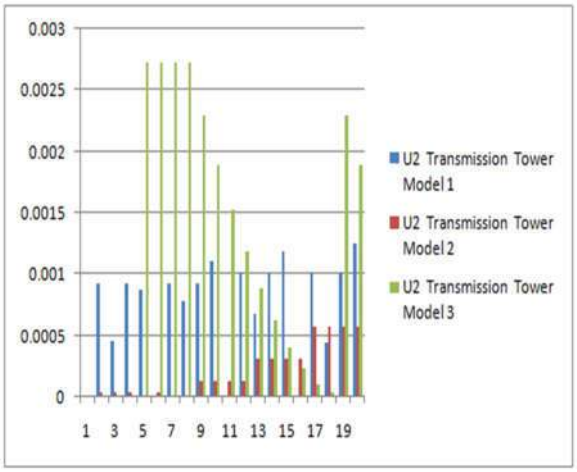

U 3 Displacements

Joint	Output Case	U3 Transmission Tower Model 1	U3 Transmission Tower Model 2	U3 Transmission Tower Model 3
Text	Text	meters	meters	meters
1	RSA	0	0	0
2	RSA	0.00033	0.000069	0
3	RSA	0.000189	0.000069	0
4	RSA	0.000676	0.000069	0
5	RSA	0.000536	0	0.000336
6	RSA	0	0.000069	0.000337
7	RSA	0.000335	0	0.000336
8	RSA	0.00023	0	0.000337
9	RSA	0.000393	0.000118	0.000348
10	RSA	0.000672	0.000118	0.000351
11	RSA	0	0.000118	0.000346
12	RSA	0.000233	0.000118	0.000331
13	RSA	0.000143	0.000133	0.000308
14	RSA	0.00042	0.000133	0.000276
15	RSA	0.000556	0.000133	0.000236
16	RSA	0	0.000133	0.000188
17	RSA	0.000331	0.00011	0.000133
18	RSA	0.000213	0.00011	0.000068
19	RSA	0.000694	0.00011	0.000349
20	RSA	0.000466	0.00011	0.000351

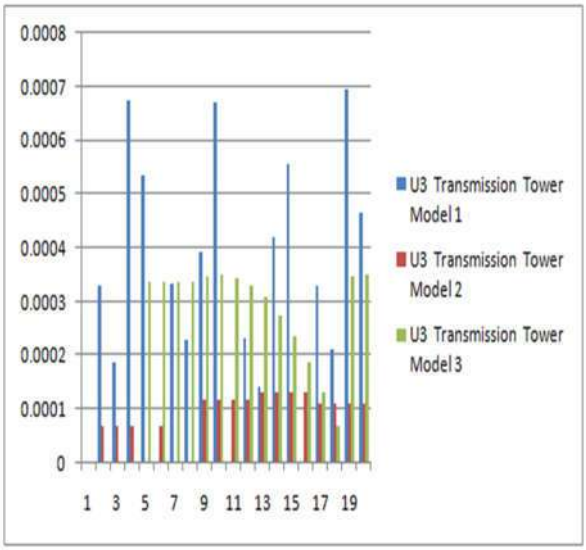

Displacements in radians (R1)

Joint	Output Case	R1 Transmission Tower Model 1	R1 Transmission Tower Model 2	R1 Transmission Tower Model 3
Text	Text	Radians	Radians	Radians
1	RSA	0.000397	0.000003146	0
2	RSA	0.000156	0.00001	0
3	RSA	0.000305	0.000011	0
4	RSA	0.000062	0.000011	0
5	RSA	0.000148	0.000003405	0.000234
6	RSA	0.000707	0.00001	0.000235
7	RSA	0.000078	0.000003308	0.000239
8	RSA	0.000395	0.000003128	0.000237
9	RSA	0.000177	0.000026	0.000228
10	RSA	0.000093	0.000027	0.000213
11	RSA	0.000588	0.000026	0.000194
12	RSA	0.00015	0.000026	0.000175
13	RSA	0.000356	0.000042	0.000153
14	RSA	0.000145	0.000044	0.00013
15	RSA	0.000145	0.000043	0.000104
16	RSA	0.000352	0.000042	0.000079
17	RSA	0.000162	0.000072	0.000054
18	RSA	0.00028	0.000079	0.000027
19	RSA	0.000074	0.000078	0.000227
20	RSA	0.000129	0.000071	0.000213

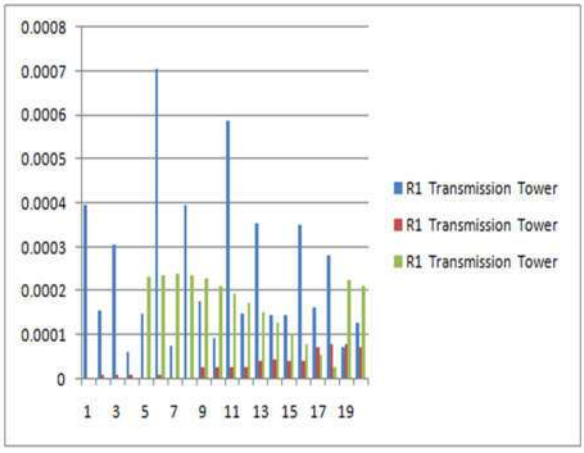

Displacements in radians (R2)

Joint	Output Case	R2 Transmission Tower Model 1	R2 Transmission Tower Model 2	R2 Transmission Tower Model 3
Text	Text	Radians	Radians	Radians
1	RSA	0.00059	0.000003433	0
2	RSA	0.000151	0.000011	0
3	RSA	0.000357	0.00001	0
4	RSA	0.000139	0.00001	0
5	RSA	0.000143	0.000003188	0.000245
6	RSA	0.000394	0.000011	0.000243
7	RSA	0.000143	0.000003097	0.000244
8	RSA	0.000298	0.000003356	0.000244
9	RSA	0.000136	0.000026	0.000227
10	RSA	0.000081	0.000026	0.000212
11	RSA	0.000341	0.000026	0.000192
12	RSA	0.000159	0.000026	0.000173
13	RSA	0.00027	0.000043	0.00015
14	RSA	0.000135	0.000042	0.000127
15	RSA	0.000076	0.000042	0.000102
16	RSA	0.000714	0.000044	0.000077
17	RSA	0.000104	0.000078	0.000052
18	RSA	0.000405	0.000072	0.000023
19	RSA	0.000111	0.000071	0.000228
20	RSA	0.000168	0.000079	0.000212

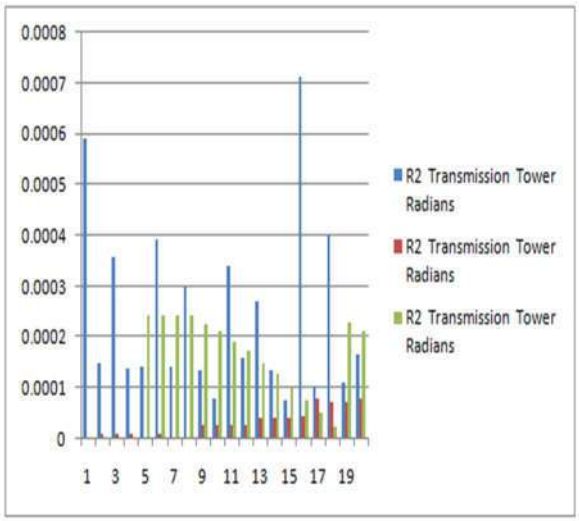

Displacements in radians (R3)

Joint	Output Case	R3 Transmission Tower Model 1	R3 Transmission Tower Model 2	R3 Transmission Tower Model 3
Text	Text	Radians	Radians	Radians
1	RSA	0.000223	0.000001388	0
2	RSA	0.000132	0.000002984	0
3	RSA	0.000171	0.00000317	0
4	RSA	0.000074	0.000002382	0
5	RSA	0.00014	7.991E-07	0.000026
6	RSA	0.00025	0.000002626	0.000028
7	RSA	0.000129	0.000001427	0.000029
8	RSA	0.000185	0.000001475	0.000025
9	RSA	0.000125	0.000003315	0.000026
10	RSA	0.000123	0.000003201	0.000023
11	RSA	0.000262	0.000003261	0.000023
12	RSA	0.000138	0.000003187	0.000023
13	RSA	0.000203	0.000004482	0.00002
14	RSA	0.000126	0.000004538	0.000018
15	RSA	0.000095	0.000002823	0.000013
16	RSA	0.000264	0.00000377	0.000012
17	RSA	0.00015	0.000003011	0.00001
18	RSA	0.000206	0.000001137	0.000015
19	RSA	0.000124	0.000003503	0.000019
20	RSA	0.000097	0.000001034	0.000019

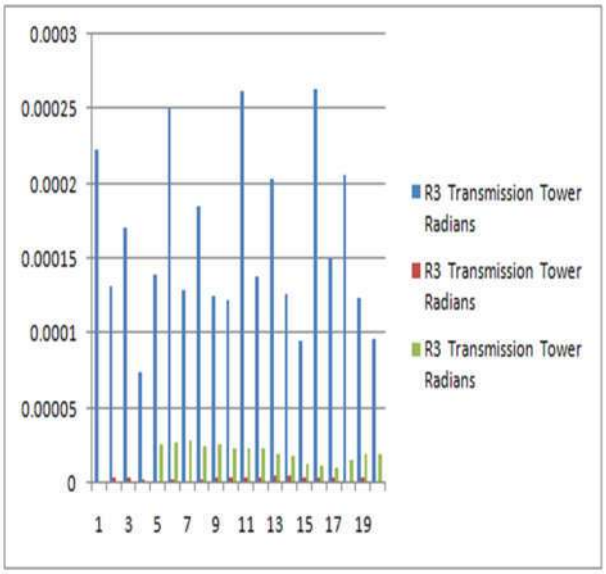

IV .CONCLUSIONS

- The difference between modeling the forces on foundations of a transmission tower using industry standard static point loads and more advanced dynamic loading techniques appears to be relatively significant.
- This indicates that it is important to model the conductors dynamically although this was not within the scope of this thesis. Maximum compression forces are also reduced by a similar amount, although this is generally a less critical design factor.
- It was observed the displacement of the model 2 transmission tower having the least values in the joint displacements and overturning moments
- The Base reactions are of the model 2 of the transmission line tower is having least values as compared to the other transmission line towers.
- The percentage of the steel used in the transmission line towers are the used less steel with best suitable structure to the transmission 220 KV line towers.
- Maximum displacement along X direction 0.653 m and maximum displacement along Y direction is 0.0653 m as compared to X the direction of Y is quite more less in the model 2 of the transmission line tower
- The seismic load and wind load are within the expectable limits as per the codal provisions as per Indian standards.
- The less seismic loads are observed in the model 2 transmission line tower as it was showing least displacements in joints as well as the base reactions of all the transmission towers (i.e. model 1, model 3)
- The wind loads calculations are calculated, and the wind load was seen a major effect on the transmission line tower.
- Considering all the above the considerations in the all three towers the best suitable structure is the square based transmission tower of model 2 is best suitable structure.

REFERENCES

[1] Albermani, F., Kitipornchai, S. and Chan, R. (2009). Failure analysis of transmission towers. Engineering Failure Analysis, 16(6), pp.1922-1928.

[2] Ambrosini, R., Riera, J. and Danesi, R. (2002). Analysis of structures subjected to random wind loading by simulation in the

frequency domain. Probabilistic Engineering Mechanics, 17(3), pp.233-239.

[3] Battista, R., Rodrigues, R. and Pfeil, M. (2003). Dynamic behavior and stability of transmission line towers under wind forces. Journal of Wind Engineering and Industrial Aerodynamics, 91(8), pp.1051-1067.

[4] Belu, R. and Koracin, D. (2013). Statistical and Spectral Analysis of Wind Characteristics Relevant to Wind Energy Assessment Using Tower Measurements in Complex Terrain. Journal of Wind Energy, [online] 2013, pp.1-12. Available at: http://dx.doi.org/10.1155/2013/739162 [Accessed 27 Apr. 2016].

[5] Bessason, B. (2010). Structural Analysis 2. C03.apogee.net. (2017). Fundamentals of Electricity - Towers.

[6] Jordan Journal of Civil Engineering, Volume 7, No. 4, 2013

[7] IS 802 Part 1 Sec 1 1995 Code of practice for use of structural steel in overhead transmission line towers, Part 1

International Journal of Computer Sciences and Engineering Open Access
Research Paper Vol.-6, Issue-11, Nov 2018 E-ISSN: 2347-2693

Robust Design of Intrusion Detection System in Wireless Mobile Adhoc Network (RDIDS-WMAN)

Syed Muqtar Ahmed[1*], Syed Abdul Sattar[2]

[1] Dept. of Computer Science, Research Scholar of Rayalaseema University, ID: PP.COM.SCI & ENG.083, Kurnool, Andhra Pradesh, India
[2] Dept. of Electronics and Communication, Nawab Shah Alam College of Engineering and Technology, Hyderabad, Telengana, India

[*]*Corresponding Author: syedmuqtar@yahoo.com, Tel.: +00-9963102912*

Available online at: www.ijcseonline.org

Accepted: 25/Nov/2018, Published: 30/Nov/2018

***Abstract*—** Presenting cutting edge research- A mobile Adhoc network is a collection of wireless devices in which nodes interact with each other in a tentative topology without using pre-defined infrastructure. Almost all networks are protected using multilayer firewalls and encryption methods, but many of them are not so effective. Therefore we proposed a Robust Design of Intrusion Detection System in Wireless Mobile Adhoc Network (RDIDS-WMAN) to detect anomalies for multi-hop networks. The purpose of this paper is to design a detail architecture of Analysis Process that operates on simple rules including four different phases namely Event management, Authentication, Duplicate request generation and Message alert monitoring phase to detect the malicious node. This paper also conducted the simulation of proposed RDIDS-WMAN with a combination of AODV protocol to show its effectiveness and resists the attacks. Meanwhile, the performance of network, such as Packet Delivery Ratio, Average End-to-End delay, Throughput and Packet Drop Ratio is tolerable according to the NS-2.35 simulation results. Our solution also uses an authentication process with hash method.

***Keywords*—** MANET, AODV, RDIDS-WMAN, Multi-hop network, Authentication, Intusion

I. INTRODUCTION

Wireless network have dynamic nature due to which it forms clusters with nearest neighbouring nodes [1]. An intrusion may be defined as "any set of actions that attempt to compromise the integrity, confidentiality or availability of a resource". Intrusion Detection Systems (IDS) help us to identify the behaviour of malicious activity in Adhoc network. IDS is broadly classified into two techniques: Signature based IDS & Anomaly based IDS. Signature based IDS uses signatures of attacks to detect the intrusion, whereas Anomaly based IDS technique help us to protect destination machine and networks against malicious behaviour. The function of an Adhoc network routing protocol is to make a correct and efficient route between neighbours so that messages would be send within the active time interval [2]. The traditional way of securing network with firewalls and encryption methods may not be sufficient. Therefore, we proposed Robust Intrusion Detection System which may provide best solution for Mobile Adhoc Network (MANET) as its applications are directly related to military, airports, university and the whole community. Many researchers have been working on Adhoc network to provide better solutions for security, but still we need to work on it.

The paper is organized as follows: Section-I discuss about the introduction to MANET, Section-II discuss about related work of different researchers with solutions, Section-III have complete Architecture of RDIDS-WMAN, Section-IV is about Simulation results and finally Section-V is about Conclusion. Our main goal is to work on the following points:

- Provide better Authenticated solution.
- Identify and detect malicious node.
- Protect legal user of MANET.

I. I Vulnerabilities of MANET

Vulnerability is the weakness in the system. MANET is open and decentralized. The use of wireless link provides the network susceptible to attack from passive eavesdropping to active interfering. Damages would be node impersonation; message contamination & leaking of secrete information. Every node in a network must be prepared to confront unexpected attacks. Some of the vulnerabilities are Dynamic nature of topology, Scalability & limited power supply and Lack of centralized management etc.

© 2018, IJCSE All Rights Reserved

I.II Attacks in MANET

One of the challenging tasks in MANET is to provide good security. MANET would be dynamically changing it's topology as the time passes. So its mechanism and shared wireless medium among nodes would be more vulnerable to attacks. Before developing any solution for MANET security, one has to understand different types of attacks which are as follows:

DOS and DDOS Attacks

The purpose of Denial-of-Service (DOS) attack is to stop all the services to the legitimate users by interrupting Server. Perpetrator generates a single request from his machine and sends it through internet, which may create thousands of copies of similar request through flood to disrupt all services of host. Routing is one of the biggest challenges in MANET with various security problems. DOS attacks namely Black-hole, Gray-hole are serious threats for MANETs [3].
Distributed Denial-of-Service (DDOS) attack is a malicious activity to interrupt normal traffic of a targeted server with a flood of Internet traffic. DDOS is more dangerous than DOS.

I.III Routing Protocols in MANET

Our Research is based on AODV. Routing protocol plays a significant role in MANET. They can control the number of nodes with restricted resources and provide optimal routes to deliver data packets quickly. The following are the routing protocol often used in MANET.

I.III.I AODV Protocol

The abbreviation of AODV is Adhoc on demand distance vector protocol. AODV protocol was developed by Nokia, University of California and Santa Barbara. AODV is a reactive protocol as it has the capability to establish the link on demand. It was developed for wireless MANET with range of 10's—100's mobile nodes and utilizes Sequence numbers for route updates. AODV works on Route Discovery and Route maintenance. The source can establish the route to destination that may have minimum number of hops through neighbours. The route established between the nodes by flooding RREQ message. One neighbour would forward the request to other neighbour and record the entry in there routing tables. The neighbour sends the RREP to source, assuring that it can provide best route to destination. AODV protocol ignore count-to-infinity problem when ever route change occur by using sequence numbers.

I.III.II Malicious Activity in AODV Protocol

Let 'A' as source, 'G' as destination and D as malicious node. Node A broadcasts a RREQ packet to all adjacent neighbours as shown in Fig-1. Neighbours scan their routing tables to check the possibility of having rout to destination. They could reply with RREP if there is a route available, otherwise, the RREQ is forwarded to another node and store a backward path in the source. The routing table store path details of the neighbour, the distance and the latest biggest sequence number [4]. If topology changes in the network then the route maintenance starts. When a broken path is detected, a RERR message is generated to inform the neighbours that the line is lost. The RREP message identifies those nodes which are not reachable by the way of the lost link. The D act as a malicious node would send a fake reply to ensure that it has the optimal route to source. When it receives data from source, simply it drops the packets or it may forward to any other malicious node.

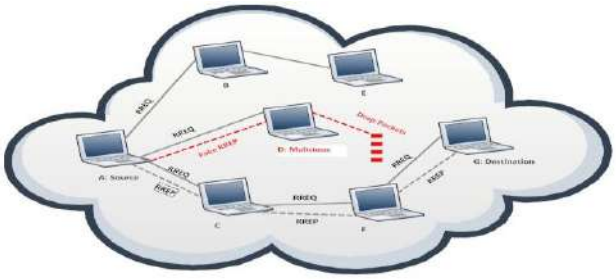

Fig-1: Establishing a new route using AODV protocol

I.III.III DSR Protocol

The abbreviation of DSR is Dynamic Source Routing protocol. It was developed for multi-hop wireless ad hoc networks. The protocol has two main characteristics, "Route Discovery" and "Route Maintenance", which could work altogether to explore and maintain routes to any destinations in MANET. DSR supports multiple routes to any destination and also manage the route while sending the packets to have load balancing. DSR support loop-less routing operations in network that may have single path using only "soft RREQ - RREP Source Destination state", and there will quick recovery when paths are updated [5].

II.RELATED WORK

This section reviews related work on IDS in MANET. Wireless Mobile Adhoc Network is an excellent field of research and less attention is paid to security aspects of routing protocols. The research community is involved to test and implement ad hoc network routing protocols. Wireless mobile ad hoc network is less secure compared to wired network. Therefore, researchers need to make new IDS systems which can handle new security challenges. Cooperative intrusion detection system has been proposed to have good security in mobile Adhoc network [6], where all the available nodes are guided to run their IDS in order to collect and identify possible intrusions. If any abnormal

© 2018, IJCSE All Rights Reserved

behaviour is found, then a global detection process is started for detecting advance intrusions. Later on, enhancement of this model was developed in, where all possible intrusions can be detected with their adjacent sources. The watchdog solution belongs to a part of IDS. The concept in this solution is to keep an eye on neighbour of each node by sensing the channel to find out whether it forwards to its successor or drops the packet. In [7], authors developed a method that resolves some of watchdog's problems. In this proposal, each node quickly checks its neighbour and authenticates Two-way-hop acknowledged message. In [8], authors, sketch an intrusion detection system to avoid the black hole attacks in AODV. In this solution, an agent is utilized to know the attacks that use the route request and the route reply packets. An agent can keep an eye on two-way packets. If any activity is non ethical, then black hole is identified. In [9], Ms. Nidhi Sha and rma Mr.Alok Sharma developed couple of solutions for black hole attack, later they compare their solutions to the original AODV based on the pause time and found low delay in MANET. In [10] a solution was proposed known as channel aware detection (CAD) that rely on two techniques, namely hop by hop loss observation and traffic overhearing. An intermediate node checks the behaviour of its predecessor and successor neighbours to find the malicious node.

III. METHODOLOGY

This section explains the Architecture, Pseudocode and Algorithm of RDIDS-WMAN.

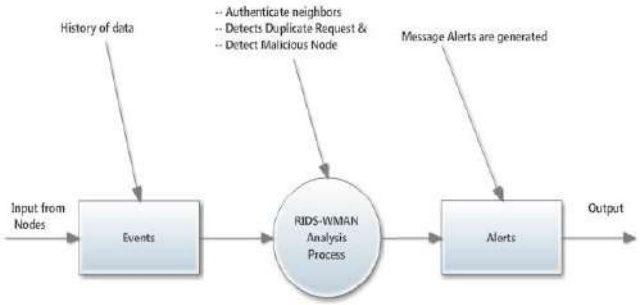

Fig-2: Top Level Architecture of RDIDS-WMAN

Events: This phase checks and store the history of data related to a particular event.
Analysis Process: carry out processes on the collected data to detect malicious signs based on Simple rules of Algorithm.
Alerts: one of the nodes would be selected for monitoring alerts that generates response to the administrator.

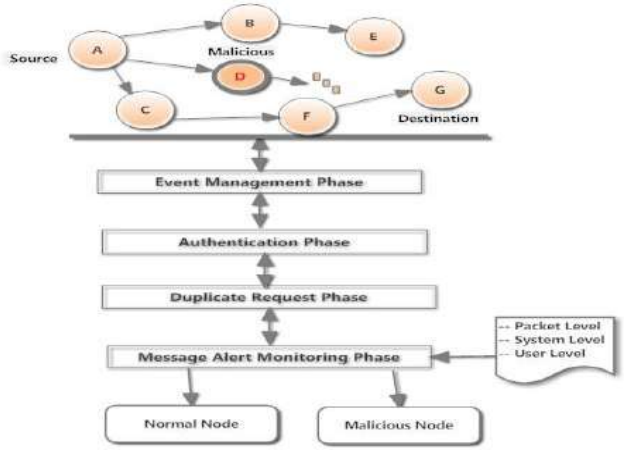

Fig-3 : Detail Architecture of Analysis Process

III.I Architecture of RDIDS-WMAN

The RDIDS-WMAN has been proposed to identify the malicious node in adhoc network with AODV Protocol. The Detail Architecture is displayed in Fig-3, with the following phases:
Event Management Phase : Keeps history of events.
Authentication Phase : Authenticates the nodes
Duplicate Request Phase : Find out whether a message is Duplicate or not.
Message Alert Monitoring Phase : Malicious node can be detected here and the alerts are sent to administrator.
Initially RDIDS-WMAN broadcast RREQ packet to all its Neighbours. In the next step the internmediate node receives a RREP, then it will calculate its hop counter value, which is bigger than Threshold value to detect as a malicious node. RDIDS-WMAN was proposed to perform the detection of malicious node and also block control messages effectively, and at the same time it reduces the tranmission of duplicate RREQ to reduce the network overhead and the time delay.

III.II Pseudocode of RDIDS-WMAN

1. Source node generates RREQ packet and broadcast to all neighbors using flooding.
2. Select one route from several routes.
3. Authentication process with hash method.
4. Check whether the packet received is duplicate or original RREQ.
5. Check whether the node is intermediate or destination node.
6. Identify the malicious node by checking hop counter value that must be greater than Time to live value.

© 2018, IJCSE All Rights Reserved

7. If malicious node is found then intermediate node will update its routing table and also broadcast its updates to all its neighbors in order to block messages.

III.III Algorithm of RDIDS-WMAN

Let {SN: Source Node, DN: Destination Node, X1, X2, X3……Xn-1…...X…...Xn+1 are Intermediate nodes, RREQ: Route Request Packet, RREP: Route Reply Packet, PTOS: Present time of System, T: Timer, TTL=Time to live, THV: Threshold Value to find malicious node, ∀ : Logical symbol for All }

```
Boolean: RREQ = 0;   //0: false & 1: true
h_cnt=0;    //Hop counter initialize to zero
-------------------------------------------------------------------------
Step 1:  //SN generates RREQ and broadcast to all its
//neighbours using flooding
      for ∀ packets of SN do send RREQ by flooding
Step 2:  Procedure Select route ();    // Select one route from
several routes
Step 3: // Authentication process with hash method,
// Where EKpub is an encryption with public key, Hs() is a
 // hashing function and + is a concatenation symbol.
              C ← EKpub (Hs (xi+xi-N)
Step 4:  // if the node is not the DN then it should be
              // One of the Intermediate nodes.
            If (Xk != DN) then      //Xk may be any one
                        // Intermediate node such as X1, X2…Xn
             Print "Intermediate Node"
             else
              Print "Destination Node"
             end if
Step 5:   // Check whether duplicate RREQ is
         //received by neighbour. Here 1 indicates Boolean true.
             If (RREQ =1) && (h_cnt=TTL) then
             Print "Duplicate RREQ"
else
 h_cnt=h_cnt-1;       // Decrement counter by 1 for next hop
Print "Original RREQ"
end if
Step 6: // When Xn-1 receives a RREP, concludes that it's a
//malicious or Normal node.
// RREP is in the range of hop count limit and threshold
value
    // to decide about malicious node.
Xn-1← RREP    // Intermediate node may receive Route Reply
If (h_cnt>THV) then
Print" Malicious Node"
             else
              Print "Normal Node"
end if
Step 7:  // if malicious node is found then Xn-1 will update
 // its routing table and also broadcast updates to all its
// neighbours.
Xn-1 ← malicious
Print "Xn-1 broadcast updates to all neighbours to block
message and   Xn broadcast message to Xn+1"
end for
```

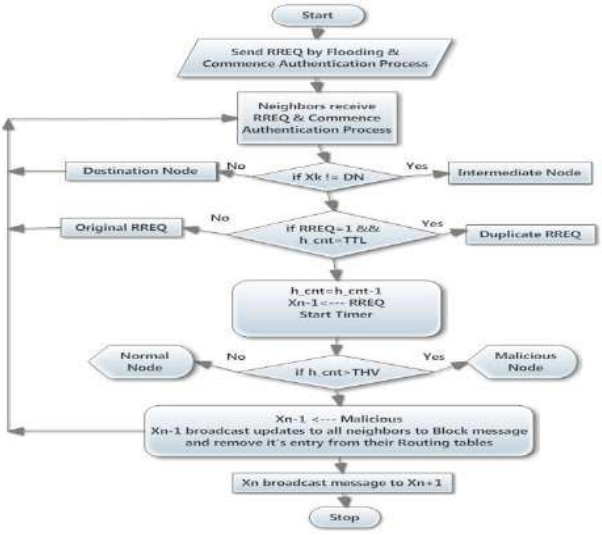

Fig-4: Flowchart of RDIDS-WMAN

1V. SIMULATION RESULTS AND DISCUSSION

We have simulated our proposed algorithm using NS-2.35. The functionality of malicious node is to either drop the packets or to forward to other malicious nodes. We took the original AODV protocol and configured one node as malicious. Our solution detects the malicious node and later immediately blocks that node by sending information to neighbours. The following table shows the simulation parameters

Fig-5: Simulation Screen Shot

1V.I Metrics for Simulation

Packet Delivery Ratio (PDR): It is defined as the ratio of sum of data packets received at destination to the sum of data packets that were send by the source. If the PDR ratio is high then the performance of the routing protocol is high. PDR is calculated as follows:

$$PDR = \sum Packets\ Received / (\sum Packets\ Send) * 100 \quad (1)$$

© 2018, IJCSE All Rights Reserved

Average End to End Delay: It is the defined as delay between the packets send by the source and its delivery at the receiving node.

$$AVG.\,End-End-Delay = delay/(Packets\ Received) \quad (2)$$

Throughput: The total number of bits forwarded to higher layers per second. It is measured in Kbps.

$$Throughput = bytes * (8/(End\ time\ of\ Packet\ transmission - Start\ time\ of\ Packet\ transmission))/1000 \quad (3)$$

Packet Drop Ratio: It is the difference between Packets send & Packets received divided by packets send.

$$Packet\ Drop\ Ratio = (Packet\ Send - Packet\ Received)/(Packets\ send) * 100 \quad (4)$$

Table-2: Simulation of AODV without malicious node

Number of Nodes	Packet Send	Packet Received	PDR (%) AODV	Avg_End-to-End delay (ms) AODV	P_Drop_Ratio (%) AODV	Throughput (Kbps) AODV
5	300	267	89.00	164.44	11	18.83
10	300	298	99.33	149.71	0.67	20.77
15	300	296	98.67	151.12	1.33	21.19
20	300	298	99.33	149.99	0.67	21.57
25	300	300	100	149.5	0	20.83
30	300	299	99.67	149.99	0.33	21.25

Table-3: Simulation of RDIDS-WMAN with a malicious node

Number of Nodes	Packet Send	Packet Received	PDR (%) RDIDS-WMAN	Avg_End-to-End delay (ms) RDIDS-WMAN	P_Drop_Ratio (%) RDIDS-WMAN	Throughput (Kbps) RDIDS-WMAN
5	300	270	90.00	166.28	10	12.23
10	300	295	98.33	148.67	1.67	15.43
15	300	290	96.66	181.98	3.33	15.21
20	300	292	97.33	179.82	2.66	17.18
25	300	298	99.33	149.99	0.66	18.01
30	300	295	98.33	181.67	1.66	17.27

The below Fig-6 graph shows that PDR for our proposed RDIDS-WMAN solution. It has been observed that our solution PDR is reduced only by 0.67% compared to AODV protocol with 25 nodes.

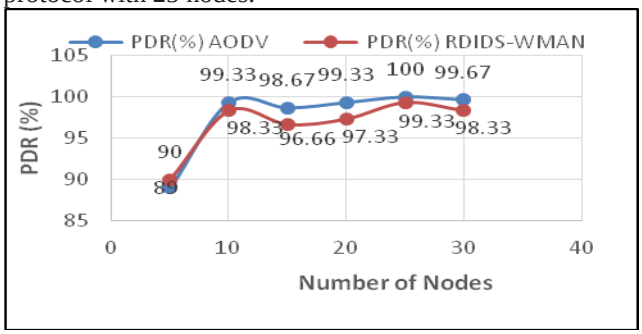

Fig-6: Number of Nodes Vs Packet Delivery Ratio

Table-1: Simulation Parameters

S. No	Simulation Parameters	Values
1	Simulator tool	NS-2.35
2	Number of Nodes (Experiment repeated 6 times to have accurate Performance)	5,10,15,20,25,30
3	Number of Malicious Node	1
4	Area Size	900m x 900m
5	Routing Protocols used	AODV
6	Wireless Standard	IEEE 802.11
7	Packet Size in Bytes	512
8	Source of Traffic	CBR/UDP
9	Model of Propagation	Two ray ground

The below Fig-7 graph shows that Average End-to-End delay of RDIDS-WMAN is almost similar to AODV at 10 and 25 nodes simulation, showing differences of 1.04ms and 0.06 ms respectively. It may vary for other number of nodes.

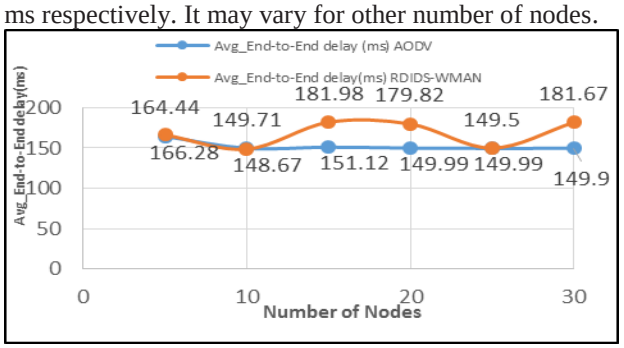

Fig-7: Number of Nodes Vs Average End-to-End delay

The below Fig-8 graph shows that Throughput of RDIDS-WMAN is close to AODV at simulation of 25 nodes, showing differences of 2.82 kbps. It may vary for other number of nodes.

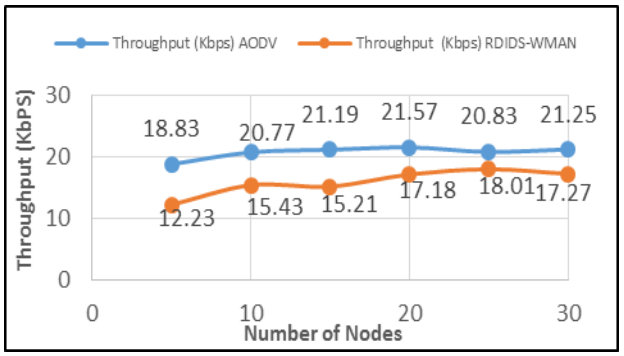

Fig-8: Number of Nodes Vs Throughput

The below Fig-9 graph indicates that Packet Drop Ratio of RDIDS-WMAN is close to AODV showing only the difference of approximately 1% in throughout.

© 2018, IJCSE All Rights Reserved

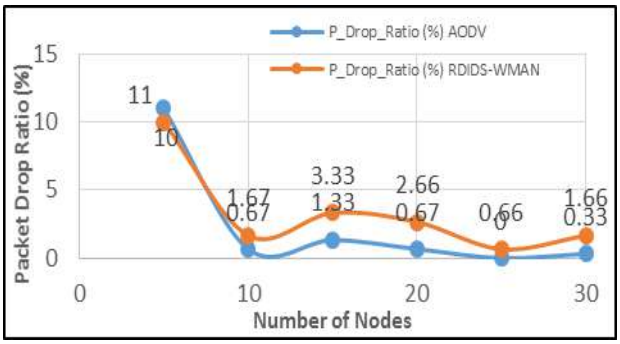

Fig-9: Number of Nodes Vs Packet Drop Ratio

V. CONCLUSION

MANET is vulnerable in terms of security. Attacker gains the access to it due to decentralized nature and undefined topology. The algorithm and architecture proposed in this paper composed by four stages namely Event Management Phase, Authentication Phase, Duplicate Request Phase and Message Alert Monitoring Phase The simulation results shows that the PDR and Average End-End-Delay of proposed solution is approximately similar to AODV. It signifies that the solution is efficient. Meanwhile, the Throughput introduced by authentication is tolerable.

REFERENCES

[1]. J. Srilakshmi1, S.S.S.N. Usha Devi N2, "Secure and Efficient Multipath Routing Using Overlay Nodes", International Journal of Scientific Research. Computer Science and Engineering, Vol.6, Issue 5, pp.16-19, October 2018.

[2]. Lubdha M. Bendale, Roshani. L. Jain, Gayatri D. Patil, "Study of Various Routing Protocols in Mobile Ad-Hoc Networks", International Journal of Scientific Research in Network Security and Communication", Vol. 6, Sp.issue.01, pp.1-5, January 2018.

[3]. Rutvij H. Jhaveri, Sankita J. Patel and Devesh C. Jinwala "DOS Attacks in Mobile Ad-hoc Networks: A Survey", In the Proceedings of the 2012 Second International Conference on Advanced Computing & Communication Technologies, India, Pages 535-541, 2012.

[4]. Swaijit Kaushal, Reena Aggarwal," A study of different types of attacks in MANET and performance analysis of AODV protocol against wormhole attack", International Journal of Advanced Research in Computer Engineering & Technology, Vol. 4 Issue 2, February 2015.

[5]. Naveen Bilandi and Harsh K Verma, "Comparative Analysis of Reactive, Proactive and Hybrid Routing Protocols in MANET", International Journal of Electronics and Computer Science Engineering Vol. 1, Issue 3, pp.1660-1667,

[6]. Y. Huang and W. Lee, "A Cooperative Intrusion Detection System for Ad Hoc Networks," Proceedings of the 1st ACM Workshop on Security of Ad Hoc and Sensor Networks, USA, Pages 135-147, 2003.

[7] D. Djenouri and N. Badache, "Struggling against selfishness and black hole attacks in MANET", Wireless Communication. Mobile Computing, vol. 6, pp. 689–704, 2008.

[8] Morigere Subramanya Bhat, Shwetha .D, Manjunath .D and DevarajuJ.T,"Scenario Based Study of on demand Reactive Routing Protocol for IEEE-802.11 and 802.15.4 Standards", Vol. 1(2), 128-135, November 2011.

[9] Ms. Nidhi Sha rma and Mr. A. Sharma, "The Black-hole node attack in MANET", Proceedings of 2012 Second International Conference on Advanced Computing & Communication Technologies, pp. 546-548, 2012.

[10] S. D. Manikantan, C. Yu and A. Trisha, "Channel-aware detection of gray hole attacks in wireless mesh networks", IEEE global telecommunications conference, pp. 1–6, December 2009.

Author's Biography

Syed Muqtar Ahmed is pursuing Ph.D. in Computer Science & Engineering, from Rayalaseema University, Kurnool, Andhra Pradesh, India. He is having 20 years of teaching experience. Worked as Assistant, Associate Professor and Head of CSE department at Deccan College of Engineering & Technology, Hyderabad, India from 1997-2008. He also worked as a faculty at Nizwa College of Technology, Sultanate of Oman from 2008-2009. He received M.Tech in Information Technology in 2003 and B.E in Computer Science & Engineering in 1997. Recently published articles in Intrusion detection system and also an author of Textbook Title: 'Data Communication and Networking', Sure Series, Hyderabad, India. His area of research is Data Communication, Wireless Network and Network Security.

Dr. Syed Abdul Sattar is a Professor, Director (R&D) at Nawab Shah Alam College of Engineering and Technology, Hyderabad, India. He had received national award as Young Scientist in year 2006 with a Gold medal from NESA New Delhi. He obtained his first Ph.D. in CSE from GSU USA in 2004 on WLAN's Efficiency and Second Ph.D. in ECE from JNTU, Hyderabad on WLAN security in year 2006. He passed Bachelors of Engineering in 1990 and obtained Master's in 2002. His publications are more than 170 in National and International Journals like IEEE, ELSEVIER and SPRINGER etc. He has guided 17 Ph.D. scholars so far and more than 20 are in pipeline. His area of Research is in Wireless communication and Image processing.

© 2018, IJCSE All Rights Reserved

International Journal of Computer Sciences and Engineering Open Access
Research Paper Vol.-6, Issue-12, Dec 2018 E-ISSN: 2347-2693

Mechanism for Detecting Black Hole Attack in Infrastructure-Less MANET (MDB-MAN)

Syed Muqtar Ahmed[1*], Syed Abdul Sattar[2]

[1]Department of Computer Science, Research Scholar of Rayalaseema University, ID: PP.COMP.SCI & ENG.083, Kurnool, Andhra Pradesh, India
[2]Department of Electronics and Communication, Nawab Shah Alam College of Engineering and Technology, Hyderabad, Telengana, India

[*]*Corresponding Author: syedmuqtar@yahoo.com, Tel.: +00-9963102912*

Available online at: www.ijcseonline.org

Accepted: 27/Dec/2018, Published: 31/Dec/2018

Abstract— Mobile Adhoc Network (MANET) is a self-organized group of wireless nodes forming a tentative network. In MANET nodes would be randomly changing their positions due to its dynamic infrastructure-less property. Therefore it is more susceptible to Black-Hole & Gray-Hole attacks, which are considered as serious attacks to the network. So far several solutions have been developed for MANET but many of them are not efficient. The main purpose of this paper is to present a solution known as mechanism for detecting Black Hole Attack in Infrastructure-Less MANET (MDB-MAN). An Algorithm is developed to detect Black-Hole node based on reactive Adhoc on demand distance vector protocol (AODV), where routes are established on demand. Several times simulations were conducted on proposed model using Network Simulator and found that the Packet Delivery Ratio (PDR) and Throughput is almost similar at time instant 50 msec. as compared to original AODV protocol. The Packet Drop Ratio keeps on changing as time changes and it can be tolerable.

Keywords— MANET, AODV, MDB-MAN, Black-Hole attack, Gray-Hole attack

I. INTRODUCTION

Mobile Adhoc network consists of group of wireless nodes which are moving freely from one end to other within the domain of network without the help of pre-existing infrastructure. The MANET is self-organized network in which mobile nodes or devices would be added or deleted dynamically at any time [1]. Therefore, MANET is suitable for that type of areas where fixed wired network could not be setup easily. In MANET, different movable & portable devices are assumed to be connected with the help of routing protocols [2]. Routing protocols have been classified into three categories namely Reactive protocols: Example: AODV & DSR Proactive Protocols: Example: OLSR and Hybrid protocols: Example: ZRP [3]. In today's wireless communication, the Adhoc network could not be isolated from our daily routine work; especially in military and emergency services.

Many researchers have been involved to show different solutions on Black-Hole attack but still they are not effective. In this paper, we present a solution to identify and detect the Black-Hole attack. Our paper is organized as follows: Section-I contains the introduction to Adhoc on demand distance vector protocol, Intrusion Detection System and Black-Hole attack, Section-II contains a related work done by several researchers with their solutions, Section-III is about the proposed Algorithm with Flow chart and configuration of Black-Hole node. Section-IV is about Simulation, Section-V describes Results and discussion and Section-VI concludes the research work.

I. I. Adhoc on Demand Distance Vector Protocol

Adhoc on demand distance vector (AODV) Protocol has been designed for mobile Adhoc networks (MANET). Our proposed solution is based on AODV protocol. This protocol would establish the link from source to destination, whenever it is required. I.e. on-demand policy. AODV would maintain the routes in the routing table with the help of different packet parameters like Source Address, Source Sequence number, Broadcast Id, Destination Address and Hop-Count. AODV works on two strategies like Route-Discovery and Route-Maintenance [4]. The first step of this protocol is to send a RREQ (Route-Request) to all the adjacent nodes that are directly connected to source node. The process of sending a RREQ simultaneously to all nodes is known as flooding. Once RREQ is received, every node would update its routing table to maintain current status. The RREP (Route-Reply) is

© 2018, IJCSE All Rights Reserved

send back to source either by intermediate neighbour or destination node to complete the round trip journey in the form of acknowledgement and to ensure that it has the optimal route to destination with less number of hops.

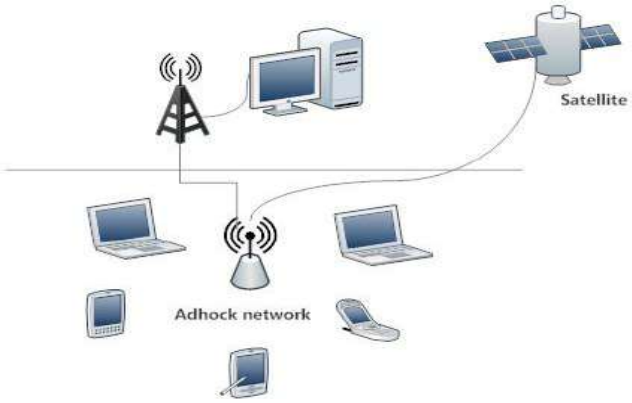

Fig-1 Mobile Adhoc Network

I.II. Intrusion Detection System

The main purpose of Intrusion Detection System (IDS) is to identify and detect the malicious behaviour of Intruder in the network. Intrusion Detection System is basically used for monitoring all operational parameters of Wired or Wireless networks. Over two decades different categories of IDS have been developed. The traditional types of IDS were failed to analyse the data properly as they work on log-files within the Operating Systems. Therefore, we need both software and hardware IDS solutions to provide full security to our data and network as well. One of the categories of IDS is Distributed IDS which could be used on several nodes to collect and analyse parameters. The main design issue in the Distributed IDS is the communication between Components within the System Architecture [5].

I.III. Black-Hole Attack

Black Hole attack is one of the most dangerous threat to the network security, which could degrade the overall performance of MANET. One of the nodes could be a Black-Hole-Node (B-H-N) node that acts like an attacker. As soon as B-H-N node receives RREQ from source, it will send RREP, ensuring that it has the best route to destination with less number of hops in order to deceive the other nodes in the network. Hence, the packets are delivered to a B-H-N and ultimately packets are drop or may be forwarded to any other B-H-N (if it is available in the network). Black Hole Attacks have been divided into two categories namely Single Black-Hole Attack and Collaborative-Hole Attack [6]. In this paper, we are working on Single-Hole Attack. To explain the Single-Hole Attack, we assume the scenario of Fig-2. In this, N0, N1, N2……N14 are the nodes. N0 is a source, N5 is Black-Hole-Node and N14 is considered as Destination.

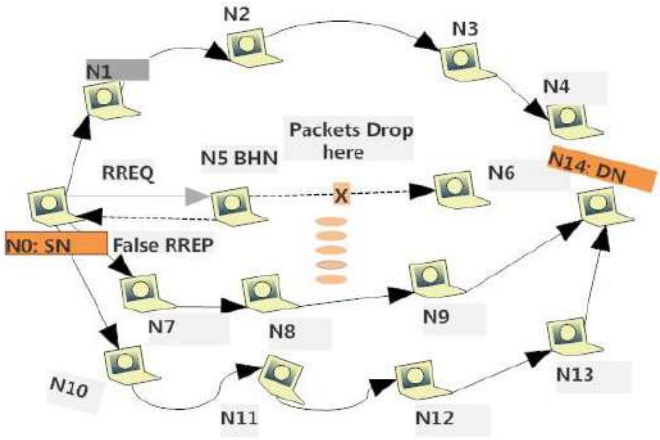

Fig-2: RREQ-RREP in Black-Hole Node (B-H-N)

The Summary of Fig-2 RREQ-RREP is conducted with AODV protocol as follows:

- N0 broadcast RREQ to all neighbours (N1, N5, N7 and N10).
- Assume that N5 is Black-Hole Node (BHN).
- N5 will backtrack to N0 by false RREP, saying that it has the optimal route to destination with less number of hops.
- N0 store the false information in its routing table and deliver packets to N5 (B-H-N). Simply N5 discard the packets instead of forwarding to N14.

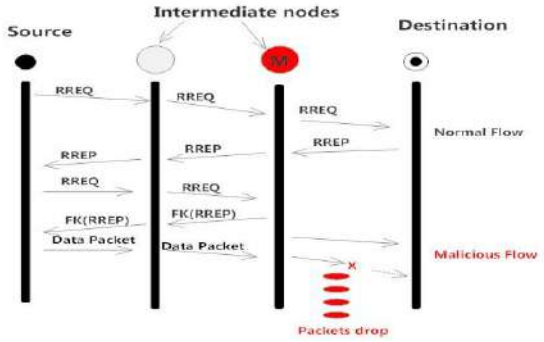

Fig-3 Sequence diagram of Black-Hole node

II.RELATED WORK

Many solutions have been presented with different techniques to solve the Black-Hole Attack in MANET which are discussed in this section:

Amol A. Bhosle, Tushar P. Thosar and Snehal Mehatre proposed a Watchdog technique which uses two different tables namely Pending-Packet table (PPT) and Node-Rating table (NRT). Both the tables store the data related with Source-Address (SA), Destination-Address (DA), Next hop-Count (H-Count) and Packet-ID (P-ID). In PPT, initially the packets are placed in the queue and later on it check the

© 2018, IJCSE All Rights Reserved

address of next neighbour and forward to it. NRT holds the data related with drop packets. In order to detect Black-Hole node, the watchdog technique uses the ratio between Packets delivered and Packets drop. If the ratio is above the Threshold value (TH) then it is assumed that node as a Black-Hole-Node [7].

BDSR scheme for DSR based MANET was proposed by Po-Chun Tsou, Jian-Ming Chang, Yi-Hsuan Lin, HanChieh Chao and Jiann-Liang Chen, which is based on Dynamic Source Routing. It uses Virtual-Address to make sure that Black-Hole node must send RREP when source node delivers RREQ [8].

Raj and Swadas presented a technique that compares the Sequence-number (SN) with Threshold updated value. If the SN>THV then the neighbour node is considered as malicious and this node is send to black list [9].

Lalit and L. Himral, V. Vig, and N. Chand, presented a method to prevent intruder node by checking the First RREP received from neighbour. If the Sequence-Number (SN) of neighbours node is much greater than the SN of Source node then it is assumed as Black-Hole node and the entry will be erased from the Routing Table [10].

Helio Mendes Salmon et al. presented a method based on Artificial-Immune System for Intrusion Detection. This method shows the results with Low-Positive value and increases efficiency of system but the Total End-End-delay is also increased [11].

Sanjay K. Dhurandher , Isaac Woungang , Raveena Mathur , Prashant Khurana proposed a GAODV Protocol which is based on Acknowledgement packets (RREP) send by neighbours to source for detecting Black hole attack. The technique shows that Data-Delivery ratio is improved compared to original AODV [12].

Rutvji proposed an approach to mitigate Black-Hole and Gray-Hole attacks. They have modified the name of previous Algorithm known as R-AODV to MR-AODV and even they have removed the limitastions from R-AODV. During Discovery phase they could able to separate Black-Hole and Gray-Hole nodes and establish a new secure path to deliver data. MR-AODV is a reliable solution configured with multiple simulation parameters that increases the Packet Delivery Ratio and acceptable Average End-End-Delay [13]. Murugan et.al presented a method which uses cluster technique and cryptography to detect Black-Hole attack. It provides better security using Secret-key and Threshold-Cryptography with in the network [14]. Michiardi and Molva proposed a Core scheme in which every node calculate a reputation value for every neighbour, based on watchdog scheme [15]. The Black-Hole attack effects on the overall performance of MANET. Its simulation is carried out in OPNET [16].

III. METHODOLOGY

This section explains an Algorithm of MDB-MAN with comments as shown below in green text.

Assume [S0: Source, Ni may be any intermediate node, RREQ: Route Request Packet, RREP: Route Reply Packet, TL=Time to live, mxt: maximum Threshold, PSA: Packet Source Address, FL: False Route, DP: Data Packet].

---

1. Procedure Black_Hole( )
2. h_count=0; //hop count is initialized to Zero
3. for i = 1 to N // 1,2,3,….N number of neighbors
4. S0:Broadcast PREQ // Send PREQ simultaneously
   //to all neighbors
5. Ni ← PREQ // Neighbors receive PREQ
6. if ($Ni_{(Addr)}$ = = PSA) /* Check if there is an entry of source and destination Address in Routing table of neighbor. */
   S0 ←Ni (FL[RREP]) /* Black-Hole node(N5) generate False RREP & send to source */
   else
   Ni+1← RREQ /* Otherwise; RREQ is appended to another neighbor. */
   end if
7. Ni ← S0[DP] /* Source send Data Packet to Malicious node and it will drop packets. */
8. If (RREQ = = TRUE && (hop_count=TL)
   Display “Drop Packets” // Drop packets
   else
   hop_count - = hop_count /* hop count is decremented by one. */
   Display “Forward Packets” // Forward packets to other node. */
   end if
9. Ni-1 ← RREP
   If (hop_count > mxt) /* Check whether hop count is greater than maximum threshold value. */
   Display “Dangerous: Black Hole Node”
   else
   Display “Normal Node”
   end if
10. All routes to Black-Hole node are blocked
    end for loop
    end Black-Hole Procedure

© 2018, IJCSE All Rights Reserved

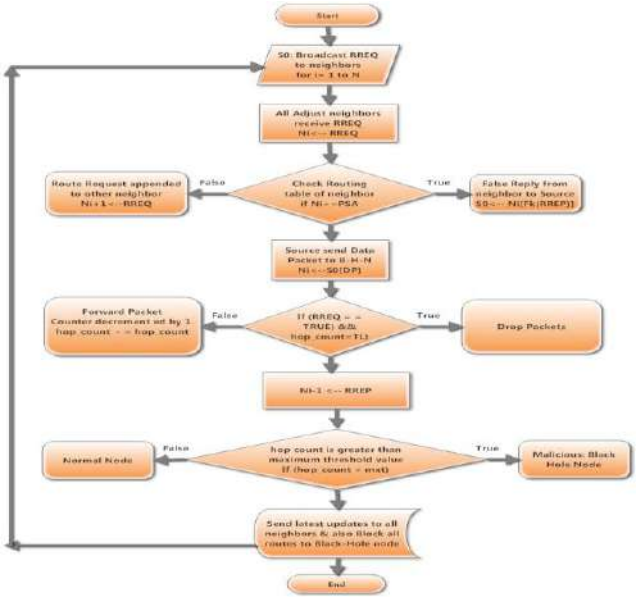

Fig-4 Flow chart of MDB-MAN

1V. SIMULATION

Simulation of MDB-MAN for adding Black-Hole node can be done with the following Steps:

1. Install ns-allinone package under Ubuntu Operating system.
2. Under Aodv.h & Aodv.cc add Black-Hole (malicious) agents.

Under Aodv.h add the following code:

bool BHN_malicious;

a) Under Aodv.cc add the following code to the constructor of Aodv class:

BHN_malicious = false;

b) Goto Aodv::command( ) class, add the following code:

If(Strcmp(argv[1], "BHN_malicious") = = 0)

{

BHN_malicious = true;

return TCL_OK;

}

c) Goto AODV: rt_resolve(packet *) class, add the following code:

#define DROP_MALICIOUS "BHN_malicious"

If (BHN_malicious = = true)

{

drop (p, DROP_BHN_malicious);

d) Goto project and clean

3. Initial route is assumed as **N0→N8→N9→N10→N14** where N0: Source node, N14: Destination node and N8, N9, N10 are Intermediate nodes.
4. Configure Black-Hole node in TCL Script (N6 is Black-Hole node for our network) with the following code:

$ ns at 0.0 "[N6 set ragent _] BHN_malicious"
$ ns color brown
$ns at 0.0 "$N6 label BHN_malicious"

V. RESULTS AND DISCUSSION

The simulation of our solution is done under NS-2.35. The Black-Hole node in our network either drops the packet or play with in the network to forward packets to another malicious node, which may degrade the overall performance of system. To resolve this issue, we have combined some functionality of our solution into AODV protocol. The proposed technique identify and detects the Black-Hole node and broadcast information to all neighbours to delete its entry from their routing tables and block all further packet transmission. The following Fig-5 is the Screenshots of simulation and table-1 shows the simulation parameters.

Fig-5 Screenshots of Simulation

V.I. Metrics for Simulation

Packet Delivery Ratio (PDR): The ratio of total of received packets to the total of send packets. If we want to have the optimal performance of network then we need to have high PDR. It is calculated by the following equation.

$$PDR(MDB) = (\sum packets\ Received / \sum Pakets\ send) * 100 \quad \text{--- (1)}$$

Throughput: The total number of bits delivered/sec.

The unit of throughput is in Kbps.

$$Throughput(MDB) = Receive\ Line * (End\ time - Start\ time) * (\frac{8}{1000})$$

© 2018, IJCSE All Rights Reserved

--- (2)

Packet Drop Ratio: It is the difference between Packets send & Packets received divided by packets send.

$$Packet - Drop - Ratio(MDB) = (Send\ Line - Received\ Line / Send\ Line) * 100$$

--- (3)

Table-1: AODV Data

Time (msec)	Packet Send	Packet Received	PDR (%) AODV	P_Drop_Ratio (%) AODV	Throughput (Kbps) AODV
10	1188	1090	91.75	8.25	597.64
20	3579	3454	96.5	3.49	808.51
30	6625	6500	98.11	1.89	965.85
40	9635	9510	98.7	1.3	1036.01
50	12655	12530	99.01	0.99	1078.44
60	15684	15559	99.2	0.8	1068.67

Table-2: MDB-MAN Data

Time (msec)	Packet Send	Packet Received	PDR (%) MDB-MAN	P_Drop_Ratio (%) MDB-MAN	Throughput (Kbps) MDB-MAN
10	1188	750	63.45	36.86	413.29
20	3579	2432	67.95	32.04	596.3
30	6625	5212	78.61	21.32	773.84
40	9635	8305	86.19	13.8	904.61
50	12655	11446	90.46	9.55	985.31
60	15684	14027	89.43	10.56	963.41

The Fig- shows that PDR for MDB-MAN is almost similar to AODV protocol at time instant 50 msec. Its keep on changing for rest of the time.

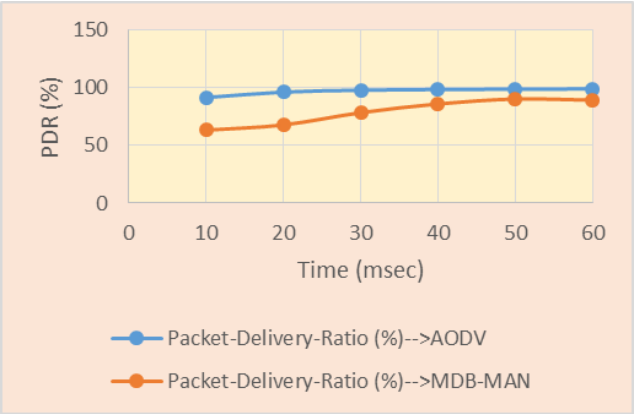

Fig-6: Time Vs Packet Delivery Ratio

Table-3: Simulation Parameters

#No.	Parameters	Items
1.	Software	NS-2
2.	Topology Area Size	850m x 850m
3.	MANET Protocol	AODV
4.	Wireless Standard	IEEE 802.11
5.	Packet Size (Bytes)	512
6.	Total Number of Nodes	15
7.	Number of Malicious Node	1
8.	Simulation Time (msec)	10,20,30,40,50,60
9.	Traffic Pattern	CBR/TCP
10.	Propagation	Two ray ground

The Fig-7 shows that Throughput of MDB-MAN is similar to AODV protocol at time instant 40 and 50 msec.

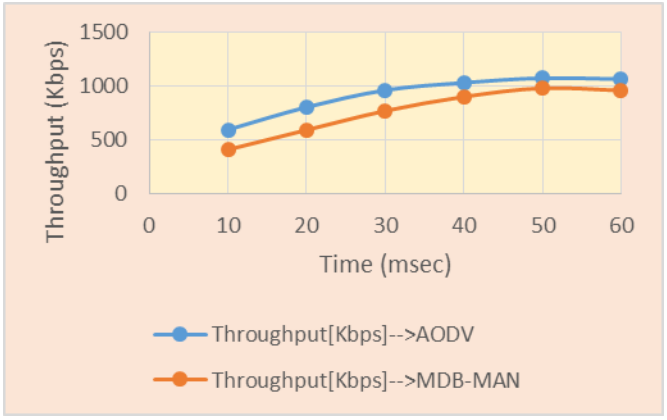

Fig-7: Time Vs Throughput

The Fig-8 shows that Packet-Drop-Ratio of MDB-MAN. It is near to AODV curve at time instant 50 msec. and for rest of the time it keeps on changing.

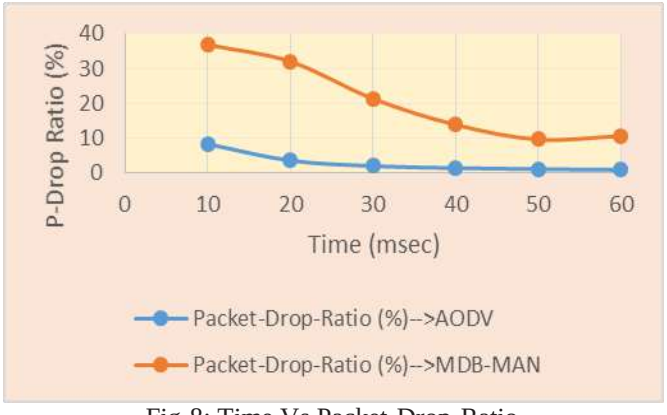

Fig-8: Time Vs Packet-Drop-Ratio

© 2018, IJCSE All Rights Reserved

VI. CONCLUSION

The Wireless mobile Adhoc network is infrastructure–less network and it is subjected to be vulnerable. Hence, security issues arises. The bad behaviour of malicious node would take the advantage of this network and try to attack on it. The proposed MDB-MAN Algorithm identify and detect the Black-Hole node, which is considered as one of danger attack on MANET. Our Simulation results presented are efficient in terms of Packet Delivery Ratio and Throughput, which is almost near to the original value of AODV protocol at time instant 50 msec. The Packet-Drop-Ratio is varied as time changes and it can be tolerable. Therefore, the proposed solution is efficient. In future, our solution could be extended with Clustering of nodes.

REFERENCES

[1] S. Jain, N. Hemrajan, S. Srivastava, "Simulation and Analysis of Performance Parameters for Black Hole and Flooding Attack in MANET Using AODV Protocol", International Journal of Scientific & Technology Research Vol. 2, Issue. 7, pp. 66-69, July 2013.

[2] A. Patel and A. Jain, "A study of various Black Hole Attack techniques and IDS in MANET", International Journal of Advanced Computer Technology, Vol. 4, Issue. 3, pp. 58-62, 2016.

[3] R. Garg, V. Mongia, " Mitigation of Black Hole Attack in Mobile Ad-Hoc Network Using Artificial Intelligence Technique", International Journal of Scientific Research in Computer Science, Engineering and Information Technology , Vol. 3, Issue. 1, pp. 1168-1174, 2018.

[4] S. Muqtar Ahmed and S. Abdul Sattar, "International Journal of Computer Science and Engineering", Vol. 6, Issue. 11, pp. 77-82, 2018.

[5] M. Jahnke, J. T¨olle, S. Lettgen, M. Bussmann, and U. Weddige, "A Robust SNMP Based Infrastructure for Intrusion Detection and Response in Tactical MANETs", Springer-Verlag Berlin Heidelberg, pp. 164–180, 2006.

[6] I. Saada, M. Z. Rashad, R. H. Sakr, "Implementing and Comparing LIDBPP (Local Intrusion Detection by Bluff Probe Packet)", International Journal of Computer Science and Network Security, Vol.16 Issue.8, pp. 20-24, August 2016.

[7] A. A. Bhosle, T. P. Thosar and S. Mehatre, "Black-Holeand Wormhole Attack in Routing Protocol AODV in MAN", International Journal of Computer Science, Engineering and Applications, Vol. 2, No.1, February 2012.

[8] P.C. TSOU, J. Ming CHANG, Y.Hsuan LIN, H.Chieh CHAO, J. Liang CHEN, "Developing a BDSR Scheme to Avoid Black Hole Attack Based on Proactive and Reactive Architecture in MANETs", 13th International Conference on Advanced Communication Technology, ICAC-2011.

[9] P. N. Raj and P. B. Swadas, "DPRAODV: A dyanamic learning system against black hole attack in aodv based manet", IJCSI International Journal of Computer Science Issues, vol. 2, pp. 54–59, 2009.

[10]. L. Himral, V. Vig, and N. Chand, "Preventing Aodv Routing Protocol From Black Hole Attack", International Journal of Engineering Science and Technology (IJEST), Vol .3, 2011.

[11]. H. M. Salmon, C. M. d. Farias, P. Loureiro, L. Pirmez, "Intrusion Detection System for Wireless Sensor Networks Using Danger Theory Immune-Inspired Techniques", International Journal of Wireless Information Networks, Vol. 20, Issue.1, pp. 39-66, 2013.

[12] S. K. Dhurandher, I. Woungang , R. Mathur , P. Khurana, "GAODV: A Modified AODV Against Single and Collaborative Black Hole Attacks in MANETs", 27th International Conference on Advanced Information Networking and Applications Workshops, 2013.

[13] Rutvij, H.J., "MR-AODV: A solution to mitigate black hole and gray hole attacks in AODV based MANETs. Pro", 3rd International Conference on Advanced Computing and Communication Technologies, CCT-2013.

[14] R. Murugan, A. Shanmugam, "Cluster Based Node Misbehaviour Detection, Isolation and Authentication Using Threshold Cryptography in Mobile Ad Hoc Networks", International Journal of Computer Science and Security 3 Vol. 6; Issue. 3; Start page: 188, 2012.

[15] U. K. Singh, J. Patidar and K. C. Phuleriya, "On Mechanism to Prevent Cooperative Black Hole Attack in Mobile Ad Hoc Networks", International Journal of Scientific Research in Computer Science & Engineering", Volume-3, Issue-1, pp. 11-16, 2015.

[16] P K. Sharma, S. Mewada and P. Nigam, "Investigation Based Performance of Black and Gray Hole Attack in Mobile Ad-Hoc Network", International Journal of Scientific Research in Network Security and Communication, Vol.1, Issue. 4, pp. 8-11, 2013.

Author's Prifile

Syed Muqtar Ahmed is pursuing Ph.D. in Computer Science & Engineering, from Rayalaseema University, Kurnool, Andhra Pradesh, India. He is having 20 years of teaching experience. Worked as Assistant, Associate Professor and Head of CSE department at Deccan College of Engineering & Technology, Hyderabad, India from 1997-2008. He also worked as a faculty at Nizwa College of Technology, Sultanate of Oman from 2008-2009. He received M.Tech in Information Technology in 2003 and B.E in Computer Science & Engineering in 1997. Recently published articles in Intrusion detection system and also an author of Textbook Title: 'Data Communication and Networking', Sure Series, Hyderabad, India. His area of research is Data Communication, Wireless Network and Network Security.

Dr. Syed Abdul Sattar is a Professor, Director (R&D) at Nawab Shah Alam College of Engineering and Technology, Hyderabad, India. He had received national award as Young Scientist in year 2006 with a Gold medal from NESA New Delhi. He obtained his first Ph.D. in CSE from GSU USA in 2004 on WLAN's Efficiency and Second Ph.D. in ECE from JNTU, Hyderabad on WLAN security in year 2006. He passed Bachelors of Engineering in 1990 and obtained Master's in 2002. His publications are more than 170 in National and International Journals like IEEE, ELSEVIER and SPRINGER etc. He has guided 17 Ph.D. scholars so far and more than 20 are in pipeline. His area of Research is in Wireless communication and Image processing.

© 2018, IJCSE All Rights Reserved

NETWORK SECURITY BASED ON CHAOTIC MAPS BASED AUTHENTICATION IN VANETS

Muqtadir
Research Scholar computer science engineering Rayalaseema University
PP. COMP SCI&ENGG. 0384
Kurnool,Andhra Pradesh,India.
.
Dr. Syed Abdul Sattar
Director R & D,
Nawab Shah Alam Khan College of Engg. & Tech. (NSAKCET),
Hyderabad
. Telangana, India

Abstract: -
With an emergence of applications of Mobile Ad-hoc Networks in several areas, vehicular ad-hoc networks are constantly evolving for traffic monitoring, reducing accidents and various other applications. However, these networks are vulnerable towards malicious nodes, which might send false signals leading towards accidents causing human life and financial losses. Thus, vehicular ad-hoc networks require a faultless security approach to protect the network environment from security threats. Recently, various security methods were developed to address the security threats through cryptography. However, security methods must cause minimum overhead with respect to delay and computation, as VANET is a delay sensitive network. To assign security in any communication medium, authenticated key agreement is a precondition. Authenticated key agreement is a procedure of authenticating communicating devises by providing session keys between them. Thus, in this paper, we design a password based light weight authenticated key agreement between communicating nodes with the help of Chaotic Maps. We compare our method with RSA based authenticated key agreement protocols. Performance results shows that proposed work time complexity is less in comparison with RSA based authenticated key agreement protocols.

Key words :- Vehicular Ad-hoc Networks, authentication, security and chaotic maps.

Introduction

Vehicular Ad-hoc Networks [2] (particularly termed as VANETs) are based on the principles of Mobile Ad-hoc Networks (MANETs). These networks are particularly used to relay the information among vehicles to facilitate vehicular communications. This inter-vehicular communication aids roadside navigation, traffic monitoring, vehicular safety and other services [3]. Each vehicle establishes its data such as time, location, speed and direction at every 300ms. The data is processed between vehicles, RSUs (Road Side Units) and DMV (Department of Motor Vehicle) [4].

Generally, the vehicular information is transmitted to the other vehicles and RSUs in range. RSUs are deployed at particular distances and act as an access point to the vehicles. They send the vehicular information towards the DMV (Department of Motor Vehicles).

A VANET infrastructure has heterogeneous configuration similar to Mobile Ad-hoc Networks, where each node acts as a router and a host. It is mainly comprised of three components i.e., Vehicles, RSUs (Road Side Units) and DMV (Department of Motor Vehicles). The information is shared between these three components to keep the connection intact and secure. This network uses a radio frequency range of 5.9 GHZ based on 802.11p IEEE standard for wireless transmission.

Vehicles: The vehicles are individual nodes recorded at a centralized Department of Motor Vehicles. They share their information such as location, time and velocity with the other nodes. The vehicles are deployed with On-board units and GPS devices to connect and share the data

using 802.11p IEEE spectrum. Vehicular nodes might be either benign or malicious depending on their characteristics and activities.

RSUs (Road Side Units): These are deployed as a Wireless Access Point (AP) at a specified range on intersection such as parking lot entrance and bus stations. It works on 802.11p IEEE and provides access to the vehicles in range. RSUs check the authenticity of vehicular information and report any malicious activity to the Department of Motor Vehicles. However, RSUs are vulnerable to attacks since these are components of a heterogeneous network. Attacks on RSBs can cause severe losses since the attackers can compromise multiple vehicles in range.

DMV (Department of Motor Vehicles): DMV is a centralized authority, which monitors the vehicular records such as registrations. DMV acts as a Trusted Authority as it cannot be manipulated by a malicious node or an attacker. However, excessive transmission between DMV and vehicles can cause congestion.

Transmission of Data: At a specified interval or occurrence of particular event, vehicles broadcast their information towards the other vehicles in range and RSUs. The data includes the time t, location l and event type e along with vehicular identity i. Broadcast takes place in a predetermined interval or a specific event such that $i = (t, l, e)$. Each vehicle has its own identity as registered at Department of Motor Vehicles. The architecture of VANET is shown in figure 1.

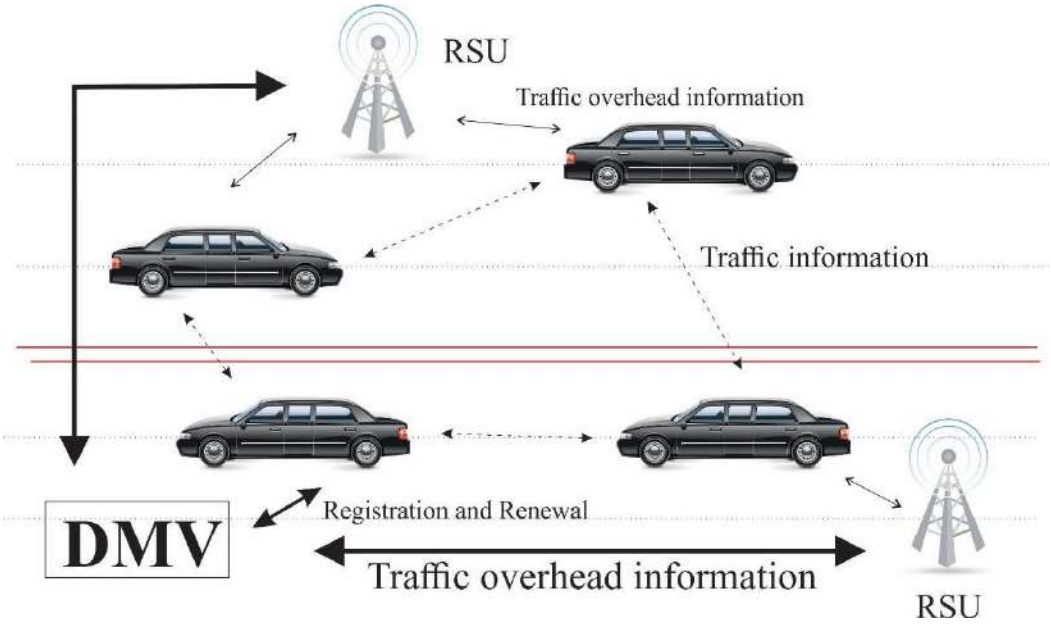

Figure 1:- Architecture of vehicular ad hoc network

VANETs use heterogeneous configuration, where each node acts as a router as well as a host. This makes communication easier between the nodes. However, it also leaves VANETs more vulnerable to threats and attacks. An attacker can be either among the nodes having access to the information or an intruder from an outside source.

The primary functions of VANETs are to prevent vehicular accidents and unnecessary traffic jams by exchanging the messages between the vehicles. VANETs also help in applications such as altering routes and avoiding collision. Due to their heterogeneity, VANETs are prone towards all the security threats affecting wireless networks. However, the security measures are different in comparison with the other wireless networks.

Some types of attacks include false information, Denial of Service (DoS), replaying events, worm hole attacks, disclosure of identity, altering messages, compromising RSB and so on.

These attacks cause severe traffic issues and accidents making human life more prone towards casualties.

Privacy must also be emphasized along with security as an intruder can have further advantage if all the vehicular information is revealed. This paper addresses various types of attacks majorly found in wireless networks.

VANETs incur various types of attacks [5] that are prominent in wireless network. These attacks are assumed according to the vulnerabilities in VANETs and the intentions of attackers. Attackers can either be among the vehicular nodes or outsiders intruding the network by compromising RSUs or other vehicles.

Vehicular Data Manipulation: An attacker collects the vehicular data from a transmitting node, modifies the information and forwards to the other nodes.

False Sensor Information: An attacker broadcasts false information to the nodes in a range to affect the behavior of drivers in order to cause accidents.

Replaying Packets: In this case, an attacker collects an event from the other nodes and replays the same in different locations and timestamps.

Denial of Service (DoS) attacks: These are severe types of attacks where an attacker causes congestion in central mediums such as RSUs. They proceed their attacks on the other nodes by averting the access to the medium.

Distributed Denial of Service (DDoS) attacks: These attacks are more severe than DoS attacks where an attacker uses several vehicular identities and sends the messages from different timestamps and locations.

Mimicking Nodes: In this case, an attacker uses the identity of other nodes to mask and sends the wrong information on behalf of those nodes.

Delay in Messages: An attacker adds timestamp to an original message such that it causes delay in receiving of message.

Sybil Attacks: In these attacks, an attacker uses an identity of different vehicles and sends multiple messages to the nodes.

Providing security and mitigation attacks in VANET is a vital issue. In order to incorporate security in any network environment easy and simple way is to provide mutual authentication [1] between communicating nodes/ devices. Thus in this paper we design the light weight password based authenticated key agreement between communicating nodes. The detail discussion of proposed protocol is available in following sections.

Mitigation of Malicious Attacks on VANETs using Chaotic Maps

Various malicious attacks can be prevented by recognizing the behavior and activity of an attacker. The types of attacks and intentions of attackers were assumed from the related work based on security of Wireless Networks.

Most of the attacks can be caused by disclosure of vehicular identities and messages. Since the messages between the nodes are sent in a plaintext form, attackers can easily manipulate the information once they intrude the network. To prevent these attacks, authenticated key agreement is helpful where messages between the source and the destination are encrypted. This work is based on chaotic maps based authenticated key agreement. In this scheme, each node requires a password to send messages to the other nodes.

Initially we computed the time complexity of chaotic map based and modular arithmetic based Diffie Hellman key exchange problem. The Sequence of steps for chaotic map based based Diffie Hellman key exchange problem as follows.

1. The Source and The Destination agree upon a specific Prime number, let X.
2. The Source computes the value of $T_n(X)$ using the following equation, by considering a large prime number 'n'.

$T_n(X)$ =2 *X*$T_{n-1}(X)$ - $T_{n-2}(X)$

3. The Source sends the computed value $T_n(X)$ towards the destination.
4. The destination in turn computes the value of $T_m(X)$ using the following equation, by considering a big prime number 'm'.

$T_m(X)$ =2 *X*$T_{m-1}(X)$ - $T_{m-2}(X)$

5. Then the destination sends the computed $T_m(X)$ value towards source node.
6. Further, the destination computes the value of $T_{mn}(X)$, with the help of a received value by the following equation.

$$T_{mn}(X) = T_m\big(T_n(X)\big)$$

7. Then, it sends the computed $T_{mn}(X)$ value back to the source node.
8. Source node validates the received value $T_{mn}(X)$ by calculating the value of $T_{nm}(X)$ by following equation.

$$T_{nm}(X) = T_n\big(T_m(X)\big)$$

Secondly we computed the time complexity of modular arithmetic [8] based Diffie Hellman key exchange problem. The Sequence of steps for modular arithmetic based Diffie Hellman key exchange problem as follows.

1. The Source and The Destination agree upon two big prime numbers i.e., P, N.
2. The Source computes the value 'J' using below equation by selecting a prime number 'A'

$$J = N^A \ mod \ P$$

3. The Source sends the value J towards the destination node.
4. The destination node computes the value 'K' using the following equation by selecting a prime number 'B'.

$$K = N^A \ mod \ P$$

5. Destination send the value J towards the source node.
6. Now, the source computes the value $K^A \ mod \ P$.
7. The destination also computes the value of $J^B \ mod \ P$.
8. The values calculated by the source as well as the destination are ensured to match.

Performance analysis of RSA and Chaotic Maps based Diffie Hellman key exchange Problem in a static identical condition

The performance of RSA [7] and Chaotic maps [6] based authenticated key agreement is evaluated based on static identical states. For performance evaluation, network simulator NS2.35 [9] is used. The hardware specifications comprised a Hard Disk of 160 Gigabytes capacity, DDR2 SDRAM with 2GB memory and clock rate of 667MHz, Dual Core 2.33 GHz processor with 2MB Cache. The computation time is evaluated for each algorithm in identical conditions. Results are shown in figure 2 and 3.

The results demonstrate that the computation time taken by Chaotic Maps is far less in comparison with RSA based authentication. Furthermore, reduction of computational time increases the network performance, occupies less buffer and consumes less energy. Chaotic maps induced less overhead on VANETs in comparison with RSA.

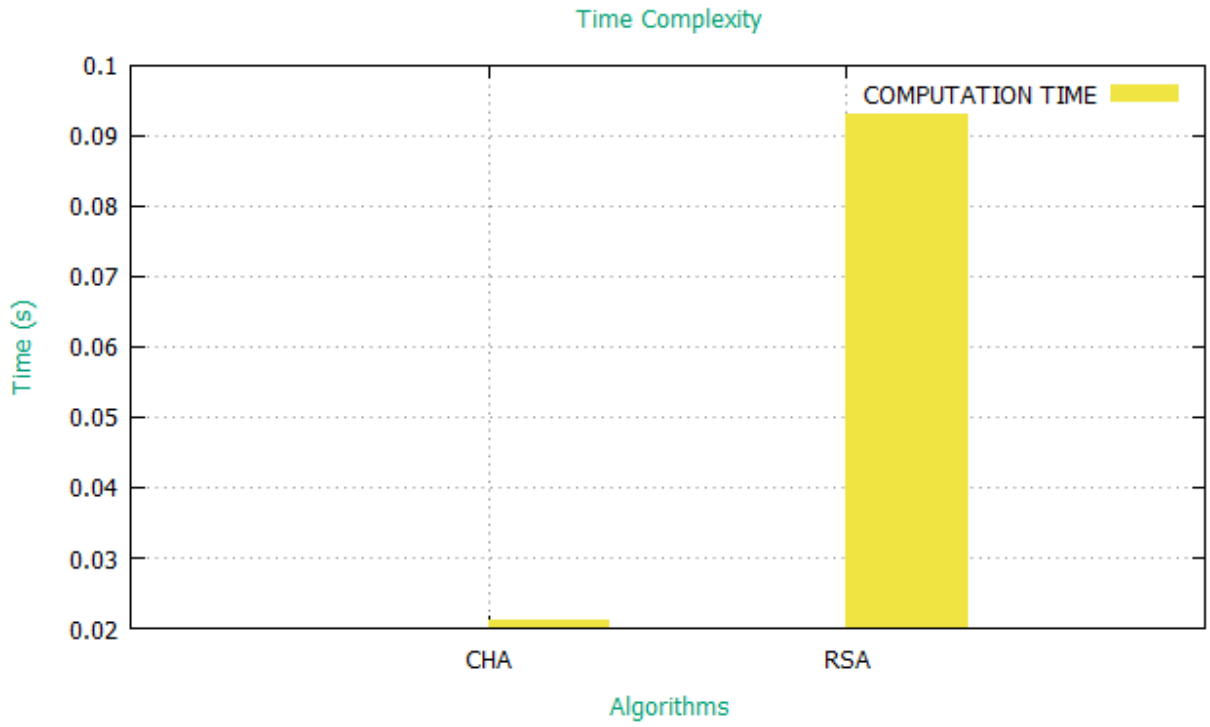

Figure 2 :- Comparison of RSA and Chaotic maps in static identical environment

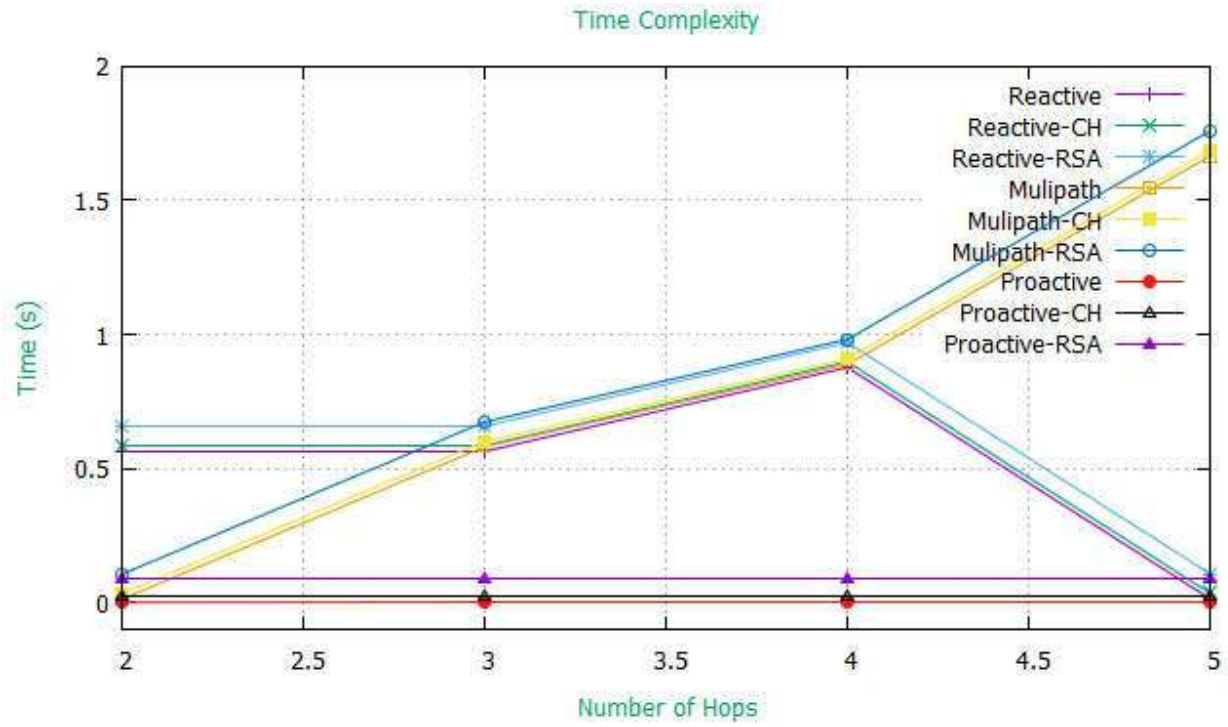

Figure 3:- Comparison of RSA and Chaotic maps in dynamic identical environment

Proposed password based Authenticated key agreement based on Chaotic maps

Proposed algorithm, i.e., password Authenticated key agreement based on Chaotic maps between two vehicles are explained as follows

1. The Source and The Destination agree vehicles upon a specific Prime number, let X.
2. The Source vehicle computes the value of $T_n(X)$ using the following equation, by considering a large prime number 'n'.

$T_n(X)$ =2 *X*$T_{n-1}(X)$ - $T_{n-2}(X)$

3. The Source select a password and compute the following value

$$Tuple = (T_n(X) \,||\, ID_s \,||\, ID_D \,||\, Password)$$

4. Source vehicle calculate the hash value of tuple

5. $Digest = H(T_n(X) \,||\, ID_s \,||\, ID_D \,||\, Password)$
6. The source sends the $\{T_n(X),\ Password,\ Digest\ \}$ towards the destination.
7. The destination in turn computes the value of $T_m(X)$ using the following equation, by considering a big prime number 'm'.

$T_m(X)$ =2 *X*$T_{m-1}(X)$ - $T_{m-2}(X)$

8. The destination select a password and compute the following value

$$Tuple = (T_m(X) \,||\, ID_s \,||\, ID_D \,||\, Password)$$

9. Destination vehicle calculate the hash value of tuple
10. $Digest = H(T_m(X) \,||\, ID_s \,||\, ID_D \,||\, Password)$
11. The destination sends the $\{T_m(X),\ Password,\ Digest\ \}$ towards the destination.
12. Further, the destination computes the value of $T_{mn}(X)$, with the help of a received value by the following equation.

$$T_{mn}(X) = T_m\big(T_n(X)\big)$$

13. Then, it sends the computed $T_{mn}(X)$ value back to the source node.
14. Source node validates the received value $T_{mn}(X)$ by calculating the value of $T_{nm}(X)$ by following equation.

$$T_{nm}(X) = T_n\big(T_m(X)\big)$$

In the above algorithm source and destination vehicles are validate the received values by comparing the received digest values.

Conclusion:

VANETs use heterogeneous infrastructure based on MANETs, which leaves VANETs more vulnerable to security issues. To prevent these issues, a chaotic maps based algorithm is

used based on Public Key Cryptography. This digested the messages sent between the nodes and thereby prevents attackers using chaos method. The Chaotic Maps based algorithm has been compared with RSA based algorithm in an identical environment, which concludes that Chaotic Maps based encryption induces less overhead when compared to RSA based encryption. Moreover, Chaotic Maps is a lightweight algorithm causing less consumption of memory, bandwidth and energy, which prevents congestion due to overhead. Hence, this paper concludes that Chaotic Maps based authentication is a lightweight and strong cryptographic technique to prevent security holes in VANETs.

References

1. Memon, I., 2015. A secure and efficient communication scheme with authenticated key establishment protocol for road networks. *Wireless Personal Communications*, *85*(3), pp.1167-1191.
2. Mukherjee, J.C., Agarwal, S. and Gupta, A., 2014, May. Distributed event notification in VANET with multiple service providers. In *Proceedings of the 8th ACM International Conference on Distributed Event-Based Systems* (pp. 334-337). ACM.
3. Chen, Z., Liu, Y., Wong, R.C.W., Xiong, J., Mai, G. and Long, C., 2014, June. Efficient algorithms for optimal location queries in road networks. In *Proceedings of the 2014 ACM SIGMOD international conference on Management of data* (pp. 123-134). ACM.
4. Wang, Y. and Li, F., 2009. Vehicular ad hoc networks. In *Guide to wireless ad hoc networks* (pp. 503-525). Springer, London.
5. Al-Kahtani, M.S., 2012, December. Survey on security attacks in Vehicular Ad hoc Networks (VANETs). In *Signal Processing and Communication Systems (ICSPCS), 2012 6th International Conference on* (pp. 1-9). IEEE.

6. Mohammad, A.A.K., Mirza, A. and Vemuru, S., 2016. Cluster based mutual authenticated key agreement based on chaotic maps for mobile ad hoc networks. *Indian Journal of Science and Technology*, *9*(26).
7. Eissa, T., Razak, S.A. and Ngadi, M.D., 2011. Towards providing a new lightweight authentication and encryption scheme for MANET. *Wireless Networks*, *17*(4), pp.833-842.
8. Ovshinsky, S.R. and Pashmakov, B., Energy Conversion Devices Inc, 2004. *Methods of factoring and modular arithmetic*. U.S. Patent 6,714,954.
9. Issariyakul, T. and Hossain, E., 2012. Introduction to Network Simulator 2 (NS2). In *Introduction to Network Simulator NS2* (pp. 21-40). Springer, Boston, MA.

A COMPARATIVE STUDY ON PUSHOVER ANALYSIS WITH LINEAR STATIC ANALYSIS OF INDUSTRIAL STEEL STRUCTURE SUBJECTED TO GRAVITY LOADS AND DYNAMIC LOADS

Mohd Abdul Atif Sulaiman[1], Shaik Mohammed Javid[2] Syed farrukh Anwar[3]

[1] Pg Student, M.tech in Structural engineering, Department of Civil Engineering, Nawab Shah Alam Khan College of Engineering and Technology, Hyderabad, Telangana 500024

[2] Assistant Professor, M.tech in Structural engineering, Department of Civil Engineering, Nawab Shah Alam Khan College of Engineering and Technology, Hyderabad, Telangana 500024

[3] Head of the Department (PHD) , Vice Principal, M.tech in Structural engineering, Department of Civil Engineering, Nawab Shah Alam Khan College of Engineering and Technology, Hyderabad, Telangana 500024

ABSTRACT :Developments in computer hardware and software have made analysis techniques that were formerly too expensive within the reach of most project budgets. Foremost among these has been equivalent static analysis and push over analysis.. This approach defines a series of forces acting on a building to represent the effect of earthquake ground motion, typically defined by a seismic design response spectrum. It assumes that the building responds in its fundamental mode. For this to be true, the building must be low-rise and must not twist significantly when the ground moves. The response is read from a design response spectrum, given the natural frequency of the building.

The applicability of this method is extended in many building codes by applying factors to account for higher buildings with some higher modes, and for low levels of twisting. To account for effects due to "yielding" of the structure, many codes apply modification factors that reduce the design forces (e.g. force reduction factors).

Shaking and ground rupture are the main effects created by earthquakes, mainly resulting damage to buildings and other rigid structures. The severity of the local effects depends on the complex combination of the earthquake magnitude, the distance from the epicenter and the local geological and geomorphologic conditions the ground motion is measured by ground acceleration .An earthquake may cause injury and loss of life, road and bridge damage, general property damage and collapse or destabilization of buildings.

Present work deals with study of seismic analysis and design of Technology Innovation and Industry Relations with different types of bracings V bracings, and X bracings was compared with the bare frame and results are analyzed like story displacements, story shear, bending moment , shear force and building torsion with the help of commercial software like ETABS9.7.4 under the static and pushover analysis.

Keywords: V bracings, X bracings, story displacements, story shear, bending moment building torsion etc.,

I.INTRODUCTION

The primary purpose of all kinds of structural systems used in the building type of structures is to transfer gravity loads effectively. The most common loads resulting from the effect of gravity are dead load, live load and snow load. Besides these vertical

loads, buildings are also subjected to lateral loads caused by wind, blasting or earthquake. Lateral loads can develop high stresses, produce sway movement or cause vibration. Therefore, it is very important for the structure to have sufficient strength against vertical loads together with adequate stiffness to resist lateral forces. Strengthening of structures proves to be a better option catering to the economic considerations and immediate shelter problems rather than replacement of buildings. Moreover it has been often seen that retrofitting of buildings is generally more economical as compared to demolition and reconstruction. Therefore, seismic retrofitting or strengthening of building structures is one of the most important aspects for mitigating seismic hazards especially in earthquake prone areas.

TYPES OF BRACINGS

There are two types of bracing systems

1) Concentric Bracing System

All kinds of the concentrically braced frames used in the seismic rehabilitation including the Cross, Chevron V braced frames, Chevron Inverted-v-braced frames, Zipper column rehabilitated Invertedv- braced frames. Axial forces including tension and compression in concentrically braced frames are regarded as Displacement control. Columns in compression are Force control (buckling of columns is critical) and in tension are displacement control.

K BRACINGS

The full diagonal bracing is not used in areas where a passage is required. In such cases, k-bracings are preferred over diagonal bracing because there is a room to provide opening for doors and windows etc.

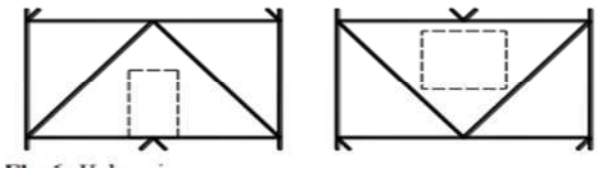

V brace: Bracing where a pair of braces joins at a single point on the beam span. Inverted V braceis that form of chevron bracing that terminates at point on beam from below.

This involves two diagonal members extending from the top two corners of a horizontal member and meeting at a centre point at the lower horizontal member, in the shape of a V. Inverted V-bracing (also known as chevron bracing) involves the two members meeting at a centre point on the upper horizontal member.

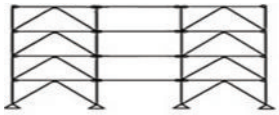

V Bracing

X brace: Bracing where two diagonal braces crosses near mid-length of the bracing members. c) K brace: Bracing where a pair of braces connected on one side of a column joins at a single point on another leg of column.

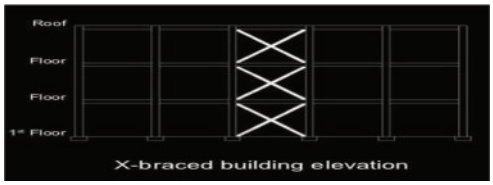

2) Eccentric Bracings

Reduce the lateral stiffness of the system and improve the energy dissipation capacity. The lateral stiffness of the system depends upon the flexural stiffness property of the beams and columns, thus reducing the lateral stiffness of the frame. The vertical component of the bracing forces due to earthquake causes lateral concentrated load on the beams at the point of connection of the eccentric bracing.

Eccentric bracing consists of diagonal braces located in the plane of the frame where one or both ends of the brace do not join at the end points of other framing members. The system essentially combines the features of a moment frame and a concentrically braced frame, while minimising the disadvantages of each system.

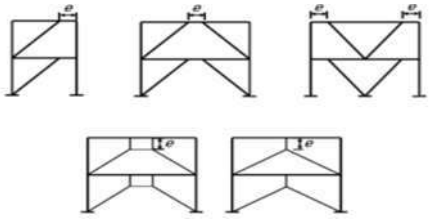

Types of eccentrically braced frames depending on the location of the link beam

OBJECTIVE OF THE STUDY

I. To understand the elastic and plastic behavior of the STEEL BUILDING building under gravity loads taken as per IS 875-1987

II. To compare the steel building with different types of bracings like X bracings and V bracings are compared with the BARE framed building .

III. To compare various parametric results such as Storey drift and Storey forces for the different models considered.

IV. To obtain pushover curves both in X and Y directions using FEM based analytical software ETABS 9.7.4.

V. To compare various parametric results such as Storey shear and column forces and beam forces for the different models considered

II.LITERATURE REVIEW

Dr. S.V. Itti[1], Prof. AbhishekPathade[2] and Ramesh B. Karadi[3] et all,.(2006) This study focuses on the comparison of the Indian Code (IS) and International Building Codes (IBC) in relation to the seismic design and analysis of Ordinary RC moment resisting frame (OMRF), Intermediate RC moment-resisting frame (IMRF) and Special RC moment-resting frame (SMRF). The analytical results of the model buildings are then compared and analyzed taking note of any significant differences. This study explores variations in the results obtained using the two codes, particularly design base shear, lateral loads, drifts and area of steel for structural members for all RC buildings in both the codes. The discussion in this study will be confined to monolithically cast reinforced concrete buildings. Specific provisions for design of seismic resistant reinforced members are presented in detail. Provisions of Indian and International Buildings Codes are identified. Target deflection of the building is achieved at a lower lateral force in SMRF IBC i.e, the concept of lesser force and more deflection is followed. However in OMRF, IMRF and SMRF of Indian Code lateral force applied in higher as a result the deflection on the top of the building exceeds the target deflection.

F. Zareian[1], D. G. Lignos[2] and H. Krawinkler[3] et all,. (2010) This paper summarizes a study focused on evaluating the design modification factors (i.e., R, Cd, Ω) for Steel Special Moment-resisting Frames (SSMFs) by application of the FEMA P695 methodology. In this study, archetype design that comprise 3-bay special SMFs that serve as lateral load resisting system of steel buildings ranging from 1 to 20 stories are designed using ASCE 7-05 and AISC 341-05design provisions. Nonlinear models are developed using latest advances in structural component modeling. Parameters for these models are extracted from a steel component database for modeling of component deterioration. The numerical models are analyzed to predict the collapse capacities of each design, and the adjusted collapse margin ratios (ACMR) are evaluated and compared to acceptance criteria.

III.METHODOLOGY

Building frame with the following geometrical types are considered for analysis in seismic zone (Zone V) for seismic and gravity loading in each case. And also the terrain category (terrain category 3 are also studied on the each case.

- PUSH OVER ANALYSIS

CASE-1: G+17building frame without bracing system (Bare Frame).

CASE-2: G+17 building frame with X bracing system.

CASE-3: G+17 building frame with V bracing system.

- EQUVALENT STATIC ANALYSIS

CASE-1: G+17building frame without bracing system (Bare Frame).

CASE-2: G+17 building frame with X bracing system.

CASE-3: G+17 building frame with V bracing system.

Push over analysis:

Pushover analysis is an approximate analysis method in which the structure is subjected to monotonically increasing lateral forces with an invariant height-wise distribution until a target displacement is reached. Pushover analysis consists of a series of sequential elastic analysis, superimposed to approximate a force-displacement curve of the overall structure. A two or three dimensional model which includes bilinear or trilinear load-deformation diagrams of all lateral force resisting elements is first created and gravity loads are applied initially. A predefined lateral load pattern which is distributed along the building height is then applied. The lateral forces are increased until some members yield. The structural model is modified to account for the reduced stiffness of yielded members and lateral forces are again increased until additional members yield. The process is continued until a control displacement at the top of building reaches a certain level of deformation or structure becomes unstable.

Pushover is a static-nonlinear analysis method where a structure is subjected to gravity loading and a monotonic displacement-controlled lateral load pattern which continuously increases through elastic and inelastic behavior until an ultimate condition is reached. Lateral load may represent the range of base shear induced by earthquake loading, and its configuration may be proportional to the distribution of mass along building height, mode shapes, or another practical means.

Output generates a static-pushover curve which plots a strength-based parameter against deflection. For example, performance may relate the strength level achieved in certain members to the lateral displacement at the top of the structure, or bending moment may be plotted against plastic rotation. Results provide insight into the ductile capacity of the structural system, and indicate the mechanism, load level, and deflection at which failure occurs.

When analyzing frame objects, material nonlinearity is assigned to discrete hinge locations where plastic rotation occurs according to FEMA-356 or another set of code-based or user-defined criteria. Strength drop, displacement control, and all other nonlinear software features, including link assignment, P-Delta effect, and staged construction, are available during static-pushover analysis.

EQUVALENT STATIC ANALYSIS

Equivalent Static Analysis:
This approach defines a series of forces acting on building to represent the effect of earthquake ground motion, typically defined by a seismic design response spectrum. It assumes that the building responds in its fundamental mode. For this to be true, the building must be low-rise and must not twist significantly when the ground moves. The response is read from a design response spectrum, given the natural frequency of the building (either calculated or defined by the building code). The applicability of this method is extended in many building codes by applying factors to account for higher buildings with some higher modes, and for low levels of twisting. To account for effects due to “yielding” of the structure, many codes apply modification factors that reduce the design forces (e.g., force reduction factors).

The seismic design of buildings fallows the dynamic nature of the load. But equivalent static analysis would become sufficient for simpler, regular in plan configuration and it will give more efficient results. This analysis will flow in a manner with the calculation of design base shear and its distribution to all storey’s by using the formula given in the code

PROBLEM OF STATEMENT

In building plan was taken in seismic zone V for seismic analysis of the building (G+17) with braced building and unbraced building (general building). The basic specifications of the building are:
Beam Size
= ISMB300
Column size
= ISMB600
Bracings
= ISMB125(BOTH V,X BRACINGS)
Storey Height
= 3.0 mts

Bottom storey
= 3.5 mts
Column spacing
= 5 mts
Materials used
= M25 & Fe415;
Depth of slab
= 150 mm
Unit weight of concrete
= 25 kN/m^3
Code Books used
=IS1893:2002,

1. BARE FRAME

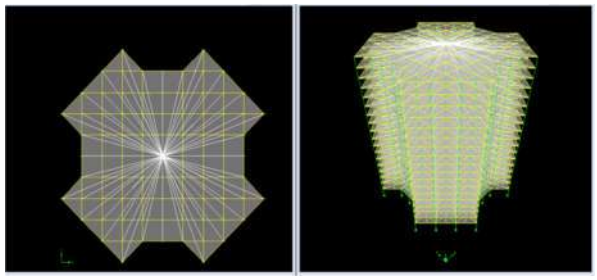

2. V BARCED FRAME BUILDING

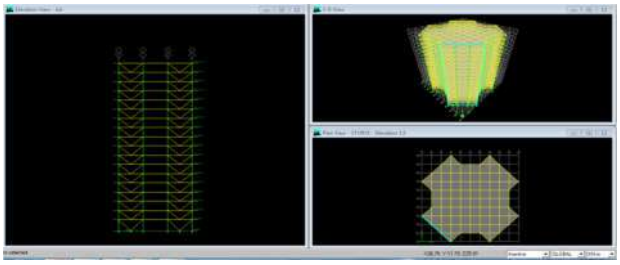

3. X BARCED FRAME BUILDING

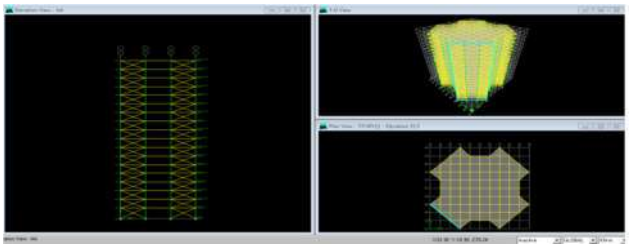

IV. RESULTS AND ANALYSIS
PUSH OVER ANALYSIS

STORY DRIFT IN X DIRECTION

Story	Load	DRIFT X in bare frame	drift x in v push	drift x in x bracing
STORY18	PUSHX	0.00225	0.000963	0.001311
STORY17	PUSHX	0.00289	0.000886	0.001257
STORY16	PUSHX	0.00368	0.000916	0.001259
STORY15	PUSHX	0.00451	0.00093	0.001281
STORY14	PUSHX	0.00535	0.000988	0.001305
STORY13	PUSHX	0.00619	0.001021	0.001328
STORY12	PUSHX	0.00703	0.001051	0.001345
STORY11	PUSHX	0.00788	0.001077	0.001355
STORY10	PUSHX	0.00869	0.001096	0.001357
STORY9	PUSHX	0.00948	0.001109	0.00133
STORY8	PUSHX	0.01021	0.001114	0.001303
STORY7	PUSHX	0.01089	0.001111	0.001303
STORY6	PUSHX	0.01148	0.001096	0.00126
STORY5	PUSHX	0.01192	0.001071	0.0012
STORY4	PUSHX	0.01208	0.001033	0.001123
STORY3	PUSHX	0.0117	0.000991	0.001023
STORY2	PUSHX	0.01017	0.000999	0.000874
STORY1	PUSHX	0.00539	0.001046	0.000574

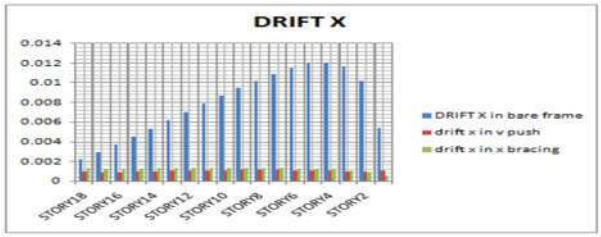

STORY DRIFT IN Y DIRECTION

Story	Load	drift y in bare frame	drift y in v push	drift y in x bracing
STORY18	PUSHY	0.00243	0.000361	0.00114
STORY17	PUSHY	0.00453	0.000613	0.001194
STORY16	PUSHY	0.00641	0.00065	0.001231
STORY15	PUSHY	0.00808	0.000685	0.001254
STORY14	PUSHY	0.00955	0.000729	0.001291
STORY13	PUSHY	0.01083	0.000771	0.001324
STORY12	PUSHY	0.01196	0.00081	0.001346
STORY11	PUSHY	0.01291	0.000844	0.001362
STORY10	PUSHY	0.0137	0.000873	0.001367
STORY9	PUSHY	0.01432	0.000896	0.001363
STORY8	PUSHY	0.01477	0.000912	0.001348
STORY7	PUSHY	0.01505	0.000921	0.00132
STORY6	PUSHY	0.01516	0.00092	0.001278
STORY5	PUSHY	0.01666	0.000911	0.001222
STORY4	PUSHY	0.01851	0.000892	0.00115
STORY3	PUSHY	0.02048	0.000869	0.001063
STORY2	PUSHY	0.02288	0.000879	0.000983
STORY1	PUSHY	0.02601	0.000951	0.000693

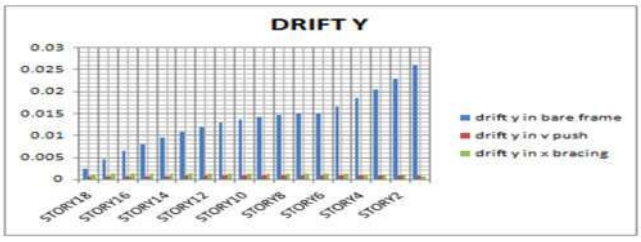

LATERAL FORCES (P)

Story	Load	Loc	p in bare frame	p in v bracing	p in x bracing
STORY18	PUSHX	Bottom	-38417.85	1592.81	5682.61
STORY17	PUSHX	Bottom	-77955.94	3199.44	11415.71
STORY16	PUSHX	Bottom	-117494	4806.1	17148.78
STORY15	PUSHX	Bottom	-157032.1	6412.76	22881.83
STORY14	PUSHX	Bottom	-196570.2	8019.43	28614.87
STORY13	PUSHX	Bottom	-236108.3	9626.1	34347.9
STORY12	PUSHX	Bottom	-275646.4	11232.78	40080.93
STORY11	PUSHX	Bottom	-315184.5	12839.48	45813.98
STORY10	PUSHX	Bottom	-354722.6	14446.18	51547.05
STORY9	PUSHX	Bottom	-394260.7	16052.91	57280.13
STORY8	PUSHX	Bottom	-433798.8	17659.64	63013.24
STORY7	PUSHX	Bottom	-473336.9	19266.39	68746.37
STORY6	PUSHX	Bottom	-512874.9	20873.16	74479.52
STORY5	PUSHX	Bottom	-552413	22479.94	80212.68
STORY4	PUSHX	Bottom	-591951.1	24086.73	85945.85
STORY3	PUSHX	Bottom	-631489.2	25693.53	91679
STORY2	PUSHX	Bottom	-671027.3	27300.3	97412.08
STORY1	PUSHX	Bottom	-710752.1	28907.8	103151.7

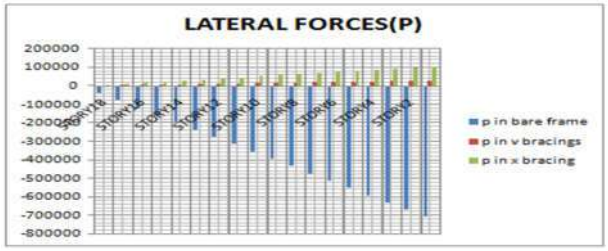

SHEAR FORCE IN X DIRECTION

Story	Load	Loc	vx in bare frame	vx in v push	vx in x bracing
STORY18	PUSHX	Bottom	936	-8.97	-34.44
STORY17	PUSHX	Bottom	1872.06	-19.24	-67.31
STORY16	PUSHX	Bottom	2808.19	-29.23	-100.01
STORY15	PUSHX	Bottom	3744.4	-38.98	-132.56
STORY14	PUSHX	Bottom	4680.7	-48.49	-164.91
STORY13	PUSHX	Bottom	5617.12	-57.75	-197
STORY12	PUSHX	Bottom	6553.74	-66.77	-228.61
STORY11	PUSHX	Bottom	7490.6	-75.58	-260.19
STORY10	PUSHX	Bottom	8427.71	-84.22	-291.54
STORY9	PUSHX	Bottom	9365.05	-92.74	-323.09
STORY8	PUSHX	Bottom	10302.58	-101.22	-354.56
STORY7	PUSHX	Bottom	11240.27	-109.73	-386.33
STORY6	PUSHX	Bottom	12177.98	-118.4	-418.39
STORY5	PUSHX	Bottom	13115.46	-127.35	-451.21
STORY4	PUSHX	Bottom	14052.31	-136.74	-485.03
STORY3	PUSHX	Bottom	14987.91	-146.65	-520.29
STORY2	PUSHX	Bottom	15921.51	-156.36	-558.35
STORY1	PUSHX	Bottom	16851.76	-158.93	-608.71

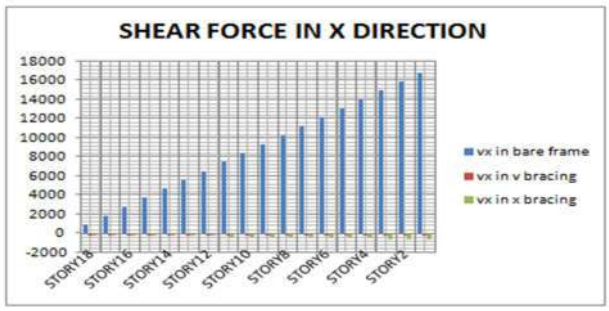

SHEAR FORCE IN Y DIRECTION

Story	Load	Loc	vy in bare frame	vy in v push	vy in x bracing
STORY18	PUSHY	Bottom	858.89	-9.74	-29.57
STORY17	PUSHY	Bottom	1717.77	-20.67	-58.79
STORY16	PUSHY	Bottom	2576.66	-31.5	-88.01
STORY15	PUSHY	Bottom	3435.55	-42.02	-117.1
STORY14	PUSHY	Bottom	4294.43	-52.25	-146.09
STORY13	PUSHY	Bottom	5153.32	-62.17	-174.99
STORY12	PUSHY	Bottom	6012.2	-71.81	-203.82
STORY11	PUSHY	Bottom	6871.09	-81.18	-232.58
STORY10	PUSHY	Bottom	7729.98	-90.31	-261.29
STORY9	PUSHY	Bottom	8588.86	-99.25	-290
STORY8	PUSHY	Bottom	9447.75	-108.04	-318.72
STORY7	PUSHY	Bottom	10306.63	-116.74	-347.43
STORY6	PUSHY	Bottom	11165.51	-125.44	-376.36
STORY5	PUSHY	Bottom	12024.4	-134.2	-405.33
STORY4	PUSHY	Bottom	12883.28	-143.12	-434.51
STORY3	PUSHY	Bottom	13742.17	-152.07	-463.91
STORY2	PUSHY	Bottom	14601.05	-160.29	-493.72
STORY1	PUSHY	Bottom	15459.94	-165.3	-526.95

BUILDING TORSION

Story	Load	Loc	t in bare frame	T in v push	t in x bracing
STORY18	PUSHX	Bottom	936.737	-96.682	-8.181
STORY17	PUSHX	Bottom	1876.364	-136.319	-124.959
STORY16	PUSHX	Bottom	2818.734	-201.683	-230.279
STORY15	PUSHX	Bottom	3766.318	-259.127	-328.172
STORY14	PUSHX	Bottom	4722.736	-314.566	-437.993
STORY13	PUSHX	Bottom	5691.668	-366.721	-500.968
STORY12	PUSHX	Bottom	6676.065	-414.908	-573.442
STORY11	PUSHX	Bottom	7678.544	-458.359	-660.607
STORY10	PUSHX	Bottom	8702.286	-496.243	-730.947
STORY9	PUSHX	Bottom	9750.64	-527.621	-766.863
STORY8	PUSHX	Bottom	10826.819	-551.42	-820.843
STORY7	PUSHX	Bottom	11934.21	-566.372	-859.661
STORY6	PUSHX	Bottom	13077.158	-570.944	-866.833
STORY5	PUSHX	Bottom	14262.297	-563.219	-865.264
STORY4	PUSHX	Bottom	15499.548	-540.894	-841.258
STORY3	PUSHX	Bottom	16803.209	-498.053	-787.296
STORY2	PUSHX	Bottom	18226.052	-436.93	-694.046
STORY1	PUSHX	Bottom	19890.283	-454.708	-589.41

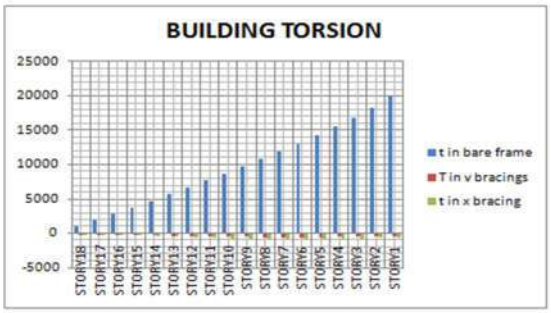

BENDING MOMENT IN X DIRECTION

Story	Load	Loc	mx in bare frame	mx in v push	Mx in x bracing
STORY18	PUSHX	Bottom	-962137.5	39857.74	142287.8
STORY17	PUSHX	Bottom	-1954585	80098.647	285968.4
STORY16	PUSHX	Bottom	-2949055	120374.26	429756.1
STORY15	PUSHX	Bottom	-3945301	160683.7	573653.1
STORY14	PUSHX	Bottom	-4943102	201026.6	717660.1
STORY13	PUSHX	Bottom	-5942257	241402.58	861777.4
STORY12	PUSHX	Bottom	-6942578	281811.3	1006006
STORY11	PUSHX	Bottom	-7943883	322252.42	1150345
STORY10	PUSHX	Bottom	-8945996	362725.63	1294795
STORY9	PUSHX	Bottom	-9948745	403230.65	1439356
STORY8	PUSHX	Bottom	-10951963	443767.26	1584027
STORY7	PUSHX	Bottom	-11955477	484335.31	1728810
STORY6	PUSHX	Bottom	-12959109	524934.73	1873702
STORY5	PUSHX	Bottom	-13962677	565565.58	2018703
STORY4	PUSHX	Bottom	-14965991	606227.97	2163812
STORY3	PUSHX	Bottom	-15968851	646921.76	2309029
STORY2	PUSHX	Bottom	-16970787	687646.73	2454349
STORY1	PUSHX	Bottom	-17977409	728495.75	2600246

BENDING MOMENT IN Y DIRECTION

Story	Load	Loc	my in bare frame	my in v push	my in x bracing
STORY18	PUSHY	Bottom	884712.14	-39861.35	-119383
STORY17	PUSHY	Bottom	1797491.5	-80101.02	-239836
STORY16	PUSHY	Bottom	2712535.5	-120371.8	-360382
STORY15	PUSHY	Bottom	3629739.2	-160675.3	-481021
STORY14	PUSHY	Bottom	4549000	-201011	-601754
STORY13	PUSHY	Bottom	5470218.1	-241378.8	-722581
STORY12	PUSHY	Bottom	6393293.2	-281778.4	-843503
STORY11	PUSHY	Bottom	7318117.8	-322209.6	-964519
STORY10	PUSHY	Bottom	8244574.6	-362672	-1085630
STORY9	PUSHY	Bottom	9172550.1	-403165.7	-1206836
STORY8	PUSHY	Bottom	10101949	-443690.5	-1328137
STORY7	PUSHY	Bottom	11032701	-484246.4	-1449532
STORY6	PUSHY	Bottom	11964778	-524833.6	-1571021
STORY5	PUSHY	Bottom	12898237	-565452.5	-1692603
STORY4	PUSHY	Bottom	13833313	-606103.6	-1814277
STORY3	PUSHY	Bottom	14770607	-646787.5	-1936040
STORY2	PUSHY	Bottom	15711493	-687503	-2057890
STORY1	PUSHY	Bottom	16670835	-728351.9	-2180226

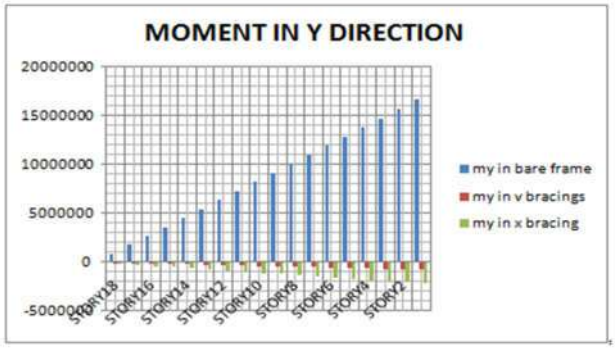

B.EQUVALENT STATIC ANALYSIS

STORY DRIFT IN X DIRECTION

Story	Item	drift x in bare frame	drift x in v bracing	drift x in x bracing
STORY18	STATIC	0.000276	0.000399	0.005673
STORY17	STATIC	0.000372	0.000482	0.005499
STORY16	STATIC	0.000483	0.00059	0.005436
STORY15	STATIC	0.000598	0.000697	0.005476
STORY14	STATIC	0.000713	0.000807	0.005526
STORY13	STATIC	0.000828	0.000918	0.005557
STORY12	STATIC	0.000943	0.001028	0.005562
STORY11	STATIC	0.001057	0.001137	0.005539
STORY10	STATIC	0.001171	0.001245	0.005481
STORY9	STATIC	0.001283	0.001349	0.005384
STORY8	STATIC	0.001395	0.001449	0.005242
STORY7	STATIC	0.001505	0.001544	0.00505
STORY6	STATIC	0.001614	0.001632	0.004802
STORY5	STATIC	0.001721	0.001735	0.00449
STORY4	STATIC	0.001827	0.001855	0.004099
STORY3	STATIC	0.001931	0.001991	0.003622
STORY2	STATIC	0.00204	0.002298	0.002992
STORY1	STATIC	0.002069	0.002446	0.001741

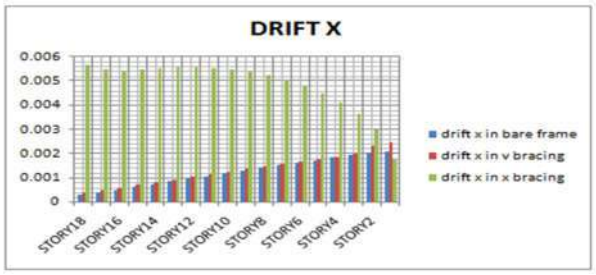

STORY DRIFT IN Y DIRECTION

Story	Item	drift y in bare frame	drift y in v bracing	drift y in x bracing
STORY18	STATIC	0.00064	0.001284	0.004215
STORY17	STATIC	0.00117	0.001426	0.004463
STORY16	STATIC	0.0017	0.001584	0.004525
STORY15	STATIC	0.00224	0.001765	0.004641
STORY14	STATIC	0.00278	0.001952	0.00475
STORY13	STATIC	0.00331	0.002142	0.004829
STORY12	STATIC	0.00385	0.002329	0.004876
STORY11	STATIC	0.00439	0.002511	0.004891
STORY10	STATIC	0.00492	0.002684	0.00487
STORY9	STATIC	0.00545	0.002844	0.00481
STORY8	STATIC	0.00598	0.002987	0.004708
STORY7	STATIC	0.00651	0.003107	0.004561
STORY6	STATIC	0.00704	0.003201	0.004366
STORY5	STATIC	0.00757	0.003282	0.004123
STORY4	STATIC	0.00809	0.003352	0.003846
STORY3	STATIC	0.00861	0.003392	0.003697
STORY2	STATIC	0.00944	0.003451	0.003113
STORY1	STATIC	0.02297	0.003871	0.002117

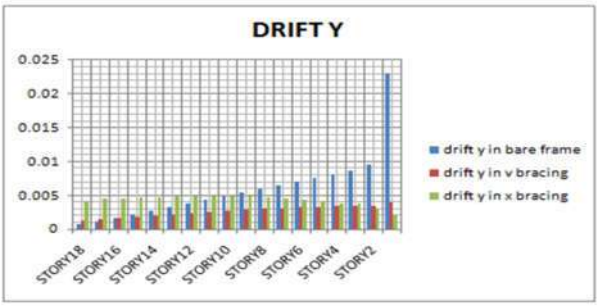

LATERAL FORCES (P)

Story	Load	Loc	p in bare frame	p in v bracing	p In x bracing
STORY18	STATIC	Bottom	28799.8	28886.79	28375.05
STORY17	STATIC	Bottom	57599.59	57731.58	56750.1
STORY16	STATIC	Bottom	86399.39	86576.37	85125.16
STORY15	STATIC	Bottom	115199.18	115421.15	113500.21
STORY14	STATIC	Bottom	143998.98	144265.94	141875.26
STORY13	STATIC	Bottom	172798.78	173110.73	170250.31
STORY12	STATIC	Bottom	201598.57	201955.52	198625.36
STORY11	STATIC	Bottom	230398.37	230800.31	227000.41
STORY10	STATIC	Bottom	259198.16	259645.1	255375.47
STORY9	STATIC	Bottom	287997.96	288489.88	283750.52
STORY8	STATIC	Bottom	316797.76	317334.67	312125.57
STORY7	STATIC	Bottom	345597.55	346179.46	340500.62
STORY6	STATIC	Bottom	374397.35	375024.25	368875.67
STORY5	STATIC	Bottom	403197.15	403869.04	397250.73
STORY4	STATIC	Bottom	431996.94	432713.83	425625.78
STORY3	STATIC	Bottom	460796.74	461558.61	454000.83
STORY2	STATIC	Bottom	489596.53	490403.4	482375.88
STORY1	STATIC	Bottom	518549.46	519407.83	511159.32

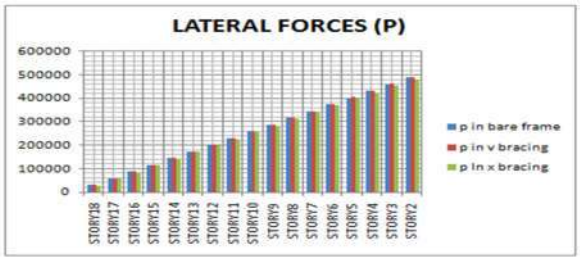

SHEAR FORCE IN X DIRECTION

Story	Load	Loc	vx in bare frame	vx in v bracing	vx in x bracing
STORY18	STATIC	Bottom	-255	-255	-127.5
STORY17	STATIC	Bottom	-510	-552	-255
STORY16	STATIC	Bottom	-765	-849	-382.5
STORY15	STATIC	Bottom	-1020	-1146	-510
STORY14	STATIC	Bottom	-1275	-1443	-637.5
STORY13	STATIC	Bottom	-1530	-1740	-765
STORY12	STATIC	Bottom	-1785	-2037	-892.5
STORY11	STATIC	Bottom	-2040	-2334	-1020
STORY10	STATIC	Bottom	-2295	-2631	-1147.5
STORY9	STATIC	Bottom	-2550	-2928	-1275
STORY8	STATIC	Bottom	-2805	-3225	-1402.5
STORY7	STATIC	Bottom	-3060	-3522	-1530
STORY6	STATIC	Bottom	-3315	-3819	-1657.5
STORY5	STATIC	Bottom	-3570	-4116	-1785
STORY4	STATIC	Bottom	-3825	-4413	-1912.5
STORY3	STATIC	Bottom	-4080	-4710	-2040
STORY2	STATIC	Bottom	-4335	-5007	-2167.5
STORY1	STATIC	Bottom	-4590	-5304	-2295

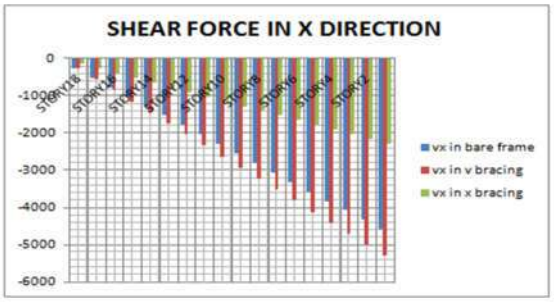

BUILDING TORSION

Story	Load	Loc	Tin bare frame	Tin v bracing	Tin x bracing
STORY18	STATIC	Bottom	-255	-255	-127.5
STORY17	STATIC	Bottom	-510	-552	-255
STORY16	STATIC	Bottom	-765	-849	-382.5
STORY15	STATIC	Bottom	-1020	-1146.001	-510
STORY14	STATIC	Bottom	-1275	-1443.001	-637.5
STORY13	STATIC	Bottom	-1530	-1740.001	-765
STORY12	STATIC	Bottom	-1785	-2037.001	-892.5
STORY11	STATIC	Bottom	-2040	-2334.001	-1020
STORY10	STATIC	Bottom	-2295	-2631.002	-1147.5
STORY9	STATIC	Bottom	-2550	-2928.002	-1275
STORY8	STATIC	Bottom	-2805	-3225.002	-1402.5
STORY7	STATIC	Bottom	-3060	-3522.002	-1530
STORY6	STATIC	Bottom	-3315	-3819.002	-1657.5
STORY5	STATIC	Bottom	-3570	-4116.003	-1785
STORY4	STATIC	Bottom	-3825	-4413.003	-1912.5
STORY3	STATIC	Bottom	-4080	-4710.003	-2040
STORY2	STATIC	Bottom	-4335	-5007.003	-2167.5
STORY1	STATIC	Bottom	-4590	-5304.003	-2295

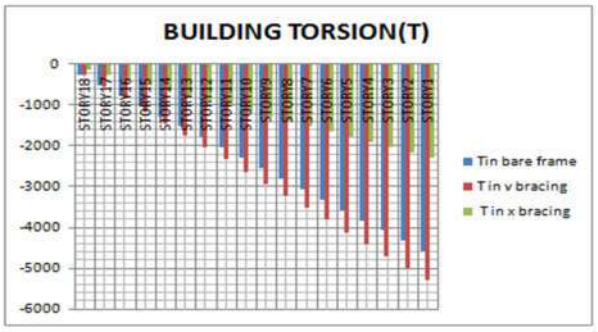

SHEAR FORCE IN Y DIRECTION

Story	Load	Loc	vy in bare frame	vy in v bracing	vy in x bracing
STORY18	STATIC	Bottom	-255	-255	-127.5
STORY17	STATIC	Bottom	-510	-552	-255
STORY16	STATIC	Bottom	-765	-849	-382.5
STORY15	STATIC	Bottom	-1020	-1146	-510
STORY14	STATIC	Bottom	-1275	-1443	-637.5
STORY13	STATIC	Bottom	-1530	-1740	-765
STORY12	STATIC	Bottom	-1785	-2037	-892.5
STORY11	STATIC	Bottom	-2040	-2334	-1020
STORY10	STATIC	Bottom	-2295	-2631	-1147.5
STORY9	STATIC	Bottom	-2550	-2928	-1275
STORY8	STATIC	Bottom	-2805	-3225	-1402.5
STORY7	STATIC	Bottom	-3060	-3522	-1530
STORY6	STATIC	Bottom	-3315	-3819	-1657.5
STORY5	STATIC	Bottom	-3570	-4116	-1785
STORY4	STATIC	Bottom	-3825	-4413	-1912.5
STORY3	STATIC	Bottom	-4080	-4710	-2040
STORY2	STATIC	Bottom	-4335	-5007	-2167.5
STORY1	STATIC	Bottom	-4590	-5304	-2295

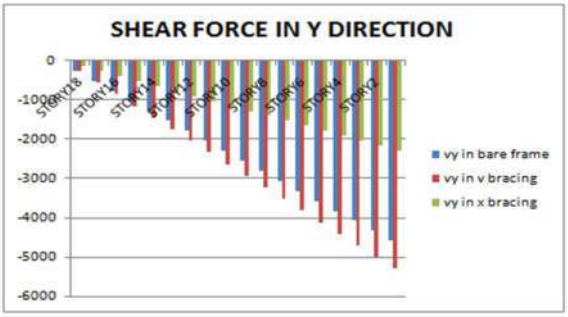

BENDING MOMENT IN X DIRECTION

Story	Load	Loc	MXin bare frame	Mxin v bracing	Mxin x bracing
STORY18	STATIC	Bottom	720504.9	723787.08	710231.4
STORY17	STATIC	Bottom	1441774.8	1447373.2	1420845.3
STORY16	STATIC	Bottom	2163809.7	2171850.2	2131841.7
STORY15	STATIC	Bottom	2886609.6	2897218.3	2843220.6
STORY14	STATIC	Bottom	3610174.3	3623477.4	3554982
STORY13	STATIC	Bottom	4334504.4	4350627.5	4267125.9
STORY12	STATIC	Bottom	5059599.3	5078668.5	4979652.3
STORY11	STATIC	Bottom	5785459.2	5807600.6	5692561.2
STORY10	STATIC	Bottom	6512084.1	6537423.7	64038526
STORY9	STATIC	Bottom	723947.4	7268137.8	7119526.5
STORY8	STATIC	Bottom	7967628.9	7999742.8	7833582.9
STORY7	STATIC	Bottom	8696548.8	8732238.9	8548021.8
STORY6	STATIC	Bottom	9426233.7	9465626	9262843.2
STORY5	STATIC	Bottom	10156684	10199904	9978047.1
STORY4	STATIC	Bottom	10887899	10935073	10693633
STORY3	STATIC	Bottom	11619878	11671133	11409602
STORY2	STATIC	Bottom	12352623	12408084	12125954
STORY1	STATIC	Bottom	13092256	13152650	12854024

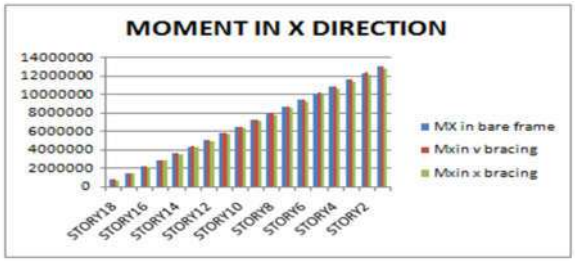

BENDING MOMENT IN Y DIRECTION

Story	Load	Loc	MY in bare frame	MY in v bracing	MY in x bracing
STORY18	STATIC	Bottom	-721014.9	-723664.3	-710031.2
STORY17	STATIC	Bottom	-1442795	-1447212	-1420445
STORY16	STATIC	Bottom	-2165340	-2171650	-2131241
STORY15	STATIC	Bottom	-2888650	-2896979	-2842420
STORY14	STATIC	Bottom	-3612725	-3623199	-3553981
STORY13	STATIC	Bottom	-4337564	-4350311	-4265924
STORY12	STATIC	Bottom	-5063169	-5078313	-4978251
STORY11	STATIC	Bottom	-5789539	-5807206	-5690959
STORY10	STATIC	Bottom	-6516674	-6536991	-6404050
STORY9	STATIC	Bottom	-7244574	-7267666	-7117524
STORY8	STATIC	Bottom	-7973239	-7999232	-7831380
STORY7	STATIC	Bottom	-8702669	-8731690	-8545619
STORY6	STATIC	Bottom	-9432864	-9465038	-9260240
STORY5	STATIC	Bottom	-10163824	-10199277	-9975244
STORY4	STATIC	Bottom	-10895549	-10934407	-10690630
STORY3	STATIC	Bottom	-11628038	-11670429	-11406399
STORY2	STATIC	Bottom	-12361293	-12407341	-12122550
STORY1	STATIC	Bottom	-13101436	-13151822	-12850408

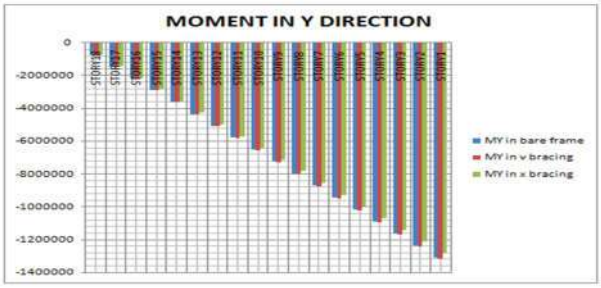

V.CONCLUSIONS

- The pushover analysis is relatively simple way to explore the non-linear behavior of buildings and it is an elegant tool to visualize the performance level of a building under a given earthquake.
- The Drift values in the V braced building shows very less storey drifts due to arrangements of the V braces in the buildings .
- The shear force in the industrial steel structure due to arrangement of the bracings , the braced building of V braced system shows very less values when compared to the other building systems.
- The bending moments of the steel structure shows the very high moments and the least moments are observed in V braced building due to its arrangement in the buildings.
- The overturning moments of the buildings observed to more in the steel building and X braced building systems , the least values are observed in the V braced systems.

Considering all the above results the V braced building systems shows the best results and next to the that is X braced building systems.

- The Drift values in the Equivalent static analysis the steel buildings also shows very high displacements when compared to the other building systems , the V braced building systems are best suitable structures.
- The shear values in the Equivalent static analysis the V braced building systems shows that the less shear values compared to the other building systems.
- The bending in the Equivalent static analysis the V braced building systems shows that the less Bending values compared to the other building systems. due to the arrangements bracings in the buildings .
- The overturning moments in the equivalent static analysis results shows that the less overturning moments in V braced building systems when compared to the other steel and X braced structures.

Comparing the above results the V braced steel Building is best suited structure according to the Pushover analysis. And the X braced building is the Best structure according to the equivalent static analysis.

SCOPE OF THE FUTURE WORK:

- By using bracings in the structures, the displacement of the structure greatly reduced can be changed or altered. Hence the further study can be done by examining the behavior of the storey building due to wind load forces and Time history analysis.
- We can also study on the behavior of Bending Moment, shear Force etc.
- We can study other types of bracings in different Zones for the different soil type conditions.
- We can study for the different sections in tall structures and compare with and without bracings.

REFERANCES

[1] Theory of Structures by Ramamrutham for literature review on kani′s method
[2] Theory of structures by B.C.Punmia for literature on moment distribution method.
[3] Reinforced concrete Structures by A.K. Jain and B.C. Punmia for design of beams, columns and slab.
[4] Fundamentals of concrete structure by N. C. Sinha.

[5] S.Mahesh and Dr.B.Panduranga Rao Comparison of analysis and design of regular and irregular configuration of multi Story building in various seismic zones and various types of soils were using STAAD Volume 11, Issue 6 Ver. I (Nov- Dec. 2014), PP 45-52

[6] Kevadkar M.D., Kodag P.B., 'Lateral load (loads due to earthquake, wind, blast, fire hazards etc) (earthquake loads, wind loads, blast, fire hazards etc) Analysis of R.C.C. Building', International Journal of Modern Engineering Research (IJMER), Vol.3, Issue.3, May-June. 2013, pp-1428-1434.

[7] Salehuddin Shamshinar, Stability of a six storey steel frame structure, International Journal of Civil & Environmental Engineering, Vol.13 No.06, 2011. User Manual STAAD.Pro.

[8] Chopra, A. K., Dynamics of Structures (1995): Theory and Applications to Earthquake Engineering, Prentice-Hall. Inc., Englewood Cliffs, New Jersey.

[9] IS 1893 : 2002, Indian Standard criteria for earthquake resistant design of frames, Part 1 General provisions and buildings, Draft of Fifth Revision, Bureau of Indian Standards, New Delhi, 2002.

[10] IS: 875(Part-1)- 1987 ‘Code of Practice for Design Loads (Other than Earthquake) buildings and frames’, Part-1 Dead load, Unit weight of building materials and stored materials, Bureau of Indian Standards, New Delhi.

A COMPARATIVE STUDY ON PUSHOVER ANALYSIS WITH LINEAR STATIC ANALYSIS OF INDUSTRIAL STEEL STRUCTURE SUBJECTED TO GRAVITY LOADS AND DYNAMIC LOADS

Mohd Abdul Atif Sulaiman[1], Shaik Mohammed Javid[2] Syed farrukh Anwar[3]

[1] Pg Student, M.tech in Structural engineering, Department of Civil Engineering, Nawab Shah Alam Khan College of Engineering and Technology, Hyderabad, Telangana 500024

[2] Assistant Professor, M.tech in Structural engineering, Department of Civil Engineering, Nawab Shah Alam Khan College of Engineering and Technology, Hyderabad, Telangana 500024

[3] Head of the Department (PHD) , Vice Principal, M.tech in Structural engineering, Department of Civil Engineering, Nawab Shah Alam Khan College of Engineering and Technology, Hyderabad, Telangana 500024

ABSTRACT :Developments in computer hardware and software have made analysis techniques that were formerly too expensive within the reach of most project budgets. Foremost among these has been equivalent static analysis and push over analysis.. This approach defines a series of forces acting on a building to represent the effect of earthquake ground motion, typically defined by a seismic design response spectrum. It assumes that the building responds in its fundamental mode. For this to be true, the building must be low-rise and must not twist significantly when the ground moves. The response is read from a design response spectrum, given the natural frequency of the building.

The applicability of this method is extended in many building codes by applying factors to account for higher buildings with some higher modes, and for low levels of twisting. To account for effects due to "yielding" of the structure, many codes apply modification factors that reduce the design forces (e.g. force reduction factors).

Shaking and ground rupture are the main effects created by earthquakes, mainly resulting damage to buildings and other rigid structures. The severity of the local effects depends on the complex combination of the earthquake magnitude, the distance from the epicenter and the local geological and geomorphologic conditions the ground motion is measured by ground acceleration .An earthquake may cause injury and loss of life, road and bridge damage, general property damage and collapse or destabilization of buildings.

Present work deals with study of seismic analysis and design of Technology Innovation and Industry Relations with different types of bracings V bracings, and X bracings was compared with the bare frame and results are analyzed like story displacements, story shear, bending moment , shear force and building torsion with the help of commercial software like ETABS9.7.4 under the static and pushover analysis.

Keywords: V bracings, X bracings, story displacements, story shear, bending moment building torsion etc.,

I.INTRODUCTION

The primary purpose of all kinds of structural systems used in the building type of structures is to transfer gravity loads effectively. The most common loads resulting from the effect of gravity are dead load, live load and snow load. Besides these vertical

loads, buildings are also subjected to lateral loads caused by wind, blasting or earthquake. Lateral loads can develop high stresses, produce sway movement or cause vibration. Therefore, it is very important for the structure to have sufficient strength against vertical loads together with adequate stiffness to resist lateral forces. Strengthening of structures proves to be a better option catering to the economic considerations and immediate shelter problems rather than replacement of buildings. Moreover it has been often seen that retrofitting of buildings is generally more economical as compared to demolition and reconstruction. Therefore, seismic retrofitting or strengthening of building structures is one of the most important aspects for mitigating seismic hazards especially in earthquake prone areas.

TYPES OF BRACINGS

There are two types of bracing systems

1) Concentric Bracing System

All kinds of the concentrically braced frames used in the seismic rehabilitation including the Cross, Chevron V braced frames, Chevron Inverted-v-braced frames, Zipper column rehabilitated Invertedv- braced frames. Axial forces including tension and compression in concentrically braced frames are regarded as Displacement control. Columns in compression are Force control (buckling of columns is critical) and in tension are displacement control.

K BRACINGS

The full diagonal bracing is not used in areas where a passage is required. In such cases, k-bracings are preferred over diagonal bracing because there is a room to provide opening for doors and windows etc.

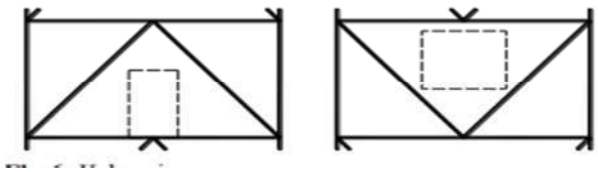

V brace: Bracing where a pair of braces joins at a single point on the beam span. Inverted V braceis that form of chevron bracing that terminates at point on beam from below.

This involves two diagonal members extending from the top two corners of a horizontal member and meeting at a centre point at the lower horizontal member, in the shape of a V. Inverted V-bracing (also known as chevron bracing) involves the two members meeting at a centre point on the upper horizontal member.

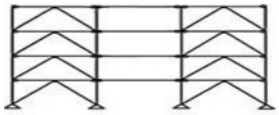

V Bracing

X brace: Bracing where two diagonal braces crosses near mid-length of the bracing members. c) K brace: Bracing where a pair of braces connected on one side of a column joins at a single point on another leg of column.

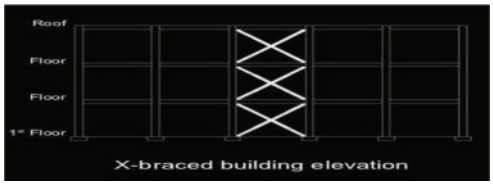

2) Eccentric Bracings

Reduce the lateral stiffness of the system and improve the energy dissipation capacity. The lateral stiffness of the system depends upon the flexural stiffness property of the beams and columns, thus reducing the lateral stiffness of the frame. The vertical component of the bracing forces due to earthquake causes lateral concentrated load on the beams at the point of connection of the eccentric bracing.

Eccentric bracing consists of diagonal braces located in the plane of the frame where one or both ends of the brace do not join at the end points of other framing members. The system essentially combines the features of a moment frame and a concentrically braced frame, while minimising the disadvantages of each system.

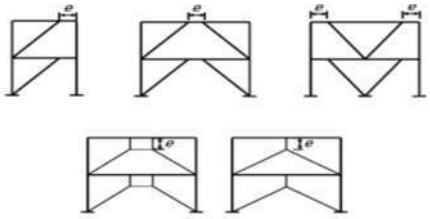

Types of eccentrically braced frames depending on the location of the link beam

OBJECTIVE OF THE STUDY

I. To understand the elastic and plastic behavior of the STEEL BUILDING building under gravity loads taken as per IS 875-1987

II. To compare the steel building with different types of bracings like X bracings and V bracings are compared with the BARE framed building .

III. To compare various parametric results such as Storey drift and Storey forces for the different models considered.

IV. To obtain pushover curves both in X and Y directions using FEM based analytical software ETABS 9.7.4.

V. To compare various parametric results such as Storey shear and column forces and beam forces for the different models considered

II.LITERATURE REVIEW

Dr. S.V. Itti[1], Prof. AbhishekPathade[2] and Ramesh B. Karadi[3] et all,.(2006) This study focuses on the comparison of the Indian Code (IS) and International Building Codes (IBC) in relation to the seismic design and analysis of Ordinary RC moment resisting frame (OMRF), Intermediate RC moment-resisting frame (IMRF) and Special RC moment-resting frame (SMRF). The analytical results of the model buildings are then compared and analyzed taking note of any significant differences. This study explores variations in the results obtained using the two codes, particularly design base shear, lateral loads, drifts and area of steel for structural members for all RC buildings in both the codes. The discussion in this study will be confined to monolithically cast reinforced concrete buildings. Specific provisions for design of seismic resistant reinforced members are presented in detail. Provisions of Indian and International Buildings Codes are identified. Target deflection of the building is achieved at a lower lateral force in SMRF IBC i.e, the concept of lesser force and more deflection is followed. However in OMRF, IMRF and SMRF of Indian Code lateral force applied in higher as a result the deflection on the top of the building exceeds the target deflection.

F. Zareian[1], D. G. Lignos[2] and H. Krawinkler[3] et all,. (2010) This paper summarizes a study focused on evaluating the design modification factors (i.e., R, Cd, Ω) for Steel Special Moment-resisting Frames (SSMFs) by application of the FEMA P695 methodology. In this study, archetype design that comprise 3-bay special SMFs that serve as lateral load resisting system of steel buildings ranging from 1 to 20 stories are designed using ASCE 7-05 and AISC 341-05design provisions. Nonlinear models are developed using latest advances in structural component modeling. Parameters for these models are extracted from a steel component database for modeling of component deterioration. The numerical models are analyzed to predict the collapse capacities of each design, and the adjusted collapse margin ratios (ACMR) are evaluated and compared to acceptance criteria.

III.METHODOLOGY

Building frame with the following geometrical types are considered for analysis in seismic zone (Zone V) for seismic and gravity loading in each case. And also the terrain category (terrain category 3 are also studied on the each case.

- PUSH OVER ANALYSIS

CASE-1: G+17building frame without bracing system (Bare Frame).

CASE-2: G+17 building frame with X bracing system.

CASE-3: G+17 building frame with V bracing system.

- EQUVALENT STATIC ANALYSIS

CASE-1: G+17building frame without bracing system (Bare Frame).

CASE-2: G+17 building frame with X bracing system.

CASE-3: G+17 building frame with V bracing system.

Push over analysis:

Pushover analysis is an approximate analysis method in which the structure is subjected to monotonically increasing lateral forces with an invariant height-wise distribution until a target displacement is reached. Pushover analysis consists of a series of sequential elastic analysis, superimposed to approximate a force-displacement curve of the overall structure. A two or three dimensional model which includes bilinear or trilinear load-deformation diagrams of all lateral force resisting elements is first created and gravity loads are applied initially. A predefined lateral load pattern which is distributed along the building height is then applied. The lateral forces are increased until some members yield. The structural model is modified to account for the reduced stiffness of yielded members and lateral forces are again increased until additional members yield. The process is continued until a control displacement at the top of building reaches a certain level of deformation or structure becomes unstable.

Pushover is a static-nonlinear analysis method where a structure is subjected to gravity loading and a monotonic displacement-controlled lateral load pattern which continuously increases through elastic and inelastic behavior until an ultimate condition is reached. Lateral load may represent the range of base shear induced by earthquake loading, and its configuration may be proportional to the distribution of mass along building height, mode shapes, or another practical means.

Output generates a static-pushover curve which plots a strength-based parameter against deflection. For example, performance may relate the strength level achieved in certain members to the lateral displacement at the top of the structure, or bending moment may be plotted against plastic rotation. Results provide insight into the ductile capacity of the structural system, and indicate the mechanism, load level, and deflection at which failure occurs.

When analyzing frame objects, material nonlinearity is assigned to discrete hinge locations where plastic rotation occurs according to FEMA-356 or another set of code-based or user-defined criteria. Strength drop, displacement control, and all other nonlinear software features, including link assignment, P-Delta effect, and staged construction, are available during static-pushover analysis.

EQUVALENT STATIC ANALYSIS

Equivalent Static Analysis:
This approach defines a series of forces acting on building to represent the effect of earthquake ground motion, typically defined by a seismic design response spectrum. It assumes that the building responds in its fundamental mode. For this to be true, the building must be low-rise and must not twist significantly when the ground moves. The response is read from a design response spectrum, given the natural frequency of the building (either calculated or defined by the building code). The applicability of this method is extended in many building codes by applying factors to account for higher buildings with some higher modes, and for low levels of twisting. To account for effects due to “yielding” of the structure, many codes apply modification factors that reduce the design forces (e.g., force reduction factors).

The seismic design of buildings fallows the dynamic nature of the load. But equivalent static analysis would become sufficient for simpler, regular in plan configuration and it will give more efficient results. This analysis will flow in a manner with the calculation of design base shear and its distribution to all storey’s by using the formula given in the code

PROBLEM OF STATEMENT

In building plan was taken in seismic zone V for seismic analysis of the building (G+17) with braced building and unbraced building (general building). The basic specifications of the building are:
Beam Size
= ISMB300
Column size
= ISMB600
Bracings
= ISMB125(BOTH V,X BRACINGS)
Storey Height
= 3.0 mts

Bottom storey
= 3.5 mts
Column spacing
= 5 mts
Materials used
= M25 & Fe415;
Depth of slab
= 150 mm
Unit weight of concrete
= 25 kN/m^3
Code Books used
=IS1893:2002,

1. BARE FRAME

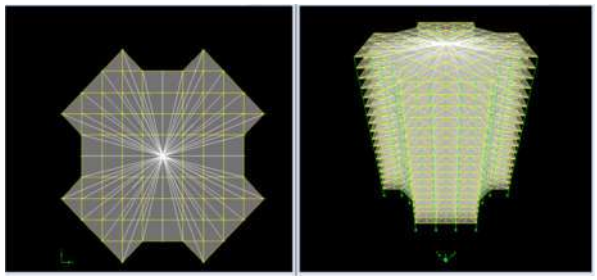

2. V BARCED FRAME BUILDING

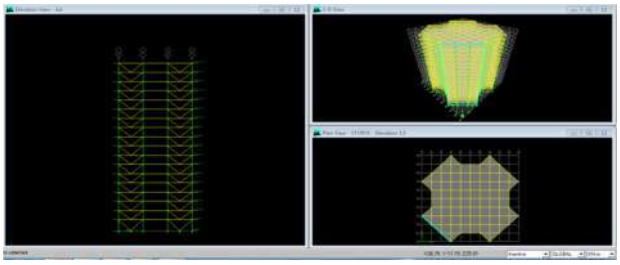

3. X BARCED FRAME BUILDING

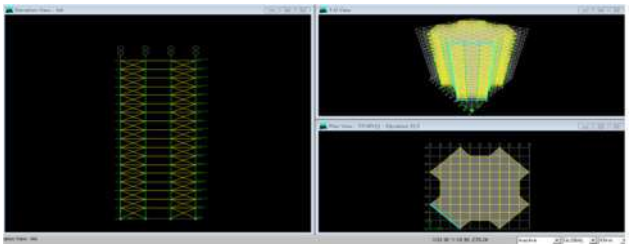

IV. RESULTS AND ANALYSIS
PUSH OVER ANALYSIS

STORY DRIFT IN X DIRECTION

Story	Load	DRIFT X in bare frame	drift x in v push	drift x in x bracing
STORY18	PUSHX	0.00225	0.000963	0.001311
STORY17	PUSHX	0.00289	0.000886	0.001257
STORY16	PUSHX	0.00368	0.000916	0.001259
STORY15	PUSHX	0.00451	0.00093	0.001281
STORY14	PUSHX	0.00535	0.000988	0.001305
STORY13	PUSHX	0.00619	0.001021	0.001328
STORY12	PUSHX	0.00703	0.001051	0.001345
STORY11	PUSHX	0.00788	0.001077	0.001355
STORY10	PUSHX	0.00869	0.001096	0.001357
STORY9	PUSHX	0.00948	0.001109	0.00133
STORY8	PUSHX	0.01021	0.001114	0.001303
STORY7	PUSHX	0.01089	0.001111	0.001303
STORY6	PUSHX	0.01148	0.001096	0.00126
STORY5	PUSHX	0.01192	0.001071	0.0012
STORY4	PUSHX	0.01208	0.001033	0.001123
STORY3	PUSHX	0.0117	0.000991	0.001023
STORY2	PUSHX	0.01017	0.000999	0.000874
STORY1	PUSHX	0.00539	0.001046	0.000574

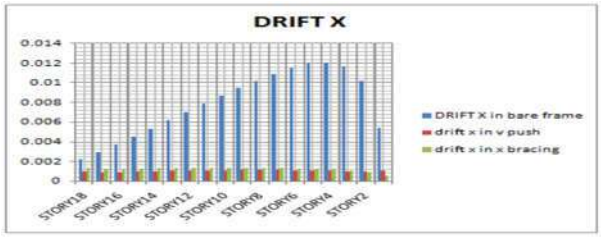

STORY DRIFT IN Y DIRECTION

Story	Load	drift y in bare frame	drift y in v push	drift y in x bracing
STORY18	PUSHY	0.00243	0.000361	0.00114
STORY17	PUSHY	0.00453	0.000613	0.001194
STORY16	PUSHY	0.00641	0.00065	0.001231
STORY15	PUSHY	0.00808	0.000685	0.001254
STORY14	PUSHY	0.00955	0.000729	0.001291
STORY13	PUSHY	0.01083	0.000771	0.001324
STORY12	PUSHY	0.01196	0.00081	0.001346
STORY11	PUSHY	0.01291	0.000844	0.001362
STORY10	PUSHY	0.0137	0.000873	0.001367
STORY9	PUSHY	0.01432	0.000896	0.001363
STORY8	PUSHY	0.01477	0.000912	0.001348
STORY7	PUSHY	0.01505	0.000921	0.00132
STORY6	PUSHY	0.01516	0.00092	0.001278
STORY5	PUSHY	0.01666	0.000911	0.001222
STORY4	PUSHY	0.01851	0.000892	0.00115
STORY3	PUSHY	0.02048	0.000869	0.001063
STORY2	PUSHY	0.02288	0.000879	0.000983
STORY1	PUSHY	0.02601	0.000951	0.000693

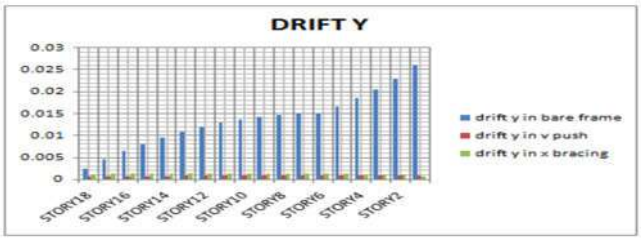

LATERAL FORCES (P)

Story	Load	Loc	p in bare frame	p in v bracing	p in x bracing
STORY18	PUSHX	Bottom	-38417.85	1592.81	5682.61
STORY17	PUSHX	Bottom	-77955.94	3199.44	11415.71
STORY16	PUSHX	Bottom	-117494	4806.1	17148.78
STORY15	PUSHX	Bottom	-157032.1	6412.76	22881.83
STORY14	PUSHX	Bottom	-196570.2	8019.43	28614.87
STORY13	PUSHX	Bottom	-236108.3	9626.1	34347.9
STORY12	PUSHX	Bottom	-275646.4	11232.78	40080.93
STORY11	PUSHX	Bottom	-315184.5	12839.48	45813.98
STORY10	PUSHX	Bottom	-354722.6	14446.18	51547.05
STORY9	PUSHX	Bottom	-394260.7	16052.91	57280.13
STORY8	PUSHX	Bottom	-433798.8	17659.64	63013.24
STORY7	PUSHX	Bottom	-473336.9	19266.39	68746.37
STORY6	PUSHX	Bottom	-512874.9	20873.16	74479.52
STORY5	PUSHX	Bottom	-552413	22479.94	80212.68
STORY4	PUSHX	Bottom	-591951.1	24086.73	85945.85
STORY3	PUSHX	Bottom	-631489.2	25693.53	91679
STORY2	PUSHX	Bottom	-671027.3	27300.3	97412.08
STORY1	PUSHX	Bottom	-710752.1	28907.8	103151.7

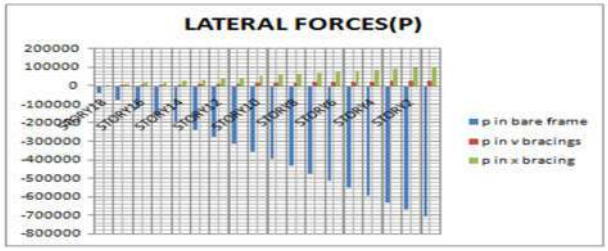

SHEAR FORCE IN X DIRECTION

Story	Load	Loc	vx in bare frame	vx in v push	vx in x bracing
STORY18	PUSHX	Bottom	936	-8.97	-34.44
STORY17	PUSHX	Bottom	1872.06	-19.24	-67.31
STORY16	PUSHX	Bottom	2808.19	-29.23	-100.01
STORY15	PUSHX	Bottom	3744.4	-38.98	-132.56
STORY14	PUSHX	Bottom	4680.7	-48.49	-164.91
STORY13	PUSHX	Bottom	5617.12	-57.75	-197
STORY12	PUSHX	Bottom	6553.74	-66.77	-228.61
STORY11	PUSHX	Bottom	7490.6	-75.58	-260.19
STORY10	PUSHX	Bottom	8427.71	-84.22	-291.54
STORY9	PUSHX	Bottom	9365.05	-92.74	-323.09
STORY8	PUSHX	Bottom	10302.58	-101.22	-354.56
STORY7	PUSHX	Bottom	11240.27	-109.73	-386.33
STORY6	PUSHX	Bottom	12177.98	-118.4	-418.39
STORY5	PUSHX	Bottom	13115.46	-127.35	-451.21
STORY4	PUSHX	Bottom	14052.31	-136.74	-485.03
STORY3	PUSHX	Bottom	14987.91	-146.65	-520.29
STORY2	PUSHX	Bottom	15921.51	-156.36	-558.35
STORY1	PUSHX	Bottom	16851.76	-158.93	-608.71

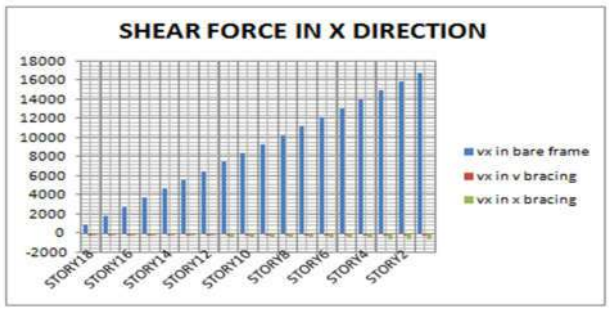

SHEAR FORCE IN Y DIRECTION

Story	Load	Loc	vy in bare frame	vy in v push	vy in x bracing
STORY18	PUSHY	Bottom	858.89	-9.74	-29.57
STORY17	PUSHY	Bottom	1717.77	-20.67	-58.79
STORY16	PUSHY	Bottom	2576.66	-31.5	-88.01
STORY15	PUSHY	Bottom	3435.55	-42.02	-117.1
STORY14	PUSHY	Bottom	4294.43	-52.25	-146.09
STORY13	PUSHY	Bottom	5153.32	-62.17	-174.99
STORY12	PUSHY	Bottom	6012.2	-71.81	-203.82
STORY11	PUSHY	Bottom	6871.09	-81.18	-232.58
STORY10	PUSHY	Bottom	7729.98	-90.31	-261.29
STORY9	PUSHY	Bottom	8588.86	-99.25	-290
STORY8	PUSHY	Bottom	9447.75	-108.04	-318.72
STORY7	PUSHY	Bottom	10306.63	-116.74	-347.43
STORY6	PUSHY	Bottom	11165.51	-125.44	-376.36
STORY5	PUSHY	Bottom	12024.4	-134.2	-405.33
STORY4	PUSHY	Bottom	12883.28	-143.12	-434.51
STORY3	PUSHY	Bottom	13742.17	-152.07	-463.91
STORY2	PUSHY	Bottom	14601.05	-160.29	-493.72
STORY1	PUSHY	Bottom	15459.94	-165.3	-526.95

BUILDING TORSION

Story	Load	Loc	t in bare frame	T in v push	t in x bracing
STORY18	PUSHX	Bottom	936.737	-96.682	-8.181
STORY17	PUSHX	Bottom	1876.364	-136.319	-124.959
STORY16	PUSHX	Bottom	2818.734	-201.683	-230.279
STORY15	PUSHX	Bottom	3766.318	-259.127	-328.172
STORY14	PUSHX	Bottom	4722.736	-314.566	-437.993
STORY13	PUSHX	Bottom	5691.668	-366.721	-500.968
STORY12	PUSHX	Bottom	6676.065	-414.908	-573.442
STORY11	PUSHX	Bottom	7678.544	-458.359	-660.607
STORY10	PUSHX	Bottom	8702.286	-496.243	-730.947
STORY9	PUSHX	Bottom	9750.64	-527.621	-766.863
STORY8	PUSHX	Bottom	10826.819	-551.42	-820.843
STORY7	PUSHX	Bottom	11934.21	-566.372	-859.661
STORY6	PUSHX	Bottom	13077.158	-570.944	-866.833
STORY5	PUSHX	Bottom	14262.297	-563.219	-865.264
STORY4	PUSHX	Bottom	15499.548	-540.894	-841.258
STORY3	PUSHX	Bottom	16803.209	-498.053	-787.296
STORY2	PUSHX	Bottom	18226.052	-436.93	-694.046
STORY1	PUSHX	Bottom	19890.283	-454.708	-589.41

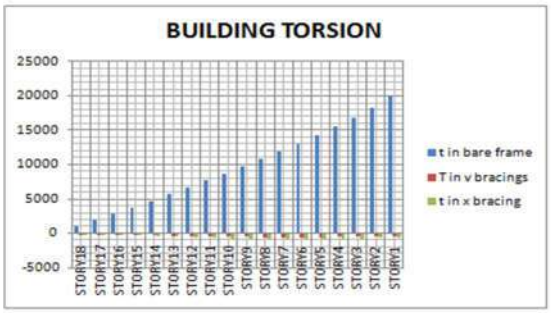

BENDING MOMENT IN X DIRECTION

Story	Load	Loc	mx in bare frame	mx in v push	Mx in x bracing
STORY18	PUSHX	Bottom	-962137.5	39857.74	142287.8
STORY17	PUSHX	Bottom	-1954585	80098.647	285968.4
STORY16	PUSHX	Bottom	-2949055	120374.26	429756.1
STORY15	PUSHX	Bottom	-3945301	160683.7	573653.1
STORY14	PUSHX	Bottom	-4943102	201026.6	717660.1
STORY13	PUSHX	Bottom	-5942257	241402.58	861777.4
STORY12	PUSHX	Bottom	-6942578	281811.3	1006006
STORY11	PUSHX	Bottom	-7943883	322252.42	1150345
STORY10	PUSHX	Bottom	-8945996	362725.63	1294795
STORY9	PUSHX	Bottom	-9948745	403230.65	1439356
STORY8	PUSHX	Bottom	-10951963	443767.26	1584027
STORY7	PUSHX	Bottom	-11955477	484335.31	1728810
STORY6	PUSHX	Bottom	-12959109	524934.73	1873702
STORY5	PUSHX	Bottom	-13962677	565565.58	2018703
STORY4	PUSHX	Bottom	-14965991	606227.97	2163812
STORY3	PUSHX	Bottom	-15968851	646921.76	2309029
STORY2	PUSHX	Bottom	-16970787	687646.73	2454349
STORY1	PUSHX	Bottom	-17977409	728495.75	2600246

BENDING MOMENT IN Y DIRECTION

Story	Load	Loc	my in bare frame	my in v push	my in x bracing
STORY18	PUSHY	Bottom	884712.14	-39861.35	-119383
STORY17	PUSHY	Bottom	1797491.5	-80101.02	-239836
STORY16	PUSHY	Bottom	2712535.5	-120371.8	-360382
STORY15	PUSHY	Bottom	3629739.2	-160675.3	-481021
STORY14	PUSHY	Bottom	4549000	-201011	-601754
STORY13	PUSHY	Bottom	5470218.1	-241378.8	-722581
STORY12	PUSHY	Bottom	6393293.2	-281778.4	-843503
STORY11	PUSHY	Bottom	7318117.8	-322209.6	-964519
STORY10	PUSHY	Bottom	8244574.6	-362672	-1085630
STORY9	PUSHY	Bottom	9172550.1	-403165.7	-1206836
STORY8	PUSHY	Bottom	10101949	-443690.5	-1328137
STORY7	PUSHY	Bottom	11032701	-484246.4	-1449532
STORY6	PUSHY	Bottom	11964778	-524833.6	-1571021
STORY5	PUSHY	Bottom	12898237	-565452.5	-1692603
STORY4	PUSHY	Bottom	13833313	-606103.6	-1814277
STORY3	PUSHY	Bottom	14770607	-646787.5	-1936040
STORY2	PUSHY	Bottom	15711493	-687503	-2057890
STORY1	PUSHY	Bottom	16670835	-728351.9	-2180226

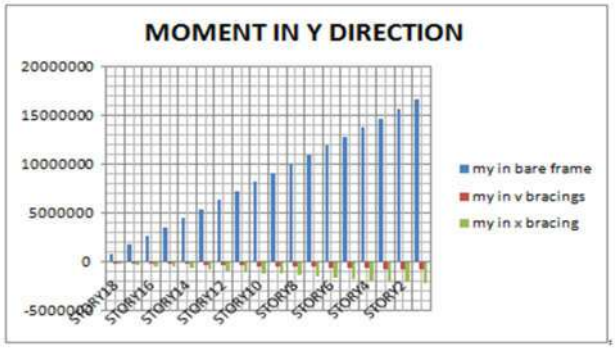

B.EQUVALENT STATIC ANALYSIS

STORY DRIFT IN X DIRECTION

Story	Item	drift x in bare frame	drift x in v bracing	drift x in x bracing
STORY18	STATIC	0.000276	0.000399	0.005673
STORY17	STATIC	0.000372	0.000482	0.005499
STORY16	STATIC	0.000483	0.00059	0.005436
STORY15	STATIC	0.000598	0.000697	0.005476
STORY14	STATIC	0.000713	0.000807	0.005526
STORY13	STATIC	0.000828	0.000918	0.005557
STORY12	STATIC	0.000943	0.001028	0.005562
STORY11	STATIC	0.001057	0.001137	0.005539
STORY10	STATIC	0.001171	0.001245	0.005481
STORY9	STATIC	0.001283	0.001349	0.005384
STORY8	STATIC	0.001395	0.001449	0.005242
STORY7	STATIC	0.001505	0.001544	0.00505
STORY6	STATIC	0.001614	0.001632	0.004802
STORY5	STATIC	0.001721	0.001735	0.00449
STORY4	STATIC	0.001827	0.001855	0.004099
STORY3	STATIC	0.001931	0.001991	0.003622
STORY2	STATIC	0.00204	0.002298	0.002992
STORY1	STATIC	0.002069	0.002446	0.001741

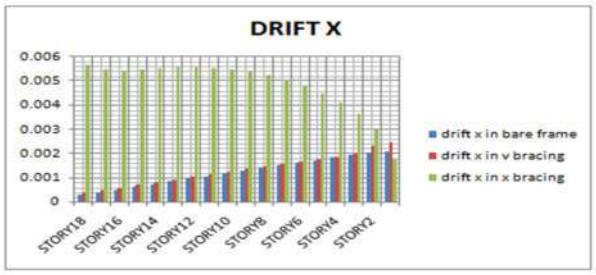

STORY DRIFT IN Y DIRECTION

Story	Item	drift y in bare frame	drift y in v bracing	drift y in x bracing
STORY18	STATIC	0.00064	0.001284	0.004215
STORY17	STATIC	0.00117	0.001426	0.004463
STORY16	STATIC	0.0017	0.001584	0.004525
STORY15	STATIC	0.00224	0.001765	0.004641
STORY14	STATIC	0.00278	0.001952	0.00475
STORY13	STATIC	0.00331	0.002142	0.004829
STORY12	STATIC	0.00385	0.002329	0.004876
STORY11	STATIC	0.00439	0.002511	0.004891
STORY10	STATIC	0.00492	0.002684	0.00487
STORY9	STATIC	0.00545	0.002844	0.00481
STORY8	STATIC	0.00598	0.002987	0.004708
STORY7	STATIC	0.00651	0.003107	0.004561
STORY6	STATIC	0.00704	0.003201	0.004366
STORY5	STATIC	0.00757	0.003282	0.004123
STORY4	STATIC	0.00809	0.003352	0.003846
STORY3	STATIC	0.00861	0.003392	0.003697
STORY2	STATIC	0.00944	0.003451	0.003113
STORY1	STATIC	0.02297	0.003871	0.002117

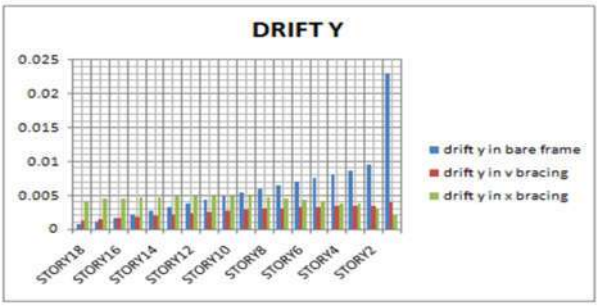

LATERAL FORCES (P)

Story	Load	Loc	p in bare frame	p in v bracing	p In x bracing
STORY18	STATIC	Bottom	28799.8	28886.79	28375.05
STORY17	STATIC	Bottom	57599.59	57731.58	56750.1
STORY16	STATIC	Bottom	86399.39	86576.37	85125.16
STORY15	STATIC	Bottom	115199.18	115421.15	113500.21
STORY14	STATIC	Bottom	143998.98	144265.94	141875.26
STORY13	STATIC	Bottom	172798.78	173110.73	170250.31
STORY12	STATIC	Bottom	201598.57	201955.52	198625.36
STORY11	STATIC	Bottom	230398.37	230800.31	227000.41
STORY10	STATIC	Bottom	259198.16	259645.1	255375.47
STORY9	STATIC	Bottom	287997.96	288489.88	283750.52
STORY8	STATIC	Bottom	316797.76	317334.67	312125.57
STORY7	STATIC	Bottom	345597.55	346179.46	340500.62
STORY6	STATIC	Bottom	374397.35	375024.25	368875.67
STORY5	STATIC	Bottom	403197.15	403869.04	397250.73
STORY4	STATIC	Bottom	431996.94	432713.83	425625.78
STORY3	STATIC	Bottom	460796.74	461558.61	454000.83
STORY2	STATIC	Bottom	489596.53	490403.4	482375.88
STORY1	STATIC	Bottom	518549.46	519407.83	511159.32

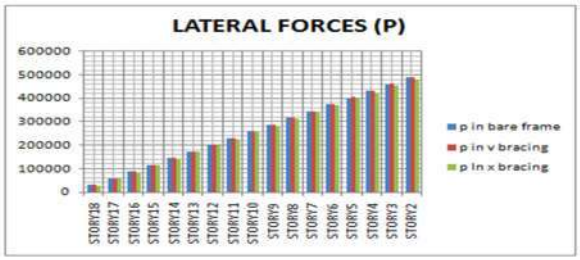

SHEAR FORCE IN X DIRECTION

Story	Load	Loc	vx in bare frame	vx in v bracing	vx in x bracing
STORY18	STATIC	Bottom	-255	-255	-127.5
STORY17	STATIC	Bottom	-510	-552	-255
STORY16	STATIC	Bottom	-765	-849	-382.5
STORY15	STATIC	Bottom	-1020	-1146	-510
STORY14	STATIC	Bottom	-1275	-1443	-637.5
STORY13	STATIC	Bottom	-1530	-1740	-765
STORY12	STATIC	Bottom	-1785	-2037	-892.5
STORY11	STATIC	Bottom	-2040	-2334	-1020
STORY10	STATIC	Bottom	-2295	-2631	-1147.5
STORY9	STATIC	Bottom	-2550	-2928	-1275
STORY8	STATIC	Bottom	-2805	-3225	-1402.5
STORY7	STATIC	Bottom	-3060	-3522	-1530
STORY6	STATIC	Bottom	-3315	-3819	-1657.5
STORY5	STATIC	Bottom	-3570	-4116	-1785
STORY4	STATIC	Bottom	-3825	-4413	-1912.5
STORY3	STATIC	Bottom	-4080	-4710	-2040
STORY2	STATIC	Bottom	-4335	-5007	-2167.5
STORY1	STATIC	Bottom	-4590	-5304	-2295

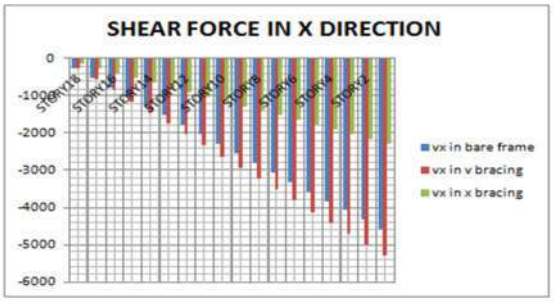

BUILDING TORSION

Story	Load	Loc	Tin bare frame	Tin v bracing	Tin x bracing
STORY18	STATIC	Bottom	-255	-255	-127.5
STORY17	STATIC	Bottom	-510	-552	-255
STORY16	STATIC	Bottom	-765	-849	-382.5
STORY15	STATIC	Bottom	-1020	-1146.001	-510
STORY14	STATIC	Bottom	-1275	-1443.001	-637.5
STORY13	STATIC	Bottom	-1530	-1740.001	-765
STORY12	STATIC	Bottom	-1785	-2037.001	-892.5
STORY11	STATIC	Bottom	-2040	-2334.001	-1020
STORY10	STATIC	Bottom	-2295	-2631.002	-1147.5
STORY9	STATIC	Bottom	-2550	-2928.002	-1275
STORY8	STATIC	Bottom	-2805	-3225.002	-1402.5
STORY7	STATIC	Bottom	-3060	-3522.002	-1530
STORY6	STATIC	Bottom	-3315	-3819.002	-1657.5
STORY5	STATIC	Bottom	-3570	-4116.003	-1785
STORY4	STATIC	Bottom	-3825	-4413.003	-1912.5
STORY3	STATIC	Bottom	-4080	-4710.003	-2040
STORY2	STATIC	Bottom	-4335	-5007.003	-2167.5
STORY1	STATIC	Bottom	-4590	-5304.003	-2295

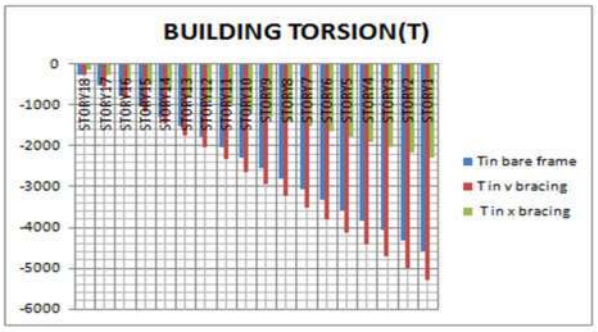

SHEAR FORCE IN Y DIRECTION

Story	Load	Loc	vy in bare frame	vy in v bracing	vy in x bracing
STORY18	STATIC	Bottom	-255	-255	-127.5
STORY17	STATIC	Bottom	-510	-552	-255
STORY16	STATIC	Bottom	-765	-849	-382.5
STORY15	STATIC	Bottom	-1020	-1146	-510
STORY14	STATIC	Bottom	-1275	-1443	-637.5
STORY13	STATIC	Bottom	-1530	-1740	-765
STORY12	STATIC	Bottom	-1785	-2037	-892.5
STORY11	STATIC	Bottom	-2040	-2334	-1020
STORY10	STATIC	Bottom	-2295	-2631	-1147.5
STORY9	STATIC	Bottom	-2550	-2928	-1275
STORY8	STATIC	Bottom	-2805	-3225	-1402.5
STORY7	STATIC	Bottom	-3060	-3522	-1530
STORY6	STATIC	Bottom	-3315	-3819	-1657.5
STORY5	STATIC	Bottom	-3570	-4116	-1785
STORY4	STATIC	Bottom	-3825	-4413	-1912.5
STORY3	STATIC	Bottom	-4080	-4710	-2040
STORY2	STATIC	Bottom	-4335	-5007	-2167.5
STORY1	STATIC	Bottom	-4590	-5304	-2295

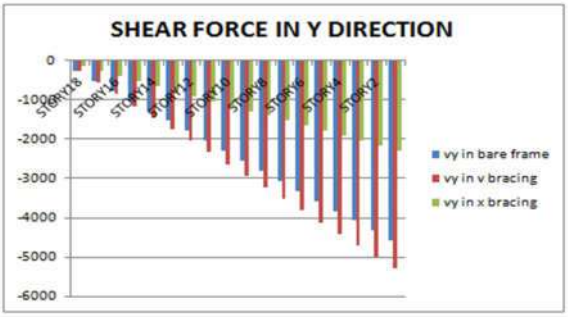

BENDING MOMENT IN X DIRECTION

Story	Load	Loc	MXin bare frame	Mxin v bracing	Mxin x bracing
STORY18	STATIC	Bottom	720504.9	723787.08	710231.4
STORY17	STATIC	Bottom	1441774.8	1447373.2	1420845.3
STORY16	STATIC	Bottom	2163809.7	2171850.2	2131841.7
STORY15	STATIC	Bottom	2886609.6	2897218.3	2843220.6
STORY14	STATIC	Bottom	3610174.3	3623477.4	3554982
STORY13	STATIC	Bottom	4334504.4	4350627.5	4267125.9
STORY12	STATIC	Bottom	5059599.3	5078668.5	4979652.3
STORY11	STATIC	Bottom	5785459.2	5807600.6	5692561.2
STORY10	STATIC	Bottom	6512084.1	6537423.7	64038526
STORY9	STATIC	Bottom	723947.4	7268137.8	7119526.5
STORY8	STATIC	Bottom	7967628.9	7999742.8	7833582.9
STORY7	STATIC	Bottom	8696548.8	8732238.9	8548021.8
STORY6	STATIC	Bottom	9426233.7	9465626	9262843.2
STORY5	STATIC	Bottom	10156684	10199904	9978047.1
STORY4	STATIC	Bottom	10887899	10935073	10693633
STORY3	STATIC	Bottom	11619878	11671133	11409602
STORY2	STATIC	Bottom	12352623	12408084	12125954
STORY1	STATIC	Bottom	13092256	13152650	12854024

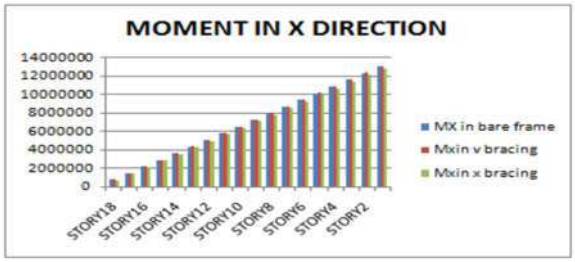

BENDING MOMENT IN Y DIRECTION

Story	Load	Loc	MY in bare frame	MY in v bracing	MY in x bracing
STORY18	STATIC	Bottom	-721014.9	-723664.3	-710031.2
STORY17	STATIC	Bottom	-1442795	-1447212	-1420445
STORY16	STATIC	Bottom	-2165340	-2171650	-2131241
STORY15	STATIC	Bottom	-2888650	-2896979	-2842420
STORY14	STATIC	Bottom	-3612725	-3623199	-3553981
STORY13	STATIC	Bottom	-4337564	-4350311	-4265924
STORY12	STATIC	Bottom	-5063169	-5078313	-4978251
STORY11	STATIC	Bottom	-5789539	-5807206	-5690959
STORY10	STATIC	Bottom	-6516674	-6536991	-6404050
STORY9	STATIC	Bottom	-7244574	-7267666	-7117524
STORY8	STATIC	Bottom	-7973239	-7999232	-7831380
STORY7	STATIC	Bottom	-8702669	-8731690	-8545619
STORY6	STATIC	Bottom	-9432864	-9465038	-9260240
STORY5	STATIC	Bottom	-10163824	-10199277	-9975244
STORY4	STATIC	Bottom	-10895549	-10934407	-10690630
STORY3	STATIC	Bottom	-11628038	-11670429	-11406399
STORY2	STATIC	Bottom	-12361293	-12407341	-12122550
STORY1	STATIC	Bottom	-13101436	-13151822	-12850408

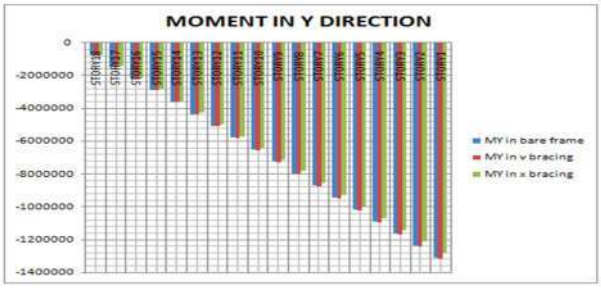

V.CONCLUSIONS

- The pushover analysis is relatively simple way to explore the non-linear behavior of buildings and it is an elegant tool to visualize the performance level of a building under a given earthquake.
- The Drift values in the V braced building shows very less storey drifts due to arrangements of the V braces in the buildings .
- The shear force in the industrial steel structure due to arrangement of the bracings , the braced building of V braced system shows very less values when compared to the other building systems.
- The bending moments of the steel structure shows the very high moments and the least moments are observed in V braced building due to its arrangement in the buildings.
- The overturning moments of the buildings observed to more in the steel building and X braced building systems , the least values are observed in the V braced systems.

Considering all the above results the V braced building systems shows the best results and next to the that is X braced building systems.

- The Drift values in the Equivalent static analysis the steel buildings also shows very high displacements when compared to the other building systems , the V braced building systems are best suitable structures.
- The shear values in the Equivalent static analysis the V braced building systems shows that the less shear values compared to the other building systems.
- The bending in the Equivalent static analysis the V braced building systems shows that the less Bending values compared to the other building systems. due to the arrangements bracings in the buildings .
- The overturning moments in the equivalent static analysis results shows that the less overturning moments in V braced building systems when compared to the other steel and X braced structures.

Comparing the above results the V braced steel Building is best suited structure according to the Pushover analysis. And the X braced building is the Best structure according to the equivalent static analysis.

SCOPE OF THE FUTURE WORK:

- By using bracings in the structures, the displacement of the structure greatly reduced can be changed or altered. Hence the further study can be done by examining the behavior of the storey building due to wind load forces and Time history analysis.
- We can also study on the behavior of Bending Moment, shear Force etc.
- We can study other types of bracings in different Zones for the different soil type conditions.
- We can study for the different sections in tall structures and compare with and without bracings.

REFERANCES

[1] Theory of Structures by Ramamrutham for literature review on kani′s method
[2] Theory of structures by B.C.Punmia for literature on moment distribution method.
[3] Reinforced concrete Structures by A.K. Jain and B.C. Punmia for design of beams, columns and slab.
[4] Fundamentals of concrete structure by N. C. Sinha.

[5] S.Mahesh and Dr.B.Panduranga Rao Comparison of analysis and design of regular and irregular configuration of multi Story building in various seismic zones and various types of soils were using STAAD Volume 11, Issue 6 Ver. I (Nov- Dec. 2014), PP 45-52

[6] Kevadkar M.D., Kodag P.B., 'Lateral load (loads due to earthquake, wind, blast, fire hazards etc) (earthquake loads, wind loads, blast, fire hazards etc) Analysis of R.C.C. Building', International Journal of Modern Engineering Research (IJMER), Vol.3, Issue.3, May-June. 2013, pp-1428-1434.

[7] Salehuddin Shamshinar, Stability of a six storey steel frame structure, International Journal of Civil & Environmental Engineering, Vol.13 No.06, 2011. User Manual STAAD.Pro.

[8] Chopra, A. K., Dynamics of Structures (1995): Theory and Applications to Earthquake Engineering, Prentice-Hall. Inc., Englewood Cliffs, New Jersey.

[9] IS 1893 : 2002, Indian Standard criteria for earthquake resistant design of frames, Part 1 General provisions and buildings, Draft of Fifth Revision, Bureau of Indian Standards, New Delhi, 2002.

[10] IS: 875(Part-1)- 1987 ‘Code of Practice for Design Loads (Other than Earthquake) buildings and frames’, Part-1 Dead load, Unit weight of building materials and stored materials, Bureau of Indian Standards, New Delhi.

Strength and Permeability Properties of concrete using fly Ash, rice husk Ash, and Ground Granulated Blast Furnace Slag

Salem Ahmed Ali[1],Salahuddin Shakeeb S.M[2] Mohd Farrukh Anwar[3]

[1] Pg Student, M.Tech in Structural engineering, Department of Civil Engineering, Nawab Shah Alam Khan College of Engineering and Technology, 6-4-1, New Malakpet, Near Railway Station, Hyderabad, Telangana 500024

[2] Assistant Professor, M.Tech in Structural engineering, Department of Civil Engineering, Nawab Shah Alam Khan College of Engineering and Technology, 6-4-1, New Malakpet, Near Railway Station, Hyderabad, Telangana 500024

[3]Head of the Department (PHD) , Vice Principal ,M.Tech in Structural engineering, Department of Civil Engineering, Nawab Shah Alam Khan College of Engineering and Technology, 6-4-1, New Malakpet, Near Railway Station, Hyderabad, Telangana 500024

Abstract: ***cement industry may be one amongst the key sources of environmental pollution so the reduction of cement demand should be improved. Fly ash(FA), Rice husk ash(RHA) and Ground granulated blast furnace slag (GGBS) are the by-products of industries and it ought to be reused to scale back the waste pollution. Therefore the present study is directed towards developing a better understanding on the combined performance of FA,RHA and GGBS on the strength properties of Ternary concrete over an Ordinary concrete. This work primarily deals with the strength characteristics such as Compressive, Split Tensile and Flexural Strength. Total 5 Different concrete mixtures were cast and tested with different cement replacement levels (5%, 10%,15%,20%,25%) of combination of three byproducts .Compressive ,Split Tensile and Flexural Strength of Ternary Blended Concrete At the ages of 7, 28, 60 and 90 days for various combinations FA,RHA, and GGBS..All Mixes were studied at water cement ratio of 0.50 and 0.40. The cement has been replaced by rice husk ash, accordingly in the range of 0%, 5 %, 10 %, 15 %, and 20 % by weight. Concrete mixture of M 30 and M40with RHA, were produced, tested and compared in terms of compressive strengths with the Conventional concrete. These tests were carried out to evaluate the mechanical properties for the test results of 7, 28, 56, 90 days for compressive strengths in normal water and in MgSO4 solution of 1% and 5%. Also the durability aspect for rice husk ash concrete for sulphate attack was tested. Similarly the above tests were also performed for FA and SCBA The experimental results shows that, the strength properties of ternary blended concrete increase with increase in cement replacement levels of FA,RHA, and GGBS.. (20%),the addition of FA,RHA, and GGBS does not improve the strength properties of compressive, Split Tensile and Flexural, durability tests are also performed.***

Key words: ***Fly Ash, Rice Husk Ash, GGBS, Concrete, M30 grade concrete M40 grade concrete, cubes, cylinders, MgSO4, durability.***

I.INTRODUCTION

These days researchers are studying different agro-based waste materials. The major quantities of waste generated from agricultural sources include sugarcane bagasse, rice husk, and coconut husk. Reusing such waste as a sustainable construction material seems to be a suitable solution for the problem of land filling and the high cost of building materials (Rabi et al 2009). These days, agricultural solid waste materials are being reused in manufacturing blended mortars and concrete for better performance and price. The use of waste materials in concrete has been a continuous procedure in different industries. These waste agricultural materials are used to heighten the mechanical properties of a building material while they are not useful in agriculture fields. Rice husk ash (RHA), sugarcane bagasse ash (SCBA), sawdust and cork granules have been used as pozzolanic materials for reactivity in concrete. They are added to concrete to partially replace cement in concrete mixtures so that the concrete will have sufficient engineering physical and chemical properties. RHA has been used as a suitable raw material to make hydraulic cement and as a good corrective admixture to reduce expansion that occurs as a result of an alkali-silicate reaction, and also to reduce the temperature in high-strength concrete SCBA is a valuable cement-replacing material for cement and concrete production because of its high content of silicon and aluminium oxides. Also, the effect of elevated temperature on strength of normal and high strength concrete with and without different ashes is investigated by different researchers.

FLY ASH

Fly ash is a fine powder which is a byproduct from burning pulverized coal in electric generation power plants. Fly ash is a pozzolana, a substance containing aluminous and siliceous material that forms cement in the presence of water. When mixed with lime and water it forms a compound similar to Portland cement. The fly ash produced by coal-fired power plants provide an excellent prime material used in blended cement, mosaic tiles, and hollow blocks among others. Fly ash can be an expensive replacement for Portland cement in concrete although using it improves strength, segregation, and ease of pumping concrete. The rate of substitution typically specified is 1 to 1 ½ pounds of fly ash to 1 pound of cement. Nonetheless, the amount of fine aggregate should be reduced to accommodate fly ash additional volume.

RICE HUSK ASH

Rice husk is an agricultural residue which accounts for 20% of the 649.7 million tons of rice produced annually worldwide[1]. The produced partially burnt husk from the milling plants when used as a fuel also contributes to pollution and efforts are being made to overcome this environmental issue by utilizing this material as a supplementary cementing material[2]. The chemical composition of rice husk is found to vary from one sample to another due to the differences in the type of paddy, crop year, climate and geographical conditions

GROUND GRANULATED BLAST FURNACE SLAG

Ground Granulated Blast furnace Slag (GGBS) is a byproduct from the blast furnaces used to make iron. These operate at a temperature of about 1500 degrees centigrade and are fed with a carefully controlled mixture of iron ore, coke and limestone. The iron ore is reduced to iron and the remaining materials from a slag that floats on top of the iron. This slag is periodically tapped off as a molten liquid. and if it

is to be used for the manufacture of GGBS it has to be rapidly quenched in large volumes of water. The quenching optimizes the cementations properties and produces granules similar to coarse sand. This „granulated" slag is then dried and ground to a fine powder. Although normally designated as "GGBS" in the UK, it can also be referred to as "GGBS" or "Slag cement" Concrete is basically a mix of fine aggregate, coarse aggregate and cement. The main problem is the original conventional materials are depleting and we are in hunt for alternate building materials which lands us here on the purpose of GGBS. Being a by product and waste using it effectively up to some extent serves as a step for a greener environment and at the same time keeping in mind that the strength of the concrete doesn't degrade by the usage GGBS.

OBJECTIVE OF THE STUDY

Depending on the suitability of Bagasse ash, it can be used as resource material in the following applications:

- Silica source as it contains high amount of silica in it.
- Brick production as BA used as additive in making bricks that have high compressive strength and low water absorption bricks.
- Farm fertilizer as it contains traces of potassium and phosphorus compounds etc.
- To compare the tests results of fly ash, rice husk ash, and sugarcane Bagasse ash with the normal concrete.
- To find the optimum usage of the percentage replacement of the fly ash , rice husk ash, baggage ash to the concrete.

SCOPE OF THE STUDY

The primary aim of experimental work is to study the properties of sugar cane bagasse ash. Preparation of mix design Replacement of cement with SCBA as different proportions with cement.

- Effect of a GGBS on workability.
- Effect of fly ash and rice husk ash on the strength of the concrete.
- Effect on compressive strength of concrete.
- Effect on split tensile strength of concrete.
- To determine the optimum dosage of the GGBS, Fly ash, Rice husk ash to be added to the concrete mix.
- Comparison of result of different tests with varying proportion of FA, RHA and GGBS.

II.LITERATURE REVIEW

Sagar Dhengare [1], Sourabh Amrodiya[2] and Mohanish Shelote[3] et all,. In developing countries, accumulation of unmanaged agricultural waste has resulted in an increased environmental concern. Recycling of such agricultural wastes is the viable solution not only to pollution problem, but also the problem of land filling. In view of utilization of agricultural waste in concrete and mortar, the present paper reviews, utilization of sugarcane Bagasse ash (SCBA) in different compositions that were added to the raw material at different levels to develop sustainable concrete and mortar. Various physic-mechanical properties of the concrete and mortar incorporating sugarcane Bagasse ash are reviewed and recommendations are suggested as the outcome of the study. The study in turn is useful for various resource SCBA material to develop sustainable construction material.

Mangesh V Madurwar, Sachin A Mandavgane, Ph.D. et al (2014) SBA-QD-L bricks are up to40%

lighter than the conventional locally available bricks and hence support in lightweight construction projects with larger design loads. Observations during the tests showed that SBA-QD-L brick composition with SBA (50% by weight), quarry dust (30% by weight), and lime (20% by weight) exhibits the water absorption of 19.70% (less than 20%) and the compressive strength of 6.59 MPa, which is almost double the conventional commercially available clay bricks (3.5 MPa) and satisfies the requirements in IS: 2185 (Part-I) (BIS 1979) and SP: 21 (BIS 1983) for a building material.

Cbatveera, P. NtmJtyonglkul. et al (1994) This research is conducted to develop new kinds of pozzolana from other agricultural wastes apart from rice husk and rice straw. The study investigated the use of coconut husk, Corn cob and peanut shell ash as pozzolana. The properties of CHA, CCA and PSA namely specific gravity, fineness, chemical composition and the strength activity index with Portland cement were determined. For properties of paste, only ordinary Portland cement and 30% PSA were investigated for normal consistency and initial and final setting time. CCA mortars have lower compressive strength than the controlled mortar (0% CCA) while PSA mortars showed higher compressive strength than the controlled mortar (0% PSA).Among the four mortars tested for chemical attack, PSA mortars showed higher resistance against sulphate attach and RHA against acidic attack.

III.METHODOLOGY

CEMENT

Cement is a binder, a substance used in construction that sets and hardens and can bind other materials together. The most important types of cement are used as a component in the production of mortar in masonry, and of concrete which is a combination of cement and an aggregate to form a strong building material.

OPC 53 GRADE CEMENT

COARSE AGGREGATE

Crushed stone aggregate of 20mm size is brought from nearby quarry. Aggregates of size more than 20mm size are separated by sieving. Tests are carried in order to find out the

• Specific gravity = 2.98

• Fineness modulus = 7.5

Coarse aggregate

FINE AGGREGATE:

Locally available fresh sand, free from organic matter is used. The result of sieve analysis confirms it to Zone-II (according to IS: 383-1970).The tests conducted and results plotted below.

- Specific gravity = 2.3
- Fineness modulus = 3.06

Fine aggregates

Super plastizers (perma super plast 220)

Perma Plast Super- 220 is a high range, low dosage, super plasticising admixture for slump retention. It is a product based on refined naphthalene formaldehyde and ligno sulfonate blends. To produce self-compacting flowing concrete. To produce high early strength concrete for delayed slump retention and for long overhauls. Ideally suited for commercial RMC plants and concrete made with crushed sand.For the production of high workability concrete where heavily congested reinforcement exist or poor access is available. To produce flowing self Compacting concrete which requires minimal labour to place. For the production of high strength, high workability concrete. Particularly beneficial in hot climatic conditions and in ready mix concrete. It is based on naphthalene formaldehyde blends.

MIX DESIGN

Final trial mix for M30 grade concrete is 1:1.64:2.55 at w/c of 0.45

GRADE OF CONCRETE	CEMENT KGS	Granulated ground blast furncace slag (GGBS)	Fly Ash	Rice husk Ash	Fine aggregates	coarse aggregates	water content	Admixture
M30	183.82	7.32	7.32	7.32	502	780	88	4
Addition of extra 10%	202.20	8.052	8.052	8.052	552.2	858	96.8	4.818

Final trial mix for M40 grade concrete is 1:2.29:3.56 at w/c of 0.40

GRADE OF CONCRETE	CEMENT KGS	Granulated ground blast furnace slag (GGBS)	Fly Ash	Rice husk Ash	Fine aggregates	coarse aggregates	water content	Admixture
M40	194	7.32 Kgs	7.32 kgs	7.32 kgs	502	780	87.2	4.38
Addition of extra 10%	213.4	8.05	8.05	8.05	552.2	858	8.72	0.44

IV.RESULTS

MATERIAL PROPERTIES

Test results on the cement

Sl.no	Test	Results	IS code used	Acceptable limit
1	Specific gravity of cement	3.10	IS:2386:1963	3 to 3.2
2	Standard consistency of cement	6mm at 32% w/c	IS:4031:1996	w/c ratio 28%-35%
3	Initial and final setting time	45 mins and 10 hours	IS:4031:1988	Minimum 30mins and should not more than 10 hours
4	Fineness of cement	4.00%	IS:4031:1988	<10%

Test results on coarse aggregates

Sl.no	Test	Results	Is code used	Acceptable limit
1	Fineness modulus	6.8	IS:2386:1963	6.0 to 8.0mm
2	Specific gravity	2.95	IS:2386:1963	2 to 3.1mm
3	Porosity	46.83%	IS:2386:1963	Not greater than 100%
4	Voids ratio	0.8855	IS:2386:1963	Any value
5	Bulk density	1.50g/cc	IS:2386:1963	-
6	Aggregate impact value	35.5	IS:2386:1963	Less than 45%
7	Aggregate crushing value	27.5%	IS:2386:1963	Less than 45%

Test results on the fine aggregates

Sl.no	Test	Result	Is code used	Acceptable limits
1	Fineness modulus	4.5	IS:2386:1963	Not more than 3.2 mm
2	Specific gravity	2.43	IS:2386:1963	2.0 to 3.1
3	Porosity	36.6%	IS:2386:1963	Not greater than 100%
4	Voids ratio	0.577	IS:2386:1963	Any value
5	Bulk density	1.5424	IS:2386:1963	-
6	Bulking of sand	4.0%	IS:2386:1963	Less than 10%

slump values for concrete

S.NO	% Replacement	Slump for M30grade	Slump for M40 grade
1	0%	55	52
2	1.67% FA+1.67% RHA+1.67% GGBS	67	68
3	3.33% FA+3.33% RHA+3.33% GGBS	72	79
4	5% FA+5% RHA+5% GGBS	78	80
5	6.67% FA+6.67% RHA+6.67% GGBS	85	92

Compaction factor Test

S.NO	% Replacement	Compaction factor for M30 grade concrete	Compaction factor for M40 grade concrete
1	0%	0.98	0.94
2	1.67% FA+1.67% RHA+1.67% GGBS	0.95	0.9
3	3.33% FA+3.33% RHA+3.33% GGBS	0.88	0.88
4	5% FA+5% RHA+5% GGBS	0.88	0.84
5	6.67% FA+6.67% RHA+6.67% GGBS	0.86	0.86

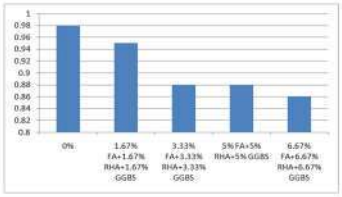

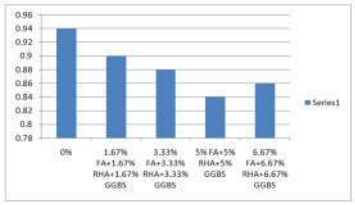

Compressive strength:

s.no	% Replacement	Compressive strength of concrete			
		M30 grade concrete		M40 grade concrete	
		7 days	28 days	7 days	28 days
1	0%	28.84	29.6	38.6	39.86
2	1.67% FA+1.67% RHA+1.67% GGBS	28.6	29.2	37.24	37.44
3	3.33% FA+3.33% RHA+3.33% GGBS	27.4	29.8	36.6	37.9
4	5% FA+5% RHA+5% GGBS	26.4	27	35.4	36.2
5	6.67% FA+6.67% RHA+6.67% GGBS	25.6	26.4	32.8	34.22

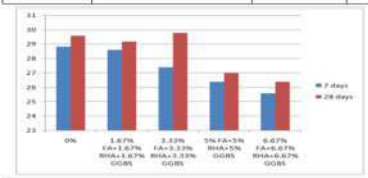

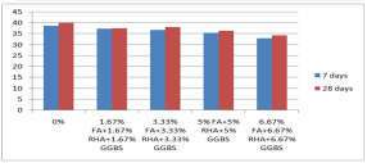

Split tensile strength of concrete

S.no	% Replacement	28 days split tensile strength for M30 grade	28 days split tensile strength for M40 grade
1	0%	4.82	5.28
2	1.67% FA+1.67% RHA+1.67% GGBS	5.21	5.16
3	3.33% FA+3.33% RHA+3.33% GGBS	5.53	5.2
4	5% FA+5% RHA+5% GGBS	5.45	5.46
5	6.67% FA+6.67% RHA+6.67% GGBS	5.8	4.8

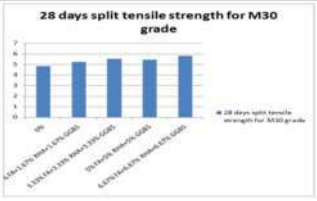

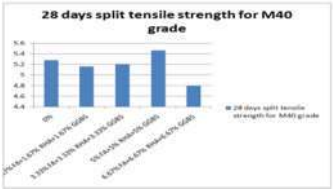

Flexural strength of concrete:

S.no	% Replacement	28 days flexural strength for M30 grade concrete	28 days flexural strength for M40 grade concrete
1	0%	5.54	5.8
2	1.67% FA+1.67% RHA+1.67% GGBS	5.71	5.6
3	3.33% FA+3.33% RHA+3.33% GGBS	5.74	5.74
4	5% FA+5% RHA+5% GGBS	5.92	6.1
5	6.67% FA+6.67% RHA+6.67% GGBS	6.36	6.4

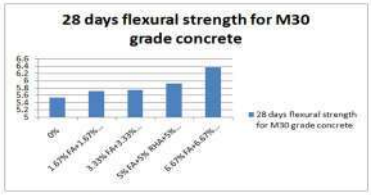

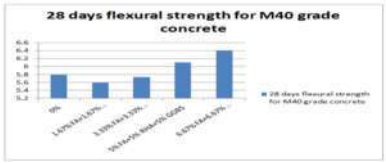

Durability

For M30 grade concrete for acid attack

Sl.no	% replacement	Initial weight of cube after 28days curing in grams	Final weight of cubes after 90days curing in grams	% loss of weight due to acid attack	Compressive strength of cube after 28days curing	Compressive strength of cubes after 90days curing	% loss of compressive strength due to acid attack
1	0%	2261	2242	0.82	29.6	26.95	8.96
2	1.67% FA+1.67% RHA+1.67% GGBS	2340	2318	0.94	29.2	26.51	9.2
3	3.33% FA+3.33% RHA+3.33% GGBS	2351	2323	1.2	29.8	26.94	9.6
4	5% FA+5% RHA+5% GGBS	2234	2202	1.44	27	24.5	9.2
5	6.67% FA+6.67% RHA+6.67% GGBS	2394	2356	1.6	26.4	23.6	10.6

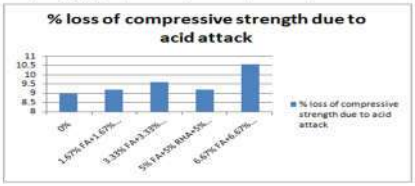

Alkaline attack

Sl. No	% replacement	Initial weight of cube after 28days curing in grams	Final weight of cubes after 90days curing in grams	% loss of weight due to alkaline attack	Compressive strength of cube after 28days curing	Compressive strength of cubes after 90days curing	% loss of compressive strength due to alkaline attack
1	0%	2266	2239	1.2	29.6	25.98	12.26
2	1.67% FA+1.67% RHA+1.67% GGBS	2340	2306	1.44	29.2	25.3	13.34
3	3.33% FA+3.33% RHA+3.33% GGBS	2280	2244	1.6	29.8	25.86	13.2
4	5% FA+5% RHA+5% GGBS	2310	2268	1.84	27	23.32	13.62
5	6.67% FA+6.67% RHA+6.67% GGBS	2296	2251	1.96	26.4	22.67	14.1

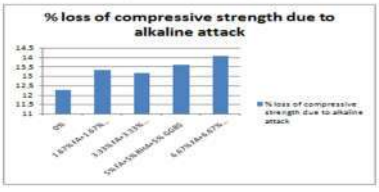

Sulphate attack test

Sl.no	% replacement	Compressive strength of cube after 28days curing	Compressive strength of cubes after 90days curing	% loss of compressive strength due to sulphate attack
1	0%	29.6	24.07	18.66
2	1.67% FA+1.67% RHA+1.67% GGBS	29.2	23.65	18.98
3	3.33% FA+3.33% RHA+3.33% GGBS	29.8	24.07	19.2
4	5% FA+5% RHA+5% GGBS	27	21.87	18.98
5	6.67% FA+6.67% RHA+6.67% GGBS	26.4	21.27	19.4

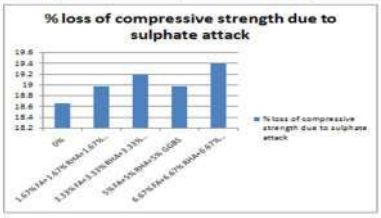

For M40 grade concrete:

Sl.no	% replacement	Initial weight of cube after 28days curing in grams	Final weight of cubes after 90days curing in grams	% loss of weight due to acid attack	Compressive strength of cube after 28days curing	Compressive strength of cubes after 90days curing	% loss of compressive strength due to acid attack
1	0%	2351	2349	0.09	39.86	35.4	11.24
2	1.67% FA+1.67% RHA+1.67% GGBS	2340	2312	1.2	37.44	33	11.84
3	3.33% FA+3.33% RHA+3.33% GGBS	2351	2318	1.4	37.9	33.5	11.6
4	5% FA+5% RHA+5% GGBS	2234	2194	1.8	36.2	31.81	12.12
5	6.67% FA+6.67% RHA+6.67% GGBS	2394	2341	2.2	34.22	29.98	12.4

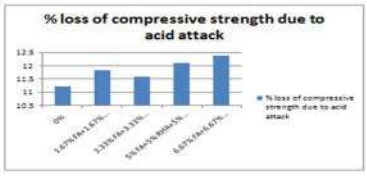

Alkaline attack

Sl. No	% replacement	Initial weight of cube after 28days curing in grams	Final weight of cubes after 90days curing in grams	% loss of weight due to alkaline attack	Compressive strength of cube after 28days curing	Compressive strength of cubes after 90days curing	% loss of compressive strength due to alkaline attack
1	0%	2351	2320	1.3	39.86	34.12	14.4
2	1.67% FA+1.67% RHA+1.67% GGBS	2340	2302	1.6	37.44	31.9	14.8
3	3.33% FA+3.33% RHA+3.33% GGBS	2260	2228	1.4	37.9	32	15.6
4	5% FA+5% RHA+5% GGBS	2245	2205	1.8	36.2	30.33	16.2
5	6.67% FA+6.67% RHA+6.67% GGBS	2260	2210	2.2	34.22	28.52	16.66

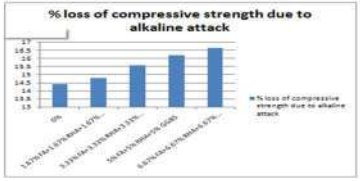

Sulphate attack test

Sl.no	% replacement	Compressive strength of cube after 28days curing	Compressive strength of cubes after 90days curing	% loss of compressive strength due to sulphate attack
1	0%	39.86	33.4	16.22
2	1.67% FA+1.67% RHA+1.67% GGBS	37.44	31.13	16.84
3	3.33% FA+3.33% RHA+3.33% GGBS	37.9	31.37	17.22
4	5% FA+5% RHA+5% GGBS	36.2	29.82	17.6
5	6.67% FA+6.67% RHA+6.67% GGBS	34.22	28	18.2

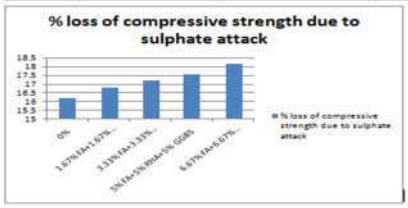

V.CONCLUSIONS

From the above experimental program the following conclusions were made

1. The material properties of the cement, fine aggregates and coarse aggregates are within the acceptable limits as per IS code recommendations so we will use the materials for research.
2. Slump cone value for the RHA, FA, GGBS concrete increases with increasing in the percentage of RHA, FA, GGBS so the concrete was not workable.
3.Compaction factor value of RHA, FA, GGBS concrete decreases with increase in the percentage of RHA, FA, GGBS
4. The compressive strength of concrete is maximum at 20% replacement of RHA, FA, GGBS and is the optimum value for 7days curing and 28days curing
5. Split tensile strength for the cylindrical specimens is maximum at 40% of replacement of copper slag for 28days curing.
6. The flexural strength of copper slag concrete is also maximum at 20% replacement of copper slag for 28 days of curing.
7. So the replacement of 5% to 20% of RHA, FA, GGBS is generally useful for better strength values in M30 And M40 grade of concrete.

FUTURE RECOMMENDATIONS:

- Using RHA, FA, GGBS with cement checking out whether the minimum strength

required for M50 and M60 grades of concrete can be achieved.

- Checking out the feasibility of utilization of HA, FA, GGBS finding the Strength characteristics of Concrete.

REFERENCES

1. Brindha, D and Nagan, S (2010). "Utilization of copper slag as a partial replacement of fine aggregate". International Journal of Earth Sciences and Engineering, Vol.3, No.4, pp.579-585

2. Wei Wu, Weide Zhang, Guowei Ma "Optimum content of copper slag as a fine aggregate in high strength concrete" Materials and Design, Elsevier science Ltd, Vol. 31, 2010, pp. 2878–2883.

3. Pazhani K, Jeyaraj R, "Study on durability of high performance concrete with industrial wastes", Peer-reviewed & Open access journal, ATI- Applied Technologies & Innovations, Vol. 2, Issue 2, August 2010, pp. 19-28.

4.Khalifa S Al-Jabri, Abdullah H Al-Saidy, Ramzi Taha, "Effect of copper slag as a fine aggregate on the properties of cement mortars and concrete", Construction and Building Materials, Vol. 25, 2011, pp. 933 – 938

5.Mostafa Khanzadi, Ali Beholds(2009), " Mechanical properties of high strength concrete incorporating copper slag as coarse aggregate" , Construction and Building Materials 23 pp 2183–2189.

6. Meenakshi Sudarvizhi, S. and Ilangovan, R. "Performance of copper slag and ferrous slag as partial replacement of sand in concrete", International Journal of Civil and Structural Engineering, Vol.1, No.4, 2011.

7. Chavan, R.R. and Kulkarni, D.B. "Performance of copper slag on strength properties as partial replacement of fine aggregate in concrete mix design", International Journal of Advanced Research and Studies, Vol.2, No.4, pp.95-98, 2013.

8. IS: 10262 – 2009, Concrete Mix Proportioning, Bureau of Indian Standards, New Delhi.

9. IS 516 (1959): Method of Tests for Strength of Concrete [CED 2: Cement and Concrete]

10.IS 2386-1 (1963): Methods of Test for Aggregates for Concrete, Part I: Particle Size and Shape [CED 2: Cement and Concrete]

Indian J.Sci.Res. 17(2): 158-161, 2018 ISSN: 0976-2876 (Print)
ISSN: 2250-0138(Online)

HEAVY FLOODS ON THE URBAN ROADS OF HYDERABAD FLOODING LOW LYING INHABITANTS OF HYDERABAD METRO CITY – A CASE STUDY

[1]Raja Kishan Rao, [2]Korapati Manga, [3]Dr.V.Lobo
[1]Department of Irrigation and CAD, Govt.of Telangana, Hyderabad
[2,3] Engineering, Aurora's Scientific Technological & Research Academy, Hyderabad

Abstract- The urban population in rapidly increasing world wide similarly the flooding of urban roads also are increasing due to the old drainage system designed limited population. In the case of Hyderabad metro city, the drainage system was developed during 1591 by th King Mohammed Quuli Qutub shah on the bank of river Musi, The urbanisation lead to more catchment area resulting to heavy floods on the roads and low lying areas of Hyderabad. In addition the agricultural lands have been converted to residential agglomating in the pheriphery of 30km radius thus creating concrete jungle. Due to the development of urbanisation concrete building area and concrete roads area increased to 90% of the city metro area. As surely total rainfall is diverted to runoff with out increasing the ground water of the city; thus flooding of roads and low lying bresidential areas. The buildings increased irregularly on the road on the flood zones tributaries of musi river resulting to floodings of residential buildings of the city. The hazards faced by the citizens will be studied and will be find out the solutions this project to study the solutions to the above problem in metro city Hyderabad under GHMC and HMDA

Keywords : Drainage System, Runoff, Ground Water, Flooding.

I. Introduction

Hyderabad is a historic city noted for its monuments, temples, mosques and bazaars. The culture was of its multitude influence shaped the character of the city in the last 400 years. Hyderabad was the capital city Qutubshahi dynasty.

Mohammed Quli Qutub shah of the Qutub shahi dynasty built the city of Hyderabad on the musi river 5 miles (8Km) east of Golconda in 1589.The roads along with the bridge called the purana phool were constructed and the city was formed during the kingdom of Mohammed Quli Qutub Shah. He ruled the city on Golconda fort, which was constructed by the Kakatiya dynasty.He also ordered the construction of iconic monument Charminar in 1591.

Heavy overnight rains created havoc in past of Hyderabad and its suburbs as water entered some residential areas and flooded roads.

The city drainage system was developed in the early 1930 after the disastrous number Musi flood of 1908 which is said to have killed 15,000 people in Hyderabad and made an equal number homeless.Since then, while additions have been made to the drainage and sewage system by successive Government, there has been no revamp.

Hazards due to flooding of Musi River in the urban roads of high density traffic in(High Tech city….

Overflowing drains, Water logging, fallen trees, wall/building collapses.

Large parts of the city were left without electricity and there by communication for several days.

Major traffic blocks suffer due to water logging and transportation of essential commodities will be affected.

Since Hyderabad lapses a separate storm-water drainage system, even mild showers can cause water logging and flooding in the city. The following table depicts the growth of population in the city of Hyderabad over the last fifty years.

Census	Population	%
1971	1,796,000	
1981	2,546,000	41.8%
1991	4,359,262	71.2%
2001	51,637,483	29.3%
2011	7,674,689	36.1%.

The city population in 1897 was 415,039 today the city of Hyderabad, covers an area of 650sq.km (250 sq.miles) has a population of 6.8 million.

There has been a steep increase in Hyderabad slum population, which attributed to ineffective implementation of planning.

The city population in1897 was 415,039 today the city of Hyderabad, covers an area of 650 sq.km (250 sq. Miles) has a population.

There has been a steep increase in Hyderabad slum population, which is attributed to ineffective implementation of planning.

Tom bell, the climate scientist from NASA godderd space flight centre points out that "Water vapour does not

[1]Corresponding Author

ordinarily, spontaneously condense into drops to form clouds".

The impact of urban water and air due to flood water and storm water "water vapour doesn't ordinarily spontaneously condense into drops to form clouds", says climate scientist Tom Bell, from NASA Goddard space flight centre.

"It needs dirt to form spherical shape. All rain needs aerosols to form clouds "in the natural world cloud – forming aerosols are things like sea salt, dust and pollen all of which are visually smaller and more numerous than natural aerosols.The impact on rain, says Bell, varies depending on where the clouds form. In some cases, urban aerosols from rain, but in others they increase it.

II. Physical Causes of Flooding

Heavy rainfall, Snowmelt, Steep slopes, Long Periods of rain, Impermeable Routs,Very Wet, Saturated Soils.

Reasons for flooding the urban roads and low lying areas:

Flooding occurs when a river discharge exceeds the capacity of its channel to carry the discharge.The nature of the drainage basin has influence on the likelihood of flooding. Some drainage basins are more likely to flood than others .The vegetation soil type and geology of surface and sub soils in areas of the world vegetated by dense forest ,interception and uptake by plants reduce the risk of flooding during time of heavy rainfall.

The impact of human activities on flooding:

- Population growth and urbanisation has led to demand for land to build on-flood plains illegally.
- As the pavement materials like cement concrete roads, bituminous roads which are being developed in the city are impermeable materials, the runoff will increases at a rapid rate
- Often surface water is channelled directly into drains and sewers, so runoff reaches the river much more quickly.

Deforestation:

Owing to the cutting of trees for developmental works like roads, road widening and building, there is a great risk of erosion and fast flowing of runoff without interception and without percolation in the urban areas increase the floods.

River Management:

The main aim of river management is to reduce the likelihood of flooding. However, in some circumstances it can actually increase the risk.

Flood embankment have been built along river banks .They are designed to increase river capacity with due protection but in the urban cities like Hyderabad no protection to the banks of Musi river were provided.

It is predicted that global warming will result in reduced rainfall in some areas, but on the other hand counter heavy rain fall will be precipitated without notice.

Higher temperatures will result in increased evaporation over the seas and oceans, leading to greater precipitation such an increase will inevitably cause more rivers to flood, particularly since most flood plains have become heavily urbanised over the last one century.

Hyderabad Climate:

Heavy rains lashed the city of Hyderabad in September and October. The areas as under Falakanuma, Ramnagar, Madhapur, Chandanagar, Darulshifa, Dabeerpura and Jama Masjid, Punjagutta, Jublihills, Raj Bhavan Road, Nagole, Ramanthapur T.V Studio Road, Krishna nagar, Madhapur, Asifnagar, Bahadurpura, Ramnagar, Singodikunta, Ambrepet, Habisguda, Shiva Rampalli, Begumbazar, Mozamjari market, Christiancolony, Vanastalipuram, Thopkhana, Nagamaiah kunta, Mehidipatnam, Gachibowli, Pathabasthi during September and October 2017.

Transport networks economic activity was hampered by stopping the movement of goods and light vechiles by the flood water in many areas of Hyderabad city.

Flooding, especially as a result of intense precipitation, is the predominant cause of weather related disruption to the transport sector and to the inhabitants of Hyderabad urban city.

Fig 2.1 Rainfall intensity of Hyderabad

Fig 2.2 punjagutta road

Fig 2.3 Gachibowli junction

III. Analysis

As the city is developing rapidly with cement concrete buildings, impervious roofs resulting to less water percolation into the ground. This increasing the run off and decreasing the ground water level. The flood plains of streams and rivers are encroached with the urban buildings restricting the vent way of the floods. As the vent way is decreased the Highest Flooding Level (H.F.L) increases entering's into residential buildings causing heavy loss to the properties and food items.

Effects:

On the movement of the public for food items and for discharging their duties at times of floods wading in rain water causes allergies, creating severe itching sensation on the skin of the human bodies.

The rain water is contaminated due to sewage water from the manholes and storm water over flooding in the city. The combined flow of storm water and sewage water is also making the health hazards.

Due to the storm water floods, water pollution and air pollution creating viral fever, cough, cold and viral diarrheaare causing health hazards.

The impact of floods on the urban roads of Hyderabad specially high density traffic areas like Kondapur leading to Model House, Falakanuma, Ramnagar, Madhapur, Chandanagar, Darulshifa, Dabeerpura and Jama Masjid, Punja gutta, Jublihills, Raj Bhavan Road, Nagole, Ramanthapur T.V Studio Road, Krishna Ragar, Madhapur, Asifnagar, Bahadurpura, Ramnagar, Singodikunta, Ambrepet, Habisguda, Shiva Rampalli, Begum Bazar, Mozamjari Market, Christiancolony, Vanastalipuram, Thopkhana, Nagamaiah Kunta, Mehidipatnam, Pathabasthi.

Impacts of Floods on Transport:

- Rain fall can reduce driver visibility, reducing the speed as a precautionary measure.
- During extreme floods, the goods carried in the transport vehicles may be damaged.
- There is every risk of transport vehicles completely overturning due to submerged road conditions.
- The light vehicles may be over turned with life risk due to heavy flood.

At Bio diversity center in Kondapur the major vehicles junction traffic leading I.T.Corridor are being delayed on the roads due to heavy water flooding.

Recently, Greater Hyderabad Municipal Cooperation GHMC, proposed to construct a culvert with a length of 215 m with an estimated cost of Rs.2.20 crores to solve the above problem permanently.

Causes:

The factors initiating the rising of flood levels of nalas/stream are as follows.

Every year illegal construction come up on the nalas/drain decreasing the vent way of the streams .The flood level in the buffer zone increases and entered into residential building creating hazzards.

GHMC and Hyderabad Metropolitan Development Authority, have regularised the illegal and structures which fills their coffers with the penalty money.As such the problems remain stand still.

The total nalas in GHMC limit is 173. All the Nala are fully or partially encroached.

The Kirlosker committee submitted a decade ago, had clearly recommended that storm water drains/nalas to be widened for the free flow of rain water in GHMC limits. Totally 28000 illegal constructions on 173 Nalas/drains required to be dismantled which will be costing around Rs.15000,crores towards compensation .As such this matter was kept in abeyence by the Govt as heavy budget was involved.

This problem is main cause of all the hazards in 826 tanks basins (Catchment Area) of . GHMC.

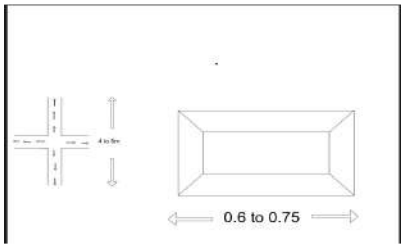

IV. Conclusion

- Flooding is a major environmental phenomenon creating severe impacts on the socio-economic and environmental aspects of human endeavour.
- It is prominent in highly built-up and low lying areas especially where little or no attention was paid to proper planning and development of infrastructure (road transport and buildings).
- At present, the over flooded water in flowing areas are being pumped to high level areas where the water scarcity is more. This water is being used for gardening, irrigation and for domestic purposes.This process is becoming costlier to maintain every year with recurring expenditure.
- Green roof gardens can be developed to absorb the rainfall and runoff
- The flood plains of streams and rivers are encroached with urban residential buildings restricting the vent way of the flood. As such the buildings, structures which are constructed in the flood plains may be removed and rehabilitated in other safe zones.
- The rainwater has to be separated from the sewage system, thereby overloading of the sewage treatment system can be avoided. The pollution of takes like Hussainsagar, Himayatsagar etc., can be avoided. In addition, air pollution can also be avoided in the twin cities of Hyderabad and Secunderbad.
- The ground water in the twin cities is in degradable condition and sub-surface water is not available even upto 150 mtdeapth in the city zones in densely populated areas. The public deciding in high rise buildings are facing scarcity of ground water.
- The ground water in the high densely residing populated areas of the city likes Banjarahills,Jublie hills is decreasing year by year.The unexpected down pour of heavy precepition with high intensity of 8 to 12 hours is creating heavy floods resulting to hazards.Due to the concrete jungle the rate of percolation into the ground is very less,and the entire runoff is diverted to Musi river in the urban city Hyderabad.
- The Nalas of 173 and 826 tanks are encroached to 40%. This problem is main cause of all the hazards in 826 tanks and 173 Nalas. The dismantling of illegal construction require huge budget of Rs.5000 crores. It is proposed to divert flood water into the water harvesting pits in the upper reaches of each basin at the junctions of the roads as per the flooding quantity. The water harvesting pits may be constructed parallel to the roads with restricted width of 0.6 to 0.75 m to a depth of 5m to 8m so that adjacent building foundations are not effected by using pre fabricated Reinforced Cement Concrete rectangular walls.
- The flood water floating from D.L.F, Gachibowli, P.T.R nagar, Cyber hills, Diamond hills is rushing to biodiversity junction creating traffic jam for 8 to 20 hrs during the flood days in Oct and Sep 2017.This main road will lead into I.T corrider having more traffic .The GHMC authorities proposed to construct a culvert at biodiversity junction of Kondapur village for a length of 215 m with an estimated cost of Rs.2.20 crores to solve the above problem.
- In the future the apartments having more than three floors must have their own septic tanks at each residential building, so, that the sewers will not be float out and mix with sewage water.

References

- Deccan chronicle news paper.
- Eenadu News Paper.
- Survey of india- Hyderabad map

Fig Hyderabad map

Indian J.Sci.Res. 17(2): 434 - 439, 2018 ISSN: 0976-2876 (Print)
ISSN: 2250-0138(Online)

STUDY OF DESALINATION METHODS

[1] Korapati Manga, [2]Kanchan Goswami, [3]Ale Akshitha
[1,2,3]Department of Civil Engineering, Aurora's Scientific, Technological and Research Academy, Hyderabad

Abstract **-**The paper presents the over view on the developments in the methods of desalination. The process of desalination aims to convert sea water into portable water or drinking water.This process of desalination was started because of deficiency of water in societies, as rains don't be available everywhere. The people need to start using sea water for their personal and drinking purposes. Different methods of converting sea water into portable water is mainly used in countries like Saudi Arabia, United Arab Emirates, Spain, Italy, Greece, Japan, China, Australia and now in India also. It is mostly seen in middle east countries because those are near to equator. The process of desalination helps in softening the hard sea water, but it also has some negative effects on the environment. But the process is more expensive. As the use of this processes are increasing it is becoming cost-effective. There are two desalination plants in India.

Keywords: Desalination, sea water.

I. Introduction

The chemical process of changing seawater into potable or fresh water is called desalination. It is a process that extracts excess salts and mineral components from saline water. Thermal distillation and membrane processes are the two main approaches used around the world to desalinize water. Salt water is desalinated to produce water suitable for human consumption or irrigation.

Fig (1).Main inputs and outputs in a desalination process. Source: CLAYTON (2007)

In most desalination processes, saltwater (also called "feed water") is treated and two streams of water are produced. Treated freshwater that has low concentrations of salts and minerals. Concentrate or brine, which has salt and mineral concentrations higher. As shown in the above.

The pure water that is obtained after desalination must be re-mineralized to be adequate for human consumption. The concentrated brine produced in desalination processes needs to be disposed of properly. Due to its energy consumption, desalinating sea water is generally more costly than fresh water from rivers or groundwater, water recycling and water conservation. However, these alternatives are not always available and depletion of reserves is a critical problem worldwide.

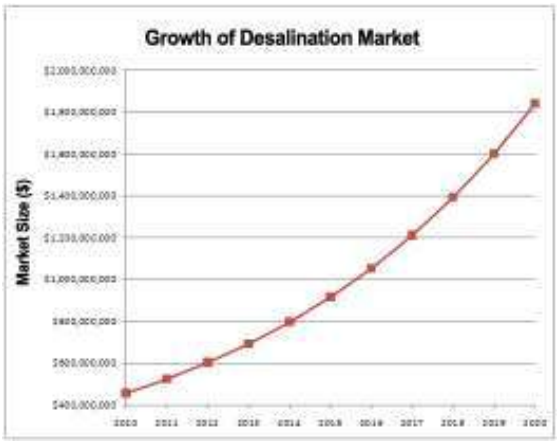

Fig (2) Increase in use of desalination in past few years.Source:Aqua membranes [TM]

Table 1: Desalination methods categories and description

Category Title	Short Hand Title	Description/Embedded Topics
Vacuum distillation	V D	Heavy hydrocarbon debris from altercation distillation unit is refining in a vacuum distillationunit for further separation of under reduced pressure.
Reverse Osmosis	RO	Filtration is the absolute clarification to improve the savor, odor and appearance of water.
Freeze-Thaw Distillation	FTD	It exudes the water by freezing technique.
Electro dialysis	EDD	In general, electro dialysis reversal are

[1]Corresponding Author

Distillation		voluntary more appurtenant for appliance in processes with low total dissolved solids.
Solar Evaporation	SED	Abolish salts from brackish or saline surface water and groundwater in adjustment to render it acceptable for human consumption or other uses.
Multi Effect Distillation	MED	The low categorization thermal process of obtaining fresh water by recovering the vapor of boiling sea water in a sequence of vessels, each maintained at lower temperature than the last.
Vapor Compression Distillation	VCD	The most attractive among the single stage desalination processes is vapor compression distillation.
Multi-Stage Flash Distillation	MSFD	MSF desalination process is mainly employed for large-scale, thermal desalination plants where thermal energy is available in the form of low-pressure steam (>2 bar a), e.g. in combination with thermal power plants or industrial complexes.
Iron Exchange Distillation	IED	Ion exchange is an eversible process, and the ion exchanger can be regenerated or loaded with desirable ions by washing with an excess of these ions.

The above figure shows that the increase in use of desalination, from 2010 and till reaching 2020 there is higher usage of desalination process.

This desalination process now has started in India also; there are only two plants in India. One in Gujarat and another in Tamil Nadu. And these plants are in progress in other states of India like Andhra Pradesh, Rajasthan, Orissa and West Bengal.

II. Methods of Desalination

A. Vacuum Distillation

The traditional process used in these operations is vacuum distillation essentially boiling it to leave impurities behind. In desalination, atmospheric pressure is reduced, thus lowering the required temperature needed. Thus, because of the reduced temperature, low-temperature "waste" heat from electrical power generation or industrial processes.

- Takahisajitsuno (2012) he develop a simple solar-powered vacuum distillation system for producing fresh water using only pipes as the main device. This system contains an evaporating pipe heated by solar-radiation and a cooling pipe cooled by air. This system only contains pipes, and no elements are consumed during operation.[21].
- Yongqing Wang(2014) he investigate experimentally the performance of a solar desalination system coupling a vacuum tube solar collector and a VMD unit. The experimental set-up was built in Xiamen, a seaside city in the southeast of China, with an average daily insulation of 12.6 MJ/m2 /d. The VMD unit used was first tested and examined using an electric heater, and then using the solar collector heater, as a combined system.[23]
- Xiaohua Liu(2014) As a new desalination method, NVD technology has many merits such as low grade thermal energy using, low electric power consumption, low corrosion and scaling rates, simple structures, convenient operation process and low cost in maintenance. These features will provide favorable conditions for its development in engineering. NVD technology developed quickly in recent 20 years. [22]
- Adnan AlhathalAlanezi (2016) An O-ring membrane module was constructed and specially designed to investigate the performance of the VMD process using PTFE and PVDF membranes. [1]

B. Reverse Osmosis

In the natural process of osmosis, when a seawater solution and pure water are separated by a semi- permeable membrane, the pure water will pass through the membrane to the seawater solution side. The natural driving force is osmotic pressure. Reverse osmosis systems require electrical energy for the high pressure pump. Fuel required to operate a reverse osmosis system is approximately 9.1liters of fuel per 3,785 liters of water produced. The Reverse Osmosis process is not maintenance free. It have some advantages like, operate at ambient sweater temperature reducing corrosion and scale formation,equipment size is small. but it also have some disadvantages like, the system's high pressure pump creates vibrations that may require special foundations, high pressure salt water requires special materials for the

system's high pressure piping and the following authors says

- Berge Djebedjian (2008) - In this paper, a methodology is developed for optimization of the reverse osmosis (RO) desalination system performance. The solution-diffusion model is used for the modeling.[3]
- Lauren F. Greenleea(2009) -The field of RO membrane desalination has rapidly grown over the past has improved, allowing significant increases in product production and cost savings.While the basic operating principles remain the same for all ROapplications, individualized applications have developed. Basedonfeed water quality. [15]
- Loreen O. Villacorte (2014) - the occurrence of HABs in seawater, their effects on the operation of seawater reverse osmosis (SWRO) plants, the indicators for quantifying/predicting these effects, and the pretreatment strategies for mitigating operational issues during algal blooms. [16]

C. Freeze Thaw Distillation

Freeze-thaw desalination uses freezing to remove fresh water from frozen seawater. One method, invented by Alexander Zarchin, used freezing and vacuuming of salt from seawater.

- Farah Hanim Ab. Hamid (2015)-s In recent century, the world is experiencing clean water supply shortage and the severity of this problem is increasing at an alarming rate. Introduction of new technologies for water purification is essential to accommodate the demand for clean water supply. [6]
- R.D.C. Shonet (1987) - The desalination of waters by freezing is a well-known process and relies on the principle that the structure of an individual ice crystal does not accommodate salts. Therefore, during the freezing of a salt solution, salts are rejected by the growing ice crystals. [19]
- J. Mauricio Pardo (2015) - It has not been implemented at an industrial level because its separation efficiency is lower than that of the traditional freeze concentration process. Therefore, numerous assisting techniques are being studied around the world to overcome this deficiency. [10]

D. Electro Dialysis Reverse Osmosis

Electro dialysis was developed in the mid-1950s to dematerialize brackish water at commercial scale. In general, electro dialysis and electro dialysis reversal are considered more appropriate for applications in processes with low total dissolved solids (TDS). Both processes have a good degree of resistance against scaling and fouling, which makes the technology attractive in brackish water desalination.

- Fernando Valero (2007) First commercial equipment based on Electro dialysis (ED) technology was developed in the 1950s to dematerialize brackish water over the past twenty years EDR has earned a reputation as a membrane desalination process that works economically and reliably on surface water supplies. [17]
- Marjolein Vanoppe (2014&2016) - This research focused on assisted reverse electro dialysis as a possible pre-treatment technology for reverse osmosis. This technology can decrease the overall energy demand for seawater desalination, without an excessive membrane area requirement, as is the case with Reverse Electro Dialysis. [18]
- Krishnaveni Venugopal (2013) - Desalination of brackish water, which is the source of drinking water in various world regions, is one of the large-scale applications of electro dialysis (ED). in the fields of both separation and purification due to its diversity, sophisticated functions and technological compatibility .[14]

E. Solar Evaporation

In 1870 the first US patent was granted for a solar distillation device to Norman Wheeler and Walton Evans. Two years later in Las Salinas, Chile, Charles Wilson, a Swedish engineer, began building a direct method solar powered distillation plant to supply freshwater to workers at a saltpeter and silver mine. Solar desalination of seawater and brackish groundwater in the modern United States extends back to the early 1950s when Congress passed the Conversion of Saline Water Act, which led to the establishment of the Office of Saline Water (OSW) in 1955.

- Amitava Bhattacharyya (2013) The author says that direct sunlight has been utilized long back for desalination of water. Solar distillation plants are used for supplying desalinated water to small communities nearby coastal remote areas. Solar stills are easy to construct, can be done by local people from locally available materials, simple in operation by unskilled personnel.[2]
- Hazim Mohameed Qiblawey (2007) The use of solar energy in thermal desalination processes is one of the most promising applications of the renewable energies. Solar desalination can either be direct; use solar energy to produce distillate directly in the solar collector, or indirect.[9]
- Hamid Mokhtari (2014): Traditional plants use fossil fuels to provide required steam but, nowadays, using

solar collectors has become more attractive to prevent global pollution. Multi objective optimization technique based on the genetic algorithm was proved to be a reliable tool for techno economic improvement of plants and has been used by many researchers.[8]

F. Multi Effect Distillation

Distillation is the oldest and most commonly used method of desalination. The world's first land-based desalination plant, a multiple-effect distillation (MED) process plant that had a capacity of 60 m^3/day, was installed on Curacao, Netherlands Antilles, in 1928. Multiple-effect distillation (MED) works through a series of steps called "effects".

- C. Frantza (2014) Decreasing water resources and steadily rising water demand drive research towards new approaches for safe and reliable water supply for the municipal, agricultural and industrial sectors. One solution for fresh water provision is sea water desalination using solar thermal energy.[4]
- Marios C. Georgiou (2013) The Multiple-Effect Distillation, or MED, process consists of several consecutive stages (or effects), maintained at decreasing levels of pressure (and temperature), leading from the first (hot) stage to the last one (cold). A schematic of a four-stage MED unit is depicted. however, typical MED plants can contain as many as 20 effects.[17]

G. Vapour-Compression Distillation

The most attractive among the single stage desalination processes. Vapor-compression evaporation involves using either a mechanical compressor or a jet stream to compress the vapor present above the liquid. The compressed vapor is then used to provide the heat needed for the evaporation of the rest of the sea water

- Jorge R. Lara - Vapor compression is a reliable and robust desalination technology that is attractive because of its capacity to treat large volumes of water with a wide range of salt concentrations. However, compared to other major desalination technologies such as reverse osmosis, mechanical vapor compression has had relatively high operating and capital costs.[12]
- JiangangJi (2015)process is generally used for small- and medium-scale desalting units. The heat for evaporating the water comes from the compression of vapor rather than the direct exchange of heat from steam produced in a boiler or other heat sources. The effects of the variations of operating condition on the system performance are investigated and analyzed.[11]

H. Multi-Stage Flash Distillation

Water is evaporated and separated from sea water through multi-stage flash distillation, which is a series of flash evaporations. Each subsequent flash process utilizes energy released from the condensation of the water vapor from the previous step and so on. The first multi stage flash plant was sold in Saudi Arabia, and Robert silver worked tirelessly to bring it on line. That plant established the commercial viability of multi stage flash process and its design was duplicated in many places. People started using it since 1950.

- S. Ravindran (2012)- In a steam power plant, the exhaust steam will be condensed in a condenser. The cooling fluid will be water, which intern gets cooled in a cooling tower. In a Multi Stage Flash (MSF) distiller, the condenser cum cooling tower units shall be replaced by a brine heater and series of flash chambers with condensers. The condensers of the MSF units are very large in terms of length and number of tubes.
- Hazim Mohameed Qibla wey (2007)- Solar desalination can either be direct; use solar energy to produce distillate directly in the solar collector, or indirect; combining conventional desalination techniques, such as multistage flash desalination (MSF), vapor compression (VC), reverse osmosis (RO), membrane distillation (MD) and electro dialysis, with solar collectors for heat generation.

I. Ion Exchange

Ion exchange is an exchange of ions between two electrolytes or between electrolytes. Using methods developed by Frank Speeding in the 1940s, ion exchange used to be the only practical way to separate them in large quantities, until the Liquid-phase (aqueous) ion-exchange desalination

- Hayani (2016) - In this work, the resin Doolittle 206A has been tested for softening, on the one hand, synthetic water containing Ca2+ and Mg2+, and secondly, brackish groundwater from the coastal area of El Jadida province (Morocco).
- L Karimi (2015) Electro dialysis reversal is a membrane based desalination process in which ions are transferred through ion exchange membranes under the influence of applied electric field. As discussed in this paper some parameters such as applied voltage and temperature.

III. Conclusion

The processes of desalination as a source for portable water have begun to become wider in country India. As being citizen sit is to be aware of the environmental aspects related to the various processes and in each case to consider the environmental costs as well as the requirements and the financial costs. In a paper, which

deals with the problems caused by processes of desalination, it is also important to go through the disadvantages and the advantages, of adding desalinated water to the existing water system. This process has been already started in India states like Tamil Nadu and Gujarat and it may also start in other states like Rajasthan, Andhra Pradesh and West Bengal. Because of water deficiencies and of lack of rains .The main purpose of seawater desalination is to offset present or future deficits in potable water, by producing water of good quality at a reasonable price. However, the amounts and the quality of the produced water highlight several additional environmental advantages. These advantages are dependent on the intended point of use of the desalinated water as well as on the volume and quality ratio between this water and the rest of the water in the water supply system.

IV. References

[1]. Adnan AlhathalAlanezi - A. AlHathal Al-Anezi, A. O. Sharif, M. I. Sanduk, and A. R.Khan, "Potential of membrane distillation—a comprehensive review," International Journal of Water, vol. 7, no. 4, pp. 317–346,2013.

[2]. Amitava Bhattacharyya -Amitava Bhattacharyya,Solar Stills for Desalination of Water in Rural Households, 2013

[3]. BergeDjebedjian - . Djebedjian, B., Gad, H., Khaled, I., and Rayan, M.A., "Reverse Osmosis Desalination Plant in Nuweiba City (Case Study)," Proceedings of IWTC11 2007, Eleventh International Water Technology Conference, 15-18 March 2007, Sharm El-Sheikh, Egypt, pp. 315-330.

[4]. C. Frantza - C. Frantz and B. Seifert, "Thermal Analysis Of A Multi Effect Distillation Plant Powered By a Solar Tower," (Diploma Thesis), 2014

[6] Farah Hanim Ab. Hamid - Farah Hanim Ab. Hamid, Zaki Yamani Zakaria, NorzitaNgadi and MazuraJusoh , Application of Progressive Freeze Concentration for Water Purification using Rotating Crystallizer with Anti-super cooling Holes,2015.

[7] Fernando Valero - Fernandez-Turiel, J.., Roig, A., Llorens, Antich, N., Carnicero, M. & Valero, F. (2000). Monitorig of drinking water treatment plants of Ter and Llobregat (Barcelona NE Spain) using ICP-MS, Toxicological and Environmental Chemistry 74: 87-103

[8] Hamid Mokhtari - Hamid Mokhtari, MokhtarBidi, and Mahdi Gholinejad, Thermoeconomic Analysis and Multiobjective Optimization of a Solar Desalination Plant,2014.

[9] HazimMohameedQiblawey - HazimMohameedQiblawey*, Fawzi Banat, Solar thermal desalination technologies, 2007.

[10] J. Mauricio Pardo - J. Mauricio Pardo*§; Ricardo Sanchez, Block freeze concentration intensification by means of vacuum and microwave pulses, 2015.

[11] JiangangJi - JiangangJi, Simulation and Analysis of a Single-Effect Thermal Vapor-Compression Desalination System at Variable Operation Conditions,2007

[12] Jorge R. Lara -Lara, J. R., Holtzapple, M. T. Experimental Investigation of Drop wise Condensation on Hydrophobic Heat Exchangers. Department of Chemical Engineering Texas A&M University, 3122 TAMU, College Station, TX 77843-3122, February 2010.

[13] .Karimi Lei -Karimi. L, Abkar, Aghajani. M, Ghassemi. A, Technical feasibility comparison of off -grid PV-EDR and PV-RO desalination systems via their energy consumption ,sep. purify. technol. 151 (2015) 82-94.

[14] .KrishnaveniVenugopal - K. Venugopal and S. Dharmalingam, "Fundamental studies on a new series of SPSEBS-PVA-QPSEBS bipolar membrane: Membrane preparation and characterization," Journal of Applied Polymer Science, vol. 127, no. 6, 2013, pp. 4983-4990, DOI: 10.1002/APP38098

[15] .Lauren F. Greenlee , Desmond F. Lawler, Benny D. Freeman , Benoit Marrot , Philippe Moulin, Reverse osmosis desalination: Water sources, technology, and today's challenges,2008.

[16]. Loreen O. Villacorte - Villacorte L.O., Tabatabai S.A.A., Dhakal N., Amy G., Shippers J.C., Kennedy M.D. (2015a). Algal blooms: an emerging threat to seawater reverse osmosis desalination. Desalination and Water Treatment, In Press, DOI:10.1080/19443994.2014.940649

[17]. Marios C - Marios C. Georgiou, Aristides M. Bonanos,1and John G. Georgiadis. Evaluationof a Multiple-Effect Distillation Unit under Partial Load Operating Conditions,2013.

[18] MarjoleinVanoppen - Vanoppen, M. et al., 2014. Reduction of specific energy demand of seawater RO by osmotic dilution/osmotic energy recovery - realistic modeling approach. In Desalination for the Environment: Clean Water and Energy.

[19] R.D.C. SHONET - SHONE, R.D.C., and HARRIES, R.e. Desalination of mine water. Symposium on Mine Water Systems, Mine

Ventilation Society of South Africa, Sun City Conference Centre, Bophuthatswana, Mar. 1985.

[20] S. Ravindran -S. RavindranMaterials Usage in Multistage Flash Distillers,2012.

[21] Takahisajitsuno- Takahisa JITSUNO and Kaoru HAMABE,Vacuum Distillation System Aiming to Use Solar-Heat for Desalination,2012.

[22] Xiaohua Liu - Xiaohua Liu, Xinchun Zhang , Yaqin Fang , Mingming Zhu ,The Natural Vacuum Desalination Technology in Seawater Desalination,2014.

[23] Yongqing Wang - X. Wang, L. Zhang, H. Yang, H. Chen, Feasibility research of potable water production via solar-heated hollow fiber membrane distillation system, Desalination 247 (2009)403-411.

SHEEP-OC with adaptive sensing; An Energy Efficient data gathering scheme in WSNs

Mohammed Moyed Ahmed[1], Dr.D. Sreenivasa Rao[2]
Department of ECE, College of Engineering Hyderabad
Jawaharlal Nehru Technological University Hyderabad, Hyderabad, India

Abstract **-** Wireless sensor networks have been the useful technology for monitoring in a remote and hostile environment, in applications such as prediction of landslides where the frequent sensing and data gathering of seismic parameters are required in the dynamic surroundings. Since the nodes of the sensor networks are inadequate in energy, a lifetime of the network becomes the major criteria for the effective design of data gathering schemes in wireless sensor networks. In this paper, we propose an efficient data gathering scheme adaptive to sensing requirements, where the sensor nodes are equipped with multiple sensors. To accomplish the task we adopt the response threshold model for sensing. The results are evaluated through simulations, our proposed algorithm can accomplish energy-efficient data gathering, satisfying dynamically changing sensing requirements.

Keywords **-** *Wireless Sensor Network, data gathering, adaptive sensing, response threshold model, Energy efficiency.*

I. INTRODUCTION

The Wireless Sensor Network (WSNs) [1,2] were extensively deployed and researched for many applications in recent years, by taking the advantage of smaller dimension, lower cost and simple structure of the sensor node. More restrictions come together with sensor nodes due to these characteristics. Therefore, the limited power of sensor nodes is the most direct and difficult problem we meet. The limitation on the energy of sensor node makes the bottlenecks for designing the suitable routing protocols. In order to solve the problem of limited energy, power loading of nodes have to be distributed as possible as it can. If the energy consumption can be shared averagely by most nodes, then the lifetime of sensor networks will be enlarged. In many applications of wireless sensor network, the sensor nodes are required in the form of error-free data transmission[3] to the Sink node. We proposed an energy-efficient data collection program. The method we proposed to reduce the data transmission is by adaptive sensing mechanism and transmitting the data to respective cluster heads on the basis of threshold values of the sensed parameter. In general, the sensor node in a wireless sensor networks that can be sensed and the information gathered can be transmitted to a distance are all fixed, and two are directly related. The greater the distance between the nodes makes greater power consumption[4]. The relation between the communication distance and power consumption are exponentially proportional. Therefore by transmitting the aggregated information to longer transmission distance with a lower power consumption to a data collection node (Sink Node), enormous amount of energy can be saved. The algorithms to improve the use of time and performance of the entire wireless sensor network environment becomes one of the most important research areas in the recent times.

II. PROPOSED WORK

Energy conservation techniques for the radio communication has been extensively proposed by many authors[5,6]. Here we are attempting to proposed a mechanism for sensing level. Adaptive response threshold technique can be applied to achieve energy conservation at the beginning of sensor level for sensing of a physical quantity to be monitored, it means switching off the transceivers system, reducing the amount of data to be transmitted to the base station one can reduce the energy consumption without losing the useful information. In fact, routing protocol used in wireless sensor network play an important role in balanced energy consumption. There are different routing protocols have been proposed, many of them want the same goal as much as possible, improving the survival time of the wireless sensor network, in order to enable them to have better usability. To minimize power consumption under the WSN premises, consider the application target, static use of environment. Efficiently maintaining the energy consumption of sensor nodes by balanced clustering, involving in multi-hop communication between the cluster heads and performing data aggregation or fusion in order to decrease the number of transmitted messages to base station is the main goal of the routing protocols (cluster based). In order to prolong the network lifetime, energy-efficient protocols should be designed to adapt the characteristic of wireless sensor networks. Clustering algorithm is a kind of key technique used to reduce energy consumption, which can increase network scalability and lifetime. Earlier the author has proposed two protocols, a Stable Energy Efficient cluster based protocol(SHEEP) [7]where the stability period has increased by making use of energy heterogeneity and Stable Energy Efficient Protocol with optimum clustering (SHEEP-OC)[8] where the optimum number of clusters have been used to overcome energy hole and coverage hole problems. This paper studies the performance of clustering algorithm in saving energy for heterogeneous wireless

sensor networks with adaptive sensing technique, and evaluated in the (SHEEP-OC) clustering scheme.

Basically in cluster based algorithms[9,10], there are two phases of cycle in each round,

- *Setup cycle* and
- *Steady state cycle.*

In Set-up Cycle network initiation, cluster head CH selection takes place and cluster formation will be done. In *steady state cycle*, sensor nodes starts sensing and transmits the sensed data to corresponding cluster heads, subsequently received data from the nodes will be aggregated and transmitted to the base station BS.

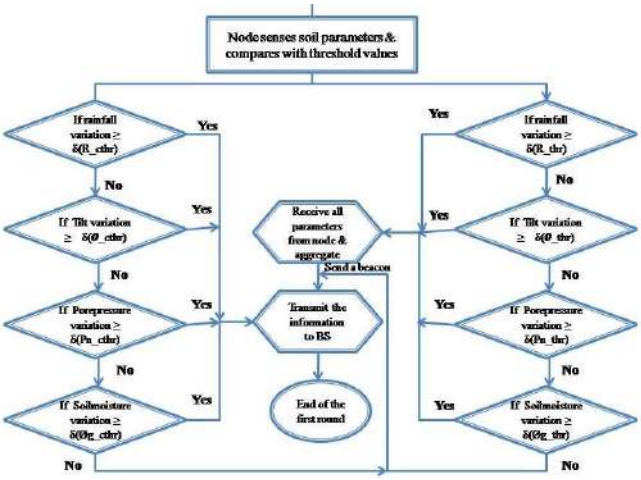

Fig. 1 Adaptive sensing algorithm during steady state phase

After one round of setup and steady state cycle, network goes back to second round of steady state phase. In the proposed algorithm, we are going to apply the adaptive sensing algorithm on **SHEEP-OC** routing protocol, where after network initialization and clustering phase, during the data transfer phase (*steady state phase*) proposed algorithm will be applied. During the steady state phase before transmission of data to cluster heads, each node measures the sensed parameters, compares the data with the defined threshold values, if they crosses the threshold then data will be transmitted to corresponding cluster heads else the node will transmit a beacon and transceiver will switch off but sensor will remain in sensing state. For the analysis purpose we have chosen an application on the landslide prediction. A spatially distributed soil information of the landslide prone area is necessary to predict the landslides. The parameters to be sensed includes, Tilt measurement (using inclinometer), Amount of rainfall (using rain gauge), Soil moisture sensor and Pore pressure (using piezometer).

Normal threshold levels for the purpose of comparison: The transceiver will be switched off in WSN node but sensor will be in sensing state, if the change in the parameters is less than mentioned below values:

1. Rainfall (reading from the rain gauge) $\delta(R_{thr}) = 1\ mm$
2. Tilt measurement (inclinometer reading) $\delta(\theta_{thr}) = 1^{\circ}$
3. Pore-pressure (Piezo-meter reading) $\delta(P_{n,thr}) = 0.1\ kPa$
4. Soil moisture (soil moisture sensor reading) $\delta(\emptyset_{g,thr}) = 3\ \%$

Nodes are connected with multiple sensors, whole sensed information will be transmitted to the CH if the variation in any of the parameters crosses the threshold value.

Critical Threshold: In case if there is significant change in the soil parameter, nodes switches on the transmitters and immediately sends the information to CH, same time CH relays the information to the Base station without delay. Following are the Critical threshold values:

1. Rainfall (reading from the rain gauge) $\delta(R_{cr}) = 10\ mm$
2. Tilt measurement (inclinometer reading) $\delta(\theta_{cr}) = 5^{\circ}$
3. Pore-pressure (Piezo-meter reading) $\delta(P_{n,cr}) = 0.5\ kPa$
4. Soil moisture (soil moisture sensor reading) $\delta(\emptyset_{g,cr}) = 5\ \%$

Fig. 1 shows the adaptive sensing algorithm implemented during the steady state phase of the round in SHEEP-OC (adaptive sensing) algorithm.

III. SIMULATION RESULTS

Table 1: Simulation Parameters

Description	Value
N, Number of sensors	100
Area (meter square)	100 x 100
E_0 , Initial energy	0.5 J
E_{elec} , Electronics energy	50 nJ/bit
E_{DA} , Energy of data aggregation	5 nJ/bit
K, Data packet size	500 bytes
k_{broad} , Broadcast packet size	25 bytes

Simulation was performed using the above scenario as shown in the Table 1. Comparison has been made with the proposed mechanism SHEEP-OC with adaptive sensing and LEACH, SEP, SHEEP. The base was assumed to be at the top middle of the area. Sensing targets are assumed to be amount of rain fall, pore pressure, soil moisture and tilt angle. For the purpose of simulation and analysis each node is assumed to be generating random number [0,1]. if the generated random number is less than set threshold value then the nodes do not transmit any information to the CH.

Nodes transmit the data in their assigned TDMA slot with following condition:

$$T_{i,tr} = \begin{cases} R_{value} + \theta + P_n + \emptyset_g;\ if\ \ RN_R \geq R_{thr} \cup RN_\theta \geq \theta_{thr} \cup \\ \qquad\qquad RN_{P_n} \geq P_{n,thr} \cup RN_{P_n} \geq \emptyset_{g,thr} \\ beacon \qquad\qquad otherwise \end{cases}$$

----(1)

In case of critical threshold condition, nodes transmit the information with a critical flag to the CH, when the CH receives any critical information immediately it transmits to the BS without delay. The following condition refers to critical information.

$$T_{i,tr,em} = \begin{cases} R_{value} + \theta + P_n + \emptyset_g; if\ RN_R \geq R_{cr} \cup RN_\theta \geq \theta_{cr} \cup \\ \qquad\qquad RN_{P_n} \geq P_{n,cr} \cup RN_{P_n} \geq \emptyset_{g,cr} \\ beacon \qquad\qquad otherwise \end{cases}$$

--(2)

On the basis of threshold values nodes of WSN send sensed data to the respective cluster heads CH. As a result, few nodes will be in idle condition transmits a beacon and go to sleep, some of the nodes transmits sensed information if there is variation of parameters and some of nodes may send critical information if there is drastic change in the sensed parameters. Cluster Heads will collect the data and transmits to Base Station after aggregation.

For the purpose of energy efficiency analysis, radio model considered as in [7,8], Energy required to transmit information (L bit) over a distance 'd' is given by

The energy required to transmit L bit of message over a distance of d is given by the equations below:

$$E_{Tx}(l,d) = \begin{cases} L.E_{elec} + L.\in_{fs}.d^2 & if\ d \leq d_0 \\ L.E_{elec} + L.\in_{mp}.d^4 & if\ d > d_0 \end{cases}$$

---- (3)

Where E_{elec} represents energy required by the circuit(transmitter and receiver) to transmit one bit. The energy required by the cluster head in one round is given by the formula,

$$E_{CH} = \left(\frac{n}{k} - (1 + N_{non-tr})\right) L.E_{elec} + \left(\frac{n}{k} - (1 + N_{non-tr})\right) L.E_{DA} + L.E_{elec} + L.\in_{fs} d^2_{to\,BS}$$

----(4)

Where E_{CH} is the energy dissipation of Cluster head, N_{non-tr} is number of non transmitting nodes, $d_{to\,BS}$ is the distance between BS and CH; $d_{to\,BS} = M\sqrt{\frac{1}{2\pi k}}$ where M is the length of the network area.

$$E_{non-CH} = \left(\frac{n}{k} - (1 + N_{non-tr})\right)(L.E_{elec} + L.\in_{fs} d^2_{to\,BS})$$

---- (5)

E_{non-CH} is the energy dissipated by all non CH nodes of the cluster, $d_{to\,BS}$ represents the distance between the cluster head and the node. Now the total energy dissipation during the one round of transmission is given by

$$E_C = E_{CH} + E_{non-CH}$$

----------(6)

if 'k' is the total number of the clusters,

$$E_t = k\ X\ E_C$$

----------(7) 'k' represents the number of clusters, 'E_{DA}' is energy required for data processing.

and energy expended by cluster member node is given by the equation,

$$E_{nonCH} = L.E_{elec} + \mathrm{L}.\in_{fs} d^2_{to\,BS}$$

Total energy consumed by the network is given by,

$$E_{tot} = L\,(2n.E_{elec} + n.E_{DA} + \in_{fs}(k\,d^2_{to\,BS} + n\,d^2_{to\,BS}))$$

a. Evaluation of simulation results

Fig. 2 shows the number of alive nodes with respect to number of rounds, it is observed that the proposed algorithm outperforms the LEACH, SEP, SHEEP AND SHEEP-OC due to reduced number of transmissions by using adaptive sensing algorithm, as a result the algorithm can increase the lifetime of the network by 33% compared to the SHEEP-OC without implementation of adaptive sampling technique

In fig.3 it can be observed that the length of stable region has been extended for different values of energy heterogeneity, proposed protocol SHEEP-OC-AS has longer stable region, almost 50% improvement over SHEEP-OC

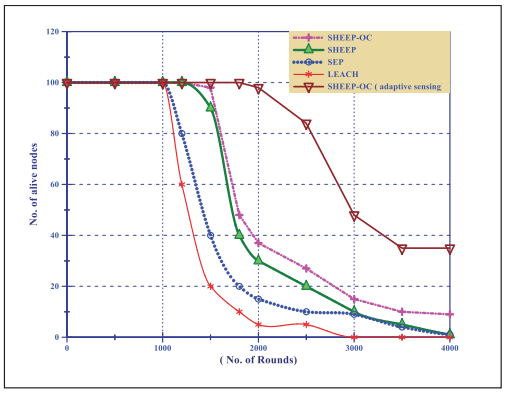

Fig.2 Network lifetime (No. of alive nodes VS simulation time) SHEEP-OC (adaptive sampling) with LEACH, SEP & SHEEP-OC

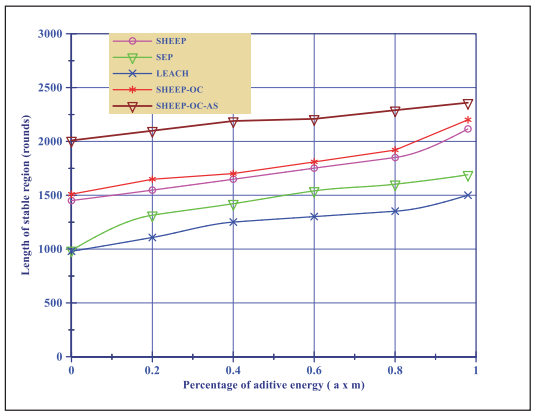

Fig.3 Length of the stable region for different values of heterogeneity comparison of SHEEP-OC-AS with LEACH, SEP, SHEEP & SHEEP-OC.

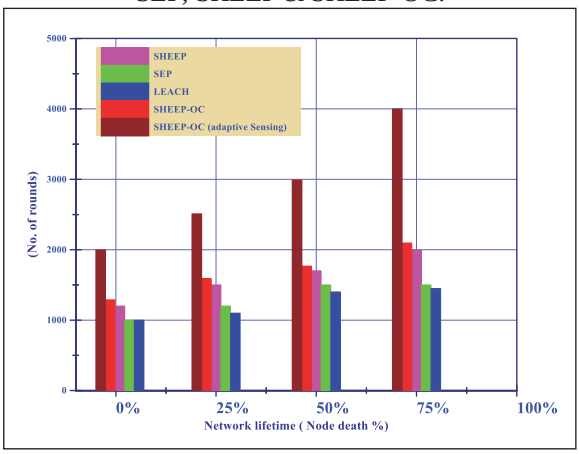

Fig.4 Node death percentage per analysis of SHEEP-OC(adaptive sampling) with LEACH, SEP, SHEEP& SHEEP-OC protocols.

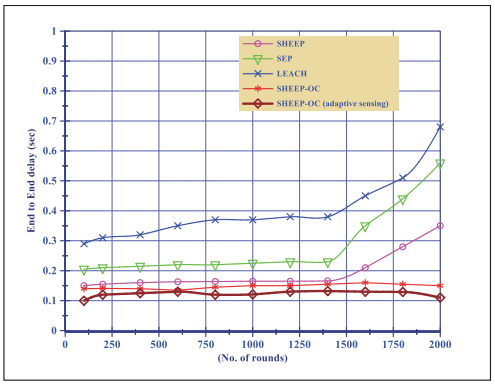

Fig.5 End to End delay comparison for the proposed with LEACH, SEP , SHEEP & SHEEP- OC.

Fig.5,6&7 shows the end to end delay, throughput analysis and PDR perfomance of the proposed SHEEP-OC-AS with the existing LEACH, SEP, SHEEP & SHEEP-OC Protocol. From the results, it shows that the proposed system can successfully transmits the data in lesser time with high rate due reduced number of transmissions.

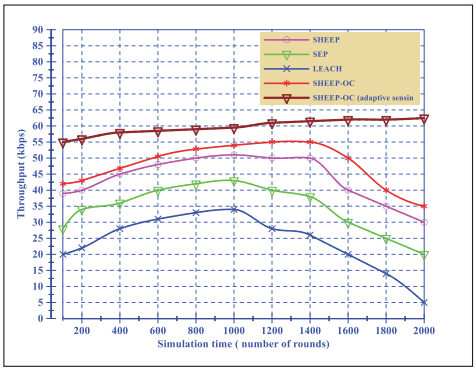

Fig. 6 Throughput analysis for proposed SHEEP-OC (adaptive sensing) with the existing LEACH, SEP, SHEEP & SHEEP-OC Protocols.

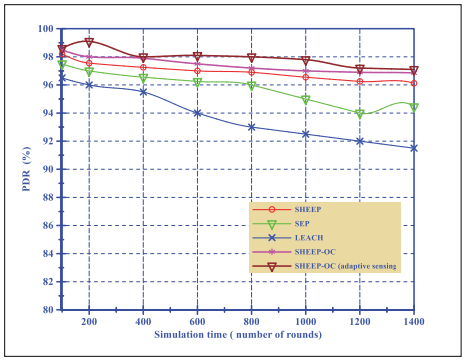

Fig. 7 Packet delivery ratio of SHEEP-OC with the existing LEACH, SEP and SHEEP Protocols.

IV. CONCLUSION

Performance evaluation of these protocols are performed by conducting comparative simulation study along with discussions in terms of well defined performance measures. These performance measures are stability period, network lifetime, throughput, end to end delay, packet delivery ratio. It has been noticed that the lifetime and stability period of the network. Fig. 2 & 4 shows that how many nodes are alive as the number of rounds increases. Results show that SHEEP-OC(adaptive sensing) has maximum network lifetime as compared to the other protocols. Maximum stability of SHEEP-OC(adaptive sensing) is also a significant achievement. Stability period of SHEEP-OC(adaptive sensing) is almost 150 %, 100 %, 75 %, 50 % greater than LEACH, SEP, SHEEP and SHEEP-OC, respectively. Main reasons behind this drastic improvement are threshold based transmissions.

V. REFERENCES

[1]. Akyildiz, Ian F, Weilian Su, Yogesh Sankarasubramaniam, and Erdal Cayirci. "A survey on sensor networks." IEEE communications magazine 40, no. 8 (2002): 102-114.

[2]. Akkaya, Kemal, and Mohamed Younis. "A survey on routing protocols for wireless sensor networks." Ad hoc networks 3, no. 3 (2005): 325-349.

[3]. Zhengwang Ye, Tao Wen, Zhenyu Liu, Xiaoying Song, "A security fault-tolerant routing for multi-layer non-uniform clustered WSNs" EURASIP Journal on Wireless Communications and Networking, 2016:192 https://doi.org/10.1186/s13638-016-0692-3.

[4]. Jinglong Zhou, Martin Jacobsson and Ignas Niemegeers," Link Quality-Based Transmission Power Adaptation for Reduction of Energy Consumption and Interference" EURASIP Journal on Wireless Communications and Networking, 2010:92013.

[5]. C. Tang, C. Raghavendra, "Compression Techniques for Wireless Sensor Networks", Wireless sensor Networks, Kluwer Academic Publishers, Boston, USA, 2004.

[6]. Mukesh Kumar, Kamlesh Datta, "LDAT: LFTM based data aggregation and transmission protocol for wireless sensor networks" ournal of Trust Management20163:2 https://doi.org/10.1186/s40493-016-0023.

[7]. Mohammed Moyed Ahmed, Dr.D. Sreenivasa Rao," Stable Heterogeneous Energy Efficient Cluster Based Protocol (SHEEP) For Application-Specific WSNs" International Journal of Emerging Technology and Advanced Engineering (ISSN 2250-2459, ISO 9001:2008 Certified Journal, Volume 8, Issue 1, January 2018).

[8]. Mohammed Moyed Ahmed, Dr.D. Sreenivasa Rao, "Stable Heterogeneous Energy Efficient Protocol with Optimum Clustering (SHEEP-OC) in Wireless Sensor Networks" International Journal of Emerging Technologies in Engineering Research, ISSN 2454-6410, Volume 6, Issue 3, March 2018).

[9]. Liu C, Liu Y, Zhang ZJ (2013) Improved reliable trust-based and energy-efficient data aggregation for wireless sensor networks. Int J Distrib Sens Netw 2013(652495):1–11.

[10]. Wenjing Guo, Wei Zhang " A survey on intelligent routing protocols in wireless sensor networks", Journal of Network and Computer Applications 38 (2014) 185–201.

[11]. Baranidharan B, Shanti BA. "Survey on energy efficient protocols for wireless sensor networks". International Journal of Computer Applications 2010;11(10):35–40.

ResearchGate

See discussions, stats, and author profiles for this publication at: https://www.researchgate.net/publication/325809951

HADOOP based image compression and amassed approach for lossless images

Article · January 2018

DOI: 10.4066/biomedicalresearch.29-17-3062

CITATIONS
2

READS
64

4 authors, including:

Nisar nisar Ahmed
Institute of Aeronautical Engineering
8 PUBLICATIONS **5** CITATIONS

SEE PROFILE

All content following this page was uploaded by Nisar nisar Ahmed on 10 January 2022.

The user has requested enhancement of the downloaded file.

Biomedical Research 2018; 29 (8): 1532-1542 *ISSN 0970-938X*
www.biomedres.info

HADOOP based image compression and amassed approach for lossless images.

Ruhiat Sultana[1*], Nisar Ahmed[2], Syed Abdul Sattar[3]

[1]Rayalaseema University, Kurnool, Andhra Pradesh, India

[2]Mewar University, Chitoghar, Rajasthan, India

[3]Department of Electronics, Mewar University, Chitoghar, Rajasthan, India

Abstract

Background: This paper develops Hadoop based image compression approach, to solve the problem of low image quality, low compression ratio and high time that occurs during lossless image compression.
Method: Lossless image is considered in this paper because in case of lossy compression it leads to information loss which cannot retrieve anymore. By the employment of Hadoop based technique this paper proposes a novel image compression for lossless images. This method makes use of Weiner filter for the cancellation of noise and image blurring.
Result: Followed by this, hybrid concepts are employed to perform segmentation and feature extraction. Finally, compression is done with the help of Hadoop map reduce concept.
Discussion: Our proposed technique is implemented in MATLAB and therefore the experimental results proved the effectiveness of proposed image compression technique in terms of high compression ratio and low noise ratio when compared with existing techniques.

Keywords: Image compression, Weiner filtering, Bray-curtis dissimilarity, Hadoop map reduce, Isomap technique, Minimum spanning tree, Non-parametric non-uniform intensity normalization.

Accepted on January 24, 2018

Introduction

In the current advancement of multimedia applications like medical imaging, image archiving, remote detecting, computerized image photography etc., image compression assumes an overwhelming part in its performance and upcoming features [1]. While compressing the images enhance the speed of the document exchange, storage capacity, network bandwidth etc. [2]. In image compression two different processes is carried out to be specific encoding and decoding. In encoding section the first image takes as an input and in the wake of processing the compressed image will be its output yet in decoding section the process is carried out in reversible order [3]. Also image compression is partitioned into two different categories such as lossy compression and lossless compression. The bandwidth, storage space and even small subtle elements from the image can be extracted utilizing the technique of lossy image compression [4].

For the most part in lossy compression, the redundant image pixels are neglected during compression process and it is more capable for achieving higher compression [5]. The compressed image is subjected to decompression process to recover the first image in lossless image compression [6]. In the current scenario, image compression assumes a noteworthy part in research areas; it is one of the sort of modern image compression technique. Encryption is an important step to be done before the process of compression [7]. Double encryption technique was discussed to be specific multiple Huffman coding where tables were actualized to secure Huffman coder and the other is secure QM coder [8]. In order to decrease the encryption and decryption time, encryption process is done somewhat [9,10].

Fractal compression process through the self-comparative properties in different fractions of images which depends on the fact that the image parts are frequently looks like different parts of a similar image [11]. However the significant drawback in Fractal Image Compression (FIC) is that, here the encoding of fractals is exceptionally complex, compressing time is high because of its complexity and consumption of time to search for the best matching block [12]. Fractal Image Compression (FIC) depends on Iterated Function System (IFS) is utilized to represent the self-similitudes of the images and is represented as a limited arrangement of contraction mapping for each image that has the fixed point which is identical to the image itself [13]. On the other hand while applying the change iteratively on the irregular introductory image, the result will orchestrated to be the first image [14]. One of the special kinds of IFS is the Partitioned Iterated Function System (PIFS), which is utilized to demonstrate the image blocks by using the

characteristic of self-similitude's in view of different parts of the images to achieve image quality and compression ratio [15].

Recent advances in image compression have prompted numerous knowledge, imaging in more extensive algorithms, and decreased stockpiling requirements are conceivable [16]. Multimedia applications like graphics, sound and video data's requires considerable bandwidth and storage capacity when it is uncompressed. Moreover this leads to a need of compression of images and all multimedia applications to save storage and transmission time [17]. Algorithms like inserted zero wavelet algorithm, convergent algorithm, Fuzzy vector quantization algorithm etc. are utilized already to compress the images with high quality and reduced size [18,19]. Be that as it may, during compression the encoding stage takes more than the decoding stage yet it achieves the resulted image with great quality [20].

The paper is sorted out as takes after. Section 2 analyses the research works related with our proposed strategy. Section 3 discussed about the proposed procedure for image compression. Section 4 illustrates the approved results. Section 5 describes the conclusion.

Related Work

This section provides an overview of the lossless image compression techniques available in the literature. Several algorithms and techniques have been proposed in the last decade, but there are considerable differences in, each with respect to the datasets used, segmentation objectives and validation. A summary of the different approaches and their features of lossless image compression are presented below.

Xinpeng et al. [21] discussed around an approach for the compression of images. Here the process of compression is done after the process of encryption of the images. Encryption is finished by producing helper data and this assistant data will be valuable during the process of image compression and decompression. At the sender side the image was compressed utilizing quantization technique in view of the ideal parameters generated from the assistant data. After that the compressed image is broadcasted alongside encrypted part. At the receiving end the image was decrypted utilizing the compressed encrypted data and secret key.

Chaurasia et al. [22] described a compression scheme named as quick fractal compression scheme in view of feature extraction and inventive method for image comparison. Here in the advancement, the complexity in view of the applicable space search was reduced by changing the issue from image area to vector area. Fractal image compression process is utilized to compress the image by parcelling the image into different geometric subsections. It uses the existence of self-symmetry and utilizations relative contractive changes.

Dar et al. [23] discussed a technique of post processing for the reduction of compression artifact. The approach managed the errand as a reverse issue with a regularization that influences on existing cutting edge image de noising algorithms. Here fitting and-Play Prior system, recommending the solution of general converse issues by means of Alternating Direction Method of Multipliers (ADMM). The principle process in their scheme was linearization of the compression-decompression process, to survey a formulation to be enhanced.

Hussain et al. [24] described around an image compression technique named as Hybrid Predictive Wavelet coding. The proposed technique incorporates the properties of predictive coding and discrete Wavelet coding. Here to evacuate between pixel redundancies, the data values are pre-processed utilizing a nonlinear neural network predictor coding. The error rates, which were the difference between the first and the predicted values, discrete wavelet coding changed.

Wu and Ming [25] developed a Genetic Algorithm (GA) in perspective of Discrete Wavelet Change (DWT) to overcome the drawback of the time-consuming for the fractal encoder. At initially, for each range block, two wavelet coefficients are used to locate the fittest Dihedral block of the space block. The comparable match is done just with the fittest block to extra seven eighths redundant MSE computations. Next implanting the DWT into the GA, a GA in light of DWT is attempted to quick formative speed encourages and keeps up incredible recovered quality.

Neoteric Image Compression for Lossless Images

To overcome the drawbacks of lossless image compression an efficient approach known as Hadoop based image compression is proposed for seeking accurate image compression. Before the process of compression there are three major steps involved here. The first phase performs preprocessing for the given input image for the removal of noise and image blurring by the employment of Weiner filter. Weiner filter is different from other filter and has the special benefit of performing inverse filtering and controls output error. The output image from the Weiner filter is used as input to the Minimum Spanning Tree (MST) to segment the images and the MST segmentation is modified with the Bray-Curtis Dissimilarity (BCD) distance method which is a dimension independent distance. The advantage of using MST is that it segments the image based on the weights, so that efficient segmentation result can be obtained. After that BCD distance method is exploited to measure the dissimilarity between images. As a result it acquires accurate segmented image and this image is given as the input for the next phase. The next phase is the feature extraction. Here, Isomap technique with N3 (Non-parametric non-uniform intensity normalization) is used to extract the feature textures and intensity which will remove the extra information and minimize the image. Isomap technique is utilized for the purpose of reducing dimensionality which transforms high dimensional space to less space and N3 is a type of normalization technique in which the accurate needed information is extracted. The extracted dimensionally reduced features are compressed by performing compression technique with Hadoop based on Map Reduce function and is carried out to improve the encoding speed. The tools employed for processing in Hadoop is basically located in same servers, due

to this the processing time will be reduced and security is cent percent guaranteed in Hadoop map reduce because it works with HDFS and HBase security that allows only approved users to operate on data stored in the system. Thus through this approach we can attain the efficient result. The process flow diagram of the proposed method is shown in the following Figure 1.

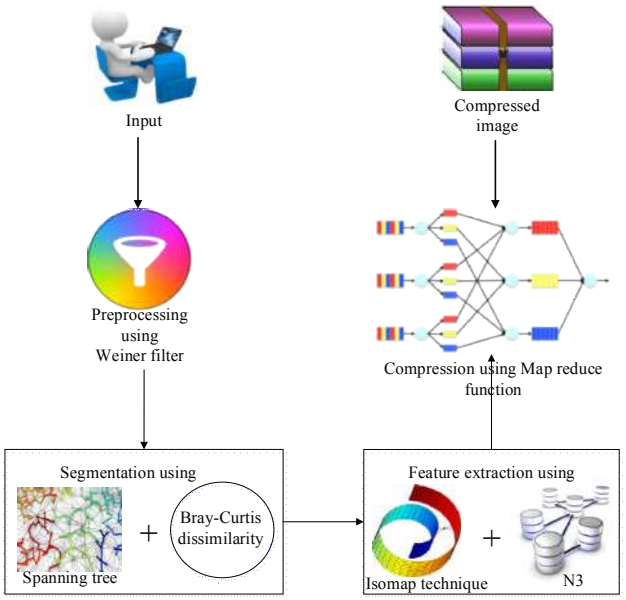

Figure 1. *Proposed architecture.*

Pre-processing using Weiner filter

Pre-processing is the first step to be carried out in image processing. This is performed by the employment of Weiner filter in [26]. Weiner filter is different from other filter and has the speciality of performing inverse filtering and controls output error. In pre-processing phase, Weiner filter is employed to remove low frequency background noise and blurred image. Normally noise will appear due to malfunctioning pixels in camera sensors. In this paper Weiner Filter is utilized which is a type of linear filter. It is used to smoothen the image at low variance and high variance. When compared to linear filters, Weiner filter provides better results (Figure 2).

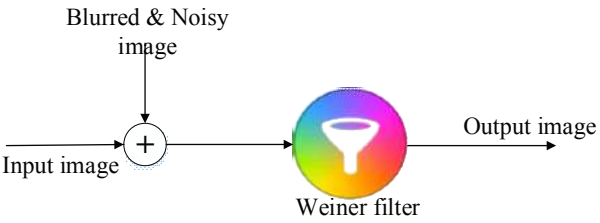

Figure 2. *Weiner filter.*

The inverse filtering is the restoration technique for de-convolution. At the point when the image is obscured by a known low pass filter, it is conceivable to get back the image by converse filtering. This converse filtering is exceptionally touchy to additive noise. The strategy for reducing one degradation at a time enables us to build up a restoration algorithm for each kind of degradation and just combine them. The Weiner filtering executes an ideal trade-off between converse filtering and noise smoothing. It expels the additive noise and modifies the obscuring in the meantime. The Weiner filtering is perfect as far as the mean square error. Weiner filter is utilized to limit the general mean square error in the process of backwards filtering and noise smoothing. The Weiner filtering is a linear estimation of the first Image. This depends on stochastic system. The output from the Weiner filter is the noiseless image.

Segmentation using Hybrid MST and BCD

After the process of noise removal the next step is the segmentation of image. In this paper, MST method in [27] performs segmentation process. The advantage of using MST is that it segments the image based on weights, so that efficient segmentation results can be obtained. The main problem in MST is finding the minimum weight for set of edges that connects all their vertices when connected graph G with positive edge weights is given. Consider an image for this MST problem,

Undirected graph $G=(V, E)$,

Where, V=the set of pixels,

E=the set of possible interconnections between pairs of pixels,

The weight of E is the difference of intensity values between neighbouring pixels. After that find an acyclic subset that connects all of the pixels and whose total weight is minimized. Eventually, the result of the segmentation is obtained by simply cutting edges whose weights are larger than a threshold value.

MST creation: The initial solution is a singleton set containing an edge with smallest weight and then current partial solution repeatedly expands by adding the next smallest weighted edge under constrain that no cycles are formed until no more edges can be added.

Steps for Mst generation

Input: A non-empty connected weighted graph with vertices V and edges E

Output: MST

Step 1: Initialize: $V_{new}=\{u\}$,where u is an arbitrary node from V, $E_{new}=\{\}$

Step 2: Repeat until $V_{new}=V$

Step 3: Select an edge$\{x, y\}$with minimal weight such that x is in V_{new} and y

Step 4. Add y to V_{new} and$\{x, y\}$ to E_{new}

This above steps explains the creation of MST. The main reason behind using Prims algorithm is to construct MST that it tends to group pixels of similar (edges with small weights) together. If an image contains number of objects, each of which has a uniform depth, then the pixels representing each object will form a sub tree for the spanning tree obtained by Prims Algorithm. In general we would expect that if an image

consists of number of objects represented by adjacent regions, Prims Algorithm would build a MST so that each object forms a sub tree. Along with the depth, height and width is taken into consideration so that, the objects will be grouped according to the depth. After the creation of adjacency graph, MST is to be constructed. MST is constructed to obtain shortest weight between points without removing the points in the point cloud. So creation of MST helps to find out all the points with minimum weight. At last an edge with largest weight is obtained as the final point. The output from the spanning tree will be segmented tree of image (Figure 3).

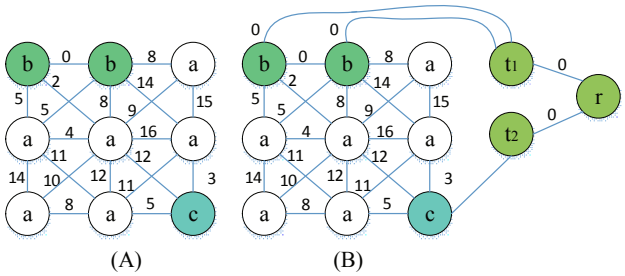

Figure 3. *MST. (a) Original image graph g, where colour vertices represent markers b and c; non-marker pixels are denoted by "a" (b) Addition of extra vertices t_1, t_2, and r to the graph. MST of the graph presented in (b).*

BCD: The segmented tree structured image which is the output from the MST is given as the input to the BCD method [28]. BCD is used to calculate the dissimilarity between images. Euclidean distance is one of the prevalent metric exploited to measure the distance between subjects. It makes use of principle of distance that is appropriate for univariate data. In literature, the other distance metrics are also appealing and that can be preferred for multivariate samples. Some of them still satisfy the basic axioms of what mathematicians call a metric, while others are not even metrics, but still make good sense as a measure of difference between two samples in the context of certain data. Among them, BCD metric is preferred that is popular in the study of environmental science problems. In ecology and science, the BCD metric is statistically used to quantify the compositional difference between two different destinations in view of counts at each site. With regards to ecological abundance, data collected from different inspecting locations quantifies the difference between tests utilizing Bray Curtis, which is one of the notable disparity metric. This measure gives off an impression of being sensible to achieve the results. Be that as it may, it doesn't fulfil the triangle disparity aphorism and hence is not a genuine distance when Bray and Curtis examine the Bray Curtis divergence metric. One of the suspicions of BCD metric is that the examples are taken from the same physical size such as area or volume. This is because uniqueness will be computed on crude counts not on relative counts as a result it leads to higher general abundance and is a piece of difference between these two samples that is, size and state of the count vectors will be considered in the metric. The computation includes summing the total differences between the counts and isolating this by the entirety of the abundances in the two samples. The general formula for calculating the BCD between two samples is given as follows.

$$l_{BCD}(V_{new}, E_{new}) = \frac{\sum_{i=1}^{M} \left| V_{new_i} - E_{new_i} \right|}{\sum_{i=1}^{M} V_{new_i} + E_{new_i}} \rightarrow (1)$$

Where, M is the dimensionality of the image, Y is the test image, X is the training image and V_{new}, E_{new} are the i^{th} values of the X and Y images to be compared. The Bray Curtis should be reversed for similarity computation is shown as below.

$l_{BCS}=1-l_{BCD} \rightarrow (2)$

The classification performance of the LBP and ALBP methods are evaluated on face databases such as Extended Yale B, Yale A and our database.

Algorithm for MST with BCD

Input: Filtered image

Output: Segmented image

Initialize number of trees, weight values, gray image

For n=1 to number of trees do

Estimate height and weight for the image

For *i*=2 to *h*i-1 do

For *j*=2 to *w*i-1 do

Calculate the distance based on weight value

End

End

End

Initialize segmented image

For *i*=1 to length of s_{img} do

Calculate distance value for the segmented image

End

The output after processing from MST and BCD is the best segmented image.

Feature extraction based on ISOMAP and N3

After the process of segmentation, the next phase is the feature extraction. In our proposed method, ISOMAP technique with N3 is employed to perform feature extraction. Iso map technique in [29] is utilized for the purpose of reducing dimensionality which transforms high dimensional space to less space and N3 [30] is a type of normalization technique in which the accurate needed information is extracted.

ISOMAP algorithm: The initial set is assumed as M real value vectors of high dimensional space R_h and is projected to low dimensional space R_l ($l<h$). The basic process of iso map is to obtain the expression of data set of observation space in a low dimensional space through distance preserving mapping when the distribution of data set possesses low dimensional

embedding manifold structure. This algorithm is divided by the following steps.

Step 1: Form the neighbour graph G

Define with the Euclidean distance l_{BCD} (V_{new}, E_{new}) between points V_{new} and E_{new}, if is located within the radius r of V_{new} or among O nearest points of V_{new} then connect V_{new} and E_{new} points. And the length of the side equals to l_{BCD} (V_{new}, E_{new})

Step 2: Calculate the shortest path

Calculate the shortest path l_G (V_{new}, E_{new}) between V_{new} and E_{new} in the neighbour graph with Floyd algorithm and estimate the geodesic distance in topologic space p based on the said path.

Step 3: Form the l dimensional embedding

By adopting the classical MDS method, form a l dimensional embedding space X that keeps the essential structure of topologic space on distance matrix $h_G=\{l_G (V_{new}, E_{new})\}$, h_X is the Euclidean distance matrix of l dimensional space, coordinate vector is obtained through the following equations which can minimize error.

$=|| (h_G)- (h_X)||_2 \rightarrow (3)$

The matrix transform operator $_h=-HSH/2$, D means distance matrix squared $\{Di_{Vnew}\ i_{Enew}=h^2\ i_{vnew}\ i_{Enew}\}$, C means centralized matrix $\{Ci_{Vnew}\ i_{Enew}=Di_{Vnew}\ i_{Enew}-1/m\}$ the min value of Equation 9 is realized by acquiring the feature vector corresponding to d max feature values of matrix (h_G).

ISOMAP gives the rules for determining the number of dimensionalities to be reduced and it defines the residual error e (l) to measure the error of dimensionality reduction.

$e (l)=l-R^2 (h_G, h_X) \rightarrow (4)$

Where R^2 is linear correlation coefficient; generally, the higher the number of dimensionalities to be reduced the lower the residual error. ISOMAP determines the number of dimensionalities to be reduced in the following two situations:

1) Inflection point appears on the residual error curve

2) The residual error is small and approaches to certain threshold value.

One advantage of ISOMAP is that, for single manifold structure, “elbow” phenomenon appears when the variance of Equation 1 is solved during dimensionality reduction, based on this, the intrinsic dimensionality of manifold is judged.

N3 technique: In this phase, the intensity is corrected by using *N3*. And the problem of correcting intensity non-uniformity is simplified when it is modelled as a smooth multiplicative field. It is consistent with multiplicative non-uniformity arising from variations in the sensitivity of reception coil and with non-uniformity to a lesser extent due to induced currents and non-uniform excitation.

Consider the image formation in MR is

$x (l)=y (l) f (l)+e (l) \rightarrow (5)$

Where, y indicates the measured signal, x indicates the true signal emitted by the tissue, f is an unknown smoothly varying bias field, and e is white Gaussian noise assumed to be independent of x at location l. The problem of compensating for intensity non-uniformity is the task of estimating f.

In the noise-free case, the true intensities x at each voxel location i are independent identically distributed random variables. Using the notation $\hat{y}\ (l)=log\ (y\ (l))$ the image formation model becomes additive.

$$\hat{x}(l) = \hat{y}(l) + \hat{f}(l) \rightarrow (6)$$

Let X, Y, F are the probability densities of $\hat{x}$, $\hat{y}$, $\hat{f}$ respectively. Making the approximation that $\hat{y}$ and $\hat{f}$ are independent or uncorrelated random variables, the distribution of their sum is found by the convolution as follows.

$$X(\hat{x}) = F(\hat{x}) \times Y(\hat{y}) = \int F\left(\hat{x} - \hat{f}\right) Y\left(\hat{f}\right) d\hat{f} \rightarrow (7)$$

The non-uniformity distribution F can be viewed as blurring the intensity distribution J.

Correction strategy: From signal processing perspective, blurring due to the field reduces the high frequency components of Y. The task of correcting intensity non-uniformity is equal to that of restoring the frequency content of Y. Our approach for correcting the non-uniformity is to find the smooth, slowly varying, multiplicative field that maximizes the frequency content of Y. As evidence of the simple form of the distribution F, consider the distribution. These have been derived from the fields fitted to manually labelled regions of white matter on 12 individuals. Each individual was scanned using the same pulse sequences but on a different MR machine. As the large scale features of F vary little between scans. Returning to the optimization criterion, one could be in a principle search through all possible fields $\hat{f}$ to find the one that maximizes the high frequency content of Y.

There are two drawbacks arises in this approach, (i) large search space for 3D fields, (ii) computation of entropy is difficult.

In this approach, we propose a distribution for Y by sharpening the distribution X, and then to estimate corresponding smooth field which produces a distribution Y close to the proposed one. If F is Gaussian, then it searches only the space of all distributions Y corresponding to F with zero mean and given variance. In this way the space of all distributions Y is collapsed down to a single dimension in the width of the F distribution.

In practice, the field distribution F is only approximately Gaussian and some of our assumptions, such as zero noise, are violated. The benefit of this approach is that between subsequent estimates of Y, corresponding smooth field $\hat{f}$ is estimated. The constraint that the field be smooth changes the shape of the proposed distribution Y to the one that is consistent with the field. These iterations proceed until no

further changes in $\hat{f}$ or X result from de-convolving narrow Gaussian distributions from X.

Field estimation: Further theory is presented here to explain the process of proposing distributions for Y and estimating corresponding fields. For notational simplicity, we will assume that the true distribution of intensities Y can be arrived at a single iteration by de-convolving a distribution F, which is Gaussian from X. The full iterative description of the method is left for a subsequent section.

For the given the distribution Y, the method for estimating corresponding field is as follows. For a measurement of $\hat{x}$ at some location l, $\hat{y}$ is estimated using the distributions Y and F. Since the choice of the location l is arbitrary, the measurement $\hat{x}$ can be treated as a random sample from the distribution X. The expected value of $\hat{y}$ gives the measurement $\hat{x}$ as follows.

$$\Re\left[\frac{\hat{y}}{\hat{x}}\right] = \int_{-\infty}^{\infty} \hat{y}s\left(\frac{\hat{y}}{\hat{x}}\right)d\hat{y} = \int_{-\infty}^{\infty} \hat{y}\left(\frac{s(\hat{y},\hat{x})}{s(\hat{x})}\right)d\hat{y} \rightarrow (8)$$

$$\Re\left[\frac{\hat{y}}{\hat{x}}\right] = \frac{1}{X(\hat{x})}\int_{-\infty}^{\infty} \hat{y}s(\hat{y},\hat{x})d\hat{y} \rightarrow (9)$$

$$= \frac{1}{X(\hat{x})}\int_{-\infty}^{\infty} \hat{y}s\left(\hat{y},\hat{f}\right)d\hat{y} \rightarrow (10)$$

$$= \frac{1}{X(\hat{x})}\int_{-\infty}^{\infty} \hat{y}p\left(\hat{y}\right)S\left(\hat{f}\right)d\hat{y} \rightarrow (11)$$

$$= \frac{\int_{-\infty}^{\infty}\hat{y}F(\hat{x}-\hat{y})Y(\hat{y})d\hat{y}}{\int_{-\infty}^{\infty}F(\hat{x}-\hat{y})Y(\hat{y})d\hat{y}} \rightarrow (12)$$

An estimate of $\hat{f}$ can be obtained using the estimate of from Equation 17 as follows.

$$= \quad \hat{f}_e(\hat{x}) = \Re\left[\frac{\hat{f}}{\hat{x}}\right] = \hat{x} - \Re\left[\frac{\hat{y}}{\hat{x}}\right] \rightarrow (13)$$

Where, $\hat{f}_e$ is an estimate of $\hat{f}$ at location l based on the single measurement of $\hat{x}$ at l. This estimate can be smoothed by the operator S_m to produce

$$\hat{f}_e(\hat{x}) = Sm\left\{\hat{f}_e(\hat{x})\right\} = Sm\left\{\hat{x} - \Re\frac{\hat{y}}{\hat{x}}\right\} \rightarrow (14)$$

An estimate of $\hat{f}$ based on all of the measurements in a neighborhood of l.

Given a distribution F and the measured distribution of intensities X, the distribution Y can be estimated using a de-convolution filter as follows:

$$\tilde{G} = \frac{\tilde{F}^*}{\left|\tilde{F}\right|^2 + \mu^2} \rightarrow * (15)$$

$$\tilde{Y} \approx \tilde{G}\tilde{X} \rightarrow (16)$$

Where, * denotes complex conjugate, $\tilde{F}$ is the Fourier transform of F, and μ is a constant term to limit the magnitude of $\tilde{G}$. This estimate of Y is then used to estimate a corresponding field $\hat{f}$.

Implementation details: The nonparametric correction process is shown in the Figure 4. Besides the processing steps described previously, there are number of steps needed for practical implementation of the algorithm.

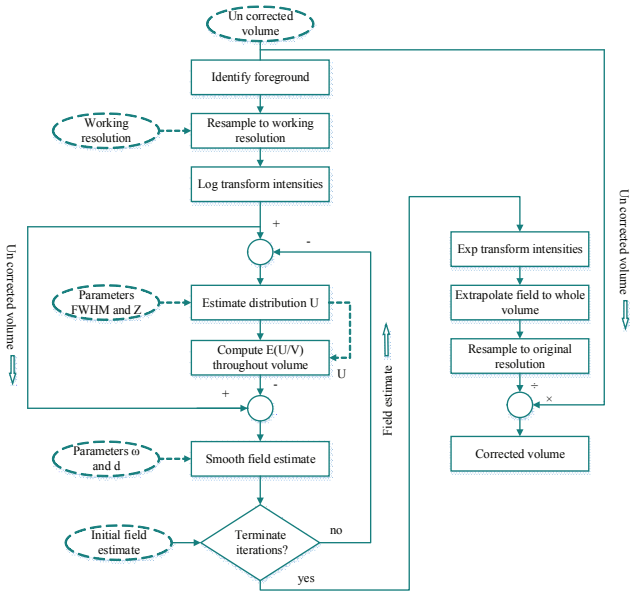

Figure 4. *Flowchart for N3.*

Here ellipses represents user-selected parameters and priors. Rectangles are processing steps. The flow of volumetric data and other data is represented by solid lines and dashed lines. Circles perform arithmetic operations on a voxel by voxel basis. The result of the process is a corrected volume.

The first step "identify foreground," is to segment and remove empty regions from the volume. Besides the numerical problems associated with transforming values near zero to the log domain, these background regions provide no information about the non-uniformity field. Since the accuracy of this segmentation is not critical, the foreground is determined using a simple threshold chosen automatically by analysing the histogram of the volume.

A histogram with equal-size bins and a triangular Parzen window is used to estimate X. Given a set of N measurements x (l_u) and locations l_u, X, is estimated as follows:

$$X(\hat{x})\frac{1}{N}\sum_{u=1}^{N}\frac{1}{d}\varphi\left[\frac{\hat{x}_v-\hat{x}(l_u)}{h}\right]\rightarrow(17)$$

$$\varphi(P)=\begin{cases}1-|P|, & |P|<1\\ 0, & \text{elsewhere}\end{cases}\rightarrow(18)$$

Where, $x\hat{}_v$ is the centers of the bins and dis the distance between them. For a typical 20% bias field, the scale factor f ranges from 0.9 to 1.1 which corresponds to $f\hat{}$ between 0.1 and 0.1. MR volumes generally have sufficient data to estimate X at a resolution d better than a tenth of this range.

Smoothing the non-uniformity field at full resolution is computationally expensive, so the MR data is sub sampled without averaging to a lower resolution. Since the non-uniformity field is slowly varying, a 1 mm iso-tropically sampled volume is reduced to 3 mm and has a negligible effect on the field estimate and substantially accelerates computation. The processing of volume with ten iterations of N3 method is reduced from 4.5 h to 7 min of CPU time on a 200 MHz Intel Pentium workstation running Linux by re sampling to the coarser resolution. The final field estimate is re sampled to the original resolution and used to correct the original volume. The measure used to terminate the iterations is computed as follows:

$$e=\frac{\vartheta\{c_n\}}{\rho\{c_n\}},n=1...N\rightarrow(19)$$

Where, c_n is the ratio between subsequent field estimates at n^{th} location, ϑ denotes standard deviation, and ρ denotes mean. This measure is chosen so as to be insensitive to global scale factors that may accumulate with iterations. Iteration is stopped when e drops below 0.001, typically after ten iterations.

Smoothing: The manner in which the field estimate is smoothed has significant impact on the performance of the correction method. Smoothing is particularly challenging for this problem because the scale over which the field varies is compared to the size of the region being smoothed. Conventional filtering techniques proved unsatisfactory for this application since boundary effects significantly degraded overall performance.

The smoothness of the approximation is determined by two parameters: ω is the smoothing parameter and d is the distance between basis functions. Since splines are being used as filter for this application, the smoothness of the approximation must be chosen rather than derived from the data. The relationship between the smoothness of the approximation and the smoothing parameter is nonlinear. However, the normalization of the Bsp line has been chosed to eliminate the dependence of ω on scale and number of data points ω, can be fixed and the distance between basis functions varied instead. The output from this hybrid technique will be optimal extracted features.

Compression based on Hadoop map reduce

After the process of feature extraction, compression is the final step. This is done by the utilization of Hadoop map reduce [31]. The tools employed for processing in Hadoop is basically located in same servers, due to this the processing time will be reduced and security is cent percent guaranteed in Hadoop map reduce because it works with HDFS and *H* Base security that allows only approved users to operate on data stored in the system.

HADOOP: It is an open source framework used to process big data or datasets in a distributed environment. It provides with huge data storage space and excessive processing power. In our proposed scheme the compression process is done by Hadoop based on map reduce function. It is used to improve the encoding speed.

Map reduce: Map Reduce is used to process the data stored within Hadoop File System. Here the output is in the form of a <key, value>pair. A map reduce program consists of following 3 parts:

1. Mapper
2. Reducer
3. Record writer

Mapper: The text line input is divided in the form of no of input splits. The mapper process the data i.e., Input splits. Each of these input splits are assigned to a mapper.

No of input splits=No of mapper

The mapper doesn't accept text line input. It allows the input to be in a key, value pair. To convert the text line input to<key, value> pair, record reader is used. The record reader converts the byte oriented input into record oriented input.

Reducer: It obtains sorted<key, value>pairs sorted by the key. The value list contains all the values with the same key produced by mappers. Reducer combines the output from all the mappers and generates the final output. This final output shouldn't have any duplicate keys.

Record writer: Record writer writes the output to the output file by converting into text line-form.

Steps for Hadoop mapreduce

Step 1: Map (key, value):

{

It takes set of large data and processes it to give output in form of smaller chunks. It takes file from Hadoop distributed

File system and input is processed line by line.

For each attribute:

Output index and its value and class label of instance to generate key value pairs.

Return output key and output value

}

Step 2: Reduce (key, value)

{

Count occurrences of combination: attribute index and its value and class Label.

Print count against each combination.

}

The output from the Hadoop map reduction will be the compressed feature after encoding.

Results

The following table contains the information about the values obtained during implementation (Table 1).

Table 1. *Meta data information.*

Name	'en_val'
Global	0
Sparse	0
Complex	0
Persistent	0
Nesting	(1 × 1 struct)
Bytes	3840
Size	(16 30)
Class	'double'
Encryption time	0.11097 s
Decryption time	0.10745 s
PSNR value	2.0108
Bit Rate	1
Compression ratio	33.584616

This section shows the performance of the proposed Hadoop based image compression and the results obtained by them. In our proposed system the main objective is to accurately compress the given input image and overcome the problems that occur during image compression. The input contains some noise and this noise is removed by means of Weiner filter. The difference between input image and noiseless image is shown below in Figure 5.

Figure 5. *Input image and Weiner filter.*

After the removal of noise the first stage should be done in image processing is the segmentation of image. Here hybrid technique namely MST with BCD is employed for the purpose of segmentation. The segmented image using MST is shown below in Figure 6.

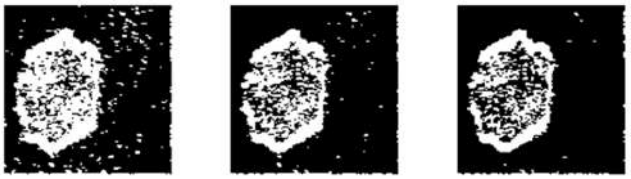

Figure 6. *Segmentation using MST.*

The segmented image after applying BCD is shown below in Figure 7.

Figure 7. *Segmentation using BCD.*

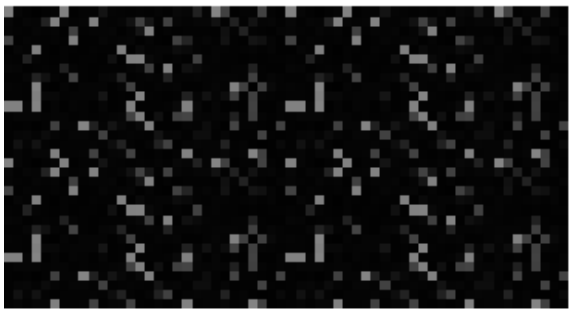

Figure 8. *Compressed image.*

After the process of segmentation the next step is the feature extraction. Here the process of extraction of feature is done by means of isomap technique and N3 (normalization technique). The features after the process of extraction is compressed and

encrypted by the employment of Hadoop map reduce. The compressed image is shown in Figure 8.

Performance result for the proposed approach

The following graph shows the results of our proposed approach *via* the parameters compression time, decompression time, compression ratio and PSNR (Figures 9-12).

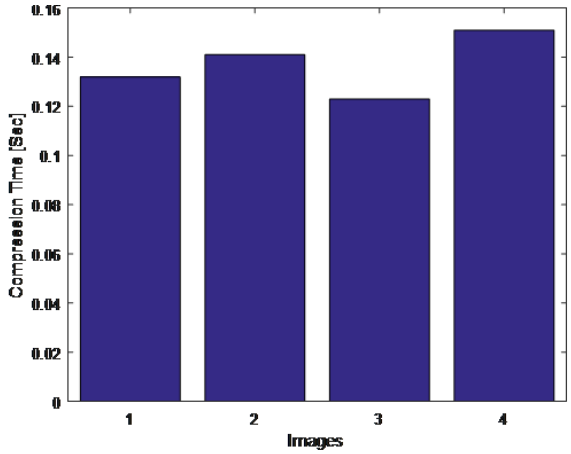

Figure 9. *Compression time.*

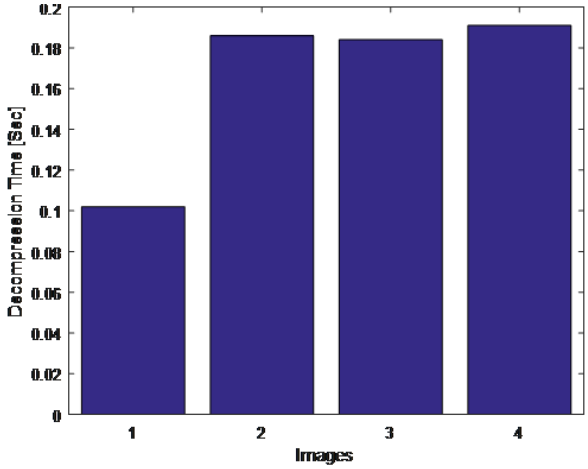

Figure 10. *Decompression time.*

Comparison result

The compression time and decompression time must always be low for obtaining efficient result. The compression and decompression time is compared with the existing QTC approach is shown below in Figure 13.

To evaluate the compression result two measures are commonly applied. The first one is the PSNR (peak signal to noise ratio) and the next is the CR (Compression Ratio).

The compression ratio for the compressed image must be always high in order to obtain good quality image. Compression is nothing but it eliminates unwanted information in order to gain high compression ratio. The compression ratio for our proposed system compared with the existing FIC approach, QTC and survey is shown below in Figure 14. PSNR is the process of measuring the quality of reconstructed image. PSNR value for accurate compressed image must be always low. The PSNR value for our proposed system compared with the existing FIC approach, QTC and survey is shown below in Figure 14.

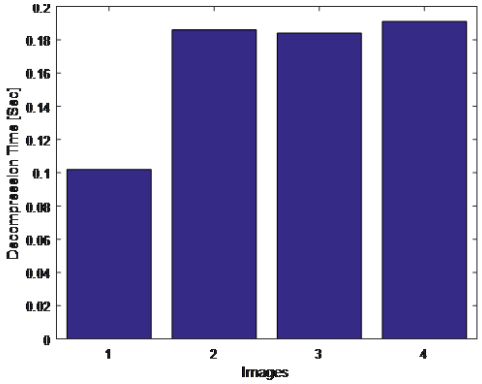

Figure 11. *Compression ratio.*

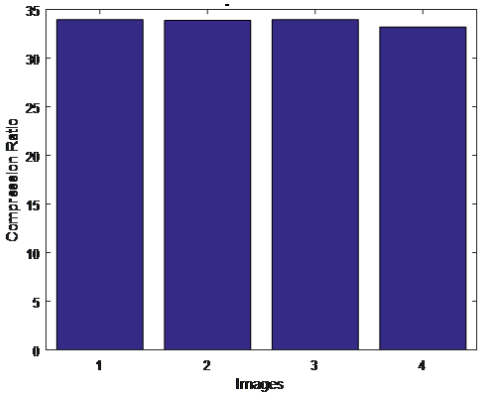

Figure 12. *PSNR.*

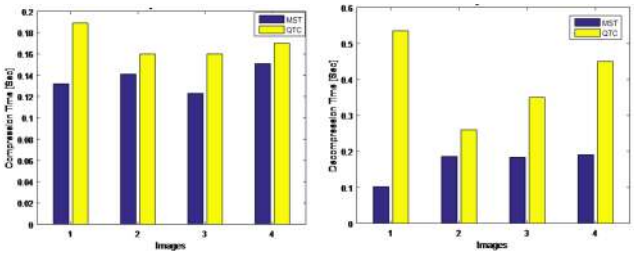

Figure 13. *Comparison of compression and decompression time.*

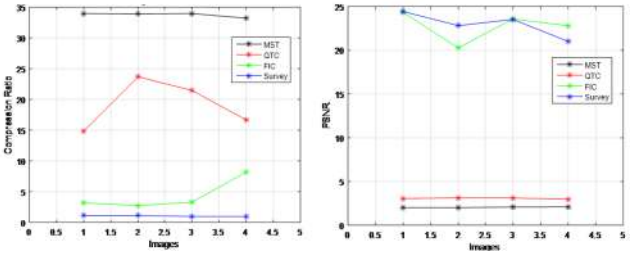

Figure 14. *Comparison of compression ratio and PSNR with [32,33].*

Conclusion

In image compression, the problem that occurs is the low image quality, compression ratio and speed. To solve and overwhelm these issues, Hadoop based image compression approach is proposed in this paper. The comparison results are obtained for the parameters compression time, decompression time, compression ratio and PSNR. The comparison tables and the graphs illustrated the performance of the proposed method with other researches. Hence with the aid of this proposed technique the problems in the existing image compression are reduced to greater extends.

References

1. Zhou N, Aidi Z, Fen Z, Lihua G. Novel image compression–encryption hybrid algorithm based on key-controlled measurement matrix in compressive sensing. Opt Laser Technol 2014; 62: 152-160.
2. Padmavati S, Vaibhar M. DCT combined with fractal quadtree decomposition and Huffman coding for image compression. Condition Assessment Techniques in Electrical Systems (CATCON) 2015; 28-33.
3. Bansal N. Image compression using hybrid transform technique. J Glob Res Comp Sci 2013; 4: 13-17.
4. Kamisli F. Block-based spatial prediction and transforms based on 2D Markov processes for image and video compression. IEEE Trans Imag Proc 2015; 24: 1247-1260.
5. Rufai AM, Gholamreza A, Hasan D. Lossy image compression using singular value decomposition and wavelet difference reduction. Dig Sig Proc 2014; 24: 117-123.
6. Xiao B, Gang L, Yanhong Z, Weisheng L, Guoyin W. Lossless image compression based on integer discrete tchebichef transform. Neuro Comput 2016; 214: 587-593.
7. Belloulata K, Amina B, Shiping Z. Object-based stereo video compression using fractals and shape-adaptive DCT. AEU Int J Electron Commun 2014; 68: 687-697.
8. Wu CP, Kuo CC. Design of integrated multimedia compression and encryption systems. IEEE Trans Multimed 2005; 7: 828-839.
9. Cheng H, Li X. Partial encryption of compressed images and videos. IEEE Trans Sig Proc 2000; 48: 2439-2451.
10. Ibrahim RA, Sherin YM, Saleh ME. An enhanced fractal image compression integrating quantized quadtrees and entropy coding. Innovations in Information Technology (IIT). Proceedings of 11th International Conference IEEE 2015: 190-195.
11. Zhou N, Aidi Z, Fen Z, Lihua G. Novel image compression–encryption hybrid algorithm based on key-controlled measurement matrix in compressive sensing. Opt Laser Technol 2014; 62: 152-160.
12. Song, C, Sud S, Madjid Mi, A robust region-adaptive dual image watermarking technique. J Vis Commun Imag Represent 2012; 23: 549-568.
13. Potluri US, Arjuna M, Renato CJ, Fabio BM, Sunera K, Amila E. Improved 8-point approximate DCT for image and video compression requiring only 14 additions. IEEE Trans Circ Sys I Regular Papers 2014; 61: 1727-1740.
14. Bairagi VK, Sapkal AM. Automated region-based hybrid compression for digital imaging and communications in medicine magnetic resonance imaging images for telemedicine applications. IET Sci Measure Technol 2012; 6: 247-253.
15. Rawat C, Sukadev M. A hybrid image compression scheme using dct and fractal image compression. Int Arab J Inf Technol 2013; 10: 553-562.
16. Lin YH, Ja LW. Quality assessment of stereoscopic 3D image compression by binocular integration behaviors. IEEE Trans Imag Proc 2015; 23: 1527-1542.
17. Qin C, Chin-Chen C, Yi-Ping C, A novel joint data-hiding and compression scheme based on SMVQ and image in painting. IEEE Trans Imag Proc 2014; 23: 969-978.
18. Zhang X. Lossy compression and iterative reconstruction for encrypted image. IEEE Trans Info Forens Secur 2011; 6: 53-58.
19. Karri C, Umaranjan J. Fast vector quantization using a Bat algorithm for image compression. Eng Sci Technol Int J 2016; 19: 769-781.
20. Kumar G, Pragati S, Scholar PG. A survey of various image compression techniques for RGB images. InT j Eng Sci 2016; 4905.
21. Zhang X, Ren Y, Shen L, Qian Z, Feng G. Compressing encrypted images with auxiliary information. IEEE Trans Multimed 2014; 16: 1327-1336.
22. Chaurasia V, Vaishali C. Statistical feature extraction based technique for fast fractal image compression. J Vis Commun Image Represent 2016; 41: 87-95.
23. Dar Y, Bruckstein AM, Elad M, Giryes R. Postprocessing of compressed images via sequential denoising. IEEE Trans Image Process 2016; 25: 3044-3058.
24. Hussain AJ, Dhiya AJ, Naeem R, Paulo L. Hybrid neural network predictive-wavelet image compression system. Neuro Comput 2015; 151: 975-984.
25. Wu MS. Genetic algorithm based on discrete wavelet transformation for fractal image compression. J Vis Commun Image Represent 2014; 25: 1835-1841.
26. MalothuNagu NV. Image de-noising by using median filter and weiner filter. Int J Innov Res Comp Commun Eng 2014; 2.
27. Geetha M, Rakendu R. An improved method for segmentation of point cloud using minimum spanning tree. Communications and Signal Processing (ICCSP). proceedings of IEEE International Conference 2014; 833-837.
28. Shyam R, Singh YN. Evaluation of eigen faces and fisher faces using bray Curtis dissimilarity metric. In Industrial and Information Systems (ICIIS). Proc Int Conf 2014; 1-6.
29. Xu XL, Chen T. ISOMAP algorithm-based feature extraction for electromechanical equipment fault

prediction. Image Sig Proc CISP09 2nd International Congress IEEE 2009; 1-4.

30. Sled JG, Zijdenbos AP, Evans AC. A nonparametric method for automatic correction of intensity nonuniformity in MRI data. IEEE Trans Med Imaging 1998; 17: 87-97.
31. Desai S, Roy S, Patel B, Purandare S, Kucheria M. Very Fast Decision Tree (VFDT) algorithm on Hadoop. Comp Commun Contr Autom (ICCUBEA) Proc IEEE Int Conf 2016; 1-7.
32. Chaudhari RE Dhok SB. Wavelet transformed based fast fractal image compression. Circ Sys Commun Info Technol Appl 2014; 2014: 65-69.
33. Bhavani S, Thanushkodi K. A survey on coding algorithms in medical image compression. Int J Comp Sci Eng 2010; 2: 1429-1434.

*Correspondence to

Ruhiat Sultana

Rayalaseema University

Andhra Pradesh

India

View publication stats

International Journal of Electronics and Communication Engineering and Technology (IJECET)
Volume 9, Issue 4, July-August 2018, pp. 22–35, Article ID: IJECET_09_04_003
Available online at
http://iaeme.com/Home/issue/IJECET?Volume=9&Issue=4
ISSN Print: 0976-6464 and ISSN Online: 0976-6472
© IAEME Publication

EFFICIENT DEFENSE SYSTEM FOR JAMMING ATTACKS IN WIRELESS SENSOR NETWORKS

Dr. Syeda Gauhar Fatima
Professor, Department of ECE,
Deccan College of Engineering and Technology, Hyderabad, India

Dr. Syed Abdul Sattar
Professor, Director (R&D) & Principal, Department of ECE,
Nawab Shah Alam Khan College of Engineering and Technology, Hyderabad, India

Mohammed Sadiq
Assistant Professor, Department of ECE,
Deccan College of Engineering and Technology, Hyderabad, India

ABSTRACT

Wireless Sensor networks (WSN) have a great potential and an emerging technology which can be employed in many critical fields such as traffic surveillance, battlefields habitat monitoring, commercial applications such as building and in many more fields. But one of the main issue that wireless networks face is about formation of the malicious node which may results in the security threats. So to avoid the formation of malicious or compromised nodes and their abnormal data packets in the wireless sensor networks we propose an Efficient Defense System for Jamming Attacks. This approach consists of mainly a control channel where the data packets of the node are sent through this control channel in order to find out the abnormal data packets. This control channel consists of five stages hopping sequence generation, hopping sequence assignment, control channel access, compromised node identification, and hopping sequence update. The data packets which are resulted as abnormal data packets are put into a safe cover with a spread code and sent to the destination node.

Key words: Wireless Sensor Networks, Control Channel and Safe Cover

Cite this Article: Dr. Syeda Gauhar Fatima, Dr. Syed Abdul Sattar and Mohammed Sadiq, Efficient Defense System for Jamming Attacks in Wireless Sensor Networks. *International Journal of Electronics and Communication Engineering and Technology*, 9(4), 2018, pp.22–35.
http://iaeme.com/Home/issue/IJECET?Volume=9&Issue=4

1. INTRODUCTION

1.1. WSN

WSN stands for "Wireless Sensor Network". It is a non- infrastructure network which is formed through mass deployment of sensor nodes (SN). The main function of WSN is to collect and monitor the related information about the specific environment. The SNs detect the surrounding environment or the given target and deliver the data to the sink using wireless communication. After that the data is analyzed to understand the state of target. Due to their hardware design, WSNs suffer from many resource constraints like low computation capability, small memory and limited energy. As it consist of many low-cost, small devices, and usually deploy to an open and unprotected region they are vulnerable to various types of attacks. In this case, preventive mechanism can be applied to protect them from group of attacks. For this more sophisticated methods like intrusion detection systems are needed to achieve a more autonomic and complete defense mechanism, even against attacks that have not been anticipated in advance.

The applications where WSNs can be implemented are military sensing, disaster response, health care and intelligent house control that can be configured to suit a wide variety of personal requirements. The two types of network topologies that occur in WSNs are flat-based WSN and Cluster-based WSN (CWSN). In flat-based WSN such as SPIN, generates large amount of information by multihop communication and require large amount of energy. CWSN works by electing one cluster head (CH) to manage the operation of its own cluster. CH aggregates data from all SN from specific target and hence efficiently reduces the amount of information in the entire network which in turn results in less energy consumption. [1][2][3].

1.2. Intrusion Detection System (IDS)

An Intrusion Detection System (IDS) can detect an attack and warn the sensors and the operator about it. It is used to detect the packets in a network and it determines whether they are attackers. It helps to develop the prevention technique through acquired nature of attack.

Two types of IDS are:

- Collaboration-based Intrusion Detection (CID): It is a continuous IDS that detects intrusion during the cluster cycle.
- Routing Tables Intrusion Detection (RTID): It is an event-driven IDS. When the attacks occur, it compares the attack data and raise alarm.

Several mechanisms are implemented in IDS to improve the detection technique of IDS. It can be coupled with a set of response mechanism to translate passively generated alerts in to automated actions. The possible action of such Intrusion prevention systems (IPS) includes blocking malicious connection, changing the configuration or restoring the application in to a clean state.
[3][4][5]

1.2.1. Issues of isolating attackers in WSN

The main issues of providing security from attackers in WSN are:

- Data Confidentiality: It is the ability to conceal messages from a passive attacker so that any message communicated via the sensor network remains confidential. It is the most important issues in providing security in network.
- Data Authentication: It ensures the reliability of the message by identifying its origin. Due to the wireless nature of the media and the unattended nature of sensor networks, it is extremely challenging to ensure authentication.

- Data Integrity: It is needed in sensor network to ensure the reliability of the data and refers to the ability to confirm that a message has not been tampered with, altered or changed.
- Data Availability: It determines whether a node has the ability to use the resources and whether the network is available for the messages to communicate.
- Data Freshness: It suggests that the data is recent, and it ensures that no old messages have been replayed.
- Self-Organization: If self-organization is lacking in a sensor network, the damage resulting from an attack or even the risky environment may be devastating.
- Secure Localization: The utility of a sensor network relies on its ability to accurately and automatically locate each sensor in the network. As an attacker can easily manipulate non secured location information by reporting false signal strengths, replaying signal it is important to provide secure localization.
- Time Synchronization: Most sensor network applications rely on some form of time synchronization.

Some of the attacks in WSN are Sybil attack, sinkhole attack, jamming attack, wormhole attack, node replication attack, data flooding attack and many more.
[1][3][6]

1.2.2. Methods to Provide Security in WSN

The security mechanism in WSN is divided into following two categories:

- Low-Level Mechanism: Low-level security primitive for securing sensor networks Include: Key establishment and trust setup, Secrecy and authentication, Privacy, Robustness to communication denial of service, secure routing and Resilience to node capture.
- High-Level Mechanism: High-level security mechanisms for securing sensor networks, includes secure group management, intrusion detection, and secure data aggregation.

  [1][3][7]

1.3. Jamming Attacks and its Impact

Act of intentionally directing electromagnetic energy towards a communication system to interrupt or avoid signal transmission in the network is defined as the jamming. In wireless sensor networks the jamming attack is one of the most and serious critical security issues at present, which spreads out sufficient confrontational signals into the radio frequencies used by normal sensor nodes in the network. These jamming attacks produces noise in the network which could reduce the chance of establishing a successful broadcasting in the wireless communication. The jammers in the network, discover lots of internal and secured data of the wireless network. So it becomes easy for jammers to jam the normal sensor nodes in the network and reduce the performance of the network. The jammers in the network will be in an idle state until the jammers are triggered by messages distributed within the sensor node's transmission range. If this continues in the network then it would become difficult for the network to detect the jamers.

- Jamming can be a severe security threat in the field of WSNs since the jammers can exploit strong high layer security mechanisms, if they are ignored in the initial WSN design.
- Even in the low powered situations the jammers have the potential to interrupt the entire network.

  [8][9][10][11]

1.4. Previous Work

In our previous paper, we have proposed an energy efficient intrusion detection system for WSN. Initially the nodes deployed in the network are analyzed for malicious activity based on

the residual energy. If the energy consumed and residual energy of the node is greater than the predicted threshold, the node is considered as malicious node and the packets emerging from these nodes is said to be abnormal. The abnormal packets are passed through the back propagation network (BPN) to analyze the data misinterpretation. In case, the output of BPN is found to be abnormal, then the attack detection is confirmed and attack type is estimated. Otherwise, there is no detection of attack.

Drawbacks

- IDS technique here considers only the energy metrics as a decision factor
- The proposed technique cannot isolate or block the attacks.

2. LITERATURE REVIEW

Rung-Ching Chen et al in paper [5] have proposed a method to combine routing tables and isolation tables to detect anomalies. The IDS depends on attack behaviors to detect malicious nodes. When the WSN is intruded by malicious nodes, IDS detects a malicious node through its unusual behavior. The IDS compares sensor node behaviors with attack behaviors to determine anomalous information. If the node is anomalous, it will be isolated and recorded in the isolation table. The SCHs send an isolation table to PCH for integration. If there is no anomaly, the SCHs periodically send information to avoid nodes being infiltrated. Finally PCH updates the isolation table to BS periodically. When the PCH is changed, the new PCH can receive the isolation table from BS to continuously isolate anomalous nodes. The IDS must consider that WSNs has limited resources; thus, the estimation method is different between WSNs and wired networks. They have listed estimation IDS performance methods that were used in their performance evaluation. The CID method focuses on energy consumption and remaining resources to determine live nodes. The RTID method uses the number of monitored nodes to calculate transmission accuracy. Their primary experiment compares live nodes with CID, and compares transmission accuracy with RTID. The primary experiment proves our ITIDS can prevent attacks effectively. From this paper future work can be done to provide efficient resource utilization technique to detect different attacks.

Sisi Liu et al in paper [7] have addressed the problem of control-channel jamming attacks from insider nodes. They proposed a randomized distributed scheme for maintaining and establishing a broadcast channel using frequency hopping. Their method differs from classical frequency hopping in that the communicating nodes are not synchronized to the same hopping sequence. Instead, each node follows a unique hopping sequence. They further proposed a mechanism for adjusting hopping sequences to dynamic spectrum conditions without incurring any extra overhead. Their scheme can identify compromised nodes through their unique sequences and exclude them from the network. They evaluated the performance of their scheme both in static and dynamic-spectrum networks, based on the metrics of evasion entropy, evasion delay, and evasion ratio. They further evaluated the Hamming distance between the jamming sequence and those assigned to compromised and uncompromised nodes. The drawback of proposed scheme is that it is a temporary solution for reestablishing the control channel until the jammer and the compromised nodes are removed from network.

Hyojin Kim et al in paper [8] have proposed the period-based defense mechanism against data flooding attacks. The data flooding attack paralyzes a victim node by consuming its resources. Hence, the throughput of the victim node is significantly reduced. However, the current defense systems focus on RREQ flooding attacks rather than the data flooding attack. They easily reduce the throughput of burst traffic by comparing with the simple threshold. Hence, they aimed to enhance the throughput of burst traffic under the data flooding attack. The proposed scheme uses a blacklist, considers the data type, and processes packets

according to the priority so as to defend against data flooding attacks; since the attacker forwards many data packets at a high rate for the whole session. From this paper future work can be done to implement the methods for different types of attack.

Jerry T. Chiang et in paper [10] have proposed a protocol that allows a broadcast communication system to dynamically change the spreading codes used by subsets of receivers so that some benign users can share a single spreading code, thereby conserving the number of spreading codes used simultaneously. They have showed a lower bound on the number of spreading codes used simultaneously in order to mitigate jamming by relying only on keying and not other physical characteristics. They optimized their protocol so that it can mitigate jamming by using twice as many spreading codes simultaneously as the lower bound. They have presented simulation results to support their theoretical results and showed that jamming can be effectively mitigated in a broadcast wireless system. The drawback of this paper is that in the proposed protocol false alarms result in unnecessary consumption of energy.

Alejandro Proano et al in paper [11] have addressed the problem of selective jamming attacks in wireless networks. They have considered an internal adversary model in which the jammer is part of the network under attack, thus being aware of the protocol specifications and shared network secrets. They showed that the jammer can classify transmitted packets in real time by decoding the first few symbols of an ongoing transmission. They evaluated the impact of selective jamming attacks on network protocols such as TCP and routing. Their findings showed that a selective jammer can significantly impact performance with very low effort. They developed three schemes that transform a selective jammer to a random one by preventing real-time packet classification. Their schemes combine cryptographic primitives such as commitment schemes, cryptographic puzzles, and all-or-nothing transformations with physical-layer characteristics. They analyzed the security of their schemes and quantified their computational and communication overhead. The drawback of this paper is that the proposed scheme has higher computational and communication overhead.

3. PROPOSED SOLUTION

3.1. Overview

Now as an extension to the previous work, we propose to design efficient techniques to block or isolate the attackers thus preventing from attacks.

Here we implement the code tree scheme [15] along with the new frequency hopping sequence method [13] to detect the jamming attack and isolate these attacks in the control channel network. The spread spectrum in the code tree scheme is implemented with hopping sequence node that consists of five stages to detect and isolate these attacks in the network. In our scheme, the hopping sequence assigned to each node consists of spreading code of the code tree scheme that consists of secret key between the sender and receiver.

The control channel consists of the hopping sequence allocated for the various nodes that are designed in such a way that it overlaps at certain time slot. The time slot of overlapping of each node in hopping sequences is kept secret. These schemes consist of the five stages that are: hopping sequence generation, hopping sequence assignment, control channel access, compromised node identification and the hopping sequence update.

The hopping sequence generation consists of random generation of the nodes in the control channel that is assigned with frequency band and about the location to each node such that no node can exchange the information with each other. The hopping sequence assignment

consists of assigning a secret PN code to each spreading node that cannot be known to the other node what they have been assigned. The control channel access consists of the hopping sequence assigned to each node about the time slot and position vector that are kept secret. The compromised node is detected based on the hamming distance metrics between the two sequences of the node. The hopping sequence update phase is implemented to update the compromised node in the network.

To isolate the jamming attacks from the network, the cover in which the attack is detected is removed and two new leaf nodes is added to that cover and different cover is chosen to transmit the spreading code.

Advantages

- The proposed scheme provides a complete security against Jamming attack as it completely removes the cover in which attack is detected in the network.
- It provides an energy efficient method to isolate the attack as it uses the tree scheme.

3.2. Control Channel Implementation

In our previously proposed approach at the beginning stage the nodes are deployed in the network. Later these nodes analyzed in order to check whether these nodes are compromised or not. While analyzing these nodes it considers the consumed energy and residual energy of the node. If the consumed energy and residual energy is greater than the predicted threshold then that particular node is considered as the malicious node or the compromised node. Finally the attack detection is confirmed and attack type is estimated through BPN.

If $N_i = MN_i$ (from previous paper sec 3.5)

i.e. if the node exhibits strange behavior based on the node type then the packet originating from MN_i is considered as abnormal packets. The nodes which are confirmed as malicious or compromised nodes in the network, those node's packets are sent to the control channel implementation. In this control channel implementation, it consists of five stages to isolate the abnormal packets in the network.

- Hopping sequence generation
- Hopping sequence assignment
- Control channel access
- Compromised node identification
- Hopping sequence update

3.2.1. Hopping sequence generation

In a network the generated hopping sequence are assigned to cluster members, which only overlap in a predefined number of slots. These slots are used to implement the control channel. This control channel is implemented so that the privacy of the control channel is protected. But the generated hopping sequence should have the knowledge of earlier hops which does not reveal any information about future ones. Also when the network is interpreted with codewords, any two hopping sequences should have a maximum Hamming distance so that a malicious/compromised node can be recognized in a network.

Suppose that the cluster consists of n nodes plus the CH, and let the set of available channels be $\{1, \ldots, K\}$. To construct n hopping sequences of length L + M, where M denotes the number of slots implementing the control channel, the CH executes the following steps

Step 1: Generate n random sequences s_j; $1 \leq j \leq n$, each of length L. For each sequence $s_j = \{s_j(1), \ldots, s_j(L)\}$, we have $Pr[s_j = k] = 1/K$, where $k = 1,2, \ldots, K$.

Step 2: Generate a random channel location vector c = {c(1), . . . , c(M)} where Pr[c(i)=k]=1/K i=1, . . , M and k=1, 2, . , K.

Step 3: Generate a random slot position vector v={v(1), . . ,v(M)}, where v(i) ϵ {1, . . , L+M}, v(i)≠v(j), ∀i≠j

Step 4: In every sequence s_j, insert element c(i) before element $s_j(v(i))$ to generate a new sequence mi

3.2.2. Hopping sequence assignment

To assign hopping sequence to each node, the CH uses a secure pairwise communication method. I makes use of preshared pairwise keys mechanism where CH establishes a pairwise shared PN codes among its member of nodes in the cluster. Here each node in the cluster disclose the PN code only with shared nodes and for rest all nodes it remains as a secret key and hence these code is used for jamming-resistant pairwise communication

The hopping sequences generated by the CH are assigned to individual cluster nodes via secure pairwise communication. Using preshared pairwise keys, the CH can establish pairwise shared PN codes with the members of its cluster. Note that the compromise of a cluster node only reveals the PN code shared between that node and the CH, while the rest of the pairwise PN codes remain secret. Thus, these codes can be used for jamming-resistant pairwise communication (but not for broadcasting of control information). The steps of the hopping sequence assignment for a node n_j are as follows:

Step 1: The cluster head (CH) and n_j node launches a pairwise PN code (this code can be preloaded or also can be generated based on a pairwise key $K_{CH,nj}$).

Step 2: The cluster head offers n_j with the hopping sequence m_j, which is encrypted using the pairwise key $K_{CH,nj}$. Using message authentication code (MAC) the message integrity is achieved.

Step 3: Node n_j removes from its memory if any information about the identity of the CH.

3.2.3. Control Channel Access

The hopping sequences that are assigned to each node in a cluster are implemented to the control channel only during the slots that are indicated by the random slot position vector v. The position vector v is designed in such a way that the nodes in a cluster are not aware of the time slots in which they have to access the channel and hence it prevents the network from jamming the control slots.

The main aim of the control channel access is to make sure that a slot in the control channel is accessed at least one time during the repetitive transmission. During this process let us assume that x be the number of retransmissions of a control message. For this x a suitable value can be probabilistically figured based on the design parameters of the hopping sequences. That is, when the value of x is tuned such that a control-channel slot occurs with a desired probability p0. This probability can be the number of occurrences z of a control slot which is larger than one in a total of x slots is

$$\Pr[z \geq 1] = 1 - \Pr[z = 0] = 1 - \left(\frac{L}{L+M}\right)^{x} \quad (1)$$

Where,

L is the length of n hopping sequences

M is the number of slots implementing the control channel

x is the number of retransmissions of a control message

3.2.4. Compromised Node Identification

If a node n_j in the cluster is compromised, the adversary will acquire the unique hopping sequence m_j that was assigned to this node. As the time slots assigned to each node to access the control channel is kept secret, the adversary will consider m_j to jam the channel. But the hopping sequence m_j will disclose the identity of compromised node n_j that is based on the Hamming distance between the sequence assigned to the nodes and the jamming hopping sequence.

Step 1: Initialize $d(s_j, s_{jam})=0, \forall j$

Step 2: Synchronize with the hopping sequence m_j of a randomly selected node n_j

Step 3: For each slot i, $i \in v$, if $m_j(i)$ is not jammed, set $d(s_j, s_{jam}) = d(s_j, s_{jam})+1$

Step 4: After some number of slots $X \geq \gamma_0$, if $d(s_j, s_{jam}) < E[d(s_j, s_{jam})]-\delta x$ then node nj is considered to be compromised

Step 5: A set of codes J on which jamming has been detected which is known as a cover C safe relative to J

Else

$C \cap J = \emptyset$. i.e. C contains no codes on which jamming was previously detected. (explained in 3.3)

Step 6: Randomly pick another node and repeat Steps 2-4 for X slots

During the compromised node process the cluster node make use of the knowledge of all the subsequences s_j which are different for all the nodes in the network. Let s_{jam} denote the subsequence which is tailed by the jammer, without the slot positions in vector v. The cluster head estimates the Hamming distance between s_{jam} and every assigned sequence s_j in order to identify the compromised node in the network. The resulted compromised nodes in the network are put into a safe cover C and then these nodes are passed to the receiver side.

3.2.5. Hopping Sequence Update

In this stage if a node is detected as compromised node the CH updates the hopping sequences by assigning a new sequence to all uncompromised nodes. It is done by synchronizing the PN code of each individual to assign a new PN code. The phase of updating the hopping sequence differs from the early hopping sequence assignment which comes in the pairwise PN code that is used for communication. Later early initial assignment, cluster nodes hop according to their m_j's. Hence, the cluster head has to follow each m_j to interact with each node individually.

Step 1: The CH synchronizes with PN code m_j (m_j is only known to the CH and n_j).

Step 2: The CH communicates to n_j a portion of m_j, which is meant to prove the CH's knowledge of m_j. This communication is secured by the pairwise key $K_{CH,mj}$.

Step 3: The CH assigns a new sequence m^*_j to n_j. This communication is secured by the pairwise key $K_{CH,mj}$.

Step 4: Node n_j erases all information regarding the identity of the CH.

3.3. Isolation of Compromised Node

In the identification of compromised node phase, the compromised nodes in the network are identified. The nodes which are resulted as the compromised nodes in the network as to be isolated or kept apart in the network. When the sender nodes sends the data packets to the destination node, the data packets are initially sent to the control channel which consists of five stages. During this process if the control channel come across any compromised node in the network. Then those data packets are sent to the destination node in a minimal safe cover on which jamming had been early detected. By this all the destination nodes in the network

can decode the packet. In order to detect the compromised nodes and jamming acts in the network, the sender node sends a spreading code which is chosen from among the nodes of the cover. This test spreading code allows the sender node and destination node to supportively detect compromised node or jamming on any spreading code in the cover. To receive a data packet from the source node, each node at the destination end simply decodes the signal using all the spreading codes the node has. If a destination node does not have enough computation ability to decode using all codes it knows then destination node will successively try all spreading codes in each time instance.

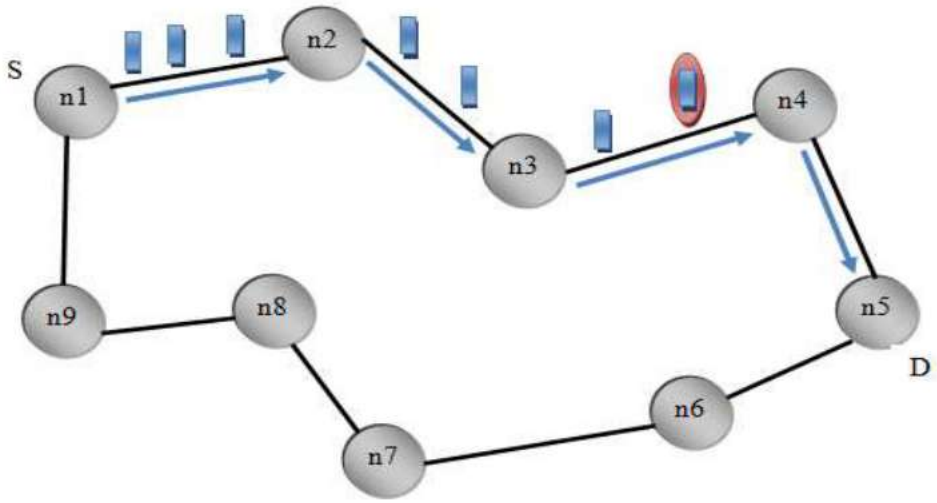

Fig 1: Isolation of Compromised node

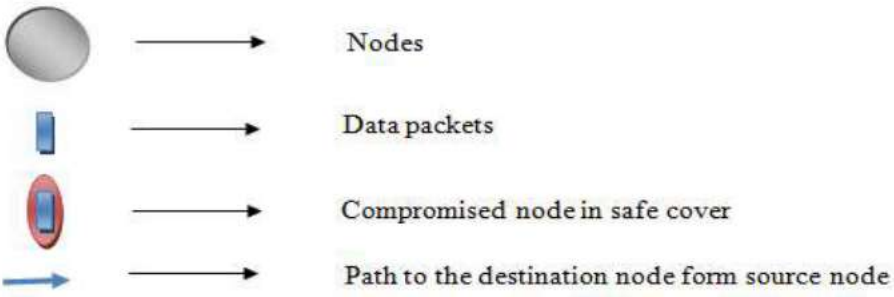

In the above figure the source node sends the data packets to the destination node. During this transmission of the data packets in the network, the data packets undergo the control channel where it consists of five stage. During this process if any compromised node is present it will be detected in the identification of compromised node stage and these compromised nodes are put in a safe cover. Then the data packets are sent to the destination node. At the destination node the compromised node are isolated. Through this way the compromised data packets in the network are isolated from the other data packets and also form the nodes of the network.

No. of Nodes	200
Area Size	500 X 500
Mac	IEEE 802.11
Transmission Range	250m
Simulation Time	25 sec
Traffic Source	CBR

Packet Size	512
Rate	50,100,150,200 and 250kb
Attackers	1,2,3,4 and 5
Initial Energy	10.3J
Transmission power	0.660
Receiving Power	0.395
Routing Protocol	AODV

4. SIMULATION RESULTS

4.1. Simulation Model and Parameters

The Network Simulator (NS2) [17], is used to simulate the proposed architecture. In the simulation, 200 mobile nodes move in a 500 meter x 500 meter region for 25 seconds of simulation time. All nodes have the same transmission range of 40 meters. The simulated traffic is Constant Bit Rate (CBR). We have consider jamming attack nodes along the same channel.

The simulation settings and parameters are summarized in table.

4.2. Performance Metrics

The proposed Efficient Defense System for Jamming Attacks (EDSJA) is compared with the Cross-Layer Jamming Detection and Mitigation (CJDM) technique [15]. The performance is evaluated mainly, according to the following metrics.

- **Packet Delivery Ratio:** It is the ratio between the number of packets received and the number of packets sent.
- **Packet Drop**: It refers the average number of packetsropped during the transmission
- **Energy Consumption**: It is the amount of energy consumed by the nodes to transmit the data packets to the receiver.
- **Delay**: It is the amount of time taken by the nodes to transmit the data packets.

4.3. Results

Based on Attackers

In our first experiment we vary the number of attackers as 1,2,3,4 and 5.

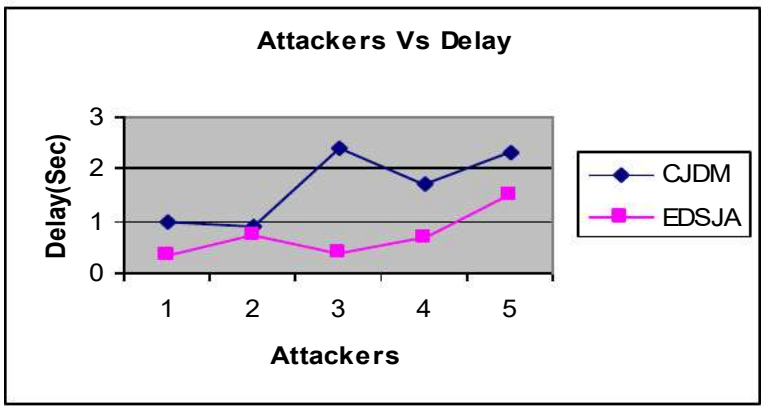

Figure 2 Attackers Vs Delay

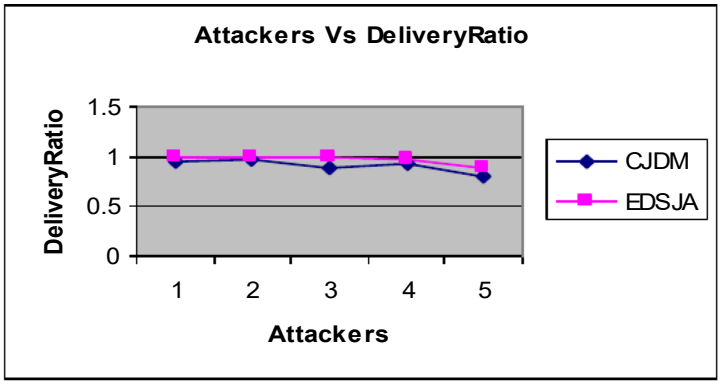

Figure 3 Attackers Vs Delivery Ratio

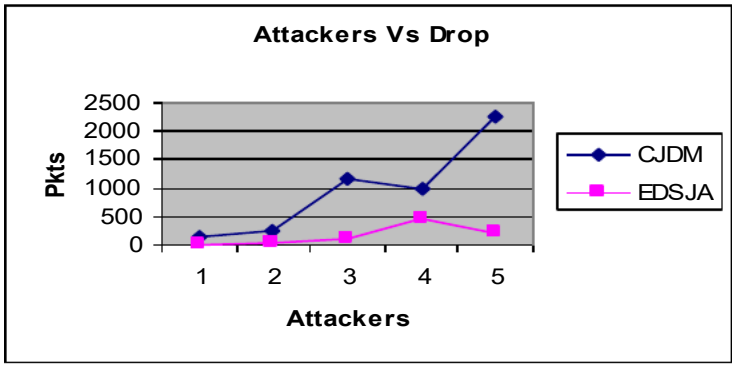

Figure 4 Attackers Vs Drop

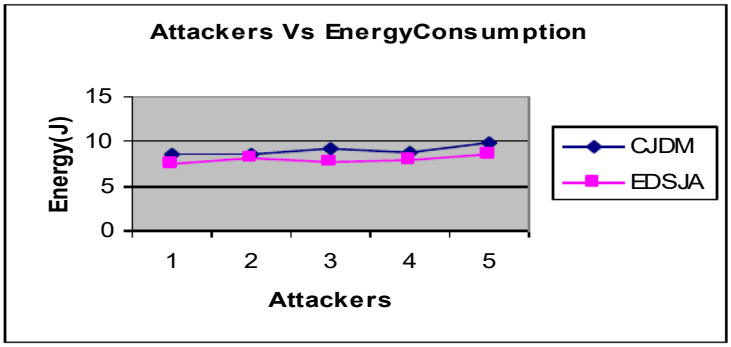

Figure 5 Attackers Vs Energy Consumption

Figure 2 shows the delay of EDSJA and CJDM techniques for different number of attacker scenario. We can conclude that the delay of our proposed EDSJA approach has 52% of less than CJDM approach.

Figure 3 shows the delivery ratio of EDSJA and CJDM techniques for different number of attacker scenario. We can conclude that the delivery ratio of our proposed EDSJA approach has 6% of higher than CJDM approach

Figure 4 shows the packet drop of EDSJA and CJDM techniques for different number of attacker scenario. We can conclude that the packet drop of our proposed EDSJA approach has 82% of less than CJDM approach.

Figure 5 shows the energy consumption of EDSJA and CJDM techniques for different number of attacker scenario. We can conclude that the energy consumption of our proposed EDSJA approach has 12% of less than CJDM approach.

Based on Rate

In our second experiment we vary the transmission rate as 50,100,150,200 and 250Kb.

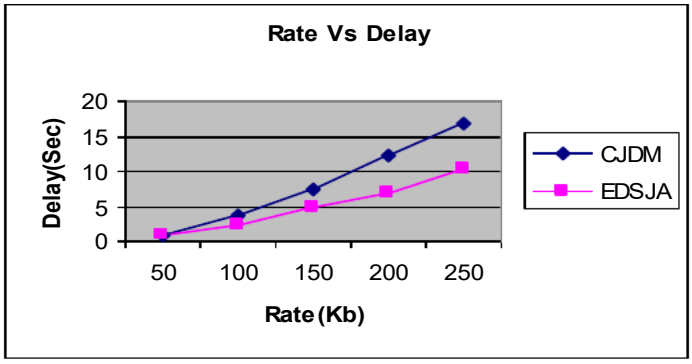

Figure 6 Rate Vs Delay

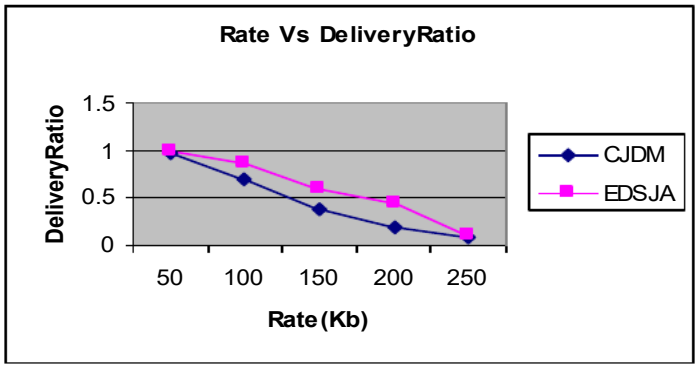

Figure 7 Rate Vs Delivery Ratio

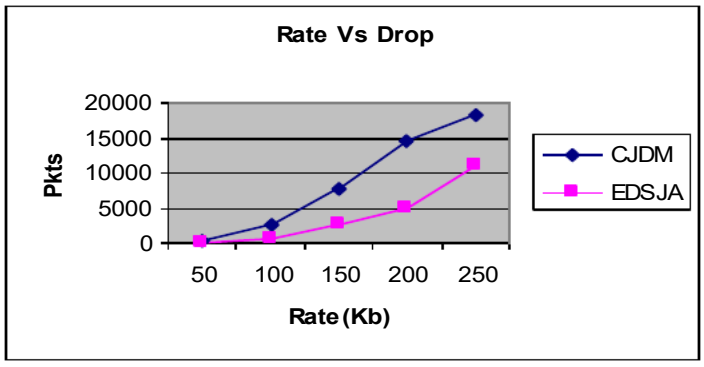

Figure 8 Rate Vs Drop

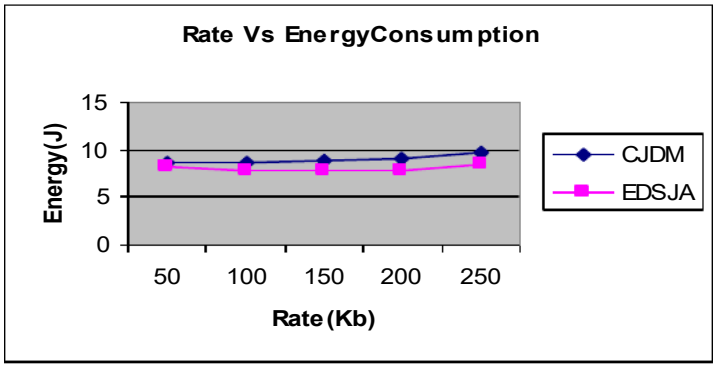

Figure 9 Rate Vs Energy Consumption

Figure 6 shows the delay of EDSJA and CJDM techniques for different rate scenario. We can conclude that the delay of our proposed EDSJA approach has 35% of less than CJDM approach.

Figure 7 shows the delivery ratio of EDSJA and CJDM techniques for different rate scenario. We can conclude that the delivery ratio of our proposed EDSJA approach has 25% of higher than CJDM approach

Figure 8 shows the packet drop of EDSJA and CJDM techniques for different rate scenario. We can conclude that the packet drop of our proposed EDSJA approach has 67% of less than CJDM approach.

Figure 9 shows the energy consumption of EDSJA and CJDM techniques for different rate scenario. We can conclude that the energy consumption of our proposed EDSJA approach has 11% of less than CJDM approach.

5. CONCLUSIONS

We propose an Efficient Defense System for Jamming Attacks. Through this approach it is possible to overcome the malicious or compromised nodes and their data packets which transmitted in the network. This approach consists of mainly a control channel where the data packets of the node are sent through this control channel in order to find out the abnormal data packets. This control channel consists of five stages hopping sequence generation, hopping sequence assignment, control channel access, compromised node identification, and hopping sequence update. The data packets which are resulted as abnormal data packets are put into a safe cover with a spread code and sent to the destination node. Through this approach the wireless networks will be able to isolate the malicious nodes and the abnormal data packets.

REFERENCES

[1] Yan, K. Q., S. C. Wang, and C. W. Liu. "A Hybrid Intrusion Detection System of Cluster-Based Wireless Sensor Networks." Proceedings of the International MultiConference of Engineers and Computer Scientists. Vol. 1. 2009.

[2] Krontiris, Ioannis, Thanassis Giannetsos, and Tassos Dimitriou. "LIDeA: A Distributed Lightweight Intrusion Detection Architecture for Sensor Networks." Proceedings of the 4th International Conference on Security and Privacy in Communication Netowrks. ACM, 2008.

[3] Krontiris, Ioannis, et al. "Cooperative Intrusion Detection in Wireless Sensor Networks." Wireless Sensor Networks. Springer Berlin Heidelberg, 2009. 263-278.

[4] Berthier, Robin, William H. Sanders, and Himanshu Khurana. "Intrusion Detection for Advanced Metering Infrastructures: Requirements and Architectural Directions." Smart Grid Communications (SmartGridComm), 2010 First IEEE International Conference on. IEEE, 2010.

[5] Zoran S. Bojkovic, Bojan M. Bakmaz, and Miodrag R. Bakmaz, “Security Issues in Wireless Sensor Networks”, “International Journal of Communications, Issue 1, Volume 2, 2008”.

[6] Stetsko, Andriy, Lukáš Folkman, and Vashek Matyas. "Neighbor-Based Intrusion Detection for Wireless Sensor Networks." Wireless and Mobile Communications (ICWMC), 2010 6th International Conference on. IEEE, 2010.

[7] Padmavathi, Dr G., and Mrs Shanmugapriya. "A Survey of Attacks, Security Mechanisms and Challenges in Wireless Sensor Networks." arXiv preprint arXiv:0909.0576 (2009).

[8] Pathan, Al-Sakib Khan, Hyung-Woo Lee, and Choong Seon Hong. "Security in Wireless Sensor Networks: Issues and Challenges." Advanced Communication Technology, 2006. ICACT 2006. The 8th International Conference. Vol. 2. IEEE, 2006.

[9] Shin, Incheol, Yilin Shen, Ying Xuan, My Tra Thai, and Taieb Znati. "Reactive jamming attacks in multi-radio wireless sensor networks: an efficient mitigating measure by identifying trigger nodes." In Proceedings of the 2nd ACM International Workshop on Foundations of Wireless Ad Hoc and Sensor Networking and Computing, pp. 87-96. ACM, 2009.

[10] Mpitziopoulos, Aristides, Damianos Gavalas, Charalampos Konstantopoulos, and Grammati Pantziou. "A Survey on Jamming Attacks and Countermeasures in WSNS." Communications Surveys & Tutorials, IEEE 11, no. 4 (2009): 42-56.

[11] Wang, Yong, Garhan Attebury, and Byrav Ramamurthy. "A Survey of Security Issues In Wireless Sensor Networks." (2006).

[12] Chen, Rung-Ching, Chia-Fen Hsieh, and Yung-Fa Huang. "An Isolation Intrusion Detection System for Hierarchical Wireless Sensor Networks." Journal of Networks Volume 5 (3), 2010, pp.335-342.

[13] Liu, Sisi, Loukas Lazos, and Marwan Krunz. "Thwarting Control-Channel Jamming Attacks from Inside Jammers." Mobile Computing, IEEE Transactions on Volume 11 (9), 2012, pp.1545-1558.

[14] Kim, Hyojin, Ramachandra Bhargav Chitti, and Jooseok Song. "Novel Defense Mechanism Against Data Flooding Attacks in Wireless Ad Hoc Networks." Consumer Electronics, IEEE Transactions on 56(2), 2010, pp.579-582.

[15] Chiang, Jerry T., and Yih-Chun Hu. "Cross-Layer Jamming Detection and Mitigation In Wireless Broadcast Networks." Proceedings of the 13th annual ACM International Conference on Mobile Computing and Networking. ACM, 2007.

[16] Proano, Alejandro, and Loukas Lazos, "Packet-Hiding Methods For Preventing Selective Jamming Attacks", Dependable and Secure Computing, IEEE Transactions on 9(1), 2012, pp.101-114.

[17] Network Simulator: http:///www.isi.edu/nsnam/ns

Use Of Outrigger, Belt Wall And Bracing Systems In High Rise Building Subjected To Wind Loads

[1]Mohammed Arsalaan Wajid, [2]Dr. S. Amaresh Babu
[1]Post Graduate Student, [2]Professor and Head of Department of Civil Engineering
Nawab Shah Alam Khan College of Engineering and Technology

Abstract - **In the fast changing and ever evolving world of today, high-rise structures with innovative designs have become the norm. Even though these structures are a marvel to look at, they have their own fair share of problems. As one goes higher, the wind forces become a huge obstacle that needs to be dealt with effectively in order to ensure the security of the residents. After extensive research and trial runs, many creative solutions have come up to tackle the effect of wind energy. In the present study, an attempt is made to effectively reduce the lateral displacement caused by wind forces with the help of a belt wall, optimally placed outriggers and a proper bracing system. In this research, with the assistance of Outrigger / Belt wall / Bracing systems, an effort has been made to assess an economical technique of decreasing lateral displacement of the structure owing to wind forces. The present study takes in consideration an elliptically planned height structure of about 320 m, the structure consists of 78 above ground level stories and 2 below. It comprises of an elliptical core as lateral load resisting system. The structure is studied with (i) Core wall (ii) Core wall with Outrigger (iii) Core wall with Belt wall (iv) Core wall with combination of Outrigger and Belt wall and (v) Core wall with Bracing systems. The thickness of outrigger/Belt wall is varied from 300mm to 500m with a step of 100. The Outrigger/Belt wall system is provided on different levels and in some cases, it is provided on two different levels. The Outrigger/Belt wall is provided only on plant floors/refuge floors/mechanical floor. The bracing system is studied only at level 70 only with cross sectional areas and with different materials (concrete and steel). There are four plant floors in the model structure, which are at level 17, 51, 70 and at roof level. The parameters discussed in this study are the lateral displacement, which occurs at the roof level of the structure along with the moment reduction shared by the elliptical core that is caused by wind forces and the moment shared by the combination system, i.e. the bracing system, outriggers and the belt wall. After much trial and error, it was established that the optimum location of a single outrigger or belt wall was level 51. For two different levels, the best location was found to be at level 17 and level 70. On the other hand, the use of bracing system drastically reduced the lateral displacement of the building right down to the permissible value but it was found to be ineffective when it came to reducing the moment shared by the core. Out of all the options and various permutations and combinations, the safest and most economical setup was found to be combination of belt wall and outrigger at two levels i.e. level 17 and level 70. This study also shows that the lateral displacement of the structure can be minimized by enlarging the size of the central core or in other words simply increasing the stiffness of the building. However, the drawback of this method is the exponential increase in the cost of the structure thereby making it profligate, because the increase in size of core directly results in the increase in volume of concrete used, which is negligible when the combination system proposed in this study is utilized.**

keywords - **Outrigger, belt wall , bracing system, wind loads**

I. INTRODUCTION

In this day and age, the construction of tall buildings has become a fast-growing trend. In order to make your presence felt in the market, companies are making it a point to construct flamboyant structures or own an office in the region's biggest skyscraper. Sky is the limit for these innovative structures as long as all proper conditions are being met. One of the biggest problems an engineer faces when designing a tall building is the considerable effect of wind on the lateral stability of the structure. This is the governing factor in the design of skyscrapers. As the building goes higher, wind pressure increases proportionally, and that is why loads associated with winds are much greater than live and dead loads. Extreme lateral displacement can cause structural and non-structural damage while too much acceleration can lead to problems to the occupants. Generally, shear walls and moment resisting frames are more than enough for low to medium height buildings, but as you go higher, these methods are rendered insufficient. At this point, belt wall system along with outriggers can be effectively used to keep the lateral displacements in check and increase the stiffness of the structure. Outriggers are a concept derived from sailing ships, which use them to resist the wind forces in their sails. Simply put, the core in the high-rise building can be related to the mast of the ship, while the outriggers act like the spreaders and the outer columns like the shroud.

1.1 Lateral Load Resisting Systems

1.1.a Outrigger System

An outrigger is a rigid horizontal structure, which is a part of a boat's rigging, which extends beyond the gunwale providing stability to the main hull preventing it from capsizing. Taking inspiration from this concept, high-rise structures are installed with outriggers and a central core. Stiff in flexure, these horizontal cantilevers connect the central core to the peripheral columns. The moment arm of the core is increased due to this connection, which in turn increases the lateral stiffness of the system. When wind

forces act on the structure, the column-restrained outriggers on the windward side restrain overturning moment through tension and the outriggers on the leeward side through compression. This minimizes lateral displacement drastically when compared to a structure without outriggers. Outrigger systems are not only efficient in controlling the lateral displacements occurring at the top, they are also significant in reducing the inner storey drifts of the structure. This is one of the most efficient system of designing a high-rise structure as it increases the structural depth of the building when it behaves as a vertical cantilever. A horizontal deep girder joins all the exterior columns, which are not directly connected to the ends of the outriggers.

Types of Outrigger Systems

- **Conventional Outrigger System** - This system consists of outrigger girders connected directly to the braced frame or the shear wall at the central core and to the peripherally located columns. These exterior columns are most commonly located at the outer edge of the building. These outrigger trusses, which are connected on one side with the central core and the exterior columns on the other side, convert the moment at the core into a vertical couple at the columns thereby resisting rotation at the core. The core is subjected to reverse curvature below the outrigger, as the rotation is minimal in most designs. In other words, the outrigger truss moves up and down due to overturning and rotation of the core caused by the wind forces. The peripheral columns restrict this movement and produce opposing forces.
- **Virtual Outrigger System** - One of the biggest problems associated with conventional outrigger system is the decline of usable space on the working floor. Functional and architectural constraints create many hurdles. To overcome these problems, virtual outrigger concept is used. The direct connection between the central core and the exterior columns used in the conventional outrigger system is eliminated which in turn solves many problems concomitant with the use of outrigger systems. The working behind the virtual outrigger concept is to make use of stiff diaphragms, which are resilient in their own plane. The moment is transmitted in the form of horizontal couple from the central core to the outrigger trusses and from there to the peripheral columns. Belt truss/walls and basements can be used as virtual outriggers

1.1.b Belt Walls

Belt walls eliminate many of the hurdles that arise when working with the outrigger system. They are provided to improve the axial and torsional stiffness of the columns. Belt walls are quite useful in controlling the settlement of columns as well as shortening and differential elongation. Extra peripheral columns are constructed in order to support restraining the overturning of the outriggers.

To achieve this phenomenon, exterior columns are tied to a wall running around the circumference of the building in the form of a belt, hence the name belt wall. The floor diaphragms are flexible in the out-of-plane vertical direction even though they are quite stiff in their own plane and are thus unaffected by differential settlement of columns.

1.1.c Bracing Systems

Bracing is a highly economical and efficient system of resisting lateral displacement in a high-rise building. This system is most suited for buildings of medium height and are generally used in steel construction. The number of bracings and their location is the most important factor during architectural planning Bracing systems usually form a triangulated vertical truss in which the diagonal members form the web and columns acting as chords. The biggest advantage of this system is that it can be used repetitively leading to a highly economical design and cost cutting in fabrication. Large-scale bracing systems are highly efficient in reducing drift ratio and uplift forces in the foundation.

1.2 Need for Present Study

It comes as no surprise that the cost of owning a piece of land these days is through the roof. To compensate for this exponential increase, builders have started going higher and higher, which presents its own set of problems. Larger height to width ratio will cause huge overturning moments while the structure deflects considerably. Taller buildings have created a need for unconventional, innovative and efficient structural systems. As fewer exterior columns are preferred, the central core wall is the one that is fully responsible of resisting lateral forces. For this concept to work, high-rise structures consist of floor spaces free of columns between the peripheral columns and the central core. This type of setup sanctions for varied utilization of the floor space, at the cost of sacrificing the core and peripheral column system, which is vital for repelling the overturning forces and moment. To overcome this hurdle, one needs some form of structural system to connect these two components in order to increase the overall resistance of the structure. The best option here is to make use of outriggers, which increase the resisting moment to overcome the lateral forces acting on the structure. They are also quite economical as the use of outriggers directly influences the quantity of steel used and it is common knowledge that controlling the cost of steel increases the overall economy of the structure.

1.3 Objectives of the Study

The primary objective of the present thesis is to find out the efficiency of belt walls, bracing systems and outriggers in resisting lateral forces at various storeys in a high-rise structure exposed to wind loads. The aim of the study is

- To observe and study the way in which displacement at roof level is reduced and how the high-rise structure behaves with the addition of belt walls and outrigger
- To study the reduction of moment shared by the central core wall by the application of outriggers and belt wall.
- To calculate the moment shared at the base of the high-rise structure.

II. LITERATURE REVIEW

Gerasimidis and Efthymiou (2009) "Optimum outrigger locations of high-rise steel buildings for wind loading" In this paper a two-dimensional model was analyzed with a concrete core at the middle of the building model and two columns at the edges of the structure. One of the outriggers was placed at the top level of the building while the study was carried out in finding the optimum location for the second outrigger. The second outrigger was moved along the height of the building and placing it on every floor level. A uniform wind loading was considered for the two-dimensional model. The number of stories were thirty with a constant story height of 3m. It was found that when the second outrigger was placed at the middle of the model, the optimum location of the outrigger was achieved, taking into consideration only the drift criteria.

Abbas and Mohsin (2012) "Optimization of outrigger locations in steel tall buildings subjected to earthquake loads**"** This paper compared the optimum outrigger locations obtained by response spectrum and nonlinear time history analysis. 3D models of 20 and 25 storey steel frame braced by outrigger and belt truss system were considered. The paper concludes that optimum outrigger and belt location resulting from response spectrum analysis are at storey 10 and 14 respectively for 20 and 25 storey models whereas for time history analysis the optimum locations were at storey 14 and 16 respectively.

Raj Kiran, Ihtesham and Suresh (2013) "Optimum position of outrigger system for high rise reinforced concrete buildings under wind and earthquake loads" The paper studied nine 30 storey 3d models of outrigger and belt truss system for both wind and earthquake loads. The paper concludes that the use of outrigger and belt truss system in high rise buildings increased the stiffness of the building and made it efficient under lateral load. The drift at the top with only core is 50.63mm when outrigger was provided at top, this reduced to 48.2mm and 47.63mm with and without belt truss. There was no reduction in drift with belt truss. Using second outrigger with cap truss gives the reduction of 18.55% and 23.01% with and without belt truss. The optimum location of the second outrigger is middle height of the building.

II.a Critical Appraisal

- Much of the literature copes with the study of steel outrigger trusses and belt trusses, no journal is studied using reinforced concrete outriggers and reinforced concrete belt walls.
- Many of the researchers studied only the optimum location of outriggers so far attempt is not made for reducing lateral displacement by providing RCC outrigger and belt walls.
- Thus, the present study is an attempt for the analysis of high-rise structure with concrete outriggers, belt walls, combination of outriggers and belt walls along with bracing systems.

III. CASE STUDY

High-rise structures are vulnerable to oscillate under high winds for long natural periods. These structures are prone to the phenomenon of dynamic resonance in wind. Vortex shedding is another type of dynamic response in wind. In vortex shedding phenomenon when high winds blown across the surface of a high-rise structure, vortices are alternately shed from one side to the other giving rise to low pressure zones on the downward side of the structure which generates a fluctuating force acting perpendicularly to the direction of the wind. For buildings higher than 40 storeys, the dynamic resonance in wind has a huge impact on the design of the building. In simpler words, the dynamic resonance in a building can be compared to that of a tuning fork. The taller the structure, the lower is the frequency. It means that as the building goes higher, its frequency is lowered proportionally which results in a structure which resonates more by the wind. At the end of the day, the biggest factor governing the design of a tall structure is the drift of the building due to wind forces and not the fully stressed state as is the common misconception.

One of the chief factors influencing the design of high-rise structure is the behaviour of the structure under the application of lateral loading. Lateral drift at roof level or top of the structure is one of the most essential condition for the design of high-rise structures. According to Indian Standard Code 456, the tolerable displacement also known as top deflection for analysis of wind loading is 1/500 of the height of the structure. It is difficult to truly understand how drift affects the structure unless one experiences acceleration. There are several methods to reduce the drift caused due to lateral loads, one of them being the core wall system which has been found to be quite effective. The main drawback of this system is that when the building increases in height, the stiffness of the core is not enough to keep the wind drift in check. As stiffness of the building increases in significance as one goes higher, the core wall system is combined with outrigger beams connected to shear walls or belt walls which are then connected to the peripheral columns. With this particular system in place, the lateral forces are controlled, wherein the rotation of the core is resisted by outriggers and columns thereby reducing the deflection at top and moment at the base which would have been present in free core system. Quite a number of studies have been carried out on this combination system.

An RCC shear walled structure of 320 m height is considered in the current study. The structure considered here is proposed building which is under construction, however the general layout, height and various other dimensions of the buildings have been greatly exaggerated to make the building susceptible to failure under wind forces so as to make use of outriggers and belt walls. In other words, a scenario is created in which the use of belt walls, bracing system and outriggers seems like a good solution.

Gust factor method is the most commonly used method for determining the way a building will behave under the dynamic effects of wind in both parallel and perpendicular directions, however, to avoid unnecessary complications, a 2 kN/m_2 uniform wind pressure is assumed to act on the building in y direction only. In high-rise structures, it has been seen that the wind base shear effect is much more substantial than the effect of seismic base shear, therefore, in this study, static wind analysis is performed on the structure. The building model was created according to the exact specifications in ETABS. The model was created using several different position combinations of outriggers, bracings and belt walls at various levels in the building. The purpose of placing the lateral force resisting systems on different levels is to investigate and govern the assortment of options that are going to be optimal to endure the loads.

III.a Description of Structure Model

The present thesis comprises of a spiral building in the shape of an egg whose dimensions are 43.2m in X-direction and 55.9m in Y-direction encompassing an area of 2415m2. The total height of the building is 292m. There are 70 floors with different heights above the ground along with 3 floors underground (12m). The structure is surrounded by a radial grid system of columns placed at regular intervals.

The central core installed in the building is of elliptical shape which will be able to comfortably house various amenities and elements like staircase, MEP risers and other forms of vertical transportation. The lateral force resisting system functions on the fundamental principle of central core wall system. Not counting the elliptical core, the structure consists of 14 different shear walls. It is common knowledge that the lower floors of the building require stronger concrete whereas the higher levels can make do with lower grades, keeping that in mind the lower levels use M45 grade and the higher levels use M85 grade.

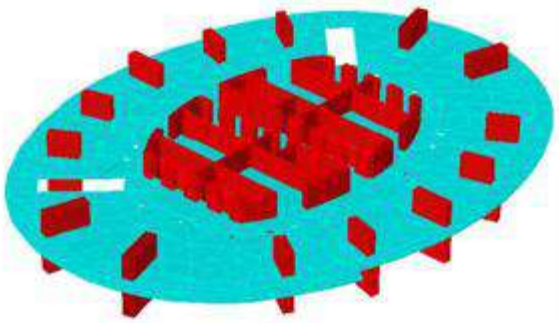

Fig. 3.B Floor plate of the Structure

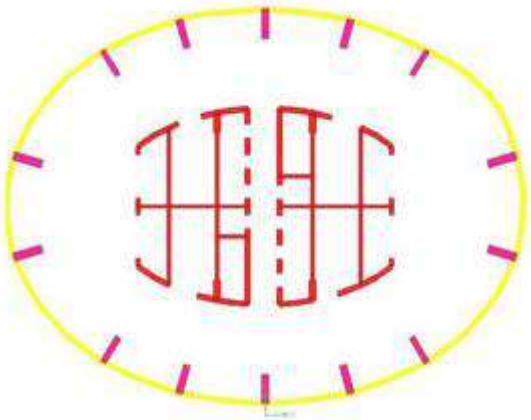

Fig. 3.A Plan of the Structure

III.b Building model analysis using ETABS

The stresses developed along with moment and displacements are calculated by using the method of static wind analysis including and excluding outriggers. The software used for this analysis is ETABS which stands for Extended Three-Dimensional Analysis of Building Systems. The points to be considered for this software are

- The slab and walls were taken as shell type to deliver plane stiffness.
- The rigid diaphragm option was used to model the slab sections and they are modelled only to take in plane diaphragm forces.
- Due to cracks appearing in the slabs at supports and also because of the effect of shrinkage and creep, the out of plane bending stiffness of slabs is neglected.
- The building was analyzed carefully after Uniformly Distributed Load was properly disturbed among all floors.

After detailed consultation and feedback from experienced engineers who are in practice, for preliminary calculations, only uniform wind pressure was adopted. After the option of outrigger is accepted by the client and architect, the calculation of different loads will be incorporated in the final detailed design. The structure is studied only for wind acting in the Y direction.

The results which were compared are as follows:

- Displacement at the roof level
- Moment shared by the elliptical core
- Moment shared by the outrigger system
- Moment shared by the belt system
- Moment shared by the outrigger and belt system

IV. RESULTS AND DISCUSSIONS

IV.a. Outrigger System

The stresses and moment shared by the elliptical core along with drift of the building under the presence of outriggers are studied carefully in this thesis. The static wind analysis was carried out in ETABS software wherein outriggers were placed in certain places with different thicknesses varying from 450mm to 650mm. The behaviour of the building was observed and appropriate results were documented.

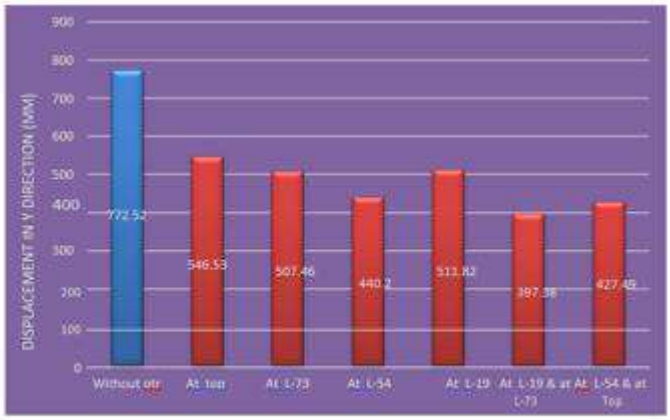

Fig 4.1 Comparison of lateral displacement at roof level with different outrigger locations.

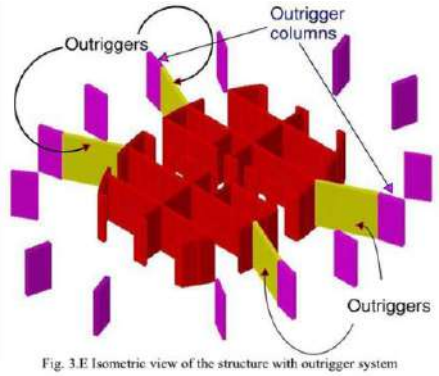

Fig. 3.E Isometric view of the structure with outrigger system

IV.b Belt Walls

The belt wall system was modelled similarly on the same floors i.e. the 73rd, 54th, and the 19th floors and a combination of 19th floor and 73rd floor along with 54th floor and the roof level.

The structure consists of a combination of outriggers along with belt wall. This system was modelled in ETABS with the thickness varying from 450mm to 650mm and its subsequent effect on the behaviour of the building i.e. drift of the building along with stresses and moment shared by the elliptical core is studied.

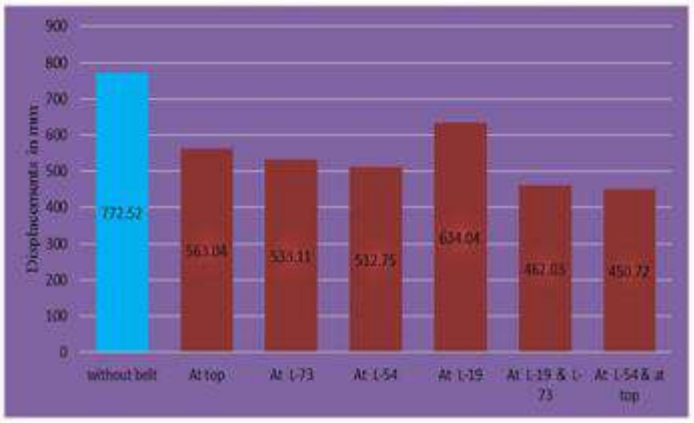

Fig 4.D.1 Comparison of lateral displacement at roof level with different belt locations

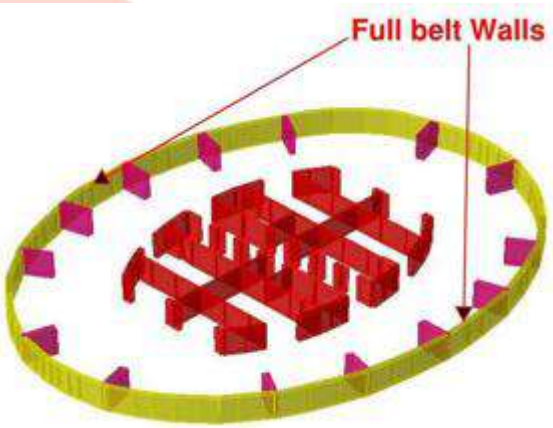

Fig. 3.N Isometric view of the structure showing belt wall system

IV.c. Bracing System

The behaviour of the building is observed by providing bracings or x-bracing of varying sizes such as 0.7mx1.75m, 1.1mx1.1m, 1.3x1.3m of grade M60 at the 73rd Floor with its ends released. The subsequent results obtained such as moment reduction and deflection in the core are studied carefully.

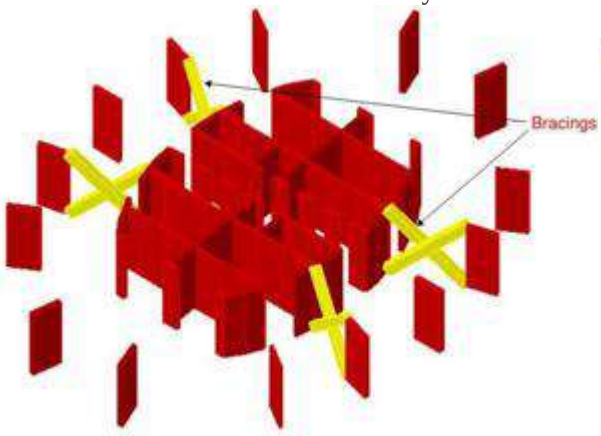

Fig. 3.Q Isometric view showing bracing system in the structure

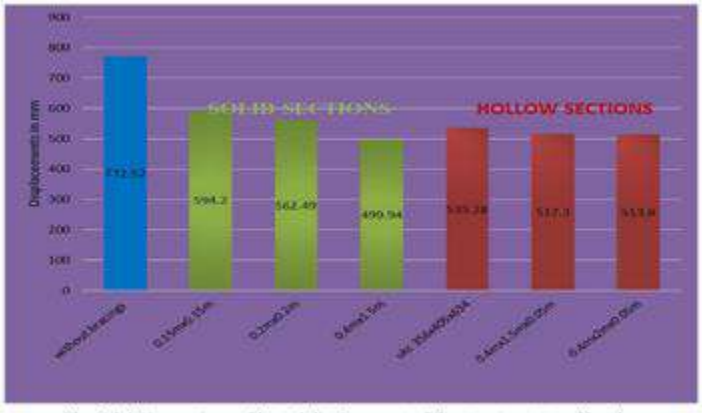

Fig 4.K.1 Comparison of lateral displacement of the structure at roof level with steel bracing of different cross sections.

IV.c. Belt wall and Outrigger System

The structure consists of a combination of outriggers along with belt wall. This system was modelled in ETABS with the thickness varying from 450mm to 650mm and its subsequent effect on the behaviour of the building i.e. drift of the building along with stresses and moment shared by the elliptical core is studied.

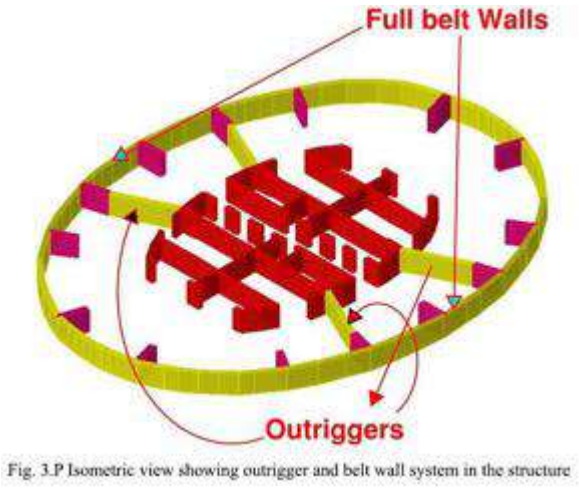

Fig. 3.P Isometric view showing outrigger and belt wall system in the structure

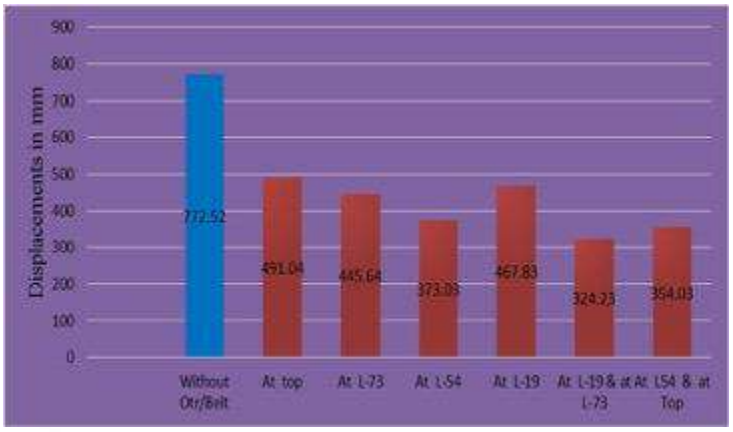

V. CONCLUSIONS

- The tall buildings with core wall as lateral load resisting system (LLRS), a large amount of moment caused by wind forces is shared by core wall. For the structure to be safe the size of the core wall should be sufficient enough, making the structure highly uneconomical.
- The addition of Outrigger makes the structure stiff to a very high level and it allows the structure to be spacious unlike if we use "Tubular Structures" which reduces the portability of the structure.
- It was observed that with the use of a 600mm outrigger at two locations (L-73 & L-19) the lateral displacement due to wind-y forces of the structure reduces by almost 50%, reduces moment shared by central core by 38% and stresses on core by 29%. The moment shared by outrigger system is about 41% of the total moment developed due to wind-y forces.
- With the use of belt walls at two level (L-73 & L-19), the lateral displacement of the structure reduces by 52%, moment shared by the central core also reduces by almost 40%. The moment shared by belt wall system in this particular model is about 40% of the total moment developed due to lateral loads.
- The combination of outrigger and belt wall reduces the lateral displacement of the structure by almost 60% when the combo was placed at two level (L-73 & L-19), the moment shared by the central elliptical core reduces by 48% and stress on core by 39%. In this model the moment shared Outrigger Belt system is of about 49% of the total moment developed.
- With the use of bracing of different cross-sectional areas, the lateral displacement of the structure reduces to the permissible limits, but the bracing fails in axial forces.

VI. REFERENCES

[1] Ali Lame (2007), "Optimization of outrigger structures", University of Tehran, Massachusetts Institute of Technology libraries.
[2] Abbas and Mohsin (2012) "Optimization of outrigger locations in steel tall buildings subjected to earthquake loads"
[3] Bryan Stafford Smith and Alex Coull, "Tall building structures-Analysis and design" A Wiley Interscience Publications-John Wiley and sons.
[4] ETABS 9.7, "Documentation and Training Manuals".
[5] Gerasimidis and Efthymiou (2009) "Optimum outrigger locations of high-rise steel buildings for wind loading"
[6] Hi sun choi, Joseph Neville mathias (2012) "Outrigger design for high rise buildings": An output of the CTBUH outrigger working group, council on tall building and urban habitat: Chicago
[7] Hi Sun Choi, Leonard Joseph, Thornton Tomasetti (2012), "Outrigger system design considerations" CTBUH research paper.
[8] IS -1893, "Criteria for Earthquake Resistant Design of Structures – Part I, General provisions and buildings (Fifth Revision)" Bureau of Indian Standards, New Delhi, 2002
[9] IS 875(Part 3)-1987, "Indian standard code of practice for design loads (other than earthquake) for buildings and structures"
[10] J.R.Wu and Q.S.Li(2003) "Structural performance of Multi-Outrigger braced Tall Buildings"
[11] John Merrick, Radu Bliuc and Mike Haysler(2009), "Design of a Composite Outrigger Structure for the Dubai Tower, Doha"
[12] Kyoung Sun Moon (2015), "Structural Design and Construction of Complex-Shaped Tall Buildings" IACSIT International Journal of Engineering and Technology, Vol. 7, No. 1, February
[13] N. Herath, N. Haritos, T. Ngo & P. Mendis (1998) "Behaviour of outrigger beams in high rise buildings under earthquake loads" Australian Earthquake Engineering Society 2009 Conference
[14] P. Mendis, T. Ngo, N. Haritos, A. Hira (2007) "Wind Loading on Tall Buildings", Electronic journal of structural engineering (EJSE) Special Issue: Loading on Structures

[15] Pankaj Agarwal and Manish Shrikhande, "Earthquake Resistant Design of Structures" PHI Learning Private Limited, New Delhi, 2010.
[16] Po seng kian and Frits torang siahaan (2001) "The use of outrigger and belt truss system for high rise concrete buildings"
[17] Raj kiran, Ihtesham and Suresh (2013) "Optimum position of outrigger system for high rise reinforced concrete buildings under wind and earthquake loads"
[18] Shankar Nair, R, "Belt Trusses and Basements as Virtual Outriggers for Tall Buildings", Engineering Journal, Fourth Quarter, American journal of steel construction, 1998.
[19] Shaun T Debanon(1999), "Optimization of outrigger structural systems" Brigham Young University, Massachusetts Institute of Technology libraries.
[20] SP-64, "Explanatory handbook on Indian standard code of practice for design loads (other than earthquake) for buildings and structures"
[21] Taranath B.S. (2001), "Reinforced concrete design of tall buildings" CRC Press
[22] Z. Bayati, M. Mahdikhani and A. Rahaei (2008), "Optimized use of multi-outriggers system to stiffen tall Buildings" The 14th World Conference on Earthquake Engineering, Beijing, China.

Use Of Outrigger, Belt Wall And Bracing Systems In High Rise Building Subjected To Wind Loads

[1]Mohammed Arsalaan Wajid, [2]Dr. S. Amaresh Babu
[1]Post Graduate Student, [2]Professor and Head of Department of Civil Engineering
Nawab Shah Alam Khan College of Engineering and Technology

Abstract - **In the fast changing and ever evolving world of today, high-rise structures with innovative designs have become the norm. Even though these structures are a marvel to look at, they have their own fair share of problems. As one goes higher, the wind forces become a huge obstacle that needs to be dealt with effectively in order to ensure the security of the residents. After extensive research and trial runs, many creative solutions have come up to tackle the effect of wind energy. In the present study, an attempt is made to effectively reduce the lateral displacement caused by wind forces with the help of a belt wall, optimally placed outriggers and a proper bracing system. In this research, with the assistance of Outrigger / Belt wall / Bracing systems, an effort has been made to assess an economical technique of decreasing lateral displacement of the structure owing to wind forces. The present study takes in consideration an elliptically planned height structure of about 320 m, the structure consists of 78 above ground level stories and 2 below. It comprises of an elliptical core as lateral load resisting system. The structure is studied with (i) Core wall (ii) Core wall with Outrigger (iii) Core wall with Belt wall (iv) Core wall with combination of Outrigger and Belt wall and (v) Core wall with Bracing systems. The thickness of outrigger/Belt wall is varied from 300mm to 500m with a step of 100. The Outrigger/Belt wall system is provided on different levels and in some cases, it is provided on two different levels. The Outrigger/Belt wall is provided only on plant floors/refuge floors/mechanical floor. The bracing system is studied only at level 70 only with cross sectional areas and with different materials (concrete and steel). There are four plant floors in the model structure, which are at level 17, 51, 70 and at roof level. The parameters discussed in this study are the lateral displacement, which occurs at the roof level of the structure along with the moment reduction shared by the elliptical core that is caused by wind forces and the moment shared by the combination system, i.e. the bracing system, outriggers and the belt wall. After much trial and error, it was established that the optimum location of a single outrigger or belt wall was level 51. For two different levels, the best location was found to be at level 17 and level 70. On the other hand, the use of bracing system drastically reduced the lateral displacement of the building right down to the permissible value but it was found to be ineffective when it came to reducing the moment shared by the core. Out of all the options and various permutations and combinations, the safest and most economical setup was found to be combination of belt wall and outrigger at two levels i.e. level 17 and level 70. This study also shows that the lateral displacement of the structure can be minimized by enlarging the size of the central core or in other words simply increasing the stiffness of the building. However, the drawback of this method is the exponential increase in the cost of the structure thereby making it profligate, because the increase in size of core directly results in the increase in volume of concrete used, which is negligible when the combination system proposed in this study is utilized.**

keywords - **Outrigger, belt wall , bracing system, wind loads**

I. INTRODUCTION

In this day and age, the construction of tall buildings has become a fast-growing trend. In order to make your presence felt in the market, companies are making it a point to construct flamboyant structures or own an office in the region's biggest skyscraper. Sky is the limit for these innovative structures as long as all proper conditions are being met. One of the biggest problems an engineer faces when designing a tall building is the considerable effect of wind on the lateral stability of the structure. This is the governing factor in the design of skyscrapers. As the building goes higher, wind pressure increases proportionally, and that is why loads associated with winds are much greater than live and dead loads. Extreme lateral displacement can cause structural and non-structural damage while too much acceleration can lead to problems to the occupants. Generally, shear walls and moment resisting frames are more than enough for low to medium height buildings, but as you go higher, these methods are rendered insufficient. At this point, belt wall system along with outriggers can be effectively used to keep the lateral displacements in check and increase the stiffness of the structure. Outriggers are a concept derived from sailing ships, which use them to resist the wind forces in their sails. Simply put, the core in the high-rise building can be related to the mast of the ship, while the outriggers act like the spreaders and the outer columns like the shroud.

1.1 Lateral Load Resisting Systems

1.1.a Outrigger System

An outrigger is a rigid horizontal structure, which is a part of a boat's rigging, which extends beyond the gunwale providing stability to the main hull preventing it from capsizing. Taking inspiration from this concept, high-rise structures are installed with outriggers and a central core. Stiff in flexure, these horizontal cantilevers connect the central core to the peripheral columns. The moment arm of the core is increased due to this connection, which in turn increases the lateral stiffness of the system. When wind

forces act on the structure, the column-restrained outriggers on the windward side restrain overturning moment through tension and the outriggers on the leeward side through compression. This minimizes lateral displacement drastically when compared to a structure without outriggers. Outrigger systems are not only efficient in controlling the lateral displacements occurring at the top, they are also significant in reducing the inner storey drifts of the structure. This is one of the most efficient system of designing a high-rise structure as it increases the structural depth of the building when it behaves as a vertical cantilever. A horizontal deep girder joins all the exterior columns, which are not directly connected to the ends of the outriggers.

Types of Outrigger Systems

- **Conventional Outrigger System** - This system consists of outrigger girders connected directly to the braced frame or the shear wall at the central core and to the peripherally located columns. These exterior columns are most commonly located at the outer edge of the building. These outrigger trusses, which are connected on one side with the central core and the exterior columns on the other side, convert the moment at the core into a vertical couple at the columns thereby resisting rotation at the core. The core is subjected to reverse curvature below the outrigger, as the rotation is minimal in most designs. In other words, the outrigger truss moves up and down due to overturning and rotation of the core caused by the wind forces. The peripheral columns restrict this movement and produce opposing forces.
- **Virtual Outrigger System** - One of the biggest problems associated with conventional outrigger system is the decline of usable space on the working floor. Functional and architectural constraints create many hurdles. To overcome these problems, virtual outrigger concept is used. The direct connection between the central core and the exterior columns used in the conventional outrigger system is eliminated which in turn solves many problems concomitant with the use of outrigger systems. The working behind the virtual outrigger concept is to make use of stiff diaphragms, which are resilient in their own plane. The moment is transmitted in the form of horizontal couple from the central core to the outrigger trusses and from there to the peripheral columns. Belt truss/walls and basements can be used as virtual outriggers

1.1.b Belt Walls

Belt walls eliminate many of the hurdles that arise when working with the outrigger system. They are provided to improve the axial and torsional stiffness of the columns. Belt walls are quite useful in controlling the settlement of columns as well as shortening and differential elongation. Extra peripheral columns are constructed in order to support restraining the overturning of the outriggers.

To achieve this phenomenon, exterior columns are tied to a wall running around the circumference of the building in the form of a belt, hence the name belt wall. The floor diaphragms are flexible in the out-of-plane vertical direction even though they are quite stiff in their own plane and are thus unaffected by differential settlement of columns.

1.1.c Bracing Systems

Bracing is a highly economical and efficient system of resisting lateral displacement in a high-rise building. This system is most suited for buildings of medium height and are generally used in steel construction. The number of bracings and their location is the most important factor during architectural planning Bracing systems usually form a triangulated vertical truss in which the diagonal members form the web and columns acting as chords. The biggest advantage of this system is that it can be used repetitively leading to a highly economical design and cost cutting in fabrication. Large-scale bracing systems are highly efficient in reducing drift ratio and uplift forces in the foundation.

1.2 Need for Present Study

It comes as no surprise that the cost of owning a piece of land these days is through the roof. To compensate for this exponential increase, builders have started going higher and higher, which presents its own set of problems. Larger height to width ratio will cause huge overturning moments while the structure deflects considerably. Taller buildings have created a need for unconventional, innovative and efficient structural systems. As fewer exterior columns are preferred, the central core wall is the one that is fully responsible of resisting lateral forces. For this concept to work, high-rise structures consist of floor spaces free of columns between the peripheral columns and the central core. This type of setup sanctions for varied utilization of the floor space, at the cost of sacrificing the core and peripheral column system, which is vital for repelling the overturning forces and moment. To overcome this hurdle, one needs some form of structural system to connect these two components in order to increase the overall resistance of the structure. The best option here is to make use of outriggers, which increase the resisting moment to overcome the lateral forces acting on the structure. They are also quite economical as the use of outriggers directly influences the quantity of steel used and it is common knowledge that controlling the cost of steel increases the overall economy of the structure.

1.3 Objectives of the Study

The primary objective of the present thesis is to find out the efficiency of belt walls, bracing systems and outriggers in resisting lateral forces at various storeys in a high-rise structure exposed to wind loads. The aim of the study is

- To observe and study the way in which displacement at roof level is reduced and how the high-rise structure behaves with the addition of belt walls and outrigger
- To study the reduction of moment shared by the central core wall by the application of outriggers and belt wall.
- To calculate the moment shared at the base of the high-rise structure.

II. LITERATURE REVIEW

Gerasimidis and Efthymiou (2009) "Optimum outrigger locations of high-rise steel buildings for wind loading" In this paper a two-dimensional model was analyzed with a concrete core at the middle of the building model and two columns at the edges of the structure. One of the outriggers was placed at the top level of the building while the study was carried out in finding the optimum location for the second outrigger. The second outrigger was moved along the height of the building and placing it on every floor level. A uniform wind loading was considered for the two-dimensional model. The number of stories were thirty with a constant story height of 3m. It was found that when the second outrigger was placed at the middle of the model, the optimum location of the outrigger was achieved, taking into consideration only the drift criteria.

Abbas and Mohsin (2012) "Optimization of outrigger locations in steel tall buildings subjected to earthquake loads**"** This paper compared the optimum outrigger locations obtained by response spectrum and nonlinear time history analysis. 3D models of 20 and 25 storey steel frame braced by outrigger and belt truss system were considered. The paper concludes that optimum outrigger and belt location resulting from response spectrum analysis are at storey 10 and 14 respectively for 20 and 25 storey models whereas for time history analysis the optimum locations were at storey 14 and 16 respectively.

Raj Kiran, Ihtesham and Suresh (2013) "Optimum position of outrigger system for high rise reinforced concrete buildings under wind and earthquake loads" The paper studied nine 30 storey 3d models of outrigger and belt truss system for both wind and earthquake loads. The paper concludes that the use of outrigger and belt truss system in high rise buildings increased the stiffness of the building and made it efficient under lateral load. The drift at the top with only core is 50.63mm when outrigger was provided at top, this reduced to 48.2mm and 47.63mm with and without belt truss. There was no reduction in drift with belt truss. Using second outrigger with cap truss gives the reduction of 18.55% and 23.01% with and without belt truss. The optimum location of the second outrigger is middle height of the building.

II.a Critical Appraisal

- Much of the literature copes with the study of steel outrigger trusses and belt trusses, no journal is studied using reinforced concrete outriggers and reinforced concrete belt walls.
- Many of the researchers studied only the optimum location of outriggers so far attempt is not made for reducing lateral displacement by providing RCC outrigger and belt walls.
- Thus, the present study is an attempt for the analysis of high-rise structure with concrete outriggers, belt walls, combination of outriggers and belt walls along with bracing systems.

III. CASE STUDY

High-rise structures are vulnerable to oscillate under high winds for long natural periods. These structures are prone to the phenomenon of dynamic resonance in wind. Vortex shedding is another type of dynamic response in wind. In vortex shedding phenomenon when high winds blown across the surface of a high-rise structure, vortices are alternately shed from one side to the other giving rise to low pressure zones on the downward side of the structure which generates a fluctuating force acting perpendicularly to the direction of the wind. For buildings higher than 40 storeys, the dynamic resonance in wind has a huge impact on the design of the building. In simpler words, the dynamic resonance in a building can be compared to that of a tuning fork. The taller the structure, the lower is the frequency. It means that as the building goes higher, its frequency is lowered proportionally which results in a structure which resonates more by the wind. At the end of the day, the biggest factor governing the design of a tall structure is the drift of the building due to wind forces and not the fully stressed state as is the common misconception.

One of the chief factors influencing the design of high-rise structure is the behaviour of the structure under the application of lateral loading. Lateral drift at roof level or top of the structure is one of the most essential condition for the design of high-rise structures. According to Indian Standard Code 456, the tolerable displacement also known as top deflection for analysis of wind loading is 1/500 of the height of the structure. It is difficult to truly understand how drift affects the structure unless one experiences acceleration. There are several methods to reduce the drift caused due to lateral loads, one of them being the core wall system which has been found to be quite effective. The main drawback of this system is that when the building increases in height, the stiffness of the core is not enough to keep the wind drift in check. As stiffness of the building increases in significance as one goes higher, the core wall system is combined with outrigger beams connected to shear walls or belt walls which are then connected to the peripheral columns. With this particular system in place, the lateral forces are controlled, wherein the rotation of the core is resisted by outriggers and columns thereby reducing the deflection at top and moment at the base which would have been present in free core system. Quite a number of studies have been carried out on this combination system.

An RCC shear walled structure of 320 m height is considered in the current study. The structure considered here is proposed building which is under construction, however the general layout, height and various other dimensions of the buildings have been greatly exaggerated to make the building susceptible to failure under wind forces so as to make use of outriggers and belt walls. In other words, a scenario is created in which the use of belt walls, bracing system and outriggers seems like a good solution.

Gust factor method is the most commonly used method for determining the way a building will behave under the dynamic effects of wind in both parallel and perpendicular directions, however, to avoid unnecessary complications, a 2 kN/m_2 uniform wind pressure is assumed to act on the building in y direction only. In high-rise structures, it has been seen that the wind base shear effect is much more substantial than the effect of seismic base shear, therefore, in this study, static wind analysis is performed on the structure. The building model was created according to the exact specifications in ETABS. The model was created using several different position combinations of outriggers, bracings and belt walls at various levels in the building. The purpose of placing the lateral force resisting systems on different levels is to investigate and govern the assortment of options that are going to be optimal to endure the loads.

III.a Description of Structure Model

The present thesis comprises of a spiral building in the shape of an egg whose dimensions are 43.2m in X-direction and 55.9m in Y-direction encompassing an area of 2415m2. The total height of the building is 292m. There are 70 floors with different heights above the ground along with 3 floors underground (12m). The structure is surrounded by a radial grid system of columns placed at regular intervals.

The central core installed in the building is of elliptical shape which will be able to comfortably house various amenities and elements like staircase, MEP risers and other forms of vertical transportation. The lateral force resisting system functions on the fundamental principle of central core wall system. Not counting the elliptical core, the structure consists of 14 different shear walls. It is common knowledge that the lower floors of the building require stronger concrete whereas the higher levels can make do with lower grades, keeping that in mind the lower levels use M45 grade and the higher levels use M85 grade.

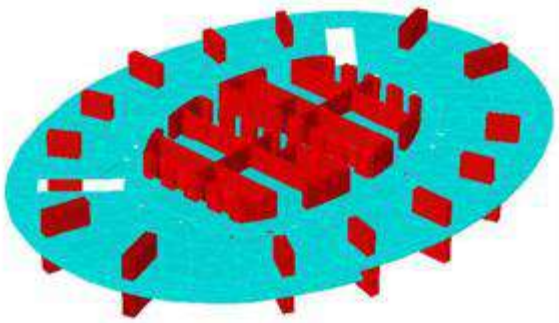

Fig. 3.B Floor plate of the Structure

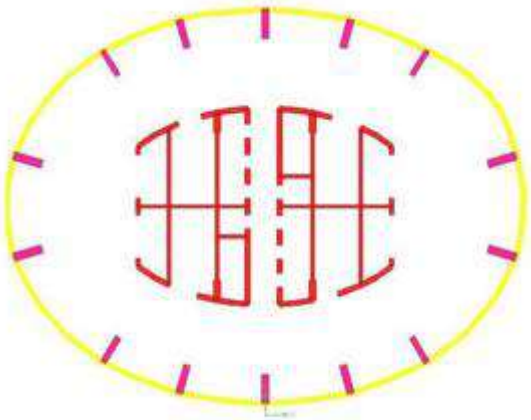

Fig. 3.A Plan of the Structure

III.b Building model analysis using ETABS

The stresses developed along with moment and displacements are calculated by using the method of static wind analysis including and excluding outriggers. The software used for this analysis is ETABS which stands for Extended Three-Dimensional Analysis of Building Systems. The points to be considered for this software are

- The slab and walls were taken as shell type to deliver plane stiffness.
- The rigid diaphragm option was used to model the slab sections and they are modelled only to take in plane diaphragm forces.
- Due to cracks appearing in the slabs at supports and also because of the effect of shrinkage and creep, the out of plane bending stiffness of slabs is neglected.
- The building was analyzed carefully after Uniformly Distributed Load was properly disturbed among all floors.

After detailed consultation and feedback from experienced engineers who are in practice, for preliminary calculations, only uniform wind pressure was adopted. After the option of outrigger is accepted by the client and architect, the calculation of different loads will be incorporated in the final detailed design. The structure is studied only for wind acting in the Y direction.

The results which were compared are as follows:

- Displacement at the roof level
- Moment shared by the elliptical core
- Moment shared by the outrigger system
- Moment shared by the belt system
- Moment shared by the outrigger and belt system

IV. RESULTS AND DISCUSSIONS

IV.a. Outrigger System

The stresses and moment shared by the elliptical core along with drift of the building under the presence of outriggers are studied carefully in this thesis. The static wind analysis was carried out in ETABS software wherein outriggers were placed in certain places with different thicknesses varying from 450mm to 650mm. The behaviour of the building was observed and appropriate results were documented.

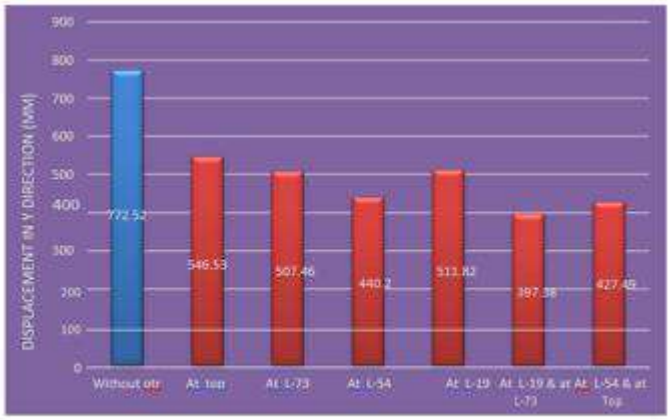

Fig 4.1 Comparison of lateral displacement at roof level with different outrigger locations.

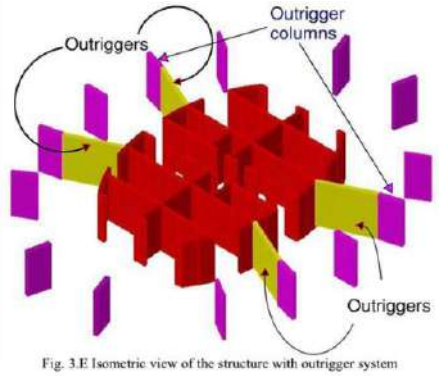

Fig. 3.E Isometric view of the structure with outrigger system

IV.b Belt Walls

The belt wall system was modelled similarly on the same floors i.e. the 73rd, 54th, and the 19th floors and a combination of 19th floor and 73rd floor along with 54th floor and the roof level.

The structure consists of a combination of outriggers along with belt wall. This system was modelled in ETABS with the thickness varying from 450mm to 650mm and its subsequent effect on the behaviour of the building i.e. drift of the building along with stresses and moment shared by the elliptical core is studied.

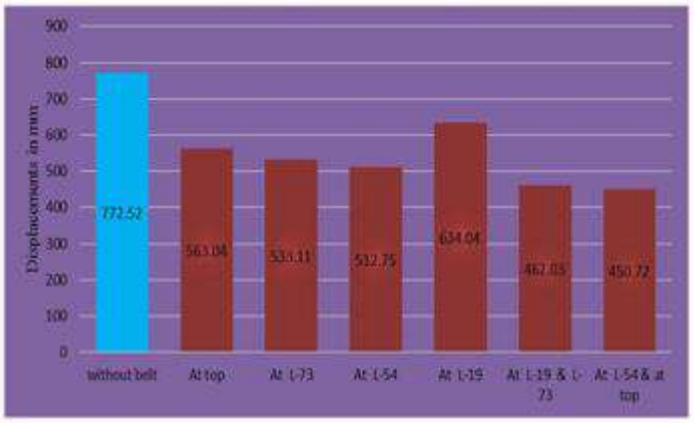

Fig 4.D.1 Comparison of lateral displacement at roof level with different belt locations

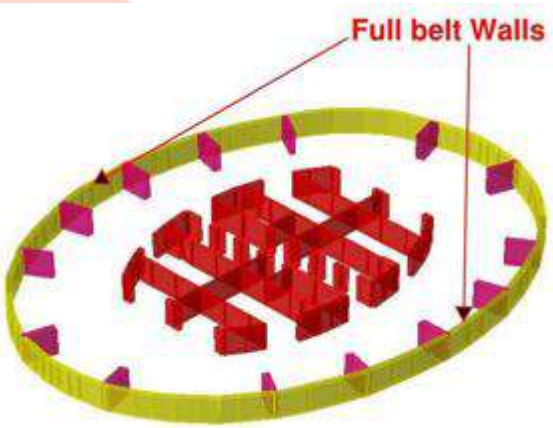

Fig. 3.N Isometric view of the structure showing belt wall system

IV.c. Bracing System

The behaviour of the building is observed by providing bracings or x-bracing of varying sizes such as 0.7mx1.75m, 1.1mx1.1m, 1.3x1.3m of grade M60 at the 73rd Floor with its ends released. The subsequent results obtained such as moment reduction and deflection in the core are studied carefully.

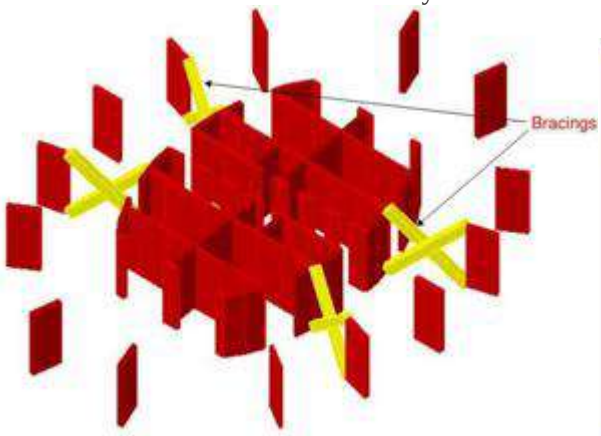

Fig. 3.Q Isometric view showing bracing system in the structure

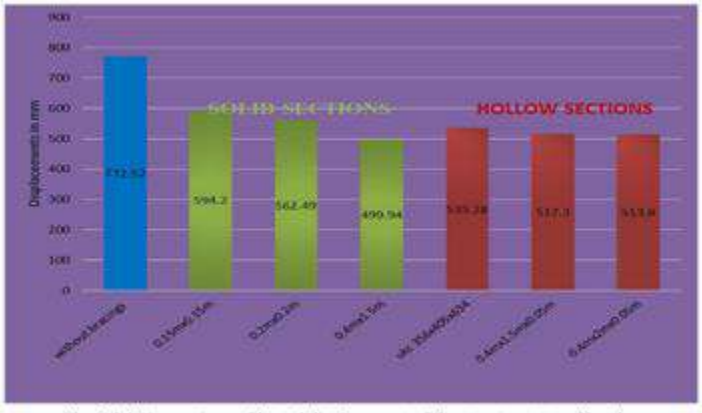

Fig 4.K.1 Comparison of lateral displacement of the structure at roof level with steel bracing of different cross sections.

IV.c. Belt wall and Outrigger System

The structure consists of a combination of outriggers along with belt wall. This system was modelled in ETABS with the thickness varying from 450mm to 650mm and its subsequent effect on the behaviour of the building i.e. drift of the building along with stresses and moment shared by the elliptical core is studied.

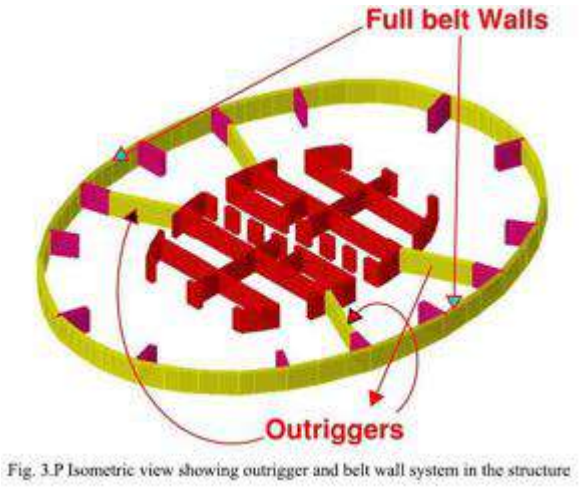

Fig. 3.P Isometric view showing outrigger and belt wall system in the structure

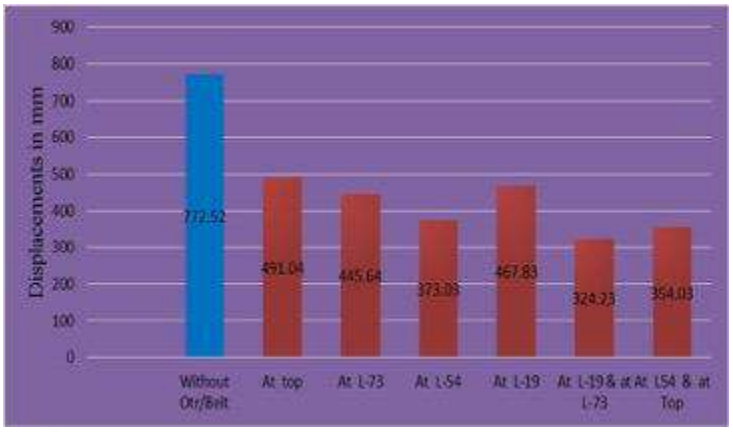

V. CONCLUSIONS

- The tall buildings with core wall as lateral load resisting system (LLRS), a large amount of moment caused by wind forces is shared by core wall. For the structure to be safe the size of the core wall should be sufficient enough, making the structure highly uneconomical.
- The addition of Outrigger makes the structure stiff to a very high level and it allows the structure to be spacious unlike if we use "Tubular Structures" which reduces the portability of the structure.
- It was observed that with the use of a 600mm outrigger at two locations (L-73 & L-19) the lateral displacement due to wind-y forces of the structure reduces by almost 50%, reduces moment shared by central core by 38% and stresses on core by 29%. The moment shared by outrigger system is about 41% of the total moment developed due to wind-y forces.
- With the use of belt walls at two level (L-73 & L-19), the lateral displacement of the structure reduces by 52%, moment shared by the central core also reduces by almost 40%. The moment shared by belt wall system in this particular model is about 40% of the total moment developed due to lateral loads.
- The combination of outrigger and belt wall reduces the lateral displacement of the structure by almost 60% when the combo was placed at two level (L-73 & L-19), the moment shared by the central elliptical core reduces by 48% and stress on core by 39%. In this model the moment shared Outrigger Belt system is of about 49% of the total moment developed.
- With the use of bracing of different cross-sectional areas, the lateral displacement of the structure reduces to the permissible limits, but the bracing fails in axial forces.

VI. REFERENCES

[1] Ali Lame (2007), "Optimization of outrigger structures", University of Tehran, Massachusetts Institute of Technology libraries.
[2] Abbas and Mohsin (2012) "Optimization of outrigger locations in steel tall buildings subjected to earthquake loads"
[3] Bryan Stafford Smith and Alex Coull, "Tall building structures-Analysis and design" A Wiley Interscience Publications-John Wiley and sons.
[4] ETABS 9.7, "Documentation and Training Manuals".
[5] Gerasimidis and Efthymiou (2009) "Optimum outrigger locations of high-rise steel buildings for wind loading"
[6] Hi sun choi, Joseph Neville mathias (2012) "Outrigger design for high rise buildings": An output of the CTBUH outrigger working group, council on tall building and urban habitat: Chicago
[7] Hi Sun Choi, Leonard Joseph, Thornton Tomasetti (2012), "Outrigger system design considerations" CTBUH research paper.
[8] IS -1893, "Criteria for Earthquake Resistant Design of Structures – Part I, General provisions and buildings (Fifth Revision)" Bureau of Indian Standards, New Delhi, 2002
[9] IS 875(Part 3)-1987, "Indian standard code of practice for design loads (other than earthquake) for buildings and structures"
[10] J.R.Wu and Q.S.Li(2003) "Structural performance of Multi-Outrigger braced Tall Buildings"
[11] John Merrick, Radu Bliuc and Mike Haysler(2009), "Design of a Composite Outrigger Structure for the Dubai Tower, Doha"
[12] Kyoung Sun Moon (2015), "Structural Design and Construction of Complex-Shaped Tall Buildings" IACSIT International Journal of Engineering and Technology, Vol. 7, No. 1, February
[13] N. Herath, N. Haritos, T. Ngo & P. Mendis (1998) "Behaviour of outrigger beams in high rise buildings under earthquake loads" Australian Earthquake Engineering Society 2009 Conference
[14] P. Mendis, T. Ngo, N. Haritos, A. Hira (2007) "Wind Loading on Tall Buildings", Electronic journal of structural engineering (EJSE) Special Issue: Loading on Structures

[15] Pankaj Agarwal and Manish Shrikhande, "Earthquake Resistant Design of Structures" PHI Learning Private Limited, New Delhi, 2010.
[16] Po seng kian and Frits torang siahaan (2001) "The use of outrigger and belt truss system for high rise concrete buildings"
[17] Raj kiran, Ihtesham and Suresh (2013) "Optimum position of outrigger system for high rise reinforced concrete buildings under wind and earthquake loads"
[18] Shankar Nair, R, "Belt Trusses and Basements as Virtual Outriggers for Tall Buildings", Engineering Journal, Fourth Quarter, American journal of steel construction, 1998.
[19] Shaun T Debanon(1999), "Optimization of outrigger structural systems" Brigham Young University, Massachusetts Institute of Technology libraries.
[20] SP-64, "Explanatory handbook on Indian standard code of practice for design loads (other than earthquake) for buildings and structures"
[21] Taranath B.S. (2001), "Reinforced concrete design of tall buildings" CRC Press
[22] Z. Bayati, M. Mahdikhani and A. Rahaei (2008), "Optimized use of multi-outriggers system to stiffen tall Buildings" The 14th World Conference on Earthquake Engineering, Beijing, China.

A Survey on secure routing protocols for VANET based on node trust

Muqtadir
Research Scholar,Computer Science & Engineering, Rayalaseema University
PP. COMP SCI&ENGG. 0384
Kurnool,Andhra Pradesh,India.
.
Dr. Syed Abdul Sattar
Director R & D,
Nawab Shah Alam Khan College of Engg. & Tech. (NSAKCET),
Hyderabad
. Telangana, India

Abstract: - Vehicular ad hoc network is developed based on mobile ad hoc networks principles to provide vehicles safety by relaying the communication between vehicles. Secure routing in one the important considerable issue to achieve reliable communication, which can be achieved by the selection route by mutual trust between communicating entities, as misbehaving nodes transmit the false information among other nodes and disturb the routing process. The VANET is vulnerable towards the misbehaving nodes that could be transmit false information leading towards accidents causing human life and financial losses. In order to overcome the problem, in literature lot of secure routing protocol has been developed based on trust. In order to give a comprehensive understanding of secure routing protocols based on trust designed for Vehicular ad hoc network and Pave the path for future research: , a survey of different secure trust based VANET routing protocols is discussed in details in this paper.

1. Introduction

Vehicular communication is one of the emerging technology and it is designed based on mobile ad hoc network technology to provide communication between vehicles, road side units (RSUs) and vehicles to roadside units [1]. In recent ears road safety is one of the considerable issue due to increase in the accidents and more congested and busy roads. The VANET establish communicating between mobile vehicles with the help of DSRC (Dedicated short range communication). Thus, vehicle directly communicate with other vehicles by single or multi hop regarding traffic jams and warning information with the help of fixed road site units. Source vehicle is present in a communication range of destination vehicle, then they communicate directly and it is called single hop communication. If both are not present in a communication range then they relay on intermediate vehicles

for communication. Vehicles also communicate with Road Site Unit (RSU) that increases range of network for communicating vehicles to RSU for sending, forwarding and receiving data with them.

The main aim of VANET is to increases the passenger safety by exchanging the information between vehicles. The major communication attacks on VANET are denial of service, modification attack and false message attack. VANET communication architecture shown in figure 1.

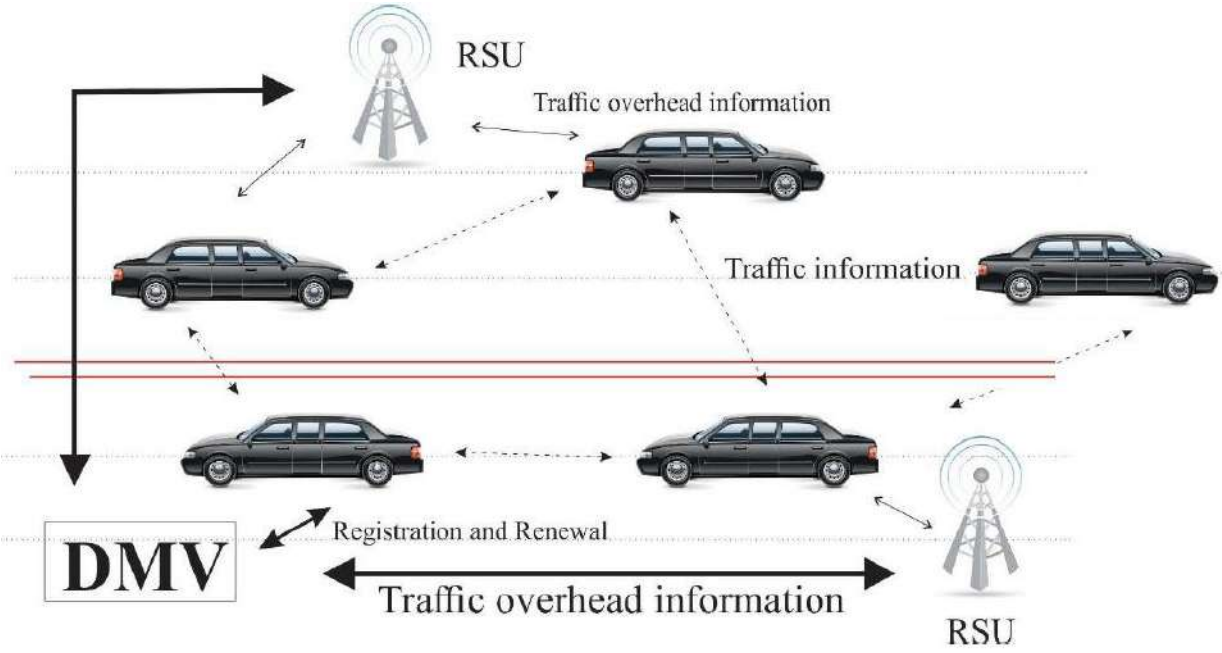

Figure 1: -Architecture of vehicular ad hoc network

Secure communication in VANET is more challenging task due to its characteristics such as absence of centralization, dynamic network topology and mobility. These characteristics make VANET to vulnerable towards the security attacks, and it is very hard to recognize misbehaving nodes or vehicles from communication channel. In literature different trust based routing protocols are designed, the main aim in these protocols are to verify and provide suitable trust values to vehicles. This trust value either provided directly or indirectly, but intention is to give clear information about the vehicles that the node is trustworthy, secure and reliable communication with other nodes in network.

Although there is a lot of review work carried out by researchers about survey of trust based routing protocols. Our work gives the state-of-the-art analysis about survey of trust based routing protocols. It is very difficult to judge which protocol is best for a given network condition. Hence, motivation is to divide the network condition into categories and then compare the performance of protocol.

The remaining paper is organized as follow. Section 2 discusses about trust based routing in VANET, Section 3 gives the discussion. Section 3 shows the conclusion.

2. Trust based routing protocols in VANET

VANET require an optimistic routing protocol due to its dynamic nature and dynamic network topology. The existing routing protocols majorly divided based on topology of network and position of vehicles. In general, vehicles in VANET are mobile with high speed due to which network topology change unpredictably. However depend on traffic condition or road condition speed of vehicle vary, and very difficult to predict the accurate position of the vehicle. Moreover, any vehicle can enter and leave the network any time, and we cannot say what next time within network for is after communication with particular vehicle. In order to establish trust in network first thing is to get the real time related information and false information must not propagate with in the network, else these factors affect the total network performance. If vehicle receive the false position information about the road then it may causes the traffic jams on road and enhances the possibility of accidents. In order to establish the trust following conditions must be considered.

- Vehicles have random speed
- Vehicles move in random direction
- Its current location is sent rapidly to other vehicles and RSU unit for establishment of trust value to vehicles.
- Traffic condition of the road is dynamic
- Node information like time and location information are accurate to all vehicles

In following section we describe the different existing approaches for establishing the trust based routing in VANET.

I. A trust based clustering with Ant Colony Routing in VANET [2]

Cluster head is selected based on real time updated position and trust value of vehicles. Ant colony optimization technique is used for creating reliable and efficient path with minimum routing overhead. Trust value is computed based on trust parameters such as traffic rule obey, data packet forward, control packet forward, data packet precession and control packet precession.

II. Countermeasure Uncooperative Behaviors with Dynamic Trust-Token in VANETs [3]

In order to provide cooperation and to prevent VANET communication, this model designs a dynamic cooperation enhancement based on dynamic trust token for VANET. This mechanism uses the both asymmetric

and symmetric cryptography methods to provide data integrity. It also apply the neighbor information for generating trust token. It achieves the latency in its network performance evaluation.

III. ART: An Attack-Resistant Trust Management Scheme for Securing Vehicular Ad Hoc Networks [4]

The work detects and isolate the malicious nodes and also provide the trustworthiness data and nodes in vehicular ad hoc network. Node trust is evaluated based on functional and recommendation trust and data trust is computed based on the data received, sensed and collected from different vehicles. This scheme is well suitable for VANET applications to increase traffic safety, movement, and environmental defense with improved trustworthiness.

IV. Towards a Novel Trust-Based Multicast Routing for VANETs [5]

This work is based on direct and indirect trust evaluation approaches. Direct trust computed based on Bayesian mechanism and indirect trust is calculated based on assessment of trustworthiness and activity. This system improves the packet delivery with slightly extra delay overhead.

V. Trusted and Secured Routing Protocol for Vehicular Ad-Hoc Networks [6]

It is the modified Ad-hoc On-demand Distance Vector routing protocol designed for MANET with evaluation of trust. Trust is calculated by direct experience of the trust initiator upon the trusty node. Recommendation trust is calculated based on the recommendation given by the recommender nodes upon the trusty node.

VI. Enhance Trust based Routing Techniques against Sinkhole Attack in AODV based VANET [7]

Every node in a network computes the trust value and appropriate status form all its neighboring nodes by the process of monitoring regarding behavior. This trust model is incorporated with reactive MANET routing protocol i.e. Ad hoc on-demand distance vector routing (AODV) protocol. However route is not decided based on the basis of first arrival of Route Reply and waits till it gets the Route Reply from all neighboring nodes and decides the path to be routed based on the nature of Association between them.

VII. A New Trusted Routing Protocol for Vehicular Ad Hoc Networks Using Trusted Metrics [8]

In order to make secure route selection and protect the communication environment from malicious activities, an optimized routing path selection routing protocol for VANET is defined based on trusted metric. On trusted metrics using a Trusted Computing Algorithm. An Optimized node selection routing protocol of VANET has been implemented using Trusted Computing Algorithms with the features of extended light weight routing and

routing messages with trust information which can be updated directly through optimized node selection Routing protocol Algorithm.

Pophali et al. [9] designed a trust based opportunistic routing algorithm for VANET to enhance the security of communication and to protect the network from misbehaving nodes. The algorithm descends the least cost devious routing to compute the node cost to send the packet from the source to the destination. The misbehaving node has been firmly restricted from joining the network. Here, there is a chance of selfish nodes can be present in the network which restricts the transmission from the source to the destination vehicle.

3. Discussion

VANET confirm that the message received from any node (vehicle) is confidentially to prevent accidents. The most important thing is how to trust the received information, as neighboring node is rapidly changing its position. Present trust based routing protocols for VANET computes the trust by voting on the decision received by several nodes, which might not be required for practical scenarios. MANET reputation based routing protocols cannot applied directly to VANET due to its ephemeral nature. Due to mobility voting based trust model causes the problem of oversampling [10]. Oversampling is a situation in which a node observing two or more nodes, takes into consideration both their opinions equally without knowing that they might have influenced each other in decision making. We show that simple voting for decision making, leads to oversampling and gives incorrect results. In our future work we will propose a routing protocol to overcome the problem of oversampling effects to ad hoc networks.

4. Conclusion

The VANET is vulnerable towards the misbehaving nodes that could be transmit false information leading towards accidents causing human life and financial losses. In order to overcome the problem, in literature lot of secure routing protocol has been developed based on trust. In order to give a comprehensive understanding of secure routing protocols based on trust designed for Vehicular ad hoc network and Pave the path for future research: , a survey of different secure trust based VANET routing protocols is discussed in details in this paper. Due to mobility voting based trust model causes the problem of oversampling. Oversampling is a situation in which a node observing two or more nodes, takes into consideration both their opinions equally without knowing that they might have influenced each other in decision making. We show that simple voting for decision making, leads to oversampling and gives incorrect results. In our future work we will propose a routing protocol to overcome the problem of oversampling effects to ad hoc networks

References

1. Muqtadir and Syed Abdul Sattar "Network security based on chaotic maps based authentication in vanets" Journal of Applied Science and Computations Volume V, Issue XII, December/2018 , Page No:280
2. Sahoo, Rashmi Ranjan, Rameswar Panda, Dhiren Kumar Behera, and Mrinal Kanti Naskar. "A trust based clustering with Ant Colony Routing in VANET." In *Computing Communication & Networking Technologies (ICCCNT), 2012 Third International Conference on*, pp. 1-8. IEEE, 2012.
3. Wang, Zhou, and Chunxiao Chigan. "Countermeasure uncooperative behaviors with dynamic trust-token in VANETs." In *Communications, 2007. ICC'07. IEEE International Conference on*, pp. 3959-3964. IEEE, 2007.
4. Li, Wenjia, and Houbing Song. "ART: An attack-resistant trust management scheme for securing vehicular ad hoc networks." *IEEE Transactions on Intelligent Transportation Systems* 17, no. 4 (2016): 960-969.
5. Xia, Hui, San-shun Zhang, Ben-xia Li, Li Li, and Xiang-guo Cheng. "Towards a Novel Trust-Based Multicast Routing for VANETs." *Security and Communication Networks* 2018 (2018).
6. Roy, Debasish, and Prodipto Das. "Trusted and Secured Routing Protocol for Vehicular Ad-Hoc Networks." *Indian Journal of Science and Technology* 10, no. 17 (2017).
7. Chinnasamy, A., S. Prakash, and P. Selvakumari PhD. "Enhance trust based routing techniques against sinkhole attack in AODV based VANET." *International Journal of Computer Applications (0975–8887) Volume* (2013): 22-28.
8. Jeyaprakash, Thangakumar, and Rajeswari Mukesh. "A New Trusted Routing Protocol for Vehicular Ad Hoc Networks Using Trusted Metrics." *IJ Network Security* 19, no. 4 (2017): 537-545.
9. M. Pophali, S. Mohod, T. S. Yengantiwar, "Trustbased opportunistic routing protocol for VANETcommunication,"International Journal Of Engineer-ing And Computer Science, vol. 3, no. 8, pp. 7408–7414, Aug. 2014
10. Huang, Zhen, Sushmita Ruj, Marcos Cavenaghi, and Amiya Nayak. "Limitations of trust management schemes in VANET and countermeasures." In *Personal Indoor and Mobile Radio Communications (PIMRC), 2011 IEEE 22nd International Symposium on*, pp. 1228-1232. IEEE, 2011.

International Journal of Trend in Scientific Research and Development (IJTSRD)
International Open Access Journal
ISSN No: 2456 - 6470 | www.ijtsrd.com | Volume - 2 | Issue – 3

IoT Integrated Energy Efficient Wireless Sensor Networks Application for Healthcare

Md Aleemuddin Ghori[1], Dr. Syed Abdul Sattar[2]
[1]MCA, M.TECH(CSE),(PhD), Research Scholar, Rayalaseema University, Kurnool, Andhra Pradesh, India
[2]B.E, M. Tech, PhD (ECE), PhD (CS), Principal
[2]Nawab Shah Alam Khan College of Engineering & Technology, Hyderabad, Telangana, India

ABSTRACT
In the Internet of Things, smart objects communicate with each other, data are gathered and certain requests of users are satisfied by different queried data. The development of energy efficient schemes for the IoT is a challenging issue as the IoT becomes more complex due to its large scale the current techniques of wireless sensor networks cannot be applied directly to the IoT. Since energy efficiency is of utmost importance to these battery constrained IoT devices, IoT-related standards and research works have focused on the device energy conserving issues.

This paper presents a comprehensive survey on energy conserving issues and solutions in using diverse wireless radio access technologies for IoT connectivity. To achieve the green networked IoT, this paper addresses energy efficiency issues by proposing a novel deployment scheme. The simulation results show that the new scheme is more energy efficient and flexible than traditional WSN schemes and consequently it can be implemented for efficient communication in the IoT.

The development of energy efficient schemes for the IoT is a challenging issue as the IoT becomes more complex due to its large scale the current techniques of wireless sensor networks cannot be applied directly to the IoT. To achieve the green networked IoT, this paper addresses energy efficiency issues by proposing a novel deployment scheme.

Keywords: *IoT, Wireless Sensor Network, Battery, Energy efficiency*

I. INTRODUCTION
The Internet of Things (IoT) has been visualized as the communication and integration of smart objects (things). The dominance of IoT leads to a novel context of upcoming services and applications. These sensors and actuators (e.g., surveillance cameras, home appliances, and environment monitoring sensors) are typically equipped with different kinds of microcontrollers, transceivers, and protocols for communication of sensing and control data.

These real life objects, either sensors or actuators, are connected with each other to transfer their sensed data to centralized servers, where information is collectively stored and made available for particular users with proper access rights.

Devices in such IoT networks will typically operate based on battery power sources, and hence, energy efficiency is naturally of utmost importance in device management. Looking into a particular Wireless Sensor Network (WSN) domain, energy efficiency for battery operated sensor nodes and lifetime prolongment have been research issues for so long, where Medium Access Control (MAC) layer protocols focus on adjusting the duty cycle for sensor nodes, and routing layer protocols are designed for data aggregation and many-to-one transmission. Similarly, since IoT devices operating in the IoT network paradigm are also battery operated, battery consumption should be kept in mind during IoT network deployment.

This paper examines the literature with a specific focus on wireless networking aspects for IoT energy conservation. The remainder of the paper is organized as follows. In Section 2, we provide basic information

about IoT network architectures, IoT device structures, and various applications. In Section 3, we discuss some possible issues that can cause battery drainage of IoT devices and hence affect the lifetime of IoT devices and networks. In Section 4, we review energy conserving solutions provided in different kinds of literature. In Section 5, we propose important research directions regarding energy conserving issues for wireless networking- based IoT and we give concludingremarks.

Internet of Things (IoT):

IoT is an emerging technology used in various applications such as, home automation, health care, industries, market, etc. It is attracting considerable attention from both public and private sectors. IoT network is referred as smart network, because the availability of intelligent and low cost devices, which works autonomously with its sensing, computation and communication capabilities.

Also the proliferation of IoT offers opportunities but may also bear risks. A hither to neglected aspect is the possible increase in power consumption. IoT devices are expected to be reachable by other devices at all times. This implies that the device is consuming electrical energy even when it is not in use for its primary function. Billions of such devices therefore raise concerns regarding excessive standby energy consumption, even if the individual device has only moderate power needs.

This paper investigates the standby power of novel mains connected IoT devies and their estimated impact on the worldwide standby energy consumption. Traditional network-enabled devices like personal computers, tablets, mobile phones, game consoles, set-top boxes, and smart TVs, as well as network infrastructure equipment and data centers, are not covered. The scope of this study is highlighted in yellow in figure 1 below. The report further assesses the related IoT communication technologies as well as the relevant standardization activities.

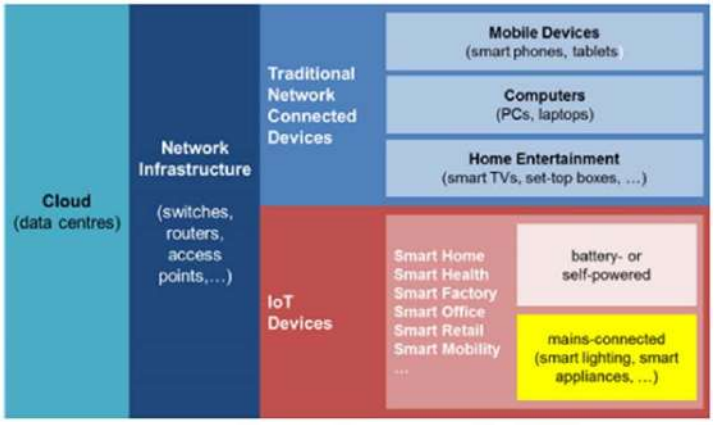

Figure 1.System overview and scope of study (yellow)

Since IoT comprises a very wide variety of industries and applications, we have first structured the IoT space according applications. Then they have been prioritized regarding their standby energy potential based on the estimated proliferation.

The IoT is a term that's bandied around quite a bit these days, simply put, the IoT consists of a patchwork of hardware, software and services all working together to gather and transport information, analyze data, and then use that data to make decisions that improve the efficiency of specific tasks The devices that populate the IoT ecosystem range from smart appliances and automobiles, to wearable and everything in between. While they may differ in application and use, each of these devices makes use of four critical components: sensing,

The project had the following objectives: Provide an overview of the structure of IoT and priorities the categories with the highest energy impact potential based on expected proliferation. Assess energy consumption for prioritised categories based on current technologies and measurements, including analysis of the impact of options to reduce energy consumption. Develop initial high-level recommendations for policy objectives and measures. Identify the most important topics, which should be investigated in further work.

The energy efficient based IoT

A lot of research has already been reported for efficient communication in WSNs for the deployment of a green IoT but little work is found concerning energy efficient communication for a scalable IoT. Routing protocols can be categorized into three types.

- Energy efficiency-based;
- Reliability and network operation-based
- Network operation-based.

The traditional technologies like home automation, wireless sensor networks and control systems will become more efficient and smarter due to involvement of IoT. IoT is having a wide range of application areas. Such as Medical applications for monitoring the health of a patient and sends the information wirelesses.

The present developing Wearable instrumentation is also based on IoT. The example wearable instrumentation is Smart wrist bands, navigation pills, etc. All this methods require an internet interface to update the health info or to control the device with a smart phone. The IoT also plays a vital role in media applications for advertising and exchanging the information worldwide. The manufacturing processes also requires IoT for supply chain management, digital control systems for monitoring the manufacturing processes. IoT in automobile applications and traffic maintenance became a most using area of automation. The automated devices in a vehicle should be connected to a cloud to update the car health within a period of time. By connecting the vehicles and traffic signalling systems to the internet, people can easily find the shortest path for their destination from the traffic monitoring systems and can navigate automatically by checking all other directions

Energy Monitoring of IoT

We realize that buildings can be very different from each other and it is extremely important to find the common "thing" or pattern among them in terms of energy efficiency. So in our project we talked to some on-campus building maintenance experts thoroughly and investigated the common structure of these buildings [12]. We found that for such small office buildings or home buildings, it is relatively simpler and easier to apply networking technologies to control or change their energy policy. In comparison, large buildings like our tested are more difficult to change and it is also one of the reasons why in this paper we primarily focus on such large office buildings. With our findings in this testbed, it is relatively easier to tailor and generalize the system to solve the issue with other buildings of the same type or different types.

ENERGY EFFICENCY ALGORITHM BASEDIOT

SystemModel

Complexity in the IoT is higher than in WSNs, as it has a large number of objects and due to this reason it has a large scale. Dynamic routing for WSN architectures is not suitable in large scale areas. Dynamic routing used in the WSN environment is difficult to use for large-scale networking such as IoT. In general, dynamic routing is difficult to use effectively because sensor transmission is highly sensitive to factors such as air, humidity, temperature, and interference. A stable topology suitable for IoT with large networks can allow static routing to participate in more energy-efficient communication than dynamic routing. Therefor we are considering the above factors we propose static and energy efficient routing for a scalable and complexIoT.

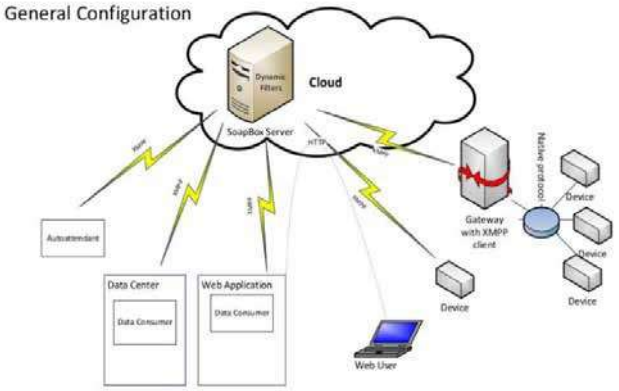

Figure 2: General configuration

We have used the same tiered framework as used except for the relay layer which is not used in our framework, as can be seen in figure 2. It presents the hierarchical network structure where all objects placed are static and follow the transmission Our proposed summarize the research on the topic into three sequential keyaspects:

1. Energy Efficiency of IoT: Through communication networks, the consumption and generation of energy are monitored and logged in different granularities including the whole building, floors, departments, labs, rooms, and even occupants.
2. Energy Modeling and Evaluation: Through off-line modeling and evaluation, identify the energy consumption patterns and factors that may influence the consumption and the extent of the irimpact.
3. IoT System to Apply Practical Changes and Strategy Adjustments: The modeling and evaluation results are used to identify the key energy components of the building, to apply adjustments, and to devise strategies to reduce energyconsumption.

The most important advantage of AODV is its ability to heal itself in case of node failures. It finds the shortest path from source to destination, based on the hop count. For resource constrained wireless sensor network, energy level of the node has to be considered. In proposed work routing residual energy considered for route discovery process. The main objective of this paper is to enhance the network lifetime to achieve an energy efficient IoT, so the optimization for IoT based on the above constraints can be modeledas:

$$T_E = \min\left[\sum_{u \in NM} E_u + \sum_{v \in RM} E_v + \sum_{x \in CH} E_x + \sum_{y \in CCO} E_y\right] \quad (1)$$

The energy optimization problem is to reduce total energy consumption TE . There are other issues for efficient IoT-like robustness, and timely delivery of data which are covered in this paper, but the first and foremost requirement is to minimize the energy depletion of the nodes which are performing various roles.

Residual Energy:

Most of the WSN applications are handled by battery operated devices, so energy is considered as an important resource. Lifetime of the entire network depends on energy usage. The nodes which are near to sink will be overloaded in multihop transmission, this leads to uneven energy drinage and node drain out its battery soon. In an IoT environment composed of WSNs, to avoid this problem, energy of the node should be considered during route discovery process. The nodes with good energy level can be considered as intermediate nodes from source to destination. The residual energy (Er) of node is defined as Units (2).

$$E_r = E_r / E_{\max}$$

Er is remaining energy of the node and Emax is maximum energy available in the node. D. RREQ packet format AODV protocol use route request (RREQ) packet for route discovery from source node to destination node. To implement the Er in AODV, it should be added in RREQ control packet. This paper proposed figure 3 describes the RREQ packet format with Residual Energy (Er) information. By adding this information in control packet, AODV selects the path based Hop Count and Residual Energy.

Type	Flags	Reserved	Hop count
RREQ (broadcast) ID			
Destination Address			
Destination Sequence Number			
Original Address			
Original Sequence number			
Residual Energy			

Figure 3. REEQ packet format

E. Route selection by destination node based in Er value

Route selection of AODV protocol is done by destination node. When the destination node receives route request, it discards further route request and starts sending the route replay to the source. The Figure 4 shows the path selection procedure of the destination node in the IoT environment considering energy efficiency.

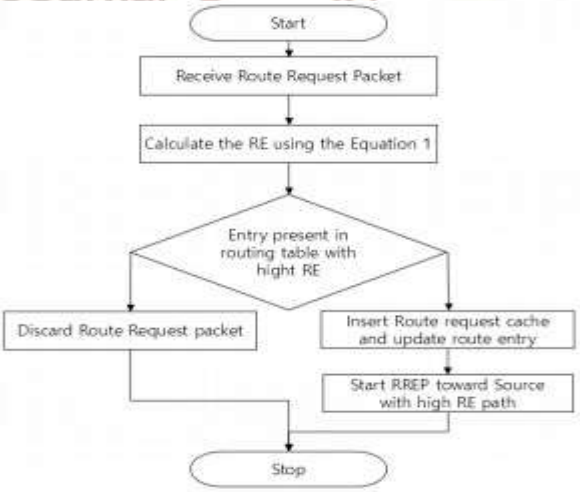

Figure 4. Minimum Er path selecting by destination node

The proposed method considers the residual energy of the IoT device to improve energy efficiency. figure 4 show the path selection step of the destination node considering the residual energy(Er) of the IoT device. It selects the node, which has good Er. After starting RREP timer, destination node sends reply RREP to each RREQ packet stored in cache. After data transmission it removes all the entries in the cache.

SIMULATION RESULTS

This paper, Performance evaluation of hierarchical relay node placement with Energy efficient routing mechanism *RE* (AODV) is done. The comparison between random node deployment and proposed architecture is evaluated by the used of NS2 (NetworkSimulator-2).

Simulation setup

Simulations of the proposed scheme have been performed by the Network Simulator version 2.35 on the Linux Ubuntu version 14.04. The experimental environment is shown in Table 1. 50 joules is used as initial energy for sensor nodes and 60 joules as initial energy for Relay nodes. Relay nodes transmit the data to sinknode.

Simulation Results:

Description	Default
Routing Protocol	AODV, AODV(RE)
MAC /Physical Layer	802.11
Channel Type	Wireless
Radion Propagation Model	Two Ray Ground
Traffic Type	Constant Bit rate
Antenna Model	Omni Directional
Initial node energy	50J
Initial relays energy	60J
Total number of nodes	68

PerformanceEvaluation

Network lifetime: The network is said to be energy efficient network based on its network lifetime. Balancing the energy consumption will prolong the network lifetime and prevent the network from energy whole problem. The lifetime of the network is estimated based on first death node, because when first node starts drain out its energy, within a short span of time all other nodes will drain out its energy. The reason for quick node death after first node death is, after first node death the second node will carry the data load of fist node, hence it will be overloaded and leads to battery drain out. After second node death, the data overload of first and second will be given to thirdnode.

Similar all the nodes in network drain out its battery. In simulation result, the first node death in random placement of relay occur at 140^{th}second, in proposed network architecture first node death occur at 200^{th}second. In random placement of relay nodes, all the nodes losses its energy in 400^{th}seconds. Also In proposed architecture, only 15 nodes losses its energy after entire simulation period. This shows, the proposed network architecture performs uniform energy consumption and gives better network lifetime.

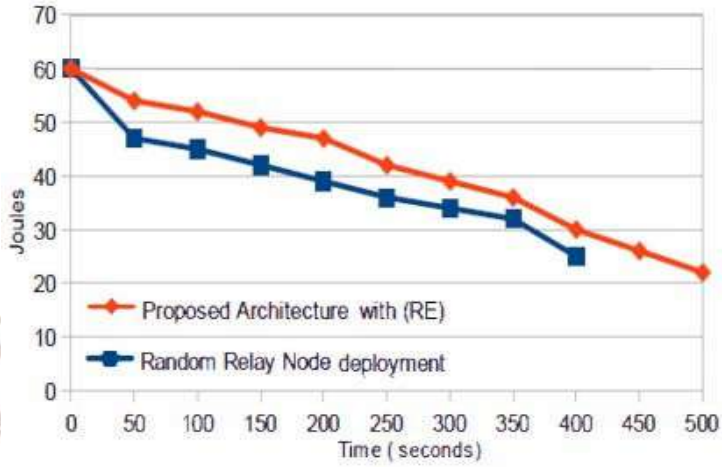

Figure 5.Average energy consumption of node

Average Energy consumption of nodes: Energy efficiency of the network is directly related to average energy consumption of nodes. The performance and lifetime of the network depends on balanced energy consumption of nodes. In Fig. 4 the average energy consumption of relay nodes are in balanced way (uniform). This says the proposed network architecture, gives balanced energy consumption of nodes. From above results it is understood that, the effective combination of node placement and routing mechanism gives energy efficient network.

CONCULSION

In this section, we suggest a few research directions for energy conservation in wireless networking-based IoT. IoT is referred as low power smart device network. Implementing required smart device for particular application and maintaining the network for long time are the two important considerations of loT network. Utilizing the energy in efficient way is the main goal of loT network.

In this paper, hierarchical network architecture is proposed to solve the energy whole problem and suitable routing mechanism is implemented to handle low power devices (battery operated). Common problem affects the network lifetime is uneven energy consumption, this problems are taken care in proposed work. Our simulation result shows, the proposed architecture gives balanced energy consumption, better network lifetime. Hence it is concluded that, proposed network architecture is more suitable for WSN and loT applications.

References

[1] H.W. Ju and Y.W. Yoo, “Efficient Packet Transmission Utilizing Vertical Handover in IoT Environment”, *Journal of the information and communication convergence engineering*, vol. 42, no. 6, pp. 807- 816,2016.

[2] J.Y. Lee, H.S. Choi and W.S. Rhee, “Development of the Web-based Participation IoT Service Brokering Platform,” *Journal of the Korea Contents Association*, vol. 15, iss. 2, pp. 40-57,2015.

[3] H.B. Lee, and K. H. Kwon, “Implementation of a DB-Based Virtual File System for Lightweight IoT Clouds”, *Journal of the KIPS Transactions on Computer and Communication Systems*, vol. 3, no. 10, pp. 311-322,2014.

[4] H.W. Kim and D.Kyue, "Technology and Security of IoT", Journal of The Korea Institute of Information Security and Cryptology, vol.22, no.1, pp.7-13,2012.

[5] K.I. Kim, “Clustering Scheme for (m, k)-Firm Streams in Wireless Sensor Networks,” *the Journal of information and communication convergence engineering*, vol.14, no. 2, pp. 84-88,2016.

International Journal of Trend in Scientific Research and Development
IJTSRD
International Journal
in Scientific
Research and
Development
ISSN: 2456-6470

Image Fusion Scheme based on Wavelet Transformation

Nisar Ahmed
Research Scholar, Mewar University
Department of Electronics and Communication
Rajasthan, INDIA

Ruhiat Sultana
Research Scholar, Rayalaseema University
Department of Computer Science and Engineering
Kurnool, INDIA

Syed Abdul Sattar, PhD
Professor
Department of Electronics and Communication
Nawab Shah Alam Khan Engineering College, Hyderabad, INDIA

ABSTRACT
The paper focuses on image fusion between multi-spectral images and panchromatic images using a gradient based wavelet analysis method with image processing traits. For highlighting the core features of source images, pre-processing is accomplished. A new gradient technique is developed based on wavelet transformation. As of gradient process, for a multi-spectral image, every pixel having 4 neighbors of each of them. The summation that we do matches those of the multi-spectral images that we have selected. Two major considerations for gradient are considered. One is for the pixel values in the multi-spectral images region and other is the gradient pixel values that are at the boundary. Once we have calculated these values, we transfer these values from the multi-spectral images onto the panchromatic image and then rest of the values outside the mask are kept as same. Since we are working on the RGB images, we copied the RGB channels directly. By calculating bigger gradient of the two images either in multi-spectral images or panchromatic images and then construct the final image using inverse wavelet transformation. The proposed method is experimented on satellite, medical and natural images. In all the cases, this method shown superiority with existing methods.

General Terms
Gradient pyramid, spatial frequency, Haar fusion, panchromatic image.

Keywords
Gradient, wavelet, fusion, Multi-spectral, pre-processing.

1. INTRODUCTION
In a multiband, few images represent only smooth variations i.e., weak features while few images have sharp and strong features: that depend on the substances exhibiting either stronger or weaker response for the given wavelength. We need to particularly preserve the weak features in the correct proportion during the fusion. Thus aim of multiband image fusion is to form a single image that merges possible features from all the source images. In the proposed method each pixel in the image band is weighted differently depending on its local details. The weight for any particular pixel in the image is computed based on its relative importance of the feature with respect to its neighborhood. Each pixel in the fused image is obtained with the normalized weighted average of all the pixels at the corresponding location in the band. Local details in the image are obtained by subtracting the 2D smoothed image from the original image. However, the smoothing filter should not blur the edges. Bilateral [1] and nonlocal means filter [2] is popular filters for preserving edges while smoothing. The fusion method based on the wavelet transformation has retained and inherited the main merits of tower-shaped transformation fusion method [3, 4, 5]. Simultaneously, because the orthogonal wavelet transformation has non-redundancy, the image data quantity after wavelet transformation will not increase. By using the direction of wavelet transformation, a better visual effect of fusion image will be able to obtain based on the vision characteristics that the human eye have different resolutions to high frequency component of different directions The image fusion realization requests to extract information (details) from each source image and obtains the effective demonstration in the final fusion image. According to the general theory of imagery processing, the image information (details) is concluded in the image high frequency component, therefore, the key point of image fusion research is to seek an appropriate processing method of fusing detailed information of source image respectively, that is, how will the information be fuse-processed effectively in the corresponding frequency band. According to the multi-resolution analysis theory, the source image after the wavelet transformation, the inner tube signal row , contains separately the image high frequency component of corresponding frequency directed in normal, horizontal and 45º of the image, therefore, using the image tower-shaped structure after wavelets decomposing, to carry on fusion processing separately according to different transformation level and different frequency band, the information detail from different images can be fused effectively.

Carry on N wavelet transformation to the two-dimensional picture, and it will finally get some (3N+1) different frequency bands, which contains a 3N high frequency bands and a low-frequency band. The image fusion program based on wavelet multi-dimensional transformation is shown as in Figure 2. Take two image fusions as an example, many image fusion methods may be analogized from this regarding. Suppose A and B are two primitive images, F is the image after fusion, its basic fusion steps are as follows:

Apart from medical and remote sensing, other fusion applications include classification [6], target identification [7] and object detection [8]. The areas in which multiband/multispectral image fusion find its applications include, geological surveying and environmental monitoring. Another popular category of fusion is in the area of remote sensing with multispectral (MS) and panchromatic (PAN) images. Multispectral images are usually characterized by its higher spectral but lower spatial resolution and vice-versa in the case of panchromatic images. There are quite a large

number of papers that discuss on the fusion techniques for such images. In [9] authors have proposed the technique of combining multispectral and satellite aperture radar (SAR) images by intensity modulation. In [10] authors have carried out fusion based on component framework, whereas in [11] a specific image model has been formed for pan-sharpening approach. Fusion algorithm based on pyramid transforms such as Laplacian and Gaussian are constructed by filtering the images successively and then down sampling. Registered images are subjected to pyramid transform and then fused in the transformed domain. The final image is obtained by performing the inverse transform. The PCA transform de-correlates the inter-correlated multispectral bands into a new set of uncorrelated components. Only the first principal component which contains the most information of the MS image is substituted with PAN image. In recent years wavelet transforms have been successfully used. In [12] authors use wavelet packet transform to fuse Quickbird panchromatic and multispectral data fusion. But there are certain drawbacks of wavelet transform worth to be mentioned. With contourlet transform it is possible to avoid the mentioned drawbacks and hence in [13] authors have used contourlet based fusion for pan sharpening. Unlike the case, where features from high spatial resolution panchromatic sensor is injected into low spatial resolution multispectral bands, authors in [14] have taken into account the physical electromagnetic spectrum response of sensors during the fusion process. Authors showed that the obtained image would be closer to the image obtained by the ideal sensor than obtained by usual wavelet-based fusion method. Authors in [15] have developed a fusion strategy based on synthetic variable ratio method to reproduce the spectral and spatial characteristics of multispectral and panchromatic images, respectively.

In this paper, we propose a novel fusion strategy by obtaining gradient weights from different images in a given multiband using wavelets. Gradient weights vary as the dominating features of the pixels in the individual image vary. Finally, a fused image is obtained with a gradient weighted sum of individual components.

The rest of the paper organized as follows: the sections 2 describe about proposed method, section 3 describes about pictorial and numerical results and discussions. Finally conclusions are derived in section 4.

2. PROPOSED METHOD

In a multi-spectral, few images represent only smooth variations i.e., weak features while few images have sharp and strong features: that depend on the substances exhibiting either stronger or weaker response for the given wavelength. We need to particularly preserve the weak features in the correct proportion during the fusion. Thus aim of multi-spectral image fusion, is to form a single image that merges strong features which are obtained from gradient of all the source images. In the proposed method each pixel in the image is gradient weighted differently depending on its local details. The gradient weight for any particular pixel in the image is computed based on its relative importance of the feature with respect to its neighborhood. Each pixel in the fused image is obtained with the normalized gradient weighted average of all the pixels at the corresponding location in the multi-spectral.

2.1 Wavelet transformation

The 1-Dwavelettransformofa1-Dsignal $f_i(x_i)$ [16]

$$W(a,b) = \int_{-\infty}^{\infty} f_i(x_i)\ h_{a,b}{}^{*}(x_i)dx_i$$

Where * represents the complex conjugate.

A set of daughter wavelets $h_{a,b}(x_i)$is generated from the mother wavelet by scale a and shift b operations

$$h_{a,b}(x_i) = \frac{1}{\sqrt{a}}\left(\frac{x_{i-b}}{a}\right)$$

Where $\sqrt{a}$ is a normalized factor.

The 2-Dwavelettransformofa1-Dsignal $f_i(x_i, y_i)$

$$W(a_1, a_2, b_1, b_2) = \int_{-\infty}^{\infty}\int_{-\infty}^{\infty} f_i(x_i, y_i)\ h_{a_1a_2b_1b_2}{}^{*}(x_i, y_i)dx_i\ dy_i$$

A set of daughter wavelets $h_{a_1a_2b_1b_2(x_i,y_i)}$ is produced from the mother wavelet $h(x_i, y_i)$ by scales (a1 and a2) and shifts (b1 and b2) operations:

$$h_{a_1a_2b_1b_2}b(x_i, y_i) = \frac{1}{\sqrt{a_1a_2}}\left(\frac{x_{i-b_1}}{a_1}, \frac{y_{i-b_2}}{a_2}\right)$$

The different daughter wavelets are spatially multiplexed with different reference-beam directions [17].

2.2 Basic steps of proposed method

Consider two images, need to perform fusion operation, in general, two images are considered as input for fusion operation.

The basic fusion steps are as follows:

1. Apply wavelet transformation separately to each source image to establish various images of the wavelet tower-shaped transformation.
2. Apply fusion processing separately to each transformation level using different fusion operator, to obtain fusion wavelet pyramid
3. For each wavelet pyramid, apply gradient to obtain dominant features. The dominant features are very useful to reconstruct the fusion image from two images.

Apply the wavelet inverse transformation (i.e. to carry on image restructuring) to gradient result, obtain restructuring image namely for fusion image.

The proposed method block diagram is given in Fig. 1.

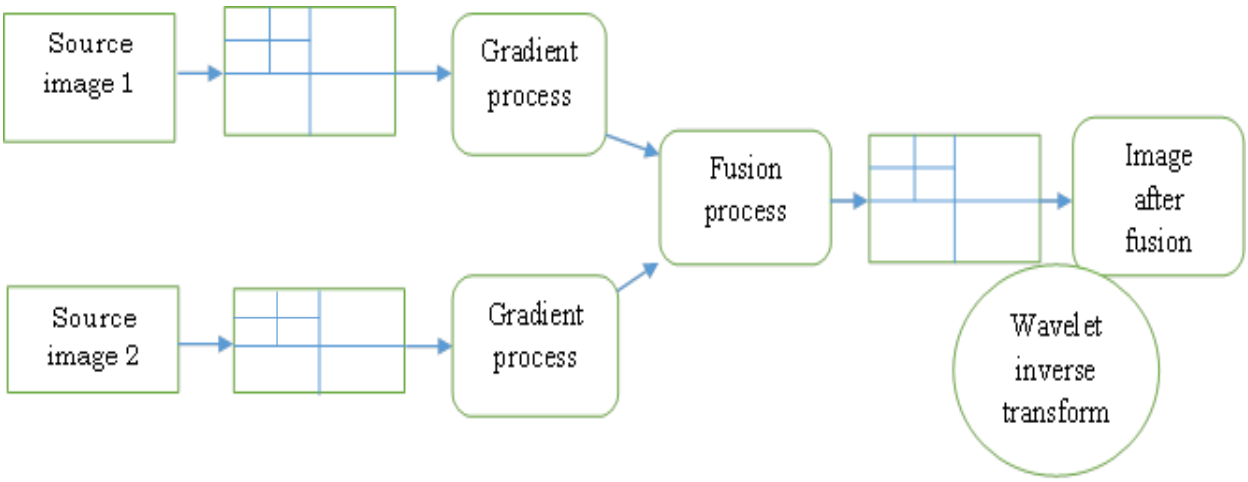

Fig 1: Block diagram of proposed method.

2.3 Basic steps of proposed method

Step 1: To highlight the dominant features of source and target images use pre-processing. By this, the source images are first padded so that they are the same size.

Step 2: Find multi spectra band images using single level 2-D discrete wavelet transformed to get $w_{LL}^1, w_{LH}^2, w_{HL}^3, w_{LL}^4$ sub-bands $[w_{LL}^1, w_{LH}^2, w_{HL}^3, w_{LL}^4] = DWT(W(x_i, y_i)$.

Step 3: Calculating the gradient of each pixel of each band.

In a band image, every pixel has 4 neighbors. Two major considerations for gradient need to be made – one is for the pixel values in the source image region and other is the gradient pixel values that are at the boundary. Once we have calculated these values, we transfer these values from the source image onto the target or background image and then rest of the values outside the mask are kept as it is.

Step 4: Construct the fusion image using wavelet inverse transformation.

3. RESULTS AND DISCUSSION

We tested the proposed method on different images like satellite, medical and natural images. From these images, it is observed that each category of images have different set features and phenomena. The purpose of fusion is to form a single image by merging possible features from all the source images. Figure 2 & Figure 3 Shows the fusion of images. The proposed method clearly identifies the image dominant features and gets success in merging them into single image. For evaluating the proposed algorithm quantitatively, we use statistical measures like average correlation, average Signal noise ratio (SNR) and entropy, mean of fusion image for qualitative measure. The correlation of first image and fusion image is C1 and correlation of second image and fusion image is C2 then considered average correlation is average of C1, C2. Similarly SNR ratio also. We compare results of multi spectral image fusion with (a) contourlet transform used in [18] and (c) bilateral approach suggested in [19] and tabulated in Table 1.

The entropy is calculated using following equation

$$Entropy = -\sum_i \sum_j f_{ij} \log f_{ij}$$

This is a measure of randomness, having its highest value when the elements of f are all equal.

The gradient of an image is given by the formula

$$\nabla f = \begin{bmatrix} g_x \\ g_y \end{bmatrix} = \begin{bmatrix} \frac{df}{dx} \\ \frac{df}{dy} \end{bmatrix}$$

Where:

$\frac{df}{dx}$ is the gradient in the x direction

$\frac{df}{dy}$ is the gradient in the y direction.

Table 1. Comparison of Counterlet Transform and Bilateral Approach.

Methods	Average Correlation	Average SNR(db)	Entropy	Gradient
Contourlet transform	85.65	17.36	4.6	4.3
Bilateral approach	90.12	19.68	5.4	4.9
Proposed method	97.25	29.98	6.2	5.9

(a) **(b)** **(c)**

Fig 2: (a) First Image (b) Second Image & (c) Fused Image

Correlation between first image and fused image =0.977748

Correlation between second image and fused image =0.981530

SNR between first image and fused image =29.92 db

SNR between second image and fused image =29.98 db

(a)

(b)

(c)

Fig 3: (a) First Image (b) Second Natural Image & (c) Fused Image

Correlation between first image and fused image =0.508583

Correlation between second image and fused image =0.843888

SNR between first image and fused image =14.30 db

SNR between second image and fused image =14.30 db

4. CONCLUSIONS

In this paper, we have proposed a novel fusion strategy for different category of images. As the information across the images in the each category is not uniformly distributed, many traditional fusion methods based on averaging the images with equal weights fail. In the proposed method gradients computed on wavelet mutli- spectral images for fusion is based on the local information in each spectral image and hence are different for different images. Fused image is formed with the dominant average gradient of the pixels at the corresponding location. Reduction in the computational cost is achieved by a separable implementation of local gradient. We are able to achieve better results by exploiting all available information at all locations from all the images in the all wavelet spectral image. Results are tested qualitatively and quantitatively with a wide number of quality metrics and also compared with other fusion based approaches.

5. REFERENCES

[1] C. Tomasi and R. Manduchi, “Bilateral filtering for gray and color images,” Proc. 6th Int. Conf. Computer vision. Washington, pp. 839–846, 1998.

[2] . A. Buades, B. Coll, and J. M. Morel, “A non-local algorithm for image denoising,” in IEEE Computer Vision and Pattern Recogognition (CVPR), 2005, pp. 60–65.

[3] JIA Yong-hong, Li de-ren, SUN Jia-bing. Multi-dimensional remote sensing imagery data fusion. Remote sensing technology and application2000,15 (1):41-44

[4] LIU Xiao-long. Study on multi-resource remote sensing imagery information maintaining fusion technology. Journal of image and graphics, 2001, 6 (7):636-641.

[5] LI Jun, LIN Zong-jian. Remote sensing imagery data fusion method based on the characteristic. Journal of image and graphics, 1997, 2 (2):103-107.

T. Westra, K. C. Mertens, and R. R. D. Wulf, “Wavelet-based fusion of SPOT/VEGETATION and ENVISAT/ASAR wide swath data for wetland mapping,” in SPOT/VEGETATION Users Conference, 2004, pp.24–26.

[6] Z. Korona and M. M. Kokar, “Multiresolution multisensory target identification,” In J. D. Irwin (Ed.), The Industrial Electronics Handbook, vol. 12, pp. 1627–1632, 1997.

[7] Z. Zhang and R. S. Blum, “A region-based image fusion scheme for concealed weapon detection,” in St Annual Conference on Information Sciences and Systems, 1997, pp. 168–173.

[8] L. Alparone, L. Facheris, S. Baronti, A. Garzelli, and F. Nencini, “Fusion of multispectral and sar images by intensity modulation,” in Int. Conf. Inf. Fusion, Stockholm, Sweden, 2004, pp. 637–643.

[9] W. Dou, Y. Chen, X. Li, and Z. Sui, “A general framework for component substitution image fusion: An implementation using the fast image fusion method,” Computational Geoscience, vol. 33, no. 2, pp. 219–228, 2007.

[10] M. Joshi, L. Bruzzone, and S. Chaudhuri, “A model-based approach to multiresolution fusion in

remotely sensed images," IEEE Trans. Geosci. Remote Sens., vol. 44, no. 9, pp. 2549–2562, 2006.

[11] W. Zhang and J. Kang, "Quickbird panchromatic and multi-spectral image fusion using wavelet packet transform," Lecture Notes in Control and Information Sciences. Berlin, Germany: Springer-Verlag, vol. 344,pp. 976–981, 2006.

[12] V. Shah, N. Younan, and R. King, "An efficient pan-sharpening method via a combined adaptive pca approach and contourlets," IEEE Trans. Geosci. Remote Sens., vol. 46, pp. 1323–1335, 2008.

[13] X. Otazu, M. Gonzlez-Audcana, O. Fors, and J. Nnez, "Introduction of sensor spectral response into image fusion methods," IEEE Transactions on Geoscience and Remote Sensing, vol. 43, no. 10, 2005.

[14] Y. Zhang, "A new merging method and its spectral and spatial effects," International Journal of Remote Sensing, vol. 20, no. 10, pp. 2003–2014, 1999.

[15] Daubechies I.The wavelet transforms time–frequency localization and signal analysis. IEEE TransInfTheory1990; 36:961–1005.

[16] Mendlovic D, Konforti N. Optical realization of the wavelet transform for two-dimensional objects. ApplOpt1993; 32:6542–6.

[17] A. Alejaily, I. Eirule, and M. Mangoud, "Fusion of remote sensing images using contourlet transform," in Intl. Conf. on Innovations and Advanced Technique in systems, Computing Sciences and Software Engineering, 2008, pp. 213–218.

[18] S. Raman and S. Chaudhuri, "Bilateral filter based compositing for variable exposure photography," in Eurographics Conf., Munich, Germany, 2009.

International Research Journal of Engineering and Technology (IRJET) e-ISSN: 2395-0056
Volume: 05 Issue: 06 | June -2018 www.irjet.net p-ISSN: 2395-0072

Intensification of Soil properties influence by Synthetic Fibre and Pond Ash

Md Ameer Khusro[1], Prof.Sharana kumar Mathad[2], Prof. A Pandurang[3]

[1]PG Student Dept. of Geotechnical Engineering, BKIT college, Bhalki
[2,3]Assistant Professor, Department of Civil Engineering, BKIT college, Bhalki

---

Abstract – Thermal power plant delivered pond ash which is a waste material. In India, Installed limit of power segment is 186 Giga watt (fifth biggest in world) and 65% of introduced limit is constitute by thermal power plant. Thermal power plant utilized 80% of coal for creating power which prompt coal ash generation. Indian coal having the low caloric esteem it prompts coal fiery remains generation rate is all the more, in this way, creation of coal ash is every year in India is around 130 million tons. Spending of huge amount on operation and maintenance of ash pond hence it is required to increment the utilization level of ash pond. However, it is possible to know the engineering behaviour of pond ash. Utilization of pond ash in the field of pavement, abutment, retaining wall, bridge etc, required to be reinforced. In this investigation ,utilizing the pond ash in soil by taking percentage as 10%, 20%, 30%, 40 % and then adding the percentage of nylon fibre in soil such as 2%,4%,6%,8% and 10% efforts are made to reinforce the pond ash with fibre which is nylon fibre in variant substitution percentage such as 2%,4%,6%,8% and 10%.The strength behaviour is examined by conducting CBR(un soaked) test.

Key Words: Black Cotton Soil, Pond ash, Nylon fibre, OMC, MDD, CBR.

1. INTRODUCTION

Thermal power plant produced pond ash which is a waste material. Pond ash strength is low examination with material of earth and having the angle of friction is less and pond ash shape is sub rounded. In India, Installed capacity of electricity sector is 186 Giga watt (5th largest in world) and 65% of installed capacity is constitute by thermal power plant. Thermal power plant used 80% of coal for generating power which lead to coal ash production. Indian coal having the low caloric value it leads to coal ash production percentage is more, thus, production of coal ash is annually in India is about 130 million tons.

By products are the waste material produced by thermal power plant which effects the environment. Now a days disposal of them is major concern it needs a more area and having many environmental issues. Mechanical or electrostatic precipitator delivered fly cinder. Gathering of base cinder from the base of boilers and blend of fly cinder and base cinder is called pond ash. Generation of pond ash is more contrasted with fly cinder and base cinder. Usage of pond ash in other arena to diminish the condition of potential risks.

Self-draining capability display in pond ash and also its weight very less compare with the natural soil before used in other fields. It is vital to know pond ash characteristics strength. Substantial measure of soil required for any developments, for example, abutments, embankments, retaining structures and earthen dam etc. Less accessibility of normal soil then scientists thought to using the power plants waste product, natural soil replaced by waste product as a replacement. Using of by product reduces the natural soil scarcity.

Now a days in India usage of pond ash is negligible in others field. It is used as commercially about 35%. Maximum extent to usage of pond ash for preservation of natural soil. In low lying areas filler material as taken as. Pond ash utilization is rare and for using purpose having the knowledge to physical properties and characteristics.

Pond ash strength is low examination with material of earth and having the angle of friction is less and pond ash shape is sub rounded. Pond ash and reinforcement which increases the geotechnical properties. It is fundamental to know the characteristics strength and reinforcement is very required.

2. EXPERIMENTAL DETAILS

A. Materials:

Black cotton soil; Utilized materials in the investigation are BC soil, Collected BC Soil from near Karanja Dam, district Bidar the soil is greyish black in color the physical properties of soil is tabulated in table 1.

Table -1: Physical properties of Black Cotton Soil

Sl No.	Property	Values
1	Specific gravity	2.45
2	Consistency Limits	
	a. Liquid Limit (%)	74.9
	b. Plastic Limit (%)	42.9

	c. Plasticity Index (%)	32
3	Compaction Properties	
	a. Maximum Dry Density (g/cc)	1.404
	b. Optimum Moisture Content %	23.04
4	Grain Size Distribution	
	a.Coefficient of Curvature	0.86
	b.Coefficient of Uniformity	6.15
5	CBR (Unsoaked) (%)	1.55
6	Differential Free Swell Index (%)	33.25

Pond ash; Collection of pond ash from Raichur Thermal Power Plant, Karnataka. India.

Table-2: shows the chemical composition of Pond ash

Parameter	Value in Percentage
Sio_2	59-61
Al_2O_3	28-28.8
Fe_2O_3	2.70-5.52
Na_2O	0.24-0.50
K_2O	1.26-1.76
CaO	0.7-1
MgO	1.40-1.90
LOI	0.5-2.5

Nylon Fibre; The fibre used in this research work is collected from islampur,Sangli District, Maharashtra, India.

Table-3: shows the physical properties of Nylon Fibre

Sl.No	Property	Value
1	Fibre Cross Section	Trilobal
2	Fibre lenght	18mm
3	Filament	3
4	Sp. Gravity	1.13
5	Color	Brilliantly White
6	Melting point	220 Degree Centigrade
7	Chemical resistance	Very good against alkalis,hydrocarbon

B. Preparation of sample:

Black cotton soil with Pond ash and Nylon fibre is tested for stabilizing clay soil ,pond ash it will be replaced with 10%, 20%, 30 %, 40% by black cotton soil and the geotechnical parameters will be tested in the laboratory by conducting standard compaction test, CBR. Addition of Nylon fibre with 2%, 4%, 6%, 8% & 10% into black soil and the geotechnical parameters will be tested in the laboratory by conducting standard compaction test, CBR test. Adding optimum percentage of pond ash who achieved more dry density then adding with Nylon fibre with 2%, 4%, 6%, 8% & 10% into black soil and the geotechnical parameters will be tested in the laboratory by conducting standard compaction test, CBR test. And after all, results were observed and the variation of properties of soil is observed.

C. Experimental work:

Following tests were carried out specific gravity test, moisture content test, atterberge limits where carried out for only black soil, standard proctor test, California bearing ratio test.

3. RESULTS AND DISCUSSION

A. OMC and MDD results for treated for different blending proportions of the soil:

Table 4: Describing result for OMC and MDD for varying percentage of pond ash

Sl.No	Particular	MDD in g/cc	OMC in %
1	0% Pond ash	1.40	23.04
2	10% Pond ash	1.46	16.66
3	20% Pond ash	1.53	18.2
4	30% Pond ash	1.5	19.10
5	40% Pond ash	1.48	20

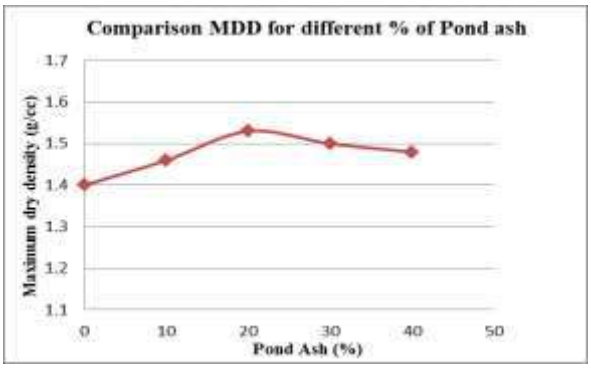

Fig 1; indicating the results for MDD for different % of Pond ash

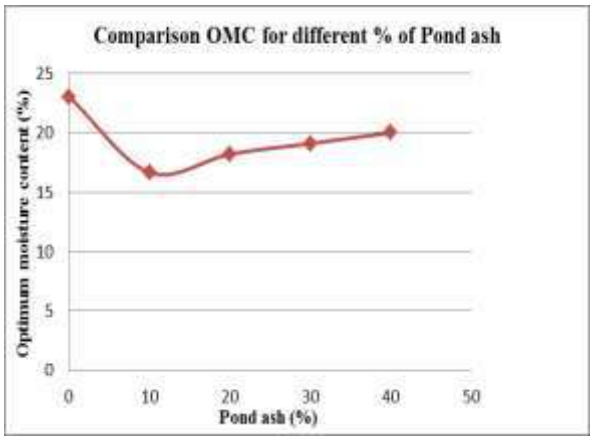

Fig 2; indicating the results for OMC for different % of Pond ash

Above figure (1) & (2) display the addition of 20% of pond ash gives the Maximum Dry Density 1.53g/cc for 18.2% of Optimum Water Content after this diminishing the dry density of rising of water content.

Table 5: Describing result for OMC and MDD for optimum 20% of pond ash varying percentage of Nylon fibre

Sl.No	Particular	MDD in g/cc	OMC in %
1	2% Nylon fibre	1.55	17.7
2	4% Nylon fibre	1.57	21.05
3	6% Nylon fibre	1.68	19.1
4	8% Nylon fibre	1.63	15.03
5	10% Nylon fibre	1.59	20
6	Optimum 20% PA +2% Nylon fibre	1.65	19.04
7	Optimum 20% PA +4% Nylon fibre	1.77	15.8
8	Optimum 20% PA +6% Nylon fibre	1.74	17.8
9	Optimum 20% PA +8% Nylon fibre	1.73	21.6
10	Optimum 20% PA +10% Nylon fibre	1.69	14.6

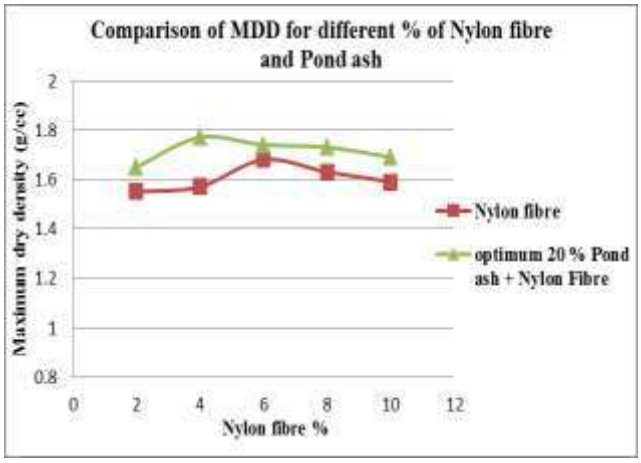

Fig 3; indicating the results for MDD for different % of Nylon fibre and Pond ash

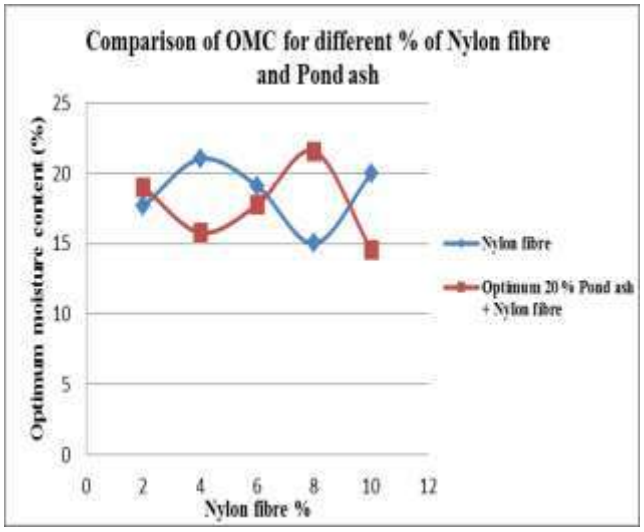

Fig 4; indicating the results for OMC for different % of Nylon fibre and Pond ash

From the above figures shows the addition 20% pond ash which gives the Maximum Dry Density 1.53g/cc for 18.2% of Optimum Water Content after this diminishing the dry density of rising of water content. Then addition of 6% of Nylon fibre into the black cotton soil gives the Maximum Dry Density 1.68g/cc for 19.10% of Optimum Water Content after this diminishing the dry density rising of water content. Combination of the addition of 20% of optimum pond ash with 4% of Nylon fibre gives the Maximum Dry Density 1.77g/cc for 15.8% of Optimum Water Content after this diminishing the dry density rising of water content. Combination of both Nylon fibre and optimum 20% of Pond ash which achieve the highest maximum dry density among all.

B.California bearing ratio test results:

Table 6: Showing the results of CBR test for variant percentage of Pond ash

POND ASH %	CBR VALUE 2.5 MM PENETRATION (%)	CBR VALUE 5 MM PENETRATION (%)
0	1.55	1.38
10	2.07	1.72
20	3.62	3.1
30	3.11	2.76
40	2.59	2.07

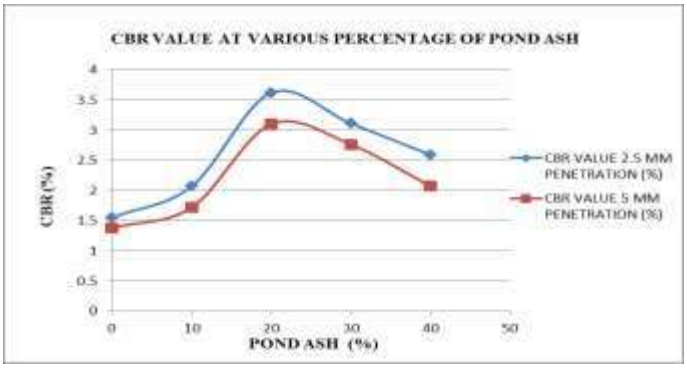

Fig 5; indicating the results of variant CBR value with variant percentage of pond ash

Fig 5; Display the addition of 20% of pond ash in soil gives highest value of CBR at 2.5 penetration is 3.62% and gives at 5mm penetration is 3.11% achieved as compared to other percentage of pond ash as taken.

Table 7: Showing the results of CBR test for variant percentage of Nylon fibre

FIBRE CONTENT %	CBR VALUE 2.5 MM PENETRATION (%)	CBR VALUE 5 MM PENETRATION (%)
0	1.55	1.38
2	2.59	2.42
4	3.62	3.11
6	4.66	3.8
8	4.14	3.45
10	3.11	2.76

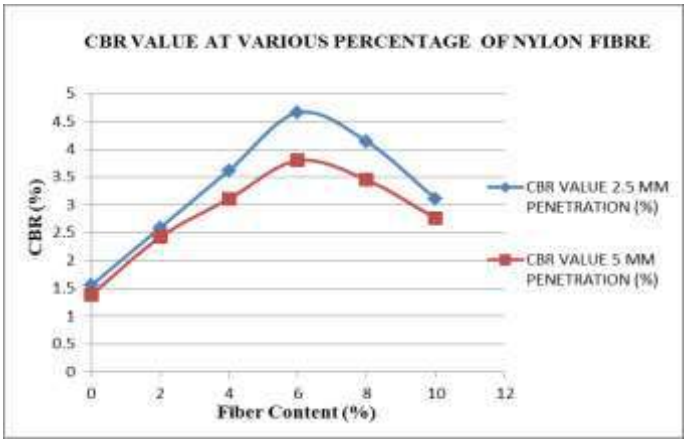

Fig 6; indicating the results of variant CBR value with variant percentage of Nylon fibre.

Fig 6; Display the addition of 6% of Nylon Fibre in soil gives the highest CBR value at 2.5 penetration is 4.66% and gives at 5mm penetration is 3.8% achieved as compared to other percentage of Nylon Fibre taken.

Table 8: Showing the results of CBR test for variant percentage of Nylon fibre

20% POND ASH + FIBRE CONTENT (%)	CBR VALUE 2.5 MM PENETRATION (%)	CBR VALUE 5 MM PENETRATION (%)
0	1.55	1.38
2	3.62	3.45
4	5.18	4.83
6	4.14	3.8
8	3.62	3.1
10	2.59	2.27

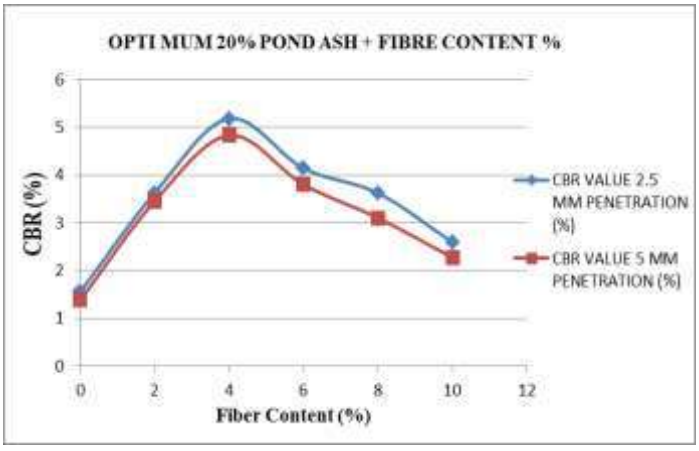

Fig 7; indicating the results of variant CBR value with variant percentage of Nylon fibre.

Fig 7; Display the addition of 6% of Nylon Fibre in soil gives the highest CBR value at 2.5 penetration is 4.66% and gives at 5mm penetration is 3.8% achieved as compared to other percentage of Nylon Fibre taken.

From the above figures shows when adding 20% of pond ash in soil gives highest value of CBR at 2.5 penetration is 3.62% and gives at 5mm penetration is 3.11% achieved as compared to other percentage of pond ash as taken. When adding the 6% of Nylon fibre in soil gives the highest CBR value at 2.5 penetration is 4.66% and gives at 5mm penetration is 3.8% achieved as compared to other percentage of Nylon fibre taken. Addition of 4% of Nylon Fibre with optimum 20 % Pond ash in soil gives the highest CBR value at 2.5 penetration is 5.18% and gives at 5mm penetration is 4.83% achieved as compared to other percentage of Nylon fibre taken. Combination of Nylon fibre and Pond ash which achieve highest CBR value among all.

4. CONCLUSIONS

The addition of Nylon fibre and Pond ash has impact the properties on index property & characteristics of BC soil. The conclusions drawn from these examinations are as per the following:-

- The CBR (unsoaked) estimation of the soil is 1.5 and after blending of ash pond in the soil, there is noteworthy change in CBR esteem. The pond ash of 20% addition raised the CBR esteem from 1.5 to 3.62, yet assist addition of pond ash caused diminish in CBR value. Thus, the optimum amount of pond ash i.e., after which the CBR esteem begins diminishing, is 20%.

- The BC soil is blended with nylon fibre at variant percentage as 2%,4%,6%,8% and 10%.the outcomes are acquired as below.

- When addition of 6% of nylon fibre content blended with soil, the most extreme esteem of CBR is accomplished which is 4.66. It is 3.1times more prominent than CBR estimation of soil.

- CBR (unsoaked) estimation blended soil increments up to 6% fibre content and after this esteem it begins diminishing.

- In this manner for the BC soil utilized as a part of the present investigation, Nylon Fibre content at 6% achieve greatest unsoaked CBR.

- The optimum amount of pond ash is blended with Nylon fibre at variant percentage of fibre in soil the outcomes acquired are.

- Addition of 4% of nylon fibre content with pond ash 20% in blended soil, the peak esteem of CBR is achieve which is 5.18. & it is 3.45 times more prominent than CBR estimation of soil.

- CBR (unsoaked) estimation of ash pond blended soil increments up to 4% fibre content and after this esteem it begins diminishing.

- In this manner for the BC soil utilized as a part of the present investigation, the ideal amount of pond ash and Nylon Fibre are 20 % and 4% respectively achieve greatest unsoaked CBR.

5. FUTURE SCOPE

In view of the examination did in this investigation, the extent of future work the scope for future work is distinguished and discussed as given below.

- Similarly laboratory facility studies might be taken up on various sorts of pond ash and fibre material.

- The present examination was done on Black cotton soil of low compressibility and ideal estimation of Nylon fibre and pond ash is computed.

- Additionally study might be taken up on other weak soils like silt and so on and different filaments might be utilized to study the impact of them on the properties of soils.

- Consolidated impact of different admixtures like lime, bitumen, chemicals and so forth with various sort of filaments can be considered.

REFERENCES

[1] Siddhartha Rokade and Rakesh Kumar (2017) "Effect of Inclusion of Fly-Ash and Nylon Fibre on Strength Characteristics of Black Cotton Soil" Electronic Journal of Geotechnical Engineering, 2017 (22.06), pp 1941-1950.

[2] Pallavi Mahta and Pradeep Singh (2016) Stabilization of Black Cotton Soil using Fly Ash and Nylon Fibre "International Research Journal of Engineering and Technology" Volume: 03 Issue:11, ISSN: 2395 -0056.

[3] Ghosh P. and Goel S. (2014) "Physical and Chemical Characterization of Pond Ash" International Journal of Environmental Research and Development. ISSN 22493131 Volume 4, Number 2 (2014), pp. 129-134.

[4] Sonawane P.G.,Dwivedi A.K. (2013) "Technical Properties of Pond Ash - Clay Fired Bricks – An Experimental Study" American Journal of Engineering Research (AJER) e-ISSN : 2320-0847 p-ISSN : 2320-0936 Volume-02, Issue-09, pp-110-117.

[5] Bhangale P.P, Nemade P.M (2013) "Study of Pond ASH (BTPS) Use as A Fine Aggregate in Cement Concrete - Case Study" (IJLTET) ,Vol. 2 Issue 2 March 2013.

[6] Patil B. M., Patil K. A. (2013) "Effect of Pond Ash and RBI Grade 81 on Properties of Subgrade Soil and Base Course of Flexible Pavement" World Academy of Science, Engineering and Technology International Journal of Civil, Architectural, Structural and Construction Engineering Vol:7 No:12, 2013 P.V.V.

[7] Bera A.K., Kumar A. (2010) "Effect of Pond Ash Content on Engineering Properties of Fine Grained Soil" Indian Geotechnical Conference–2010, Geo trendz December 16–18, 2010 IGS Mumbai Chapter & IIT Bombay.

[8] Bera A.K.,Ghosh A., Ghosh A. (2009) "Shear strength response of reinforced pond ash" Construction and Building Materials 23 (2009) 2386–2393.

[9] Sharan A. (2008) "Strength Characteristics of fibre reinforced compacted pond ash" Department of civil engineering, NIT Rourkela odisha.

International Research Journal of Engineering and Technology (IRJET) e-ISSN: 2395-0056
Volume: 07 Issue: 05 | May 2020 www.irjet.net p-ISSN: 2395-0072

Experimental Investigation on Fiber Reinforced Concrete by Addition of Steel Fibers and Glass Fiber

Salahuddin Shakeeb S.M[1], Syed Mohammed Isahqui[2], Sayyed Furqan Hussain[3], Mohammed Baseerullah[4], Syed Murtuza Ahmed[5]

[1]Assistant Professor, Department of Civil Engineering, NSAKCET, Hyderabad, Telangana, India
[2-5]BTECH student, Department of Civil Engineering, NSAKCET, Hyderabad, Telangana, India

---

Abstract – The purpose of this investigation is to find the usefulness of fiber reinforced concrete (FRC) in various civil engineering applications by addition of glass and steel fiber. Fiber reinforced concrete has so far been successfully used in slabs on grade, architectural panels, precast products, offshore structures, structures in seismic regions, thin and thick repairs, crash barriers, footings, hydraulic structures and many other applications. Fiber Reinforced Concrete (FRC) is gaining attention as an effective way to improve the performance of concrete. Fibers are currently being specified in tunneling, bridge decks, pavements, loading docks, thin unbounded overlays, concrete pads, and concretes slabs. These applications of fiber reinforced concrete are becoming increasingly popular and are exhibiting excellent performance. Fiber-reinforced concrete (FRC) is concrete containing fibrous material which increases its structural integrity. It contains short discrete fibers that are uniformly distributed and randomly oriented. Fibers include steel fibers, glass fibers, synthetic fibers and natural fibers this study presents understanding strength of fiber reinforced concrete. Mechanical properties and durability of fiber reinforced concrete.

Key Words: Fibre Reinforced Concrete, synthetic fibre, glass fibre, steel fibre….

1. INTRODUCTION

Concrete is a composite material containing hydraulic cement, water, coarse aggregate and fine aggregate. The resulting material is a stone-like structure which is formed by the chemical reaction of the cement and water. This stone like material is a brittle material which is strong in compression but very weak in tension. This weakness in the concrete makes it to crack under small loads, at the tensile end. These cracks gradually propagate to the compression end of the member and finally, the member breaks. The formation of cracks in the concrete may also occur due to the drying shrinkage. These cracks are basically micro cracks. These cracks increase in size and magnitude as the time elapses and they finally make the concrete to fail. The formation of cracks is the main reason for the failure of the concrete. To increase the tensile strength of concrete many attempts have been made. One of the successful and most commonly used method is providing steel reinforcement. Steel bars, however, reinforce concrete against local tension only. Cracks in reinforced concrete members extend freely until they encounter steel bars. Thus, need for multidirectional and closely spaced steel reinforcement arises. That cannot be practice call possible. Fiber reinforcement gives the solution to this problem so to increase the tensile strength of concrete, a technique of introduction of fibers in concrete is being used. These fibers act as crack arrestors and prevent the propagation of the cracks (glass, carbon, steel, natural, sisal. etc.)

1.1 Glass Reinforced Fibers

Glass fibers were first used to reinforce cement and concrete in Russia. However they were corroded by the highly alkaline Portland cement matrix. Therefore, alkali resistant glass fibers have been subsequently developed in UK and other countries.

Glass fibers are available in the form of continuous roving, chopped strand mats, Wool, ropes and woven fabric. Glass fibers coated with epoxy resin compounds have also been Tried out to protect them from alkali attack by Portland cement.

1.2 Steel Reinforced Fibers

During recent years, steel fiber reinforced concrete has gradually advanced from a new, rather unproven material to one which has now attained acknowledgment in numerous engineering applications. Lately it has become more frequent to substitute steel reinforcement with steel fiber reinforced concrete. The applications of steel fiber reinforced concrete have been varied and widespread, due to which it is difficult to categorize. The most common applications are tunnel linings, slabs, and airport pavements.

2. Objectives

The main objective of this experimental investigation is to study the performance of Steel & Glass Fiber in concrete under variable amplitude loading by varying the percentages of Steel & Glass fiber by the weight of coarse aggregates and cement respectively.

Experimental investigation include the basic tests carried out to check the physical properties of material used and properties of concrete in fresh state like Compaction factor

test, Slump test, Vee-Bee test. Testing on hardened concrete like compressive strength for cubes and split tensile for cylinders is carried out.

3. Physical Properties of Steel Fiber

Length of: Generally the length of the fiber is 30mm, the length of fibers were measured using steel ruler and 10 pieces were randomly chosen to find out the length of steel fiber.
Diameter: Filament diameter 14 microns. Steel fibers are pieces of steel wire from 0.3 to 1.1 mm in diameter
Cross-section: Round, flat, crescent, etc.
Deformations: Straight, wavy, end hook
Length 19-60 mm
Aspect Ratio (length/diameter): 30-100
Tensile strength: 345-1700 N/mm2
Young´s modulus: 205kN/mm2

4. Physical Properties of Glass Fiber

Length: Glass fibers of 10mm to 50mm in length and a few microns in diameter can be added up to 5% by weight and premixed with cement and water in a pan or a paddle mixer.
Material thickness: Typically range from 1/16"to 1/2".
Corner radius 1/8" or larger
Shrinkage: .002in/in
Young's Modulus: 51.7-86.9 GPa
Density: 2.11-2.72 g/cm^3

5. Results and Discussions

This chapter consists of two types of hardened concrete testing. They are compression test and tensile test. All the procedure used was according to the Indian Standard Code. Experiments were conducted on normal concrete and modified concrete by addition of steel & glass fiber with varying percentages of 0.5%, 1.5%, 1% & 2% by weight of cement

5.1 Compressive Strength

Compressive strength of concrete can be defined as the measured maximum resistance of a concrete to axial loading. Compression test is the most common test used to test the hardened concrete specimens because the testing is easy to make. The strength of the concrete specimens with different percentage of fibers can be indicating through the compression test.

Table -1: Compressive strength for 7 days

Specimen	W/C Ratio	% steel fiber	% glass fiber	Total % of fiber	Compressive Strength (7 days)
1.	0.5	0	0	0	8.76
2.	0.5	0.25	0.25	0.5	9.40
3.	0.5	0.5	0.5	1	10.51
4.	0.5	0.75	0.75	1.5	12.38
5.	0.5	1	1	2	11.2

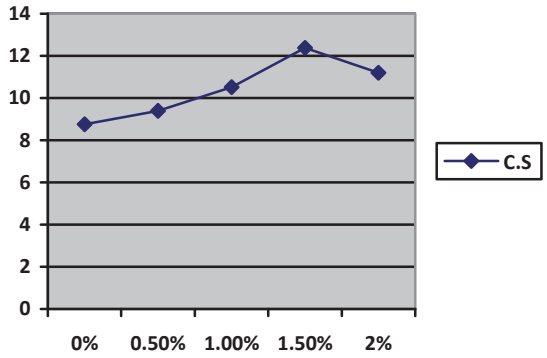

Chart -1: Compressive Strength

The value obtained for 1.5% and water cement ratio 0.5 yielded highest results for compressive strength. However, the compressive strength decreased on the increase in fiber addition. Therefore there is an optimum value of fiber to cement ratio, beyond which the compressive strength decreases. Hence 0.5 was taken as the optimum water cement ratio and optimum fiber.

Table 2- Compressive strength for 28 days.

Specimen	W/C Ratio	% of steel fiber	% of glass fiber	Total % of fiber	Compressive Strength (28 Days)
1.	0.5	0	0	0	9.5
2.	0.5	0.25	0.25	0.5	10.12
3.	0.5	0.5	0.5	1	16.85
4.	0.5	0.75	0.75	1.5	18.65
5.	0.5	1	1	2	16.9

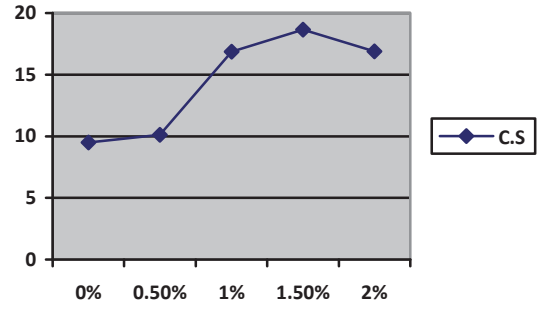

Chart 2: Compressive Strength

From the graph it is seen that when fibre content is increased there is an increase in tensile strength with a maximum at 1.5% fiber. However when the fiber content is increased beyond this value a downward slope of the graph is observed

5.2 Split Tensile Strength

Split tensile strength tests were conducted on standard cylinders of dimension 15cm diameter and 30cm depth, specimens each for plain concrete, Steel & glass fiber reinforced concrete were cast at varying percentages of RCA (0%, 0.5%, 1%, 1.5%, and 2%).For each case7 &28days strength values were obtained by loading under a compression testing machine.

Table 1: Split Tensile Strength for 7 days

Specimen	W/C Ratio	% of Steel fiber	% of Glass Fiber	Total % of Fiber	Tensile Strength (7 Days)
1.	0.5	0	0	0	2.131
2.	05	0.25	0.25	0.5	2.344
3.	0.5	0.5	0.5	1	2.557
4.	0.5	0.75	0.75	1.5	2.770
5.	0.5	1	1	2	2.599

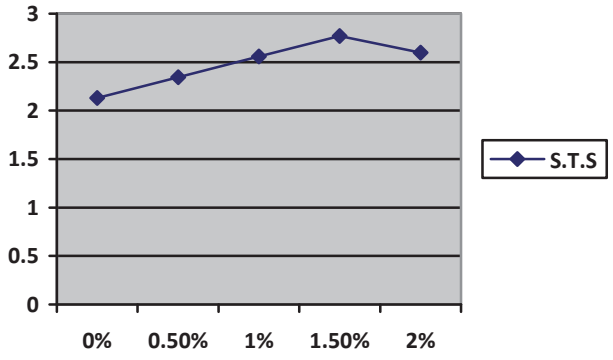

Chart 1: Split Tensile Strength

Table 2: Split Tensile Strength for 28 Days

Specimen	W/C Ratio	% of Steel Fiber	% of Glass Fiber	Total % of Fiber	Tensile Strength (28 days)
1.	0.5	0	0	0	2.15
2.	0.5	0.25	0.25	0.5	2.46
3.	0.5	0.5	0.5	1	2.62
4.	0.5	0.75	0.75	1.5	2.88
5.	0.5	1	1	2	2.93

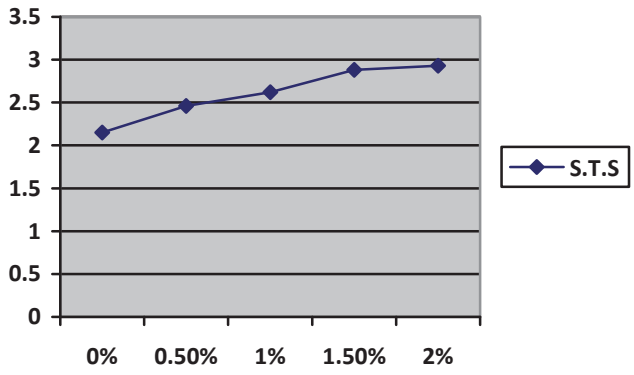

Chart 2: Split Tensile Strength

The value obtained for 2% addition of fiber and water cement ratio 0.5 yielded highest results for tensile strength. However, the tensile strength decreased on the increase in Fiber addition. Therefore there is an optimum value of Fiber to cement ratio, beyond which the tensile strength decreases. Hence 0.5 was taken as the optimum water cement ratio and optimum fiber content was taken as 2%.

3. CONCLUSIONS

Experimental works on the use of glass fibers and steel fibers have proven that good quality concrete could be produced with glass fibers and steel fibers. Based on the experimental investigation reported in the work, the Following conclusions are drawn:

- The workability of glass fibers and steel fiber concrete mix is satisfactory compare to natural aggregate, concrete mix with 2% steel fibers and 1% glass fibers has satisfied workable concrete.
- The glass fibers concrete has a convenient compressive strength and appreciable improvement in tensile strength, which means it, can be convenient for structural elements in concrete structures.
- Although glass fibers can be applied in the high strength concrete structure, but one issue must not be neglected as glass fibers with reduce water content would have low workability. Whenever glass fibers is used, water content in the concrete mix has to be monitored carefully.

ACKNOWLEDGEMENT

This research work was done under the distinguish guidance of our professor Salahuddin Shakeeb, and his mentorsh

REFERENCES

1. Some Properties of the Crushed Tile Concretes Exposed to Elevated – Journal of Construction and Building Materials, Vol. 25, pp. 1883 1689, 2011.

2. Journal of Construction and Building Materials, Vol. 25, pp. 4088 4094, 2011.
3. Rock material and cementing our future, 2005.
4. Blended Pastes of Cement and Quartz Powder under the Effect of - Journal of Construction and
Building Materials, Vol. 29, pp. 672 681, 2012.
5. Metakaolin Modified Cement Mortar with Quarry Dust as Fine in Civil Engineering (ACEE), pp. 54 59, 2010.
6. Manufacturing Technologies, Vol. 3, No. 1, 2009. Arundeb Gupta, Saroj Ma
7. ARPN Journal of Engineering and Applied Sciences, Vol.7, No. 1, pp. 100 107, 2012.
8. Aggregate Concrete Journal of Researchers in Engineering (E), Vol. XII, Issue III, Version I,2012. 203
9. Binu Sukumar, SrinivaRagavan, R., Chandrasekaran, E.and Sand) by Cru pp.186-192, 2003.
10. - Last Five Year Price Hike -8, 2012.
11. National Seminar (NSFCCE 2003) at S.R.M Engineering College, Kattankulathur, pp. 1.1 1.7, 2003.
12. International Conference on Building Education and Research (BEAR) -1341, 2008.

BIOGRAPHIES

SALAHUDDIN SHAKEEB S M[1]
received Diploma in Civil Engineering from HKE Polytechnic Raichur, Karnataka and B.E Civil Engineering degree from Government Engineering College Raichur, Karnataka, India, and M.Tech in Construction Technology from VTU Belgaum, Karnataka. He is presently working as Asst Prof in Civil Engineering Dept, Nawab Shah Alam Khan College of Engineering and technology, Hyderabad, Telangana, India

Syed Mohammed Ishaqui[2]
He is presently pursuing B.Tech in Civil Engineering from Nawab Shah Alam Khan College of Engineering and technology, Hyderabad, Telangana, India.

Sayyed Furqan Hussaain[3]
He is presently pursuing B.Tech in Civil Engineering from Nawab Shah Alam Khan College of Engineering and technology, Hyderabad, Telangana, India.

Mohammed Baseerullah[4]
He is presently pursuing B.Tech in Civil Engineering from Nawab Shah Alam Khan College of Engineering and technology, Hyderabad, Telangana, India.

Syed Murtuza Ahmed[5]
He is presently pursuing B.Tech in Civil Engineering from Nawab Shah Alam Khan College of Engineering and technology, Hyderabad, Telangana, India

Energy-efficient Expected Transmission Count protocol for WSN

S ANURADHA
Research Scholar,ECE
JNTUH
Hyderabad, India

Dr.D.Sreenivasa rao
Professor ,ECE
JNTUHCEH
Hyderabad, India

Abstract

The applications of wireless sensor networks comprise a wide variety of scenarios. In most of them, the network is composed of a significant number of nodes deployed in an extensive area in which not all nodes are directly connected. Then, the data exchange is supported by multihop communications. Routing protocols are in charge of discovering and maintaining the routes in the network. However, the appropriateness of a particular routing protocol mainly depends on the capabilities of the nodes and on the application requirements. This paper proposes an Energy-efficient expected transmission count protocol in WSNs, and a Route Optimization Technique (ROT) using expected transmission metric count in clustered WSNs among obstacles. ROT forms an energy-efficient path between the CHs and other members in clusters and CHs to the sink

Keywords: WSN, Cluster, ROT, ETX

1 Introduction

Wireless sensor network (WSN) consists of several tiny and low-power sensors which use radio frequencies to perform distributed sensing tasks. WSNs find their applications in many areas that include plant monitoring, battlefield surveillance, fire detection, and leakage of toxic chemicals, radiations, and gas detection [1]–[5]. In such WSNs, a large number of sensors are deployed in a field of interest (FoI) in stochastic manner. In stochastic deployment, sensors are usually dropped randomly in large numbers to guarantee reliability [1], [4], [6], [7].

Due to limited capacity of wireless communication media and lossy wireless links, it is extremely important to carefully select the route that can maximize the end-to-end throughput, especially in multi-hop wireless networks. a fundamental problem with existing wireless routing protocols is that minimizing the overall number (or time) of transmissions to deliver a single packet from a source node to a destination node does not necessarily maximize the end-to-end throughput. So we are going to propose a new routing protocol to increase high throughput in multi-hop wireless networks, to achieve high end-to-end throughput considering inter flow spatial reusability.

Minimising the energy consumed while ensuring the connectivity of a network is an important issue to be addressed in WSNs because the batteries powering the sensors may not be accessible for recharging often. Cluster-based routing in WSNs has been investigated by researchers to achieve the network scalability and management, which maximizes the lifetime of the network by using local collaboration among sensors [2]–[5], [8]–[10]. In a clustered WSN, every cluster has a cluster head (CH). CHs periodically collect, aggregate, and forward data to the sink.

We propose an Energy-efficient expected transmission count technique in WSNs, that selects the CHs to create a backbone to the network. EEETX is a distributed technique, where sensors are communicated to the CH in a distributed manner. We design Route Optimization Technique (ROT) using expected transmission metric count in clustered WSNs among obstacles. ROT forms an energy-efficient path between the CHs and other members in clusters and CHs to the sink, based on this process which it increases increase high throughput in multi-hop wireless networks, to achieve high end-to-end throughput considering inter flow spatial reusability.

2 ETX

The expected transmission count metric (ETX), which finds high-throughput paths on multi-hop wireless networks. ETX [11] minimizes the expected total number of packet transmissions (including retransmissions) required to successfully deliver a packet to the ultimate destination. The ETX metric incorporates the effects of link loss ratios, asymmetry in the loss ratios between the two directions of each link, and interference among the successive links of a path. In contrast, the minimum hop-count metric chooses arbitrarily among the different paths of the same minimum length, regardless of the often large differences in throughput among those paths, and ignoring the possibility that a longer path might offer higher throughput.

We can calculate ETX by using the following equation

$$\mathbf{ETX} = \frac{\mathbf{1}}{\mathbf{P_f} \times \mathbf{P_r}}$$

Where

P_f : Probability of a successful forward packet delivery ratio

Pr : Probability of a successful reverse acknowledgement delivery ratio

3 Energy-efficient Expected Transmission Count Protocol

In this paper, we design an Energy-efficient expected transmission count protocol (EEETX) for WSNs. This Protocol is the combination of three different schemes; one is for cluster formation in the entire network, cluster head selection, optimal multi-hop route selection, In the protocol, the entire network is divided into different circles, and clusters are formed within each circle. The cluster formation procedure presents the clustering process which is discussed in section 3.1, once the network was clustered, the cluster head selection process procedure was shown in 3.2, optimal route discovery process for data distribution was presented in 3.3.

3.1 Cluster Formation

A cluster is formed with fixed radius by choosing (either arbitrarily or with highest cooperating neighbor density within range of 2 hop distance) a node as center and randomly small distance as radius. Center of the new cluster is calculated as mean of the points within the zone whereas the radius is increased by the distance of two successive centers. The nodes then reply back and in this way clusters are formed which is shown in Fig (2).
It consist of the following parameters:

- Set of nodes $N_i = \{n_1, n_2, \ldots, n_{i-1}\}\{\}$
- A matrix of node (n_i and n_j)
- Random length r

Algorithm -1 Cluster formation

1) *First select a node n_i which is 2 hop distance apart from other participating node with a random length r_1.*
2) *Perform the cluster formation technique*

Do
$B=b_i$, $r=r_1$;
Draw a circle with b_i as center and r as radius
Compute new radius $r_1 = r + |b_i - b_j|$
While $b_i \neq b_j$
Cluster-1 is formed with all cooperating nodes lying within the circles.

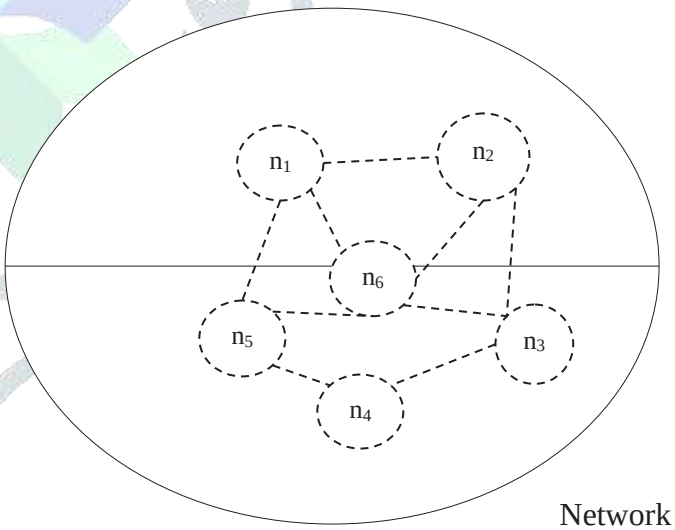

Fig 1: Cluster Formatic

3.2 Cluster Head Selection

A cluster head selection process computed all the nodes characteristics such as energy threshold, node degree (Number of neighbour nodes), node position, distance to the sink node, to elect a suitable cluster

head. To know each node characteristics, here we maintain node characteristics table, this table represents each node characteristics. Table-1 represents node characterstic table. The node energy status is measure as follows

Let consider each node status such as sensing, receiving, transmitting and idle status as $S = \{S_0, S_1, S_2, \ldots, S_n\}$

The state of node keeps changing during the process of data transmission or reception at time t_1. In time duration t_n, the probability that the node changes its state is denoted using Equation (1) [9]

$$P_{xy}^{n} = P\{S_n = y \mid S_0 = x\} \quad (1)$$

Where x and y represents two different stats

The node state probability P_{xy}^{n} is computed using the following equations:

$$P_{xy}^{n} = \sum_{z=0}^{n} P_{xz}^{(i)} P_{zy}^{(n-i)} \quad (2)$$

The probability of each node state in a same status is derives with the time duration T u using the equation (3)

$$TS = \sum_{t=1}^{T} P_{xy}^{n} \quad (3)$$

The energy dissipated in the subsequent time duration TS is estimated using Eq (4), which consider the four different node stats as sensing, transmission, receiving and idle.

$$E_d = \sum_{y=1}^{4} \left(\sum_{t=1}^{T} P_{xy}^{n} * E_y \right) \quad (4)$$

The remaining energy (RE_i) of each node (N_i) in the susbsequent time duration is measure as

$$REi = Eini - (Etx + Erx) \quad (5)$$

Where E_i = Initial energy of the node

E_{tx} & E_{rx} = energy utilized at the time of transmission and reception of data.

3.2.1 Node Degree

Each node have defined communication range, some of the nodes are placed at different positions, while choosing suitable cluster head its essential to consider number of neighbour nodes surrounded to the node. To determine node velocity, first we estimate the distance by using Euclidian distance function, this function contains distance across set of nodes in a cluster, in equation (6) we derive the each node distance, afterwards , the node degree threshold presents the threshold rate value to extract a neighbour nodes. The flowing equation (6) derives the node degree of each node.

$$D_{N_i} = \sum_{i=1}^{n-1} \sqrt{(X_i - X_{i-1})^2 + (Y_i - Y_{i-1})^2} \quad (6)$$

D_{N_i} represent distance of each node, X,Y represent each node coordinates. Based on the node distance from node to the sink node we determine the group of neighbour nodes

$$for\ i: 1\ to\ n$$
$$if\ \left(D_{N_i} \leq CR\right)$$
$$Add\ node\ i\ to\ neighbor\ set\ \{S_i\}$$
$$end\ if$$
$$end\ for$$

Where CR is communication range, S_i is neighbour set

Nodes	Energy Threshold	Neighbor nodes/ node Degree	Distance to Sink	Node position
A	RE_A	B,C,D,E,F / 5	D_A	(A_x, A_y)
B	RE_B	C,D,E,F,G / 5	D_B	(B_x, B_y)
C,	RE_C	E,F,G / 3	D_C	(C_x, C_y)
D	RE_D	E,G / 2	D_D	(D_x, D_y)
E	RE_E	B,C, / 2	D_E	(E_x, E_y)
F	RE_F	C,D,A /3	D_F	(F_x, F_y)
G	RE_G	E,F,C,D /4	D_G	(G_x, G_y)

Table 1: Node characteristics table

The CH selection derived based on the table-1 data, the following technique derives the CH selection process

Step 1: First, Initialize the parameters to 0 or null.

$CH_{cur} \leftarrow 0$

$CH_{prev} \leftarrow 0$

$Time_{prev} \leftarrow 0$

Curr () $\leftarrow 0$

Step 2: Calculate the Average Node character data based on the equations (5) (6)

$$CH_{i,j} = \sum_{i=1}^{n-1} P_E(i,j) + P_{Dist}(i, Sink) + P_{ND}(i)$$

P_E is energy probability, P_{Dist} distance probability, P_{ND} node degree proabability

Step 3: Compare the given condition to select CH

While ($Time_{prev}$_Curr () ≤ 1=true) do

CH_{prev} remains as Cluster Head

End while

Step 4: Compare Average node character data of previous and current Cluster Head

If $Avg(CH_{prev})=Avg(CH_{cur})$ and $Cost(CH_{prev})=Cost(CH_{cur})$

then

both CH_{prev} and CH_{cur} remains as cluster heads

Else

select new Cluster Head

Select new cluster head(s)

end if

3.3 Expected any-path transmissions metric (EATX)

The expected any-path transmissions metric EATX [12] for opportunistic any-path forwarding captures the expected number of transmissions between them under opportunistic forwarding and selection. Prioritization method based on EATX. Opportunistic routing that exploit the broadcast nature of wireless transmissions for selecting the best next-hop at that instant among a set of candidates are being actively explored.

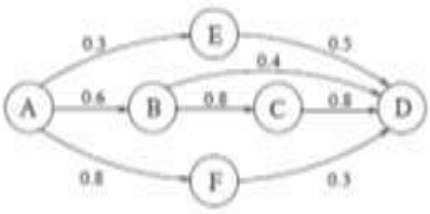

EATX metric was defined to reflect overall transmissions in any-path forwarding.

Figure 2: EATX estimation process

$$EATX = \frac{1+\sum_i EATX\left(A_i^{S,R},R\right)p_i\prod_{j=1}^{i-1}(1-p_i)}{1-\prod_i(1-pi)}$$

Where

S : Sender

R : Receiver

Metric	*A*	*B*	*C*	*D*	*E*	*F*
ETX	*4.17*	*2.50*	*1.25*	*0*	*2*	*3.33*
EATX	*3.24*	*1.82*	*1.25*	*0*	*2*	*3.33*

A_i : Adjacent set of links

P_i : Probability of link failure

j : is the set of links to be consider from the current Sender

3.3.1 Expected Transmission Count(ETX)

The goal of the metric is to choose a high-throughput path between a source and a destination. Our metric assigns weights to individual links based on the Expected Transmission Count (ETX) of a packet over the link. The ETX is a function of the loss rate and the bandwidth of the link. The individual link weights are combined into a path metric called Weighted Cumulative ETX (WCETX) that explicitly accounts for the interference among links that use the same channel. The WCETT metric is incorporated into a routing protocol that we call Multi-Radio Link-Quality Source Routing. The expected transmission time is a function of the loss rate and the bandwidth of the link.

ETX = ETX x [Packet size / Bandwidth]

Algorithm 2 :ETX Algorithm

INPUT : Paths (p'), cost of each link(ci).

OUTPUT : Path cost (C) and path P.

Step 1: Identify the set of path {pi'} from source to destination.

Step 2: Find the cost for the path(Ci').

Step 3: Find the set of non-interfering links (nil) in that path (p)

if nil = NULL

then path of the cost is C=min(Ci').

Step 4: From the set of non-interfering links find the maximum cost.

nil(c') = max{nil}

nil(c) =∑{nili}- nil(c')

then path cost is C=Ci'- nil(c).

Step 5: Compare the cost of all paths with the new cost C.

Step 6: The minimum cost C and path P.

4 Simulation Results

This section presents the performance evolution of energy efficient expected transmission count protocol for HWSN to determine the efficiency for various network scenarios and various energy rates, we configure multiple network models to achieve energy efficiency in Heterogenous WSN by configuring different energy rates to nodes, we measure the proposed model efficiency by considering various data rates. This section presents the comparative results between EEETX and a dynamic multipath routing algorithm (IDDR) [13]

4.1 Simulation Model and Parameters

We use Network Simulator Version-2 (NS2) to simulate our proposed protocol. In our simulation, the channel capacity of sensor nodes is set to the same value: 2 Mbps. We use the distributed coordination function (DCF) of IEEE 802.11 for wireless LANs as the MAC layer protocol. It has the functionality to notify the network layer about link breakage.

In our simulation, sensor nodes are deployed within the area of 1000 meter x 1000 meter region for 20 seconds simulation time. All nodes have the same communication range of 250 meters. Our simulation settings and parameters are summarized in table 2

No. of Nodes	50,100,150 and 200.
Area Size	1000 X 1000
Mac	802.11
Radio Range	250m
Simulation Time	20 sec
Traffic Source	CBR
Packet Size	512
Receiving Power	0.395
Sending power	0.660
Idle Power	0.035
Initial Energy	10.3 J
Rate	50,100,150,200 and 250Kb

Table 2: Simulation Settings

4.2 Performance Metrics

We evaluate mainly the performance according to the following metrics.

Average Packet Delivery Ratio: It is the ratio of the number .of packets received successfully and the total number of packets transmitted.

Average Throughput: It is the average number of packets reached at sink node at time instance

End-to-End Delay: It is the time taken by the packets to reach the receiver.

Energy Consumption: It is the amount of energy consumed by the nodes for the data transmission.

A. Based on Nodes

In our first experiment we vary the number of nodes as 50,100,150 and 200.

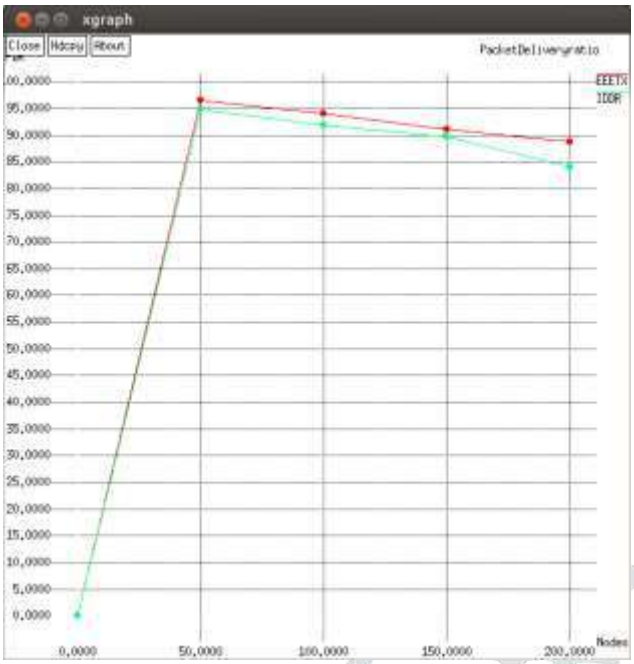

Fig 3: PDR : EEETX vs IDDR

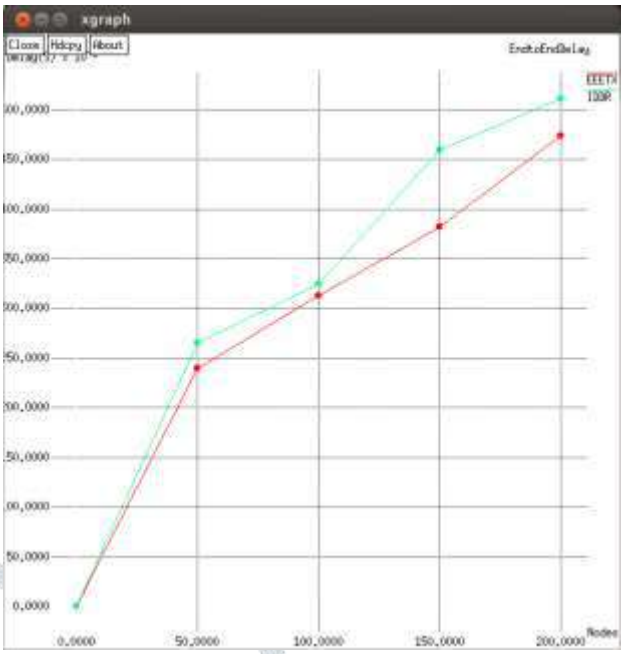

Fig 5: End-to-End Delay : EEETX vs IDDR

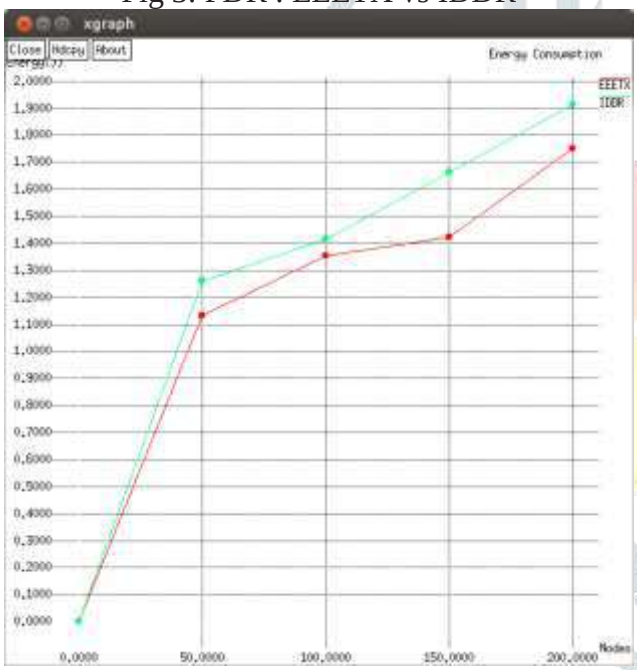

Fig 4: Energy Consumption : EEETX vs IDDR

Fig 6 : Avg Throughput: EEETX vs IDDR

From figure 3, we can see that the delivery ratio of our proposed EEETX is higher than the existing IDDR technique.

From figure 4, we can see that the energy consumption of our proposed EEETX is less than the existing IDDR technique.

From figure 5, we can see that the delay of our proposed EEETX is less than the existing IDDR technique.

From figure 6, we can see that the throughput ratio of our proposed EEETX is higher than the existing IDDR technique.

Conclusion

In this paper, we proposed an Energy-efficient expected transmission count protocol for WSN to meet the desired connectivity requirements. We mainly focused on energy-efficient for WSNs to prolong the lifetime of WSNs. We also proposed a technique to optimize the routing path among obstacles in clustered WSNs by designing Expected Transmission Count path mechanism. We simulated the performance of the proposed EEETX for different network scenarios and demonstrated that the energy consumption and average hop count in WSNs are reduced due to the clustering of sensors and optimization of routing path, hence the lifetime of WSNs is increased. The results demonstrated that the geometry and location of the obstacles should be considered to compute an optimized routing path

References

References

[1] J. H. Lee, T. Kwon, and J. Song, "Group connectivity model for
industrial wireless sensor networks," *IEEE Trans. Ind. Electron.*, vol. 57,
no. 5, pp. 1835–1844, May 2010.
[2] J.-S. Lee and W.-L. Cheng, "Fuzzy-logic-based clustering approach for
wireless sensor networks using energy predication," *IEEE Sensors J.*,
vol. 12, no. 9, pp. 2891–2897, Sep. 2012.
[3] Z. Ha, J. Wu, J. Zhang, L. Liu, and K. Tian, "A general self-organized
tree-based energy-balance routing protocol for wireless sensor network,"
IEEE Trans. Nucl. Sci., vol. 61, no. 2, pp. 732–740, Apr. 2014.
[4] D. C. Hoang, P. Yadav, R. Kumar, and S. Panda, "Real-time implementation
of a harmony search algorithm-based clustering protocol for
energy-efficient wireless sensor networks," *IEEE Trans. Ind. Informat.*,
vol. 10, no. 1, pp. 774–783, Feb. 2014.
[5] M. Tarhani, Y. S. Kavian, and S. Siavoshi, "SEECH: Scalable energy
efficient clustering hierarchy protocol in wireless sensor networks," *IEEE
Sensors J.*, vol. 14, no. 11, pp. 3944–3954, Nov. 2014.
[6] P. T. A. Quang and D.-S. Kim, "Enhancing real-time delivery of
gradient routing for industrial wireless sensor networks," *IEEE Trans.
Ind. Informat.*, vol. 8, no. 1, pp. 61–68, Feb. 2012.
[7] J. Niu, L. Cheng, Y. Gu, L. Shu, and S. K. Das, "R3E: Reliable reactive
routing enhancement for wireless sensor networks," *IEEE Trans. Ind.
Informat.*, vol. 10, no. 1, pp. 784–794, Feb. 2014.
[8] R. Xie and X. Jia, "Transmission-efficient clustering method for wireless
sensor networks using compressive sensing," *IEEE Trans. Parallel
Distrib. Syst.*, vol. 25, no. 3, pp. 806–815, Mar. 2014.
[9] H. Lu, J. Li, and M. Guizani, "Secure and efficient data transmission for
cluster-based wireless sensor networks," *IEEE Trans. Parallel Distrib.
Syst.*, vol. 25, no. 3, pp. 750–761, Mar. 2014.
[10] D. Wei, Y. Jin, S. Vural, K. Moessner, and R. Tafazolli, "An energyefficient
clustering solution for wireless sensor networks," *IEEE Trans.
Wireless Commun.*, vol. 10, no. 11, pp. 3973–3983, Nov. 2011.
[11] D. S. J. D. Couto, D. Aguayo, J. C. Bicket, and R. Morris, "A high-throughput path
metric for multi-hop wireless routing," in MOBICOM, 2003.
[12] S. Biswas and R. Morris, "Exor: opportunistic multi-hop routing for wireless
networks," in SIGCOMM, 2005.
[13] Jiao Zhang, Fengyuan Ren, Shan Gao, Hongkun Yang, and Chuang Lin, "Dynamic Routing for Data Integrity and Delay Differentiated Services in Wireless Sensor Networks", IEEE TRANSACTIONS ON MOBILE COMPUTING, VOL. 14, NO. 2, FEBRUARY 2015

QUERY PROCESSING & OPTIMIZATION TECHNIQUE FOR TEMPORAL DATABASES

[1]Mir Abid Ali, [2]Dr. Syed Abdul Sattar
[1]Research Scholar, Department of Computer Science Engineering, PP.COMP.SCI.0578, Rayalaseema University, A.P, India.
[2] Director, Research & Development, Nawab Shah Alam Khan College of Engineering & Technology, Hyderabad.

Abstract: Conventional relational systems are frequently incident for temporal query processing for new characteristics are not taken into concern. As an example, a temporal join often contains a conjunction of several inequalities involving only timestamps. With a conventional relational query processor, this type of query is processed using the nested-loop join algorithm, which may not be the most efficient method. This paper explains a stream processing approach for temporal query processing and improvement. Given appropriately arranged information, the usage of temporal joins and semi-joins as stream processors can be exceptionally powerful. We also talk over the tradeoffs between sort orders, the amount of local workspace and multiple scans over input streams; in particular, we are interested in the effect of sort ordering on the local workspace requirement. We present stream processing algorithms for various temporal joins and semi-joins, and their workspace requirements for various data sort orderings. Finally, we communicate how semantic query optimization can show a vital and natural role in optimization of temporal queries.

IndexTerms - Temporal query processing, temporal queries, temporal joins.

I. INTRODUCTION

Many real database applications intrinsically involve time-varying information. With the availability of cheap processing and storage units, there is a developing interest in temporal databases which store the evolving history of the "enterprise" of interest. Maximum studies on temporal databases can be roughly categorized into three areas [3]. The first is the formulation of the semantics of time [3, 9] and is closely related to research issues in knowledge representation. The second area concerns physical implementation issues [2, 3]; the focus is mainly on new access methods and data organization strategies. The third area is the logical modeling of temporal data [5]. Many of these studies emphasize distribute the relational data model to capture time semantics and to support relational temporal query languages. These extended models generally augment relations of the snapshot data model with several time attributes (such as ValidF'rom and ValidTo attributes [5]) which store the relevant timestamps. New temporal operators are also defined in these extended data models, based upon traditional relational algebraic operators [6], to allow users to query time attributes but not update them directly.

'This work was done under the Tangram Project, supported by DARPA contract F29601-87-C0072.

This paper explains the query processing and optimization for temporal databases, a topic which is seldom discussed in the literature (a notable exception is [8]). We observe that there are numerous interesting characteristics which are peculiar to temporal queries: (1) a temporal query often involves patterns of events; (2) a temporal query often contains a conjunction of several inequalities over the time domain and no equality conditions; and (3) temporal data is rich in semantics, and semantic query optimization is particularly desirable in the existence of a number of inequalities. These characteristics provide new opportunities for optimization. Ignoring these, as in conventional relational systems, can result in poor performance.

We discuss join and semijoin operations which are the most common and expensive computations in database systems. We introduce a stream processing approach which takes advantage of data ordering. As temporal data often has certain implicit ordering by time, the stream processing approach, as we demonstrate, is a good alternative. We should emphasize, however, that the stream processing algorithms that we present are merely additional strategies that a query optimizer should consider, and are by no means substitutes for traditional query processing methods.

The idea of stream processing has also appeared in [6]. These studies share the basic principle of the stream processing paradigm which is that input data should be in a certain order before the processing commences. This paper explanations are more concerned with (1) the impact of various data orderings on performance issues, mainly memory workspace requirements, and (2) efficient processing algorithms for join and semijoin operations. As we show, the optimal sort ordering for these temporal operators may depend on the statistics of data instances as well as the operator itself. [10] presents a more detailed comparison with related work which is omitted herein consideration of space limitations.

One might argue that stream processing algorithms are *not* useful when data are not sorted properly. With an abundant amount of main memory and processing cycles available, one can sort the input streams "on the fly" with marginal additional cost as assumed in [10]. The algorithms we describe would still be applicable although the streams are actually memory resident.
We informally discuss the role of semantic query optimization in Section 5, and finally, conclude with instructions for upcoming work.

2 IMPLEMENTATION AND CHALLENGES OF TEMPORAL DATABASE

Few out of every odd database requires a temporal database implementation, however, some do. We can enable you to begin. As examined in our past article, the SQL-2011 standard included clauses for the meaning of temporal tables as a component of the SQL/Foundation. In any case, this standard is new and not yet broadly adopted, For the time being, the majority of you should stretch out your current database tables to fuse temporal concepts. In this article, we'll concentrate on temporal tables. These tables are the building blocks of temporal databases.

Temporal Tables – The Important Theories

Theory #1: Valid-Time State Tables

From Wikipedia: "Valid time is the time period during which a reality is valid with respect to the real world." A valid time state table gives a chance to manage data whose values change over time. A valid time state table lets you manage data whose values change over time. For a sample, the interest rate on a loan can be 5% for the first year, and 6% for the second year. During the second year, you still want to know that the rate was 5% in the previous year.

Theory #2: Transaction-Time State Tables

Semantic query optimization has been discussed in the literature [8] but apparently has not been widely used in conventional systems. Semantic constraints in temporal databases occur more naturally and are more plentiful, and consequently, a query optimizer should profitably exploit the semantics. We will briefly discuss the role of semantic query optimization in temporal databases after discussing more basic query optimization issues.

The rest of the paper is structured as follows. Section 2 provides an outline of the temporal data model that we adopt from [6] and discusses the basic categories of temporal queries. We illustrate, in Section 3, the conventional approach to processing a complex temporal query. In the 4th Section, we discuss a stream processing approach for the implementation of temporal operators.

Theory #2: Transaction-Time State Tables

From Wikipedia: "Transaction time is the time period through which a fact deposited in the database is considered to be true." When you effectively catch the sequence of states for an evolving table, you have made a substantial transaction-time state table. The tables independent from anyone else now contain the expected data to return in time or to "rewind" to a specific minute and see the information that was substantial right then and there.

Theory #3: BiTemporal Tables

From Wikipedia: "Bitemporal data combines both Valid and Transaction Time." Valid-time state tables and transaction-time state tables are orthogonal. You don't have to implement both at once; you can do one or the other, and even if you do both, you don't have to keep the information in a single table. For example, it is common to find designs where the transaction information is stored in different tables. In such cases, only the latest valid information is stored in one table while the other table contains the historical records.

On the off chance that you choose to make a table both a valid-time and a transaction-time table, at that point, you have made a bitemporal table. Utilizing Snodgrass' words, "a bitemporal table permits a magnificent expressiveness while investigating and separating data" from

such tables. Step by step instructions to Implement a Temporal Table:

How to Implement a Temporal Table:

In the accompanying three areas, we quickly depict what you have to do with your tables to actualize a temporal database.

We will allude to the Hudson Foods hamburger review referenced in our first article. This is a precedent given in Richard Snodgrass' book, outlining an unmistakable instance of an association enduring noteworthy budgetary punishments because of not having a time-varying database. This model includes following dairy cattle between various pens, and how that information changes after some time. The data beneath is a super disentanglement of the model incorporated into Chapter 2 of the book.

In a feed yard, cattle are grouped into "lots". Cattle from one lot can be partitioned into numerous pens. We characterize a table LOT_LOC that tracks what number of cattle from each part live in each pen of each feed yard. cattle from each lot are moved from pen to pen, in this way the information is changing after some time.

LOT_LOC(LOT_ID_NUM, PEN_ID, HD_CNT, FROM_DATE, TO_DATE)

How about we center around two segments: FROM_DATE and TO_DATE.

These two columns render the table a "valid time state table": it records information valid at some time in the modeled reality, and it records states; that is, facts that are true over a period of time. The FROM_DATE and TO_DATE sections delimit the "valid time" or "period of validity" of the data in the line. A key idea in this structure is thinking about your "temporal granularity." You should pick the correct granularity for your concern. This could be days, hours, minutes, seconds, or whatever you require as a granularity level. For the past table, the granularity level is multi-day.

Think about the accompanying three lines:

(100, 3001, 32, 2014-06-01, 2014-06-02)

(100, 3001, 30, 2014-06-02, 9999-12-31)

(100, 3002, 02, 2014-06-02, 9999-12-31)

We can tell the accompanying from the information: from June first, 2014, to June second, 2014, there were 32 cows from part 100 in pen 3001; on June second, 2014, the cattle from lot 100 were part in two unique pens. Thirty cows stayed in pen 3001, and two cows were moved to pen 3002.
This is the latest valid data. The primary column is presently invalid for the current date. As should be obvious, we can proceed to include and change this information. It will be conceivable to question the information with the end goal that we see a real perspective of the information as it existed at a specific time. We could compose questions that would enable us to follow back every one of the pens containing cows from a specific lot before or on a specific date.

The Design Works, Be that as it may, it's entangled.

This plan would have understood Hudson Foods information issues and would have brought about a more engaged and lessened sustenance review. This plan idea can be utilized to execute temporal concepts into any standard database table. There are, nonetheless, difficulties to this plan, which we will talk about in the following article.

Few out of every odd database requires a temporal database implementation, yet some do. We can enable you to begin. As discussed in our past two articles, the SQL-2011 standard included conditions for the meaning of temporal tables as a feature of the SQL/Foundation. Be that as it may, this standard is new and not yet broadly embraced. For the present, the vast majority of you should stretch out your present database tables to consolidate temporal concepts. We have demonstrated to you that expanding your present database tables is moderately simple.

In this article, we'll concentrate on the difficulties in broadening your current tables into temporal tables, and why executing a genuine temporal database is less demanding.
The Challenges of Implementing a Temporal Table

Challenge-1
SQL comes up short on a time-range data type, so you need to utilize two diverse time columns to capture that data. As a result, both time columns must turn out to be a piece of the essential key, so they shouldn't be permitted to be NULL. (You could utilize NULL, yet in specific cases, you may get stuck in an unfortunate situation. For instance, read this blog: The Index You've Added is Useless. Why? To stay away from a NULL value, the TO_DATE was given a non-null value of 9999-12-31 for lines that are as of now legitimate in time.

Why a temporal database is less demanding - > temporal databases bolster a time-range data type. The presence of this time extends deliberation rearranges the structure. Contemplations, for example, the likelihood of a NULL in the from/to essential key column, are not any more pertinent.

Challenge-2
Without the FROM_DATE and TO_DATE columns, the essential keys would be LOT_ID_NUM and pen once you include the FROM_DATE and TO_DATE columns, the primary key must incorporate four columns: FROM_DATE, TO_DATE, LOT_ID_NUM, and PEN_ID. A same lot and pen could exist in various focuses in time; they are not anymore one of a kind for each line, and you have to incorporate the time run with the end goal to look after uniqueness. Characterizing the FROM_DATE and TO_DATE segments as a major aspect of the essential key is a test with non-temporal databases. In a non-temporal database, the semantic significance presently is something like "LOT_ID_NUM, PEN_ID, FROM_DATE, and TO_DATE are the exceptional identifiers".

Why a temporal database is less demanding - > A temporal database would enable you to characterize just LOT_ID_NUM and PEN_ID as the primary keys, which would have the semantic importance of "LOT_ID_NUM and PEN_ID are the remarkable identifiers at any minute in time."

Challenge -3
All inquiries must be time-mindful. Regardless of whether you just need to inquire the last substantial information in time, despite everything you need to add a WHERE clause to ensure you get only the most recent information. As a rule, every one of your inquiries will presently be somewhat more intricate (or much more unpredictable).

Why a temporal database is less demanding - >
On the off chance that you were utilizing a temporal database, your tables would follow time-varying legitimacy naturally. You would inquiry the most recent legitimate information (without a WHERE proviso) as a matter of course.

You additionally would gain admittance to other decent highlights, for example, "time breakpoints." For instance, you could set a breakpoint at 2012-12-01, and starting there on the entirety of your inquiries would be for information that was legitimate until 2012-12-01 just; for instance, "select the pens that contained cattle from part 55 preceding 2012-12-01". Your breakpoint could likewise be a period go like TIME_RANGE (2012-11-01, 2012-12-01); for instance, "select the pens that contained dairy cattle from part 55 between 2012-11-01 and 2012-12-01".

Challenge-4

Every one of your updates is currently more unpredictable. Each refresh now includes evolving (at least one) existing row(s) and making (at least one) new row(s).

Why a temporal database is easier

A temporal database will consequently guarantee that once a row is refreshed its earlier data isn't lost. In a temporal database, you are not by any stretch of the imagination refreshing columns yet rather changing their time legitimacy.

Challenge-5.

In a temporal table, you don't erase information. You change the time range with the end goal to demonstrate that the information isn't substantial any longer. On the off chance that distinctive clients and applications are getting to your tables, it is hard to control and check that everyone regards the presumptions for this table.

A temporal database will guarantee that all clients/applications executing inquiries against the "current valid time" will get precise outcomes. Invalid/erased information won't be returned.

A temporal database will naturally authorize the principles for a DELETE task to guarantee earlier information isn't lost, paying little heed to the customer.

3 TEMPORAL DATA MODEL

In our temporal data model, we consider time as a sequence of discrete, consecutive, equally-distanced points, i.e. Time = *{to, t l,. . .,* now} which are totally ordered. The sequence of time points can simply be treated as isomorphic *to* the natural numbers, and therefore we do not specify the time unit.

We adopt a modified version of the Time Sequence concept in [11]' as the basic data construct in our temporal data model. A temporal data value is a 4-tuple <S, V, ValidFrom, ValidTo>

Where S is the surrogate or the identity of the object, V is a time-varying attribute of concern, and [ValidFrom, ValidTo) represents the lifespan of the tuple. Naturally, within a tuple, the ValidFrom value is always smaller than the ValidTo value. Semantically, the object S has attribute value V during the period [ValidFrom, ValidTo)2. A temporal relation is a set of temporal data values (i.e. a set of 4-tuples).

An example of a temporal relation is Faculty (Name, Rank, ValidFrom, ValidTo) Together with the following integrity constraints

and assumptions, this example is used in subsequent sections for illustration purposes. The name is the identity of a faculty member. For attribute Rank, we consider only three different ranks - 'Assistant', 'Associate' and 'Full'.

We will assume in this example that an assistant professor can be promoted only to an associate professor and then to full professor. In other words, there is a chronological ordering among the data values that the Rank attribute can assume. For the same faculty member, e.g. "Smith" as illustrated in Figure 1, UValidTol<ValidFrom2" and "ValidTozSValidRoms" must hold. The period [ValidFrom, ValidTo) in a tuple is the time during which the faculty member holds the indicated rank. We also assume that a faculty member is at exactly one rank at any time between becoming an assistant

professor and termination as a full professor. As we mentioned above, for any tuple t, "t.ValidFrom<t.ValidTo" always holds.

Smith	Assistant	$ValidFrom_1$	$ValidTo_1$
Smith	Associate	$ValidFrom_2$	$ValidTo_2$
Smith	Full	$ValidFrom_3$	$ValidTo_3$

Fig-1. A Sample Faculty Relation

'A Time Sequence is a totally ordered sequence of temporal data values <Surrogate, Attribute-value, Time>. For continuous Time Sequence, the attribute due of an object between any two-time points (i.e. between consecutive temporal data values) can be computed using an interpolation function.'We consider only the valid times in TQuel temporal database taxonomy [7]. Also, for simplicity, we often use TS (which stands for Time Start) to abbreviate ValidFrom, and TE (which stands for Time End) to abbreviate ValidTo. A stepwise-constant interpolation function is applied between the lime points ValidFrom and ValidTo. V can be generated as a list of attributes.'Borrowed from 1321. Also, the relation is in TNF

4 CONVENTIONAL APPROACHES

In this section, we describe the deficiencies of conventional relational database systems in processing temporal queries. Allen [3] presents thirteen elementary temporal operators of time-intervals which are listed in Figure 2. These temporal operators are actually just syntactic sugar for the query-specific constraints which are given in the right-hand column of Figure 2 and can be easily incorporated into query languages like SQL and Quel.

Temporal queries using these extended constructs are usually processed in the following way. First, they are translated into equivalent queries in a relational language such as Quel. The translated queries are then optimized and processed by conventional relational query processors. This approach is generally not effective for temporal query processing as we demonstrate below.

Suppose we have a relation Faculty (Name, Rank, ValidFrom, ValidTo) as described in the previous section. Consider the following
Quel query modified from [3214: *Superstar - Who got* promoted from assistant to full professor while at least one other faculty remained at the associate rank?

```
        Range of fl is Faculty
        Range of f2 is Faculty
        Range of f3 is Faculty
 Retrieve into Stars (Name=fl.Name,ValidRom=fl.ValidFrom,
                ValidTo=B.ValidTo)
        Where fl.Name=B.Name and f3.Rank="Associate"
        And fl.Rank="Assistant" and f2.Rank="Full"
        And (fl overlap f3) and (f2 overlap f3)'
```

These "overlap" operators can be translated directly into equivalent
Clauses (e.g. in Quel) involving inequalities. That is,

```
(fl overlap f3) = fl.ValidFkom<f3.ValidTo
                  ^fJ.ValidFrom<fl.ValidTo
(0 overlap f3) = f2.ValidFrom<f3.ValidTo
                  ^f3.ValidFrom<f?.ValidTo
```

'The original TQuel query in is:
The range of fl is Faculty
The range of f2 is Faculty
Range of a is Associate
Retrieve into Stars(Name=fl.Name) Valid from beginning of fl to begin of E!
Where fl.Named2.Name When (fl overlap a) and (f2 overlap a)
and fl.Rank="Assistant" and f2.Rank="Full" 'This overlap operator defined in [11] is different from "overlaps" in [3]; it is defined in a general sense and therefore it may also mean the "equal", "start", "finishes" or "during" relationships in Figure 2. For the sake of exposition, we follow [11].

Temporal Operators	Time axis →	Explicit Constraints
(1) X equal Y	xxxx yyyy	X.TS=Y.TS∧X.TE=Y.TE
(2) X meets Y	xxxyyy	X.TE=Y.TS
(3) X starts Y	xxxx yyyyyyy	X.TS=Y.TS∧X.TE<Y.TE
(4) X finishes Y	xxxx yyyyyyy	X.TE=Y.TE∧X.TS>Y.TS
(5) X during Y	xxxx yyyyyyy	X.TS>Y.TS∧X.TE<Y.TE
(6) X overlaps Y	xxxx yyyy	X.TS<Y.TS∧X.TE>Y.TS ∧X.TE<Y.TE
(7) X before Y	xxx yyy	X.TE<Y.TS

TS ≡ ValidFrom, TE ≡ ValidTo
Integrity Constraints: X.TS<X.TE ∧ Y.TS<Y.TE

Figure-2 The 13 possible temporal relationships

The corresponding relational algebra expression for the Superstar query is:

$$\pi_L(\sigma_\theta(\text{Faculty}_{f1} \times \text{Faculty}_{f2} \times \text{Faculty}_{f3}))$$

where L is f1.Name, f1.ValidFrom, f2.ValidTo
θ is f1.Name=f2.Name ∧ f1.Rank="Assistant"
∧ f2.Rank="Full" ∧ f3.Rank="Associate" ∧ θ'
θ' is f1.ValidFrom<f3.ValidTo ∧ f3.ValidFrom<f1.ValidTo
∧ f2.ValidFrom<f3.ValidTo ∧ f3.ValidFrom<f2.ValidTo

This algebraic expression can be represented as a parse tree[9], as depicted in Figure 3(a). The parse tree can then ameliorated by applying well-known traditional algebraic manipulation methods, e.g. the selections and projection are pushed as far down the parse tree as possible(see Figure 3(b)).

There are several interesting observations about the "conventionally optimized" parse tree in Figure 3(b):

1. There are three references to the Faculty relation in the parse tree implying that it is joined with itself twice conventional systems would scan the relation several times. If we view the query as a "Superstar" pattern matching in the Faculty relation, one might wonder if we are able to answer this query with only a single scan of the relation. Roughly speaking, we are looking for a pattern composed of three-tuples - an assistant professor, a full professor and an associate professor. That is, instead of performing multiple joins, a single scan might be possible by recognizing this query qualification as describing a pattern in the data.

2. The first join in the parse tree can be efficiently implemented as an equi-join using a conventional approach such as nested-loop join, merge join or hash join. The second join, a scaled less-than join, is a Cartesian product charted by a selection with the condition being a conjunction of inequality predicates - 6' '. Traditionally, the best strategy for processing less-than joins appears to be the
'Note that range search (e.g. salary > 10K and salary < 20K) is different
from this form of query qualification.

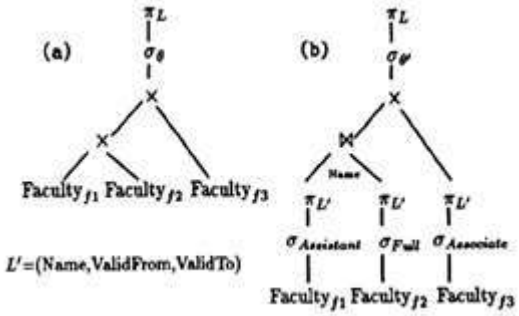

Figure-3 (a) Parse tree for the superstar expression (b) its optimized version

Conventional nested-loop join method. With only a single inequality as the join condition, we have no optimal but the nested-loop join method. Since time points are totally ordered and the join condition is a concurrence of several inequalities over time domain, one might wonder if there are any more efficient processing alternatives. In the past, little courtesy has been given to this form of qualification because: in traditional database applications, queries seldom contain less-than joins, and when inequalities do occur, in most situations the join condition has d y a single inequality predicate; for example, in an Employee/Department database, we might want to retrieve employees who earn more than their manager. The situation is quite different when we consider temporal databases: less-than joins appear more frequently and naturally because temporal queries often involve patterns of events, and therefore less-than joins need to be *ex*plicitly considered in query optimization, the join condition often contains a conjunction of several Inequality predicates which further indicates that optimization might be possible. Recall that there is an integrity constraint in the Faculty relation: a chronological ordering of data dues – 'Assistant', 'Associate' and 'Full'. This ordering implies that being an assistant professor must occur before being promoted to a full professor i.e. "fl.ValidTo<f2.ValidFrom" always holds in the presence of (fl.Name=D.Name).

These constraints, together with the "intra-tuple" integrity constraints,

$$fi.ValidFrom<fi.ValidTo \text{ for } i=1,2,3$$

imply "fl.ValidTo<f2.ValidFrom" and "f3.ValidFrom< f2. ValidTo". Therefore these inequalities in 6' are redundant i.e. they are subsumed by other inequalities. The important point is not so much this particular case; rather it is the process of semantic query optimization each department: emp is the employee, $dept_h$ is the department that the employee works with, salary is the employee's salary

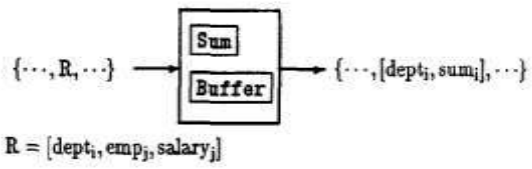

Figure 4: A stream processor to sum all employees' salaries in

The above Observations suggest that, in addition to traditional set-oriented relational operators, we may need other alto process temporal queries. In subsequent sections, we will present and discuss a number of such alternatives.

4 STREAM PROCESSING APPROACH

We discuss a stream processing approach for temporal query processing in this section. Algorithms that implement temporal operators are presented. The tradeoffs between sort orders, the amount of indigenous workspace and multiple passes over input streams are discussed. For properly sorted streams of tuples, we show that temporal operators can often be carried out with a single pass of input streams and the amount of workspace required can be small.

4.1 What is stream processing?

Abstractly, a *stream* can be demarcated as an ordered arrangement of data objects [1,10]. Stream processing resembles the notion of data flow processing in database systems [4,7]. A classic example of stream processing is the merge-join; it is efficiently executed and the sort ordering of its output can be utilized by subsequent operations [10].
There are several intrinsic characteristic s of stream processing in database systems. First, a computation on a stream has access only to one element at a time and only in the specified ordering of the stream. Second, the implementation of a function as a stream processor may keep some local state information in order to avoid multiple readings of streams. The state information represents a summary of the history of a computation on the portion of a stream that has been read so far; the state may be composed of copies of some objects or some summary information of the objects previously read (e.g. sum, min, count etc.) Using the local state information, the implementation of a stream processor can be expressed in terms of functions on the individual objects at the head of each input stream and the current state. For example, a simple stream processor, which is depicted in Figure 4, lists all the departments and computes the total salaries of all employees in each department. The point here is that the state contains summary information (i.e. the partial sum), and the function (i.e. sum) is expressed in terms of the current state and an input object.
Third, there are often tradeoffs among the following factors:
(1) The minimal size of the local workspace which depends on the function itself and the statistics of a specific instance of the data stream,
(2) Sort order of input streams, and
(3) Multiple passes over input streams.

Very often stream processing requires input streams to be properly sorted in order to perform the computation while only reading the input streams once. In addition, the sort orderings of input streams greatly affect the size of local workspace required. Conversely, suppose there is enough local workspace to keep all data objects. Then only a single pass over the input streams is required and (theoretically) the sort ordering would not be important. In the next section, we discuss the application of stream processing algorithms to temporal databases. In these discussions, the sort ordering of streams plays a major role.

4.2 Sort Orderings

Suppose we have temporal relations X(S, V,TS,TE)7 and Y(S,V, TS,TE). We are interested in the effect of various sort orderings on the efficiency with which it is possible to implement the temporal operators (listed in Figure 2) in the stream processing paradigm. Because of space limitation, we concentrate on the "during" relationship which has only inequalities in its explicit constraints? The implementation of Overlap and before operators in the stream processing paradigm are discussed in [16]. Before we proceed, we should note that the temporal operators listed in Figure 2 are in fact join and semi join operations. Because of this, the only form of state information we need consider in subsets of the tuples previously read and not any summary information such as sum, min, etc.

4.2.1 Contain-join(X ,*Y*)

Contain-join(X,Y) outputs the concatenation of tuples X and Y if the lifespan of X contains that of Y; that is, "X.ValidFrom < Y.ValidFrom *h* Y.ValidTo<X.ValidTo" - i.e. the "during" relationship in Figure 2. The generic algorithm for Contain-join(X,Y) is shown in Figure *5*. The specific instance of this generic algorithm depends on the sort orderings of streams. In this paper, we present the Contain-join algorithm in more detail for the case when both relations X and Y are sorted on the attribute ValidFrom in ascending order (see Figure 6(a)). The following conventions and notations are used in the algorithm:

(1) there is
an input buffer for reading tuples from each stream (denoted
as <Buffer-x, Buffer-y>), and the tuples in these buffers are denoted as Xb and Yb respectively;
(2) the expected difference
between ValidFrom values of two consecutive X tuples is *r*, (similarly, *RV* for Y tuples), and
(3) *2* denotes the absolute value of
the difference between yb.validFrom and xb.ValidFrom.

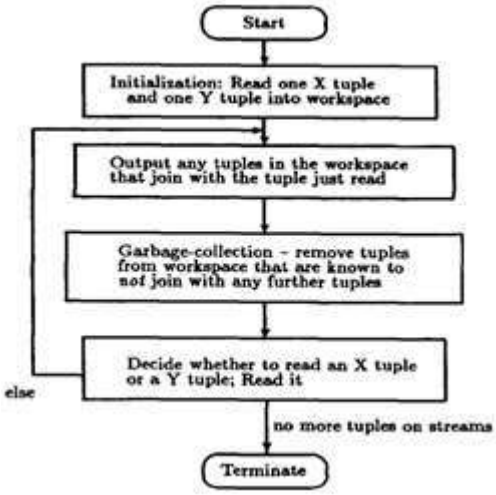

Figure-5 Generic Join Algorithm

'Recall that TS and TE stand for ValidFrom and ValidTo respectively. 'For a temporal operator with equality predicate(s), an obvious stream processing method appears to be sorting both relations on attributes that are involved in the equalities followed by a conventional merge-join (and perhaps combined with filtering using other predicates of the operator.)

Contain-join(X,Y): [9]

1 Initially the first tuple from each stream is read and stored in the buffer.

2 Join phase: Output any tuples in the workspace (i.e. the state) that join with the tuple just read. Note that additional housekeeping must be done for maintaining the output sort ordering.

3 Garbage-collection phase: discard X tuples in the state if "X.ValidTo<y_b.ValidFrom". Also discard Y tuples if "Y.ValidFrom<x_b.ValidFrom". The garbage-collection conditions must guarantee that the Y (and X respectively) tuples being discarded do not satisfy the join condition with any subsequent X (and Y respectively) tuples.

4 Read phase: Copy the previously read tuple(s) into the workspace as state tuple(s). There are two different situations in deciding which stream of tuples is to be read. The first case is when "y_b.ValidFrom<x_b.ValidFrom" as shown in Figure 6(b). As all Y tuples read so far do not join with x_b, clearly the optimal step is to read the next Y tuple.

The second case is when "y_b.ValidFrom≥x_b.ValidFrom" as shown in Figure 6(c). The workspace contains
(1) X tuples whose lifespan span y_b.ValidFrom and
(2) Y tuples whose ValidFrom value is in region I.
A possible heuristic to decide whether to read the next X tuple or Y tuple is presented below.

5 The algorithm terminates if either stream has been exhausted and there is no corresponding state tuple. Otherwise, go to Step 2.

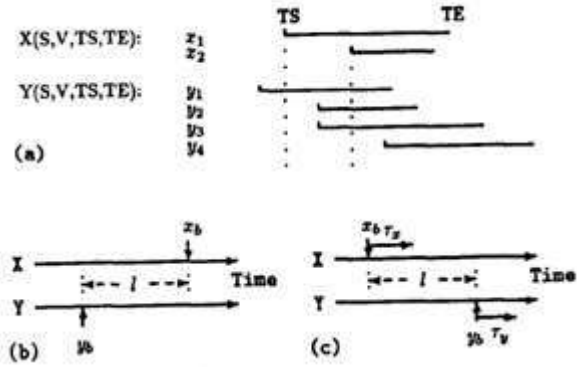

Figure-6 Contain-join: Both X and Y are sorted on TS in ascending order (only time attributes are shown)

The heuristic algorithm which can be used to decide whether to read an X tuple or a Y tuple is as follows. If the next X tuple is read, the expected ValidFrom due is Zb.ValidFrom+r_x. The number of Y tuples that would be garbage-collected *can* be estimated as the number of Y tuples in the workspace with ValidFrom value in the interval [za.ValidRom, Zb.ValidFrom+r_x. If the next Y tuple is read, the expected ValidFrom value is yb.ValidFrom+t_y. The number of disposable X tuples can be estimated as the number of X tuples in the workspace with ValidTo value in the interval [ya.ValidRom, by.ValidFrom+t_y]. Based on these two estimations, a decision is made on which would yield a greater reduction in the number of tuples in the workspace. Using this heuristic, the state (i.e. workspace contents) can be characterized as follows: (1) if we keep reading X tuples such
that all Y tuples in the state have been garbage-collected, the maximal set of X tuples that are required consists of all X tuples that span the time instant ya.ValidFrom. (2) conversely, if we keep reading Y tuples such that there is no X state tuple, the maximal set of Y state tuples that is required consists of those whose ValidFrom value lies in the lifespan of Zb.

We now summarize the state information requirements of processing the Contain-join for other sort orderings in Table 1. The algorithm for the case (b), i.e. when the relation X is sorted on ValidFrom and the relation Y is sorted on ValidTo, is similar to the one presented above (readers may refer to 1161 for details). Note that (1) it is generally inappropriate to have one relation sorted in ascending order and the other in descending order. (2) sorting both relations X and Y on attribute ValidTo in descending order would have the same effect as sorting them on attribute ValidFrom in ascending order because of symmetry
(although the ValidFrom and ValidTo attributes exchange their roles); the lower half of Table 1 is, therefore, the mirror image *of* the upper half.

Table-1 Effect of various sort orders on Contain-join, Contain-semijoin & Contained- semijoin

Sort Orders X		Sort Orders Y		Contain-join(X,Y)	Contain-semijoin(X,Y)	Contained-semijoin(X,Y)
TS	↑	TS	↑	(a)	(c)	(c)
TS	↓	TS	↓	-	-	-
TS	↑	TE	↑	(b)	(d)	-
TS	↓	TE	↓	-	-	(d)
TE	↑	TS	↑	-	-	(d)
TE	↓	TS	↓	(b)	(d)	-
TE	↑	TE	↑	-	-	-
TE	↓	TE	↓	(a)	(c)	(c)

↑ Sorting the corresponding attribute in ascending order.

↓ Sorting the corresponding attribute in descending order.

\- The sort ordering is not appropriate for stream processing – no garbage-collection criteria.

(a) state = {X tuples whose lifespan span y_b.TS} ∪ {Y tuples whose TS value lie in region *l*}

(b) state = {X tuples whose lifespan span y_b.TE} ∪ {Y tuples whose lifespans are contained within region *l*}

(c) state ⊆ {X tuples whose lifespan span x_b.TS} ∪ {Y tuples whose TS values lie in region *l*}

(d) local workspace = <Buffer-x, Buffer-y>.

4.2.2 Contained- & Contain-semijoin(X,Y)"

Contain-semijoin(X, Y) is defined as {x I x belongs to X and 3 y belong to Y s.t. 2's lifespan contains y's lifespan}. Contained-semijoin(X, Y) is
defined as {z I z EX and 3 y E Y s.t. 2's lifespan is contained in y's lifespan}. In a later section, we show that Contained-semijoin may be used to efficiently process the Superstar query.

For semijoins, a stream processor can output a tuple as soon as it finds the first matching tuple. Based on this observation, we devise an optimized algorithm which requires just one buffer for each input stream. Suppose the relation X is sorted on attribute ValidFrom and the relation Y is sorted on ValidTo in ascending order as shown in Figure 7. The Contain-semijoin(X, Y) algorithm for this sort order is as follows.
'The separation of this join algorithm into several phases is primarily for the sake of explanation; it is possible that Steps 2, 3 and 4 can be combined
together to gain better performance.

Figure-7 Contain-semi joins: X is sorted on TS and Y is on TE in ascending order

Contain-semijoin(X,Y):

Contain-semijoin(X,Y):

Repeat the following steps until one stream of tuples is exhausted. Suppose we have x_b and y_b tuples in the workspace. Then, one of the following conditions must hold:

- "x_b.ValidFrom<y_b.ValidFrom ∧ y_b.ValidTo<x_b.ValidTo" — i.e. x_b and y_b satisfy the semijoin condition, or
- "x_b.ValidFrom≥y_b.ValidFrom"[11], or
- "y_b.ValidTo≥x_b.ValidTo".

If the semijoin condition is satisfied, x_b is output and the next X tuple is read. If "x_b.ValidFrom≥y_b.ValidFrom" holds, the next Y tuple should be read because y_b cannot be contained in further X tuples. On the other hand, if "y_b.ValidTo≥x_b.ValidTo" holds the next X tuple should be read because x_b cannot be joined with further Y tuples.

It can be easily verified that only one tuple from each stream needs to be in the workspace. For example, in Figure 7, when x_1 is fetched, the local workspace contains <x_1, y_2> and for x_2 it is <x_2, y_4>.

It should be mentioned that the above algorithm can be applied to Contained-semi join(Y, X) for the same sort ordering with a slight modification - when the semi join condition is satisfied, yb is output and the next Y tuple is read. For other sort orderings (e.g. both streams are sorted on ValidFrom), we list the local workspace requirements in Table 1. We note that for Contain-semijoin(X, X) and Contained-semijoin(X, X), the stream of tuples may be scanned twice if we apply the semijoin algorithm presented above. To avoid this kind of inefficiency, we, therefore, devise a more efficient algorithm which scans the stream only once provided that it is sorted properly. As an example, suppose the relation X has primary sort ordering on the attribute ValidFrom and secondary sort ordering on ValidTo in ascending order. The algorithm for Contained-semijoin(X, X) is as follows.

Contained-semijoin(X,X):

1 Read the first tuple from the stream and store it as the state tuple (denoted by x_s).

2 Read the next X tuple (x_b) and do :

if "x_s.ValidFrom=x_b.ValidFrom", replace x_s with x_b as the state tuple
else (i.e. "x_s.ValidFrom<x_b.ValidFrom")
if "x_s.ValidTo≤x_b.ValidTo", replace x_s with x_b as the state tuple
else (i.e. x_b's lifespan is contained within that of x_s) x_b is output
and x_s remains as the state tuple.

3 Repeat Step 2 until all tuples have been read.

"It does not matter what the relationship between ZB.ValidTo and yb.ValidTo is.

It is interesting to consider using a semijoin algorithm as a preprocessor for a join operation. Intuitively, the advantages are: (1) the output stream from a semijoin operation has the same sort ordering as the input stream - *&-preserving;* (2) with proper sort orderings, the semijoin algorithms scan input streams only once, and a number of "dangling" tuples may be eliminated, which may reduce the size of workspace to join operations.

5 SEMANTIC QUERY OPTIMIZATION

Semantic query optimization techniques have been introduced and shown to be potentially useful in many studies [8]. However, the technique has not been widely used in conventional systems. The reason, we speculate, might be that conventional application domains ax seldom rich enough in semantics, i.e. they contain only a few useful semantic constraints which the query optimizer can profitably exploit.

For temporal databases, time is unarguably rich in semantics and many temporal semantic properties/constraints do occur naturally. It is, therefore, our belief that, unlike conventional applications, semantic query optimization can play a significant role in temporal databases. In this section, we discuss informally the significance of semantic query Optimization in temporal query processing; its formal treatment is now underway. Earlier we mentioned an interesting integrity constraint in the Faculty relation, namely the chronological ordering of data values which the attribute Rank can assume - 'Assistant', 'Associate' and 'FUI'.

For every faculty, being an assistant professor must occur before being promoted to an associate professor, which must then occur before becoming a full professor. There are two consequences if the database system does not capture and use this constraint. First, and most important, the optimizer would not be able to recognize that the less-than join in the Superstar example is, in fact, a Contained-semijoin. The less-than join operation shown in Figure 3(b) can be described pictorially using Figure 8. The equi-join on "fl.Name=fL.The name" (in Figure 3(b)) concatenates those fl and f2 tuples corresponding

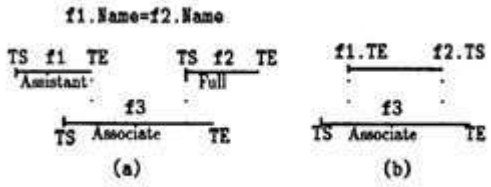

Figure-8 (a) The less-than join in the superstar query, and (b) its equivalent contained-semijoin condition after sematic optimisation

to those assistant professors promoted to full professors. The less than join then selects those fl and f2 tuple pairs which satisfy the less-than join condition *(0')* as shown in Figure 8(a). With the above semantic constraint, it is not " It to see that fl.ValidFrom<B.ValidTo and B.ValidFiom<f2.ValidTo is redundant and the less-than join condition *can* be reduced to a Contained-semijoin condition as shown in Figure 8(b). Being able to recognize a Contained-semijoin allows the database system to make use of sort orderings and therefore the stream
processing techniques mentioned in the previous section. The second consequence of the constraint on the Rank attribute is that we are able to eliminate two redundant inequalities in *0';* their presence makes it harder to recognize the join as Contained-semijoin and there is also some overhead due to testing redundant qualification. Eliminating redundant qualifications is indeed a by-product of semantic query optimization.

6 CONCLUSIONS & FUTURE WORK

We have illustrated deficiencies of conventional systems for temporal query processing using the complex Superstar query. This example leads to several observations which suggest new requirements for temporal query processing strategies.
The most interesting and important observation is that less-than joins occur more often and naturally in temporal queries, and usually contain a conjunction of a number of inequalities. For the Superstar example, it may be more efficient to implement the less-than join using Contain-semijoin instead of using nested-loop join algorithm especially when tuples are properly sorted. These observations motivate our investigation of the stream processing strategies and suggesting new avenues of research in temporal query optimization techniques. We have considered stream processing techniques for processing various temporal join and semijoin operators.
Given data integrity constraints and a temporal query, we discussed the effect of various sort orderings of streams of tuples on the efficiency with which the operator is implemented and the local workspace requirement in the stream processing environment. In particular, we note that the optimal sort order may depend on the query itself and the statistics of data instances.
We have also discussed semantic query optimization in temporal databases. In temporal databases such as in (321, relations are augmented with time attributes such as Validation and ValidTo. Users are not allowed to update these attributes directly although a set of temporal operators are provided for data manipulation. From an algebraic manipulation point of view, these system-defined attributes are the same as any user-defined attributes. The main difference becomes evident when the semantics of Validfiom and ValidTo attributes are utilized in the semantic query optimization process. As we can see from the
Superstar example, the system might not be able to evaluate the query using Contained-semijoin without knowing the “intra-tuple” integrity constraint. There are many directions for future research. We are currently pursuing the following areas: a complete temporal data model, statistical information gathering and formalizing semantic query optimization in temporal databases.

REFERENCES

[l] Abelson H. and Sussman G.J. ‘Structure and Interpretation of Computer Programs,’ The MIT Press, 1985.

[2] Ahn I. ‘Towards an Implementation of Database Management Systems with Temporal Support,’ Proceedings of the Int. Conf. on Data Engineering, February 1986, pp.374-381.

[3] Allen James F. ‘Maintaining Knowledge about Temporal Intervals,’ Communications of the ACM, Vo1.26, No.11, November 1983, pp.832-843.

[4] Batory D.S., Leung T.Y. and Wise T.E. ‘Implementation Concepts for an Extensible Data Model and Data Language,’, ACM %ns. on Database Systems, vo1.13, No.3,n September 1988, pp.231-262.

[5] Ben-Zvi J. ‘The Time Relational Model,’ (Unpublished) Ph.D. Thesis, Dept. of Computer Science, University of California,

Los Angeles, 1982.

[6] Bentley J. 'Algorithms for Reporting and Counting Geometric Intersections,' IEEE 2"s. on Computers, Vo1.C-28,No.9, September 1979, pp.643-647.

[7] Boral H., Dewitt D. 'Applying Data Flow Techniques to Data Bae Machines,' IEEE Computer, Vo1.15, No.8, August 1982, pp.57-63.

[8] Chakravarthy U.S., Fishman D.H., and Minker J. 'Semantic Query Optimization in Expert System and Database Systems,' Expert Database Systems, 1984, pp.32G-341.

[9] Clifford J., and Warren D.S. 'A Model for Historical Databases,' ACM Tmns. on Database Systems, Vo1.8, No.2, June 1983, pp.214-254.

[l0] Clifford J., and Tansel A. 'On an Algebra for Historical Relational Databases: Two Views,' Proceedings of the ACM SIGMOD Int. Conf. on Management of Data, May 1985, pp.247-265.

[ll] Clifford J., and Croker A. 'The Historical Relational Data Model (BRDM) and Algebra Based on Lifespans,' Proceedings of the Int. Conf. on Data Engineering, February 1986, pp.474-481.

ALGORITHMS FOR EVENT – JOIN OPTIMIZATION FOR EFFICIENT PERORMANCE & AN ACCESS STRUCTURE FOR TEMPORAL DATA

[1]Mir Abid Ali, [2]Dr. Syed Abdul Sattar
[1]Research Scholar, Department of Computer Science Engineering, PP.COMP.SCI.0578, Rayalaseema University, A.P, India.
[2] Director, Research & Development, Nawab Shah Alam Khan College of Engineering & Technology, Hyderabad.

Abstract: An Event-Join consolidates temporal join and external join properties into a single operation. It is, for the most part, used to group transient characteristics of an element into a single relation. This paper motivates the need to support the efficient processing of event-joins, & introduce several optimization algorithms, both for a general information association and for specific associations (arranged and annex just databases). For the affix just information base we present an information structure that can enhance the execution of event-joins and additionally different questions we depict another ordering system, the time index, for enhancing the performance of specific classes of temporal queries. The time index can be used to recover versions of objects that are valid during a specific time period. It supports the preparing of the temporal When administrator and temporal aggregate functions efficiently. The time indexing scheme is additionally reached out to enhance the execution of the temporal SELECT administrator, which recovers objects that fulfill a specific condition amid an explicit era. We will portray the ordering system and its search and insertion algorithms.

IndexTerms **- temporal join, temporal queries, time index, database, event-join .**

I. INTRODUCTION AND MOTIVATION

Temporal data models are designed to capture the complexities of many time-dependent phenomena, something that traditional approaches, like the relational model, were not intended to do. Numerous new administrators are required with the end goal to abuse the maximum capacity of fleeting information models in upgrading the recovery intensity of a database the executives' framework (DBMS). Numerous fleeting administrators have been presented in the writing, (e.g. [Clifford and Tansel 4, Adiba and Quang 1, Clifford and Croker 3, Snodgrass 6]), yet with couple of special cases (e.g., tLurn et al 10, Rotem & Segev 7, Snodgrass & Ahn 6]), the issues of performance and optimization have not received as much attention. In an earlier paper [Gunadhi & Segev 11, 12], A set of temporal joins are identified and carried out initial investigation into their optimization. This paper explains the study of optimization of event-join operations. It was first introduced by [Segev & Shoshani 9]; it is unique in that it cartels temporal join and outer join components into a single operation. It is used primarily to group temporal attributes of an entity into a single relation; temporal attributes be appropriate to the same entity, but which are not synchronous in their event points, are probable to be stored in separate relations.

Numerous inquiries require that they are gathered together as one connection, however, contrasts in their conduct after some time raises the likelihood that invalid qualities are engaged with the operands and the join result.

It deals with streamlining occasion participates in fleeting social databases. Its commitments are the accompanying: a. Rousing and showing the need to support the proficient preparing of event-joins. As traditional handling can't bolster event-joins, we have created optimization algorithms for different circumstances, including static arranged databases and dynamic databases with general information organization and attach just association.

With regards to the append-only database, we have built up another information structures called the AP-Tree (Append-Only Tree). This tree is a variety of an ISAM and a B+-tree blend and is valuable for other transient inquiries other than an event- joins.

We consider our time index to be a fundamental indexing technique for temporal data. It very well may be joined with a regular credit ordering plan to productively process worldly choices and transient join operations.

II. RELATIONAL REPRESENTATION OF TEMPORAL DATA

A suitable way to look at temporal data is through the perceptions of Time Sequence Collection (T_X) and Time Sequences (T_S) [Segev & Shoshani 9]. A T_S represents a history of a temporal attribute(s) associated with a particular instance of an entity or a relationship.

Table-1 Representing SWC Data with Lifespans = [1,20]

MANAGER	E#	MGR	T_S	T_E
	E1	TOM	1	5
	E1	MARK	9	12
	E1	JAY	13	20
	E2	RON	1	18
	E2	RON	1	20
COMMISSION	**E#**	**C_RATE**	**T_S**	**T_E**
	E1	10%	2	7
	E1	12%	8	20
	E2	8%	2	7
	E2	10%	8	20

In this paper, we are fretful with two types -- stepwise constant and discrete.

Stepwise constant (SWC) data speaks to a state variable whose qualities are controlled by events and continues as before between events: the pay trait represents to SWC information. Discrete data speaks to a trait of the event itself, e.g. number of things sold. Time sequences of a similar surrogate and quality sorts can be assembled into a time sequence collection (T_X), e.g. the history of the salary of all employee forms a TSC.

III EVENT JOINS

Event-Join group's numerous temporal attributes of an entity into a single relation. This activity is critical in light of the fact that because of standardization, temporal attributes is probably going to reside in separate relations. To explain this point, an employee relation is considering in a conventional database. If the database is normal, we are likely to find all the attributes of the employee entity in a single relation. If we now define temporal as a subset of the attributes (e.g., salary, job code, manager, commission-rate, etc.) and they are put away in a single relation, a tuple will be made at whatever point an occasion influences something like one of those attributes. Thusly, gathering temporal attributes into a single relation ought to be done if their event points are synchronized. Despite the idea of temporal attributes, in any case, a physical database design may prompt putting away the temporal attribute8 of a given element in a few relations. The similarity in a conventional database is that the database creator may make 3NF tables, however clearly, the client is permitted to join them and make a unnormalized outcome

Let $r_i(R_i)$ be a relation on scheme $R_i = \{S_i, A_{i1}, \ldots, A_{im}, T_S, T_E\}$. In many instances we illustrate the concepts using a single temporal attribute, that is, $m = 1$; all apply to any $m > 1$. Also, when the two surrogate *types* S_i of R_i and S_j of R_j are the same, we simply use S. Instances of surrogate S are denoted by $s1, s2, \cdots$. We use x_i to refer to an arbitrary tuple of r_i; $x_i(A)$ is the value of attribute A in tuple x_i. In order to describe the event-join between r_1 and r_2, we first present two basic operations *TE–JOIN* and *TE–OUTERJOIN*. TE-JOIN is the temporal equivalent of a standard equijoin; two tuples $x_1 \in r_1$ and $x_2 \in r_2$ are concatenated † if their join attribute's values are equal and the intersection of their time intervals is non-empty; the T_S and T_E of the result tuple correspond to the intersection interval. Semantically, this join condition is "where the join values are equal at the same time". In the case of event-joins, we are concerned only with a special case of TE-JOINs where the joining attribute is the surrogate. A TE-OUTERJOIN is a directional operation from r_1 to r_2 (or vice versa). For a given tuple $x_1 \in r_1$, outerjoin tuples are generated for all points $t \in [x_1(T_S), x_1(T_E)]$ where there does not exist $x_2 \in r_2$ such that $x_2(S) = x_1(S)$ and $t \in [x_2(T_S), x_2(T_E)]$. Note that all consecutive points t that satisfy the above condition generate a single outerjoin tuple. Using those operations the event-join, r_1 EVENT-JOIN r_2, is done as: temp1 $\leftarrow r_1$ TE-JOIN r_2 on S; temp2 $\leftarrow r_1$ TE-OUTERJOIN r_2 on S; temp3 $\leftarrow r_2$ TE-OUTERJOIN r_1 on S; result $\leftarrow$ temp1 $\cup$ temp2 $\cup$ temp3. Table 2 shows the result of an event-join performed between the MANAGER and COMMISSION relations of Table 1.

Table 2: Results of Event-Joint

Result	E#	MGR	C_RATE	T_S	T_E
	E1	TOM	Ø	1	1
	E1	TOM	10%	2	5
	E1	Ø	10%	6	7
	E1	Ø	10%	8	8
	E1	MARK	12%	9	12
	E1	JAY	12%	13	20
	E2	RON	12%	1	1
	E2	RON	Ø	2	7
	E2	RON	8%	8	18
	E2	Ø	10%	19	20
	E3	RON	Ø	1	20

The most troublesome segments of the event- join are the external joins. The circumstance is additionally confused when time interval predicate related with the TE-external join, keeping the use of non-fleeting external join methods [Rosenthal and Reiner 14, Dayal 13]. A simple arrangement that rings a bell is to store all non-presence tuples explicitly, e.g., tuples like (1, Ø, 6,8) are added to the MANAGER connection of Table 1. All things considered, the external join parts vanish, and the issue decreases to a TE: JOIN on S. Unfortunately, there are numerous circumstances where such a 'fix' will debase by and large execution as opposed to enhancing it. For instance, if the entire Si domain is spoken to in connection RI, speaking to all non-presence information unequivocally will in the most pessimistic scenario twofold the extent of the table (this is the situation of rotating state changes among presence and non-presence). A much more awful issue may emerge when a connection contains just a small amount of the S-domain values, e.g., if, on the normal, just 5% of the workers of an extensive organization win commissions, adding to the non-presence information for the 95% different representatives to the commission connection will add to capacity cost, questioning cost (counting event joins), and upkeep of the commission relation and any of its related optional records. Thus, we partition divide event-joins into two sorts - 'simple' and 'troublesome'. Simple cases are those where the relations contain explicit tuples for all non-presence information and are arranged by (S, 7's) (the arranged case is point by point in the following segment). Different cases are respected troublesome. In the rest of the paper, we are for the most part worried about the difficult cases.

IV. EVENT- JOIN OPTIMIZATION

Optimizations of event-joins were discussed in this section where the relations are either sorted or unsorted. Before we ensue with details of the algorithms, the significant concept of tuple covering, which is used throughout the discussions, is presented first.

4.1. The concept of Tuple Covering:

We first introduce the notion of covering which is used in all the event-join algorithms. To illustrate the concept, consider the example of Table 3.

Table 3 Example of Tuple Covering

r_1	r_2	Cover of x_1	Modified x_1
*s*1,*a*,5,15	*s*1,*b*,1,2	*None*	*s*1,*a*,5,15
	*s*1,*c*,3,7	*s*1,*a*,*c*,5,7	*s*1,*a*,8,15
	*s*1,*d*,9,12	*s*1,*a*,Ø,8,8 *s*1,*a*,*d*,9,12	*s*1,*a*,13,15
	*s*1,*e*,16,20	*s*1,*a*,Ø,13,15	*Full cover*

Relation r_1 has a scheme $R_1 = (S, A_1, T_S, T_E)$ and a single tuple $<s1, a, 5, 15>$. r_2 has a scheme $R_2 = (S, A_2, T_S, T_E)$ and four tuples as shown in the table. During the event-join, $x_1 \in r_1$ has to be compared with tuples $x_2 \in r_2$; assume that the order of comparisons is as shown in the table (top-down). A tuple x_2 contributes to the covering of x_1 if one or two result tuples $[x_1(S), x_1(A_1), x_2(A_2), I_C]$ can be derived, where $I_C \subseteq [x_1(T_S), x_1(T_E)]$. I_C can be viewed as a covered portion of x_1. The 'modified x_1' column in the table represents the uncovered portion of x_1. Note that in the covering process we have relied on the ordering of r_2 by time in deriving the outerjoin tuples (those with $x_2(A_2) = \emptyset$). Also, the covering column of the table contains only a subset of the final result since the covering of r_2's tuples is incomplete. The remaining result tuples should be derived from a TE-outerjoin from r_2 to r_1. In this particular example, the remaining result tuples are $<s1, \emptyset, b, 1, 2>$, $<s1, \emptyset, c, 3, 4>$ and $<s1, \emptyset, e, 16, 20>$.

Determining and maintaining the information about the covered portion of a tuple is substantially different if the relations are not sorted by T_s. In the sorted case we can determine outer-join tuples as the scanning progresses and the information about the covered portion of the tuple is maintained by simply modifying its T_s.

In the general case, the covered subintervals can be encountered in a random order; moreover, an outer-join result tuple associated with x 1 E rl can be determined only when the scanning of r2 is complete. We first present an algorithm for the case where r1 and r2 are sorted by S (primary order) and by T_s (second order). In the next subsection, we discuss the general case. As can be seen from the above example, the particular values of A1 and A2 are immaterial as far as the logic of the event-join is concerned &, we are only interested in existence or non- existence of these attributes. Consequently, in the remainder of the paper, whenever convenient, we use examples with relation schemas of (Si, T_s, TE), but the reader should keep in mind that at least ON Ai attribute is part of the actual tuples. Also, the algorithms presented in this paper involve lots of housekeeping details. For lack of space, we omit the details and provide only an outline of the algorithms. The logic of all algorithms is described ignoring blocking of tuples; it is trivially extended to handle blocking.

4.2 Event-Join Sort-Merge Algorithm

The Sort-Merge algorithm processes the event- join by taking advantage of the fact that both relations are in sort order. Unlike a conventional relation which requires only the primary key order for sorting, the temporal relation needs to be sorted on S as the primary order and T_s as the second order. The event-join sort-merge algorithm, which will be referred to as Algorithm One, scans each relation just once in order to produce the result relation. At each iteration, two tuples (possibly with modified T_s), x1 E r1 and x2 E r2, are compared to each other and one or two result tuples will be produced based on the relationship between the tuples on their surrogate values and time intervals.

The first comparison in Algorithm One is on the surrogate value if they are unequal, it means that the tuple with the lower S value, say xl, does not have any matching surrogates in the other relation; this implies that x1 is fully covered, an outer-join result tuple is generated, and the next x1 tuple is read. If on the other hand x1(S) = x2(S), there are many possible relationships that can exist between the time intervals of the two tuples; but there are just three distinct possibilities in terms of result tuples that have to be generated. The three cases are identified in Step 3 of Algorithm One.

Algorithm One

(1). Read x_1 and x_2. Repeat steps 2 to 4 until End-of-File (EOF). If EOF occurred for r_i, generate outerjoin tuples for the remainder of r_j's tuples (including the current tuple if not fully covered).

(2). If $x_i(S) < x_j(S)$, generate an outerjoin result tuple for x_i.

(3). For the situation where $x_1(S) = x_2(S)$, there are three cases to consider.

Case 1: $x_i(T_S) = x_j(T_S)$. Write an intersection result tuple.

Case 2: $x_i(T_S) < x_j(T_S)$ and $x_i(T_E) \geq x_j(T_S)$. Write one outerjoin tuple for x_i and one intersection tuple. Modify x_1 and x_2 and read next tuple(s).

Case 3: $x_i(T_E) < x_j(T_S)$. Write an outerjoin tuple for x_i.

(4). Modify x_1 and x_2 and read next tuple(s).

The next tuple of r_i is read-only when the current tuple has been fully covered. Note that whenever we use the subscripts i and j in Algorithm One, i=1, and j=2 or i=2 and j=l. Also, an intersection result tuple is equivalent to a TE-JOIN result tuple.

4.3 Event - Join Nested-Loop Algorithm

The Nested-Loop method described below does not assume any kind of ordering among the tuples in either relation. The event-join is achieved in two stages, the first of which is nested-loop with r1 and r2 being the inner and outer relations respectively. Tuples produced in the first stage are the result of either intersections or outer joins from r1 to r2. In the second stage, the order of relations are now reversed for another nested-loop, but the only result tuples created here will be outer joins from r2 to r1.

Unlike the sorted case, maintaining the information about the covered portion Of Xi's time interval can't be done by simply modifying T_s, and the following procedure is followed. In the first nested-loop, whenever a tuple x1 from r1 is first to read a list U is initialized with the pair of time-stamps associated with x1. This list corresponds to the uncovered portions of x1. For each tuple x2, the algorithm applies the test of equality on the surrogate values and a non-null intersection over time. The second condition is needed because if two tuples share a common surrogate value but are disjoint over time, no conclusion can be derived (in contrast to the sorted case) as to whether an outer- join is appropriate unless the EOF for r2 has been reached. Thus, while scanning r2, the covering of x1 is achieved only through interval intersections, and for each x2, at most one intersection result tuple will be produced. Once this is accomplished, the uncovered subintervals associated with x1 are determined, and appropriate outer join result tuples are generated. At the end of r2's scan, the interval of x1 will either be completely covered, has one uncovered segment, or at most two segments. For each uncovered segment, the time pair's representing them are inserted into U in place of the original entry. This ensures that U remains an ordered list; the ordering within U helps the search for the appropriate interval that is relevant for a TE-JOIN in subsequent iterations through r2. Regardless of the number of entries in the list, any tuple x2 can only intersect with one entry, otherwise, it would mean that there are two or more tuples in r2 having the same surrogate value and overlap in time. This implies that the condition of 1TNF has not been satisfied.

Unlike conventional nested-loop procedures, we need not retrieve all the tuples of the outer relation, since an empty U indicates that the original xi has been fully covered. In the event that the loop terminates because the end of file r2 is reached, either the whole or parts of xi's time interval were left uncovered. An outer join result tuple is generated from each time pair in U; the time pair determines the time-start and time-end of the result tuple.

The second nested-loop differs from the first in that it produces only outer join tuples from r2. Thus no result tuple duplicating a tuple already produced in the first stage is created. In order to reduce the number of unnecessary scans of ri, the Algorithm uses a hash-filter [Bloom 2] created during the first stage as follows: when r2 is scanned, each time an x2 is found that participates in a TE-JOIN, the hash-filter is updated for that tuple. The hash-filter maintains H bits to represent N_{r2} tuples, where $H<=N_{r2}$. The hash-filter entries corresponding to h(x2), where h is the hash- function, are initialized to 0, and whenever an x2 generates an intersection result tuple for the current x1, h (~9 is set to 1). This table is kept in main memory, and in the best case scenario where there is sufficient memory to maintain one bit per tuple, the hash function is the count of x2 tuples already accessed, and the table is a one-dimensional array indexed by this count. During the second stage, for each tuple in the inner relation r2, if it hashes to a value of 0, then an outer join tuple is produced without scanning r1. Otherwise, as in the first nested-loop, we carry out the same updates on the coverage of x2, although no intersection tuples are produced. As before, outer join tuples are produced when it can be determined that no x1 exists to cover the current x2. Below we outline the steps of the algorithm, labeled as Algorithm TWO. U_i denotes the list U for X_i, i =I, 2.

Algorithm Two

(1). [*Nested-Loop-1*] For each tuple in r_1: read r_2 and execute Step 2 until EOF for r_2 or x_1 is fully covered. If EOF for r_2, produce outerjoin tuples for x_1 based on U_1.

(2). If $x_1(S) = x_2(S)$ and the two time intervals intersect, then do: write an intersection result tuple. Update U_1. Set hash-filter entry for x_2 to 1.

(3). [*Nested-Loop-2*] For each tuple x_2 of r_2: if hash-filter bit = 0 produce outerjoin tuple immediately, and read next x_2. Otherwise read r_1 and execute Step 4 until EOF for r_1 or x_2 is fully covered.

(4). if $x_2(S) = x_1(S)$ and the two time intervals intersect then update U_2.

In the case of having space for a second bit for each of r2's tuples, Algorithm Two can be further improved if a second filter is used. During the first stage, while covering x1 it is possible that the time interval of x2 contains that of xi. In that case, we set the corresponding filter entry to 1. Then, in Step 3 we also avoid the scan of r1 if the first filter bit is 1 and the second filter bit is also 1.

V. THE TIME INDEX ACCESS STRUCTURE

In this section, we first give a storage model for temporal data based on the object versioning approach' [SA 15]. The time indexing technique can be adapted to other temporal database proposals, such as time normalization [NA 16] or attribute versioning [GY17]. We use object versioning because it is a simpler approach for storage management, and allows us to concentrate our presentation on the properties of the time index itself. In Section 5.2, we will describe our time index, and provide search, insertion, and deletion algorithms. Sections 5.3 and 5.4 show how the time index may be used to efficiently process the temporal WHEN operator and aggregate functions.

5.1 The Temporal Storage Model

The time dimension is represented, as in [GY17, CW18, Gad19, and others, using the concepts of discrete time points and time intervals. A time interval, denoted by [t1,t2], is defined to be a set of consecutive equidistant time instants (points), where t1 is the first time instant and t2 is the last time instant of the interval. The time dimension is represented as a time interval [0, now], where 0 represents the starting time of our database mini-world application, and now is the current time, which is continuously expanding. The distance between two consecutive time instances can be adjusted based on the granularity of the application to be equal to months, days, hours, minutes, seconds, or any other suitable time unit. A single discrete time point t is easily represented as an interval [t, t] or simply [t].

We will assume an underlying record-based storage system which supports object versioning. Records are used to store versions of objects. In addition to the regular record attributes, Ai, each record will have an interval attribute, called valid-time, consisting of two sub-attributes t_s (valid start time) and t_e (valid end time). The valid-time attribute of an object version is a time interval during which the version is valid. In object versioning, a record r with r.valid-time.t_e = now is considered to be the current version of some object. However, numerous past versions of the object can also exist. We assume that the versions of an object are linked to the current version using one of the basic storage techniques (chaining, clustering, accession list) proposed in [AS88, Lum84]. In addition, we assume that the current version of an object can be efficiently located from any other version; for example, by using a pointer to a linked list header, which in turn points to the current version.

Whenever an object o is updated with new attribute values, the current version, r, becomes the most recent past version, and a new current version T' is created for o. If the valid time of the update is t_u, then the update is executed as follows:

r.valid-time.t_e <- (t_u, - 1) ;
create a new object version r^l by setting r^l <- r ;
for each modified regular attribute Ai
set $r^l.A_i$ <- the new attribute value ;
set r^l.valid-time.t_s <- t_u ;
set r^l.valid-time.t_e <- now;

Such a database is called append only since older object versions are never deleted, so the file of records continually has object versions appended to it. An operation to delete an object o at time t_d is executed as follows:

find the current version r of the object o;
set r.valid_time.t_e <- t_d ;

Finally, an operation to insert an object o at time t_i is executed as follows:

create the initial version T for o ;
set r.valid-time.t_s <- t_i ;
set r.valid-time.t_e <- now ;

Because the append-only nature of such a temporal database will eventually lead to a very large file, we assume that a purge(t_p) operation is available. This operation purges all versions r with r.valid-time.t_e < t_{ps} by moving those versions to some form of archival storage, such as optical disk or magnetic tape.

Name	Dept	Valid_Time
emp1	A	[0, 3]
emp1	B	[4, now]
emp2	B	[0, 5]
emp3	C	[0, 7]
emp3	A	[8, 9]
emp4	C	[2, 3]
emp4	A	[8, now]
emp5	B	[10, now]
emp6	C	[12, now]
emp7	C	[11, now]

The EMPLOYEE table

Dept	Manager	Valid_Time
A	Smith	[0, 3]
A	Thomas	[4, 9]
A	Chang	[10, now]
B	Cannata	[0, 6]
B	Martin	[7, now]
C	Roberto	[0, now]

The DEPARTMENT table

Figure 1 A Temporal Database

5.2 Description of the Time Index

Conventional indexing schemes assume that there is a total ordering on the index search values. The properties of the temporal dimension make it difficult to use traditional indexing techniques for time indexing. First, the index search values, the valid-time attribute, are intervals rather than points. The valid-time intervals of various object versions will overlap in arbitrary ways. Because one cannot define a total ordering on the interval values, a conventional indexing scheme cannot be used. Second, because of the nature of temporal databases, most updates occur in an append mode, since past versions are kept in the database. Hence, deletions of object versions do not generally occur, and insertions of new object versions occur mostly in increasing time value. In addition, the search condition typically specifies the retrieval of versions that are valid during a particular time interval.

A time index is defined over an object versioning record-based storage system, TDB, which consists of a collection of object versions, TDB = {el, e2,....en}, and supports an interval-based search operation. This operation is formally defined as follows.

Given a Search Interval, Ts = [ta, ta], find the following set of versions:

S(Is) = {ej E TDB | (ej.validtime n Is) ≠ 0 }

A simple but inefficient implementation of this search operation is to sequentially access the entire storage system, TDB, using linear search, and to retrieve those records whose valid-time intersects with Is. Such a search will require O(N*M) accesses to the storage system, where N is the number of objects and M is the maximal number of versions per object.

Notice that the interval-based search problem is identical to the k-dimensional spatial search problem, where k = 1. There have been a number of index methods proposed for k-dimensional spatial search [Gut20, OSD21], which are not suitable for the time dimension for the reasons discussed below. These index methods support the spatial search for 2-dimensional objects in CAD or geographical database applications. The algorithms proposed in [Gut20, OSD21] use the concept of a region to index spatial objects. A search space is divided into regions which may overlap with each other. A sub-tree in an index tree contains pointers to all spatial objects located in a region. Since spatial objects can overlap with each other, handling the boundary conditions between regions is quite complex in these algorithms. In temporal databases, there can be a very high degree of overlap between the valid-time intervals of object versions. A large number of long or short intervals can exist at a particular time point. Furthermore, the search space is continuously expanding and most spatial indexing techniques assume a fixed search space. In addition, temporal objects are appended mostly in increasing time value, making it difficult to maintain tree balance for traditional indexing trees. Because of these differences between temporal and spatial search, we do not consider the spatial algorithms in [Gut20, OSD21] to be suitable for temporal data if they are directly adapted from 2-dimensions to a single dimension.

The idea behind our time index is to maintain a set of linearly ordered indexing points on the time dimension. An indexing point is created at the time points where (a) a new interval is started, or (b) the time point immediately after an interval terminates. The set of all indexing points is formally defined as follows:

(PR1) BP = {t_i | €j E TDB ((t_i = ej.validtime.t_s) V (t = ej.validtime.t_e + 1))) U {now}
The concept of indexing points is illustrated in Figure 2 for the temporal data shown in the EMPLOYEE table of Figure 1. In Figure 2, e_{ij} refers to version j of object e_i. There exist 9 indexing points in BP for all employee versions, BP = {0,2,4,6,8,10,11,12,now). Time point 2 is an index point since the version e41 starts at 2. Time point 6 is an index point since e21 terminates at 5. Before proceeding to describe our index structure, we define some additional notation that will be useful in our discussion. Let tj be an arbitrary time point, which may or may not be a point in BP.

Let t_j be an arbitrary time point, which may or may not be a point in BP. We define t_j- (t_j+) to be the point in BP such that t_j- < t_j (t_j < t_j+) and there does not exist a point t_m E BP such that t_j- < t_m < t_j (t_j < t_m, < t_j+). In other words, t_j- (t_j+) is the point in BP that is immediately before (after) t_j. We also define t_{j-} = as follows:

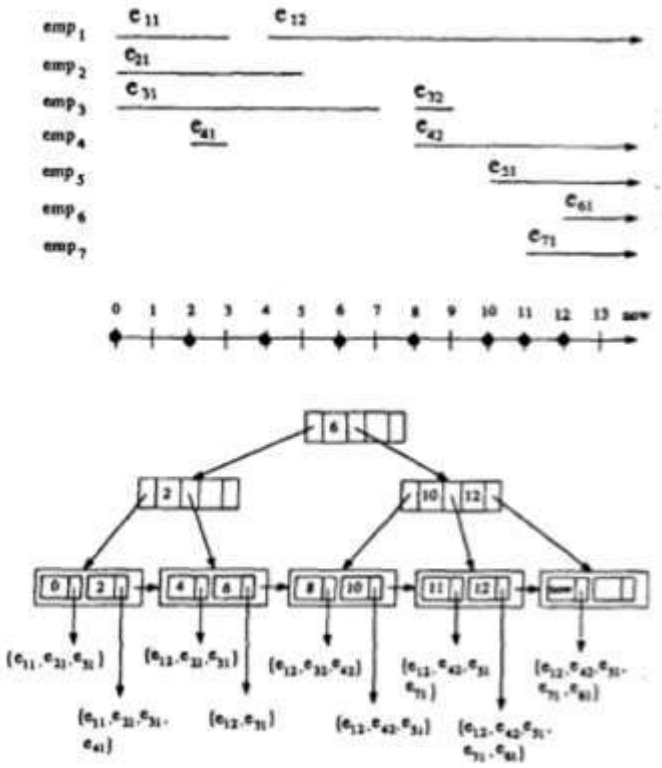

Figure 2 Versions of Employees Object and Time Index

1. If there exists a point t_k E BP such that t_j = t_k, then t_{j-}= = t_k.
2. Otherwise, tj-= = t_i

Since all the indexing points t_i in BP can be totally ordered, we can now use a regular B+tree [Com22, EN23] to index these time points. Each leaf node entry of the B+-tree at point t_s is of the form:

[t_s, bucket]

where the bucket is a pointer to a bucket containing pointers to object versions. Each bucket B(t_i) in our index scheme is maintained such that it contains pointers to

all object versions whose *valid_time* contains the interval $[t_i, t_i^+ - 1]$. Such a property can be formally specified as follows:

(PR2) $B(t_i) = \{e_j \in TDB \mid ([t_i, t_i^+ - 1] \subseteq e_j.valid_time)\}$

Figure 2 shows a B^+-tree of order 3, which indexes the *BP* set of points of the EMPLOYEE versions. Each node in the B^+-tree contains at most two search values and three pointers. Consider the leaf entry for search time point 4, for instance; (PR2) indeed holds.

$$B(4) = \{e_{12}, e_{21}, e_{31}\}$$
$$= \{e_j \in TDB \mid ([4,5] \subseteq e_j.valid_time)\}$$

In a real temporal database, there can be a large number of object versions in each bucket, and many of those may be repeated from the previous bucket. For example, in Figure 2 the object version e12 appears in multiple consecutive buckets. To reduce this redundancy and make the time index more practical, an incremental scheme is used. Rather than keeping a full bucket for each time point entry in BP, we only keep a full bucket for the first entry of each leaf node. Since most versions will continue to be valid during the next indexing interval, we only keep the incremental changes in the buckets of the subsequent entries in a leaf node. For instance, in Figure 3 the entry at point 10 stores {+e31, -e32} in its incremental bucket indicating e31 starts at point 10 and e32 terminates at the point immediately before point 10. Hence, the incremental bucket $B(t_i)$ for a non-leading entry at time point t_i can be computed as follows:

$B(t_i) = B(t_l) \cup (U_{tj \in BP,\ t_i < t_j < t_l} SA(tj)) - (U_{tj \in BP}, t, <tj<ti\ SE(tj))$

Where $B(t_l)$ is the bucket for the leading entry in the leaf node where point t; is located, $SA(t_j)$ is the set of object versions whose start time is t_j and $SE(t_j)$ is the set of object versions whose end time is t_j - 1.

We now describe our search algorithm as follows:

1. Suppose the time search interval is I_s = [ta, tb]. Perform a range search on the B+-tree to find

(C1) PI(Is) = {ti E BP/t_a < ti < t_b) U {t_a-=}

2. Then compute the following set as the result of the algorithm.

(C2) $T(I_s) = U_{ti \in PI}\ B(t_i)$

Insertion or deletion of a new object version should maintain the properties (PR1) and (PR2). The algorithms for inserting and deleting an object version ek are shown in Algorithm A.

Note that, in general, version deletion will not occur in append-only databases except for an exception such as correction of an error. It is easy to argue that (PR1) and (PR2) is maintained after each execution of the Insert or Delete operation. We will not show the proof argument here due to the lack of space.

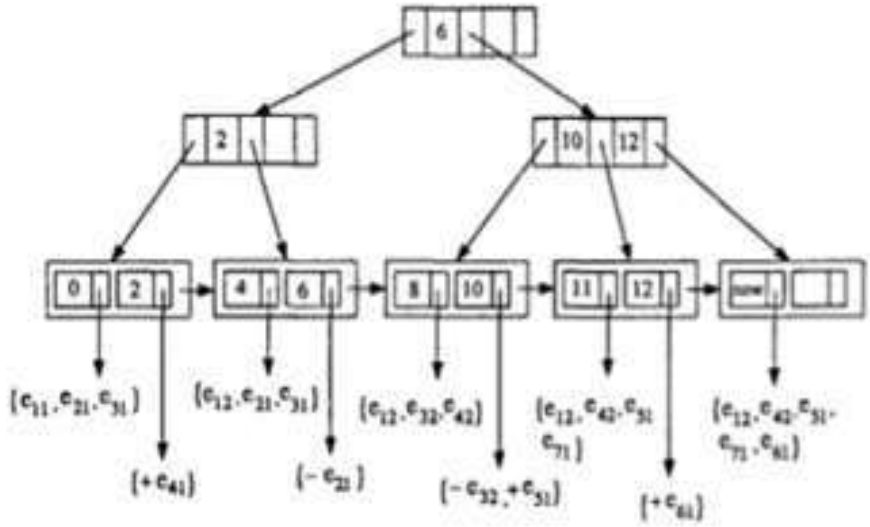

Figure 3 Storing Incremental changes in Time Index Buckets

Algorithm A

```
Insert(e_k)
begin
   t_a ← e_k.valid_time.t_s ;
   t_b ← e_k.valid_time.t_e + 1 ;
   search the B+-tree for t_a;
   if (¬found) then
        insert t_a in the B+-tree;
   if entry at t_a is not a leading entry in a leaf node
        add e_k into SA(t_a);
   search the B+-tree for t_b;
   if (¬found) then
        insert t_b in the B+-tree;
   if entry at t_b is not a leading entry in a leaf node
        add e_k into SE(t_b);
   for each leading entry t_l of a leaf node
   where t_a ≤ t_l < t_b
        add e_k in B(t_l);
end
```

```
Delete(e_k)
begin
   t_a ← e_k.valid_time.t_s ;
   t_b ← e_k.valid_time.t_e + 1 ;
   search the B+-tree for t_a;
   if entry at t_a is not a leading entry in a leaf node
     remove e_k from SA(t_a);
   search the B+-tree for t_b;
   if entry at t_b is not a leading entry in a leaf node
     remove e_k from SE(t_b);
   for each leading entry t_l of a leaf node
   where t_a ≤ t_l < t_b
     remove e_k from B(t_l);
end
```

5.3 Using the Time Index for Processing the WHEN Operator

The time index can be used to efficiently process the WHEN operator [GY17] with a constant projection time interval. An example of the type of query is: List the salary history for all employees during the time interval [4, 51]. The result of such a query can be directly retrieved using the time index on the EMPLOYEE object versions shown in Figure 3. We will discuss in Section 3 how an extension to the time index will permit efficient processing of temporal SELECT operations. Notice that a simple query such as the one given above is very expensive to process if there was no index on time.

5.4 Using the Time Index for Processing Aggregate Functions

In this section, we will describe how the time index scheme is used to process aggregate functions at different time points or intervals. In a non-temporal conventional database, the aggregate functions, such. as COUNT, EXISTS, SUM, AVERAGE, MIN, and MAX are applied to sets of objects or attribute values of sets of objects. In temporal databases, an aggregate function is applied to a set of temporal entities over an interval. For instance, the query 'GET COUNT EMPLOYEE: [3, 81' [EW24] should count the number of employees at each time point during the time interval [3, 81]. The result of the temporal COUNT function is a function mapping from each time point in [3, 81 to an integer number that is the number of employees at that time point. For instance, the above query is evaluated to the following result if applied to the database shown in Figure 1:

{ [3] → 4, [4, 5] -> 3, [6, 7] → 2, [8] → 3 }

Our time index can be easily used to process such aggregate functions. Let 1s be the interval over which the temporal aggregate function is evaluated. The query performs a range search to find Pl(Is). Each point in Pl(ls) p represents a point of state change in the database. That is, the database mini-world changes its state at each change point and stays in the same state until the next change point. Therefore the aggregate function only needs to be evaluated for the points in Pl(ls). The query is evaluated by applying the function on the bucket of object versions at each point. If the incremental index shown in Figure 3 is used, the running count from the previous change point is updated at the current change point by adding the number of new

versions and subtracting the number of removed versions at the change point. Similar techniques can be used for other aggregate functions that must be computed at various points over a time interval

VI CONCLUSION

In this paper, we have addressed the problem of optimizing event-joins in a temporal relational database. Event-joins are important because normalization considerations are likely to split the temporal attributes of an entity among several relations. The event-join combines a temporal equijoin component and a temporal outer join component. Unlike a conventional outer join, the temporal counterpart consists of two asymmetric outer joins, a fact that complicates its optimization. The complexity of processing event-join strategies depends on the nature of the data, its organization, and whether or not all non-existing data are represented explicitly. We addressed three cases of data organization; these are (in increasing order of complexity) data sorted by surrogate and time, append-only, and general optimization. For the sorted case (appropriate for static databases), the processing of an event-join is the most efficient since each relation has to be read only once. We described a new indexing technique, the time index, for temporal data. The index is different from regular B+-tree indexes because it is based on objects whose search values are intervals rather than points. We create a set of indexing points based on the starting and ending points of the object intervals and use those points to build an indexing structure. At each indexing point, all object versions that are valid during that point can be retrieved via a bucket of pointers. We used incremental buckets to reduce the bucket sizes. Search, insertion, and deletion algorithms are presented.

Our structure can be used to improve the performance of several important operations associated with temporal databases. These include temporal selection, temporal projection, aggregate functions, and certain temporal joins.

REFERENCES

1. Adiba, M, Quang, N.B., Historical Multi-Media Data- bases, Proc. ht. Co& on VLDB, pp. 63-70, 1986.
2. Bloom, B.H., Space/Time Trade-offs in Hash Coding with Allowable Errors, Comm. of the ACM, 13, 7, 1970.
3. Clifford, J., Croker, A., Historical Relational Data Model (HRDM) and Algebra Based on Lifespans, Proc. ht. Co@. on Data Engineering, pp. 528-537, 1987.
4. Clifford, J., Tansel, A., On an Algebra for Historical Relational Databases: Two Views, Proc. ACM SIG- MOD ht. Co@ on Mgt. of Data, pp. 247-265, 1985
5. I. Ahn. Towards an implementation of database management systems with temporal support. In IEEE Data Engineering Conference, February 1986.
6. I. Ahn and R. Snodgrass. Partitioned storage for temporal databases. Information Systems, 13(4), 1988.
7. Rotem D, Segev. A, Physical design of Temporal Databases. to appear in Proceedings of the Third International Conference on Data Engineering. February. 1987.
8. Snodgrass. R .. The Temporal Query Language TQuel. Proceedings of the Third ACM SIG- .\lOD S.vmposium on Principles of Database SJ'stems (PODS). Waterloo .. Canada. April 1984. pp. 204-213.
9. Arie Segevt and Arie Shoshani, LOGICAL MODELING OF TEMPORAL DATA ,School of Business Administration The University of California Berkeley, CA 04720 +Computer Science Research Department Lawrence Berkeley Laboratory University of California Berkeley, California 04720 March, 1987.
10. Lum, V., Dadam. P, Erbe, R., Guenauer. J, Pistor. P., Walch. G , Werner. H , Woodfill .. J , Designing Dbms Support for the Temporal Dimension. Proceedings of the ACM SIGMOD International Conference on Management of Data. June 1984. pp. 115-130. March. 1986.
11. Gunadhi, H., Segev, A. A Framework for Query Optimization in Temporal Databases, Lawrence Berkeley Lab Technical Report LBL-26417, 1988.
12. Gunadhi, H., Segev, A. Indexing Structures for Temporal Database, Lawrence Berkeley Lab Technical Report, 1989.
13. Dayal, U., Of Nests and Trees: A Unified Approach to Processing Queries That Contain Nested Subqueries, Aggregates, and Quantifiers, Pro. ht. Conf on VLDB, pp.197-208, 1987.
14. Rosenthal, A., Reiner, D., Extending the Algebraic Framework of Query Processing to Handle Outerjoins Proc. ht. Conf. on VLDB, pp. 334-343,1984.
15. R. Snodgrass and I. Ahn. A taxonomy of time in databases. In ACM SIGMOD Conference, May 1985.

16. S.B. N avathe and R. Ahmed. A temporal relational model and a query language. In Infomnation Sciences, North-Holland, Vol. 49, No. 1, 2, and 3, 1989.

17. S. Gadia and C. Yeung. A generalized model for a temporal relational database. In ACM SIGMOD Conference, June 1988.

18. J. Clifford and D. Warren. Formal semantics for time in databases. ACM TODS, 8(2), June 1983.

19. S. Gadia. A homogeneous relational model and query language for temporal databases. ACM TODS, 13(4), December 1988.

20. A. Guttman. R-trees: A dynamic index structure for spatial searching. In A CM SIGMOD Conference, May 1984.

21. K. Ooi, B. McDonell and R. Sacks-Davis. Spatial kd-tree: Indexing mechanism for spatial database. In IEEE COMPSAC 87, 1987.

22. D. Comer. The ubiquitous b-tree. ACM Computing Surveys, 11(12), June 1979.

23. R. Elmasri and S. Navathe. Fundamentals of Database Systems. Benjamin/Cummings, 1989.

24. R. Elmasri and G. Wuu. A temporal model and language for er databases. In IEEE Data Engineeting Conference, February 1990.

Received: 5 June 2018 | Revised: 8 November 2018 | Accepted: 12 November 2018

DOI: 10.1002/ima.22302

Check for updates

WILEY

RESEARCH ARTICLE

Denoising and segmentation of MR images using fourth order non-linear adaptive PDE and new convergent clustering

Sreedhar Kollem[1] | Katta Rama Linga Reddy[2] | Duggirala Srinivasa Rao[3]

[1]Department of ECE, JNTUH University, Hyderabad, Telangana, India

[2]Department of ETM, G. Narayanamma Institute of Technology and Science (GNITS), Hyderabad, Telangana, India

[3]Department of ECE, JNTUH College of Engineering, Hyderabad, Telangana, India

Correspondence
Sreedhar Kollem, Research Scholar, Department of ECE, JNTUH University, Hyderabad 500085, Telangana, India.
Email: ksreedhar829@gmail.com

Abstract

At present, digital image processing plays a vital role in medical imaging areas and specifically in magnetic resonance imaging (MRI) of brain images such as axial and coronal sections. This article mainly focused on the MRI brain images. The existing methods such as total variation (MC), parallel MRI, modified pyramidal dual-tree direction filter, adaptive dictionary selection algorithm, classifier methods, and fuzzy clustering techniques are poor in image eminence and precision. Thus, this article presents a novel approach consisting of denoising followed by segmentation. The objective of these proposed methods was visual eminence improvement of medical images to examine tumor extent using an adaptive partial differential equation (APDE)-based analysis with soft threshold function in denoising. The fourth order, nonlinear APDE was used to denoise the image depending on gradient and Laplacian operators associated with the new adaptive Haar-type wavelet transform. A second approach was the new convergent K-means clustering for segmentation. The convergent K-means procedure diminishes the summation of the squared deviations of structures in a cluster from the center. The significance of these proposed methods was to compute their performances in terms of mean squared error, peak signal-to-noise ratio, structure similarity, segmentation accuracy, false hit, missed-term, and elapsed time. The results were analyzed with the MATLAB software.

KEYWORDS

adaptive Haar wavelet transform, false-hit, missed-term, new convergent K-means clustering, non-linear APDE

1 | INTRODUCTION

Imaging science visualizes an object and quantitatively characterizes its structure and function. The aim of biomedical image processing technology is to interact with multidimensional images. Medical applications for imaging include computer-aided mammography diagnosis and tumor imaging. Multimodality types of images are essential for diagnosis. It is used to identify, locate, and diagnose a tumor. After the highest diffuse tumor is detected, this tumor's image is then used to supervise radiotherapy planning and therapeutic assessment. Image modalities such as computed tomography, single photon emission computed tomography, magnetic resonance imaging (MRI), positron emission tomography, and others provide more information for understanding tumor structure and function. Image denoising gives a qualitative representation of the image, and it is very convenient for real-time applications in different medical fields but the interpretation of image segmentation relies upon the image denoising. Image segmentation is a widespread and active area not only for medical imaging but also for computer vision and satellite imaging. The main aim of image segmentation[1] is to segment images into different components, which are used to give more information about the image.

A different number of denoising and segmentation methods have been applied to MRI images, including a new MRI

 © 2018 Wiley Periodicals, Inc.

denoising technique that takes rough measurements of a low-slung-rampant tensor that may appear similar to regional MRI signals. The scheme contains a division of cubic patches similar to the tensor-4 for each three-dimensional (3D) model, using the similarity of reinforcements. The specified operational resemblance of 3D reinforcements, a low-slung-rampant tensor, remains on and disintegrates through higher-order singular value decomposition. The position of different tensor modes is adaptively determined by a noise level with indigenous image data. The 3D-MRI reinforcement baskets are efficiently riddled using a low-level tensor adaptive guesstimated using the sophisticated BM4D and adaptive nonlocal means denoising (ANLMD) threshold procedures. The proposed method goes beyond the latest determining procedures, including nonlocal transform domain filter for volumetric data (BM4D) and ANLMD methods implemented by Dong and Ying.[2]

Zhang and Shen[3] recommended an MRI denoising structure that uses structural correlations between subjects for adequate assessment of the no-noise signal. Nonlocal means denoising (NLMD) avoids the need for many acquisitions that require a lot of time. The aim of the NLMD is to expand the proposed auxiliary noise elimination framework to work with distributed weighted images. This method supports the consistency of study of the virtue of disorders.

Huang et al.[4] demonstrated frame-based image segmentation with additive noise and inhomogeneity of multiplicative intensity. On this background, local compute unified device architecture accelerators are mainly used to remove additional noise. Next, an embedded fuzzy c-means (FCM) method with bias correction is anticipated to segment the image with inhomogeneity of multiplicative intensity. The projected framework has been tested for both selected synthetic and actual images in addition to the public Berkeley Segmentation Dataset (BSD), Brain Web, and internet brain segmentation repository datasets. In BSD images, the approach demonstrates that the number of objects in each image is moderately different, and the primary goals of the model is to identify objects on the surface. The procedure is essential to recognize in advance how many classes should be shared, and the method is based on pixels that detect objects even if they are small. Consequently, the proposed method forecasts the number of objects in advance, analyzes statistical data with respect to intensity and presents a way of multiplying the method for segmentation results.

Chen and Yang[5] designed a competent image denoising procedure, which employs a partial differential equation (PDE) and generalized cross-validation (GCV) in a tetrolet transform field. The procedure uses the GCV model to yield the finest threshold value of noise statistics. In addition, to the other three analogous denoising procedures (curvelet, shearlet with Perona and Malik1 [PM1], and PM2) Tetrolet with GCV is the best when the noise level is high. The GCV with PM1 image stays flat, which supports supplementary superiorities in the original image.

Wang and Xinbo[6] suggested a method that consists of an image set level based on suspending the developing contour according to the size in the active pixel that must be inside or outside of the evolving contour. It has achieved this using an FCM partition matrix with the help of the Lattice Boltzmann Method and graphics processing unit. Hypothetical results from medical and real-world images showed good results for speed, efficiency and intensity inhomogeneities, accuracy, and noise immunity, based on the suggested method regardless of original contour. The system is faster and more appropriate for segmentation of three-dimensional images than other methods. The segmentation result can also be increased by presenting spatial information to the fuzzy external force, but care must be taken not to disrupt the parallelism of the method.

Liu et al.[7] recommended minmax concave total variation (MCTV) and applied it to the reconstruction of the MR brain image. MCTV is a method that is compatible with the alternating direction method of the multiplier algorithm. For each iteration, the convexity of cost-effectiveness can be preserved. The MCTV penetration has the ability to improve the gradient density of MR brain images compared to standard total variation and non-local total variation, thus reducing sample rates in brain imaging for better neuroscience results.

Bhaskar Rao et al.[8] presented a novel approach to reduce complications and to increase accuracy in the medical image segmentation procedure. In this regard, Berkeley Wavelet Transformation-based brain tumor segmentation and SVM-based classifier techniques were proposed.

Xing et al.[9] demonstrated a new method using an automatic cell detection algorithm with an adaptive dictionary learning procedure. An adaptive dictionary selection algorithm (ADSA) is used to control the appearance of cells. The recommended algorithm works well for cells with different images that present large differences in appearances and shapes. This method can effectively cope with the brain tumor's image.

The rest of the article is prepared in several sections: (1) The materials and methods are clearly explained (such as Adaptive PDE-based denoising and new convergent K-means clustering segmentation algorithms) in section 2; (2) The experimental results are presented in section 3; (3) Discussion about different parameters is given in section 4; and (4) Finally, the conclusion in section 5 is presented.

2 | MATERIALS AND METHODS

2.1 | Proposed denoising and segmentation algorithms

2.1.1 | Adaptive PDE-based denoising

Image denoising remains an essential component of processing images. An important attribute of the dynamic image

denoising method is to completely eradicate noise with perpetuate edges. One of these models is a linear model, and the other is non-linear. In some techniques, linear models are used because they have the advantage of speed.

Linear models cannot process the image's edges, and the image's boundaries are blurred. However, non-linear models can recognize the corners better than linear models. One of the non-linear models is the adaptive partial differential equation method. We demonstrated that this method can be used to denoise the image provided by $NI = OI + N$, in which OI is the original image, N is a value-added white Gaussian noise with an unknown variation or standard deviation (SD), and NI is the noisy image. In the fourth order, the PDE-derived method can minimize the functional energy of the Laplace image. Noise can be predicted as accelerated oscillating signals of small areas. It is essential to avoid high-frequency signals while retaining important image functions when it comes to digital images. It is the best method to handle truncated reckon time, which suppresses noise and smooths out the edges in the image. The adaptive PDE method is widely used in satellite and medical applications.

The APDE algorithm is a powerful method for denoising and has good relationships to image segmentation. The resulting image noise reduction directly affects the accuracy of image segmentation. This algorithm works to yield better images when compared with other traditional methods. Its performance is calculated in terms of mean squared error (MSE) and peak signal to noise ratio (PSNR). A small MSE value indicates a minor error that leads to a large PSNR. A high PSNR value indicates a better image quality. To get the denoised image, APDE-based denoising can be described according to a specific procedure: an MRI brain tumor noisy image is applied to a new adaptive Haar-type wavelet transform. This transform divides the entire image's coefficient based on the shapes of tetrominoes into different coefficients such as multiple lower and higher coefficients. After that, the threshold value of multiple higher coefficients can be determined using the soft thresholding method. Both of these coefficients are applied to the inverse wavelet transform. After getting a denoised image, it can be analyzed by the fourth order APDE method. Its purpose is to find the fourth order image using gradient and Laplacian operators. Finally, the difference between noisy and fourth order images is the perfect denoised image. Sections The contemporary adaptive Haar-type wavelet transform and Steps for determining fourth order APDE give the implementation shown in Figure 1 and is described below.

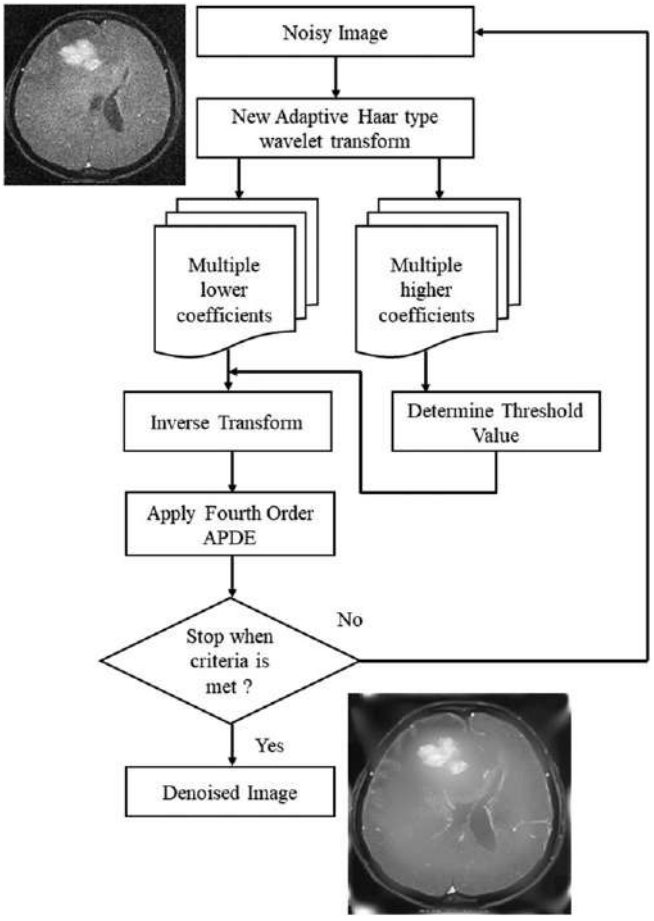

FIGURE 1 Flowchart of the APDE-based denoising algorithm

The contemporary adaptive Haar-type wavelet transform

To represent an image efficiently, we introduce a contemporary adaptive Haar wavelet transform,[10] termed Tetrolet Transform. There are five main shapes that fall into different image blocks. Each block has different coefficients such as multiple lower and higher coefficients as shown in Figure 2.

Figure 3 explains the principles of the Haar-type wavelet transform. After considering a case in which the input image size is 256 × 256 and the image is divided into 4 × 4 blocks using different shapes of tetrominoes, nearly 117 solutions are available. Now, we will have different filter coefficients such as low and high pass filter coefficients. For example, 256 × 256 can be arranged into 4 × 4 blocks in terms of low pass filter coefficients whose image size is 128 × 128 rearranged into 2 × 2 blocks or high pass filter coefficients whose image size is 64 × 64 rearranged into 2 × 2 blocks. It is then repeated to obtain low-frequency tetrolet coefficients and each time high-frequency coefficients are stored. Finally, an output image in the form of a decomposed image is produced.

To compute multiple lower coefficients the given formula is used (Equation (1)):

$$K^1 = \left(k^1[l,m]\right)_{l,m=0}^{\frac{M}{2}-1} \text{with } k^1[l,m] = \sum_{d \in f} \in [0,Q(d)]k[d] \quad (1)$$

The formula for multiple higher coefficients (Equation (2)) is

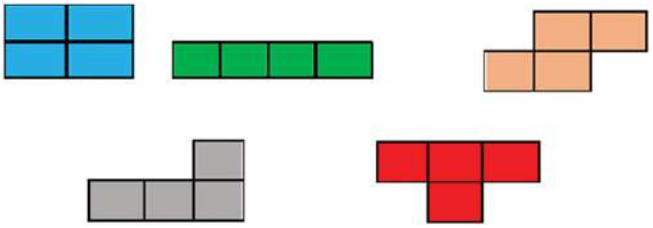

FIGURE 2 Different shapes of the tetrominoes [Color figure can be viewed at wileyonlinelibrary.com]

$$H_t^1 = \left(h_t^1[l,m]\right)_{l,m=0}^{\frac{M}{2}-1} \text{ with } h_t^1[l,m] = \sum_{d\in f} \in [t,Q(d)]k[d] \quad (2)$$

in which l, m, $d = (l', m')$ are integers or a set of integers, Q is used to align the pixels in a unique order, $f = P_{l,m}$ is the image index set, $k^1[l, m]$ is the input image in the form of multiple lower elements, $\in[0, Q(l', m')]$ and $\in[t, Q(d)]$ are the entries of the Haar wavelet transform matrix, $k[d]$ is the input image in the form of submultiple lower elements, t is an integer ($t = 1,2,3$), and M is the image size.

Determination of a threshold value

The threshold concept plays an essential role in denoising in addition to segmentation algorithms. In many algorithms, this concept is used because it is straightforward and robust for image processing. Depending on the type of noise detected in the image, the threshold is divided into two profiles: (1) soft thresholding and (2) hard thresholding.

We only use soft thresholding with generalized cross-validation. At a reasonable threshold, threshold image coefficients are set to zero, and the threshold value is subtracted from the image coefficients beyond the threshold value. The graphical representation of soft thresholding[11] as shown in Figure 4 indicates that a wavelet coefficient w between $-k$ and k is set to zero, while the others shrink in absolute value.

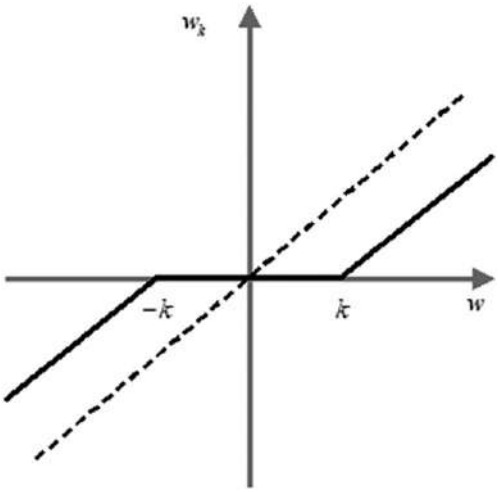

FIGURE 4 Concept of the soft thresholding

For example, set the threshold value at 2 and image coefficients at 0-5. Its threshold image coefficients are 0, 0, 0, 1, 2, 3.

The soft thresholding function is computed as shown in Equation (3):

$$\mathrm{ST} = \begin{cases} 0 \ if \left|r_{lm}^x\right| < k \\ r_{lm}^x - k \ \text{ otherwise} \end{cases} \quad (3)$$

The generalized cross-validation is computed as shown in Equation (4):

$$k = \frac{\frac{1}{m\times n}\left\|r_{lm}^x - \left(r_{lm}^x\right)'\right\|^2}{\left(\frac{(m\times n)-s}{m\times n}\right)^2} \quad (4)$$

in which r_{lm}^x is the coefficient after threshold function, $\left(r_{lm}^x\right)'$ is the coefficient before threshold function, k is a threshold value, m and n are the image's rows and columns, s is the number of coefficients that have been set to zero after the

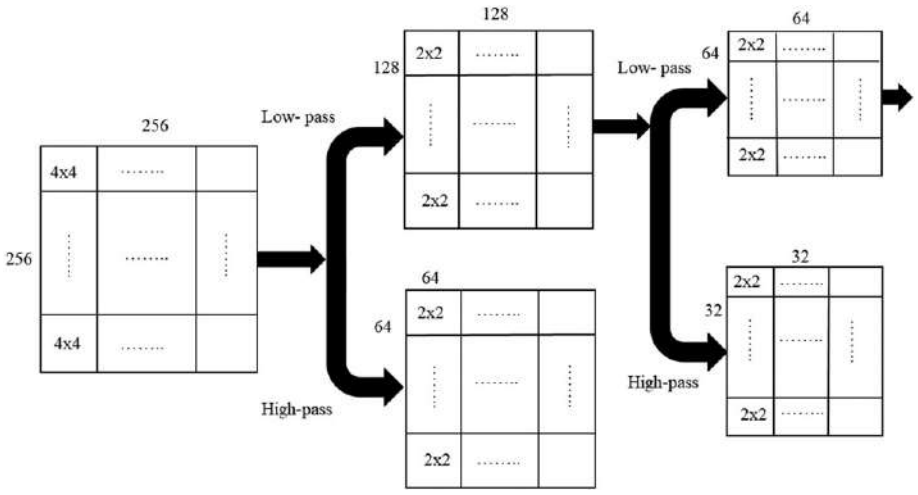

FIGURE 3 Diagram of the adaptive Haar-type wavelet transform of the image (256 × 256)

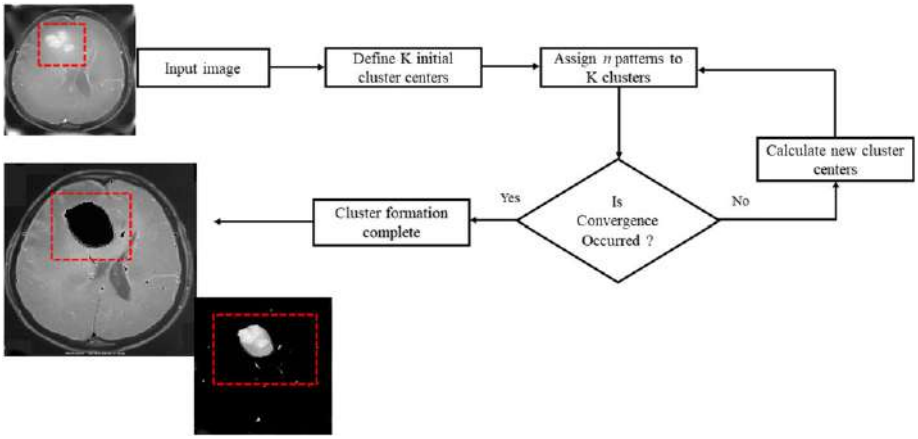

FIGURE 5 Flowchart of the new convergent clustering (NCKMC) [Color figure can be viewed at wileyonlinelibrary.com]

threshold has been managed, and ST is the soft thresholding function.

Steps for determining fourth order APDE

The fourth order APDE procedure is shown in the series of steps:

Step 1: Apply Laplacian operator mask for an input image.

Step 2: Laplacian is used to find the second order of the image and second order differential equation in matrix form:

$$\begin{bmatrix} 0 & -1 & 0 \\ -1 & 4 & -1 \\ 0 & -1 & 0 \end{bmatrix}$$

The second-order function depends on the first-order equation and is obtained by the gradient function (∇) and is depicted in the form of a first-order matrix: $\begin{bmatrix} 0 & -1 \\ -1 & 0 \end{bmatrix}$

$$D\left(\nabla^2 e\right) = h'\left(\left|\nabla^2 e\right|\right)\frac{\nabla^2 e}{\left|\nabla^2 e\right|} = c\left(\left|\nabla^2 e\right|\right)\nabla^2 e \qquad (5)$$

To obtain the coefficient $D(\nabla^2 e)$, the gradient of the processed image (∇e) is used to find the first-order matrix. It is known as first order mask is represented with $\begin{bmatrix} 0 & -1 \\ -1 & 0 \end{bmatrix}$.

By applying the first-order mask to Equation (5), it delivers the second order mask represented as $\begin{bmatrix} 0 & -1 & 0 \\ -1 & 4 & -1 \\ 0 & -1 & 0 \end{bmatrix}$.

Finally, the second order image will then be formed. Thus, this forms the relationship between Equation (5) and the first order matrix.

Equation (5) is used for determining the gradient for the whole convolution image (second-order image) in which c ($|\nabla^2 e|$) is the diffusion coefficient, Laplacian magnitude is $|\nabla^2 e|$, D is the differential operator, e is the processed image, and the higher order parameter is $h'(\circ)$.

Step 3: Step 2 is used to find the fourth order PDE.[12]

$$D^n_{k,m} = D\left(\nabla^2 e^n(i,j)\right) \qquad (6)$$

Equation (6) is the second-order image gradient ($n = 1$). This is done using Laplace convolution. If $n = 2$, then the Equation (6) is known as fourth order image gradient in which *i, j, n, m,* and *k* are integers and ∇ and ∇^2 are gradient and Laplacian operators.

Step 4: Output image = Input image fourth-order image.[13] This image is the denoised image.

2.1.2 | New convergent K-means clustering algorithm for segmentation

Medical image segmentation is a difficult task because of noise and artifacts. Often, we are looking for an object in an image that is smooth and has a closed boundary. The clustering techniques consist of different types, including hard and soft clustering. We have different types of hard clusterings. One is hierarchical, and the other is partitional. Partitional

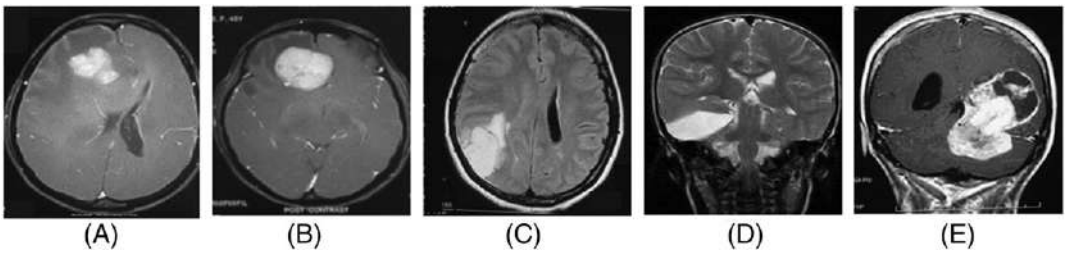

FIGURE 6 Five different MRI brain tumor images: (A) Axial1, (B) Axial2, (C) Axial3, (D) Coronal1, (E) Coronal2

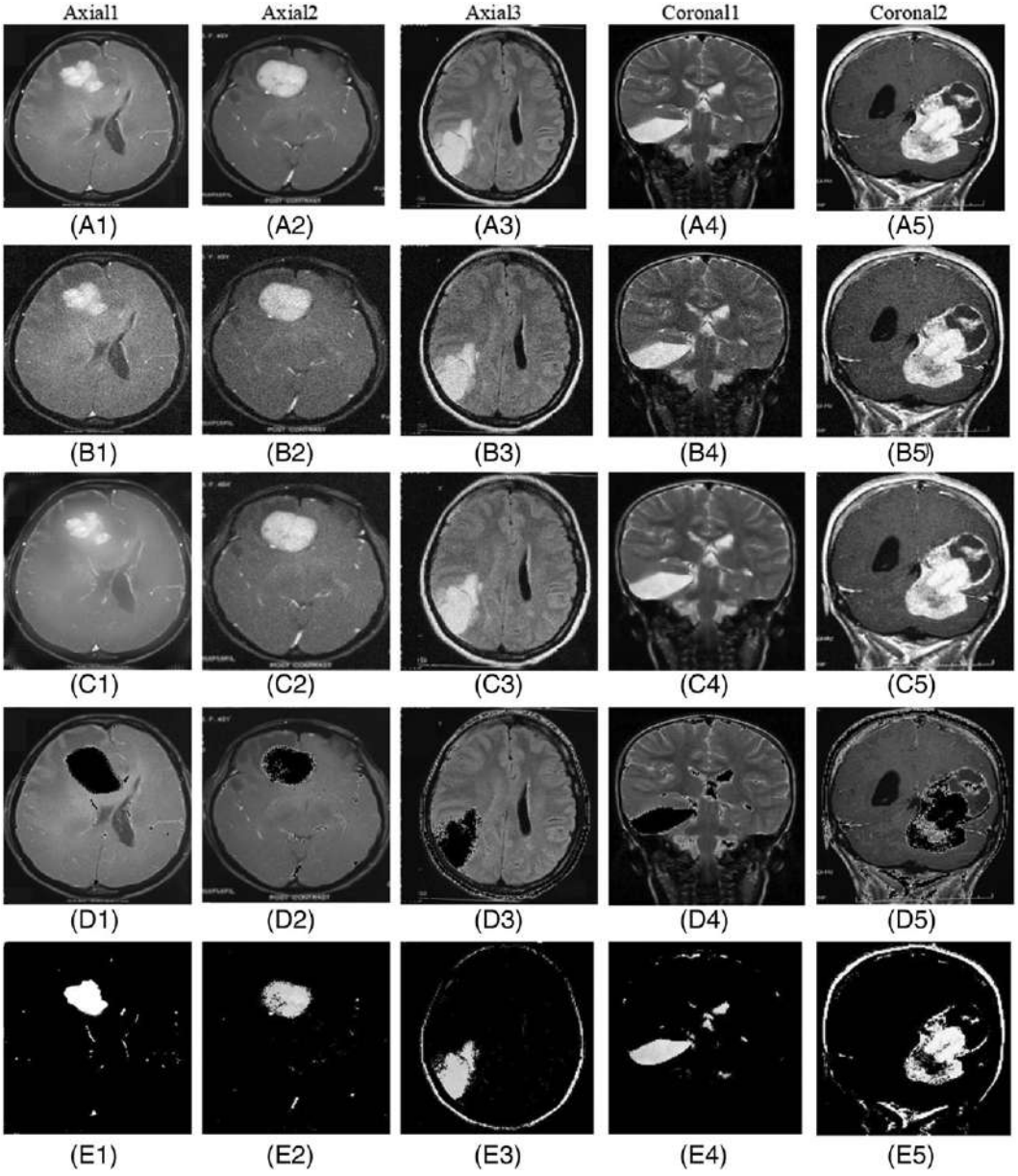

FIGURE 7 Denoised and segmented Axial1, Axial2, Axial3, Coronal1, Coronal2 brain tumor images using proposed algorithms (APDE and NCKMC): (A1-A5) brain tumor images, (B1-B5) noisy brain tumor images with $\sigma = 5$, (C1-C5) denoised brain tumor images, (D1-D5) segmented non-tumor images, (E1-E5) segmented tumor images

clustering algorithms create a hard or soft partition. The most widely used algorithm for this category is the new convergent K-means clustering (NCKMC) algorithm.[14]

The proposed segmentation algorithm works by searching for abnormal regions (tumor areas in MRI brain images) and to segment these areas from the normal regions (non-tumor areas in MRI brain images). Implementing this algorithm is simple and provides high-quality performance. The performance of the algorithm depends on the segmentation accuracy, a number of false-hits, missed-terms, and elapsed time. Segmentation accuracy results allow complete isolation of the tumor from abnormal MRI brain images. False-hit describes the number of wrongly sensed tumor pixels. Missed-term refers to the number of wrongly sensed non-tumor pixels. The time taken for the segmentation process to separate the tumor areas from the normal areas is the elapsed time. For the best-proposed segmentation algorithm, the SA is high, and false-hits, missed-terms, and the elapsed time is low.

The new convergent K-means clustering approach segments the tumor region from the abnormal brain image and can be described: NCKMC is a mathematical model that defines the way in which to automatically group different objects (tumor and non-tumor pixels). Group the objects based on minimum distance. Here, we used simple geometrical distance (also termed as the Euclidean distance [d]), which is calculated within each cluster between centroids and data points and between clusters. The main objective of NCKMC algorithm is to match each cluster with its respective centroid. Centroids are the center of each cluster.

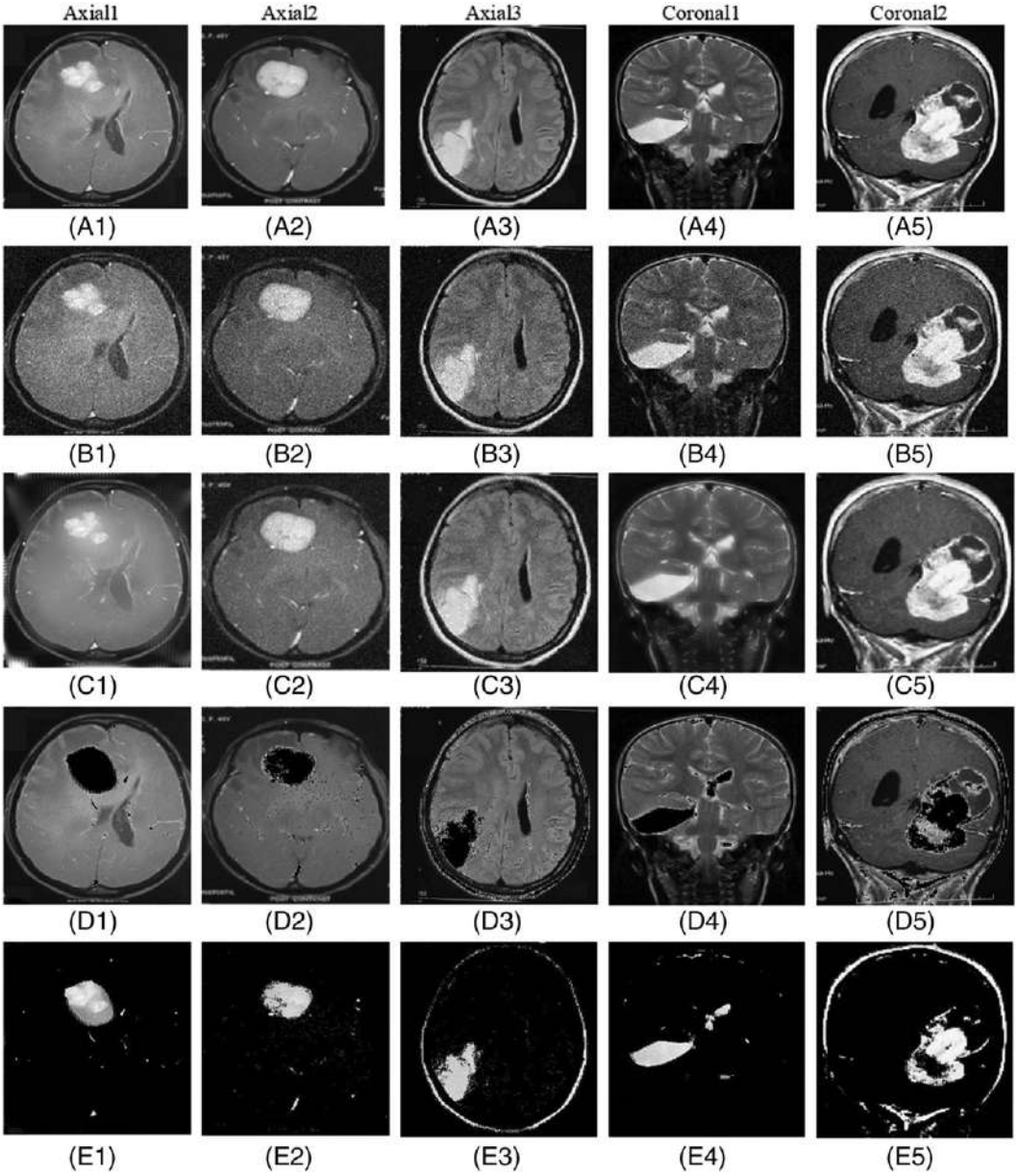

FIGURE 8 Denoised and segmented Axial1, Axial2, Axial3, Coronal1, Coronal2 brain tumor images using proposed algorithms (APDE and NCKMC): (A1-A5) brain tumor images, (B1-B5) noisy brain tumor images with $\sigma = 10$, (C1-C5) denoised brain tumor images, (D1-D5) segmented non-tumor images, (E1-E5) segmented tumor images

As an example: Suppose, we are looking at the MRI brain tumor image that is constructed with normal (non-tumor) and abnormal (tumor) pixels. Suppose the datasets represent tumor and non-tumor pixels. We decided to form two clusters (K_1 and K_2). This algorithm uses two centroids at first, and the algorithm randomly assigns these centroids simply because it does not know where the center of each cluster is. Next, distances come into play after a straight line is drawn between the two centroids and then a perpendicular bisector divides the line into two halves. This is called the boundary line, and its purpose is to establish the two clusters' regions (K_1 and K_2) and any data point that lies toward the left of the first cluster (K_1). Any point that is closer to the first cluster centroid is marked as a member of the first cluster while any data point closer to the second cluster centroid is marked as the member of the second cluster. This is dataset clustering (S), but some data points do not seem to belong to the second cluster as they are closer to the first cluster and should have been placed in the first cluster. In this case, K-means iterations come into play.

In the first iteration, the distances within each cluster are calculated once these distances are computed. The centroid is pulled toward the center of the cluster using the mean of these distances. The same happens with the second cluster centroid in which all of the distances are computed. The second cluster centroid moves closer to the center of its respective cluster. The same computing distance step between the two clusters is then repeated, and a new boundary line is drawn since centers have shifted. This shift occurs because data points that were previously in the second cluster now

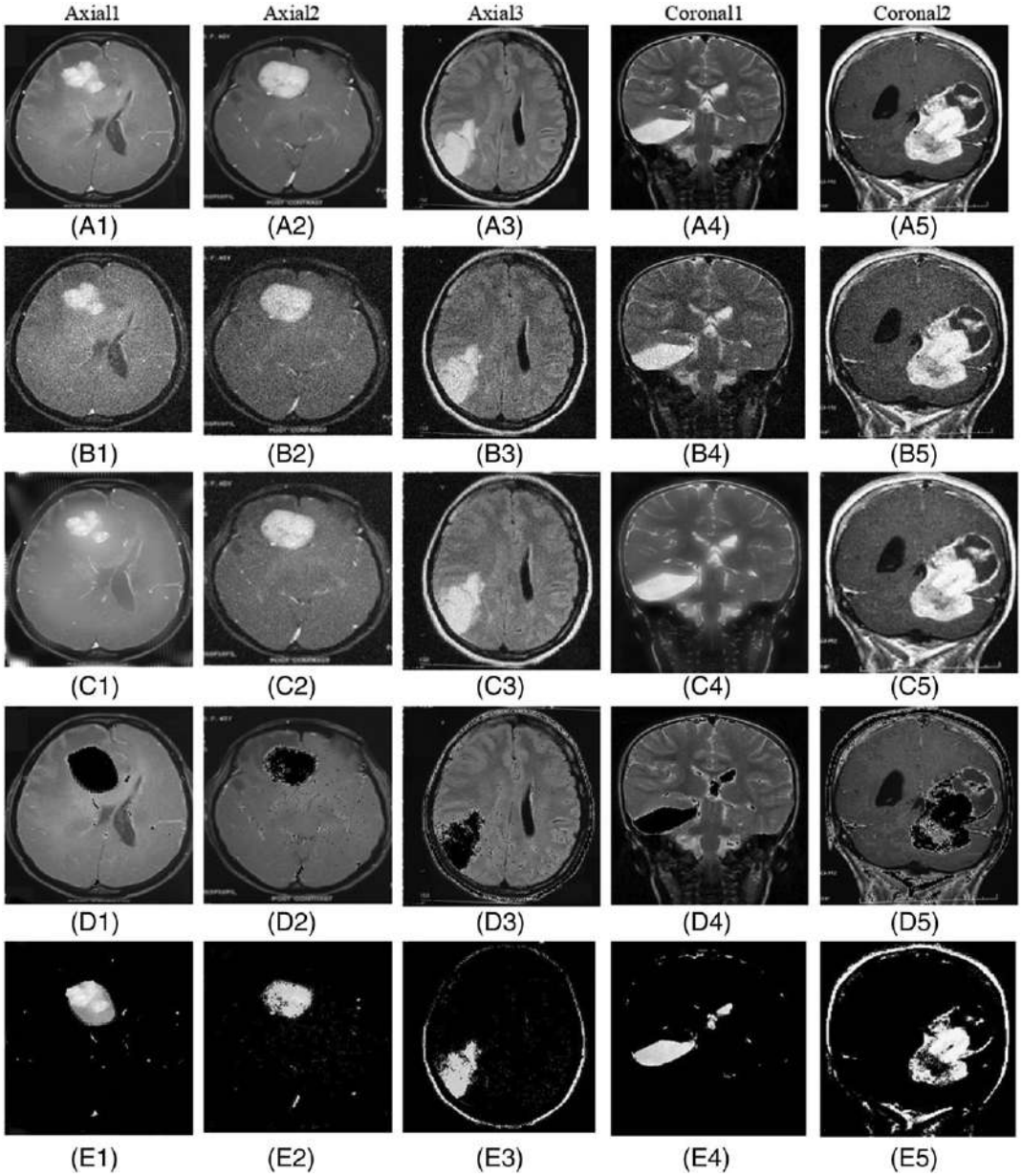

FIGURE 9 Denoised and segmented Axial1, Axial2, Axial3, Coronal1, Coronal2 brain tumor images using proposed algorithms (APDE and NCKMC): (A1-A5) brain tumor images, (B1-B5) noisy brain tumor images with $\sigma = 20$, (C1-C5) denoised brain tumor images, (D1-D5) segmented non-tumor images, (E1-E5) segmented tumor images

lie to the left of boundary line and will now be placed within the first cluster. This process continues until there are no more changes in the positions of both centroids and the boundary line after this iteration is completed. Once convergence is finished, cluster formation is complete. In this regard, the pixel of a tumor and the non-tumor is now isolated.

The flowchart of Figure 5 is described as follows.

Step 1: Select the *K*'s initial cluster centers. Define all *n* patterns in one of the *K*-clusters. The pattern is allocated to the nearest center/cluster.

Step 2: Calculate the cluster center to create the current pattern.

Step 3: Set all *n* patterns to the nearest center/cluster.

Step 4: If there is no alteration in assigning patterns for clusters in the course of two consecutive iterations, stop; otherwise, go to step 2.

Step 5: Once convergence is finished, cluster formation is then complete. Otherwise, repeat all of the above steps until the cluster is formed.

The new convergent K-means clustering algorithm reduces the number of abnormalities in squares from the inside of the cluster. If this a_r is the *r*th-cluster's centroid and *p*, *t*, and *M* are integers, the algorithm then has a minimized function (Equation (7)):

$$\sum_{r=1}^{M} \sum_{p \in \mathrm{r^{th}cluster}} (p-a_r)^t (p-a_r) \tag{7}$$

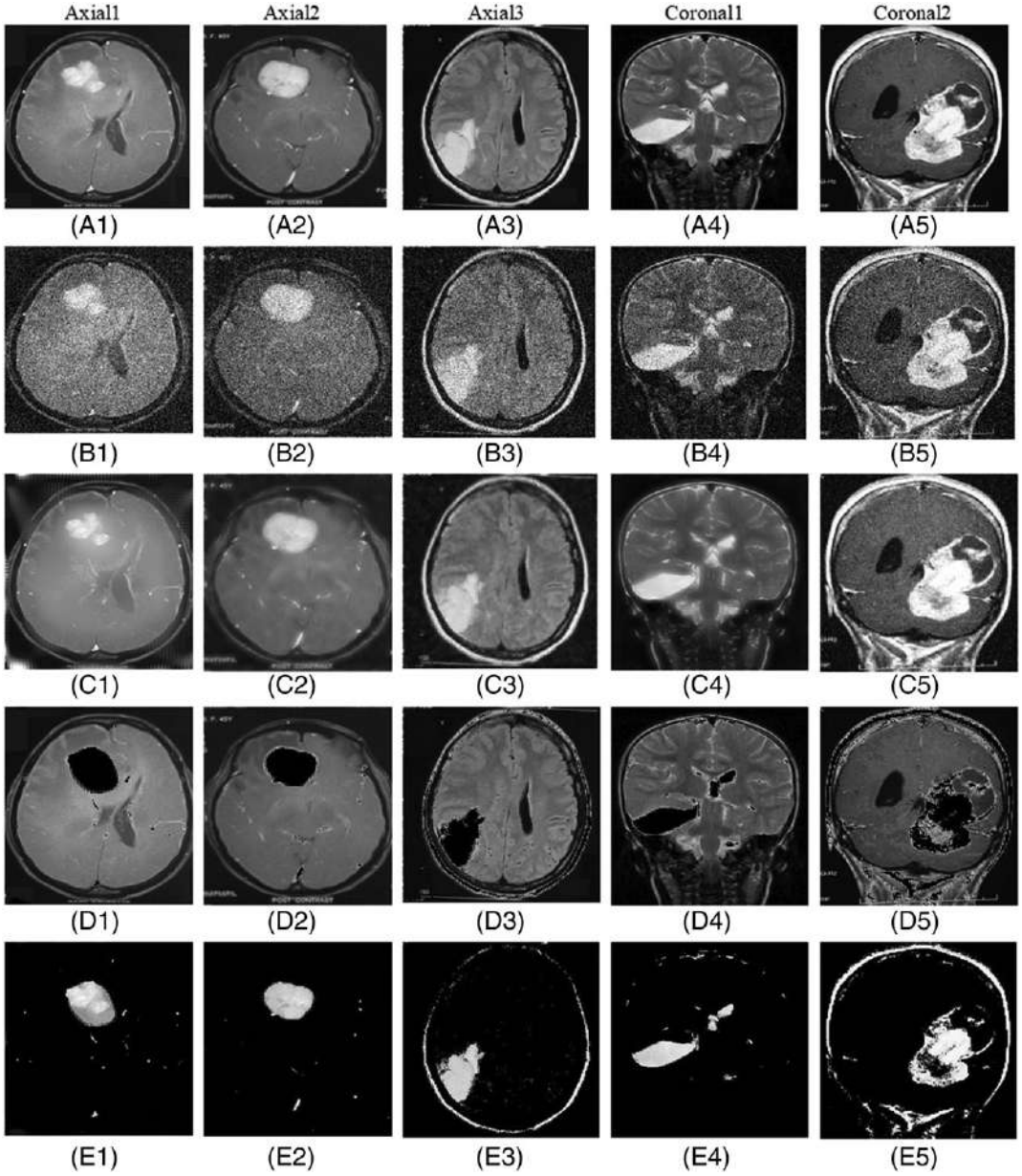

FIGURE 10 Denoised and segmented Axial1, Axial2, Axial3, Coronal1, Coronal2 brain tumor images using proposed algorithms (APDE and NCKMC): (A1-A5) brain tumor images, (B1-B5) noisy brain tumor images with $\sigma = 30$, (C1-C5) denoised brain tumor images, (D1-D5) segmented non-tumor images, (E1-E5) segmented tumor images

The following is the mathematical form of new convergent K-means clustering algorithm.

Let a number of clusters is equal to K (Assume $K = 2$). S is the input dataset.

$S = \{x_1, x_2, \ldots\ldots x_n\} \subset R^M$ and d is the Euclidean distance.

Step 1: $A_{l1}, A_{l2}, \ldots..A_{lk}$. Partition of S into k subsets.

Step 2:$A_{21} = A_{22} = \ldots A_{2k} = \Phi$

Step 3*:* Y_i = mean of A_{1i} and $i = 1, 2,\ldots k.$

Step 4: For $j = 1, 2,\ldots\ldots n.$

Put x_j in A_{2i}.

If $d\ (x_j, y_i) < (x_j, y_{i1}),\ i_1 \neq i.$

Step 5: If $A_{1i} = A_{2i}$ for all $i = 1, 2\ldots k$ then stops. Otherwise, rename A_{2i} as A_{1i} for all $i = 1,2\ldots.k$ and go to step 2.

3 | EXPERIMENTAL RESULTS

The performance of the proposed denoising (APDE)[15] and segmentation (NCKMC) algorithms are computed by PSNR, mean square error, structural similarity, segmentation accuracy, false-hits, missed-terms, and elapsed time. In testing the proposed algorithms, we have taken the MRI database images of size 256×256 from NeuroImaging Tools and Resources Collaboratory[16] and Brainweb.[17] In this case, all of the brain images are added using a Gaussian white noise with SDs, and its average value was zero. These two algorithms ran on the MATLAB R2015a software with the help of Lenovo IdeaPad 520 laptop, and its processor was Intel (R) Core (TM) i5-7200 CPU@ 2.50 GHz and

TABLE 1 Evaluation parameters of the proposed denoising algorithm (APDE) on five different medical images

σ(variance)	Tested images	MSE	PSNR	SSIM
5 (0.005)	Axial1	0.0099	68.1332	0.70309
	Axial2	0.0091	69.1522	0.41638
	Axial3	0.0099	68.1735	0.47432
	Coronal1	0.0045	71.5727	0.67445
	Coronal2	0.0105	67.8964	0.54269
10 (0.01)	Axial1	0.0163	65.9973	0.67964
	Axial2	0.0115	67.4943	0.34024
	Axial3	0.0116	67.4737	0.41521
	Coronal1	0.0068	70.2855	0.62833
	Coronal2	0.0091	68.5277	0.59695
20 (0.02)	Axial1	0.0153	64.1367	0.66453
	Axial2	0.0115	67.4936	0.34043
	Axial3	0.0114	67.5328	0.41654
	Coronal1	0.0071	69.5897	0.62206
	Coronal2	0.0112	67.6355	0.51314
30 (0.03)	Axial1	0.0152	63.9233	0.65231
	Axial2	0.0063	70.1303	0.62112
	Axial3	0.0097	68.2288	0.48923
	Coronal1	0.0062	70.1524	0.63191
	Coronal2	0.0112	67.6169	0.50895

2.71 GHz. The installed memory (RAM) was 4 GB (DDR4 2133 MHz), and the operating system was Windows 10 Home edition 64-bit based processor.

TABLE 2 Evaluation parameters of the proposed segmentation algorithm (NCKMC) on five different medical images

σ(variance)	Tested images	Accuracy (elapsed time[s])	True P/N	False P/N
5 (0.005)	Axial1	0.9415(08.154)	2000/59 686	3380/470
	Axial2	0.9755(04.336)	1900/62 034	1200/402
	Axial3	0.9618(15.480)	1886/61 147	2056/447
	Coronal1	0.9270(02.980)	1926/58 828	4300/482
	Coronal2	0.8827(23.071)	1909/55 942	7296/389
10 (0.01)	Axial1	0.9368(47.051)	2366/59 033	3613/524
	Axial2	0.9727(07.527)	1944/61 808	1460/324
	Axial3	0.9529(08.844)	2168/60 284	2824/260
	Coronal1	0.9218(28.149)	2016/58 399	4775/346
	Coronal2	0.8727(08.399)	2365/54 830	7906/435
20 (0.02)	Axial1	0.9166(42.226)	1894/58 181	5059/402
	Axial2	0.9723(06.155)	1986/61 737	1519/294
	Axial3	0.9602(10.128)	1911/61 019	2314/292
	Coronal1	0.9226(16.795)	1852/58 613	4548/523
	Coronal2	0.8851(15.011)	1966/56 045	7107/418
30 (0.03)	Axial1	0.9024(25.123)	2133/57 009	5906/488
	Axial2	0.9818(01.899)	1994/62 354	890/298
	Axial3	0.9638(02.498)	2110/61 055	2212/159
	Coronal1	0.9250(28.200)	2044/58 581	4412/499
	Coronal2	0.8886(05.211)	1988/56 251	6842/455

Abbreviations: True P/N-True Positive and Negative; False P/N- False Positive and Negative.

TABLE 3 Comparison of PSNR (dBs) of the proposed method (APDE) with different image denoising algorithms

σ(variance)	Tested images	MPDTDF (2017)[22]	PMRI (2017)[23]	SVM (PC) (2017)[8]	MCTV (2018)[7]	Proposed method
5 (0.005)	Axial1	31.0045	43.3359	55.4510	39.7445	**68.1332**
	Axial2	31.3002	42.5333	68.2100	37.1177	**69.1522**
	Axial3	31.2200	43.8339	56.2812	31.1177	**68.1735**
	Coronal1	29.0178	42.0011	58.7945	32.1129	**71.5727**
	Coronal2	30.5320	41.4450	59.6510	30.1266	**67.8964**
10 (0.01)	Axial1	31.0012	41.5001	54.6601	38.6444	**65.9973**
	Axial2	29.4560	40.2300	66.1433	36.5682	**67.4943**
	Axial3	30.4533	39.1214	55.1332	30.6927	**67.4737**
	Coronal1	31.5644	38.0135	57.0015	32.0384	**70.2855**
	Coronal2	28.2238	37.0123	56.7836	30.0224	**68.5277**
20 (0.02)	Axial1	30.8956	43.0145	53.4011	37.0011	**64.1367**
	Axial2	31.3312	41.2355	64.5610	35.1456	**67.4936**
	Axial3	31.0770	39.1044	55.1220	30.0498	**67.5328**
	Coronal1	30.4400	38.6612	58.0013	31.8799	**69.5897**
	Coronal2	29.8990	37.0123	56.0125	30.0015	**67.6355**
30 (0.03)	Axial1	31.3500	42.1122	52.0345	36.1200	**63.9233**
	Axial2	30.1245	41.0125	63.4450	34.1055	**70.1303**
	Axial3	29.1450	40.1253	56.4310	31.0076	**68.2288**
	Coronal1	29.3322	39.1245	52.0019	30.4410	**70.1524**
	Coronal2	25.6601	40.3322	55.1298	29.9880	**67.6169**

Abbreviations: MPDTDF, modified pyramidal dual-tree direction filter; PMRI, parallel magnetic resonance imaging; SVM(PC), support vector machine (proposed classifier); MCTV, minmax concave total variation.

3.1 | Subjective evaluation of algorithms

To evaluate the denoising[18] and segmentation algorithms, we considered five different MRI brain tumor images taken in the MRI databases such as www.nitrc.org[16] and Brainweb[17] as shown in Figure 6.

In Figure 6, the brain tumor images accompanied by white Gaussian noise was dependent on variance or SD and mean. If the mean value is zero for different values of σ and σ^2, the variance should be taken in the range 0-1. In this study, the standard deviations were taken as 5, 10, 20, and 30.

3.1.1 | Parameter analysis of the adaptive PDE-based denoising algorithm

The performance of the denoising algorithm depends on the mean square error, PSNR, and structural similarity.

MSE (Equation (8))[19] indicates the squared error between the enhanced and original image:

$$\mathrm{MSE} = \frac{1}{\mathrm{MN}} \sum_{p=1}^{M} \sum_{q=1}^{N} \left[A(p,q) - \widetilde{A}(p,q) \right]^2 \tag{8}$$

in which M and N are the rows and columns of the image, A and $\widetilde{A}$ are the original and enhanced images associated with variance or SD, and p and q are integers.

TABLE 4 Comparisons of false-hit, missed-term, and segmentation accuracy of the proposed method (NCKMC) with different segmentation algorithms

Methods	Tested images	False-hit	Missed-term	Total	Segmentation accuracy
Proposed method	Axial1	**3380**	**470**	**3850**	**0.9415**
	Axial2	**890**	**298**	**1188**	**0.9818**
	Axial3	**2212**	**159**	**2371**	**0.9638**
	Coronal1	**4300**	**482**	**4782**	**0.9270**
	Coronal2	**6842**	**455**	**7297**	**0.8886**
SVM(PC) (2017)[8]	Axial1	4512	991	5503	0.9112
	Axial2	1400	1000	2400	0.9651
	Axial3	4500	912	5412	0.9214
	Coronal1	6421	1100	7521	0.9100
	Coronal2	9543	1285	10 828	0.8454
ADSA (2017)[9]	Axial1	3501	1402	4903	0.9211
	Axial2	1600	1245	2845	0.9600
	Axial3	4986	1450	6436	0.9499
	Coronal1	7215	1432	8647	0.9156
	Coronal2	10 223	1489	11 712	0.8501
NNC (2017)[25]	Axial1	4655	1244	5899	0.9189
	Axial2	1900	1389	3289	0.9228
	Axial3	5443	1658	7101	0.9320
	Coronal1	7800	1756	9556	0.9122
	Coronal2	11 056	1896	12 952	0.8699
SRM(2015)[26]	Axial1	5148	1344	6492	0.8111
	Axial2	2546	1687	4233	0.8025
	Axial3	6870	2458	9328	0.8145
	Coronal1	8122	2188	10 310	0.8215
	Coronal2	10 288	2010	12 298	0.8300

Abbreviations: SVM(PC), support vector machine (proposed classifier); ADSA, adaptive dictionary selection algorithm; NNC, neural network classifier; SRM, Selvaraj Raghavan method.

PSNR (Equation (9)) used to compute the peak error and is represented in terms of decibels:

$$\mathrm{PSNR} = 10\log_{10}\left(\frac{\left(2^b-1\right)^2}{\mathrm{MSE}}\right) \tag{9}$$

in which b denotes the number of bits in an image. Consider an image size of 256×256 and the number of bits is 8. Thus, the PSNR for an 8-bit image is $10\log_{10}\left(\frac{255\times 255}{\mathrm{MSE}}\right)$ in decibels (dBs). If the image size is 512×512 and the number of bits is 9, then PSNR for the 9-bit image is $10\log_{10}\left(\frac{511\times 511}{\mathrm{MSE}}\right)$ dBs. The small MSE value indicates a minor error that will lead to a large PSNR. A high PSNR value indicates the better quality of the image.[20]

SSIM (Equation (10)) is a method to determine image eminence built on the decomposition of structural data. It is cast-off to associate the structures of the original and threshold image.

SSIM is computed as

TABLE 5 Comparison of elapsed time of the proposed method (NCKMC) with different segmentation algorithms

Methods	Tested images	Elapsed time (s)
Proposed method	Axial1	**08.154**
	Axial2	**01.899**
	Axial3	**02.498**
	Coronal1	**02.980**
	Coronal2	**05.211**
CBFCT (2017)[27]	Axial1	20.183
	Axial2	13.982
	Axial3	18.485
	Coronal1	16.641
	Coronal2	18.114
MFCM (2017)[28]	Axial1	33.001
	Axial2	19.523
	Axial3	18.011
	Coronal1	16.247
	Coronal2	19.445
BCFCM (2016)[29]	Axial1	1492
	Axial2	1488
	Axial3	1245
	Coronal1	1158
	Coronal2	1478
PSFCM (2015)[30]	Axial1	1671
	Axial2	1549
	Axial3	1332
	Coronal1	1450
	Coronal2	1436

Abbreviations: CBFCT, Cuckoo-based fuzzy clustering technique; MFCM, modified fuzzy c means; BCFCM, bias corrected fuzzy c means; PSFCM, partial supervision fuzzy c means.

$$\mathrm{SSIM}(p,q) = \frac{\left(2\mu_p\mu_q + D_1\right)\left(2\sigma_{pq} + D_2\right)}{\left(\mu_p^2 + \mu_q^2 + D_1\right)\left(\sigma_p^2 + \sigma_q^2 + D_2\right)} \tag{10}$$

in which μ_p and μ_q denotes the mean gray level of the image of p and q respectively, p and q are integers, σ_p and σ_q gives the SDs of p and q respectively, and σ_{pq} is the native sample correlation coefficient between p and q. D_1 and D_2 are constants and help to prevent instability if $\mu_p^2 + \mu_q^2$ are very close to zero. Here, $D_1 = D_2 = 0.8$. The SSIM[21] ranges from -1 to 1.

3.1.2 | Parameter analysis of the new convergent K-means clustering segmentation algorithm

The performance of the proposed segmentation algorithm is analyzed using the following evaluation parameters, which are defined as follows:

$$\text{Segmentation accuracy} = \frac{(\text{True P} + \text{True N})}{(\text{True P} + \text{False P} + \text{True N} + \text{False N})} \tag{11}$$

in which True P is true positive that delivers a number of suitable sensed tumor pixels, True N is true negative that delivers a number of suitable sensed non-tumor pixels, False

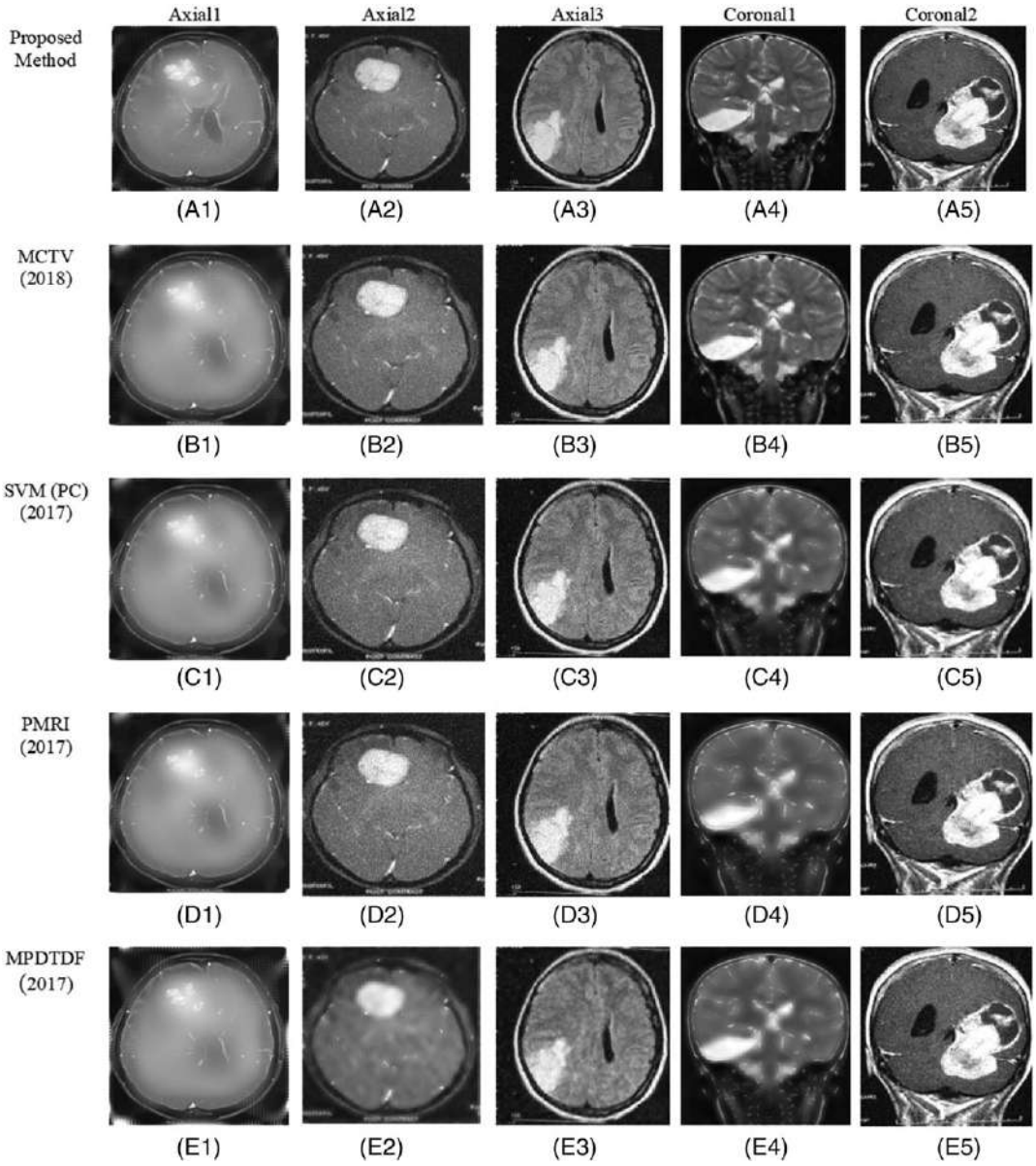

FIGURE 11 Comparison of different denoising algorithms with the proposed denoising method (APDE) by taking Axial1, Axial2, Axial3, Coronal1, and Coronal2 images with $\sigma = 5$: (A1-E1), (A2-E2), (A3-E3), (A4-E4), and (A5-E5) are denoised images of Axial1, Axial2, Axial3, Coronal1, and Coronal2

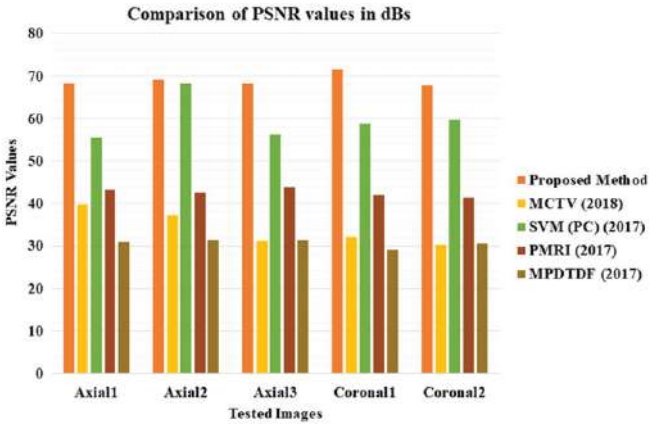

FIGURE 12 Comparison of PSNR (dBs) of the proposed method (APDE) with different image denoising algorithms [Color figure can be viewed at wileyonlinelibrary.com]

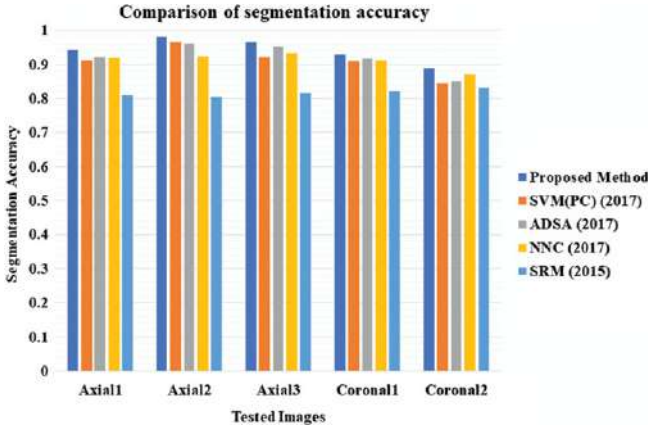

FIGURE 13 Comparison of the segmentation accuracy of the proposed method (NCKMC) with different segmentation algorithms [Color figure can be viewed at wileyonlinelibrary.com]

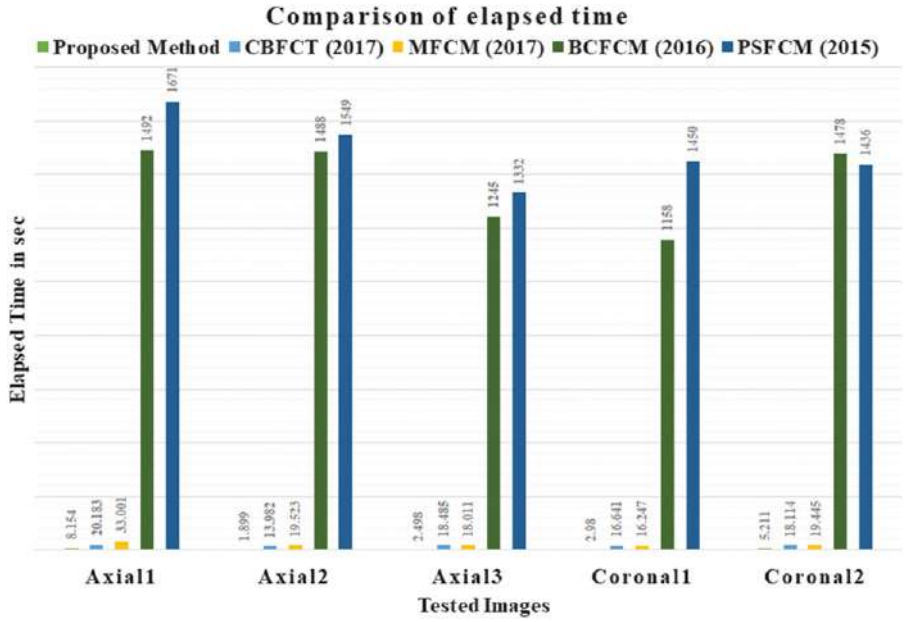

FIGURE 14 Comparison of elapsed time of the proposed method (NCKMC) with different segmentation algorithms [Color figure can be viewed at wileyonlinelibrary.com]

P is false positive (false-hits) that gives the number of unsuitable sensed tumor pixels, and False N is false negative (missed-terms) that gives the number of unsuitable sensed non-tumor pixels, respectively.

The time required to complete the segmentation process of the input image is known as elapsed time and is reported in seconds. The proposed segmentation method (NCKMC) requires less time to process input images.

The noisy brain tumor images of size 256 × 256 associated with SDs are 5, 10, 20, and 30 and act as an input to the denoising algorithm (APDE). The output of the denoising algorithm is applied as input into the segmentation algorithm (NCKMC). Thus, we have a denoised, segmented tumor, and non-tumor output images as shown in Figures 7–10.

4 | DISCUSSION

To compute performance parameters such as MSE, PSNR, SSIM, segmentation accuracy, and elapsed time in the proposed denoising (APDE) and segmentation algorithms (NCKMC) using different SD values was the aim of this study. In this article, we used the values such as 5,10, 20, and 30 as SDs as shown in Table 1.

We have chosen 5, 10, 20, and 30 as SDs for MSE, PSNR, and SSIM values of images from Axial1 to Coronal 2. Coronal1 had the best MSE value of 0.0045, PSNR was 71.5727, SSIM was 0.67445 under the SD of 5 (variance = 0.005). If the SD was set at 10 (Variance = 0.01), Coronal 1 had the best MSE of 0.0068, PSNR was 70.2855, and SSIM was 0.62833. If the SD was set at 20 (Variance = 0.02), Coronal1 had the best MSE of 0.0071, PSNR was 69.5897, and SSIM was 0.62206. When SD was set at 30 (Variance = 0.03), Coronal1 had the best MSE of 0.0062, PSNR was 70.1524, and SSIM was 0.63191 as shown in Table 1. Thus, lower MSE and higher PSNR and SSIM give the best results.

We have selected the SDs of 5, 10, 20, and 30 for the evaluation of performance parameters such as segmentation accuracy and elapsed time of images from Axial1 to Coronal2. Axial2 has the best accuracy of 0.9755 (SD = 5 and Variance = 0.005), Axial2 has the best accuracy of 0.9727 (SD = 10 and Variance = 0.01), Axial2 has the best accuracy of 0.9723 (SD = 20 and Variance = 0.02), Axial2 has the best accuracy of 0.9818 (SD = 30 and Variance = 0.03). Coronal1 has the best elapsed time of 2.980 seconds (SD = 5 and Variance = 0.005). Axial2 has the best elapsed time of 7.527 seconds (SD = 10 and Variance = 0.01). Axial2 has the best elapsed time of 6.155 seconds (SD = 20 and Variance = 0.02). Axial2 has the best elapsed time of 1.899 seconds (SD = 30 and Variance = 0.03) as shown in Table 2. Therefore, the best results are the most accurate and less elapsed time was the least important result.

According to Figure 1, the denoised image suffers from minor artifacts such as edge blurring and speckles. We suggest two reasons: (1) First, the proposed denoising APDE algorithm uses the GCV theory; it can achieve the optimal threshold noise reduction without knowing the statistical noise features. Thus, this method suppresses the high-frequency part such as noise and edges and maintains the low-frequency part of the image and (2) Second, the inappropriate choice of $c(|\nabla^2 e|)$ as the spatial varying coefficient or diffusion coefficient causes an image blur. So, this impact shows up on the proposed segmentation method. However, the proposed denoising and segmentation algorithms are better than the traditional methods as described in section 4.1.

4.1 | Comparison with other methods

In Table 3, PSNR values for all five methods are calculated using different types of MRI brain tumor images. Table 3 clearly states that the best PSNR of the proposed method (APDE) is 71.5725 dBs, which is better than the PSNR values of the existing methods such as minmax concave total variation (MCTV-39.7445 dBs),[7] support vector machine (proposed classifier) (SVM[PC]-68.2100 dBs),[8] parallel magnetic resonance imaging (PMRI-43.8339 dBs),[23] modified pyramidal dual-tree direction filter (MPDTDF-31.3500 dBs).[22] This is for denoising.[24]

Segmentation accuracy (SA), false-hit, and missed-term values were computed using different types of MRI brain tumor images as shown in Table 4. The comparison showed the best SA, false-hit, and missed-term values of the proposed method. NCKMC was 98.18%, 890, and 298, respectively, which was better than the existing methods such as support vector machine proposed classifier (SVM[PC]-96.51%, 1400, 1000),[8] adaptive dictionary selection algorithm (ADSA-96%, 1600, 1245),[9] neural network classifier (NNC-93.20%, 5443, 1658),[25] or Selvaraj Raghavan Method (SRM-83%, 10 288, 2010)[26] as shown in Table 4.

The elapsed time with all methods is given in Table 5. The proposed segmentation method (NCKMC) takes less time to find better results (1.899 seconds) than the other methods for segmentation and was better than the existing methods such as cuckoo-based fuzzy clustering technique (CBFCT-20.183 seconds),[27] modified fuzzy c means (MFCM-33.001 seconds),[28] bias corrected fuzzy c means (BCFCM-1492 seconds),[29] or partial supervision fuzzy c means (PSFCM-1671 seconds).[30] This is for segmentation.[31] Finally, the results of the proposed method presented in Tables 3–5 are highlighted in bold as compared to conventional methods.

Figures 11–14 show that the proposed methods for denoising are best represented by PSNR, SA, and elapsed time compared to the existing methods such as MCTV, SVM(PC), PMRI, MPDTDF for segmentation, SVM(PC), ADSA, NNC, SRM, CBFCT, MFCM, BCFCM, and PSFCM.

5 | CONCLUSION

In this article, we have two algorithms. One is for denoising, and the other is for segmentation. Experimental results show that these methods (APDE and NCKMC) are robust for medical images, particularly MRI brain tumor images, compared to other existing methods such as MCTV, SVM(PC), PMRI, MPDTDF, ADSA, NNC, SRM, CBFCT, MFC, BCFCM, and PSFCM. The performance of these two algorithms (APDE and NCKMC) were evaluated in terms of MSE, PSNR, and SSIM for denoising, SA, and elapsed time for segmentation. The proposed denoising algorithm (APDE) offers the best PSNR of 71.5727 dBs, and the utmost SA and elapsed time were 98.18% and 1.899 seconds provided by the proposed segmentation algorithm (NCKMC).

ACKNOWLEDGMENTS

The authors wish to thank the JNTUH University, G. Narayanamma Institute of Technology and Science (GNITS), and S.R Engineering College (Autonomous), India.

CONFLICT OF INTEREST

The authors declare that there is no conflict of interest regarding the publication of this article.

DATA AVAILABILITY

The MRI TumorSim and Brainweb data used to support the findings of this study were supplied by NITRC under license and so cannot be made freely available. Requests for access to these data should be made to NITRC, https://www.nitrc.org/projects/tumorsim, and www.bic.mni.mcgill.ca/brainweb.

ORCID

Sreedhar Kollem https://orcid.org/0000-0002-9203-0404

REFERENCES

1. Ma X, Cui B, Ma Y. Classification of visible and infrared HS images based on image segmentation and edge-preserving filtering. *Int J Infrar Phy Technol*. 2017;81:79-88.
2. Dong WH, Fu Y. 3D magnetic resonance image denoising using a low-rank tensor approximation. *J Neur Comput Lett*. 2016;195:30-39.
3. Zhang Pie YPT, Shen DG. Denoising MRI images using collaborative non-local means. *Neurocomputing*. 2016;177:215-227.
4. Huang M, Zhao D, Feng C. Image segmentation using CUDA accelerated non-local means denoising and bias correction embedded fuzzy C-means. *Int J Sig Process*. 2016;122:164-189.
5. Chen Y, Yang Y. Image denoising by using PDE and GCV in tetrolet transform domain. *Int J Eng Appl Artif Intell*. 2015;48:204-229.
6. Wang B, Xinbo G. A fast and robust L-set method for image segmentation using FC and lattice Boltzmann method. *IEEE Trans Cybern*. 2013;43(3):910-920.
7. Liu Y, Du H, Wang Z, Mei W. Convex MR brain image reconstruction via nonconvex total variation minimization. *Int J Imaging Syst Technol*. 2018;28(4):1-8.
8. Bhaskar Rao NB, Arun Kumar R, Harpal T. Image analysis for MRI based brain tumor detection and feature extraction using biologically inspired BWT and SVM. *Int J Biomed Imag*. 2017;2017:1-12.
9. Xing F, Yang L, Su H. Robust cell detection of histopathological brain tumor images using sparse reconstruction and adaptive dictionary selection. *IEEE Trans Med Imaging*. 2016;35:1575-1586.
10. Jens K. TT: a new adaptive HW algorithm for sparse image representation. *J Vis Comm Image Repres*. 2010;21(4):364-374.
11. Bhandari AK, Kumar D, Singh GK. Optimal sub-band adaptive thresholding-based edge preserved satellite image denoising using AD evolution algorithm. *Neurocomputing*. 2016;174:698-721.
12. Wang Z, Zhang Li KK. Bayesian reconstructions with PDE image model for emission tomography. In: Proceedings of the IEEE Nuclear Science Symposium Conference Record. Honolulu, HI, USA, 2007:4410-4414.

13. Lysaker M, Arvid L. Noise removal using fourth-order PDE with applications to MRI in space and time. *IEEE Trans Image Process*. 2003;12(12):1579-1590.
14. Waqas M, Khan A. Image de-noising using noise ratio estimation, K-means clustering, and non-local means-based estimator. *Int J Comput Electric Eng*. 2016;45:1-12.
15. Cong W, Wang X, Yang J. Denoising filters evaluation for MRI. *Int J Light Electro-Opt*. 2015;126:3844-3850.
16. MRI TumorSim database. https://www.nitrc.org/projects/tumorsim.
17. Brainweb database. http://brainweb.bic.mni.mcgill.ca/brainweb/.
18. Suman KM, Ashish P. Rough set based bilateral filter design for denoising brain MR images. *J Appl Soft Comput*. 2014;33:1-14.
19. Kang YH, Li Y. Tetrolet shrinkage with PDE for image denoising. *Nat Sci J Hain Univ*. 2011;29(2):166-171.
20. Jacques L, Oumar N. PDE-based approach for E-mode decomposition: application on image analysis. *IEEE Trans Image Process*. 2012;21(9):3991-4001.
21. Wang QL. DST: a new directional transform and compactly supported shearlet frames. *IEEE Trans Image Process*. 2010;19(5):1166-1180.
22. Teng L, Li H, Shoulin Y. Modified pyramid dual tree direction filter-based image denoising via curvature scale and nonlocal mean multigrade remnant filter. *Int J Commun Syst*. 2017;31(16):1-12.
23. Korti A. Regularization in parallel magnetic resonance imaging. *Int J Imaging Syst Technol*. 2017;00:1-7.
24. Chang WC, Zhang J. A novel segmentation-based video-denoising method with noise level estimation. *Int J Inform Sci*. 2014;281:507-520.
25. Borase V, Naik G, Londhe V. Brain MR. image segmentation for tumor detection using artificial neural. *Int J Eng Comput Sci*. 2017;6:20160-20163.
26. Selvaraj D, Raghavan D. Combining tissue segmentation and neural network for brain tumor detection. *Int Arab J Inf Technol*. 2015;12:42-52.
27. Alagarsamy S, Kamatchi K, Govindaraj V, Thiyagarajan A. A fully automated hybrid methodology using cuckoo-based fuzzy clustering technique for magnetic resonance brain image segmentation. *Int J Imaging Syst Technol*. 2017;27:317-332.
28. Almazrooie M, Vadiveloo M, Abdullah R. *GPU based Fuzzy C-Means Clustering Algorithm for Image Segmentation.* 2017;1–13: arXiv:1601.00072.
29. Aitali N, Cherradi B, Bouattane O, Youssfi M. Parallel implementation of bias field correction fuzzy C-means algorithm for image segmentation. *Int J Adv Comput Sci Appl*. 2016;7:375-383.
30. Cherradi B, Ali NA, Abbassi AE, Bouattane O, Youssfi M. CPU and GPU behaviour modelling versus sequential and parallel bias field correction fuzzy C-means algorithm implementations. *Contemp Eng Sci*. 2017;10:423-438.
31. Paul EC, Duarte JM, Guillermo S. Multiscale representation and segmentation of HS imagery using GPDE and AM Methods. *IEEE Trans Geosci Remote Sens*. 2008;46(8):2418-2434.

How to cite this article: Kollem S, Reddy KRL, Rao DS. Denoising and segmentation of MR images using fourth order non-linear adaptive PDE and new convergent clustering. *Int J Imaging Syst Technol*. 2018;1–15. https://doi.org/10.1002/ima.22302

Hu Moments Based Gesture Recognition using Back Propagation Neural Networks

[1]P.P.S.Subhashini,[2]Dr. M.SatyaSairam, [3]Dr. D.Sreenivasa Rao

[1]RVR& JC College of Engg,[2]CIET,[3]JNTUH
[1]saraswathi0859@gmail.com

Abstract

Day by day lots of efforts are being put towards developing an intelligent and natural interface between computer systems and users. Looking at the technologies .Now-a-days it has become possible by means of variety of media information like visualization, audio, paint etc. Gestures have become an important part of human communication to convey the information. Thus in this paper a method is proposed for Gesture Recognition which includes Hand Segmentation, Hand Tracking and various algorithms. The objective of this system is to explore the utility of a neural network-based approach to the recognition of the hand gestures that create a system that will easily identify the gestures and use them for device control and convey information instead of nor-mal input devices such as mouse and keyboard. The system consists of four modules: Hand Tracking and Segmentation, Feature Extraction, Neural Training and Testing.

Feed-Forward and Back Propagation algorithms are used for Gesture Recognition. Feed-forward normally refers to multi layer perception network in which the outputs from all neurons go to following layers but not preceding layers. So, there is no feed-back loops. Back propagation algorithm is used to identify the similarity between new input vector and previous trained patterns. The aim of this paper is to overcome the vision based challenges, such as dynamic background removal, variable lighting condition, skin color detection for Human Computer Interface. The main goal of this project is to design a system that will help the interaction between computer and human through the use of gestures.

1. Introduction

Neural Networks have seen explosion of interest over the last few years and are being successfully applied across an extraordinary range of problem domains, in areas as diverse as finance, medicine, engineering, geology, physics and biology. The excitement stems from the fact that these attempt to model the human brain's capabilities. Neural networks have emerged as a powerful tool because of its potential to predict and classify problems.

An ANN is based on a collection of connected units or nodes called artificial neurons which loosely model the neurons in a biological brain. Each connection, like the synapses in a biological brain, can transmit a signal from one artificial neuron to an-other. An artificial neuron that receives a signal can process it and then signal additional artificial neurons connected to it.

In common ANN implementations, the signal at a connection between artificial neurons are real number, and the output of each artificial neuron is computed by some non-linear function of the sum of its inputs. The connections between artificial neurons are called edges. Artificial neurons and edges typically have a weight that adjusts as learning proceeds. The weight increases or decreases the strength of the signal at a connection. Artificial neurons may have a threshold such that the signal is only sent if the

aggregate signal crosses that threshold. Typically, artificial neurons are aggregated into layers. Different layers may perform different kinds of transformations on their inputs. Signals travel from the first layer (the input layer), to the last layer (the output layer), possibly after traversing the layers multiple times.

The paper is organized as follows: In Section B contains technological background about the proposed model. In Section C contains experimental details and results. Finally conclusion is described in Section D.

2. Proposed Model

2.1 Gesture Recognition System

The hand gesture recognition system , consists of the following stages. The first stage is the hand gesture image capture stage where the images are taken using digital camera under different conditions such as scaling, translation and rotation [1].

The second stage is a pre-processor stage in which edge detection, smoothing, and other filtering processes occur. In the next stage, the features of the images of hand gesture are extracted using two methods, namely, region properties and invariant moments. The last stage is the classification using Artificial Neural Network (ANN), where the recognition rate is calculated and comparison is carried out. The following is a description of these stages. Block diagram of Gesture Recognition system is shown in the Figure 1.

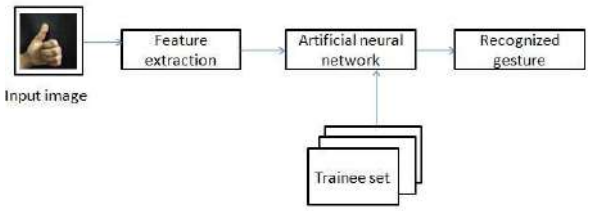

Figure 1. Gesture Recognition system

The input image is captured and given as input. The features of the input image are extracted and are given to a neural network. The neural network then compares it with the training set and gives the best suited gesture as output. The construction of a database for hand gesture (i.e., the selection of specific hand gestures) generally depends on the intended application. The gesture images have different sizes. In image capture stage, a digital camera of 16MP and 4x optical zoom is used to capture the images and each gesture is performed at various scales, translations, rotations and illuminations.

The database consists of 50 images (ten samples for each gesture). Employing relatively few training images facilitates the measurement of the robustness of the proposed methods, given that the use of algorithms that require relatively modest resources either in terms of training data or computational resources is desirable. In addition, it is generally considered that using a small data set to represent each class is of practical value especially in problems where it is difficult to get a lot of examples for each class. The primary goal of the pre-processing stage is to ensure a uniform input to the classification network. This stage includes hand segmentation to isolate the foreground (hand gesture) from the background and the use of special filters to remove any noise caused by the segmentation process [2].

2.2 Gesture Feature Extraction Methods

The objective of the feature extraction stage is to capture and distinguish the most relevant characteristics of the hand gesture image for recognition. The selection of good features can greatly affect the classification performance and reduce computational time. The features used must be suitable for the application and the applied classifier. Two different feature extraction methods were used as part of the proposed hand gesture recognition algorithm:

- Hu Moments
- Region Properties

2.3 Hu moments and Region Properties Feature extraction

Extracting invariant moments from a gesture involves a series of steps. They can be explained as follows: Represent image in the form of matrix. The image is then resized to fit the requirements of accuracy and further operations in feature extraction. The image is converted into a gray-scale image. Thresholding is done in order to convert the gray-scale image into a binary image. It separates the background from the actual gesture.

The following steps are performed to obtain features from the gesture image:Represent image in the form of matrix. The image is then resized to fit the requirements of accuracy and further operations in feature extraction. The image is converted into a gray-scale image. Thresholding is done in order to convert the gray-scale image into a binary image. It separates the background from the actual gesture. The Matlab function, regionprops () is used to calculate the required features namely Area, Perimeter, Major axis length, Minor axis length.

2.4 Multi-Layer Perceptron Neural Network

The Multi-Layer Perceptron Neural Network is used for implementation of the Ges-ture Recognition System. Multi-Layer Perceptron (MLP) is a type of artificial network for applications to problems of supervised learning such as pattern classification. A feed-forward network has a layered structure. Each layer consists of units which re-ceive their input from units from a layer directly below and send their output to units in a layer directly above the unit. There are no connections within a layer. The inputs are fed into the first layer of hidden units. No processing takes place in input units. The training output values are vectors of length equal to the number of classes. After training, the network responds to a new pattern [3].

This network consists of three layers, one input layer, number of hidden layers and one output layer. The activation of a hidden units of layer of $N_{h;1}$ is a function f of the weighted inputs plus a bias .The output of the hidden units is distributed over the next layer of $N_{h;2}$ hidden units, until the last layer of hidden units, of which the outputs are fed into a layer of N_0 output units [4].

The output of each hidden neuron is then weighted and passed to the output layer. The outputs of the network consist of sums of the weighted hidden layer neurons. The design of an MLP requires several decisions that include the number of hidden units in the hidden layer, values of the prototypes, the functions used at the hidden units and the weights applied between the hidden layer and the output layer. The performance of an MLP network depends on the number of inputs, the shape of the sigmoid function at the hidden units and the method used for determining the network weights. MLP networks are trained by selecting the weights randomly from the training data. Back propagation of errors is then used to assign correct weights to each node in the hidden and output layers.

The following are the steps to be followed in order to train the neural network. Consider a neural network having architecture consisting of the number of input nodes I, the number of hidden nodes J and the number of output nodes K. The 1-dimensional input z is passed directly to a hidden layer as shown in Figure 2.

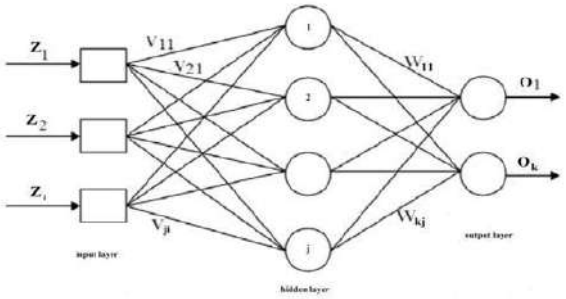

Figure 2. Multi Layer Perceptron Neural Network

By applying the feature vectors one by one to the input layer the output of hidden layer is computed by using equation 1. For j = 1, 2, …. J, where J is the number of neurons in hidden layer. The function f1(:) is unipolar Sigmoid Function .Output of output layer is computed by using equation 2 . for k=1,2,. . . K. Where K is the number of neurons in output layer. The function f2(:) is Generalized Sigmoid Function. The error value is computed by using equation 3.

$$y_j = f_1(v_j^t z) \tag{1}$$

$$O_k = f_2(w_k^t y) \tag{2}$$

$$E = \frac{1}{2}(d_k - o_k)^2 \tag{3}$$

3. Experimental Results

3.1 Input Consideration

The Input Dataset consists of 5 different gestures shown in Figure 3. Ten images of different orientations of each gesture are considered there by forming a dataset that consists of 50 images. Out of these, 35 images i.e. 7 different images of each gesture are used for training the neural network and 15 images i.e. 3 different images of each gesture are used for testing purpose.

3.2 Input vector

Input vector is extracted from Hu moments and Region properties and can be illustrated as shown in Figure 4 and Figure 5 for Guesture 1 .

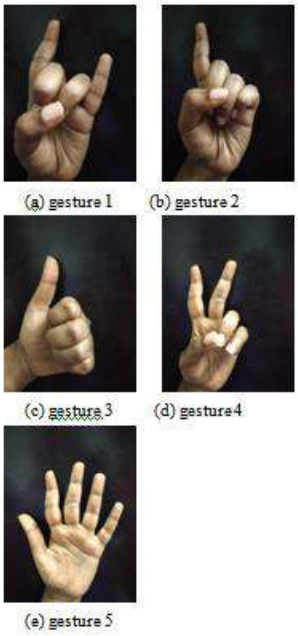

Figure 3. Gestures

GESTURE MODEL 1	Hu moments						
	I1	I2	I3	I4	I5	I6	I7
	0.2875	0.0054	0.0014	0.000102	2.73E-08	7.55E-06	2.73E-08
	0.2898	0.0055	0.0014	0.000135	2.73E-08	7.96E-06	2.31E-08
	0.2810	0.0056	0.0014	9.75E-05	1.87E-08	6.01E-06	1.59E-08
	0.2917	0.0053	0.0016	0.000126	2.95E-08	6.04E-06	1.75E-08
	0.2754	0.0054	0.0015	0.000118	1.29E-08	7.67E-06	1.78E-08
	0.2710	0.0057	0.0014	9.98E-05	1.87E-08	7.01E-06	2.59E-08
	0.2898	0.0053	0.0013	9.91E-05	1.87E-08	7.51E-06	1.65E-08
	0.2810	0.0053	0.0014	9.45E-05	1.87E-08	7.29E-06	1.97E-08
	0.2810	0.0056	0.0014	9.98E-05	1.87E-08	8.91E-06	1.64E-08
	0.2810	0.0055	0.0014	9.65E-05	1.87E-08	8.99E-06	1.99E-08

Figure 4. Hu Moments of Gesture 1

Gesture model 1	Region properties			
	Area	Perimeter	Major Axis Length	Minor Axis Length
	6167	1.26E+02	1.26E+02	97.26984
	6413	1.20E+02	1.20E+02	90.95424
	6433	1.20E+02	1.20E+02	88.50091
	6350	1.27E+02	1.27E+02	93.28359
	6121	1.22E+02	1.22E+02	93.00061
	6167	1.09E+02	1.51E+02	5.19E+02
	5413	1.86E+02	1.24E+02	77.13002
	6333	1.52E+02	1.21E+02	93.44799
	6350	1.22E+02	1.23E+02	93.63508
	5921	1.64E+02	1.35E+02	86.77585

Figure 5. Region Properties of Gesture 1

3.3 Target vector

The target Vector is represented in the form of a 50 X 5 matrix in which, 1 represents the expected output. The output is obtained at respective nodes for different gestures. The target vector for gesture 1 is shown in Figure 6.

Output	Node 1	Node 2	Node 3	Node 4	Node 5
G	1	0	0	0	0
E	1	0	0	0	0
S	1	0	0	0	0
T	1	0	0	0	0
U	1	0	0	0	0
R	1	0	0	0	0
E	1	0	0	0	0
1	1	0	0	0	0
	1	0	0	0	0
	1	0	0	0	0

Figure 6. Target vector of gestures

4. CONCLUSION

A gesture recognition system is designed to recognize 5 gestures .An input vector of 50×11 is obtained from feature extraction and a target vector of 50×5 is considered. 70% of the images are used for training, 15% are used for validation and 15% of images are used for testing by the back propagation neural network. The designed Gesture Recognition system has 96% accuracy.

5. REFERENCES

[1] Xia Liu and Kikuo Fujimura. (2004). "Hand Gesture Recognition using Depth Data", Proc. of the Sixth IEEE International conference on automatic Face and Gesture Recognition, pp. 529- 534.

[2] Dr. Jane J. Stephan, Sana'a Khudayer, " Gesture Recognition for Human-Computer Interaction (HCI)" International Journal of Advancements in Computing Technology Vol. 2, No. 4, October 2010.

[3] Deep Learning; Ian Goodfellow, Yoshua Bengio, Aaaron Courville; MIT Press; 2016, p 196.

[4] Hand Gesture Recognition Using Neural Networks by Klimis Symeonidis.

A Review of Image Denoising and Segmentation Methods Based on Medical Images

Sreedhar Kollem, Katta Rama Linga Reddy, and Duggirala Srinivasa Rao

***Abstract*—Image denoising and segmentation are required to use in digital image processing. For researchers' point of view, still, these two methods are challenging task in medical images. At present, image denoising and segmentation take part in real-world applications such as computer graphic, computer vision, satellite, and medical fields. These two methods are analyzed by using different images but mainly concentration on medical images such as computed tomography, single photon emission computed tomography, magnetic resonance imaging, positron emission tomography. Medical images can break into noise, major research has created solutions to this complication, various techniques are being proposed. Image segmentation is a widespread and active area not only for medical imaging but also for computer vision and satellite imaging. The foremost plan of image segmentation remains to segment images into different components, which are used to give more information about the medical image. Here is an overview of the different methods after a brief introduction. These methods are classified as the basis for the techniques used.**

***Index Terms*—Image denoising, Image segmentation, performance parameters, derivative based image denoising, clustering methods.**

I. Introduction

Digital image processing requires a computer to work with images, so it is fit aimed at image investigation, pattern recognition, together with human reflection. By means of computer knowledge, digital image processing has several applications over different industries such as face recognition, medical imaging, computer vision, remote sensing, and medical sciences.

Medical images such as computed tomography, single photon emission computed tomography, magnetic resonance imaging, positron emission tomography contains rich information, both anatomy, and functionality that can be used to diagnose, plan, and investigate operations. These images can be either a two-dimensional image or a three-dimensional image, which is solved in terms of both time and non-time.

A large amount of information on these pictures can be evaluated with simple visualization, but for quantitative measurements, the object must be divided into segments. Possible quantitative measurements such as organs size, heart infarct size, muscle weakness, tumor size, as well as tumor progression or regression or other developmental disorders [1].

Medical imaging analyzes image denoising and segmentation. First, Image denoising [2] stays regular process in digital image processing. It remains a pre-processing period to eradicate certain unidentified such as Additive White Gaussian noise (AWGN) from an image to get a clean image used in favor of image processing, such as image segmentation. Image segmentation is an alternative outlet of the image. A representative instance of the image processor is image denoising prototypical. This method incorporates a disintegrated prototypical giving to some prior information of a corrupted image. To reestablish the distorted image in favor to obtain an auspicious result.

In this instance, n_0 tells about noisy medical image and w is an original, nevertheless usually known or unknown image i.e.,

$$n_0 = Dw + n_1 \quad (1)$$

in which D is a linear or non-linear operator representing the distortion and n_1 is additive noise.

Second, segmentation is the most important technique for image processing to identify image objects. Image segmentation stays a progression which splits images into different sections or objects originate on a number of features such as intensity, color or location of the pixels. Segmentation of images is a central theme of analysis about medical image because there are many different types of images and the solution to this problem is different from the application. Some segmentation methods often have poor results, as they do not use previous information about objects containing elements to be segmented [3]. Finally, the image segmentation depends on the image denoising. In recent years, many techniques have been implemented in both image denoising and segmentation. Here is an overview of some techniques, including simple methods that have improved the results in this area. The techniques were explained sequentially in the next section.

The rest of the article is prepared into several sections: i) Literature survey on image denoising and image segmentation methods are offered in Section II; ii) Data availability is introduced in Section III; and iii) Lastly, the conclusion in Section IV is represented.

II. Literature Survey

A. Image Denoising Methods

Image denoising is a key issue of image processing applications, such as computer vision and medical science. The performance of the Image denoising method is measured

Manuscript received December 5, 2018; revised April 15, 2019.

Sreedhar Kollem is with the JNTUH University, Telangana, India and also Dept of ECE, S R Engineering College (Autonomous), Warangal, India (e-mail: ksreedhar829@gmail.com).

K. Rama Linga Reddy was with G. Narayanamma Institute of Technology and Science, Hyderabad, Telangana, India. He is now with the Department of ETM (e-mail: kattareddy2000@yahoo.com).

D. srinivasa Rao is with the ECE Department, JNTUH College of engineering, Hyderabad, Telangana, India (e-mail: dsraoece@gmail.com).

doi: 10.18178/ijmlc.2019.9.3.800

by using the important factors such as Mean or Average pixel intensity, Standard Deviation, Mean Square Error, Root Mean Square Error, Mean Absolute Error, Peak Signal to Noise Ratio, Structural Similarity, Universal Image Quality Index, and Entropy [4].

B. Performance Parameters of Image Denoising Methods

1) Mean

It determines the dissimilarity of the image by adding all the pixels and dividing the total pixels of the image.

$$Mn = \frac{\sum_{x_1=1}^{A}\sum_{x_2=1}^{B} Q(x_1, x_2)}{A \times B} \tag{2}$$

where $Q(x_1, x_2)$ is the intensity value at the pixel location (x_1, x_2), Mn is mean or average pixel intensity, A and B are the rows and columns of the image [5].

2) Standard Deviation (SD)

It refers to the current value of the pixel intensity relative to the image's pixel intensity.

$$SD = \sigma = \left(\frac{\sum_{x_1=1}^{A}\sum_{x_2=1}^{B} \left(Q(x_1, x_2) - Mn\right)^2}{A \times B} \right)^{\frac{1}{2}} \tag{3}$$

3) Average gradient (Ag)

It gives the sharpness and clarity of the image is

$$Ag = \frac{\sum_{x_1=1}^{A}\sum_{x_2=1}^{B} \left(\left(Q(x_1, x_2) - Q(x_1+1, x_2)\right)^2 + \left(Q(x_1, x_2) - Q(x_1, x_2+1)\right)^2 \right)^{\frac{1}{2}}}{A \times B} \tag{4}$$

4) Mean Square Error (MSE)

It remains to calculate image fidelity or to find the difference between two images respectively.

$$MSE = \frac{1}{A \times B} \sum_{x_1=1}^{A}\sum_{x_2=1}^{B} \left[Q(x_1, x_2) - \tilde{Q}(x_1, x_2) \right]^2 \tag{5}$$

where A and B are the rows and columns of the image, Q and $\tilde{Q}$ are the original and enhanced images, x_1 and x_2 are integers [6].

5) Root Mean Square Error (RMSE)

The representation of RMSE is

$$RMSE = (MSE)^{\frac{1}{2}} = \left(\frac{1}{A \times B} \sum_{x_1=1}^{A}\sum_{x_2=1}^{B} \left[Q(x_1, x_2) - \tilde{Q}(x_1, x_2) \right]^2 \right)^{\frac{1}{2}} \tag{6}$$

6) Mean Absolute Error (MAE)

The MAE measurement is accomplished to find proximity between fused and source image. Its mathematical equation is

$$MAE = \frac{1}{A \times B} \sum_{x_1=1}^{A}\sum_{x_2=1}^{B} \left| Q_f(x_1, x_2) - Q_I(x_1, x_2) \right| \tag{7}$$

in which $Q_f(x_1, x_2)$ is a fused image, $Q_I(x_1, x_2)$ is the source image respectively.

7) Peak Signal to Noise Ratio (PSNR)

PSNR tells about the revamped image is defined as

$$PSNR(dB) = 10 \log_{10} \left(\frac{\left(2^q - 1\right)^2}{MSE} \right) \tag{8}$$

where q gives the number of bits in an image, MSE means mean square error respectively.

8) Structural Similarity (SSIM)

It tells about the image quality in image processing. SSIM depends on three parameters such as luminance, contrast and structural term. The product of these parameters gives the SSIM of the image. The parameter $L(x_1, x_2)$ is the luminance assessment function determines the quality of having only a small margin between two images in terms of mean luminance (μ_{x_1} and μ_{x_2}). The parameter $C(x_1, x_2)$ is the contrast assessment function compute the quality of having only a small margin between two images in terms of standard deviations (σ_{x_1} and σ_{x_2}). The parameter $S(x_1, x_2)$ is the structure assessment function determines the correlation coefficient between two images in terms of covariance ($\sigma_{x_1 x_2}$).

$$SSIM(x_1, x_2) = \left\lfloor L(x_1, x_2) \right\rfloor a_1 \times \left\lfloor C(x_1, x_2) \right\rfloor b_1 \times \left\lfloor S(x_1, x_2) \right\rfloor c_1 \tag{9}$$

where,

$$L(x_1, x_2) = \frac{2\mu_{x_1}\mu_{x_2} + U_1}{\mu_{x_1}^2 + \mu_{x_2}^2 + U_1} \tag{10}$$

$$C(x_1, x_2) = \frac{2\sigma_{x_1}\sigma_{x_2} + U_2}{\sigma_{x_1}^2 + \sigma_{x_2}^2 + U_2} \tag{11}$$

$$S(x_1, x_2) = \frac{\sigma_{x_1 x_2} + U_3}{\sigma_{x_1}\sigma_{x_2} + U_3} \tag{12}$$

where μ_{x_1} and μ_{x_2} are the local mean, σ_{x_1} and σ_{x_2} are the standard deviation, $\sigma_{x_1 x_2}$ is the cross-covariance of x_1, x_2 for the image. Assume $a_1 = b_1 = c_1 = 1$, $U_1 = (R \times S_1)^2$ and $U_2 = (R \times S_2)^2$.

where R is the size of the image (256 for 8-bit grayscale images), U_1 is a small constant value at $S_1 << 1$, U_2 is positive constant value at $S_2 << 1$ and $U_3 = U_2/2$.

The simplified version of SSIM is

$$SSIM(x_1, x_2) = \frac{\left(2\mu_{x_1}\mu_{x_2} + U_1\right)\left(2\sigma_{x_1 x_2} + U_2\right)}{\left(\mu_{x_1}^2 + \mu_{x_2}^2 + U_1\right)\left(\sigma_{x_1}^2 + \sigma_{x_2}^2 + U_2\right)} \tag{13}$$

9) Universal Image Quality Index (UQI)

It determines image distortion by combining three factors, such as contrast distortion, loss of correlation, and luminance distortion.

$$UQI = \frac{\left(4 \times \sigma_{x_1 x_2}\right)\left(\mu_{x_1} + \mu_{x_2}\right)}{\left(\mu_{x_1}^2 + \mu_{x_2}^2\right)\left(\sigma_{x_1}^2 + \sigma_{x_2}^2\right)} \tag{14}$$

10) Entropy

Entropy statistical action demonstrates the ailment or intricacy of the image

$$E = -\sum_{x_1=0}^{A-1}\sum_{x_2=0}^{B-1} g(x_1, x_2) \times \log\left(g(x_1, x_2)\right) \qquad (15)$$

where $g(x_1, x_2)$ is the intensity value at the pixel location (x_1, x_2), x_1 and x_2 are integers respectively.

There are other algorithms and general technologies designed intended for image denoising. These are listed below:

Statistical Modeling based image denoising

In this category, various authors suggest new algorithms to set up statistical models. New algorithms are discussed below.

Wang *et al.* (2018) [7] demonstrated the non-convex total variation minimization and it is a general technique used in the gradient field as a cross-sectional image. The author discusses the problem of MR brain image reconstruction of extremely subordinate Fourier measurements. The author presents the minimax-concave TV (MCTV) to reconstruct the MR brain image. MCTV is non-convex, mainly to represent the nonconvexity parameter properly and at the same time maintain a convexity for every iteration step. MCTV may receive promotional applications in the area of neurology in the future.

Park *et al.* (2016) [8] presented parallel imaging using multilayer perception for MR image denoising. The author has several contrasting MR images with similar structural information and noise patterns on images used to realize PI technologies. The author suggested a method of learning-based denoising. This significantly reduces PI noise and the start-up time is much faster. It creates high-quality images that do not have degrading information to increase speed.

Zhang *et al.* (2016) [9] demonstrated an MRI denoising framework that structurally correlates between users to evaluate the models efficiently to reduce noise in the signal. This eliminates the need for long-term multi-acquisition. This will help the reliability in a survey of the integrity of white material on the development, aging, and disorders.

Waqas *et al.* (2016) [10] highlighted significant issues in confiscating random noise as of digital images with control filter, in detecting impulse noise, which is a random, shadowed disparity of the image. New noise detection algorithms were proposed based on the grouping of K-means clustering with Non-Local Means based filter. Luo-statistic has been developed a non-local means-based estimator. In this work, the first step in assessing the noise ratio before detecting noise. This estimate agrees to choose appropriate constraints aimed at noise detection procedure. In a faulty phase, pixels are restored to interfere with their actual values. Using this global dataset, this method shows that noise cancellations can be effectively erased. A widespread evaluation of counterfeit results with already reported results reveals that the anticipated process is excessive operative than existing noise abatement technology for both noise and image enhancement.

Derivative-based image denoising

Magudeeswaran *et al.* (2017) [11] have launched the concept of a new approach for machine learning and is used to enhance and segment the medical image. The author develops a novel level-set technique originate from the active contour prototypical. This technique diminishes the costly initialization of a level set technique further efficiently. Primarily, images are pre-processed with the Contrast Limited Fuzzy Adaptive Histogram Equalization (CLFAHE) improvement technique to enhance dissimilarity of the image. The improved images remain segmented by means of the projected system. This technique associated the GAC and Chan-Vese (C-V) prototypical with the advantages of local and global segmentation. In conclusion, image entropy, Absolute Mean Brightness Error (AMBE), PSNR and Feature Similarity Index (FSIM) were found and this gave the best results.

Yang *et al.* (2016) [12] proposed for image denoising algorithm using PDE and GCV. Through the proposed algorithm, the blocking effect is reduced by tetrolet transformation and is considered to be good. Because suggested procedure used the GCV theory to get finest denoising threshold short of knowledge of the statistical possessions of noise. Related to various comparable denoising procedures, Tetrolet + GCV + PM1 supports PSNR images are best once noise intensity is high. The images taken through T_GCV_PM1 are flat with maintaining the boundaries, facts of the original image.

Sedaaghi *et al.* (2016) [13] state that diffusion has even been made is an important element of the partial differential equation (PDE) imaging denoising procedures. Generally, diffusion coefficient, Perona-Malik (PM) are extensively cast-off algorithm for noise cancellation based on PDE. Diffusion coefficient PM analyzes the flux. Based on the PM flux analysis aimed at areas with a slope height, the brightness can lead to unwanted ambiguities and conflicts. To solve these problems, the image remains bisected into three slices, depending on gradient level: the area where the slope is inferior to the smoothness of the area, where the slope is between the smoothness and the flux point and the slope area is higher than the flux point. The author defines conditions to remain taken into account in these three parts. Then, all of these terms are calculated after the diffusion is even made. The test results confirm that the proposed method is best by means of signal-to-noise ratio, mean structural similarity, universal quality index, and feature similarity.

Lundervold *et al.* (2003) [14] confirmed the novel technique aimed at image smoothing about the fourth order PDE technique. This scheme remains monitored in many realistic medical MRI and non-medical synthesized test images are represented with different domains. This algorithm has a good noise reduction without destroying a substantial anatomical or functional detail.

To overcome overshoots and avoid the edge blurring, the author defines the FODE-based edge-conversing regularization filter aimed at noise elimination and is one of non-linear anisotropic diffusion. The comparison with the results clearly shows that the proposed scheme is better than the LLT model about eliminating noise whereas sharply preserving the edge structures by Huang *et al.* (2011) [15].

The author presented piecewise planarity conditions aimed at FO variational denoising methods in the field. Ineffective imitation of FO variational schemes, the author has come up with mathematical approaches for instances variable constraint parameter and stable step size. While PPCs are not fulfilled with the same information, they can be a valuable mathematical tool for creating the ultimate method for PDE-based denoising. The PPC model demonstrated the ability to take measurements measured in PSNR (and visual inspection) better than the PPC model. The FO variational methods can reinstate improved images than other systems, predominantly after embracing the PPCs. FO methods take reinstated texture areas positively, whereas other methods have a tendency on the way to re-establish the boundaries of huge differences evidently by Lim *et al*. (2009) [16].

To eradicate the staircasing consequence aimed at TV filter together with evading boundaries distorting in support of fourth-order PDE filter, the author suggested the anisotropic diffusion in favor of image denoising. In anticipated prototypical, the H−1 -model is treated by way of reliability tenure remains possessed of a TV regularization together with a fourth-order filter. When the pixels are on the boundaries, the TV filter is nominated so that they can retain the edges. If the pixels are part of the flat area, a fourth-order filter is accepted that can remove the staircase artifacts. Hypothetical consequences are seen that the anticipated prototypical exceeds most modern models presented in the form of qualitative and quantitative assessments by Tan *et al.* (2016) [17].

C. Image Segmentation Methods

Image segmentation remains an important issue of image processing applications, such as computer vision and medical science. The segmentation purpose is to split the image into parts, which are a specific application. The quality of image segmentation scheme is estimated according to factors like Similarity Index, Dice Score, Sensitivity or Overlap fraction, Extra Fraction, Specificity, Accuracy.

D. Performance Parameters of Image Segmentation Methods

1) Similarity Index (SI)

SI tells about the mutual value among input MRI brain image and segmented output image.

$$SI = \frac{2 \times Tru\ Pos}{2 \times Tru\ Pos + Fal\ Pos + Fal\ Neg} \tag{16}$$

where *Tru Pos* is the True Positive, it tells the volume of positive pixels properly segmented. *Fal Pos* is the False Positive, it gives the volume of positive pixels imperfectly segmented. *Fal Neg* is the False Negative, it gives the volume of negative pixels incorrectly segmented. *Tru Neg* is the True Negative, it gives the volume of negative pixels properly segmented.

2) Dice Score (DS)

It gives comparisons among the segmented section and ground truth section [18].

$$DS = \frac{2 \times Tru\ Pos}{(Tru\ Pos + Fal\ Neg) + (Fal\ Pos + Tru\ Pos)} \tag{17}$$

3) Sensitivity or overlap fraction

It describes appropriate segmentation associated with input MR brain images. It provided the ability of the test to identify positive results.

$$\text{Sensitivity} = \frac{Tru\ Pos}{(Tru\ Pos + Fal\ Neg)} \tag{18}$$

4) Extra Fraction

Total voxels not detected as a tumor region given by the extra fraction.

$$\text{Extra Fraction} = \frac{Fal\ Pos}{(Tru\ Pos + Fal\ Neg)} \tag{19}$$

5) Specificity

It is based on the ability of the test to identify negative results [19].

$$\text{Specificity} = \frac{Tru\ Neg}{(Tru\ Neg + Fal\ Pos)} \tag{20}$$

6) Accuracy

It is cast-off to estimate the accomplishment of the tumor detection and segmentation system

$$\text{Accuracy} = \frac{Tru\ Neg + Tru\ Pos}{(Tru\ Neg + Tru\ Pos + Fal\ Neg + Fal\ Pos)} \tag{21}$$

Various algorithms and techniques are considered to segment the image. These are shown below.

Clustering methods

Machine learning is an effective way to automatically analyze and diagnose medical images [20]. It can diminish the burden on scientists in the form of radiology, which can study complex or experimental relationships of the empirical data and make the accurate decision [21]. Machine learning algorithms can be planned into different groups based on different ideologies. This methodology is classified into supervised learning, semi-supervised learning, and unsupervised learning algorithms have its origin in the use of model labels of training. During unsupervised learning, we only have one observation and no label information for each sample. In general, these observations or attributes are not caused by perceived or hidden variables. The main objective of unsupervised learning is to explore the relationship between patterns or to find hidden variables behind the observations. The clustering algorithm is a demonstrative method of unsupervised learning. Semi-supervised learning incorporates supervised and unsupervised learning. It uses labeled and unlabelled data during the training process.

In utmost cases, the most commonly used brain tumor segmentation procedures depend on clustering approaches like Fuzzy C-Means, k-mean, Artificial Neural Networks, Vector Machine Support etc. FCM algorithms are discussed in the next section for segmenting brain tumor.

FCM based methods

FCM remains a clustering technique that splits two or more clusters in the data collection. This scheme [22] is often cast-off in pattern recognition. This procedure works through

allocating every point allocated to each cluster center through the length amid the cluster and information point. Further details are in the cluster center, where its members are likely to move towards a special cluster center.

The advantages of FCM algorithms are: (1) providing better results for overlapped datasets and better than the rule of k-means. (2) Contrasting the k-means, data points must belong to a single cluster center, sharing a data component with more than one cluster center is provided. As a result, data points can be more than one cluster. (3) the implementation of FCM data into MR data shows the incentive result. Consequently, the FCM for tumor segmentation becomes fertile. In brain tumor segmentation, the brain tumors are divided into tissues, including activated cells, necrotic core, and edema using the unsupervised FCM clustering procedure [23]. With this algorithm, segmentation images can be generated which are the clinically relevant neuro-anatomical and neuropathological tissue contrast media for raw MR images. Then, some researchers learn more about using FCM as functional vectors. MRI images have been processed by a scheme that combines knowledge-based methods through a multispectral histogram study of the action of brain tumor segmentation [24]. According to fuzzy information, a new image segmentation method, for example, the Fuzzy Knowledge-Based Seeded Region Growing [25], is proposed. Investigational outcomes demonstrated that the FKSRG technique has a multi-spectral MR image efficient than automotive segmentation device, k-means, and SVM methods. Because FCM remains an iterative procedure make use of more time. Different solutions, such as Fast Generalized FCM (FGFCM) algorithms and BCSM algorithms, are proposed to reduce the time of implementation of this algorithm. The newly fast and secure FCM framework was assigned for brain tumor segmentation, called FGFCM cluster algorithms, by adding local information [26]. The BCFCM algorithm offers high-quality segmented brain images in actual high-speed ways, it is an outstanding device for virtual brain endoscopy so that segmentation of brain tumor occurs [27].

In order to diminish the sensitivity of the conventional FCM algorithm with Gaussian and impulse noises, a modified FCM-based method was suggested to perform the fast and exact segmentation [28]. The purpose of the method is a scalar feature value in all pixels adjacent to the context-dependent filtering technique, which uses spatial and gray level distances. These functions remain monitored by means of the advanced FCM algorithm histogram-based approach. Towards recover the quality of the FCM algorithm, some investigators introduced a neighborhood attraction that relies on comparative position with the properties of adjacent pixels. Genetic algorithms (GA) are good for finding the best solution, but it is difficult to find a precursor, while particle swarm optimization (PSO) increases the optimum solution. Combining GA and PSO has been presented to determine the optimal value of attractiveness [29]. To improve the precision of tumor stage and size, a combined method of k-means and fuzzy C-mean procedures aimed at the treatment of a tumor segmentation was suggested [30]. This process permits the tumor gain to be segmented with precision and reproduction, which is comparable to the manual segmentation. Additionally, for the segmentation process, it decreases the time.

Traditional methods

In this article, traditional brain tumor segmentation techniques typically involve typical image processing approaches, like threshold and region-based systems [31]. Two-dimensional image segmentation [32] use threshold-based and region-based approaches.

Threshold-based methods

The threshold-based approach is modest, efficient method compared to its intensity by one or more thresholds. Current threshold-based approaches remain categories as global and local thresholding. If an image has objects with the same intensity or dissimilarity amid items furthermore high contextual, the global thresholding remains the best option to separate objects and backgrounds. Local threshold values are typically assessed with local statistical properties like average MRI intensity with prior knowledge. In addition, the Gaussian distribution was used to determine the thresholds for common brain MRI images [33].

Due to the specific structure of brain tumors, global and local thresholds are used primarily to regulate the estimated position of brain tumors in the brain. In most cases, the threshold is castoff initial stage in the brain segmentation procedure.

Region-based (RB) methods

The RB segregation methods scrutinize pixels in the picture furthermore create anonymous regions due to combining zone pixels escorted by characteristics locate over predetermined criterion of similarity [34]. The region growing and watershed segmentation schemes remain part of regional methods are mainly employed in brain tumor segments. The area is an increasingly frequent and widespread regional segmentation method and is used to separate the pixels of the region into an image. Growing areas begin with the unique kernel, which fits the pattern of interest. Neighbors of the kernel remain examined together with the area is accompanied by similar criteria. The range of pixels, intensity pixels, or other image functions decides the similar criteria. Kernels are selected physically or via collecting kernels automatically [35]. The benefit of region growing can divide similar areas and establish connectivity areas.

Some researchers have shown the RG based area remains fulfilled method than NR based approaches with regard to segmentation of the MR images, especially in similar tissues and regions [36].

The main drawback of the RG based approach is the incomplete capacity outcome that restricts the precision of MR image segmentation. Multi-scale watershed transformation methods used by researchers to segment brain tumors [37]. An investigation of watershed segmentation approaches of MRI brain tumor information was achieved. Quantitative and qualitative findings indicate that segmentation time and accuracy have improved considerably and managed segmentation successfully. The investigation also recognized some drawbacks of brain tumor segmentation in the watershed approach. A method has been proposed to improve these disadvantages. A multi-parameter watershed segmentation algorithm used to detect an MRI 2-D and 3-D

brain tumor [38]. A marker-based better-quality watershed procedure by using the prior information about test images for the brain tumor segmentation was proposed [39]. The watershed segmentation procedure frequently agonizes about over-segmentation. To evade over segmentation and yield a sensible segmentation, some cutting-edge approaches have been projected [40].

The virtuous outcomes of brain tumor segmentation by means of predictable approaches are rigid to achieve. In utmost circumstances, these procedures were considered as a pre-processing period in the brain tumor segmentation. Consequently, more progressive automatic approaches were planned to consensus with the necessities of medical doctors.

Deformable based methods

Because of the 3-D MRI data presentation, segmentation of the data is difficult [41]. The difficult task is to develop the rudiments of the same construction and participate these rudiments addicted to a coherent and reliable method of structures. Additionally, model-based segmentation approaches with parametric (PDBM) and geometric deformable based methods (GDBM) remain suggested to recover the problem. The normally accepted authority of deformable methods has the capability to segment the image of anatomical structures using the boundaries of image statistics composed through prior information of position, extent, and outline of the constructions. Deformable representations have the opportunity to manage changes in the biological structure. In addition, deformable representations can be used to provide high-quality instinctive mechanisms that enable medical professionals and doctors to acquire the skills needed to perform the interpretive tasks they need.

Various techniques such as PDBM and GDBM are discussed in the subsequent sections.

PDB methods

Active contour approaches are known as parametric deformable based methods (PDBM) and it is introduced in 1988. Once the initialization has been made, the snake will be able to find the object contour well. In parametric deformable models, the main stage in segmenting the brain tumor is the detection of brain tumor borders. Snakes are widely used for sensing the brain tumor boundary. The reality has shown that identifying the boundary by the snake method is well than traditional edge-detection procedures, such as Laplacian, Canny, and Sobel [42].

Some researchers believe that the external energy of snake function is null at the corners and is positive inhomogeneous regions. Many investigators remain annoying to advance the presentation of snake's process. Gradient Vector Flow (GFF) snake and balloon model remained wished-for to recover brain tumor segmentation on T_1 brain tumor [43].

The GVF technique was advised to follow the snake difficulties of the rapid capture range and incapability towards snakes' problems. The balloon prototypical licenses to expand the snake's capture range. Parametric deformation model was projected as a phase of spatial relationships as an improvement to accurately calculate T_1 MRI of any type of brain tumor [44]. A method is available that includes the merging of brain scanning of segmentation and deformation of the glioma patients' brain into a standard atlas. The projected technique remains created on the Expectation Maximization (EM) procedure, which includes the glioma development prototypical intended for the atlas, a procedure that replaces the usual atlas with the tumor and edema. The altered atlas remains enumerated in the patient's area in addition to evaluate the posterior probability of the labels of different tissues. EM is an iterative improvement of enumerated constraints, the posterior probability of tissue labels and the constraints of tumor development prototypical. It is noteworthy that sometimes the PDM's initial position requires the manual to be nearly enough to the anticipated limit to evade intersecting inappropriate restrictions.

GDB methods

Using deformable parametric methods for segmentation of 3-D MRI data, one of the drawbacks is the severity of topological changes managed naturally by splitting and merging of contours. Geometric deformable based methods (GDBM, correspondingly known as level sets) have been wished-for to solve this problem. Even though these methods have greatly amended the initiation of parametric active outlines, and only if the original outline is symmetrically positioned in relation to dominant boundaries, it is difficult to do in practice because many methods of segmenting brain tumors cannot cope with objects formulated regularly [45]. As continuous reproduction snakes have to be carefully initiated and liberated by weak or missing boundary parts, level-set snakes have been offered and have more significant advantages than traditional statistical classification and mathematical morphology. A Charged Fluid Framework (CFF) was presented by some researchers and ruled by Poisson's equation in place of a deformable model to accomplish brain tumor segmentation. Level set formula comprised of a regulatory tenure from which the curve development equation aimed at dynamism reduction was obtained. The consistency of level set functions identified was essentially maintained at the level set regularization tenure in order to confirm a precise calculation, evading costly re-use of the changing fixed level set function.

Some researchers created a local intensity clustering of a brain tumor and other images with the intense disorder have established a local clustering principle function for intensity criteria at each point in the neighborhood. The local clustering principle has been integrated into the Neighbourhood Center to define the energy functionality that has been transformed into a defined level set design. The transmission of dynamism was accomplished in the development of mutually level set progress and a field of bias. A tumor cut procedure was implemented that combines tumor segmentation with cellular automata, and the level set is determined by a tumor map of the probability of introducing spatial smoothness.

In utmost cases, the deformable model is not used alone but is used in conjunction with other procedures such as FCM, MRF, ANN, etc. This may include the advantages of two or more procedures to polish the accuracy of brain tumor segmentation.

III. Data Availability

All brain tumor images are taken from the following

databases, which are itemized in Table I.

TABLE I: DIFFERENT DATABASES

Name	Link
TumorSim	https://www.nitrc.org/projects/tumorsim
3D Slicer	https://www.slicer.org
ISTB	http://www.istb.unibe.ch/research/index_eng.html
BrainWeb	http://brainweb.bic.mni.mcgill.ca/brainweb/

IV. CONCLUSION

This article emphasizes a few non-linear image-denoising methods, even though linear methods remain modest, efficient, and then relaxed to put into action, nevertheless they are limited by high noise density and complex noise patterns. Nonlinear methods were the stage of art denoising approaches. The approaches differ in relation to the category of noise used. All kinds of noise, such as impulse, Gaussian white noise, and speckle, have been studied with techniques related to denoising approaches. Each method in its problematic area has its own performance indicators that may not work and meet requirements in another problem zone. However, complete approaches allied by wavelet domain have achieved excellent results due to their adaptation and noise. But the majority of the approaches gives the better results and appearance can be calculated in terms of Mean or Average pixel intensity, Standard Deviation, Mean Square Error, Root Mean Square Error, Mean Absolute Error, Peak Signal to Noise Ratio, Structural Similarity, Universal Image Quality Index, and Entropy.

This article also delivered an outline of MRI-based brain tumor segmentation approaches.

Different types of present brain tumor segmentation approaches work on the MRI images due to the non-invasive with good tissue contrast of MRI and use classification and clustering approaches, using a variety of features and taking more precisely by region. The persistence of these methods is to make a preliminary decision on the diagnosis, the development of tumor diffusion and treatment planning. Although the majority of tumor segmentation algorithms in the MRI brain have relatively good results in medical image analysis.

Different approaches remain discussed in the paper and each approach has its own unique principle such as precision, validity, and toughness of MRI-based brain tumor segmentation and its associated approaches are previously revealed excessive latent in sensing and investigating tumors in medical training. Nevertheless, the majority of the approaches gives the better results and appearance can be calculated in terms of Similarity Index (SI), Dice Score (DS), Sensitivity or Overlap fraction, Extra Fraction, Specificity, and Accuracy.

ACKNOWLEDGMENT

The author thanks JNTUH University, G. Narayanamma Institute of Technology and Science, and S R Engineering College (Autonomous).

REFERENCES

[1] M. Raza, I. Irum, and M. Sharif, "A review of image denoising methods," *Jr Eng Sci Tech Rev*, vol. 8, no. 5, pp. 41-48, Dec 2015.

[2] K. R. L. Reddy, D.S. Rao, and K. Sreedhar, "Image denoising by using modified sghp algorithm," *Int Jr Electr and Comp Eng*, vol. 8, no. 2, pp. 971-978, April 2018.

[3] J. Wang, J. Liu, and Y. Pan, "A survey of MRI-based brain tumor segmentation methods," *Tsing Sci and Tech*, vol. 19, no. 6, pp. 578-595, Dec 2014.

[4] M. Hussain, S. Rathore, and I. Aksam, "Robust brain MRI denoising and segmentation using enhanced non‐local means algorithm," *Int Jr Img Syst and Tech*, vol. 24, no. 1, pp. 52-66, Mar 2014.

[5] A. Prabha, and S. Saladi, "Analysis of denoising filters on MRI brain images," *Int Jr Img Syst and Tech*, vol. 27, no. 3, pp. 201-208, Aug. 2017.

[6] V. Kollu and D. P. Bavirisetti, "Fusion of MRI and CT images using guided image filter and image statistics," *Int Jr Img Syst and Tech*, vol. 27, no. 3, pp. 227-237, Aug. 2017.

[7] Z. Wang, W. Mei, and H. Du, "Convex MR brain image reconstruction via non‐convex TV minimization," *Int Jr Img Syst and Tech*, vol. 28, no. 4, pp. 1-8, Dec 2018.

[8] H. Park and K. Kwon, "Multi-contrast MR image denoising for parallel imaging using multilayer perceptron," *Int Jr Img Syst and Tech*, vol. 26, no. 1, pp. 65-75, April 2016.

[9] P. Zhang, and D. Shen, "Denoising MRI using collaborative non-local means," *Neu comp*, vol. 177, pp. 215-227, Feb 2016.

[10] M. Waqas and S. Alshomrani, "Image de-noising using noise ratio estimation, K-means clustering, and NLM-based estimator," *Comp & Electr Eng*, vol. 54, pp. 370-381, Aug 2016.

[11] V. Magudeeswaran and J. Singh, "A machine learning approach for brain image enhancement and segmentation," *Int Jr Img Syst and Tech*, vol. 27, no. 4, pp. 311-316, Dec 2017.

[12] Y. Yang and Y. Chen, "Image denoising by using PDE and GCV in tetrolet transform domain," *Eng Appl Artif Intell*, vol. 48, pp. 204-229, Feb 2016.

[13] M. H. Sedaaghi and S. Saryazdi, "Efficient diffusion coefficient for image denoising," *Comp & Math with Appl*, vol. 72, no. 4, pp. 893-903, Aug. 2016.

[14] A. Lundervold and X. C. Tai, "Noise removal using the fourth-order PDE with applications to medical MRI in space and time" *IEEE Trans on Img Proc*, vol. 12, no. 12, pp. 1579-1590, Dec. 2013.

[15] L. Huang and G. Guo, "Adaptive fourth-order PDE filter for image denoising," *Appl Math Lett*, vol.24, no. 8, pp. 1282-1288, Aug. 2011.

[16] H. Lim, "Fourth-order PDE for effective image denoising," *Electr J Diff Equ*, vol. 17, pp. 107-121, Jan. 2009.

[17] J. Tan and L. Ai, "Hybrid regularizers-based adaptive anisotropic diffusion for image denoising," *SprinPlu*, vol. 5, no. 1, p. 404, Dec. 2016.

[18] G. L. Priya, "Walsh Hadamard kernel-based texture feature for multimodal MRI brain tumor segmentation," *Int Jr Img Syst and Tech*, vol. 28, no. 4, pp. 254-266, Dec. 2018.

[19] A. K. Ray and H. P. Thethi, "Image analysis for MRI based brain tumor detection and feature extraction using biologically inspired BWT and SVM," *Int Jr Biomed Img*, Mar. 2017.

[20] V. Govindaraj and A. Thiyagarajan, "A fully automated hybrid methodology using Cuckoo-based fuzzy clustering technique for MRI brain image segmentation," *Int Jr Img Syst and Tech*, vol. 27, no.4, pp. 317-332, Dec. 2017.

[21] N. M. Nasrabadi, "Pattern recognition and machine learning," *Jr Electr Img*, vol. 16, no. 4, Oct. 2016.

[22] A. Farag and T. Moriarty, "A modified fuzzy c-means algorithm for bias field estimation and segmentation of MRI data," *IEEE Trans Med Img*, vol. 21, no. 3, pp. 193-199, Mar. 2002

[23] M. S. Silbiger and J. C. Bezdek, "A comparison of neural network and fuzzy clustering techniques in segmenting MRI of the brain," *IEEE Trans Neur Net*, vol. 3, no. 5, pp. 672-682, Sep. 1992.

[24] M. L. Silbiger, "Application of fuzzy c-means segmentation technique for tissue differentiation in MRI of a hemorrhagic glioblastoma multiforme," *Magn Reson Img*, vol. 13, no. 2, pp. 277-290, Jan. 1995.

[25] C. C. Kang and C. M. Wang, "Multispectral MRI segmentation based on fuzzy knowledge and modified seeded region growing," *Magn Reson Img*, vol. 30, no. 2, pp. 230-246, Feb. 2012.

[26] S. M. Szilagyi and H. S. Adam, "MR brain image segmentation using an enhanced fuzzy c-means algorithm," *Int Conf IEEE*, vol. 1, pp. 724-726, Sep. 2003.

[27] S. Chen and D. Zhang, "Fast and robust fuzzy c-means clustering algorithms incorporating local information for image segmentation," *Patt Recog*, vol. 40, no. 3, pp. 825-838, Mar. 2007.

[28] S. M. Szilagyi and Z. Benyo, "A modified fuzzy c-means algorithm for MR brain image segmentation," *Int Conf Img Anal Recog*, pp. 866-877, Aug. 2007.

[29] N. Forghani and M. Teshnehlab, "Parameter optimization of improved fuzzy c-means clustering algorithm for brain MR image segmentation," *Eng Appl Artif Intel*, vol. 23, no. 2, pp.160-168, Mar. 2010.
[30] M. M. Shringirishi, "Implementation of brain tumor segmentation in brain MRI using k-means clustering and fuzzy c-means algorithm," *Int Jr Comp Tech*, vol. 5, no. 1, pp.54-59, April 2013.
[31] L. Bischof, "Seeded region growing," *IEEE Trans Patt Anal Mach Intel*, vol.16, no. 6, pp. 641-647, Jun. 1994.
[32] D.C. Gharpure, "Development of image-processing software for automatic segmentation of brain tumors in MRI," *Jr Med Phy/Assoc Med Phys of Ind*, vol. 36, no. 3.
[33] R. Fahlbusch and O. Ganslandt, "Improved delineation of brain tumors: An automated method for segmentation based on pathologic changes of 1H-MRSI metabolites in gliomas," *Neu Img*, vol. 23, no. 2, pp. 454-461.
[34] K. P. Wong, "Medical image segmentation: methods and applications in functional imaging," Handbook *of Biomed Img Anal*, pp. 111-182, 2005.
[35] F. A. Jolesz and R. Kikinis, "Automated segmentation of MRI of brain tumors," *Radiogy*, vol. 218, no. 2, pp. 586-591, Feb. 2001.
[36] S. M. Alian and M. E. M Bayome, "Validation techniques for quantitative brain tumors measurements," in *Proc. Annl Int Conf*, 2005, pp. 7048-7051.
[37] D. Bloyet and J. M. Constans, "A framework of fuzzy information fusion for the segmentation of brain tumor tissues on MRI," *Img Vis Comp*, vol. 25, no. 2, pp. 164-171, Feb. 2007.
[38] S. K. Sharma, "Multiparameter segmentation and quantization of brain tumor from MRI images," *Ind Jr Sci Tech*, vol. 2, no. 2, pp. 11-15, Feb. 2009.
[39] A. Bahrani, "Segmentation of tumor tissue in gray medical images using the watershed transformation method," *Int Jr Advan in Comp Tech*, vol. 2, no. 4, Oct. 2010.
[40] Y. Li and B. Zhang, "A novel approach for segmentation of MRI brain images," in *Proc. IEEE Mediterranean Electr Conf*, 2006, pp. 525-528.
[41] D. L. Arnold and D. L. Collins, "Review of automatic segmentation methods of multiple sclerosis white matter lesions on conventional magnetic resonance imaging," *Med img Anal*, vol. 17, no. 1, pp. 1-18, Jan. 2013.
[42] J. L. Prince, "Snakes, shapes, and gradient vector flow," *IEEE Trans img proc*, vol. 7, no. 3, pp. 359-369, Mar 1998.
[43] S. Ourselin, "A new deformable model using dynamic gradient vector flow and adaptive balloon forces," *APRS Workshop on Dig Img Comp*, pp. 9-14, Feb. 2003.
[44] I. Bloch, "3D brain tumor segmentation in MRI using fuzzy classification, symmetry analysis, and spatially constrained deformable models," *Fu Sets Sys*, vol. 160, no. 10, May 2009.
[45] D. Valentino, "An electrostatic deformable model for medical image segmentation," *Comput Med Img and Grap*, vol. 32, no. 1, pp. 22-35, Jan. 2008.

Sreedhar Kollem is a Ph.D. research scholar in the Department of ECE at JNTUH University, Hyderabad, Telangana, India. He received the B.Tech. degree in electronics and communication engineering from JNTUH University, Hyderabad, India in 2005 and M. Tech degree in communication systems from JNTUH University, Hyderabad, India in 2009. He has a life membership in ISTE and IETE. He qualified UGC NET in Electronic Science. His areas of interests are digital image processing, signal processing, and wireless communications.

Katta Ramalinga Reddy is working as a professor, head of the Department of Electronics and Telematics (ETM) in G. Narayanamma Institute of Technology and Science (GNITS), Hyderabad, Telangana, India. He completed his B.E. from Vasavi Engineering College in 1989 and M. Tech from SVU Engineering College in 1991, Ph.D. from JNTU Hyderabad. He won the academic excellence award in 2005 for his academic contribution in GNITS. He has more than 40 research papers to his credit. His areas of interests are digital image processing, signal processing, and wireless communications.

Duggirala Srinivasa Rao is working as a professor of Electronics and Communication Engineering Department at JNTUH College of Engineering, Kukatpally, Hyderabad, Telangana, India. He completed his Ph.D. from Central University Hyderabad. He handled the research projects like Quality of Service in mobile Ad-hoc networks, funded by UGC from 2012 to 2014. He has more than 35 research papers to his credit. His areas of interests are computer networks, wireless networks, and communications.

Journal of Engineering and Applied Sciences 12 (Special Issue 1): 5814-5820, 2017
ISSN: 1816-949X
© Medwell Journals, 2017

Energy Aware on Demand Routing for MANETs based on Intermediate Node Residual Status

[1]Mahabubul Haq Atif and [2]Syed Abdul Sattar
[1]Department of CSE, Rayalaseema University, Kurnool, Andhra Pradesh (AP), India
[2]Department of CSE, Nawab Shah Alam College of Engineering, Hyderabad, Telangana (TS), India

Abstract: MANETs (Mobile Ad-hoc Networks) are self-configuring network that comprised of mobile nodes having no fixed infrastructure. These devices are dynamic and move freely so that they form varying network topology. The challenge for successful communication is to form an appropriate route to maintain connectivity consistently between mobile nodes having limited battery power. Therefore, MANETs need to have improved network lifetime to perform a streamlined and dynamic routes between multiple mobile nodes. This research focuses on designing a protocol for MANETs which is energy efficient and congestion avoidance between mobile nodes. In this mechanism, two important attributes, i.e., link stability and network lifetime are addressed. We used NS-2 Network Simulator to analyze the performance. The outcome of this simulated demonstration that developed energy aware mechanism is better than the existing EDDSR, MDR and LEAR routing protocols.

Key words: MANETs, node, network lifetime, link stability, routing, LEAR

INTRODUCTION

MANETs (Muhammad *et al*., 2015) (Mobile Ad-hoc Networks) are self-configuring and infrastructure less networks that comprises of a set of mobile nodes forming peer-to-peer communications. The network topology of MANETs is autonomous, dynamic and consisting of number of intermediate mobile nodes between communicating peer nodes. Each node in a network has to act as a source, receiver and router to forward the packets. MANETs have many applications such as environment monitoring, wireless sensor network, military and law enforcement. These applications need to be cost and/or time effective. Communicating nodes in MANETs depends upon intermediate nodes for communication when they are not in radio range of each other. Moreover, forwarding packets by other nodes consume resources of node particularly energy. The primary issue in MANETs is availability of limited power as they are powered by batteries that have limited lifetime.

Mobile nodes are equipped with batteries that have a limited amount of power and lifetime. These batteries cannot be recharged or replaced during the mission and hence, energy management is considered as a necessary factor. The nodes consume the energy during data reception, data processing and data transmission. MANETs consist of single and multiple communicating entities have peer-to-peer connectivity and are required to route the traffic properly. To improve the performance of communication and lifetime of network, we need to design a routing mechanism in such a way that the packets are routed with minimum energy consumption and based on energy awareness of nodes. One of the important goal of routing in MANETs is to create a cost optimum as well as energy efficient path. Hence, we chose energy aware routing as the best procedure of managing the energy in Mobile Ad-hoc Networks. However, properties and resources of MANETs make this task more challenging. To solve the issues of energy management, in literature many routing protocols have been put forwarded. These protocols were broadly classified into three categories:

- Energy efficient routing path
- Reliable routing path and
- Routing path with higher energy nodes

The protocol designed based on energy efficient routing path concentrates on reduction of energy usage during transmission and reception to minimize the amount of energy required for communications by the mobile nodes present in a network. This goal is achieved either by reducing the energy consumption when the nodes are in idle state or by minimizing the amount of energy required for packet delivery. A routing path with higher energy nodes has the protocol that uses higher energy nodes to find the routes whereas a reliable routing path has the protocol that detects the route according to

Corresponding Author: Mahabubul Haq Atif, Department of CSE, Rayalaseema University, Kurnool, Andhra Pradesh (AP), India

anticipated energy count. To recover from packet loss, this type of link routing used a concept of minimum amount of retransmission. Each protocol has its own merits and demerits and accordingly it is judged which protocol is suitable for a specified network condition.

In order to deep analyze the routing protocols performance, network condition is divided into categories and then the performance of different routing protocols is analyzed and compared. Researchers can have an effective use of the results produced in our project for their experimentations. Though in literature various researchers carried out a lot of analyses and research to contrast the routing protocols for energy management, this project has a new technical performance system such as forwarding packets from various sources through conversion of node into bottleneck intermediate node, which is one of the best procedure in assessing the multi-hop environment routing protocols for energy management. This system of performance analysis is an innovative feature of this study.

In the first part of our study, the state of the art analysis of proactive and reactive routing protocol performances such as DSDV (Moravejosharieh *et al*., 2013), AODV (Chaubey *et al*., 2015) and DSR are defined. For a particular network condition, it is difficult to judge which mechanism is suitable for routing protocols. Thus, we divided the network condition into broader categories and then compared the different performance systems by analyzing routing protocol performances with various network conditions with mobility considerations such as variable radio area, variable packet size and variable hop-count. The outcome of this analysis can be used by the researchers in their experiments. Ultimately, we considered DSR to be the best suited to develop a routing protocol in MANETs energy efficiency. Due to heterogeneous mobile nodes batteries with limited power, energy efficiency is a necessary issue in designing of MANETs. It is essential to have reduced amount of energy consumed during wireless communications. If the routing protocol does not consider the power required and relies upon shortest path, then the affect is caused on the lifetime of network by power failure of a node. The goal of energy efficient routing protocol is to find the route that consumes minimum amount of energy during end to end packet travelling as well as to make residual energy of a node and have reliable routing through links. This improves the network lifetime as well as the overall performance. Therefore, a routing protocol is still required to address these issues in MANETs.

In second part of our study, we designed "Energy aware routing for MANETs based on a current processing state of Node". In this protocol, we make use of DSR to achieve energy efficiency. DSR (Dynamic Source Routing) is a protocol that stores all nodes from source to destination. It is a source initiated protocol similar to "AODV" protocol. Proposed work enhances DSR protocol to improve network lifetime and to reduce routing cost upon mobile networks. Though the researchers carried out a lot of experiments and thesis for the development of energy efficient routing protocols with different performance analyses, our research has a new technical performance system which makes nodes possible to become a "Bottleneck node". It is the mediator condition for forwarding the traffic through intermediate node. Hence, we create a routing process to avoid the node to become "Bottleneck node" which results in improvement of performance and lifetime of a network.

Routing in manets: According to literature review of routing in MANETs, it seems more challenging over infra-structured networks. The literature shows a lot of routing protocols that were developed with extra attempts to manage the attributes of MANETs environment. The work of routing in MANETs is more taxing by the limiting factors such as mobility, heterogeneity and dynamic network topology. In most of the existing protocols, there are different patterns of designs that are followed by MANETs according to reactive and proactive approaches. In proactive routing protocols, the nodes are allowed to have a clear vision over the network topology. Therefore, all nodes in traffic can be routed quickly and properly. An extra overhead is made by periodic messages. DSDV, ABR and OSLR are the few examples of proactive routing (Mohammad *et al*., 2015; Varshney *et al*., 2016; Chaubey *et al*., 2015; Moravejosharieh *et al*., 2013; Dulman *et al*., 2003).

The reactive or source initiative routing follows on-demand approach and is an alternative to proactive routing mechanism. The establishment of route occurs only when there is a transmission or communication between a source and a destination. The route request function of source node follows a route reply function of a destination node to initiate the route. The route maintenance function maintains the initiated route till it is required. AODV and DSR are the examples of reactive source initiative routing protocol.

The DSR protocol is similar to AODV protocol which forms a route when it is requested by a transmitting node but instead of depending upon a routing table, DSR protocol uses source routing. In DSR protocol, the complete path is discovered by the sender of the packet through which the packets are forwarded. This route is listed in the packets by the sender which takes the address of next node to identify each hop to be forwarded

through which the packets are transferred to the destination host. The performance of DSR routing protocol is better than that of AODV and DSDV protocol. Unlike table driven approach, DSR uses a reactive approach to avoid the need to flood the network periodically through the table update messages.

Need of energy awareness in MANETs: The battery power of mobile nodes is finite in MANETs. MANET's properties are highly suitable for various applications like disaster recovery and battlefield but recharging and changing of batteries looks very difficult. After losing the power completely, nodes cannot be used further for communication as they are removed from the network. In MANETs, it is necessary to manage the energy because it is difficult to change or substitute the battery, shortage of central coordination, peer to peer characteristics network and finite energy storage. The utilization of active energy in MANETs occurs through packet communication such as packet reception and packet transmission. Inactive utilization of energy occurs through rest state of node but as they are listening medium they can respond to any feasible communication requests by other nodes and it utilized the energy when the node is at rest. Most of the researchers developed the routing protocols such as correct path between source and destination, simply based on energy efficient beside this they are also developed the energy management as they can provide the network functions for a longer time.

Literature review: In the first stage of our research, we have done the analysis of performance of DSDV, AODV and DSR concerning radio area, traffic mobility and hop count regarding variable packet size. Performance of this routing protocol is analyzed based on reactive and proactive approach. The simulator used for calculating the performance of DSR, AODV and DSDV is NS-2 Network Simulator in terms of throughput, packet loss and end to end delay. The outcome of this simulation shows that DSR performance is slightly better than AODV and DSDV, which is shown in Fig. 1-5.

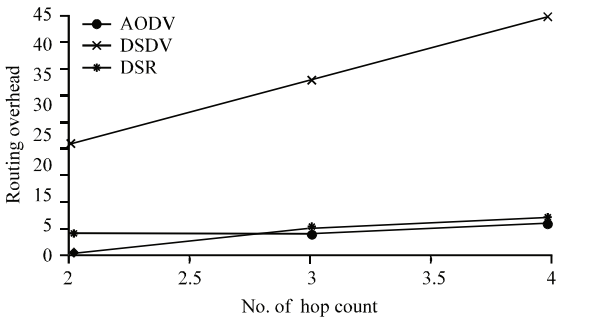

Fig. 1: Routing overhead comparison of routing protocols (AODV, DSDV, DSR)

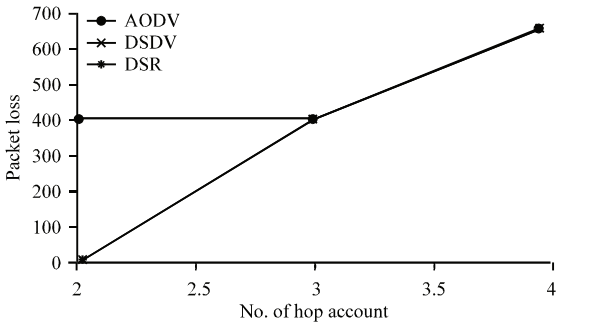

Fig. 2: Packet loss comparison of routing protocols (AODV, DSDV, DSR)

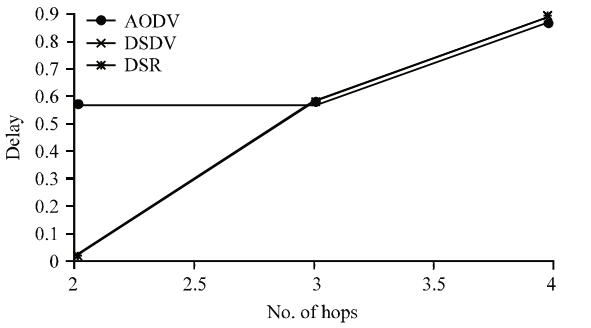

Fig. 3: End to end delay comparison of routing protocols (AODV, DSDV, DSR)

DSR based energy efficient routing: We have done literature review on DSR based energy management routing protocols as its performance is better than other routing protocols such as AODV and DSDV. In Dynamic Source Routing (DSR), the complete system of nodes is carried by each data packet which needs to be passed to reach the destination. DSR is based upon the process route discovery and route maintenance. A Route Request (RREQ) is broadcast by a node in the process of route discovery. After reaching the destination or intermediate node, RREQ process is terminated and Route Reply (RREP) is sent back to the source. The source node uses the route from RREP to transmit the packets towards the destination. A broken link or a link in disconnection is detected by route maintenance process which sends the Route Error packet (RERR) to the source. The source discovers a new route towards the destination and deletes the broken link from its cache.

To estimate the lifetime of a node, a new cost function is described by the Minimum Drain Rate (MDR)

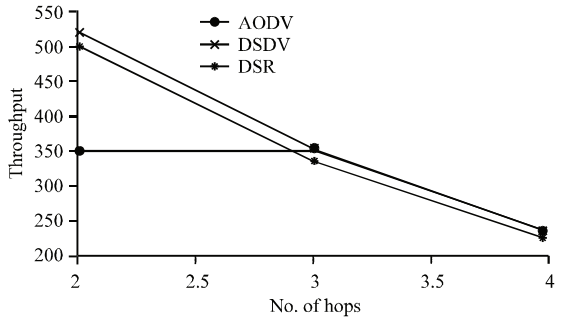

Fig. 4: Throughput comparison of routing protocols (AODV, DSDV, DSR)

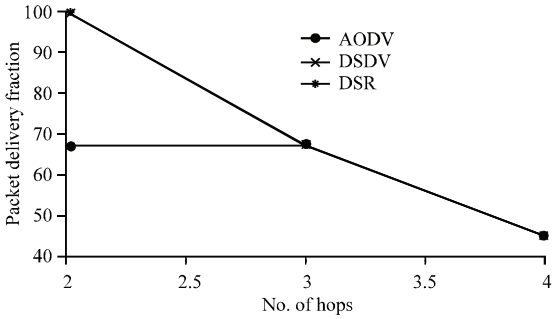

Fig. 5: Packet delivery fraction comparison of routing protocols (AODV, DSDV, DSR)

mechanism. The cost function is based upon the conditions of traffic load and battery power (Woo *et al*., 2001; Vazifehdan *et al*., 2014). MDR is fully based upon source-destination based mechanism. Only the source or destination makes decision during transmission and intermediate nodes can piggyback their current costs through the messages in routing.

To distribute the packets to all energy-rich nodes, the "Local Energy-Aware Routing" (LEAR) is introduced. A node discovers a node only when its current amount of energy exceeds a specific threshold. Otherwise, it creates a message known as Drop Route Request (DR- REQ) and drops Route Request (RREQ). RREQ reaches the destination node only when it passes through all intermediate nodes with sufficient amount of energy. If RREQ does not reach the destination, then the source does not receive RREP from the destination. It then starts a second attempt to discover a route towards destination.

A route cache is used in this protocol where an intermediate node generates a message known as Route Cache (RCAC) and sends towards a destination. The destination node responds either to first route request or to route cache and ignores all the other messages. Route cache will be replied only when power is above specific threshold. Otherwise Drop Route Cache (DR-CAC) or

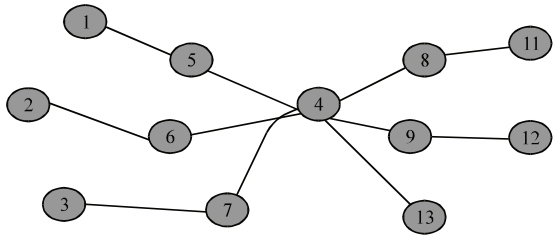

Fig. 6: Scenario of node to become bottleneck

Cancel Route Cache (CR-CAC) is replied to the node which sends route cache. The node then attempts to discover the other paths after getting next route request.

However, all the above discussed protocol does not concentrate the issue of node to become bottleneck. It is a situation in the network where multiple source node forwarding the packets through an identical intermediate node. If node receives the packets greater than its resource capacity of handling packets, then packets get drop from intermediate node and if this situation continue for some extend may cause complete network to congestion (Mohammad *et al*., 2016a, b). Bottleneck intermediate node is shown in Fig. 6.

MATERIALS AND METHODS

Proposed energy aware routing protocol: The Energy Dependent DSR (EDDSR) mechanism is proposed which can be used in the route discovery process of DSR. We devised a new mechanism whose aim is to increase the lifetime of node with low amount of energy stored. In this mechanism, each node shows its readiness to forward packets according to its current energy level. Each node in the medium calculates its Residual Battery Power known as "RBP_i". If RBP_i is lower than the specific threshold, then the rebroadcasting of RREQ by a node is delayed. If residual power of a node is enough, then it behaves as a DSR nodes and proceeds its network activities.

A predicted node lifetime n_i is described by the ratio RBP_i, DR_i in which RBP_i represents residual battery power and Dr_i represents drain rate which described the amount of energy consumed per second.

In EDDSR mechanism, the nodes with shorter lifetime are prevented from route discovery process to increase their lifetime. Therefore, the route requests sent by a node having small lifetime will be cancelled by the nodes closer to destination. RERR packets are sent to the sourc to inform the source when the energy of a node is below critical levels. EDDSR mechanism finally uses RCAC as suggested by Local Energy-Aware Routing (LEAR) protocol. Hence, the behavior of intermediate nodes with RRCAC message is similar to RREQ.

We proposed a new mechanism called as "Energy Aware Proactive Routing for MANETs based on intermediate node current condition" to find the energy aware route from source to destination. We named it as EDDSR as it is extension of existing DSR routing protocol with energy awareness. In proposed algorithm, a route is selected according to "Contemporary Processing State" of an intermediate node to achieve extended network lifetime and link reliability in terms of node's input buffer and residual energy. A major handout over the work proposed is classified as follows:

- Energy required to process K Kilobytes of packets through an intermediate node
- Current Processing State (CPS) of node in terms of energy and its input buffer traffic
- Priority of node by describing value of threshold
- Selecting path of route according to priority of a node

When threshold condition is satisfied by a node in terms of energy, then it can participate in routing. The information processing capability optimizes the metric node based on residual energy and current traffic to prevent the node from becoming a bottleneck. In DSR protocol, it uses first priority message of a node to discover an optimistic route.

To calculate the CPS (Contemporary Processing State) of a node in terms of input buffer traffic and energy consumed, consider a node N_x having energy E_x in joules and B as buffer in kilobytes which must process the x kilobytes of packets in a present state.

Consider a packet termed as K_x which requires energy e_x joules of energy and buffer space b kilobytes to process from an intermediate node. To calculate the contemporary processing state, we need to calculate subset of packets so that firstly, all communication packets are combined with size in bytes at the most of energy E_x in joules. Secondly, a sufficient amount of packets must be processed by an intermediate node in a contemporary state and also, part of the packets must not be processed. To successfully process packet K_x, a node need to consume the energy $e(K_x)$ within multi-hop mobile ad-hoc network environment and it is computed by the equation given:

$$e(K_x) = T(K_x) + R(K_x) + D(K_x)$$

Where, $T(K_x)$, $R(K_x)$ and $D(K_x)$ send, receive and process node energy which needs to be sent, received and processed in K_x Kilobytes of packets through an intermediate node.

For calculation of the Contemporary Processing State (CPS) of a node according to energy and input buffer traffic, the data packets need to be processed through an intermediate node N_x in kilobytes (where x = 1, 2, 3, ...). The packets need to be processed completely because partial processing of packets impossible. N-Topples with positive values are considered as given below: number of packets for processing N_x from a given node is in K_x (Kilobytes where x = 1, 2, 3). E (K_x) is the energy required by a node for processing of packet K_x.

Now, we use Knapsack algorithm design in two-dimensional arrays to get optimal results. The equation is as follows:

$$S[0,..., n, 0...e_x]1 \le x \le n \forall \text{ and } 0 \le e(K_x) \le e$$

Where, $SS[T(K_x), e_x]$ processes maximum number of packets with "K_x" Kilobits of data (where x = 1, 2, 3, ...,) (Algorithm 1).

Algorithm 1; the algorithm calculates contemporary processing state of a node:

$S[0, e(kx)] = 0$ $\quad 0 \le e(kx) \le ex$

no packet process through the node

$S[x, e(kx)] = \forall -\infty e(kx) < 0$, illegal condition

Optimization as:

$S[i,e(kx)] = \max(S[x-1,e(kx)], \quad Sx+S[x-1,e(k)-e(kx)]) \quad \forall \quad 1 \le I \le x$ and $0 \le e(kx) \le ex$

We designed an algorithm for calculation of contemporary processing state of a node. Our protocol is based upon DSR but we use CPS as route selection metric instead of hop count. Each node has to calculate the value of CPS in a network and the rest of mechanism follows DSR protocol (Algorithm 2).

Algorithm 2; for proposed protocol:

Step 1.: (loop, initialization)
for $e(k_y) \leftarrow 0$ to e_y till node energy
set $S[0,e(k_y)] \leftarrow 0$
Step 2.: (loop)
for $y \leftarrow 1$ to m (set number of packets)
set $S[y,0] \leftarrow 0$
Step 3.: (loop inspecting the packet to process or not)
for $i \leftarrow 1$ to m
for $e(k_y) \leftarrow 0$ to e_y
if$(e(k_y)) \leftarrow 0$ to e_y(then packets can be processed by a node)
if $(k_y + S[Y-1,e(k_y)-e_y] > S[Y-1,e_y])$ then
set $S[Y, e_y] \leftarrow k_y + s[Y-1, e_y] - e_y$
else
set $S[Y,e_y] \leftarrow s[Y-1,e_y] + (e(k_y) > e_y)$
Step 4.: (finish)
Exit

RESULTS AND DISCUSSION

Performance evaluation of proposed protocol (MDDSR): After calculating the EDDSR mechanism, we have compared this with LEAR, MDR and pure DSR in a

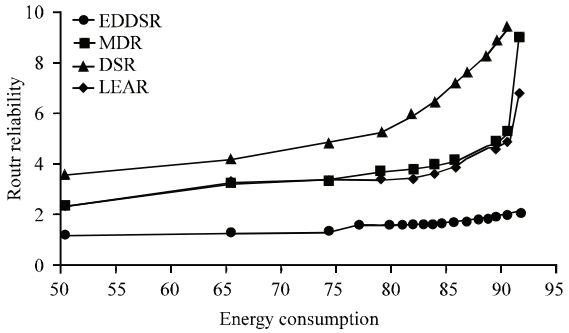

Fig. 7: Routing reliability comparison between proposed and existing mechanisms

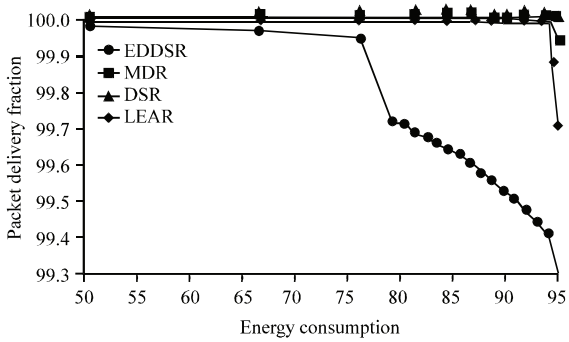

Fig. 8: Packet delivery fraction comparison between proposed and existing

Table 1: Simulation parameters

Parameters of network	Values
Time for simulation	300 (sec)
Total number of nodes	10-100
Type of link layer	Logical link
Type of MAC layer	802.11
Type of radio propagation	Two-ray ground
Type of queue	Drop tail
Node's initial enargy	15 Joules
Range of transmission	250 m
Antenna	OMNI antenna
Receiving and transmission power	350 and 650 MW
Routing protocol	DSR
Traffic	FTP, CBR
Network area	500×500 m
Type of mobility	Random wave propogation

scenario of sparse and dense network; we compared four mechanisms with respect to energy parameter. Moreover, our main focus is to compute node life time, i.e., due to lack of battery capacity it takes some time for a node to stop working. The network parameters consider in our simulation shown in Table 1. To investigate the overheating effects, we consider the energy cost and repeat all the simulations because of overheating activities.

Figure 7-9 compares number of nodes died over time after the capacity of a battery expires in a static network

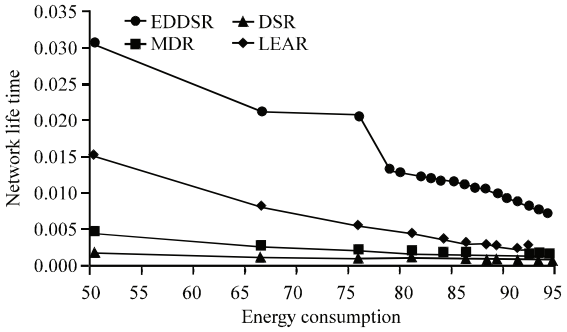

Fig. 9: Network lifetime comparison between proposed and existing mechanisms

environment. All protocols have a similar behavior but there is a slight amount of improvement found in EDDSR when simulation ends. This attitude is because of use of EDDSR rerouting techniques which helps us to avoid using a node with a weak battery.

When we consider overheating activity, balancing of energy consumption by the power aware algorithm fails because of large amount of energy consumed during overhearing activities.

In dynamic network scenario (Siddiqua *et al*., 2015), EDDSR and MDR outperform DSR. In addition, DSR consumes large amount of energy because of routing activities and the LEAR mechanism induces a large amount of energy consumption. This effect occurs due to frequent use of process of route discovery which uses DDREQ packets sent by broadcasting.

The perspective of MDR and EDDSR seems to have a better outcome from the mobility of a node which allows new routes after breakage of route. Therefore, EDDSR and MDR are able to balance the utilization of node and energy consumption accordingly. MDR is independent of the route cache and it has the capability to acquire fresh routes through periodical initiation of route discovery procedure. These routes reflect the node's residual power as well as the actual topology which removes the overhead caused due to route discovery. EDDSR does not allow an intermediate node to send RREP consisting an invalid route towards the source. In a manner of this appreciation, we also observed a small amount of expenditure of routing energy for both mechanisms.

CONCLUSION

In this research, we proposed a Energy Dependent DSR (EDDSR) method to improve energy efficiency in MANETs. Initially we compared the basic routing algorithms of MANETs designed based on hop count routing metric, through simulation we conclude that DSR is best suited protocol for achieving energy efficiency

as it is designed based on demand source initiative mechanism. Thus, we developed a on demand reactive energy dependent routing based on DSR. Through simulation, we conclude that our proposed work out perform with respect to energy efficiency parameters.

LIMITATION

The proposed on-demand routing protocol considers only few parameters in routing like energy, congestion control and neglects other parameters of QOS.

SUGGESTION

In future another on-demand routing protocol can be designed which considers other parameters of QOS also.

REFERENCES

Chaubey, N., A. Aggarwal, S. Gandhi and K.A. Jani, 2015. Performance analysis of TSDRP and AODV routing protocol under black hole attacks in MANETs by varying network size. Proceedings of the 5th International Conference on Advanced Computing and Communication Technologies, February 21-22, 2015, Rohtak, India, pp: 320-324.

Dulman, S., J. Wu and P. Havinga, 2003. An energy efficient multipath routing algorithm for wireless sensor networks. Proceedings of the IEEE International Symposium on Autonomous Decentralized Systems, April 9-11, 2003, Pisa, Italy.

Mohammad, A.A.K., A. Mirza and M.A. Razzak, 2015. Reactive Energy Aware Routing Selection Based on Knapsack Algorithm (RER-SK). In: Emerging ICT for Bridging the Future-Proceedings of the 49th Annual Convention of the Computer Society of India CSI, Satapathy, S., A. Govardhan, K. Raju and J. Mandal (Eds.). Springer, Berlin, Germany, ISBN: 978-3-319-13730-8, pp: 289-298.

Mohammad, A.A.K., A. Mirza and S. Vemuru, 2016a. Analytical model for evaluating the bottleneck node in MANETs. Indian J. Sci. Technol., 9: 1-6.

Mohammad, A.A.K., A. Mirza and S. Vemuru, 2016b. Cluster based mutual authenticated key agreement based on chaotic maps for mobile ad hoc networks. Indian J. Sci. Technol., 9: 1-11.

Moravejosharieh, A., H. Modares, R. Salleh and E. Mostajeran, 2013. Performance analysis of AODV, AOMDV, DSR, DSDV routing protocols in vehicular ad hoc network. Res. J. Recent Sci., 2: 66-73.

Siddiqua, A., K. Sridevi and A.A.K. Mohammed, 2015. Preventing black hole attacks in MANETs using secure knowledge algorithm. Proceedings of the 2015 International Conference on Signal Processing and Communication Engineering Systems (SPACES), January 2-3, 2015, IEEE, Guntur, India, pp: 421-425.

Varshney, P.K., G.S. Agrawal and S.K. Sharma, 2016. Relative performance analysis of proactive routing protocols in wireless ad hoc networks using varying node density. Invertis J. Sci. Technol., 9: 161-169.

Vazifehdan, J., R.V. Prasad and I. Niemegeers, 2014. Energy-efficient reliable routing considering residual energy in wireless ad hoc networks. Mobile Comput. IEEE. Trans., 13: 434-447.

Woo, K., C. Yu, H.Y. Youn and B. Lee, 2001. Non-blocking, localized routing algorithm for balanced energy consumption in mobile ad hoc networks. Proceedings of 9th International Symposium on Modeling, Analysis and Simulation of Computer and Telecommunication Systems, August 15-18, 2001, Cincinnati, OH., USA., pp: 117-124.

International Journal of Electrical and Computer Engineering (IJECE)
Vol. 8, No. 2, April 2018, pp. 971~978
ISSN: 2088-8708, DOI: 10.11591/ijece.v8i1.pp971-978

Image Denoising by using Modified SGHP Algorithm

Sreedhar Kollem[1], K. Ramalinga Reddy[2], D. Sreenivasa Rao[3]
[1]Department of Electronics and Communication Engineering, SR Engineering College, Warangal, Telangana, India
[2]Department of Electronics and Telematics Engineering,
G. Narayanamma Institute of Technology and Science Hyderabad, Telangana, India
[3]Department of Electronics and Communication Engineering, JNTUH CEH, Kukatpally, Hyderabad, Telangana, India

Article Info

Article history:

Received Sep 20, 2017
Revised Dec 27, 2017
Accepted Jan 7, 2018

Keyword:

Gradient histogram
Noise estimation
Principal component analysis
PSNR
S-GHP
SSIM

ABSTRACT

In real time applications, image denoising is a predominant task. This task makes adequate preparation for images looks prominent. But there are several denoising algorithms and every algorithm has its own distinctive attribute based upon different natural images. In this paper, we proposed a perspective that is modified parameter in S-Gradient Histogram Preservation denoising method. S-Gradient Histogram Preservation is a method to compute the structure gradient histogram from the noisy observation by taking different noise standard deviations of different images. The performance of this method is enumerated in terms of peak signal to noise ratio and structural similarity index of a particular image. In this paper, mainly focus on peak signal to noise ratio, structural similarity index, noise estimation and a measure of structure gradient histogram of a given image.

Copyright © 2018 Institute of Advanced Engineering and Science.
All rights reserved.

Corresponding Author:

Sreedhar Kollem
Department of Electronics and Communication Engineering,
SR Engineering College,
Warangal, Telangana, India.
Email: ksreedhar446@gmail.com

1. INTRODUCTION

Images affected by unwanted noise from different sources like traditional film cameras and digital cameras. These noise elements will create some serious issues for further processing of images in practical applications such as computer vision, artistic work or marketing and also in many fields. So, different classification of noises likes salt and pepper, Gaussian, shot and quantization. In salt and pepper noise, all the images are constructed with pixels in a two-dimensional array. In that pixel to pixel, the difference is observed when the image is affected by noise that is in terms of intensity of neighbouring pixels. So, it is identified pixels and neighbouring pixels only the small number of pixels is affected in an image. The salt and pepper noise is clearly identified in an image by it contains black and white speckles. When we viewed an image which is affected by salt and pepper noise, the image contains black and white dots, hence it terms as salt and pepper noise.

In Gaussian noise, noisy pixel value will be a small change of the original value of a pixel. A diagram consisting of rectangles whose area is proportional to the frequency of a variable or PSNR and whose width is equal to the different noise standard deviations is a histogram. Other Gaussian models are present mainly depends upon the central limit theorem shows that addition of different noises from different sources to associated with Gaussian distribution.

Denoising of an image involves the manipulation of the image data to produce a visually high-quality image. There are numerous models that have been published so far which are used for denoising an image [1]. Sparse representation for image restoration [2], [3], Total variation model [4], Wavelet-based model [5], BM3D [6] model and histogram preservation algorithm [7] are some of them. Each method has its own characteristics, benefit and also demerit. Two major classes of denoising methods are (a) model based

and (b) Learning-based method. In the model, based method, a statistical/mathematical model will be used for the denoising. Whereas in Learning based method, an algorithm will be trained by using sufficient parameters and then the model is allowed to work based on its weightage function [8].

2. PROPOSED METHOD

In the present work, the denoising is done in a more realistic way as in practical situations, only the noisy image will be available. A noisy image is taken as input to the algorithm is shown in Figure 1. We have adopted patch-based noise level estimation algorithm by Xinhao Liu et al [9]. Patches are generated from the single noisy image and its weak textured patches are identified. The Noise level is estimated from the Principal Component Analysis [10], [11].

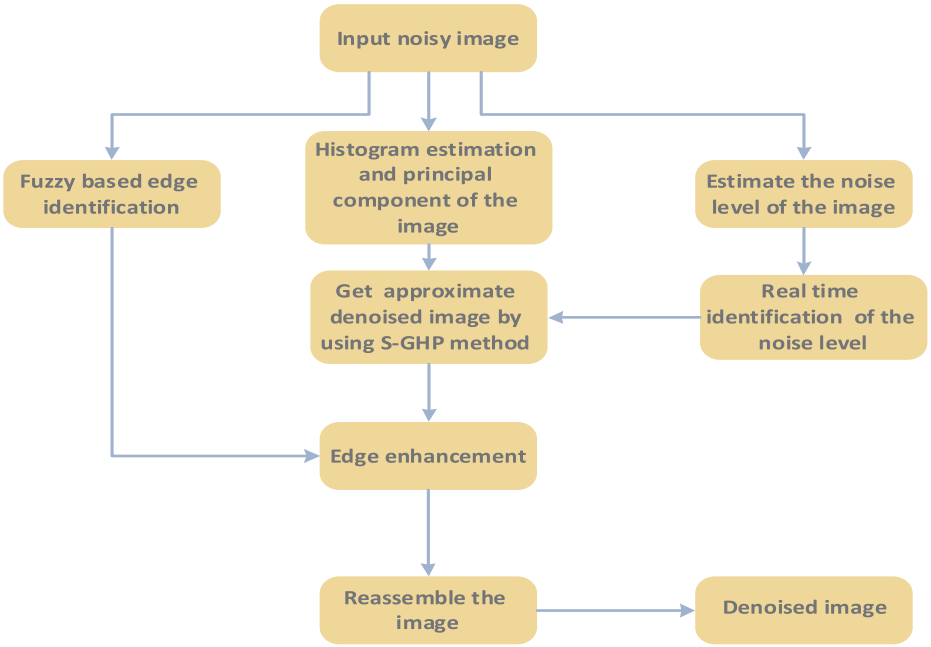

Figure 1. Flowchart of the proposed algorithm

In most of the denoising method, it is seen that, after its implementation, the image will be blurred than that of the original image. Also, the edge of the denoised image gets smoothened and will have lesser details than that of the original image. A study has been conducted to find the edge of the original and noisy image by using sample data. In this study, it is found that there fewer details of edges in the denoised image. To address this issue, we have employed fuzzy based edge detection and then the edge is enhanced in the denoised image that we have received by using our method. Now the denoising is performed based on the modified parameter S-GHP focus on smoothing of the image by implementing the gradient histogram preservation.

2.1. Noise estimation

Input image is decomposed into overlapping patches by

$$y_i = z_i + n_i \quad (1)$$

Where z_i has represented the original image patch with the ith pixel at its centre and $\mathbf{y}_i$ is the observed vectorized patch corrupted by zero-mean Gaussian noise [12] vector n_i. The objective of the noise level estimation is to compute the standard deviation σ_n of the noisy image is given. In this method, the Horizontal and vertical derivative ($D_h y$ and $D_v y$ are calculated and then the gradient vector $\mathbf{G}_y$ is obtained by taking $[D_h y D_v y]$.

Now the covariance matrix Cov_y is calculated by

$$Cov_y = G_y^T G_y \tag{2}$$

The Directional Derivative in both Horizontal Direction and Vertical Direction is calculated and trace of Gradient Matrix is calculated by

$$D = tr\left(D_h \times D_h + D_V \times D_V\right) \tag{3}$$

Now the initial noise level is estimated by computing the First component of Eigenvalue of the covariant matrix. This is taken as the initial value for calculating noise level by using iterative noise estimation [13]

$$\tau_0 = \Gamma_{inv}(\delta, \alpha, \beta) \tag{4}$$

Now the noise level estimation form weak textured patch is performed [14]. For this Inverse gamma function $\tau_0 = \Gamma_{inv}(\delta, \alpha, \beta)$ with the shape parameter α and scale parameter β is used

$$\tau = \sigma(k-1) \times \tau_0 \tag{5}$$

If the selected patch size is less than τ then the patch is selected as a Weak Texture Patch. Maximum eigenvalues of the gradient covariance are computed when the strength of image patches are to be estimated.

Now the Noise Level of Weak Texture Patch is found by using the EigenValue of Covariance Matrix of the weak textured patch and its principal component [15], [16]. The iteration is continued until the difference between sigma in step n-1 and n is less than 10^{-4}.

2.2. Image denoising frame work

The noisy image is defined by the Equation (6) that is

$$y = x + v \tag{6}$$

Where the noisy image is represented with y, the Original image is represented with x, Additive white Gaussian noise (AWGN) with zero mean is represented with v and the standard deviation is denoted with σ. The main purpose of image denoising is to compute the clean image x from noisy image y. The vibrational method is the best denoising approach is obtained by

$$\hat{x} = \arg\min_x \left\{ \frac{1}{2\sigma^2} \|y - x\|^2 + \lambda R(x) \right\} \tag{7}$$

Where regularization term is denoted with R(x) and positive constant is with λ. The R(x) relies on existing images.

Image denoising methods have a general issue that image quality scale characteristics such as structures like texture will be over-smoothed. The original image has substantial gradients than the gradients of over smoothed image. Inherently, a structure like texture doesn't depend on over smoothing and the texture have an indistinguishable gradient distribution of x for good evaluation of x. For this reason, we propose a modified parameter in S-GHP method by taking different database images. The gradient histogram of the denoised image $\hat{x}$ very close to the reference histogram h_r based on the compute of the gradient histogram of x, denote h_r. The following proposed S-GHP denoising method is defined as

$$\hat{x} = \arg\min_{x,F} \left\{ \frac{1}{2\sigma^2} \|y - x\|^2 + \lambda R(x) + \mu \|F(\nabla x) - \nabla x\|^2 \right\} \text{ s.t. } h_F = h_r \tag{8}$$

Where the odd function is *F* uniformly non-descending, h_F is histogram of the transformed gradient image |*F* (∇x) |, ∇is gradient operator and positive constant is μ. The proposed modified parameter in S-GHP method acquires the alternating optimization approach. For given *F*, then $\nabla x_0 = F(\nabla x)$ and update to x. For given x, based on equation $\nabla x_0 = F(\nabla x)$ *F* is updated by using modified parameter S-GHP specification operator.

Another case in the S-GHP method is what way to perceive the reference histogram h_r of unspecified image x. Computation of h_r depends on the noisy observation y. For finding h_r, new methods are proposed first one is a regularized deconvolution method and the second one is an iterative deconvolution method from the noisy image [17] depends upon different noise levels [18]. After reference histogram is attained, then modified parameter in S-GHP method is applied for image denoising.

3. S-GRADIENT HISTOGRAM PRESERVATION DENOISING METHOD

S-GHP is a proposed method based on the patch method. Let $x_i = R_i x$ is a patch take out at position *i* = 1, 2... *N*, where patch extraction operator is R_i and N indicates pixels in the image. Given a dictionary D, infrequently encode the patch x_i over D, gives the sparse coding vector α_i. Image patches having coding vectors are attained, the image x can be renovated by

$$x = D \circ \alpha \overset{\Delta}{=} \left(\sum_{i=1}^{N} R_i^T R_i \right)^{-1} \sum_{i=1}^{N} R_i^T D\alpha_i \tag{9}$$

Where concatenation belongs to α for all the values of α_i.

Images are taken from databases are testing modified parameter S-GHP Method. So, the combination regarding identical priors refines the modified parameter S-GHP. For example, the estimation procedures in [19]-[23] merge image non-local NSS prior to image local sparsity prior and we have better denoising results. In the method modified parameter in S-GHP, the R(x), which is sparse non-local regularization term proposed in the non-locally centralized sparse representation (NCSR) model [24] is

$$R(x) = \sum_i \left\| \alpha_i - \beta_i \right\|_1 \tag{10}$$

Where weighted average of α_i^q is β_i then

$$\beta_i = \sum_q w_i^q \alpha_i^q \tag{11}$$

and coding vector of the *q*th nearest patch (x_i^q) to x_i is α_i^q. Weight is denoted as $w_i^q = \frac{1}{W} \exp\left(-\frac{1}{h} \left\| \hat{x}_i - \hat{x}_i^q \right\|^2 \right)$, where the predefined constant is *h* and normalization factor is *W*.

The formula for modified parameter S-GHP method is defined as by using Equation (3) is

$$\hat{x} = \arg\min_{x,F} \left\{ \frac{1}{2\sigma^2} \left\| y - x \right\|^2 + \lambda \sum_i \left\| \alpha_i - \beta_i \right\|_1 + \mu \left\| F(\nabla x) - \nabla x \right\|^2 \right\} \tag{12}$$

Such that

$$x = D \circ \alpha, \; h_F = h_r \tag{13}$$

From the S-GHP method, using Equation (7), *F* (∇x) is approximate to ∇x when histogram parameter leads to larger and we can achieve required histogram parameter for S-GHP. When the histogram h_F of |*F* (∇x)| is

required and approximate to the h_r, (histogram of $\nabla x = h_r$) then acquire the required gradient histogram parameter for S-GHP.

4. RESULTS AND DISCUSSION

4.1. Performance analysis

The proposed method is verified by using three different images like image-3, image-4 and image-5. Here, three images are grey-scale images having a range between 0 to 255. For image-3, image-4 and image-5 are taking five different noise levels are 20, 25, 30, 35 and 40 with respect to that different PSNR and SSIM values are obtained. In Figure 2, Figure 3 and Figure 4, there is original image and different enhanced images with different noise levels. In Figure 5, numbers of iterations are increased then PSNR value increases. When noise standard deviation is increased then the structural similarity index is decreased. From the Figure 5, image-3 having more structural similarity index. In Table 1, Table 2 and Table 3 give the structural similarity index and PSNR values of image-3, image-4 and image-5 by using a modified parameter in S-GHP method.

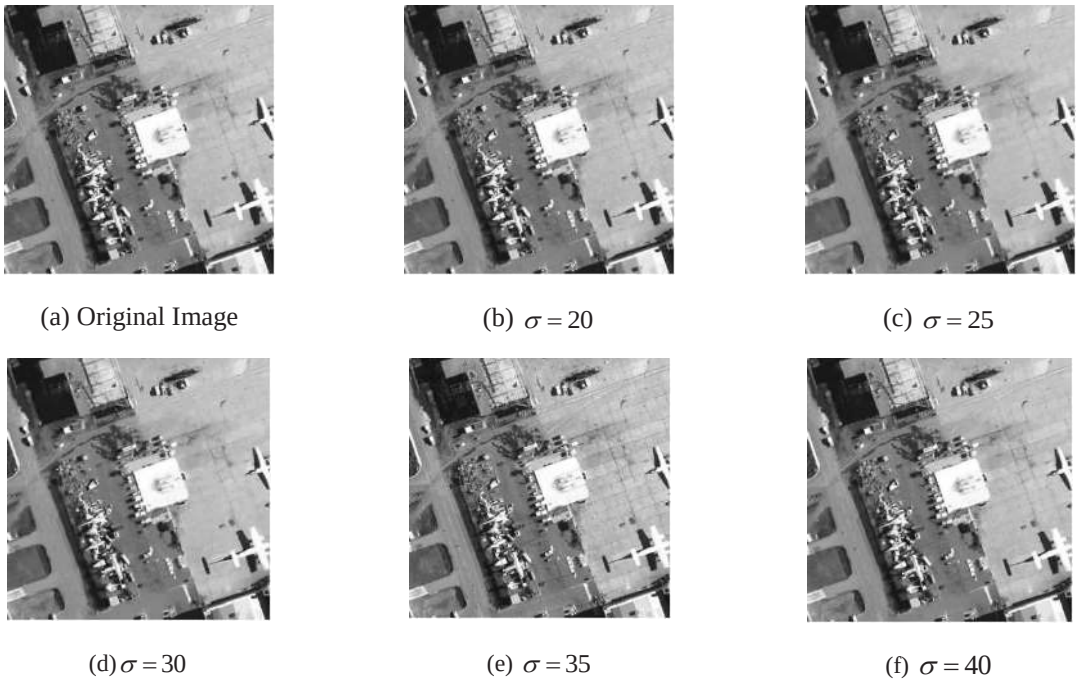

(a) Original Image (b) $\sigma = 20$ (c) $\sigma = 25$

(d) $\sigma = 30$ (e) $\sigma = 35$ (f) $\sigma = 40$

Figure 2. Denoised image-3 under different noise levels

Table 1. Structural similarity index (SSIM) and PSNR (dB) results of s-gradient histogram preservation of image-3

No. of Iterations	Sigma=20 S-GHP	Sigma=25 S-GHP	Sigma=30 S-GHP	Sigma=35 S-GHP	Sigma=40 S-GHP
1	27.766	26.440	25.297	24.842	24.031
	0.738	0.678	0.621	0.600	0.556
2	27.957	26.771	25.779	25.400	24.766
	0.748	0.698	0.651	0.640	0.608
3	28.093	27.015	26.138	25.684	25.127
	0.755	0.713	0.675	0.660	0.637
4	28.161	27.147	26.334	25.736	25.190
	0.757	0.719	0.687	0.660	0.638
5	28.174	27.193	26.406	25.727	25.186
	0.755	0.719	0.689	0.656	0.634
6	28.157	27.192	26.417	25.708	25.169
	0.752	0.716	0.687	0.654	0.632
Average PSNR	28.051	26.959	26.061	25.516	24.911
and SSIM	0.750	0.707	0.668	0.645	0.617

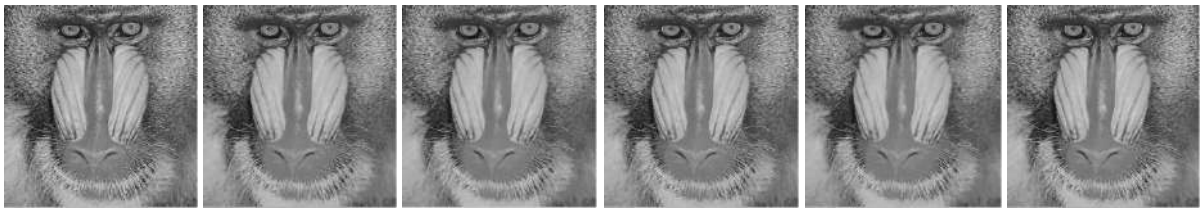

(a) Original Image (b) $\sigma = 20$ (c) $\sigma = 25$ (d) $\sigma = 30$ (e) $\sigma = 35$ (f) $\sigma = 40$

Figure 3. Denoised image-4 using under different noise levels

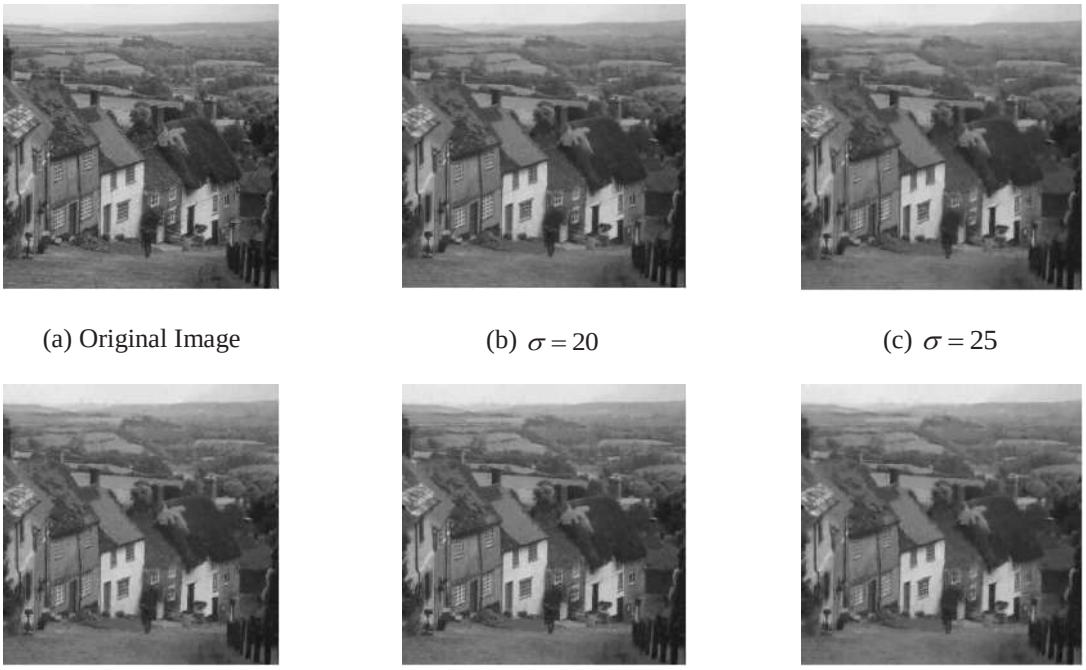

(a) Original Image (b) $\sigma = 20$ (c) $\sigma = 25$

(d) $\sigma = 30$ (e) $\sigma = 35$ (f) $\sigma = 40$

Figure 4. Denoised image-5 using under different noise levels

Table 2. Structural similarity index (SSIM) and PSNR (dB) results of s-gradient histogram preservation of image-4

No. of Iterations	Sigma=20 S-GHP	Sigma=25 S-GHP	Sigma=30 S-GHP	Sigma=35 S-GHP	Sigma=40 S-GHP
1	26.449	25.120	24.033	23.495	22.770
	0.772	0.708	0.648	0.615	0.568
2	26.547	25.256	24.213	23.715	23.068
	0.780	0.720	0.663	0.637	0.595
3	26.638	25.396	24.405	23.927	23.326
	0.788	0.733	0.681	0.662	0.627
4	26.704	25.506	24.556	24.020	23.421
	0.795	0.745	0.699	0.673	0.639
5	26.741	25.577	24.654	24.036	23.428
	0.800	0.753	0.711	0.674	0.638
6	26.744	25.600	24.689	24.018	23.398
	0.801	0.757	0.715	0.672	0.637
Average PSNR and SSIM	26.637	25.409	24.425	23.868	23.235
	0.789	0.736	0.686	0.655	0.617

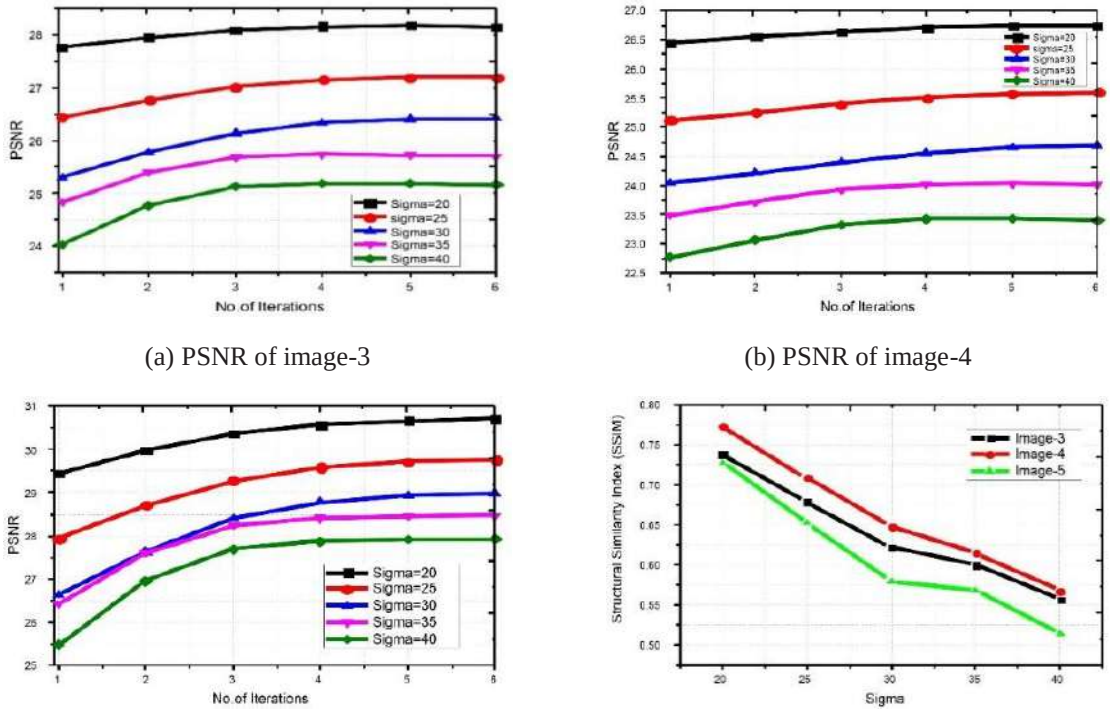

(a) PSNR of image-3

(b) PSNR of image-4

(c) PSNR of image-5

(d) Comparison of Sigma and SSIM

Figure 5. Variation of PSNR of image-3, image-4, image-5 using different sigma values and its SSIM

Table 3. Structural similarity index (SSIM) and PSNR (dB) results of s-gradient histogram preservation of image-5

No. of Iterations	Sigma=20 S-GHP	Sigma=25 S-GHP	Sigma=30 S-GHP	Sigma=35 S-GHP	Sigma=40 S-GHP
1	29.451	27.936	26.617	26.421	25.469
	0.728	0.652	0.580	0.568	0.513
2	29.972	28.703	27.637	27.606	26.939
	0.760	0.701	0.647	0.655	0.620
3	30.361	29.280	28.398	28.243	27.690
	0.785	0.742	0.703	0.709	0.687
4	30.570	29.585	28.779	28.403	27.863
	0.799	0.764	0.733	0.722	0.701
5	30.667	29.711	28.930	28.454	27.914
	0.804	0.772	0.744	0.724	0.704
6	30.707	29.761	28.986	28.473	27.930
	0.806	0.774	0.747	0.726	0.706
Average PSNR	30.288	29.163	28.224	27.933	27.300
and SSIM	0.780	0.734	0.692	0.684	0.655

4.2. Comparative analysis

The existing methods and proposed method verified by using three different images like image-3, image-4 and image-5 with five different noise levels are 20, 25, 30, 35 and 40. Performance of these methods is mentioned in terms of Peak signal to noise ratio and structural similarity index [25], [26] as shown in Table 4.

Table 4. Comparison of Existing methods and proposed method in terms of PSNR (dB) results

Image No	Existing Methods		Proposed Method
	B-GHP PSNR	APBS PSNR	Modified S-GHP PSNR
3	27.01	26.05	28.051
4	25.49	25.11	26.637
5	29.90	28.66	30.288

5. CONCLUSION

In this paper, the proposed method modified Structure gradient histogram preservation used for enhancing the different images by taking different noise levels like 20, 25, 30 and 40. Based on the noise levels, the PSNR and SSIM values are improved compared to other methods like APBS and B-GHP. All the above-mentioned results proved that the modified parameter S-GHP is better compared to B-GHP and APBS.

REFERENCES

[1] Buades, B. Coll, and J. Morel, "A review of image denoising methods, with a new one", *Multiscale Model. Simul.*, vol. 4, no. 2, pp. 490530, 2005.

[2] K. Dabov, A. Foi, V. Katkovnik, and K. Egiazarian, "Image denoising by sparse 3-D transform-domain collaborative filtering", *IEEE Trans. Image Process.*, vol. 16, no. 8, pp. 2080-2095, Aug. 2007.

[3] W. Dong, L. Zhang, G. Shi, and X. Li, "Nonlocally centralized sparse representation for image restoration", *IEEE Trans. Image Process*, vol. 22, no. 4, pp. 1620-1630, Apr. 2013.

[4] L. Rudin, S. Osher, and E. Fatemi, "Nonlinear total variation based noise removal algorithms", *Phys. D*, vol. 60, nos. 14, pp. 259-268, Nov. 1992.

[5] Pankaj Hedaoo and Swati S Godbole, "Wavelet Thresholding Approach for Image Denoising", *International Journal of Network Security Its Applications (IJNSA)*, vol. 3, no. 4, July 2011.

[6] H. C. Burger, C. J. Schuler, and S. Harmeling, "Image denoising: Canplain neural networks compete with BM3D", *in Proc. Int. Conf. CVPR*, Jun. 2012, pp. 2392-2399.

[7] S. Subha, I. Jesudass and K. Thanushkodi, "Image denoising by using iterative histogram and preservative algorithm", *ARPN Journal of Engineering and Applied Sciences*, vol. 10, no. 11, June 2015.

[8] P. Koltsov, "Comparative study of texture detection and classification algorithms," *Comput. Math. Math. Phys.*, vol. 51, no. 8, pp. 1460-1466, 2011.

[9] Liu, Xinhao, Mitsuru Tanaka, and Masatoshi Okutomi, "Noise level estimation using weak textured patches of a single noisy image", *Image Processing (ICIP), 2012 19th IEEE International Conference on. IEEE*, 2012.

[10] S. Pyatykh, J. Hesser and L. Zheng, "Image Noise Level Estimation by Principal Component Analysis," in IEEE Transactions on Image Processing, vol. 22, no. 2, pp. 687-699, Feb. 2013.doi: 10.1109/TIP.2012.2221728.

[11] Jolliffe, "Principal component analysis," in *Encyclopedia of Statistics in Behavioral Science*. New York: Springer-Verlag, 2002.

[12] D. Pastor, "A theoretical result for processing signals that have unknown distributions and priors in white Gaussian noise," *Comput. Stat. Data Anal.*, vol. 52, no. 6, pp. 3167–3186, 2008.

[13] Liu, "A fast method of estimating Gaussian noise," in *Proc. 1st Int. Conf. Inf. Sci. Eng.*, 2009, pp. 441–444.

[14] C. Kervrann and J. Boulanger, "Optimal spatial adaptation for patch-based image denoising," *IEEE Trans. Image Process.*, vol. 15, no. 10, pp. 2866–2878, Oct. 2006.

[15] R. Bilcu and M. Vehvilainen, "New method for noise estimation in images," in *Proc. IEEE-Eurasip Nonlinear Signal Image Process.*, May 2005.

[16] G. Smith and I. Burns, "Measuring texture classification algorithms," *Pattern Recognit. Lett.*, vol. 18, no. 14, pp. 1495–1501, 1997.

[17] D. Makovoz, "Noise variance estimation in signal processing," in *Proc. IEEE Int. Symp. Signal Process. Inf. Technol.*, Jul. 2006, pp. 364–369.

[18] M. Uss, B. Vozel, V. Lukin, S. Abramov, I. Baryshev, and K. Chehdi, "Image informative maps for estimating noise standard deviation and texture parameters," *EURASIP J. Adv. Signal Process.*, vol. 2011, pp. 806516-1–806516-12, Mar. 2011.

[19] M. Elad and M. Aharon, "Image denoising via sparse and redundant representations over learned dictionaries", *IEEE Trans. Image Process.*, vol. 15, no. 12, pp. 3736-3745, Dec. 2006.

[20] J. Jancsary, S. Nowozin, and C. Rother, "Loss-specific training of nonparametric image restoration models: a new state of the art," in *Proc. Eur. Conf. Comput. Vis.*, 2012.

[21] M. Hashemi and S. Beheshti, "Adaptive noise variance estimation in Bayes shrink", *IEEE Signal Process. Lett.*, vol. 17, no. 1, pp. 12-15, Jan. 2010.

[22] T. Tasdizen, "Principal components for non-local means image denoising," in *Proc. IEEE Int. Conf. Image Process.*, Feb. 2008, pp. 1728-1731.

[23] V. Rajanesh and Kollem Sreedhar, "A New Approach to Image Denoising by Patch-Based Algorithm", in *International Journal of Advanced Research in Computer and Communication Engineering*, vol. 5, no. 12, pp. 212-218, 2016.

[24] Yasmin, Sabina, and Md Masud Rana, "Performance Study of Soft Local Binary Pattern over Local Binary Pattern under Noisy Images", *International Journal of Electrical and Computer Engineering*, vol. 6, no. 3 (2016), p. 1161.

[25] Omidiora, E. O., S. O. Olabiyisi, J. A. Ojo, Abayomi-Alli Adebayo, O. Abayomi-Alli, and K. B. Erameh, "Facial Image Verification and Quality Assessment System-FaceIVQA", *International Journal of Electrical and Computer Engineering*, vol. 3, no. 6 (2013), p. 863.

[26] Subramanyam, M. V., and Giri Prasad, "A New Approach for SAR Image Denoising", *International Journal of Electrical and Computer Engineering*, vol. 5, no. 5 (2015).

International Journal of Engineering Technology Science and Research
IJETSR
www.ijetsr.com
ISSN 2394 – 3386
Volume 4, Issue 10
October 2017

Design of Improved Remote Data Transfer Using Concurrent Multipath through Mobile Device

Rajeshwari M Goudar[1]
Research Scholar, UniversityCollege of Engg, JNTU, Kakinada[1]
Syed Abdul Sattar[2]
Nawab Shah Alam Khan, College of Engg& Technology, Hyderabad[2],
Ch Satyanarayana[3]
University College of Engg, JNTU,Kakinada[3]

ABSTRACT

With faster growth of mobile technology and internet more and more technical features are provided through mobile devices which made the ease of day to day activities of the users of mobile devices. Millions of users are making use of mobile devices for making faster communication, sending and receiving of data or information seamlessly from remote places. Today's mobile devices are having the features of personal computers (pcs) and hence the integration of the devices between mobile and pcs can be monitored and better interaction can be accomplished.

Due to the widespread use of wireless technologies convergence of wired and wireless networks made easy to perform tasks on mobile devices. Today's corporate world is handling most of the work through remote place by controlling the activities over different networks. Administrator of the network will handle all the activities of network through mobile device without his presence in a server room of the network. Research activities are being carried out that allow remote control of devices.

An effort is made to explore multipath aggregation problem in order to get solutions which will improve throughput by making effective use of multiple paths of heterogeneous wireless networks concurrently. This work is mainly tested at application layer by forwarding single data transport connection over the multiple paths. The purpose of logical segmentation of a file streaming is made by using multi-homed clients is to be developed at application layer. The new approach uses CMT-SCTP protocol with existing server infrastructure client based manner.

KEYWORDS

Concurrent Multi-path, Bandwidth Aggregation, Interface

I INTRODUCTION

The first computer communication network started since the birth of Internet which covered area more than laboratory among three American universities and Stanford Research Institute by using 50 Kbit/s links [1]. The packet switched network was used for the first datagram in the world is sent for long distance and their onwards technology of communication journey started its progress. The fast growing wired and wireless technology of communication enabled, use of mobile devices, smartphones by millions of people to access the data of huge size by using Internet. The increasing data access demands for high speed of data transfer at the end hosts. This can be achieved by aggregating multiple network interfaces (paths) and using multiple paths simultaneously. The aggregation of bandwidth is useful when media of data is accessible by using slow wireless networks. The single wireless network path is, unable to provide the required data rate of transmission.

Today's wireless devices like smartphones and laptops are equipped with multiple number of interface which will be enabled to communicate with wireless local area networks. These devices are located in the coverage areas of wireless networks. Operating systems use single interface only for data transmission and other

International Journal of Engineering Technology Science and Research
IJETSR
www.ijetsr.com
ISSN 2394 – 3386
Volume 4, Issue 10
October 2017

interfaces will be idle in spite of available multiple interfaces. TCP and UDP transport protocols are used for majority of data transfer. However TCP and UDP protocols are not supporting for multiple number of IP addresses. By using multiple paths, packet reordering is essential and it can affect the performance.

Main goal of this proposed work is to improve data transfer speed by using multiple-paths i.e. interfaces available in the network at user's end host. This can be achieved by aggregating multiple network interfaces(paths) and using multiple paths simultaneously. This will be very much useful when the media of data access is possible through several slow networks. The single wireless network path is, unable to provide the required data rate of transmission like high quality multimedia streaming.

Smartphones and laptops devices equipped with multiple interfaces are commonly used for communicating different wireless technologies such as 3G, Wi-Fi, cellular networks and wireless local area networks. These mobile devices are present in the coverage areas of networks. Whenever the device is in the range of access networks then the device which executes the application can send the data simultaneously by using multiple paths as shown in fig. 1.

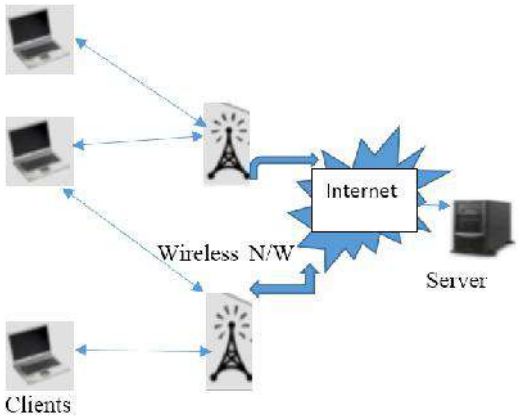

Fig. 1: Multipath network for data transmission

Remainder of the paper is organized as below. Section II briefs about the related work of bandwidth aggregation at different layers of standard protocol stack. Section III presents CMT-SCTP protocol which is followed by architecture of system in section IV and conclusion is given in Section V.

II Related work:

The main aim of aggregation of multiple paths is to improve the throughput. Solution of aggregation of multipath should attain at least average throughput, equivalent to the total addition of throughput of each individual paths.Continuous research work is carried out by researchers in order to provide the bandwidth aggregation on different layers of the protocol stack which use multi-homed devices.

Link layer

Multipath aggregation at link layer is also called as bonding or bundling at link layer as more number of physical channels are bundled into one logical channel [2]. Ethernet channel allows many of the hosts to be connected in order to obtain improved throughputby using multiple cables of Ethernet. Ethernet bundling prevents reordering of frames by making use of same port of Ethernet for the data flow. Ethernet speed is always more than the requirement of single application. Multilink Point to Point Protocol (PPP) also uses aggregation of the links[3]. At link layer, bandwidth aggregation works for two systems only. It is not useful for connecting multiple systems. Generic link layer (GLL) approach for bandwidth aggregation for link layer is proposed by Koudouridis[14]. Multiple radio access networks are used for communication with destination node.

International Journal of Engineering Technology Science and Research
IJETSR
www.ijetsr.com
ISSN 2394 – 3386
Volume 4, Issue 10
October 2017

Network layer

Multipath routing in network layer uses different paths(end to end) between the source and thedestination. Forwarding of IP traffic data over the multiple paths require the host to be multi-homed. The multi-homed system is one which has multiple providers of IP address ranges.

Aggregation of multiple paths at network layers use tunneling mechanism for transfer of packets from server to all IP addresses at client side. Bandwidth aggregation with infrastructure for network layer was proposed by Chebrolu et al. [4,5].Knowing the addresses of multi-homed clients, server calculates the packet delivery time to send the packetsintelligently with the aim of reducing reordering of packets at receiver. Earliest Delivery Path First (EDPF) is used for bandwidth aggregation at network layer is used by the author Kameshwari Chebrolu [5] at Network Layer, where minimal changes are made for existing infrastructure. EDPF works mainly based on the principle of ensuring packets which meet playback deadlines. Here scheduling of packets is based on estimation of transmission time ofthe packets. EDPF well performs similar to the Aggregated Single Link (ASL), where single interface will replace multiple interfaces which are having same kind of aggregated bandwidth.

Transport layer:

Single path transport protocols are not able to support for multimedia and other business applications which demand for reliability and fault tolerance. Multipath techniques can solve deficiencies of single path protocols by using inverse multiplexing of resources to send packets over multiple paths which provide fault tolerance, better reliability and enhanced throughput. Use of multipath transport layer is suitable for the devices which provide heterogeneous access technologies like Wi-Fi, 3G,Wi-max etc. Mobile devices by using multiple paths provide improved reliability and the ability to shift from one technology to other. It is also possible for the mobile nodes to pool their low bandwidth which can support for high bandwidth demanding applications. CMT-SCTP protocol is useful for multiple paths aggregation at transport layer for failover of multiple IP addresses and not for use of simultaneous data transfer. Iyengar etal.[7,8] developed concurrent multipath transfer protocol, the extension of SCTP supports for data transfer forone end to other end paths. Different capacity of the paths and delay will cause packet reordering and faster transmission. Authors propose for virtual queues to be used at the sender side to know the packet reordering and packet losses.

Many of researchers continued the work in order to strengthen idea of CMT, by developing CMT-SCTP, load sharing SCTP(LS-SCTP). Fiore et al. [9] and Perotto et al. [10] suggested to use Westwood's bandwidth estimation in order to send the chunks over available paths efficiently.

Dreibholz and Adhari etal. [11, 12] proposed SCTP-based multipath aggregation solution over the asymmetric paths.Distributed Stream Control Transmission Protocol (DSCTP) makes use of [15] multi-streaming and multi-homing for the aggregation of the bandwidths of interfaces. It makes use theavailable active streams simultaneously.

Application layer:

The application which wants to transfer the data on multiple paths will establish several transport connections and binding them to IP addresses. Data to be transferred is distributed as per the available capacity of the path. The data file to be sent is split into number of logical segments and transmitted concurrently over different paths.

Application Layer Protocol based Aggregation (ALPA) is a protocol used at the application layer for bandwidth aggregation is proposed in the paper[16] by considering the dynamics of wireless links. The objective this work is mainly to minimize energy consumption and guaranteed quality of service by dynamically scheduling of data transmission for both network interfaces.

IIICMT SCTP Protocol

Stream control transmission protocol (SCTP) is a standard transport layer protocol developed by Internet Engineering Task Force (IETF). CMT SCTP is an extension of SCTP protocol. It provides services

International Journal of Engineering Technology Science and Research
IJETSR
www.ijetsr.com
ISSN 2394 – 3386
Volume 4, Issue 10
October 2017

equivalent to TCP and UDP apart from multi-homing and multi-streaming. SCTP is one of the reliable protocol. It supports for multiple IP addresses. It is useful for addressing interfaces which are connected to different networks. It uses one single identified path for data transmission and other are used for the purpose of backup and retransmissions. Today's mobile devices like laptops and smart phones are having multiple interfaces. The multi-homing service allow these devices for establishment of connection with more number of networks similar to smart phone with 4G and Wi-Fi connections.

In an SCTP association, one of the path is usedfor transmission of data and others are used for retransmissions or backup whenever path failure occurs.The multi-streaming service is used for concurrent transmission of streams.SCTP supports forthe transfer of simultaneous data over multiple paths by using CMTSCTP so as to updatethroughput of aggregated transmission [13]. CMT-SCTP protocol allows for utilization of multi paths simultaneously. It facilitates for higher data transmission among the hosts, having multiple interface devices so as to maximize aggregated transmission throughput.

CMT-SCTP allows for the payload data to be distributed across all of available paths at the same time. An example for association of two paths SCTP and CMT-SCTP is as shown in the fig 2 a) and Figure 2 b). Apart from increase in the performance by using CMT SCTP but there are some issues related to reordering of the data at the receiver end. However main issues related are fast retransmission and selective acknowledgement traffic. In order to avoid these issues, algorithms for CMT-SCTP are proposed [13].

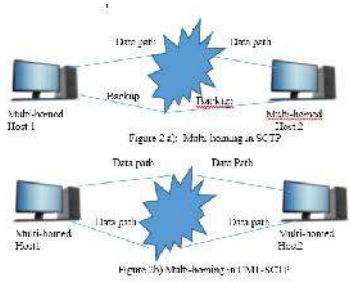

Fig. 2b) Multi-homing in CMT-SCTP

Association buffer is used to keep data chunks irrespective of the path on which these data chunks were transmitted. It supports for multi-buffer structure. CMT-SCTP association is as shown in the fig.3.

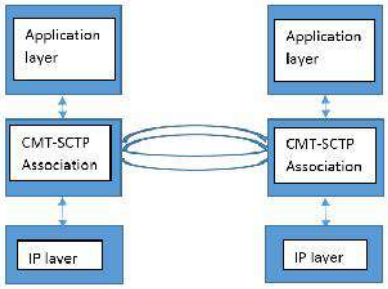

Fig. 3: CMT-SCTP Association

IV Architecture of system

The general architecture for multipath data transfer consists of multiple clients and server from which data is to be fetched are connected in a wired/wireless network. Let the client C makes request for required file transfer from server S. The server S transmits the requested file using multiple paths where concurrent transmission takes place in the form of data chunks. Each path connected through an intermediate node which forwards the incoming packets from first path P_1 towards the client on second path P_2 based on the optimum selection of path based on estimation of path selection for communication which is as shown in figure 4. Client can be smartphone, mobile device or laptop and nodes can be access point, base station, Wi-Fi, Wi-

International Journal of Engineering Technology Science and Research
IJETSR
www.ijetsr.com
ISSN 2394 – 3386
Volume 4, Issue 10
October 2017

max, wireless routers or personal computers used as clients. Server is connected through buffer interfaces in the form of FIFO queue. The paths between server and client are of variable bandwidth. Variable bandwidth is the rate at which the paths send the data from server buffers as a function of time. Intermediate nodes just forward the data packets received as it is to the client.

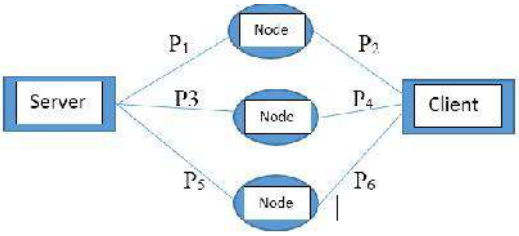

Fig. 4: Bandwidth aggregation architecture

The overall architecture of system mainly consists of following modules.

A Creation of Network:

A simulation environment is created by connecting multiple machines in wireless network including a server. Some of the nodes will work as transportation media of Wi- fi /wi-max. Each of these nodes have their own unique speed of transmission and others will act as clients. Database is maintained for both the files to be transmitted at the server side and database for keeping the received files at client side. Receiving buffers are used at the client side to receive incoming packets. Clients will make request for the required data for the server and server will check for the requested file in its database and responds by sending the file requested using multi-paths of the network available using optimal paths for communication using bandwidth aggregation. CMT-SCTP association is created between client and server and socket is used for the process of transportation. Compressed data to be sent is received by data splitter and there by divided into number of data chunks and these chunks are sent on different paths based on the selection of paths of communication using path estimation and selection of paths as shown in system architecture diagram represented in the fig. 5.

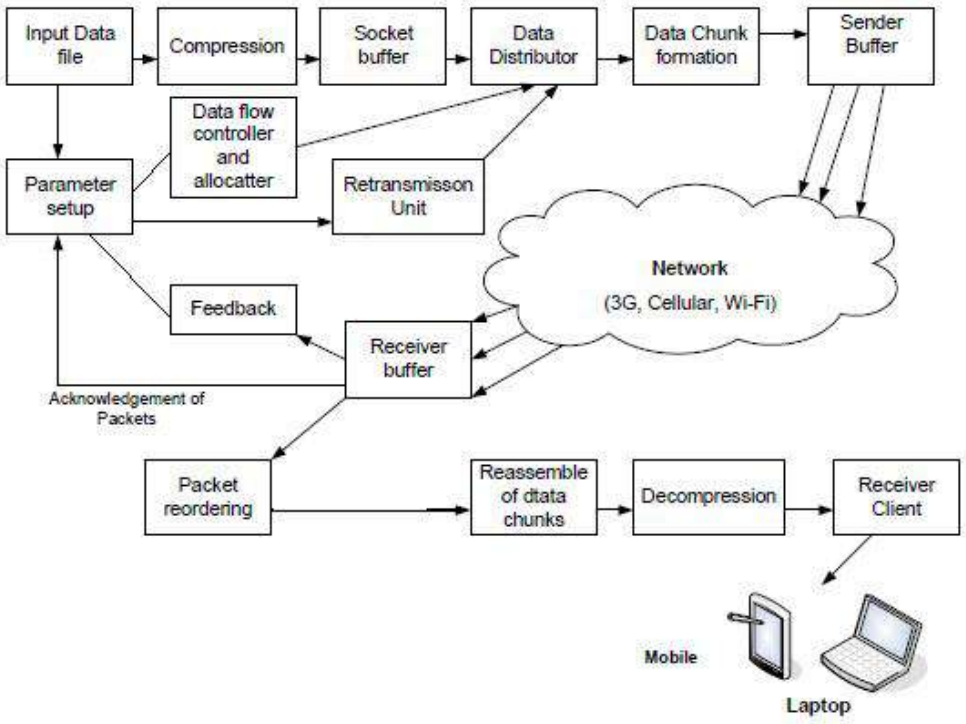

Fig. 5: System architecture

International Journal of Engineering Technology Science and Research
IJETSR
www.ijetsr.com
ISSN 2394 – 3386
Volume 4, Issue 10
October 2017

B. Server activity:

Server activity module starts first to collect list of clients activated/started in the network. It is ready to provide the following information/services.

1. List of clients connected in the network
2. List out the processes which are being executed at the selected client
3. Facility to kill a particular process, shutdown or termination of client machine
4. Sending and receiving of messages from server to the clients
5. Transfer of requested file by the client from server using bandwidth aggregation

Various operations will be executed remotely for controlling of process, file operations, sending a message, capturing of screenshots. All these operations are controlled by mobile device. Mobile device can be connected either through internet connection or through Wi-Fi connection. The server module performs operations such as control of processes, and killing of the running process of the client node. One has to select the process which is to be terminated from the list of the processes. In order to read a particular file one has to enter the path of the file and can have the access to the file. Other operations like broadcasting of message and sending notification to particular client is also possible.

C. Client activity:

Client gets started and have the facilities for requesting a file required from server end, Sending and receiving of messages. Activities of client are controlled by server.

D. Data flow rate controller and allocator:

Data flow rate controller and allocator is mainly concerned with choosing of best paths from the subset of communication paths and assign the transmission or bandwidth allocation rates to each of the path. Bandwidth allocation vector R =(r_0,r_1,r_2,r_3 … r_{n-1}) is maintained to keep track of number of transmission paths and bandwidth allocation values(n) along each of the path and is arranged in ascending order so that a path with maximum available bandwidth value is selected. r_i is thebandwidth allocated to the source i so that there is no congestion in the network and it is always less than the capacity of the link. If the available bandwidth is allocated with equal amount of bandwidth among all the connections and there is no proper utilization of bandwidth as each of the application is not utilizing the bandwidth. So there is a need of utility maximization algorithm for maximizing bandwidth allocation to each of the application.

E. Packets forwarding: Server is connected to the clients with multiple paths in the network. Each of path in the network is independent of each other path and has its own transmission speed. Each of these communication paths are having the properties as listed below.

a) Bandwidth available (B_a): It is measured in terms of bits transferred in the given unit amount of time.

b) Round trip time (RTT_p): It is total time taken for sending of data packet and receiving of acknowledgement for the data packet.

c) Path loss rate(L_p): It is the rate of loss of packets for that path of communication.

Each of the communication path is assigned with transmission capacity. Optimal throughput is obtained by using flow rate controller and allocator using utility maximization algorithm.

F. Reordering of packets:

The end to end delay of each path differs in the network. During the transfer of packets using concurrent multipath, there are chances of receiving the packets out of order. So packet scheduling [11] [12] [13] [15] is used to arrange transmission sequence in order to minimize the delay caused due to the reordering of packets at receiver end. The desired output at the receiver is generated by reordering of packets received through concurrent multi-paths.

V Conclusion:

Bandwidth aggregation for improving the throughput is proposed for accessing remotely required data by the clients connected in a network using mobile device. It is useful for remote monitoring and sharing of data. A terminal equipped with multiple network interfaces can access data through concurrent multi-paths. By using services of bandwidth aggregation, significant enhancement in the performance is achieved in terms of throughput, reliability and resource sharing over the use of single interface. A virtual bigger logical link with high bandwidth can be created by using multiple links of lower bandwidth in order to meet demands of applications which require higher bandwidth. Here a dynamic bandwidth aggregation is used at transport layer of the network. Compression and decompression of data is implemented in order to enhance the transmission throughput and better quality of service. Bandwidth aggregation is attained by using lower bandwidth channels and thereby achieving increase in transmission throughput.

In future, mobile and wireless communication systems will support for the increase in volume of data and thereby increase in the range of application domains which demand for high speed of transmission of data. The popularity of multi-homed mobile terminals facilitate for bandwidth aggregation to provide improved data transmission, throughput and reliability. In this work, the design of system is addressed to get aggregate bandwidth when a mobile device has several interfaces for communication and transfer of data. The extension of this research work can be useful for high streaming of video where dynamic availability of access networks with multiple interfaces of mobile device.

REFERENCES

[1] Zakon, R. H. Hobbes' Internet Timeline. IETF RFC 2235, November 1997.

[2] Association, I. S. Link aggregation for local and metropolitan area networks. IEEE Standard 802.1AX-2008, November 2008.

[3]Simpson, W. A. The Point-to-Point Protocol (PPP). IETF RFC 1661, July 1994.

[4] Chebrolu, K., Raman, B., and Rao, R. R. A network layer approach toenable TCP over multiple interfaces. Wireless Networks 11, 5 (2005), 637–650.

[5] Chebrolu, K., and Rao, R. R. Bandwidth aggregation for real-time applicationsin heterogeneous wireless networks. IEEE Transactions on Mobile Computing 5, 4(2006), 388–403.

[6] C. Paasch, G. Detal, F. Duchene, C. Raiciu, and O. Bonaventure, "Exploringmobile/WiFi handover with multi-path TCP," in Proceedings ofthe 2012 ACM SIGCOMM workshop on Cellular networks: operations,challenges, and future design. ACM, 2012, pp. 31–36.

[7] Allman, M., Balakrishnan, H., and Floyd, S. Enhancing TCP's Loss RecoveryUsing Limited Transmit. IETF RFC 3042, January 2001.

[8] Allman, M., Kruse, H., and Ostermann, S. An Application-Level Solutionto TCP's Satellite Inefficiencies. In Proceedings of the First International Workshopon Satellite-based Information Services (WOSBIS) (Rye, New York, USA, 1996).

[9] Fiore, M., Casetti, C., and Galante, G. Concurrent multipath communicationfor real-time traffic. Comput. Commun. 30, 17 (2007), 3307–3320.

[10] Perotto, F., Casetti, C., and Galante, G. SCTP-based Transport Protocolsfor Concurrent Multipath Transfer. WCNC (2007).

[11] Dreibholz, T., Becke, M., Rathgeb, E. P., and Tuxen, M. On the Useof Concurrent Multipath Transfer over Asymmetric Paths. In Proceedings of theIEEE Global Communications Conference (GLOBECOM), ISBN 978-1-4244-5637-6 (December 2010).

[12] Adhari, H., Dreibholz, T., Becke, M., Rathgeb, E. P., and Tuxen, M.Evaluation of Concurrent Multipath Transfer over Dissimilar Paths. In Proceedingsof the 1st International Workshop on Protocols and Applications with Multi-HomingSupport (PAMS), Singapore (March 2011).

[13]J. R. Iyengar, P. D. Amer, and R. Stewart, "Concurrent multipath transferusing SCTP multi-homing over independent end-to-end paths," Networking,IEEE/ACM Transactions on, vol. 14, no. 5, pp. 951–964, 2006.

[14]Koudouridis GP,Aguero R, AlexandriE, ChoqueJ, DimouK,KarimiHR, LedererH, Sachs J, Sigle , "Generic link layer functionality for multiradio access networks". In Proceedings of mobile summit, 2005.

[15] Mohammad Mamun Elahi, Shahin Khan, "A DistributedSCTP Scheme for Bandwidth aggregation", 16th International Conference of Computer and Information Technology, 8-10 March 2014.

[16] Zaiyang Tang, Zirui Wang, Peng Li, Song Guo, Xiaofei Liao, and Hai Jin "An Application Layer Protocol for Energy-Efficient Bandwidth Aggregation with Guaranteed Quality-of-Experience", IEEE Transactions on Parallel and Distributed Systems2014.

A Network Coded Mobile Agent Based Energy Efficient Data Gathering Scheme for Heterogeneous Wsns

S Anuradha, D Sreenivasa rao

Abstract*: *Latest centuries have observed a rising attention in organizing huge amounts of micro-sensors which cooperate in a distributed method on information gathering as well as handling. Sensors remain estimated towards being economical and might remain positioned in a huge measure in strict atmospheres which concludes that sensors remain normally operative unattended. Through inadequate battery control, Energy-efficient information distribution remains critical as sensor nodes activate. Presently, maximum energy-efficient applications in Heterogeneous wireless sensor network (WSN) remain based on the customer or server calculating model, where every sensor node sends its information towards a sink node. A sensor network's information traffic might exceed the network capability as the link bandwidth of a WSN remains normally far lower compared to that of a connected network. For reducing the energy consumption in the network, it remains verified several times that clustering is one of the favorable approaches. In this effort, for collecting the combined information openly from the CHs, here we suggest and study a new energy-effective information assembly method NCMA (Novel Energy-Efficient Data Gathering Scheme) which hires mobile representatives and cluster head (CH) consumes the charge of collaborating by the mobile representative as well as the participant nodes. For limiting the information communication in the network, Network coding and TDMA programing is utilized.

Index Terms*:*Heterogeneous WSNs, cluster head selection, TDMA, Network coding, multi-hop routing, energy efficiency, Mobile agent, Network lifetime.

I. INTRODUCTION

WSNs are developing equally fundamental and widespread methods of delivering certain calculating atmospheres for numerous submissions owing to characteristics such as minor extent, less-price, less-power, as well as multi-purposes by improvements in wireless transmissions, micro electromechanical networks (MEMS) expertise as well as low-power electronics [1].

In these type of presentations, hundreds otherwise even thousands of less-price sensor node remain distributed greater than the controlling region, using nodes wisely established in a wireless network, wherein every sensor node occasionally informs its sensed information towards base station. While they run in unfriendly atmospheres, it remains problematic for replacing or recharging batteries of the sensor nodes.

Energy saving remains a significant subject for WSN. Several methods aimed at energy savings remain advanced, containing sleep arranging as well as media access control (MAC) procedures, routing procedures, information accumulation, topological control, etc. [2]. Amongst them, routing procedure remains a significant subject for planning WSN and may remain categorized into twofold collections: planar routing as well as hierarchical routing. Hierarchical routing typically achieves a network through separating the network to dissimilar clusters that ensure a cluster head liable in place of fusing information from cluster members thenit is transferred towards base station (BS). The gain of little energy consumption, modest routing tabletops as well as upright scalability, has prepared hierarchical routing remaina hot investigation region of WSN [3].

Entire sensor nodes remain indistinguishable in relations of battery capability and hardware difficulty in homogeneous networks. Using clustering in a homogeneous network, nodes in a cluster track information and transfers towards cluster head (CH) that sequentially collects the information which remains terminated as well as extremely connected from entire cluster members and transfers towards the base station through single-hop otherwise multi-hop. Clustering saves energy thus improving the lifespan of the network. Similarly it may remain practiced for huge sensor networks. Since it remains informal to achieve the cluster heads compared to the complete network. Clustering may remain very operative in one-to-many, many-to-one, otherwise one-to-all (broadcast) transmissions [4]. Built on hierarchical clustering in addition to a traditional hierarchical routing procedure in Heterogeneous WSNs, Low energy adaptive clustering hierarchy (LEACH) [5] remains a leading routing procedure. An excessive agreement of resolution suggestions occurs aimed at energy-efficient clustering afterward LEACH [6–12]. In Ref. [6], Mahmood et al. suggested a routing procedure named MODLEACH and cluster wouldn't alter in following stagewhenever residual energy of the head node remains above a threshold, thus the energy spent for cluster establishment might remain protected. In Refs [7–8], Zhao et al. proposed a comparable approach of choosing the cluster heads as well as their preservation, however all of Refs. [6–8] do not deliberate the transmission amongst the CH as well as BS. Indeed, in conservative heterogeneous networks, the foremost energy consumption originates after the communicating processes amid CH and the BS. Consequently, while scheming routing algorithms, we ought to integrate a trade-off amid distance between CH and SINK are more, we performing three objectives.

Revised Manuscript Received on May 31, 2019

S Anuradha, Department of ECE, JNTUH, Hyderabad, India.
Dr.D. Sreenivasa rao, Department of ECE, JNTUHCEH, Hyderabad, India.

In this broadsheet, we discourse the following complications:

1) Frequent re-clustering happens due to the energy imbalance among the nodes
2) Overhead is increases particularly in inter-cluster communication
3) Large number of nodes participate in clustering
4) Re-clustering happens after certain rounds of communication due to the depletion of energy on previously elected CH's.

We solve the above problems using our proposed method it's involving with following criteria's:

- Mobile agents between CHs and SINK node
- Network coding technique
- TDMA Scheduling technique

II. EXISTING WORK

Numerous heuristics have likewise remained offered for routing in Heterogeneous WSNs. LEACH [13] remains a prevalent cluster-grounded routing procedure, which actively replaces the load of the CHs among the sensor node that remains suitable aimed at load balancing. Nevertheless, the chief drawback of this method is that a node using very small energy might remain chosen by means of a CH that might expire rapidly. Furthermore, the CHs interact with base station through single-hop that remains difficult for Heterogeneous WSNs by huge coverage region. Hence, a huge amount of procedures have been established towards improving LEACH that can remain originated in [14], [15]. In [16], author has offered a price-focused distributed energy composed clustering as well as routing procedure for CH choice and cluster establishment. Nevertheless, the procedure undergoes connectivity issue of the chosen CHs.

A sum of metaheuristic built clustering procedures has been described for Heterogeneous WSNs. Nevertheless, extreme of them have allocated using CH choice only. In recent times, a GA grounded weight composed clustering procedure for Heterogeneous WSNs [17] was suggested. The procedure customs group in such an approach that the extreme weight of every entry remains reduced and the aforementioned workings aimed at both the identical and inadequate capacity of the sensor node. The procedure consumes quicker convergence as well as improved load balancing compared to customary GA [18]. Nevertheless, it consumes the disadvantage that the CHs responsively communicate by the BS that might not remain accurate aimed at wide region networks. Furthermore, the procedure does not assume residual energy of the sensor node and gateways in cluster establishment that might direct towards varying energy consumption of the sensor node. In [19], author has offered a GA-grounded procedure for information routing amid gateways in a two-tire wireless sensor network. Selection of gateways is supported by the Roulette-wheel selection process as well as the suitability role remains well-defined using network lifespan in terms of series. A GA-grounded routing procedure named GAR was proposed where the complete transmission distance from the gateways towards the BS remains reduced [20]. Nevertheless, both of the procedures [19] [20] assume only routing of combined information from the gateways towards the BS without assuming information transmission from the sensor node towards the gateways in every cluster.

In [21],focusing on lessening the communication distance amongst the nodes in addition to lessening the amount of network overhead necessaryaimed at setting up a cluster, author presents the Energy-aware and layering-based clustering and routing algorithm (EA-CRA). It remains more problematical to scheme a network as the sum of power constrained nodes rises. This is caused by the massive overhead that arriveswhenever the network expandsenormously. Its limitations include Overhead increases particularly in inter-cluster communication when applied in highly dense networks and Re-clustering is also one of the major issue in this method as no mechanism to monitor and control the load and energy of the nodes.

In [22], author presents the Cluster-head Restricted Energy-efficient protocol (CREEP) and critically analyzed the numerousstatic heterogeneous clustering procedures and estimated their lifespan and throughput performance in mobile node setscorrespondingly.In a two-level heterogeneous WSNbytransforming the CH selection thresholds, it enhances network lifespan. Itincludes the limitation that the system complexity may increase if hugenumber of nodes partakes in the clustering method.

For extending network timeby a combining of a clustering methodin addition tooptimum relay selection procedure,author anticipated a novel routing procedure for WSNs named Novel energy aware hierarchical cluster-based routing protocol (NEAHC)in [23]. The suggestion is for determining optimal routing path commencing the source towards the destination inapprovingmaximumresidual battery power, minimal energy consumption in multi-hop path, as well asoptimal fairness between sensor nodes. Its limitation increase the work load among the cluster head nodes and energy is depleted more quickly in the CH nodes, which leads to frequent re-clustering and CH rotation. Also this method would increase the traffic at the nodes surrounding near to the sink node.

III. PROPOSED FRAMEWORK

So, to improve the clustering efficiency and to reduce the frequent re-clustering in the network, we proposed a method called NCMA. The introduction of MA's reduces the load among the CHs and the surrounding nodes. Also energy is not a primary parameter for CH selection. So CH rotation is limited and prolong for a long time. The network coded methods is used for data aggregation. The working process of proposed method shows in figure 1.

3.1 Clustering phase

At this time, we propose a LEACH-alike clustering method, where the network is subdivided into a group of clusters by single cluster head in every cluster. Communication amongst cluster head as well as Base Station remains straight. The Base Station transmits a "hello" message to entire nodes at an assured power point in the network deployment level. Using this method, every node may calculate the estimated distance for the nodes based on the expected signal power. It supports nodes for selecting the appropriate power point for communicating through the Base Station.

In cluster head selection level, finely distributed cluster heads remain selected using a slight control overhead. A new task is presented towards forming clusters in cluster development stage.

3.2 Cluster head (CH) selection phase

Many cluster heads are selected in this point. Towards advertising their determinations, Nodes turn out to be CANDIDATE nodes through a possibility T and then transmit the COMPETE_HEAD_MSGs inside radio extent R. Every CANDIDATE node verifies whether here exists a CANDIDATE node by small distance in the range R. When the CANDIDATE node discovers an extra significant CANDIDATE node, it will hand over the competition without getting sub-consecutive COMPETE_HEAD_MSGs. It will remain selected as HEAD in the conclusion otherwise.

3.3 Cluster formation

In this stage, every HEAD node transmits the HEADAD-MSG across the network while the PLAIN nodes accept all the HEAD_AD_MSGs and select which cluster to link. The metric for PLAIN nodes for making choices remains the distance metric. For instance, the PLAIN nodes select the cluster head that demand least communication towards the established signal strength. Nevertheless, tracking effective energy consumption of the PLAIN nodes merely direct HEAD nodes drained fast throughout the information communication level.

3.4 Network coding technique

The package dealing out process of a node in the network coding layer is presented. Every single node in the network coding layer preserves a received queue (RecvQueue ()) as well as a sensed queue (SensQueue ()). By getting a package Pi, a node places the package in RecvQueue (Pi). Suppose the package remains previously administered using the node than it is rejected, or else the node practices the package additionally. The node verify its role from EncoderNodeSet (), whether it is an encoder or else a modest transmit nodule. Suppose the package is a natural (non-coded) package and the node remains an encoder, the nodule appeals the technique XorEncode (). The node conveys the coded packet towards the sink on effectively producing an encrypting packet. The processed package remains implanted in the forwarding set ForwardSet () that stocks forward packets and support in confining additional terminated broadcasts. Nevertheless, the arrived package Pi is formerly an encoded package and it remains rejected by the node. Additionally, if the node is a decoder, it performances by means of an unsure relay and transmits the estimated packet Pi towards the Drop.

3.5 Decoding of packets

The sink node or else the delivery node obtain natural packages from the modest relay nodes as well as coded packets from the network coder node. In COPE the internal node encrypts and decrypts packets. The sink preserves a group of packets, in which it stores every customary native packet. The sink recovers the equivalent native packets in sequence from the group of packets when the sink accepts an encrypted packet containing of ˆ k native packets. The Drop XORs the ˆ k − 1 native packets using the received coded packet recover the misplaced packet that remains completely misplaced or else delivered by fault at the sink.

3.6 TDMA scheduling

The bandwidth of frequency is shared among several stations on the basis of interval in TDMA. Every single location is assigned by a period opening through which it may deliver its information i.e. every location could convey its statistics in its assigned time slot. Every single location need to recognize the starting of its slot as well as the position of its slot. TDMA involves synchronization amid dissimilar locations. Synchronization remains attained by means of consuming certain synchronization bits (preamble bits) on the opening of every slot. Though they remain theoretically same, TDMA remains altered from TDM. TDM remains a physical layer method which groups the information from relaxed networks and communicates then by means of consuming a quicker network. This procedure implements the physical multiplexer. TDMA, on other hand, remains an admission technique in the data link layer. The data link layer in every station expresses its physical layer to practice the assigned time slot. There is no physical multiplexer at the physical level.

3.7 Flow Chart

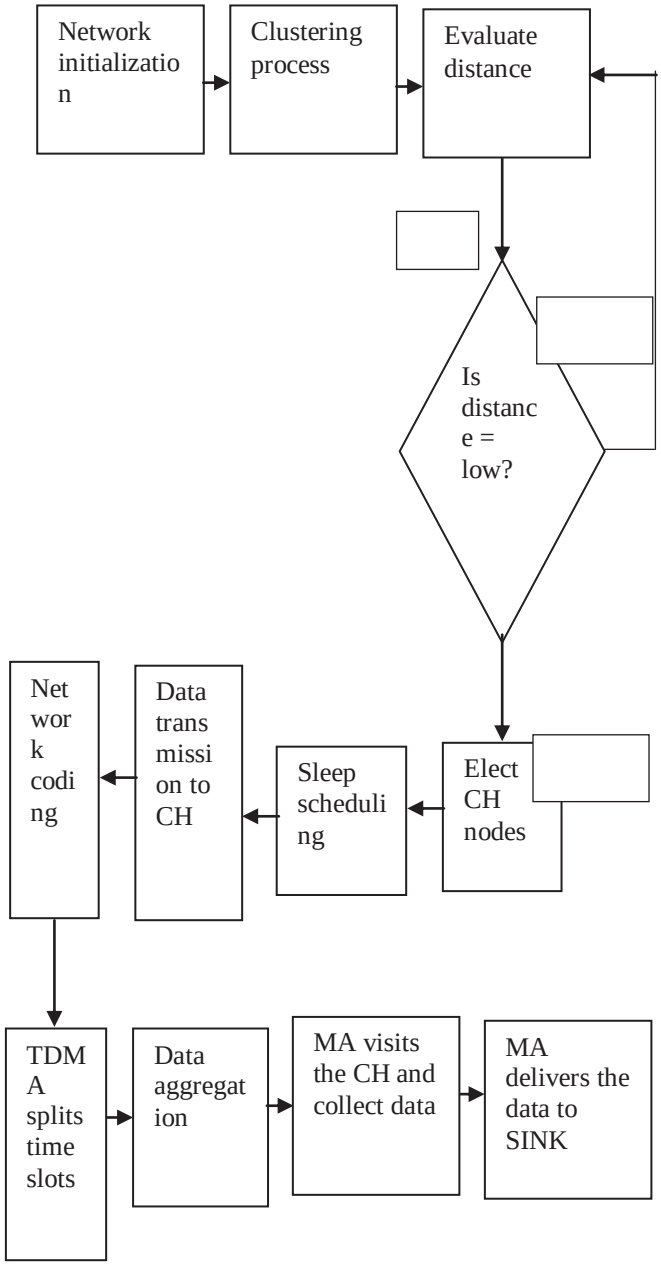

Fig. 1: Flowchart of Proposed method

IV. RESULTS AND DISCUSSION

Byachievingrelative simulations,wecalculate the realization of NCMA. Byconsuming Network simulator-2,the anticipatedprocedure, NEAHC, EA-CRA, and CREEP protocols are simulated.Aimed at NEAHC, EA-CRA, CREEP protocols and NCMA, the energy model appliedremainsequal. 76 sensor nodes remainaccidentally deployed in a geographical area A of dimension 1000 m x 500 minthe presenting simulation. Significantlimitations for our simulation are presented in table 1.

Table 1 expresses the network parameters employed in our simulations. In this paper, with the intention of simplifying scheduling for the mobile sink, we accept that the information gathered using sensor nodes remains the deferral tolerant information i.e. they can wait for the mobile sink to come and boost them up.

Weassume the resulting metricsaimed atstudying and comparing the presentation of our protocol by existing protocols.

1) Network performance: The number of transmitted packets evaluated by Megabits per sec.
2) Propagation Delay: The propagation of a packet from source node to destination node in an average time.
3) Energy consumption: The overall energyutilized by the nodes in the network.

Table1: Simulation Specifications

Parameter	Value
Application traffic	CBR
Transmission rate	512 bytes / 0.05ms
Communication range	250m
Data Packet size	4096 bits
Number of sensor nodes	76
Number of simulation iterations	220
Initial energy	100j
Network area	1000x500
Number of clusters	8
Routing methods	NCMA, EA-CRA, CREEP, NEAHC.
Routing protocol	AODV

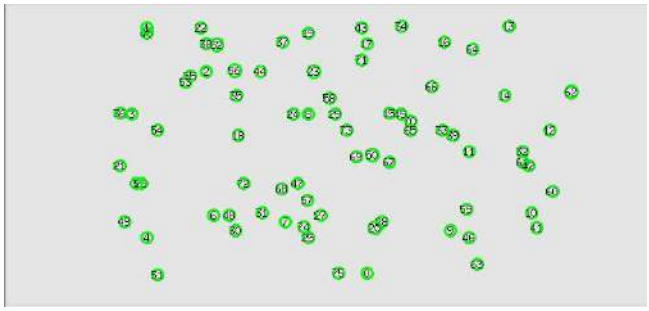

Fig. 2: Network deployment

Figure2 represents the network deployment. All the nodes are physically located in anindiscriminate way.

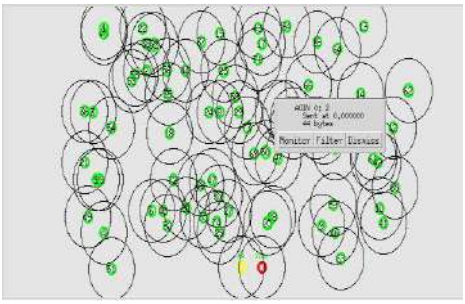

Fig.3: Broadcasting in network

Figure3 represents the broadcasting process in network. Here all the nodes request their neighbor nodes for route reply. In this network, routing protocol decides the RREQ and RREP processes.

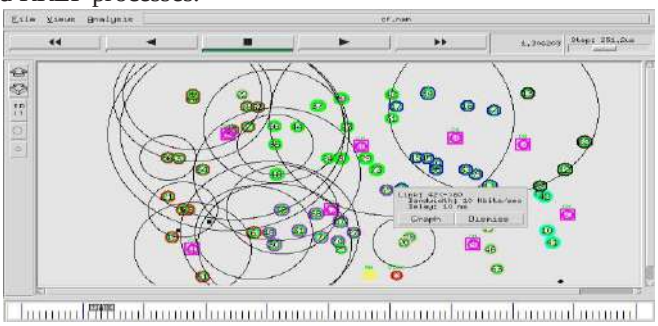

Fig.4: Cluster member to Cluster head transmission

Figure4 represents the cluster member to cluster head data transmission. After cluster formation, cluster heads are selected based on their distance from node to node in each cluster. Here link must be represented between the cluster member and cluster head process.

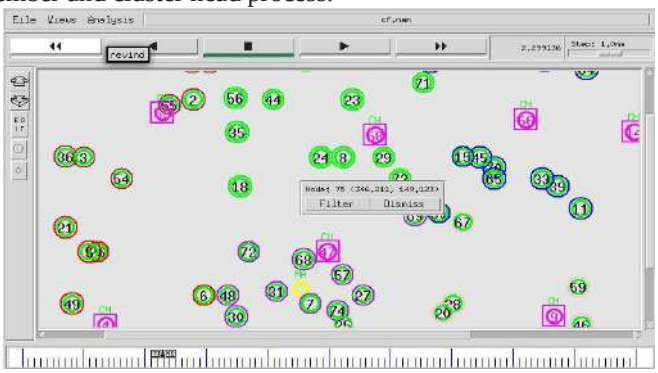

Fig. 5: Mobile node moving to nearby CH

Figure5 represents the mobile node movement in network. Here mobile node starts travelling towards CH nodes from SINK node.

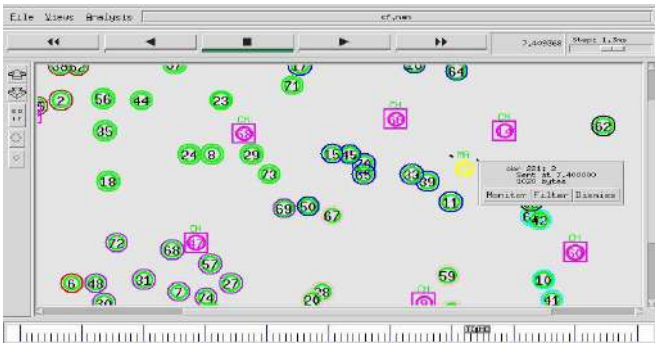

Fig. 6: CH to MA Data transmission

Figure6 represents the cluster head (CH) to mobile agent (MA) data transmission. Here MA collects the data from all the cluster heads while travelling in network.

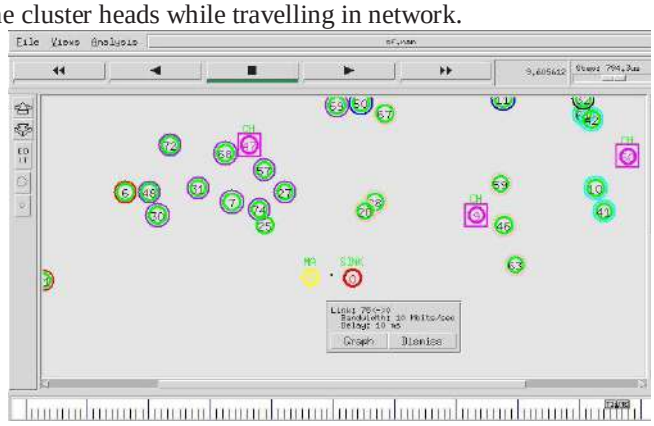

Fig. 7: MA to SINK data transmission

Figure7 represents mobile sink as SINK node data transmission. Here SINK node collects all the data present in the MA. In this figure, SINK node act as data storage point.

We analyze network performance of EA-CRA, CREEP, NEAHC, and our protocols.Asthe network progresses,westudy the technique of simulation time variation.Itremainsfair that the anticipated protocol consumesenhanced throughput compared to existing protocols in figure 8.

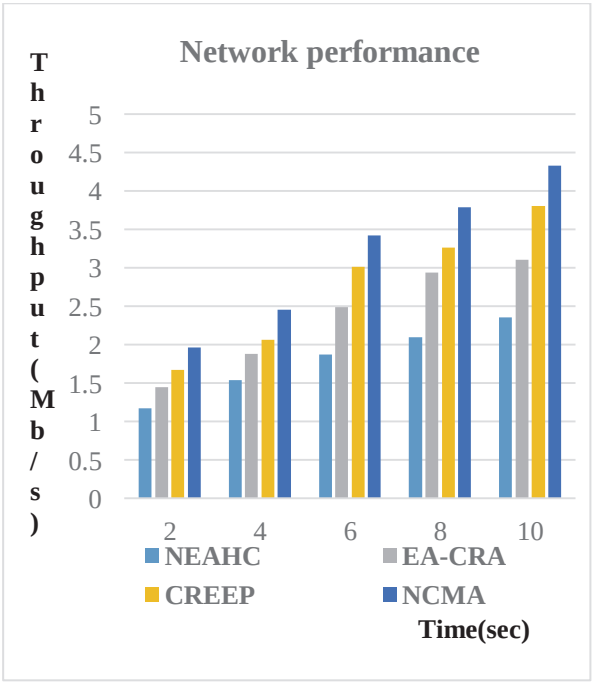

Fig8: Throughput

Figure 9 shows delay of network. For large networks, some data packets remain delayed sincespecific cluster heads doesn't existin the range of others. Delay of network is suitable for proposed protocol than EA-CRA, CREEP, and NEAHC.

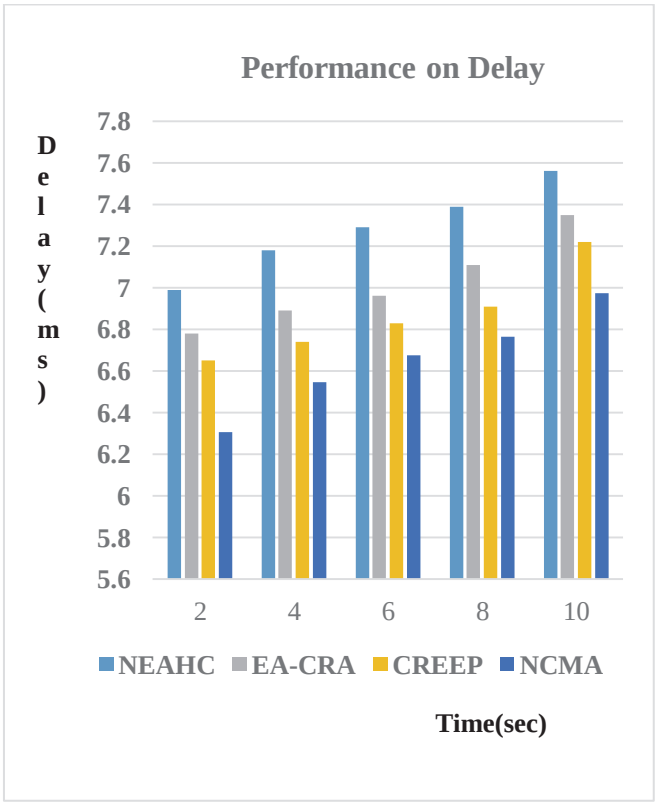

Fig9: End to End Delay

In figure 10, the proposed protocol has less energy consumption than EA-CRA, NEAHC, and CREEP because of choosing a multi-hop path with minimum communication cost.

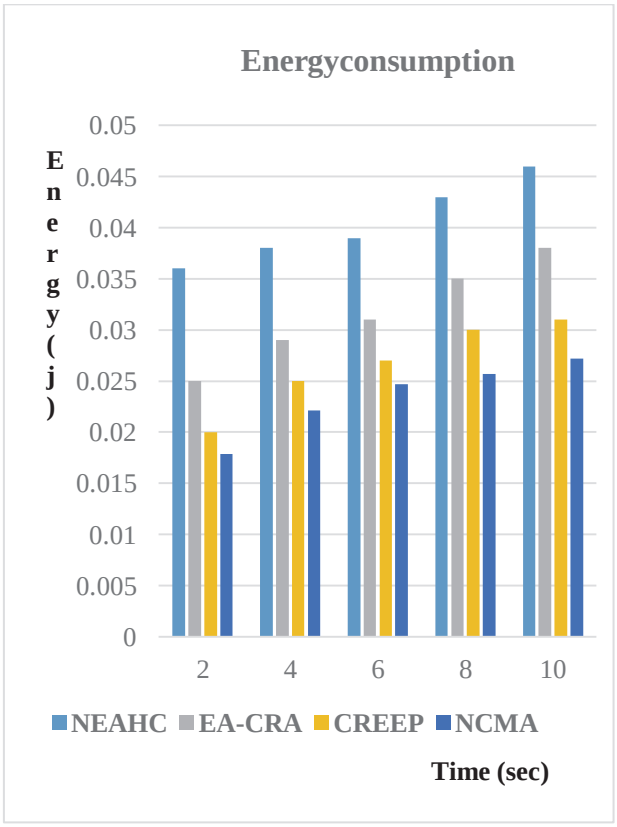

Fig10: Energy consumption

Published By:
Blue Eyes Intelligence Engineering
& Sciences Publication

V. CONCLUSION

Achieving Energy efficiency is the major task for WSNs, since these networks are energy constrained. Most of the previously proposed clustering algorithms achieves energy efficiency in intra clustering but failed to maintain the tradeoff between inter and intra cluster routing. In this paper, we proposed a novel energy-efficient data gathering scheme (NCMA). This method employs moving sinks between the BS and CHs to collect the data that are aggregated using network coding technique. This would reduce the communication overhead between BS and CHs. Time division based scheduling is used for reducing the redundant data transmission. The simulation outcomes show that the proposed NCMA completely outperforms the protocols like EA-CRA, NEAHC, and CREEP and improves the network lifetime. In this paper, 30% improvement of the anticipatedscheme over the existentschemesconsidered stands observed with respect to the performance parameters given.

REFERENCES

1. Jiang C F, Yuan D M, Zhao Y H. Towards clustering algorithms in wireless sensor networks: a survey. Proceedings of the 2009 IEEE Wireless Communications and Networking Conference (WCNC'09), Apr 5−8, 2009, Budapest, Hungary. Piscataway, NJ, USA: IEEE, 2009: 6p
2. Thakkar A, Kotecha K. Cluster head election for energy and delay constraint applications of wireless sensor network. IEEE Sensors Journal, 2014, 14(8), 2658−2664
3. Zhu K, Dou Q, Shao A H, et al. An energy-efficient routing protocol based on hotspot-aware uneven clustering and dynamic path selection. Proceedings of the 22nd Wireless and Optical Communication Conference (WOCC'13), May 16−18, 2013, Chongqing, China. Piscataway, NJ, USA: IEEE, 2013: 315−320
4. Ben Alla S, Ezzati A. Coverage and connectivity preserving routing protocol for heterogeneous wireless sensor networks. Proceedings of the 2012 Next Generation Networks and Services (NGNS'12), Dec 2−4, 2012, Faro, Portugal. Piscataway, NJ, USA: IEEE, 2012: 141−148
5. Heinzelman WR, Chandrakasan A, Balakrishnan H. Energy-efficient communication protocol for wireless microsensor networks. Proceedings of the 33rd Annual Hawaii International Conference on Network Sciences (HICSS'00), Jan 4−7, 2000, Maui, HI, USA. Piscataway, NJ, USA: IEEE, 2000: 10p
6. Mahmood D, Javaid N, Mahmood S, et al. MODLEACH: a variant of LEACH for WSNs. Proceedings of the 8th International Conference on Broadband and Wireless Computing, Communication and Applications (BWCCA'13), Oct 28−30, 2013, Compiegne, France. Piscataway, NJ, USA: IEEE, 2013: 158−163
7. Zhao H R, Zhou W N, Gao Y. Energy efficient and cluster based routing protocol for WSN. Proceedings of the 8th International Conference on Computational Intelligence and Security (CIS'12), Nov 17−18, 2012, Guangzhou, China. Piscataway, NJ, USA: IEEE, 2012: 107−111
8. Gnanambigai J, Rengarajan N, Jenifer Prarthana R. An analytical approach for quadrant based leach: an energy efficient routing protocol for WSNs. Proceedings of the 2nd International Conference on Devices, Circuits and Networks (ICDCS'14), Mar 6−8, 2014, Combiatore, India. Piscataway, NJ, USA: IEEE, 2014: 6p
9. Ataul, B.,etal..Clustering strategies for improving the lifetime of two-tiered sensor networks. Comput. Commun, 2008.31,3451–3459.
10. Kuila,P.,Jana,P.K..Approximationschemesforloadbalancedclusteringin wireless sensornetworks.J.Supercomput.68,87–105, 2014. http://dx.doi.org/ 10.1007/s11227-013-1024-6.
11. Gupta, G.,Younis,M..Load-balanced clustering of wireless sensor networks. In: IEEEICC2003,pp.1848–1852.
12. Kuila,P.,Jana,P.K..Energyefficientload-balancedclusteringalgorithmfor wirelesssensornetwork.In:ICCCS2012,ProcediaTechnology,vol.6,pp.771–777.
13. Heinzelman, W.B.,etal..Application specific protocol architecture for wireless micro sensor networks. IEEE Trans. Wirel. Commun, 2002.1,660–670.
14. Tyagi,S.,Kumar,N..Anetworkaticreviewonclusteringandroutingtechniques based upon LEACH protocol for wireless sensor networks. J.Netw. Comput. Appl, 2013 36,623–645.
15. Al-Refai,H.,etal..Efficient routing LEACH(ER-LEACH) enhanced on LEACH protocol in wireless sensor networks. Int. J.Acad. Res.(PartI), 2011.3,42–48.
16. Kuila, P.,Jana, P.K..An energy balanced distributed clustering and routing algorithmforwirelesssensornetworks.In:PDGC2012,IEEEXplore, pp. 220–225.
17. Kuila,P.,Gupta,S.K.,Jana,P.K..Anovelevolutionaryapproachforload balanced clustering problem for wireless sensor networks. SwarmEvol. Comput, 2013 12,48–56.
18. Goldberg, D.E. Genetic Algorithms: Search Optimization and Machine Learning. Addison Wesley, Massachusetts, 2007.
19. Ataul,B.,etal..Ageneticalgorithmbasedapproachforenergyefficient routing in two-tiered sensor networks. Ad-Hoc Network, 2009.7,665–676.
20. Gupta, S.K., Kuila, P. Jana, P.K..GAR: an energy efficient GA-based routing for wireless sensornetworks.In:ICDCIT2013,LNCS7753,pp.267–277.
21. K. A. Darabkh, N. J. Al-Maaitah, I. F. Jafar and A. F. Khalifeh, "Energy efficient clustering algorithm for wireless sensor networks," *2017* International Conference on Wireless Communications, Signal Processing and Networking(WiSPNET*)*, Chennai, 2017, pp. 590-594.doi: 10.1109/WiSPNET.2017.8299826.
22. Dutt, S., Agrawal, S. & Vig, R. Wireless Pers Commun (2018) 100: 1477. https://doi.org/10.1007/s11277-018-5649-x.
23. Wang Ke, Ou Yangrui, Ji Hong, Zhang Heli, Li Xi, " Energy aware hierarchical cluster-based routing protocol for WSNs", Volume 23, Issue 4, August 2016, Pages 46-52. https://doi.org/10.1016/S1005-8885(16)60044-4.

Published By:
Blue Eyes Intelligence Engineering
& Sciences Publication

Galore International Journal of Applied Sciences and Humanities
Vol.3; Issue: 4; Oct.-Dec. 2019
Website: www.gijash.com
Short Communication *P-ISSN: 2456-8430*

Improving Stress and Stress Curve of Concrete by Reinforcing Glass Fibers

Syed Uzair Ali[1], Mohammed Zaker[2]

[1]M.Tech (Structural Engineering). Nawab Shah Alam Khan College of Engineering and Technology, Hyderabad, Telangana, India.
[2]Assistant Professor. Department of Civil Engineering. Nawab Shah Alam Khan College of Engineering and Technology, Hyderabad, Telangana, India.

Corresponding Author: Syed Uzair Ali

ABSTRACT

Concrete is the most widely used construction material on the planet. The reason being its strength in compression. But it is very weak in tension. Therefore, many microcracks will be developed. These occur due to shrinkage in general. Concrete also has very little ductility and resistance to the cracks developed. To improve the nature of the concrete, Glass Fibers have been added while testing to improve the mentioned characteristics. The cement used is Ordinary Portland Cement (OPC) without any admixtures. In this investigation, glass fibers have been added in percentages ranging from 0.00% to 0.10%. The results after each interval of addition have been described and the changes in the properties (both mechanical and ductility) have been shown.

Keywords: Concrete, Ductility, Glass Fibers, Reinforcement, Investigation.

I. INTRODUCTION

Concrete is widely used and it was observed concrete developed cracks under excess loading. These cracks develop due to various factors such as plastic shrinkages, drying shrinkages and due to the practices followed during laying the concrete. In addition, there are many factors that play a role in decrease in strength.

In order to decrease the crack formation and to increase the strength of concrete in flexure, fibers can be added. These fibers will keep the concrete linked and prevent the propagation of microcracks. These fibers are also an additional reinforcement in the concrete, covering the complete volume along with weighing less and not disturbing the properties of the derived concrete.

II. Reinforcing using Fibers

Fibers of very thin, short in length and random shapes are used. These are embedded in the concrete during the mixing. Due to this, there are 2 effects: First, there will be drastic reduction in the rate of workability; Second there will be very viscous mixture preventing the segregation and bleeding. All the aggregate particles will be engulfed in the fibers and hence there will be strong contact between the aggregate particles and the cement. Since there is locking, the fibers shall act as a reinforcement in addition to the steel reinforcement provided.

III. About Fiber Reinforced Concrete

Fiber Reinforced Concrete (FRC) is made of conventional concrete added with a limited amount of fibers. It is to be noted that the fibers are discontinuous and of random lengths.

Fibers are the main load carrying entities while their surrounding cement keeps them in the fixed position. Therefore, they are less exposed to the surroundings. Hence the structural properties provided by these materials will remain unaffected even after years. The fibers in length, but here fibers of length 6mm, 12mm have been used.

IV. Experiment

The experiment has been carried out using 6mm, 12mm glass fibers in M20 and M40 concrete respectively. M20 and M40 concrete cubes without any addition of fibers are also prepared to correlate the findings.

The cube that has been used as a mold for carrying out the experiment has been shown in Figure 1.

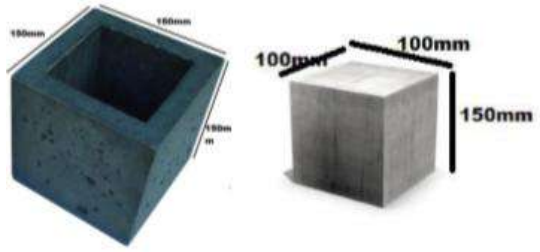

Figure 1: Dimensions of the mold used

Its outer dimensions are 150×150×150 (all in mm) and the inner dimensions are 100×100×150 (all in mm).

	Grade of Concrete	Length of Fibers (mm)	Concrete type	Glass Fiber Percentage	Number of cubes
1	M20	6	no fibers	0	3
			with fibers	0.03	3
				0.06	3
				0.09	3
2	M20	12	no fibers	0	3
			with fibers	0.03	3
				0.06	3
				0.09	3
3	M40	6	no fibers	0	3
			with fibers	0.03	3
				0.06	3
				0.09	3
4	M40	12	no fibers	0	3
			with fibers	0.03	3
				0.06	3
				0.09	3

Figure 2: Number of cubes prepared for testing

a. Materials needed

The following are the materials that are needed to make the cubes.

- Ordinary Portland Cement (Grade 53)
- Fine Aggregates
- Coarse Aggregates
- Glass Fibers (6mm and 12 mm length)
- Water

i. Ordinary Portland Cement

OPC conforming to IS 12269 the has been used.

Properties of the cement are as follows

Specific gravity	:	3.14
Standard Consistency	:	34%
Initial Setting Time	:	36 min
Final Setting Time	:	214 min

ii. Fine Aggregates

Fine aggregate conforming to Zone 2 of IS 383 has been procured and used.

Properties of the fine aggregate are as follows

Bulk Density	:	1.40g/cc
Specific Gravity	:	2.69
Fineness Modulus	:	2.85

iii. Coarse Aggregates

Coarse aggregate conforming to IS 383 has been used. 20mm size well-graded aggregates have been used.

Properties of the coarse aggregate are as follows

Bulk Density	:	1.47g/cc
Specific Gravity	:	2.79
Fineness Modulus	:	7.2

iv. Water

Potable water has been used for mixing and curing the special concrete.

b. Mixing

Mix all the ingredients dry in the pan mixer. This shall ensure uniformity when adding water. At the end of dry mixing, water is added. The mixing is continued for the next 4 minutes.

c. Casting

Molds were filled so that there was no gap between the walls of the mold and the specimen filled.

d. Curing

After casting is complete, specimens were stored at 27 degrees temperature for 24 hours. After drying, they were placed in water bath and were cured for 28 days.

e. Testing

At the end of the 28-day curing period, the specimen cubes are taken out and tested for Ultimate Strength on the Universal Testing Machine (UTM). The capacity of the UTM is 2000 KN.

V. RESULTS

Table 1: Results for all specimens with 6mm fibers

Fiber Percentage	Specimen	Compressive Strength	Average of 3 cubes
0	1	28.46	28.48
	2	28.43	
	3	28.55	
0.03	1	34.19	31.76
	2	31.99	
	3	29.1	
0.06	1	36.32	36.33333333
	2	36.26	
	3	36.42	
0.09	1	37.64	37.49666667
	2	38.23	
	3	36.62	

Table/Figure 2: Compressive Strength of concrete specimens with 6mm fibers used during production

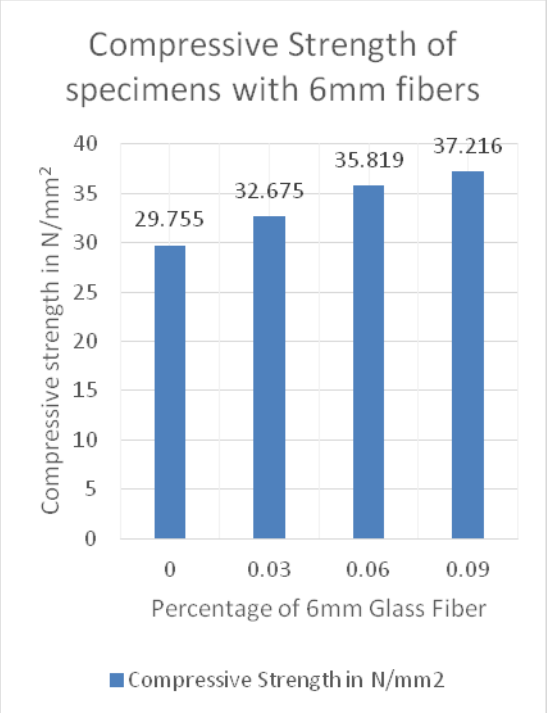

Table 3: Results for all specimens with 12mm fibers

Fiber Percentage	Specimen	Compressive Strength	Average of 3 cubes
0	1	29.369	29.75533333
	2	29.721	
	3	30.176	
0.03	1	33.698	32.67533333
	2	32.324	
	3	32.004	
0.06	1	35.129	35.81933333
	2	35.989	
	3	36.34	
0.09	1	38.017	37.21633333
	2	37.02	
	3	36.612	

Table/Figure 4: Compressive Strength of concrete specimens with 12mm fibers used during production

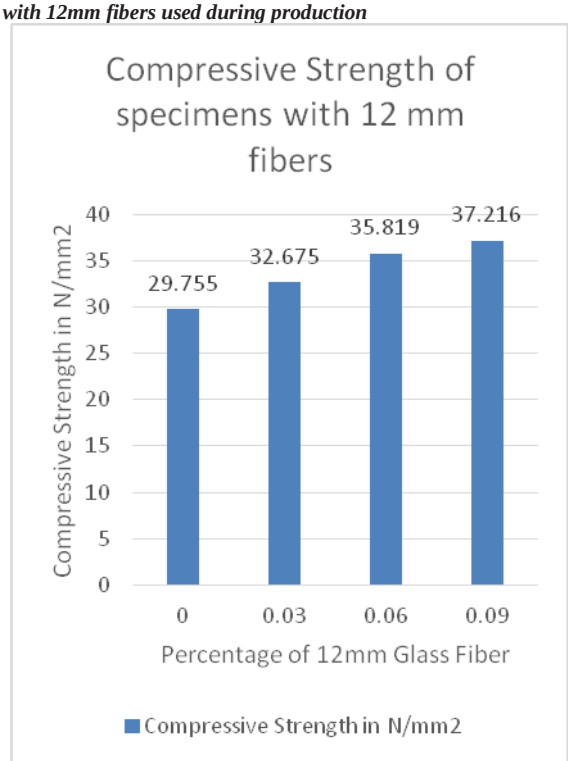

VI. CONCLUSION

The following are the points that have been deduced from conducting these experiments.

The compressive strength of the concrete cubes increased with addition of the fibers.

The fiber content of 0.09% gave the highest compressive strength of all.

The FRC specimens showed improved deformation capacity even after reaching the ultimate load.

There was an increase in the ductility of the concrete specimen.

VII. ACKNOWLEDGEMENT

I, Syed Uzair Ali, the author of this paper acknowledge that I have done this work solely by myself and have not copied it from any journal or article. This is a bonafide work done under the esteemed guidance of Mr. Ahmed Hussain (Head of Department, Civil Engineering).

VIII. REFERENCES

- Deshmukh S.H. et al. Effect of glass fibres on Ordinary Portland Cement. IOSR Journal of Engineering. June 2012 Edition. Volume 2. Page 1308-1312

- Chandramouli K. et al. Rapid Chloride Permeability Test for durability studies on glass fiber reinforced concrete. ARPN Journal of Engineering and Applied Sciences. March 2010 Issue. Volume 5. Number 10.
- K Chandramauli, P Sreenivas Rao, N Pannirselvam, T Sheshadhri Shekhar, P Sravana. Strength properties of glass fiber concrete. ARPN Journal of Engineering and Applied Sciences. April 2010 Issue. Volume 5. Number 4.
- S Shaikh, M Homam. A decade of performance of FRP Repaired Concrete Structures. ISIS-SHM Workshop. 2004. Manitoba, Canada. Page 751-758.
- IS 10262. (1982). Recommended guidelines for concrete mix design. Bureau of Indian Standards, New Delhi.
- IS 383. (1970). Indian Standard Specification for coarse and fine aggregate from natural sources Concrete.

IX. Codes of Practice

- IS 456-2000. Plain and Reinforced Concrete-Code of Practice.
- IS 516-1959. Method of Test for strength of Concrete.
- IS 2386-1963. Methods of test for aggregates for concrete: Particle shape and size.
- IS 12269-1987. Specifications for 53 Grade Ordinary Portland Cement.

How to cite this article: Ali SU, Zaker M. Improving stress and stress curve of concrete by reinforcing glass fibers. Galore International Journal of Applied Sciences & Humanities. 2019; 3(4): 14-17.

******

An Energy Efficient Data Aggregation Technique Using Multi-Sink Infrastructure in Heterogeneous Wireless Sensor Network

S Anuradha, D Sreenivasa Rao

Abstract: ***The energy consumption of sensors adjacent to sink or upon critical paths remains excessively fast along with additional drawbacks in wireless sensor networks using single sink node. Therefore, we propose Energy-efficient secondary level base station (EE-SLB) based data aggregation in wireless sensor network. Multi-sink infrastructure permits sensor nodes for choosing various sink nodes with respect to their individual situation compared to single-sink topology. As a result, the usual transmission distance amid sensor nodes as well as sink nodes may be decreased. The benefits of dispersion, stability as well as robustness are given by the deployment of multi-sink nodes.***

Keywords: Wireless sensor networks, Clustering, TDMA, Network code method, Energy level routing, Secondary level base station, mobile agent, Data aggregation, Data integrity.

I. INTRODUCTION

A WSN includes a huge quantity of minute and small power sensor nodes that remain aimlessly or physically arranged above an unattended objective area. WSNs guarantee possible submissions in atmosphere monitoring, disaster alerting systems, healthcare, defence investigation as well as reconnaissance systems [1]. Nevertheless, the major limitation of WSNs is restricted power sources of the sensor nodes. Consequently, energy preservation of the sensor nodes remains the utmost stimulating concern for the extended course of WSNs. Many concerns are assumed for this resolution which comprises low-power radio communication hardware [2], energy-aware medium access control (MAC) layer protocols [3,4], etc. Moreover, energy efficient clustering as well as routing algorithms [5, 6] remains the supreme capable regions that are assumed broadly by the way. Within a dual-tier WSN, sensor nodes remain distributed into numerous collections termed as clusters. Each single cluster has a leader recognised by means of a cluster head (CH). The entire sensor nodes identify local information and later forward that one towards their resultant CH. At that time, the CHs combine the local information and lastly direct it towards the base station (BS) otherwise through additional CHs. The performance of a cluster-built WSN is presented in Figure. 1. Clustering sensor nodes consumes the resulting benefits: (1) it allows information collection at cluster head towards discarding the redundant as well as uncorrelated information; here, in the above-mentioned preserves energy of the sensor nodes. (2) Routing may be accomplished definitely since only CHs are necessary for maintaining the local route arrangement of additional CHs and therefore require small routing information; this in turn progresses the scalability of the network expressively. (3) The above-mentioned similarly maintains communication bandwidth as the sensor nodes just interconnect by their CHs and therefore stops interchange of redundant messages amongst themselves.Nevertheless, CHs withstand certain additional amount of work assured by means of their participant sensor nodes as they obtain the sensed information from their participant sensor nodes, combine them as well as interconnect it towards the BS. Furthermore, in several WSNs, the CHs remain commonly elected amongst the usual sensor nodes that may die quickly for this added amount of effort. In this perspective, numerous investigators [7-11] have offered the usage of certain distinctive nodes named as gateways that remain delivered by additional energy. These gateways perform similar to cluster heads and remain accountable for the identical performance of the CHs. Thus, gateways as well as CHs remain employed conversely in the remainder of the paper.

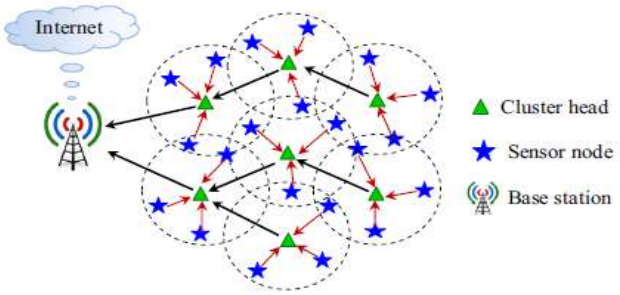

Figure 1: A Wireless sensor network model

Nevertheless, certain submissions remain exactly time-critical by nature. Therefore, they must fulfil strict delay limitations as a result that the BS could obtain the sensed information in a definite time limit. Nevertheless the delay remains comparable to the amount of forwards on the distribution route in the middle of a source as well as the BS. With the intention of minimizing the delay, it remains essential to decrease the amount of forwards that can remain attained by increasing the distance in the middle of successive forwards. While designing routing algorithms we must include a trade-off distance amid CH and SINK, therefore we consider certain objectives. Particularly, depleting energy at mobile agents is a serious problem when the sensor nodes are not distributed in a uniform manner. In this paper we address the problems mentioned below:

Revised Manuscript Received on June 07, 2019.
S Anuradha, Department of ECE, JNTUH, Hyderabad, India.
Dr.D. Sreenivasa rao, Department of ECE, JNTUHCEH, Hyderabad, India.

1. In larger networks, the distance between SINK and CHs are more.
2. As a result, the mobile agents have to travel longer distances, which is also depleting energy at mobile agents.
3. Long distance travel may increase the delay in delivering the data to BS.

In Multi-hop LEACH offered by Fan et al. [12], energy effectiveness has remained enhanced as multi-hop routing occupies smaller amount of energy than direct information towards the BS openly, particularly in huge sensor systems every CH chooses the adjoining CH in single hop series by means of its succeeding hop. However the major disadvantage of multi-hop LEACH and certain additional solutions which simply combined clustering and multi-hop transmission [13–14] is that CHs around the SINK tends to include great relay traffic and the nodes would expire shortly, therefore reducing the lifetime of the network. Here exist certain resolutions that target at exploiting the interval till the leading node turn out of energy in addition to the work towards reducing energy consumption [15–16]. The difficulty of these max-min lifespan routing procedures is that they may not safeguard energy on the base of complete system measure. Preserving energy aimed at the complete system remains more significant compared to that of distinct node in a big measure sensor system. Finally, though there exists a proportion of investigation effort on energy-aware routing in sensor systems, limited preceding mechanisms has deliberated the objectivity in energy consumption amongst sensor nodes.In some cases, particularly in large networks, the moving agent has to travel for longer distances which seriously affect the network performance in terms of delay and energy consumption. So here we introduce secondary level base station to reduce the travel time of the moving agents as well as to reduce the energy consumption. Here our paper presents three objectives performing which is shown below:

1) Data gathering between CHs and member nodes using energy aware routing protocol.
2) Involving Secondary Level Base station (SLB) in the network.
3) Mobile Agent is used to collect maximum data in routing and send it to near BS.

II. EXISTING WORK

On behalf of dynamic grouping of wireless sensor systems, [17] have offered an evolutionary aware routing protocol (EAERP). In selecting a customary of effective group heads commencing the standard sensor nodes and complete non-CH sensor nodes define adjoining CH towards joining, here the writers have prepared a challenge for minimizing the energy consumption all over the system. Furthermore, EAERP involves re-clustering in every single round for rotating the additional load of CH. Miserably, being an integrated method; EAERP involves complete system data in every single round aimed at re-clustering. Singh [18] and [19] have employed the PSO for CH selection amongst the usual sensor nodes and do not pay attention towards the cluster establishment. PSO as well as ant colony optimization (ACO) are employed in WSNs aimed at additional optimization difficulties correspondingly and they can remain found in [20], [21], and [22]. Nevertheless, not a bit of the exceeding procedures deliberate the overhead of the information routing in group establishment stage. Moreover, none of them excludes [23] attention on cluster establishment by means of nature-motivated method. Numerous workings have remained projected aimed at CH collection. Nevertheless, collection of the CHs simply cannot practice the groups. Here exists no nature-stimulated grouping procedure such as PSO that deliberates cluster establishment instead of CH assortment aimed at WSNs for the finest of our understanding. In [24], author's contribution towards EECCP is to further influence the calculation ability of sensor nodes in computing and considering a joint optimization of both computation as well as communication energy across mobile wireless sensor node for transferring and processing sensor data and distribute results to suitable parties. To the best of knowledge, this is the primary effort that considers sensor node as a service and realize cooperative calculating in MWSN. Its limitation includes the computational cost of this algorithm is very high and increases the overhead. Also, the candidate node (CN) selection affects overall energy consumption. In [25], a secured recoverable CDA scheme in heterogeneous WSN was proposed by author. In this method, only a common node can produce valid cipher text if not the node is compromised as the basis for producing cipher texts is only shared in-between the node as well as the base station that remains useful to avoid DoS attacks near the base station as specified previously. In order to protect the data privacy as well as recoverability, we use a symmetric HEBDA scheme. The base station can acquire overall original information and implement arbitrary aggregation operations. Additionally, we apply an effective signature scheme supporting batch verification that not only delivers data reliability check, but moreover can obtain in-network false data filtering as well as approved aggregation. Its limitation includes that, data aggregation creates overhead when an enormous amount of data are collected from a huge amount of sensor nodes.In [26], a Novel energy aware hierarchical cluster-based routing protocol (NEAHC) was proposed by the author for extending the lifespan of the WSNs by combining clustering technique as well as an optimal relay selection procedure. The objective is to find an optimal routing path from the source towards the destination by favoring the maximum remaining battery power, minimum energy consumption in multi-hop path, as well as optimum fairness among sensor nodes. Its limitation increase the work load among the cluster head nodes and energy is depleted more quickly in the CH nodes, which leads to frequent re-clustering and CH rotation. Also this method would increase the traffic at the nodes surrounding near to the sink node.

III. PROPOSED FRAMEWORK

In order to improve efficiency, we propose a method called EE-SLB which involves secondary base station in a network. It reduces the overhead and improves the data delivery process. The introduction of MA's reduces the load among the CHs and the surrounding nodes. Also energy is not a primary parameter for CH selection. So CH rotation is limited and prolong for a long time. The network coded methods is used for data aggregation. In this method, we use two base stations. In order to verify the data between the base stations, this data integrity check is used.

The data integrity is nothing but ensuring the sent data is received without any loss or any alteration and also to check the authenticity of the data at the receiver side. The working process of proposed method shows in figure 2.In this paper, to simplify scheduling for the mobile agent, we accept that the information gathered by sensor nodes remains the deferral tolerant information, i.e., they can wait for the mobile agent to arrive and lift them up. Here mobile agent receiving data, send it to base station. In this paper, mobile agent will deliver the data to secondary level base station, in case primary base station is not nearby. As a result, maximum data delivery progresses in network. Here cluster head node forwards the data towards nearest base station so time saving in routing level.We consider the network remains collected of N sensor nodes, represented as: 1 2 {s1, s2, s3……..Sn} correspondingly. They unceasingly supervise their adjoining atmosphere and remain equally distributed in a rectangle field. There exist k sink nodes (or Base Station, BS) that have remained arranged by indiscriminate location, signified by means of 1 2 BS1, BS2….BSk}. We build the succeeding suppositions:Entire nodes remain heterogeneous and fixed after the deployment. The sink node remain pre-located in the sensing field indiscriminately. Nodes may modify their transmitting power along with the relative distance towards its receiver and Links remain there uniformly.In every cluster there exists only one cluster head. The additional nodes in similar cluster direct information towards the cluster head. At that moment, cluster head forwards combined information towards the aforementioned significant sink. Firstly, information combination decreases traffic load. Additionally, the cluster heads located in similar mode compares itself with the probabilistic deployment in LEACH. The aforementioned remains additionally relevant on behalf of the large-scale deployed networks. Lastly, it may extend the network lifespan, by means of a majority of nodes near the communication module aimed at comparatively lengthy period. We will then select every single cluster head once similarly distributing the sensing field into numerous identical regions. We define every single cluster head using its residual energy since the network remains deliberated towards being heterogeneous. We motivate the sensor node S_i that is placed at the center of each cluster, when the selection process starts. The aforementioned remains considered by means of the cluster head. In the vicinity of radius R, it transmits single message. Aimed at the struggle of the cluster head, this message wishes towards motivating additional nodes. The aforementioned comprises the node's id as well as the aforementioned residual energy. Though the external nodes stay futile, only in the communication range, the nodes may obtain the message and turn out to be dynamic. If any node Sj consumes greater residual energy compared to S_i, it turns out to be a new cluster head applicant and transmits novel message by its individual data towards others. If Sj consumes equivalent residual energy by S_i, then relate the ID, then the node by a lesser ID succeeds. If Sj consumes lesser residual energy compared to Si, the aforementioned still transmits the message of Si. When the assessment remains achieved, the unselected node turn out to be idle once more. Entire nodes in the cluster must be paralleled merely one time. Thus, the node is selected as cluster head by the leading residual energy. The cluster-selection procedure may be expressed in the same way to find MAX ($E_{residual}$).

3.1 Inter cluster routing

The cluster heads must send collected data towards sink nodes after the data fusion. We can make better usage of the secondary level-sink topology. Every single cluster head chooses one optimum sink individually in our procedure. Our topmost interest is to minimize the energy consumption. For any cluster head CH, the energy consumption towards sink: BS is represented as E (CH, BS). Its calculation follows the energy model. E (CH, BS) == d (CH, BS), where d is the distance between the CH and BSFrom the above mentioned formula we can observe that the energy consumption i.e., E (CH, BS) is reduced if the distance, d (CH, BS) between CH and BS is low. In this scenario, the data from cluster head can be sent directly towards the sink node within single hop. Hence, we must compare the distances from every cluster head towards various sinks and then select the shortest path. In this manner, the cluster head will determine the optimal sink with minimum energy consumption.

3.2 Intra cluster routing

Sensor nodes in the identical cluster transmit information straightly towards the cluster head in numerous clustering procedures. Certain sensor nodes might consume relatively huge quantity of energy because of long-distance communication owing towards the point of their numerous locations. As a result, we fix a multi-hop routing protocol.
Aimed at every participant node Si in single cluster, the energy consumption charges towards sending information openly towards its cluster head CHsi remains characterized by means of E (S_i, CHS_i)Meanwhile, it remains promising that Si attempts towards finding additional sensor node Sj to forward information for saving energy through openly avoiding communication by CHS_i.En route for delivering a l-length packet towards the cluster head and the energy consumption E(S_i, Sj, CHS_i) remains intended in this manner as well as the optimal relay node remains defined grounded on the least assessment of E(S_i, S_j, CHSi) where ε and α differ in dissimilar circumstances along with the energy model.E(S_i, S, CHsi) = Etx (l,d, (S_i,Sj) + Erx (l) + Etx (l, d, (S_j, CHS_i))Every single Si selects S_j by the least value of E(S_i, S_j, CHS_i) by means of the relay node if needed.E (S_i, CHSS) = Min (E (S_i, Sj, CHS_i))Nevertheless, the sink nodes remain accidentally situated in our procedure. Hence, certain nodes might consumption a smaller amount of energy by transmitting information openly towards the sink instead of towards its cluster head. Therefore it remains essential for comparing E (S_i, CHS_i) as well as E (S_i, BSk) and decides the ultimate route.Aimed at easiness, the intra-cluster procedure can remain expressed as towards finding MIN (E (Si, CHS_i), E (S_i, BSk)).

3.3 Flowchart

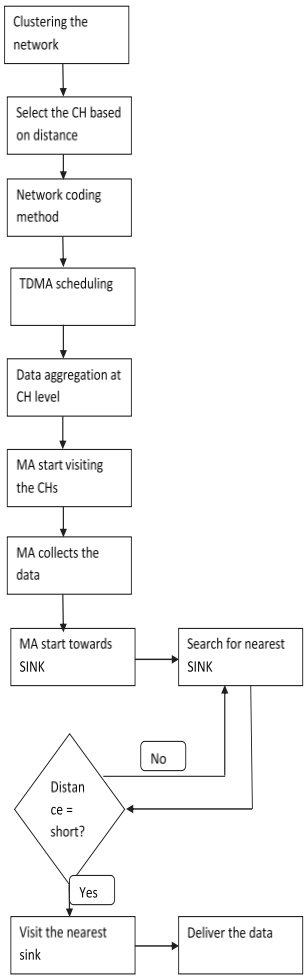

Figure. 2: Flowchart of Proposed system

IV. RESULT AND DISCUSSION

A. Simulation Environment & Parameters

The simulation environment parameters are summarized in table 1 and considered as default values unless otherwise specified in the paper.

Table 1
The Simulation Environment Parameters

PARAMETER	VALUE
Application Traffic	CBR
Transmission rate	1000 bytes/0.1 ms
Radio range	250m
Packet size	1000 bytes
Initial energy	100j
Simulation time	10s
Number of nodes	77
Area	1000x500
Grid size	50m
No. Clusters	8
Base stations	2
Routing protocol	AODV
Routing methods	EE-SLB, EE-CCP, HEBDA, NEAHC

In this paper, we consider that 77 sensor nodes are randomly spread over a 1000x500m^2 field. In this paper, we accept that no gap is present in the detecting field and static sensors remains equal in their abilities. In the meantime, we assume that the mobile agent is located initially in the top-left corner of the two-dimensional territory and its coordinates are (50 m, 50 m). After cluster head collecting the data from cluster member, the mobile agent initiates its periodical movement from beginning point and running towards to cluster heads and finally returns. Table1 presents the system parameters utilized in our simulations.

B. Performance metrics

The performance of the proposed optimal solution is evaluated via simulation results using Network simulator-2. Number of simulation experimentations has been conducted to calculate the performance of our algorithm. For evaluating the performance of our proposed algorithm, we use key metrics named energy consumption, delay and throughput based on which the performance from first deployment till the last node is carried out.

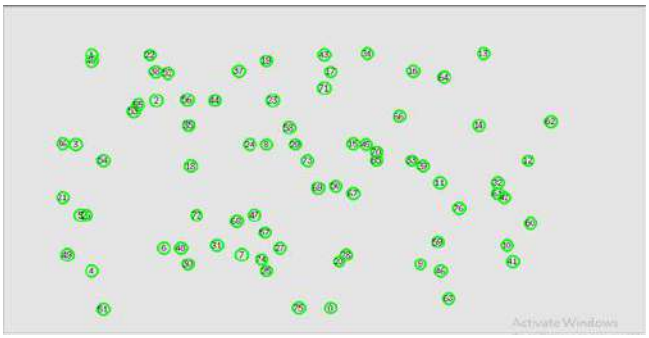

Figure. 3: Network deployment

Figure 3 demonstrates that all nodes are placed in the network (1000x500m) and the deployment of nodes is properly done in the network. At this point, the entire nodes that are represented are on the basis of random topology values and it should mention the overall properties of NAM window.

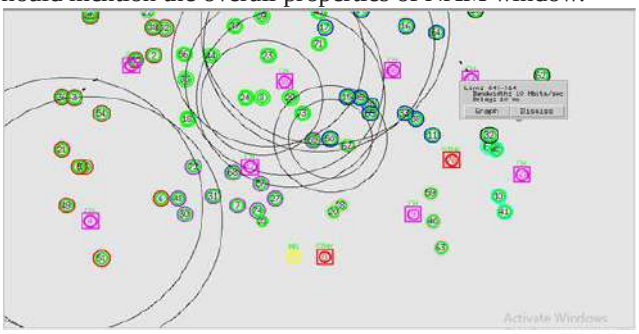

Figure. 4: Cluster level routing

Figure 4 displays that, all nodes participate and which node is to be considered and the type of the node is mentioned in NAM. All cluster heads which are considered based on distance parameter are displayed. At this point, cluster member to cluster head data transmission is performed.

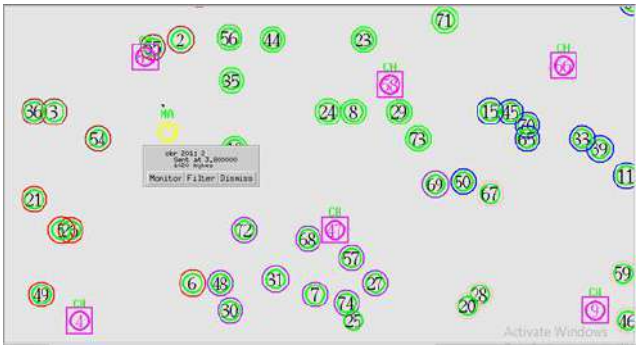

Figure. 5: Mobile agent collection

Figure 5 represents the data collection of mobile agent. In NAM, node 75 is considered as mobile agent and it starts moving towards the CH and collects data from all the cluster heads.

Figure. 6: MA to SBS data link routing

Figure 6 represents the data link between the mobile agent and secondary level BS. Here we consider node 0 as primary base station, as it is located at far distance from the mobile agent. Therefore, we choose secondary level base station to collect the data from mobile agent. Here Bandwidth and delay demonstrates the data transmission between two nodes in average time.

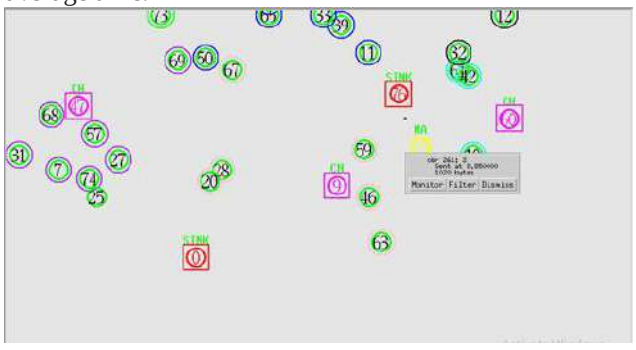

Figure. 7: MA to SBS data processing

Figure 7 demonstrates the data level routing process between MA and SBS (secondary Base station). Here CBR indicates traffic level protocol and measures the number of iterations, dual communication, packet size, and time interval. In this NAM, node 76 is considered as SINK (secondary BS).

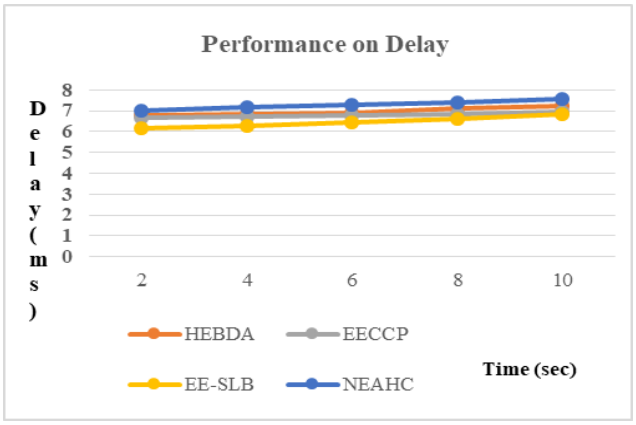

Figure. 8: Delay performance in network

We define that processing delay denotes the execution time versus varying delay in network. Figure 8 represents the delay of sensor node that is processing the data and it is much lower compared to others, since it allocates the traffic load through the CHs in the network to balance their transmission charge. But after few rounds, it rises rapidly due to the rise in transmission cost as some number of CHs reaches their level and starts data transmission directly towards the BS. If there exist long distance communication between CH and BS, mobile agent moves towards to CH and collects the data and gets it back to BS.

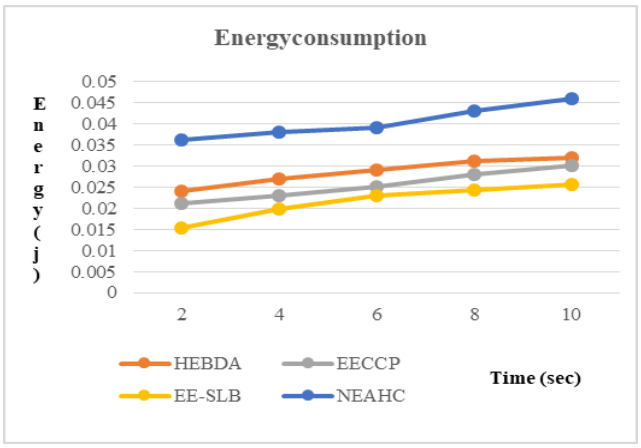

Figure. 9: Energy consumption in network

Figure 9 represents the energy consumption in network and it is much lower than others, as it allocates the traffic load through the CHs in the network to balance their transmission cost. But after few rounds, it rises suddenly due to rise in the transmission cost as some number of CHs reach their energy level and start sending data straight towards the BS. Whenever the CHs are near to BS, it directly transmits the data otherwise searches for the nearest BS without the loss of energy.

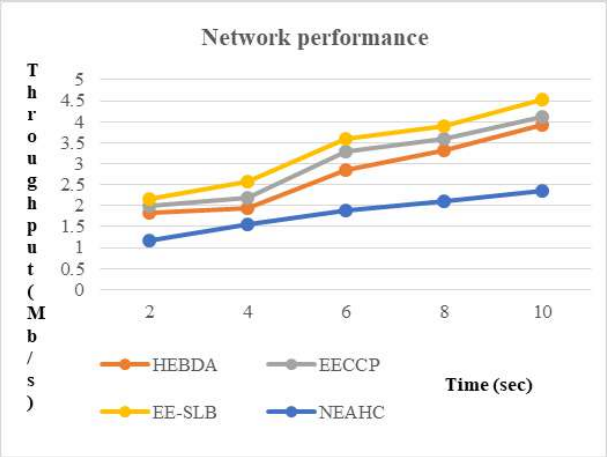

Figure. 10: Network performance

Figure 10 represents the overall network performance. Here, the number of data packets received by the BS in EE-SLB is higher at all times compared to existing methods. The average number of data packets received by BS and their network performance is computed using various number of sensor nodes as well as estimates how much data is to be stored in each sensor node for future transmission purpose. Secondary level BS is helpful for increasing the data in network in the proposed system.

V. CONCLUSION

The main design encountered in routing protocol aimed at WSNs is efficient energy usage as well as operational network lifespan. This paper defines the benefits of the secondary level base station in the network. The projected EE-SLB protocol precedes the benefits of clustering as well as secondary level base station towards optimizing the energy consumption in intra cluster routing. Simulation result proves that proposed EE-SLB outperforms equivalent procedures similar to EECCP, HEBDA as well as NEAHC protocols in terms of energy consumption and data distribution. In this paper, 38% improvement of the proposed method over the existing methods considered is observed with respect to the performance parameters given.

REFERENCES

1. Akyildiz,I.F.,etal..Wirelesssensornetworks:asurvey.Comput.Netw.38, 393–422. 2002.
2. Calhoun,B.H.,etal..Designconsiderationsforultra-lowenergywireless microsensor nodes.IEEETrans.Comput.54,727–740, 2005.
3. Ahmad,A.,etal..MAClayeroverviewforwirelesssensornetworks.In:CNC S 2012,pp.16–19, 2012.
4. Aykut,Y.M.,etal..QoSawareMACprotocolsforwirelesssensornetworks:a survey.Comput.Netw.55,1982–2004, 2011.
5. Abbasi,A.A.,Mohamad,Y..Asurveyonclusteringalgorithmsforwireless sensor networks.Comput.Commun.30,2826–2841, 2007.
6. Kemal,A.,Mohamed,Y..Asurveyonroutingprotocolsforwirelesssensorne tworks.AdHocNetw.3,325–349,2005.
7. Gupta, G.,Younis,M.,2003.Load-balancedclusteringofwirelesssensornetworks. In: IEEEICC2003,pp.1848–1852, 2003.
8. Low, C.P.,etal..Efficient load-balanced clustering algorithms for wireless sensor networks.Comput.Commun.31,750–759, 2008.
9. Ataul,B.,etal..Ageneticalgorithmbasedapproachforenergyefficient routing intwo-tieredsensornetworks.AdHocNetw.7,665–676, 2009.
10. Kuila,P.,Jana,P.K..Improvedloadbalancedclusteringalgorithmforwireles s sensor networks.In:ADCONS2011,LNCS7135,pp.399-404, 2012.
11. Kuila, P., Gupta, S.K, Jana, P.K., A Novel evolutionary approach for load balanced clustering problem for wireless sensor networks. Swarm Evol. Comput. 12, 48-56.
12. Fan X N, Song Y L. Improvement on LEACH protocol of wireless sensor network. Proceedings of the 2007 International Conference on Sensor Technologies and Applications (SensorComm'07), Oct 14−20, 2007, Valencia, Spain. Piscataway, NJ, USA: IEEE, 2007: 260−264.
13. Priyankara S, Kinoshita K, Tode H, et al. A clustering/multi-hop hybrid routing method for wireless sensor networks with heterogeneous node types. Proceeding of the 2010 IEEE GLOBECOM Workshops (GC Wkshps'10), Dec 6−10, 2010, Miami, FL, USA. Piscataway, NJ, USA: IEEE, 2010: 207-212
14. Javaid N, Aslam M, Djouani K, et al. ATCEEC: a new energy efficient routing protocol for wireless sensor networks. Proceedings of the 2014 IEEE International Conference on Communications (ICC'14), Jun 10−14, 2014, Sydney, Australia. Piscataway, NJ, USA: IEEE, 2014: 263−268.
15. Van Giang D, Taleb T, Hashimoto K, et al. A fair and lifetime-maximum routing algorithm for wireless sensor networks. Proceedings of the IEEE Global Telecommunications Conference (GLOBECOM'07). Nov 26−30, 2007, Washington, DC, USA. Piscataway, NJ, USA: IEEE, 2007: 581−585.
16. Zhang L, Chen S G, Jian Y, et al. Maximizing lifetime vector in wireless sensor networks. IEEE/ACM Transactions on Networking, 2013, 21(4): 1187−1200.
17. Enan,A.,etal..Energy aware evolutionary routing protocol for dynamic clustering of wireless sensor networks.SwarmEvol.Comput.1,195–203, 2011.
18. Singh,B.,Lobiyal,D.K..Energy-aware cluster head selection using particle swarmoptimizationandanalysisofpacketretransmissioninWSN.Procedia Technol.4,171–176, 2012.
19. Abdul,L.N.M.,etal..Energy-aware clustering for wireless sensor networks using particleswarmoptimization.In:IEEEPIMRC,pp.1–5, 2007.
20. Saleem,M.,etal..Swarm intelligence based routing protocol for wireless sensor networks:surveyandfuturedirections.Inf.Sci.181,4597–4624, 2011.
21. Kulkarni,R.V.,etal..Particleswarmoptimizationinwireless-sensornetwor ks:a briefsurvey.IEEETrans.Syst.,Man,Cybern.–PartC:Appl.Rev.41,262–26 7, 2011.
22. Zungeru,A.M.,etal..Classicalandswarmintelligencebasedroutingprotoco ls for wirelesssensornetworks:asurveyandcomparison.J.Netw.Comput.Appl. 35, 1508–1536, 2012.
23. Kuila,P.,Gupta,S.K.,Jana,P.K..Anovelevolutionaryapproachforload balanced clustering problem for wireless sensor networks. Swarm Evol. Comput. 12,48–56, 2013.
24. Z. Sheng, C. Mahapatra, V. C. M. Leung, M. Chen and P. K. Sahu, "Energy Efficient Cooperative Computing in Mobile Wireless Sensor Networks," in *IEEE Transactions on Cloud Computing*, vol. 6, no. 1, pp. 114-126, 1 Jan.-March 2018. Doi: 10.1109/TCC.2015.2458272.
25. Hong Zhong, Lili Shao, Jie Cui, Yan Xu, "AN efficient and secure recoverable data aggregation scheme for heterogeneous wireless sensor networks", Volume 111, Janguary, 2018, pages 1-12. Doi: https://doi.org/10.1016/j.jpdc.2017.06.019.
26. Wang Ke, Ou Yangrui, Ji Hong, Zhang Heli, Li Xi, " Energy aware hierarchical cluster-based routing protocol for WSNs", Volume 23, Issue 4, August 2016, Pages 46-52. https://doi.org/10.1016/S1005-8885(16)60044-4

International Journal of Advanced Research in Engineering and Technology (IJARET)
Volume 8, Issue 3, May - June 2017, pp. 25–36, Article ID: IJARET_08_03_004
Available online at http://iaeme.com/Home/issue/IJARET?Volume=8&Issue=3
ISSN Print: 0976-6480 and ISSN Online: 0976-6499
© IAEME Publication

TRUST ENHANCED DYNAMIC ROUTING FOR MANET

Syeda Kausar Fatima
Research Scholar, ECE Department,
Jawaharlal Nehru Technological University (JNTUH), Hyderabad, Telangana India

Dr. Syed Abdul Sattar
Professor and Dean, Nawab Shah Alam Khan College of Engineering & Technology (NSAKCET), Hyderabad, Telangana India

Dr. D. Srinivasa Rao
Professor, ECE Department, Jawaharlal Nehru Technological University, Hyderabad, Telangana India

Syeda Gauhar Fatima
Associate Professor, ECE Department,
Deccan College of Engineering and Technology (DCET), Telangana, India

ABSTRACT

Nowadays Mobile Adhoc Network (MANET) is becoming more popular due to its mobile and ease of deployment nature. However due to wireless and dynamic nature of network topology, it make them more exposed to various types of attacks. The main issue is to assure secure network services. In order to overcome this issue, a Trust Enhanced Dynamic Routing for MANET with Threshold Signature and Randomization process is proposed. In this technique, a secure cluster is formed based on the trust probability value where each node monitors trust value to determine the node trust level and minimum trust level of neighbor node. The node with high trust value is considered as the Cluster Head. In order to overcome the eavesdropping attacks during routing process randomization process is employed which monitors the each node to block malicious and increases node security level. The simulation results determines the comparative study results with the combination of attacks and without attacks.

Key words: MANET, security, trust, attacks.

Cite this Article: SyedaKausar Fatima, Dr. Syed Abdul Sattar, Dr. D. Srinivasa Rao and Syeda Gauhar Fatima. Trust Enhanced Dynamic Routing for MANET. *International Journal of Advanced Research in Engineering and Technology,* 8(3), 2017, pp 25–36.
http://iaeme.com/Home/issue/IJARET?Volume=8&Issue=3

1. INTRODUCTION

1.1. MANET

MANETs are highly vulnerable to various security attacks. Providing secure communication in MANET is proved to be a significant challenge. Authentication and trust model which are developed for wired network cannot be used in wireless network. Common authentication schemes are not applicable in Ad hoc network since public key infrastructure is hard to deploy [1] [2].Security supports are a significant factor in the design of security system in ad hoc networks. It is particularly important to protect the identities of individual nodes to avoid personal privacy concerns. For this a security system for ID-based anonymous cluster-based MANETs and a threshold signature [9] is proposed to protect the privacy of nodes. Here the basic operations consist of generating pairing parameters, private keys, and secret sharing.

Each node is having the ability to build a network by finding the node to communicate and share the data via radio waves. MANETs have several significant characteristics and challenges [4] for e.g. dynamic topology, distributed operation, light weighted terminal etc. Mobile ad hoc networks are vulnerable to security problems than the wired networks, different types of security solutions are used like cryptography and IDS etc. to avoid the security attacks but the malicious attackers block or modify the data traffic traversing them by refusing the cooperation and violates authenticity and confidentiality of network so these type of nodes are difficult to identify as they act as a validate user, so we use a concept of trust to solve such problems, trust is calculated on the basis of reputation, direct, indirect trust (recommendation). In which we calculate the degree of dependence on other nodes by which we then decide whether to communicate with that node or not.

2. LITERATURE REVIEW

Peng Zhou, Siwei Jiang, Athirai Irissappane, Jie Zhang, Jianying Zhou, and Joseph Chee Ming Teo et al [1]propose a suite of optimization methods to minimize the energy cost of watchdog usage, while keeping the system's securityin a sufficient level. Watchdog optimization algorithms have demonstrated excellent performance in saving energy and maintaining security, they are still subject to some challenges, which may need further investigation.

Bijon, Khalid Zaman, Md Munirul Haque and Ragib Hasanet al [2] proposes model that provides a feature of multi-hop recommendation where every valid recommendation comes only from DTNs. This model also reduces traffic in a great volume by updating multiple trust fields of intermediate nodes. It also introduces the concept of path reliability based aging. It also successfully reflects uncertainty while combining multiple recommendations.

N. Bhalaji, A. Shanmugam et al [4] proposed the trust model and analysed each node calculates trust value and association status for all its neighboring nodes through monitoring its behavior in the network. Then this trust model is integrated into the Dynamic Source Routing (DSR) protocol which is the most common on demand routing protocol used in MANET. In the proposed scheme the route is not selected on the basis of first arrival of RREP and waits till it gets the RREP from all neighboring nodes and decides the path to be routed based on the nature of association between them.

Abderrezak Rachedi and Abderrahim Benslimane [6] have proposed an anonymous protocol to secure nodes which have important roles in the network. Also they presented an Anonymous Dynamic Demilitarized Zone (ADDMZ) to protect the CA node identity and to avoid the single point of failure in the cluster. ADDMZ is formed by a set of confident nodes which have a high trust level between them and their goal is to filter the communication between the cluster member node and the CA node. They present protocol to realize these

mechanisms by using the identity based cryptographic from bilinear maps. However, it is possible to attack RA nodes by selecting randomly nodes at the attacker's neighborhood, but the risk to detect the attacker is high.

Yo Han Park et al [7] have proposed a security system for ID-based anonymous cluster-based MANETs to protect the privacy of nodes. Moreover, they propose a threshold signature scheme without pairing computations, which diminishes the computation load on each node. Their proposal satisfies most properties for an anonymous security system and effectively copes with dynamic environments with greater efficiency by using secret sharing schemes. As long as the CH does not reveal the respective polynomials, anonymity of each node is guaranteed.

Raihana Ferdous et al [8] have proposed a Cluster head(s) selection algorithm based on an efficient trust model. This algorithm aims to elect trustworthy stable cluster head(s) that can provide secure communication via cooperative nodes. However the way the messages passed through may overload the Cluster head, creating a bottleneck due to additional message exchanges. Another possible limitation is the way that the message authentication between intermediate Cluster heads are treated, where there can be adelay in identifying a malicious neighboring node.

Yao Yu and Lincong Zhang et al [9] have proposed a secure clustering algorithm based on reputation in defense of threats in clustering. In the algorithm, the nodes reputation is used to improve security, which is evaluated by combining the experience of the node in the routing process. In addition, they consider degree and relative mobility in the clustering to guarantee the stability of clusters. Moreover, it is efficient in the cluster rebuilding and healing. The proposed algorithm can effectively improve the security and stability of network. However there occurs overhead in the system.

Noman Mohammed et al [10] have proposed a solution for balancing the resource consumption of IDSs among all nodes while preventing nodes from behaving selfishly. To address the selfish behavior, they design incentives in the form of reputation to encourage nodes to honestly participate in the election scheme by revealing their cost of analysis. To address the optimal election issue, they propose a series of local election algorithms that can lead to globally optimal election results with a low cost. However the percentage of leaders is less in this model.

Hard security, designed to protect data and system integrity, may not be enough to protect nodes from misbehavior by other malicious nodes. At the present time, soft security threats are most effectively countered using trust and reputation management (TRM) systems.

3. TRUST DYNAMICVECTORROUTING PROTOCOL (TEDR)

A Trusted Dynamic Vector routing organize trusted dynamic routing which is rely on existing distance information exchanged among neighboring nodes for seeking a routing paths. The nodes maintains a routing table (Table -1) with corresponding tuple $(d, W_{N_{i,d}})$, where $d$denotes new destination node and $W_{N_{i,d}}$ minimum estimated path cost to send a packet from node i to node d.

Corresponding routing table (Table -1) extended with node trust representation. The corresponding routing table (Table -2) determines the extended trusted routing table $(d, W_{N_{i,d}}, C_t^{N_i}, H_t^{N_i}, T_{N_{i,d}})$, with node candidate, interactivity history, trust count. Here each tuple associated with a set of node candidates $C_t^{N_i}$for the next hop with minimal cost is marked.$H_t^{N_i}$, represents a interactive history from node t to node i, and each tuple (N_j, H_{N_j}) in $H_t^{N_i}$, is used to represent that N_i previously used the node H_{N_j}as the next hop to forward the

packet from the source node N_j to the destination node d. $T_{(N_{i,h}),(N_{h,d})}$, a set of trust count values from node to next hop node and next hop node to destination node. Each tuple $\left(N_j, h_{N_j}\right)$in $H_t^{N_i}$, is used to represent that $N_i$previously used the node h_{N_j}as the nexthop to forward the packet from the source node N_j to the destination node d.

Assume that a node n has m number of neighbor nodes at particular instance. Each neighbor monitors independently with probability p. The probability at node n is monitored at trust level l. Let assume each node monitors the neighbor nodes with minimum probability of P_i^{min}, where neighbor nodes are monitored with desired trust level. According to the figure -1 node – 5 represents three neighbor nodes (1,4,6). Assume trust level l =1, the node 5 monitors the neighbor nodes (0.81, 0.94 and 0.98) respectively, with the trust level probability of$P_5^{min} = \max(0.81, 0.94, 0.98) = 0.96$

$$P(l/m) = \sum_{i=1}^{m} \binom{m}{i} p^i (1-p)^{m-1}$$

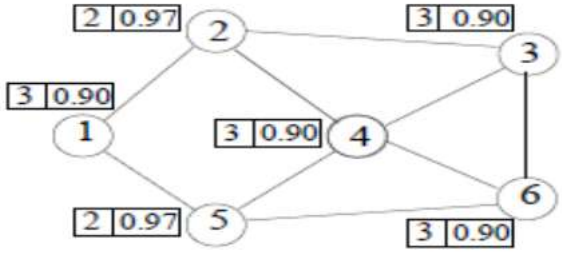

Figure 1 Calculation of Minimum Monitoring Probability

To determine node corresponding neighbors trust level probability by exchanging node degree, we define a degree as a number of neighbor nodes at instance of time. Based on that let r will be the minimum degree of node i. For the time instance t, let 5 will be the node degree of node i, to obtain the optimal trust level of node with minimum probability will be measured as

$$P_i^{min} = \sum_{j=1}^{m_i} \binom{m_i}{j} p^j (1-p) \geq T$$

The term T, as explained earlier denotes a threshold value, which is the minimum probability with which the desired trust level l. Each node in the network is monitored with the desired trust level (l) when $P_i^{min}$of each node i iscalculated using minimum degree of its neighbors (m_i)

Table 1 The routing table for the original distance-vector-based routing.

Destination Node (t)	Cost ($W_{Ni,t}$)	Nexthop
N_1	7	N_6
N_2	8	N_{21}
N_3	9	N_9

Table 2 The routing table for the security-enhanced routing algorithm

Destination Node (t)	Cost ($W_{Ni,t}$)	Nexthop Candidates (C_t^{Ni})	History Record for Packet Deliveries to the Destination Node t(H_t^{Ni})
N_1	7	{ $\hat{}N_6, N_{20}, N_{21}$}	{(N_2, N_{21}), (N_3, N_6),..(N_{31}, N_{20})}
N_2	8	{N_9 , $\hat{}N_{21}$}	{(N_1 , N_9), (N_3, N_9),..(N_{31}, N_{21})}
N_3	9	{ $\hat{}N_9$}	{(N_1, N_9), (N_2, N_9),..(N_{31}, N_9)}

The Mechanism employed by each node in the network o determine the minimum monitoring probability , which is derived in Minimum Degree for k. Fig -2 described more pictorially about *MDK* algorithm. According to the fig -3, each node intitiates this algorithm to know the probability which are the nodes it has to monitor its neighborhood. Once this algorithm derived the node neighbourhood monitoring probability, then the node (M) broadcast the message (Send Degree) to one hop neighbours, once the 1-hop neighbour of node M reply back with their respective degree. The minimum of these degree is assigned to k, and the minimum monitoring probability of node M is calculated.

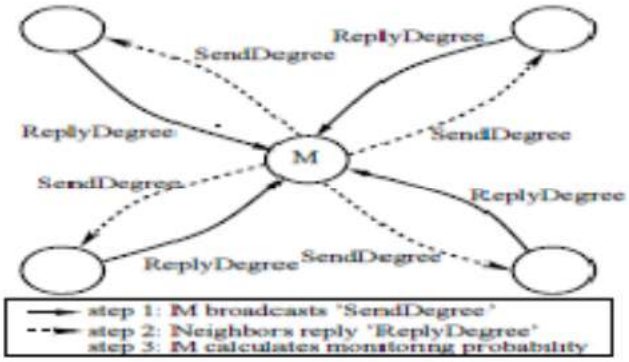

Figure 2 Description of MDK

Algorithm 1: MDK

Input : Node M, send degree, reply degree

Output : Minimum degree of k and minimum probability

1. Node Mbroadcast a message of send degree to neighbours

$$M \rightarrow brodcast : (Senddegree)$$

2. On receiving of the Send Degree message from node M, each neighbour node, $S$of M replies a Reply Degree message.

$$S \rightarrow M : (Replydegree)$$

3. On receiving of each reply degree messages of neighbour node S of M, Node M performs following operations :

- For each message dodegree = ReplyDegree;
- ii. k = Minimum(degree);
- If l > k then P_{min}M = 1.
- Otherwise, pmin M is assigned the minimum value of p (where *l*is the desired trust level of the neighbor, T +ϙ=1, ϙ is a very small positive number)such that

$$\sum_{i=1}^{k} \binom{k}{l} p^i (1-p)^{k-i} \geq T$$

3.1. Cluster Head Selection Based on TEDR

This section describes about the selection of Cluster Head (CH) in a MANET based on node fitness, node degree, node mobility, residual energy level and trust-value. For this purpose, initialize the initial trust rate value as (1), energy rate (10J), and mobility rate. Compute node fitness, the node fitness function derives based on sum of node energy level and node trust leve. The node degree represents how many number of neighbor nodes for each node in a network. The following procedure determines the election of efficient and trusted CH.

Step 1: Calculate the percentile of node degree as PN_d

$PN_d \leftarrow \left\{Numberof\ 1-hopnodesinsidethe\frac{cluster}{N}\right\} * 100$ where N is number of nodes

Step 2: Calculate the percentile of node energy level.

$$PN_E = \left\{\frac{RE_n}{T}\right\} * 100$$

Step 3: Calculate the percentile of node mobility

$$P_m = \{Avg(MS)/T \times 100\}$$

Step 4: Compute the percentile of node trust

$$P_{TV} = w1.PN_d + w2.PN_E + w3.P_m$$

where w1, w2, and w3 are weight factors given to different parameters such as node degree, energy, and mobility.

$$w1 + w2 + w3 = 1$$

Based on section 3.1 and Table 1 and 2, the Cost (WN_i, t) and history record for Packet Deliveries to the Destination Node $t(H_t, N_i)$. The node TV is determined as

$$TV_{i,j} = \sum_{\substack{0 \le i \le m \\ 0<j<n}} \frac{P_{TV}(i,j)}{cost(WN_i, t)}$$

Where $i, j \in nodes$, TVi, j represents node i's TRUST_VALUE for node j.

The CH selection technique can be explained as below:

Step 1: First, Initialize the parameters to 0 or null.

CHcur ⟵ 0

CHprev ⟵ 0

Timeprev ⟵ 0

Curr () ⟵ 0

Step 2: Calculate the TV of each node from the equation ()

$TV_{i,j} = \sum_{\substack{0 \le i \le m \\ 0<j<n}} \frac{P_{TV}(i,j)}{cost(WN_i t)}$

Step 3: Compare the given condition to select CH

While (Timeprev_Curr () or TRUST_VALUE (CHprev) ≤ 1 =true) do

CHprevremains as Cluster Head

End while

Step 4: Compare Trust Value of previous and current Cluster Head

If Trust_Value(CHprev)=Trust_Value(CHcur) and Cost(CHprev)=Cost(CHcur) then

bothCHprev and CHcurremains as cluster heads

Else

select new Cluster Head
Select new cluster head(s)
end if

4. AUTHENTICATION TECHNIQUE USING THRESHOLD SIGNATURE

4.1. Generation of Pseudonyms

The CH generates pseudonyms for all the node inside the cluster by using corresponding polynomial.

For this it performs (S1, n1)-KK of km. Also each CH calculate $id_R = H_0(ID_R)$ and secret sharing $f^{CH_j}_m(x) : PK_R = f^{CH_j}_m(x)(id_A)\ where(1 \le R \le n_1)$

4.1.2. Authentication Technique

The authentication process starts with the generation of threshold signature.

The network consist of the following parameters:

Cluster Head (CH)

A set of Member Node X = {N1……N_{S2}) where N_{S2} represents identity of the ith ($1 \le i \le S1$) member.

A set of signer $Y = \{K1,.....K_{S2}\}$ where K is a subset of N and K_{S2} represents the identity of the jth ($1 \le i \le S2$) member

Verifier V

4.2 Generation of Threshold Signature

In order to generate a threshold signature for message N, a number of S2 (b_1, b_2, b_3, b_4, b_5) nodes including the members of N perform the following steps as shown in Fig (3):

Step 1: In the first step, all the member node request for threshold signature. This is started by one of the signers by sending a threshold generation request to selected CH along with list of signers as(TK1… TK_{S2}).

Step 2: In the next step they sends tokens. For this CH selects a random token $T_R \in Z*_q$ where $(1 \le R \le S_2)$ and sends them to the corresponding signers very securely.

Step 3: After that each signer creates a signature: $Sig_{PK_R} = H_0(N).K_{PK_R}$ and calculates with a corresponding token: $T \cdot Sig_{PK_R} = TA \cdot Sig_{PK_R}$

Step 4: After that start sending signature along with pseudonym public key. Here, each node sends the message tuple to the verifier V and CH_j.

$$((N, Q_{PK_R}, Q_{PK_V}, T \cdot Sig_{PK_R}, HMAC_{PK_R}(M, Q_{PK_V}, T.Sig_{PK_A})) \quad (2)$$

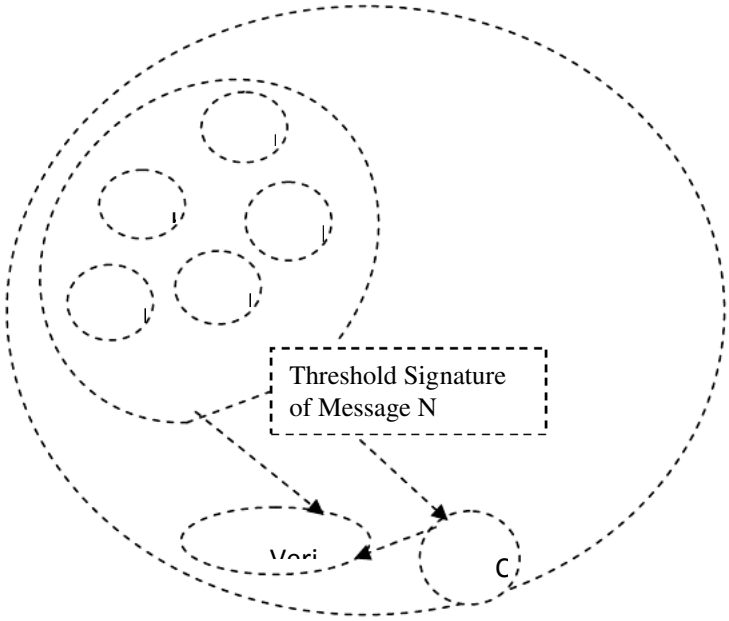

Figure 3 Representation of Authentication Technique Using Threshold

5. RANDOMIZATION PROCESS

Consider the delivery of a packet with the destination t at a node N_i. In order to minimize the probability that packets are eavesdropped over a specific link, a randomization process for packet deliveries shown in Procedure 1 is adopted. In this process, the previous nexthop h_s (defined in H_t^{Ni} of Table 2) for the source node s is identified in the first step of the process (line 1). Then, the process randomly picks up a neighboring node in C_t^{Ni} excluding h_s as the nexthop for the current packet transmission. The exclusion of h_s for the nexthop selection avoids transmitting two consecutive packets in the same link, and the randomized pickup prevents attackers from easily predicting routing paths for the coming transmitted packets.

Procedure 1

RANDOMIZEDSELECTOR (s, t, pkt)

1: Let h_s be the used nexthop for the previous packet delivery for the source node *s*.
2: if $h_s \in C_t^{Ni}$ then
3:if $| C_t^{Ni} | > 1$ then
4: Randomly choose a node *x* from $\{ C_t^{Ni} - h_s \}$ as anexthop, and send the packet pkt to the node *x*
5: $h_s \leftarrow x$, and update the routing table of N_i.
6: else
7: Send the packet *pkt* to h_s.
8: end if
9: else
10: Randomly choose a node *y* from C_t^{Ni} as nexthop, and send the packet *pkt* to the node *y*.
11:$h_s \leftarrow y$, and update the routing table of N_i.
12: end if.

5.1. Trust Table Maintenance

Let every node in the network be given a routing table and a link table. We assume that the link table of each node is constructed by an existing link discovery protocol, such as the Hello protocol. On the other hand, the construction and maintenance of routing tables are revised based on the well-known Bellman-Ford algorithm and described as follows:

Initially, the routing table of each node (e.g., the node N_i) consists of entries {(Nj, W_{Ni}, C_t^{Ni}= {N_j}, H_t^{Ni} = 0) }, where $N_j \in Nbr_i$ and $W_{Ni, Nj} = w_{Ni, Nj}$. By exchanging distance vectors between neighboring nodes, the routing table of N_i is accordingly updated. The exchanging for distance vectors among neighboring nodes can be based on a predefined interval. The exchanging can also be triggered by the change of link cost or the failure of the link/node. TEDR considers cases when N_i receives a distance vector from a neighboring node N_j. Each element of a distance vector received from a neighboring node N_j includes a destination node t and a delivery cost

$W_{Nj,t}$from the node N_j to the destination node t. The algorithm for the maintenance of the routing table of N_i is shown in Procedure 2, and will be described below.

Procedure 2

DVPROCESS (t,$W_{Ni,t}$)
1: if the destination node t is not in the routing table then
2: Add the entry (t, ($w_{Ni,Nj}$+ $W_{Nj, t}$), C_t^{Ni} = { N_j }, H_t^{Ni} = 0)
3: else if ($w_{Ni,Nj}$+ $W_{Nj, t}$) < $W_{Ni, t}$ then
4: $C_t^{Ni} \leftarrow$ { N_j} and N_j is marked as the minimal-cost nexthop.
5: $W_{Ni, t} \leftarrow (w_{Ni,Nj}+ W_{Nj, t})$
6: for each node $N_k \in Nbr_i$ except N_j do
7: if $W_{Nk, t} < W_{Ni, t}$ then
8: $C_t^{Ni} \leftarrow C_t^{Ni} \cup \{ N_K \}$
9: end if
10: end for
11: Send (t, $W_{Ni, t}$) to each neighboring node $N_k \in Nbr_i$
12: else if ($w_{Ni,Nj}$ + $W_{Nj, t}$) > $W_{Ni, t}$ then
13: if ($N_j \in C_t^{Ni}$) then
14: if N_j was marked as the minimal-cost nexthop then
15: $W_{Ni, t} \leftarrow MIN_{Nk \in Nbri}$ ($w_{Ni,Nk}$ + $W_{Nk, t}$)
16: $C_t^{Ni} \leftarrow 0$
17: for each node $N_k \in Nbr_i$ do
18: if $W_{Nk,t} < W_{Ni,t}$ then
19: $C_t^{Ni} \leftarrow C_t^{Ni} \cup \{ N_j \}$
20: end if
21: end for
22: Send (t, $W_{Ni, t}$) to each neighboring node $N_k \in Nbr_i$.
23: else if $W_{Nj,t} < W_{Ni,t}$ then
24: $C_t^{Ni} \leftarrow C_t^{Ni} - \{ N_j \}$
25: end if
26: else if ($N_j \in C_t^{Ni}$) $\wedge$ ($W_{Nj,t} < W_{Ni,t}$) then
27: $C_t^{Ni} \leftarrow C_t^{Ni} \cup \{ N_j \}$
28: end if
29: end if

Initially for the elements that do not exist in the routing table, new entries for the corresponding destination nodes will be inserted. Otherwise, $w_{Ni,Nj} + W_{Nj,,t}$ is compared with $W_{Ni,t}$ saved in the routing table of N_i, and the following four cases are considered:

$w_{Ni,Nj} + W_{Nj,\ t} < W_{Ni,\ t}$ (lines 3-11). The corresponding minimal cost is updated in the routing table, and N_j is marked as the minimal-cost nexthop. Any neighboring node N_k which has an estimated packet delivery cost from N_k to t (i.e., $W_{Nk,t}$) no more than $(w_{Ni,Nj} + W_{Nj,\ t})$ joins the candidate set C_t^{Ni} .It is to aggressively include more candidates for the nexthop to t with reasonable packet delivery cost (i.e., $W_{Nk,t} < W_{Ni,t}$). Compared to the Bellman-Ford algorithm, more one neighboring node can be selected as the nexthop candidates in this step (lines 6-10) to accommodate multiple packet-delivery paths to the destination node t. Also, the selection policy described above can prevent the algorithm from generating the routing loops.

$w_{Ni,Nj} + W_{Nj,\ t} > W_{Ni,\ t}$ and N_j is in the set C_t^{Ni} of nexthop candidates (lines 13-25). Based on whether N_j is marked as the minimal-cost nexthop in the routing table of Ni, the following two cases are further considered.

N_j was marked as the minimal-cost nexthop (lines 14-22). For all neighboring nodes of N_i, the minimal cost to the destination node t is recomputed according to the distance vectors received from the neighboring nodes. Also, the nexthop candidates for the destination node t are reselected, and the selection policy is the same as lines 7-9 for Case 1.

N_j was not marked as the minimal-cost nexthop (lines 23 and 24). If $W_{Nj,t} > W_{Ni,t}$, N_j is removed

from C_t^{Ni}.

$(w_{Ni,Nj} + W_{Nj,\ t}) > W_{Ni,\ t}$ and N_j is not in the set C_t^{Ni} of nexthop candidates (lines 26 and 27). If $W_{Nj,t} > W_{Ni,t}$, N_j is inserted into C_t^{Ni}.

Otherwise, nothing is done.

When a node N_i receives a distance vector from a neighboring node, Procedure 2 is used to maintain the nexthop candidates for each entry in the routing table of N_i. Based on Procedures 1 and 2, our security-enhanced dynamic routing can be achieved without modifying the existing distance-vector-based routing protocols

6. SIMULATION RESULTS

Table 3 Simulation Parameters

No. of Nodes	50,100,150,200
Area Size	1000 X 1000
Mac	802.11
Routing protocol	TEDR
Simulation Time	40 sec
Traffic Source	CBR
Packet Size	512
Attacker	1,2,3,4 and 5
Antenna	OmniAntenna
Speed	5,10,15,20,25

6.1. Performance Metrics

The performance of TEDR Trust Enhanced Dynamic Routing for MANET with Threshold Signature and Randomization process technique is compared with TSCP Trust Based Routing

Protocol. The performance is evaluated mainly, according to the following metrics: .Average Packet Delivery Ratio,PDR ratio measured with respective of attack and without attacks**.**

6.2. Results

Based on Attackers

In our initial experiment, number of attackers are varied as 1, 2, 3,4and 5.

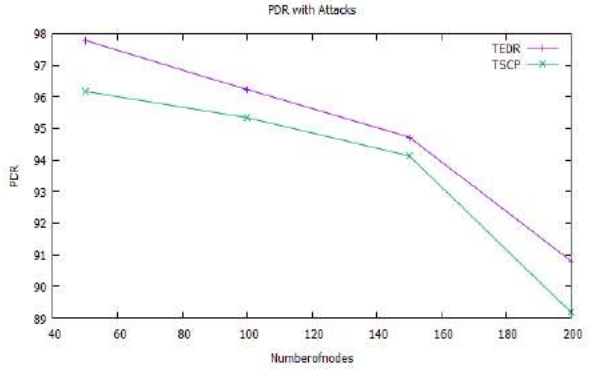

Figure 6 (a) NodesVs Delivery Ratio…

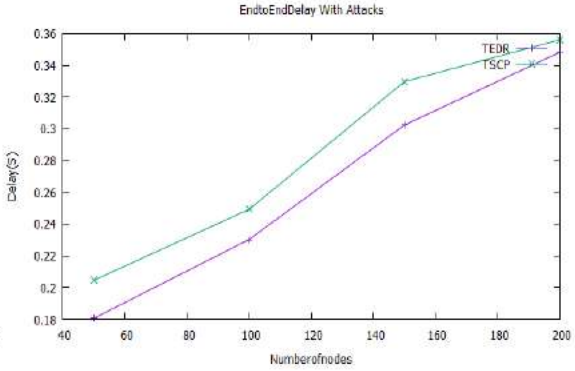

Figure 6(b) 2: Nodes Vs End2End Delay

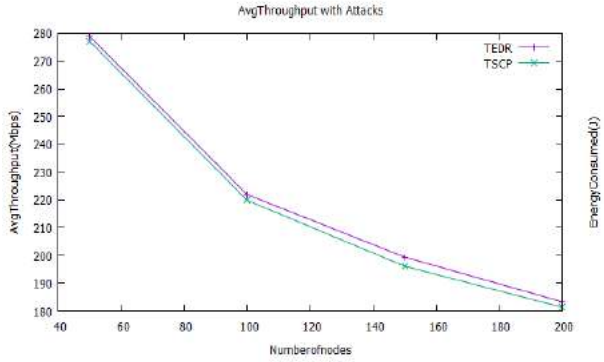

Figure 6 (c) Nodes VsAvg Throughput

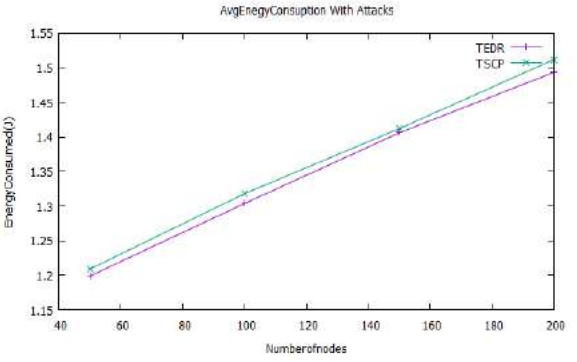

Figure 6 (d) NodesVs Avg Energy Consumption

From above figures we can see that the delivery ratio of our proposed TEDR is 5.2% higher than the existing TSCP technique. End to end delay of our proposed TEDR is 11% less than the existing TSCP technique. Average throughput of our proposed TEDR is 9.1% higer than the existing TSCP technique and energy consumption of our proposed TEDR is 11.2% less than the existing TSCP technique.

7. CONCLUSION

A trust enhanced dynamic routing protocol is proposed for MANET. In this technique, a secure cluster is formed based on the trust value. For each node participating in the cluster formation trust value is calculated. The node with high trust value is considered as the Cluster Head. In order to increase the security, the selected cluster head is further verified by using Threshold Signature. In order to overcome the eavesdropping attacks during routing process, randomization process is employed which monitor each node to block malicious and increases node security level.

REFERENCES

[1] Peng Zhou, Siwei Jiang, Athirai Irissappane, Jie Zhang, Jianying Zhou, and Joseph Chee Ming Teo Toward Energy-Efficient Trust System Through Watchdog Optimization for WSNs IEEE Transactions on InformationForensics and Security, VOL. 10, NO. 3, March 2015.

[2] Bijon, Khalid Zaman, Md Munirul Haque and Ragib Hasan. "A trust based Information sharing model (TRUISM) in MANET in the presence of uncertainty." Privacy, Security and Trust (PST), 2014 Twelfth Annual International Conference on. IEEE, 2014.

[3] Balakrishnan, Venkatesan and et al. "Team: Trust enhanced security architecture for mobile ad-hoc networks." Networks, 2007. ICON 2007. 15th IEEE International Conference on. IEEE, 2007.

[4] N.Bhalaji, A.Shanmugam Association between nodes to Combat Blackhole attack in DSR based MANET in Proceedings of the Sixth IFIP-IEEE WOCN, April 28-30 Procedia Engineering, 2012 - Elsevier

[5] Hajami, Abdelmajid, Kamal Oudidi, and Mohammed ElKoutbi. "An enhanced algorithm for MANET clustering based on multi hops and network density", New Technologies of Distributed Systems (NOTERE), 2010 10th Annual International Conference on. IEEE, 2010.

[6] Abderrezak Rachedi and Abderrahim Benslimane, "Security and Pseudo-Anonymity with a Cluster-based approach for MANET", Global Telecommunications Conference, 2008, IEEE GLOBECOM 2008, IEEE, 2008.

[7] YoHan Park, YoungHo Park and SangJae Moon, "Anonymous Cluster-Based MANETs with Threshold Signature", Hindawi Publishing Corporation International Journal of Distributed Sensor Networks Volume 2013, Article ID 374713.

[8] Raihana Ferdous, Vallipuram Muthukkumarasamy and Elankayer Sithirasenan, "Trust-based Cluster head Selection Algorithm for Mobile Ad hoc Networks", Trust, Security and Privacy in Computing and Communications (TrustCom), 2011 IEEE 10th International Conference on. IEEE, 2011.

[9] Yao Yu and Lincong Zhang, "A Secure Clustering Algorithm in Mobile Ad Hoc Networks", IPCSIT vol. 29 (2012).

[10] Noman Mohammed, Hadi Otrok, Lingyu Wang, Mourad Debbabi and Prabir Bhattacharya, "Mechanism Design-Based Secure Leader Election Model for Intrusion Detection in MANET", Dependable and Secure Computing, IEEE Transactions on 8.1 (2011).

[11] Syeda Kausar Fatima, Syed Abdul Sattar, D. Sreenivasa Rao, "Trusted and Secured Clustered Protocol in MANET", International Journal of Computer Applications (0975-8887) Volume 153-N04, November (2016) pp14-20 ©IJCA.

[12] S. Radha Rammohan. Anomaly Detection in Mobile Adhoc Networks (MANET) using C4.5 Clustering Algorithm. International Journal of Information Technology & Management Information System (IJITMIS), 7 (1), 2015, pp. 01-10.

[13] Aniket Deshpande and Dr. Ashok Kaushal, Identification of Important Sampling Parameters in Extrapolating the Performance of TCP in MANETs. International Journal of Computer Engineering and Technology, 7(6), 2016, pp. 01–08.

A Study On Durability Of Concrete By Partial Replacement Of Cement With Steel Slag Powder Using Robo Sand

[1]SHAIK YASEEN, [2]Mohd Yousuf Ahmed
[1]M.Tech Student (Structural Engineering), [2]Assistant Professor
Nawab Shah Alam Khan College Of Engineering & Technology

Abstract - **Durability can be explained as the concrete ability to counteract the abrasion, chemical attack, weathering action or any other process of degradation. Durability also includes the effects of serviceability and quality of concrete when exposed to acid and sulphate attacks. Steel Slag powder as partial substitute for cement and ROBO sand as complete alternative for natural sand are combined mostly on basis of the criteria of durability properties and costing qualities. Not only these properties, pollution in environment can also be lowered upto some extent due to the fact that emission of unsafe gases like CO(carbon monoxide) & CO2(carbon dioxide) are limited. In this research paper our study is mostly limited to the evaluation and observation of changes in both weight reduction & compressive strength in 6 different mixes of concrete grade M30 namely CAC(Conventional Aggregate Concrete), concrete mix manufactured by altering 0%, 10%, 20%, 30%and 40% of cement with Steel Slag powder proportions and by using the substitute ROBO sand as fine aggregate in 100% proportions in all 5 subsituted samples. After the 28days curing done for specimen the adverse effect of 5% of HCL(Hydrochloric acid) and MgSO4(Magnesium Sulphate) with water content on these concrete cubes are observed and determined by immersing completely. These specimens(cubes) for 56 days & 90 days in these acidic solutions, the changes in properties in weight reduction & compressive strength was observed and upto a great extent. Finally, we can conclude that concretes made up of that ROBO sand and Steel Slag powder really got durable properties and good strength when compared with regular aggregate in extreme harm environment.**

keywords - **Concrete, Steel Slag Powder, Durability of Concrete, Robo Sand, Compressive Strength, Durability Tests.**

I. INTRODUCTION

1.1 General: In these days, concrete is commonly used material for construction because the ingredients used in making concrete like cement, aggregates etc, are of availability of raw materials, low cost, abundantly, huge durability and good strength. Nowadays the construction technology has enhanced, thus resulting in the rise of construction materials costing. The deficiency of Construction materials from various environmental sources affected the rise of cost. So search for some other or new materials through which environmental issues are not caused is important. This search leads to this research in which the study of durability and strength of partially replaced concrete**.**

1.2 Durability: The property of the concrete to prevent it from getting damage for great duration is called Durability. It can be explained as the capability of concrete property to withstand abrasion actions, chemical attack, & weathering action, at the same time keeping its desirable and acceptable characteristics simultaneously. It normally referred as the life span or duration of very low trouble performance. Different concretes has distinct durability degree properties depending upon exposure of environment and desirable properties. For ex, concrete exposure to tides in seawater will be having different durability requirements than the indoor concrete.

1.2.1 Factors Affecting Concrete Durability

Cement content: Concrete mix should be designed in such a way that it ensures cohesive property and avoids segregation & bleeding of concrete. If cement content is decreased, at the fixed water-cement ratio the workability might be affected and gets reduced leading to insufficient compaction. However, to improve workability the water is added and thereby the water-cement ratio increases & causing in increase in permeability of the material.

Compaction: The concrete mix as a whole has voids could be formed cause of insufficient compaction. Commonly it is being because of the used compaction equipment, steelwork density and type of formworks in structure.

Curing: Its necessary to allow suitable strength increasing moisture holding aid & to make certain hydrating technique take place definitely.

Cover: It is the thickness of concrete provided beyond reinforcement to avoid reinforcement damage, cover should to be observed within the restrictions of codes**.**

Permeability: Its regarded as the vital thing for durability, it could be observed that greater permeability is commonly induced because of greater porosity .Hence, curing appropriately, ample cement, perfect compaction & appropriate clear cover ought to serve in less permeability.

1.2.2 Types of Durability of Concrete

Physical Durability: This kind of durability resists the below list

1. In Temperature stresses during hydration reaction

2. Permeability & Percolation of water
3. Thawing & Freezing action

Chemical Durability: This kind of durability resists the below list

1. Reinforcement corrosion
2. Delay Ettringite Formation(DEF)
3. Admission chloride
4. In Sulphate Attack
5. In Alkali Aggregate Reaction

1.2.3 Reasons for Lack of Concrete Durability

i) External Causes:

a. During Extreme Weathering Conditions
b. At Extreme Temperatures
c. In Extreme Humidity
d. Abrasion value
e. During Electrolytic Action
f. Gases attacks or Natural & industrial liquids.

ii) Internal Causes

a) Physical

- Variation in volume occurs because of changing thermal characteristics of cement paste & aggregates
- Cause of freezing.

b) Chemical

- Corrosion of Steel
- Alkali Aggregate Reactions

1.2.4 Determination of Concrete Durability

The various factors mentioned above cause losses in concrete structures. These can be summarized as follows-

- Loss of concrete strength
- Concrete is responsible to get affected by deterrents with ease.
- Reinforcement bars corrosion
- Loss of concrete serviceability
- Poor aesthetics and unpleasant appearance
- Folks and property danger
- Expensive maintenance costs
- Poor ability of materials
- Poor ability of involved agencies
- Decrease of service life
- Effects of external agencies like weathering, attack by Industrial or natural liquids, Gases, bacterial Growth etc
- Reaction between alkali & aggregates
- Ingression of moisture content/air facilitating the reinforcement corrosion and concrete cover cracking

Therefore determination and testing on concrete's durability are must for quality restraint and validity, safety assurance of the structure. Various tests and methods are used to ascertain the same. Few most regularly used methods according to IS456 are -

- Water Absorption test
- Acid test
- Sulphate attack test.
- Alkali test

II. LITERATURE REVIEW

- **"Studies On Strength And Durability Of Concrete Consisting Ggbfs And Foundry Sand" by Roshni K G , Vineeth P** presents a very comprehensive and concise analysis on the distinct views of durability of concrete when cement is substituted by fraction with GGBFS and normal sand is substituted with artificial sand. This paper has formed the groundwork for the present proposed lookup work. This work was once performed to initiate the outcomes of used foundry sand and GGBFS on strength and concrete durability.
- K. Nagamani, N. Mahendrana & R. Ilangovana of PSNA Engineering College, Dindigul, India published "**Strength And Durability Properties Of Concrete Containing Quarry Rock Dust As Fine Aggregate**" published in October 2008 in ARPN Journal of Engineering and Applied Sciences contains studies about the aspects of concrete durability with quarry rock combination as first class fine aggregate as an alternative to conventional river sand. 150 mm measured cubes of concrete & concrete beams having dimension in mm as 100x100x500 as L x B x D have been used as specimens for tests to know the respective flexural & compressive strength of specimens. Models were casted for concrete mix M20, M30 & M40 grades and for C.A(coarse aggregates) of measurement 20mm(millimeter) was made use. The main objective of this study of durability of concrete was to checkout & investigate the studies on drying and shrinkage properties, water

absorption and deterioration studies for both the Quarry Rock Dust concrete & Conventional Concrete according to the codal provisions. The durability studies conducted were able to draw the following conclusions –

- The quarry rock dust having chemical properties & physical properties satisfies all the requirements of provisions of IS codes.
- If 100% of conventional sand is substituted by Quarry Rock Dust obtained from the quarry. It sometimes shall give better, at least equal strength than the referred concrete mix of traditional Sand, in particularly of flexural strength studies & compressive investigations. The reported *f* Studies here and everywhere has showed that the concrete strength with Quarry Rock Dust as F.A(fine aggregate) is observed 10%-12% more than identical traditional mix.
- The Durability of a mix consisting the F.A as Quarry Rock Dust under acidic & sulphate activity is much lesser compared with that of normal Concrete mix. Analysis of tests on permeability sincerely verifies, permeability property of concrete mix with Quarry Rock Dust was low when observed to that of concrete mix with conventional river sand.
- Therefore, it could be wind up that alternative of normal sand is the Quarry Rock Dust material as ingredient in concrete, as there is a possibility of complete replacement. However, greater research analysis are still carried out on Quarry Rock Dust material, which are quite vital for Quarry Rock Dust as F.A(Fine Aggregate) in practical application.

➢ In the publication **"COMPRESSIVE STRENGTH OF STEEL SLAG AGGREGATE AND ARTIFICIAL SAND IN CONCRETE"** in website IJCIET (on Feb 2015) by Professor Mrs. A. I. Tamboli and other professors, concrete cubes were put on experiment for compressive strength according to codal provisions of IS456, while cement is replaced by steel slag & natural sand with artificial sand.

Designing of concrete mix was done accordingly to the IS 456-2000 and IS 10262-1982 by assuming the mix has conditions like good tier of quality supervision and tolerant vulnerabilities. M20 mix was designed with 100% replaced natural sand by artificial sand and coarse aggregate is substituted with 0%, 10%, 20% and 30% of steel slag. They came to following conclusions as listed below -

- A 20% increase could be seen in the concrete's compressive strength because of replacement ratio i.e., with 100% natural sand substituted with the artificial sand.
- The improvement in concrete's compressive strength was seen to be 10% more to that of our regular concrete, cured for 28 days.
- Such kind of concrete mixes should be used in our regular construction works to have green engineering concept and good strength.

III. MATERIALS

The experimental program to determine the possibility of using the robo sand and waste steel slag powder & their outcomes on the concrete mechanical and physical characteristics with respect to its durability aspects, was based on following procedure as entailed in coming topics. After proper determination of various material properties involved, a design mix of M30 grade was prepared. Steel slag powder & robo sand were added to conventional concrete in various volume fractions and cubes were casted for each percentage. Robo sand should completely replace fine aggregate.

Tests on compression, for conventional concrete, and those on cubes after submerging them in the respective chemicals were conducted on 7, 28& 56 days respectively. A mean of 3 readings was taken as the final reading. Graphs been plotted b/w volume fraction and the different strengths to observe and mark the effects of the introduced materials on the different characteristics of concrete.

Cement: Locally available OPC of grade 53 was used. The cement brand named C.C.I was used during the entire course of this experiment.

Table 1 Physical Properties of OPC (Ordinary Portland cement)

S.no	Property	Test Method	Test Result
1	Specific Gravity	specific gravity bottle (IS 4031-part11)	3.14
2	initial setting time	Vicat apparatus (IS 4031-part 5)	35 min
3	normal consistency	vicat apparatus (IS 4031-part 4)	30%
4	Fineness	Sieve test on sieve no.9 (IS 4031 -part 11)	7%

Fine aggregate: Substances like crushed stone, gravel, sand together with OPC(Portland cement) & water are vital ingredients for concrete. To have a great mix, aggregates should be strong, clean, clean and should be free of clay, chemicals absorbed & few other tiny substances which can lead to degradation of cement. Aggregates which are 60-75% of total concrete quantity can be branched into 2 definite divisions i.e. coarse and fine. Commonly fine aggregates contains crushed sand or natural sand along elements mostly pass over a 3/8inch or 4.75mm sieve. Sand is generally mixed as fine aggregate & it's commonly dredged from a river, seabed & lake. After completion of digging, aggregate should be processed in following order: enough crushed, screened with sieves & washed with water to get proper gradation and cleanliness. If required, the benefaction process like separation of heavy media or jigging can be done for upgrading the quality of sand. Once it is processed, these are handled, stored to reduce segregation, degradation and to avoid contamination. Aggregates strongly affect the fresh concrete mix and its hardening

properties, proportions of concrete mix, and also economy. Consequently, the choosing of aggregates is a vital procedure and sure assessments are to be performed to verify these properties. Although few changes in aggregate properties are expected.
Fine aggregate is none other than normal sand available from nearby market. The properties like gradation, specific gravity, fineness modulus, bulk density were examined according to IS2386.

Table 1 Sieve Analysis chart of natural sand - (fine aggregate)

s.no	Sieve tube	Weight retained in gms	cumulative weight retained	cumulative % weight retained
1	10	0	0	0
2	4.75	5	5	0.5
3	2.36	9	14	1.4
4	1.18	91	105	10.5
5	600	397	502	50.2
6	300	387	889	88.9
7	150	102	991	99.1
8	pan	9	1000	Nil

Table 2 Sieve Analysis chart of robo sand - (fine aggregate)

s.no	Sieve tube	Weight retained in gms	cumulative weight retained	cumulative % weight retained
1	10	0	0	0
2	4.75	4	4	0.4
3	2.36	8	12	1.2
4	1.18	95	107	10.7
5	600	385	492	49.2
6	300	387	879	87.9
7	150	107	986	98.6
8	pan	14	1000	Nil

Robo Sand, its a fine aggregate which is manufactured from crushing slag, gravel, stone. Commonly, used for aggregate material not more to 4.75 mm size which is prepared from gravel, crushed rock & other material intended for construction purpose. Robo sand is a high-quality material, in comparision to non-refined surplus from coarse aggregate production.

Manufactured sand is a substitute for river sand. The demand for sand has increased tremendously due to fast growing construction industry leading to insufficiency of suitable river sand in most part of the world. Due to reduction of quality river sand to use in construction industry, the use of manufactured sand has escalated. Another reason for use of M-Sand is its availability and transportation cost. Seeing that this sand can be grounded from hard granite rocks, it can be obtained from the surrounding places, which reduces the cost of transportation from river sand bed which is far-off.

Table 3 Comparison of river sand and robo sand

	RIVER SAND	ROBOSAND
Specific Gravity	2.68	2.72
Water absorption % by wt.	0.20	2.5%
Material finer than 75 micron (% by weight)	0.04	0.08

Table 4 Chemical comparison of river sand and robo sand

	RIVER SAND	ROBOSAND
Marine Products	2- 4%	Nil
Over Sized Material	6- 8%	Nil
Clay & Silt	5-8%	Nil
Moisture	4-5%	Nil
Total	17- 25%	Nil

Coarse Aggregate: Particles larger than 4.75mm or commonly ranges b/w 4.75 and 20mm in diameter are coarse aggregates. Majority of coarse aggregates consists of gravels which is used in mix along crushed stone taking utmost proportion. Coarse aggregate is prepared by process of crushing, large size gravel or boulders quarry rock, cobbles. The same properties and characteristics are desired in coarse aggregate as that of fine aggregate and hence appropriate experiments were done to evaluate these characteristics for concrete mix design.

Table 5 Coarse aggregate physical properties(20mm)

S.No	Property	Test Method	Value
1	Fineness Modulus	Sieve Analysis (IS 2386-1963 Part 2)	7.07
2	Specific gravity	Pycnometer (IS 2386 -1963 Part 3)	2.74

Water: The conditions specified in IS456:2000 state that "the type of water used as cement ingredient and for curing shall be clean and shall be restricted from any harmful quantities of sugar, alkalis, salts, acids, oils, organic substances and any other elements that may degrade the steel or concrete."
Generally portable water is treated adequate for concrete mixing. Therefore, the locally available portable water is used for all purposes. The pH shouldn't be under value 6 as mentioned in code.

IV. METHODOLOGY

Mixing

Ingredients are blend in a rotating drum or hand mixing using trowels. The cementitious materials were wholly mixed with hand and after that the aggregates were added followed by slow addition of water and blending. In fiber reinforced concrete, fibers were sprinkled evenly during mixing of the matrix. Wet mixing was done till a mixture of uniform color, consistency were achieved which was then considered ready for casting. Compaction factor tests were done before casting for each batch.
Workability: Every batch of concrete, soon after mixing, was tested for consistency by any procedure explained in IS1199-1959, given that care was taken to assure that no water or any other material was lost. The concrete was remixed after compaction

test with the remaining batch prior to casting. The period of remixing was kept to a minimal to avoid drying yet enough to make a homogenous mass.

Compaction: The compaction was done by hand, with the help of standard tamping rod conforming to IS10086-1982 was used and the strokes of the bar were applied evenly all over the mould cross s/n for both the cubical and beam specimens, a total of 35 strokes per layer. The strokes were applied in a way such that they go deep into the bottom layer & the bottom layer was rodded completely at depth.

Curing of specimens: After casting, samples made are left undisturbed in the moulds for 24hrs at room temperature. The samples are then taken out from the mould and immediately moved into the curing pond having fresh and clean water.

Casting of Specimens: The cast iron moulds are made free from any mineral oil & dust particles is applied inside the mould before concrete is taken into it. The moulds are of size 150mm for cubes and 15x150x700mm for the beam specimens were used conforming to IS procedures. The moulds were kept on a level surface. Excess concrete left was removed using a trowel and the finished level was smoothed over using the same.

Compressive strength: It depends on various factors like quality control during production of concrete, cement strength, water-cement ratio, quality of concrete material etc and is taken as the primary and indicative property of concrete. Most quality control aspects of concrete are based upon its characteristic strength, which can be explained as strength of specimen, which was cured for 28 days.

Test for compressive strength can be done either on cylinder or cube. Various IS codes suggests concrete cube or concrete cylinder as the std specimen for the test.

For cube test 2 types of specimens either cubes of 15X15X15cm or else 10X10X10cm which counts on aggregate size are recommended as per IS456. For the purpose of this research cubical moulds of size 10m x 10cm x 10m were used. This concrete was poured into the mould, tampered in a manner so that no voids are present. After completing 24hrs these moulds were taken out & specimens were kept for curing. The top surface of these specimen was leveled with a trowel and made smooth and even. These specimens were tested by compression testing machine or Universal Testing Machine (UTM) after 7 & 28 days curing. Load was applied slowly by the machine at 140kg/cm2/min till the specimens. This load was taken as the failure load for the specimen at that age. An average of three readings was taken as the final reading for each variation.

Summary: All the aforementioned tests were conducted under laboratory conditions abiding by the regulations and limits set forth by the relevant codes of IS456 and IS516 after a mix was designed based on IS10262. An average of three readings for every test for every batch of concrete was taken to reduce chances of negligence and error. All calculations, readings and recordings were taken as per SI system, and relevant conversions were made wherever necessary. All the samples were hand mixed and tamped and therefore certain deviations in the characteristic strengths were observed and accounted for. The recordings and observations of the tests and are represented in their tabular and graphical forms in the subsequent chapter.

Acid Attack test: This test was done after the curing of specimens(cubes) for 28 days and the specimens were dried for 1 day then again were immersed in water with 5% dilution in Hydrochloric acid for 56 days and 90 days and there compressive tests and weight reduction tests were conducted.

Sulpahte Attack Test: This test was done after the curing of specimens(cubes) for 28 days & those were dried for 1 day then again were submerged in water with 5% dilution in Magnesium Sulphate for 56& 90 days and there compressive tests and weight reduction tests were conducted.

V. TESTS RESULTS AND DISCUSSION

Table 6 Compressive strength of concrete after 7 and 28 days curing in water

	7 Days	28 days
Cube 1	25.7	38.162
Cube 2	26.717	39.576
Cube 3	27.311	39.958
Average	26.576	39.232

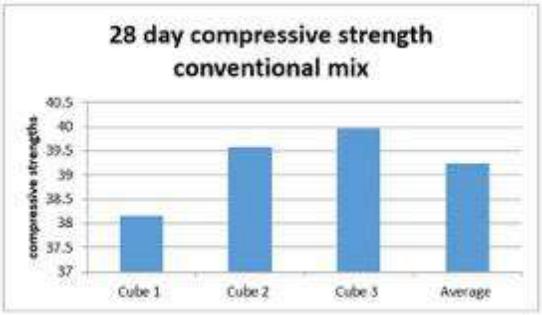

Graph 1 28 day compressive strength conventional mix

Table 7 Compressive strengths with SS and Robo Sand

S.No.	% of slag	7 Days (Mpa)	28 Days (MPa)
1	M30(KR)	26.576	39.23
2	0%(K1)	27.31	40.63
3	10%(K2)	28.35	42
4	20%(K3)	29.62	44.65
5	30%(K4)	31	46.32
6	40%(K5)	28.66	42.95

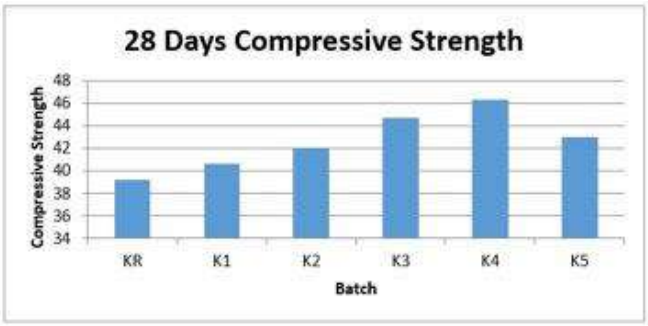

Graph 2 28 Days Compressive Strength

Table 8 Compressive strengths for 56 and 90 days after submerging in HCl

S.No	% of slag	56 Days	90 Days
1	M30 concrete	37.63	36.06
2	0%	39.26	37.64
3	10%	39.6	36.91
4	20%	41.36	36.51
5	30%	41.87	36.93
6	40%	37.69	31.83

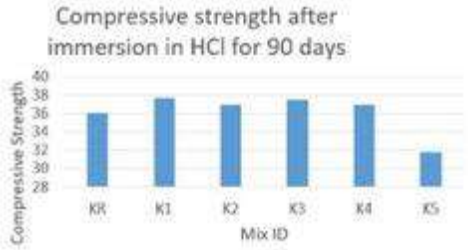

Graph 3 Compressive strengths for 90 days after submerging in HCl

Table 9 Compressive strengths for 56 and 90 days after submerging in MgSo4

S.No.	% of slag	56 Days (MPa)	90 Days (MPa)
1	M30	38.43	37.65
2	0%	39.85	38.77
3	10%	40.68	38.91
4	20%	42.06	41.09
5	30%	44.21	41.71
6	40%	40.75	38.08

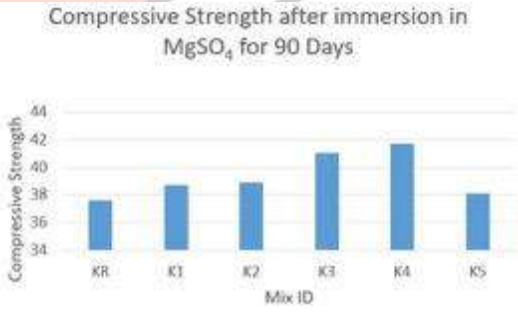

Graph 4 Compressive strengths for 90 days after submerging in MgSo4

Table 10 Weight loss in HCl

S.No.	ID	Wt.	Wt. after immersion in HCl			
			56 Days	% decrease	90 Days	% decrease
1	KR	2.48	2.44	1.61%	2.41	2.82%
2	K1	2.51	2.46	1.99%	2.43	3.19%
3	K2	2.54	2.45	3.54%	2.38	6.30%
4	K3	2.59	2.43	6.18%	2.34	9.65%
5	K4	2.63	2.43	7.6%	2.28	13.31%
6	K5	2.66	2.39	10.15%	2.09	21.43%

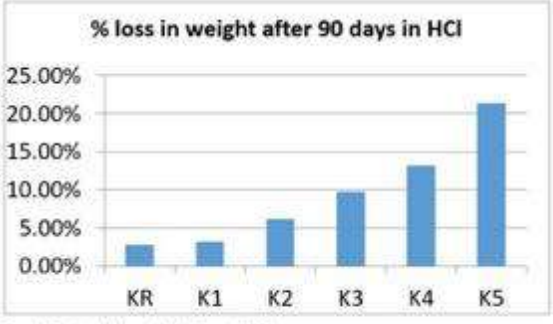

Graph 5 % weight loss after 90 days in HCl

The observations show that there is a drop in the weight with the rise in percentage of steel slag powder in cement after 56 & 90 days. These analysis represent that steel slag in cement is sensitive to the action of HCl as indicated by the increase in weight loss with rise in percentage of substitute of cement.

Table 11 Weight loss in MgSO4

S.No	ID	Wt.	Wt. after immersion in MgSo4			
			56 Days	% decrease	90 Days	% decrease
1	KR	2.48	2.45	1.21%	2.43	2.02%
2	K1	2.51	2.47	1.59%	2.45	2.39%
3	K2	2.54	2.48	2.36%	2.44	3.94%
4	K3	2.59	2.51	3.09%	2.4	6.18%
5	K4	2.63	2.53	3.80%	2.43	7.60%
6	K5	2.66	2.54	4.51%	2.41	9.40%

Graph 6 % weight loss after 90 days in MgSo4

Submerging in $MgSO_4$ for 56 & 90 days shows the weight decreases with time because of sulphate attack. Maximum loss of strength occurs at 40% replacement level as indicated by the graph.

Graph 7 Comparison for 90 Days weight loss

The comparison of the rates of weight losses for HCl and MgSO4 reveal that the loss rate is higher for HCl when contrast with MgSO4.The trend is observed for both 56 & 90 days. It is also seen that loss increases with rise in content of steel slag powder.

Table 12 Strength loss in HCl

S.No	Mix ID	% loss in strength for 56 days (HCl)	% loss in strength for 90 days (HCl)
1	KR	4.1	8.1
2	K1	4.5	8.9
3	K2	5.7	12.1
4	K3	7.4	18.2
5	K4	9.6	20.3
6	K5	12.2	25.9

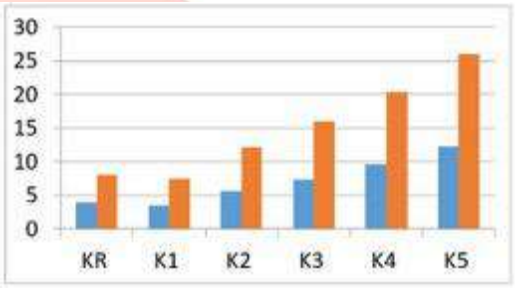

Graph 8 Strength loss in HCl

The strength loss pattern shows a similar trend to that of weight loss for both 56 and 90 days. The strength loss becomes significant after 20% of steel slag powder in cement by weight.

Table 13 Strength loss in MgSO4

S.No	Mix ID	% strength loss for 56 days (MgSO4)	% strength loss for 90 days (MgSO4)
1	KR	2.0	4.0
2	K1	1.9	4.6
3	K2	3.1	7.4
4	K3	4	8.0
5	K4	4.6	10.0
6	K5	5.1	11.3

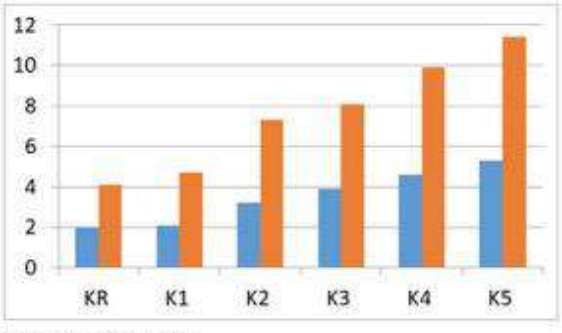

Graph 9 Strength loss in MgSO4

Strength loss for 56 & 90 days submerged in MgSO4 follow an increasing pattern with rise in Steel Slag powder. Here too the maximum loss in strength occurs at 40% replacement.

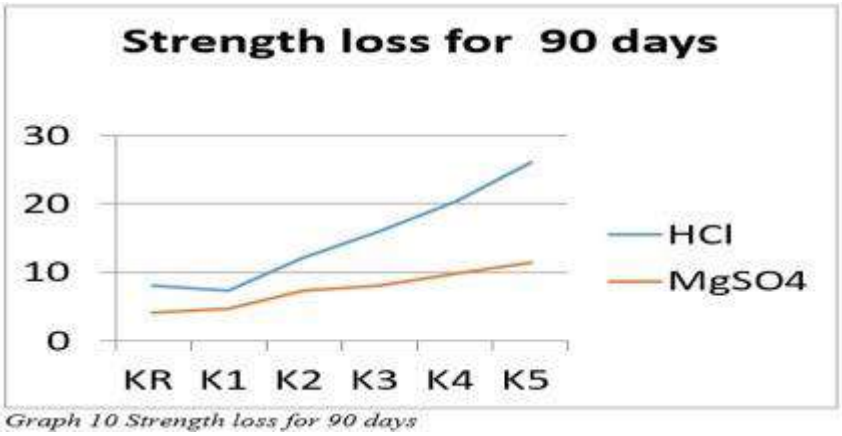

Graph 10 Strength loss for 90 days

The graphs represent that strength loss for HCl is greater than MgSO4.
The maximum loss in strength occurs for the combination K5, that is 40% cement altered with steel slag powder.
These graphs give a clear indication that the combination of these materials gives concrete that is vulnerable to HCl but offers a good cover against to sulphate attack.

VI. CONCLUSION

General conclusion

- The maximum increase in compressive strength was achieved at 30% STEEL SLAG POWDER as partial substitute of 24% in comparision to normal concrete.
- The optimal percentage of Steel Slag powder as alternative of cement is 30%.
- The concrete mix K_4 (30% STEEL SLAG POWDER) showed better resistance to sulphate attack than acid attack. The decrease in the compressive strength was marginal for all mixes at 56 & 90 days of submerging for sulphate solution. The compressive strength decreases by 5% for 56 days and 10% for 90 days
- The decrease in the compressive strength was considerable for all mixes at 56 & 90 days of submerging in HCl. The compressive strength decreases by 10% for 56 & decreases by 20% for 90 days.
- The concrete workability increases with rise of STEEL SLAG POWDER content as cement alternative.

Scope for further Investigation

- The above experimental program can be further extended can by conducting various other tests such as water absorption, carbonation etc.
- By conducting experiments on concrete using partial replacements of sand by artificially prepared sand.

REFERENCES

[1] Prof. Mrs. A. I. Tamboli –"Compressive strength of steel slag aggregate and artificial sand in concrete" in IJCIET (Feb 2015)
[2] Lohani T.K. , Padhi M., Dash K.P., Jena S.- "Optimum utilization of Quarry dust as partial replacement of sand in concrete"
[3] R. Ilangovana , N. Mahendrana and K. Nagamanib- "Strength and durability properties of concrete containing quarry rock dust as fine aggregate"
[4] Huang Yi , Guoping Xu, Huigao Cheng, JuSteel Slag powderhi Wang, Yinfeng Wan, Hui Chen, -"An overview of utilization of steel slag"
[5] "Utilization of steel slag as coarse and fine aggregate" by Gozde Inan Sezeretal.
[6] "Experimental Investigation of Coarse aggregate with Steel Slag In Concrete" by T.Subramani, G.Ravi
[7] www.wikipedia.com
[8] www.slagcement.org

Lateral Stability Analysis of High Rise Structure with variation of plan configuration with respect to height and the Effect of Outrigger and Belt Trusses Systems

[1]Syed Ammar Ahmed Maaz, [2]Mohd Mubasheer Shazeb
[1]Student, [2]Assistant Professor
Nawab Shah Alam Khan College Of Engineering And Technology

Abstract - **The outrigger and belt truss system is one of the most efficient systems used to effectively control the excessive drift due to lateral load, so that, during small or medium lateral load due to either wind or earthquake load, the risk of structural and non-structural damage can be minimized. For high-rise buildings, particularly in seismic active zone or wind load dominant, this system can be chosen as an appropriate structure. This paper studies the efficient use of outrigger and belt truss system for high-rise concrete building subjected to wind or earthquake load. Seven 44-storey models of outrigger and belt truss system are subjected to wind and earthquake load, analyzed and compared to find the lateral displacement reduction related to the types of outrigger and belt system. The analysis has been carried out to study the effect and performance of outrigger system in 40-storey building. The outrigger system is provided at different levels along the height of the building. The depth of the Outrigger and belt trusses is equal to the height of the typical story and maintained same in all the models. The key parameters discussed in this paper include lateral deflection, storey drifts, base shear and fundamental time periods. Loads are considered as per Indian Standards IS: 875(Part1)-1987, IS: 875(Part2)-1987, IS: 875(Part3)-1987 and IS: 1893(Part-1) - 2002. The modeling and analysis were performed using finite element software ETABS 16.**

keywords - **Outrigger and belt truss system, lateral load, lateral displacement, storey drifts, base shear and fundamental time periods**

I. INTRODUCTION

Improvement of the large structures has been rapidly increasing the general knowledge of new challenges that need to be met through building judgement. In present high constructions, wind or earthquake often induce lateral loads by arranging paired shear walls. However, when structure increases in height, the stiffness of the structure turns out to be increasingly important to provide the structure with sufficient lateral stiffness. The lateral load resisting system effectively controls over the top drift because of lateral load, so that, amid little or medium lateral load because of wind or earthquake load, the danger of auxiliary and non-basic harm can be limited. For tall structures, especially either in wind load or seismic zone overwhelming, these frameworks are chosen as a suitable structure. Outrigger and belt truss system have recently been widely used to minimize lateral drift. In order to attain the necessary rigidity of the large structure bracing sizes, extra lateral load resistant system such as outriggers and belt truss was needed. Outriggers and belt truss was required. The location of the outrigger truss increases the structure's efficient depth and improves the lateral stiffness owing to horizontal load effectively. Conventionally high buildings are built for the goal of office buildings, commercial, shopping malls and hotels, suburban. Improvement of tall buildings includes Different composite elements for instance economic matters, necessities, construction regularities, technology and so on. The challenges increments for the designer with the unpredictability of the height of the building and building plan. Without considering the detailed forbearance of denoting factors that affect the selection of tall buildings for the structural system, economic and adequate tall buildings cannot be intended. Building self-weight, live load, and seismic loads and along with wind forces will play valuable role as significant variables of the design. Adequate increases in the building's deflection, stress, strain, lateral displacement and deformation will result in elevated construction costs owing to the size and composition of the building components.

II. OUTRIGGER AND BELT TRUSS STRUCTURAL SYSTEM

Outriggers are rigid horizontal structure i.e. beam or truss which connects to the core wall and outer column of building for improving building strength and overturning stiffness. Outriggers are being utilized in tall structures from nearly half century, but innovative design framework has improved its proficiency. Outrigger system is the sort of structural system that is created from a horizontal cantilever part linking to the internal and outer columns of the structure. The moment arm of the core rises with the connection leading to greater lateral rigidity of the system. The central core of a structure acts as a cantilever; the outriggers are positioned to decrease the moment of overturning in the heart and transfer moment from core to exterior column by linking the core and column. Wall frame outrigger trusses are the found they connected to the foundation through outer columns is Wall frame outrigger trusses .The wall and outrigger trusses will rotate, causing downwind column compression and upwind side column tension, these axial forces will withstand the wall rotation when the structure is performed with horizontal forces.

Outriggers and columns withstand core rotation and thus considerably decrease the base moment and lateral deflection that would have occurred in a free core when the structure is subjected to lateral forces. A belt truss can be used at the outrigger concentrations to mobilize the extra axial stiffness of various columns and ensure torsional stiffness. As building height rises, column decrease is the critical issue in building methods, belt truss plays much effective in the control of settlement of columns. Belt trusses helps in limiting differential elongation and shortening of columns. Outrigger behavior with belt truss shown to be more effective when compare to the outrigger without belt truss. The outer columns and belt truss system resist rotation of central shear core and reduce the lateral deformation including bending moment at base of the structure.

III. OBTECTIVES

- To study the effect of introduction of Outriggers in high-rise building subjected to dynamic wind loading.
- To study the impact of X braced outriggers with core wall and braced core wall.
- To examine the parameters with various types of Plan Configurations with Outriggers, i.e. X Bracings and belt truss systems.
- To study the impact of steel outrigger in comparison with concrete outrigger.

IV. SCOPE OF PRESENT STUDY

The research aims to understand the seismic qualities and steadiness of the structure of the frame. The Outrigger and Belt Truss System can be used to increase this. Steel outriggers are used to counter seismic forces in steel framed structures. Steel options to use Steel Outriggers for RC frame buildings. This technique seeks to study and compare storey displacement, storey drift and base shear with distinct kinds of Outrigger Plan Configurations, i.e. X Bracings systems and belt trusses. The present research is useful for multiple academics involved in thin designing the tall structures by using outrigger and belt truss system.

V. PARAMETERS OF STUDY

- Effect of Outriggers with RC frame building when applied with Earthquake and dynamic wind loading for various Plan Configurations with Outriggers, i.e. X Bracings and belt truss systems for zone V.
- Lateral Displacement: The study emphases on the improvement of the RC frame building in terms of lateral displacement with most proficiently use of Outriggers and belt truss systems.
- Story Drifts: This parameter is considered in this research for the Optimum utilization of the Outriggers.
- The Base shear and Fundamental periods are considered as the parameters in this study.

VI. MODEL DESCRIPTION

The structures are modelled as a sequence of components that resist load. The lateral loads applied to the construction are based on the codal norms of India. The research is conducted according to IS 1893 (Part1): 2002 for seismic areas V. The adopted construction comprises of components of reinforced concrete and brick masonry. It is presumed that the structures are strongly fixed at the bottom floor and the interaction of the soil structure is overlooked. The building's complete height was set at 123.2 m (i.e. 40 stories) while the size of the members was distinct. Initially, the frame parts were intended to meet the requirements for stress analysis.

Table 1 : Y Shape Model geometry

Plan Configuration	Plan /Shape Area (sq.m)	No of Storey
Y Shape	1659.46	GF to 10
Y Shape	1315.66	10-20
Y Shape	1129.37	20-30
Y Shape	914.79	30-40

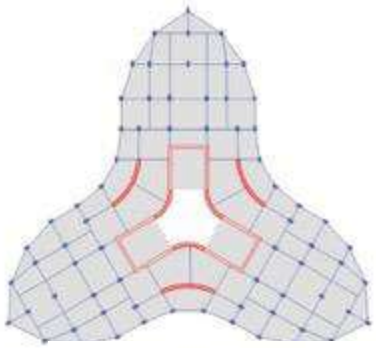

Fig 1 : Y Shape layout Plan

Table 2 : Circular Shape Model geometry

Plan Configuration	Plan /Shape Area (sq.m)	No of Storey
Circular Shape	1659.01	GF to 10
Circular Shape	1315.11	10-20
Circular Shape	1129.34	20-30
Circular Shape	914.34	30-40

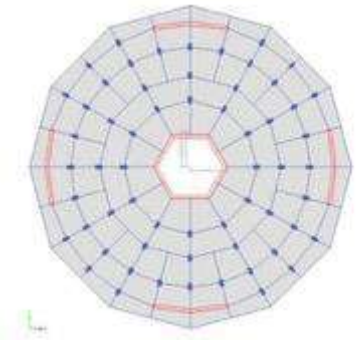

Fig 2 : Circular Shape layout Plan

Table 3 : Fillet Shape Model geometry

Plan Configuration	Plan /Shape Area (sq.m)	No of Storey
Fillet Shape	1659.46	GF to 10
Fillet Shape	1315.66	10-20
Fillet Shape	1129.37	20-30
Fillet Shape	914.79	30-40

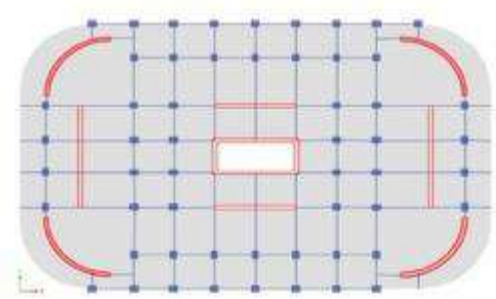

Fig 3 : Fillet Shape layout Plan

Models

The models that were chosen for the study are listed as follows,

Model 1 – Y Shape Bare frame model without Outrigger.
Model 2 – Y Shape Model with Concrete Core wall and braced Outriggers (Concrete X Bracings).
Model 3 – Y Shape Model with Concrete core wall and braced Outriggers (Steel X Bracings).
Model 4 – Circular Shape Bare frame model without Outrigger.
Model 5– Circular Shape Model with Concrete Core wall and braced Outriggers (Concrete X Bracings).
Model 6 – Circular Shape Model with Concrete core wall and braced Outriggers (Steel X Bracings).
Model 7 – Fillet Shape Bare frame model without Outrigger.
Model 8 – Fillet Shape Model with Concrete Core wall and braced Outriggers (Concrete X Bracings).
Model 9– Fillet Shape Model with Concrete core wall and braced Outriggers (Steel X Bracings).

VII. ABOUT THE ANALYSIS

The building analysis is done using widely used design software ETABS.

The design data used in the analysis are the following:

Design Data

Material Properties:

Grade of Concrete = M25 for all members
= M25 for columns
Grade of Rebar = Fe 415 Grade
Grade of Steel = Fe 345 Grade
Young's modulus of concrete (M45) = 33.541×10^6 KN/m2
Young's modulus of concrete (M60) = 38.729×10^6 KN/m2
Density of Reinforced Concrete = 25 KN/m3
Poisons' ratio of concrete = 0.2
Modulus of elasticity of brick masonry = 3500x103 KN/m2
Density of brick masonry = 8 KN/m3
Poisons' ratio of masonry = 0.15

Member Properties:

Slab = 150mm thick
Column = 500mmX1000mm
Beam = 300mmX600mm
Masonry wall (Brick) = 230mm thick
Reinforced Concrete Shear/Core wall = 400mm thick
Concrete Outriggers = 300mmX1000mm
Steel Outriggers = ISA 130X130X12mm

Load Calculations:

Assumed dead load intensities
Floor finishes = 1.5 KN/m2
Live load on floor = 3 KN/m2
Live load on roof = 1.5 KN/m2
Wall load on roof = 1x0.15x8 = 12 KN/m
Wall load on other levels = (3.2-0.6) x0.23x8 = 5 KN/m
Earthquake Live Load on slabs as per clause 7.3.1 and 7.3.2 of IS 1893 (Part-1)-2002
Roof = 0.5KN/m2
Floor = 0.5x3 =1.5 KN/m2

Seismic Data:

Structure = SMRF
Seismic Zone = V
Zone factor = 0.36
Importance factor = 1.5
Response reduction factor =5

Soil type	= Medium
Basic Wind Speed	= 44 m/s
Terrain Category	= 3
Terrain Class	=C

VIII. ANALYSIS RESULTS AND DISCUSSIONS

In this section, the results of the selected buildings are presented and discussed in detail. The consequences of base shear, lateral displacement, story shear, and vibration and in general execution for the distinctive structure models are displayed and thought about.

In this examination, an endeavor has been made for assessing the seismic exhibition of RC structures with focal center divider with outrigger and without outrigger. The outriggers of shape like 'X', of concrete and steel materials are contrasted in this examination with assess their adequacy in lessening horizontal removals and different parameters. Likewise Braced center divider is supplanted with strong center divider in the examination, and the effectiveness is watched. The idea of virtual outrigger or belt support truss was additionally contrasted and the customary outrigger for their general execution. From this examination we will likewise come to know the effectiveness of steel outriggers when contrasted with solid outriggers.

In the accompanying part, the outcomes are processed with proportional static technique for examination, reaction range investigation and static investigation. The modeling and analysis of various building models are carried by the use of ETABS software package. After the analysis, the results of base shear, lateral displacement for different models of the building are accumulated and analyzed.

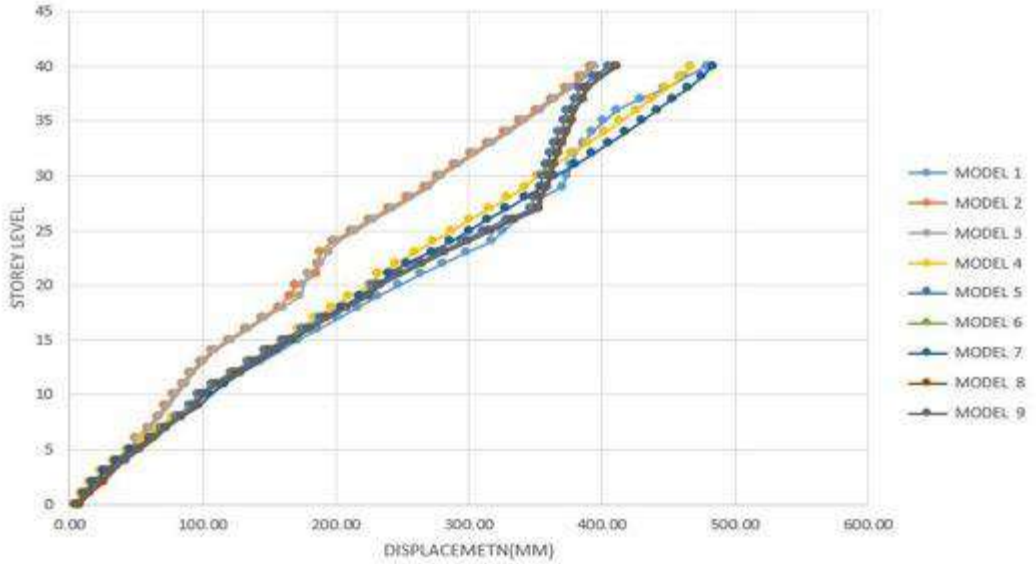

Fig 4 : Lateral Displacement for Response spectrum method along longitudinal direction for Zone V

Lateral Displacement for Response spectrum method along longitudinal direction for Zone V

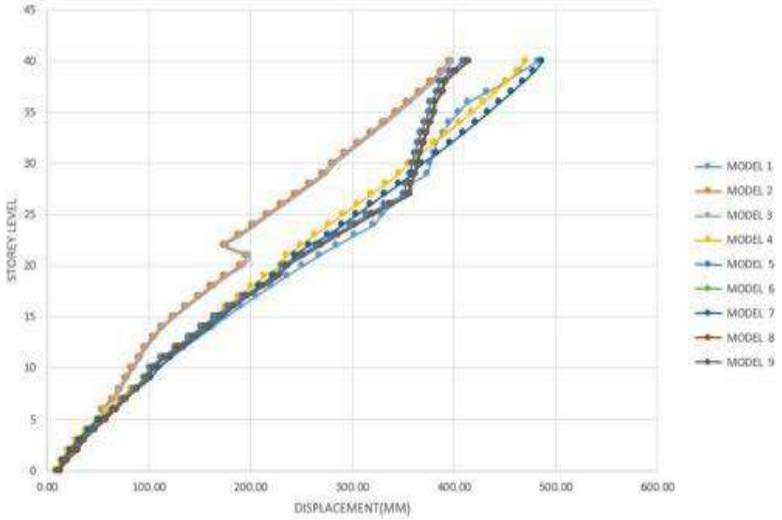

Fig 5 : Lateral Displacement for Response spectrum method along transverse direction for Zone V

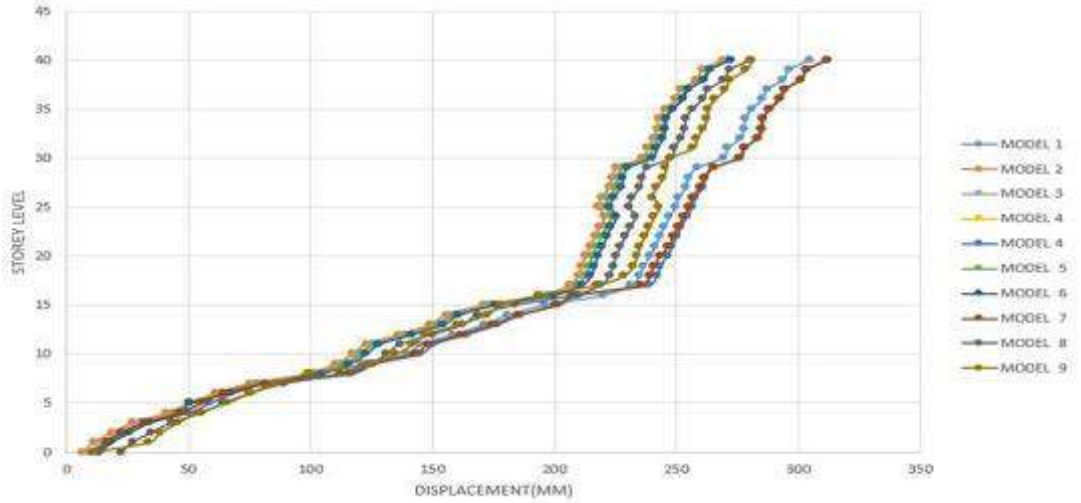

Fig 6 : Lateral Displacement for Static Wind Analysis along Longitudinal direction for Zone V

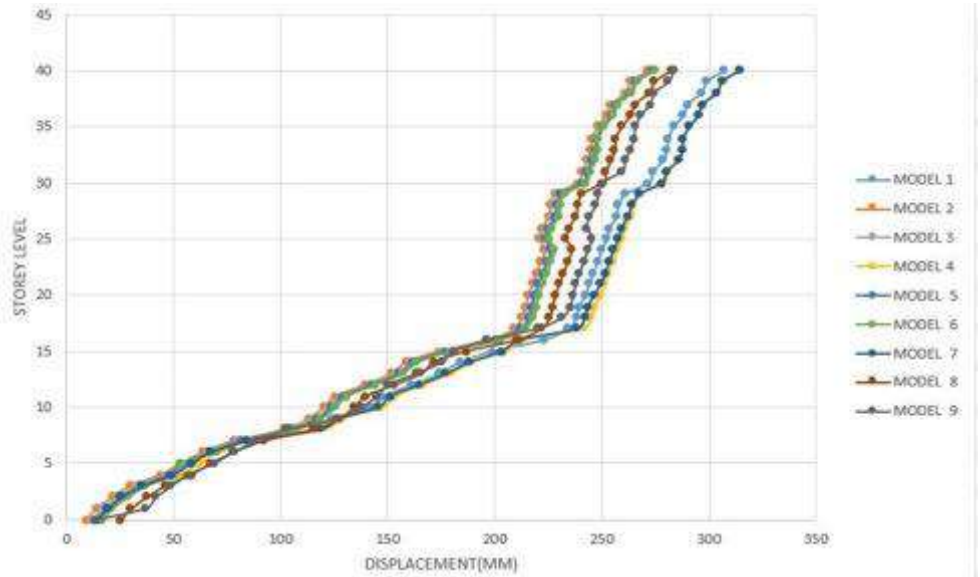

Fig 7 : Lateral Displacement for Static Wind Analysis along Transverse direction for Zone V

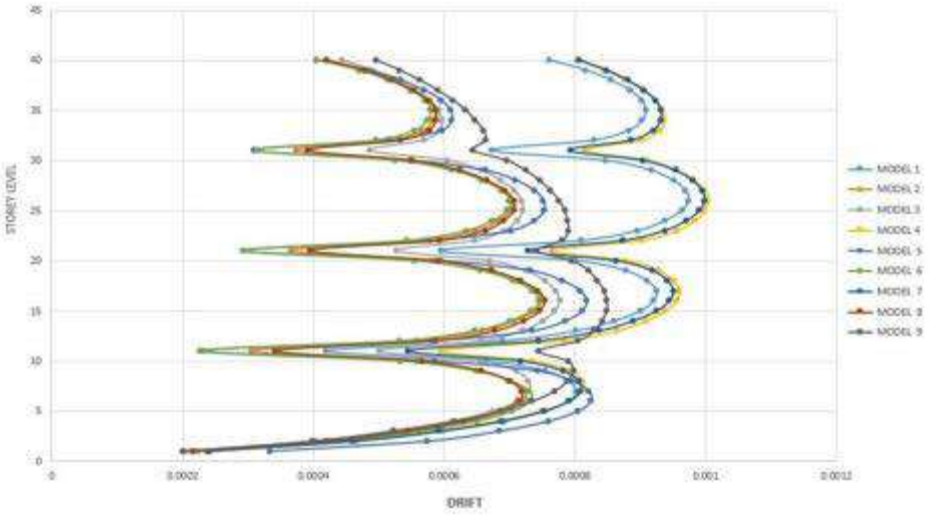

Fig 8 : Storey Drift for Response spectrum analysis along longitudinal direction for zone V

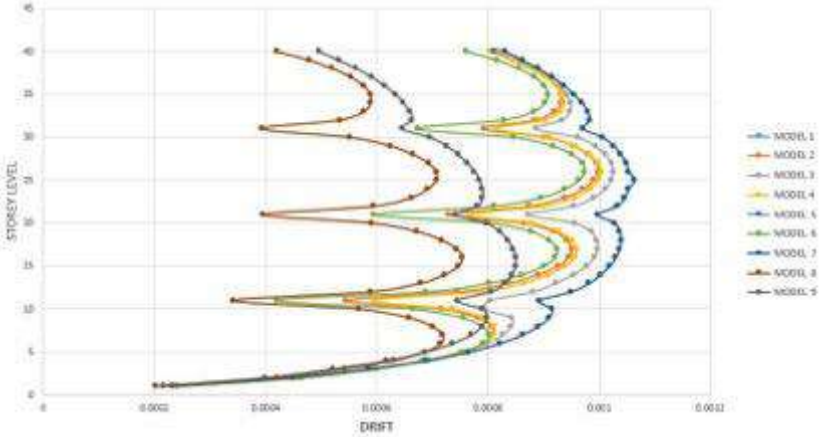

Fig 9 : Storey Drift for Response spectrum analysis along transverse direction for zone V

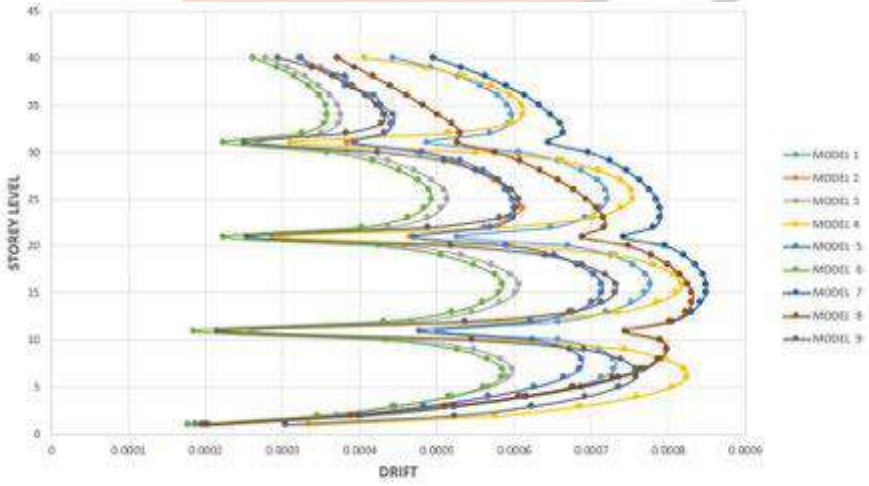

Fig 10 : Storey Drift for Static wind analysis along longitudinal direction for zone V

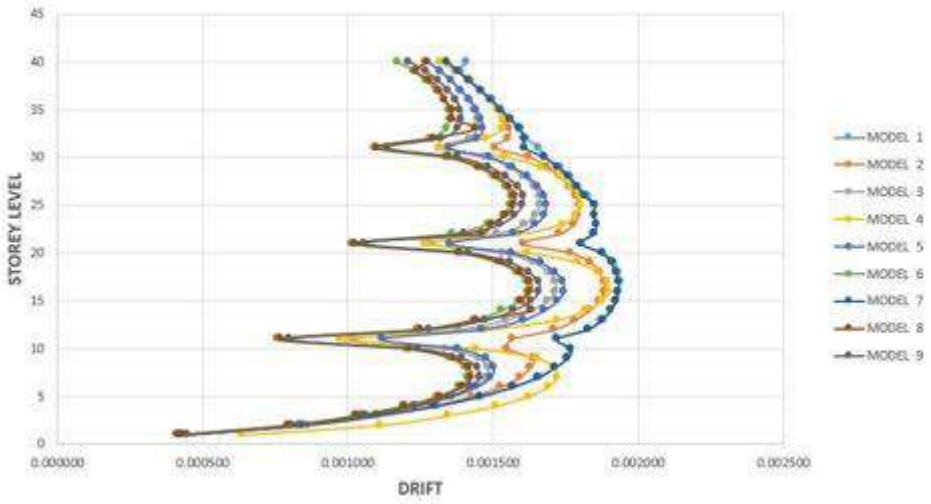

Fig 11 : Storey Drift for Static wind analysis along transverse direction for zone V

Table 4 : Base Shear by Response Spectrum Analysis and Wind Analysis along Longitudinal and Transverse direction

BASE SHEAR (KN)					
Model No.	**Type of Models**	Response Spectrum Analysis		Static Wind Analysis	
		RSA-X	RSA-Y	WIND-X	WIND-Y
1	Y Shape Bare frame model without Outrigger	16428.91	16467.95	12221.26	13541.28
2	Y Shape Model with Concrete Core wall and braced Outriggers (Concrete X Bracings)	17307.96	17937.91	11197.62	11315.69
3	Y Shape Model with Concrete core wall and braced Outriggers (Steel X Bracings)	17907.76	18312.724	11758.44	11812.36
4	Circular Shape Bare frame model without Outrigger	14610.79	14210.21	12267.97	12156.23
5	Circular Shape Model with Concrete Core wall and braced Outriggers (Concrete X Bracings)	15824.02	15924.21	12065.75	12099.73
6	Circular Shape Model with Concrete core wall and braced Outriggers (Steel X Bracings)	15470.13	15670.75	12024.84	12121.94
7	Fillet Shape Bare frame model without Outrigger	15324.22	15413.36	13351.69	13451.21
8	Fillet Shape Model with Concrete Core wall and braced Outriggers (Concrete X Bracings)	16228.86	16031.39	12562.33	12762.31
9	Fillet Shape Model with Concrete core wall and braced Outriggers (Steel X Bracings)	16404.48	16435.67	12758.44	12957.22

IX. OBSERVATIONS

- It is seen that 29.21% of top storey displacement and 26.64% of maximum story drift is constrained by providing Y Shape Plan Configurations, 28.1% of top storey displacement and 25.44% of maximum story drift by Circular Shape Plan Configurations and 22.32%of top storey displacement and 19.50% of maximum story drift is controlled with Fillet Shape Plan Configurations.
- Also 8.22% of displacement and 9.64% of storey drift is controlled if braced core wall is employed with X-braced outriggers (Model 2,3,5,6,8,9) and is compared with X-braced outriggers (Model 1, 4, 7).
- The model with Steel Outriggers demonstrates to be less productive in controlling displacement by 19.49% and of storey drift by 17.27%.This perception validates the literature [10].
- The Outriggers with Belt truss (Model 3) experienced less displacement and controlled lateral displacement by about 34.57% and about 30.75% inter storey drift is controlled.
- The natural period decreases as the stiffness of the building increases and thus leading in increment of frequency.

- The Y Shape building frame with X-braced Outriggers will have least possible lateral displacements in contrast to other building shapes of Outriggers.

X. CONCLUSIONS

The accompanying Conclusions were drawn dependent on the Observations made

- The Y plan Configuration with X-supported Outriggers is particularly powerful; as it indicates least minimum lateral displacement pursued by Circular Plan Configuration Outriggers and Fillet Plan Configuration Outriggers.
- The Outriggers provided with Braced core wall were less viable in reducing lateral displacement compared with Solid Core wall by a small margin, hence it can be employed as the cost effective construction.
- The Outriggers gave in the inside casings of a structure examined are observed to be viable when contrasted with Outriggers gave in the outside edges for example.
- The steel outriggers are discovered least compared to Concrete one. Despite the fact that Steel outriggers can be utilized as the light weight substitute for concrete.
- From the examination it tends to be reasoned that that wind is a dominating factor and outriggers are successful in lessening wind impact as looked at tremor powers.
- Steel Outriggers can be utilized as an option in contrast to the next to the other strengthening techniques available as the total weight of the current structure will remain practically same

XI. REFERENCES

[1] Krunal Z. Mistry, Prof. Dhruti J. Dhyani,"Optimum outrigger location in outrigger structural system for high rise building" International Journal of Advance Engineering and Research Development Volume 2, Issue 5, May -2015.

[2] Akshay Khanorkar, Shruti Sukhdeve, S. V. Denge & S. P. Raut, "Outrigger and Belt Truss System for Tall Building to Control Deflection: A Review" GRD Journals- Global Research and Development Journal for Engineering | Volume 1 | Issue 6 | May 2016.

[3] B.S.Taranath, "Structural Analysis & Design of Tall Buildings", New York, McGraw Hill, 1998.

[4] M. H. Gunel, and H.E. Ilgin, A proposal for the classification of structural systems of tall buildings, Faculty of Architecture, Middle EastTechnical University, Ankara 06531, Turkey, 4 July 2006.

[5] Iyengar Hal, Composite and Steel High Rise Systems, Habitat and The High- Rise, Tradition & Innovation. In Proceedings of the Fifth World Congress. 14-19 May 1995.Amsterdam, The Netherlands, Bethlehem, Council on Tall Building and Urban Habitat, Lehigh University.

[6] P.S. Kian and F.T.Siahaan, "The use of outrigger and belt truss system for high-rise concrete buildings". Dimensi Teknit Sipil, Volume 3, No1,Maret 2001, Page 36-41,ISSN1410-9530.

[7] R. S. Nair, "Belt Trusses and Basements as „Virtual" Outriggers for Tall Buildings". Engineering Journal / Fourth Quarter/ 1998.

[8] Shivacharan K, Chandrakala S, Narayana G, Karthik N.M., "Analysis of Outrigger System for Tall Vertical Irregularites Structures Subjected to Lateral Loads"IJRET: International Journal of Research in Engineering and Technology, Volume: 04 Issue: 05 | May-2015.

[9] M.R Suresh, Pradeep K.M, "Influence of Outrigger System in RC Structures for Different Seismic Zones" IJSRD - International Journal for Scientific Research & Development| Vol. 3, Issue 05, 2015 | ISSN (online): 2321-0613.

[10] Abdul Karim Mullah, Srinivas B. N, "A Study on Outrigger System in a Tall R.C Structure with Steel Bracing" International Journal of Engineering Research & Technology (IJERT), Vol. 4 Issue 07, July-2015.

[11] S. Fawzia and T. Fatima, "Deflection Control in Composite Building by Using Belt Truss and Outriggers Systems" World Academy of Science, Engineering and Technology 48 2010.

[12] Prateek N. Biradar & Mallikarjun S. Bhandiwad. "A Performance Based Study on Static and Dynamic Behavior of Outrigger Structural System for Tall Buildings" International Research Journal of Engineering and Technology (IRJET), Volume: 02 Issue: 05 | Aug-2015.

[13] Bryan Stafford Smith and Alex Coull, "Tall Building Structures: Analysis and Design", New York, John Willey & Sons, 1991.

[14] Indian Standard Code of Practice for Design Loads (other than earthquake) For Buildings and Structures, Part – 2 Live Loads, IS: 875 (Part 2) – 1987 (Second Revision), Bureau of Indian Standards, New Delhi, India.

[15] Indian Standard Code of Practice for Design Loads (other than earthquake) For Buildings and Structures, Part – 3 Wind Loads, IS: 875 (Part 3) – 1987 (Second Revision), Bureau of Indian Standards, New Delhi, India.

[16] Indian Standard Criteria for Earthquake Resistant Design of Structures, IS: 1893 (Part 1) 2002, Part 1 General Provision and Buildings (Fifth Revision), Bureau of Indian Standards, New Delhi, India.

Energy Based Pushover Analysis Of Higher Mode Dominant Structure

[1]Mohammed GousePasha, [2]Mohammed Imtiyaz
[1]Student, [2]Assistant Professor
Nawab Shah Alam Khan College of Engineering and Technology

Abstract - **The storey inertial forces and accelerations at all storeys and shear forces at higher storeys are significantly underestimated by methods which neglect or do not take into account the higher modes even for first mode dominated structures. Tall buildings are more susceptible to be influenced by the effects of higher modes on their response. Several studies suggest that numerous failures or even collapse of buildings were induced by large floor accelerations in which the higher modes were not taken into account. In this study conventional Pushover Analysis (POA) is carried out and since we know that it gives accurate results for structures whose response is controlled by the fundamental mode then there are bound to be anomalies in the higher mode pushover curves in the form of mode reversal. These can be corrected by performing Energy Based Pushover Analysis (EBPOA) as it takes into account the higher modes and then the performance level of the building for that mode in which the reversal took place is also determined**

keywords - **Energy based pushover analysis, Higher mode dominant structures, Mode reversal.**

1. INTRODUCTION

The seismic assessment and design of structures is required because of the occurrence of earthquakes. Earthquakes are caused by differential movements of the earth's crust. The result of these movements is the well known 'ground shaking' that can lead to significant damage and/or collapse of buildings, infrastructure systems (e.g. dams, roads, bridges, viaducts etc), landslides, when soil slopes loose their cohesion, liquefaction in sand and destructive waves or 'tsunamis' in the maritime environments.

Buildings should be designed like the ductile chain. For example, consider the common urban residential apartment construction - the multi-storey building made ofreinforced concrete. It consists of horizontal and vertical members, namely beams and columns. The seismic inertia forces generated at its floor levels are transferred through the various beams and columns to the ground.

As per IS: 1893-2002 (Part 1), Clause 6.1.3, "Actual forces that appear on structures during earthquakes are much higher than the design forces specified in the code". It is recognized that neither complete protection against earthquakes of all sizes is economically feasible nor design alone based on strength criterion is justified.

Modes are the inherent properties of a structure, and are determined by material properties (mass, damping and stiffness), and boundary conditions of the structure. Each mode is defined by a natural frequency, modal damping and a mode shape. If at all the material properties or the boundary conditions of a structure change, its modes will change. For instance, if a mass is added to a structure then it will vibrate differently

Every structure has a tendency to vibrate at a certain frequency known as the natural frequency. Each natural frequency is associated with a particular deflection pattern of the structure and this pattern is known as mode shape. When structure is properly excited by dynamic loads with frequency that coincides with natural frequency of the structure, it undergoes large displacements and stresses. In such cases the static analysis cannot be used

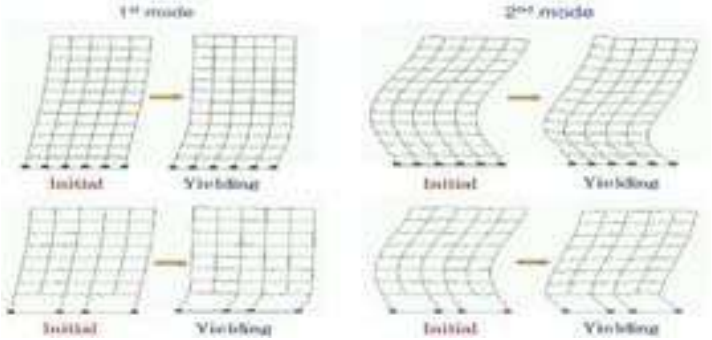

Fig.1 Variation of Modes due to Change in Stiffness.

In vapour compression cycle having compressor. It delivers the vapour refrigerant at high temperature to condenser. The Compressor uses power from engine itself. Cooling effect is produsedby cooling of refrigerant in the condenser. The vapour compression air conditioning system has some drawbacks, that's why another better alternative is needed. That is adsorption air conditioning system. it is used in this project.

Adsorption is the processes in which liquid molecules fixed on the solid surface. If molecules is fix then they looses the some form of energy. So that's why adsorption is exothermic reaction. Example silica gel is used in many process this will act like an

adsorbent. Silica gel adsorbs the water molecules. So it will forms the pair with water. In this project adsorption-desorption processes and some thermodynamic process takes place.

1.1 Literature review:

Newer analysis methodologies are being proposed with focus on a realistic characterization of seismic structural damage and its direct incorporation in the design methodology. In addition, a major emphasis is given to the characterization of all the uncertainties in the process of design In general, these approaches are categorized under performance-based seismic design (PBSD). The various ways of modeling structural damage for PBSD lead to various design approaches.

Yi Jiang and Yang (2010) developed an energy balance concept based Multimode Pushover Analysis to estimate the seismic demand of new and retrofitted buildings, which incorporates the concept of modal energy demand and capacity. The buildings were assumed to be linearly elastic. The dynamic target displacement was determined based on the interaction of the two diagrams. The proposed procedures accuracy is evaluated for buildings subjected to a variety of ground motions, including near-fault ground motions with fling-step. The statistical predictions of seismic demands of building under selected ground motions compared with the estimates of NL-THA and MMPA demonstrate that the proposed procedure is an attractive alternative for practical application.

Grigorious Manoukas et al., (2011) in their paper "Static Pushover Analysis based on an Energy-Equivalent SDOF system: Application to Spatial Systems", have proposed an efficient NSP based on energy equivalence. The energy equivalence of the structure is used as a margin to estimate the rood displacement under the monotonically increasing loads those are characterized by the modal shape of the structure (the fundamental mode shape). The work done in displacing the structure is a better index to estimate the performance of the structure and to determine the characteristics of the same. The proposed methodology was demonstrated using a framed structure and the results were compared with that of CSM. Good results for 2D and 3D framed buildings can be obtained using the procedure and is applicable for structures with regular or irregular multi-story planar frames. It is clear that the method's good approximation of the roof displacements shown in this paper does not ensure analogous accuracy for other quantities of interest, e.g. plastic rotations.

Angelo and Marco (2014) has proposed an energy-based method for Non-linear static analysis in which both the capacity curve and the demand curve are in terms of energy. The capacity curve was referred to as virtual displacement defined such that at each load step the equivalent SDOF system has the same deformation energy of the MDOF system. Integrating the capacity curve with respect to the virtual displacement, deformation energy is obtained. The demand is expressed as an energy quantity called as pseudo-energy. The definition of the performance point does not require iterative procedures. The results were compared with NL-THA and EC8 NSA procedure and were considered to be fairly accurate

1.2 Non-Linear Static Pushover Analysis:

The ATC-40 (1996) document has been a source of great knowledge for researchers working on the NSPs (Capacity Spectrum Method, Coefficient Method etc.). Excerpts from the documents that would give a better picture of the pushover analysis have been presented in the following paragraphs discussing the background and the development of the performance based analysis. The NSP may be used for any structure and any Rehabilitation Objective, with the following exceptions and limitations.

The NSP should not be used for structures in which higher mode effects are significant, unless an LDP evaluation is also performed.

To determine the response, if higher modes are significant, a modal response spectrum analysis should be performed for the structure using sufficient modes to capture 90% mass participation and a second response spectrum analysis should be performed considering only the first mode participation. Higher mode effects should be considered significant if the shear in any story calculated from the modal analysis considering all modes required to obtain 90% mass participation exceeds 130% of the corresponding story shear resulting from the analysis considering only the first mode response.

The NSP should not be used unless comprehensive knowledge of the structure has been obtained.

2 OBJECTIVE OF THE STUDY:

To identify the buildings in which higher modes are predominant to illustrate the inefficiency of Conventional Pushover Analysis (POA) on higher mode dominant structures. To perform Energy Based Pushover Analysis (EBPOA) for higher mode dominant structures. To obtain the performance level of higher mode dominant structures using EBPOA.

METHODOLOGY:

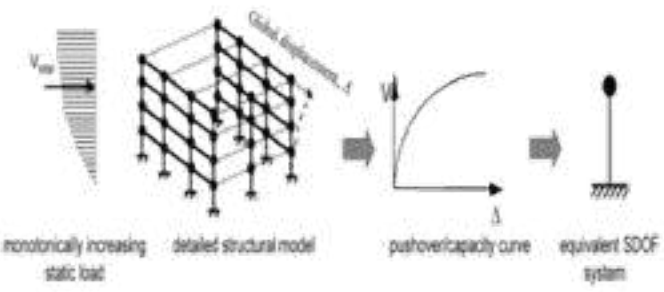

Fig. 2 Schematics Depicting the Development of an Equivalent SDOF System from a Pushover/Capacity Curve

The realistic force demands on potentially brittle elements, such as axial force demands on columns, force demands on brace connections, moment demands on beam-to-column connections, shear force demands in deep reinforced concrete spandrel beams, shear force demands in unreinforced masonry wall piers, etc.

Estimates of the deformation demands for elements that have to deform in- elastically in order to dissipate the energy imparted to the structure by ground motions.
Consequences of the strength deterioration of individual elements on the behaviour of the structural system.
Identification of the critical regions in which the deformation demands are expected to be high and that have to become the focus of thorough detailing.
Identification of the strength discontinuities in plan or elevation that will lead to changes in the dynamic characteristics in the inelastic range. Estimates of the inter-story drifts that account for strength or stiffness discontinuities and that may be used to control damage and to evaluate P-delta effects.
Verification of the completeness and adequacy of load path, considering all the elements of the structural system, all the connections, the stiff non-structural elements of significant strength, and the foundation system.
Where yielding is more gradual, disproportionate increases in the roof displacement may, in addition, affect the effective yield strength that is determined for the structure: when methods such as those described in ATC-40 are used

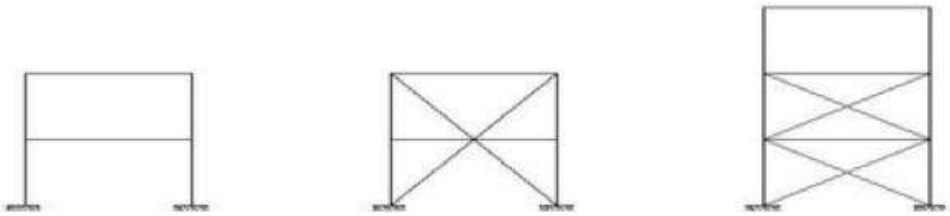

Fig. 3 Different Types of Frames

2.1 MODAL ANALYSIS PROCEDURE:

The nonlinear response of a MDOF system with N degrees of freedom subjected to an horizontal earthquake ground motion $\ddot{u}g$ can be expressed as the sum of the responses of N SDOF systems, each one corresponding to a vibration "mode" $\dot{t}$, having mass equal to the effective "modal" mass M^* and displacement equal to $Di = uNi/ vi\ \varphi Ni$ where uNi, vi and φNi are the roof displacement parallel to the excitation direction, the "modal" participation factor and the component of the vector $\boldsymbol{\varphi i}$ corresponding to uNi respectively. the inelastic resisting force of each SDOF system is equal to the "modal" base shear Vi parallel to the direction of excitation the external work of "modal" forces F_{Si} on the displacements $du_i = v_i\ \boldsymbol{\varphi}_i\ dD_i$ in a differential time interval dt its equal to the work of the resisting force (or the strain energy) of the corresponding SDOF system on the displacement dD_i. It is worthnoticing that Mi^*, Vi, $\boldsymbol{Fsi}$, Di, uNi, vi, $\boldsymbol{\varphi i}$ and φNi refer to the elastic vibration mode i. However, those conclusions are derived on the basis of the aforementioned assumptions and cannot be true all together when a pushover analysis is conducted. Thus, the EBMPA keeps conclusions 1) and 3) and uses the energy to determine modified resisting forces the system.

3. CASE STUDY DESCRIPTION

Table .1 Assumed Preliminary Data Required for the Analysis of Structural Model

Sl.no	Variable	Data
1	Type of structure	RC special moment resisting frame
2	Number of stories	20
3	Floor height	3.2m
4	Bottom story height	4m
5	Imposed load	$3kN/m^2$
6	Floor finish	$1kN/m^2$
9	Size of beams	300 x 450mm
8	Size of columns	C1 - 450 x 450mm ; C2 - 500 x 500mm
7	Materials	Concrete (M25) and Reinforced with HYSD bars (Fe415)
8	Depth of slab	125mm
10	Specific weight of RCC	$25kN/m^3$
11	Zone	III
12	Importance factor	1
13	Response reduction factor	5
14	Type of Soil	Medium

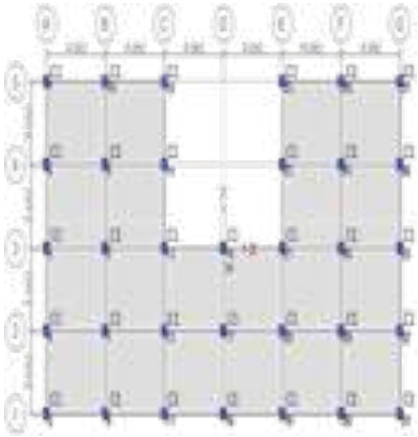

Fig. 4 Plan View of Model-1

Fig. 5 Isometric View of Model-1

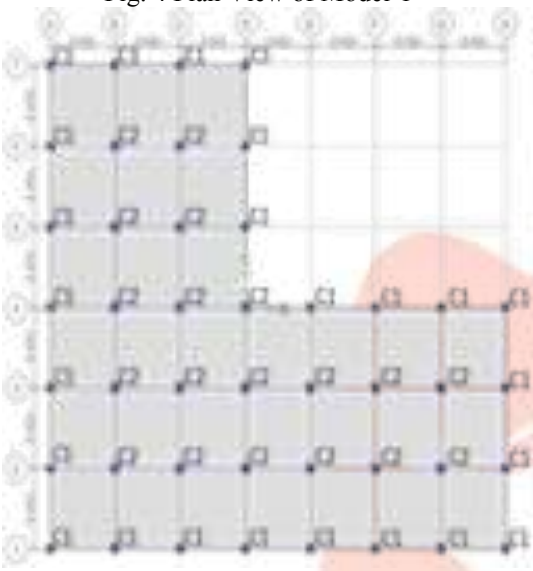

Fig. 6 Plan View of Model-2

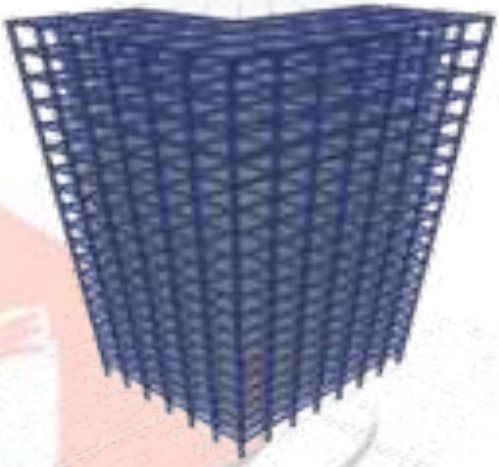

Fig. 7 Isometric View of Model-2

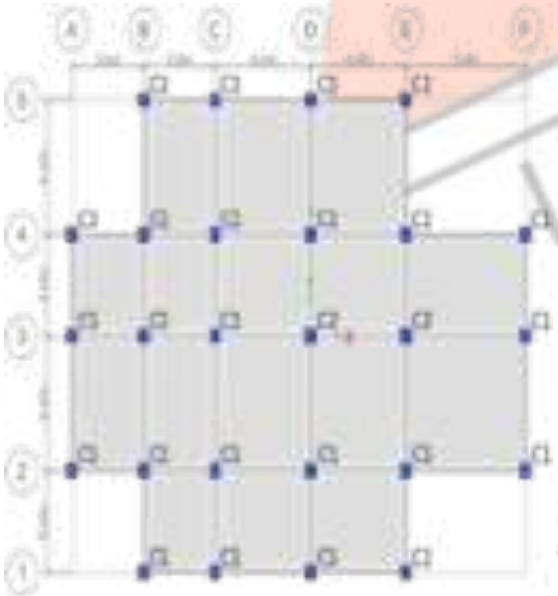

Fig. 8 Plan View of Model-3

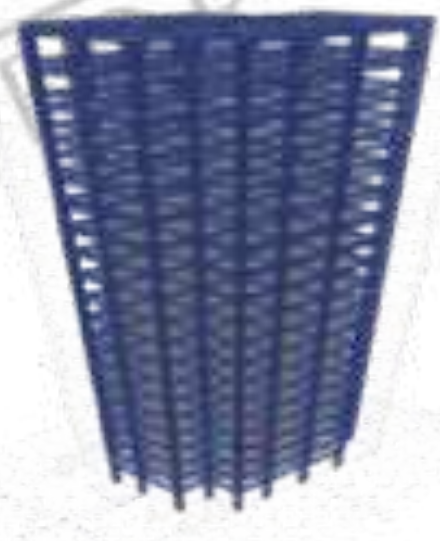

Fig.9 Plan View of Model-3

3.1 Structural Systems of the Buildings:

The beams are of size 300x450mm and columns are designated as C1 and C2 having sizes as 450x450mm and 500x500mm respectively. In the calculation the unit weights of the materials adopted, have been taken according to the IS-875 (Part 1) and the seismic loads considered according to IS:1893 (Part 1)- 2002 i.e. 25% of the live load has to be considered if the LL $\leq$ 3kN/m^2.

Fig. 10 Geometry of the Structure

General Data of Buildings

The building model is located in zone III. Tables 1 and Table 2 present a summary of the building parameters.

Table .2 General Data Collection and Condition Assessment of Buildings

Sl.no	Description	Information	Remarks
1	Building height	64.8m	Above ground level
2	Open ground storey	Yes	----
3	Special hazards	None	----
4	Horizontal floor system	Beams and slabs	
5	Software used	ETABS 15.2.2	----

3.2 Analysis Using Response Spectrum Method

Analysis methods are broadly classified as linear static, linear dynamic, nonlinear static and nonlinear dynamic methods. In these the first two methods are suitable when the structural loads are small and no point, the load will reach to collapse load and are differs in obtaining the level of forces and their distribution along the height of the structure. Whereas the non-linear static and non-linear dynamic analysis are the improved methods over linear approach. During earthquake loads the structural loading will reach to collapse load and the material stresses will be above yield stresses. So in that case material nonlinearity and geometrical nonlinearity should be incorporated into the analysis to get better results. These methods also provide information on the strength, deformation and ductility of the structures as well as distribution of demands.

Linear dynamic analysis of the building models is performed using ETABS 15.2.2. The lateral loads generated by ETABS 15.2.2 correspond to the seismic zone 3 and 5% damped response spectrum given in IS 1893-2002 (Part 1). The fundamental natural period values are calculated by ETABS 15.2.2, by solving the eigen value problem of the model. Thus, the total earthquake load generated and its distribution along the height corresponds to the mass and stiffness distribution as modelled by ETABS 15.2.2. The response spectrum for the structure is defined in the ETABS 15.2.2 as Spec 1 (Spectrum) and the response spectrum analysis data is defined in the load cases defined. The following Fig. 4.8 & 4.9 show the details of the Response history analysis case. The response spectrum analysis is run and the members are designed for the analysis results obtained, by IS: 456-2000 design specifications.

ETABS 15.2.2 has predefined member reinforcement details, these are overwritten by selecting the Reset all Concrete Overwrites button.

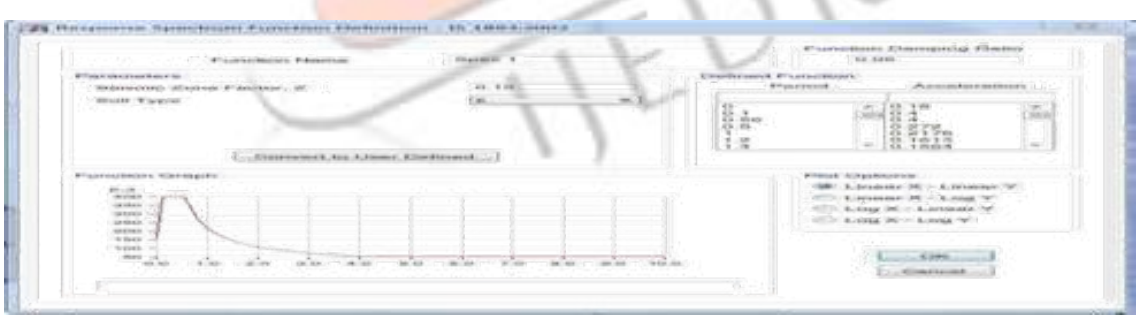

Fig. 11 Details of the Response Spectrum Defined for Response Spectrum Analysis

Fig. 12 Details of the Response Spectrum Load Case for the Structure

3.3 Pushover Analysis for Different Modes:

Pushover analysis provides important features of structural response, such as theinitial stiffness of the structure, total strength and yield displacement. In addition, it provides reasonable estimates for the post peak behaviour of the structure. Lateral load

patterns involved in determining pushover curve of the building structure should represent characteristics of inertia forces developed in the building under the input ground motion excitation.

Fixed load patterns suggested by seismic codes are usually sufficient for the determination of the envelopes of the building inertia forces. These load patterns have invariant distribution through the height of the building but gradually increase until a target value of roof displacement is reached. The displacement at an ultimate state of the building, when a global mechanism exists, is set as the target displacement for comparison purposes

software is used to perform the pushover analysis of buildings using displacement control strategy, where gravity loads (set as nonlinear) of each building are applied prior to the pushover analysis.

Fixed lateral load patterns used to push the buildings are chosen such that they represent the common patterns recommended by the seismic regulation provisions of FEMA-273. Additionally, a fixed pattern based on the first mode of vibration for the building considering an ultimate deformed configuration is investigated.

The common lateral load patterns of FEMA-273 are as follows:

The uniform load pattern (ULP)

The equivalent lateral force pattern (ELP)

The first mode load pattern (FLP)

Deformed shape of the building (DLP) (Adaptive Pushover Analysis)

For defining the POA case we start with the assignment of the hinges to the members of the structure. Default hinge definitions according to the FEMA-356 guidelines have been provided at the ends, where the formation of the potential plastic hinges is more probable for beams and columns with degree of freedom as M3 and the shear value for the hinge is taken from the Dead load case.

Default hinge definitions according to the FEMA-356 guidelines have been provided at the ends, where the formation of the potential plastic hinges is more probable for beams and columns with degree of freedom as M3 and the shear value for the hinge is taken from the Dead load case. The hinges are set so that they drop the load after reachi ng the point E of the performance level as shown in Fig.14.

Fig. 13 Hinge Assignments at the Ends of the Beams and Columns

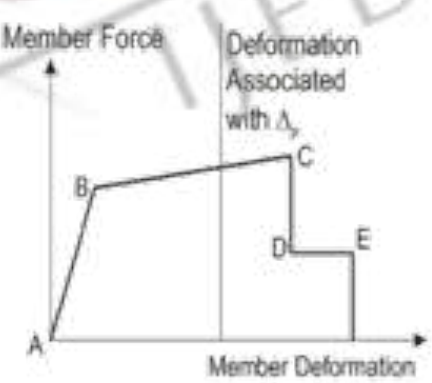

Fig. 14 Performance Levels According to Hinge States.

Force-displacement or moment-rotation curve for a hinge definition used in SAP2000 is referred to as a plastic deformation curve. The plastic deformation curve is characterized by the following points as:

Point A represents the origin.

Point B represents the yielding state.

No deformation occurs in the hinge up to point B, regardless of the deformation value specified for point B.

The displacement (rotation) at point B will be subtracted from the deformations at points C, D, and E. Only the plastic deformation beyond point B will be exhibited by the hinge.

Point C represents the ultimate capacity for pushover analysis.

Point D represents the residual strength for pushover analysis.

Point E represents total failure. Beyond point E the hinge will drop load down to point F directly below point E on the horizontal axis. If the users do not want the hinge to fail this way, a large value for the deformation at point E can be specified.

After assignment of the hinges, the pushover cases are defined under the conjugate monitored displacement. The top displacement of the structure is set to a certain percentage of the total height of the structure at one of the top storey nodes. The degree of freedom (U1) for the structure is in the direction of the application of the pushover loads i.e., along the x-axis.

The RSM and Load cases are set to run at first, the structure is then designed according to IS: 456-2000 and then pushover cases are run on the designed structure, for the analysis results. The Dead loads case is assigned to non-linear static case, and the pushover case data is given as shown in the Fig.

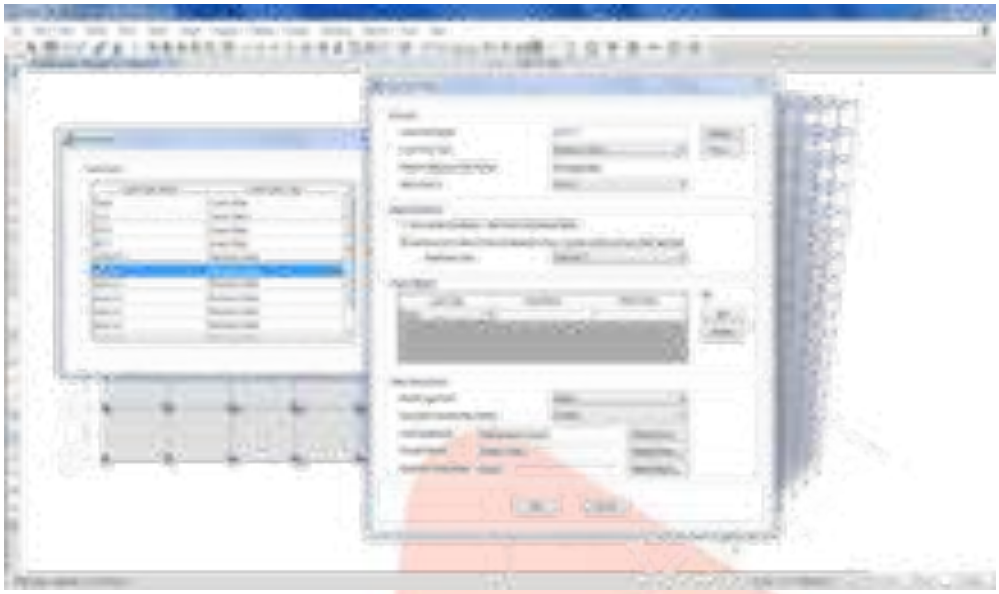

Fig. 15 Pushover Analysis Load Case Data

4 Results and Discussions:

The following tables contains the results of the pushover analysis and energy based pushover analysis carried out for the three structures as discussed earlier. The result are of different pushover cases and each pushover case is for specific mode and directioni.e. PUSH-1X represents pushover in mode 1 and in X-direction. The values tabulated are of the critical modes of the structure, which have been considered in the analysis.

Table 3 Results of the POA and EBPOA of Model-1

Case:	POA		EBPOA	
	Max Base Shear (kN)	**Max Displacement** (m)	**Max Base Shear** (kN)	**Max Displacement** (m)
PUSH-1X	1302.42	0.114	1302.42	0.092
PUSH-2Y	1371.51	0.383	1371.51	0.357
PUSH-4X	1758.46	-0.079	1758.46	0.456

Table 4 Results of the POA and EBPOA of Model-2.

Case:	POA		EBPOA	
	Max Base Shear (kN)	**Max Displacement** (m)	**Max Base Shear** (kN)	**Max Displacement** (m)
PUSH-1Y	1914.09	0.358	1914.09	0.325
PUSH-2X	1978.13	0.101	1978.13	0.087
PUSH-4Y	2541.08	-0.033	2541.08	0.347

Table 5 Results of the POA and EBPOA of Model-3.

Case:	POA		EBPOA	
	Max Base Shear (kN)	**Max Displacement** (m)	**Max Base Shear** (kN)	**Max Displacement** (m)
PUSH-1Y	1252.94	0.188	1252.94	0.153
PUSH-2X	1346.74	0.159	1346.74	0.128
PUSH-4Y	1633.37	-0.148	1633.37	0.534

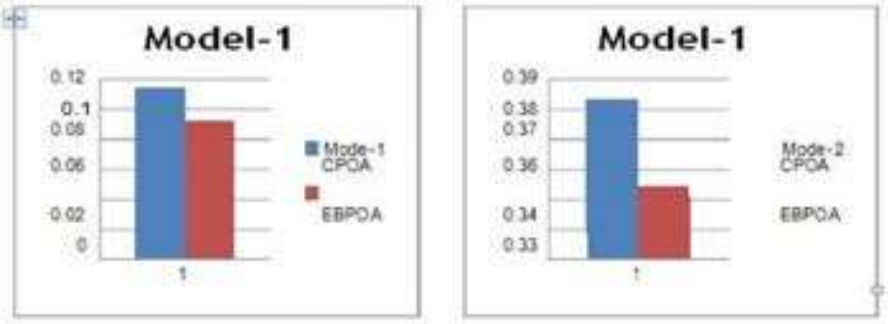

Fig. 16 Comparison of Maximum Displacement of Model-1 for Mode 1 and 2 Using CPOA and EBPOA

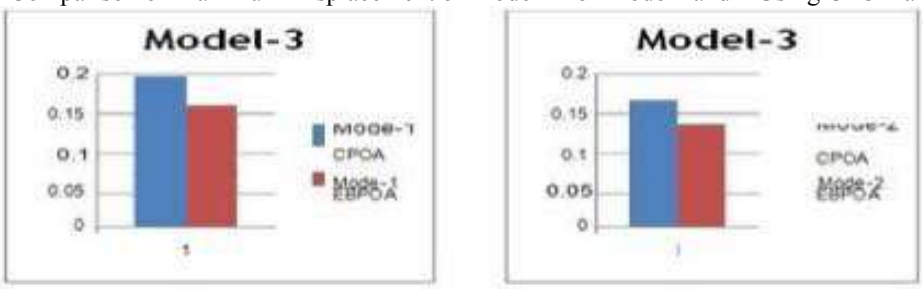

Fig. 17 Comparison of Maximum Displacement of Model-3 for Mode 1 and 2 Using CPOA and EBPOA

By carefully observing the Tables 16 to 17 there is some amount of variation in roof displacement took place when the Energy based pushover analysis (EBPOA) is applied to the different models.

The variations when EBPOA is applied are as follows: Roof displacement reduced by 20% and 7% for the 1st and 2nd modes of model-1 respectively.

Roof displacement reduced by 9% and 14% for the 1st and 2nd modes of model-2 respectively.

Roof displacement reduced by 19% and 20% for the 1st and 2nd modes of model-3 respectively.

This indicates that the conventional POA procedure overestimates the roof displacements of the structure when compared with EBPOA.

The results for EBPOA are obtained from the equations proposed by Hernandez Montes, while the results for POA have been obtained directly from the ETAB 15.2.2 output file. The use of the roof displacement in the conventional POA approach leads to an apparent stiffening in the post – yield response, while the energy-based approach shows monotonic softening with increasing displacement. Because each plastic hinge has a bilinear moment -rotation relationship the apparent stiffening after initial yielding is not physically reasonable, but instead must be viewed as a consequence of the arbitrary choice to index the capacity curve by displacement that increases disproportionately in the nonlinear regime.

4.1 Capacity curves

The pushover curves are obtained using the procedure given by Prof. Hernandez Montes.The pushover analysis for different modes is performed and the capacity curves are plotted from the analysis results obtained for POA and Energy-Based Pushover analysis. Fig. 5.2 shows the capacity curves of conventional pushover and Energy based pushover for different modes of the structure. It is seen that the energy based curve for the first mode response nearly coincides with the conventional first mode pushover capacity curve.

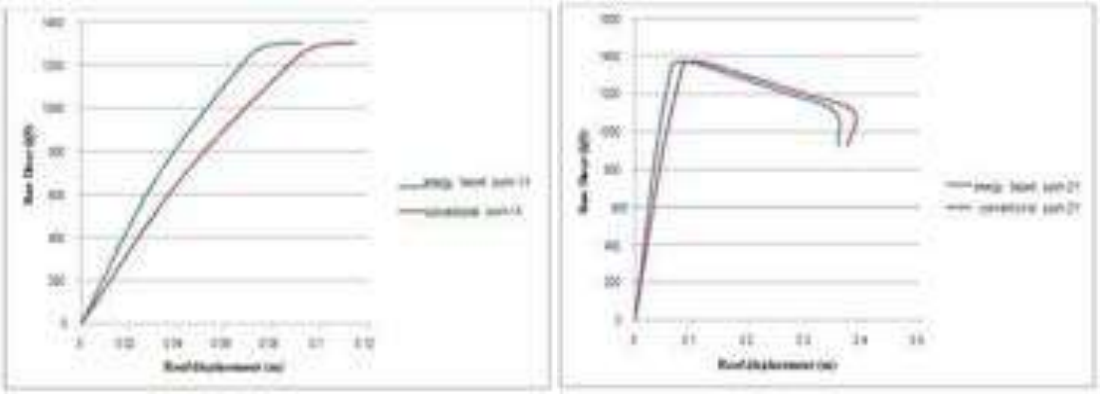

Fig. 18 Pushover Curve of Model-1 for Mode-2, Fig.19 Curve for Model-1 for Mode-4

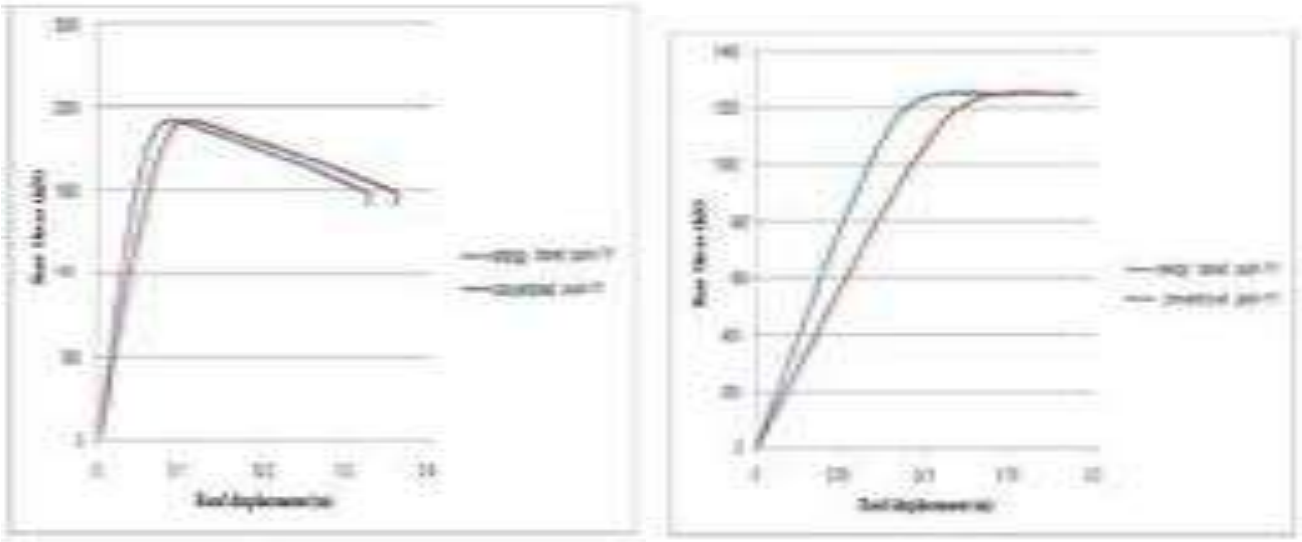

Fig. 20 Pushover Curve of Model-3 for Mode-2, Fig.21 Curve for Model-3 for Mode-4

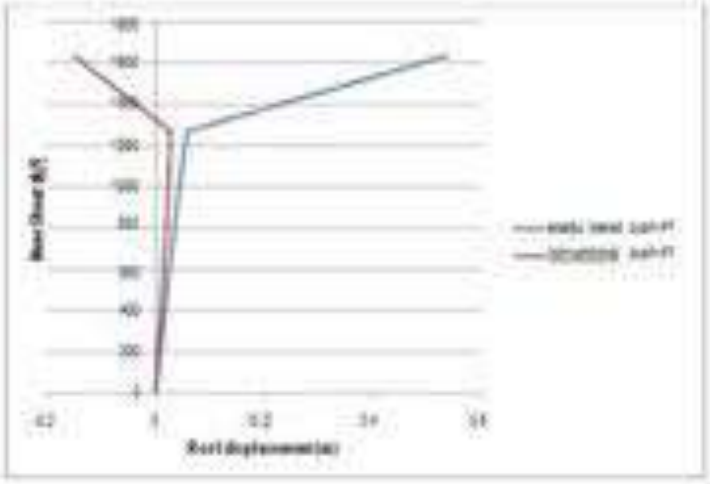

Fig. 22 Pushover Curve of Model-3 for Mode-4

4.2 Mode Shape Profiles of the Structure in Different Modes Under the Action of Loads

The following are the mode shape profiles of model-3 for different modes at each step. The first mode shows displacements only in one direction to the mean position of the building. By taking a closer look at the 4th mode shape, we can observe that the displacement of the roof of the building has shifted from the initial side to the other side of the building due to the action of the pushover forces acting on the structure at lower levels, i.e. the mode shape is reversed. This phenomenon is called as the Mode reversal and it is because of mode reversals that the pushover curves for these modes turn to the negative side of the plot shown in the figures below

Storey Level

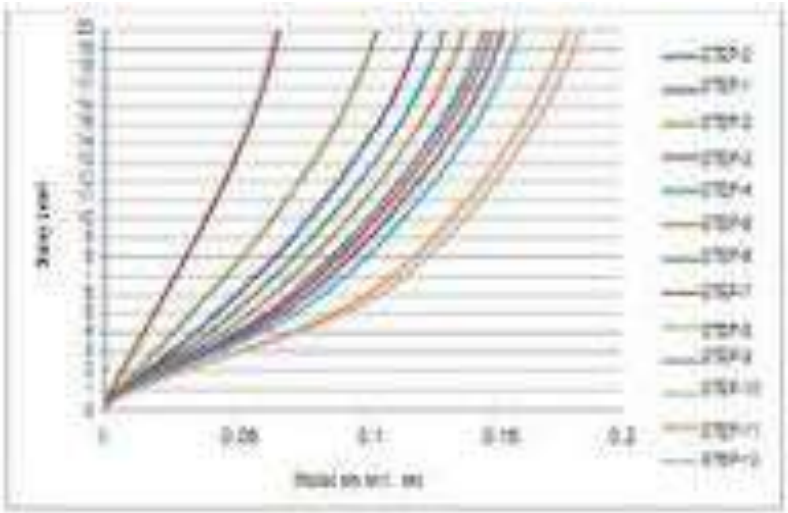

Fig. 23 Storey Level vs. Displacement Plot for the 1st Mode POA of Model-3

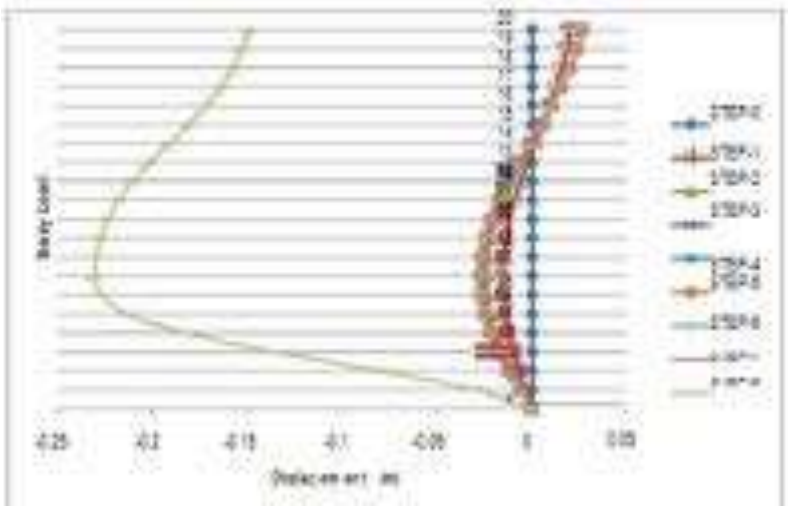

Fig. 24 Storey Level vs. Displacement Plot for the 4th Mode POA of Model-3

The major cause for the out-right reversals is due to the application of the pushover loads in proportion to the displaced shape of the structure (adaptive pushover), in this way, more force is applied at the story level where more storey displacement takes place, the first mode shape profile is a good example.

Response Spectra and Demand Curves

Response spectra is plotted for zone factor of 0.16 and effective peak acceleration (EPA) of the ground is 1*g as per ATC-40. It is then converted into Acceleration Displacement Response Spectra (ADRS) format i.e. spectral acceleration vs. spectral displacement as shown in Figures and then a series of family of response spectra is plotted corresponding to different effective damping values (βeff) starting from 5% to maximum of 20% for type C structure as shown in Fig Demand curve is generated using procedure given in ATC-40. Fig. The energy capacity and demand curves are shown in Figures. Using the intersection points of the demand and capacity curves as the maximum displacement values, the roof displacement and drift demands could be determined.

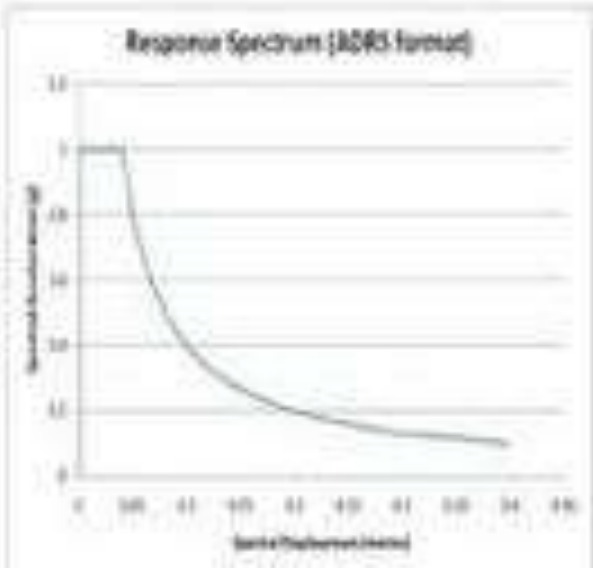

Fig.25 Response Spectrum ,

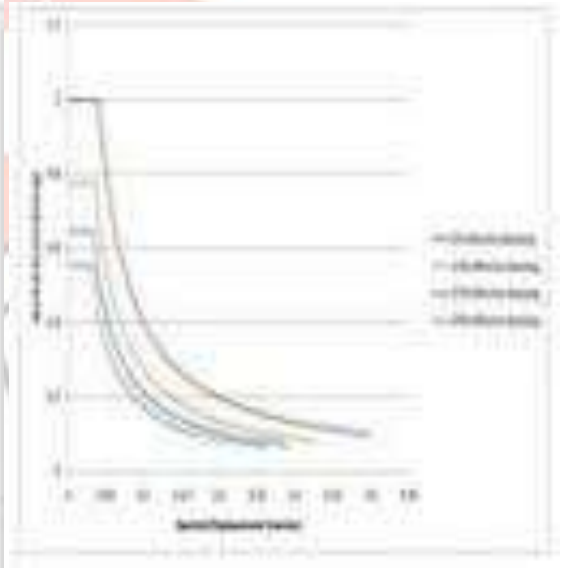

Fig.26 Family of Reduced Response Spectra

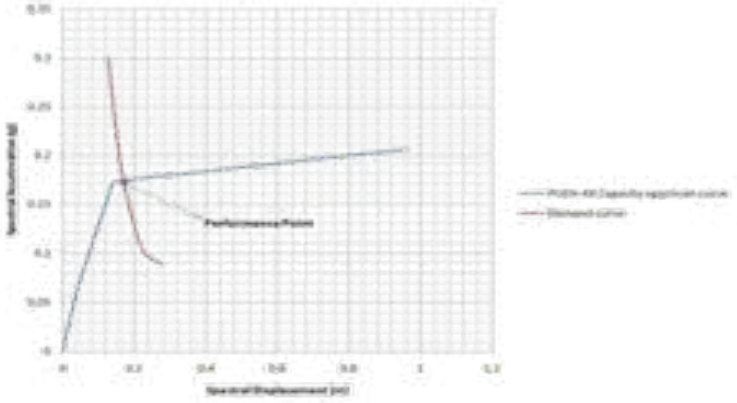

Fig. 27 Demand Curve and Capacity Curve for Mode-4 in Model-1

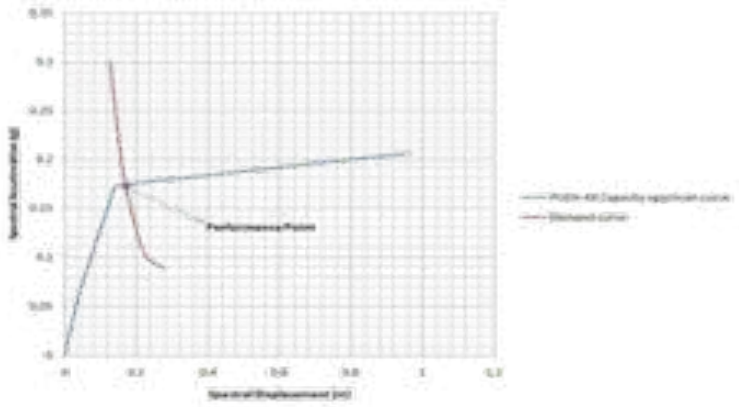

Fig. 28 Demand Curve and Capacity Curve for Mode-4 in Model-2

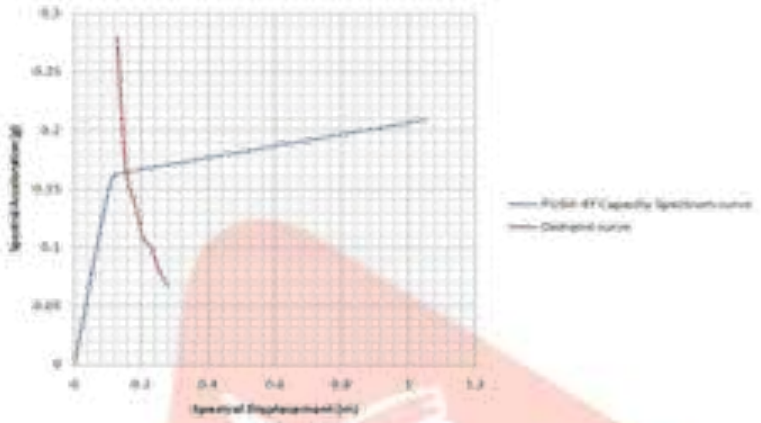

Fig. 29 Demand Curve and Capacity Curve for Mode-4 in Model-3

Table 6 Performance of Building Models for Mode-4

Model	Case	Sd(m)	Sa(g)	Performance level
1	Mode 4	0.173	0.175	**I.O**
2	Mode 4	0.165	0.19	**I.O**
3	Mode 4	0.152	0.165	**I.O**

In the table 6, the performance of the building is represented in terms of spectral acceleration (Sa) and spectral displacement (Sd). For the structural models selected for the study, the performance level of the buildings lies in the immediate occupancy stage. Since the work is targeted for studying the higher mode, the performance point is obtainedusing EBPOA which is not possible in conventional POA because of mode reversal.

5 CONCLUSIONS

The Energy-based POA has been applied to 3 models of 20 storey moment resisting 3D space frames, designed according to the Indian Standards (IS: 456-2000) for seismic loading using response spectrum analysis as specified by IS: 1893-2002. The frames are subjected to dead, live and dynamic loading as specified in IS: 1983-2002 & IS-875 Codes of Practice and designed according to IS: 456-2000.

The first mode is not dominant for both models-1 and 3 but for model-2, the first mode which is characterized along the Y-direction is dominant. Even for this type of structure in which the fundamental mode is dominant, due to neglecting the effects of higher modes leads to early mode reversal by using Conventional POA as seen in the observations. This anomaly was corrected by performing an Energy Based POA. Higher mode pushover analyses reveal local storey mechanisms at different levels in the structure not detected by the traditional pushover analysis using first mode distributions. Base shear vs. Roof displacement is a poor index for judging the response of the structure which gives good results for the first mode only when compared to the Base shear vs. Energy based roof displacement. Energy based POA shows a gradual softening of the structure rather than a quick failure. The backdrop of the mode reversals can be easily removed by EBPOA procedure. The conventional POA procedure overestimates the roof displacements of the structure when compared with EBPOA. Demand curve can be generated for higher modes in energy based approach which is difficult in conventional POA method especially where the mode reversal takes place. Performance for the higher modes where there is reversal of mode is obtained which is not possible in conventional POA. With the total work done in the structure involved, this method provides better results for the structural evaluation under seismic loading and for consideration of higher mode effects and as the total energy absorbed is considered, the method doesn‘t overestimate the response of the structure like conventional POA. From the observations made during the

calculations it can be concluded that the energy-based formulation provides a stronger theoretical basis for establishing the capacity curves of the first and higher mode equivalent SDOF systems. Overall, the performance level of different models considered falls under the same category mode.

REFERANCESS

[1] Angelo D'Ambrisi and Marco Mezzi, (2014). "An energy-based approach for nonlinear static analysis of structures". *Bulletin of Earthquake Engineering*, Vol. 13(5), Pp. 1513- 1530.

[2] Ashraf Habibullah and Stephen Pyle, (1998). "Practical Three Dimensional Nonlinear Static Pushover Analysis". S.E.2 (Published in *Structure Magazine*).

[3] ATC-40 (1996). "Seismic evaluation and retrofit of concrete buildings", *California Seismic Safety Commission*, Vol-1.

[4] Chandrashekaran, S. and Anubhab Roy, (2005)**.** "Seismic evaluation of multi storey RC frame building using modal pushover analysis". *Non-linear Dynamics*, Pp. 329-342.

[5] Charilaos Maniatakis, Psycharis, N. and Constantine Spyrakos, (2013). "Effect of higher modes on the seismic response and design of moment-resisting RC frame structures". National Technical University of Athens.

[6] Chopra, A.K. and Goel, (2002). "A modal pushover analysis procedure for estimating seismic demands for buildings". *Earthquake Engineering and Structural Dynamics*, Vol.31, Pp. 561-582.

[7] Chopra, A.K. and Goel, (2004). "A modal Pushover analysis procedure for Seismic analysis of the buildings". *Earthquake Engineering and Structural Dynamics*, Vol. 33(8), Pp. 903–927.

[8] Chou, C.C. and Uang, C.M., (2002). "Establishing absorbed energy spectra-An attenuation approach". *Earthquake Engineering and Structural Dynamics*, Vol. 29(10), Pp. 1441–1455.

[9] Chou, C.C. and Uang, C.M., (2001). "A procedure for evaluating seismic energy demand of framed structures". Department of Structural Engineering, University of California; San Diego; La Jolla; CA 92093; U.S.A.

Effect Of Combined Plan, Vertical And Mass Irregularity On Torsional Performance Of High Raised Buildings

[1]S K Shanawaz, [2]S. Amaresh Babu
[1]Student, [2]Professor
[1]Nawab Shah Alam Khan College Of Engineering & Technology,
[2]Nawab Shah Alam Khan College Of Engineering & Technology

Abstract - **Recently, reports showing the damage caused by earthquakes indicate that, torsional effects often cause considerable damage to structures leading to their collapse. The response of asymmetric buildings towards torsion is one of the most crucial factors for their damage. Torsion in such buildings is due to irregularity in plan, mass and stiffness which may cause severe damage in structural systems. Due to various reasons structures acquire asymmetry. Asymmetric structures have irregular distribution of plan, stiffness and mass, its centre of mass and centre of rigidity do not coincide and hence cause the torsional effect on the structures which is one of the most important factor influencing the seismic damage of the structure. For the purpose of study, asymmetrical buildings of 12 storeys, 15 storeys and 18 storeys with same columns sizes subjected to gravity loads and seismic loads are analysed using non-linear dynamic analysis. The structure is evaluated in accordance with IS 456-2000 and seismic code IS: 1893-2002 using non-linear time history method with the help of ETABS. Percentage of torsion and joint rotation are significantly decreased by minimizing the stiffness eccentricity. Torsion reduces to 72%, 76% and 72% for 12 storey U shaped building, 15 storeys U shaped building and 18 storeys U shaped building. Similarly torsion reduces to 79%, 85% and 90% for 12 storey building with openings, 15 storey building with openings and 18 storey building with openings. Joint rotation reduced to 84%, 58%, and 65% for 12 storey U shaped building, 15 storeys U shaped building and 18 storeys U shaped building. Joint rotation reduced to 78%, 75 %, and 86% for 12 storey building with openings, 15 storey building with openings and 18 storey building with openings. Thereby a maximum decrease in torsion is 90% for 18 storey building with openings. And maximum decrease in joint rotation is 86% for 18 storey building with openings.**

keywords - **Plan irregularity, Vertical irregularity, Mass irregularity, Torsion**

I. INTRODUCTION

1.1 General: The earthquakes are the most unpredictable and devastating among all natural disaster. Earthquake is a phenomenon that occurs due to the geotechnical activities in the strata of the earth and causes heavy loss to both life and property if it occurs in populated regions. Thus, it is the responsibility of a structural engineer to draw out the parameters from previous experiences and consider all the possible hazards that the structure may be subjected to, in the future, for the purpose of safe design of the structure. For the simplicity of the practicing engineers, different societies in different countries have specified different earthquake codes for the design of the structures subjected to different type of hazards, which are modified as and when newer knowledge is acquired, keeping in view the hazards of the natural calamities.

1.2 Types of Structural Irregularities: There are various types of irregularities in the buildings depending upon their location and scope, but mainly, they are divided into two groups- plan and vertical irregularities. In the present paper, the irregularities are considered and described as follows.

Plan Irregularities: According to clause 7.1 from Sixth revision of IS 1893-2002 (Part 1). Plan irregularities are classified as torsion irregularity, re-entrant corners, floor slabs having excessive cut-outs or openings, out-of-plane offsets in vertical elements and non-parallel lateral force system.

Torsion Irregularity: A building is said to be torsionally irregular, when maximum horizontal displacement of any floor in the direction of the lateral force at one of the floor is more than 1.5 times its minimum horizontal displacement at the far end in that direction

Vertical Irregularities: According to clause 7.1 from Sixth revision of IS 1893-2002 (Part 1). Vertical irregularities are classified as mass irregularity, vertical geometrical irregularity, stiffness irregularity, In-plane Discontinuity in Vertical Elements Resisting Lateral Force and

Mass Irregularity: Mass irregularity shall be considered to exist, when the seismic weight of any floor is more than 150 percent of that of its adjacent floors. This provision of 150 percent may be relaxed in case of roofs.

Vertical Geometric Irregularity: Vertical geometric irregularity shall be considered to exist, when the horizontal dimension of the lateral force resisting system in any storey is more than 125 percent of that in its adjacent storey

1.3 Importance of Seismic Analysis

The prediction of the response of a structure to a particular type of loading is of utmost importance for the design of structure. Basically the codes and previous experiences provide us with a lot of information regarding the type of loads and their intensities for different types of structure and the site condition. The analysis procedure to be adopted purely depends upon the engineers choice as per the accuracy of the work required. The non-linear time history method analysis can be regarded as the most accurate method of seismic demand prediction and performance evaluation of structures. A non-linear dynamic analysis or inelastic time history analysis describes the actual behavior of the structure during an earthquake. The method is based on the direct numerical integration of the motion differential equations by considering the elasto-plastic deformation of the structure element. This method captures the effect of amplification due to resonance, the variation of displacements at diverse levels of a frame, an increase of motion duration and a tendency of regularization of movements result as far as the level increases from bottom to top. Seismic analysis is a subset of structural analysis and is the calculation of the response of a building to earthquakes. It is part of the process of structural design, earthquake engineering or structural assessment in regions where earthquakes are prevalent.

Equivalent Static Analysis: Linear static analysis or equivalent static analysis can only be used for regular structure with limited height. All design against seismic loads must consider the dynamic nature of the load. However, for simple regular structures, analysis by equivalent linear static methods is often sufficient. This is permitted in most codes of practice for regular, low-to medium-rise buildings. It begins with an estimation of base shear load and its distribution on each story calculated by using formulas given in the code. The base shear is the total horizontal force on the structure which is calculated on the basis of structure mass and fundamental period of vibration and corresponding mode shape.

Response Spectrum Analysis: It is a representation of the maximum response of idealized single degree freedom system having certain period and damping, during earthquake ground motions. The maximum response plotted against undamped natural period, for various damping values, can be expressed in terms of maximum absolute acceleration, maximum relative velocity or maximum relative displacement. For this purpose, response spectrum case of analysis has been performed according to IS 1893. In the calculation of structural response (whether modal analysis or otherwise), the structure should be so represented by means of an analytical or computational model that reasonable and rational results can be obtained by its behavior.

Non-linear Static Analysis: This method is also known as push-over analysis. This method is an improvement over the linear static and dynamic analysis in the sense that it allows the inelastic behavior of the structure. The method still assumes a set of static incremental lateral load over the height of the structure. It provides information on the strength, deformation and ductility of the structure and the distribution of demands. These permits to identify critical members likely to reach limit states during the earthquake, for which attention should be given during design and detailing process. The pushover analysis of a structure is a static nonlinear analysis is a static nonlinear analysis under permanent vertical loads and gradually increasing lateral loads.

Non-linear Dynamic Analysis: A non-linear dynamic analysis or inelastic time history analysis describes the actual behavior of the structure during an earthquake. The method is based on the direct numerical integration of the motion differential equations by considering the elasto-plastic deformation of the structure element. This method captures the effect of amplification due to resonance, the variation of displacements at diverse levels of frame, an increase of motion duration and a tendency of regularization result as far the level increases from bottom to top.

1.4 Need of the Study: Structural eccentricity is a useful parameter which is responsible to co-relate the seismic elastic response of asymmetric structures. When the structural system is excited into the inelastic range, yielding of the resisting elements complicates the behaviour. Therefore there is a need to study this parameter that captures the inelastic response of the structure.

1.5 Objectives of the Study: Based on the study, the following objectives are drawn:
- To study the variation in torsion by minimizing the stiffness eccentricity.
- To study the effect of stiffness variation on joint rotation of the structure.
- Comparison of torsion and joint rotation before and after varying the stiffness eccentricity.

1.6 Scope of the Study: The present work aims at an objective to identify the non-linear response of asymmetrical structures with respect to stiffness assignments. The buildings studied in this section are asymmetrical buildings of 12 storeys, 15 storeys and 18 storeys with same columns sizes subjected to gravity loads and seismic loads using non-linear dynamic analysis. The structure is evaluated in accordance with IS: 456-2000 and seismic code IS: 1893-2002 using non-linear time history method with the help of ETABS.

1.7 Organization of Dissertation: Chapter 1 is the discussion of the importance of earthquake and torsional behaviour of buildings, types of structural irregularities and introduction to importance of seismic analysis. The scope and objective of the study has also been discussed.
Chapter 2 deals with the various literatures that have been published on effect of irregularities on buildings.
Chapter 3 covers the complete study on analysis procedures and procedure adopted in the present work.
Chapter 4 completely take care of the case study of building under consideration and the various building data surveys done to gather the information for modelling of the structure.
Chapter 5 copes with the numerical study and presentation of results of non linear dynamic analysis of for the current buildings under study

Chapter 6 details of discussions drawn based on the present work and the scope of the study.

II. LITERATURE REVIEW

The general philosophy for earthquake-resistant design of structures has undergone some major change in the past 15 years, following some of the most devastating earthquakes all over the world. The prediction of the earthquake response of a structure became more significant for the engineers to design the structures and this became more significant for the engineers to design the structures and this became much easier with the availability of seismic data and software enhancement. Newer analysis methodologies are being proposed with focus on a realistic characterization of seismic structural damage and its direct incorporation in the design methodology. In addition, a major emphasis is given to the characterization of all the uncertainties in the process of design. In general, these approaches are categorized under performance-based seismic design (PBSD). The various ways of modelling structural damage for PBSD lead to various design approaches. The most commonly adopted approach for PBSD so far is the displacement based design approach, where the design criterion is set usually by a limit on the peak roof (inelastic) displacement, the peak (inelastic) inter-story drift, or the peak ductility demanded. Generally when the earthquake hits a structure, before actual failure of the building, it passes both the linear and nonlinear stages. The linear analysis has been the source of interest of the researchers as mentioned before, but the non-linearity of the structure has now taken the stage. The strength of structure in the non-linear yield is significant for the structures and could be utilized with application of several limit states for a monitored performance and damage. Most buildings have some degree of irregularity in the geometric configuration or the distribution of mass, stiffness or strength.

2.2 Non-Linear Dynamic Procedures: The response of buildings to earthquakes is a complex, three dimensional, nonlinear, dynamic problems. Limitations in technology and the depth of our understanding of this problem have lead to the profession developing a number of simplified methods for representing it, most of which disregard one or more of its fundamental aspects: the Linear Dynamic Procedure (LDP) ignores nonlinearity; the Nonlinear Static Procedure (NSP) ignores dynamic effects; the Linear Static Procedure (LSP) ignores both. In contrast, the Nonlinear Dynamic Procedure (NDP) attempts to fully represent the seismic response of buildings without any of these major simplifying assumptions.

2.3 Overview: Moehle (1984) studied the seismic response of four irregular reinforced concrete test structures. These test structures were simplified models of 9-story 3 bay building frames comprised of moment frames and frame-wall combinations. Irregularities in the vertical plane of these structures were introduced by discontinuing the structural wall at various levels. Based upon measured displacements and distributions of storey shears between frames and walls, it was apparent that the extent of the irregularity could not be gauged solely by comparing the strengths and stiffness's of adjacent stories in a structure. Structures having the same stiffness interruption, but occurring in different stories didn't perform equally. It was observed that the curvature ductility demand in beams varied from 3.9 to 7.2 and for columns from 1.8 to 2.9, for an abrupt termination of shear walls at different levels along the height.

Han Seon Lee and Dong Woo Co (2002) they studied the seismic response of high rise RC wall buildings with different irregularities. In this study they have consider three models with three different cases. First model has a symmetrical moment resisting frame, second has in-filled shear wall at the central frame and third one is with in-filled shear walls in most exterior frames at the bottom two storey.

Dubey and Sangamnerkar (2011) have studied torsional response due to plan and vertical irregularity to analyze T-shaped building, while earthquake forces acts and to calculate additional shear due to torsion in the columns, and concluded that additional shear due to torsional moments needs to be considered because, this increase in shear forces causes columns to collapse, so in design procedure this additional shear must be taken into account.

Gupta and Pajagade (2012) have presented a review about the investigation done on torsional behaviour of multi-storey buildings with plan as well as vertical irregularities. It also focused on codal provision made for torsion.

2.4 Critical Appraisal: Despite a lot of researches being done in this field of non linear dynamic analysis, a few shortcomings in the available literature have been observed such as Dubey and Sangamnerkar, having carried out the work on T-shaped building with vertical geometrical irregularity, have not considered the torsion irregularity and mass irregularity. Similarly, Sagar and Gururaj have studied the parameters like deflection, story displacement response due to plan and vertical irregularity for cross shape, + and T shape buildings. But they have not considered the torsion parameter. Gowthami et al. carried out work on torsional effect on buildings with re entrant corners but they have not performed the work on vertical irregularities. Hence, the proposed study concentrates on torsional performance of buildings with combined plan, vertical and mass irregularity that are subjected to earthquake.

III. METHODOLOGY

3.1 The purpose of the non-linear dynamic analysis is evaluating non-linear response of the structure with respect to torsion. Nonlinear dynamic analysis utilizes the combination ofground motion records with a detailed structural model, therefore is capable of producing results with relatively low uncertainty. In nonlinear dynamic analyses, the detailed structural model subjected to a ground-motion record produces estimates of component deformations for each degree of freedom in the model and the modal responses are combined using schemes such as the square-root-sum-of-squares.

3.2 Analysis Procedure

Already the methods for the assessment of the vulnerability of building based on score assignment are rather elaborate and therefore time consuming. More sophisticated methods, implying a more detailed analysis method and more refined models, take even more times and serve therefore for evaluation of individual buildings only, possibly as a further step after the rapid screening of potential hazardous buildings in multi phase procedure. They are not suitable for the earthquake scenario projects where a large number of buildings have to be evaluated. Nevertheless, the concept behind those methods can be valuable for the development of a new simple method and hence, the main analysis procedure shall be briefly outlined. The analysis procedure can be divided into linear procedure (linear static and linear dynamic) and non linear procedure (non-linear static and nonlinear dynamic).

3.2.1 Linear Static Analysis: In a linear static analysis procedure, the building is modelled as an equivalent single degree of freedom (SDOF) system with the linear elastic stiffness and an equivalent viscous damping. The seismic is modelled by an equivalent lateral force with the objective to produce the same stress and strain as the earthquake it represents. Based on an estimation of the first fundamental frequency of the building using empirical relationships or Rayleigh's method, the spectral acceleration is determined from the appropriate response spectrum which, multiplied by the mass of the buildings, results in the equivalent lateral force. The coefficient take into account not only issue like second order effect, stiffness degradation, but also force reduction due to anticipated inelastic behaviour. The lateral force is then distributed over the height of the building and the corresponding internal force and displacements are determined using linear static analysis. These linear static procedures are used primarily for design purpose and are incorporated in most codes. Their expenditure is rather small. However, their applicability is restricted to regular buildings for which the first mode of vibration is predominant.

3.2.2 Linear Dynamic Analysis: In a linear dynamic procedure the building is modelled as a multi degree freedom (MDOF) system with a linear elastic stiffness matrix and an equivalent viscous damping matrix.

$$V = Sa * m * \sum Ci \qquad (3.1)$$

The seismic input is modelled using spectral analysis or time history analysis. Modal spectral analysis assumes that the dynamic response of a building can be found.

3.2.4 Non-Linear Dynamic Analysis: In a non-linear dynamic analysis procedure, the building model is similar to the one used in nonlinear static procedure incorporating directly the inelastic, lateral response using general finite elements. The main difference is that the seismic input is modelled using a time-history analysis which involves time-step-by-time-step evaluation of building response. This is the most sophisticated analysis procedure for predicting force and displacement under seismic input. However, the calculated response can be very sensitive to the characteristic of the individual ground motion used as seismic input therefore several time-history analysis are required using different ground motion records.

3.3 Non-Linear System: The force-deformation relationship in the structure after a deformation point becomes non-linear. This point is called as yield deformation, because at this point the yielding begins. On initial loading this yielding system is linearly elastic as long as the force is less than fy (i.e. the stiffness is zero). fy generally is called as the yield strength. The structure now enters into the plastic zone and it exhibits elasto-plastic behaviour. Now the deformation increases at constant force. The pattern of cyclic loading unloading and reloading continues till the material deformation comes to rest. This implies that the force Fs corresponding to deformation u is not single valued and depends on the history of the deformations and on whether the deformation is increasing (positive velocity) or decreasing (negative velocity) as shown in Fig. 3.1

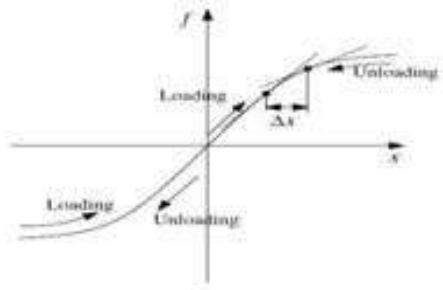

3.4 Governing Equation of Motion for SDOF and MDOF System

$$M\ddot{u} + c\dot{u} + f_s(u,\dot{u}) = -m\ddot{u}_g \qquad (3.2)$$

Where $f_s(u,\dot{u})$ is the resisting force for an elasto-plastic system

M is the mass of the structure

C is the damping coefficient

The function $f_s(u,\dot{u})$ describes the force-deformation relation in partially dimensionally form. Numerical methods are discussed in the subsequent topics to solve for the single degree of freedom system equation of motion. finalally the equation of motion for MDOF system subjected to external force or earthquake excitation for inelastic systems

$$[M]\{\ddot{u}\} + [C]\{\dot{u}\} + [K]\{u\} = -[m]\ddot{u}_g(t) = p_{eff}(t) = -s\ddot{u}_g(t) \qquad (3.3)$$

Fig. 3.1 General Non-Linear Force-Deformation Relationships

Where

[M] = Mass matrix of the MDOF system.
[C] = Damping matrix of the MDOF system.
[K] = Stiffness matrix of the MDOF system.

3.5 Centre of Mass and Centre of Rigidity: Centre of mass is the point where entire mass of the system is concentrated. During an earthquake, acceleration induced inertia forces will be developed at each floor level, where the mass of the entire storey may be assumed to be calculated. Hence the location if particular level will be determined by the centre of accelerated mass at that level. The coordinates of centre of mass is given by

XCM = ∑wxi xi/ ∑ wi
YCM = ∑wxi yi/ ∑ wi

Centre of rigidity is the point that position of storey shear which will cause only relative floor translation. It also referred as centre of stiffness of the system. The coordinates of centre of stiffness is given by

XCR = ∑ kyi xi/ ∑ki
YCR = ∑kxi yi/ ∑ ki

3.6 Development of Torsion in Buildings: When a building is subjected to seismic excitation, horizontal inertia forces are generated in the building. The resultant of these forces is assumed to act through the centre of mass of the structure. The vertical members in the structure resist these forces and the total resultant of these systems of forces act through a point called as centre of stiffness (C.S). When the centre of mass and centre of stiffness does not coincide, eccentricities are developed in the buildings which further generate torsion. The following Fig. 3.2 showsthe development of torsion in buildings.

Fig. 3.2 Development of Torsion in Buildings

3.7 Eccentricity: Stiffness Eccentricity is defined as a system with non-coincident centre of mass and centre of stiffness. When such system is subjected to dynamic excitations (like earthquake, wind), the inertia force can be modelled as acting through centre of mass while the resultant of resisting forces respond through the centre of stiffness. This creates a moment between the two opposing forces, resulting into a torsional effect. Strength eccentricity is defined as the distance between centre of mass and centre of strength for a considering floor.

V. CASE STUDY DESCRIPTION

4.1 Models of the Buildings: Model 1(a) is an U shaped 12 storied building which is asymmetric in X direction and symmetric in Y direction in plan with vertical irregularity and mass irregularity, all column sizes are 750X300mm, except C2&C3 for first storey and beam sizes are 500X300mm. Model 1(b) is an 15 storied building which is asymmetric in X direction and symmetric in Y direction in plan with vertical irregularity and mass irregularity, all column sizes are 750X300mm, except C2&C3 for first storey and beam sizes are 500X300mm. Model 1(c) is an 18 storied building which is asymmetric in X direction and symmetric in Y direction in plan with vertical irregularity and mass irregularity, all column sizes are 750X300mm, except C2&C3 for first storey and beam sizes are 500X300mm.

Model 2(a) is floors having excessive cut-outs or openings having 12 storied building with openings and symmetric in X direction and asymmetric in Y-direction in plan with vertical irregularity and mass irregularity, all columns sizes are 750X300mm and beam sizes are 500X300mm. Model 2(b) is floors having excessive cut-outs or openings having 15 storied building with openings and symmetric in X direction and asymmetric in Y-direction in plan with vertical irregularity and mass irregularity, all columns sizes are 750X300mm and beam sizes are 500X300mm. Model 2(c) is floors having excessive cut-outs or openings having 18 storied building with openings and symmetric in X direction and asymmetric in Y-direction in plan with vertical irregularity and mass irregularity, all columns sizes are 750X300mm and beam sizes are 500X300mm.

4.2 Torsion Irregularity Condition for U Shaped Models:

Model 1(a) is 12 storeys U shaped building:

Δmin= 21.783 mm
Δmax= 34.795 mm
Δmax> 1.5x (Δmin)
Δmax> 1.5x (34.795)
Δmax> 32.674 mm

Model 1(b) is 15 storeys U shaped building:

Δmin= 23.004 mm
Δmax= 38.387 mm
Δmax> 1.5x (Δmin)
Δmax> 1.5x (23.004)
Δmax> 34.506 mm

Model 1(c) is 18 storeys U shaped building:

Δmin = 29.085 mm
Δmax= 50.045 mm
Δmax> 1.5x (Δmin)
Δmax> 1.5x (29.085)
Δmax> 43.627 mm

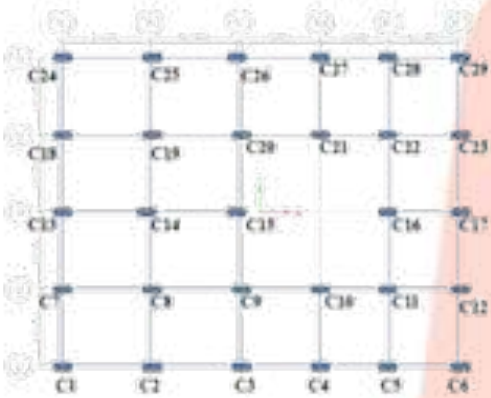

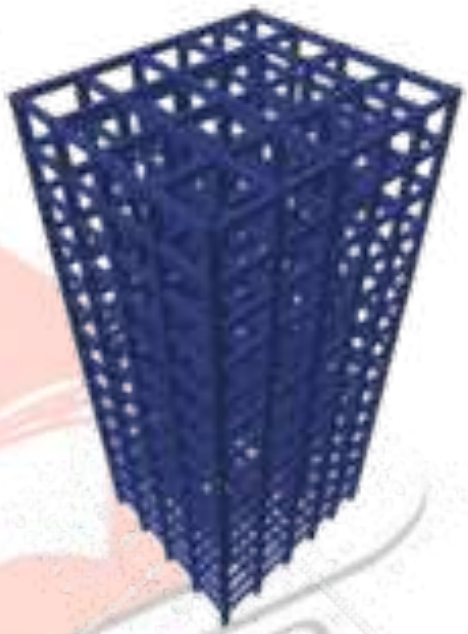

Fig. 4.3 Plan View of Model 2 Columns sizes = 750X300mm Beam sizes = 500X300mm Fig. 4.4 Isometric View of Model 2

VI. RESULTS AND DISCUSSIONS

The following results are obtained by carrying out the non linear dynamic analysis (FNA) in ETABS to study the combined effect of plan, vertical and mass irregularity on torsion. Subsequent discussions are made about the torsion in buildings by non linear dynamic analysis and reducing torsion with respect to stiffness eccentricity.

5.1 Comparison of Torsion

Model	Number of storeys	Eccentricity	Torsion (kN-m)
Model 1(a)	12	1.776	5825.631
Modified model 1 (a)	12	0.639	1588.826

Table 5.1 Results of Eccentricity and Torsion for Model 1(a) and Modified model 1(a)

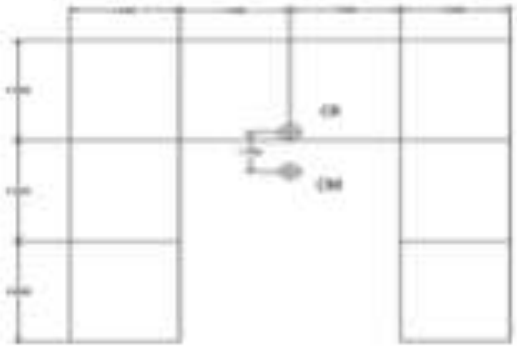

Fig. 5.1 Position of Centre of Mass and Centre of Rigidity for Model 1(a)

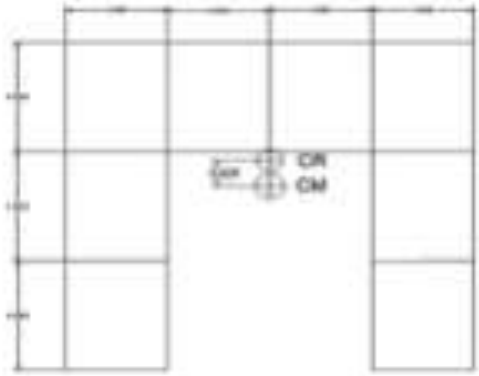

Fig. 5.2 Position of Centre of Mass and Centre of Rigidity for Modified Model 1(a)

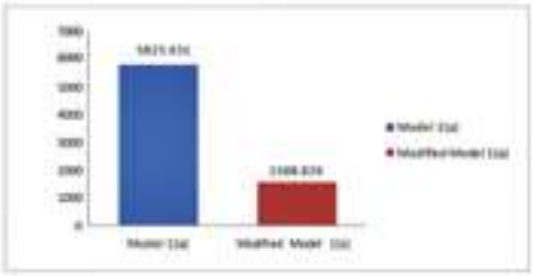

Fig. 5.3 Results of Torsion for Model 1(a) and Modified model 1(a)

It is observed that the variation of torsion for 12 storey 'U' shaped building is decreased by 72.72% after varying the stiffness parameters as shown in Fig. 5.3

Model	Number of storeys	Eccentricity	Torsion (kN-m)
Model 1(b)	15	2.058	7466.670
Modified model 1(b)	15	1.046	1749.878

Table 5.2 Results of Eccentricity and Torsion for Model 1(b) and Modified Model 1(b)

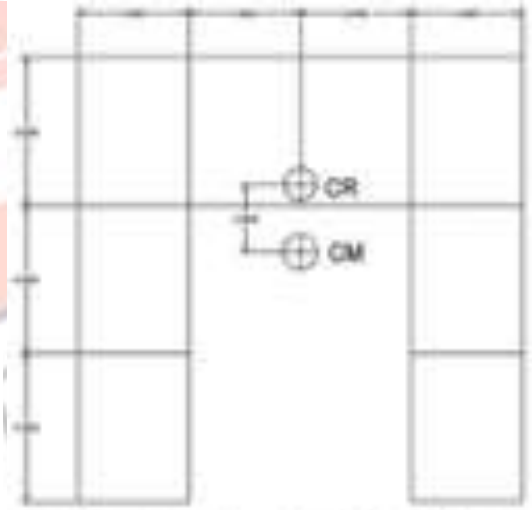

Fig. 5.4 Position of Centre of Mass and Centre of Rigidity for Model 1(b)

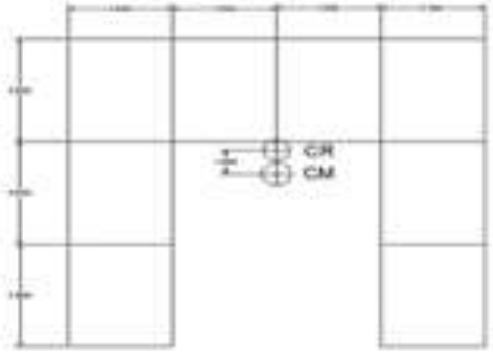

Fig. 5.5 Position of Centre of Mass and Centre of Rigidity for Modified Model 1(b)

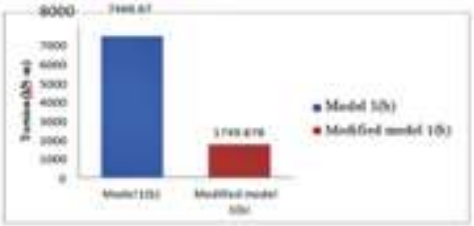

Fig. 5.6 Results of Torsion for Model 1(b) and Modified Model 1(b)

It is observed that the variation of torsion for 15 storey 'U' shaped building is decreased by 76.56% after varying the stiffness parameters as shown in Fig. 5.6

Model	Number of storeys	Eccentricity	Torsion (kN-m)
Model 1(c)	18	2.32	9344.246
Modified model 1(c)	18	1.39	2566.915

Table 5.3 Results of Eccentricity and Torsion for Model 1(c) and Modified Model 1(c)

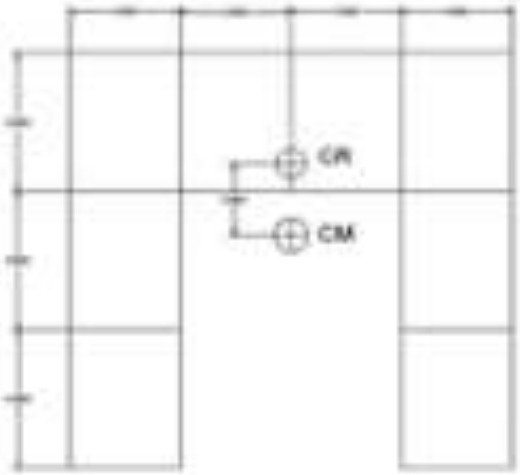

Fig. 5.7 Position of Centre of Mass and Centre of Rigidity for Model 1(c)

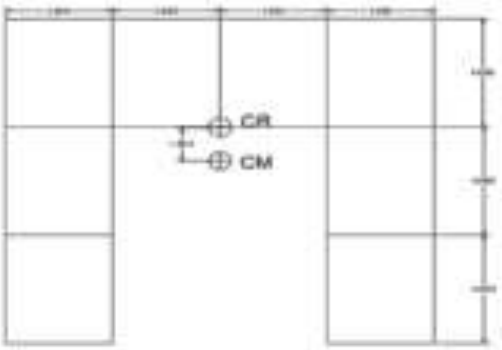

Fig. 5.8 Position of Centre of Mass and Centre of Rigidity for Modified Model 1(c)

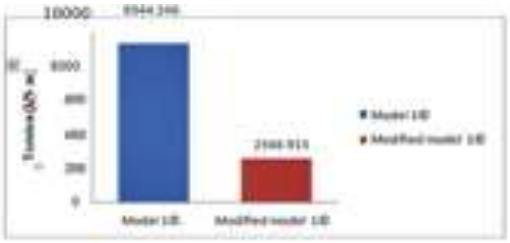

Fig. 5.9 Results of Torsion for Model 1(c) and Modified Model 1(c)

It is observed that the variation of torsion for 18 storey U shaped building is decreased by 72.53% after varying the stiffness parameters as shown in Fig. 5.9

Fig. 5.10 Position of Centre of Mass and Centre of Rigidity for Model 2(a)

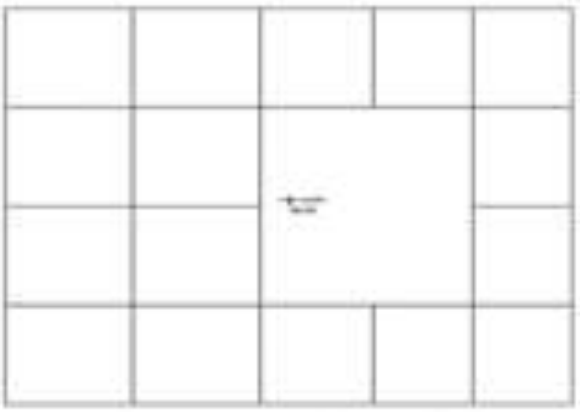

Fig. 5.11 Position of Centre of Mass and Centre of Rigidity for Modified Model 2(a)

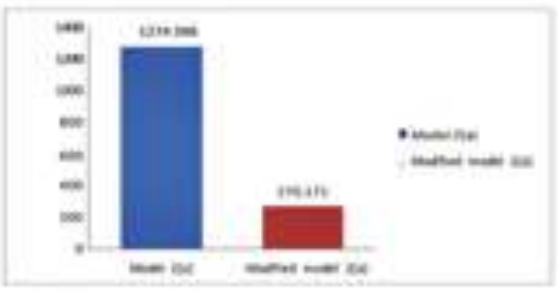

Fig. 5.12 Results of Torsion for Model 2 and Modified Model 2(a)

It is observed that the variation of torsion for 12 storey building with openings is decreased by 78.80% after varying the stiffness parameters as shown in Fig. 5.12

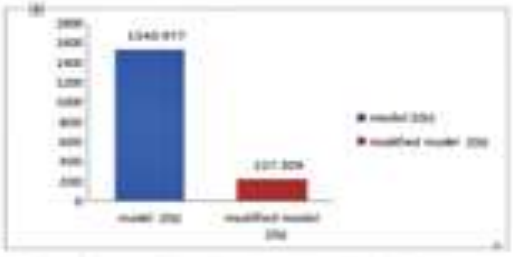

Fig. 5.13 Results of Torsion for Model 2(b) and Modified Model 2(b)

It is observed that the variation of torsion for 15 storey building with openings is decreased by 85.21% after varying the stiffness parameters as shown in Fig. 5.13

Model	Number of storeys	Eccentricity	Torsion (kN-m)
Model 2(c)	18	0.258	1678.938
Modified model 2(c)	18	0.017	162.205

Table 5.6 Eccentricity and Torsion Values of Model 2(c) and Modified Model 2(c)

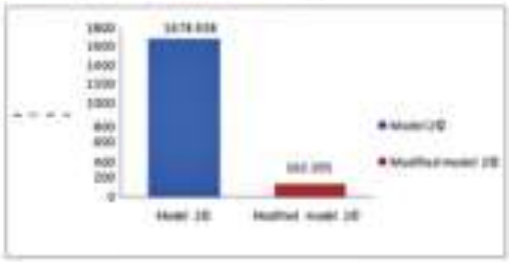

Fig. 5.18 Results of Torsion for Model 2(c) and Modified Model 2(c)

It is observed that the variation of torsion for 18 storey building with openings is decreased by 90.33% after varying the stiffness parameters as shown in Fig. 5.18

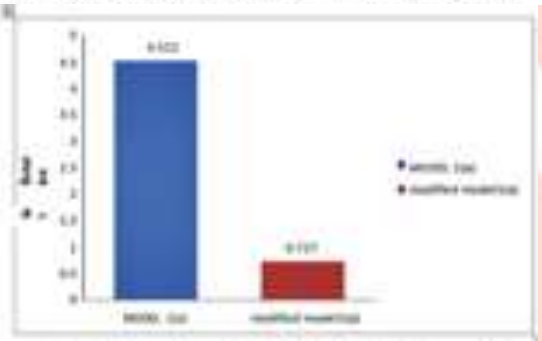

Fig. 5.19 Joint rotation Variation for Model 1(a) and Modified model 1(a)

It is observed that the variation of joint rotation for 12 storey U shaped building is decreased by 83.88% after varying the stiffness parameters as shown in Fig. 5.19

Fig. 5.17 Position of Centre of Mass and Centre of Rigidity for Modified Model 2(c)

5.2 Comparison of Joint Rotation

Model	Number of storeys	Rotation at a joint (Rz)	
		NLTH_X Max($x10^{-3}$)	NLTH_Y Max
Model 1(a)	12	4.512	0
Modified model 1(a)	12	0.727	0

Table 5.7 Results of Joint Rotation of Model 1(a) and Modified Model 1(a)

Model	Number of storeys	Rotation at a joint (Rz)	
		NLTH_X Max($x10^{-3}$)	NLTH_Y Max
Model 1(b)	15	7.476	0
Modified Model 1(b)	15	3.119	0

Table 5.8 Results of Joint Rotation for Model 1(b) and Modified Model 1(b)

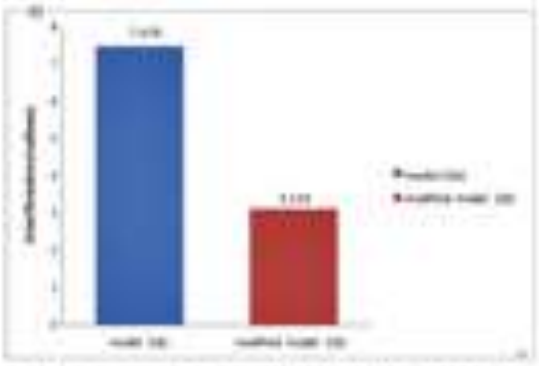

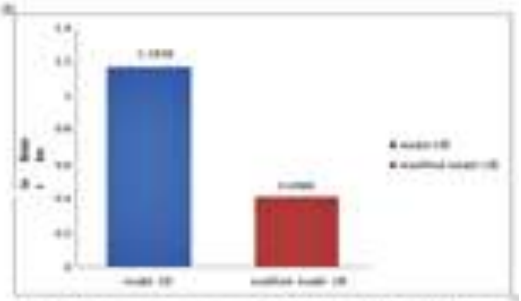

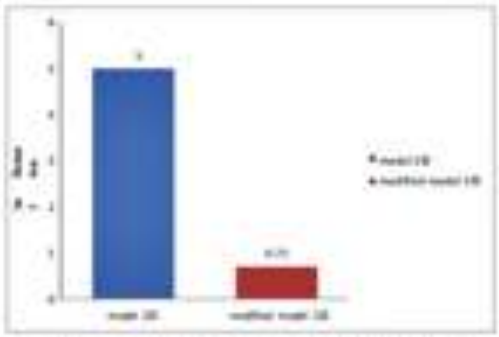

VII. CONCLUSION

The following conclusions drawn from the present work:

- Torsion percentage in asymmetrical buildings is significantly decreased by minimizing the stiffness eccentricity. Torsion reduces to 72%, 76% and 72% for 12 storey U shaped building, 15 storeys U shaped building and 18 storeys U shaped building.
- Percentage of torsion in asymmetrical buildings is decreased by minimizing the stiffness eccentricity. Torsion reduces to 79%, 85% and 90% for 12 storey building with openings, 15 storey building with openings and 18 storey building with openings.
- Percentage of joint rotation is significantly reduced by varying the stiffness parameters. Joint rotation reduced to 84%, 58%, and 65% for 12 storey U shaped building, 15 storeys U shaped building and 18 storeys U shaped building.
- Percentage of joint rotation is significantly reduced by varying the stiffness parameters. Joint rotation reduced to 78%, 75 %, and 86% for 12 storey building with openings, 15 storey building with openings and 18 storey building with openings.
- Thereby a maximum decrease in torsion is 90% for 18 storey building with openings. And maximum decrease in joint rotation is 86% for 18 storey building with openings.

6.3 Scope for Further Study

As the various researches are getting attracted towards the computer software, the scope of the studies under the particular topic can be done using different seismic zones and also using different earthquake data and effect of bracing systems on torsion for buildings with combined plan, stiffness and mass irregularity.

REFERENCES

1. Anil Chopra (2004). "Seismic Response of Vertical irregular Frames: Response History and Modal Pushover Analysis". Journal of Structural Engineering, Vol. 130(8).
2. Anvesh (2015). "Effect of Mass Irregularity on Reinforced Concrete Structures using Etabs". International Journal of Innovative Research in Science, Engineering andTechnology, Vol. 4(10).
3. Devesh Soni, P. and Bharat Mistry, B., (2006). "Qualitative review of seismic response of vertically irregular building frames". ISET Journal of Earthquake Technology, Vol. 43 (4), Pp. 121-132.
4. Gowthami, V., Satheesh, V.S. and Suresh Babu, S., (2016). "An Epitome on 3D Plan Irregularities of RC Buildings with Seismic Analysis". International Journal forScientific Research & Development, Vol. 4(1).

5. Gunay Ozmen, Konuralp Girgin and Durgun, (2014). "Torsional Irregularity in Multi-Story Structures". International Journal of Advanced Structural Engineering(IJASE), Vol.6(4), Pp. 121–131.
6. Gupta and Pajagade, P.S., (2012). "Torsional behaviour of multi-storey buildings with plan as well as vertical irregularities". International Journal for Scientific Research &Development, Vol. 7(3).
7. Han Seon Lee and Dong Woo Co, (2002)."Seismic response of high-rise RC bearing-wall structures with irregularities at bottom stories". 13th World Conference onEarthquake Engineering Vancouver.
8. IS: 1893-2002. "Criteria for Earthquake resistant design of structures", Part-1 General provisions and buildings (Sixth revision), Bureau of Indian Standards, New Delhi, India.
9. IS 456:2000. Indian standard Plain and reinforced concrete – Code of Practice, Bureau ofIndian standard, New Delhi.
10. Kusuma, B., (2017). "Seismic Analysis of a High-rise RC Framed Structure with Irregularities". International Research Journal of Engineering and Technology (IRJET),Vol.4(7).
11. Lakshmi Subash, (2017). "Seismic Behaviour of Vertically Irregular Reinforced Concrete Buildings with P-Delta Effect". International Research Journal of Engineering andTechnology, Vol. 4(4).
12. Moehle, (1984). "Seismic Response of Vertically Irregular Structures". Journal ofStructural Engineering, Vol. 110(9).
13. Neha Modakwar, P., Sangita Meshram, S. and Dinesh Gawatre, W., (2014). "Seismic Analysis of Structures with Irregularities". Journal of Mechanical and Civil Engineering, Pp. 63-66.
14. Rahila Thaskeen and Shinu Shajee, (2016). "Torsional Irregularity of Multi-storey Structures". International Journal of Advances in Engineering and Technology, Vol. 5(9).
15. Sagar Patil, B. and Gururaj Katti, B., (2015). "Study of Behavior of Plan & Vertical Irregularity by Seismic Analysis". International Journal for Scientific Research andDevelopment, Vol. 3(4).
16. Dubey, S.D. and Sangamnerkar, P.D., (2011). "Seismic Behaviour of Asymmetric RC Buildings". International Journal of Advances in Engineering and Technology, Vol. 2(4).
17. Shaikh Abdul Aijaj Abdul Rahman and Girish Deshmukh, (2013). "Seismic Response of Vertically Irregular RC Frame with Stiffness Irregularity at Fourth Floor". InternationalJournal of Emerging Technology and Advanced Engineering, Vol. 3(8).
18. Sumit Gurjar and Lovish Pamecha, (2017). "Seismic Behaviour of Buildings Having Vertical Irregularities". International Journal of Engineering Science Invention Researchand Development; Vol. 3(10).
19. Varadharajan, S., Sehgal, V.K. and Saini, B., (2011). "Review of different Structural irregularities in buildings". Journal of Structural Engineering, Vol. 39(5), Pp. 393-418
20. Vipin Gupta and Pajgade, P.S., (2015). "Torsional Behavior of Multistorey Buildings with Different Structural Irregularities". International journal of research in engineering,science and Technologies.

Study on Soil Structure Interaction and Base Isolated System for Seismic Performance of Structures Resting on Different Types of Soils

[1]Dr. S.Amaresh Babu, [2]Ahmed Zubedi
[1]Professor, [2]Student
[1]Nawab Shah Alam Khan College of Engineering and Technology,
[2]Structural Engineering, Nawab Shah Alam Khan College of Engineering and Technology

Abstract - **The conventional approach to seismic resistant design is to incorporate adequate strength, stiffness and inelastic deformation capacity into the building structure so that it can withstand induced inertia forces. This was with the presumption that during strong ground motion, whenever inertia forces exceed their design earthquake levels, the structure will dissipate this excess energy through deformations at predefined locations scattered over the structural framework. It was observed that, even with members designed for ductility, the structures did not always perform as desired. It was realized that a design based only on the principle of incorporating ductility as a safeguard against seismic effects needs a critical review. Engineers came up with the innovative idea of introducing a flexible medium between supporting ground and the building, thereby decoupling the structure from the energy rich components of seismic ground motion. This strategy came to be known as the Base Isolation method.This thesis aims to determine the significance of using Base Isolation as a technique to withstand the seismic forces. This thesis also aims to show the importance to consider soil structure interaction rather than analyzing the structure as fixed base. The comparison is mainly done between structures with soil structure interaction effects and base isolated structures. The analysis is done using computer program SAP2000 v18. The method of analysis is Fast Nonlinear Analysis (FNA). There are 18 models which are analyzed in which there are symmetric and asymmetric in plan models, which are analyzed as fixed base models, models with the consideration of soil structure interaction, and models with base isolation (lead rubber bearing). These models are assumed to be resting on three soil types namely limestone, stiff clay, and loose sand. All the models are G+13 storey. The results show that considering soil structure interaction effects for structures resting on medium and soft soils is more significant when compared to structures resting on hard soil because there is not much difference noticed in the response of structures with and without soil structure interaction effects resting on hard. Also base isolation system is best suited for structures resting on hard soil. The base shear, storey displacements, and torsion are reduced to a great extent**

keywords - **Base Isolation, Soil Structure Interaction, Fast Nonlinear Analysis.**

1. INTRODUCTION

1.1 General: An earthquake is the perceptible shaking of the surface of the Earth due to underground movement along a fault plane or from volcanic activity. The severity of the shaking can range from barely felt to violent enough to toss people around. An Earthquake is the result of sudden release of energy in the Earth's crust creating seismic waves, which causes vibration of the ground and structures resting on it. Depending on the characteristics of these vibrations, the ground may develop cracks, fissures and settlements. Shaking and ground rupture are the main effects, principally resulting in more or less severe damage to buildings and other rigid structures.Earthquakes generate two types of seismic waves namely Body Waves and Surface Waves. Body waves travel through the interior of the Earth. They create ray paths refracted by the varying density and modulus (stiffness) of the Earth's interior. The density and modulus, in turn, vary according to temperature, composition, and phase. This effect resembles the refraction of light waves. Body Waves include Primary and Secondary waves. Primary waves (P-waves) are compressional waves that are longitudinal in nature. P waves are pressure waves that travel faster than other waves through the earth to arrive at seismograph stations firstly, hence the name "Primary". These waves can travel through any type of material, including fluids, and can travel at nearly twice the speed of S waves. In air, they take the form of sound waves, hence they travel at the speed of sound. Typical speeds are 330 m/s in air, 1450 m/s in water and about 5000 m/s in granite.Secondary waves (S-waves) are shear waves that are transverse in nature. Following an earthquake event, S-waves arrive at seismograph stations after the faster-moving P-waves and displace the ground perpendicular to the direction of propagation. S-waves can travel only through solids, as fluids (liquids and gases) do not support shear stresses. S-waves are slower than P-waves, and speeds are typically around 60% of that of P-waves in any given material. Seismic surface waves travel along the Earth's surface. They can be classified as a form of mechanical surface waves. They are called surface waves, as they diminish as they get further from the surface. They travel more slowly than seismic body waves (P and S). In large earthquakes, surface waves can have an amplitude of several centimeters. The possible risk of loss of life adds a very serious dimension to seismic design, putting a moral responsibility on structural engineers. Objective of Earthquake Resistant Design is to make such buildings that can resist effect of ground motion and would not collapse during the strong Earthquake.All the components of the structure and foundations are designed to resist inertia forces in addition to the normal forces. All the walls

must be jointed properly, so that they can act together against the earthquake shaking at the time of seismic force transferring to the ground.

1.2 Soil Structure Interaction: Normally, in the conventional method of the dynamic analysis of a building under seismic conditions, base of the structure is considered to be fixed and subjected to the free field ground motion. Such ground motion is that which is not influenced by the presence of the structure. This is applicable to rock formations because due to extremely high stiffness of rock, seismic wave motions therein is not constrained by the structure supported thereon. Hence, it can be termed as Free Field Motion. However, if the structure is supported on soft soil of considerable thickness overlying the rock, then the structure and soil will interact with one another to influence the behaviour of both. This is termed as Soil Structure Interaction. If a lightweight flexible structure is built on a very stiff rock foundation, a valid assumption is that the input motion at the base of the structure is the same as the free-field earthquake motion. If the structure is very massive and stiff, and the foundation is relatively soft, the motion at the base of the structure may be significantly different than the free-field surface motion. For code design buildings it is important to consider the effect of the SSI.

1.3 Base Isolation : It is a system that may be defined as a flexible or sliding interface positioned between a structure and its foundation, for the purpose of decoupling the horizontal motions of the ground from the horizontal motions of the structure, thereby reducing earthquake damage to the structure and its contents. Base isolation system absorbs and deflects the energy released from the earthquake before it is transferred to the structure. Base isolation is a passive control system meaning thereby that it does not require any external force or energy for its activation. The base-isolation techniques prove to be very effective for the seismic protection of new framed buildings as well as for the seismic retrofitting of existing ones. An isolation system should be able to support gravity loads (including those due to vertical seismic acceleration), be sufficiently stiff to minimize displacements under repeated small magnitude lateral loads such as those due to wind, be highly flexible to absorb the energy during strong motion earthquakes and possess capability to self-centre after an earthquake event. Quite clearly, this means that the isolator should possess non-linear stiffness characteristics. It should also possess adequate damping characteristics to assist dissipation of seismic energy and not have excessive lateral displacement across the isolator interface. Midrise structures with 10 to 15 stories are the most suitable to be base-isolated. Base isolation provides an excellent substitute for fixed base design where earthquakes are frequent. The economy of base isolation is not viewed in terms of its initial installment but over the design period of the structure during which it is expected to experience earthquake. After an event of earthquake, the repair of structure, and loss of non-structural components may be a more costly affair than installing base isolation. So far, base isolation technology has been adapted in very important structures such as hospitals, laboratories, and data centres etc. Also, base isolation has been found to be extremely useful for retrofitting of the old structures where the aesthetic, architectural and heritage value is required to be maintained intact.

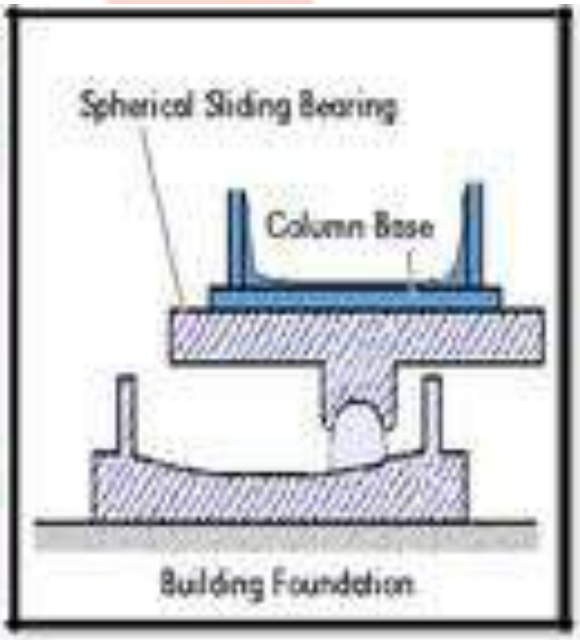

Fig.1. Elastometric Isolators Fig.2 Flat Sliding Bearing being used as an Isolator

1.4 Objectives of the Study

- To study the response of structures for Soil Structure Interaction effects resting on different types of soils subjected to seismic effects.
- To study the response of structures for Base Isolated system resting on different soils subjected to seismic effects.
- To compare the response of structures for Soil Structure Interaction effects & Base Isolated system resting on different types of soils.

2. LITERATURE REVIEW

Subramani et al.(2014) studied the ”Earthquake Analysis of structure by Base Isolation technique in SAP”. Their objectives were to Study the Effectiveness of Isolated base structures over Fixed base structure in terms of immediate occupancy and life safety by pushover analysis and To compare the storey drifts of both the structures. Their research work did not include

asymmetric in plan structures and also soil structure interaction was not considered during analysis. Hard and medium soils were also not considered for analysis. These research gaps have been overcome in this dissertation.

Chandak (2013) studied the "Effect of Base Isolation on the Response of Reinforced Concrete Building". Their main objective was to investigate the differences caused by the use of different codes in the dynamic analysis of multistoried RC buildings with fixed and isolated base conditions. The analysis was done by response spectrum method using computer program SAP2000. The design spectra recommended by IS 1893-2002 part 1 and Euro Code 8 were considered for comparison. Two types of base isolators, rubber bearing and friction isolator were used. The research work does not take soil structure interaction into consideration. This dissertation overcomes the research gap by considering soil structure interaction.

Dia Eddin Nassani and Mustafa Wassef Abdulmajeed (2015) studied the effectiveness of "Seismic Base Isolation in Reinforced Concrete Structures". Their objective was to study the effectiveness of isolated base(HDR) structures over fixed base structures. The analysis was performed in SAP2000 following time history analysis using El-centro earthquake data. 4 structures were analysed in which two are symmetrical and two are asymmetrical in plan. Their research work did not consider soil structure interaction. This dissertation covers the research gap.

Meena Noorzai et al.(2015) studied the "Response of Fixed Base and Isolation Base (LRB)", on G+25 storied buildings using ETABS software. LRB was used as base isolator. The soil structure interaction is not considered. This dissertation covers up this research gap.

Sabu et al.(2014) studied the "Effectiveness of Lead Rubber Base Isolators, for seismic resistance of Buildings, supported on different soil stratas", on G+7 storey building by comparing the analysis with and without LRBs in seismic zone V on different soil types using computer program ETABS. In this case study the soil structure interaction was not considered and also asymmetric in plan buildings were not considered. This dissertation fills the research gap.

Jenifer Priyanka et al.(2012) performed "Studies on Soil Structure Interaction of Multi Storeyed Buildings with Rigid and Flexible Foundation", analysed G+10 storey buildings with Fixed and Flexible supports subjected to seismic loads under different soil conditions like hard, medium and soft using software STAAD Pro v8i. Size of the plan was 30 x 30 m in zone V. Asymmetric in plan structure was not considered and base isolation technique was not considered in this project. This dissertation fills these research gaps.

3. METHODOLOGY

3.1 General

Earthquake and its occurrence and measurement, its vibration effect and structural response have been continuously studied for many years in earthquake history and thoroughly documented in literature. Since then the structural engineers have tried hard to examine the procedure, with an aim to counter the complex dynamic effect of seismically induced forces in structures, for designing of earthquake resistant structures in a refined and easy manner. This reexamination and continuous effort has resulted in several revision of Indian standard: 1893: (1962, 1966, 1970, 1975, 1984 & 2002) code of practice on the ―criteria of earthquake resistant‖ by the bureau of Indian standards (BIS), New Delhi. In order to properly interpret the codes and their revisions, it has become necessary; that the structural engineer must understand the basic design criteria and procedures for determining the lateral forces. Various approaches to seismic analysis have been developed to determine the lateral forces, ranging from purely linear elastic to non-linear inelastic analysis. Many of the analysis techniques are being used in design and incorporated in codes of practices of many countries. However, this chapter is restricted to method of analysis described or employed in IS 1893 (part 1): 2002 of ―criteria for earthquake resistant design of structures, essentially to building although in some cases that may be applied to other type of structures as well.

3.2 Analysis : Various analysis procedures can be used out of which Fast Nonlinear Analysis has been adopted for this dissertation

3.2.1 Fast Nonlinear Analysis

Fast Nonlinear Analysis (FNA) is a modal analysis method useful for the static or dynamic evaluation of linear or nonlinear structural systems. Because of its computationally efficient formulation, FNA is well-suited for time-history analysis, and often recommended over direct-integration applications. During dynamic-nonlinear FNA application, analytical models should be primarily linear-elastic and have a limited number of predefined nonlinear members.

In addition to nonlinear material force-deformation relationships, these link objects may simulate concentrated damping devices, isolators, and other energy-dissipating technologies. If fuse mechanisms are not integral to the design intention, an initial elastic analysis may reveal locations where inelasticity is likely to occur. However, it is always best to predefine inelastic mechanisms such that their design may provide for sufficient ductility, while elastic systems are ensured sufficient strength. Capacity Design provides for a more reliable model and a better-performing structure.

The efficiency of FNA formulation is largely due to the separation of the nonlinear-object force vector RNL(t) from the elastic stiffness matrix and the damped equations of motion, as seen in the fundamental equilibrium equation of FNA, expressed as:

$$M\,\ddot{u}(t) + C\,\dot{u}(t) + K\,u(t) + RNL\,(t) = R(t)$$

Stiffness and mass orthogonal load dependent ritz vectors represents the equilibrium relationships within the elastic structural system. At each time increment, the uncoupled modal equations are solved exactly, while forces within the predefined nonlinear DOF, indexed within RNL(t), are resolved through an iterative process which converges to satisfy equilibrium. Following this procedure, FNA is an efficient and accurate dynamic-nonlinear application which satisfies equilibrium, force deformation, and compatibility relationships

4. Case Study Description

4.1 General

There are 18 structures which are analysed using the CSI software SAP2000 v18. These 18 structures are divided into three categories. 6 structures are analysed as Fixed Base buildings, 6 structures are analysed considering Soil Structure Interaction, and 6 structures are analysed by introducing Base Isolation technique (LRB). The design of LRB is shown in chapter III Methodology.

All the 18 structures are G+13 storey. All these structures are analysed by Fast Nonlinear Analysis method. For each category there are 3 buildings symmetric in plan and 3 buildings asymmetric in plan. Each 3 buildings are analysed on three different soil conditions namely Limestone (Hard), Stiff Clay (Medium), and Loose Sand (Soft). For better understanding, the different models are categorised using flow chart below:

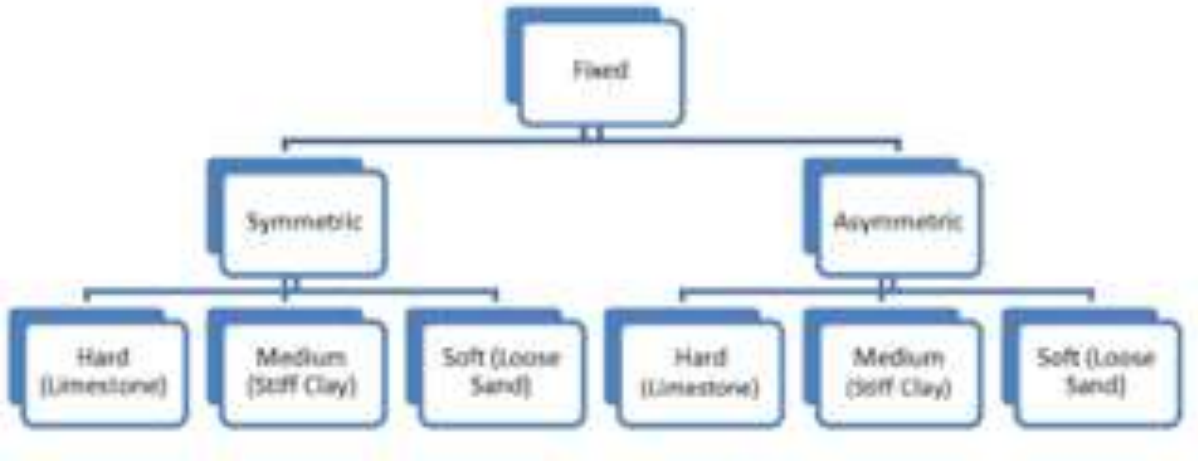

Fig. 3 Classification of Fixed Base Structures

Similarly SSI and BI structures are also Classified as shown above.

4.2 Details of Plan, Member Sizes and Materials used

The plan details are shown below:

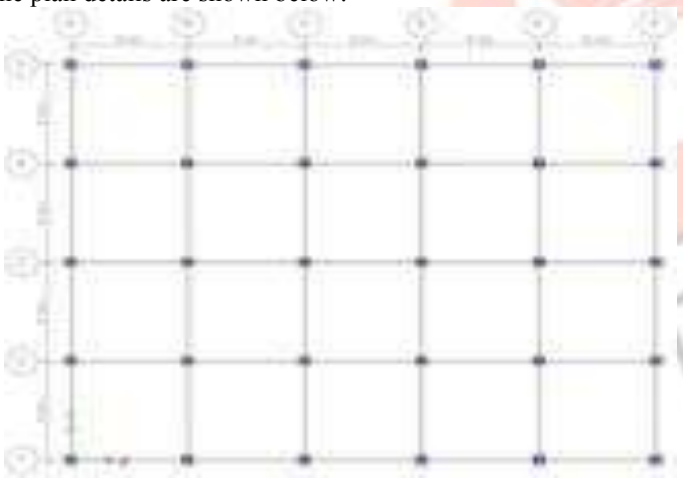

Fig. 4 Plan of Symmetric Building

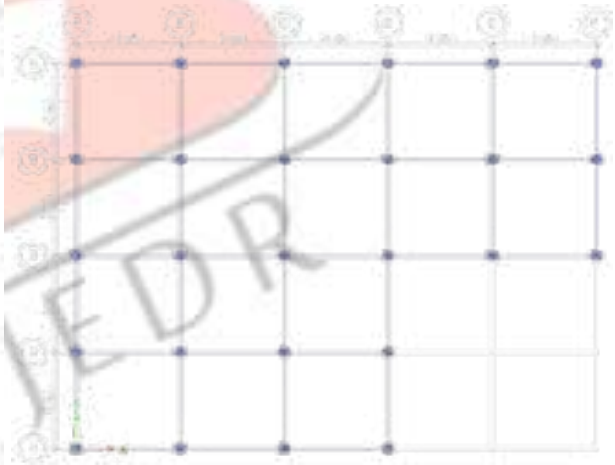

Fig. 5 Plan of Asymmetric Building

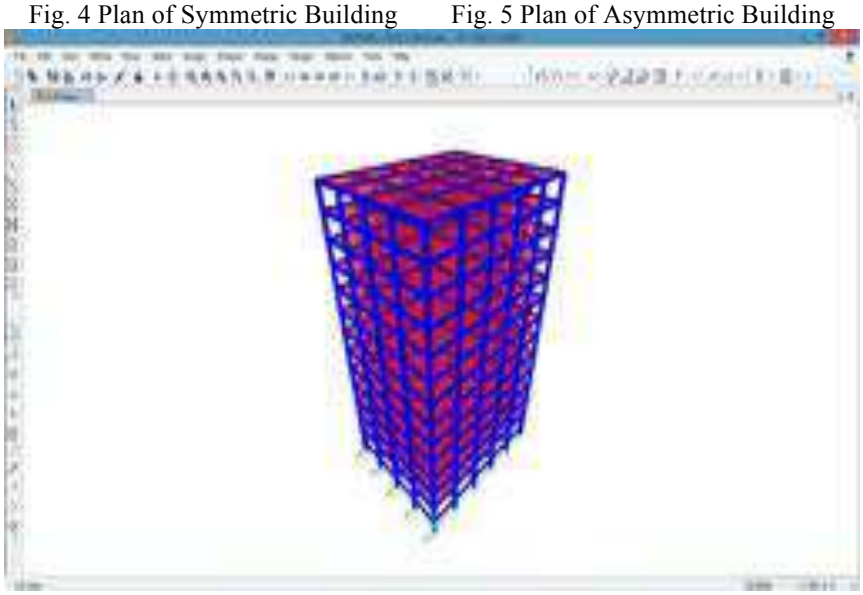

Fig.6. View of Symmetric Building in SAP2000

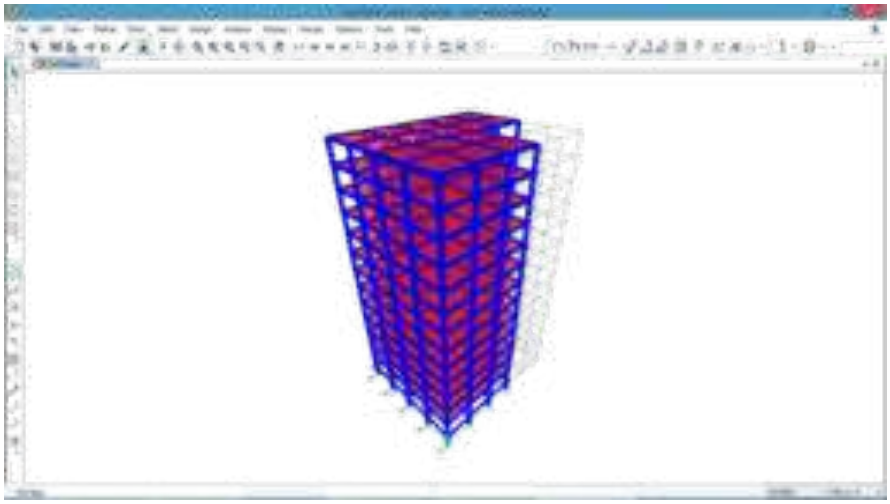

Fig .7 View of Asymmetric Building in SAP2000

S No.	Building Description	
1	Zone	V
2	[illegible]	0.24
3	[illegible]	5
4	[illegible]	1
5	[illegible]	41.6 m
6	[illegible]	550/500 mm
7	[illegible]	300x450 mm
8	[illegible]	120 mm
9	[illegible]	3 m
10	[illegible]	3 m
11	[illegible]	415 N/
12	[illegible]	3 kN/m
13	[illegible]	17 kN/m
14	[illegible]	M 30

5. Results and Discussions

5.1 General

In this chapter, dynamic analysis is performed by using SAP2000 v18.0.1. The results and discussion are presented for eighteen G+13 storey Reinforced Concrete Frame models Symmetric and Asymmetric in plan which are Fixed base models, models with the consideration of soil structure interaction, and Base Isolated (LRB) models on different soil conditions that are Limestone (Hard), Stiff Clay (Medium), and Loose Sand (Soft). The results are compared in terms of base shear, storey displacement and torsion.

5.2 Base Shear

Base shear is an estimate of the maximum expected lateral force that will occur due to seismic ground motion at the base of a structure.

5.2.1 Base Shear for Asymmetric in plan building on Hard Soil (Limestone) for X-direction

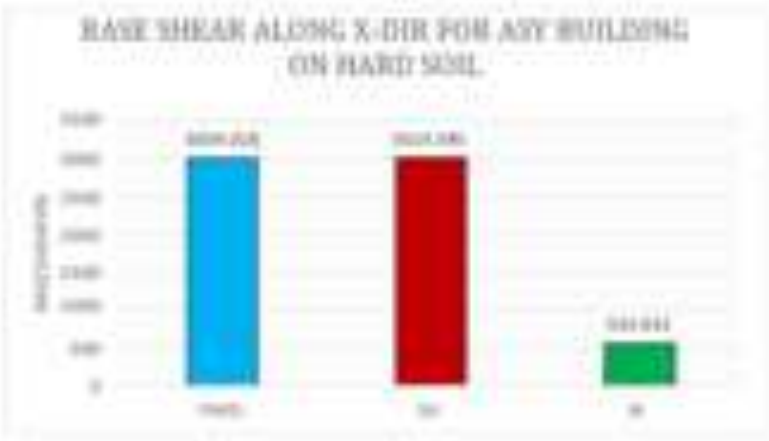

Fig 5.1 Base Shear for Asymmetric building on Hard Soil in X-direction

From Fig. 5.1, it is found that the Base Shear for Fixed Base building is 3004.018 KN. But when the structure is analysed considering soil structure interaction, the Base Shears increased to 3014.395KN. When the Base Isolated structure is analysed, it is found that the Base Shear has reduced by 81.6% i.e., 554.642 KN when compared with structure with the consideration of SSI as the response of model considering soil structure interaction is close to real values when compared to Fixed Base model.

5.2.2 Base Shear for Asymmetric in plan building on Medium Soil (Stiff Clay) for X – direction

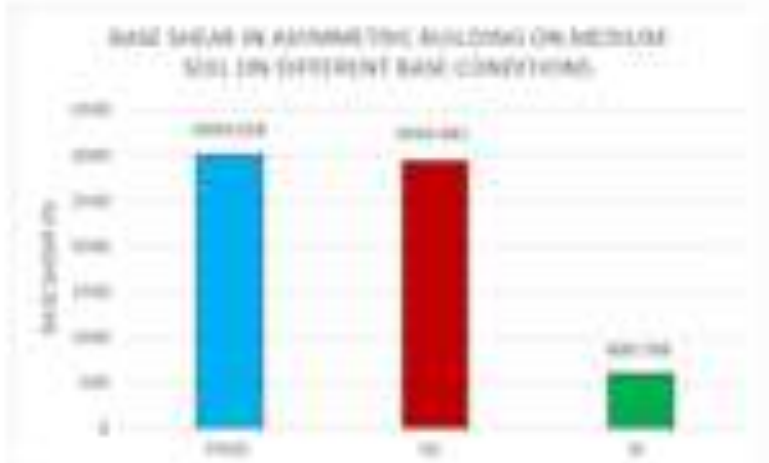

Fig 5.2 Base Shear for Asymmetric Building on Medium Soil in X-direction

From Fig. 5.2, it is found that Base Shear for fixed base model is 3004.018 KN. But when soil structure interaction is considered, the base shear reduces to 2930.581 KN i.e., 2.44% reduction. When the base isolated model was analysed, the Base Shear reduced to 600.706 KN i.e., 79.5% reduction.

5.2.3 Base Shear for Symmetric in plan building on Soft soil (Loose Sand) in X-direction

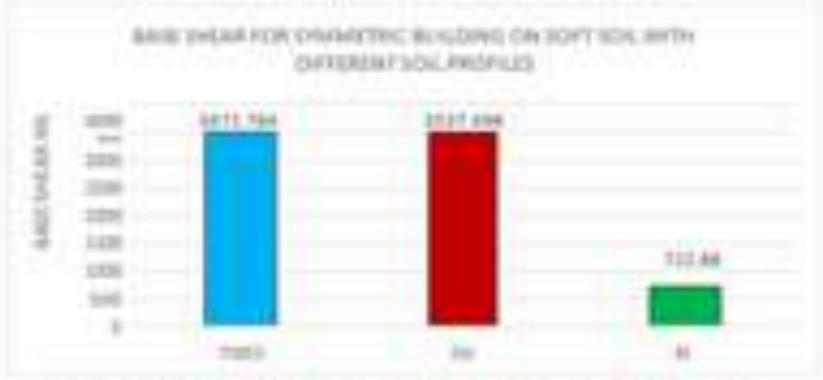

Fig. 5.3 Base Shear for symmetric building on Soft soil in X-direction

It is observed from Fig. 5.6 that the base shear for fixed base structure is found to be 3671.784 KN. When soil structure interaction was considered, the base isolation was found to be 3537.498 KN. When base isolated building is analysed, the base shear reduced to 722.88 KN which is 79.595% less.

5.2.4 Base Shear for Symmetric in plan building on Medium Soil (Stiff Clay) in X-direction

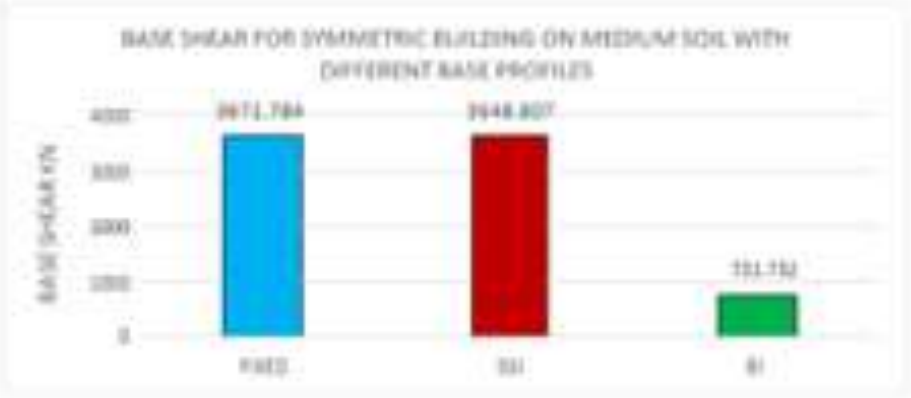

Fig. 5.4 Base Shear for symmetric building on Medium soil in X-direction

It is observed from Fig. 5.5 that the base shear of fixed base structure is 3671.784 KN. The base shear of structure whose analysis included soil structure interaction effects was found to be 3648.804 KN. The base shear of base isolated structure is 721.732 KN that is there is a reduction of 80.22%.

5.3 Storey Displacements

5.3.1 Storey Displacements for Asymmetric structure on hard soil in X-direction

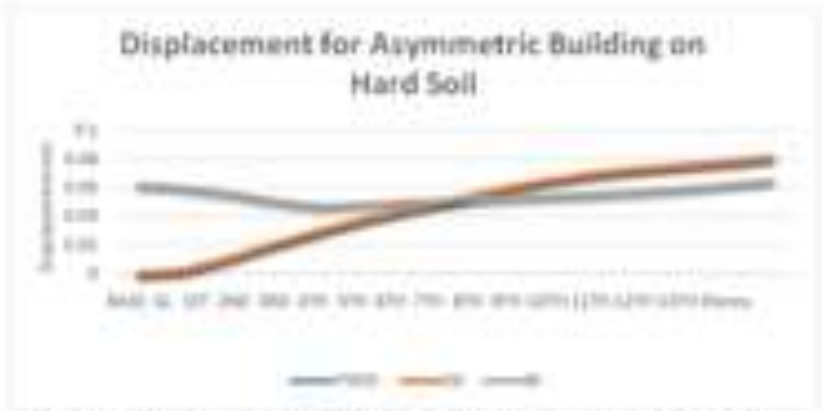

Fig. 5.5 Storey displacements for Asymmetric structure on hard soil in X-direction

In these structures, it is observed from Fig. 5.7 and Table 5.1, the displacements are increasing in fixed base from bottom to top and same goes for structure with soil structure interaction effects. But it is not the same for base isolated structure. The

displacements decreases upto almost half the height of structure and then increases. But the maximum displacement is reduced by 20.3% when compared to structure with soil structure interaction effects.

5.3.2 Storey Displacements for Symmetric Structure on Limestone in X-direction

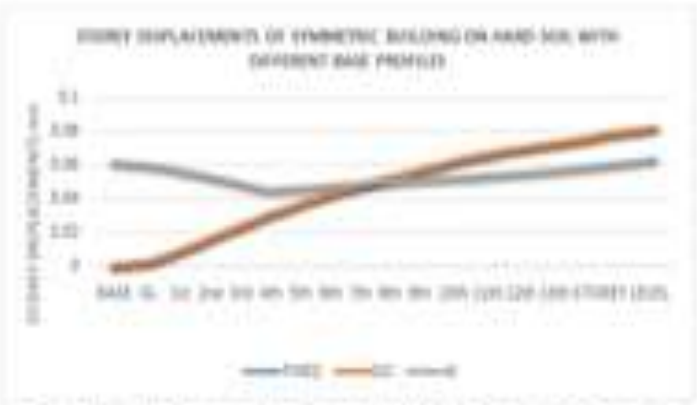

Fig. 5.6 Storey displacements for Symmetric building on Limestone in X-direction

Table 5.2 Storey Displacements for Symmetric building on Limestone in X-direction

Storey	Fixed	SSI	BI
Base	0		
G			
1st			
2nd			
3rd			
4th			
5th			
6th			
7th			
8th			
9th			
10th			
11th			
12th			

In these structures, it is observed from Fig. 5.6 and Table 5.2 that the displacements are increasing in fixed base from bottom to top and same for structure with soil structure interaction effects. But for base isolated structure, the displacements decreases upto almost half the height of structure and then increases. But the maximum displacement is reduced by 22.75% when compared to structure with soil structure interaction effects.

5.4 Torsion

Torsion is the action of twisting or the state of being twisted. It is produced when the centre of mass and centre of rigidity do not coincide.

Fig. 5.8 Torsion for Asymmetric structure resting on Limestone

It is found from Fig.5.8 that the torsion experienced by the fixed base model is 33549.0139 KN-m. When considering soil structure interaction, the torsion increased to 33620.8532 KN-m. But when base isolated structure was analysed, the torsion reduced to 6666.3944 KN-m which is 80.17% less when compared to structure with soil structure interaction

6.Summary and Conclusions

6.1 Summary

This project report deals with the analysis of 18 models which are fixed base models, models with soil structure interaction effects, and base isolated models. The models are analysed using Fast Nonlinear Analysis method which is discussed in detail in Chapter 3, Methodology. The models are analysed on three types of soils namely Limestone, Stiff Clay, and Loose Sand. The structures are of two types i.e. symmetric in plan and asymmetric in plan. All these models are G+13 storey.

The results show that the consideration of soil structure interaction effects is more significant for models resting on stiff clay and loose sand when compared to limestone. The Base Isolation system is most effective for structures resting on limestone when compared to structures resting on stiff clay and loose sand.

6.2 Conclusions

6.2.1 General Conclusions

After the analysis was carried out, and the results were compared, it is found that considering soil structure interaction for structures resting on medium (stiff clay) and soft soils (loose sand) is more significant when compared to structures resting on hard soil (limestone) as there is not much difference in the response of structures resting on hard soil with and without the consideration of soil structure interaction Base isolation system is found to be most effective for structures resting on hard soil (limestone) when compared to structures resting on medium soil (stiff clay) and soft soil (loose sand). .

6.2.2 Specific Conclusions

Through the comparison in the response of structures for soil structure interaction effects and base isolation system, it is found that:

The base shear for structures resting on limestone is 81.5% less for base isolated system when compared to structures with soil structure interaction effects.

The base shear for structures resting on stiff clay is 80% less for base isolated system when compared to structures with soil structure interaction effects.

The base shear for structures resting on loose sand is 78.5% less for base isolated system when compared to structures with soil structure interaction effects.

The storey displacements for structures resting on limestone is 21.5% less for base isolated system when compared to structures with soil structure interaction effects.

The storey displacements for structures resting on stiff clay is 43% less for base isolated system when compared to structures with soil structure interaction effects.

The storey displacements for structures resting on loose sand is 45% less for base isolated system when compared to structures with soil structure interaction effects.

The torsion for structures resting on limestone is 80.5% less for base isolated system when compared to structures with soil structure interaction effects

The torsion for structures resting on stiff clay is 76% less for base isolated system when compared to structures with soil structure interaction effects.

The torsion for structures resting on loose sand is 75% less for base isolated system when compared to structures with soil structure interaction effects.

6.3 Scope for further study

The effectiveness of base isolation technique can be checked on different gradients of sloping ground differing the number of storeys on different soil strata.

Base Isolation along with different bracing systems could be used to further minimise the storey deflections.
Base Isolation could be implemented on vertical irregular and mass irregular buildings on different soil strata

References

[1] Chandak N. R., (2013), "Effect of Base Isolation on the Response of Reinforced Concrete Building", *Journal of Civil Engineering Research*, *3(4), 135-142.*

[2] Criteria for Earthquake Resistant Design of Structures,*Indian Standard 1893 Part- I2002,* New Delhi

[3] Dhananjay A. Chikhalekar, Murudi M.M., (Sept.2015) "Seismic Performance of Structures with Fixed Base, Base Isolated Structure and Structure with Viscous Damper", *International Journal of Research in Engineering and Technology, 4(9), 158-166*.

[4] Dhiraj Raj, "Non-linear Static Analysis of Building-Foundation System considering Soil-Structure Interaction using SAP 2000 v 14", *Research Scholar, Department ofEarthquake Engineering, IIT Roorkee.*

[5] Dia Eddin Nassani, Mustafa Wassef Abdulmajeed, (February 2015), "Seismic Base Isolation in Reinforced Concrete Structures", *International Journal of Research Studiesin Science, Engineering and Technology, 2(2), 1-13*.

[6] Jenifer Priyanka R.M., Anand N., Justin S., (December 2012) "Studies on Soil Structure Interaction of Multi Storeyed Buildings with Rigid and Flexible Foundation", *International Journal of Emerging Technology and Advanced Engineering, 2(12), 111-118*

[7] Ketan Bajaj, Jitesh Chavda T., Bhavik Vyas M., (December 2013), "Seismic Behaviour of Buildings on different types of Soils", *Proceedings of Indian GeotechnicalConference, Roorkee*,

[8] Meena Noorzai, M.N. Bajad, Neha Dodal, (May 2015), "Study Response of Fixed Base and Isolation Base", *International Journal of Innovative Research in Science,Engineering and Technology, 4(5), 3674-3681*.

[9] Sabu S.K., Chore H.S., Patil S.B., (2014), "Effectiveness of Lead Rubber Base Isolators, for Seismic resistance of Buildings, supported on different soil stratas", *2(4), 53-59*.

[10] Seismic Rehabilitation of Existing Buildings, *American Society of Civil Engineers 41-06,* United States of America.

[11] Sharad Manohar, Suhasini Madhekar, (2015), "Seismic Design of RC Buildings, Theory and Practise", *Springer Publications*.

[12] Subramani T., Jothi J., Kavitha M., (June 2014), "Earthquake Analysis of structure by Base Isolation Technique in SAP", *Int. Journal of Engineering Research andApplications, 4(6), 296-305*.

[13] Syed Ahmed Kabeer K I, Sanjeev Kumar K.S., (Oct 2014), "Comparison of two similar buildings with and without Base Isolation", *International Journal of AdvancedResearch, Ideas and Innovations in Technology, 1(1), 28-36.*

[14] Vinod Kumar Parma, Hiremath G.S., (June 2015) "Effect of Base Isolation in Multistoried RC Irregular Building using Time History Analysis", *InternationalJournal of Research in Engineering and Technology, 4(6), 289-292* .

Lateral Stability Analysis of High Rise Structure with variation of plan configuration with respect to height and the Effect of Outrigger and Belt Trusses Systems

[1]Syed Ammar Ahmed Maaz, [2]Mohd Mubasheer Shazeb
[1]Student, [2]Assistant Professor
Nawab Shah Alam Khan College Of Engineering And Technology

Abstract - **The outrigger and belt truss system is one of the most efficient systems used to effectively control the excessive drift due to lateral load, so that, during small or medium lateral load due to either wind or earthquake load, the risk of structural and non-structural damage can be minimized. For high-rise buildings, particularly in seismic active zone or wind load dominant, this system can be chosen as an appropriate structure. This paper studies the efficient use of outrigger and belt truss system for high-rise concrete building subjected to wind or earthquake load. Seven 44-storey models of outrigger and belt truss system are subjected to wind and earthquake load, analyzed and compared to find the lateral displacement reduction related to the types of outrigger and belt system. The analysis has been carried out to study the effect and performance of outrigger system in 40-storey building. The outrigger system is provided at different levels along the height of the building. The depth of the Outrigger and belt trusses is equal to the height of the typical story and maintained same in all the models. The key parameters discussed in this paper include lateral deflection, storey drifts, base shear and fundamental time periods. Loads are considered as per Indian Standards IS: 875(Part1)-1987, IS: 875(Part2)-1987, IS: 875(Part3)-1987 and IS: 1893(Part-1) - 2002. The modeling and analysis were performed using finite element software ETABS 16.**

keywords - **Outrigger and belt truss system, lateral load, lateral displacement, storey drifts, base shear and fundamental time periods**

I. INTRODUCTION

Improvement of the large structures has been rapidly increasing the general knowledge of new challenges that need to be met through building judgement. In present high constructions, wind or earthquake often induce lateral loads by arranging paired shear walls. However, when structure increases in height, the stiffness of the structure turns out to be increasingly important to provide the structure with sufficient lateral stiffness. The lateral load resisting system effectively controls over the top drift because of lateral load, so that, amid little or medium lateral load because of wind or earthquake load, the danger of auxiliary and non-basic harm can be limited. For tall structures, especially either in wind load or seismic zone overwhelming, these frameworks are chosen as a suitable structure. Outrigger and belt truss system have recently been widely used to minimize lateral drift. In order to attain the necessary rigidity of the large structure bracing sizes, extra lateral load resistant system such as outriggers and belt truss was needed. Outriggers and belt truss was required. The location of the outrigger truss increases the structure's efficient depth and improves the lateral stiffness owing to horizontal load effectively. Conventionally high buildings are built for the goal of office buildings, commercial, shopping malls and hotels, suburban. Improvement of tall buildings includes Different composite elements for instance economic matters, necessities, construction regularities, technology and so on. The challenges increments for the designer with the unpredictability of the height of the building and building plan. Without considering the detailed forbearance of denoting factors that affect the selection of tall buildings for the structural system, economic and adequate tall buildings cannot be intended. Building self-weight, live load, and seismic loads and along with wind forces will play valuable role as significant variables of the design. Adequate increases in the building's deflection, stress, strain, lateral displacement and deformation will result in elevated construction costs owing to the size and composition of the building components.

II. OUTRIGGER AND BELT TRUSS STRUCTURAL SYSTEM

Outriggers are rigid horizontal structure i.e. beam or truss which connects to the core wall and outer column of building for improving building strength and overturning stiffness. Outriggers are being utilized in tall structures from nearly half century, but innovative design framework has improved its proficiency. Outrigger system is the sort of structural system that is created from a horizontal cantilever part linking to the internal and outer columns of the structure. The moment arm of the core rises with the connection leading to greater lateral rigidity of the system. The central core of a structure acts as a cantilever; the outriggers are positioned to decrease the moment of overturning in the heart and transfer moment from core to exterior column by linking the core and column. Wall frame outrigger trusses are the found they connected to the foundation through outer columns is Wall frame outrigger trusses .The wall and outrigger trusses will rotate, causing downwind column compression and upwind side column tension, these axial forces will withstand the wall rotation when the structure is performed with horizontal forces.

Outriggers and columns withstand core rotation and thus considerably decrease the base moment and lateral deflection that would have occurred in a free core when the structure is subjected to lateral forces. A belt truss can be used at the outrigger concentrations to mobilize the extra axial stiffness of various columns and ensure torsional stiffness. As building height rises, column decrease is the critical issue in building methods, belt truss plays much effective in the control of settlement of columns. Belt trusses helps in limiting differential elongation and shortening of columns. Outrigger behavior with belt truss shown to be more effective when compare to the outrigger without belt truss. The outer columns and belt truss system resist rotation of central shear core and reduce the lateral deformation including bending moment at base of the structure.

III. OBTECTIVES

- To study the effect of introduction of Outriggers in high-rise building subjected to dynamic wind loading.
- To study the impact of X braced outriggers with core wall and braced core wall.
- To examine the parameters with various types of Plan Configurations with Outriggers, i.e. X Bracings and belt truss systems.
- To study the impact of steel outrigger in comparison with concrete outrigger.

IV. SCOPE OF PRESENT STUDY

The research aims to understand the seismic qualities and steadiness of the structure of the frame. The Outrigger and Belt Truss System can be used to increase this. Steel outriggers are used to counter seismic forces in steel framed structures. Steel options to use Steel Outriggers for RC frame buildings. This technique seeks to study and compare storey displacement, storey drift and base shear with distinct kinds of Outrigger Plan Configurations, i.e. X Bracings systems and belt trusses. The present research is useful for multiple academics involved in thin designing the tall structures by using outrigger and belt truss system.

V. PARAMETERS OF STUDY

- Effect of Outriggers with RC frame building when applied with Earthquake and dynamic wind loading for various Plan Configurations with Outriggers, i.e. X Bracings and belt truss systems for zone V.
- Lateral Displacement: The study emphases on the improvement of the RC frame building in terms of lateral displacement with most proficiently use of Outriggers and belt truss systems.
- Story Drifts: This parameter is considered in this research for the Optimum utilization of the Outriggers.
- The Base shear and Fundamental periods are considered as the parameters in this study.

VI. MODEL DESCRIPTION

The structures are modelled as a sequence of components that resist load. The lateral loads applied to the construction are based on the codal norms of India. The research is conducted according to IS 1893 (Part1): 2002 for seismic areas V. The adopted construction comprises of components of reinforced concrete and brick masonry. It is presumed that the structures are strongly fixed at the bottom floor and the interaction of the soil structure is overlooked. The building's complete height was set at 123.2 m (i.e. 40 stories) while the size of the members was distinct. Initially, the frame parts were intended to meet the requirements for stress analysis.

Table 1 : Y Shape Model geometry

Plan Configuration	Plan /Shape Area (sq.m)	No of Storey
Y Shape	1659.46	GF to 10
Y Shape	1315.66	10-20
Y Shape	1129.37	20-30
Y Shape	914.79	30-40

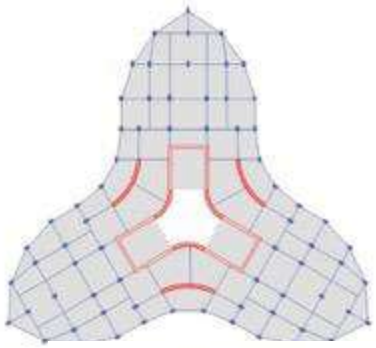

Fig 1 : Y Shape layout Plan

Table 2 : Circular Shape Model geometry

Plan Configuration	Plan /Shape Area (sq.m)	No of Storey
Circular Shape	1659.01	GF to 10
Circular Shape	1315.11	10-20
Circular Shape	1129.34	20-30
Circular Shape	914.34	30-40

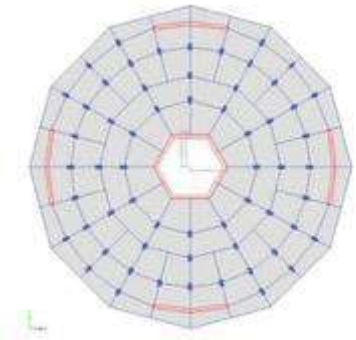

Fig 2 : Circular Shape layout Plan

Table 3 : Fillet Shape Model geometry

Plan Configuration	Plan /Shape Area (sq.m)	No of Storey
Fillet Shape	1659.46	GF to 10
Fillet Shape	1315.66	10-20
Fillet Shape	1129.37	20-30
Fillet Shape	914.79	30-40

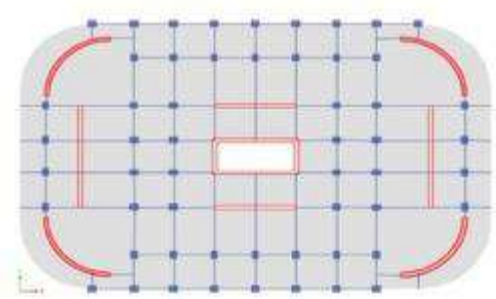

Fig 3 : Fillet Shape layout Plan

Models

The models that were chosen for the study are listed as follows,

Model 1 – Y Shape Bare frame model without Outrigger.
Model 2 – Y Shape Model with Concrete Core wall and braced Outriggers (Concrete X Bracings).
Model 3 – Y Shape Model with Concrete core wall and braced Outriggers (Steel X Bracings).
Model 4 – Circular Shape Bare frame model without Outrigger.
Model 5– Circular Shape Model with Concrete Core wall and braced Outriggers (Concrete X Bracings).
Model 6 – Circular Shape Model with Concrete core wall and braced Outriggers (Steel X Bracings).
Model 7 – Fillet Shape Bare frame model without Outrigger.
Model 8 – Fillet Shape Model with Concrete Core wall and braced Outriggers (Concrete X Bracings).
Model 9– Fillet Shape Model with Concrete core wall and braced Outriggers (Steel X Bracings).

VII. ABOUT THE ANALYSIS

The building analysis is done using widely used design software ETABS.

The design data used in the analysis are the following:

Design Data

Material Properties:

Grade of Concrete = M25 for all members
= M25 for columns
Grade of Rebar = Fe 415 Grade
Grade of Steel = Fe 345 Grade
Young's modulus of concrete (M45) = 33.541×10^6 KN/m2
Young's modulus of concrete (M60) = 38.729×10^6 KN/m2
Density of Reinforced Concrete = 25 KN/m3
Poisons' ratio of concrete = 0.2
Modulus of elasticity of brick masonry = 3500x103 KN/m2
Density of brick masonry = 8 KN/m3
Poisons' ratio of masonry = 0.15

Member Properties:

Slab = 150mm thick
Column = 500mmX1000mm
Beam = 300mmX600mm
Masonry wall (Brick) = 230mm thick
Reinforced Concrete Shear/Core wall = 400mm thick
Concrete Outriggers = 300mmX1000mm
Steel Outriggers = ISA 130X130X12mm

Load Calculations:

Assumed dead load intensities
Floor finishes = 1.5 KN/m2
Live load on floor = 3 KN/m2
Live load on roof = 1.5 KN/m2
Wall load on roof = 1x0.15x8 = 12 KN/m
Wall load on other levels = (3.2-0.6) x0.23x8 = 5 KN/m
Earthquake Live Load on slabs as per clause 7.3.1 and 7.3.2 of IS 1893 (Part-1)-2002
Roof = 0.5KN/m2
Floor = 0.5x3 =1.5 KN/m2

Seismic Data:

Structure = SMRF
Seismic Zone = V
Zone factor = 0.36
Importance factor = 1.5
Response reduction factor =5

Soil type	= Medium
Basic Wind Speed	= 44 m/s
Terrain Category	= 3
Terrain Class	=C

VIII. ANALYSIS RESULTS AND DISCUSSIONS

In this section, the results of the selected buildings are presented and discussed in detail. The consequences of base shear, lateral displacement, story shear, and vibration and in general execution for the distinctive structure models are displayed and thought about.

In this examination, an endeavor has been made for assessing the seismic exhibition of RC structures with focal center divider with outrigger and without outrigger. The outriggers of shape like 'X', of concrete and steel materials are contrasted in this examination with assess their adequacy in lessening horizontal removals and different parameters. Likewise Braced center divider is supplanted with strong center divider in the examination, and the effectiveness is watched. The idea of virtual outrigger or belt support truss was additionally contrasted and the customary outrigger for their general execution. From this examination we will likewise come to know the effectiveness of steel outriggers when contrasted with solid outriggers.

In the accompanying part, the outcomes are processed with proportional static technique for examination, reaction range investigation and static investigation. The modeling and analysis of various building models are carried by the use of ETABS software package. After the analysis, the results of base shear, lateral displacement for different models of the building are accumulated and analyzed.

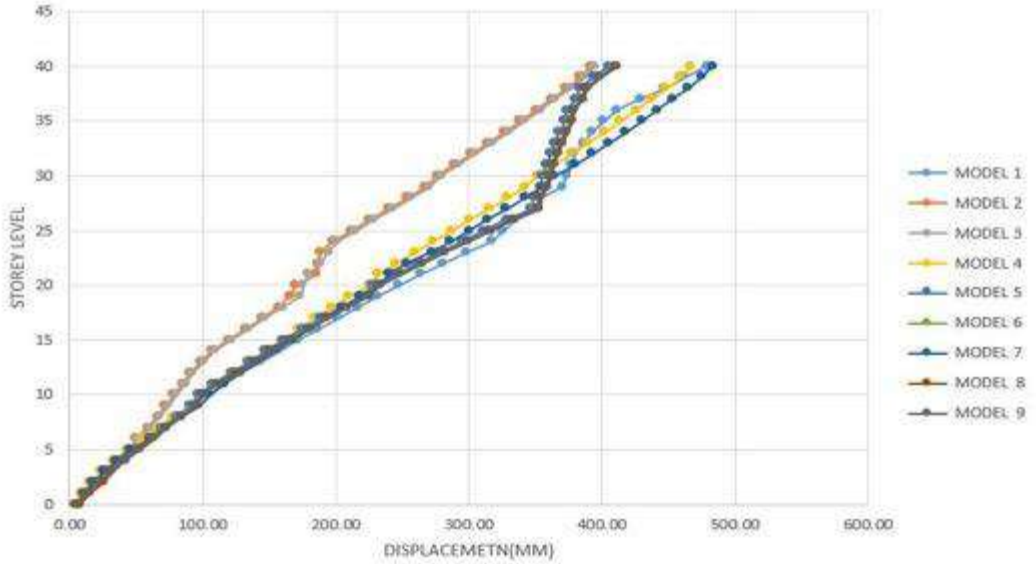

Fig 4 : Lateral Displacement for Response spectrum method along longitudinal direction for Zone V

Lateral Displacement for Response spectrum method along longitudinal direction for Zone V

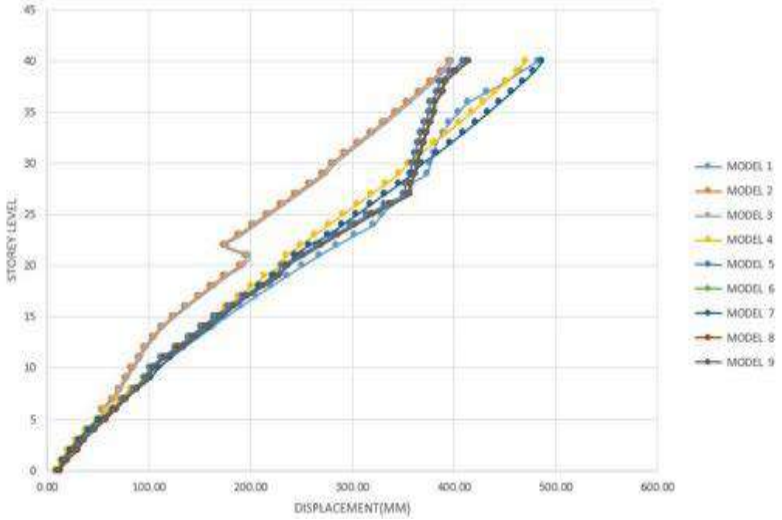

Fig 5 : Lateral Displacement for Response spectrum method along transverse direction for Zone V

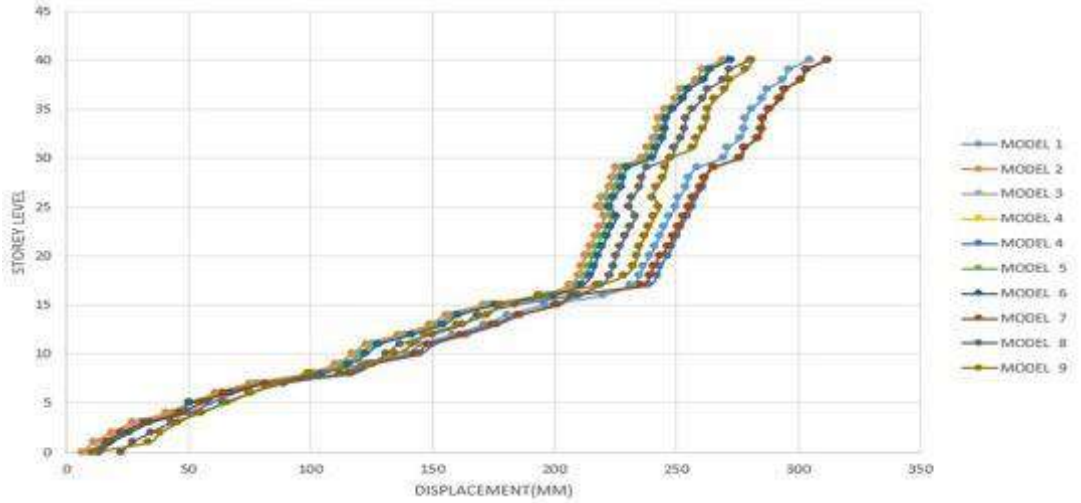

Fig 6 : Lateral Displacement for Static Wind Analysis along Longitudinal direction for Zone V

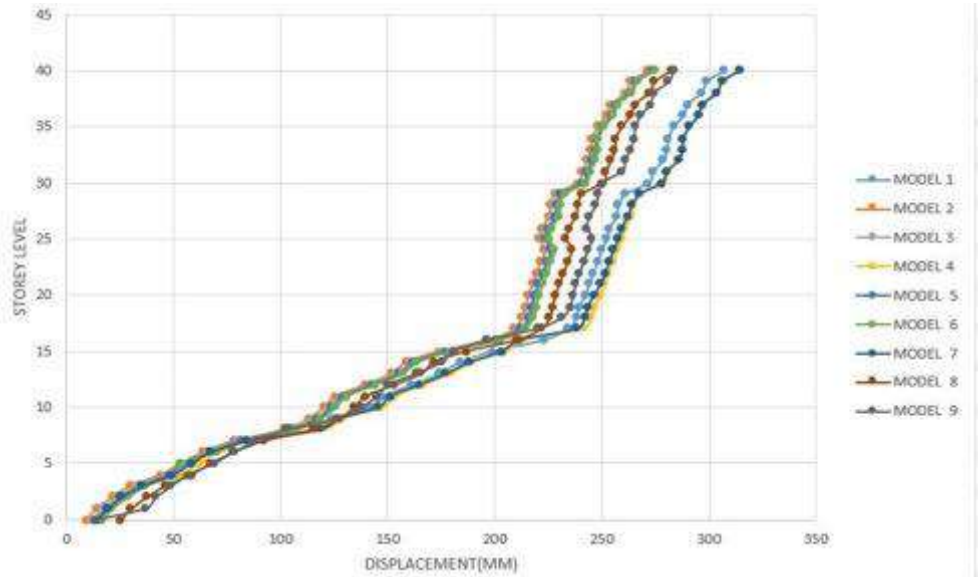

Fig 7 : Lateral Displacement for Static Wind Analysis along Transverse direction for Zone V

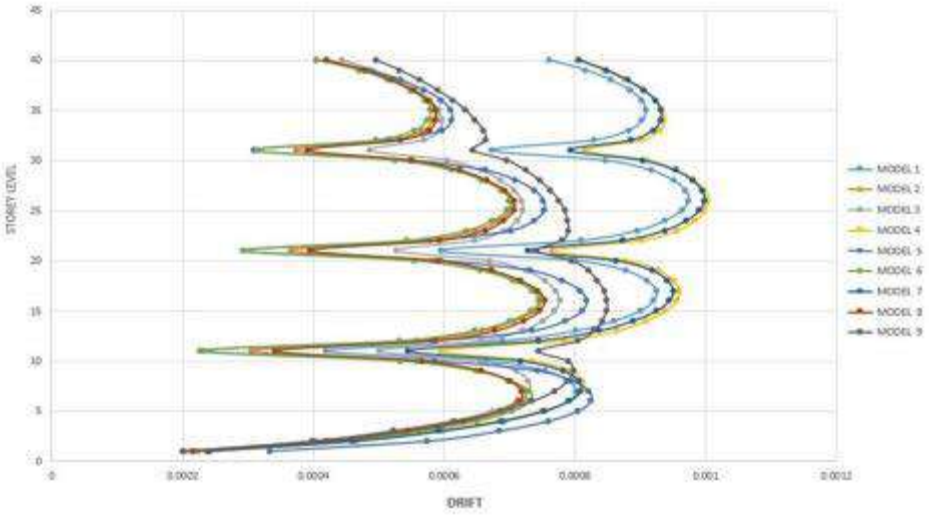

Fig 8 : Storey Drift for Response spectrum analysis along longitudinal direction for zone V

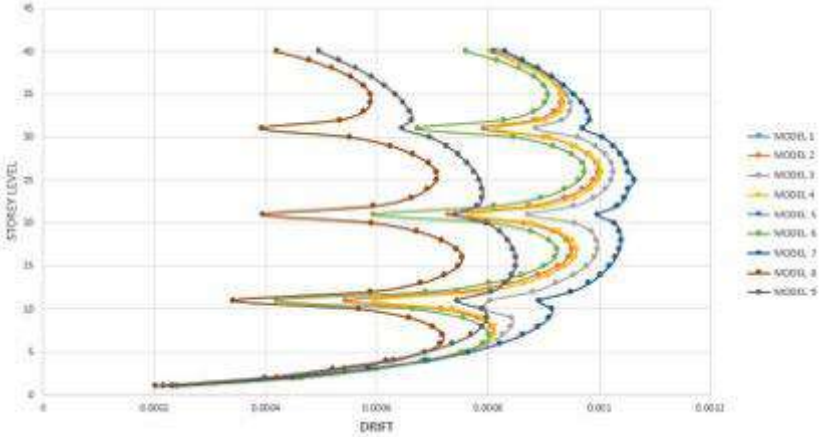

Fig 9 : Storey Drift for Response spectrum analysis along transverse direction for zone V

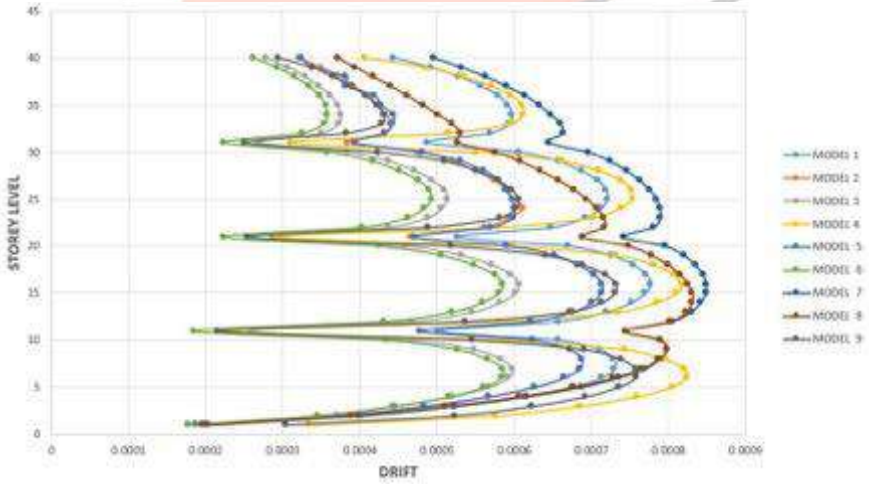

Fig 10 : Storey Drift for Static wind analysis along longitudinal direction for zone V

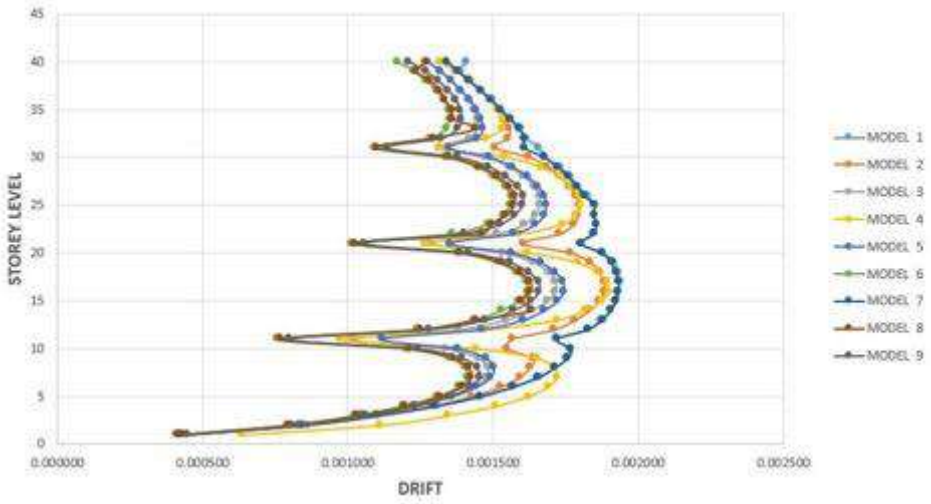

Fig 11 : Storey Drift for Static wind analysis along transverse direction for zone V

Table 4 : Base Shear by Response Spectrum Analysis and Wind Analysis along Longitudinal and Transverse direction

BASE SHEAR (KN)					
Model No.	**Type of Models**	Response Spectrum Analysis		Static Wind Analysis	
		RSA-X	RSA-Y	WIND-X	WIND-Y
1	Y Shape Bare frame model without Outrigger	16428.91	16467.95	12221.26	13541.28
2	Y Shape Model with Concrete Core wall and braced Outriggers (Concrete X Bracings)	17307.96	17937.91	11197.62	11315.69
3	Y Shape Model with Concrete core wall and braced Outriggers (Steel X Bracings)	17907.76	18312.724	11758.44	11812.36
4	Circular Shape Bare frame model without Outrigger	14610.79	14210.21	12267.97	12156.23
5	Circular Shape Model with Concrete Core wall and braced Outriggers (Concrete X Bracings)	15824.02	15924.21	12065.75	12099.73
6	Circular Shape Model with Concrete core wall and braced Outriggers (Steel X Bracings)	15470.13	15670.75	12024.84	12121.94
7	Fillet Shape Bare frame model without Outrigger	15324.22	15413.36	13351.69	13451.21
8	Fillet Shape Model with Concrete Core wall and braced Outriggers (Concrete X Bracings)	16228.86	16031.39	12562.33	12762.31
9	Fillet Shape Model with Concrete core wall and braced Outriggers (Steel X Bracings)	16404.48	16435.67	12758.44	12957.22

IX. OBSERVATIONS

- It is seen that 29.21% of top storey displacement and 26.64% of maximum story drift is constrained by providing Y Shape Plan Configurations, 28.1% of top storey displacement and 25.44% of maximum story drift by Circular Shape Plan Configurations and 22.32%of top storey displacement and 19.50% of maximum story drift is controlled with Fillet Shape Plan Configurations.
- Also 8.22% of displacement and 9.64% of storey drift is controlled if braced core wall is employed with X-braced outriggers (Model 2,3,5,6,8,9) and is compared with X-braced outriggers (Model 1, 4, 7).
- The model with Steel Outriggers demonstrates to be less productive in controlling displacement by 19.49% and of storey drift by 17.27%.This perception validates the literature [10].
- The Outriggers with Belt truss (Model 3) experienced less displacement and controlled lateral displacement by about 34.57% and about 30.75% inter storey drift is controlled.
- The natural period decreases as the stiffness of the building increases and thus leading in increment of frequency.

- The Y Shape building frame with X-braced Outriggers will have least possible lateral displacements in contrast to other building shapes of Outriggers.

X. CONCLUSIONS

The accompanying Conclusions were drawn dependent on the Observations made

- The Y plan Configuration with X-supported Outriggers is particularly powerful; as it indicates least minimum lateral displacement pursued by Circular Plan Configuration Outriggers and Fillet Plan Configuration Outriggers.
- The Outriggers provided with Braced core wall were less viable in reducing lateral displacement compared with Solid Core wall by a small margin, hence it can be employed as the cost effective construction.
- The Outriggers gave in the inside casings of a structure examined are observed to be viable when contrasted with Outriggers gave in the outside edges for example.
- The steel outriggers are discovered least compared to Concrete one. Despite the fact that Steel outriggers can be utilized as the light weight substitute for concrete.
- From the examination it tends to be reasoned that that wind is a dominating factor and outriggers are successful in lessening wind impact as looked at tremor powers.
- Steel Outriggers can be utilized as an option in contrast to the next to the other strengthening techniques available as the total weight of the current structure will remain practically same

XI. REFERENCES

[1] Krunal Z. Mistry, Prof. Dhruti J. Dhyani,"Optimum outrigger location in outrigger structural system for high rise building" International Journal of Advance Engineering and Research Development Volume 2, Issue 5, May -2015.

[2] Akshay Khanorkar, Shruti Sukhdeve, S. V. Denge & S. P. Raut, "Outrigger and Belt Truss System for Tall Building to Control Deflection: A Review" GRD Journals- Global Research and Development Journal for Engineering | Volume 1 | Issue 6 | May 2016.

[3] B.S.Taranath, "Structural Analysis & Design of Tall Buildings", New York, McGraw Hill, 1998.

[4] M. H. Gunel, and H.E. Ilgin, A proposal for the classification of structural systems of tall buildings, Faculty of Architecture, Middle EastTechnical University, Ankara 06531, Turkey, 4 July 2006.

[5] Iyengar Hal, Composite and Steel High Rise Systems, Habitat and The High- Rise, Tradition & Innovation. In Proceedings of the Fifth World Congress. 14-19 May 1995.Amsterdam, The Netherlands, Bethlehem, Council on Tall Building and Urban Habitat, Lehigh University.

[6] P.S. Kian and F.T.Siahaan, "The use of outrigger and belt truss system for high-rise concrete buildings". Dimensi Teknit Sipil, Volume 3, No1,Maret 2001, Page 36-41,ISSN1410-9530.

[7] R. S. Nair, "Belt Trusses and Basements as „Virtual" Outriggers for Tall Buildings". Engineering Journal / Fourth Quarter/ 1998.

[8] Shivacharan K, Chandrakala S, Narayana G, Karthik N.M., "Analysis of Outrigger System for Tall Vertical Irregularites Structures Subjected to Lateral Loads"IJRET: International Journal of Research in Engineering and Technology, Volume: 04 Issue: 05 | May-2015.

[9] M.R Suresh, Pradeep K.M, "Influence of Outrigger System in RC Structures for Different Seismic Zones" IJSRD - International Journal for Scientific Research & Development| Vol. 3, Issue 05, 2015 | ISSN (online): 2321-0613.

[10] Abdul Karim Mullah, Srinivas B. N, "A Study on Outrigger System in a Tall R.C Structure with Steel Bracing" International Journal of Engineering Research & Technology (IJERT), Vol. 4 Issue 07, July-2015.

[11] S. Fawzia and T. Fatima, "Deflection Control in Composite Building by Using Belt Truss and Outriggers Systems" World Academy of Science, Engineering and Technology 48 2010.

[12] Prateek N. Biradar & Mallikarjun S. Bhandiwad. "A Performance Based Study on Static and Dynamic Behavior of Outrigger Structural System for Tall Buildings" International Research Journal of Engineering and Technology (IRJET), Volume: 02 Issue: 05 | Aug-2015.

[13] Bryan Stafford Smith and Alex Coull, "Tall Building Structures: Analysis and Design", New York, John Willey & Sons, 1991.

[14] Indian Standard Code of Practice for Design Loads (other than earthquake) For Buildings and Structures, Part – 2 Live Loads, IS: 875 (Part 2) – 1987 (Second Revision), Bureau of Indian Standards, New Delhi, India.

[15] Indian Standard Code of Practice for Design Loads (other than earthquake) For Buildings and Structures, Part – 3 Wind Loads, IS: 875 (Part 3) – 1987 (Second Revision), Bureau of Indian Standards, New Delhi, India.

[16] Indian Standard Criteria for Earthquake Resistant Design of Structures, IS: 1893 (Part 1) 2002, Part 1 General Provision and Buildings (Fifth Revision), Bureau of Indian Standards, New Delhi, India.

ISSN: 0976-9102 (ONLINE)
DOI: 10.21917/ijivp.2017.0230

FRACTAL COMPRESSION TECHNIQUE FOR COLOR IMAGES USING VARIABLE BLOCK

Nisar Ahmed[1] and Syed Abdul Sattar[2]

[1]Department of Electronics and Communication Engineering, Mewar University, India
[2]Department of Electronics and Communication Engineering, Nawab Shah Alam Khan College of Engineering and Technology, India

Abstract

The main intention of Fractal Image Compression is to reduce the size of image and maintain good level of their reconstructed image. A major issue in Fractal Image Compression is decrease in image quality, compression ratio and PSNR. To overcome these issues we employ Fractal transformation with entropy coding. There are two phases in the proposed approach. In the first phase color images are separated into three RGB planes using variable range block size. In second phase by applying the inverse transform and iterative functions the image is restored. It is observed that the results are improving in fractal compression for both gray images as well as color images. In this work high CR and PSNR is observed compared to fixed block range and other existing methods. The proposed work yields better CR of 20 and high PSNR.

Keywords:

Fractal Image Compression, Variable Block Size, CR, PSNR

1. INTRODUCTION

Images are interpreted as accumulation of bits (a bit is a binary unit of information) and stored in digital media storages in the computer. These bits are denoted as pixels or points that form the picture elements. A human eye progresses large amount of information of approximately 8 million bits to create a single image. Profuse pixels constitute the formation of a reasonable quality image which, the eye arbitrates the 8 million bits from 'yes' and 'no' answers to develop the image progression. Redundancy of the pixels enriches the absorption capability of the eye to interpret the images into prominence, thus making them more apprehensible. This redundancy can be manipulated and reduced through algorithms for optimum storage and restored for recovery. An image can be alternated in many ways that are either not noticed by the human eye or do not contribute to the decay of the image. The current most famous method of image compression depend on elimination of high frequency wavelengths of the signal and storing only the low frequency components.

Fractal based image compression (FIC) technique exploit redundancy due to self-similarity properties in images to achieve compression [1]. A domain optimization technique in fractal image compression [2] deals with reducing complexity and increasing accuracy that is range and domain block alignment and matching. Fractal Image Compression is a separated image that can be a part of parts; the main motto of the fractal image compression is to reduce the redundancy or the image as well as image irrelevance to store [3]. Moreover image compression is a transformation called relative transformation. Fractal image compression is proposed in [4] based on Lossy compression principle which provides a very high compression ratio by completely eliminating the redundant information. The drawback of this technique is the degradation during reproduction of the image because of insufficient pixels for the filler sections comprising the redundant pixels. The image which is reconstructed contains degradation relative to the original image because the compression scheme completely neglects the redundant information and is more capable for achieving higher compression [5]. Fractal image compression (FIC) is based on the theory of Iterated Function System (IFS) which is used to represent the self-similarities of the images and is represented as a finite set of contraction mapping for each image that has the fixed point which is identical to the image itself [6]-[8]. Fractal image compression (FIC) seems to be one of the favorable methods of lossy image compression due to its advantages like resolution independence, high compression ratio, and fast decompression [9]. This technique was initially proposed by Jacquin and is based on the method of lossy compression. Here the images are considered to be fractals rather than pixels, which will be mainly suitable for natural images for encoding, analyzing with other image compression methods [10], [11] Suggested another system focused In the current scenario, fractal image compression plays a major role in research areas, it is one of the kind of modern image compression technique coefficients. Gohar and Habib [12] suggested in image compression two different processes is carried out namely encoding and decoding. In encoding section the original image takes as an input and after processing the compressed image will be its output but in decoding section the process is carried out in reversible order. In the event that the neighborhood heights are not fulfilled, the second phase of the calculation is completed keeping in mind the end goal to investigate further likenesses from the complete picture. Kharate and Patil [13] proposed fractal compression process through the self-similar properties in various fractions of images which relies on the fact that the image parts are often resembles other parts of the same image. Sekhar and Aruna [14] proposed a fractal is a rough or fragmented geometric shape that can be subdivided into parts, each of which is reduced/size copy of the whole. Khalil [15] found a major drawback in Fractal image compression (FIC), where encoding of fractals is very complex, compressing time is very high due to its complexity and consumption of time to search for the best matching block and more powerful. Anson [16] has recommended the IFIC using range block size. Barnsley and Hurd [17] have recommended applying the transformation iteratively on the random initial image and the result will be re-arranged as the original image. Banu [18] has proposed an efficient search of the domain pools for color image compression using Genetic Algorithm (GA). The proposed method reduces the coding process time and intensive computation tasks. Image quality factor, compression ratio and coding time are analyzed in this approach and comparative results are obtained but this method is suitable for only limited categories like facial, building and vegetable images.

2. FRACTAL COMPRESSION

Fractal Image compression is one of the popular demanding research field in the current trend, mainly it deals with the images, video sequences, graphics, animations etc. Fractal compression is one of the kind of lossy image compression technique, here it will partition the images into blocks then perform some transformations and then compress it. Normally based on lossy compression, the compression ratio will be high but the quality of the images will not attain the expected results and there will be a loss of information's too. There are many technologies developed in different research areas to improve the image quality while compressing the images. In image compression consumption of time is more in encoding and decoding. There are some limitations existing too. This has motivated us to develop an efficient compression technique for color images to enhance high compression ratio and PSNR.

Various compression algorithms are used to reduce the size of the images without reducing the quality of images [19]. Algorithms like embedded zero wavelet algorithm, convergent algorithm, Fuzzy vector quantization algorithm etc. are used previously to compress the images with high quality [20].

3. PROPOSED ALGORITHM

The main objective of this research is to compress the image with high ratio and increase the PSNR of the encoding phase

Step 1: Divide color image into sub windows. Each sub window block is called R- block.

Step 2: For each R-block, find a Domain block, which most likely represents current R-block after a certain transform.

Step 3: For every R-block, find D-block from D-pool which is most likely parallel to it.

Crop the D-block size to the size of R-block by Shrink operation and, mark the D-block as D′-block after Shrink operation is applied.

Transpose the D′- block by using the following eight relative transformation equation matrices proposed by Jacquin. The eight relative transformations matrices are represented in the equations as follows,

Consider $T = [a_{ij}]_n$ with $n = 2$ where $1 \le (i,j) \le 2$, $\begin{bmatrix} a_{11} & a_{12} \\ a_{21} & a_{22} \end{bmatrix}$.

Relative transformations matrices can be represented with the following Eq.(1) to Eq.(8),

$$T_0 \text{ is } a_{ij} = \begin{cases} 1 & \text{if } i = j \\ 0 & else \end{cases} \tag{1}$$

$$T_1 \text{ is } a_{ij} = \begin{cases} (-1)^{2^i + j} & \text{if } i \neq j \\ 0 & else \end{cases} \tag{2}$$

$$T_2 \text{ is } a_{ij} = \begin{cases} -1 & \text{if } i = j \\ 0 & else \end{cases} \tag{3}$$

$$T_3 \text{ is } a_{ij} = \begin{cases} (-1)^{i+2^j} & \text{if } i \neq j \\ 0 & else \end{cases} \tag{4}$$

$$T_4 \text{ is } a_{ij} = \begin{cases} (-1)^{ij} & \text{if } i = j \\ 0 & else \end{cases} \tag{5}$$

$$T_5 \text{ is } a_{ij} = \begin{cases} (-1)^{ii+1} & \text{if } i = j \\ 0 & else \end{cases} \tag{6}$$

$$T_6 \text{ is } a_{ij} = \begin{cases} (-1)^{i+j} & \text{if } i \neq j \\ 0 & else \end{cases} \tag{7}$$

$$T_7 \text{ is } a_{ij} = \begin{cases} 1 & \text{if } i \pm j \\ 0 & else \end{cases} \tag{8}$$

Above eight relative transformation blocks are generated for each D′-block and these blocks are composite new D-pool.

Compare each R-block with the blocks which are in D′- pool and obtain nearly all like block. The parallelism can be measured with normal conflict MSE using the Eq.(9).

$$MSE = \left\| X_k D_k + Y_k I - R_k \right\| \tag{9}$$

where X and Y are the coefficients and should have the values for making the MSE minimum. The X_k and Y_k are represented in Eq.(10) and Eq.(11) respectively,

$$X_k = \frac{B^2 \langle D_k, R_k \rangle - \langle D_k, I \rangle \langle R_k, I \rangle}{B^2 \langle D_k, R_k \rangle - \langle D_k, I \rangle^2} \tag{10}$$

$$Y_k = \frac{\langle R_k, I \rangle - \langle D_k, I \rangle}{B^2} \tag{11}$$

$$W = \{D_k(x,y),\ T_k,\ X_k,\ Y_k\} \tag{12}$$

where R_k represents the relative transformation W for each R-block.

Fractal image coding, the original image is segmented into non-collaborating regions called range blocks and collaborating regions called domains blocks. For each range block affine transformations given in the Eq.(13) is used to match as best domain block.

$$W_i \begin{bmatrix} x \\ y \\ z \end{bmatrix} = \begin{bmatrix} a_i & b_i & 0 \\ c_i & d_i & 0 \\ 0 & 0 & s_i \end{bmatrix} \begin{bmatrix} x \\ y \\ z \end{bmatrix} + \begin{bmatrix} e_i \\ f_i \\ o_i \end{bmatrix} \tag{13}$$

where S_i controls the contrast and 0_i controls the brightness and a_i, b_i, c_i, d_i, e_i, f_i denote the eight symmetries such as identity, reflection about mid-vertical and horizontal axis, first and second diagonal.

The Fig.1 is the proposed fractal image compression.

1. Partition each plane image into non-overlapping blocks, called Range or R-block.
2. Select the maximum Range block of size (R_{max}) as 16 or 8 and minimum block of size (R_{min}) of 4 or 8. R-blocks are compared with domains from the domain pool, which are double the range size.
3. A window size of $\alpha \times \alpha$ is slided on 3 images in $\alpha/2$ or $\alpha/4$. The pixels are averaged in groups to reduce to the size.
4. After partitioning and transformation, fractal encoding finds suitable candidate from all blocks to encode any particular R block.

5. To increase encoding speed classification of sub-image into upper right, upper left, lower right and lower left quadrants is done as shown in Fig.2. It is shown that in any one of the three ways as canonical ordering [21].

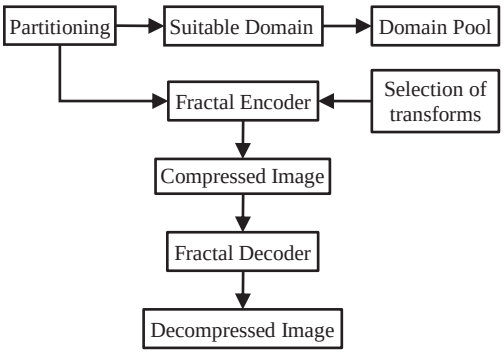

Fig.1. Proposed Fractal Compression Technique

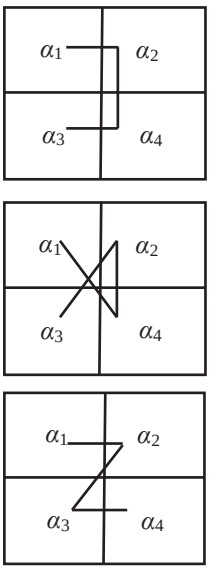

Fig.2. Arrangement of Sub Blocks Images

Classification Schemes are

- Major Class 1: $\alpha_1 > \alpha_2 > \alpha_3 > \alpha_4$
- Major Class 1: $\alpha_1 > \alpha_4 > \alpha_2 > \alpha_3$
- Major Class 1: $\alpha_1 > \alpha_2 > \alpha_4 > \alpha_3$

Entropy of coding is used to achieve fractal compression for mapping the range block to the domain block in the coding process.

4. RESULTS AND DISCUSSION

To find the effectiveness of the proposed method by means of the experimental results. The Satellite urban and rural images are reduced to standard size 256×256. The standard Lena images of size 512×512 has been used for fractal compression analysis. The first phase consists of applying color and gray images to a set of five images. We have used five different test images in our experiment. In the final phase we have calculated the CR and PSNR with the resultant images. The imageries are subjected to fractal compression scheme by using the variable range block size for three cases namely,

a) R_{max} = 16 and R_{min} = 4
b) R_{max} = 16 and R_{min} = 8
c) R_{max} = 8 and R_{min} = 4,

Three different variable range methods are displayed in Table.1 and Table.2, respectively. The novelty is, the proposed method is applied on both grey level and color images. The proposed method gives the comparable results when applied on both color and grey images. It is seen from Table.1 that the CR and PSNR values derived from Lena, Satellite Rural, Rose, Satellite Urban and Bird imageries do not show significant difference between the CR and PSNR values. However, Table.1 clearly demonstrates that CR and PSNR values derived for the Lena and other imageries show maximum values for case (b) where the variable range block size R_{max} = 16 and R_{min} = 8. It is clearly seen from Table.1 and Table.2 shows for Color and Grey images values for CR and PSNR for all the types of imageries. The variable range block sizes shows higher CR and PSNR compared to fixed and other methods. This comparison is shown in Table.3, Table.4, Table.5, and Table.6, respectively.

Table.1. CR and PSNR of Test Color Images

Test Images	**R_{max} =16 and R_{min} = 4**		**R_{max} =16 and R_{min} = 8**		**R_{max} = 8 and R_{min} = 4**	
	CR	**PSNR**	**CR**	**PSNR**	**CR**	**PSNR**
Lena Image	2.99	27.88	15.45	20.16	3.16	30.15
Satellite Rural Image	3.87	19.75	18.08	17.88	3.33	35.65
Rose Image	4.44	27.01	17.85	20.11	4.02	35.66
Satellite Urban Image	3.55	24.55	18.90	22.89	3.37	32.59
Bird Image	3.68	18.88	17.45	24.95	3.11	31.79

Table.2. CR and PSNR of Test Gray Images

Test Images	**R_{max}=16 and R_{min} = 4**		**R_{max}=16 and R_{min} = 8**		**R_{max}=8 and R_{min} = 4**	
	CR	**PSNR**	**CR**	**PSNR**	**CR**	**PSNR**
Lena Image	2.99	27.88	15.45	20.16	3.16	30.15
Satellite Rural Image	3.87	19.75	18.08	17.88	3.33	35.65
Rose Image	4.44	27.01	17.85	20.11	4.02	35.66
Satellite Urban Image	3.55	24.55	18.90	22.89	3.37	32.59
Bird Image	3.68	18.88	17.45	24.95	3.11	31.79

Variable range block size R_{max} = 16 and R_{min} = 8 are shown in Fig.3(a)-(b), Fig.4(a)-(b), Fig.5(a)-(b), Fig.6(a)-(b), Fig.7(a)-(b) and Fig.8(a)-(b). These are the reconstructed images for Color and Grey Lena, Rose, urban satellite, bird and rural satellite imageries. As seen in the figure and tables that the proposed IFIC method for the images of Lena, Bird, Satellite Rural, Rose and urban satellite gives significantly large CR values exhibits a very good quality of the reconstructed imageries.

(a) (b)

Fig.3. Results of Lena color image (a) Lena Image (b) reconstructed Lena image

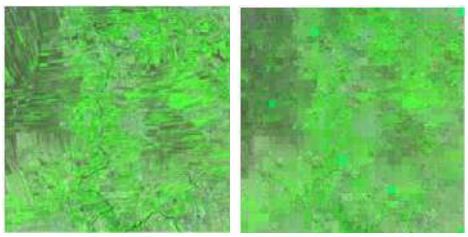

(a) (b)

Fig.4. Results of Satellite Urban color image (a) original satellite urban Image (b) re-constructed satellite image

(a) (b)

Fig.5. Results of Lena gray image (a) original lena gray Image (b) reconstructed lena image

(a) (b)

Fig.6. Results of Rose gray image (a) original rose gray Image (b) reconstructed rose image

(a) (b)

Fig.7. Results of Bird gray image (a) original gray bird Image (b) reconstructed bird image

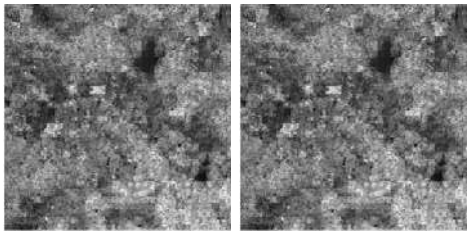

(a) (b)

Fig.8. Results of satellite rural gray image (a) original gray satellite Image (b) reconstructed satellite image

4.1 COMPARISON WITH OTHER EXISTING METHODS

The present Fractal Image Compression [FIC] is compared with the other existing methods, like standard algorithm of quadtree technique [22], fractal with quadtree and DCT technique [23], and Fractal image compressions based on variable size range block method [24]. The CR and PSNR values obtained from the present method of variable range block size for test imageries are compared with the results of existing methods [22], [23], [24]. Standard algorithm of quadtree technique (SAQT), fractal with quadtree and DST technique (FQandDST), FIC based on variable size range block method (FICVRB), Proposed FIC in both color and gray level image with range block size R_{max} = 16 and R_{min} = 8 are comparatively shown in the Table.3 to Table.6.

Table.3. Comparison of CR with other available methods for color images

Test Images	SAQT	FQ and DST	FIC VRB	FIC
Lena Image	10.01	14.44	13.0	17.53
Satellite Rural Image	8.68	13.35	15.5	18.99
Rose Image	8.32	12.56	15.4	18.13
Satellite Urban Image	10.66	13.87	13.87	17.78
Bird Image	9.99	14.98	16.56	16.55

The comparison chart of CR and PSNR values for the proposed method and other existing methods in both case i.e. color and grey image when applied on test images i.e. Lena, Satellite rural image, Satellite urban image, Bird and Rose images are shown in Fig.9 to Fig.12.

Table.4. Comparison of CR with other available methods for grey images

Test Images	SAQT	FQ and DST	FIC VRB	FIC
Lena Image	8.78	13.55	16.87	19.99
Satellite Rural Image	9.77	13.33	15.75	18.89
Rose Image	9.85	12.15	15.75	19.9

Satellite Urban Image	9.15	13.03	17.71	18.53
Bird Image	8.98	13.01	15.99	19.54

Table.5. PSNR of the proposed method and other available methods of color images.

Test Images	SAQT	FQ and DST	FIC VRB	FIC
Lena Image	24.89	29.45	18.55	30.33
Satellite Rural Image	26.33	30.98	23.01	33.55
Rose Image	26.08	32.01	21.50	35.55
Satellite Urban Image	25	30	16	32
Bird Image	26.45	31.67	23.80	33.11

Table.6. PSNR of the proposed method and other available methods of gray level images

Test Images	SAQT	FQ and DST	FIC VRB	FIC
Lena Image	23.13	29.88	26.5	32.25
Satellite Rural Image	25.15	31.19	24.55	31.15
Rose Image	24.33	29.10	18.55	32.01
Satellite Urban Image	25.36	31.87	25.55	31.95
Bird Image	25.15	30.48	23.76	32.78

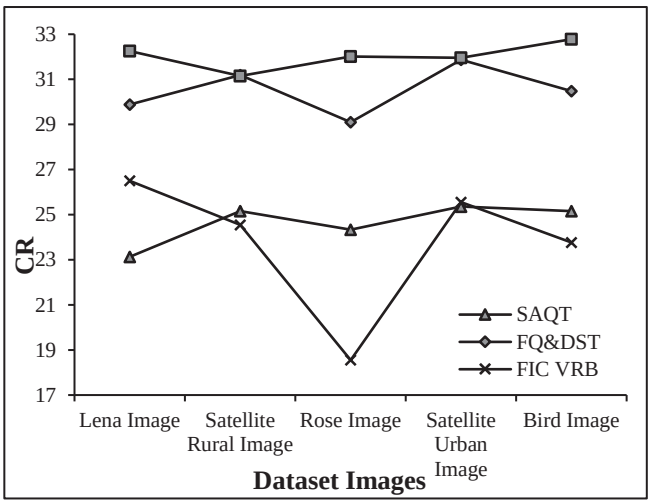

Fig.9. Comparison chart of CR of the proposed method with other existing methods when applied on color test images

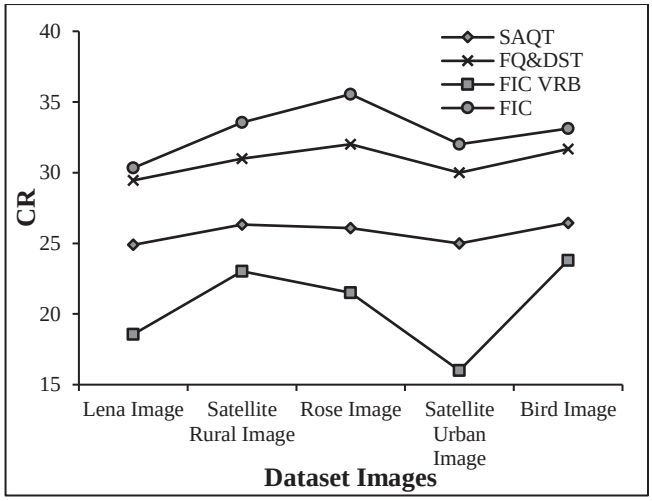

Fig.10. Existing methods when applied on gray test images Comparison chart of CR of the proposed method with other

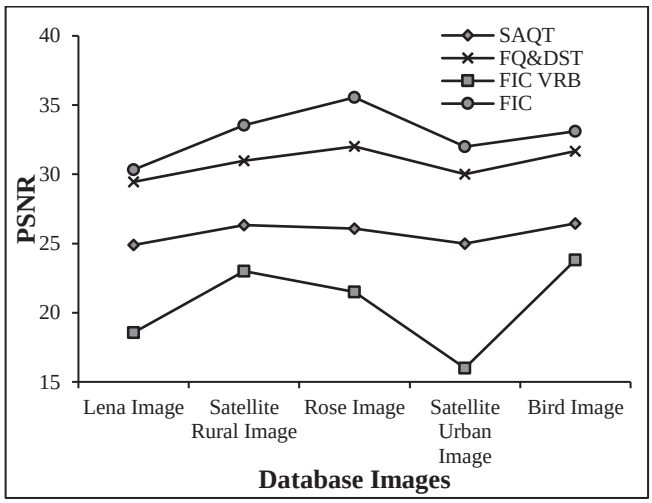

Fig.11. Comparison chart of PSNR of the proposed method with other existing methods when applied on color test images

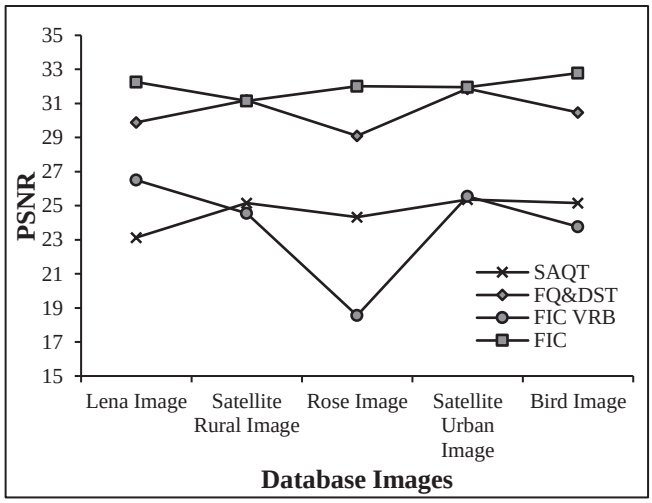

Fig.12. PSNR of the proposed method and other available methods of gray level images

5. CONCLUSION

In the present paper, an experimental work is done to get an improved fractal image compression. The experimental results clearly depict that for the variable range block size of R_{max} = 16 and R_{min} = 8 a better result is yielded with good image quality and low computational cost. The uniqueness of the proposed method is, the RGB image is divided into three planes and using range block fractal concept it is compressed with reduced computational cost. When compare with the fixed block size method of fractal compression schemes, the present method exhibits higher compression ratio and PSNR values for all types of imageries. When the proposed method is applied on both color and gray scale images it gives approximately same CR and PSNR values. The proposed method when applied on different types of images like satellite image, standard color images and natural image, gives comparatively good results. The PSNR values obtained in this approach is always nearer to 30.

REFERENCES

[1] Gagnpreet Kaur, Hitashi Hitashi and Gurdev Singh, "Performance Evaluation of Image Quality based on Fractal Image Compression", *International Journal of Computers and Technology*, Vol. 2, No.1, pp. 20-27, 2012.

[2] Zhuang Wu and Bixi Yan, "An Effective Fractal Image Compression Algorithm", *Proceedings of IEEE International Conference on Computer Application and System Modeling*, pp. 139-143, 2010.

[3] Sumathi Poobal and G.Ravindran, "Analysis on the Effect of Tolerance Criteria in Fractal Image Compression", *Proceedings of IEEE International Workshop on Imaging Systems and Techniques*, pp. 119-124, 2005.

[4] A. Selim, M.M. Hadhoud, M.I. Dessouky and F.E. Abd El-Samie, "A Simplified Fractal Image Compression Algorithm", *Proceedings of IEEE International Conference on Computer Engineering and Systems*, pp. 53-58, 2008.

[5] Dietmar Saupe, "Accelerating Fractal Image Compression by Multi-Dimensional Nearest Neighbor Search", *Proceedings of IEEE Data Compression*, pp. 222-231, 1995.

[6] Arnaud E. Jacquin, "Image Coding based on a Fractal Theory of Iterated Contractive Image Transformations", *IEEE Transaction on Image Processing*, Vol. 1, No. 1, pp. 18-30, 1992.

[7] M. Barnsley, "*Fractals Everywhere*", 2nd Edition, San Diego Academic Press, 1993.

[8] Y. Fisher, "*Fractal Image Compression*: *Theory and Application*", Springer, 1995.

[9] Brendt Wohlberg and Gerhard De Jager, "A Review of the Fractal Image Coding Literature", *IEEE Transactions on Image Processing*, Vol. 8, No. 12, pp. 1716-1729, 1999.

[10] Guojun Lu and Toon Lin Yew, "Applications of Partitioned Iterated Function Systems in Image and Video Compression", *Journal of Visual Communication and Image Representation*, Vol. 7, No. 2, pp. 144-154, 1996.

[11] Douda Sofia, Bagri Abdallah, Abdel Hakim and Amer Elimrani, "A Reduced Domain Pool based on DCT for a Fast Fractal Image Encoding", *Electronic Letters on Computer Vision and Image Analysis*, Vol. 10, No. 1, pp. 11-23, 2011

[12] Vahdati Gohar, Khodadadi Habib, Yaghoobi Mahdi and Akbarzadeh-T Mohammad, "Fractal Image Compression Based on Spatial Correlation and Hybrid Particle Swarm Optimization with Genetic Algorithm", *Proceedings of 22nd International Conference on Software Technology and Engineering*, pp. 134-138, 2010.

[13] G.K. Kharate and V.H. Patil, "Color Image Compression Based on Wavelet Packet Best Tree", *International Journal of Computer Science Issues*, Vol. 7, No. 2, pp. 31-35, 2010.

[14] D. Venkatasekhar and P. Aruna, "A Fast Fractal Image Compression using Huffman Coding", *Asian Journal of Computer Science and Information Technology*, Vol. 2, No. 9, pp. 272-275, 2012.

[15] M. Khalil, "Image Compression using New Entropy Coder", *International Journal of Computer Theory and Engineering*, Vol. 2, No. 1, pp. 39-42, 2010.

[16] Fractal Image Compression, Available at: http://www.math.psu.edu/tseng/class/Fractals.html.

[17] Michael Barnsley and Lyman Hurd, "*Fractal Image Compression*", AK Peters Limited, 1992.

[18] A.R. Nadira Banu Kamal and P. Priyanga, "Iteration Free Fractal Compression using Genetic Algorithm for Still Colour Images", *ICTACT Journal on Image and Video Processing*, Vol. 4, No. 3, pp. 785-790, 2014.

[19] Mohammed Ismail and S.M. Basha, "Improved Fractal Image Compression using Range Block Size", *Proceedings of IEEE International Conference on Computer Graphics, Vision and Information Security*, pp. 284-289, 2015.

[20] S.V. Veena Devi, A.G. Ananth, "Fractal Image Compression of Satellite Imageries using Variable Size of Range Block", *Proceedings of IEEE International Conference on Signal and Image Processing Applications*, pp. 172-175, 2013.

[21] Mario Polvere and Nappi Michele, "Speed-Up in Fractal Image Coding: Comparison of Methods", *IEEE Transaction on Image Processing*, Vol. 9, No. 6, pp. 1002-1009, 2000.

[22] A.H. Husseen, S.Sh. Mahmud and R.J. Mohammed, "Image Compression using Proposed Enhanced Run Length Encoding Algorithm", *Ibn AL- Haitham Journal for Pure and Applied Science*, Vol. 24, No. 1, pp. 18-25, 2011.

[23] K. Sharmila and K. Kuppusamy, "A New Color Image Compression Based on Fractal and Discrete Cosine Transform", *International Journal of Engineering and Computer Science*, Vol. 3, No. 7, pp. 7054-7057, 2014.

[24] S.V. Veenadevi and A.G. Ananth, "Fractal Image Compression of Satellite Color Imageries using Variable Size of Range Block", *International Journal of Image Processing*, Vol. 8, No. 1, pp. 1-8, 2014.

International Journal of Research and Review
www.ijrrjournal.com E-ISSN: 2349-9788; P-ISSN: 2454-2237

Short Communication

A Structural Study on Bubble Deck Slab and Its Properties

Mir Shahed Ali[1], Dr. S. Amaresh Babu[2]

[1]M.Tech Structural Engineering, Department of Civil Engineering, Nawab Shah Alam Khan College of Engineering and Technology, Hyderabad-24, TS.
[2]Head of Department, Department of Civil Engineering, Nawab Shah Alam Khan College of Engineering and Technology, Hyderabad-24, TS.

Corresponding Author: Mir Shahed Ali

ABSTRACT

Housing all over the world majorly comprises of concrete structures. They provide isolation and thermal comfort to the occupants. Majority of the concrete structures have flooring/roofing of thick concrete to bear the design loads. Due to his, the complete volume (eliminating the negligible volume of the reinforcement) of the roof slab comprises of concrete. Due to this, production of concrete has increased. Concrete production is not environment friendly. It is the primary producer of Carbon dioxide. In addition to this, the problem of concrete waste is at rise. Concrete waste can be reduced by two ways: recycling and using efficient volumes. Recycling is using the concrete waste in concrete generation which is of course of lower quality. Efficient volume is the way of using concrete in the most efficient way possible by substituting materials. In this paper, polyethylene balls are used in the slab to reduce concrete volume while maintaining the structural properties of the concrete. A comparison of strength of slab with the polyethylene balls and without them has been done to show the effectiveness of the new method. Various other strength tests were carried out and have been tabulated. At the end, cost effectiveness of the proposed slab has also been given.

Index terms: Bubble deck slab, Polyethylene balls, recycling concrete, concrete slabs systems.

1. INTRODUCTION

Concrete is strong in compression and weak when under tension. While considering a reinforced concrete slab, all the concrete above the neutral axis is subject to compressive forces and all the concrete below the neutral axis is subject to tensile forces. This supports the fact that concrete is the tension zone is of little use and contributes to making the slab heavier and reducing its overall efficiency. Upon having more slabs, it shall contribute to increased dead load of the structure. This dead load which is additional in nature and does not serve any positive purpose can be removed. This is done by introducing voids in the slab. Since voids cannot be made to form on their own, hollow balls or low weight balls are placed in the concrete to reduce the overall weight of the concrete. This concept bubble deck slab has hollow spheres made from recycled plastic placed between two layers or meshes of reinforcement. In this paper, we are going to study two-way slabs and design two ways slabs (both conventional and bubble deck and its types).

If weight of slab is reduced, then dimensions of other supporting structural members (such as beams and columns) shall also decrease. Since there is decrease in both the slab and supporting member volumes, reduction in total load of the structure and the volume of concrete used is evident.

A bubble deck slab reduces volume of concrete up to 33% in the slab itself and up to 18% reduction in the supporting structural members. This reduction is done by removing the volume of concrete in the center portion where there is no need of concrete structurally. Such a practice of removal of concrete from regions where there is little or no structural requirement is a very old practice, but in this case the approach is different due to use of recyclable plastic (polyethylene) balls. It also provides greater insulation due to air trapped inside since air is a bad conductor of heat. The structure shall retain the heat inside for a long period of time. This causes efficiency in energy utilization to heat up the room or cool down the room depending on the region of construction.

Time is also saved in laying a bubble deck slab as the amount of concrete needed to be handled is far less than a conventional slab. The number of manual labors involved in the task can also be reduced for the same area of the slab. It was observed that a bubble deck slab is developed 20% fast that a conventional slab of same area. All the previous statements show the savings done in terms of concrete volume, time, manual effort and transport timings.

2. Objectives

- To use hollow polyethylene balls in a slab.
- To show the procedure of the experiment and a comparison of all parameters between a bubble deck slab and a conventional slab.
- To estimate concrete volume saved
- To study and compare the self-weights of the slabs
- from the Universal Testing Machine.
- To study failure or cracking patterns on both the slab types
- To analyze the results of M20 and M25 grades of concrete on the slabs

3. Properties of materials used

3.1 Polyethylene bubbles

Bubbles are made of high-density polyethylene. It is a non-porous material which does not react chemically with concrete or the reinforcement. The bubbles usually have high stiffness and strength to support the concrete in conjunction with the reinforcement provided safely during both placing the concrete and after.

Diameter of bubbles ranges from 90mm to 120mm. Due to this, the depth of slab varies from 140mm to 170mm.

Bubble spacing should be more than $1/9^{th}$ of bubble diameter.

3.1.1 Chemical properties:

Table 1: Chemical properties

Property	Description
Marketing name of product	HDPE (High Density Poly-Ethene)
Chemical name	Polyethylene
Chemical designation	$(-CH_2-CH_2-)_n$
Genus	Polyolefin
Hazardous substance	NO
Color	desired color can be obtained
Odor	feebly of paraffin
Relative Density	950 kg/m^3
Melting point	135˚C
Softening point	123˚C
Solubility	Insoluble in water

3.2 Concrete

Concrete used for filling the slab should be more than M30. It is an added advantage if a self-compacting concrete variant is used. This way, there will be proper compaction ensured in every unreachable region inside the slab. Aggregate used in this concrete should be less than 15mm.

For the experiment,

Table 2: Properties of concrete

Material	Description
Concrete	M30 Concrete mix design as pe IS 10262: 2009 Slump Value: 74mm
Cement	Ordinary Portland Cement (OPC) 53 Grade Testing done as per IS 456: 2000 Fineness: 9.2% Specific gravity: 3.14 Consistency: 31.06%
Coarse aggregate	10mm Conforming to IS 383 Specific Gravity: 2.8
Fine aggregate	River sand 4.75mm to 150 microns Conforming to IS 383 Specific Gravity: 2.59 Sieve Analysis: C_c = 0.863, C_u = 9.702, D_{10} = 0.17
Water	Potable water used for curing and mixing Conforming to IS 456: 2000

3.3 Reinforcing bars:

This is an integral part of the whole assembly. The top and bottom slab of concrete have one mesh each, which can be either tied or welded. Transverse ribs are used to keep these meshes intact after the bubbles are placed in the allocated positions between the meshes. Height difference between the bars is related to the bubble diameter. If the bubble diameter is greater, the height difference is greater and vice versa.

For the experiment,

F_y = 500 N/mm^2 were used.

Diameter of the bars used is as per the design.

4. Advantages

Following are the advantages of bubble deck slabs that have been justly outlined.

1) Structure
   a) Less weight than a conventional slab
   b) Depth of foundation is less
   c) More strength for same volume of slab
   d) Use of beams can be nullified if the span allows
   e) Columns used are of less thickness
   f) Has similar stiffness and bending strength of that of a conventional slab
2) Fabrication
   a) Light weight
   b) Less equipment or cheap lifting equipment
   c) Less work for manual labors
3) Engineering properties
   a) Less time required to cure the slab due to less volume of concrete
   b) Lower creep due to less concrete in the center and less heat generation
   c) High explosion resistance due to bi-axial design of the slab
   d) High earth-quake resistance due to less weight and rigid design
4) Environment
   a) Less CO_2 emissions
   b) Less concrete used
   c) Recycling of plastic possible
   d) Less efforts for transporting
5) Safety
   a) Fire proofing design
   b) Moisture or condensation proof design
   c) Earthquake resistance to an extent due to reduced weight
6) Cost
   a) Savings in concrete costs
   b) Savings in manual labor costs
   c) Decrease in construction and/or fabrication time
   d) Savings in transportation costs due to low weight handling
   e)

5. Experiment

5.1 Design of concrete specimen

Design of concrete mix was carried out as per the IS 10262: 2009. Size of the specimen is taken as 0.5m×0.5×0.1m for calculation purposes. Material required for the said dimensions is given below in table

Table 3: Experiment material specification

Material	Weight in kg and volume in liter
Cement	438 kg
Fine aggregate (Sand)	583 kg
Coarse aggregate	920 kg
Water (from water: cement ratio taken as 0.45)	198 liters

5.2 Design of the reinforcement specimen

Dimension of the specimen is 0.5m×0.5m×0.1m

Cover for the specimen is 20mm in both directions

5 bars of 8mm diameter have been used

Figure 1: Cover and specimen Reinforcement

5.3 Compressive strength of Conventional Concrete Slab:

Testing was done on the UTM after curing for 28 days. Dimensions of the block for testing was 0.5m×0.5m×0.1m. Its weight when measured was 22.76Kg.Maximum load on the slab was observed as 640 KN.

Equation 1: Calculation of compressive strength

$$\text{Compressive strength of the block} = \frac{\text{Ultimate Load}}{\text{Area of Slab}}$$

From the above equation, the compressive strength of the concrete slab is 25.6 N/mm^2.

5.4 Compressive strength of Bubble Deck Slab:

Testing was done on the UTM after curing for 28 days. Dimensions of the block for testing was 0.5m×0.5m×0.1m. Its weight when measured was 20.43 Kg. It can be noted that the weight of the bubble deck slab is lighter in weight than the conventional slab. Maximum load on the slab was observed as 655 KN.

Equation 2: Calculation of compressive strength of the bubble deck

$$\text{Compressive strength of the block} = \frac{\text{Ultimate Load}}{\text{Area of Slab}}$$

From the above equation, the compressive strength of the concrete slab is 26.2 N/mm^2.

6. Testing procedure

1. This testing is done at 28-day age as described. The test slabs are simply supported and load at a single point.
2. To ensure uniformity, the cover distances from the either sides of the loading frame are checked and ensured that the load is acting at the center.
3. These specimens were placed on the Universal Testing Machine and load was made to act at the centerline.
4. All gauges were kept in appropriate locations and initial readings were noted.
5. After every load increment made, the values on gauges were recorded for both middle span deflection and cracks developed along with their propagation.
6. All deflections were measured at their middle-span. When the loading was advanced, the increment of load was made smaller till failure was reached.
7. At failure, the load indicator stopped working and deflection increased very fast without any increase in the load application.
8. All the values of load and deflection were noted for every 5KN interval.

Cracking patterns on the slab can be seen in the figure below.

Figure 2: Crack patterns while testing the slabs

7. Observation

The first observation is that the behavior of the bubble deck slab is very much dependent on the ratio of bubble diameter to the thickness of the slab.

For M20 concrete

Table 4: M20 concrete slab load and deflections

Load in KN	Conventional Slab	Bubble Deck Slab 1	Bubble Deck Slab 2
30	0.29	0.89	0.84
60	0.89	1.23	1.42
90	1.07	1.91	1.99
120	1.85	2.89	3.42
150	2.01	4.23	4.82
180	3.49	6.19	6.79
210	4.25	8.09	9.01

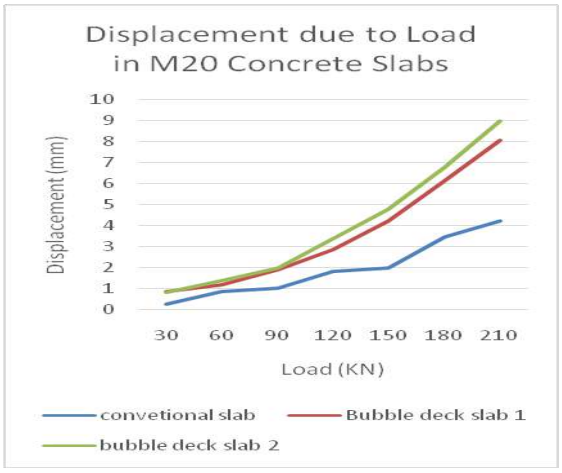

Graph 1: Displacement due to load in M20 Concrete slabs

For M25 Concrete used in the slab

Table 5: M25 concrete load and deflections

Load in KN	Conventional Slab	Bubble Deck Slab 1	Bubble Deck Slab 2
30	0.069	0.91	0.91
60	0.091	1.11	0.67
90	0.121	1.21	1.12
120	0.29	2.01	1.31
150	0.44	2.41	2.49
180	1.03	2.9	3.31
210	1.35	3.5	3.52
240	2.39	4.07	4.21
270	3.02	5.7	4.71
300	3.39	6.98	5.81
330	4.19	7.59	6.84

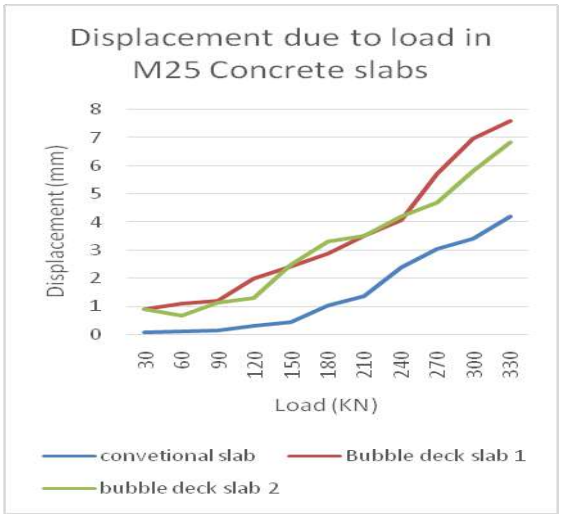

Graph 2: Displacement due to load in M25 concrete slabs

8. DISCUSSION

From this experiment, we can say that the bubble deck slab has a reduced volume of concrete which ultimately decreases the dead load on the slab. Parallelly, the load bearing capacity also increases with respect to a conventional concrete slab.

Type of arrangement of bubbles also plays a major role on the load carrying capacity of the slab. In alternative arrangement of the bubbles, there is an increase in the load bearing capacity than the convention slab but less than that of a continuous bubble deck slab. There is also a considerable change in the deflections shown by the bubble deck slabs which are nearer in deflection the conventional slabs.

Bubbles in the bubble deck slab improved the elasticity of the slab. A conventional slab deflects less than a bubble deck slab before failure. Based on the deflection, the failure can be estimated, and other preventive measures can be taken. Quantity of bubbles in the slab affects the elasticity property.

For a given volume, the compressive strength of a bubble deck slab is higher than the compressive strength of the conventional slab.

Comparison between the two slabs:

In a conventional slab, with dimensions 500mm×500mm×180mm, the maximum shear load taken by the slab was 160 KN. Crack propagation occurred at 75 KN.

In a bubble deck slab, with dimensions 500mm×500mm×180mm, the maximum shear load taken by the slab was 156 KN. Crack propagation occurred at 59 KN.

9. CONCLUSION

Bubble deck slabs give greater flexural strength, stiffness and shear force capacity. It was observed that when same quantity of concrete and reinforcement were used, the said structural properties of the slab increased by at least 60% than that of a conventional slab. The economy of construction increased by 40% when compared to a conventional slab.

For various experimental cases, the bubble deck slab had had deflections equal to that of conventional slabs under same loading conditions. Similarly, moments were 7-10% reduced to that of a conventional slab. The base shear of the structure also reduced (12-14%) due to decrease in loads by the concrete.

Economy in the corresponding structural members (such as beams and columns) was also obtained. It is due to the decrease in dead load and achievability of longer spans without increasing any dimension of the beams or columns.

There is an increased load bearing capacity in the bubble deck slab when compared to a conventional slab of same volume.

Usage of concrete is drastically decreased since 1kg of plastic replaced 100kg of concrete. This makes the bubble

deck a green initiative due to decrease in cement production and its CO_2 production.

Foundation sizes decrease for buildings as overall concrete weight decreases (in slabs, beams and columns).

Since concrete weight is decreased, the concrete handling time is also greatly reduced making the time to lay a slab lesser than that of a conventional slab. Time saving practice leads to money saving as the project will require less time and less labor to be completed.

If spacing between the balls increase the flexural strength also increases without any relation to the thickness of the slab.

Voids present in the slab due to the balls give it great thermal insulation compared to a conventional slab.

10. REFERENCES

- AarathiShethkar, Nagesh Bhanche. (2015). An Experimental Study on Bubble Deck Slab System with Elliptical Balls. Volume 12. Issue 1. Pages 21 -27.
- Annamiya, Anup Willson, Khadeehga, Mithoon, Mohammed Sheebili, Nincy C.K. (2018). Bubble deck slab. International Journal of Advance Engineering and Research Development (IJAERD). Volume 5. Issue 4. April 2018. Pages 2012-2015.
- Aron Maake, MeenaksiKhadao. (2018). Experimental study on bubble deck slab by using HDPE balls. International Journal of Advanced Innovative Technology in Engineering (IJAITE). Volume 3. Issue 2. March 2018. Pages 96-100.
- Bhagyasree Bade, Barelikhar. (2016). An Experimental Study on Two Way Bubble Deck Slab with Spherical Hollow Balls. International Journal of Recent Scientific Research (IJRSR). Volume 7. Issue 6. June 2016. Pages 11621-11626.
- Bhagyasree Bade, Suryavanshi. (2017). Structural Behavior on Two Way Bubble Deck Slab Using Hollow Spherical Balls. Vishwakarma Journal of Engineering Research (VJER). Volume 1. Issue 2. June 2017. Pages 116-124.
- Cobaix Engineering Manual. (2010). Retrieved from https://www.scribd.com/doc/200144278/Cobiax-Engineering-Manual-2010
- Deepan K., Sai Sharanya, Sai Ashwini. (2017). Experimental Study on Bubble Deck Slab using Polypropylene Balls. International Journal of Engineering Development and Research (IJEDR). Volume 5. Issue 4. Pages 716-721.
- Harshith Vanshrey, NithishJhauhari, Himansu Batt. (2017). A Review study on Bubble Deck Slab. International Journal for Research in Applied Science and Engineering Technology (IJRASET). Voume 5. Issue X. October 2017. Pages 2136-2139.
- Mohammed ShafeeqMushfeeq, ShikaShaini, Nishanth Raj. (2017). Experimental Study on Bubble Deck Slab. International Research Journal of Engineering and Technology (IRJET). Volume 4. Issue 5. May 2017. Pages 1000-1004.
- Najma Fathima, Vinay Singh. (2018). To Study Comparison Between Conventional Slab and Bubble Deck Slab. International Advanced Research Journal in Science Engineering and Technology. Volume 5. Issue 1. January 2018. Pages 70-76.
- Niraj Tewari, SaniaZaffar. (2016). Structural Behavior of Bubble Deck Slabs and Its Application. International Journal for Scientific Research and Development (IJSRD). Volume 4. Issue 2. Pages 433-437.
- Sonaal Nayak, DineyshJosi. (2017). A Voided Slab and Conventional Flat Slab- A Comparative Study. International Journal of Science Technology and Engineering (IJSTE). Volume 4. Issue 1. July 2017. Pages 44-50.
- Surendhar, Ranjitam. (2016. Numerical and Experimental Study in Bubble Deck Slab. International Journal of Engineering Science and Computing (IJESC). Volume 6. Issue 5. Pages 5959-5962.

How to cite this article: Ali MS, Babu SA. A structural study on bubble deck slab and its properties. International Journal of Research and Review. 2019; 6(10):352-357.

******

International Journal of Research and Review
www.ijrrjournal.com E-ISSN: 2349-9788; P-ISSN: 2454-2237

Short Communication

A Structural Study on Bubble Deck Slab and Its Properties

Mir Shahed Ali[1], Dr. S. Amaresh Babu[2]

[1]M.Tech Structural Engineering, Department of Civil Engineering, Nawab Shah Alam Khan College of Engineering and Technology, Hyderabad-24, TS.
[2]Head of Department, Department of Civil Engineering, Nawab Shah Alam Khan College of Engineering and Technology, Hyderabad-24, TS.

Corresponding Author: Mir Shahed Ali

ABSTRACT

Housing all over the world majorly comprises of concrete structures. They provide isolation and thermal comfort to the occupants. Majority of the concrete structures have flooring/roofing of thick concrete to bear the design loads. Due to his, the complete volume (eliminating the negligible volume of the reinforcement) of the roof slab comprises of concrete. Due to this, production of concrete has increased. Concrete production is not environment friendly. It is the primary producer of Carbon dioxide. In addition to this, the problem of concrete waste is at rise. Concrete waste can be reduced by two ways: recycling and using efficient volumes. Recycling is using the concrete waste in concrete generation which is of course of lower quality. Efficient volume is the way of using concrete in the most efficient way possible by substituting materials. In this paper, polyethylene balls are used in the slab to reduce concrete volume while maintaining the structural properties of the concrete. A comparison of strength of slab with the polyethylene balls and without them has been done to show the effectiveness of the new method. Various other strength tests were carried out and have been tabulated. At the end, cost effectiveness of the proposed slab has also been given.

Index terms: Bubble deck slab, Polyethylene balls, recycling concrete, concrete slabs systems.

1. INTRODUCTION

Concrete is strong in compression and weak when under tension. While considering a reinforced concrete slab, all the concrete above the neutral axis is subject to compressive forces and all the concrete below the neutral axis is subject to tensile forces. This supports the fact that concrete is the tension zone is of little use and contributes to making the slab heavier and reducing its overall efficiency. Upon having more slabs, it shall contribute to increased dead load of the structure. This dead load which is additional in nature and does not serve any positive purpose can be removed. This is done by introducing voids in the slab. Since voids cannot be made to form on their own, hollow balls or low weight balls are placed in the concrete to reduce the overall weight of the concrete. This concept bubble deck slab has hollow spheres made from recycled plastic placed between two layers or meshes of reinforcement. In this paper, we are going to study two-way slabs and design two ways slabs (both conventional and bubble deck and its types).

If weight of slab is reduced, then dimensions of other supporting structural members (such as beams and columns) shall also decrease. Since there is decrease in both the slab and supporting member volumes, reduction in total load of the structure and the volume of concrete used is evident.

A bubble deck slab reduces volume of concrete up to 33% in the slab itself and up to 18% reduction in the supporting structural members. This reduction is done by removing the volume of concrete in the center portion where there is no need of concrete structurally. Such a practice of removal of concrete from regions where there is little or no structural requirement is a very old practice, but in this case the approach is different due to use of recyclable plastic (polyethylene) balls. It also provides greater insulation due to air trapped inside since air is a bad conductor of heat. The structure shall retain the heat inside for a long period of time. This causes efficiency in energy utilization to heat up the room or cool down the room depending on the region of construction.

Time is also saved in laying a bubble deck slab as the amount of concrete needed to be handled is far less than a conventional slab. The number of manual labors involved in the task can also be reduced for the same area of the slab. It was observed that a bubble deck slab is developed 20% fast that a conventional slab of same area. All the previous statements show the savings done in terms of concrete volume, time, manual effort and transport timings.

2. Objectives

- To use hollow polyethylene balls in a slab.
- To show the procedure of the experiment and a comparison of all parameters between a bubble deck slab and a conventional slab.
- To estimate concrete volume saved
- To study and compare the self-weights of the slabs
- from the Universal Testing Machine.
- To study failure or cracking patterns on both the slab types
- To analyze the results of M20 and M25 grades of concrete on the slabs

3. Properties of materials used

3.1 Polyethylene bubbles

Bubbles are made of high-density polyethylene. It is a non-porous material which does not react chemically with concrete or the reinforcement. The bubbles usually have high stiffness and strength to support the concrete in conjunction with the reinforcement provided safely during both placing the concrete and after.

Diameter of bubbles ranges from 90mm to 120mm. Due to this, the depth of slab varies from 140mm to 170mm.

Bubble spacing should be more than $1/9^{th}$ of bubble diameter.

3.1.1 Chemical properties:

Table 1: Chemical properties

Property	Description
Marketing name of product	HDPE (High Density Poly-Ethene)
Chemical name	Polyethylene
Chemical designation	$(-CH_2-CH_2-)_n$
Genus	Polyolefin
Hazardous substance	NO
Color	desired color can be obtained
Odor	feebly of paraffin
Relative Density	950 kg/m^3
Melting point	135˚C
Softening point	123˚C
Solubility	Insoluble in water

3.2 Concrete

Concrete used for filling the slab should be more than M30. It is an added advantage if a self-compacting concrete variant is used. This way, there will be proper compaction ensured in every unreachable region inside the slab. Aggregate used in this concrete should be less than 15mm.

For the experiment,

Table 2: Properties of concrete

Material	Description
Concrete	M30 Concrete mix design as pe IS 10262: 2009 Slump Value: 74mm
Cement	Ordinary Portland Cement (OPC) 53 Grade Testing done as per IS 456: 2000 Fineness: 9.2% Specific gravity: 3.14 Consistency: 31.06%
Coarse aggregate	10mm Conforming to IS 383 Specific Gravity: 2.8
Fine aggregate	River sand 4.75mm to 150 microns Conforming to IS 383 Specific Gravity: 2.59 Sieve Analysis: C_c = 0.863, C_u = 9.702, D_{10} = 0.17
Water	Potable water used for curing and mixing Conforming to IS 456: 2000

3.3 Reinforcing bars:

This is an integral part of the whole assembly. The top and bottom slab of concrete have one mesh each, which can be either tied or welded. Transverse ribs are used to keep these meshes intact after the bubbles are placed in the allocated positions between the meshes. Height difference between the bars is related to the bubble diameter. If the bubble diameter is greater, the height difference is greater and vice versa.

For the experiment,

F_y = 500 N/mm^2 were used.

Diameter of the bars used is as per the design.

4. Advantages

Following are the advantages of bubble deck slabs that have been justly outlined.

1) Structure
   a) Less weight than a conventional slab
   b) Depth of foundation is less
   c) More strength for same volume of slab
   d) Use of beams can be nullified if the span allows
   e) Columns used are of less thickness
   f) Has similar stiffness and bending strength of that of a conventional slab
2) Fabrication
   a) Light weight
   b) Less equipment or cheap lifting equipment
   c) Less work for manual labors
3) Engineering properties
   a) Less time required to cure the slab due to less volume of concrete
   b) Lower creep due to less concrete in the center and less heat generation
   c) High explosion resistance due to bi-axial design of the slab
   d) High earth-quake resistance due to less weight and rigid design
4) Environment
   a) Less CO_2 emissions
   b) Less concrete used
   c) Recycling of plastic possible
   d) Less efforts for transporting
5) Safety
   a) Fire proofing design
   b) Moisture or condensation proof design
   c) Earthquake resistance to an extent due to reduced weight
6) Cost
   a) Savings in concrete costs
   b) Savings in manual labor costs
   c) Decrease in construction and/or fabrication time
   d) Savings in transportation costs due to low weight handling
   e)

5. Experiment

5.1 Design of concrete specimen

Design of concrete mix was carried out as per the IS 10262: 2009. Size of the specimen is taken as 0.5m×0.5×0.1m for calculation purposes. Material required for the said dimensions is given below in table

Table 3: Experiment material specification

Material	Weight in kg and volume in liter
Cement	438 kg
Fine aggregate (Sand)	583 kg
Coarse aggregate	920 kg
Water (from water: cement ratio taken as 0.45)	198 liters

5.2 Design of the reinforcement specimen

Dimension of the specimen is 0.5m×0.5m×0.1m

Cover for the specimen is 20mm in both directions

5 bars of 8mm diameter have been used

Figure 1: Cover and specimen Reinforcement

5.3 Compressive strength of Conventional Concrete Slab:

Testing was done on the UTM after curing for 28 days. Dimensions of the block for testing was 0.5m×0.5m×0.1m. Its weight when measured was 22.76Kg.Maximum load on the slab was observed as 640 KN.

Equation 1: Calculation of compressive strength

$$\text{Compressive strength of the block} = \frac{\text{Ultimate Load}}{\text{Area of Slab}}$$

From the above equation, the compressive strength of the concrete slab is 25.6 N/mm^2.

5.4 Compressive strength of Bubble Deck Slab:

Testing was done on the UTM after curing for 28 days. Dimensions of the block for testing was 0.5m×0.5m×0.1m. Its weight when measured was 20.43 Kg. It can be noted that the weight of the bubble deck slab is lighter in weight than the conventional slab. Maximum load on the slab was observed as 655 KN.

Equation 2: Calculation of compressive strength of the bubble deck

$$\text{Compressive strength of the block} = \frac{\text{Ultimate Load}}{\text{Area of Slab}}$$

From the above equation, the compressive strength of the concrete slab is 26.2 N/mm^2.

6. Testing procedure

1. This testing is done at 28-day age as described. The test slabs are simply supported and load at a single point.
2. To ensure uniformity, the cover distances from the either sides of the loading frame are checked and ensured that the load is acting at the center.
3. These specimens were placed on the Universal Testing Machine and load was made to act at the centerline.
4. All gauges were kept in appropriate locations and initial readings were noted.
5. After every load increment made, the values on gauges were recorded for both middle span deflection and cracks developed along with their propagation.
6. All deflections were measured at their middle-span. When the loading was advanced, the increment of load was made smaller till failure was reached.
7. At failure, the load indicator stopped working and deflection increased very fast without any increase in the load application.
8. All the values of load and deflection were noted for every 5KN interval.

Cracking patterns on the slab can be seen in the figure below.

Figure 2: Crack patterns while testing the slabs

7. Observation

The first observation is that the behavior of the bubble deck slab is very much dependent on the ratio of bubble diameter to the thickness of the slab.

For M20 concrete

Table 4: M20 concrete slab load and deflections

Load in KN	Conventional Slab	Bubble Deck Slab 1	Bubble Deck Slab 2
30	0.29	0.89	0.84
60	0.89	1.23	1.42
90	1.07	1.91	1.99
120	1.85	2.89	3.42
150	2.01	4.23	4.82
180	3.49	6.19	6.79
210	4.25	8.09	9.01

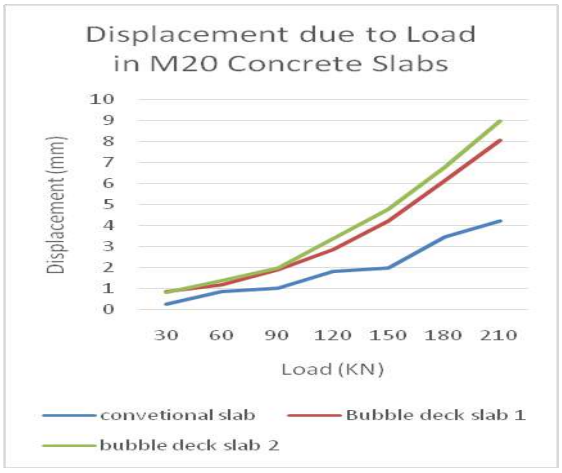

Graph 1: Displacement due to load in M20 Concrete slabs

For M25 Concrete used in the slab

Table 5: M25 concrete load and deflections

Load in KN	Conventional Slab	Bubble Deck Slab 1	Bubble Deck Slab 2
30	0.069	0.91	0.91
60	0.091	1.11	0.67
90	0.121	1.21	1.12
120	0.29	2.01	1.31
150	0.44	2.41	2.49
180	1.03	2.9	3.31
210	1.35	3.5	3.52
240	2.39	4.07	4.21
270	3.02	5.7	4.71
300	3.39	6.98	5.81
330	4.19	7.59	6.84

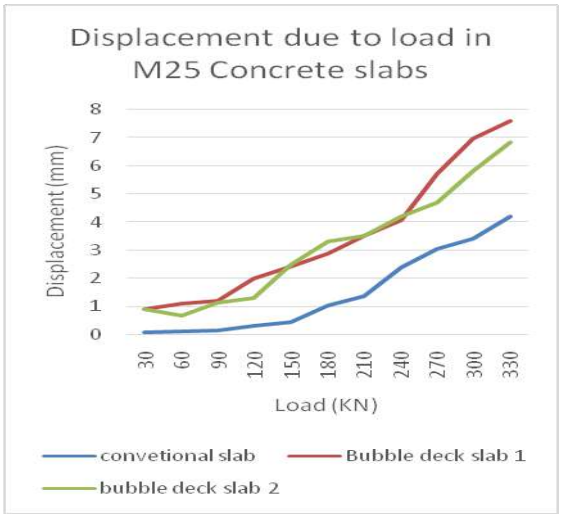

Graph 2: Displacement due to load in M25 concrete slabs

8. DISCUSSION

From this experiment, we can say that the bubble deck slab has a reduced volume of concrete which ultimately decreases the dead load on the slab. Parallelly, the load bearing capacity also increases with respect to a conventional concrete slab.

Type of arrangement of bubbles also plays a major role on the load carrying capacity of the slab. In alternative arrangement of the bubbles, there is an increase in the load bearing capacity than the convention slab but less than that of a continuous bubble deck slab. There is also a considerable change in the deflections shown by the bubble deck slabs which are nearer in deflection the conventional slabs.

Bubbles in the bubble deck slab improved the elasticity of the slab. A conventional slab deflects less than a bubble deck slab before failure. Based on the deflection, the failure can be estimated, and other preventive measures can be taken. Quantity of bubbles in the slab affects the elasticity property.

For a given volume, the compressive strength of a bubble deck slab is higher than the compressive strength of the conventional slab.

Comparison between the two slabs:

In a conventional slab, with dimensions 500mm×500mm×180mm, the maximum shear load taken by the slab was 160 KN. Crack propagation occurred at 75 KN.

In a bubble deck slab, with dimensions 500mm×500mm×180mm, the maximum shear load taken by the slab was 156 KN. Crack propagation occurred at 59 KN.

9. CONCLUSION

Bubble deck slabs give greater flexural strength, stiffness and shear force capacity. It was observed that when same quantity of concrete and reinforcement were used, the said structural properties of the slab increased by at least 60% than that of a conventional slab. The economy of construction increased by 40% when compared to a conventional slab.

For various experimental cases, the bubble deck slab had had deflections equal to that of conventional slabs under same loading conditions. Similarly, moments were 7-10% reduced to that of a conventional slab. The base shear of the structure also reduced (12-14%) due to decrease in loads by the concrete.

Economy in the corresponding structural members (such as beams and columns) was also obtained. It is due to the decrease in dead load and achievability of longer spans without increasing any dimension of the beams or columns.

There is an increased load bearing capacity in the bubble deck slab when compared to a conventional slab of same volume.

Usage of concrete is drastically decreased since 1kg of plastic replaced 100kg of concrete. This makes the bubble

deck a green initiative due to decrease in cement production and its CO_2 production.

Foundation sizes decrease for buildings as overall concrete weight decreases (in slabs, beams and columns).

Since concrete weight is decreased, the concrete handling time is also greatly reduced making the time to lay a slab lesser than that of a conventional slab. Time saving practice leads to money saving as the project will require less time and less labor to be completed.

If spacing between the balls increase the flexural strength also increases without any relation to the thickness of the slab.

Voids present in the slab due to the balls give it great thermal insulation compared to a conventional slab.

10. REFERENCES

- AarathiShethkar, Nagesh Bhanche. (2015). An Experimental Study on Bubble Deck Slab System with Elliptical Balls. Volume 12. Issue 1. Pages 21 -27.
- Annamiya, Anup Willson, Khadeehga, Mithoon, Mohammed Sheebili, Nincy C.K. (2018). Bubble deck slab. International Journal of Advance Engineering and Research Development (IJAERD). Volume 5. Issue 4. April 2018. Pages 2012-2015.
- Aron Maake, MeenaksiKhadao. (2018). Experimental study on bubble deck slab by using HDPE balls. International Journal of Advanced Innovative Technology in Engineering (IJAITE). Volume 3. Issue 2. March 2018. Pages 96-100.
- Bhagyasree Bade, Barelikhar. (2016). An Experimental Study on Two Way Bubble Deck Slab with Spherical Hollow Balls. International Journal of Recent Scientific Research (IJRSR). Volume 7. Issue 6. June 2016. Pages 11621-11626.
- Bhagyasree Bade, Suryavanshi. (2017). Structural Behavior on Two Way Bubble Deck Slab Using Hollow Spherical Balls. Vishwakarma Journal of Engineering Research (VJER). Volume 1. Issue 2. June 2017. Pages 116-124.
- Cobaix Engineering Manual. (2010). Retrieved from https://www.scribd.com/doc/200144278/Cobiax-Engineering-Manual-2010
- Deepan K., Sai Sharanya, Sai Ashwini. (2017). Experimental Study on Bubble Deck Slab using Polypropylene Balls. International Journal of Engineering Development and Research (IJEDR). Volume 5. Issue 4. Pages 716-721.
- Harshith Vanshrey, NithishJhauhari, Himansu Batt. (2017). A Review study on Bubble Deck Slab. International Journal for Research in Applied Science and Engineering Technology (IJRASET). Voume 5. Issue X. October 2017. Pages 2136-2139.
- Mohammed ShafeeqMushfeeq, ShikaShaini, Nishanth Raj. (2017). Experimental Study on Bubble Deck Slab. International Research Journal of Engineering and Technology (IRJET). Volume 4. Issue 5. May 2017. Pages 1000-1004.
- Najma Fathima, Vinay Singh. (2018). To Study Comparison Between Conventional Slab and Bubble Deck Slab. International Advanced Research Journal in Science Engineering and Technology. Volume 5. Issue 1. January 2018. Pages 70-76.
- Niraj Tewari, SaniaZaffar. (2016). Structural Behavior of Bubble Deck Slabs and Its Application. International Journal for Scientific Research and Development (IJSRD). Volume 4. Issue 2. Pages 433-437.
- Sonaal Nayak, DineyshJosi. (2017). A Voided Slab and Conventional Flat Slab- A Comparative Study. International Journal of Science Technology and Engineering (IJSTE). Volume 4. Issue 1. July 2017. Pages 44-50.
- Surendhar, Ranjitam. (2016. Numerical and Experimental Study in Bubble Deck Slab. International Journal of Engineering Science and Computing (IJESC). Volume 6. Issue 5. Pages 5959-5962.

How to cite this article: Ali MS, Babu SA. A structural study on bubble deck slab and its properties. International Journal of Research and Review. 2019; 6(10):352-357.

******

International Journal of Research and Review
www.ijrrjournal.com E-ISSN: 2349-9788; P-ISSN: 2454-2237

Short Communication

A Structural Study on Bubble Deck Slab and Its Properties

Mir Shahed Ali[1], Dr. S. Amaresh Babu[2]

[1]M.Tech Structural Engineering, Department of Civil Engineering, Nawab Shah Alam Khan College of Engineering and Technology, Hyderabad-24, TS.
[2]Head of Department, Department of Civil Engineering, Nawab Shah Alam Khan College of Engineering and Technology, Hyderabad-24, TS.

Corresponding Author: Mir Shahed Ali

ABSTRACT

Housing all over the world majorly comprises of concrete structures. They provide isolation and thermal comfort to the occupants. Majority of the concrete structures have flooring/roofing of thick concrete to bear the design loads. Due to his, the complete volume (eliminating the negligible volume of the reinforcement) of the roof slab comprises of concrete. Due to this, production of concrete has increased. Concrete production is not environment friendly. It is the primary producer of Carbon dioxide. In addition to this, the problem of concrete waste is at rise. Concrete waste can be reduced by two ways: recycling and using efficient volumes. Recycling is using the concrete waste in concrete generation which is of course of lower quality. Efficient volume is the way of using concrete in the most efficient way possible by substituting materials. In this paper, polyethylene balls are used in the slab to reduce concrete volume while maintaining the structural properties of the concrete. A comparison of strength of slab with the polyethylene balls and without them has been done to show the effectiveness of the new method. Various other strength tests were carried out and have been tabulated. At the end, cost effectiveness of the proposed slab has also been given.

Index terms: Bubble deck slab, Polyethylene balls, recycling concrete, concrete slabs systems.

1. INTRODUCTION

Concrete is strong in compression and weak when under tension. While considering a reinforced concrete slab, all the concrete above the neutral axis is subject to compressive forces and all the concrete below the neutral axis is subject to tensile forces. This supports the fact that concrete is the tension zone is of little use and contributes to making the slab heavier and reducing its overall efficiency. Upon having more slabs, it shall contribute to increased dead load of the structure. This dead load which is additional in nature and does not serve any positive purpose can be removed. This is done by introducing voids in the slab. Since voids cannot be made to form on their own, hollow balls or low weight balls are placed in the concrete to reduce the overall weight of the concrete. This concept bubble deck slab has hollow spheres made from recycled plastic placed between two layers or meshes of reinforcement. In this paper, we are going to study two-way slabs and design two ways slabs (both conventional and bubble deck and its types).

If weight of slab is reduced, then dimensions of other supporting structural members (such as beams and columns) shall also decrease. Since there is decrease in both the slab and supporting member volumes, reduction in total load of the structure and the volume of concrete used is evident.

A bubble deck slab reduces volume of concrete up to 33% in the slab itself and up to 18% reduction in the supporting structural members. This reduction is done by removing the volume of concrete in the center portion where there is no need of concrete structurally. Such a practice of removal of concrete from regions where there is little or no structural requirement is a very old practice, but in this case the approach is different due to use of recyclable plastic (polyethylene) balls. It also provides greater insulation due to air trapped inside since air is a bad conductor of heat. The structure shall retain the heat inside for a long period of time. This causes efficiency in energy utilization to heat up the room or cool down the room depending on the region of construction.

Time is also saved in laying a bubble deck slab as the amount of concrete needed to be handled is far less than a conventional slab. The number of manual labors involved in the task can also be reduced for the same area of the slab. It was observed that a bubble deck slab is developed 20% fast that a conventional slab of same area. All the previous statements show the savings done in terms of concrete volume, time, manual effort and transport timings.

2. Objectives

- To use hollow polyethylene balls in a slab.
- To show the procedure of the experiment and a comparison of all parameters between a bubble deck slab and a conventional slab.
- To estimate concrete volume saved
- To study and compare the self-weights of the slabs
- from the Universal Testing Machine.
- To study failure or cracking patterns on both the slab types
- To analyze the results of M20 and M25 grades of concrete on the slabs

3. Properties of materials used

3.1 Polyethylene bubbles

Bubbles are made of high-density polyethylene. It is a non-porous material which does not react chemically with concrete or the reinforcement. The bubbles usually have high stiffness and strength to support the concrete in conjunction with the reinforcement provided safely during both placing the concrete and after.

Diameter of bubbles ranges from 90mm to 120mm. Due to this, the depth of slab varies from 140mm to 170mm.

Bubble spacing should be more than $1/9^{th}$ of bubble diameter.

3.1.1 Chemical properties:

Table 1: Chemical properties

Property	Description
Marketing name of product	HDPE (High Density Poly-Ethene)
Chemical name	Polyethylene
Chemical designation	$(-CH_2-CH_2-)_n$
Genus	Polyolefin
Hazardous substance	NO
Color	desired color can be obtained
Odor	feebly of paraffin
Relative Density	950 kg/m^3
Melting point	135˚C
Softening point	123˚C
Solubility	Insoluble in water

3.2 Concrete

Concrete used for filling the slab should be more than M30. It is an added advantage if a self-compacting concrete variant is used. This way, there will be proper compaction ensured in every unreachable region inside the slab. Aggregate used in this concrete should be less than 15mm.

For the experiment,

Table 2: Properties of concrete

Material	Description
Concrete	M30 Concrete mix design as pe IS 10262: 2009 Slump Value: 74mm
Cement	Ordinary Portland Cement (OPC) 53 Grade Testing done as per IS 456: 2000 Fineness: 9.2% Specific gravity: 3.14 Consistency: 31.06%
Coarse aggregate	10mm Conforming to IS 383 Specific Gravity: 2.8
Fine aggregate	River sand 4.75mm to 150 microns Conforming to IS 383 Specific Gravity: 2.59 Sieve Analysis: C_c = 0.863, C_u = 9.702, D_{10} = 0.17
Water	Potable water used for curing and mixing Conforming to IS 456: 2000

3.3 Reinforcing bars:

This is an integral part of the whole assembly. The top and bottom slab of concrete have one mesh each, which can be either tied or welded. Transverse ribs are used to keep these meshes intact after the bubbles are placed in the allocated positions between the meshes. Height difference between the bars is related to the bubble diameter. If the bubble diameter is greater, the height difference is greater and vice versa.

For the experiment,

F_y = 500 N/mm^2 were used.

Diameter of the bars used is as per the design.

4. Advantages

Following are the advantages of bubble deck slabs that have been justly outlined.

1) Structure
   a) Less weight than a conventional slab
   b) Depth of foundation is less
   c) More strength for same volume of slab
   d) Use of beams can be nullified if the span allows
   e) Columns used are of less thickness
   f) Has similar stiffness and bending strength of that of a conventional slab
2) Fabrication
   a) Light weight
   b) Less equipment or cheap lifting equipment
   c) Less work for manual labors
3) Engineering properties
   a) Less time required to cure the slab due to less volume of concrete
   b) Lower creep due to less concrete in the center and less heat generation
   c) High explosion resistance due to bi-axial design of the slab
   d) High earth-quake resistance due to less weight and rigid design
4) Environment
   a) Less CO_2 emissions
   b) Less concrete used
   c) Recycling of plastic possible
   d) Less efforts for transporting
5) Safety
   a) Fire proofing design
   b) Moisture or condensation proof design
   c) Earthquake resistance to an extent due to reduced weight
6) Cost
   a) Savings in concrete costs
   b) Savings in manual labor costs
   c) Decrease in construction and/or fabrication time
   d) Savings in transportation costs due to low weight handling
   e)

5. Experiment

5.1 Design of concrete specimen

Design of concrete mix was carried out as per the IS 10262: 2009. Size of the specimen is taken as 0.5m×0.5×0.1m for calculation purposes. Material required for the said dimensions is given below in table

Table 3: Experiment material specification

Material	Weight in kg and volume in liter
Cement	438 kg
Fine aggregate (Sand)	583 kg
Coarse aggregate	920 kg
Water (from water: cement ratio taken as 0.45)	198 liters

5.2 Design of the reinforcement specimen

Dimension of the specimen is 0.5m×0.5m×0.1m

Cover for the specimen is 20mm in both directions

5 bars of 8mm diameter have been used

Figure 1: Cover and specimen Reinforcement

5.3 Compressive strength of Conventional Concrete Slab:

Testing was done on the UTM after curing for 28 days. Dimensions of the block for testing was 0.5m×0.5m×0.1m. Its weight when measured was 22.76Kg.Maximum load on the slab was observed as 640 KN.

Equation 1: Calculation of compressive strength

$$\text{Compressive strength of the block} = \frac{\text{Ultimate Load}}{\text{Area of Slab}}$$

From the above equation, the compressive strength of the concrete slab is 25.6 N/mm^2.

5.4 Compressive strength of Bubble Deck Slab:

Testing was done on the UTM after curing for 28 days. Dimensions of the block for testing was 0.5m×0.5m×0.1m. Its weight when measured was 20.43 Kg. It can be noted that the weight of the bubble deck slab is lighter in weight than the conventional slab. Maximum load on the slab was observed as 655 KN.

Equation 2: Calculation of compressive strength of the bubble deck

$$\text{Compressive strength of the block} = \frac{\text{Ultimate Load}}{\text{Area of Slab}}$$

From the above equation, the compressive strength of the concrete slab is 26.2 N/mm^2.

6. Testing procedure

1. This testing is done at 28-day age as described. The test slabs are simply supported and load at a single point.
2. To ensure uniformity, the cover distances from the either sides of the loading frame are checked and ensured that the load is acting at the center.
3. These specimens were placed on the Universal Testing Machine and load was made to act at the centerline.
4. All gauges were kept in appropriate locations and initial readings were noted.
5. After every load increment made, the values on gauges were recorded for both middle span deflection and cracks developed along with their propagation.
6. All deflections were measured at their middle-span. When the loading was advanced, the increment of load was made smaller till failure was reached.
7. At failure, the load indicator stopped working and deflection increased very fast without any increase in the load application.
8. All the values of load and deflection were noted for every 5KN interval.

Cracking patterns on the slab can be seen in the figure below.

Figure 2: Crack patterns while testing the slabs

7. Observation

The first observation is that the behavior of the bubble deck slab is very much dependent on the ratio of bubble diameter to the thickness of the slab.

For M20 concrete

Table 4: M20 concrete slab load and deflections

Load in KN	Conventional Slab	Bubble Deck Slab 1	Bubble Deck Slab 2
30	0.29	0.89	0.84
60	0.89	1.23	1.42
90	1.07	1.91	1.99
120	1.85	2.89	3.42
150	2.01	4.23	4.82
180	3.49	6.19	6.79
210	4.25	8.09	9.01

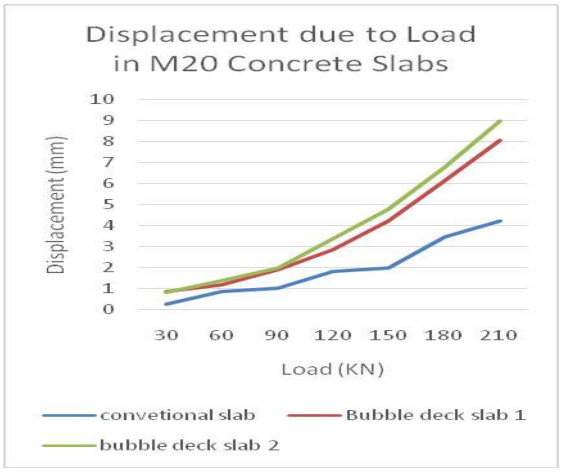

Graph 1: Displacement due to load in M20 Concrete slabs

For M25 Concrete used in the slab

Table 5: M25 concrete load and deflections

Load in KN	Conventional Slab	Bubble Deck Slab 1	Bubble Deck Slab 2
30	0.069	0.91	0.91
60	0.091	1.11	0.67
90	0.121	1.21	1.12
120	0.29	2.01	1.31
150	0.44	2.41	2.49
180	1.03	2.9	3.31
210	1.35	3.5	3.52
240	2.39	4.07	4.21
270	3.02	5.7	4.71
300	3.39	6.98	5.81
330	4.19	7.59	6.84

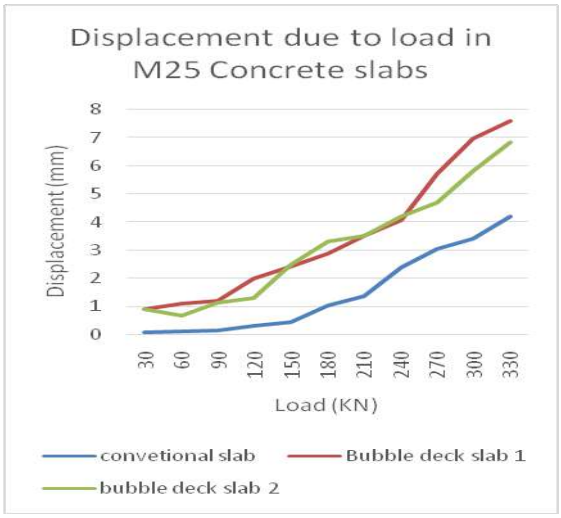

Graph 2: Displacement due to load in M25 concrete slabs

8. DISCUSSION

From this experiment, we can say that the bubble deck slab has a reduced volume of concrete which ultimately decreases the dead load on the slab. Parallelly, the load bearing capacity also increases with respect to a conventional concrete slab.

Type of arrangement of bubbles also plays a major role on the load carrying capacity of the slab. In alternative arrangement of the bubbles, there is an increase in the load bearing capacity than the convention slab but less than that of a continuous bubble deck slab. There is also a considerable change in the deflections shown by the bubble deck slabs which are nearer in deflection the conventional slabs.

Bubbles in the bubble deck slab improved the elasticity of the slab. A conventional slab deflects less than a bubble deck slab before failure. Based on the deflection, the failure can be estimated, and other preventive measures can be taken. Quantity of bubbles in the slab affects the elasticity property.

For a given volume, the compressive strength of a bubble deck slab is higher than the compressive strength of the conventional slab.

Comparison between the two slabs:

In a conventional slab, with dimensions 500mm×500mm×180mm, the maximum shear load taken by the slab was 160 KN. Crack propagation occurred at 75 KN.

In a bubble deck slab, with dimensions 500mm×500mm×180mm, the maximum shear load taken by the slab was 156 KN. Crack propagation occurred at 59 KN.

9. CONCLUSION

Bubble deck slabs give greater flexural strength, stiffness and shear force capacity. It was observed that when same quantity of concrete and reinforcement were used, the said structural properties of the slab increased by at least 60% than that of a conventional slab. The economy of construction increased by 40% when compared to a conventional slab.

For various experimental cases, the bubble deck slab had had deflections equal to that of conventional slabs under same loading conditions. Similarly, moments were 7-10% reduced to that of a conventional slab. The base shear of the structure also reduced (12-14%) due to decrease in loads by the concrete.

Economy in the corresponding structural members (such as beams and columns) was also obtained. It is due to the decrease in dead load and achievability of longer spans without increasing any dimension of the beams or columns.

There is an increased load bearing capacity in the bubble deck slab when compared to a conventional slab of same volume.

Usage of concrete is drastically decreased since 1kg of plastic replaced 100kg of concrete. This makes the bubble

deck a green initiative due to decrease in cement production and its CO_2 production.

Foundation sizes decrease for buildings as overall concrete weight decreases (in slabs, beams and columns).

Since concrete weight is decreased, the concrete handling time is also greatly reduced making the time to lay a slab lesser than that of a conventional slab. Time saving practice leads to money saving as the project will require less time and less labor to be completed.

If spacing between the balls increase the flexural strength also increases without any relation to the thickness of the slab.

Voids present in the slab due to the balls give it great thermal insulation compared to a conventional slab.

10. REFERENCES

- AarathiShethkar, Nagesh Bhanche. (2015). An Experimental Study on Bubble Deck Slab System with Elliptical Balls. Volume 12. Issue 1. Pages 21 -27.
- Annamiya, Anup Willson, Khadeehga, Mithoon, Mohammed Sheebili, Nincy C.K. (2018). Bubble deck slab. International Journal of Advance Engineering and Research Development (IJAERD). Volume 5. Issue 4. April 2018. Pages 2012-2015.
- Aron Maake, MeenaksiKhadao. (2018). Experimental study on bubble deck slab by using HDPE balls. International Journal of Advanced Innovative Technology in Engineering (IJAITE). Volume 3. Issue 2. March 2018. Pages 96-100.
- Bhagyasree Bade, Barelikhar. (2016). An Experimental Study on Two Way Bubble Deck Slab with Spherical Hollow Balls. International Journal of Recent Scientific Research (IJRSR). Volume 7. Issue 6. June 2016. Pages 11621-11626.
- Bhagyasree Bade, Suryavanshi. (2017). Structural Behavior on Two Way Bubble Deck Slab Using Hollow Spherical Balls. Vishwakarma Journal of Engineering Research (VJER). Volume 1. Issue 2. June 2017. Pages 116-124.
- Cobaix Engineering Manual. (2010). Retrieved from https://www.scribd.com/doc/200144278/Cobiax-Engineering-Manual-2010
- Deepan K., Sai Sharanya, Sai Ashwini. (2017). Experimental Study on Bubble Deck Slab using Polypropylene Balls. International Journal of Engineering Development and Research (IJEDR). Volume 5. Issue 4. Pages 716-721.
- Harshith Vanshrey, NithishJhauhari, Himansu Batt. (2017). A Review study on Bubble Deck Slab. International Journal for Research in Applied Science and Engineering Technology (IJRASET). Voume 5. Issue X. October 2017. Pages 2136-2139.
- Mohammed ShafeeqMushfeeq, ShikaShaini, Nishanth Raj. (2017). Experimental Study on Bubble Deck Slab. International Research Journal of Engineering and Technology (IRJET). Volume 4. Issue 5. May 2017. Pages 1000-1004.
- Najma Fathima, Vinay Singh. (2018). To Study Comparison Between Conventional Slab and Bubble Deck Slab. International Advanced Research Journal in Science Engineering and Technology. Volume 5. Issue 1. January 2018. Pages 70-76.
- Niraj Tewari, SaniaZaffar. (2016). Structural Behavior of Bubble Deck Slabs and Its Application. International Journal for Scientific Research and Development (IJSRD). Volume 4. Issue 2. Pages 433-437.
- Sonaal Nayak, DineyshJosi. (2017). A Voided Slab and Conventional Flat Slab- A Comparative Study. International Journal of Science Technology and Engineering (IJSTE). Volume 4. Issue 1. July 2017. Pages 44-50.
- Surendhar, Ranjitam. (2016. Numerical and Experimental Study in Bubble Deck Slab. International Journal of Engineering Science and Computing (IJESC). Volume 6. Issue 5. Pages 5959-5962.

How to cite this article: Ali MS, Babu SA. A structural study on bubble deck slab and its properties. International Journal of Research and Review. 2019; 6(10):352-357.

******

Efficient Priority Based Scheduling Scheme with Multi Sink Infrastructure in Heterogeneous Wireless Sensor Networks

S Anuradha[1], Dr.D Sreenivasa rao[2]

[1]Research Scholar, Department of ECE, JNTUH, Hyderabad, India.

[2]Professor, Department of ECE, JNTUHCEH, Hyderabad, India.

Abstract

The efficient Data transmission is an important task in WSNs along with environment monitoring. Most of WSNs are deployed in the hostile environments where manual intervention is less possible. So the data generated by these WSNs are sensitive data and needed to be transmitted immediately for further actions. Also, due to hostile environments, where providing constant power supply is a difficult task, these sensor nodes have to be energy efficient in order to prolong the network lifetime. The packet setting up would play a crucial part in lessening end-to-end transmission delay of data. This would support in decreasing sensors consumption of energy, hence extends the lifetime of the WSN (wireless sensor network). There are several traditional packet scheduling algorithms with different characteristics. But most of these scheduling algorithms schedule the data transmission in FIRST COME FIRST SERVE basis. Several packets might have to wait for a long duration as the outcome & this would lead to the expiration of packet. These results in long end-to end transmission delay, high energy consumption, and data loss. This nature affects the QoS of the entire network. Here we propose an Efficient Priority Based Packet Scheduling Scheme (EPBS), which schedule the data transmission based on packet priority. Our proposed scheme maintains three levels of queues such as HPQ (High Priority queue), LPQ (Low Priority queue) and NPQ (Non-Priority queue). Our EPBS scheme assigns priority to each data packets and allocates them in appropriate queues. The high priority data are allocated to HPQ, low priority packets are allocated with LPQ and the normal data are loaded with NPQ. This allocation reduces the tradeoff between priority and fairness and reduces the waiting time of the high priority data packets, which improves the QoS of the network. Our packet scheduling scheme which has been proposed would outperform the schemes that are conventional in terms of average data waiting duration as well as end-to-end delay of transmission & it also would decrease the consumption of sensor energy.

Keywords: Routing, WSN, Scheduling policy, Clustering, Transmission Delay, Priority scheduling, Energy efficient Protocol, NS-2.

I. Introduction

A WSN is a self-ordered network would contain many sensor nodes. Each node sensor involves a processing unit, sensing unit, transceiver unit as well as the unit of power. It is an ad-hoc network if they would classify and communicate amongst themselves. The perceptive of WSN has been organized in various application like systems of health care, environment identification systems as well as home automation. All these applications would need the cost-effective services & tiny manual intervention. The sensor nodes are normally small, & furnished with low powered source. Generally, it is not viable to charge or replace the drained sources in WSN. As the utilization of energy is the network lifetime indicator, the sensor nodes lifetime prolonging is very crucial. The energy efficiency would become the most significant quality of QoS enhancement for WSNs. Some other QoS characteristics' improvement is latency, fairness, ratio of delivery, & bandwidth. Communication among the sensor nodes is a primary aspect; Protocols as well as the algorithms

have to give surety to the challenges that have been connected like increase in the life span, self-configuration, robustness & tolerance of fault. The utilization of energy is the most crucial QoS restraint in WSN [1]. Scheduling the priority is the method through which the classification could decide the task to be carried out with respect to time. It has been utilized for effective load allocation along with aspired QoS [2]. According to the schedule of working, numerous data forwarding tasks have to be given priority hence that the loads could be regulated across the sensors. Most of the WSNs would function utilizing FCFS setting up the algorithm which would be transferring the packets in accordance with their time of arrival & this would require additional time to be conveyed to a BS (Base Station) at present.

WSNs would be consisting thousands or hundreds of sensors which have the capability for communicating along with each other [3]. The energy of each sensor node is restricted & regularly they are not rechargeable, so every sensor's consumption of energy has to be reduced for prolonging the existence span of WSNs. The prime causes of energy wastage are collision, idle listening, control overhead & overhearing [4]. Amongst all these, idle listening is a governing feature in many of the sensor network applications [5]. There are various techniques for prolonging the existence period of WSNs, for instance efficient deployment of sensors [6], optimization of WSN coverage [7], & scheduling the sleep/wake-up [8].

II. Literature survey

Lin Tang et al [9] propose a WDQS (wireless differentiated queuing service) algorithm for meeting the diverse delay requirements of multimedia transmission over WSNs. WDQS would convey the latest LDT (Latest Departure Time) scheduling measures for analyzing and forwarding by taking into consideration regarding the Packets lifetime. They also have projected a helpful method to delay for rest of the journey without adding any overhead by utilizing the query practice of the sink.

The presentation by Jandaeng et al [10] states the PSA (packet scheduling algorithm) for reducing the blocking packet in layer of MAC which would lead to lessen the whole packet conflict in the structure. PSA has been compared along with plain CA/ CSMA & other methods utilizing the topology of network standards in mathematical way. All the PSA performances are better than the CA/ CSMA standards. The PSA would yield better throughput than any other algorithms. The delay in average PSA is much greater than the previous tasks on the other side. Though, PSA would utilize the channel better than all the other algorithms.

Sensor MAC (S-MAC) [11] [12] would provide a cycle of periodic responsibility by means of all the nodes' synchronization of time. Periodic scheduling would reduce the utilization of energy in the state of listen & would assist a state of sleep to save the energy. The sensor nodes utilize CTS/ RTS messages for keeping away from collisions in the listen state. It does it in the next cycle if a sensor node does not transmit any data in the listen state which would cause a delay of transmission. Neighboring nodes would form virtual clusters for handling the planning.

The author suggests a latest routing method in [13] for WSNs known as NEAHC (Novel energy aware hierarchical cluster-based routing protocol) for extending the lifetime network utilizing the combination of a clustering method as well as an optimal relay algorithm selection. The scheme is to conclude an optimal routing course from the source to the destination by favoring the highest rest of the battery power, minimum consumption of energy in multi-hop path, & optimum fairness amongst sensor nodes.

In [14], author propose a method for WSNs called Network coded Mobile agent routing protocol (NCMA) to improve the clustering efficiency and to reduce frequent re-clustering in the network. In this proposed protocol, the introduction of MA's reduces the load among the CHs and the surrounding nodes. Also energy is not a primary parameter for CH selection. So CH rotation is

limited and prolong for a long time. Also, this method can be used for data aggregation. Its limitation is that it increases the delay for large networks. Here MA should travel for longer distance if total number of clusters is high.

In [15], author propose a method for WSNs called Energy efficient secondary level base stations (EE-SLB) to reduce the overhead and improve the data delivery process. In this method, we use multiple base stations. In order to verify the data between the base stations, data integrity check is used. The data integrity is nothing but ensuring the sent data is received without any loss or any alteration and also to check the authenticity of the data at the receiver side. Its limitation is multiple BS are vulnerable to attackers. The cost effective to deploy multiple BS.

In the previously proposed algorithms like NCMA & EE-SLB, the mechanism to properly schedule the data transfer from the nodes to SINK node is not exist. Due to this, the data flow cannot be properly managed and there might be the delay for the data packets which supposed to be delivered immediately. There are lot of traditional scheduling algorithms to properly schedule the data. But most of these scheduling algorithms schedule the data transmission in FIRST COME FIRST SERVE basis. Several packets as the consequence might have to wait for a long duration and this might lead to expiration of packet. These results in long end-to end transmission delay, high energy consumption, and data loss. So a scheduling algorithm that schedules the data according to data priority is proposed.

III. Proposed system

The nodes in the suggested plan with similar distance of hop from the BS have been believed to be placed at the identical hierarchical level. Data packets have been sensed by nodes at diverse stages have been practiced utilizing the plan of TDMA. The nodes that have been placed at the lowest phase & 1 level upper to the lowest level could be dealt time slots 1 & 2, correspondingly. Every node would be maintaining 3 phases of priority queues i.e. the utmost number of levels in the ready queue has been categorized as (i) High priority data packets have been located into the highest priority queues. (ii) Low priority data packets are placed into the Low priority queues. (iii) Non-priority data packets that have been sensed at the node are placed into the NPQ. In proportion to the priority of the packet and queue availability, node would plan the packet for the transmission.

The sizes of queue vary depending on the requirements of application in the advised arrangement. As the preemptive priority scheduling would incur overhead because of the storage context & switching in resource restraint networks of sensor, the ready queue size for non-preemptive priority scheduler has been anticipated to be slighter than that of the preemptive priority scheduler. The thought behind this is that the highest priority data have been practiced along with a least probable delay. And they have been located in non-preemptive priority assignments queue & could preempt data that is running currently. Hence, they have been supposed not to preserve a location of queue for an elongated span of time. Non-real-time packets that have been arrived from the sensor nodes at lower level have been positioned in the preemptive priority queue on the other side. This data packets' processing could be preempted by the top priority real-time tasks. The packets along with equal priority are procedure relied on the application / type of sensor in real time networks. It is relied on the packet priority in the simulation. When two equal priority packets would turn up at the ready queue at similar point of time, data packet has been produced at the lower level that will have top preference. Such happening would lessen the end-to-end delay of the lower level data to attain the BS. The smaller task will have top priority for two tasks of the similar phase.

The data generated in these sensor nodes are very sensitive and need to be delivered to the sink node without any time delay. In this work, we introduce the priority based scheduling algorithm that schedules the data transmission according to the priority of the data. This scheduling based on data priority eliminates the waiting time of the data

packets. Also to ensure the easy data delivery, multiple sinks are used to optimize the resource consumption and the delay caused due to the distance between the CH and SINK location.

Timeslots at every phase have not been fixed. Rather, they have been evaluated depending on the period of data sensing, rate of data transmission, and speed of CPU. They have been improved as the progress of phases by BS. Though, if there is any data of real-time/emergency at a specific stage, the time needed for transmitting such data would be short & wouldn't increase at the upper phases till there is no data aggregation. Rest of the time of a timeslot of nodes at a specific level has been utilized for processing the packets of data at other queues. As the possibility of having real-time emergency data is low, it is assessed that this scenario would not degrade the performance of system. It might enhance the perceived QoS (Quality of Service) by delivering real-time data quick as a substitute. If any node at a specific phase would finish its task prior to the expiration of its allotted timeslot additionally, node goes to sleep by turning its radio off for the sake of efficient energy.

The nodes of sensor in WSNs have been processed utilizing TDMA plan in this algorithm, & communication packages have been planned in 3 priority ready queues HPQ, LPQ and NPQ respectively. The higher priority queue HPQ would store the real-time packages of communication, & the packets in HPQ have been scheduled by their priority, which is a combination of deadline as well as the number of hop distance. Finally, least priority queue NPQ would store the rest non-real time communication packages whose destination is i node. The packets with deadlines that are expired have to be eliminated at the commencement of data packets processing. The packets at LPQ have been processed if there are no data packets existing at HPQ. At last, data in NPQ have been processed. If data packet turns up in HPQ while the packets in LPQ or NPQ initiate the processing, the packages in HPQ would preempt the packages' processing in LPQ or NPQ, by saving the lower priority packages context.

Algorithm

Pri(packet) = packet priority

HPQ = High Priority queue; LPQ = Low Priority queue; NPQ = Non- Priority queue;

###############

For all the nodes

Divide the nodes into 'n' clusters

Select CH nodes

End

Sensor nodes start generating the data packets

While (packet received by node) do

If Pri(packet) == high then

Add packet to High Priority queue HPQ

Else

If Pri(packet) == low then

Add packet to Low Priority queue LPQ

Else

Add packet into Non Priority queue NPQ

End If

End while

Priority queues have been filled with packets of data

Start transmitting the data packets to the destination node

Data processing in accordance with data priority

While (HPQ&& LPQ &&NPQ! = Empty)

If (HPQ! = Empty)

Process the HPQ data

End if

If (HPQ == empty &&LPQ! = Empty)

Process the LPQ data

End if

If (HPQ == empty && LPQ ===empty &&NPQ! = Empty)

Process the NPQ data

End if

End while

IV. esult and Discussion

4.1 imulation setup

We would utilize NS2 software for simulating the suggested Efficient Priority Based Packet Scheduling Scheme. The simulation configuration parameters have been summarized in Table 1.

Table1: Simulation Parameters

Parameter	Value
Area	1000x500m2
Traffic pattern	Constant bit rate (CBR)
Number of nodes	50
MAC	IEEE 802.11
Initial energy	1joule, 2 joule
Packet rate	1024 bytes / 0.1ms
Routing protocol	NCMA, EE-SLB, EPBS
Simulation time	40 sec

4.2 Performance metrics

We have assessed the performance of the Efficient Priority Based Packet Scheduling protocol in accordance with the parameters that are following. We would be comparing the NCMA, EE-SLB, protocols with the suggested protocol of EPBS.

- **elay:** It is the time quantity that has been taken by the packets to attain the respective destination.
- **nergy Consumption:** It is the amount of energy that has been consumed by the sensor nodes for the transmission of data.
- **hroughput:** It is the number of received packets successfully in a unit time and it is represented in bps.

4.3 R esult analysis

S

The delay, throughput & energy consumption have been assessed by varying the time of simulation in sec. for performance evaluation in EPBS and available protocols it represented in figures 1 to 3.

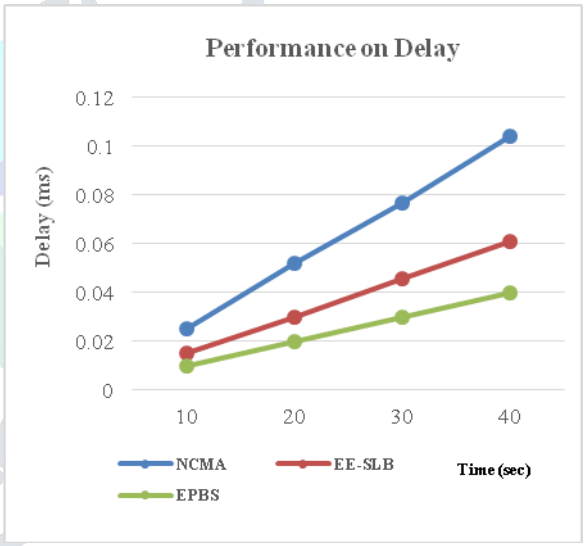

Fig1. Delay Performance

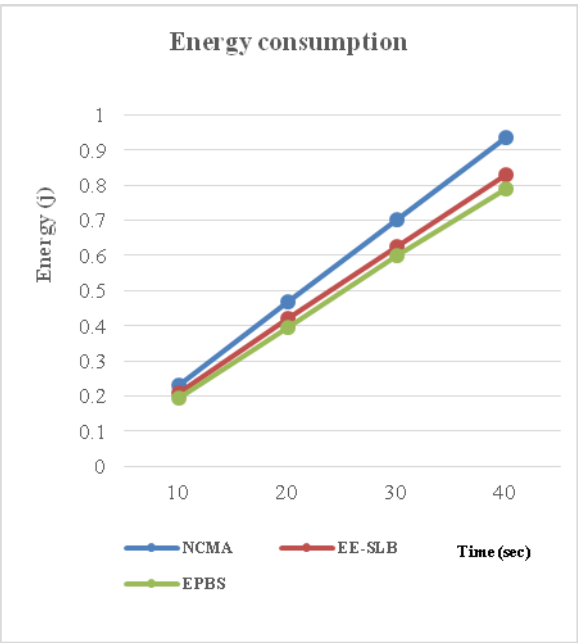

Fig2. Energy Consumption

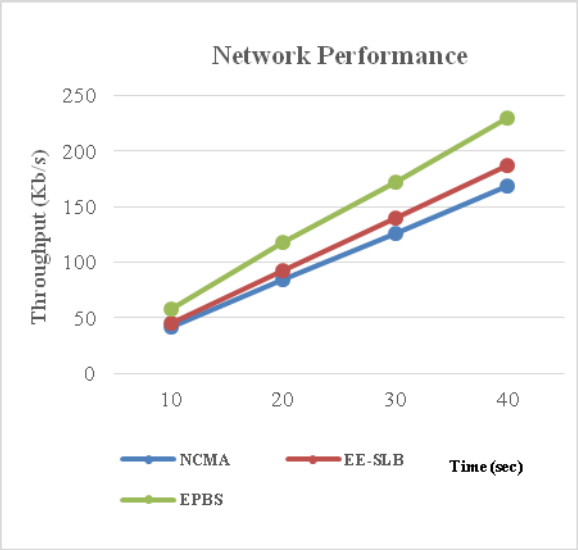

Fig3. Throughput

The scheduling would happen depending on the priority and priority scheduling would lessen the waiting time of the packets in each node. It would increase the throughput & decrease the delay of the data packets. The diminished delay in transmission of data would consume less energy when it is compared to the other methods.

Conclusion

This paper has proposed Efficient Priority Based Packet Scheduling Scheme (EPBS), which schedule the data transmission based on packet priority. The WSN data are more sensitive and application oriented and need to be transmitted according to data priority. Our EPBS method assigns each data packet with certain priority to transmit them on priority basis. For this purpose, our algorithm maintains three levels of queues namely HPQ (High Priority queue), LPQ (Low Priority queue) and NPQ (Non- Priority queue). The packets of data have been allocated to the queues depending on priority of data. The data packets in the HPQ is processed further as the data in the remaining queues have to be wait until all the data in the HPQ are processed. This will ensure that the high priority data are transmitted without any delay that reduces the total transmission delay of the network. Our simulation results show that the EPBS scheme which has been suggested attains more throughput, less end to end delay and less energy consumption compared with the formerly proposed protocols.

References

[1] Ali, M. Shoukath. "Priority Based Packet Scheduling Scheme in Wireless Sensor Networks.", IJARF, Volume 3, Issue 8, August 2016.

[2] SezerUzungenc and Tamer Dag, "A QoS Efficient Scheduling Algorithm for Wireless Sensor Networks ", *International Journal of Innovative Technology and Exploring Engineering (IJITEE)* ISSN: 2278-3075, Volume- 4 Issue-12, May 2015.

[3] M. Li, Z. Li, and A. V. Vasilakos, "A survey on topology control in wireless sensor networks: Taxonomy, comparative study, and open issues," *Proc. IEEE*, vol. 101, no. 12, pp. 2538–2557, Dec. 2013.

[4] W. Ye, J. Heidemann, and D. Estrin, "An energy-efficient MAC protocol for wireless sensor networks," in *Proc. IEEE INFOCOM*, New York, NY, USA, Jun. 2002, pp. 1567–1576.

[5] W. Ye, F. Silva, and J. Heidemann, "Ultra-low duty cycle MAC with scheduled channel polling," in *Proc. ACM SenSys*, Boulder, CO, USA, USA, Nov. 2006, pp. 321–334.

[6] X. Liu, "A deployment strategy for multiple types of requirements in wireless sensor networks," *IEEE Trans. Cybern.*, vol. 45, no. 10, pp. 2364–2376, Oct. 2015.

[7] C.-P. Chen *et al.*, "A hybrid memetic framework for coverage optimization in wireless sensor networks," *IEEE Trans. Cybern.*, vol. 45, no. 10, pp. 2309–2322, Oct. 2015.

[8] P. Guo, T. Jiang, Q. Zhang, and K. Zhang, "Sleep scheduling for critical event monitoring in wireless sensor networks," *IEEE Trans. ParallelDistrib. Syst.*, vol. 23, no. 2, pp. 345–352, Feb. 2012.

[9] Lin Tang, Quansheng Guan, Shengming Jiang, Bingyi Guo, "A Deadline-Aware and Distance-Aware Packet Scheduling Algorithm for Wireless Multimedia Sensor Networks", *International Journal of Distributed Sensor Networks*, Vol.11, Issue 3, March 2015.

[10] C. Jandaeng W. Suntiamontut, N. Elz ,"PSA: The Packet Scheduling Algorithm for Wireless Sensor Networks", *International journal on applications of graph theory in wireless ad hoc networks and sensornetworks (GRAPHHOC)* Vol.3, No.3, September 2011.

[11] W. Ye, J. Heidemann, D. Estrin, "An energy-efficient MAC protocol for wireless sensor networks", in: Proceedings of the Joint Conference of the IEEE Computer and Communications Societies (InfoCom), Vol. 3, 2002.

[12] W. Ye, J. Heidemann, and D. Estrin, "Medium Access Control with Coordinated Adaptive Sleeping for Wireless Sensor Networks," IEEE/ACM Trans. Net., vol. 12, no. 3, June 2004

[13] Wang Ke, Ou Yangrui, Ji Hong, Zhang Heli, Li Xi, " Energy aware hierarchical cluster-based routing protocol for WSNs", Volume 23, Issue 4, August 2016, Pages 46-52. https://doi.org/10.1016/S1005-8885(16)60044-4.

[14] S Anuradha, D Sreenivasa Rao, "A Network Coded Mobile agent based Energy Efficient Data Gathering Scheme for Heteronomous WSN's ", International Journal of Recent Technology and Engineering, Volume 8, Issue 1, May 2019.

[15] S Anuradha, D Sreenivasa Rao, "An Energy Efficient Data Aggregation Technique Using Multi-Sink Infrastructure in Heterogeneous Wireless Sensor Network", International Journal of Innovative Technology and Exploring Engineering, Volume 8, Issue 8, June 2019.

AN EXPERIMENTAL INVESTIGATION ON BEHAVIOUR OF CONCRETE BY PARTIAL REPLACEMENT OF CEMENT USING GGBS IN ADDITION WITH HYBRID FIBRE

MD.Rehanaj[1], Mr.Mohammed.Rafi[2]

[1]PG Scholar, Department of Civil Engineering, NSAKCET Hyderabad, India,

[2]Assistant Professor, Department of Civil Engineering, NSAKCET Hyderabad, India.

Abstract— In addition to hybrid fibers, an experimental analysis on concrete behaviour by partial replacement of cement using GGBS to boost engineering properties such as compressive strength, splitting tensile strength and flexural strength of normal concrete (NC) and hybrid fibre reinforced concrete (HFRC) with partial replacement of GGBS in cement was obtained from standard tests and compared with partial replacement of GGBS in cement. The chemical inorganic strength inhibitors used were alkali resistive glass fibre (GF) and polypropylene fibre (PF). In this analysis various percentages of glass and polypropylene fibers (0 percent, 0.2 percent, 0.4 percent, 0.6 percent, 0.8 percent and 1.00 percent) together act as a hybrid fibre with different percentages of GGBS (0 percent, 10 percent, 20 percent, 30 percent, 40 percent and 50 percent) are used to understand their effect on the reinforced concrete hybrid fibre. It is noted that the addition of fibers and up to 20 percent replacement of GGBS as the binder will boost the properties of concrete at 1.4 percent (0.6 percent polypropylene and 0.8 percent glass fibers).

Keywords— Hybrid Fibers, Hybrid Fibre reinforced concrete, Glass fibre, Polypropylene fibre, Ground granulated blast furnace slag, compressive strength, Split tensile strength and flexural strength.

1. INTRODUCTION

Concrete is the most commonly used commodity in the world for construction. Cement replacement experiments are being carried out to overcome its harmful effects on the environment and to minimize its use. In the concrete mix, fibers can disperse evently, such that surface cracking is often observed. This supplement converts large single cracks into a system of many smaller cracks, which is desired from the standpoint of protection and durability[4]. Optimum doses of PP and GF were collected from 7 days and 28 days of HFRC compressive strength with a combination of glass fibre (0.2 percent, 0.4 percent, 0.6 percent, 0.8 percent and 1 percent) and polypropylene fibers (0.2 percent, 0.4 percent, 0.6 percent, 0.8 percent and 1 percent) and cement replacement by GGBS (0 percent, 10 percent, 20 percent, 30 percent), and cement replacement by GGBS (0 percent, 10 percent, 20 percent, 30 percent).

- Research Significance: This study offers details on the conduct of HFRC with GGBS replacement for higher concrete strength relative to standard concrete. The optimum fibre material mixture was derived from the compressive strength of the concrete. In this paper, under compression, stress and flexure, hybrid FRC mixes carrying different combinations of polypropylene and glass fibers were examined.

2. LITERATURE REVIEW

Alaa M. Rashad * *et.al* :

In this study , the potential was explored to improve the compressive efficiency of high-volume GGBS (HVS) glue when viewed at elevated temperatures using small-scale metabolite (MK)(MMK). To produce HVS glue, Portland concrete (PC) was somewhat subjected to GGBS at a level of 70 percent, by weight. Afterword, with an addition of 2 percent by weight, GGBS was halfway subjected to MMK at levels ranging from 2 percent to 10 percent. Ready for six exclusive blends. The key blend was formed from 30 per cent PC and 70 per cent GGBS to produce HVS glue (with no MK expansion). This blend was allocated as mMK0. The remaining five blends were developed by halfway supplanting GGBS with MMK at different levels ranging from 2% to 10% with a 2%, by weight point. MMK particles are much better than GGBS particles just as MMK has higher Al_2O_3 content that causes much higher pozzolanic motion. But the compressive consistency has improved. Six cement blends have been selected for analysis. Which integrate control blend without filaments, steel fiber fortified cement (SFRC) with 0.5 percent steel strands and four half breed fiber reinforced cement (HFRC) of steel and polyester strands with a full volume component as 0.5 percent and attempts were made to link the various design properties with the amount of strands used.

Anithu Dev[1]*et.al*:

Their concentration was obtained from standard tests on mechanical properties such as compressive strength, dividing rigidity, break module, flexibility modulus of ordinary solid (NC), steel fiber enhanced cement (SFRC) and a mixture of fiber enforced cement. The full strand volume was set at 0.5 per cent of the absolute cement volume. A decrease in polyester fiber content (HFRC4) quality was found at 0.2 per cent. This may be due to the effect of fiber balling on higher fiber content. For SFRC, 0.5 percent steel filaments with an expansion of 11.19 percent are acquired with a greater compressive strength than NC. There was negligible variation of compressive quality among HFRC. Split rigidity is greatly influenced by the expansion of the filaments. HFRC3 (0.35% steel and 0.15% polyester) provides the most extreme level of split rigidity, which is 3.2% higher than SFRC.

Doo-Yeol Yoo [a]*et.al*:

This study expects to examine the flexural conduct of bars of steel-fibre-strengthened cement (SFRC) under semi-static and impact loads. For this reason , different SFRC pillars with three different compressive qualities (f 0c of approximately 49, 90, and 180 MPa) and four distinctive fiber volume substances (vf 0, 0.5, 1.0, and 2.0 percent) were developed and evaluated. For example of effect load, by expanding the probable vitality and efficiency, an expansion in the heap conveying limit was acquired, and an improvement in post-top behavior was seen by expanding the fiber material. The increase in fiber substance and quality also prompted improvements in the execution of leftover flexural after effect damage. The fiber content slightly affected the compressive consistency and versatile modulus while the strain limit (resisting the pinnacle) increased discernibly with the fiber material. Because of NC and HSC, the decline of the incline in the diving portion of the compressive anxiety strain bend was acquired with an expansion of fiber material, but, for example UHSC, the expansion of steel filaments had no enormous effect on the under pressure durability.

3. EXPERIMENTAL INVESTIGATION

Materials: In present work various materials are used; OPC 53 Grade, GGBS, fine aggregate: natural river sand, coarse aggregate, water and steel fibres.

Fig.1 (a): Glass Fibre

Fig.1 (b): Polypropylene fibre

Fig.1 (c): GGBS

Cement: Ordinary Portland 53 grade cement compliant with IS 12269-1987 (I.S.12269,1987) was used. 3.15 was the specific gravity of the cement. Physical characteristics of cement obtained as per IS12269-1987 (I.S. 12269, 1987) while conducting necessary tests. The results in Table.1 are shown.

TABLE 1 PROPERTIES OF CEMENT

Properties	Cement	GGBS
Fineness: Specific Surface	3.75	4.25
Specific gravity	3.15	2.87
Standard consistency of cement (%)	24%	34%
Setting time of cement A. Initial setting time(min) B. Final setting time (min)	 135 240	180

GGBS: The GGBS used in this experimental work is collected from local distributors from JSW cement Limited. The byproduct of melting ore to purify metals is ground granulated blast furnace slag. Slag has a pozzolanic reaction which allows compressive strength to increase. As per IS 4031-1988 (IS 4031, 1988),
Table 1 presents the physical properties of GGBS.

Fine aggregates: As a fine aggregate, locally available river sand conforming to the grading zone II of IS 383-1970 was used. The modulus of fineness is 2.75, with a specific gravity of 2.54. Coarse Aggregates: The coarse aggregate used is the IS383:1970 (IS383-1970) compliant crushed (angular) aggregate. The scale of the aggregates used in the test is 20 mm. The results of the sieve analysis were performed according to the IS 383-1970 (IS383-1970) specification. The modulus of fineness is 6.25 and the real gravity is 2.823.

Water: Clean drinking water is used for the process of casting and curing for the job.

Glass fibre: As shown in Figure 1(a), alkali resistant glass fibers are used in this study. Table 2 demonstrates the properties of glass fibers.

TABLE 2 PROPERTIES OF GLASS FIBER

Properties	Values
Tensile strength (MPa)	4028 to 4650
Elongation of break (%)	5.81
Diameter (μ)	10
Melting temperature bond	1558
Length of the fibre (mm)	12-13mm

Polypropylene fibre: Soft polypropylene fibers were used in this analysis as shown in Figure 1(b). Table 3 demonstrates the properties of polypropylene fibre.

TABLE 3
PROPERTIES OF POLYPROPYLENE FIBER

Properties	Values
Tensile strength (kg/cm2)	6000
Elongation of break (%)	45-55
Diameter (μ)	33-35
Length of the fibre (mm)	12-13

- **Mix Proportion**

Mix design was carried out using (I.S. 10262:2009). Mix proportions shown in Table 4

TABLE 4
MIX PROPORTIONS

Unit of batch	Water (Liters)	Cement (Kg)	F.A. (Kg)	C.A. (Kg)	Size of Agg. (mm)
Cubic meter content	168	350	695	1238	20
Ratio	0.48	1	1.98	3.53	

EXPERIMENTAL RESULTS AND DISCUSSIONS

As per IS: 10262(2009), mix design for M25 concrete grade was conducted with a mixing ratio of 1:1.98:3.53 with a water cement ratio of 0.48. Standard format test samples of 150 mm x 150 mm x 150 mm cubes for compressive strength with a mixture of different percentages of glass and polypropylene fibers (0 percent, 0.2 percent, 0.4 percent, 0.6 percent, 0.8 percent and 1.00 percent) were cast and healed for 28 days. In order to achieve the optimal dose of the mixture of fibers in the concrete, the specimens were tested. For 7 days and 28 days, cubes and cylinders with ideal hybrid fibre dosage and varying GGBS percentages (0 percent, 10 percent, 20 percent, 30 percent, 40 percent and 50 percent) were cast and cured. The specimens were tested to achieve the dosage of GGBS to be used for hybrid fibers in concrete under a compression testing machine. Beam samples of 500 mm x 100 mm x 100 mm with ideal hybrid fibre dose and various GGBS percentages (0 percent, 10 percent, 20 percent, 20 percent, 30 percent, 40 percent and 50 percent) were cast and healed for seven days and 28 days. To research the flexural behaviour of hybrid fibre reinforced concrete, the specimens were tested under the Universal Testing Machine according to IS: 516-1979. The workability of HFRC and GGBS-HFRC concrete was determined with the help of slump cone test. Decrease in workability was observed when there is an increase in percentage of GGBS in GGBS HFRC concrete.

a. Compressive Strength of the Hybrid Fibre Reinforced Concrete:

To find out the behaviour of normal concrete and HFRC in compression, the compressive strength was determined. By dividing the full load by the area of a cross section of the specimen, compressive strength was obtained. Hybrid fibre reinforced concrete compressive strengths with different percentages of PP and GF are shown in Table 5. Compressive resistance= F/A N/mm2.

TABLE 5
COMPRESSIVE STRENGTH OF HYBRID FIBRE REINFORCED CONCRETE

Mix No. (M)	*Percentage of Fibers*		*Average Compressive Strength for 28 Days (Mpa)*
	Polypropylene Fibre (P.F)	*Glass Fibre (G.F)*	
0	0	0	34.67
1	0.2	0.2	35.56
2		0.4	25.13
3		0.6	26.67
4		0.8	24.65
5		1.0	29.27
6	0.4	0.2	25.36
7		0.4	29.16
8		0.6	27.26
9		0.8	25.96
10		1.0	26.67
11	0.6	0.2	32.36
12		0.4	27.5
13		0.6	33.9
14		0.8	38.28
15		1.0	35.08
16	0.8	0.2	32.71
17		0.4	34.13
18		0.6	33.3
19		0.8	35.44
20		1.0	28.92
21	1.0	0.2	32
22		0.4	33.07
23		0.6	32.71
24		0.8	34.79
25		1.0	31.29

It was observed from the above results that cubes cast with a combination of glass fibre and polypropylene fibre developed a strong compressive strength of 38.28 MPa at 0.6 percent PP and 0.8 percent GF, which is comparatively higher than traditional concrete compressive strengths.

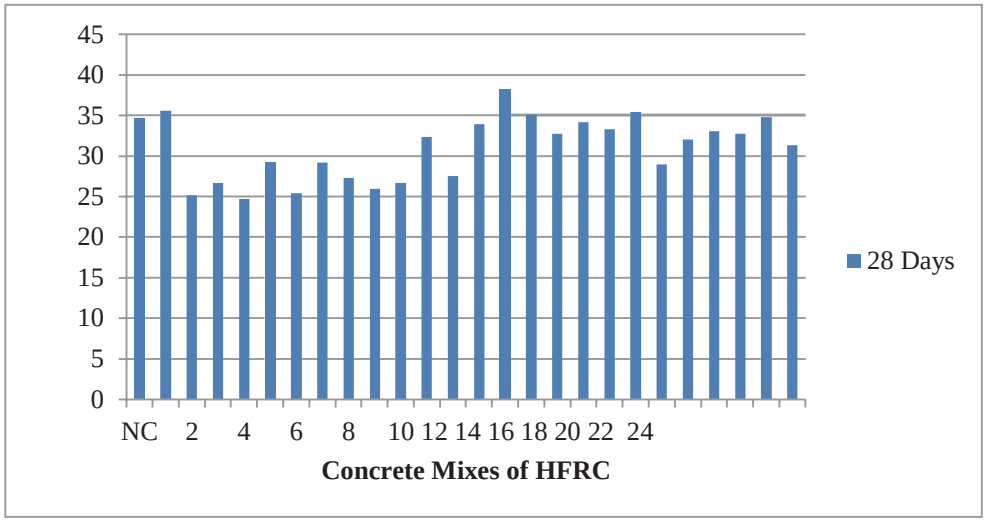

Fig. 2: Compressive Strength of HFRC (PP & GF)

b. Compressive and Split Tensile Strengths of Hybrid Fibre Reinforced Concrete with Partial Replacement of cement by GGBS:

Hybrid fibre reinforced concrete compressive and break tensile strengths with different percentages of GGBS are shown in Table 6.

Fig.3: Compressive Strength test.

Fig.4: Split tensile Strength test

c. TABLE 6

d. COMPRESSIVE AND SPLIT TENSILE STRENGTH OF HYBRID FIBRE REINFORCED CONCRETE WITH GGBS REPLACEMENT

Mix No. (M)	Percentage of Fibres		Percentage of GGBS (%)	Average Compressive Strength		Split Tensile Strength	
	Polypropylene Fibre (P.F)	Glass Fibre (G.F)		for 7 Days (Mpa)	for 28 Days (Mpa)	For 7 Days (Mpa)	for 28 Days (Mpa)
NC	0	0	0	21.22	36.43	1.92	3.31
0	0.6	0.8	0	22.79	38.28	2.07	3.48
1	0.6	0.8	10	21.48	36.59	1.95	3.32
2	0.6	0.8	20	21.63	40.07	1.96	3.64
3	0.6	0.8	30	22.22	36.44	2.02	3.31
4	0.6	0.8	40	24.15	35.26	2.19	3.20
5	0.6	0.8	50	19.85	31.85	1.80	2.89

From the above results it was found that cubes and cylinders cast with a mixture of 0.80 percent glass fibre and 0.60 percent polypropylene fibres with 20 percent GGBS cement replacement gave a compressive strength of 0.80 percent glass fibre and 0.60 percent polypropylene fibres with 20 percent cement replacement. 40.07 MPa and 3.64 MPa split tensile strength, higher than traditional concrete and hybrid fibre reinforced concrete cast compressive and split tensile strengths with maximum hybrid fibre dosage.

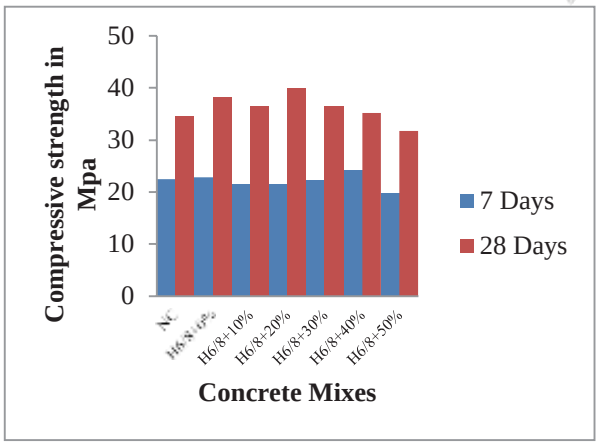

Fig.5: Compressive Strength of HFRC with GGBS

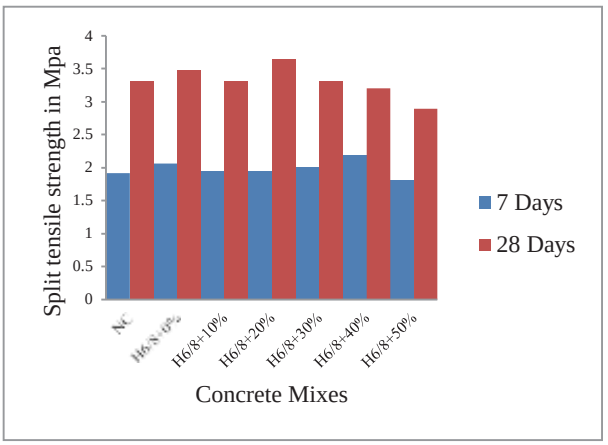

Fig.6: Split Tensile Strength of HFRC with GGBS

Flexural strength:

For 42 prism specimens, flexural strength was carried out and an average of three prisms were tested for each mix to assess the flexural strength of the concrete. The bending power of GGBS reinforced hybrid fibre concrete is shown in Table 7. The findings show that the flexural strength of concrete is maximal at 20 percent of GGBS replacement. Concrete At the age of 7 days and 28 days, the flexural strength test was performed on prisms of 100 mm × 100 mm × 500 mm and verified to IS 516-1959 to determine the action of beams and other flexural members when cast with regular concrete, HFRC and GGBS HFRC. The specimen was mounted on the universal test machine and two points of loading were applied to induce downward deflection via a hydraulic jack arrangement. The loading was carried on until the ultimate failure of the samples was achieved. The flexural intensity appears in Figure 4.

The flexural strength of prisms was calculated as follows:

Flexural strength = $3PL/2bd^2$

Where, P = Maximum load applied to the specimen, b = Measured width of the specimen, d = Measured depth of the specimen and L = Length of the span.

TABLE 7
AVERAGE FLEXURAL STRENGTH OF DIFFERENT CONCRETE MATRIX

	Flexural strength at 7 days (Mpa)	**Flexural strength at 28 days (Mpa)**
NC	2.24	3.2
HFRC (0.6%+0.8%)	2.31	3.3
GGBS 10%	2.45	3.5
GGBS 20%	2.66	3.8
GGBS 30%	2.59	3.7
GGBS 40%	2.52	3.6
GGBS 50%	2.38	3.4

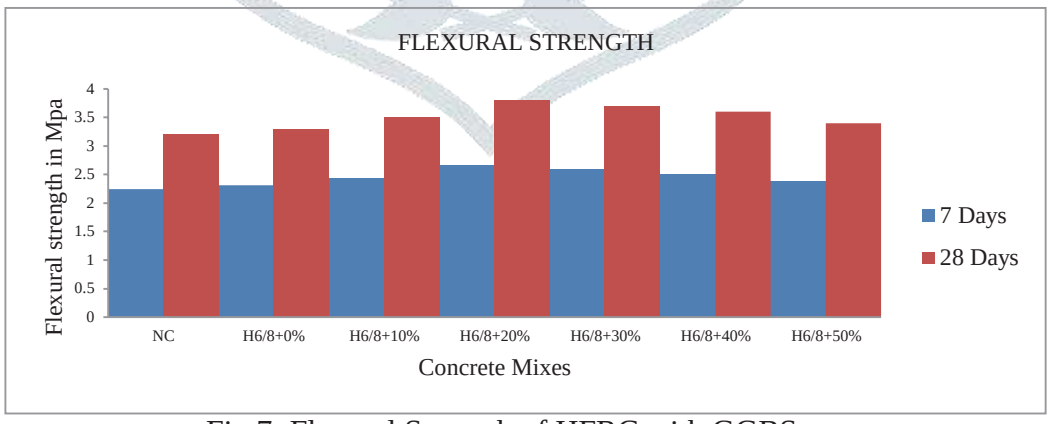

Fig.7: Flexural Strength of HFRC with GGBS

CONCLUSIONS

1) The optimal dosage of hybrid fibers in reinforced concrete hybrid fibers reached 1.4% of fibres, i.e. a mixture of 0.6% of polypropylene fibers and 0.8% of glass fibers. With the addition of fibers, the strength of regular concrete can increase by 10 percent.

2) With a 20 percent replacement of cement by GGBS, the compressive and split tensile strength of the hybrid fibre reinforced concrete cast with 1.4 percent hybrid fibers (0.6 percent polypropylene fibre and 0.8 percent glass fibre) resulted in a 10 percent improvement in both compressive and split tensile strengths of 40.07 Mpa and 40.07 Mpa respectively, i.e. MPa 3.64.

3) It was found that hybrid fibre reinforced concrete cast with 1.4% hybrid fibers (0.6% polypropylene fibre and 0.8% glass fibre) with 20% GGBS cement replacement gave a maximum flexural strength of 3.8 MPa with a flexural strength improvement of 18.75% compared to regular concrete.

4) Thus, hybrid fibre reinforced concrete (0.6 percent polypropylene fibre and 0.8 percent glass fibre) with up to 20 percent GGBS use as partial cement substitute not only enhances concrete's mechanical properties, but also protects the environment from GGBS hazards.

REFERENCES

[1] Alaa M. Rashad *, Dina M. Sadek," An investigation on Portland cement replaced by high-volume GGBS pastes modified with micro-sized metakaolin subjected to elevated temperatures", Elsevier/ International Journal of Sustainable Built Environment (2017) 6, 91–101.

[2] Anithu Dev1, Dr. Sabeena M.V2, "Mechanical Properties of Hybrid Fiber Reinforced Concrete" International Research Journal of Engineering and Technology (IRJET) Volume: 05 Issue: 04 | Apr-2018.

[3] Kutalmıs Recep Akçaa, Özgür Çakırb, Metin Ipeka,*, "Properties of polypropylene fiber reinforced concrete using recycled aggregates", Elsevier/ Construction and Building Materials 98 (2015) 620–630.

[4] Malgorzata Pajaka,*,"Investigation on Flexural Properties of Hybrid fiber Reinforced Self-Compacting Concrete", Elsevier/Procedia Engineering 161 (2016) 121 – 126.

[5] N. Banthiaa,1, F. Majdzadeha,1,2, J.Wua,1, V. Bindiganavileb,*,"Fiber synergy in Hybrid Fiber Reinforced Concrete (HyFRC) in flexure and direct shear", Elsevier/ Cement & Concrete Composites 48 (2014) 91–97.

[6] Suchita Hirde† and Pravin Gorse†, "Effect of Addition of Ground Granulated Blast Furnace Slag (GGBS) on Mechanical Properties of Fiber Reinforced Concrete" International Journal of Current Engineering and Technology, E-ISSN 2277 – 4106, P-ISSN 2347 – 5161.

[7] IS 456:2000, "Code of practice for plane and reinforced concrete, Bureau of Indian Standards, New Delhi, India).

[8] IS 516:1959 "Indian Standard methods of tests for strength of concrete", Bureau of Indian Standards, New Delhi, India.

[9] IS 383:1987, "Specification for Coarse and Fine Aggregates from Natural Sources for Concrete (Second Revision)", Ninth Reprint, September 1993, Bureau of Indian Standards, New Delhi, India.

[10] IS: 12269-2013, "Indian Standard specifications for 53 grade of cement", Bureau of Indian Standards, New Delhi, India.
IS: 10262-2009," Recommended guidelines for Concrete mix design". Bureau of Indian Standards, New Delhi, India

COMPARATIVE STUDY OF MODELLING AND DESIGNING OF PILE AND PILE RAFT FOUNDATION USING SAP 2000 AND CSI-SAFE

Prof. DR.AMARESH BABU

Department of Civil Engineering

NSAKCET, India

MOHAMMED ABDUL AJAZ

Department of Civil Engineering

NSAKCET, India

ABSTRACT: In recent years, the use of piled raft foundation has become more widespread, as the combined movement of raft and piles will increase the bearing capacity, minimize settlement and organize the piles to decrease unequal deflections in the raft. The piled raft foundation is a new phenomenon wherein the raft partially transfers the overall load from the superstructure by contact with soil. For the analysis and comparison of raft pile foundation and pile base modelling and design of pile raft foundation for a multi-storey structure, a standard construction is chosen for this project. It's a performance with and where SAP has been used to build the 3D analytical model, and the pile base is built with safe tools. The following criteria, story drifts, story displacements, forces, and time, shapes of modes have been tested, and the foundation falls under sub-structure.

1. INTRODUCTION

A geotechnical engineer who faces the foundation's architecture finds a shallow base to support a specific basic structure. As the structure's weight rises and the ground's carrying capacity compromises the structure's durability or functionality, one must resort to other kinds of base. Piles are an excellent solution in circumstances where low room capacity and complete installations are required. When constructing stacks as support for structures, a pile cap is commonly used to connect the pile heads. To study the effect of the raft and pile raft foundation on the structure subjected to earthquake loading.

- To study the effect of different soil types (soft clay, medium soil, and weather soil) on the raft and pile raft foundation's effect.
- To study various parameters like story displacement, story drift, and time period of the structure and compare with other models.

2 Literature Review

(Randolph, 1983; 1994) has developed very preliminary equations for the rigidity and load-sharing of the piled raft system between the piles and the raft. This approach is limited to the linear behavior of piled rafts' structure, which means that the base is constructed as a collection of piles with load allocations borne by the raft. By combining (Poulos & Davis, 1980) and this approach, an updated approach can be developed. The Poulos-Davis-Randolph (PDR) approach aims to use the components' stiffness to measure the piles' load percentage share and the raft.

(Maharaj, 2004) introduced the piled raft base, under the application of uniformly distributed load (UDL), three-dimensional nonlinear finite element analysis. Drucker-Prager Yield Criterion, Drucker, and Prager (1952) found that the soil medium's material nonlinearity was idealized. The raft and pile stiffness effect on the load settling action of the uniformly distributed load (UDL) piled raft base has been studied. As a production of the analysis, several plots of load settlement curves have been made. The figures below reveal the UDL (uniformly spread load) versus Raft and piled raft base settlement curves

(Cunha, Poulos, & Small, 2001), detailing the effect of the main external variables affecting their construction under concentrated column loads. The most significant parameters affecting the nature of the piled raft base, according to the authors, are those related to the characteristics of the pile (number, length, and disposition), the characteristics of the raft (thickness), and the total cost of the base, among others

3 MODELLING PARAMETERS

A G+20 storied reinforced concrete frame building situated in zone V, with a raft foundation and raft pile foundation on two soils, is taken for study. The building's plan area is 63 x 39 m, with 3m as each typical story's height. It consists of 16 bays in X-direction and 14 bays in Y-direction. The total heights of the buildings were 63m.

***Model* 1**: raft and raft pile foundation with soft soil
Model* 2:* raft and raft pile foundation with medium soil
Model* 3:* raft and raft pile foundation with hard soil

Dimensions of Structural Members

1.	Specifications	20 Storey
2.	Raft thickness	1000mm
3.	Slab thickness	125 mm
4.	Beam dimensions	300x500 mm 300x500 mm
5.	Column dimensions	750x750 mm
6.	Grade of concrete	M30
7.	Grade of steel	HYSD500
8.	Unit weight of concrete	25 KN/m^3
9.	Live loads (a) Floor loads (b) Floor finishes	 4 KN/m^3 1.5 KN/m^2
10.	Importance factor	1.0
11.	Seismic zone factor	0.36
12.	Response reduction factor	5

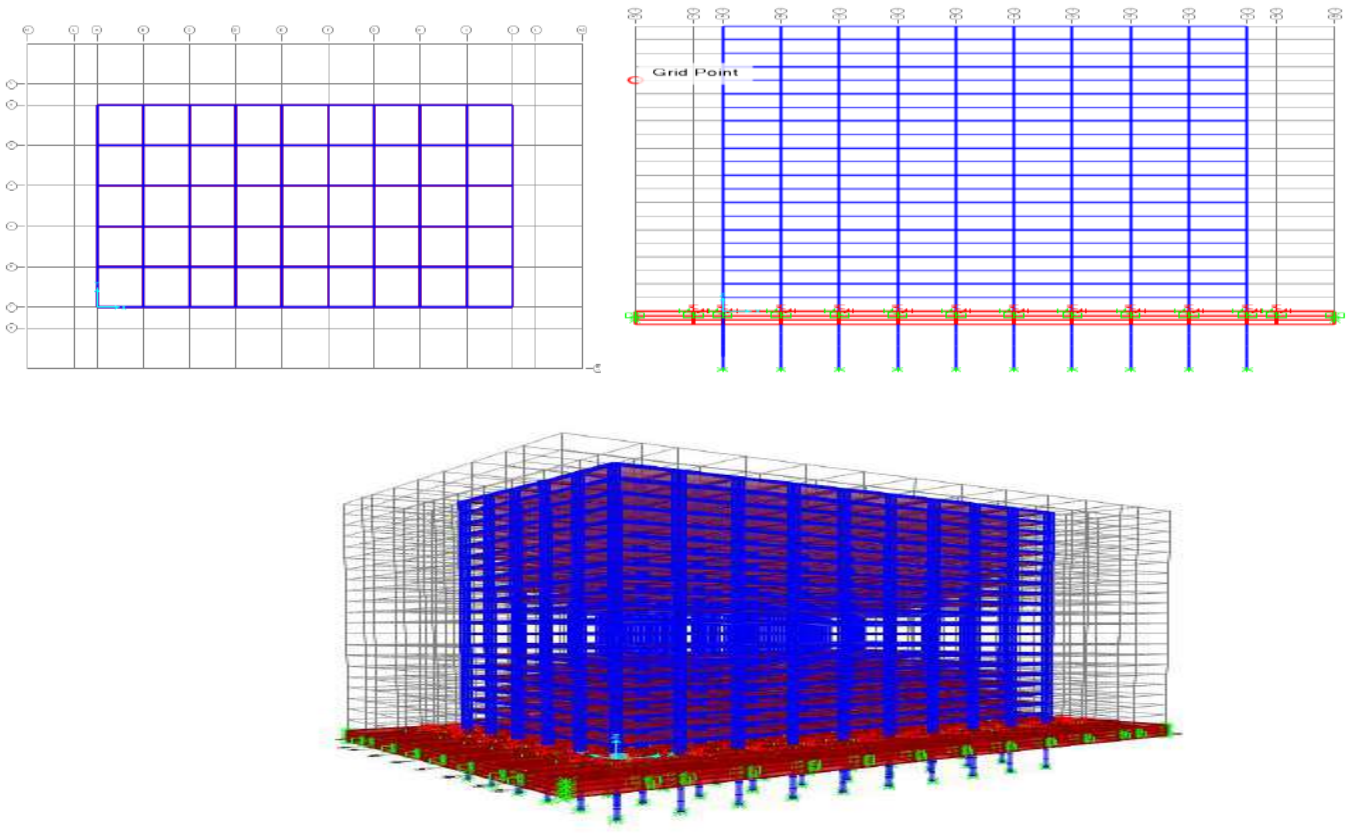

Fig No 1: Typical floor Plan 3D View

4. ANALYSIS RESULTS

STORY DISPLACEMENT						
	SOFT SOIL		MEDIUM SOIL		WEATHER SOIL	
STORIES	RAFT PILE SOFT SOIL	RAFT SOFT SOIL	RAFTPILE MEDIUM SOIL	RAFT MEDIUM SOIL	RAFT PILE WEATHER SOIL	RAFT WEATHER SOIL
BASE	0.94	5.14	0.1	0.9	0.034	0.122
STORY 1	9.32	14.08	8.57	9.35	8.36	8.48
STORY 2	16.07	21.7	15.33	16.19	15.04	15.14
STORY 3	22.16	28.82	21.43	22.44	21.07	21.14
STORY 4	27.98	35.72	27.26	28.4	26.83	26.8
STORY 5	33.68	42.5	32.96	34.27	32.46	32.41
STORY 6	39.36	49.2	38.57	40.09	38.02	37.86
STORY 7	44.83	55.82	44.11	45.6	43.59	43.19
STORY 8	50.27	62.34	49.55	51.15	48.87	48.41
STORY 9	55.6	68.72	54.88	56.53	54.13	53.48
STORY 10	60.78	75.06	60.06	61.75	59.25	58.38
STORY 11	65.79	81.2	65.06	66.78	64.19	63.09
STORY 12	70.58	87.18	69.85	71.59	68.92	67
STORY 13	75.13	92.9	74.39	76.16	73.41	71.81
STORY 14	79.39	98.5	78.64	80.46	77.6	75.5
STORY 15	83.31	103.8	82.55	84.83	81.46	79.3
STORY 16	86.86	108.9	86.07	88.06	84.94	82.62
STORY 17	89.98	113.7	89.17	91.3	87.99	85.48
STORY 18	92.63	118.13	91.7	94.1	90.57	87.8
STORY 19	94.78	122.2	93.9	96.5	92.65	89.9
STORY 20	96.4	125.97	95.49	98.4	94.2	91.326
STORY 21	97.58	129.41	96.62	100	95.3	92.46

STORY DISPLACEMENT						
	SOFT SOIL		MEDIUM SOIL		WEATHER SOIL	
STORIES	RAFT PILE SOFT SOIL	RAFT SOFT SOIL	RAFTPILE MEDIUM SOIL	RAFT MEDIUM SOIL	RAFT PILE WEATHER SOIL	RAFT WEATHER SOIL
BASE	0.72	4.95	0.19	0.87	0.022	0.09
STORY 1	8.13	16.6	7.51	10.3	7.32	9.2
STORY 2	14.16	27.11	13.5	18.21	13.24	16.7
STORY 3	19.64	37.09	18.93	25.46	18.61	23.5
STORY 4	24.9	46.85	24.17	32.44	23.75	29.36
STORY 5	30.06	55.15	29.29	39.28	28.8	36.25
STORY 6	35.16	66.13	34.35	46.03	33.79	42.43
STORY 7	40.27	75.6	39.35	52.67	38.72	48.5
STORY 8	45.18	85.03	44.28	59.2	43.59	54.45
STORY 9	50.06	94.5	49.12	65.59	48.36	60.26
STORY 10	54.83	103	53.84	71.83	53	65.88
STORY 11	59.45	112.5	58.42	77.8	57.52	71.3
STORY 12	63.89	121	62.81	83.7	61.85	76.49
STORY 13	68.12	130.24	67	89.29	65.96	81.41
STORY 14	72.11	138.7	70.93	94.59	69.83	86.01

STORY 15	75.81	147	74.56	99.56	73.41	90.26
STORY 16	79.18	155	77.87	104	76.66	94.13
STORY 17	82.19	162.69	80.81	108	79.53	97
STORY 18	84.78	170.07	83.33	112.19	82	100
STORY 19	86.94	177	85.4	115	84.03	102.9
STORY 20	88.66	183.7	87.02	118.4	85.6	104.97
STORY 21	89.98	190	88.25	120.88	86.78	106

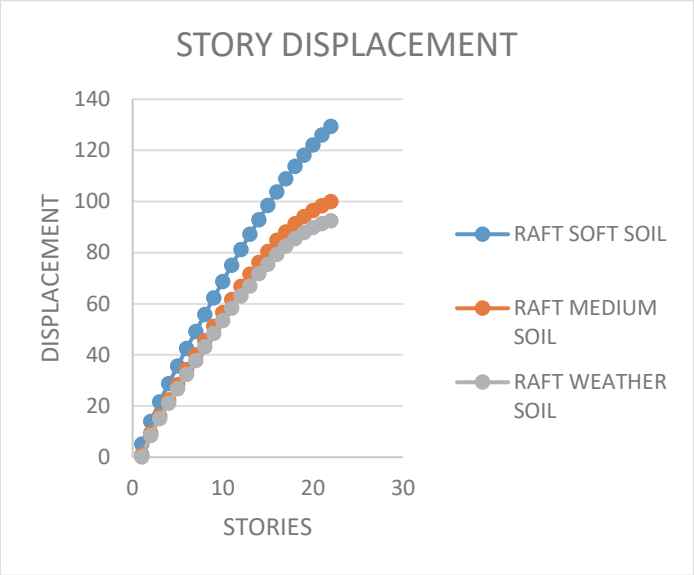

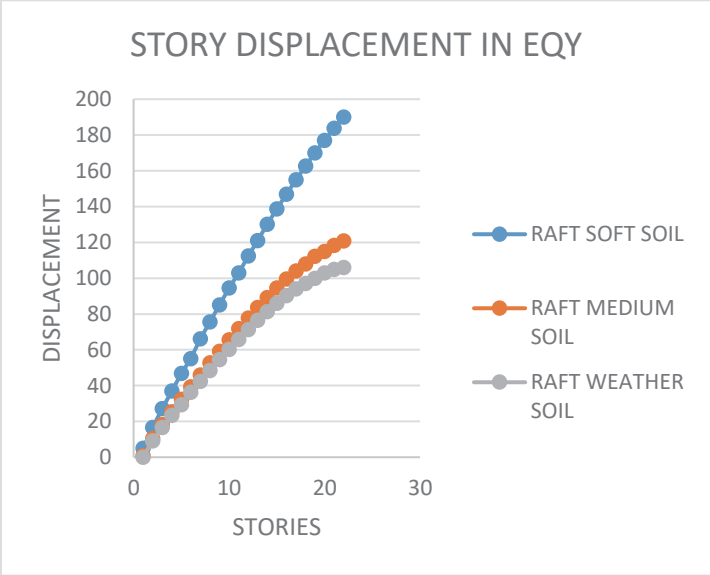

STORY DRIFT						
	SOFT SOIL		MEDIUM SOIL		WEATHER SOIL	
STORIES	RAFT PILE SOFT SOIL	RAFT SOFT SOIL	RAFTPILE MEDIUM SOIL	RAFT MEDIUM SOIL	RAFT PILE WEATHER SOIL	RAFT WEATHER SOIL
BASE	0.000313	0.001713	3.33E-05	0.0003	1.13E-05	4.07E-05
STORY 1	0.002793	0.00298	0.002823	0.002817	0.002775	0.002786
STORY 2	0.00225	0.00254	0.002253	0.00228	0.002227	0.00222
STORY 3	0.00203	0.002373	0.002033	0.002083	0.00201	0.002
STORY 4	0.00194	0.0023	0.001943	0.001987	0.00192	0.001887
STORY 5	0.0019	0.00226	0.0019	0.001957	0.001877	0.00187
STORY 6	0.001893	0.002233	0.00187	0.00194	0.001853	0.001817
STORY 7	0.001823	0.002207	0.001847	0.001837	0.001857	0.001777
STORY 8	0.001813	0.002173	0.001813	0.00185	0.00176	0.00174
STORY 9	0.001777	0.002127	0.001777	0.001793	0.001753	0.00169
STORY 10	0.001727	0.002113	0.001727	0.00174	0.001707	0.001633
STORY 11	0.00167	0.002047	0.001667	0.001677	0.001647	0.00157
STORY 12	0.001597	0.001993	0.001597	0.001603	0.001577	0.001303
STORY 13	0.001517	0.001907	0.001513	0.001523	0.001497	0.001603
STORY 14	0.00142	0.001867	0.001417	0.001433	0.001397	0.00123
STORY 15	0.001307	0.001767	0.001303	0.001457	0.001287	0.001267
STORY 16	0.001183	0.0017	0.001173	0.001077	0.00116	0.001107
STORY 17	0.00104	0.0016	0.001033	0.00108	0.001017	0.000953

STORY 18	0.000883	0.001477	0.000843	0.000933	0.00086	0.000773
STORY 19	0.000717	0.001357	0.000733	0.0008	0.000693	0.0007
STORY 20	0.00054	0.001257	0.00053	0.000633	0.000517	0.000475
STORY 21	0.000393	0.001147	0.000377	0.000533	0.000367	0.000378

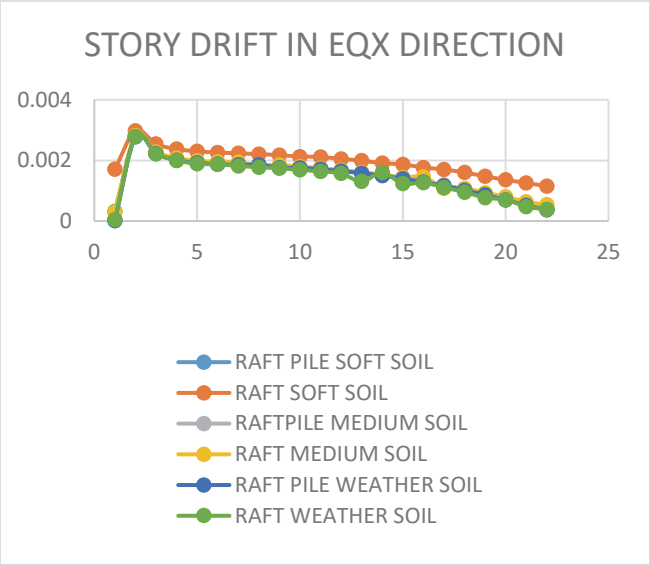

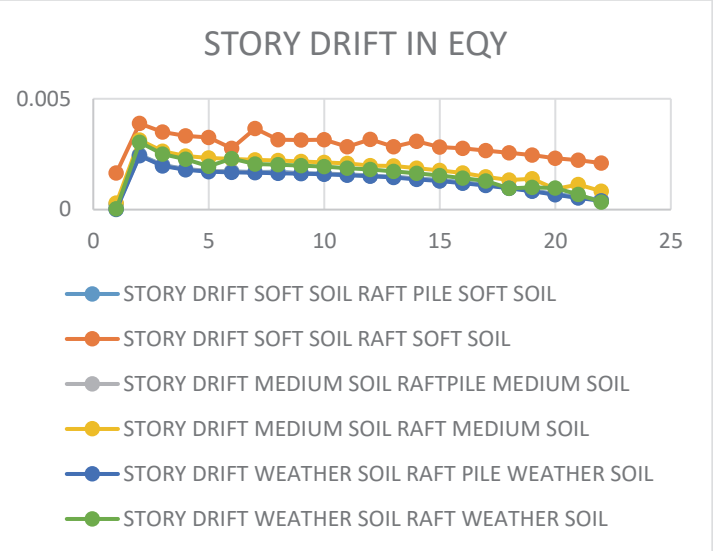

TIME PERIOD						
MODES	SOFT SOIL		MEDIUM SOIL		WEATHER SOIL	
	RAFT SOFT SOIL	RAFT PILE SOFT SOIL	RAFT MEDIUM SOIL	RAFT PILE MEDIUM SOIL	RAFT WEATHER SOIL	RAFT PILE WEATHER SOIL
1	2.711956	4.31501	2.670031	2.997921	2.658942	2.728597
2	2.604919	3.512787	2.575325	2.730213	2.568429	2.603015
3	2.531383	2.762935	2.508966	2.575722	2.503537	2.524171
4	0.868952	1.550811	0.862052	0.882918	0.860871	0.865342
5	0.841169	1.106024	0.834751	0.851785	0.83374	0.836974
6	0.81675	1.007663	0.811953	0.815479	0.811201	0.812851
7	0.489371	0.87041	0.485937	0.704483	0.485472	0.486331
8	0.478342	0.832815	0.474709	0.562682	0.474244	0.474981
9	0.463642	0.676255	0.46081	0.4959	0.460446	0.46081
10	0.32941	0.657509	0.325839	0.478223	0.325474	0.341289
11	0.322979	0.655689	0.31922	0.463012	0.31887	0.326858
12	0.311658	0.654586	0.308688	0.445901	0.308415	0.320826

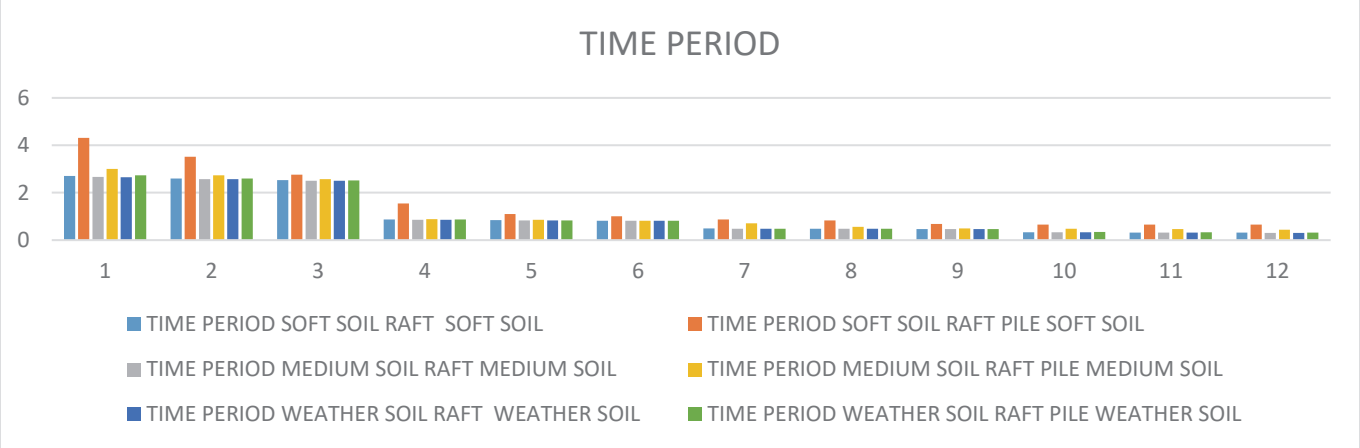

5 CONCLUSIONS

- In contrast to a single piling base or raft base, the Raft platform piling is economical. As the piles are introduced below the raft in the present work piled with raft foundation, the load sharing of pile and raft results in gradual reduction of soil settling. By using safe methods to determine the basis of multi-storey residential buildings.

- The piled raft foundation is implemented to mitigate the total and differential settlement of foundations and, thus, the estimation of the settlement profile of the piled raft foundation forms an important modelling exercise.

- In compliance with IS CODE 1904: 1986 and Geo-technical report respectively, the Settlement and Soil bearing pressure has been decreased within the allowable amount.

- The design of piled raft foundations has been seen to have substantial benefits relative to traditional foundations for certain soft clay for high-rise buildings.

- The lengthening of the lateral fundamental span of the pile supported raft superstructure method tends to be maximal in the case of a rigid frame supported by slender piles.

- The study indicates that SSI has a negligible effect, although it can lead to a substantial increase in seismic lateral force in piles due to the additional inertia force given by the foundation's heavy mass, which is not accounted for in the fixed base state.

- Piled raft structures have the ability to have, under the necessary geotechnical conditions, economic base structures. The design theory should also be

based on both the final load potential and the conditions for settlement.

- It is observed that the maximum displacement values are greater than silty sand in soft clay. It is also easily shown that the displacement values are improved for soft soil.

- It is found that the overall displacement values in the raft foundation are high. It is also easily shown that the displacement values for the pile raft foundation are decreased.

6. SCOPE FOR FURTHER STUDY

- In this project work only effect of raft and raft pile are considered and result are compared with different soil conditions

- Further study can be considered for pile foundation with varying length and diameter of pile

- Further study can be done by considering effect of different configuration of pile and pile group.

REFERENCES

- Steven L. Kramer (1996). "*Geotechnical Earthquake Engineering"* University of Washington, Prentice-Hall

- Joseph W. Tedesco, William G. McDougal and C Allen Ross (1999). *"Structural Dynamics, Theory and Application"* Addison Wesley Longman

- Anil K. Chopra (2001). *"Dynamics of Structures, Theory and Applications to Earthquake Engineering Second Edition"* Prentice-Hall

- T. K. Datta (2010). *"Seismic Analysis of Structures"* John Wiley and Sons (Asia)

- Frederick K. Lutgens and Edward J. Tarbuck (2003). *"Essentials of Geology Eighth Edition"* Prentice-Hall

- Roberto Villaverde (2009). *"Fundamental Concepts of Earthquake Engineering"* Taylor and Francis Group, LLC

- Jhonny et. al. (2010) "Seismic Pattern in Peninsular Malaysia" *Map Asia 2010 and ISG 2010*

- Mark Peterson et. al. (2007). "*Documentation for the Southeast Asia Seismic Hazard Maps, Administrative Report September 30 2007*" U.S. Department of the Interior U.S. Geological Survey

- M. Paknahad, J. Noorzaei, M.S, M.S. Jaafar and Waleed A. Thanoon (2008). "Non- linear Soil Structure Interaction of Shear Wall System with Super Element" *The 12th International Conference of International Association for Computer Methods and Advances in Geomechanics (IACMAG) 1-6 October, 2008 Goa, India*.

- Peizhen Li, Xilin Lu and Yueqing Chen (2006) "Study and Analysis On Shaking Table Tests of Dynamic Interaction of Soil-Structure Considering Soil Liquefaction" *4th International Conference on Earthquake Engineering Taipei, Taiwan, October 12-13, 2006*.

- Azlan Adnan, Hendriyawan, Aminaton Marto and Masyhur Irsyam. "Development of Synthetic Time Histories at Bedrock for Kuala Lumpur" *Proceedings of the 6th Asia-Pacific Structural Engineering and Construction*

Conference (APSEC 2006), 5 – 6 September 2006, Kuala Lumpur, Malaysia

- Ku Safirah (2010).*Seismic Behaviour of Tunnels with Different Soil Types and Depths*. University of Technology Malaysia: Master Degree Thesis.

- Ehsan Noroozinejad (2010). *Seismic Vulnerability Analysis of Various Types of Dams with Finite Element Methods.* University of Technology Malaysia: Master Degree Thesis.

- Nik Zainab (2010).*Building Performance with Different Bedrock Response Spectrum.* University of Technology Malaysia: Master Degree Thesis

- Naresh Bellana (2009). *Shear Wave Velocity as Function of SPT Penetration Resistance and Vertical Effective Stress at California Bridge Sites*. University of California: Master Degree Thesis.

- Aghei Araei et. al (2010). Dynamic Properties of Gravelly Material. *Vol. 17, Scientia Iranica, No. 4, pp. 245-261, Sharif University of Technology.*

- D.B McCallen and L.J. Hutchings (1995). Ground Motion Estimation and Nonlinear Seismic Analysis. *12th Conference on Analysis and Computation of the American Society of Civil Engineers Chicago,* Illinois April 15-18, 1996.

- L. GovindaRaju1 et.al (2004). Site Specific Ground Response Analysis. Current Science, Vol. 87, No.10 pp. 1354-1362

- R. Uma Maheswari et al (2009). Use of Surface Waves in Statistical Correlations of Shear Wave Velocity and Penetration Resistance of Chennai Soils. *Geotechnical Geology Engineering (2010)*. Vol 28 pp 119-137.

- IS 2950 (P-I)-1981, " Indian Standard code of practice for design and construction of raft foundation, " BIS, New Delhi.

- H.G. Poulos, " Simplified design procedure for piled raft Foundation." ASCE.

- Apurba Tribedi, Correlation between Soil Bearing Capacities and Modulus of Subgrade reaction," apurba,tribedi@bentley.com

- P.D. Long," Piled Raft - A cost effective Foundation Method for High Rises," Geotechnical Engineering journal of SEAGS & AGSSEA vol.41 no.3 sept2010

- A.M. Ibrahim, " Pile raft foundation with piles as settlement reducer,"abdelazimin@yahoo.com

- H.G. Poulos," Piled raft foundation : design and applications," Geotechnique 51 no.2, 95-133 (2001)

- Balkema V," A Design Method for Piled Raft Foundations," Simplex infrastructure Limited, Chennai, Tamil Nadu, India.

- H.G. Poulos (2001), " Methods of analysis of Piled raft Foundations," International Society of soil Mechanics and geotechnical Engineering

ASSESSMENT AND FORECASTING OF STUDENT EDUCATIONAL CONDUCT USING DATA MINING APPROACHES

[1]Aqsa Mahreen, [2]Mohammed Abdul Rawoof, [3]Mohammad Sanaullah Qaseem
[1]PG Scholar, Department of Computer Science Engineering and Technology,
[2]Associate Professor, Department of Computer Science and Engineering,
[3]Professor and Head, Department of CSE, Vice Principal (Academics) IQAC Coordinator,
Nawab Shah Alam Khan College of Engineering & Technology, Hyderabad

ABSTRACT

The nature of instruction in any establishment can be accomplished by assessing the understudy execution which should be possible by forecast and investigation. It ends up being successful if the instructive organizations have the data or the information on the understudies in their separate foundations. This will assist them with sifting through the feeble, normal and splendid understudies. In this, we have made a framework that can assist colleges with assessing the exhibition of understudies previously. For this reason, a few information mining philosophies, for example, characterization have been utilized. We have made an informational collection that has data about understudies regarding their sex, rank and checks in placement test and the outcomes in third year of past bunch of students. Later the informational collections have been assessed to get the eventual outcome. The characterization procedures partition the information into classes and the regulated learning technique is utilized to generate rules for arranging test information into foreordained gatherings marked preparing information is required. The total cycle goes through two stages. Initially, the learning stage where the preparation information is investigated and runs are created. The subsequent stage includes the test information to be characterized into classes concerning truing informational collection. Atlas, the assessment of third year understudies for future tests is finished utilizing the ID3 (Iterative Dichotomize 3), C4.5, Improved weighted altered ID3 grouping calculations on this data. In this way we would have the option to decide the future extent of understudies

INTRODUCTION

So as to anticipate performance of understudies in future scholastics, it's appropriate if an instructive association have an estimated earlier skill of all selected understudies in their establishment. This earlier information will turn into an important aspect for instructional organization to upgrade understudies the individuals who might presumably to get significantly less checks and also find good student. As an answer we are attempting to help a framework which will help a scholarly organization to prefigure the general exhibition of understudies from their previous working. So as to accomplish this we will utilize standards of information mining strategies below Classification. The significant goal of this project is to utilize information mining philosophies to consider understudies generally execution in the courses. Information mining gives numerous obligations that should be utilized to get some answers concerning the understudy execution.

Understudies under different classes from various areas, instructive foundation and with different rankings in selection tests like CAT, JEE take affirmations in instructive establishments every year. This placement test helps in enrolment of understudies in different fields. In addition, designing schools may likewise be associated with a lot college. Every school has sizable assortment of subjects in their educational plan. So as to flexibly a superior perspective on most probably working of undergrads in future, past in general execution of conceded understudies are needed to be investigated. It has gotten hard for the colleges and universities to keep up the people execution in their tests. In this we have thought about a few elements to decide the future exhibition of understudies. As the opposition develops between different organizations, an ever-increasing number of procedures have been concocted to assess the understudy execution. This eventually prompts the positioning of the organization dependent on understudy appraisal. The information mining strategies alongside the AI calculations have been demonstrated to be full of feeling in actualizing this task by the utilization of information mining grouping calculations this can appropriately be finished by our framework. It has been seen that for instructive network of higher learning, it is urgent issue to uncover the development of understudy's instructional exercise execution.

Students are the fundamental resource for different colleges. Colleges and students assume a significant function in delivering alumni of high characteristics with its scholarly presentation accomplishment. Scholarly execution accomplishment is the degree of accomplishment of the understudies' instructive objective that can be estimated and tried through assessment, appraisals and other type of estimations. Be that as it may, the scholarly exhibition accomplishment shifts as various sort of understudies may have distinctive degree of execution

accomplishment. The student academic performance is usually stored in student management system, in different formats such as files, document, records, images and other formats. These available students' data could be extracted to produce useful information. However, the increasing amount of students' data becomes hard to be analysed by using traditional statistic techniques and database management tools [4]. Thus, a tool is necessary for universities to extract the useful information.

LITERATURE SURVEY

DSS are an exact kind of modernized realities device that helps business endeavor and organizational decision-production exercises. A true planned DSS is an intuitive programming-based gadget proposed to help leaders unite valuable records from uncooked information, archives, non-public information, or potentially endeavor models to recognize and resolve issues and decide. A DSS is a PC programming that examines business endeavor realities and manages it so clients can make business determinations extra without any problem.

Choice tree picking up information on calculation has been solidly utilized in master structures in taking pictures information. The foremost task completed in these structures is utilizing inductive techniques to the given point of attributes of an ignorant item to choose awesome characterization as per choice standards with the assistance of utilizing C4.5 calculation. Verifiably ID3 calculation used to be utilized to assemble the Decision tree. ID3algorithm is to settle on the decision tree through by method of on down, greedy search with offered units to survey each ascribe at each hub. We built up a metric data gain which helps in choosing the characteristic for grouping given dataset. C4.5 is an expansion of Quinlan's up to this point ID3 calculation. C4.5 is normally named as a statistical classifier. At the stop of stage ID3 is analyze with C4.5 by method of improving Prediction precision & computational intricacy of DT.

DESCRIPTION OF THE PROJECT WORK

Prior it was exceptionally hard for the colleges to examine the presentation of the understudies selecting into the different courses. The educators would not be capable of recognize the brilliant and the frail understudies which by implication prompted the moderate development of an association or the foundation. On the off chance that this data about future execution of the understudies is known already, the foundation would do investigation on it and help the understudies in improving their scholastic records. The instructors will have the option to guide the understudies who are west in specific subjects. This earlier information prepares for the achievement of the foundation. In the event that the forecast is done on understudy assessment conduct, it gets simpler for the colleges to screen the advancement and guide them to achieve a lot better grade. All these cycles have been utilized information mining grouping calculations, for example, ID3 AND C4.5 algorithms.

Faculty Support System

Shana and Venkatacalam has proposed a structure named Faculty Support System (FSS) which is low in cost as it utilizes savvy open source examination programming, WEKA to dissect the understudies' presentation in a course offered by Coimbatore Institute of Technology of Anna University [1]. FSS can examine the understudies' information progressively as it can refresh of understudies' information powerfully with the progression of time to make or add another standard. The update of new standard is conceivable with the assistance from space master and the standard is controlled by information mining procedure, for example, characterization method. Characterization strategy is utilized to foresee the understudies' presentation. Furthermore, FSS center on the ID of elements that add to execution of understudies in a specific course.

Student Performance Analyser

SPA is existing secure online electronic programming that empowers instructors to see the understudies' exhibition and monitor the school's information. The SPA is an instrument intended for examining, showing, putting away, and getting criticism of understudy evaluation information [3]. It is a ground-breaking analyser apparatus utilized by schools worldwide to perform investigation and showcases the examination information once crude understudy information is transferred to the framework. The investigation is finished by following the understudy or class to get the general exhibition of understudy or class. It assists with distinguishing the understudies' presentation which is beneath the normal level, at anticipated level or over the normal level. This would permit the instructors or staffs to recognize the current understudies' presentation without any problem. Other than that, it empowers different sorts of understudies' presentation report, for example, progress report and accomplishment report to be created.

Intelligent Mining and Decision Support System (InMinds)

InMinds assists Universiti Malaysia Sarawak (UNIMAS) with monitoring the exhibition of different zones in each UNIMAS's specialties [2]. The framework empowers top and mid-administration in

UNIMAS to have an unmistakable look on the regions that required consideration by taking a gander at the figures, incomes and dangers. The highlights, usability and adaptability gave by the framework makes the exhibition examination in UNIMAS to be acted in an ideal arrangement. Graphs are given by the framework to simplicity of understudy execution's translation.

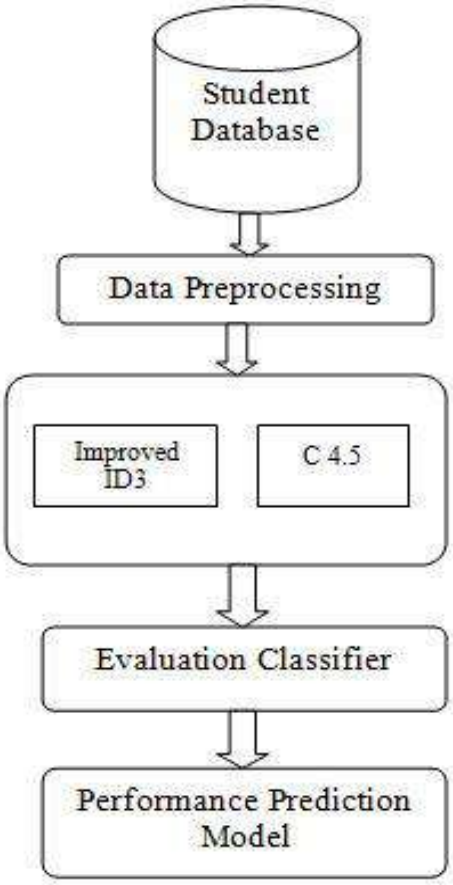

Fig 1: System Architecture

The cycle is completed in a few stages. The initial step includes putting away the information in the understudy information base on which the investigation is finished. The educators transfer information into the information base. At that point the preprocessing is performed to eliminate the traits that are no longer considered for future handling and any commotion or futile information is additionally taken out. The ID3 and C4.5 and improved ID3 is applied on the training information to get the choice trees. The understudy information is applied in fourth stage lastly the outcome is achieved giving production of execution in the type of diagrams and charts.

PROPOSED RESEARCH WORK

In this framework, we made an endeavor to make a framework that benefits the establishments in evaluating the understudy's performance. An informational collection has been fabricated dependent on understudy imprints, sexual orientation and results in third year understudies of past understudies. The directed learning calculations are utilized to deliver rules so as to classify information into classes. The whole cycle is done in two stages which is surveying the training information to get the characterization controls and acquired and in the second stage the test information is orders into classes. Different AI algorithms are performed on the informational index, for example, previous ID3 and C4.5 calculations. In this venture, we attempt to improve the ID3 classifier so we get the precise outcomes and improve the exactness of the classifier. We settled on a comparison between various choice tree calculations, for example, ID3 and C4.5 and improved ID3.

PROPOSED ADVANTAGES

- This system has made easier for universities to analyse performance with the help of graphs and charts.
- Reports can be produced easily on student performance.
- Tracking of the student performance in various course and semester is easily done with the help of this system.

MODULES

Data Source

The understudy data is put away in information base. The data like personality number, marks, name, gender, affirmation name, course id is put away in the document configurations or records. The information about the teachers related with every division is additionally given to the data set on which the information mining calculations are performed. This is gainful technique for examining understudy conduct in future and constantly evaluate the advancement of them.

Pre-processing

This is the initial phase in any information mining measure which channel out the superfluous information which might be commotion or exceptions or the attributes that is of no utilization in the later phases of framework improvement. It is basically the information cleaning measure that is essential to be done in the information revelation and expectation techniques.

Evaluation Classifier

In this the metrics utilized for the classifier is the information gain and top down ravenous hunt which discovers the attribute at every hub of the tree. The

characteristic is picked at each progression and to acquire a tree, it utilizes ideas, for example, entropy and data gain. The proposed framework eliminates the hindrance of characteristic having more qualities. Differentiating the differences in calculations happens among ID3, C4.5 and Improved ID3 giving the student forecast in his scholastics.

Student Analysis

Finally, the investigation of the third-year understudies is done to anticipate their last year results. The various diagrams and outlines are acquired demonstrating the measurements and from them a report are settled recognizing the more splendid and more vulnerable understudies.

RESULTS

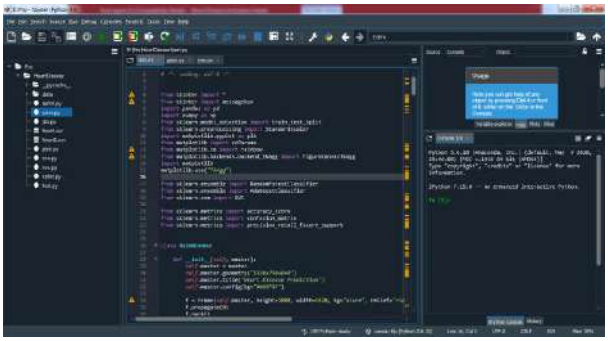

Fig 2: Home Page

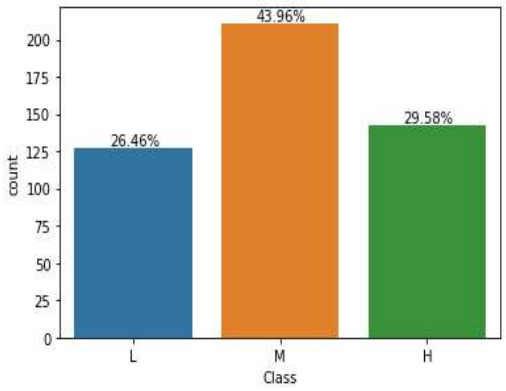

Fig 3: Class vs Count

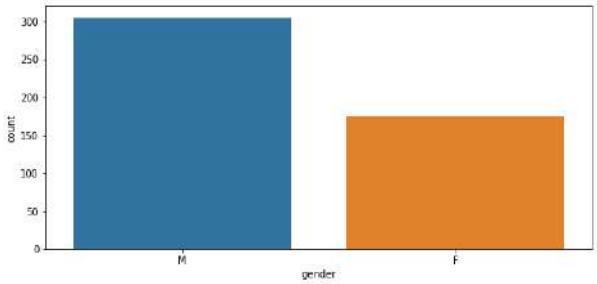

Fig 4: Gender vs Count

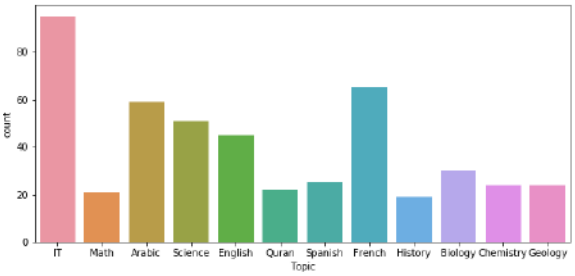

Fig 5: Topics Vs count

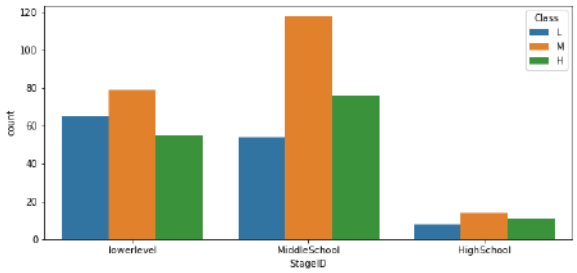

Fig 6: Count vs classes

```
Minimum Accuracy Score:   0.48611111
Maximum Accuracy Score:   0.77083333
Average Accuracy Score:   0.65036111
Minimum Prediction Misses:   33
Maximum Prediction Misses:   74
Average Prediction Misses:   50.35
RBF Minimum Accuracy Score:   0.63194444
RBF Maximum Accuracy Score:   0.84027778
RBF Average Accuracy Score:   0.74305556
-------------------------------------------------
Linear Minimum Accuracy Score:   0.66666667
Linear Maximum Accuracy Score:   0.85416667
Linear Average Accuracy Score:   0.75804861
-------------------------------------------------
```

Fig 7: Accuracy Score

CONCLUSION

The positioning of any educational establishment is estimated regarding the exhibition of the understudies. Hence it has gotten vital to decide the imprints and grades of the understudies in their forthcoming appraisal. A few approaches has been intended to help this need. The information found from

the understudy's current performance can be examined so as to anticipate their future result. This will profit the colleges in giving the high-quality education to understudies. The instructors would have the option to recognize brilliant and frail understudies which help them to guide the more fragile ones for advancement.

In this, a framework is intended to predict the understudy conduct in scholastics with the use of information ming philosophies of classification. The task likewise exhibits the total result in definite year of third year understudies. The prior approaches managed calculations like ID3, C4.5 which end up being inadequate. In our framework we attempted to draw a correlation between these algorithms and has effectively improved accuracy of the ID3 calculation while indicating the investigation on understudies as diagrams and graphs.

REFERENCE:

[1] "Prediction Students Performance using ID3 and C4.5Classification Algorithms" -International Journal of Data Mining& Knowledge Management Process (IJDKP) Vol.3, No.5, September 2013.

[2] "Student's Performance Prediction Using Weighted Modified ID3Algorithm" - International Journal of Scientific Research Engineering & Technology (IJSRET), ISSN 2278 – 0882 Volume4, Issue 5, May 2015.

[3] "Predicting Students' Performance using Modified ID3Algorithm"- ISSN: 0975-4024 Vol 5 No 3 Jun-Jul 2013

[4] Student Performance Analysis System (SPAS)" - Chew Li Sa,Dayang Hanani bt. Abang Ibrahim, Emmy Dahliana Hossain, Mohammad bin Hossin Faculty of Computer Science and Information System Universiti Malaysia Sarawak (UNIMAS)94300, Kota Samarahan, Sarawak, Malaysia.

[5] " Efficient Processing of Decision Tree Using ID3 & improvedC4.5 Algorithm "- Sonal Patil. et al, / (IJCSIT) International Journal of Computer Science and Information Technologies, Vol.6 (2) , 2015, 1956-1961.

[6]" Implementation of Improved ID3 Algorithm to Obtain more Optimal Decision Tree. International Journal of Engineering Research and Development e-ISSN: 2278-067X, p-ISSN: 2278-800X, www.ijerd.com Volume 11, Issue 02 (February 2015), PP.44-47

[7] "Implementation of ID3 Algorithm" International Journal of Advanced Research in Computer Science and Software Engineering

COMPARATIVE STUDY OF R.C. TALL BUILDINGS BETWEEN SYMMENTRICAL AND UNSYMMENTRICAL SHAPES IN CONSIDERATION OF NON DUCTILE USING WITH AND WITHOUT OUTRIGGER AND BELT TRUSS SYSTEM

Mohd Parvez Affani[1], Shaik Mohd Javeed[2] Mohd Farrukh Anwar[3]

[1] Pg Student, M.tech in Structural engineering, Department of Civil Engineering, Nawab Shah Alam Khan College of Engineering and Technology, Hyderabad, Telangana

[2] Assistant Professor, M.tech in Structural engineering, Department of Civil Engineering, Nawab Shah Alam Khan College of Engineering and Technology, Hyderabad, Telangana

[3]Head of the Department (PHD) , Vice Principal ,M.tech in Structural engineering, Department of Civil Engineering, Nawab Shah Alam Khan College of Engineering and Technology, , Hyderabad, Telangana

ABSTRACT: Should be met through engineering judgment. In Metro cities like Mumbai, Delhi, Chennai, Bangalore, Kolkata, Hyderabad etc multi-storied buildings are common and disregarding that individuals are willing to remain in elevated structure (36 storeys').The analysis and outline of tall building structural system require more concentration than that of regular multi-storied building. The lateral stability of tall building assumes an important role in safe analysis and plan. demonstrate is generated in ETABS, the state of building like a rectangular(symmetrical) Y-formed and C molded buildings i.e. (Non symmetrical) The building is strengthened in lateral direction by providing Outrigger and Belt non truss system at every 9 to 10 ,18 to 19, 27 to 28 story levels Two strategies for analysis have been considered for lateral stability analysis viz linear static and linear dynamic for both seismic and wind. The various parameters like (1) Lateral displacement story.

I. INTRODUCTION

Tall building is need of developing scenario. Rapid improvement of tall building in the world has been creating impact on innovative advancement of structural system for tall building, result of which buildings are growing taller. There is no specific definition of tall building however Council on Tall Building and Urban Habitat (CTBUH) gives a few measures to define tall building. Tall building phenomenon will continue in a greater scale to address the issues of the growing populace in future large cities. The advancement in concrete technology over the twentieth century covering materials, structural systems, analysis and construction techniques, made it conceivable to manufacture concrete tall buildings. Structural system like minute resisting frame and shear divider and bracing system fulfill primary need of building . As building increases in stature there is effect of lateral load i.e. wind and earthquake on building structure. The

impact of wind and seismic forces acting on tall building becomes an important aspect of the outline. Improving the structural systems of tall buildings can control their dynamic response Wind and earthquake stack plays major impact on building deflection. To overcome lateral load because of earthquake and wind, concrete core has been provided at center of building. Concrete core is a very effective and practical structural system which supportive in reducing the deflection because of seismic and wind forces. During recent years, the frame-concrete core divider hybrid structure has been rapidly created and profoundly concerned by owners with its performance and economic favorable circumstances. The outrigger and belt truss system is commonly utilized as one of the structural system to effectively control the excessive drift because of lateral load, so that, during little or medium lateral load due to either wind or earthquake stack, the risk of structural and non-structural harm can be minimized. For elevated structures, particularly in seismic active zone or wind stack dominant, this system can be chosen as an appropriate structure. Outriggers have been utilized in the sailing ship industry for some years. They are utilized to resist wind. The slender pole provides the utilization of outriggers. As a comparison the core can be related to the pole, the outriggers resemble the spreaders and the exterior columns resemble the shrouds or remains. Innovative structural schemes are continuously being looked for in the field. Structural Design of High Rise Structures with the intention of limiting the Drift because of Lateral Loads as far as possible without paying a high premium in steel tonnage.

OUTRIGGER AND BELT TRUSS SYSTEM

Outriggers are rigid horizontal structure i.e. truss or shaft which connect core divider and outer column of building to improve building strength and overturning stiffness. Outriggers have been utilized in tall building for nearly 50 years, however innovative plan principle has been improving its efficiency. Outrigger system is one sort of structural system which is formed from a cantilever molded horizontal member connected to structures inner core and outer columns. Through the connection, the minute arm of the core will be increased which prompt higher lateral stiffness of the system. Central core in a building act as cantilever, outriggers are provided to reduce overturning minute in core and to transfer minute from core to outer column by connecting the core and column. Divider frame outrigger trusses is a standout amongst the most efficient and economical structures in tall building, at outer end they connected to the establishment through exterior columns. At the point when the structure is subjected to horizontal loading, the divider and outrigger trusses will rotate, causing compression in the downwind column and strain in column on the upwind side, these hub forces will resist the rotation in the divider. The outrigger systems can be produced in any combination of steel, concrete and composite construction. Normally in steel structure outrigger are in the form of trusses and in the form of divider or profound bar in concrete structure. Outrigger might be stretched out to both side of central core or core might be located at one side of building with outrigger extending to other side columns. Belt truss connects outer perimeter column of a building and offer a wider perimeter to resist lateral deflection of building. This efficient structural form consists of a central core, comprising either Braced Frames or Shear Walls, with horizontal cantilever trusses or girders known as outrigger Trusses, connecting the core to the outer columns.

The core might be centrally located with outriggers extending on both.

TYPES OF OUTRIGGER TRUSS SYSTEM

Conventional Outrigger Concept

In the conventional outrigger concept, the outrigger trusses or girders are connected directly to shear dividers or braced frames at the core and to columns located outboard of the core. Typically (however not necessarily), the columns are at the outer edges of the building. Figure 1 is a romanticized section through a tall building with two arrangements of outrigger trusses, including one at the best. The outrigger trusses configuration. Shallower and deeper trusses have been utilized, with diagonals of various configurations.

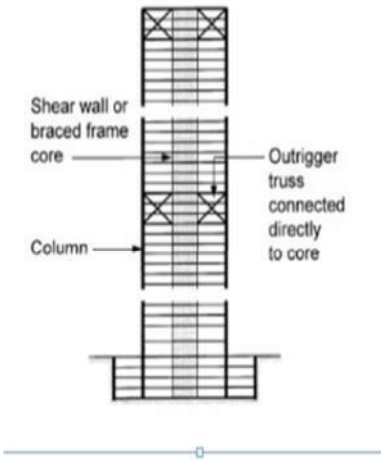

Tall building with conventional outriggers

Virtual Outrigger Concept

In the "virtual" outrigger, a similar transfer of overturning from the core to components outboard of the core is achieved, yet without a direct connection between the outrigger trusses and the core. The basic thought behind the virtual outrigger concept is to utilize floor diaphragms, which are typically very solid and strong in their own plane.

Belt Trusses As Virtual Outriggers

The utilization of belt trusses as virtual outriggers keeps away from a considerable lot of the problems associated with the utilization of conventional outriggers. The principle is the same as when belt trusses are utilized as virtual outriggers. Some fraction existing apart from everything else in the core is converted into a horizontal couple in the floors at the best and the base of the storm cellar.

NEED OF THE PROJECT

Accumulation of growing populace especially in developing countries has resulted in an increased tallness of buildings, this need creating impact on structural improvement of tall building. As building increases in tallness there is effect of wind and earthquake forces, to increase stiffness of building against lateral load extra structural system such as belt truss and outriggers is required. The reviewed approach for the outline and improvement of tall building using outrigger and belt truss is helpful to provide a potential arrangement. The study in turn is helpful for various research persons involved in outline the tall buildings by using outrigger and belt truss system

OBJECTIVE OF THE STUDY

To study the effect of introduction of Outriggers in tall structure subjected to dynamic wind loading. To study the influence of core divider and braced core divider with X braced outriggers C. To stud influence of concrete outrigger. To study the effect of Outriggers with Peripheral Belt Truss. To study the different configuration of the building under different

arrangement molded building i.e symmetrical and Unsymmetrical Buildings (Rectangular and Y formed building , C formed Building

II. METHODOLOGY

ANALYSIS OF A 36 STOREY BUILDING

The model considered for this study is 111.5 m skyscraper reinforced concrete building frame. The building represents a 36 storied office building. The stature of each story is 3m and every one of the floors are considered as Typical Floors. The location of the building is thought to be at Bhuj (Gujarat) . All divider piers are identical with a uniform divider thickness of 230mm over the entire stature. The Bracing bars (outriggers) and every other bar are 600mm wide and 600mm profound, Grade 40 concrete is considered (Compressive strength 40 N/mm²) throughout the tallness of the building. And number of stories considered for every one of the cases is 36 stories, and roof tallness is considered as 111.5 m. And story to story tallness is 3.0 m. And the outer columns sizes are considered as 800X800 mm and Inner columns measure are consider as 550X600 mm. shear divider thickness is considered as 230 mm.The technique for analysis of the previously mentioned system is construct up in light of the presumptions that the outriggers are rigidly attached to the core; The core is rigidly attached to the establishment; The sectional properties of the core, shafts and columns are uniform throughout the stature; Tensional effects are not considered; Material behavior is in linear elastic range; The Outrigger Beams are flexural rigid and induce just pivotal forces in the columns; The lateral resistance is provided just by the bending resistance of the core and the secure action of the exterior columns connected to the outrigger; The rotation of the core because of the shear deformation is immaterial.

STRUCTURAL MODELLNG

SL No	Structural details	Type of location
1	Utility of Buildings	Office Building
2	No of Storey	G+36
3	Area	2308 sq mts
4	Height of Building	111.5 mts
5	Shape of the Building	Rectangle, Y shaped, C shaped building
6	Types of Walls	SHEAR Wall -230 mm thickness Masonry wall – 230 mm thickness
7	**Geometric Details** Ground Floor	3.5 mts
	Story to story height	3.0 mts
	Beam	0.60X0.60 mts
	Columns (outer)	0.80X0.80 mts
	Columns (Inner)	0.55X0.60 mts
	Slab	0.150 mts
8	**Material Details** Concrete Grade All Steel Grades	M40 (All structural elements) FE 415 (All structural elements)
9	Type Of Construction	R.C.C FRAMED STRUCTURE
10	Place of construction	Bhuj - Gujarat
11	Loads considered in Buildings	Dead load, Live load, Earthquake ,Wind load
12	Wind Speed	50 m/s (Bhuj wind speed)
13	Seismic Zone	Zone – V (Bhuj)
14	Method of Analysis	RESPONSE SPECTRUM ANALYSIS EQUIVALENT STATIC ANALYSIS
15	NON Ductile properties	5 (Response reduction factor)
16	STATIC COMBINATION USED	1.2(Dead load+ Live load+ Earthquake in X direction)
17	IS codes used	IS456 :2000,IS1893:2002,IS 16700:2017,IS 875:1987 (Part 1, Part 2, Part 3)

Rectangle Building

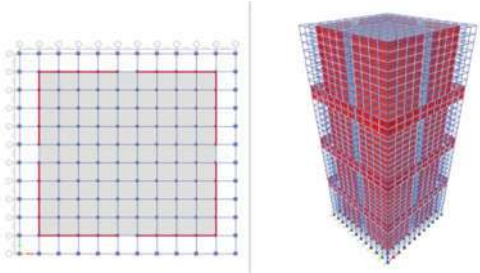

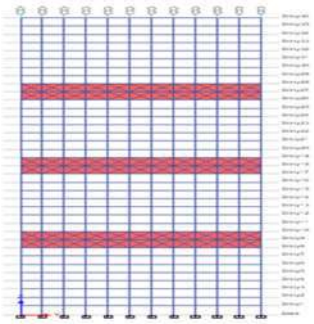

Y shaped building

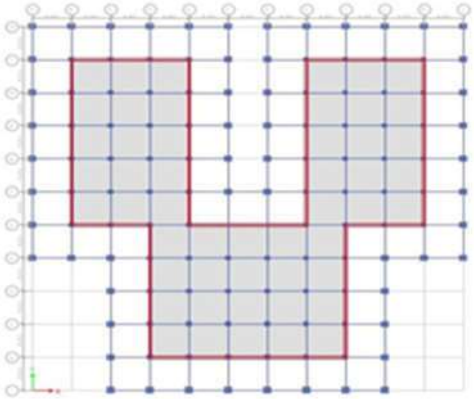

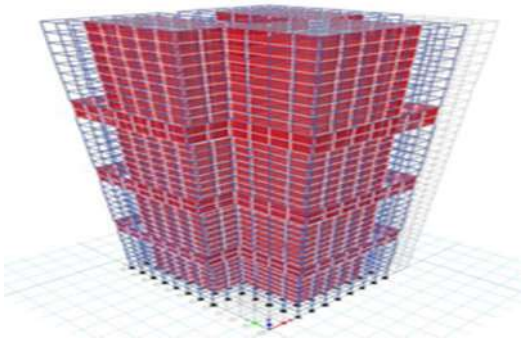

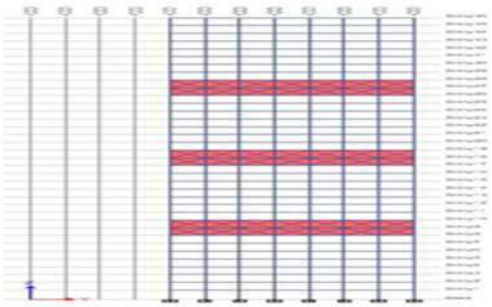

C shaped building

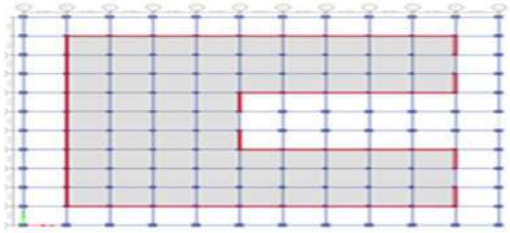

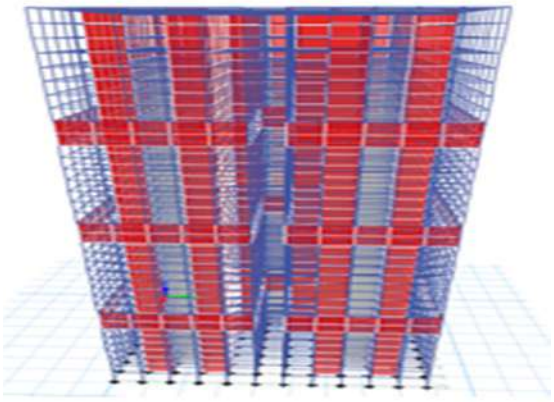

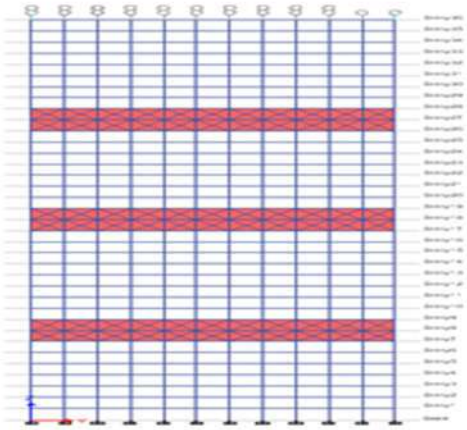

COMPARASTION OF EQUIVALENT STATIC ANALYSIS AND RESPONSE STRECTRUM ANALYSIS.

A.STOREY DRIFT

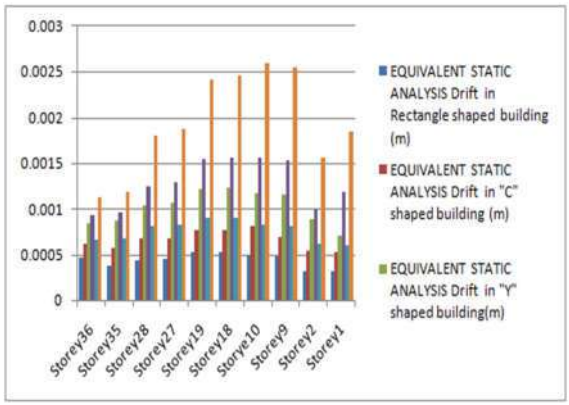

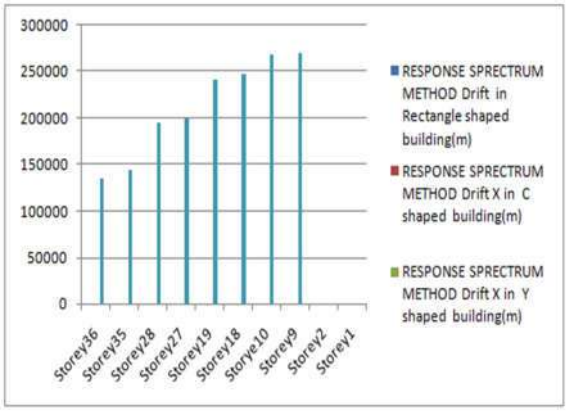

B.STOREY SHEAR FORCE

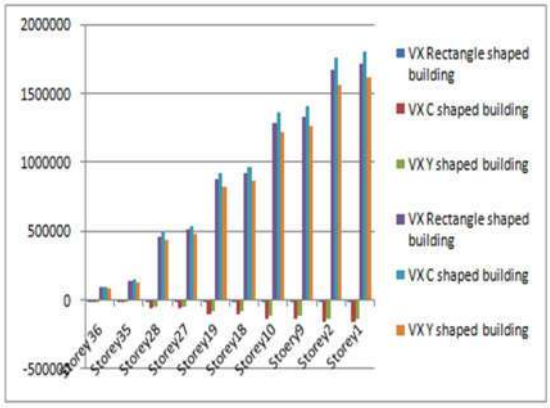

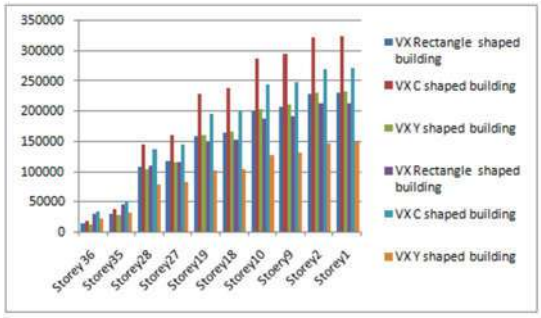

C.MOMENT FORCE

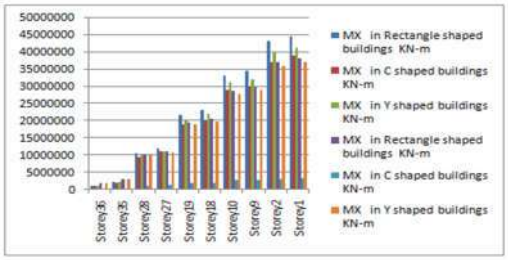

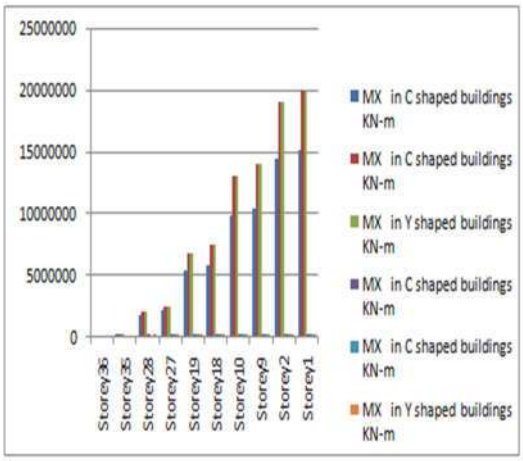

III. .CONCLUSIONS

After performing analysis and studying the results we can come to the below conclusion's:

1) The behavior of a structure under earthquake load is different from earthquake to earthquake. This well known phenomenon is well presented in the lateral displacement results obtained for both of the options. The location of the outrigger beam has a critical influence on the lateral behavior of the structure under earthquake load and the optimum outrigger locations of the building have to be carefully selected in the building design.
2) Comparison drift values both in the equivalent static analysis and response spectrum analysis the drift values show the less values in Rectangle shaped building(symmetrical) in static analysis. The response spectrum analysis shows much higher values due to the combination of all forces including static and dynamic loadings.
3) Considering the shear force in the both static and response spectrum analysis the

static analysis is having the least values in negative as compared to the response spectrum analysis.

4) The building minute demonstrates that the minute in response spectrum having less qualities as compared to the static analysis.
5) Considering all the above results and graphs the best reasonable structure is C formed building for the unsymmetrical shapes as compared to other building Y molded building both in static and response spectrum technique.
6) The utilization of outrigger and belt truss system in elevated structures increase the stiffness and make the structural form efficient under lateral burdens. Outrigger system is observed to be efficient in controlling the lateral loads and has proved to be Economical.

IV. REFERENCES

1.S. Fawzia, A. Nasir, T. Fatima (2011) Study of effectiveness of outrigger system for high rise composite buildings for cyclonic region, World Academy of Science Engineering and Technology, volume 5, 12-29.

2. J. Kim, Y. Jun and J. Park (2010) Performance of building structures with outrigger trusses subjected to loss of a column, 2nd Specialty Conference on Disaster Mitigation, Winnipeg, Manitoba.

3. Jaehong Lee, Minsik Bang, Jae-Yeol Kim (2008) an Analytical model for high-rise wall-frame structures with outriggers, The Structural Design of Tall and Special Buildings, 17, 839–851.

4. Pramod kumar Sharma, Vinay kumar singh chandrakar, Dr. P. D. Purey (2017)-"Lateral Stability analysis of High Rise building with the help of STAAD PRO"

5. Abbas Haghollahi, Mohsen Besharat Ferdous. Mehdi kastriet (2012). "Optimization of outrigger location in steel tall buildings subjected to Earthquake loads"

COMPARATIVE STUDY OF R.C. TALL BUILDINGS BETWEEN SYMMENTRICAL AND UNSYMMENTRICAL SHAPES IN CONSIDERATION OF NON DUCTILE USING WITH AND WITHOUT OUTRIGGER AND BELT TRUSS SYSTEM

Mohd Parvez Affani[1], Shaik Mohd Javeed[2] Mohd Farrukh Anwar[3]

[1] Pg Student, M.tech in Structural engineering, Department of Civil Engineering, Nawab Shah Alam Khan College of Engineering and Technology, Hyderabad, Telangana

[2] Assistant Professor, M.tech in Structural engineering, Department of Civil Engineering, Nawab Shah Alam Khan College of Engineering and Technology, Hyderabad, Telangana

[3]Head of the Department (PHD) , Vice Principal ,M.tech in Structural engineering, Department of Civil Engineering, Nawab Shah Alam Khan College of Engineering and Technology, , Hyderabad, Telangana

ABSTRACT: Should be met through engineering judgment. In Metro cities like Mumbai, Delhi, Chennai, Bangalore, Kolkata, Hyderabad etc multi-storied buildings are common and disregarding that individuals are willing to remain in elevated structure (36 storeys').The analysis and outline of tall building structural system require more concentration than that of regular multi-storied building. The lateral stability of tall building assumes an important role in safe analysis and plan. demonstrate is generated in ETABS, the state of building like a rectangular(symmetrical) Y-formed and C molded buildings i.e. (Non symmetrical) The building is strengthened in lateral direction by providing Outrigger and Belt non truss system at every 9 to 10 ,18 to 19, 27 to 28 story levels Two strategies for analysis have been considered for lateral stability analysis viz linear static and linear dynamic for both seismic and wind. The various parameters like (1) Lateral displacement story.

I. INTRODUCTION

Tall building is need of developing scenario. Rapid improvement of tall building in the world has been creating impact on innovative advancement of structural system for tall building, result of which buildings are growing taller. There is no specific definition of tall building however Council on Tall Building and Urban Habitat (CTBUH) gives a few measures to define tall building. Tall building phenomenon will continue in a greater scale to address the issues of the growing populace in future large cities. The advancement in concrete technology over the twentieth century covering materials, structural systems, analysis and construction techniques, made it conceivable to manufacture concrete tall buildings. Structural system like minute resisting frame and shear divider and bracing system fulfill primary need of building . As building increases in stature there is effect of lateral load i.e. wind and earthquake on building structure. The

impact of wind and seismic forces acting on tall building becomes an important aspect of the outline. Improving the structural systems of tall buildings can control their dynamic response Wind and earthquake stack plays major impact on building deflection. To overcome lateral load because of earthquake and wind, concrete core has been provided at center of building. Concrete core is a very effective and practical structural system which supportive in reducing the deflection because of seismic and wind forces. During recent years, the frame-concrete core divider hybrid structure has been rapidly created and profoundly concerned by owners with its performance and economic favorable circumstances. The outrigger and belt truss system is commonly utilized as one of the structural system to effectively control the excessive drift because of lateral load, so that, during little or medium lateral load due to either wind or earthquake stack, the risk of structural and non-structural harm can be minimized. For elevated structures, particularly in seismic active zone or wind stack dominant, this system can be chosen as an appropriate structure. Outriggers have been utilized in the sailing ship industry for some years. They are utilized to resist wind. The slender pole provides the utilization of outriggers. As a comparison the core can be related to the pole, the outriggers resemble the spreaders and the exterior columns resemble the shrouds or remains. Innovative structural schemes are continuously being looked for in the field. Structural Design of High Rise Structures with the intention of limiting the Drift because of Lateral Loads as far as possible without paying a high premium in steel tonnage.

OUTRIGGER AND BELT TRUSS SYSTEM

Outriggers are rigid horizontal structure i.e. truss or shaft which connect core divider and outer column of building to improve building strength and overturning stiffness. Outriggers have been utilized in tall building for nearly 50 years, however innovative plan principle has been improving its efficiency. Outrigger system is one sort of structural system which is formed from a cantilever molded horizontal member connected to structures inner core and outer columns. Through the connection, the minute arm of the core will be increased which prompt higher lateral stiffness of the system. Central core in a building act as cantilever, outriggers are provided to reduce overturning minute in core and to transfer minute from core to outer column by connecting the core and column. Divider frame outrigger trusses is a standout amongst the most efficient and economical structures in tall building, at outer end they connected to the establishment through exterior columns. At the point when the structure is subjected to horizontal loading, the divider and outrigger trusses will rotate, causing compression in the downwind column and strain in column on the upwind side, these hub forces will resist the rotation in the divider. The outrigger systems can be produced in any combination of steel, concrete and composite construction. Normally in steel structure outrigger are in the form of trusses and in the form of divider or profound bar in concrete structure. Outrigger might be stretched out to both side of central core or core might be located at one side of building with outrigger extending to other side columns. Belt truss connects outer perimeter column of a building and offer a wider perimeter to resist lateral deflection of building. This efficient structural form consists of a central core, comprising either Braced Frames or Shear Walls, with horizontal cantilever trusses or girders known as outrigger Trusses, connecting the core to the outer columns.

The core might be centrally located with outriggers extending on both.

TYPES OF OUTRIGGER TRUSS SYSTEM

Conventional Outrigger Concept

In the conventional outrigger concept, the outrigger trusses or girders are connected directly to shear dividers or braced frames at the core and to columns located outboard of the core. Typically (however not necessarily), the columns are at the outer edges of the building. Figure 1 is a romanticized section through a tall building with two arrangements of outrigger trusses, including one at the best. The outrigger trusses configuration. Shallower and deeper trusses have been utilized, with diagonals of various configurations.

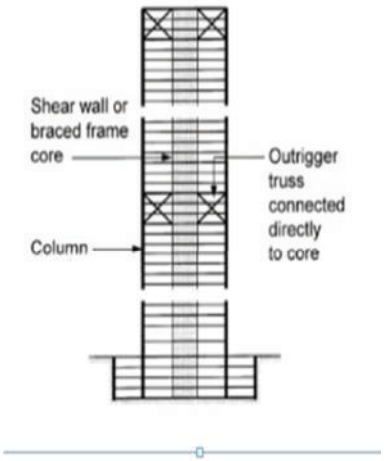

Tall building with conventional outriggers

Virtual Outrigger Concept

In the "virtual" outrigger, a similar transfer of overturning from the core to components outboard of the core is achieved, yet without a direct connection between the outrigger trusses and the core. The basic thought behind the virtual outrigger concept is to utilize floor diaphragms, which are typically very solid and strong in their own plane.

Belt Trusses As Virtual Outriggers

The utilization of belt trusses as virtual outriggers keeps away from a considerable lot of the problems associated with the utilization of conventional outriggers. The principle is the same as when belt trusses are utilized as virtual outriggers. Some fraction existing apart from everything else in the core is converted into a horizontal couple in the floors at the best and the base of the storm cellar.

NEED OF THE PROJECT

Accumulation of growing populace especially in developing countries has resulted in an increased tallness of buildings, this need creating impact on structural improvement of tall building. As building increases in tallness there is effect of wind and earthquake forces, to increase stiffness of building against lateral load extra structural system such as belt truss and outriggers is required. The reviewed approach for the outline and improvement of tall building using outrigger and belt truss is helpful to provide a potential arrangement. The study in turn is helpful for various research persons involved in outline the tall buildings by using outrigger and belt truss system

OBJECTIVE OF THE STUDY

To study the effect of introduction of Outriggers in tall structure subjected to dynamic wind loading. To study the influence of core divider and braced core divider with X braced outriggers C. To stud influence of concrete outrigger. To study the effect of Outriggers with Peripheral Belt Truss. To study the different configuration of the building under different

arrangement molded building i.e symmetrical and Unsymmetrical Buildings (Rectangular and Y formed building , C formed Building

II. METHODOLOGY

ANALYSIS OF A 36 STOREY BUILDING

The model considered for this study is 111.5 m skyscraper reinforced concrete building frame. The building represents a 36 storied office building. The stature of each story is 3m and every one of the floors are considered as Typical Floors. The location of the building is thought to be at Bhuj (Gujarat) . All divider piers are identical with a uniform divider thickness of 230mm over the entire stature. The Bracing bars (outriggers) and every other bar are 600mm wide and 600mm profound, Grade 40 concrete is considered (Compressive strength 40 N/mm²) throughout the tallness of the building. And number of stories considered for every one of the cases is 36 stories, and roof tallness is considered as 111.5 m. And story to story tallness is 3.0 m. And the outer columns sizes are considered as 800X800 mm and Inner columns measure are consider as 550X600 mm. shear divider thickness is considered as 230 mm.The technique for analysis of the previously mentioned system is construct up in light of the presumptions that the outriggers are rigidly attached to the core; The core is rigidly attached to the establishment; The sectional properties of the core, shafts and columns are uniform throughout the stature; Tensional effects are not considered; Material behavior is in linear elastic range; The Outrigger Beams are flexural rigid and induce just pivotal forces in the columns; The lateral resistance is provided just by the bending resistance of the core and the secure action of the exterior columns connected to the outrigger; The rotation of the core because of the shear deformation is immaterial.

STRUCTURAL MODELLNG

SL No	Structural details	Type of location
1	Utility of Buildings	Office Building
2	No of Storey	G+36
3	Area	2308 sq mts
4	Height of Building	111.5 mts
5	Shape of the Building	Rectangle, Y shaped, C shaped building
6	Types of Walls	SHEAR Wall -230 mm thickness Masonry wall – 230 mm thickness
7	**Geometric Details** Ground Floor	3.5 mts
	Story to story height	3.0 mts
	Beam	0.60X0.60 mts
	Columns (outer)	0.80X0.80 mts
	Columns (Inner)	0.55X0.60 mts
	Slab	0.150 mts
8	**Material Details** Concrete Grade All Steel Grades	M40 (All structural elements) FE 415 (All structural elements)
9	Type Of Construction	R.C.C FRAMED STRUCTURE
10	Place of construction	Bhuj - Gujarat
11	Loads considered in Buildings	Dead load, Live load, Earthquake ,Wind load
12	Wind Speed	50 m/s (Bhuj wind speed)
13	Seismic Zone	Zone – V (Bhuj)
14	Method of Analysis	RESPONSE SPECTRUM ANALYSIS EQUIVALENT STATIC ANALYSIS
15	NON Ductile properties	5 (Response reduction factor)
16	STATIC COMBINATION USED	1.2(Dead load+ Live load+ Earthquake in X direction)
17	IS codes used	IS456 :2000,IS1893:2002,IS 16700:2017,IS 875:1987 (Part 1, Part 2, Part 3)

Rectangle Building

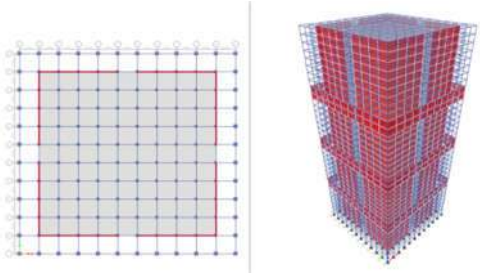

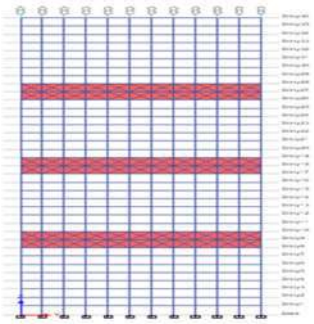

Y shaped building

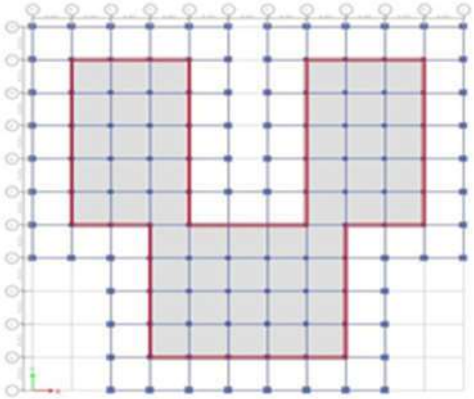

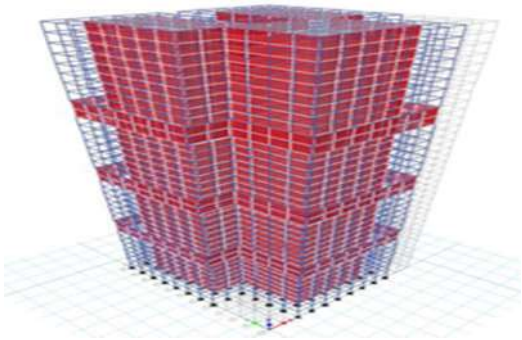

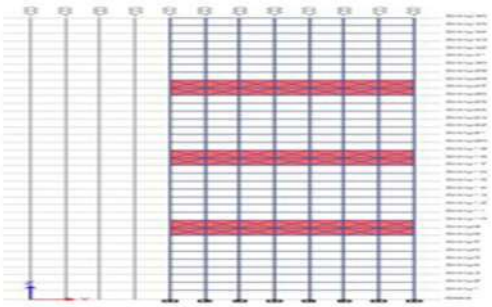

C shaped building

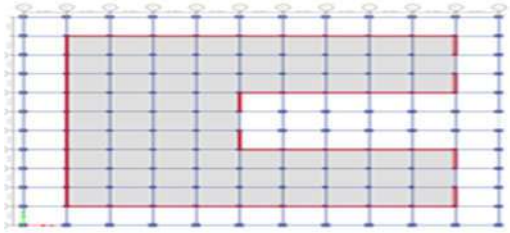

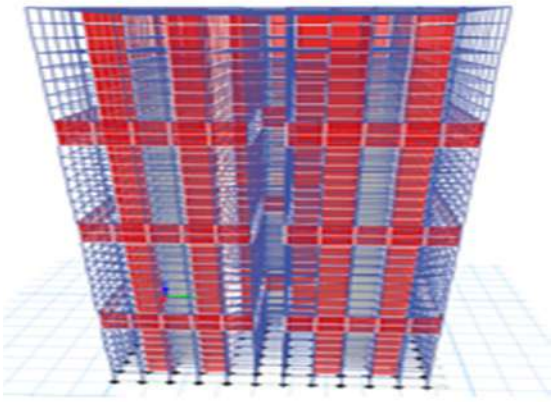

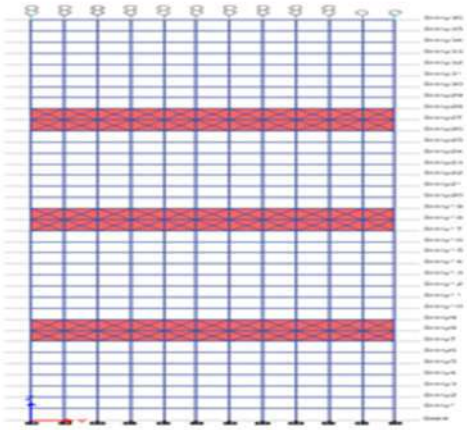

COMPARASTION OF EQUIVALENT STATIC ANALYSIS AND RESPONSE STRECTRUM ANALYSIS.

A.STOREY DRIFT

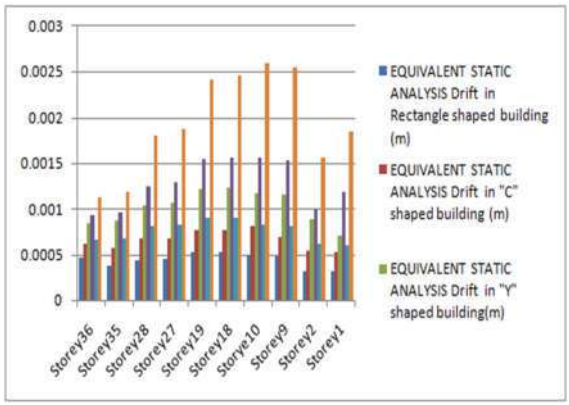

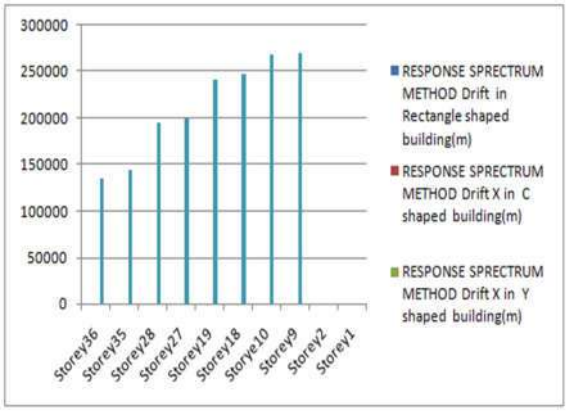

B.STOREY SHEAR FORCE

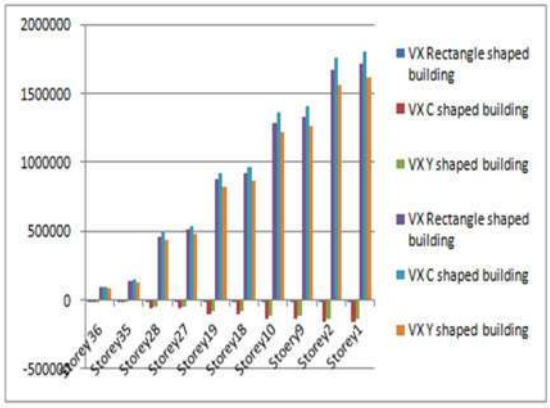

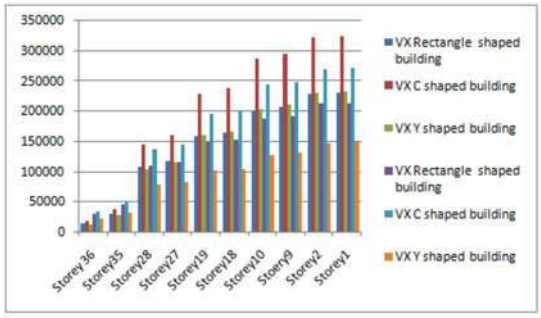

C.MOMENT FORCE

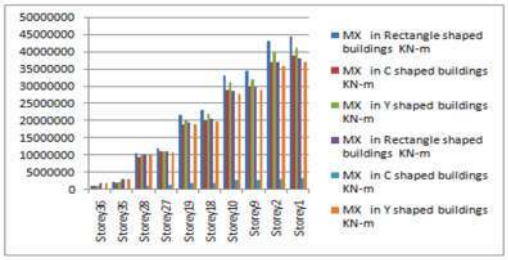

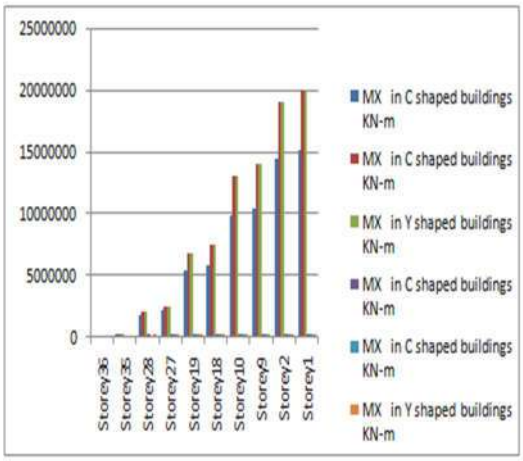

III. .CONCLUSIONS

After performing analysis and studying the results we can come to the below conclusion's:

1) The behavior of a structure under earthquake load is different from earthquake to earthquake. This well known phenomenon is well presented in the lateral displacement results obtained for both of the options. The location of the outrigger beam has a critical influence on the lateral behavior of the structure under earthquake load and the optimum outrigger locations of the building have to be carefully selected in the building design.
2) Comparison drift values both in the equivalent static analysis and response spectrum analysis the drift values show the less values in Rectangle shaped building(symmetrical) in static analysis. The response spectrum analysis shows much higher values due to the combination of all forces including static and dynamic loadings.
3) Considering the shear force in the both static and response spectrum analysis the

static analysis is having the least values in negative as compared to the response spectrum analysis.

4) The building minute demonstrates that the minute in response spectrum having less qualities as compared to the static analysis.
5) Considering all the above results and graphs the best reasonable structure is C formed building for the unsymmetrical shapes as compared to other building Y molded building both in static and response spectrum technique.
6) The utilization of outrigger and belt truss system in elevated structures increase the stiffness and make the structural form efficient under lateral burdens. Outrigger system is observed to be efficient in controlling the lateral loads and has proved to be Economical.

IV. REFERENCES

1.S. Fawzia, A. Nasir, T. Fatima (2011) Study of effectiveness of outrigger system for high rise composite buildings for cyclonic region, World Academy of Science Engineering and Technology, volume 5, 12-29.

2. J. Kim, Y. Jun and J. Park (2010) Performance of building structures with outrigger trusses subjected to loss of a column, 2nd Specialty Conference on Disaster Mitigation, Winnipeg, Manitoba.

3. Jaehong Lee, Minsik Bang, Jae-Yeol Kim (2008) an Analytical model for high-rise wall-frame structures with outriggers, The Structural Design of Tall and Special Buildings, 17, 839–851.

4. Pramod kumar Sharma, Vinay kumar singh chandrakar, Dr. P. D. Purey (2017)-"Lateral Stability analysis of High Rise building with the help of STAAD PRO"

5. Abbas Haghollahi, Mohsen Besharat Ferdous. Mehdi kastriet (2012). "Optimization of outrigger location in steel tall buildings subjected to Earthquake loads"

DETERMINATION OF BLAST LOAD PARAMETERS ON 3D BUILDING STRUCTURE USING SAP 2000

HUZAIFA YAMAN

(ASSISTANT PROFESSOR)

Department of Civil Engineering

NSAKCET, India

MOHAMMED IDREES UDDIN

Department of Civil Engineering

NSAKCET, India

ABSTRACT: The effects of blast damage on the buildings targeted and glass exposures were significant contributors to death and injury. Explosions lead to massive dynamic loads more significant than the initial design loads, and the system is tested and planned for them. The fundamental cause of progressive frame structure failure in the column is usually column failure. As a time-history analysis, the blast loads were analytically calculated.

So my research focused primarily on G+13 building with 500,1000,2000,3000 and 4000 kg TNT at 10, 20 30, and 40 m standoff distance using sap 2000 surface blast study, manually performed to detect pressure on successful structures

1. INTRODUCTION

The blast loading analysis was initiated only in the 1960s. The protection of civilian buildings from the threat of terrorist activity for structural engineers is one of the most critical challenges today. Most of the studies used high energy explosive vehicle-driven cargo to simulate a terrorist attack on concrete / composite masonry wall. Terrorism and threats are becoming a growing problem worldwide, and the protection of people from terrorist attacks means that these events can be predicted, prevented, and mitigated. In many countries, extensive research has been initiated into blast effect analysis and building protection techniques to develop critical infrastructure protection methods and the built-in environment. The main aims are to develop design and building procedures to protect personnel and equipment against mass detonation explosion.

- The secondary objective is for the design of protective structures to identify parameters of the blast load.
- To study the response of G+13 building considering blast load of varies intensity (500,1000,2000,3000 and 4000 kgs)
- The response of building with standoff distance is 10,20,30,40 m from the building.

2 Literature Review

Draganic et al. have studied, described, and presented numerous examples of the fictional structure exposed to this load in determining the explosive charge of structures. The objective was to get to know the problem of bursting cargo, given the growing terrorist threat and the absence of national and European regulations in the guidelines for monitoring nuclear infrastructure.SAP2000 analyzed the explosive charge as a history of the pressure-time and established a numerical structure model.

Koccaz, Zeynep et al. In particular, in recent years, the numbers of terrorist attacks have been discussed, showing that the effect of burning loads on buildings must be considered an essential issue in the design process. This study highlights explosive design theories, improves building safety against hazards, and design techniques to be used both in architectural and structural design. The first explained the types of explosives and explosives briefly. Also, the general aspects of the explosion process were discussed to clarify the impact of explosives on buildings.

Andrew Sorensen The recent rise of a terrorist bombing and exploding that have led to a higher need for researchers after the explosion has been studied by Andrew Sorensen, Ph.D., etc. Many advances have been made in chemical analysis on explosive residues, but few works have been done to help post-explosive investigators determine explosive weight with structural damage after the explosive explosion.

3 MODELLING PARAMETERS

In the first model, a reinforced concrete frame building situated in the V zone is taken for study. The building's plan area is 12 x 12 m, with 3m as the height of each typical story. It consists of 4 bays in X-direction and four bays in Y-direction.

Dimensions of Structural Members

S. No.	Specifications	G+13
1	Slab Thickness	150mm
2	Beam dimensions	
		230x500 mm
3	Column dimensions	700x700 mm,
4	Grade of concrete	M30
5	Grade of steel	Fe-550
6	Unit weight of concrete	25kN/m^3
7	Live loads	3kN/m^2
	(a) Floor load	1.5kN/m^2
10	Importance factor	1
11	Seismic zone	V
12	Response reduction factor	5

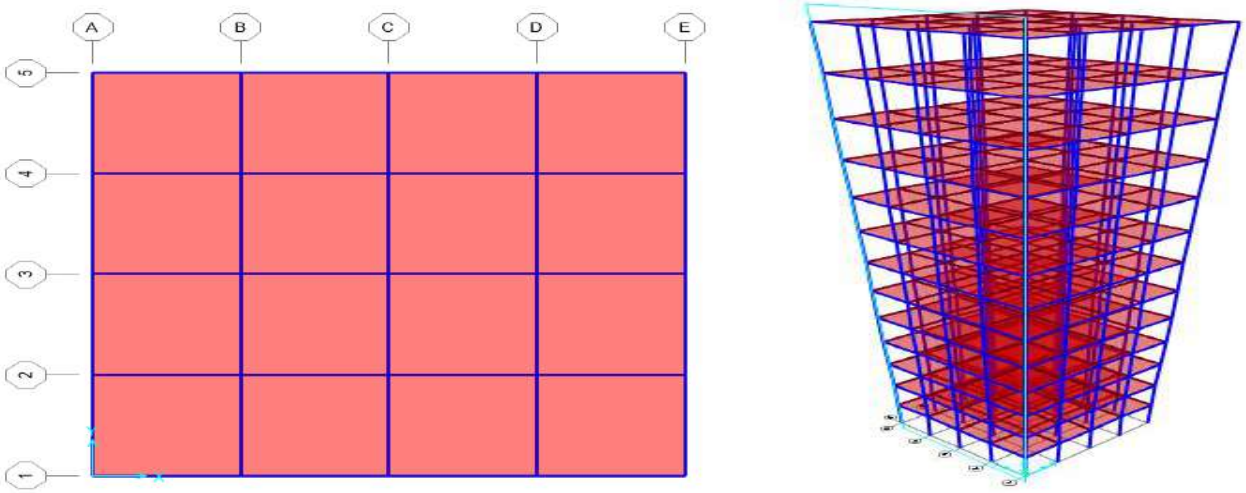

Fig No 1: Typical floor Plan 3D View

4. ANALYSIS RESULTS

Table No 1 BLAST LOAD PARAMETERS FOR 10m DISTANCE WITH CHARGE WT:- 500Kg TNT

Floor	Scaled Distance (m/$Kg^{1/3}$)		P_r (Kg/m^2)	P_{so} (Kg/m^2)	I_r (Kg/m^2-ms)	I_s(Kg/m^2-ms)	t_A (ms)	t_o (ms)	U (m/ms)	L_w (m)
G Floor	Z	2.99	512920.41	94930.38	602385.63	181876.20	5.38	18.21	1.01	2.08
1st floor	Z	3.22	413580.41	80431.51	546730.07	172066.84	6.18	18.65	0.94	2.30
2nd floor	Z	3.83	244495.95	54209.81	437804.08	147921.93	8.54	18.12	0.80	3.01

3rd floor	Z	4.67	134916.48	34273.53	341439.75	122613.18	12.39	17.20	0.67	4.05
4th floor	Z	5.64	76556.17	22256.62	271158.79	102712.20	17.60	17.92	0.57	4.98
5th floor	Z	6.68	46934.41	15260.85	221402.57	88058.84	23.99	20.83	0.51	5.85
6th floor	Z	7.77	31155.27	11059.26	185547.16	77106.94	31.35	24.41	0.47	6.64
7th floor	Z	8.89	22151.59	8407.79	158945.85	68632.89	39.50	26.87	0.44	7.34
8th Floor	Z	10.02	16657.73	6649.29	138631.13	61853.65	48.27	28.79	0.42	7.97
9th Floor	Z	11.17	13095.43	5428.55	122704.36	56279.63	57.53	30.34	0.41	8.52
10th Floor	Z	12.32	10663.09	4547.44	109931.99	51599.75	67.16	31.64	0.40	9.01
11th Floor	Z	13.49	8929.22	3889.86	99491.14	47609.44	77.08	32.77	0.39	9.45
12th Floor	Z	14.65	7644.00	3384.55	90810.99	44162.35	87.22	33.77	0.39	9.85
13th Floor	Z	15.83	6610.64	2986.78	83490.05	41155.06	97.53	34.68	0.38	9.21

Table No 2 BLAST LOAD PARAMETERS FOR 20m DISTANCE WITH CHARGE WT:- 500Kg TNT

Floor	Scaled Distance ($m/Kg^{1/3}$)		P_r (Kg/m^2)	P_{so} (Kg/m^2)	I_r (Kg/m^2-ms)	I_s(Kg/m^2-ms)	t_A (ms)	t_o (ms)	U (m/ms)	L_w (m)
G Floor	Z	5.98	64547.84	19525.46	252824.66	97369.56	19.59	18.56	0.55	5.28
1st floor	Z	6.10	60977.17	18688.88	246959.48	95647.94	20.31	18.84	0.54	5.38
2nd floor	Z	6.44	52154.51	16562.82	231422.71	91051.57	22.42	19.90	0.53	5.66
3rd floor	Z	6.97	41742.57	13927.33	210665.13	84821.69	25.87	21.95	0.50	6.07
4th floor	Z	7.65	32410.35	11411.88	188814.19	78123.67	30.54	24.11	0.48	6.56
5th floor	Z	8.45	25079.68	9297.19	168327.07	71665.46	36.28	25.99	0.45	7.08
6th floor	Z	9.34	19649.18	7623.06	150205.17	65755.08	42.94	27.69	0.44	7.60
7th Floor	Z	10.28	15700.00	6328.35	134614.00	60472.21	50.38	29.18	0.42	8.10
8th Floor	Z	11.28	12819.15	5330.71	121346.67	55778.54	58.45	30.48	0.41	8.57
9th Floor	Z	12.31	10689.33	4557.01	110076.80	51654.91	67.04	31.63	0.40	9.00
10th Floor	Z	13.37	9083.65	3949.53	106605.20	47992.53	76.05	32.66	0.39	9.41
11th Floor	Z	14.45	7847.63	3465.71	92249.89	44742.36	85.40	33.60	0.39	9.78
12th Floor	Z	15.54	6877.27	3075.06	85158.05	41850.00	95.02	34.47	0.38	10.13
13th Floor	Z	16.65	6101.47	2755.31	79000.95	39264.87	104.85	35.28	0.38	10.45

Table No 3 BLAST LOAD PARAMETERS FOR 30m DISTANCE WITH CHARGE WT:- 500Kg TNT

Floor	Scaled Distance ($m/Kg^{1/3}$)		P_r (Kg/m^2)	P_{so} (Kg/m^2)	I_r (Kg/m^2-ms)	I_s(Kg/m^2-ms)	t_A (ms)	t_o (ms)	U (m/ms)	L_w (m)
G Floor	Z	8.97	21668.33	8258.38	157322.30	68102.69	40.11	27.02	0.44	7.39
1st floor	Z	9.05	21209.71	8115.32	155744.72	67585.51	40.71	27.16	0.44	7.44
2nd floor	Z	9.28	19939.63	7715.67	151265.58	66108.30	42.50	27.59	0.44	7.57
3rd floor	Z	9.66	18145.05	7138.62	144558.36	63865.66	45.42	28.22	0.43	7.78
4th Floor	Z	10.16	16131.27	6473.57	136447.49	61105.08	49.40	29.00	0.42	8.04
5th Floor	Z	10.78	14149.25	5797.57	127709.87	58060.25	54.34	29.85	0.41	8.34
6th Floor	Z	11.48	12341.27	5159.87	118937.01	57985.16	60.13	30.72	0.41	8.66

7th Floor	Z	12.26	10766.93	4585.69	107266.42	51817.34	66.67	31.58	0.40	8.99
8th Floor	Z	13.11	9430.76	4082.82	102647.07	48833.04	73.85	32.42	0.39	9.32
9th Floor	Z	14.01	8311.21	3648.97	95433.40	46013.46	81.58	22.25	0.39	9.64
10th Floor	Z	14.94	7376.65	3277.36	88884.79	43380.84	89.76	34.00	0.38	9.94
11th Floor	Z	15.92	6595.62	2959.71	82975.18	40941.30	98.33	34.75	0.38	10.24
12th Floor	Z	16.92	5939.51	2687.68	77654.00	38689.47	107.22	35.47	0.38	10.52
13th Floor	Z	17.94	5384.65	2453.91	72866.08	36618.46	116.39	36.16	0.37	10.79

Table No 4 BLAST LOAD PARAMETERS FOR 40m DISTANCE WITH CHARGE WT:- 500Kg TNT

Floor	Scaled Distance ($m/Kg^{1/3}$)		P_r (Kg/m^2)	P_{so} (Kg/m^2)	I_r (Kg/m^2-ms)	I_s(Kg/m^2-ms)	t_A (ms)	t_o (ms)	U (m/ms)	L_w (m)
G Floor	Z	11.96	11344.26	4798.60	113702.41	53004.17	64.07	31.25	0.40	8.86
1st Floor	Z	12.01	11230.93	4756.17	113074.13	52772.02	64.57	31.32	0.40	8.89
2nd Floor	Z	12.19	10898.61	4634.47	111248.31	52092.41	66.06	31.50	0.40	8.96
3rd Floor	Z	12.48	10392.95	4446.54	108384.29	51018.98	68.50	31.81	0.40	9.07
4th Floor	Z	12.88	9769.15	4211.64	104710.15	49624.51	71.85	32.20	0.40	9.23
5th Floor	Z	13.37	9083.65	3949.53	100654.21	47992.53	76.05	32.66	0.39	9.41
6th Floor	Z	13.94	8383.23	3677.16	95914.57	47204.25	81.02	33.17	0.39	9.61
7th Floor	Z	14.59	7702.27	3407.86	91227.03	44330.91	86.69	33.72	0.39	9.83
8th Floor	Z	15.31	7063.60	3150.78	86564.77	42430.00	92.97	34.29	0.38	10.06
9th Floor	Z	16.08	6476.43	2910.65	82035.06	40547.47	99.81	34.87	0.38	10.29
10th Floor	Z	16.91	5945.79	2690.34	77706.86	38712.45	107.13	35.46	0.38	10.52
11th Floor	Z	17.77	5469.72	2489.98	73619.25	36947.92	114.86	36.05	0.37	10.75
12th Floor	Z	18.67	5044.94	2309.10	69790.60	35266.14	122.97	36.64	0.37	10.97
13th Floor	Z	19.61	4666.78	2146.37	66223.99	33674.76	131.39	37.23	0.37	11.18

Table No 5 BLAST LOAD PARAMETERS FOR 50m DISTANCE WITH CHARGE WT:- 500Kg TNT

Floor	Scaled Distance ($m/Kg^{1/3}$)		P_r (Kg/m^2)	P_{so} (Kg/m^2)	I_r (Kg/m^2-ms)	I_s(Kg/m^2-ms)	t_A (ms)	t_o (ms)	U (m/ms)	L_w (m)
G Floor	Z	14.94	7376.65	3277.36	88884.79	43380.84	89.76	34.00	0.38	9.94
1st Floor	Z	14.99	7334.08	3260.27	87042.11	43255.19	90.18	34.04	0.38	9.96
2nd Floor	Z	15.13	7211.05	3210.51	87665.78	42882.05	91.43	34.15	0.38	10.00
3rd Floor	Z	15.37	7015.94	3131.45	86206.96	42282.89	93.49	34.33	0.38	10.08
4th Floor	Z	15.69	6763.32	3028.44	84210.27	41484.52	96.33	34.58	0.38	10.17
5th Floor	Z	16.09	6468.75	2907.51	81973.77	40521.42	99.91	34.88	0.38	10.29
6th Floor	Z	16.58	6148.58	2774.92	79390.18	39430.37	104.18	35.23	0.38	10.43
7th Floor	Z	17.13	5816.97	2636.39	76622.70	38248.14	109.10	35.61	0.38	10.58
8th Floor	Z	17.74	5485.00	2496.47	73754.86	37006.92	114.59	36.03	0.37	10.74
9th Floor	Z	18.41	5160.99	2358.72	70854.07	35735.81	120.63	36.47	0.37	10.90

10th Floor	Z	19.14	4850.45	2225.57	67974.73	34458.57	127.14	36.94	0.37	11.07
11th Floor	Z	19.91	4556.94	2098.84	65158.99	33194.36	134.09	37.41	0.37	11.25
12th Floor	Z	20.72	4282.19	1979.44	62434.42	31957.73	141.43	37.90	0.37	11.42
13th Floor	Z	21.56	4027.34	1867.92	59820.95	30757.88	149.11	38.39	0.37	11.59

Incident Pressure (P_{so}):

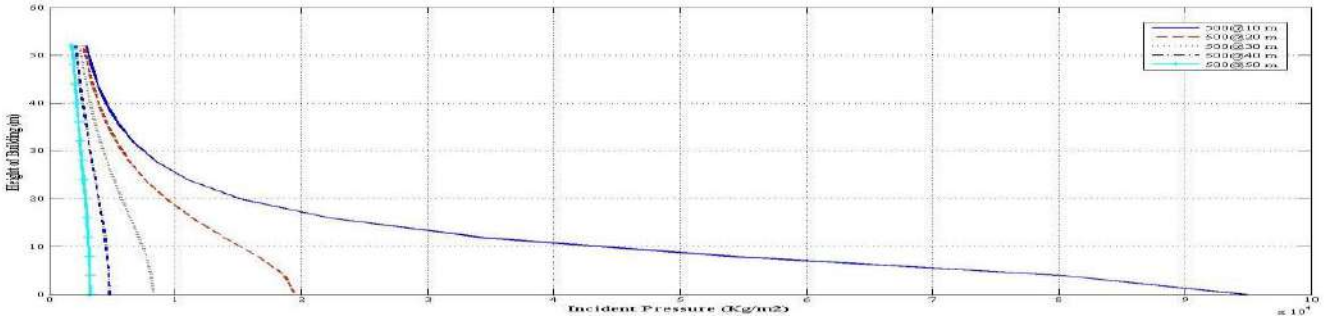

Figure 2 Incident Pressures @ 500kg TNT

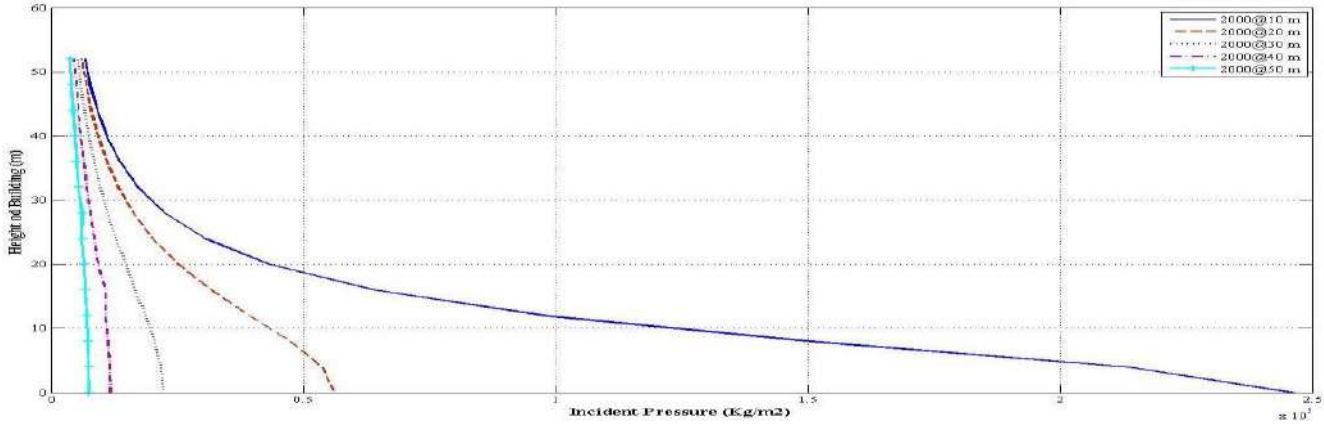

Figure 3 Incident Pressures @ 2000kg TNT

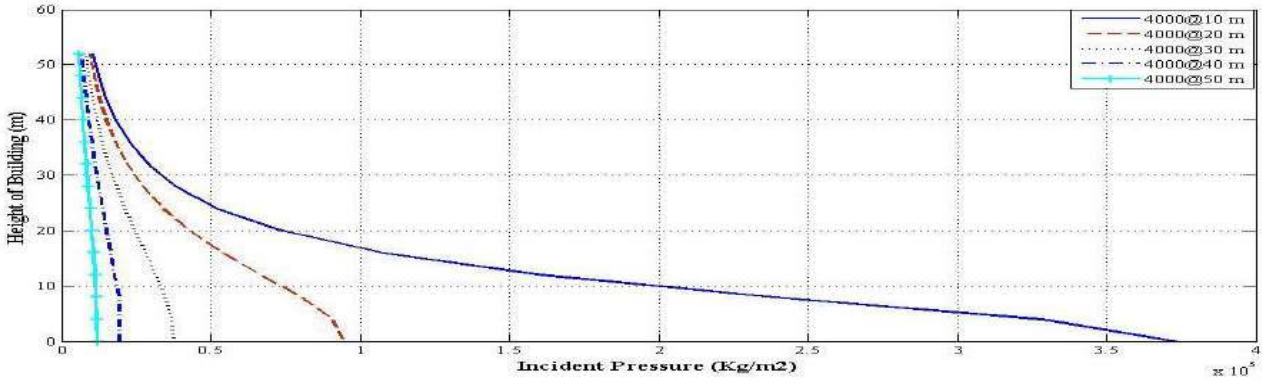

Figure 4 Incident Pressures @ 4000kg TNT

Reflected Pressure (P_r):

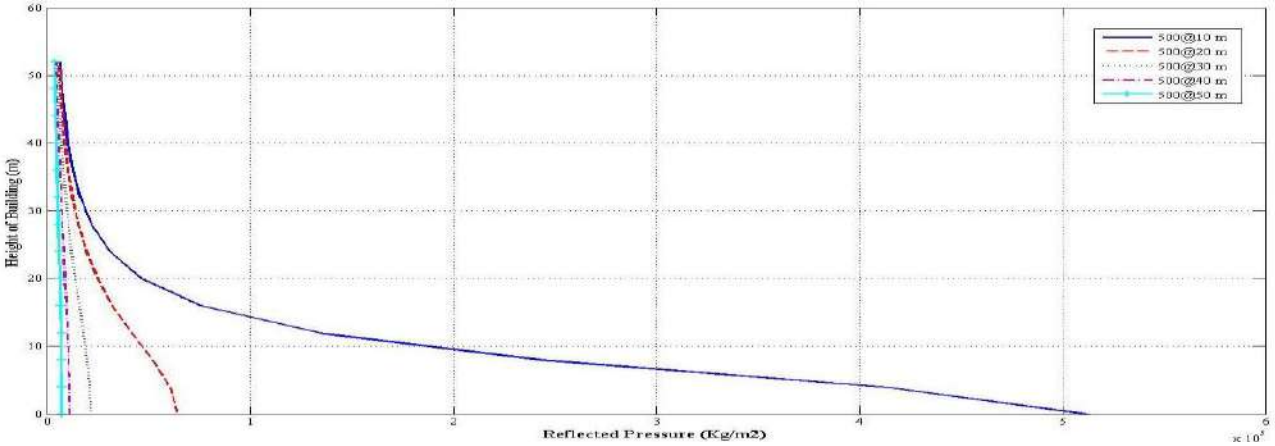

Figure 5 Reflected Pressures @ 500kg TNT

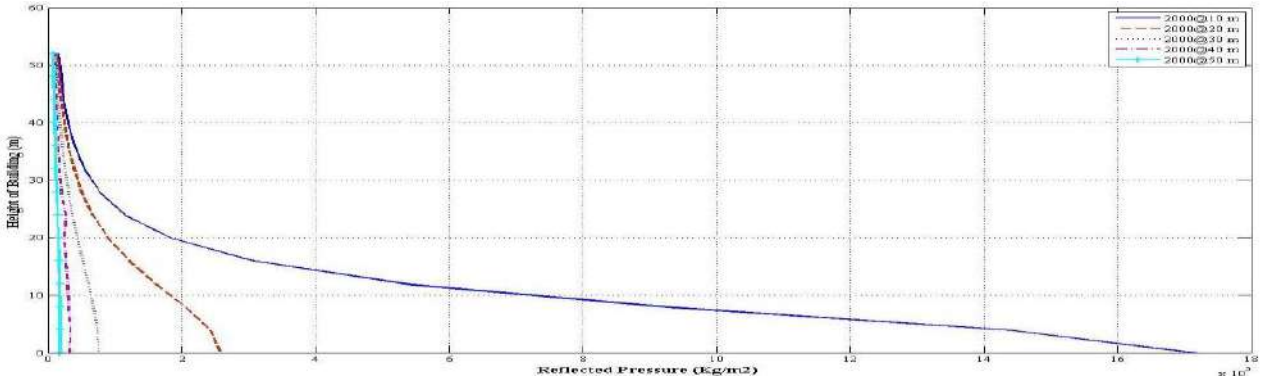

Figure 6 Reflected Pressures @ 2000kg TNT

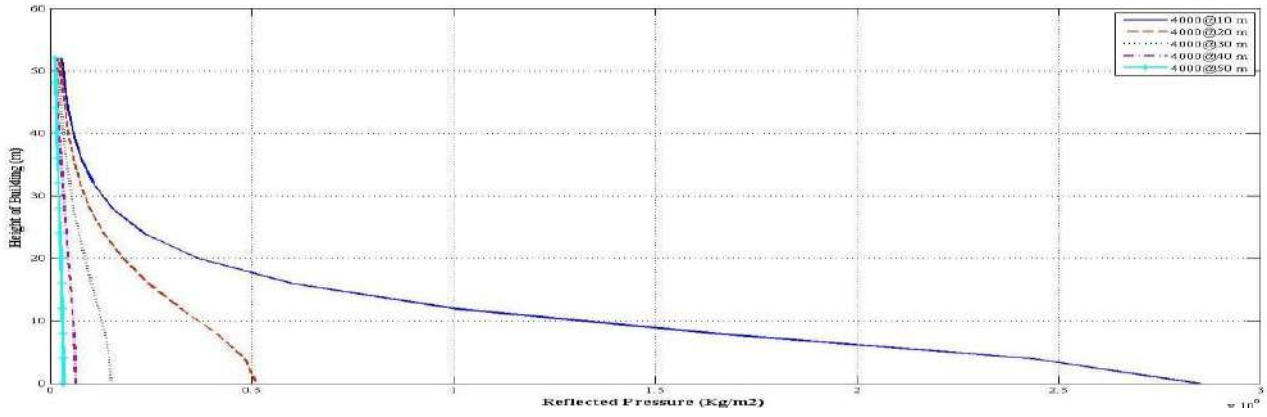

Figure 7 Reflected Pressures @ 4000kg TNT

5 CONCLUSIONS

- The Surface blast analysis was performed manually, in which the loading weights from structure to the explosion were found for the pressures induced on efficacy structures with different TNT (Trinitrotoluene).
- The reflected pressure distribution decreases for blasts over the façade of the structure at the structure height.
- The measure of the reflected pressure for the combinations mentioned above of range and charge weight shows that the charge weight effect, i.e., the change is reflected stress between the floors, is much greater for lower floors and the upper floors change less pronounced.
- · The distribution for blasts of wide range is approximately uniform, and this assumption is not valid for shorter ranges
- Due to the high reflected pressure in low ranges, the lower stories will initially collapse locally, leading to the entire structure collapsing progressively.
- The structure's local response is more in the case of small ranges. For high range, because of the low-pressure variation on a façade of the structural structure that is noticeable in reflected pressure contours across a façade, the structure rates globally rather than locally.
- For all charging weights, the reflected pressure at the top of the structure in the 10 m range is more than the 20, 30, 40, and 50 m range
- For the 10 m range, the reflected load pressure factor has increased in the third and fifth floors, between 400 to 600 incident angles, from 4000 kilos of TNT to 2000 kilos of TNT and 500 kg of TNT.
- The variation in reflected momentum is more pronounced in lower floors in low-range load weights and less in the case of lower-range load weights.
- In all combinations of ranges and load weights, the top floors' reflected impulses are almost uniform.
- The time of entry (tA) and the sum of the times and the excellent phase reflected pressure (TA+tO) increase and decrease in the load's weight.
- The change in the times and (tA, tA+tO) of the above is nonlinear in the lowest and roughly linear in the top levels due to the expansion of the shocked face from the explosion and decreases the incident pressure, and also the distance to the explosion, to the environmental pressure.

6. SCOPE FOR FURTHER STUDY

- The broad conclusion derived from this work has been reported within the limited scope of the present work. In the following fields, however, further study may be conducted.

- The study can be extended further to the air explosion as well.
- Any simulation software may be used in the present study manual design.
- Towards manual and software simulation analysis, the work can be extended as a comparative study.
- Time history analysis may be carried out using these graphs in the present study impulse diagrams.

REFERENCES

1) http://engagedscholarship.csuohio.edu/cgi/viewcontent.cgi?article=1021&context=encee_facpub, Ronan Point Apartment England in1968.

2) Unified Facilities Criteria (UFC), Structures to resist the effects of accidental explosions, US Army Corps of Engineers, Naval Facilities Engineering Command, Air Force Civil Engineer Support Agency, UFC 3-340-02, 5 December 2008.

3) https://en.wikipedia.org/wiki/1999_Athens_earthquake, in 1999 Athens Earthquake Occurred.

4) https://en.wikipedia.org/wiki/1999_%C4%B0zmit_earthquake, in 1999 Izmir Earthquake.

5) https://en.wikipedia.org/wiki/1999_D%C3%BCzce_earthquake,in 1999 Duzce Earthquake occurred.

6) https://simple.wikipedia.org/wiki/1999_Chi-Chi_earthquake, in the 1999 Chi-Chi Earthquake.

7) https://en.wikipedia.org/wiki/2001_Gujarat_earthquake, in 2001 Bhuj Earthquake occurred.

8) https://en.wikipedia.org/wiki/2003_Boumerd%C3%A8s_earthquake, in 2003 Boumerdes Earthquake occurred.

9) https://en.wikipedia.org/wiki/April_2015_Nepal_earthquake, in2015 Gorkha Earthquake occurred.

10) https://en.wikipedia.org/?title=Oklahoma_City_bombing, Alfred P. Murrah Federal office building in Oklahoma City, USA

11) https://en.wikipedia.org/wiki/Khobar_Towers_bombing, Khobar Tower bombing, Saudi Arabia

12) 12) H. 12) ISSN 1330-3651 UDC / UDK 624.01.04:662 from Draganic, V. Sigmund. Fifteen. Blast structural loading.

13) 13) Koccaz Zeynep Fatih Sutch, Torunbalci Necdet. 13. for blast resistant buildings, architectural and structural design.

14) 14) The threat against structure induced by Manmohan Das Goel Blast.

15) John E. Crawford and Kenneth and L. Javier Malvar. To resist exposure, use of composites

16) The Research & Development Setting (Engineering) CK Gautham and R.C. Pathak, Pune-41015. Structures resistant to blast design. Journal of Defence Sciences, vol-47, No 2, April 1997.

17) The explosion in various structures by Andrew Sorenson.

18) Ranjan Kumar, S.M.ASCE, Choudhury M.ASCE Deepankar, and Bhargava Kapilesh, respectively. Prediction of vibration parameters induced by the bubble in soil sites.

19) Shlomo Ginsburg Protective structure analysis and design against explosion.

20) Avinash C. Songhay Studies on various thickness flexible aluminium panels.

21. The process for determining a blast-resistant wheel is in use in Giovanna A. Naselli.

TEMPERATURE STRESS OF RCC AND COMPOSITE STRUCTURE WITH BRB FRAME

ASST Prof. MOHAMMED ABDUL AQUIL
Department of Civil Engineering
NSAKCET, India

MOHAMMED ABDUL RAHMAN
Department of Civil Engineering
NSAKCET, India

ABSTRACT:

The strength of the building in dangerous load conditions such as earthquakes and explosion is one of the most critical challenges for structural engineers. The primary function of the horizontal braking system is to maintain wind and earthquake structural load. Buckling-restrained brace systems (BRBFs) are typically used as seismic resistant systems for buildings in seismic areas. The use of the Buckling stretched brace system has been increased in recent decades, and the performance of BRBs under static and seismic charges at room temperature has been tested because of their best positive behavior in earthquake conditions.

This comparative analysis includes the 20 story R.C.C. and standardized composite frameworks. BRBF with specific temperature charges is evaluated using non-linear time-history analyses through the seismic conduct of the system of studies developed using the proposed methodology. The software SAP 2000 v 16 offers 3D modelling and structural analysis. In this study, the main parameters evaluated are lateral displacement, interstitial drifting, base shear, rotation, maximum axial strength, and maximum bending.

1. INTRODUCTION

Most Indian buildings fall into the low-level building category. Therefore, reinforced cement components are always used in such systems because they are very efficient and straightforward. However, as the population grows exponentially in cities and the territory is limited, vertical construction in these towns is needed. These days, therefore, there are a large number of medium- to high buildings. It has been found that composites are more realistic and cost-effective when constructing such highrise buildings than reinforced cement beams. Due to its advantage over standard reinforced construction, the significance of composite concrete buildings in cities can be. For low altitude buildings in which the charge is small, R.C.C. frames are used.

- To study the response of Rcc and composite Structure under temperature loading.
- Study of Seismic demands of regular R.C and composite buildings using the Non-linear time history analysis.
- To illustrate the effects of Buckling resistance brace on the response of the High-rise Symmetric Buildings.
- To evaluate the performance of a building to suggest some retrofitting techniques, if required.

2 Literature Review

Takanori OYA, Takashi Fukazawa, et al (2009),

In its paper, a new form of BRB has been applied to various structures. The bracelet has two hinges (steel mortarboards), which snap in the central platter under axial forces. Both sections are welded together and contain the core layer of plastic behavior that prevents deformation and humps out of the plane. The paper includes material properties on the history of the BRBF and a description of the various issues concerning code enforcement, agency approvals, research, and design, detailing, and building problems.

Uang and Kiggins (2006)

The study is built on the research of Sabella et al. (2003). The SMRFs were added to the original three and 6-story buildings as a dual system and their seismic responses with the initial BRBF systems. Twenty-five percent of the overall necessary shear was designed for the SMRFs. Including SMRFs in BRBFs, the study showed a 10 to 12 percent lower average drift demands and a 46-55 percent lower residual drift than the initial BRBFs. There is, therefore, extreme standard deviation from the residual drift result, which shows that several predictions are uncertain.

R.D. Panchal et P.M. Marathe

Use a comparative method of study in the G+30 commercial building in seismic Zone IV to identify R.C.C., composite, and steel options. Equivalent Static Method and ETABS software were used for this purpose. The comparative studies were also based on scale, deflections, members' material use in R.C.C. and steel components, and carefully investigated composite components.

.

3 MODELLING PARAMETERS

In the first model, R.C.C building is prepared for which plan & the isometric view is given in Fig 4.1 & Fig 4.2, respectively, to prepare this plan stepwise procedure is explained. Materials have been defined for the same ex; M_{25}& fe_{500}. Detailed dimensions of the frame section are given in table 4.1. For this model, the average temperature is inculcated (25^0C).

Dimensions of Structural Members

S.No	Variable	Data
1	Type of Structure	Moment Resisting Frame
2	Number of Stories	20
3	Floor height	3m
4	Live Load	2.0 kN/m^2
5	Dead load	1.25 kN/m^2 & wall load of 10 kN/m^2
6	Materials	Concrete (M35) and Reinforced with HYSD bars (Fe500)
7	Size of Columns	R.C.C. structure 300x900 mm
		Composite structure 500X700 mm encased with ISMB 350
8	Size of Beams	R.C.C. structure 300x600 mm
		Composite structure ISMB 350
9	Depth of slab	125 mm thick
10	The specific weight of R.C.C.	25 kN/m^3
11	Zone	V
12	Importance Factor	1
13	Response Reduction Factor	3
14	Type of soil	Medium

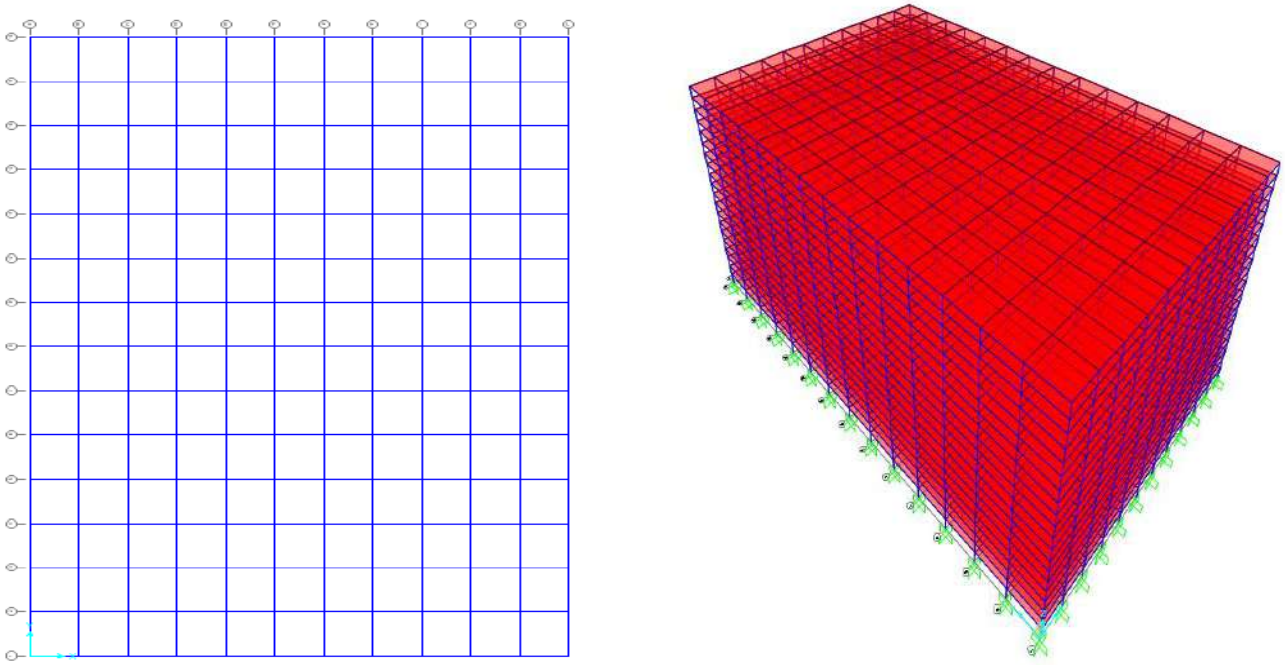

Fig No 1: Typical floor Plan 3D View

4. ANALYSIS RESULTS

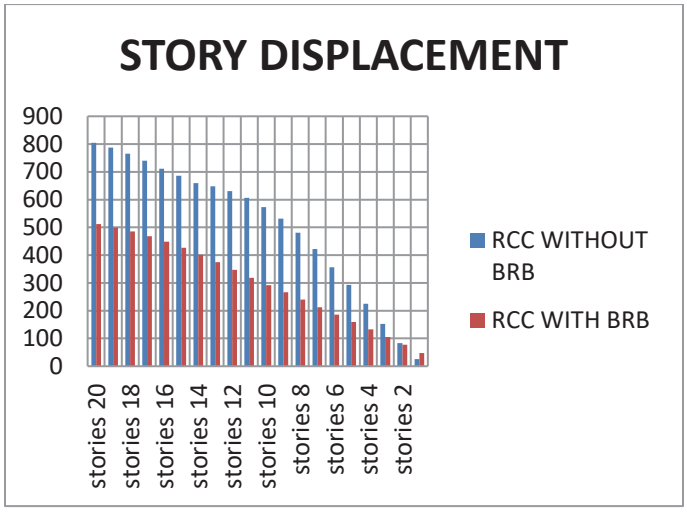

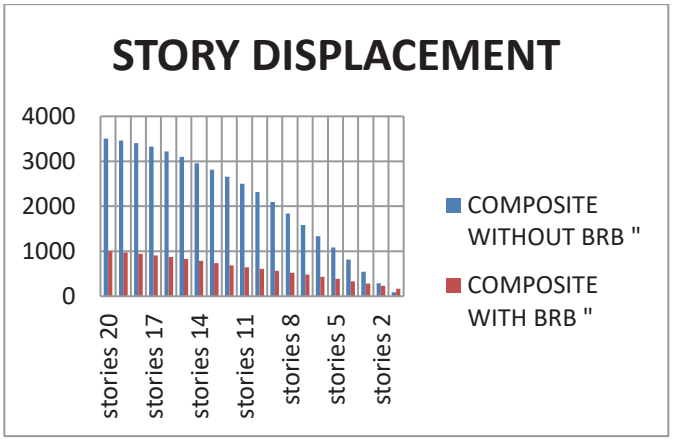

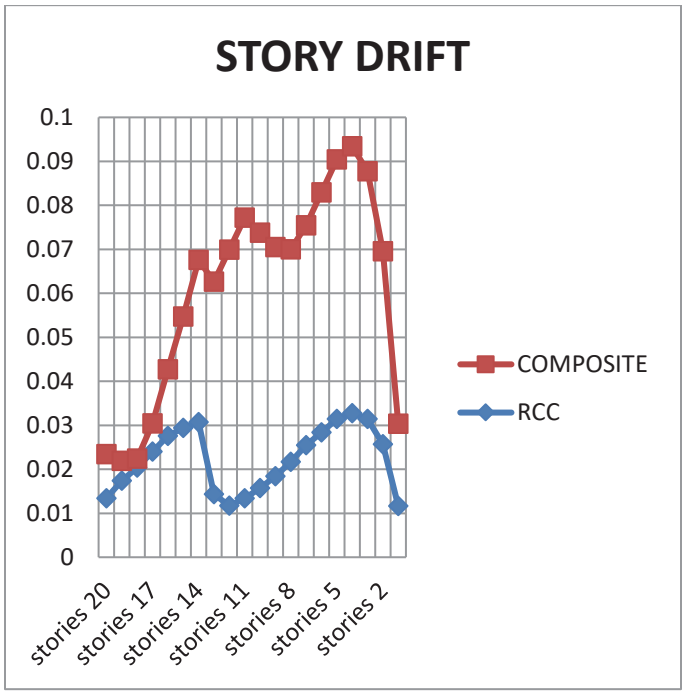

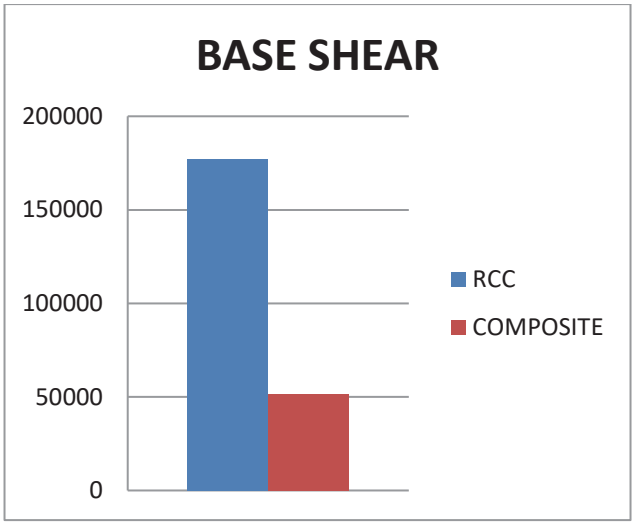

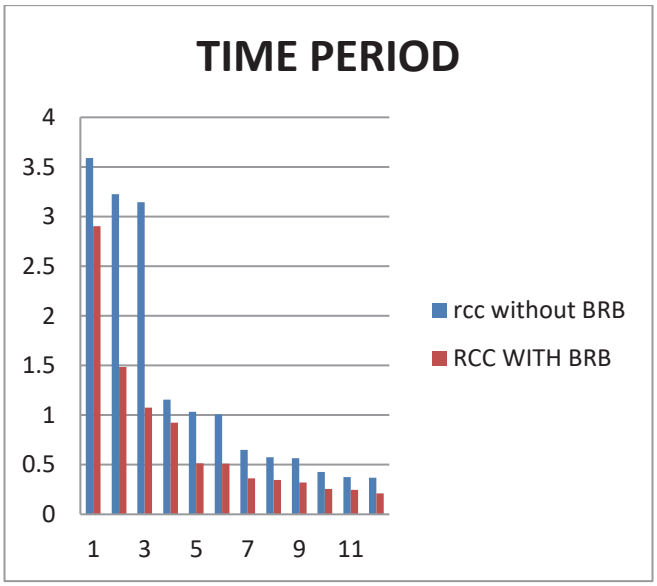

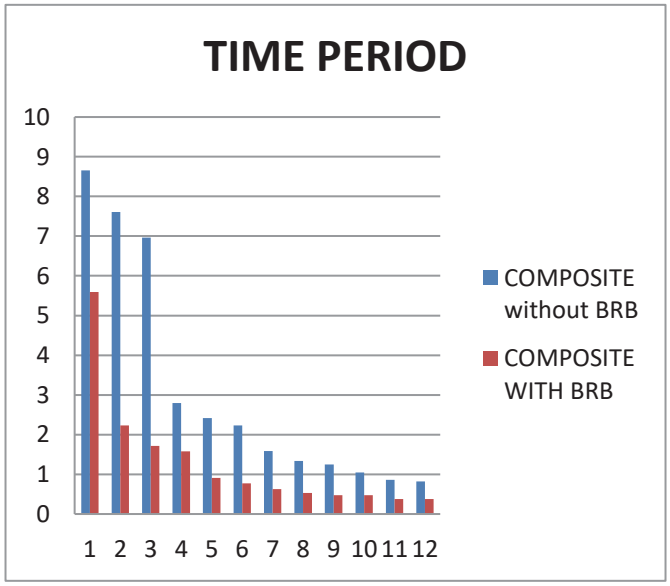

TEMPERATURE LOADING OF TWENTY STOREY RCC AND COMPOSITE SYMMETRIC BUILDING

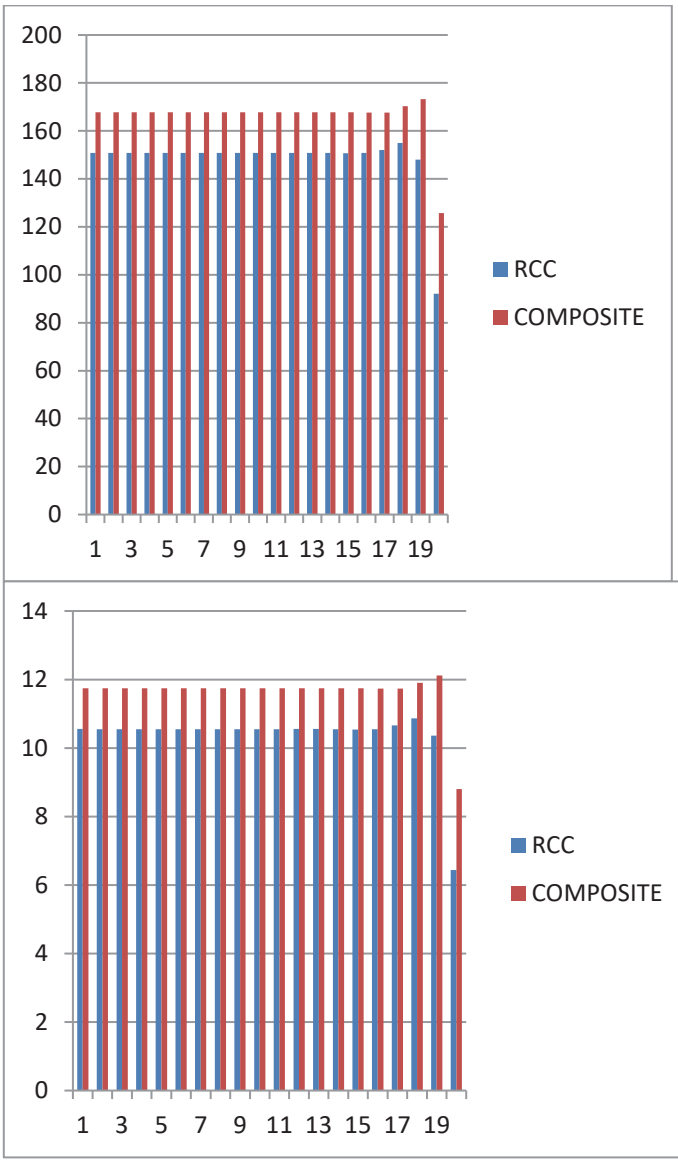

5 CONCLUSIONS

1. The story displacement was decreased by 37% for twenty-story R.C.C. symmetric building and decreased by 70% for twenty-story composite symmetric buildings suggesting the effectiveness of BRB for (both symmetric).
2. The BRB was found to be excellent seismic control devices for twenty-story buildings in controlling forced Responses such as base shear for symmetric buildings and in controlling base shear as well as base torsion moment for symmetric buildings because of the reduction in Base shear by 70% for symmetric Buildings and by reducing the base torsion moment by 52% Respectively.
3. The overall results suggested that BRB were excellent seismic control devices for symmetric composite building as the roof displacement is reduced by 71%, but for Rcc, it is reduced only by 37%. It suggests that they are excellent for a composite structure.
4. Lateral displacement and story drift observed more in symmetric composite building models of a fixed base and BRB building as compared with symmetric R.C.C. building model of fixed and BRB building.
5. The deflection & story drift in a composite structure is nearly double that of R.C.C. Structure, but the deflection is within the permissible limit.
6. The axial force in composite columns is 57% less than R.C.C. columns in non-linear dynamic analysis.
7. The primary direction in composite columns is 40% less than R.C.C. in non-linear dynamic analysis.
8. The maximum displacements of structures generally decrease as the stiffness of BRB increases. The use of low strength steel for BRB, which undergoes more considerable plastic deformation and dissipates more energy, is beneficial for reducing structural damage.
9. The displacement of the Rcc structure is less compared to the composite structure. As the flexibility of the Rcc structure is more than that of the composite structure.

6. SCOPE FOR FURTHER STUDY

1. The research needs regarding composite structures using precast concrete and even pre-stressed concrete in specific applications and steel should also have good market potential due to the economy that can be achieved by saving time, labour, and money.

2. The research needs regarding composite structures for different soil conditions, different zones, different column orientations, and different utility of buildings.

3. Different shapes of highrise buildings can be compared for R.C.C., Steel, and Composite options for better guidelines for selecting the system.

4. Seismic performance under non-linear pushover analysis by considering stiffness irregularity and viscous dampers with BRB.

REFERENCES

1. Kim Sd, Hong Wk, Ju YK "A modified dynamic inelastic analysis of tall buildings considering changes of dynamic characteristics" the structural design of tall Buildings 02/1999.
2. Aiken, I.D., Mahin, S.A., and Uriz, P.R. (2002). "Large-scale testing of buckling restrained braced frames." Proceedings of the Japan Passive Control Symposium, Tokyo Institute of Technology, Japan, December 2002.
3. Black, C. J., Makris, N., and Aiken, I. D. (2004). "Component testing, seismic evaluation, and characterization of buckling-restrained braces." J. of Struct. Eng., 130:6, 880-894.
4. Carr, A. (2004). Ruaumoko Manual. University of Canterbury, New Zealand.

5. Chi, W.-M., Kanvinde, A. M., and Deierlein, G. G. (2006). "Prediction of ductile fracture in steel connections using SMCS criterion." J. of Struct. Eng., 132:2, 171-181.
6. Coy, B. B. (2007). "Buckling-restrained brace connection design and testing." Master's thesis, Brigham Young University, Provo, UT.

7. Christopulos, A. (2006). "Improved Seismic Performance of Buckling Restrained Braced Braces," Master's Thesis, University of Washington, Seattle, WA.

8. Fahnestock, L.A., Ricles, J.M, and Sause, R. (2007). "Experimental evaluation of a large-scale buckling-restrained braced frame," J. of Struct. Eng., 133:9, 1205-1214

9. Asgarian, B., & Amirhesari, N. (2008). Comparing the dynamic non-linear behavior of ordinary and buckling restrained braced frames is subjected to steady ground motion. The structural design of tall and unique buildings, 17, 367–386.

10. Deulkar, W., Modhera, C., & Patil, H. (2010). Buckling Restrained Braces for Vibration Control of Building Structures. IJRRAS 4, 363-372.
11. FEMA-273, NEHRP Guidelines for the Seismic Rehabilitation of Buildings, Federal Emergency Management Agency, Washington DC, U.S.A., 1997.
12. Indian Standard Code of Practice for Earthquake Resistant Design of Structure, I.S. 1893:2000, Bureau of Indian Standards, New Delhi
13. Iwata, M., Kato, T. and Wada, A., Buckling-restrained braces as hysteretic dampers, Behaviour of Steel Structures in Seismic Areas: STESSA 2000, Balkema, 2000, pages 33-38.
14. Ku, W, Non-linear analyses of three-story steel concentrically braced frame building with the application of buckling-restrained (unbounded) brace, Dept. of Civil and environmental engineering, University of California, Berkeley, Calif., 1999.
15. Buckling Restrained Braces Provide the Key to the Seismic Retrofit of the Wallace F. Bennett Federal Building A. Parry Brown, S.E. Ian D. Aiken, Ph.D., P.E. F. Jeff Jafarzadeh, and P.E.
16. Innovative Use OF Buckling Restrained Braces at the University of Auckland. L. Beazley and R. J. Built
17. Behavior and design of structures with buckling-restrainedbracesJinkoo Kim, Hyunhoon Choi
18. Performance-based seismic design and behavior of composite Buckling restrained braced frame Prabuddha Dasgupta, Subhash c. Goel, Gustavo Parra-Montesinos, and k. C. Tsai.

SEISMIC ANALYSIS OF G+30 STOREY BUILDING OF DIFFERENT SHAPES ON VARIOUS SLOPES WITH AND WITHOUT BASE ISOLATION

DR.S. AMARESH BABU
Department of Civil Engineering

NSAKCET, India

MOHAMMED YAHIYA
Department of Civil Engineering

NSAKCET, India

ABSTRACT: The most popular and efficient way of protecting structures from earthquake forces is seismic isolation. Base isolators are standard in many earthquake-prone regions worldwide, like Lead-Rubber bearings (LRB), HDBs, or Friction Pendle Systems (FPS). The study aims to determine that the base isolators can be useful in eliminating structural vibrations. The study's preliminary findings show that Rubber Base isolators' use significantly improves dynamic efficiency during the analyzed building's seismic excitement. The present study is carried out based on base isolators, a building structure of 30-story structures square, L – type, and U- type with the slopy ground (5,10 and 15 degrees)was considered with a fixed and an isolated base. The buildings in the Earth Quake Zone III are analyzed with medium soil following IS 1893-2002. The results are compared.

1. INTRODUCTION

Base isolation has been a viable structural option to decrease a building's vulnerability to damage during an earthquake. It is an advanced practical solution to improve a building's seismic response by minimizing structural damage previously deemed inevitable by strong ground motions. Give this deformable medium a low horizontal rigidity that alters a stiff structure's total duration to a considerably higher level than that of high-energy terrestrial movements.

The present work aims at the study of the following objectives:

- TO study the symmetrical RCC building(square, L, and U- type) resting on slope ground under linear dynamic analysis (response spectrum).
- Comparative study of the building by considering the different slope of ground angle with and without base isolation. To study various responses such as story displacement, inter-story drift, story shear, and time period, etc. of buildings

2 Literature Review

Patel et al. (2014) Studied Three dimensional analytical model of eight storied Buildings using analytical tool ETabs with an asymmetric and asymmetric model to measure column height variation due to steep slopes and the impact of the concrete shear wall at various locations during the earthquake. In the present study, lateral load analysis as per seismic code was performed to study the effect of seismic load and evaluate the seismic vulnerability through pushover analysis.

Sreerama and Ramancharla (2013) Note that more than 375,000 people have been killed, and over 100,000 buildings have been destroyed by recent earthquakes like Bihar-Nepal (1980), the Shillong Plateau, and the Kangra earthquake. The structures are dynamically different from those on the slopes because both vertically and horizontally, the building's geometry differs. This irregularity prevents the center of weight and rigidity from coinciding and produces a torsional response.

Ravikumar et al. (2012) The plan irregularities with geometric and diaphragm inconsistency and vertical irregularity with a reversal and sloped ground were studied in two types of building model irregularities. The Pushover analysis took different lateral load cases to detect seismic demands in all three directions. All considered buildings are three-story buildings with varying patterns of design and irregularities

3 MODELLING PARAMETERS

A G+30 storied reinforced concrete frame building situated in zone III, with base isolation, is taken for study. The building's plan area is 35 m x 35 m, with 3m as each typical story's height. It consists of 7 bays in X-direction and 7 bays in Y-direction. The total heights of the buildings were 103.72 m.

***Model* 1**: square plan model

Model* 2:* L-type plan model

Model* 3:* U- type plan model

S. No.	Specifications	G+30
1	Slab Thickness	150mm
2	Beam dimensions	500X500 mm
		500x500 mm
3	Column dimensions	750x750 mm,
4	Grade of concrete	M30
5	Grade of steel	Fe-550
6	Unit weight of concrete	25kN/m^3
7	Live loads	3kN/m^2
	(a) Floor load	1.5kN/m^2
10	Importance factor	1
11	Seismic zone	III
12	Response reduction factor	3

S. No.	Description	Information
1	Plan size	35mx35m
2	Building heights	103.72m
3	Number of story's above ground level	30
4	Number of basements below ground	0
5	Type of Structure	R.C. frame
6	Open ground story	Yes
7	Ground slope	5,10 and 15 degree
8	Type of Building	Regular frame with open ground story
9	Horizontal floor system	Beams & Slabs
10	Software used	ETABS 2018

Table 1 Data of R.C. Frames considered in the study

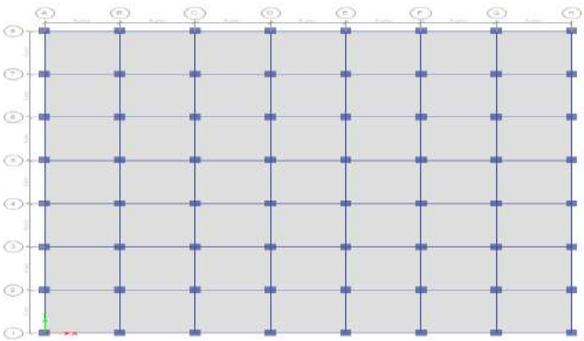

Fig 1: plan view of the square building

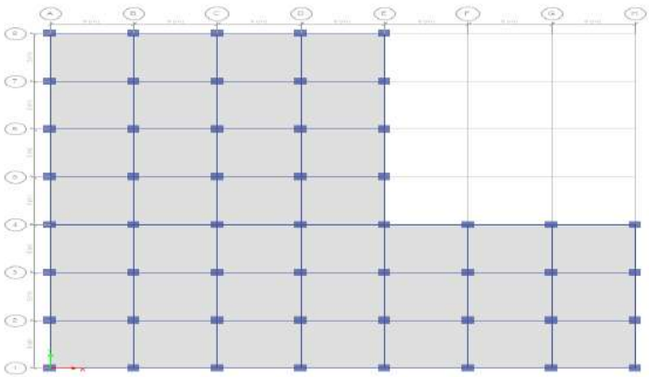

Fig 2 plan view of the L-Type building

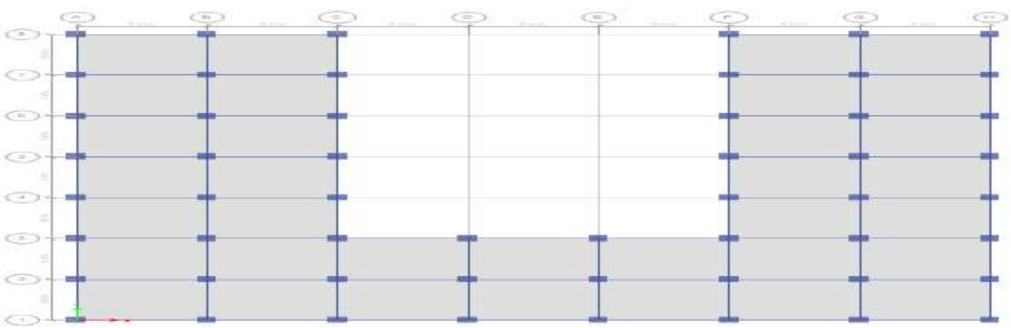

Fig 3 plan view of U-Type Building

4. ANALYSIS RESULTS

The results obtained are of different parameters such as story displacement, Storey drifts, story shear, Modal Periods, etc. The results were obtained by response spectrum Analysis for G+30 Storey Buildings with a ground slope of 5 degrees, 10 degrees, and 15 degrees as listed. Subsequent Discussions are made about the Results Obtained based on the story drifts, story shear, etc. buildings individually and considering the base isolation effect of Symmetric buildings by comparing the structure's responses for 30 story Buildings.

4.1 DISPLACEMENT RESULT OF 30 BUILDING WITH 5 DEGREE SLOPE

STORY DISPLACEMENT						
STORIES	square	L TYPE	U TYPE	SQ WITH ISOLATOR	L TYPE WITH ISOLATOR	U TYPE WITH ISOLATOR
BASE	0	0	0	125.146	129.383	154.954
PLINTH	3.842	6.144	2.866	169.714	164.733	160.17
GROUND	19.503	21.672	15.687	195.917	189.254	181.079
Story1	40.566	41.124	38.741	219.056	210.652	203.104
Story2	63.361	61.792	65.095	240.902	230.765	225.531
Story3	86.505	84.187	92.659	262.048	250.218	247.891
Story4	109.451	108.648	120.545	282.69	269.22	270.159
Story5	131.973	132.8	148.359	302.884	287.832	292.317
Story6	153.985	156.517	175.927	322.642	306.068	314.344
Story7	175.461	179.751	203.177	341.957	323.923	336.221
Story8	196.406	202.491	230.085	360.819	341.385	357.926
Story9	216.827	224.737	256.643	379.21	358.437	379.435
Story10	236.729	246.489	282.848	397.113	375.062	400.723
Story11	256.107	267.74	308.686	414.51	391.239	421.763
Story12	274.946	288.474	334.137	431.379	406.95	442.525
Story13	293.228	308.669	359.174	447.701	422.174	462.979
Story14	310.928	328.299	383.769	463.454	436.889	483.092
Story15	328.023	347.339	407.89	478.618	451.075	502.831
Story16	344.491	365.762	431.503	493.168	464.709	522.16
Story17	360.306	383.54	454.573	507.081	477.769	541.041
Story18	375.44	400.642	477.06	520.334	490.231	559.433
Story19	389.867	417.035	498.92	532.899	502.071	577.295
Story20	403.554	432.684	520.105	544.752	513.265	594.582
Story21	416.47	447.55	540.563	555.864	523.786	611.247
Story22	428.583	461.594	560.24	566.207	533.609	627.242
Story23	439.856	474.774	579.073	575.75	542.705	642.517
Story24	450.247	487.039	596.997	584.463	551.047	657.02
Story25	459.707	498.332	613.933	592.314	558.605	670.699
Story26	468.177	508.589	629.795	599.272	565.352	683.502
Story27	475.595	517.742	644.498	605.311	571.265	695.386
Story28	481.909	525.741	657.975	610.421	576.334	706.33
Story29	487.119	532.588	670.227	614.63	580.585	716.36
Story30	491.373	538.448	681.439	618.079	584.146	725.635

Table 1: story displacement of 30 story building on the 5-degree ground slope with and without base isolation

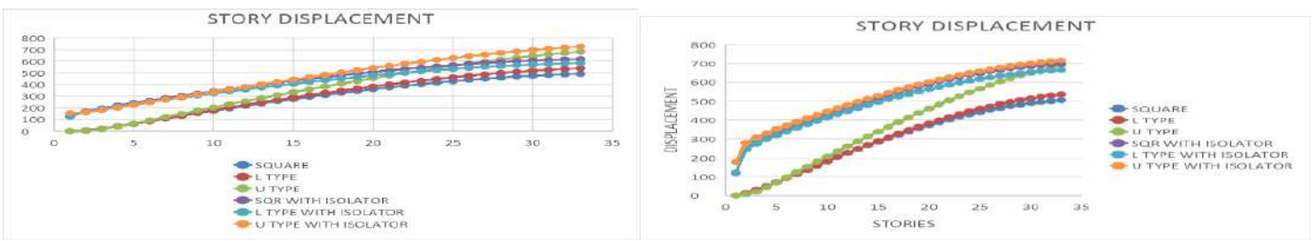

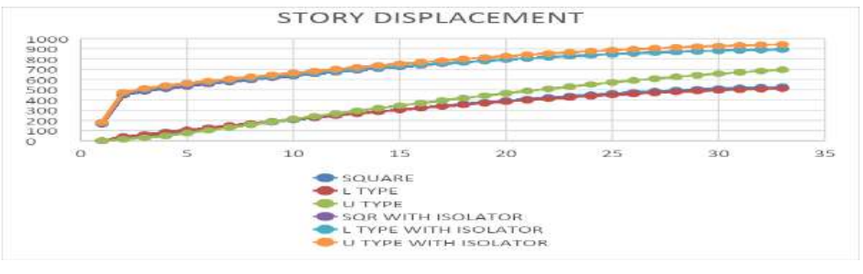

Figure 1: story displacement for square building with and without base isolation at 5,10&15-degree slope ground

4.2 STORY DRIFT RESULT OF 30 BUILDING WITH 5 DEGREE SLOPE

STORY DRIFT						
STORIES	SQUARE	L TYPE	U TYPE	SQR WITH ISOLATOR	L TYPE WITH ISOLATOR	U TYPE WITH ISOLATOR
BASE	0	0	0	0	0	0
PLINTH	0.00203	0.001804	0.002172	0.013241	0.01235	0.010313
GROUND	0.00522	0.005177	0.004869	0.008739	0.008178	0.007489
Story1	0.007022	0.007063	0.007686	0.007728	0.007147	0.007522
Story2	0.007603	0.007914	0.00879	0.007318	0.006738	0.007542
Story3	0.00773	0.008166	0.009205	0.007115	0.006587	0.007564
Story4	0.007687	0.008187	0.009338	0.006984	0.006534	0.007587
Story5	0.007585	0.00812	0.009357	0.006876	0.006479	0.007609
Story6	0.00747	0.008027	0.009337	0.006773	0.006421	0.007627
Story7	0.007359	0.007931	0.009309	0.006669	0.006358	0.007637
Story8	0.007255	0.007839	0.009282	0.006559	0.006288	0.007638
Story9	0.007152	0.007749	0.009255	0.006441	0.006211	0.007628
Story10	0.007044	0.007653	0.009221	0.006316	0.006125	0.007606
Story11	0.006927	0.007548	0.009175	0.006183	0.006031	0.007573
Story12	0.006798	0.007431	0.009117	0.006043	0.005929	0.007526
Story13	0.006658	0.007303	0.009045	0.005894	0.005818	0.007466
Story14	0.006511	0.007166	0.008961	0.005738	0.005699	0.007392
Story15	0.006357	0.00702	0.008866	0.005572	0.00557	0.007303
Story16	0.006196	0.006865	0.008757	0.005396	0.005431	0.007196
Story17	0.006025	0.006699	0.008633	0.00521	0.00528	0.007071
Story18	0.005843	0.00652	0.008489	0.005012	0.005117	0.006927
Story19	0.005649	0.006326	0.008324	0.004802	0.00494	0.006761
Story20	0.005444	0.006117	0.008136	0.004578	0.004748	0.006573
Story21	0.005228	0.005893	0.007925	0.004338	0.004539	0.006361
Story22	0.004997	0.005649	0.007685	0.004082	0.004311	0.006122
Story23	0.004745	0.00538	0.00741	0.003804	0.00406	0.005854
Story24	0.004459	0.005073	0.007088	0.003502	0.003783	0.005554
Story25	0.004122	0.004714	0.006706	0.003173	0.003477	0.00522
Story26	0.003723	0.004293	0.006252	0.002817	0.00314	0.004854
Story27	0.003253	0.003804	0.005725	0.002434	0.002775	0.004459
Story28	0.002721	0.003257	0.005141	0.002034	0.002392	0.004048
Story29	0.002162	0.002692	0.004546	0.001638	0.002013	0.003647
Story30	0.001669	0.002203	0.004043	0.001301	0.001695	0.003317

Table 2: story drift of 30 story building on a 5-degree ground slope with and without base isolation

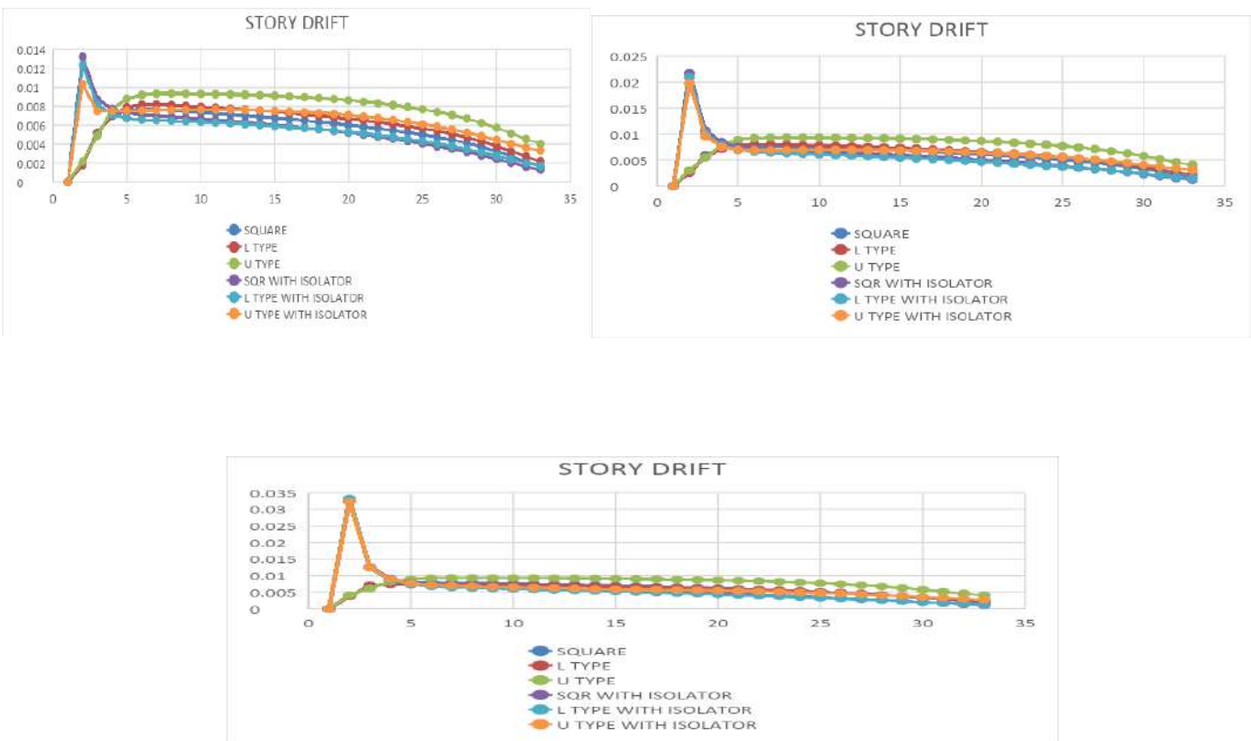

Figure 2: story drift for building's with and without base isolation at 5,10&15-degree slope ground

4.3 TIME PERIOD RESULT OF 30 BUILDING WITH 5 DEGREE SLOPE

TIME PERIOD							
MODES		SQUARE	L TYPE	U TYPE	SQR WITH ISOLATOR	L TYPE WITH ISOLATOR	U TYPE WITH ISOLATOR
Modal	1	2.978	3.037	3.279	3.644	3.712	3.957
Modal	2	2.969	3.009	2.879	3.628	3.671	3.665
Modal	3	2.658	2.727	2.704	3.305	3.397	3.512
Modal	4	0.973	0.987	1.041	1.192	1.22	1.316
Modal	5	0.97	0.978	0.938	1.19	1.205	1.19
Modal	6	0.877	0.896	0.889	1.068	1.101	1.122
Modal	7	0.559	0.56	0.574	0.659	0.662	0.689
Modal	8	0.557	0.557	0.536	0.658	0.66	0.646
Modal	9	0.515	0.521	0.517	0.608	0.617	0.621
Modal	10	0.389	0.389	0.395	0.447	0.448	0.461
Modal	11	0.387	0.387	0.373	0.447	0.447	0.435
Modal	12	0.359	0.363	0.36	0.415	0.419	0.42

Table 3: Time period of 30 story building on the 5-degree ground slope with and without base isolation

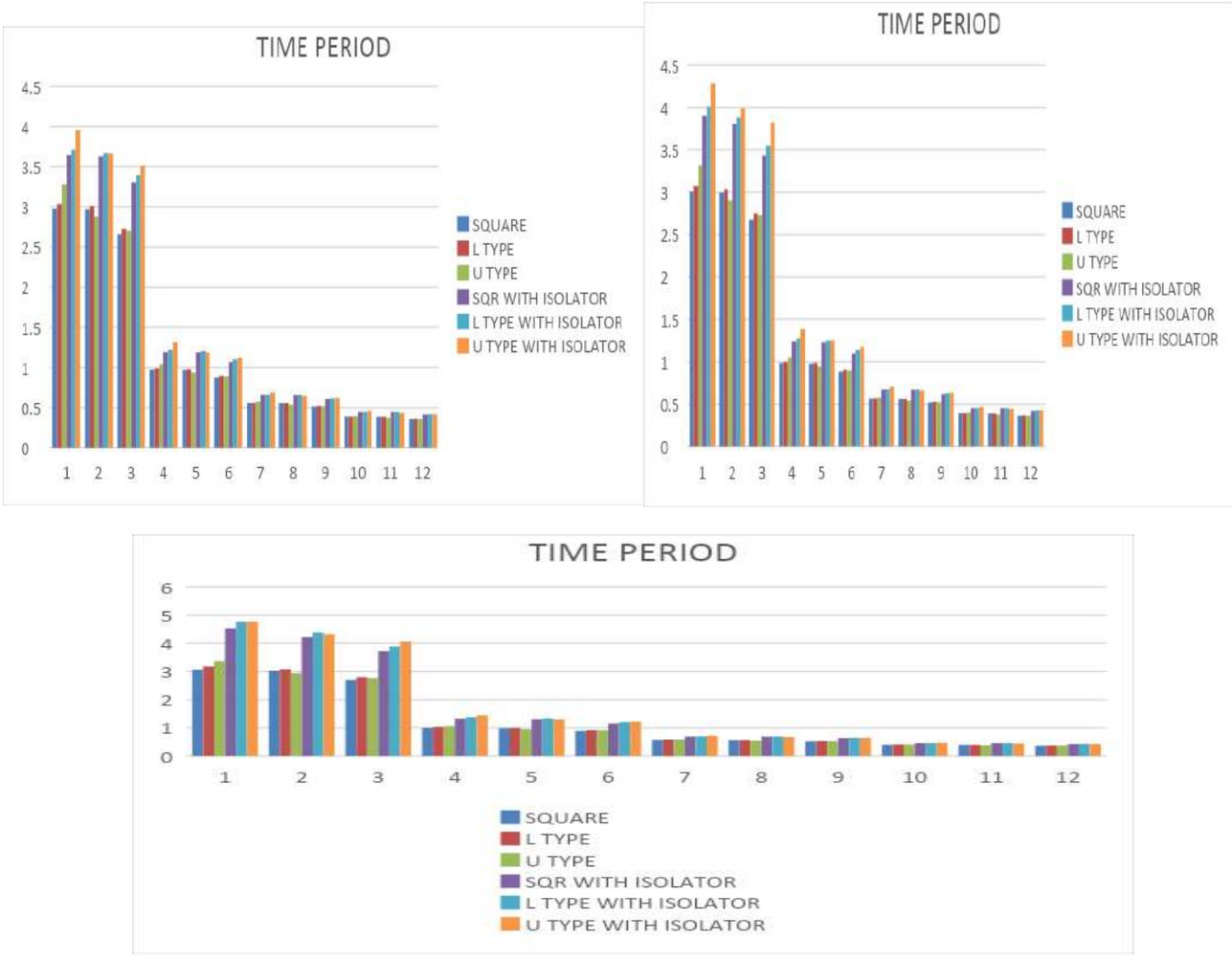

Figure 3: Time period for building's with and without base isolation at 5,10&15-degree slope ground

5 CONCLUSIONS

From analytical results, it is observed that the base isolation technique is very significant to reduce the seismic response of both symmetric as well as asymmetric models as compared to fixed base building and control the damages in the building during firm ground shaking. By comparing the dynamic properties of structures following conclusions are made:

1. It has been observed that maximum shear force, bending moment, story acceleration, and base shear decreases, whereas an increase in lateral displacements was observed for the bottom story then gradually decreases for the base-isolated top story building as compared with the fixed base building model.

2. From an analytical study, it is observed that for both models of symmetric and asymmetric, fixed base building has zero displacements at the base of the structure whereas, base-isolated building models show an appreciable amount of lateral displacements at the bottom. Also, it has been observed that as floor height increases, lateral displacements increase drastically in the fixed-base building as compare to the base-isolated building. Due to this reduction in lateral displacement during earthquake damages of structural as well as non-structural is minimized.

3. At base, more story drift was observed for the base-isolated model as compared to the model of fixed base building. As story height increases, the story drifts in the base-isolated building model drastically decrease compared to the fixed base building model.

4. From the study of symmetric and asymmetric building models, it can be concluded that shear force, bending moment, story drift, and acceleration have not changed appreciably in the asymmetrical building than symmetric building model. Therefore, the symmetrical structure with base isolation remains strong enough during the earthquake compared to asymmetric buildings.
5. In both of the model's fixed base and base-isolated, there is a reduction in bending moment. Thus it will require less reinforcement. Therefore the cost is reduced considerably.
6. Finally, it is concluded that the base isolation system is significantly effective in protecting the structures against moderate and robust earthquake ground motion.

6. SCOPE FOR FURTHER STUDY

- In this study, the only effect of base isolation studies for sloppy ground building with a different slope.
- The effect of base isolation with other energy dissipating devices can be studied.
- Different types of isolation systems can be included in this study, and the effect of this on the sloppy ground can be studied.

REFERENCES

[1] Kilar V. And Koren D., "Usage Of Simplified N2 Method For Analysis Of Base Isolated Structures," The 14th World Conference on Earthquake Engineering, October 12-17, 2008, Beijing, China.

[2] Saiful Islam A. B. M., Jameel M., Ahmad S.I. And Jumaat M. Z., "Study On Corollary of Seismic Base Isolation System On Buildings With Soft Storey," International Journal of the Physical Sciences Vol. 6(11), pp. 2654-2661, 4 June 2011 ISSN1992-1950 ©2011 Academic Journals.

[3] Di Sarno, L., Cosenza, E.and Peace, M.R., "Application Of BaseIsolation To A Large Hospital In Naples, Italy," 10 World Conference on Seismic Isolation, Energy Dissipation and Active Vibrations Control of Structures, Istanbul, Turkey, May 27-30, 2007.

4 Construction Nakashima M., Chusilp P., "A Partial View of Japanese Post-Kobe Seismic

Design and Practices," Disaster Prevention Research Institute, Kyoto University, Uji, Kyoto 611-0011, Japan.

[5] Ramallo J. C., Johnson E. A., Spencer B.F., Jr., And Sain M.K, "Semiactive Building Base Isolation," The 1999 American Control Conference, San Diego, California, June 2–4, 1999.

[6] Ramallo J. C.; Johnson E. A., A. M. Asce; and B. F. Spencer Jr., M.Asce, "Smart Base Isolation Systems," 10.1061/ASCE/0733-9399/2002/128:10/1088.

[7] A. Jalali1 and P. Narjabadifam, "Optimum Modal Characteristics for Multi-Story Buildings Isolated with Lead rubber bearings," 4th International Conference on Earthquake Engineering, Taipei, Taiwan, October 12-13, 2006, Paper No. 187.

[8] Wen P. And Baifeng S., "Two-Step Design Method For Base Isolation Structures," The 14th World Conference on Earthquake Engineering, October 12-17, 2008, Beijing, China.

[9] Pradeep Kumar T. V. And D. K. Paul, "Force-Deformation Behavior of Isolation Bearings," 10.1061/ASCE/1084-0702/2007/12:4/527.

[10] Indian Standard Criteria for Earthquake Resistant Design Structure 1839-2002

[11] Shrikhande M. and Agrawal P., "Earthquake Resistant Design structure," Tata McGraw Hill Publication, 10th Edition 2004.

[12] Duggle S.K., "Earthquake Resistant Design Structure," Tata McGraw Hill Publication, 10th Edition 2004.

[13] Zanaica L., "Design of Storey-Isolation System in multi-story Building" MEEES programmed, May 2007.

DIFFERENTIAL ASSESSMENT OF REGULAR RCC BUILDINGS.

Prof. SYED FARRUKH ANWAR

Department of Civil Engineering

NSAKCET, India

ASIYA

Department of Civil Engineering

NSAKCET, India

ABSTRACT: Lateral rigidity is one of the building's most essential properties, which determines tolerance to displacements under lateral forces and has an immense effect on a structure's natural period. Different stiffness values can eventually influence a structure's action under quake loads and lateral forces that are applied to it. The other parameter for the study is the stiffness modification factor introduced in IS 1893-2016 on the shear wall. In this comparative study on mid-rise (G+10) and high rise (G+30), storied RCC structured framed is considered. Linear analyses evaluate the seismic behaviour of the frame designed by the proposed methodology by considering the Shear wall at a different location and using stiffness modifiers given in IS 1893-2016. Three-Dimensional modelling and analysis of the Structure are carried out with ETABS 2016 software. The core constraints in this study are Lateral displacement, Interstory drift response, Stiffness, periods.

.

1. INTRODUCTION

Shear wall is among the excellent ways to provide quake resistance to multi-storeyed concrete construction. During earthquakes, the Structure remains damaged due to some of the other reasons. Structural inappropriate behaviour during earthquake movement depends on weight distribution, rigidity, and intensity in horizontal and building planes. The vital role that Stiffness of the Structure has in the analysis and design of shear wall-frame structures is the focus of this study. The concentration is mainly on shear walls, and how various parameters can affect the Stiffness of these walls and other design factors explained. Different shear wall distributions in a plan can result in different stiffness values for the same Structure. The effects of shear wall configurations are studied for mid-rise buildings and high rise buildings. The intention is to investigate how cracking can reduce the Stiffness of shear walls and how critical the influence can be in terms of lateral displacements of the Structure

2 Literature Review

S. Zubair and e.tal [2] suggested that multi-story buildings with an open ground floor are inherently susceptible to earthquake load collapse; their construction is still typical in developing countries due to the social and logistical need to have ground-level parking space. The engineering community has sometimes cautioned against these buildings. Along with constructing the gravity load, it has to endure lateral load that can produce high stresses that lead to buildings being demolished. The R.C.C. building is modelled and evaluated in three cases in this case study. I) Platform without a wall of infill (Bare Platform). II) The pattern opens with the tale at the bottom. III) A standard with a base story steel bracing system. ETABS performs complex analyzes of the building models.

Bertero: This proposed dual system could incorporate the advantages of their constituent parts. When needed, ductile frames, interacting with the walls, can provide a considerable amount of energy dispersion, especially in the building's upper stories. On the other hand, strong story-drifts stability can be accomplished during an earthquake due to the broad Stiffness of the walls.

Chandurkar and Pajgade: In this study, the shear wall position and shear wall efficiency solution were studied using four different models. Model one is a basic frame design, and the other three are structural dual-type systems. From the test, it is concluded that the shear wall in the short span at the corner of the building in 10 story building is economical relative to other models with a wide span.

3 MODELLING PARAMETERS

In the model, a reinforced concrete frame building situated in zone II is taken for study. The building's plan area is 30 x 30 m, with 3m as the height of each typical story. It consists of 5 bays in X-direction and 5 bays in Y-direction.

Model 1: RCC building with and without with stiffness modifier without shear wall

Model 2: RCC building with and without with stiffness modifier central shear wall

Model 3: RCC building with and without with stiffness modifier perimeter shear wall

Model 4: RCC building with and without with stiffness modifier intermediate shear wall

S. No.	Specifications	G+10,G+30 storey
1	Slab Thickness	150mm
2	Beam dimensions	
	10 STORIES	230X 450 mm
	30 STORIES	230X 600 mm
3	Column dimensions	230X530 mm, 800X800 mm
4	Grade of concrete	M30
5	Grade of steel	Fe-550
6	Unit weight of concrete	25kN/m^3
7	Live loads (a) Floor load	3kN/m^2 1.5kN/m^2
10	Importance factor	1
11	Seismic zone	II
12	Response reduction factor	3

Element	Moment of inertia
columns	0.7Ig
Beams	.35Ig
wall	0.7Ig

Table 1 Data of R.C. Frames considered in the study

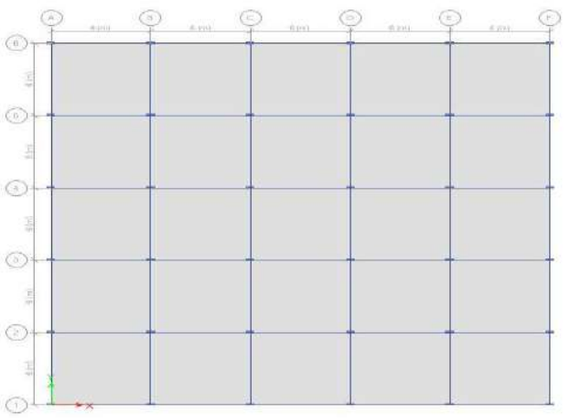

Fig 1: normal building

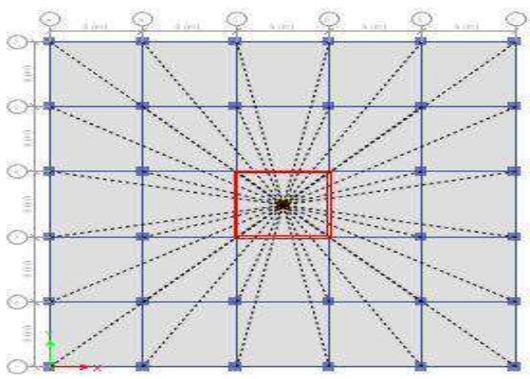

Fig 2: building with shearwall at core

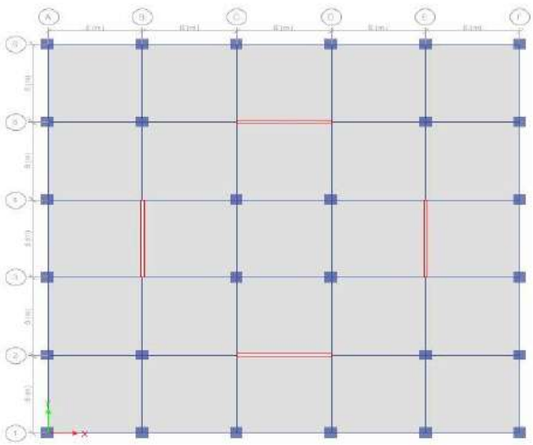

Fig 3 building with shearwall at intermediate position

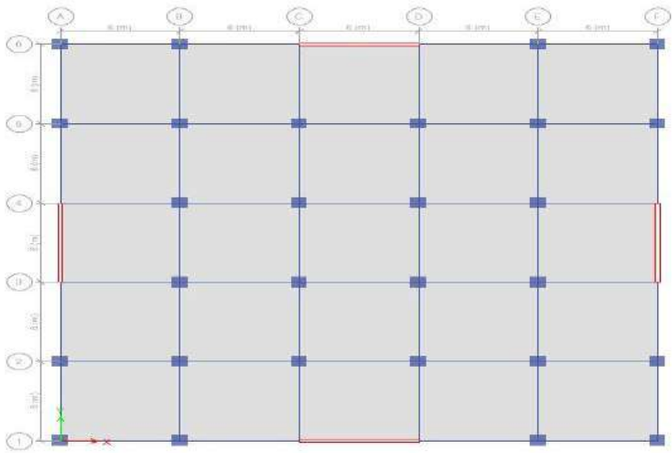

Fig 4 building with shearwall at corner position

4. ANALYSIS RESULTS

The results obtained are of different parameters such as story displacement, Storey drifts, Base shear, Modal Periods, etc. The results were obtained by carrying out by linear static Analysis for G+10, G+30 Storey Buildings, as listed. Subsequent Discussions are made about the Results Obtained based on the story drifts, Base shear, etc.

for Symmetric buildings individually and also considering the Storey effect of Symmetric buildings by comparing the responses of the Structure for 10, 30 story Buildings.

4.1 DISPLACEMENT RESULT OF (G+10) BUILDING

STORY DISPLACEMENT								
	NORMAL		SW CENTER		SW AT PERIMETER		SW AT INTERMEDIATE	
Story	EQX	EQY	EQX	EQY	EQX	EQY	EQX	EQY
Base	0	0	0	0	0	0	0	0
Story1	1.222	2.456	0.274	0.278	0.338	0.349	0.337	0.347
Story2	3.181	5.446	0.801	0.826	1.094	1.165	1.089	1.144
Story3	5.255	8.447	1.529	1.598	2.163	2.348	2.146	2.29
Story4	7.33	11.419	2.423	2.558	3.457	3.813	3.423	3.698
Story5	9.366	14.324	3.445	3.668	4.905	5.485	4.848	5.293
Story6	11.329	17.121	4.561	4.893	6.443	7.297	6.359	7.009
Story7	13.181	19.755	5.741	6.201	8.019	9.189	7.903	8.79
Story8	14.878	22.166	6.956	7.56	9.587	11.114	9.436	10.587
Story9	16.371	24.282	8.181	8.945	11.114	13.03	10.925	12.363
Story10	17.604	26.022	9.395	10.332	12.576	14.91	12.346	14.09
Story11	18.52	27.299	10.585	11.704	13.965	16.739	13.693	15.758
Story12	19.084	28.025	11.731	13.045	15.28	18.516	14.963	17.366

with stiffness modifier								
STORY DISPLACEMENT								
	NORMAL with stiffness modifier		SW CENTER with stiffness modifier		SW AT PERIMETER with stiffness modifier		SW AT INTERMEDIATE with stiffness modifier	
Story	EQX	EQY	EQX	EQY	EQX	EQY	EQX	EQY
Base	0	0	0	0	0	0	0	0
Story1	1.504	2.971	0.275	0.278	0.347	0.358	0.344	0.352
Story2	4.058	6.746	0.821	0.838	1.161	1.222	1.143	1.183
Story3	6.808	10.545	1.59	1.637	2.343	2.498	2.294	2.394
Story4	9.565	14.301	2.545	2.636	3.806	4.103	3.712	3.901
Story5	12.267	17.968	3.648	3.798	5.476	5.961	5.321	5.628
Story6	14.865	21.493	4.865	5.089	7.286	8.003	7.055	7.506
Story7	17.309	24.809	6.163	6.473	9.176	10.167	8.857	9.476
Story8	19.541	27.837	7.512	7.92	11.097	12.399	10.677	11.486
Story9	21.495	30.489	8.885	9.401	13.008	14.654	12.477	13.496
Story10	23.099	32.663	10.258	10.892	14.88	16.898	14.23	15.475
Story11	24.279	34.247	11.616	12.374	16.7	19.111	15.922	17.406
Story12	25	35.132	12.937	13.83	18.458	21.285	17.547	19.285

Table 2: Story Displacement of G+10 building

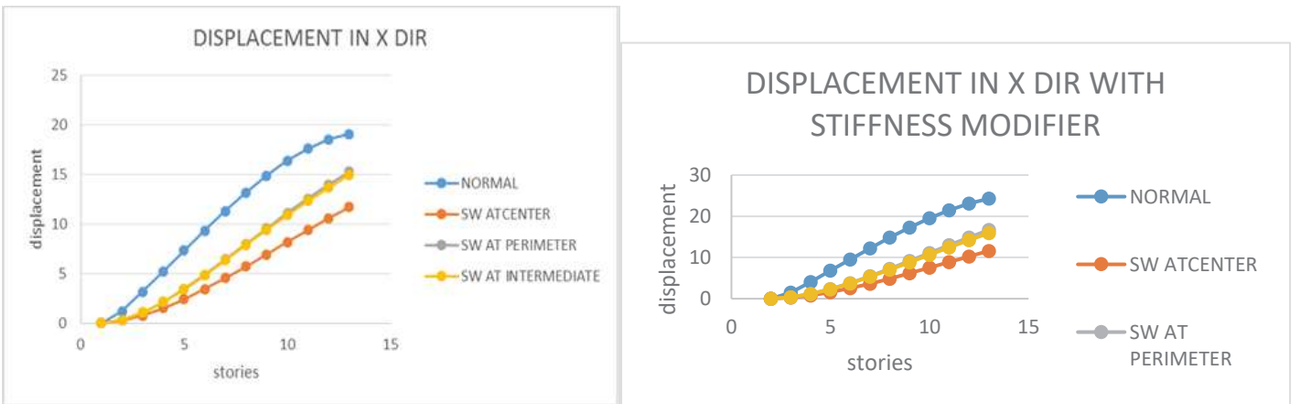

Figure 1: Displacements of G+10 buildings in x dir

4.2 DRIFT RESULTS OF G+10

STORY DRIFT								
	NORMAL		SW CENTER		SW AT PERIMETER		SW AT INTERMEDIATE	
Story	EQX	EQY	EQX	EQY	EQX	EQY	EQX	EQY

Base	0	0	0	0	0	0	0	0
Story1	0.000407	0.000819	9.10E-05	9.30E-05	0.000113	0.000116	0.000112	0.000116
Story2	0.000653	0.000997	0.000176	0.000183	0.000252	0.000272	0.00025	0.000266
Story3	0.000692	0.001001	0.000243	0.000258	0.000356	0.000394	0.000352	0.000382
Story4	0.000692	0.00099	0.000298	0.00032	0.000432	0.000488	0.000426	0.000469
Story5	0.000679	0.000969	0.000341	0.00037	0.000483	0.000557	0.000475	0.000532
Story6	0.000654	0.000932	0.000372	0.000408	0.000513	0.000604	0.000504	0.000572
Story7	0.000617	0.000878	0.000393	0.000436	0.000525	0.000631	0.000515	0.000594
Story8	0.000566	0.000804	0.000405	0.000453	0.000523	0.000641	0.000511	0.000599
Story9	0.000498	0.000705	0.000408	0.000462	0.000509	0.000639	0.000496	0.000592
Story10	0.000411	0.00058	0.000405	0.000462	0.000487	0.000627	0.000474	0.000576
Story11	0.000305	0.000426	0.000397	0.000457	0.000463	0.00061	0.000449	0.000556
Story12	0.000188	0.000242	0.000382	0.000447	0.000438	0.000592	0.000423	0.000536

STORY DRIFT								
	NORMAL with stiffness modifier		SW CENTER with stiffness modifier		SW AT PERIMETER with stiffness modifier		SW AT INTERMEDIATE with stiffness modifier	
Story	EQX	EQY	EQX	EQY	EQX	EQY	EQX	EQY
Base	0	0	0	0	0	0	0	0
Story1	0.000501	0.00099	9.20E-05	9.30E-05	0.000116	0.000119	0.000115	0.000117
Story2	0.000851	0.001259	0.000182	0.000187	0.000272	0.000288	0.000266	0.000277
Story3	0.000917	0.001266	0.000256	0.000266	0.000394	0.000425	0.000384	0.000404
Story4	0.000919	0.001252	0.000318	0.000333	0.000488	0.000535	0.000473	0.000502
Story5	0.0009	0.001223	0.000368	0.000387	0.000557	0.000619	0.000536	0.000576
Story6	0.000866	0.001175	0.000406	0.00043	0.000603	0.000681	0.000578	0.000626
Story7	0.000815	0.001105	0.000433	0.000461	0.00063	0.000721	0.000601	0.000657
Story8	0.000744	0.00101	0.00045	0.000482	0.00064	0.000744	0.000607	0.00067
Story9	0.000651	0.000884	0.000458	0.000494	0.000637	0.000752	0.0006	0.00067
Story10	0.000535	0.000725	0.000458	0.000497	0.000624	0.000748	0.000584	0.000659
Story11	0.000393	0.000528	0.000453	0.000494	0.000607	0.000738	0.000564	0.000644
Story12	0.00024	0.000295	0.00044	0.000485	0.000586	0.000724	0.000541	0.000626

Table 3: Story Drift of G+10 building

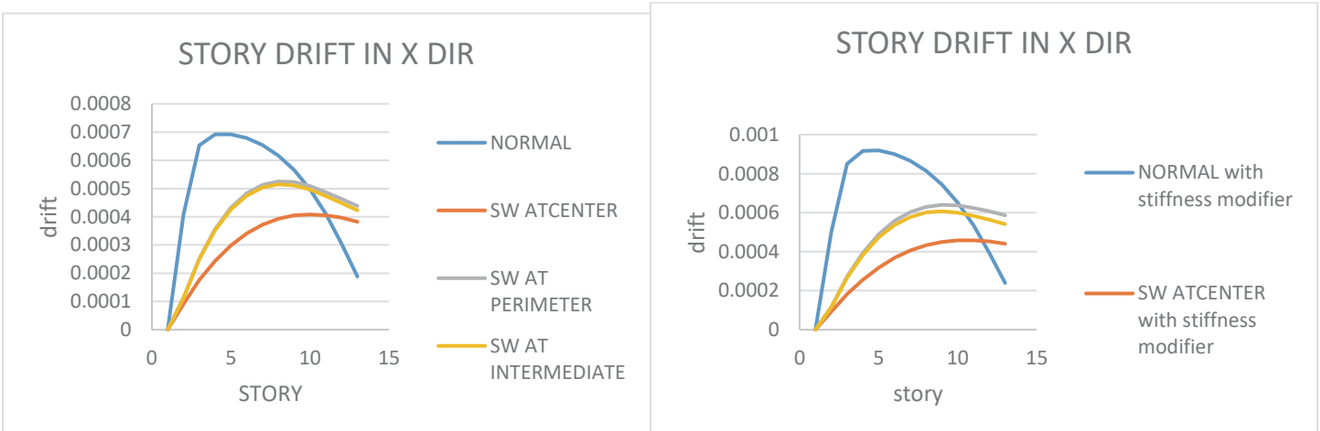

FIGURE 2: Drift of G+10 buildings in x-dir with and without stiffness modifier

4.3 TIME PERIOD RESULTS OF G+10

TIME PERIOD FOR 10 STORY								
MODEL	NORMAL	SW AT CENTER	SW AT PERIMETER	SW AT INTERMEDIATE	NORMAL WITH STIFFNESS MODIFIER	SW ATCENTER WITH STIFFNESS MODIFIER	SW AT PERIMETER WITH STIFFNESS MODIFIER	SW AT INTERMEDIATE WITH STIFFNESS MODIFIER
1	2.76	0.987	1.43	1.355	3.462	1.039	1.614	1.482
2	1.92	0.906	1.216	1.195	2.551	0.98	1.427	1.367
3	1.84	0.901	0.908	1.179	2.411	0.952	1.036	1.355
4	0.918	0.302	0.334	0.327	1.151	0.318	0.35	0.339
5	0.632	0.219	0.308	0.305	0.837	0.223	0.333	0.326
6	0.603	0.212	0.206	0.303	0.787	0.218	0.216	0.324
7	0.547	0.182	0.141	0.14	0.685	0.191	0.144	0.142
8	0.391	0.13	0.136	0.135	0.487	0.137	0.14	0.139
9	0.37	0.102	0.086	0.134	0.487	0.108	0.088	0.138

10	0.349	0.099	0.082	0.082	0.453	0.1	0.083	0.082
11	0.304	0.097	0.08	0.079	0.377	0.099	0.081	0.081
12	0.257	0.084	0.056	0.079	0.334	0.089	0.057	0.08

Table 4: time period of G+10 building

4.4 STORY STIFFNESS RESULTS OF G+10

STORY STIFFNESS								
	NORMAL		SW CENTER		SW AT PERIMETER		SW AT INTERMEDIATE	
Story	EQX	EQY	EQX	EQY	EQX	EQY	EQX	EQY
Base	0	0	0	0	0	0	0	0
Story1	552049.9	183039	5312244	4780507	3172258	2605998	3234037	2770997
Story2	343804.9	150133	2755583	2416832	1413165	1113578	1449497	1203842
Story3	322607.9	148607.2	1980632	1704153	994717.8	763368.9	1023837	832863.7
Story4	317942.4	148011.7	1592317	1352381	809093.1	607602.4	835045.3	668003.9
Story5	315901.2	147518.7	1356576	1139507	705067.1	518944	729432.9	574596
Story6	314344.2	147048.4	1190692	990039.2	636456.6	459316.4	659944.9	512123.2
Story7	312833.5	146562.3	1057450	870621.3	583272	412568.6	606170.3	463264.9
Story8	311132.3	146000.6	935389.1	762571.5	533685	369604.7	555971.2	418099
Story9	308893.4	145257.7	808977.3	652954	478127.6	323734.2	499416.5	369079.7
Story10	305227.9	144097.4	664513.1	530887.8	406700.6	268830.5	426075.3	308996.4
Story11	296706	141849.8	487290.3	385727.8	307647.2	198630.2	323356.4	230153.3
Story12	257331.9	133352.1	266336.4	207449	171392	107756.5	180659	125772.8

Table 5: Story Stiffness of G+10 building

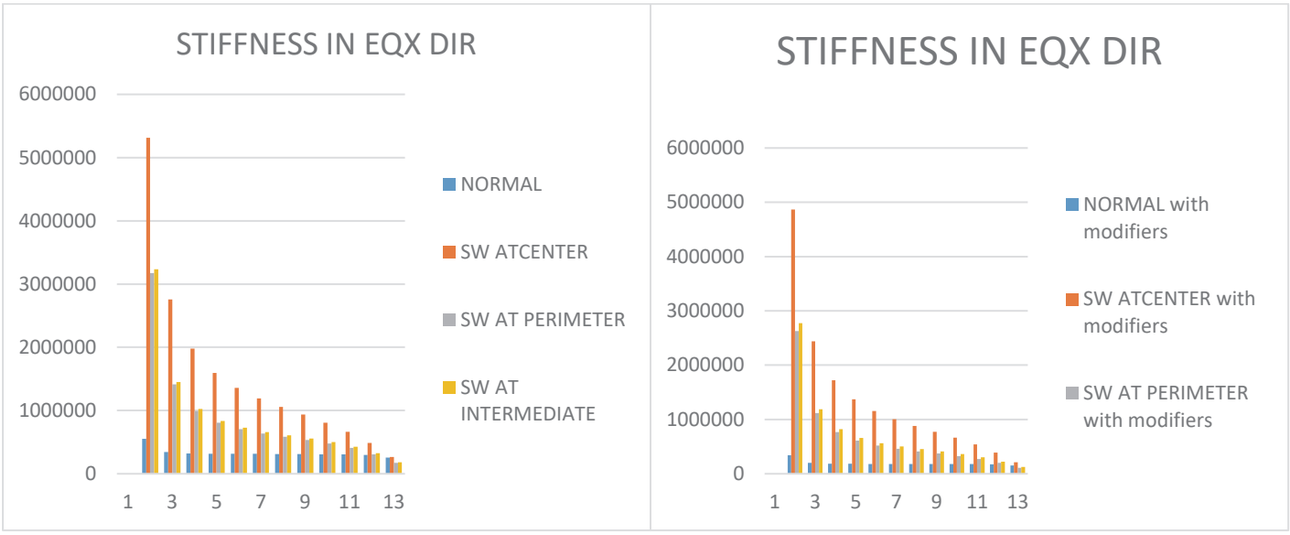

FIGURE 3: stiffness of G+10 buildings in x-dir with and without stiffness modifier

5.1 DISPLACEMENT RESULT OF (G+10) BUILDING

STORY DISPLACEMENT								
	NORMAL		SW CENTER		SW AT PERIMETER		SW AT INTERMEDIATE	
Story	EQX	EQY	EQX	EQY	EQX	EQY	EQX	EQY
Base	0	0	0	0	0	0	0	0
Story1	0.5	0.5	0.229	0.229	0.289	0.289	0.29	0.29
Story2	1.578	1.578	0.712	0.712	0.94	0.94	0.943	0.943
Story3	2.917	2.917	1.376	1.376	1.838	1.838	1.843	1.843
Story4	4.375	4.375	2.195	2.195	2.917	2.917	2.925	2.925
Story5	5.892	5.892	3.143	3.143	4.127	4.127	4.14	4.14
Story6	7.438	7.438	4.199	4.199	5.433	5.433	5.45	5.45
Story7	8.999	8.999	5.343	5.343	6.808	6.808	6.829	6.829
Story8	10.568	10.568	6.56	6.56	8.232	8.232	8.257	8.257
Story9	12.141	12.141	7.836	7.836	9.688	9.688	9.718	9.718
Story10	13.712	13.712	9.158	9.158	11.165	11.165	11.201	11.201
Story11	15.279	15.279	10.515	10.515	12.653	12.653	12.694	12.694
Story12	16.838	16.838	11.897	11.897	14.143	14.143	14.19	14.19
Story13	18.385	18.385	13.294	13.294	15.629	15.629	15.683	15.683
Story14	19.916	19.916	14.698	14.698	17.105	17.105	17.164	17.164
Story15	21.427	21.427	16.102	16.102	18.564	18.564	18.63	18.63
Story16	22.914	22.914	17.499	17.499	20	20	20.073	20.073

Story17	24.372	24.372	18.881	18.881	21.409	21.409	21.489	21.489
Story18	25.795	25.795	20.243	20.243	22.786	22.786	22.873	22.873
Story19	27.179	27.179	21.579	21.579	24.124	24.124	24.218	24.218
Story20	28.519	28.519	22.884	22.884	25.418	25.418	25.52	25.52
Story21	29.808	29.808	24.153	24.153	26.664	26.664	26.773	26.773
Story22	31.041	31.041	25.381	25.381	27.856	27.856	27.972	27.972
Story23	32.211	32.211	26.565	26.565	28.99	28.99	29.113	29.113
Story24	33.313	33.313	27.702	27.702	30.06	30.06	30.19	30.19
Story25	34.34	34.34	28.788	28.788	31.062	31.062	31.2	31.2
Story26	35.284	35.284	29.823	29.823	31.993	31.993	32.138	32.138
Story27	36.141	36.141	30.806	30.806	32.85	32.85	33.003	33.003
Story28	36.902	36.902	31.737	31.737	33.632	33.632	33.792	33.792
Story29	37.563	37.563	32.619	32.619	34.341	34.341	34.509	34.509
Story30	38.121	38.121	33.456	33.456	34.981	34.981	35.156	35.156
Story31	38.579	38.579	34.253	34.253	35.562	35.562	35.744	35.744
Story32	38.952	38.952	35.005	35.005	36.091	36.091	36.281	36.281

STORY DISPLACEMENT								
	NORMAL stiffness modifier		SW CENTER stiffness modifier		SW AT PERIMETER stiffness modifier		SW AT INTERMEDIATE stiffness modifier	
Story	EQX	EQY	EQX	EQY	EQX	EQY	EQX	EQY
Base	0	0	0	0	0	0	0	0
Story1	0.803	0.803	0.232	0.232	0.33	0.33	0.326	0.326
Story2	2.642	2.642	0.747	0.747	1.122	1.122	1.105	1.105
Story3	5.016	5.016	1.487	1.487	2.267	2.267	2.227	2.227
Story4	7.669	7.669	2.425	2.425	3.693	3.693	3.623	3.623
Story5	10.468	10.468	3.536	3.536	5.34	5.34	5.232	5.232
Story6	13.341	13.341	4.797	4.797	7.161	7.161	7.009	7.009
Story7	16.252	16.252	6.187	6.187	9.116	9.116	8.914	8.914
Story8	19.178	19.178	7.688	7.688	11.173	11.173	10.916	10.916
Story9	22.106	22.106	9.282	9.282	13.306	13.306	12.991	12.991
Story10	25.026	25.026	10.953	10.953	15.493	15.493	15.116	15.116
Story11	27.93	27.93	12.687	12.687	17.714	17.714	17.273	17.273
Story12	30.811	30.811	14.47	14.47	19.954	19.954	19.447	19.447
Story13	33.661	33.661	16.29	16.29	22.197	22.197	21.624	21.624
Story14	36.475	36.475	18.135	18.135	24.432	24.432	23.792	23.792
Story15	39.242	39.242	19.994	19.994	26.647	26.647	25.939	25.939
Story16	41.957	41.957	21.858	21.858	28.83	28.83	28.057	28.057
Story17	44.61	44.61	23.717	23.717	30.973	30.973	30.134	30.134
Story18	47.192	47.192	25.563	25.563	33.066	33.066	32.163	32.163
Story19	49.693	49.693	27.387	27.387	35.1	35.1	34.134	34.134
Story20	52.104	52.104	29.184	29.184	37.066	37.066	36.041	36.041
Story21	54.415	54.415	30.945	30.945	38.959	38.959	37.875	37.875
Story22	56.614	56.614	32.666	32.666	40.769	40.769	39.629	39.629
Story23	58.69	58.69	34.342	34.342	42.491	42.491	41.298	41.298
Story24	60.631	60.631	35.969	35.969	44.119	44.119	42.875	42.875
Story25	62.425	62.425	37.544	37.544	45.649	45.649	44.356	44.356
Story26	64.061	64.061	39.066	39.066	47.077	47.077	45.739	45.739
Story27	65.527	65.527	40.534	40.534	48.404	48.404	47.023	47.023
Story28	66.813	66.813	41.95	41.95	49.63	49.63	48.208	48.208
Story29	67.911	67.911	43.315	43.315	50.761	50.761	49.299	49.299
Story30	68.819	68.819	44.636	44.636	51.804	51.804	50.305	50.305
Story31	69.55	69.55	45.919	45.919	52.775	52.775	51.241	51.241
Story32	70.138	70.138	47.155	47.155	53.685	53.685	52.117	52.117

Table 6: Story Displacement of G+30 building

5.2 DRIFT RESULT OF (G+30) BUILDING

STORY DRIFT								
	NORMAL		SW CENTER		SW AT PERIMETER		SW AT INTERMEDIATE	
Story	EQX	EQY	EQX	EQY	EQX	EQY	EQX	EQY
Base	0	0	0	0	0	0	0	0
Story1	0.000167	0.000167	7.60E-05	7.60E-05	9.60E-05	9.60E-05	9.70E-05	9.70E-05
Story2	0.000359	0.000359	0.000161	0.000161	0.000217	0.000217	0.000218	0.000218

Story3	0.000446	0.000446	0.000222	0.000222	0.000299	0.000299	0.0003	0.0003
Story4	0.000486	0.000486	0.000273	0.000273	0.00036	0.00036	0.000361	0.000361
Story5	0.000506	0.000506	0.000316	0.000316	0.000404	0.000404	0.000405	0.000405
Story6	0.000515	0.000515	0.000352	0.000352	0.000435	0.000435	0.000437	0.000437
Story7	0.00052	0.00052	0.000382	0.000382	0.000458	0.000458	0.00046	0.00046
Story8	0.000523	0.000523	0.000406	0.000406	0.000474	0.000474	0.000476	0.000476
Story9	0.000524	0.000524	0.000425	0.000425	0.000485	0.000485	0.000487	0.000487
Story10	0.000524	0.000524	0.000441	0.000441	0.000492	0.000492	0.000494	0.000494
Story11	0.000522	0.000522	0.000452	0.000452	0.000496	0.000496	0.000498	0.000498
Story12	0.00052	0.00052	0.000461	0.000461	0.000497	0.000497	0.000499	0.000499
Story13	0.000516	0.000516	0.000466	0.000466	0.000495	0.000495	0.000497	0.000497
Story14	0.00051	0.00051	0.000468	0.000468	0.000492	0.000492	0.000494	0.000494
Story15	0.000504	0.000504	0.000468	0.000468	0.000486	0.000486	0.000488	0.000488
Story16	0.000496	0.000496	0.000465	0.000465	0.000479	0.000479	0.000481	0.000481
Story17	0.000486	0.000486	0.000461	0.000461	0.00047	0.00047	0.000472	0.000472
Story18	0.000474	0.000474	0.000454	0.000454	0.000459	0.000459	0.000461	0.000461
Story19	0.000461	0.000461	0.000445	0.000445	0.000446	0.000446	0.000448	0.000448
Story20	0.000446	0.000446	0.000435	0.000435	0.000432	0.000432	0.000434	0.000434
Story21	0.00043	0.00043	0.000423	0.000423	0.000415	0.000415	0.000418	0.000418
Story22	0.000411	0.000411	0.000409	0.000409	0.000397	0.000397	0.0004	0.0004
Story23	0.00039	0.00039	0.000395	0.000395	0.000378	0.000378	0.00038	0.00038
Story24	0.000367	0.000367	0.000379	0.000379	0.000357	0.000357	0.000359	0.000359
Story25	0.000342	0.000342	0.000362	0.000362	0.000334	0.000334	0.000337	0.000337
Story26	0.000315	0.000315	0.000345	0.000345	0.00031	0.00031	0.000313	0.000313
Story27	0.000285	0.000285	0.000328	0.000328	0.000286	0.000286	0.000288	0.000288
Story28	0.000254	0.000254	0.00031	0.00031	0.000261	0.000261	0.000263	0.000263
Story29	0.00022	0.00022	0.000294	0.000294	0.000236	0.000236	0.000239	0.000239
Story30	0.000186	0.000186	0.000279	0.000279	0.000213	0.000213	0.000216	0.000216
Story31	0.000152	0.000152	0.000266	0.000266	0.000193	0.000193	0.000196	0.000196
Story32	0.000125	0.000125	0.000251	0.000251	0.000176	0.000176	0.000179	0.000179

STORY DRIFT								
	NORMAL with stiffness modifier		SW CENTER with stiffness modifier		SW AT PERIMETER with stiffness modifier		SW AT INTERMEDIATE with stiffness modifier	
Story	EQX	EQY	EQX	EQY	EQX	EQY	EQX	EQY
Base	0	0	0	0	0	0	0	0
Story1	0.000268	0.000268	7.70E-05	7.70E-05	0.00011	0.00011	0.000109	0.000109
Story2	0.000613	0.000613	0.000172	0.000172	0.000264	0.000264	0.00026	0.00026
Story3	0.000791	0.000791	0.000247	0.000247	0.000382	0.000382	0.000374	0.000374
Story4	0.000884	0.000884	0.000313	0.000313	0.000475	0.000475	0.000465	0.000465
Story5	0.000933	0.000933	0.00037	0.00037	0.000549	0.000549	0.000536	0.000536
Story6	0.000958	0.000958	0.00042	0.00042	0.000607	0.000607	0.000592	0.000592
Story7	0.00097	0.00097	0.000463	0.000463	0.000652	0.000652	0.000635	0.000635
Story8	0.000975	0.000975	0.0005	0.0005	0.000686	0.000686	0.000668	0.000668
Story9	0.000976	0.000976	0.000531	0.000531	0.000711	0.000711	0.000692	0.000692
Story10	0.000973	0.000973	0.000557	0.000557	0.000729	0.000729	0.000708	0.000708
Story11	0.000968	0.000968	0.000578	0.000578	0.00074	0.00074	0.000719	0.000719
Story12	0.00096	0.00096	0.000594	0.000594	0.000747	0.000747	0.000725	0.000725
Story13	0.00095	0.00095	0.000607	0.000607	0.000748	0.000748	0.000726	0.000726
Story14	0.000938	0.000938	0.000615	0.000615	0.000745	0.000745	0.000723	0.000723
Story15	0.000923	0.000923	0.00062	0.00062	0.000738	0.000738	0.000716	0.000716
Story16	0.000905	0.000905	0.000621	0.000621	0.000728	0.000728	0.000706	0.000706
Story17	0.000884	0.000884	0.00062	0.00062	0.000714	0.000714	0.000692	0.000692
Story18	0.000861	0.000861	0.000615	0.000615	0.000698	0.000698	0.000676	0.000676
Story19	0.000834	0.000834	0.000608	0.000608	0.000678	0.000678	0.000657	0.000657
Story20	0.000804	0.000804	0.000599	0.000599	0.000656	0.000656	0.000636	0.000636
Story21	0.00077	0.00077	0.000587	0.000587	0.000631	0.000631	0.000611	0.000611
Story22	0.000733	0.000733	0.000574	0.000574	0.000603	0.000603	0.000585	0.000585
Story23	0.000692	0.000692	0.000559	0.000559	0.000574	0.000574	0.000556	0.000556
Story24	0.000647	0.000647	0.000542	0.000542	0.000543	0.000543	0.000526	0.000526
Story25	0.000598	0.000598	0.000525	0.000525	0.00051	0.00051	0.000494	0.000494
Story26	0.000545	0.000545	0.000507	0.000507	0.000476	0.000476	0.000461	0.000461
Story27	0.000489	0.000489	0.000489	0.000489	0.000442	0.000442	0.000428	0.000428
Story28	0.000429	0.000429	0.000472	0.000472	0.000409	0.000409	0.000395	0.000395
Story29	0.000366	0.000366	0.000455	0.000455	0.000377	0.000377	0.000364	0.000364

Story30	0.000303	0.000303	0.00044	0.00044	0.000348	0.000348	0.000335	0.000335
Story31	0.000244	0.000244	0.000428	0.000428	0.000324	0.000324	0.000312	0.000312
Story32	0.000196	0.000196	0.000412	0.000412	0.000303	0.000303	0.000292	0.000292

Table 7: Story Drift of G+30 building

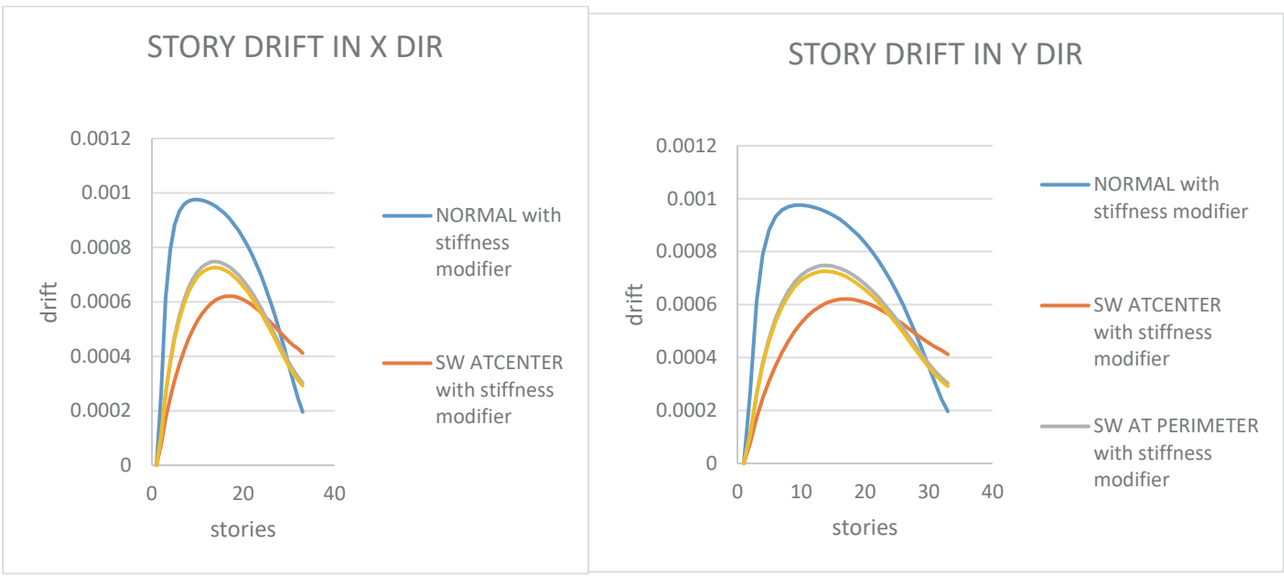

FIGURE 3: Drift of G+30 buildings in x-dir with and without stiffness modifier

6 CONCLUSIONS

Based on the findings of the study, on overall view, the aim of the study has been achieved, and the conclusions for each objective which can be drawn out are as follows;

- Results of study of multiple models undertaken for medium and high-rise buildings usually followed the same trend. All models had a comparatively higher rigidity with a central core and, as a result, less displacement and shorter natural time. A common practice among engineers is to achieve the most effective wall distribution around the plane's perimeter in resisting torsion if significant torsional moments are generated for some purpose.
- The explanation is that the torsion resisted by a wall has been associated with its lateral rigidity, compounded by the distance from the mass center, so that the more distant the shear wall from the mass core, the further it will resist torsion.
- On the basis of the theoretical findings in this analysis, therefore, it can be inferred that if the structure is symmetrical and where the centre of mass is not far from the centre of rigidity (in other words, no major torsion exists in the structure), the shear walls do not have to be positioned in the circumference of the plan. If a priority is to minimize lateral displacements and improve rigidity with the same number of shear walls, it will be a more effective architecture if the system considers a central concrete centre.
- This central core action and its effectiveness in minimizing lateral shifts are more effective in high-height towers since these towers typically encounter considerably greater lateral load and have restrictions on lateral shifts.
- Based on the results of analyses, the rigidity of a structure can be greatly affected by cracked parts of a concrete product. The study revealed that a single round of inspection cannot reach the entire number of broken elements in a shear wall, and that a more reliable method-need more runs. Owing to the transfer of loads, cracked elements move further loads to neighbouring elements at each point of the study (which have not yet been cracked and have a moment of inertia greater than cracked elements). Extra load passed to uncracked elements may help to raise the stress above the rupture value, meaning an element which was not cracked during the first test round could fracture in the second round. Results demonstrate that this form of analysis inevitably stabilizes and that the number of cracked products converges. Once this is done, further analyses are not mandatory and no new cracked elements will be possible.

REFERENCES

1. **Bertero, V.V**. (1980). "Seismic Behavior of Reinforced Concrete Wall Structural Systems". Proceedings of 7th world conference on Earthquake Engineering, Istanbul, Vol. 6, 323-330.

2. **Sudarshan Brahma, R and Kaustubh Dasgupta**, "Influence of structural wall area ratio on seismic design of reinforced concrete wall-frame building", International Journal of Earth Science and Engineering, ISSN 0974-5904, Volume 04, No.06 SPL, 2011, Pages 560-564.

3. **Romy, M, and Prabha, C** (2011), "Dynamic Analysis of RCC Buildings with Shear Wall", International Journal of Earth Sciences and Engineering, ISSN 0974- 5904, Vol. 4, No. 6 SPL, pp. 659-662.

4. **AL-Mekhlafy, N (2013),** "Some parameters affecting the behavior of RC frames designed for gravity loads only and subjected to Earthquakes", Journal of Engineering Sciences, Vol. 42, No. 01, pp. 93-111.

5. **Satpute, S.G, and Kulkarni, D.B**(2013), "Comparative Study of Reinforced Concrete Shear Wall Analysis in Multistoried Building with Openings by Nonlinear Methods", International Journal of Structural and Civil Engineering Research, ISSN 2319-6009, Volume 02, No.03.

6. **Patil, A.S and Kumbhar, P.D**(2013), "Time History Analysis of Multistoried RCC Buildings for Different Seismic intensities", International Journal of Structural and Civil Engineering Research, ISSN 2319-6009, Volume 02, No.03.

7. **Chandurkar, P.P, and Pajgade, P.S** (2013), "Seismic Analysis of RCC Buildings with and without Shear Wall", International Journal of Modern Engineering Research, ISSN 2249- 6645, Vol. 3, pp. 1805-1810.

8. **Anshul Sud, Raghav Singh Shekhawat and Poonam Dhiman** (2014), "Best Placement of Shear wall in an RCC space frame Based on Seismic Response", International Journal of Engineering Research and Applications, ISSN 2248- 9622, pp. 38-35.

9. **ASCE** (2007). Seismic Rehabilitation of Existing Buildings, ASCE/SEI 41-06, American Society of Civil Engineering, Virginia, USA.

10. **Applied Technology Council**. (1996). Seismic Evaluation and Retrofit of Concrete Buildings. ATC-40 Volume 1-2. Redwood City. California.

11. **Oesterle, R.G, Aristizabal-Ochoa, J.D., Fiorato, A. E., Russel, H.G., and Corley, W.G.** (1979). Earthquake Resistant Structural Walls-Test of Isolated Walls – Phase2, Construction Technology Laboratory/National Science Foundation, Washington D.C.

12. **IS 13920-1993** "Code of Practice for ductile detailing of reinforced concrete structures subjected to seismic forces", Bureau of Indian Standards, New Delhi.

13. **Paulay T, and Priestely M.J.N**. (1992). Seismic Design of Reinforced concrete & Masonry Buildings. A Wiley Interscience Publication, New York, USA.

14. **Farrukh Anwar, A. K. Asthana** Evaluation of Seismic Design Forces of Indian Building Code. An International Journal of Engineering Research & Technology (IJERT) ISSN: 2278-0181 Vol. 2 Issue 6, June – 2013

15. **Mahesh N. Patil, Yogesh N. Sonawane** Seismic Analysis of Multistore Building International Journal of Engineering and Innovative Technology (IJEIT) Volume 4, Issue 9, March 2015

16. **FEMA**, NEHRP guidelines for the "Seismic Rehabilitation of Buildings" (FEMA 273). Washington (DC): Building Seismic Safety Council; 1997.

17. **IS 1893 Part 1** (2002)," Indian Standard Criteria for Earthquake Resistant Design of Structures", Bureau of Indian Standards, New Delhi.

18. **IS 875: Part 1**, (1987). Code of practice for design loads (other than earthquake) for buildings and structures Part 1 Dead loads - Unit weights of building material, Bureau of Indian Standards, New Delhi.

19. **IS 875: Part 2**, (1987). Code of practice for design loads (other than earthquake) for buildings and structures: Part 2 Imposed loads, Bureau of Indian Standards, New Delhi.

20. **S. Zubair Ahmed, K.V. Ramana, Ramancharla Pradeep Kumar** Seismic Response of RC Frame Structure with Soft Storey IJRET: International Journal of Research in Engineering and Technology

STRESS ANALYSIS IN REINFORCED CONCRETE SLAB WITH DIFFERENT END CONDITIONS.

ASST PROF. HUZAIFA YAMAN

Department of Civil Engineering

NSAKCET, India

FARHEEN KHAN

Department of Civil Engineering

NSAKCET, India

ABSTRACT: In order to acquire detailed information to construct a safe and usable structure, it is very important to consider the behaviour of reinforced concrete (RC) components in systems subjected to varying loading conditions. Condition tracking of systemic structures has recently drawn scientists and researchers to establish online resources for detecting damage. In this work, using ANSYS and SAFE tools, a reinforced concrete slab was modelled to consider the slab's behaviour as a fixed support and a simple assisted slab with different end conditions and to compare stress and displacement due to different end conditions
.

1. INTRODUCTION

Several approximate methods for the analysis of two-way slabs were developed over the past years. Some of these methods include equivalent frame method (E.F.M.) and direct design method (D.D.M.), which have restrictions on their use or may be time-consuming. This research aims to study variable approximate approaches used in the analysis of two-way slabs Indian code and compare the values of load distribution factors based on bending moment results only with corresponding values using the finite element method

• To review available analysis approaches for two-way slabs systems,

• To compare numerical results with each method,

• To study the effect of different boundary condition as per IS 456-2000, and

• To recommend appropriate analysis method for two-way slab system

2 Literature Review

Dev et al. (2017) analyzed the waffle slab by an approximate method using the RankineGrashoff method and compared it with Timoshenko's plate theory and ETABS 2015. The results showed that finite element results and plate theory are in good agreement, but the Rankine-Grashoff method overestimates critical bending moment Mx and shear force Qx because they neglect negative moments.

Davies : Used finite elements' strategy to test deflections and moments in Corner with rectangular slab support. Both basic aids and fixed supports were taken into account. Several loading conditions have been considered, and scale model experiments have been correlated with empirical findings. Davies found a clear association between analytical and experimental experiments and demonstrated that tested basic and fixed support models were usually limited to real slab-to-column connections

Nishan and Shenoy (2013) made a parametric study of two-way slab analysis using various methods, including the Rankine-Grashoff method, Plate Theory, Stiffness Matrix Method, and STAAD program. The study shows that Plate theory underestimates the bending moment shear force values when compared to other methods, but the most important result is that Rankine- Grashoff method and plate theory can be only used when the slab is simply supported on all sides since each of the methods does not take into consideration the deflection of boundary and their stiffness.

.

3 MODELLING PARAMETERS

The dimension of the slab studied are 6000mm x4000mm x125 mm. The slab is made up of M 20 grade of concrete with thickness 125 mm. the load acting on the slab is considered as uniformly distributed load of self-weight of slab +live load +floor finish load.

Self-weight of slab = 0.125*25 = 3.125 kn/m2, Live load as per is 875 = 3 kn/m2

Floor finish load = 1kn/m2

Total load at slab = 7.125 kn/m2

4.1 slab with interior support:

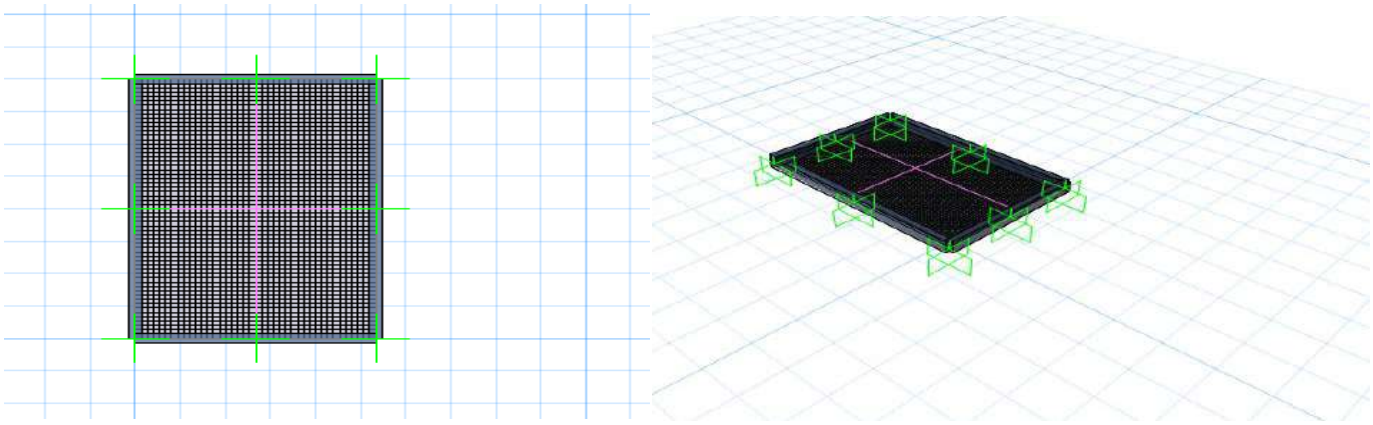

Figure1 isometric view of interior panel slab

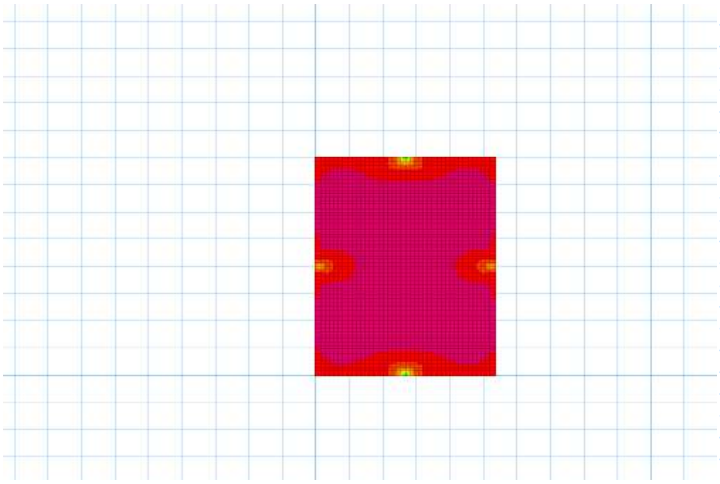

Figure2 stress of interior panel slab in short direction

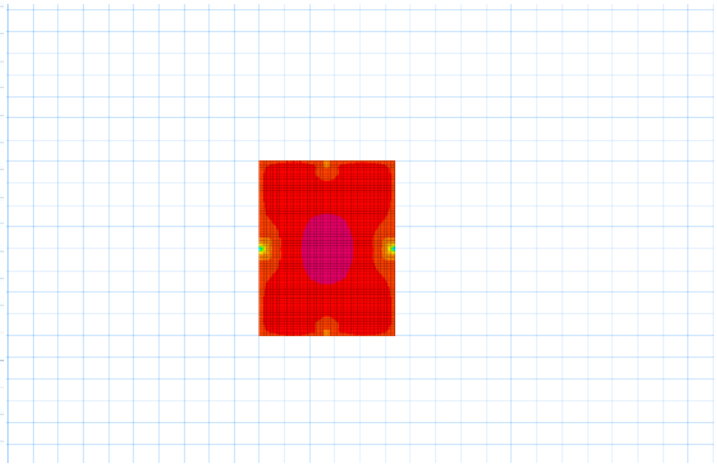

Figure 3 stress of interior panel slab in long direction

4.2 slab with One Short Edge Continuous support:

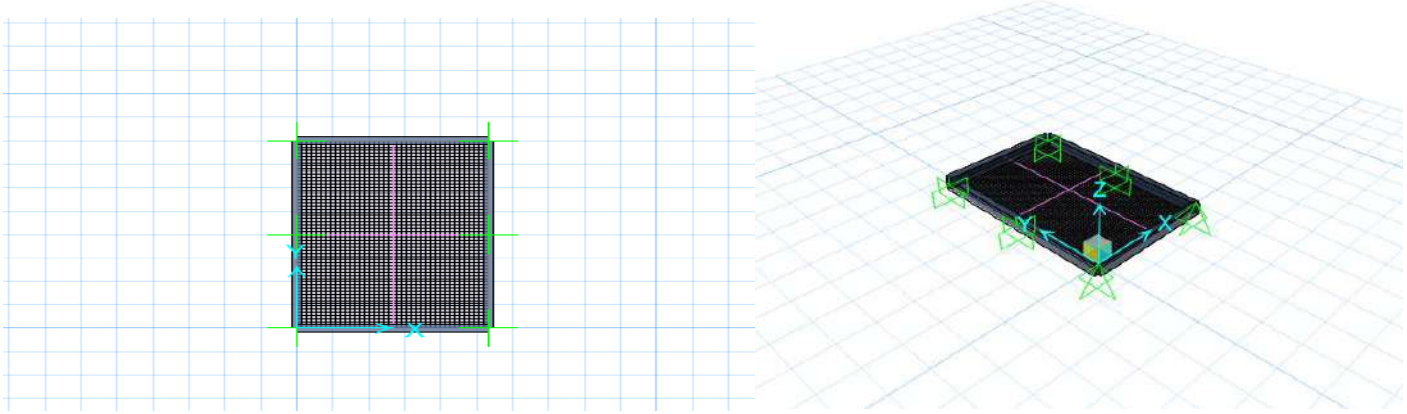

Figure 4 isometric view of One Short Edge Continuous support panel

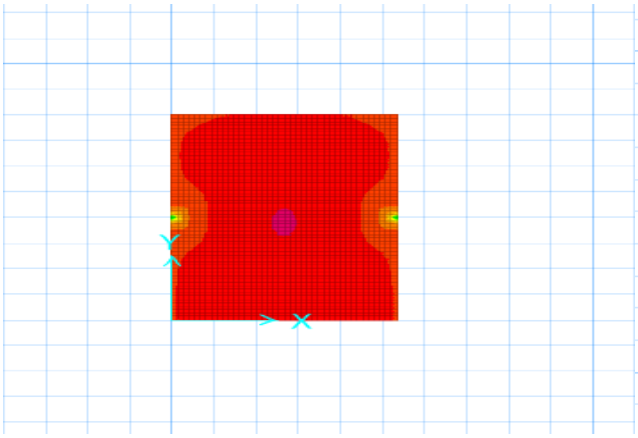

Figure5 stress in longer direction

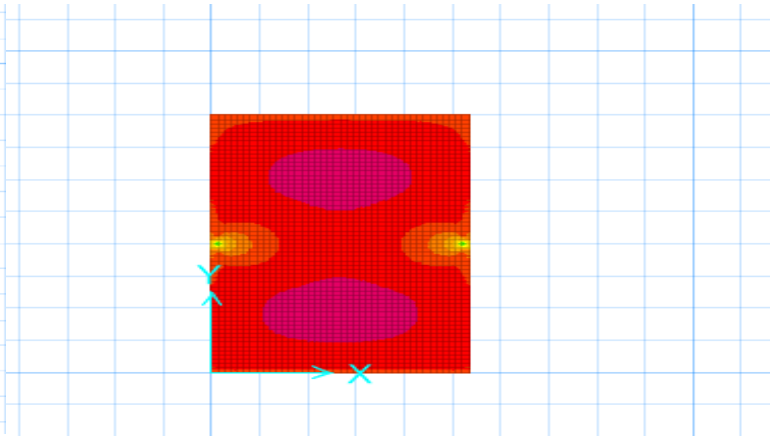

Figure6 stress in short direction

4.3 slab with one long Edge Discontinuous

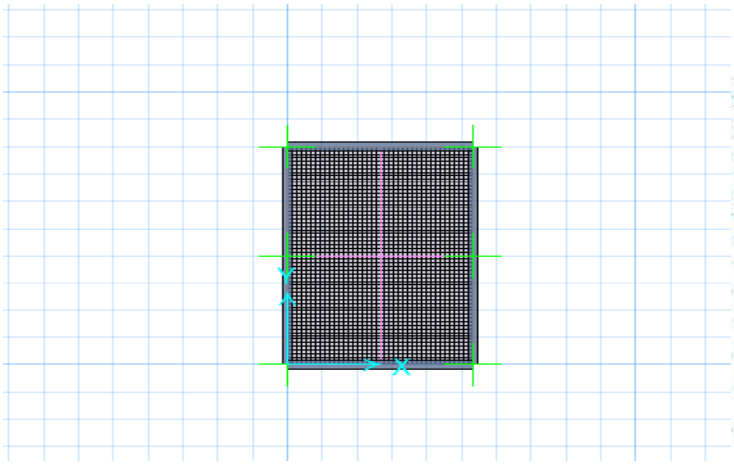

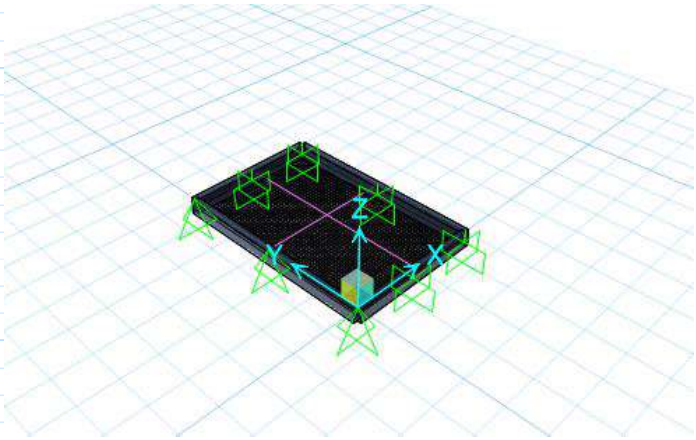

Figure 7 isometric view of one long Edge Discontinuous support panel

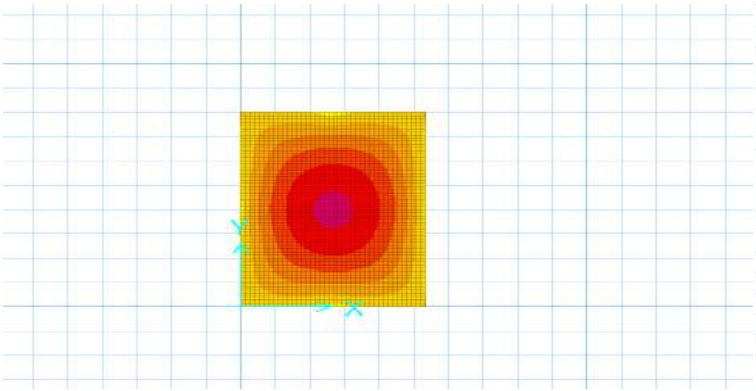

Figure 8 stress in longer direction

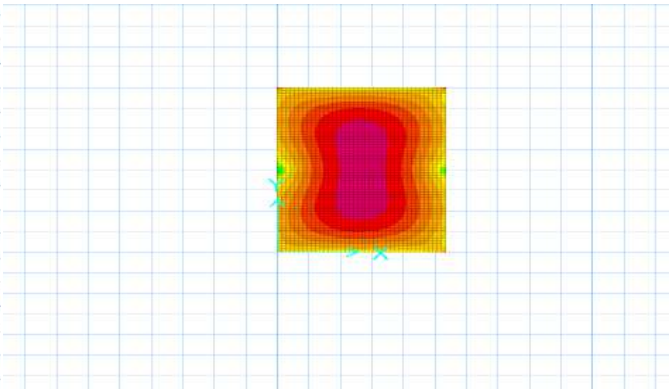

Figure 9 stress of one long Edge Discontinuous support panel short direction

4.4 slab with two Adjacent Edges Discontinuous

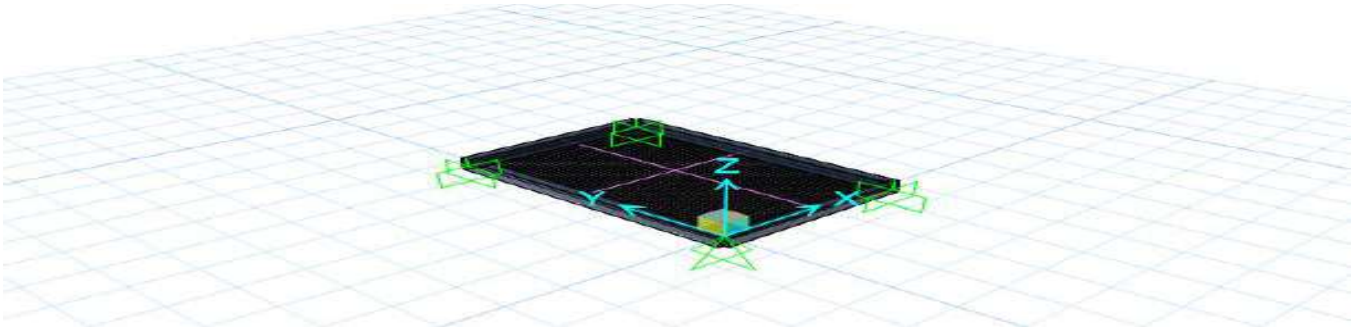

Figure 10 isometric view of two Adjacent Edges Discontinuous support panel

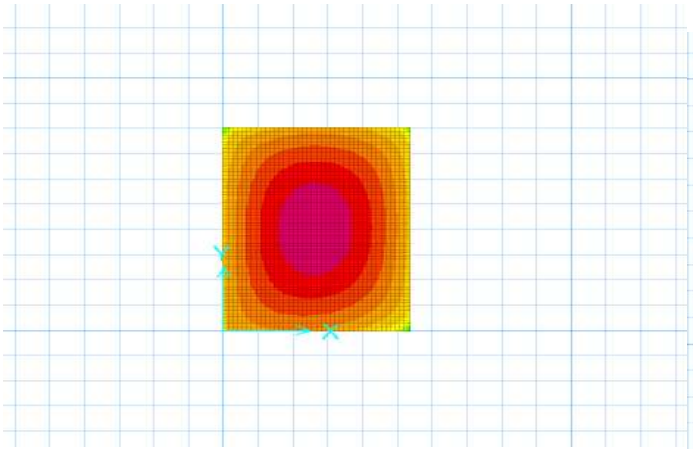

Figure11 stress of two Adjacent Edges in longer direction

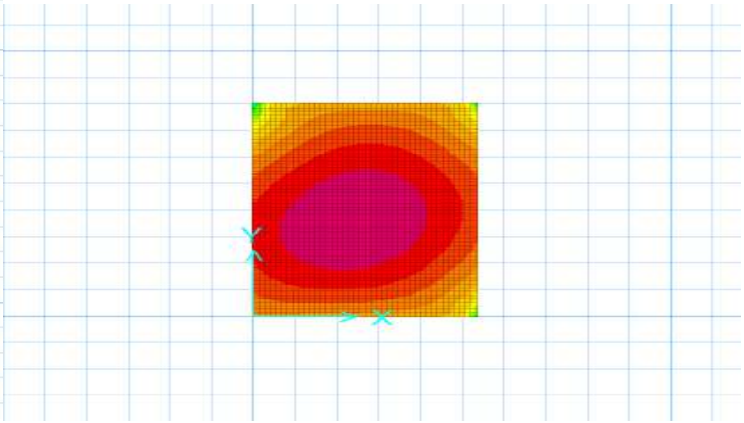

Figure12 stress of two Adjacent Edges Discontinuous support panel short direction

4.5 slab with two short Edges Discontinuous

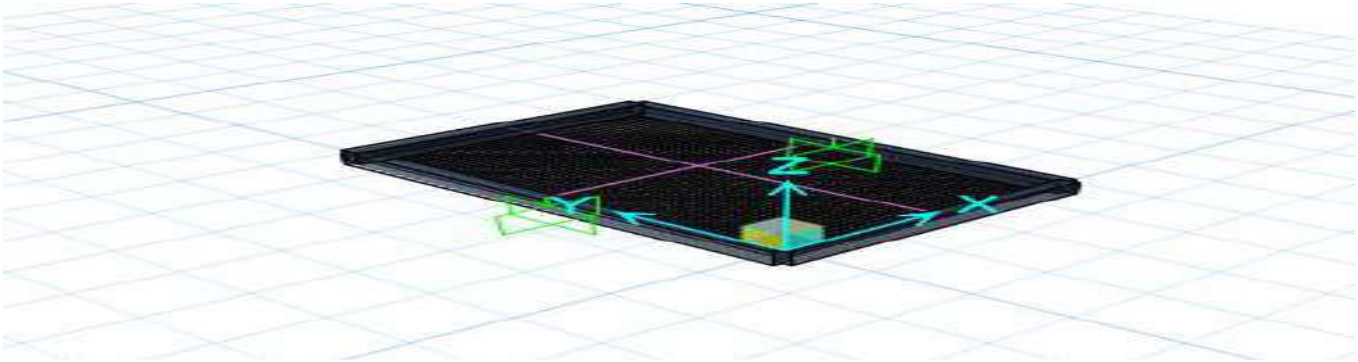

Figure 13 isometric view of two short Edges Discontinuous support panel

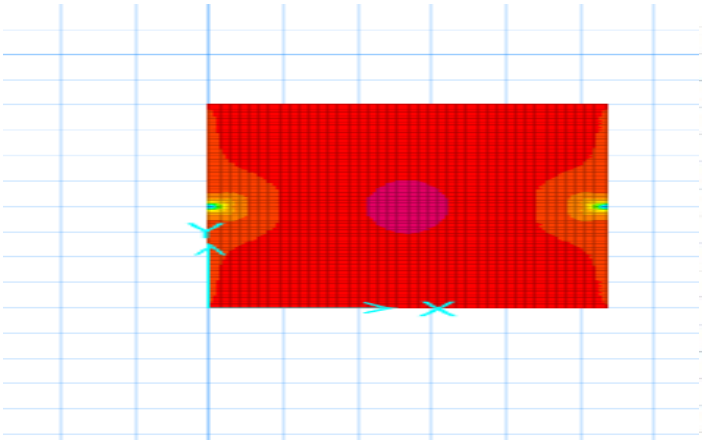

Figure 14 stress in longer direction

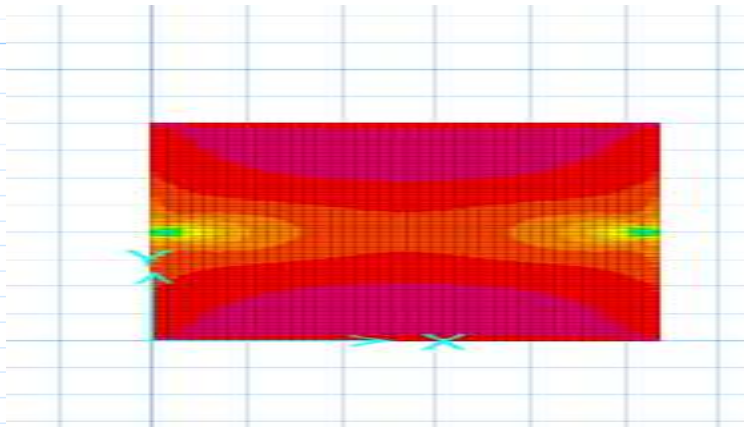

Figure15 stress of two short Edges Discontinuous short direction

4.6 slab with two long Edges Discontinuous

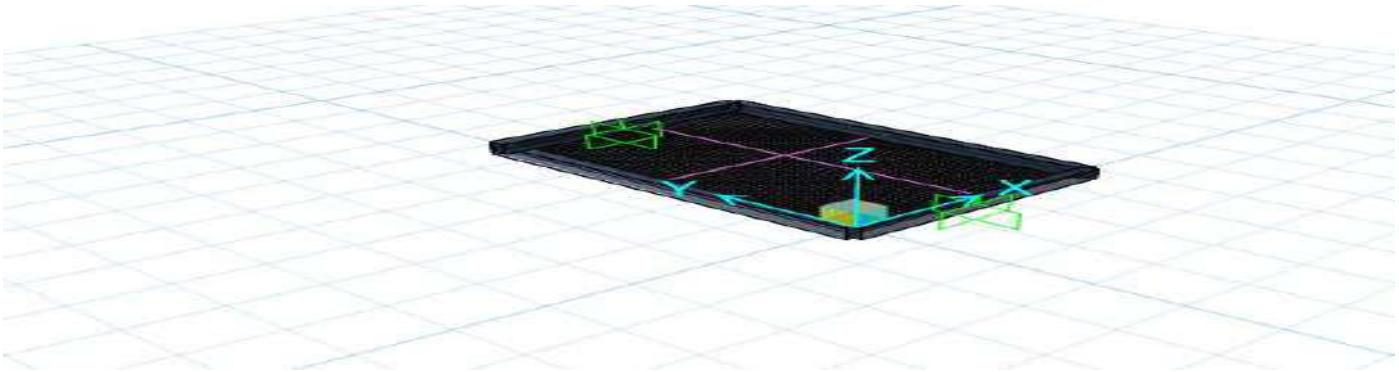

Figure16 isometric view of two long Edges Discontinuous support panel

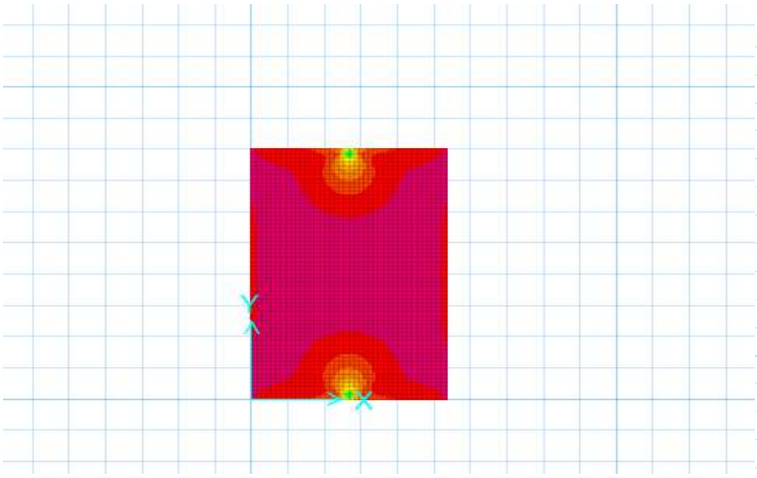

Figure17 stress in longer direction

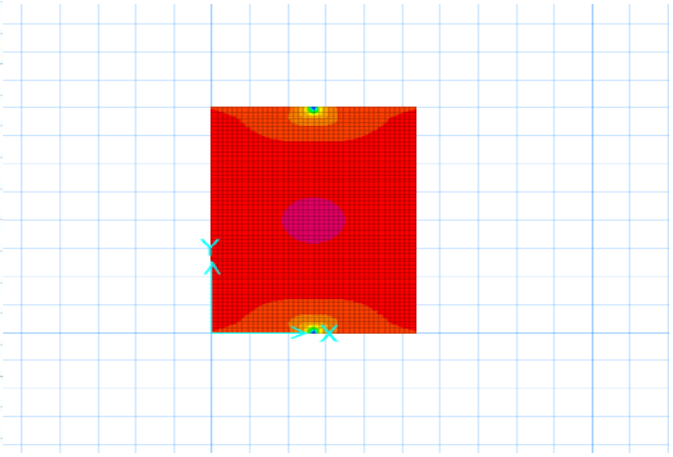

Figure18 stress of two long Edges Discontinuous in short direction

4.7 slab with Three Edges Discontinuous (One Long Edge Continuous):

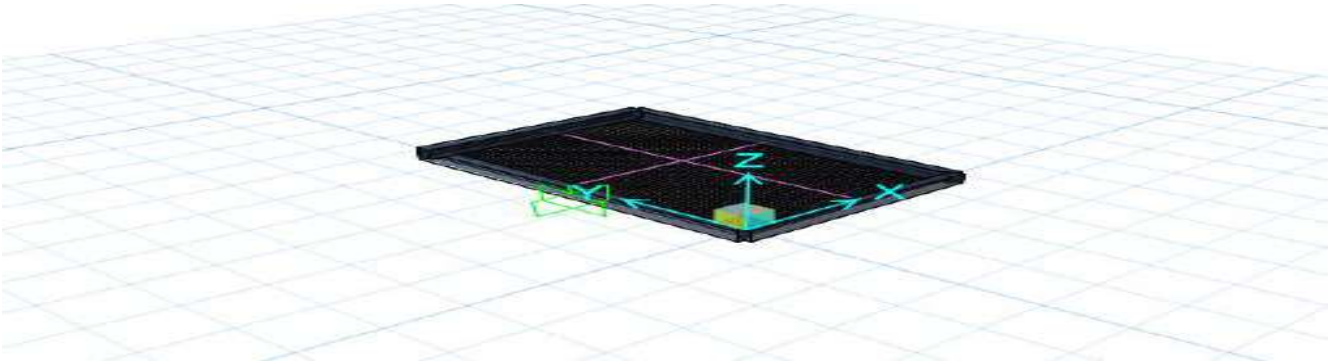

Figure19 isometric view of Three Edges Discontinuous (One Long Edge Continuous): support panel

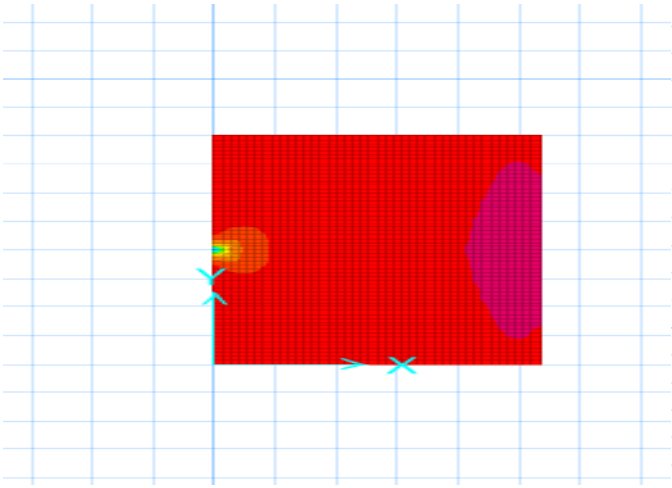

Figure 20 stress of Three Edges Discontinuous in longer direction

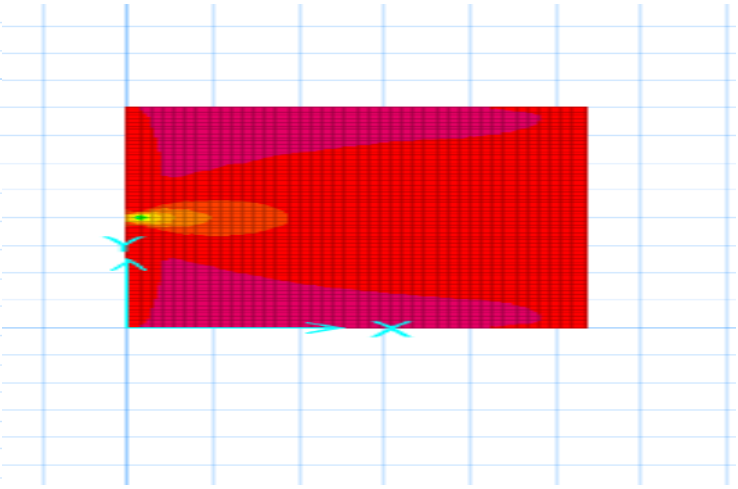

Figure21 stress of Three Edges Discontinuous short direction

4.8 slab with Three Edges Discontinuous (One Short Edge Continuous):

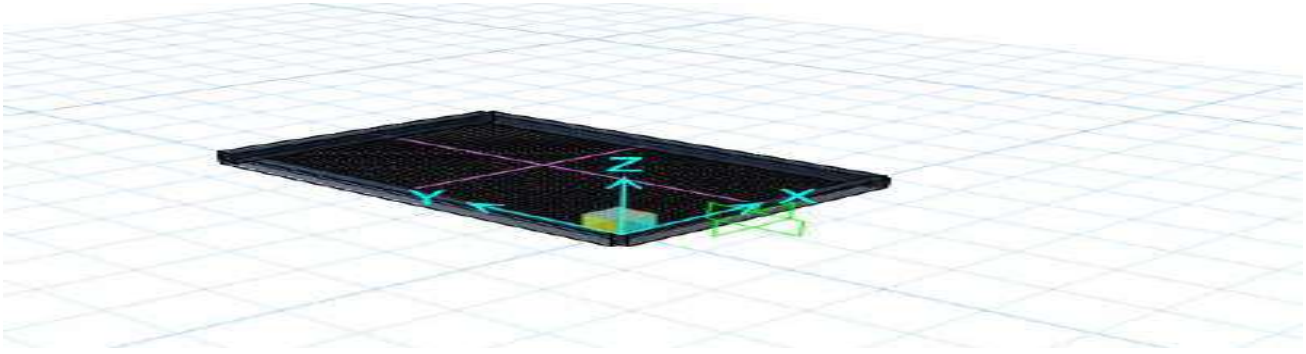

Figure 22 isometric view of Three Edges Discontinuous (One Short Edge Continuous): support panel

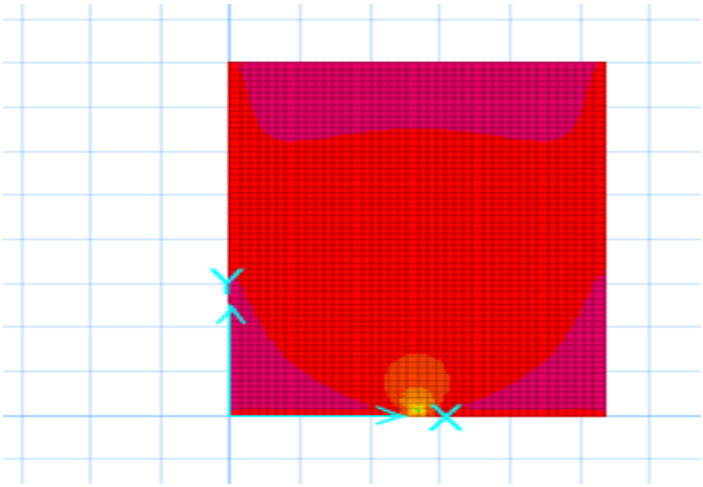

Figure 23 stress of Three Edges Discontinuous in longer direction

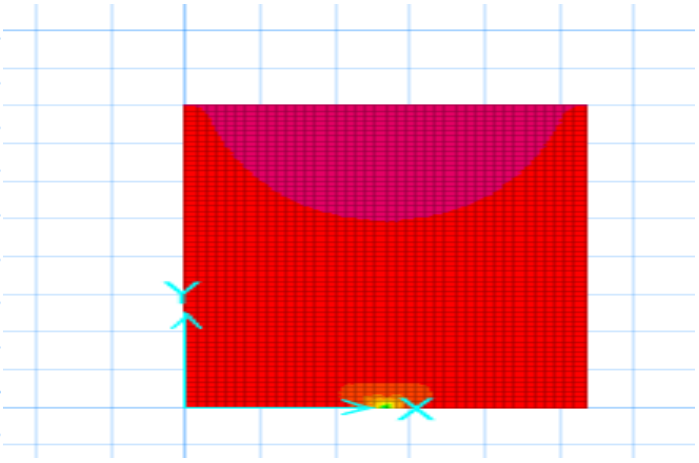

Figure 24 stress of Three Edges short direction

4.9 slab with Four-Edges Discontinuous:

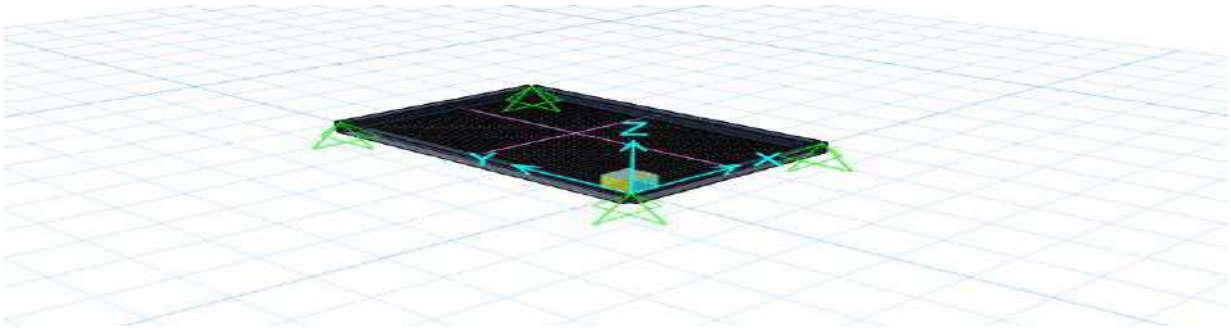

Figure2 5 isometric view of Four-Edges Discontinuous support panel

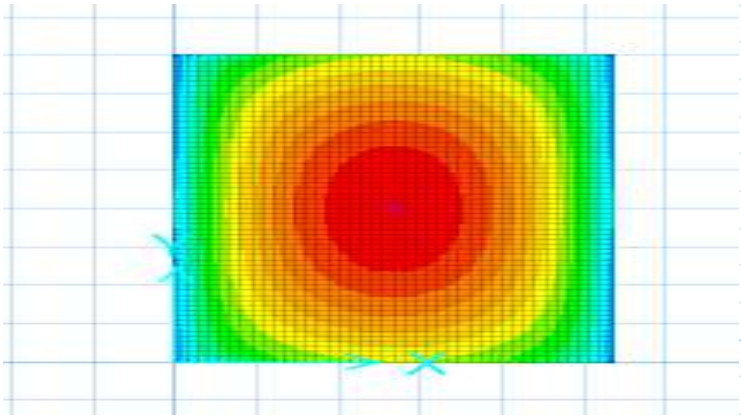

Figure26 stress of Four-Edges Discontinuous in longer direction

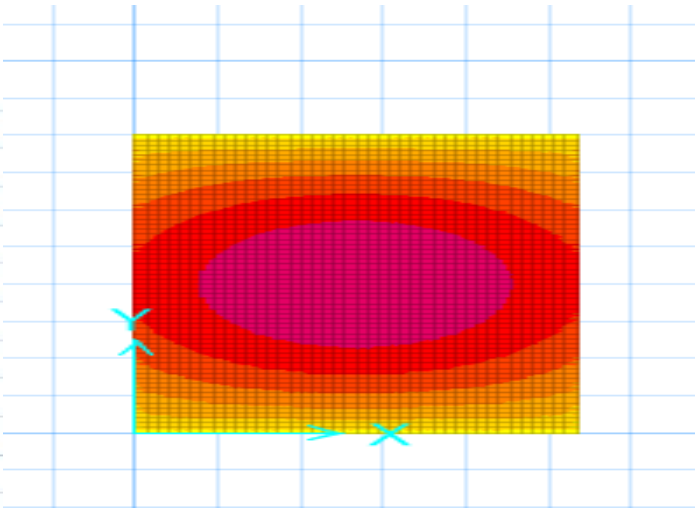

Figure 27 stress of Four-Edges Discontinuous short direction

6 CONCLUSIONS

Based on the findings of the study, on overall view,

the aim of the study has been achieved, and the conclusions for each objective which can be drawn out are as follows;

- The primary purpose of this research is to consider the action of two-way RC slabs and approximate the coefficients of the bending moment.
- Analysis was conducted and the creation of yield lines at various sections of the slab panel was observed at different loading stages in order to find out the values.
- In linear analysis, bending moment coefficients don't depend on loading and panel scale.
- Bending moment coefficients are determined on the basis of content yield at the edges and mid-span.

6.1 SCOPE

The following recommendations are proposed for further research:

1. Develop an approximate method based on finite element results.

2. Expand the analysis for varying slab thickness and the aspect ratio with different loading conditions.

3. Compare finite element results with experimental and analytical results.

4. Study the one way and two-way waffle slabs, and compare between analysis methods

REFERENCES

- Abdel-Karim, R., & Mahmood, I. M. (2016). The effect of beams stiffness's on the load distribution in a single simply supported two-way ribbed slab. IUG Journal of Natural Studies, Vol.14(1). P.191-208,
- ACI Committee. (1963). Building code requirements for reinforced concrete (ACI 318-63). American Concrete Institute.
- IS 456. Building code requirements for reinforced concrete design.
- Al- Qadamani J. (1998). Finite Element Analysis of Slab of Uniform Thickness in both Direction Versus Different Applied Methods. Master Thesis. An-Najah National University,
- BSI. (1997). BS 8110-1: 1997: Structural use of concrete. Code of practice for design and construction.35-40
- Deaton, J. B. (2005). A finite element approach to reinforced concrete slab design (Doctoral dissertation, Georgia Institute of Technology).
- Dev A., Jasmin S.P., Shajee S. (2017). Analysis and Parametric Study of Waffle Slabs, International Journal of Innovative Research in Science, Engineering and Technology IJIRSET, Vol.6, 5850-5857.
- Kamara, M., Mahamid, M., & Novak, L. C. (2012). Historical Perspective on the Evolution of Two-Way Slab Design. Special Publication, 287, 1-10.
- Mosley, W. H., Hulse, R., & Bungey, J. H. (2012). Reinforced concrete design: to Eurocode 2. Macmillan International Higher Education.
- Nishan B., Shenoy P. (2013). Automated Analysis and Parametric Study of Grid Floors, International Journal of Innovative Research in Science, Engineering and Technology IJIRSET, Vol.6, 20897-20903.
- Park, R., & Gamble, W. L. (2000). Reinforced concrete slabs. John Wiley & Sons.

- Rusinowski, P. (2005). Two-way concrete slabs with openings: experiments, finite element analyses and design. Sinha, S. N. (2014). Reinforced concrete design. Tata McGraw-Hill Education.
- Szilard, R. (2004). Theories and applications of plate analysis: classical, numerical and engineering methods. John Wiley & Sons.
- Varma, M., Pendharkar, U., & Sharma, R. K. (2012). Experimental study to evaluate short-term deflections for two-way RC slabs. International Journal of civil and structural Engineering, 2(3), 901-913.

STRESS ANALYSIS IN REINFORCED CONCRETE SLAB WITH DIFFERENT END CONDITIONS.

ASST PROF. HUZAIFA YAMAN

Department of Civil Engineering

NSAKCET, India

FARHEEN KHAN

Department of Civil Engineering

NSAKCET, India

ABSTRACT: In order to acquire detailed information to construct a safe and usable structure, it is very important to consider the behaviour of reinforced concrete (RC) components in systems subjected to varying loading conditions. Condition tracking of systemic structures has recently drawn scientists and researchers to establish online resources for detecting damage. In this work, using ANSYS and SAFE tools, a reinforced concrete slab was modelled to consider the slab's behaviour as a fixed support and a simple assisted slab with different end conditions and to compare stress and displacement due to different end conditions
.

1. INTRODUCTION

Several approximate methods for the analysis of two-way slabs were developed over the past years. Some of these methods include equivalent frame method (E.F.M.) and direct design method (D.D.M.), which have restrictions on their use or may be time-consuming. This research aims to study variable approximate approaches used in the analysis of two-way slabs Indian code and compare the values of load distribution factors based on bending moment results only with corresponding values using the finite element method

• To review available analysis approaches for two-way slabs systems,

• To compare numerical results with each method,

• To study the effect of different boundary condition as per IS 456-2000, and

• To recommend appropriate analysis method for two-way slab system

2 Literature Review

Dev et al. (2017) analyzed the waffle slab by an approximate method using the RankineGrashoff method and compared it with Timoshenko's plate theory and ETABS 2015. The results showed that finite element results and plate theory are in good agreement, but the Rankine-Grashoff method overestimates critical bending moment Mx and shear force Qx because they neglect negative moments.

Davies : Used finite elements' strategy to test deflections and moments in Corner with rectangular slab support. Both basic aids and fixed supports were taken into account. Several loading conditions have been considered, and scale model experiments have been correlated with empirical findings. Davies found a clear association between analytical and experimental experiments and demonstrated that tested basic and fixed support models were usually limited to real slab-to-column connections

Nishan and Shenoy (2013) made a parametric study of two-way slab analysis using various methods, including the Rankine-Grashoff method, Plate Theory, Stiffness Matrix Method, and STAAD program. The study shows that Plate theory underestimates the bending moment shear force values when compared to other methods, but the most important result is that Rankine- Grashoff method and plate theory can be only used when the slab is simply supported on all sides since each of the methods does not take into consideration the deflection of boundary and their stiffness.

.

3 MODELLING PARAMETERS

The dimension of the slab studied are 6000mm x4000mm x125 mm. The slab is made up of M 20 grade of concrete with thickness 125 mm. the load acting on the slab is considered as uniformly distributed load of self-weight of slab +live load +floor finish load.

Self-weight of slab = 0.125*25 = 3.125 kn/m2, Live load as per is 875 = 3 kn/m2

Floor finish load = 1kn/m2

Total load at slab = 7.125 kn/m2

4.1 slab with interior support:

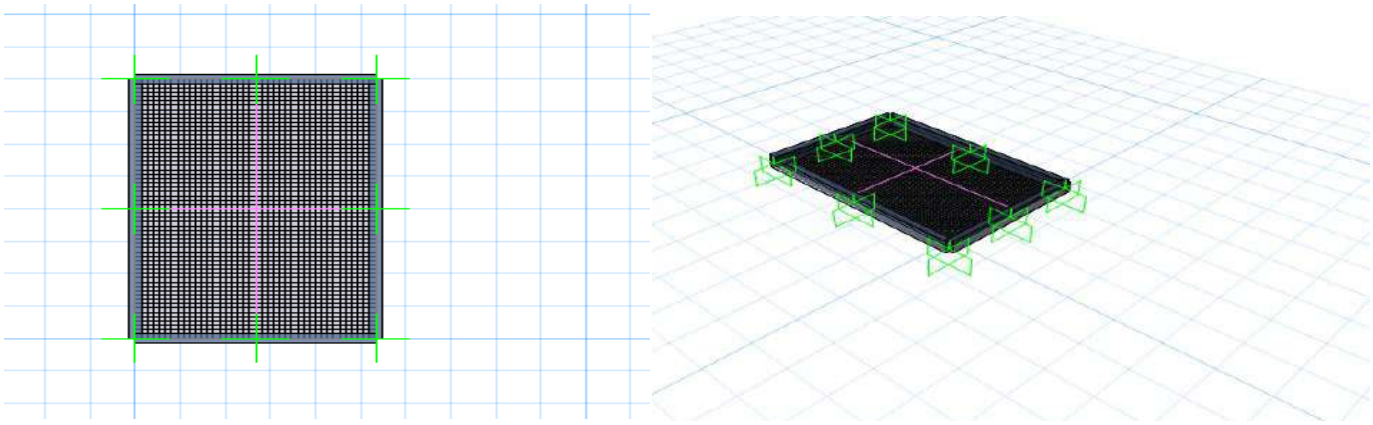

Figure1 isometric view of interior panel slab

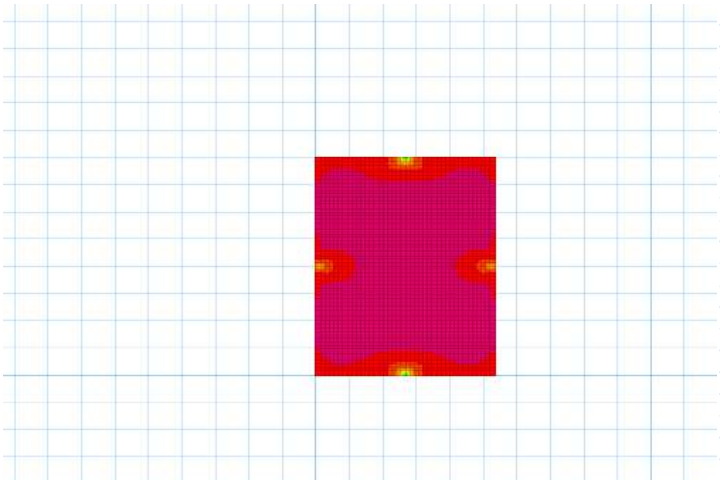

Figure2 stress of interior panel slab in short direction

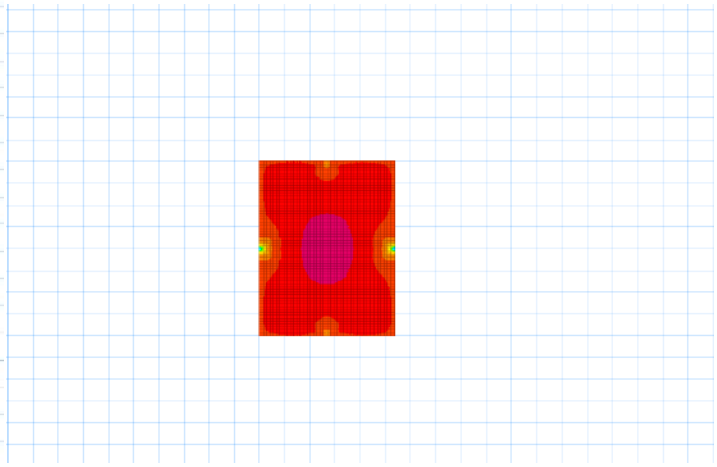

Figure 3 stress of interior panel slab in long direction

4.2 slab with One Short Edge Continuous support:

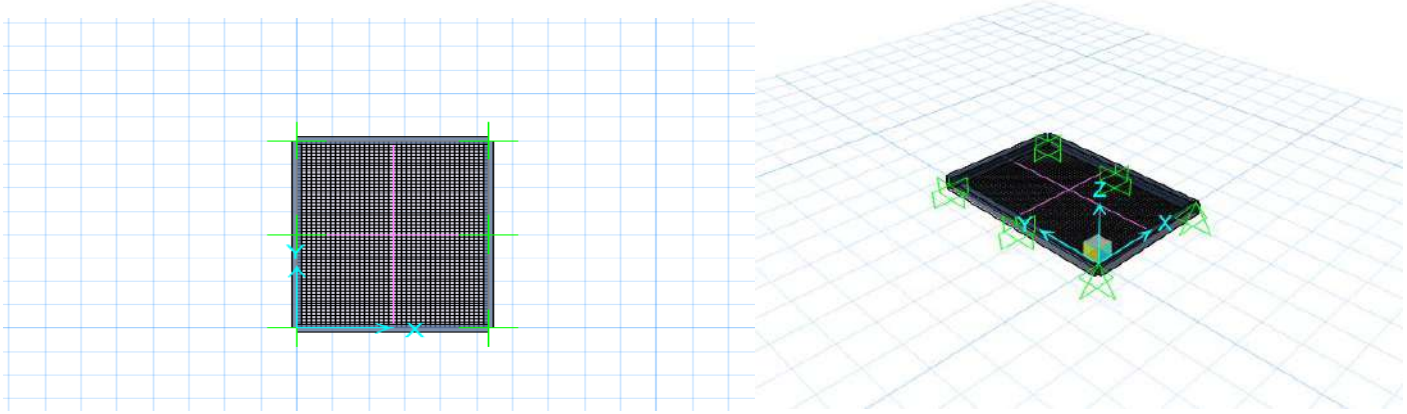

Figure 4 isometric view of One Short Edge Continuous support panel

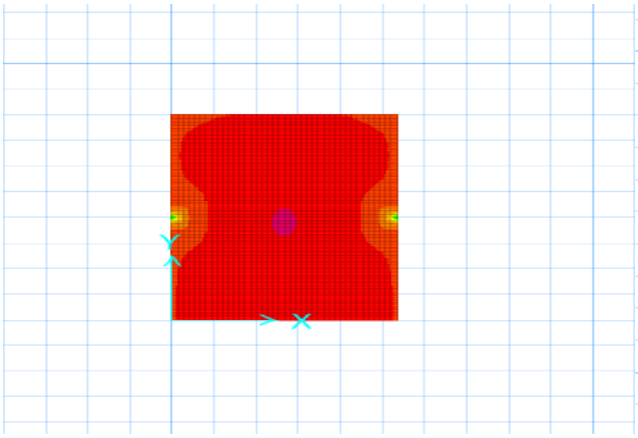

Figure5 stress in longer direction

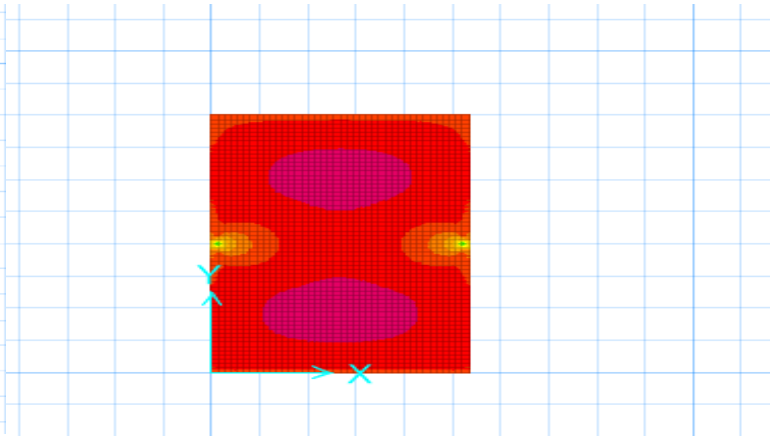

Figure6 stress in short direction

4.3 slab with one long Edge Discontinuous

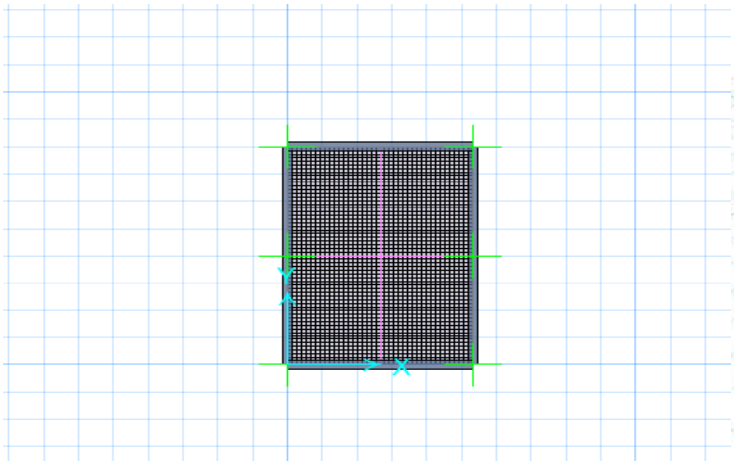

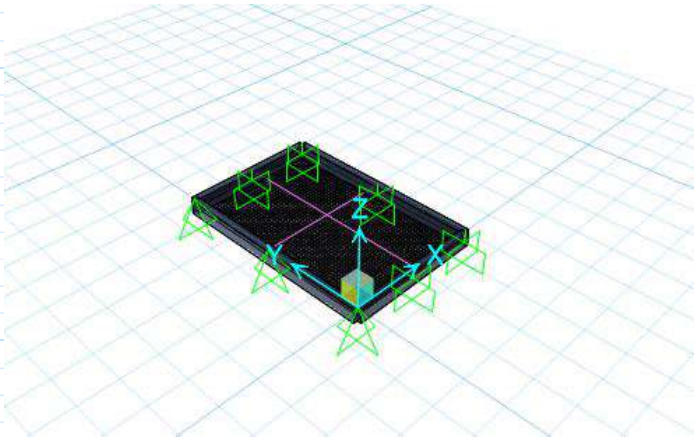

Figure 7 isometric view of one long Edge Discontinuous support panel

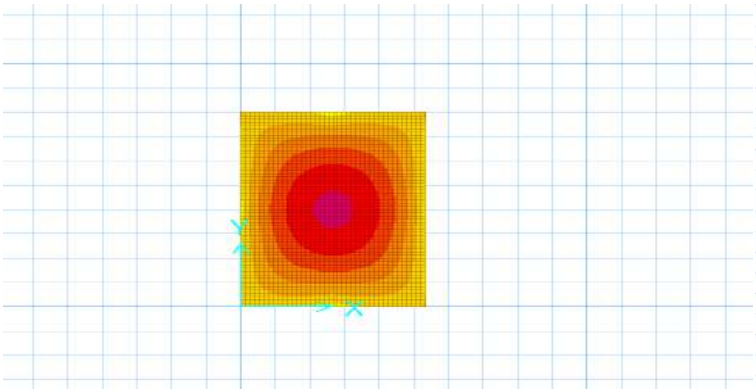

Figure 8 stress in longer direction

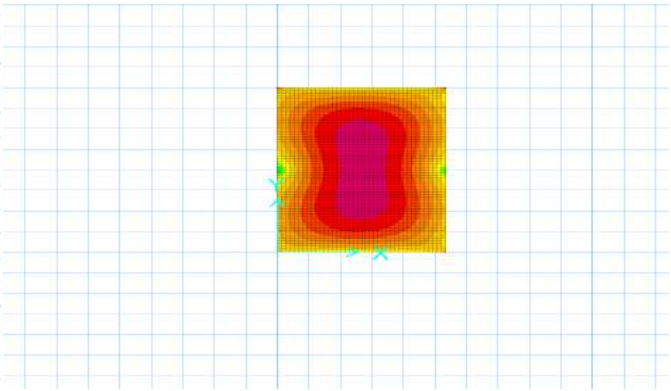

Figure 9 stress of one long Edge Discontinuous support panel short direction

4.4 slab with two Adjacent Edges Discontinuous

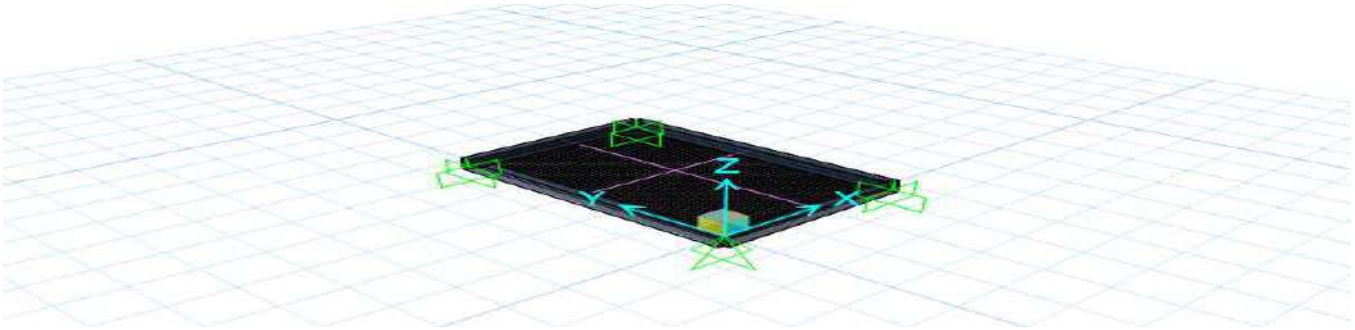

Figure 10 isometric view of two Adjacent Edges Discontinuous support panel

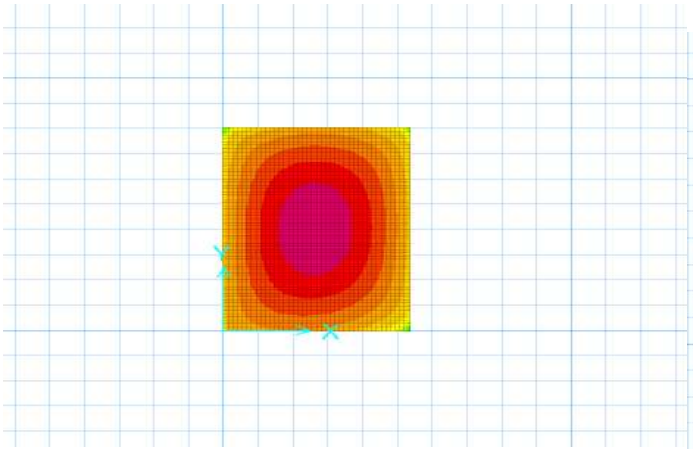

Figure11 stress of two Adjacent Edges in longer direction

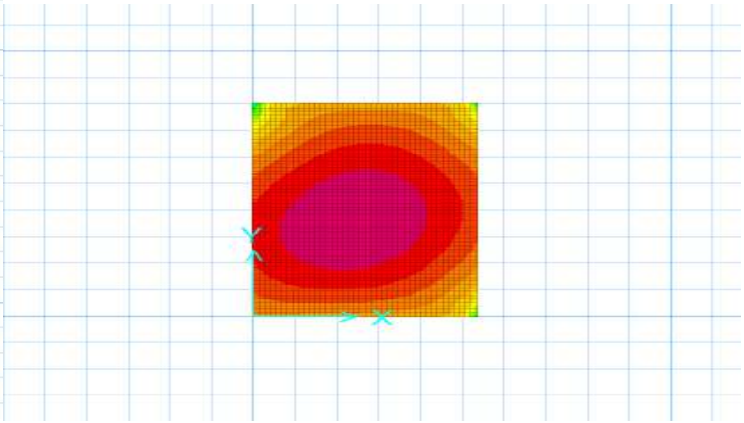

Figure12 stress of two Adjacent Edges Discontinuous support panel short direction

4.5 slab with two short Edges Discontinuous

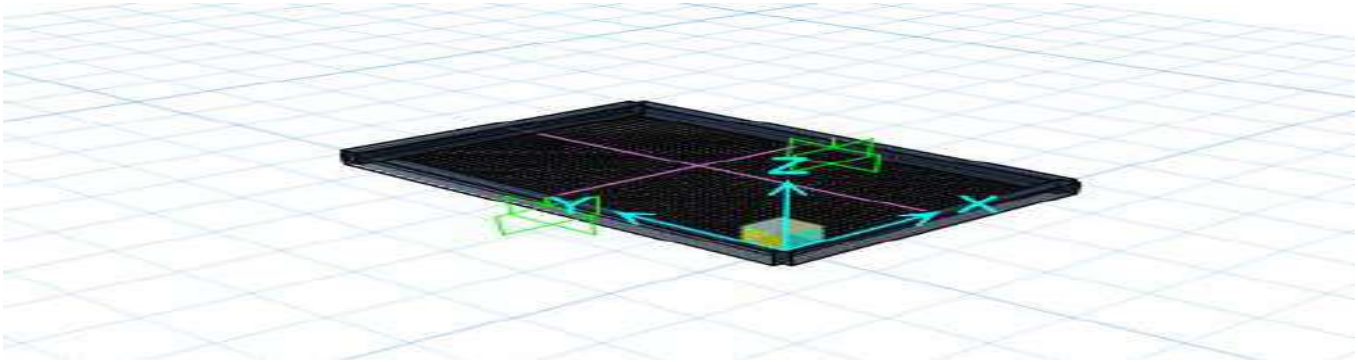

Figure 13 isometric view of two short Edges Discontinuous support panel

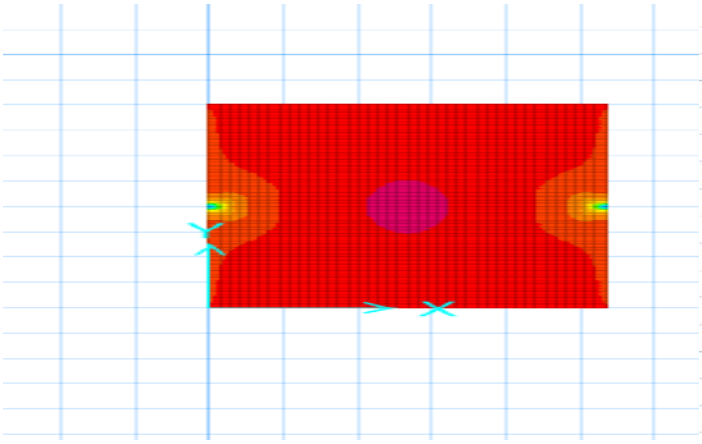

Figure 14 stress in longer direction

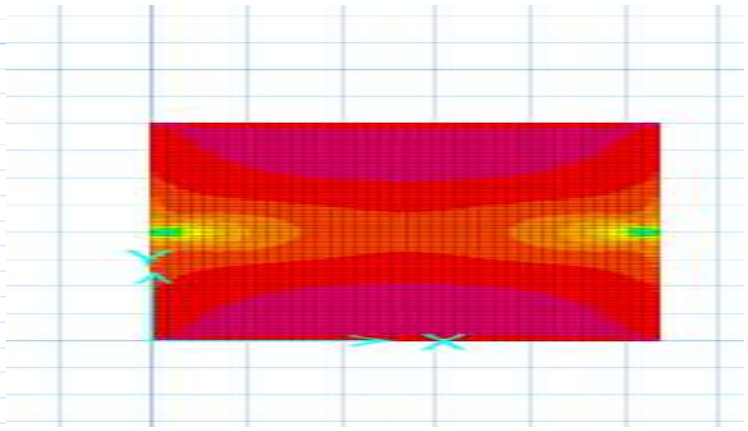

Figure15 stress of two short Edges Discontinuous short direction

4.6 slab with two long Edges Discontinuous

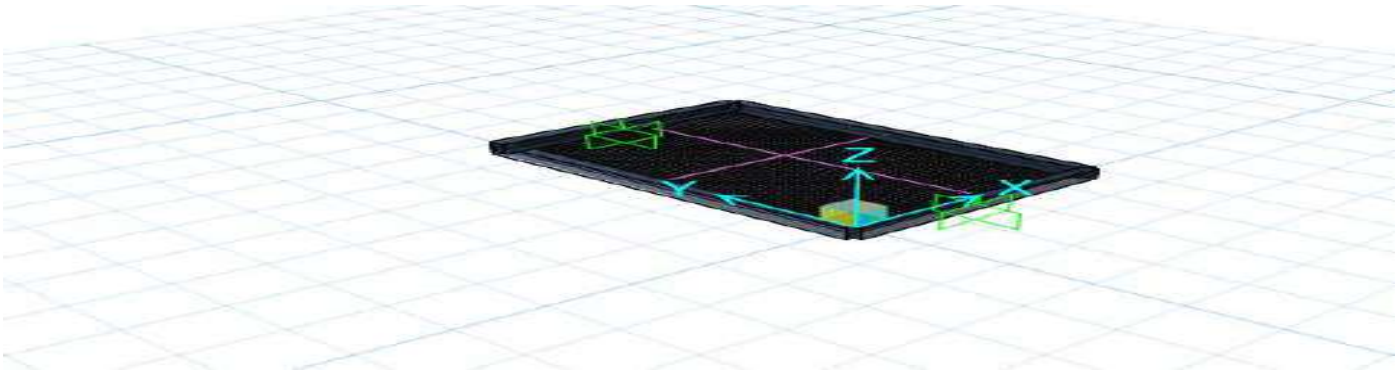

Figure16 isometric view of two long Edges Discontinuous support panel

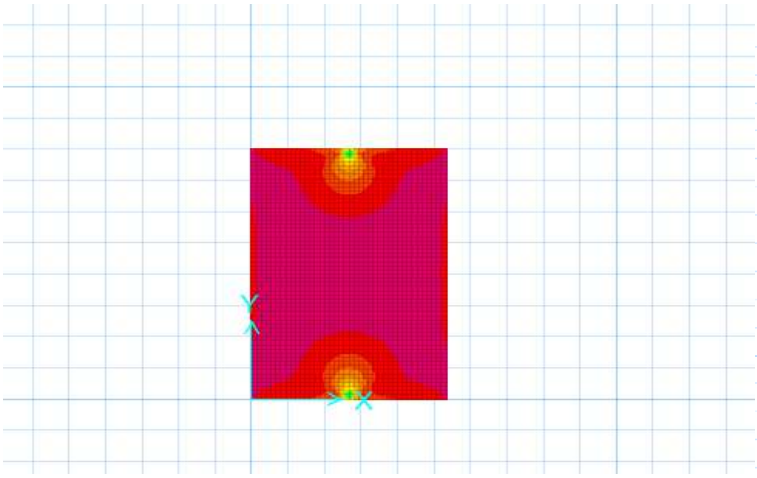

Figure17 stress in longer direction

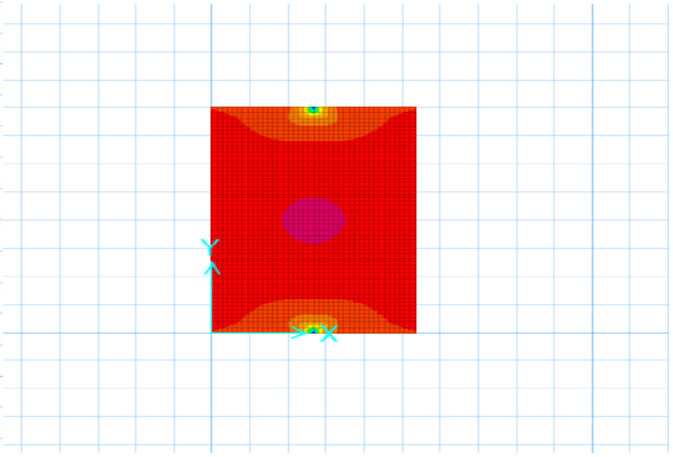

Figure18 stress of two long Edges Discontinuous in short direction

4.7 slab with Three Edges Discontinuous (One Long Edge Continuous):

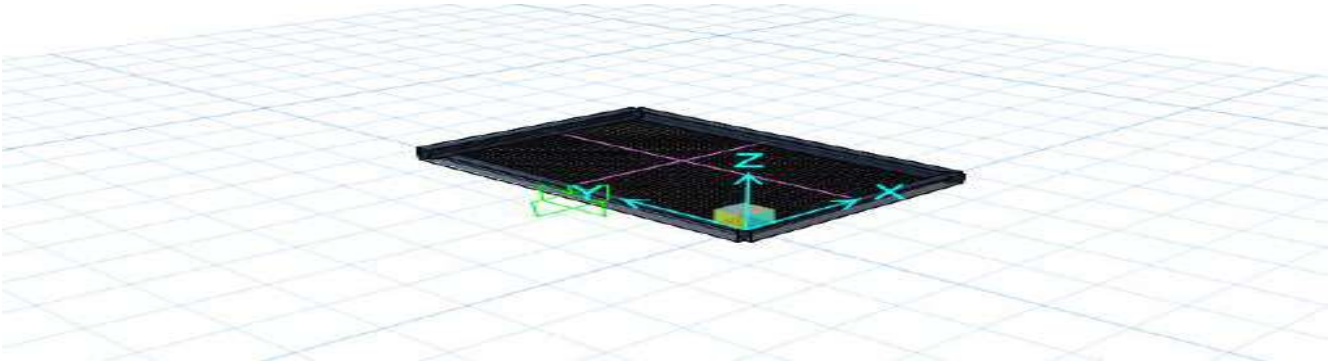

Figure19 isometric view of Three Edges Discontinuous (One Long Edge Continuous): support panel

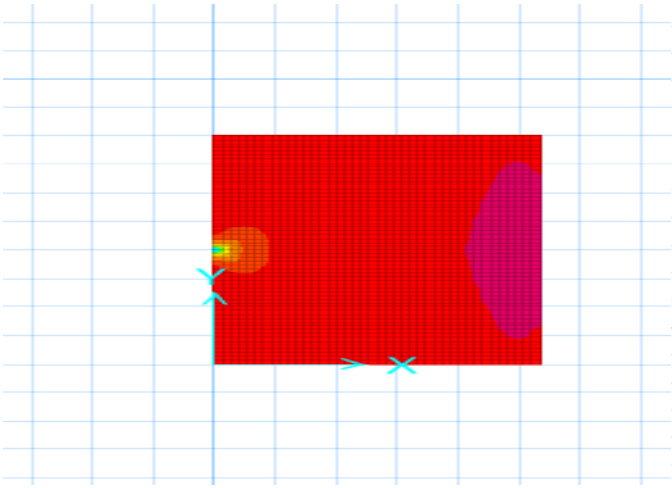

Figure 20 stress of Three Edges Discontinuous in longer direction

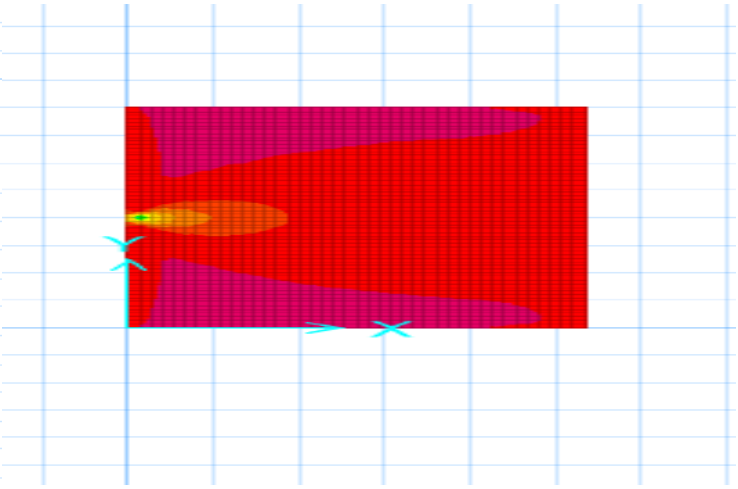

Figure21 stress of Three Edges Discontinuous short direction

4.8 slab with Three Edges Discontinuous (One Short Edge Continuous):

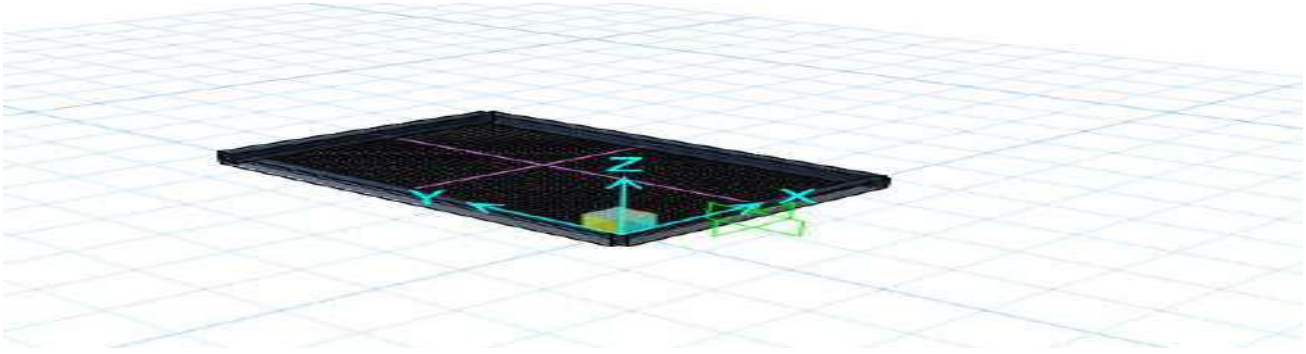

Figure 22 isometric view of Three Edges Discontinuous (One Short Edge Continuous): support panel

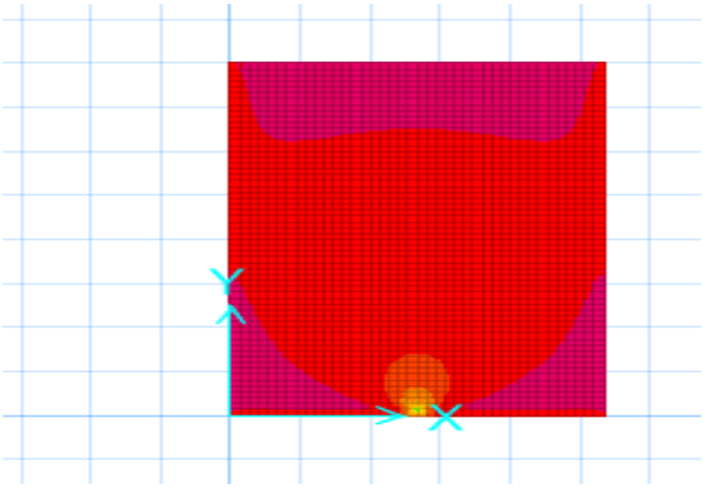

Figure 23 stress of Three Edges Discontinuous in longer direction

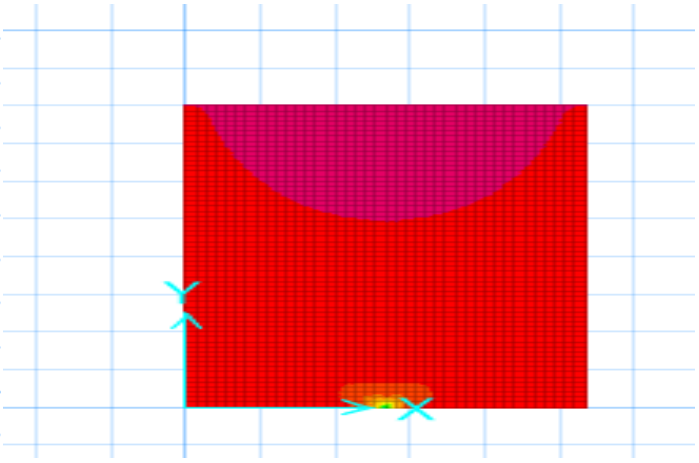

Figure 24 stress of Three Edges short direction

4.9 slab with Four-Edges Discontinuous:

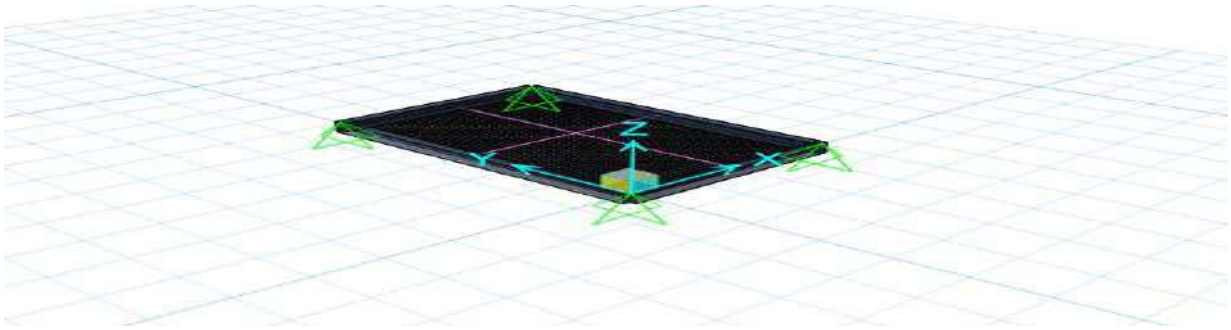

Figure2 5 isometric view of Four-Edges Discontinuous support panel

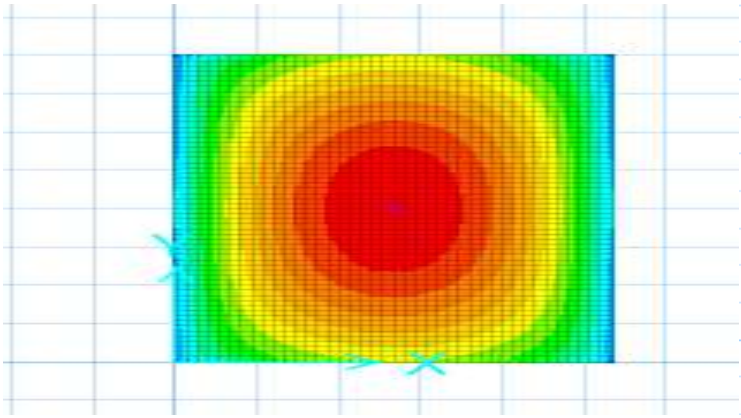

Figure26 stress of Four-Edges Discontinuous in longer direction

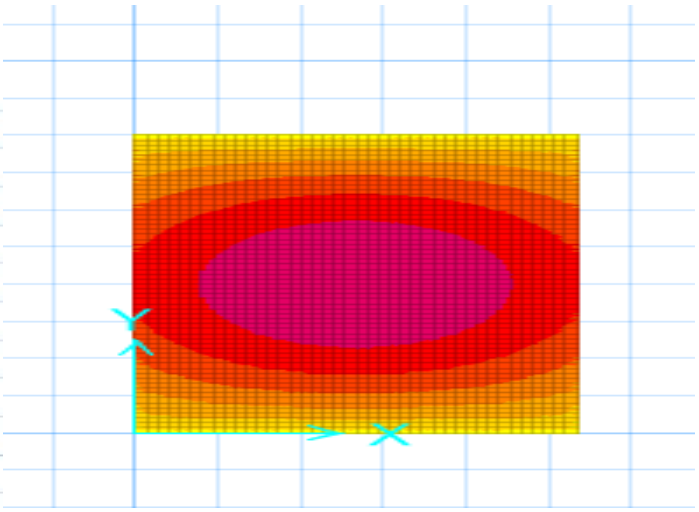

Figure 27 stress of Four-Edges Discontinuous short direction

6 CONCLUSIONS

Based on the findings of the study, on overall view,

the aim of the study has been achieved, and the conclusions for each objective which can be drawn out are as follows;

- The primary purpose of this research is to consider the action of two-way RC slabs and approximate the coefficients of the bending moment.
- Analysis was conducted and the creation of yield lines at various sections of the slab panel was observed at different loading stages in order to find out the values.
- In linear analysis, bending moment coefficients don't depend on loading and panel scale.
- Bending moment coefficients are determined on the basis of content yield at the edges and mid-span.

6.1 SCOPE

The following recommendations are proposed for further research:

1. Develop an approximate method based on finite element results.

2. Expand the analysis for varying slab thickness and the aspect ratio with different loading conditions.

3. Compare finite element results with experimental and analytical results.

4. Study the one way and two-way waffle slabs, and compare between analysis methods

REFERENCES

- Abdel-Karim, R., & Mahmood, I. M. (2016). The effect of beams stiffness's on the load distribution in a single simply supported two-way ribbed slab. IUG Journal of Natural Studies, Vol.14(1). P.191-208,
- ACI Committee. (1963). Building code requirements for reinforced concrete (ACI 318-63). American Concrete Institute.
- IS 456. Building code requirements for reinforced concrete design.
- Al- Qadamani J. (1998). Finite Element Analysis of Slab of Uniform Thickness in both Direction Versus Different Applied Methods. Master Thesis. An-Najah National University,
- BSI. (1997). BS 8110-1: 1997: Structural use of concrete. Code of practice for design and construction.35-40
- Deaton, J. B. (2005). A finite element approach to reinforced concrete slab design (Doctoral dissertation, Georgia Institute of Technology).
- Dev A., Jasmin S.P., Shajee S. (2017). Analysis and Parametric Study of Waffle Slabs, International Journal of Innovative Research in Science, Engineering and Technology IJIRSET, Vol.6, 5850-5857.
- Kamara, M., Mahamid, M., & Novak, L. C. (2012). Historical Perspective on the Evolution of Two-Way Slab Design. Special Publication, 287, 1-10.
- Mosley, W. H., Hulse, R., & Bungey, J. H. (2012). Reinforced concrete design: to Eurocode 2. Macmillan International Higher Education.
- Nishan B., Shenoy P. (2013). Automated Analysis and Parametric Study of Grid Floors, International Journal of Innovative Research in Science, Engineering and Technology IJIRSET, Vol.6, 20897-20903.
- Park, R., & Gamble, W. L. (2000). Reinforced concrete slabs. John Wiley & Sons.

- Rusinowski, P. (2005). Two-way concrete slabs with openings: experiments, finite element analyses and design. Sinha, S. N. (2014). Reinforced concrete design. Tata McGraw-Hill Education.
- Szilard, R. (2004). Theories and applications of plate analysis: classical, numerical and engineering methods. John Wiley & Sons.
- Varma, M., Pendharkar, U., & Sharma, R. K. (2012). Experimental study to evaluate short-term deflections for two-way RC slabs. International Journal of civil and structural Engineering, 2(3), 901-913.

BEHAVIOUR OF MULTISTOREYS RC BUILDING WITH SKY-BRIDGE UNDER THE SESMIC EFFECT.

ASST PROF HUZAIFA YAMAN

Department of Civil Engineering

NSAKCET, India

ABDUL MOIZ

Department of Civil Engineering

NSAKCET, India

ABSTRACT

The need for high-rise buildings is inevitable while the land in the rapidly developing towns and cities is becoming scarce due to increasing population numbers. Apart from the scarcity of the land, some part of our world is always hit by natural disasters such as earthquake, hurricane, tornado, tsunami, etc. Sky-bridges serve that need. Sky-bridges between buildings are becoming common, and its effect on structural behavior and design need to be understood. Responses to earthquake lateral loads are one of the guiding factors of the structural design. Current trends include horizontally connecting adjacent high buildings for various purposes. In this project, Twin RCC structures are considered with the connecting bridge in seismic zone V and II, and the story of the structure is G+45. The analysis is done by considering earthquake loads with the effect of sky-bridge at different levels. And after analyzing the above structure the Displacement, story drift, time period, are compared. A comparison of various design parameters is also done and interesting results have been obtained.

1.INTRODUCTION: The need for high-rise buildings is inevitable as land in fast-growing towns and cities become scarce as the population is growing. In addition to the scarcity of land, natural disasters like earthquakes, hurricanes, tornadoes, tsunamis, etc. continue to affect some parts of the world. These earthquakes are caused by the sudden movement of the earth's tectonic plate. The movement occurs on fault lines and the released energy is transferred by the earth in the form of waves that cause soil movement many miles from the epicenter. Regions next to active fault lines are the most susceptible to earthquakes.

The present work aims at the following objectives:

- Study of Seismic demands of regular R.C twin buildings using the dynamic analysis.
- To study the effect of connecting bridge at different levels by varying the height of connecting building.
- To illustrate the effects of seismic zone V and II, on the response of the Twin connected Buildings.
- To study various responses such as story shear, story displacement, inter-story drift, time period, etc. of buildings

2 LITERATURE REVIEW

- **Sayed Mahmoud (2019):** Reactions to lateral charges triggered by wind and earthquakes are among the main factors in the design of these structures. In the most recent design, neighbouring high buildings for different purposes are horizontally linked. However, such horizontal connexions can change the behavior of the structure, limiting the validity of design codes. In this paper, the response of connected high-rise structures under quake loads will be thoroughly

examined according to design code criteria. It is also investigated the impact of placing only the sky-bridge on the inducted responses. The building configurations were excited by the collection of ground movement data from various top speeds. The connecting location of the bridge affected the predicted dynamic responses from the building systems, but dramatically in some cases.

- **Imad Shakir Abood (2018):** In this paper, the effect of structural relations on earthquake responses was discussed using the finite element modelling technique for a connected building system. For this study, double 40-story Rcc frame-wall buildings, linked horizontally by longitudinal ties, depict the linked building system. It is believed that the two adjacent buildings were similar in this related building system so that an inter-story connexion might carry the two adjacent stories to the very same level. The linked tower system is designed as a rigid tower floor diaphragm and fixed to the structural perimeter of the buildings as a framework for each link.

- **Verma (2014)** The wind pressure coefficients for Sky Bridge were determined by studies performed for rectangular tall buildings on rigid models with incidence angles of 0 °, 45 °, and 90 °. "The models were tested at the Civil Engineering Department of the Indian Technology Institute Roorkee in the Closed Circuit Wind tunnel with a 1.3 m (width) x0.85 m (height) cross-section. Perspex sheet 5 mm thick is used for the manufacture of two construction models, each of which has square design of 50 mm to 50 mm in size to 300 mm. The study showed that negative pressure on the opposite faces is significantly increased when models are close.

3. CASE STUDY

The Layout of the plan having20x16 bays of equal length of 6m. The buildings considered are Reinforced concrete ordinary moment-resisting space frames of 42 story symmetric. The stiffness of the infill is neglected to account for the Nonlinear Behavior of Seismic demands. All these buildings have been analyzed by the NLTHA method. The story height is kept uniform of 3m for all kinds of building models which are as below. The analysis illustrates the step-by-step procedure for the determination of forces.

The Plan configuration consists of

1. Model 1 – Twin connecting building with the same height
2. Model 2 –. Twin connecting building for one building at 1/2 height
3. Model 3 –. Twin connecting building for one building at 1/4 height
4. . Model 4 –. Twin connecting building for one building at 3/4 height

Sl.no	Variable	Data
1	Type of structure	Moment Resisting Frame
2	Number of Stories	42
3	Floor height	3m
4	Live Load	3.0 kN/m^2
5	WALL load	10KN/m
6	Materials	Concrete (M30) and Reinforced with HYSD bars (Fe500)
7	Size of Columns	900X900 mm
8	Size of Beams	300x500 mm in the longitudinal direction 300x500 mm in the transverse direction
9	Depth of slab	150mm thick
10	The specific weight of RCC	25 kN/m^3
11	Zone	V
12	Importance Factor	1
13	Response Reduction Factor	5
14	Type of soil	Medium

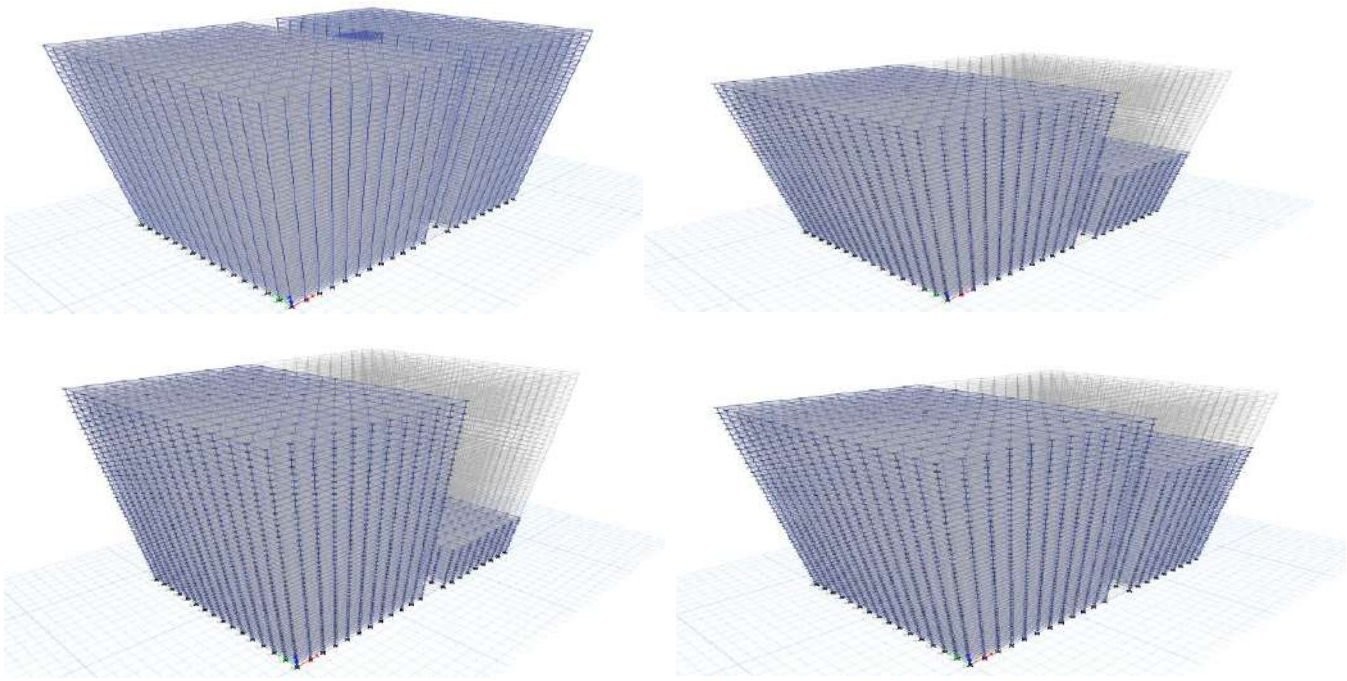

Figure 1: Isometric Views of Model

4. RESULT AND DISCUSSION

The software ETABS is used to analyses the buildings considered in the present work by using non-linear dynamic analysis. Seismic zones II and V are utilized to evaluate the seismic behavior of the structure

STORY DISPLACEMENT				
	top	1/4 TH HEIGHT	3/4 TH HEIGHT	1/2 TH HEIGHT
Base	0	0	0	0
Story1	4.484	5.276	4.594	5.702
Story2	14.992	17.586	15.364	19.06
Story3	28.75	33.653	29.474	36.539
Story4	44.053	51.46	45.182	55.96
Story5	59.813	69.715	61.384	75.935
Story6	75.335	87.565	77.372	95.542
Story7	90.113	104.425	92.641	114.179
Story8	103.837	119.894	106.846	131.41
Story9	116.257	133.698	119.789	146.938
Story10	127.229	145.753	131.28	160.612
Story11	136.668	156.097	141.272	172.341
Story12	144.529	164.732	149.694	182.12
Story13	150.795	171.698	156.568	190.031
Story14	155.486	176.986	161.948	196.235
Story15	158.638	180.657	165.883	200.972
Story16	160.268	182.665	168.456	204.522
Story17	160.447	183.17	169.762	207.129
Story18	159.275	182.447	169.896	208.917
Story19	160.583	180.906	168.933	209.957
Story20	164.909	179.418	166.962	210.281
Story21	168.449	178.805	164.079	209.833
Story22	171.083	178.777	160.41	208.556
Story23	172.735	178.813	156.065	206.413
Story24	173.348	178.307	155.886	203.371
Story25	172.891	176.85	161.173	198.141
Story26	171.364	174.169	166.575	191.284
Story27	175.865	170.159	172.032	183.555
Story28	181.739	167.999	177.468	175.618
Story29	187.553	174.581	182.799	168.344
Story30	193.222	180.979	187.931	174.349
Story31	198.661	187.105	192.775	180.897
Story32	203.792	192.89	197.239	187.114
Story33	208.546	198.275	201.241	192.904
Story34	212.867	207.078	204.702	198.843
Story35	216.716	215.612	208.857	210.399
Story36	220.071	222.802	214.139	222.418
Story37	222.929	228.72	218.962	235.086
Story38	230.486	233.489	223.091	247.592
Story39	241.453	237.316	226.499	259.732
Story40	252.606	240.443	229.328	271.945
Story41	263.451	243.231	231.84	284.242
Story42	273.531	246.063	234.377	295.93
Story43	282.539	249.105	237.179	306.735
Story44	290.251	252.312	240.193	316.383
Story45	296.49	255.477	243.143	324.651
Story46	301.241	258.417	245.981	331.52
Story47	304.662	261.09	251.977	337.249

Table 1 story displacement of twin building with different levels of Sky Bridge for zone 5

STORY DRIFT				
	top	1/4 TH HEIGHT	3/4 TH HEIGHT	1/2 TH HEIGHT
Base	0	0	0	0
Story1	0.001495	0.001759	0.001531	0.001901
Story2	0.003503	0.004105	0.00359	0.004453
Story3	0.004586	0.005359	0.004703	0.005826
Story4	0.005102	0.005937	0.005237	0.006474
Story5	0.005258	0.006086	0.005404	0.00666
Story6	0.005182	0.00595	0.005331	0.006543
Story7	0.004953	0.00562	0.005099	0.006226
Story8	0.004626	0.005158	0.00476	0.00578
Story9	0.004243	0.004612	0.004359	0.005273
Story10	0.003831	0.004036	0.003939	0.004795
Story11	0.003414	0.003463	0.003529	0.004416
Story12	0.003294	0.003635	0.003144	0.004144
Story13	0.00324	0.004616	0.002792	0.003942
Story14	0.00317	0.004536	0.002841	0.003768
Story15	0.003071	0.004591	0.00296	0.003592
Story16	0.002936	0.004631	0.003018	0.003399
Story17	0.002891	0.004545	0.003008	0.003364
Story18	0.002907	0.004327	0.002929	0.00346
Story19	0.003157	0.003993	0.003225	0.003497
Story20	0.003433	0.00438	0.003555	0.003486
Story21	0.003671	0.004856	0.003856	0.003442
Story22	0.003867	0.005266	0.004117	0.003392
Story23	0.004015	0.005599	0.004329	0.003358
Story24	0.004112	0.005843	0.004483	0.00344
Story25	0.004157	0.005996	0.004573	0.004631
Story26	0.004152	0.006052	0.004594	0.005658
Story27	0.004105	0.006013	0.004543	0.006335
Story28	0.004028	0.005885	0.004419	0.006785
Story29	0.003954	0.005674	0.004227	0.007082
Story30	0.003957	0.005515	0.004018	0.007275
Story31	0.004189	0.006036	0.004257	0.007393
Story32	0.004484	0.006484	0.004419	0.007457
Story33	0.004704	0.006853	0.004497	0.007485
Story34	0.004848	0.007136	0.004483	0.007488
Story35	0.004914	0.007327	0.004479	0.007468
Story36	0.004903	0.00742	0.005565	0.007419
Story37	0.004817	0.007409	0.006301	0.00732
Story38	0.004659	0.007287	0.006556	0.007157
Story39	0.004433	0.007051	0.006493	0.006912
Story40	0.004183	0.0067	0.00621	0.006569
Story41	0.003884	0.006236	0.00577	0.006125
Story42	0.00352	0.005668	0.005216	0.005582
Story43	0.003096	0.005013	0.004578	0.004951
Story44	0.002624	0.004296	0.003894	0.004255
Story45	0.002119	0.00356	0.003201	0.003535
Story46	0.001602	0.002868	0.002562	0.002855
Story47	0.001154	0.002352	0.002066	0.002319

Table 2: story drift of twin building with different levels of Sky Bridge for zone 5

TIME PERIOD				
Mode	top	1/4 TH HEIGHT	3/4 TH HEIGHT	1/2 TH HEIGHT
1	6.738	6.509	6.405	6.358
2	6.58	6.157	6.001	5.667
3	6.443	5.907	5.075	4.235
4	2.204	2.142	2.136	2.482
5	2.159	2.098	2.086	2.314
6	2.115	1.993	1.821	2.167
7	1.272	1.444	1.332	1.243
8	1.253	1.302	1.301	1.222
9	1.228	1.276	1.25	1.105
10	0.874	1.22	0.885	0.901
11	0.864	0.959	0.877	0.894
12	0.847	0.911	0.856	0.86

Table 3: Time period of twin building with different levels of Sky Bridge For zone 5

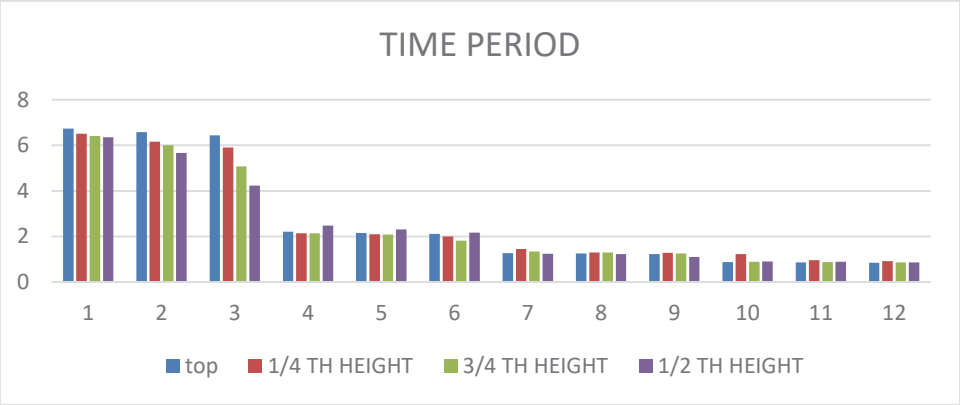

Figure 2: Time period of twin building with different levels of Sky Bridge

	top	1/4 TH HEIGHT	3/4 TH HEIGHT	1/2 TH HEIGHT
BASE SHEAR	113263	121158	125906	137113
BASE MOMENT	4874394	5677180	4984217	6200188

Table 4: Base shear and base moment of twin building with different levels of Sky Bridge for zone 5

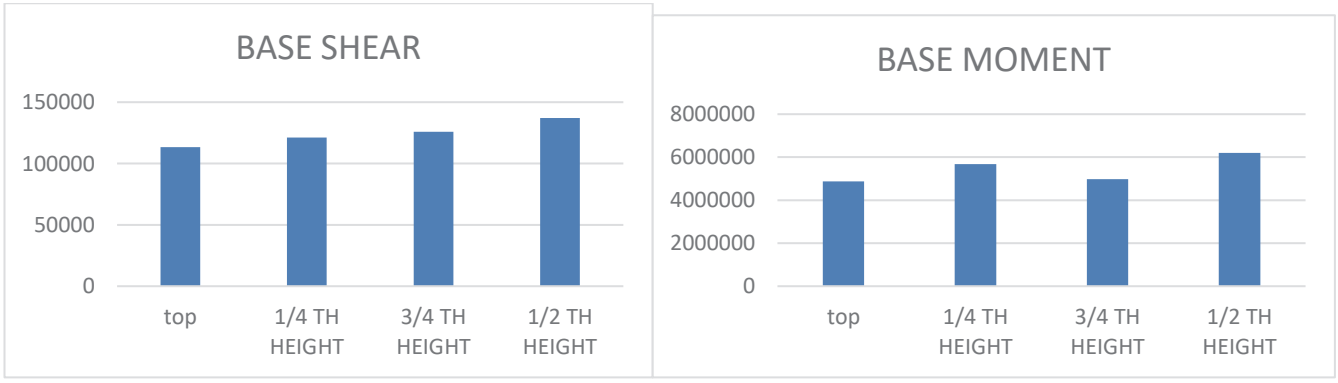

Figure 3: Base shear and base moment of twin building with different levels of Sky Bridge

STORY DISPLACEMENT				
	top	1/4 TH HEIGHT	3/4 TH HEIGHT	1/2 TH HEIGHT
Base	0	0	0	0
Story1	1.168	1.42	1.215	1.531
Story2	3.905	4.731	4.064	5.115
Story3	7.484	9.05	7.792	9.803
Story4	11.459	13.834	11.939	15.007
Story5	15.545	18.732	16.21	20.353
Story6	19.558	23.513	20.415	25.593
Story7	23.366	28.017	24.419	30.564
Story8	26.884	32.136	28.132	35.146
Story9	30.053	35.793	31.497	39.261
Story10	32.831	38.961	34.465	42.864
Story11	35.194	41.648	37.024	45.936
Story12	37.131	43.852	39.156	48.474
Story13	38.643	45.58	40.865	50.501
Story14	39.726	46.837	42.165	52.066
Story15	40.386	47.645	43.075	53.231
Story16	40.636	47.989	43.618	54.075
Story17	40.498	47.92	43.817	54.67
Story18	41.735	47.509	43.695	55.041
Story19	43.092	46.865	43.277	55.217
Story20	44.259	46.21	42.585	55.197
Story21	45.196	45.806	41.647	54.97
Story22	45.881	45.577	40.493	54.521
Story23	46.293	45.379	39.158	53.84
Story24	46.416	45.044	39.945	52.91
Story25	46.241	44.46	41.315	51.361
Story26	45.768	43.55	42.724	49.353
Story27	45.006	42.278	44.153	47.101
Story28	46.487	43.083	45.582	44.798
Story29	48.005	44.813	46.987	43.139
Story30	49.49	46.497	48.342	44.92
Story31	50.917	48.111	49.622	46.644
Story32	52.266	49.63	50.8	48.28
Story33	53.517	51.038	51.854	49.803
Story34	54.656	52.977	52.767	51.193
Story35	55.67	55.281	53.542	52.752
Story36	56.553	57.219	54.835	55.947
Story37	57.306	58.809	56.124	59.338
Story38	58.595	60.092	57.227	62.7
Story39	61.635	61.119	58.143	65.967
Story40	64.76	61.969	58.903	69.247
Story41	67.815	62.739	59.59	72.565
Story42	70.679	63.528	60.297	75.734
Story43	73.243	64.383	61.085	78.667
Story44	75.446	65.281	61.927	81.289
Story45	77.25	66.168	62.745	83.544
Story46	78.634	66.984	63.484	85.415
Story47	79.648	67.727	64.139	86.974

Table 5: Story displacement of twin building with different levels of Sky Bridge for zone 2

STORY DRIFT				
	top	1/4 TH HEIGHT	3/4 TH HEIGHT	1/2 TH HEIGHT
Base	0	0	0	0
Story1	0.000389	0.000473	0.000405	0.00051
Story2	0.000912	0.001104	0.000949	0.001195
Story3	0.001193	0.001441	0.001243	0.001563
Story4	0.001325	0.001595	0.001382	0.001735
Story5	0.001364	0.001633	0.001424	0.001783
Story6	0.00134	0.001594	0.001402	0.001749
Story7	0.001277	0.001502	0.001338	0.001661
Story8	0.001189	0.001373	0.001244	0.001538
Story9	0.001085	0.001222	0.001135	0.001399
Story10	0.000974	0.001061	0.001021	0.001268
Story11	0.000901	0.000904	0.000909	0.001166
Story12	0.000886	0.000938	0.000805	0.001093
Story13	0.000871	0.001193	0.000711	0.00104
Story14	0.000851	0.001177	0.000716	0.000994
Story15	0.000824	0.001195	0.000751	0.000948
Story16	0.000787	0.001208	0.00077	0.000897
Story17	0.000742	0.001186	0.00077	0.000882
Story18	0.000749	0.001127	0.000753	0.000911
Story19	0.000819	0.001036	0.000852	0.000924
Story20	0.000899	0.001166	0.000945	0.000923
Story21	0.000969	0.0013	0.00103	0.000913
Story22	0.001027	0.001415	0.001104	0.000902
Story23	0.001071	0.001509	0.001165	0.000895
Story24	0.001102	0.001579	0.001209	0.00092
Story25	0.001118	0.001623	0.001236	0.001243
Story26	0.00112	0.00164	0.001243	0.001523
Story27	0.001109	0.001631	0.001231	0.001709
Story28	0.00109	0.001597	0.001198	0.001833
Story29	0.001069	0.00154	0.001146	0.001917
Story30	0.001065	0.001476	0.001076	0.001972
Story31	0.001115	0.001624	0.001145	0.002006
Story32	0.00118	0.001751	0.001193	0.002026
Story33	0.001246	0.001856	0.001218	0.002036
Story34	0.001291	0.001937	0.001218	0.00204
Story35	0.001315	0.001993	0.00122	0.002037
Story36	0.001318	0.002022	0.001519	0.002026
Story37	0.0013	0.002022	0.001722	0.002001
Story38	0.001263	0.001991	0.001793	0.001959
Story39	0.001219	0.001929	0.001777	0.001893
Story40	0.00116	0.001834	0.001701	0.001801
Story41	0.001081	0.001708	0.001581	0.00168
Story42	0.000984	0.001553	0.00143	0.001532
Story43	0.000871	0.001374	0.001255	0.001359
Story44	0.000744	0.001178	0.001067	0.001169
Story45	0.000606	0.000976	0.000877	0.000971
Story46	0.000465	0.000786	0.000702	0.000784
Story47	0.000341	0.000644	0.000566	0.000636

Table 6: Story drift of twin building with different levels of Sky Bridge for zone 2

TIME PERIOD				
MODES	top	1/4 TH HEIGHT	3/4 TH HEIGHT	1/2 TH HEIGHT
1	6.763	6.509	6.405	6.358
2	6.601	6.157	6.001	5.667
3	6.449	5.907	5.075	4.235
4	2.212	2.142	2.136	2.482
5	2.166	2.098	2.086	2.314
6	2.117	1.993	1.821	2.167
7	1.277	1.444	1.332	1.243
8	1.258	1.302	1.301	1.222
9	1.23	1.276	1.25	1.105
10	0.878	1.22	0.885	0.901
11	0.867	0.959	0.877	0.894
12	0.847	0.911	0.856	0.86

Table 7: Time period of twin building with different levels of Sky Bridge For zone 2

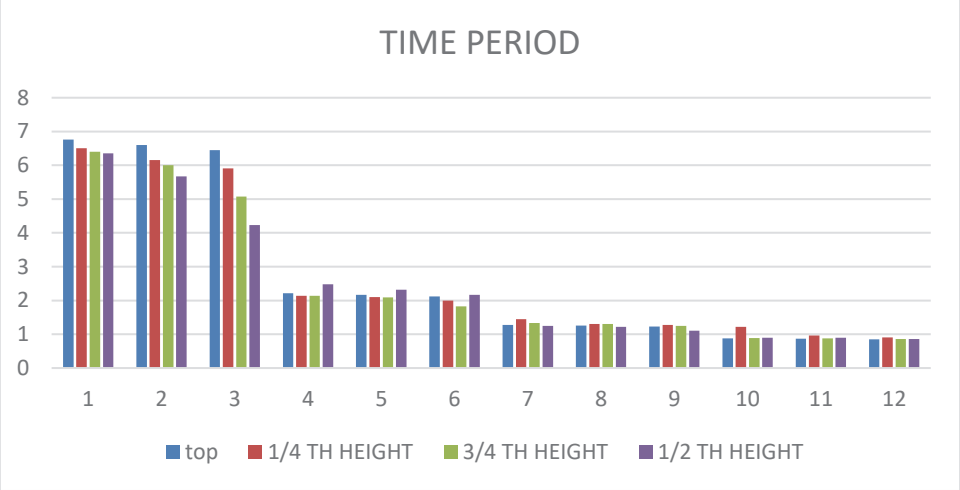

Figure 4: Time period of twin building with different levels of Sky Bridge for zone 2

	top	1/4 TH HEIGHT	3/4 TH HEIGHT	1/2 TH HEIGHT
BASE SHEAR	33462.5	34978	36753.7	39616.5
BASE MOMENT	1272256	1528940	1320370	1666566

Table 8: base shear and base moment of twin building with different levels of Sky Bridge for zone 2

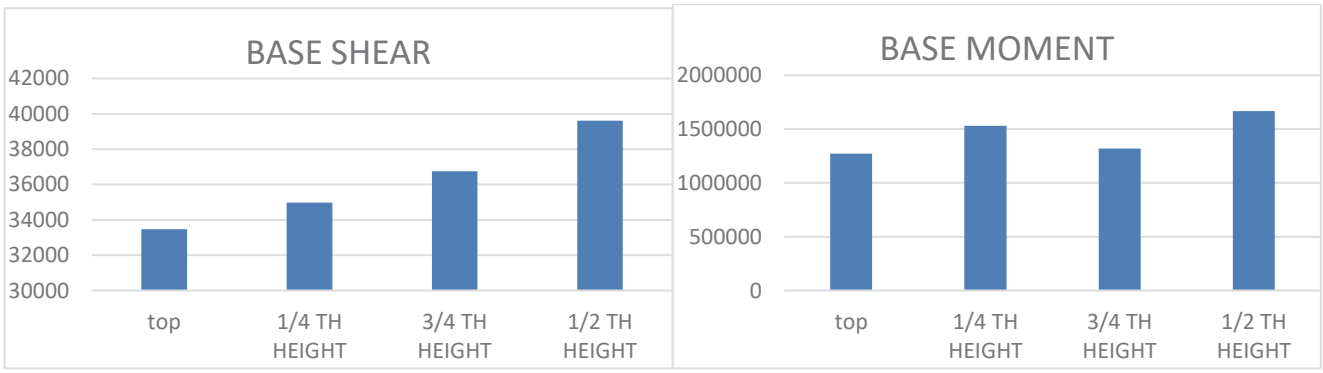

Figure 5.: Base Shear and base moment of twin building with different levels of Sky Bridge for zone 2

5 Conclusions

In this work, the analysis is carried out to study the lateral effect of the structurally coupled buildings connected by sky bridges using earthquake dynamic analysis. The buildings are 45 stories high. The comparisons are drawn between the responses, namely, drift and displacement of connected structures by varying height of connecting building in zone II and zone V. The following conclusions are drawn:

1. From Tables 5.1 and 5.6, it can be observed that for connecting building at $3/4^{th}$ height of the structure has less story displacement compared to other models around 25% and 26.67% reduction in displacement for zone 5 and zone 2 can be obtained. This is because the sky bridge is connected in the X direction so it provides lateral stability in that particular direction.

2. A maximum reduction in drift can be obtained for connecting the building of the same height and the Sky Bridge at the top story. From Tables 5.2 and 5.7, these have 50.93% and 47% reduction in drift values respectively for zone 5 and zone 2.

3. Thus from tables 5.3 and 5.8, overall story shear saw a reduction of 14.7% and 27.37% for connecting building at 3/4 the height.

4. The base shear and base moment for connecting building with same height are less compare to other models we can see in table 5.5 and 5.10, as the connecting building is of same height the response of lateral force are less.

5. The time period of the structure depends on the stiffness of the structure it can be seen that the time period is less for connecting building at 3/4 th height of the structure.

6. From the results it can be seen that connecting building at 3/4 the height has less response is terms of displacement, whereas building with 3/4 height and building with same height has less response and it is effective in both seismic zones II and V.

6.Future scope of the work

The following studies can be done for a more accurate and better understanding of the present study:

- Further studies can be carried out

using a different type of structure like steel-framed structure or shear wall-plate slab structure, etc.

- Wind Dynamic analysis can be carried for a proper understanding of Sky Bridge and across wind behavior of the structure.
- More studies can be done by increasing the overall height of the building so that wind loads govern the design. Also for the same purpose shape of the structure can be changed.
- Moreover, studies can be done by changing earthquake and wind parameters like soil type, terrain category, etc.

REFERENCES

- Abada, G. (2004). "2004 on Site Review Report: Petronas Office Towers, Kuala Lumpur, Malaysia."
- CSI Knowledgebase (2010). "Etabs."< https://wiki.csiamerica.com/display/etabs/Home > (July 3, 2017).
- CSI Knowledge base (2010). "P-Delta Analysis Parameters."
- < https://wiki.csiamerica.com/display/etabs/P-Delta+analysis+parameters> (March 23, 2017).
- CED 38 (10639) WC (Bureau of Indian Standards), 2016.Criteria for Structural Safety of Tall Buildings.
- Davidson, B.J., Fenwick, R.C., and Chung, B.T. (1992). "P-delta effects in multi-story structural design." The 10th World Conference on Earthquake Engineering, Balkema, Rotterdam.
- Engineers, (2010). "The Pinnacle@Duxton." *The Singapore Engineer*, Jun 2010
- Haklar, T. (2009). "10 Fascinating Skybridge."
- <http://www.theworldgeography.com/2013/08/skybridges.html>. (July 3, 2017)
- Holl, S.A. (2009) "Linked Hybrid."
- <http://www.stevenholl.com/projectdetail.php?id=58>. (July 4, 2017).
- IRC: 6 (Indian Roads Congress). 2014. Standard Specifications and Code of Practice for Road Bridges. Section-II Loads and Stresses.
- IS 1893 (Bureau of Indian Standards). 2002. Indian Standard Criteria for Earthquake Resistant Design of Structures. Part 1 General Provisions and Buildings (Fifth Revision).

- IS 875 (Bureau of Indian Standards). 1989. Indian Standard Code of Practice for Design Loads for Buildings and Structures. Part 1 Dead loads- Unit Weights of Building Materials and Stored Materials (Second Revision).
- IS 875 (Bureau of Indian Standards). 1989. Indian Standard Code of Practice for Design Loads for Buildings and Structures. Part 3 Wind Loads (Second Revision)
- Kareem, A., Kijewski, T., and Tamura, X., (1999). “Mitigation of Motions of Tall Buildings with Specific Examples of Recent Applications” *Wind and Structures*. 2(3), 201-251.
- Kheyari, P., Dalui, S.K. (2015). “Estimation of Wind Load on a Tall Building under Interference effects: A Case Study.” Jordan Journal of Civil Engineering. 9(1).
- Kim, W., Tamura, Y., and Yoshida, A., (2009). “Interference effects of Two Buildings on Peak Wind Pressures.” The Seventh Asia-Pacific Conference on Wind Engineering, Taipei, Taiwan.
- Kiran, M. U, Shivananda, S. M., and Mahantesha, O. (2016). “A Study of Lateral Drift Controlling Between Two Buildings by Connecting Sky Bridge.” International Journal of Civil and Structural Engineering Research. 4(1), 266-273.
- Lu, X. (2009). "Shaking table model tests on a complex high-rise building with two towers of different height connected by trusses." Structural Design of Tall and Special Buildings, 18(7), 765-788.
- Luong, A., and Kwok, M. (2012). "Finding Structural Solutions by Connecting Towers."
- *CTBUH Journal* (III), 26-31.
- McCall, A. J.T. (2013). "Structural Analysis and Optimization of Skyscrapers Connected with Skybridge and Atria”. *All Theses and Dissertations.* Paper 3829.
- Ming, L. J., Suan, T. P., and Toh, W. (2010). "HDB's next generation of eco-districts at Punggol and eco-modernization of existing towns." *The IES Journal Part A: Civil & Structural Engineering*, 3(3), 203-209.
- New Scientist (2006). "No way out?" New Scientist, 189(2538), 40-43.
- Nishimura, A. (2011). "Base-isolated super high-rise RC building composed of three connected towers with vibration control systems." Structural Concrete, 12(2), 94-108.
- Seima. (2012). “Shanghai World Financial Center at Night.”

BEHAVIOUR OF MULTISTOREYS RC BUILDING WITH SKY-BRIDGE UNDER THE SESMIC EFFECT.

ASST PROF HUZAIFA YAMAN

Department of Civil Engineering

NSAKCET, India

ABDUL MOIZ

Department of Civil Engineering

NSAKCET, India

ABSTRACT

The need for high-rise buildings is inevitable while the land in the rapidly developing towns and cities is becoming scarce due to increasing population numbers. Apart from the scarcity of the land, some part of our world is always hit by natural disasters such as earthquake, hurricane, tornado, tsunami, etc. Sky-bridges serve that need. Sky-bridges between buildings are becoming common, and its effect on structural behavior and design need to be understood. Responses to earthquake lateral loads are one of the guiding factors of the structural design. Current trends include horizontally connecting adjacent high buildings for various purposes. In this project, Twin RCC structures are considered with the connecting bridge in seismic zone V and II, and the story of the structure is G+45. The analysis is done by considering earthquake loads with the effect of sky-bridge at different levels. And after analyzing the above structure the Displacement, story drift, time period, are compared. A comparison of various design parameters is also done and interesting results have been obtained.

1.INTRODUCTION: The need for high-rise buildings is inevitable as land in fast-growing towns and cities become scarce as the population is growing. In addition to the scarcity of land, natural disasters like earthquakes, hurricanes, tornadoes, tsunamis, etc. continue to affect some parts of the world. These earthquakes are caused by the sudden movement of the earth's tectonic plate. The movement occurs on fault lines and the released energy is transferred by the earth in the form of waves that cause soil movement many miles from the epicenter. Regions next to active fault lines are the most susceptible to earthquakes.

The present work aims at the following objectives:

- Study of Seismic demands of regular R.C twin buildings using the dynamic analysis.
- To study the effect of connecting bridge at different levels by varying the height of connecting building.
- To illustrate the effects of seismic zone V and II, on the response of the Twin connected Buildings.
- To study various responses such as story shear, story displacement, inter-story drift, time period, etc. of buildings

2 LITERATURE REVIEW

- **Sayed Mahmoud (2019):** Reactions to lateral charges triggered by wind and earthquakes are among the main factors in the design of these structures. In the most recent design, neighbouring high buildings for different purposes are horizontally linked. However, such horizontal connexions can change the behavior of the structure, limiting the validity of design codes. In this paper, the response of connected high-rise structures under quake loads will be thoroughly

examined according to design code criteria. It is also investigated the impact of placing only the sky-bridge on the inducted responses. The building configurations were excited by the collection of ground movement data from various top speeds. The connecting location of the bridge affected the predicted dynamic responses from the building systems, but dramatically in some cases.

- **Imad Shakir Abood (2018):** In this paper, the effect of structural relations on earthquake responses was discussed using the finite element modelling technique for a connected building system. For this study, double 40-story Rcc frame-wall buildings, linked horizontally by longitudinal ties, depict the linked building system. It is believed that the two adjacent buildings were similar in this related building system so that an inter-story connexion might carry the two adjacent stories to the very same level. The linked tower system is designed as a rigid tower floor diaphragm and fixed to the structural perimeter of the buildings as a framework for each link.

- **Verma (2014)** The wind pressure coefficients for Sky Bridge were determined by studies performed for rectangular tall buildings on rigid models with incidence angles of 0 °, 45 °, and 90 °. "The models were tested at the Civil Engineering Department of the Indian Technology Institute Roorkee in the Closed Circuit Wind tunnel with a 1.3 m (width) x0.85 m (height) cross-section. Perspex sheet 5 mm thick is used for the manufacture of two construction models, each of which has square design of 50 mm to 50 mm in size to 300 mm. The study showed that negative pressure on the opposite faces is significantly increased when models are close.

3. CASE STUDY

The Layout of the plan having20x16 bays of equal length of 6m. The buildings considered are Reinforced concrete ordinary moment-resisting space frames of 42 story symmetric. The stiffness of the infill is neglected to account for the Nonlinear Behavior of Seismic demands. All these buildings have been analyzed by the NLTHA method. The story height is kept uniform of 3m for all kinds of building models which are as below. The analysis illustrates the step-by-step procedure for the determination of forces.

The Plan configuration consists of

1. Model 1 – Twin connecting building with the same height
2. Model 2 –. Twin connecting building for one building at 1/2 height
3. Model 3 –. Twin connecting building for one building at 1/4 height
4. . Model 4 –. Twin connecting building for one building at 3/4 height

Sl.no	Variable	Data
1	Type of structure	Moment Resisting Frame
2	Number of Stories	42
3	Floor height	3m
4	Live Load	3.0 kN/m^2
5	WALL load	10KN/m
6	Materials	Concrete (M30) and Reinforced with HYSD bars (Fe500)
7	Size of Columns	900X900 mm
8	Size of Beams	300x500 mm in the longitudinal direction 300x500 mm in the transverse direction
9	Depth of slab	150mm thick
10	The specific weight of RCC	25 kN/m^3
11	Zone	V
12	Importance Factor	1
13	Response Reduction Factor	5
14	Type of soil	Medium

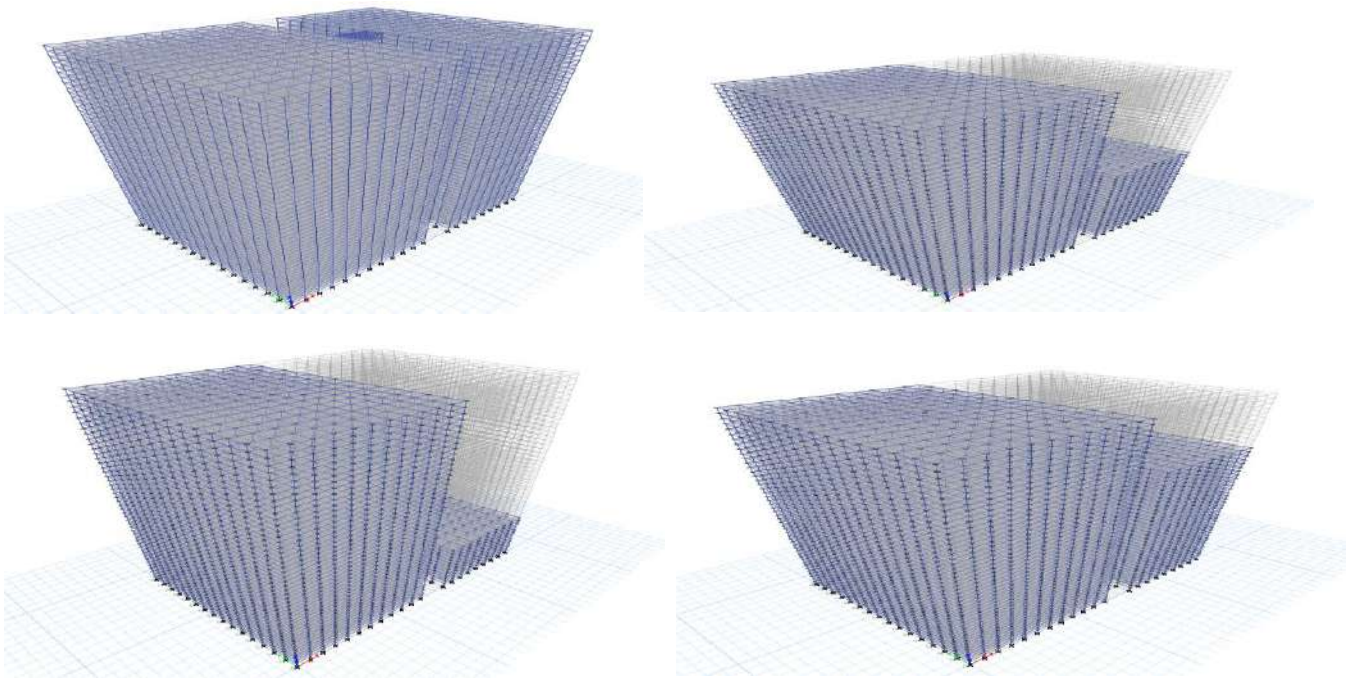

Figure 1: Isometric Views of Model

4. RESULT AND DISCUSSION

The software ETABS is used to analyses the buildings considered in the present work by using non-linear dynamic analysis. Seismic zones II and V are utilized to evaluate the seismic behavior of the structure

STORY DISPLACEMENT				
	top	1/4 TH HEIGHT	3/4 TH HEIGHT	1/2 TH HEIGHT
Base	0	0	0	0
Story1	4.484	5.276	4.594	5.702
Story2	14.992	17.586	15.364	19.06
Story3	28.75	33.653	29.474	36.539
Story4	44.053	51.46	45.182	55.96
Story5	59.813	69.715	61.384	75.935
Story6	75.335	87.565	77.372	95.542
Story7	90.113	104.425	92.641	114.179
Story8	103.837	119.894	106.846	131.41
Story9	116.257	133.698	119.789	146.938
Story10	127.229	145.753	131.28	160.612
Story11	136.668	156.097	141.272	172.341
Story12	144.529	164.732	149.694	182.12
Story13	150.795	171.698	156.568	190.031
Story14	155.486	176.986	161.948	196.235
Story15	158.638	180.657	165.883	200.972
Story16	160.268	182.665	168.456	204.522
Story17	160.447	183.17	169.762	207.129
Story18	159.275	182.447	169.896	208.917
Story19	160.583	180.906	168.933	209.957
Story20	164.909	179.418	166.962	210.281
Story21	168.449	178.805	164.079	209.833
Story22	171.083	178.777	160.41	208.556
Story23	172.735	178.813	156.065	206.413
Story24	173.348	178.307	155.886	203.371
Story25	172.891	176.85	161.173	198.141
Story26	171.364	174.169	166.575	191.284
Story27	175.865	170.159	172.032	183.555
Story28	181.739	167.999	177.468	175.618
Story29	187.553	174.581	182.799	168.344
Story30	193.222	180.979	187.931	174.349
Story31	198.661	187.105	192.775	180.897
Story32	203.792	192.89	197.239	187.114
Story33	208.546	198.275	201.241	192.904
Story34	212.867	207.078	204.702	198.843
Story35	216.716	215.612	208.857	210.399
Story36	220.071	222.802	214.139	222.418
Story37	222.929	228.72	218.962	235.086
Story38	230.486	233.489	223.091	247.592
Story39	241.453	237.316	226.499	259.732
Story40	252.606	240.443	229.328	271.945
Story41	263.451	243.231	231.84	284.242
Story42	273.531	246.063	234.377	295.93
Story43	282.539	249.105	237.179	306.735
Story44	290.251	252.312	240.193	316.383
Story45	296.49	255.477	243.143	324.651
Story46	301.241	258.417	245.981	331.52
Story47	304.662	261.09	251.977	337.249

Table 1 story displacement of twin building with different levels of Sky Bridge for zone 5

STORY DRIFT				
	top	1/4 TH HEIGHT	3/4 TH HEIGHT	1/2 TH HEIGHT
Base	0	0	0	0
Story1	0.001495	0.001759	0.001531	0.001901
Story2	0.003503	0.004105	0.00359	0.004453
Story3	0.004586	0.005359	0.004703	0.005826
Story4	0.005102	0.005937	0.005237	0.006474
Story5	0.005258	0.006086	0.005404	0.00666
Story6	0.005182	0.00595	0.005331	0.006543
Story7	0.004953	0.00562	0.005099	0.006226
Story8	0.004626	0.005158	0.00476	0.00578
Story9	0.004243	0.004612	0.004359	0.005273
Story10	0.003831	0.004036	0.003939	0.004795
Story11	0.003414	0.003463	0.003529	0.004416
Story12	0.003294	0.003635	0.003144	0.004144
Story13	0.00324	0.004616	0.002792	0.003942
Story14	0.00317	0.004536	0.002841	0.003768
Story15	0.003071	0.004591	0.00296	0.003592
Story16	0.002936	0.004631	0.003018	0.003399
Story17	0.002891	0.004545	0.003008	0.003364
Story18	0.002907	0.004327	0.002929	0.00346
Story19	0.003157	0.003993	0.003225	0.003497
Story20	0.003433	0.00438	0.003555	0.003486
Story21	0.003671	0.004856	0.003856	0.003442
Story22	0.003867	0.005266	0.004117	0.003392
Story23	0.004015	0.005599	0.004329	0.003358
Story24	0.004112	0.005843	0.004483	0.00344
Story25	0.004157	0.005996	0.004573	0.004631
Story26	0.004152	0.006052	0.004594	0.005658
Story27	0.004105	0.006013	0.004543	0.006335
Story28	0.004028	0.005885	0.004419	0.006785
Story29	0.003954	0.005674	0.004227	0.007082
Story30	0.003957	0.005515	0.004018	0.007275
Story31	0.004189	0.006036	0.004257	0.007393
Story32	0.004484	0.006484	0.004419	0.007457
Story33	0.004704	0.006853	0.004497	0.007485
Story34	0.004848	0.007136	0.004483	0.007488
Story35	0.004914	0.007327	0.004479	0.007468
Story36	0.004903	0.00742	0.005565	0.007419
Story37	0.004817	0.007409	0.006301	0.00732
Story38	0.004659	0.007287	0.006556	0.007157
Story39	0.004433	0.007051	0.006493	0.006912
Story40	0.004183	0.0067	0.00621	0.006569
Story41	0.003884	0.006236	0.00577	0.006125
Story42	0.00352	0.005668	0.005216	0.005582
Story43	0.003096	0.005013	0.004578	0.004951
Story44	0.002624	0.004296	0.003894	0.004255
Story45	0.002119	0.00356	0.003201	0.003535
Story46	0.001602	0.002868	0.002562	0.002855
Story47	0.001154	0.002352	0.002066	0.002319

Table 2: story drift of twin building with different levels of Sky Bridge for zone 5

TIME PERIOD				
Mode	top	1/4 TH HEIGHT	3/4 TH HEIGHT	1/2 TH HEIGHT
1	6.738	6.509	6.405	6.358
2	6.58	6.157	6.001	5.667
3	6.443	5.907	5.075	4.235
4	2.204	2.142	2.136	2.482
5	2.159	2.098	2.086	2.314
6	2.115	1.993	1.821	2.167
7	1.272	1.444	1.332	1.243
8	1.253	1.302	1.301	1.222
9	1.228	1.276	1.25	1.105
10	0.874	1.22	0.885	0.901
11	0.864	0.959	0.877	0.894
12	0.847	0.911	0.856	0.86

Table 3: Time period of twin building with different levels of Sky Bridge For zone 5

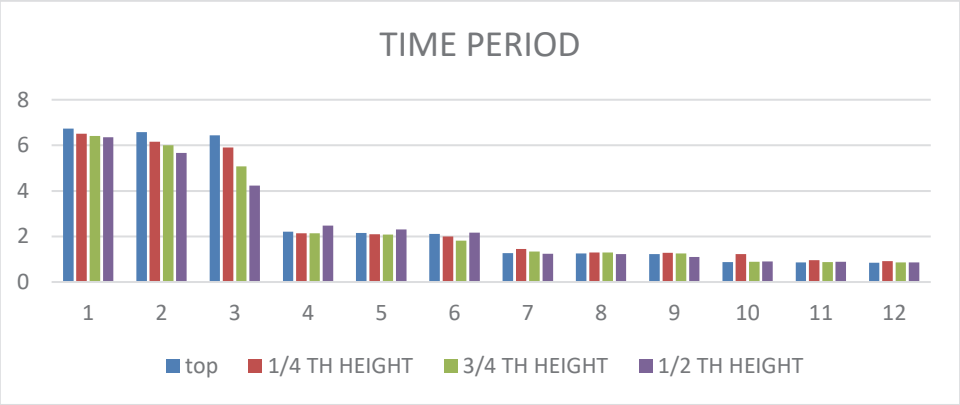

Figure 2: Time period of twin building with different levels of Sky Bridge

	top	1/4 TH HEIGHT	3/4 TH HEIGHT	1/2 TH HEIGHT
BASE SHEAR	113263	121158	125906	137113
BASE MOMENT	4874394	5677180	4984217	6200188

Table 4: Base shear and base moment of twin building with different levels of Sky Bridge for zone 5

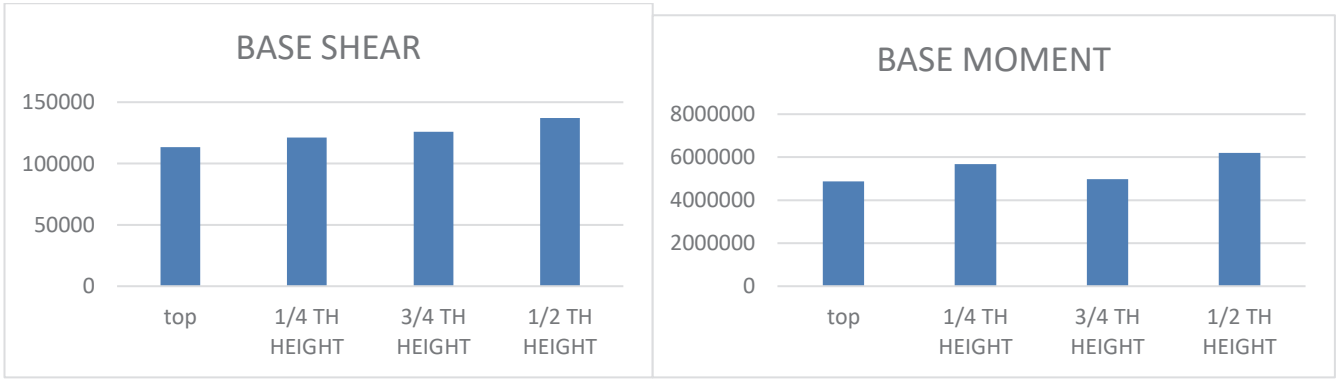

Figure 3: Base shear and base moment of twin building with different levels of Sky Bridge

STORY DISPLACEMENT				
	top	1/4 TH HEIGHT	3/4 TH HEIGHT	1/2 TH HEIGHT
Base	0	0	0	0
Story1	1.168	1.42	1.215	1.531
Story2	3.905	4.731	4.064	5.115
Story3	7.484	9.05	7.792	9.803
Story4	11.459	13.834	11.939	15.007
Story5	15.545	18.732	16.21	20.353
Story6	19.558	23.513	20.415	25.593
Story7	23.366	28.017	24.419	30.564
Story8	26.884	32.136	28.132	35.146
Story9	30.053	35.793	31.497	39.261
Story10	32.831	38.961	34.465	42.864
Story11	35.194	41.648	37.024	45.936
Story12	37.131	43.852	39.156	48.474
Story13	38.643	45.58	40.865	50.501
Story14	39.726	46.837	42.165	52.066
Story15	40.386	47.645	43.075	53.231
Story16	40.636	47.989	43.618	54.075
Story17	40.498	47.92	43.817	54.67
Story18	41.735	47.509	43.695	55.041
Story19	43.092	46.865	43.277	55.217
Story20	44.259	46.21	42.585	55.197
Story21	45.196	45.806	41.647	54.97
Story22	45.881	45.577	40.493	54.521
Story23	46.293	45.379	39.158	53.84
Story24	46.416	45.044	39.945	52.91
Story25	46.241	44.46	41.315	51.361
Story26	45.768	43.55	42.724	49.353
Story27	45.006	42.278	44.153	47.101
Story28	46.487	43.083	45.582	44.798
Story29	48.005	44.813	46.987	43.139
Story30	49.49	46.497	48.342	44.92
Story31	50.917	48.111	49.622	46.644
Story32	52.266	49.63	50.8	48.28
Story33	53.517	51.038	51.854	49.803
Story34	54.656	52.977	52.767	51.193
Story35	55.67	55.281	53.542	52.752
Story36	56.553	57.219	54.835	55.947
Story37	57.306	58.809	56.124	59.338
Story38	58.595	60.092	57.227	62.7
Story39	61.635	61.119	58.143	65.967
Story40	64.76	61.969	58.903	69.247
Story41	67.815	62.739	59.59	72.565
Story42	70.679	63.528	60.297	75.734
Story43	73.243	64.383	61.085	78.667
Story44	75.446	65.281	61.927	81.289
Story45	77.25	66.168	62.745	83.544
Story46	78.634	66.984	63.484	85.415
Story47	79.648	67.727	64.139	86.974

Table 5: Story displacement of twin building with different levels of Sky Bridge for zone 2

STORY DRIFT				
	top	1/4 TH HEIGHT	3/4 TH HEIGHT	1/2 TH HEIGHT
Base	0	0	0	0
Story1	0.000389	0.000473	0.000405	0.00051
Story2	0.000912	0.001104	0.000949	0.001195
Story3	0.001193	0.001441	0.001243	0.001563
Story4	0.001325	0.001595	0.001382	0.001735
Story5	0.001364	0.001633	0.001424	0.001783
Story6	0.00134	0.001594	0.001402	0.001749
Story7	0.001277	0.001502	0.001338	0.001661
Story8	0.001189	0.001373	0.001244	0.001538
Story9	0.001085	0.001222	0.001135	0.001399
Story10	0.000974	0.001061	0.001021	0.001268
Story11	0.000901	0.000904	0.000909	0.001166
Story12	0.000886	0.000938	0.000805	0.001093
Story13	0.000871	0.001193	0.000711	0.00104
Story14	0.000851	0.001177	0.000716	0.000994
Story15	0.000824	0.001195	0.000751	0.000948
Story16	0.000787	0.001208	0.00077	0.000897
Story17	0.000742	0.001186	0.00077	0.000882
Story18	0.000749	0.001127	0.000753	0.000911
Story19	0.000819	0.001036	0.000852	0.000924
Story20	0.000899	0.001166	0.000945	0.000923
Story21	0.000969	0.0013	0.00103	0.000913
Story22	0.001027	0.001415	0.001104	0.000902
Story23	0.001071	0.001509	0.001165	0.000895
Story24	0.001102	0.001579	0.001209	0.00092
Story25	0.001118	0.001623	0.001236	0.001243
Story26	0.00112	0.00164	0.001243	0.001523
Story27	0.001109	0.001631	0.001231	0.001709
Story28	0.00109	0.001597	0.001198	0.001833
Story29	0.001069	0.00154	0.001146	0.001917
Story30	0.001065	0.001476	0.001076	0.001972
Story31	0.001115	0.001624	0.001145	0.002006
Story32	0.00118	0.001751	0.001193	0.002026
Story33	0.001246	0.001856	0.001218	0.002036
Story34	0.001291	0.001937	0.001218	0.00204
Story35	0.001315	0.001993	0.00122	0.002037
Story36	0.001318	0.002022	0.001519	0.002026
Story37	0.0013	0.002022	0.001722	0.002001
Story38	0.001263	0.001991	0.001793	0.001959
Story39	0.001219	0.001929	0.001777	0.001893
Story40	0.00116	0.001834	0.001701	0.001801
Story41	0.001081	0.001708	0.001581	0.00168
Story42	0.000984	0.001553	0.00143	0.001532
Story43	0.000871	0.001374	0.001255	0.001359
Story44	0.000744	0.001178	0.001067	0.001169
Story45	0.000606	0.000976	0.000877	0.000971
Story46	0.000465	0.000786	0.000702	0.000784
Story47	0.000341	0.000644	0.000566	0.000636

Table 6: Story drift of twin building with different levels of Sky Bridge for zone 2

TIME PERIOD				
MODES	top	1/4 TH HEIGHT	3/4 TH HEIGHT	1/2 TH HEIGHT
1	6.763	6.509	6.405	6.358
2	6.601	6.157	6.001	5.667
3	6.449	5.907	5.075	4.235
4	2.212	2.142	2.136	2.482
5	2.166	2.098	2.086	2.314
6	2.117	1.993	1.821	2.167
7	1.277	1.444	1.332	1.243
8	1.258	1.302	1.301	1.222
9	1.23	1.276	1.25	1.105
10	0.878	1.22	0.885	0.901
11	0.867	0.959	0.877	0.894
12	0.847	0.911	0.856	0.86

Table 7: Time period of twin building with different levels of Sky Bridge For zone 2

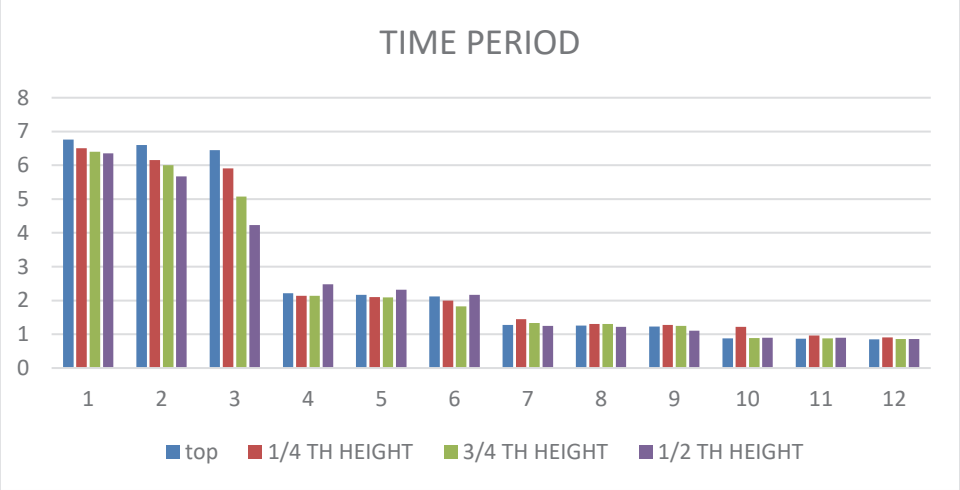

Figure 4: Time period of twin building with different levels of Sky Bridge for zone 2

	top	1/4 TH HEIGHT	3/4 TH HEIGHT	1/2 TH HEIGHT
BASE SHEAR	33462.5	34978	36753.7	39616.5
BASE MOMENT	1272256	1528940	1320370	1666566

Table 8: base shear and base moment of twin building with different levels of Sky Bridge for zone 2

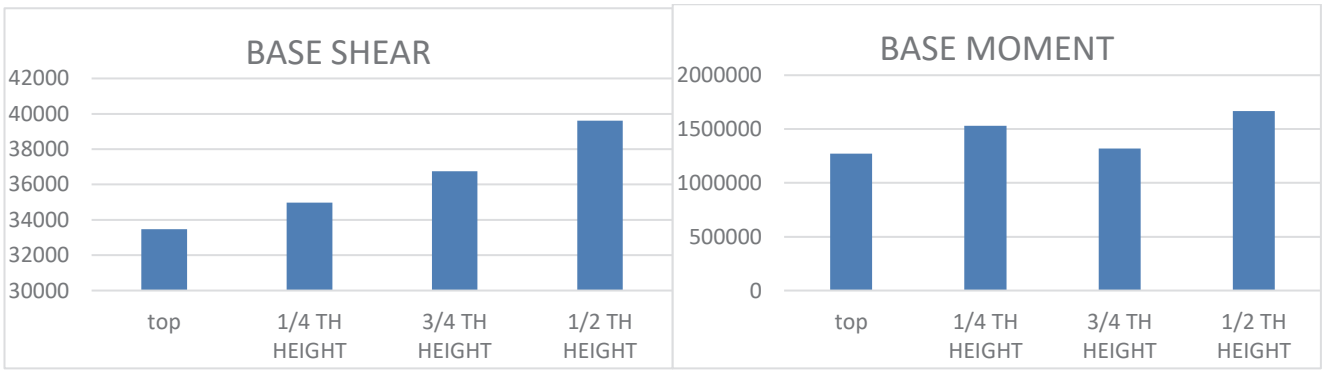

Figure 5.: Base Shear and base moment of twin building with different levels of Sky Bridge for zone 2

5 Conclusions

In this work, the analysis is carried out to study the lateral effect of the structurally coupled buildings connected by sky bridges using earthquake dynamic analysis. The buildings are 45 stories high. The comparisons are drawn between the responses, namely, drift and displacement of connected structures by varying height of connecting building in zone II and zone V. The following conclusions are drawn:

1. From Tables 5.1 and 5.6, it can be observed that for connecting building at $3/4^{th}$ height of the structure has less story displacement compared to other models around 25% and 26.67% reduction in displacement for zone 5 and zone 2 can be obtained. This is because the sky bridge is connected in the X direction so it provides lateral stability in that particular direction.

2. A maximum reduction in drift can be obtained for connecting the building of the same height and the Sky Bridge at the top story. From Tables 5.2 and 5.7, these have 50.93% and 47% reduction in drift values respectively for zone 5 and zone 2.

3. Thus from tables 5.3 and 5.8, overall story shear saw a reduction of 14.7% and 27.37% for connecting building at 3/4 the height.

4. The base shear and base moment for connecting building with same height are less compare to other models we can see in table 5.5 and 5.10, as the connecting building is of same height the response of lateral force are less.

5. The time period of the structure depends on the stiffness of the structure it can be seen that the time period is less for connecting building at 3/4 th height of the structure.

6. From the results it can be seen that connecting building at 3/4 the height has less response is terms of displacement, whereas building with 3/4 height and building with same height has less response and it is effective in both seismic zones II and V.

6.Future scope of the work

The following studies can be done for a more accurate and better understanding of the present study:

- Further studies can be carried out

using a different type of structure like steel-framed structure or shear wall-plate slab structure, etc.

- Wind Dynamic analysis can be carried for a proper understanding of Sky Bridge and across wind behavior of the structure.
- More studies can be done by increasing the overall height of the building so that wind loads govern the design. Also for the same purpose shape of the structure can be changed.
- Moreover, studies can be done by changing earthquake and wind parameters like soil type, terrain category, etc.

REFERENCES

- Abada, G. (2004). "2004 on Site Review Report: Petronas Office Towers, Kuala Lumpur, Malaysia."
- CSI Knowledgebase (2010). "Etabs."< https://wiki.csiamerica.com/display/etabs/Home > (July 3, 2017).
- CSI Knowledge base (2010). "P-Delta Analysis Parameters."
- < https://wiki.csiamerica.com/display/etabs/P-Delta+analysis+parameters> (March 23, 2017).
- CED 38 (10639) WC (Bureau of Indian Standards), 2016.Criteria for Structural Safety of Tall Buildings.
- Davidson, B.J., Fenwick, R.C., and Chung, B.T. (1992). "P-delta effects in multi-story structural design." The 10th World Conference on Earthquake Engineering, Balkema, Rotterdam.
- Engineers, (2010). "The Pinnacle@Duxton." *The Singapore Engineer*, Jun 2010
- Haklar, T. (2009). "10 Fascinating Skybridge."
- <http://www.theworldgeography.com/2013/08/skybridges.html>. (July 3, 2017)
- Holl, S.A. (2009) "Linked Hybrid."
- <http://www.stevenholl.com/projectdetail.php?id=58>. (July 4, 2017).
- IRC: 6 (Indian Roads Congress). 2014. Standard Specifications and Code of Practice for Road Bridges. Section-II Loads and Stresses.
- IS 1893 (Bureau of Indian Standards). 2002. Indian Standard Criteria for Earthquake Resistant Design of Structures. Part 1 General Provisions and Buildings (Fifth Revision).

- IS 875 (Bureau of Indian Standards). 1989. Indian Standard Code of Practice for Design Loads for Buildings and Structures. Part 1 Dead loads- Unit Weights of Building Materials and Stored Materials (Second Revision).
- IS 875 (Bureau of Indian Standards). 1989. Indian Standard Code of Practice for Design Loads for Buildings and Structures. Part 3 Wind Loads (Second Revision)
- Kareem, A., Kijewski, T., and Tamura, X., (1999). “Mitigation of Motions of Tall Buildings with Specific Examples of Recent Applications” *Wind and Structures*. 2(3), 201-251.
- Kheyari, P., Dalui, S.K. (2015). “Estimation of Wind Load on a Tall Building under Interference effects: A Case Study.” Jordan Journal of Civil Engineering. 9(1).
- Kim, W., Tamura, Y., and Yoshida, A., (2009). “Interference effects of Two Buildings on Peak Wind Pressures.” The Seventh Asia-Pacific Conference on Wind Engineering, Taipei, Taiwan.
- Kiran, M. U, Shivananda, S. M., and Mahantesha, O. (2016). “A Study of Lateral Drift Controlling Between Two Buildings by Connecting Sky Bridge.” International Journal of Civil and Structural Engineering Research. 4(1), 266-273.
- Lu, X. (2009). "Shaking table model tests on a complex high-rise building with two towers of different height connected by trusses." Structural Design of Tall and Special Buildings, 18(7), 765-788.
- Luong, A., and Kwok, M. (2012). "Finding Structural Solutions by Connecting Towers."
- *CTBUH Journal* (III), 26-31.
- McCall, A. J.T. (2013). "Structural Analysis and Optimization of Skyscrapers Connected with Skybridge and Atria”. *All Theses and Dissertations.* Paper 3829.
- Ming, L. J., Suan, T. P., and Toh, W. (2010). "HDB's next generation of eco-districts at Punggol and eco-modernization of existing towns." *The IES Journal Part A: Civil & Structural Engineering*, 3(3), 203-209.
- New Scientist (2006). "No way out?" New Scientist, 189(2538), 40-43.
- Nishimura, A. (2011). "Base-isolated super high-rise RC building composed of three connected towers with vibration control systems." Structural Concrete, 12(2), 94-108.
- Seima. (2012). “Shanghai World Financial Center at Night.”

AN EXPERIMENTAL INVESTIGATION ON HIGH STRENGTH BINARY BLENDED POLYMER HYBRID CONCRETE USING POLYCARBOXYLATE SUPER PLASTICIZER

MOHD AHMED[1] & MOHD ZAKER[2]

[1]*PG Student, Department of Civil Engineering, Nawab Shah Alam Khan College Of Engineering & Technology, Hyderabad India.*

[2]*Assistant Professor, Department of Civil Engineering, Nawab Shah Alam Khan College Of Engineering & Technology, Hyderabad India.*

ABSTRACT

Concrete the worlds most consumed material after water on the earth planet. Concrete is the material which is said to be strong in compression and weak in the tension. Steel is the ductile material to withstand tension in the concrete. Cement is the non-acidic and alkaline which prevent the steel from corrosion. The main focus on this experimental study in the past is made to make concrete strong in tension with less use of steel and with the use of some replacements. The Steel crimped fibre are said to be used to improve the properties of concrete which have the improvement to the age factor of concrete. The use of Polypropylene fibre to improve the flexural property in the concrete. Past Experimental studies by some of the past researchers. The use of polycarboxylate superplasticizers to improve the workability and to reduce the water content in the concrete and improve the compressive strength with the emphases on the different properties of concrete to overcome the different botheration in concrete. In this undertaking to be centre around attributes quality of solid evaluation of cement with various corresponding of supplanting of concrete with and we including pleated steel fibre. To utilizing steel fibre, improve the flexural quality of cement in various variety blend. The solid of blend to be casted with steel fibre and without steel fibre in vary rates 0%,0.6% 1.6% 2.2% and 3.3%. To believe the expense of development to be examine.

KEYWORDS: Hybrid Fibre, Polypropylene Fibre, Steel Fibre Concrete, Polycarboxylate.

INTRODUCTION

Concrete is by far the most widely used construction material today. It is versatile, has desirable engineering properties, can be moulded into any shapes and more importantly is produced with cost-effective materials. There is an old saying that broken stone, sand, and cement make good concrete. But the same proportion of broken stone, sand and cement also make bad concrete. To make good concrete now variety of innovative materials such as fibres, admixtures and construction chemicals, pozzolanas and different concrete making techniques are adopted in present day construction. In recent years, intensive research has resulted in advances and innovation in the technology of fibres such as glass, polypropylene, carbon etc., and more basic knowledge has been gained on the behaviour of cement concrete containing these fibres. Concrete containing hydraulic cement, water, aggregate, and discontinuous discrete fibres is called fibre-reinforced concrete. The incorporation of short discrete fibres (steel, polypropylene, glass, carbon) can lead to useful improvements in the mechanical behaviour of tension weak concrete.

OBJECTIVE

The main aim of this experiment is to study the strength properties of steel fibre and polypropylene fibre reinforced concrete with 0%, 0.6%, 1.6%, 2.2amd 3.3% by volume of concrete. The strength properties of fibre reinforced concrete are compared with normal concrete (reference mix) without any fibres.

MATERIALS AND METHODOLOGY

Constituent Materials Used

Cement

In this experiment 53 grade ordinary Portland cement (OPC) with brand name Ultra Tech Cement was used for all concrete mixes. The physical properties of cement used are as given in table.1.

Table 1: Physical Properties of Cement

Sl. No	Properties	Value	IS Specification and Test Procedure
1	Specific gravity	3.125	IS:4031
2	Fineness modulus	2%	IS:4031 & IS269
3	Initial Setting time in minutes	60	>30, IS:4031 & IS269
4	Final Setting time in minutes	260	<600, IS:4031 & IS269

Fine Aggregate

The fine aggregate used for the study was manufactured sand which was free from deleterious materials like clay, silt content and chloride contamination. The physical properties of fine aggregate used are as given in table.2.

Table 2: Physical Properties of Fine Aggregate

Sl No.	Properties	Value
1	Specific gravity	2.67
2	Fineness modulus	2.69
3	Grading of sand	zone II

Coarse Aggregate

The coarse aggregates used for the work is of 20mm and 12mm size which is free from deleterious materials like clay, silt content and chloride contamination.

Table 3: Physical Properties of Coarse Aggregate

Sl No.	Properties	Value
1	Specific gravity	2.49
2	Fineness modulus	4.66

Water

Clean potable tap water available in the laboratory, which satisfies drinking standards, was used for the preparation of specimens and for the curing of specimens.

Super Plasticizer

Super plasticizers, also known as high range water reducers, are chemical admixtures used where well-dispersed particle suspension is required. In my study Polycarboxylate was used as super plasticizer.

Steel Fibres and Polypropylene Fibres

Steel fibres and Polypropylene fibres were obtained from Tilak Road Abids Hyderabad. The length of crimped steel fibres used are 25mm of equivalent diameter 0.5mm leading to an aspect ratio of 50 .The young's modulus of steel fibres was found to be 2×10^5 MPa. The density of steel fibre was found to be 7900 N/m^3. The ENDURO-600 macro synthetic polypropylene fibres were having a length of 50mm and their average thickness was found to be 1mm leading to an aspect ratio of 50. The density of polypropylene fibres was found to be 9460 N/m^3

Figure 1: Polypropylene Fibres

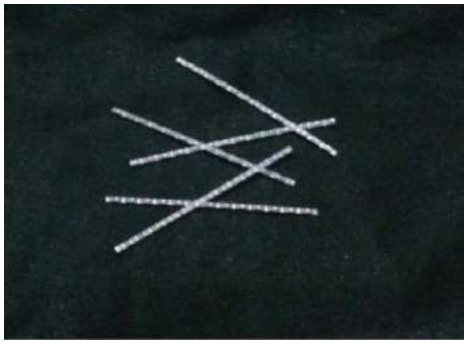

Figure 2 : Crimped Steel Fibres

Concrete Mix Design

Mix design was done as per IS 10262. The super plasticizer dosage was adopted as 1 % of cement.

Table 4: Mix Proportion for M30

Material	Calculated Quantity
Cement	437.77 kg
Coarse aggregate : 20 mm (60%)	733.8 kg
Coarse aggregate : 12 mm (40%)	489.2 kg
Fine aggregate	655.175 kg
Water	197liters

Testing Procedure

Concrete test specimen consist of 150x150x150mm cubes, Cylinders of 150mm diameter and 300mm height. Concrete cube specimen were tested at 7 and 28 days to obtain the compressive strength of concrete. Cylindrical specimen were tested at 7 and 28 days to obtain the split tensile strength of concrete.

EXPERIMENTAL RESULTS

Compressive Strength Test Results

The following table gives the overall results of compressive strength for reinforced concrete with steel and polypropylene fibres reinforced concrete. The table also gives the percentage increase of compressive strength with respect to plain reinforced concrete (reference mix).

Table 5: Overall Test Results of Compressive Strength

COMPRESSIVE STRENGTH AFTER 3 DAYS IN MPA

	Percentage of POLYPROPYLENE replaced				
Percentage of fiber	0	0.6	1.6	2.2	3.3
0	32.97	27.64	27.55	24.57	39.51
1	31.51	28.53	22.93	27.20	44.08

Table 17

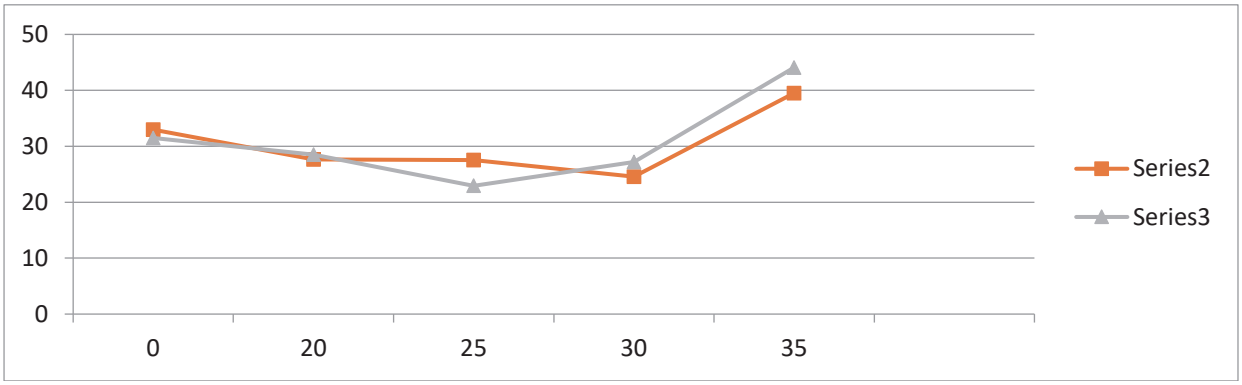

Graph 1 of Compressive Strength After 3 Days In Mpa

COMPRESSIVE STRENGTH AFTER 14 DAYS IN MPA

	Percentage of POLYPROPYLENE replaced				
Percentage of fiber	0	0.6	1.6	2.2	3.3
0	42.59	36.80	44.0	28.92	40.3
1	24.72	32.65	52.0	33.41	44.7

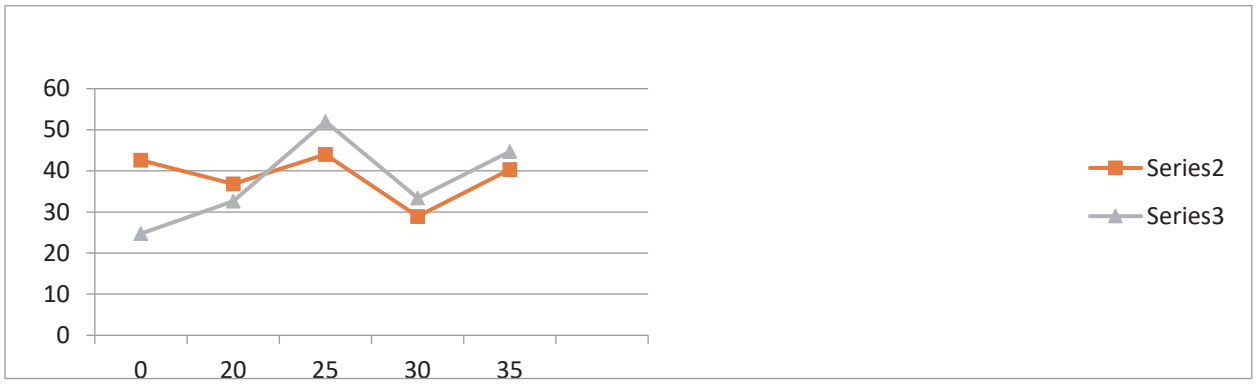

Graph 2 **Compressive Strength After 14 Days In Mpa**

SPLIT TENSILE STRENGTH AFTER 3 DAYS IN MPA

	Percentage of POLYPROPYLENE replaced				
Percentage of fiber	0	0.6	1.6	2.2	3.3
0	2.10	2.27	2.41	1.65	1.93
1	2.46	2.0	2.19	1.72	2.18

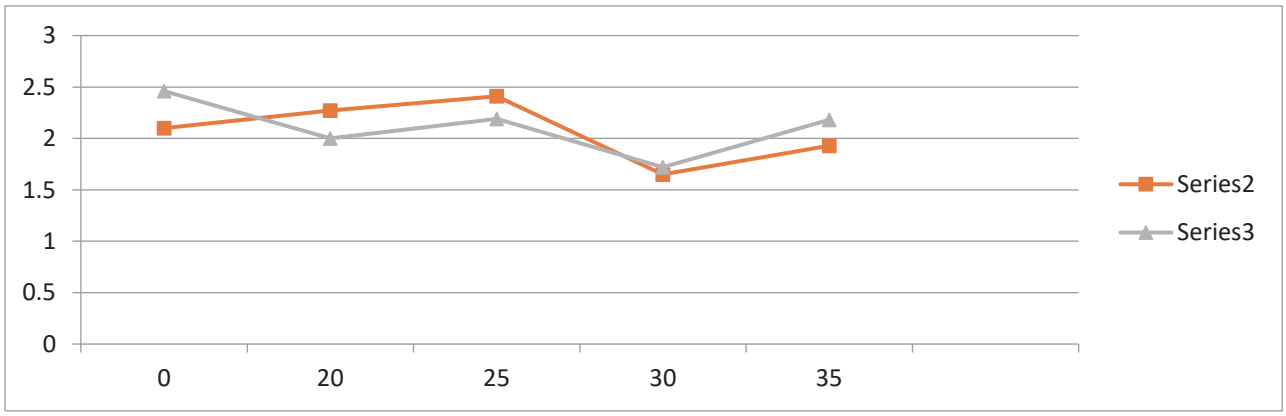

Graph 3

SPLIT TENSILE STRENGTH AFTER 14 DAYS IN MPA

	Percentage of POLYPROPYLENE replaced				
Percentage of fiber	0	0.6	1.6	2.2	3.3
0	2.12	3.46	2.92	2.91	2.09
1	1.51	3.03	2.85	1.88	3.04

CONCLUSIONS

The steel fibre reinforced concrete yield higher compressive strength with addition of 0.6% steel fibre by volume of concrete. Fibre reinforced concrete with crimped steel fibre of 25mm length with aspect ratio 50 yields better compressive strength than hooked end steel fibre of 30mm length with aspect ratio 50. The steel fibre reinforced concrete yield higher splitting tensile strength with addition of 0.6% steel fibre by volume of concrete. The polypropylene fibre reinforced concrete yield higher splitting tensile strength with addition of 1.6% polypropylene fibre by volume of concrete. Fibre reinforced concrete with crimped steel fibre of 25mm length with aspect ratio 50 yields better splitting tensile strength than hooked end steel fibre of 30mm length with aspect ratio 50. The steel fibre reinforced concrete yield higher flexural strength with addition of 2.2% steel fibre by volume of concrete. The polypropylene fibre reinforced concrete yield higher flexural strength with addition of 0.5% polypropylene fibre by volume of concrete. Fibre reinforced concrete with crimped steel fibre of 25mm length with aspect ratio 50 yields better flexural strength than hooked end steel fibre of 30mm length with aspect ratio 50.

REFERENCES

1. MR. Mehul J Patel, MRS. S. M Kulkarni, *"Effect of polypropylene fiber on the High Strength Concrete", Journal of Information, Knowledge and Reserch in Civil Engineering,* Volume 2, Issue 3, Nov-12-Oct-13.

2. Roohollah Bagherzadeh Ph.D, Hamid Reza Pakravan, Adol-Hossein Sadeghi, Mazoud Latifi, Ali Akbar Merati, *"An Investigation on Adding Polypropylene Fibers to Reinforce Lightweight Cement Composites", Journal of Engineered Fibers and Fabrics,* Volume7. Issue 4, 2012

3. Eray Baran, Tolga Akis, Seda Yesimen, *"Pull-out behavior of Prestressing strands in steel fiber reinforced concrete", Construction and Building Materials* 28(2012) 362-371

4. Budia Aulia. (2002), *"Effects of polypropylene fibers on the properties of high strength concrete", Lacer journal no*. 7, pp. 21-26.

5. Shetty M. S., *"Concrete Technology",* Chand S. and Company Limited, New Delhi, 6th Edition, 2005.

6. IS: 456- 2000, *"Plain and reinforced concrete- code of practice (fourth revision)"*, Bureau of Indian Standards, New Delhi, India.

7. Marco Orgrass and Yvette Klug. (2004), *"Steel Fiber Reinforced Ultra High Strength Concretes", Lacer journal no* -9, pp. 31-36.

8. Balasubramanian. K, Bharatkumar. B. H, and Gopalkrishnan S. (1996), *"Impact resistance of steel fiber reinforced concrete using drop weight impact method"*, The Indian Concrete Journal, mar, pp. 257-262.

9. Amir A. Mirsayah and Nemkumar Banthia. (2002), *"Shear Strength of Steel Fiber Reinforced Concrete"*, ACI Materials Journal, Vol. 99, No. 5, pp. 473-479.

10. Talukdar S. and Baruah P. (2007), *"A Comparative Study of Compressive, Flexural, Tensile and Shear Strength of Concrete with Fibers of Different Origins",* Indian Concrete Journal, Oct, pp 17-24.

AN EXPERIMENTAL INVESTIGATION ON HIGH STRENGTH BINARY BLENDED POLYMER HYBRID CONCRETE USING POLYCARBOXYLATE SUPER PLASTICIZER

MOHD AHMED[1] & MOHD ZAKER[2]

[1]*PG Student, Department of Civil Engineering, Nawab Shah Alam Khan College Of Engineering & Technology, Hyderabad India.*

[2]*Assistant Professor, Department of Civil Engineering, Nawab Shah Alam Khan College Of Engineering & Technology, Hyderabad India.*

ABSTRACT

Concrete the worlds most consumed material after water on the earth planet. Concrete is the material which is said to be strong in compression and weak in the tension. Steel is the ductile material to withstand tension in the concrete. Cement is the non-acidic and alkaline which prevent the steel from corrosion. The main focus on this experimental study in the past is made to make concrete strong in tension with less use of steel and with the use of some replacements. The Steel crimped fibre are said to be used to improve the properties of concrete which have the improvement to the age factor of concrete. The use of Polypropylene fibre to improve the flexural property in the concrete. Past Experimental studies by some of the past researchers. The use of polycarboxylate superplasticizers to improve the workability and to reduce the water content in the concrete and improve the compressive strength with the emphases on the different properties of concrete to overcome the different botheration in concrete. In this undertaking to be centre around attributes quality of solid evaluation of cement with various corresponding of supplanting of concrete with and we including pleated steel fibre. To utilizing steel fibre, improve the flexural quality of cement in various variety blend. The solid of blend to be casted with steel fibre and without steel fibre in vary rates 0%,0.6% 1.6% 2.2% and 3.3%. To believe the expense of development to be examine.

KEYWORDS: Hybrid Fibre, Polypropylene Fibre, Steel Fibre Concrete, Polycarboxylate.

INTRODUCTION

Concrete is by far the most widely used construction material today. It is versatile, has desirable engineering properties, can be moulded into any shapes and more importantly is produced with cost-effective materials. There is an old saying that broken stone, sand, and cement make good concrete. But the same proportion of broken stone, sand and cement also make bad concrete. To make good concrete now variety of innovative materials such as fibres, admixtures and construction chemicals, pozzolanas and different concrete making techniques are adopted in present day construction. In recent years, intensive research has resulted in advances and innovation in the technology of fibres such as glass, polypropylene, carbon etc., and more basic knowledge has been gained on the behaviour of cement concrete containing these fibres. Concrete containing hydraulic cement, water, aggregate, and discontinuous discrete fibres is called fibre-reinforced concrete. The incorporation of short discrete fibres (steel, polypropylene, glass, carbon) can lead to useful improvements in the mechanical behaviour of tension weak concrete.

OBJECTIVE

The main aim of this experiment is to study the strength properties of steel fibre and polypropylene fibre reinforced concrete with 0%, 0.6%, 1.6%, 2.2amd 3.3% by volume of concrete. The strength properties of fibre reinforced concrete are compared with normal concrete (reference mix) without any fibres.

MATERIALS AND METHODOLOGY

Constituent Materials Used

Cement

In this experiment 53 grade ordinary Portland cement (OPC) with brand name Ultra Tech Cement was used for all concrete mixes. The physical properties of cement used are as given in table.1.

Table 1: Physical Properties of Cement

Sl. No	Properties	Value	IS Specification and Test Procedure
1	Specific gravity	3.125	IS:4031
2	Fineness modulus	2%	IS:4031 & IS269
3	Initial Setting time in minutes	60	>30, IS:4031 & IS269
4	Final Setting time in minutes	260	<600, IS:4031 & IS269

Fine Aggregate

The fine aggregate used for the study was manufactured sand which was free from deleterious materials like clay, silt content and chloride contamination. The physical properties of fine aggregate used are as given in table.2.

Table 2: Physical Properties of Fine Aggregate

Sl No.	Properties	Value
1	Specific gravity	2.67
2	Fineness modulus	2.69
3	Grading of sand	zone II

Coarse Aggregate

The coarse aggregates used for the work is of 20mm and 12mm size which is free from deleterious materials like clay, silt content and chloride contamination.

Table 3: Physical Properties of Coarse Aggregate

Sl No.	Properties	Value
1	Specific gravity	2.49
2	Fineness modulus	4.66

Water

Clean potable tap water available in the laboratory, which satisfies drinking standards, was used for the preparation of specimens and for the curing of specimens.

Super Plasticizer

Super plasticizers, also known as high range water reducers, are chemical admixtures used where well-dispersed particle suspension is required. In my study Polycarboxylate was used as super plasticizer.

Steel Fibres and Polypropylene Fibres

Steel fibres and Polypropylene fibres were obtained from Tilak Road Abids Hyderabad. The length of crimped steel fibres used are 25mm of equivalent diameter 0.5mm leading to an aspect ratio of 50 .The young's modulus of steel fibres was found to be 2×10^5 MPa. The density of steel fibre was found to be 7900 N/m^3. The ENDURO-600 macro synthetic polypropylene fibres were having a length of 50mm and their average thickness was found to be 1mm leading to an aspect ratio of 50. The density of polypropylene fibres was found to be 9460 N/m^3

Figure 1: Polypropylene Fibres

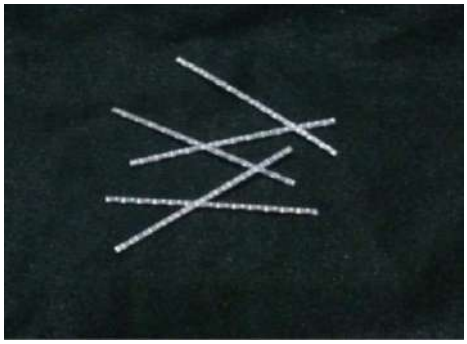

Figure 2 : Crimped Steel Fibres

Concrete Mix Design

Mix design was done as per IS 10262. The super plasticizer dosage was adopted as 1 % of cement.

Table 4: Mix Proportion for M30

Material	Calculated Quantity
Cement	437.77 kg
Coarse aggregate : 20 mm (60%)	733.8 kg
Coarse aggregate : 12 mm (40%)	489.2 kg
Fine aggregate	655.175 kg
Water	197liters

Testing Procedure

Concrete test specimen consist of 150x150x150mm cubes, Cylinders of 150mm diameter and 300mm height. Concrete cube specimen were tested at 7 and 28 days to obtain the compressive strength of concrete. Cylindrical specimen were tested at 7 and 28 days to obtain the split tensile strength of concrete.

EXPERIMENTAL RESULTS

Compressive Strength Test Results

The following table gives the overall results of compressive strength for reinforced concrete with steel and polypropylene fibres reinforced concrete. The table also gives the percentage increase of compressive strength with respect to plain reinforced concrete (reference mix).

Table 5: Overall Test Results of Compressive Strength

COMPRESSIVE STRENGTH AFTER 3 DAYS IN MPA

	Percentage of POLYPROPYLENE replaced				
Percentage of fiber	0	0.6	1.6	2.2	3.3
0	32.97	27.64	27.55	24.57	39.51
1	31.51	28.53	22.93	27.20	44.08

Table 17

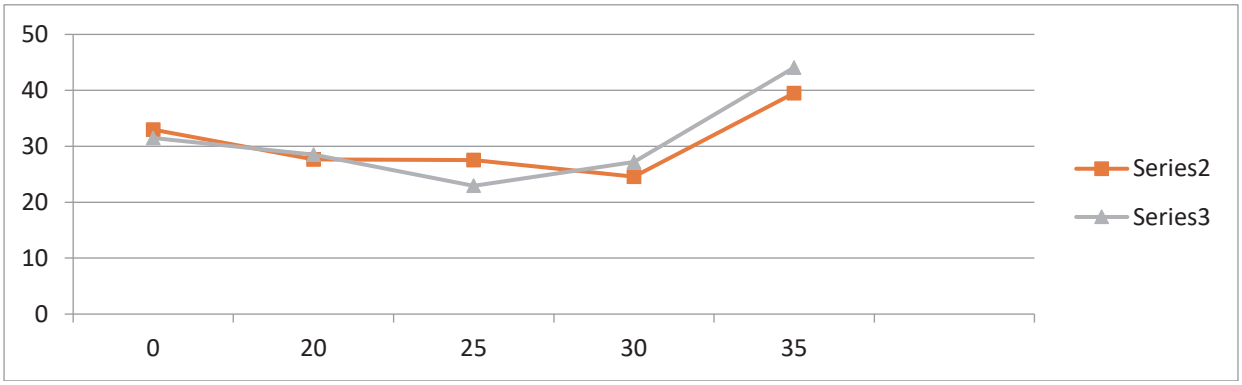

Graph 1 of Compressive Strength After 3 Days In Mpa

COMPRESSIVE STRENGTH AFTER 14 DAYS IN MPA

	Percentage of POLYPROPYLENE replaced				
Percentage of fiber	0	0.6	1.6	2.2	3.3
0	42.59	36.80	44.0	28.92	40.3
1	24.72	32.65	52.0	33.41	44.7

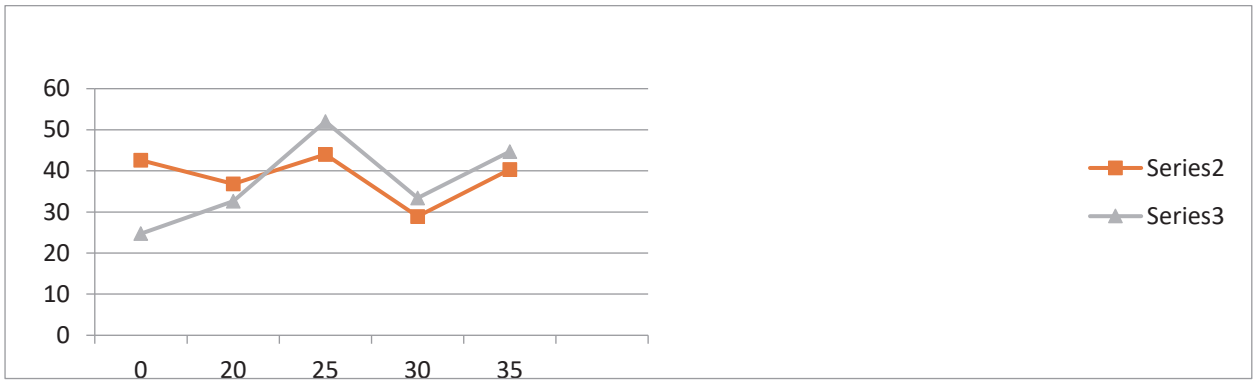

Graph 2 **Compressive Strength After 14 Days In Mpa**

SPLIT TENSILE STRENGTH AFTER 3 DAYS IN MPA

	Percentage of POLYPROPYLENE replaced				
Percentage of fiber	0	0.6	1.6	2.2	3.3
0	2.10	2.27	2.41	1.65	1.93
1	2.46	2.0	2.19	1.72	2.18

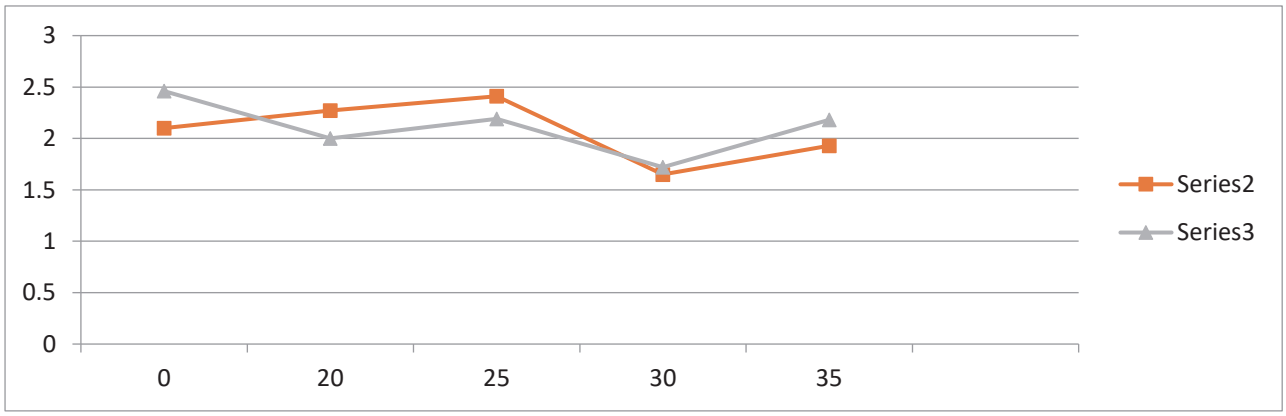

Graph 3

SPLIT TENSILE STRENGTH AFTER 14 DAYS IN MPA

	Percentage of POLYPROPYLENE replaced				
Percentage of fiber	0	0.6	1.6	2.2	3.3
0	2.12	3.46	2.92	2.91	2.09
1	1.51	3.03	2.85	1.88	3.04

CONCLUSIONS

The steel fibre reinforced concrete yield higher compressive strength with addition of 0.6% steel fibre by volume of concrete. Fibre reinforced concrete with crimped steel fibre of 25mm length with aspect ratio 50 yields better compressive strength than hooked end steel fibre of 30mm length with aspect ratio 50. The steel fibre reinforced concrete yield higher splitting tensile strength with addition of 0.6% steel fibre by volume of concrete. The polypropylene fibre reinforced concrete yield higher splitting tensile strength with addition of 1.6% polypropylene fibre by volume of concrete. Fibre reinforced concrete with crimped steel fibre of 25mm length with aspect ratio 50 yields better splitting tensile strength than hooked end steel fibre of 30mm length with aspect ratio 50. The steel fibre reinforced concrete yield higher flexural strength with addition of 2.2% steel fibre by volume of concrete. The polypropylene fibre reinforced concrete yield higher flexural strength with addition of 0.5% polypropylene fibre by volume of concrete. Fibre reinforced concrete with crimped steel fibre of 25mm length with aspect ratio 50 yields better flexural strength than hooked end steel fibre of 30mm length with aspect ratio 50.

REFERENCES

1. MR. Mehul J Patel, MRS. S. M Kulkarni, *"Effect of polypropylene fiber on the High Strength Concrete", Journal of Information, Knowledge and Reserch in Civil Engineering,* Volume 2, Issue 3, Nov-12-Oct-13.

2. Roohollah Bagherzadeh Ph.D, Hamid Reza Pakravan, Adol-Hossein Sadeghi, Mazoud Latifi, Ali Akbar Merati, *"An Investigation on Adding Polypropylene Fibers to Reinforce Lightweight Cement Composites", Journal of Engineered Fibers and Fabrics,* Volume7. Issue 4, 2012

3. Eray Baran, Tolga Akis, Seda Yesimen, *"Pull-out behavior of Prestressing strands in steel fiber reinforced concrete", Construction and Building Materials* 28(2012) 362-371

4. Budia Aulia. (2002), *"Effects of polypropylene fibers on the properties of high strength concrete", Lacer journal no*. 7, pp. 21-26.

5. Shetty M. S., *"Concrete Technology",* Chand S. and Company Limited, New Delhi, 6th Edition, 2005.

6. IS: 456- 2000, *"Plain and reinforced concrete- code of practice (fourth revision)"*, Bureau of Indian Standards, New Delhi, India.

7. Marco Orgrass and Yvette Klug. (2004), *"Steel Fiber Reinforced Ultra High Strength Concretes", Lacer journal no* -9, pp. 31-36.

8. Balasubramanian. K, Bharatkumar. B. H, and Gopalkrishnan S. (1996), *"Impact resistance of steel fiber reinforced concrete using drop weight impact method"*, The Indian Concrete Journal, mar, pp. 257-262.

9. Amir A. Mirsayah and Nemkumar Banthia. (2002), *"Shear Strength of Steel Fiber Reinforced Concrete"*, ACI Materials Journal, Vol. 99, No. 5, pp. 473-479.

10. Talukdar S. and Baruah P. (2007), *"A Comparative Study of Compressive, Flexural, Tensile and Shear Strength of Concrete with Fibers of Different Origins",* Indian Concrete Journal, Oct, pp 17-24.

AN EXPERIMENTAL INVESTIGATION ON HIGH STRENGTH BINARY BLENDED POLYMER HYBRID CONCRETE USING POLYCARBOXYLATE SUPER PLASTICIZER

MOHD AHMED[1] & MOHD ZAKER[2]

[1]*PG Student, Department of Civil Engineering, Nawab Shah Alam Khan College Of Engineering & Technology, Hyderabad India.*

[2]*Assistant Professor, Department of Civil Engineering, Nawab Shah Alam Khan College Of Engineering & Technology, Hyderabad India.*

ABSTRACT

Concrete the worlds most consumed material after water on the earth planet. Concrete is the material which is said to be strong in compression and weak in the tension. Steel is the ductile material to withstand tension in the concrete. Cement is the non-acidic and alkaline which prevent the steel from corrosion. The main focus on this experimental study in the past is made to make concrete strong in tension with less use of steel and with the use of some replacements. The Steel crimped fibre are said to be used to improve the properties of concrete which have the improvement to the age factor of concrete. The use of Polypropylene fibre to improve the flexural property in the concrete. Past Experimental studies by some of the past researchers. The use of polycarboxylate superplasticizers to improve the workability and to reduce the water content in the concrete and improve the compressive strength with the emphases on the different properties of concrete to overcome the different botheration in concrete. In this undertaking to be centre around attributes quality of solid evaluation of cement with various corresponding of supplanting of concrete with and we including pleated steel fibre. To utilizing steel fibre, improve the flexural quality of cement in various variety blend. The solid of blend to be casted with steel fibre and without steel fibre in vary rates 0%,0.6% 1.6% 2.2% and 3.3%. To believe the expense of development to be examine.

KEYWORDS: Hybrid Fibre, Polypropylene Fibre, Steel Fibre Concrete, Polycarboxylate.

INTRODUCTION

Concrete is by far the most widely used construction material today. It is versatile, has desirable engineering properties, can be moulded into any shapes and more importantly is produced with cost-effective materials. There is an old saying that broken stone, sand, and cement make good concrete. But the same proportion of broken stone, sand and cement also make bad concrete. To make good concrete now variety of innovative materials such as fibres, admixtures and construction chemicals, pozzolanas and different concrete making techniques are adopted in present day construction. In recent years, intensive research has resulted in advances and innovation in the technology of fibres such as glass, polypropylene, carbon etc., and more basic knowledge has been gained on the behaviour of cement concrete containing these fibres. Concrete containing hydraulic cement, water, aggregate, and discontinuous discrete fibres is called fibre-reinforced concrete. The incorporation of short discrete fibres (steel, polypropylene, glass, carbon) can lead to useful improvements in the mechanical behaviour of tension weak concrete.

OBJECTIVE

The main aim of this experiment is to study the strength properties of steel fibre and polypropylene fibre reinforced concrete with 0%, 0.6%, 1.6%, 2.2amd 3.3% by volume of concrete. The strength properties of fibre reinforced concrete are compared with normal concrete (reference mix) without any fibres.

MATERIALS AND METHODOLOGY

Constituent Materials Used

Cement

In this experiment 53 grade ordinary Portland cement (OPC) with brand name Ultra Tech Cement was used for all concrete mixes. The physical properties of cement used are as given in table.1.

Table 1: Physical Properties of Cement

Sl. No	Properties	Value	IS Specification and Test Procedure
1	Specific gravity	3.125	IS:4031
2	Fineness modulus	2%	IS:4031 & IS269
3	Initial Setting time in minutes	60	>30, IS:4031 & IS269
4	Final Setting time in minutes	260	<600, IS:4031 & IS269

Fine Aggregate

The fine aggregate used for the study was manufactured sand which was free from deleterious materials like clay, silt content and chloride contamination. The physical properties of fine aggregate used are as given in table.2.

Table 2: Physical Properties of Fine Aggregate

Sl No.	Properties	Value
1	Specific gravity	2.67
2	Fineness modulus	2.69
3	Grading of sand	zone II

Coarse Aggregate

The coarse aggregates used for the work is of 20mm and 12mm size which is free from deleterious materials like clay, silt content and chloride contamination.

Table 3: Physical Properties of Coarse Aggregate

Sl No.	Properties	Value
1	Specific gravity	2.49
2	Fineness modulus	4.66

Water

Clean potable tap water available in the laboratory, which satisfies drinking standards, was used for the preparation of specimens and for the curing of specimens.

Super Plasticizer

Super plasticizers, also known as high range water reducers, are chemical admixtures used where well-dispersed particle suspension is required. In my study Polycarboxylate was used as super plasticizer.

Steel Fibres and Polypropylene Fibres

Steel fibres and Polypropylene fibres were obtained from Tilak Road Abids Hyderabad. The length of crimped steel fibres used are 25mm of equivalent diameter 0.5mm leading to an aspect ratio of 50 .The young's modulus of steel fibres was found to be 2×10^5 MPa. The density of steel fibre was found to be 7900 N/m^3. The ENDURO-600 macro synthetic polypropylene fibres were having a length of 50mm and their average thickness was found to be 1mm leading to an aspect ratio of 50. The density of polypropylene fibres was found to be 9460 N/m^3

Figure 1: Polypropylene Fibres

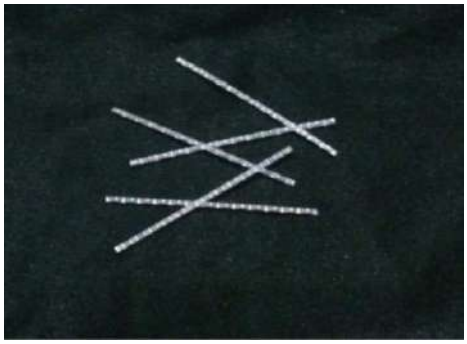

Figure 2 : Crimped Steel Fibres

Concrete Mix Design

Mix design was done as per IS 10262. The super plasticizer dosage was adopted as 1 % of cement.

Table 4: Mix Proportion for M30

Material	Calculated Quantity
Cement	437.77 kg
Coarse aggregate : 20 mm (60%)	733.8 kg
Coarse aggregate : 12 mm (40%)	489.2 kg
Fine aggregate	655.175 kg
Water	197liters

Testing Procedure

Concrete test specimen consist of 150x150x150mm cubes, Cylinders of 150mm diameter and 300mm height. Concrete cube specimen were tested at 7 and 28 days to obtain the compressive strength of concrete. Cylindrical specimen were tested at 7 and 28 days to obtain the split tensile strength of concrete.

EXPERIMENTAL RESULTS

Compressive Strength Test Results

The following table gives the overall results of compressive strength for reinforced concrete with steel and polypropylene fibres reinforced concrete. The table also gives the percentage increase of compressive strength with respect to plain reinforced concrete (reference mix).

Table 5: Overall Test Results of Compressive Strength

COMPRESSIVE STRENGTH AFTER 3 DAYS IN MPA

	Percentage of POLYPROPYLENE replaced				
Percentage of fiber	0	0.6	1.6	2.2	3.3
0	32.97	27.64	27.55	24.57	39.51
1	31.51	28.53	22.93	27.20	44.08

Table 17

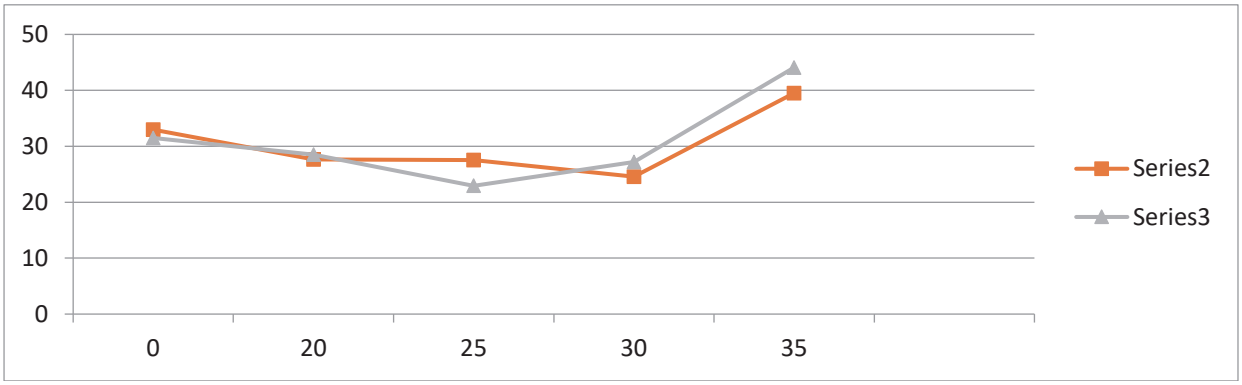

Graph 1 of Compressive Strength After 3 Days In Mpa

COMPRESSIVE STRENGTH AFTER 14 DAYS IN MPA

	Percentage of POLYPROPYLENE replaced				
Percentage of fiber	0	0.6	1.6	2.2	3.3
0	42.59	36.80	44.0	28.92	40.3
1	24.72	32.65	52.0	33.41	44.7

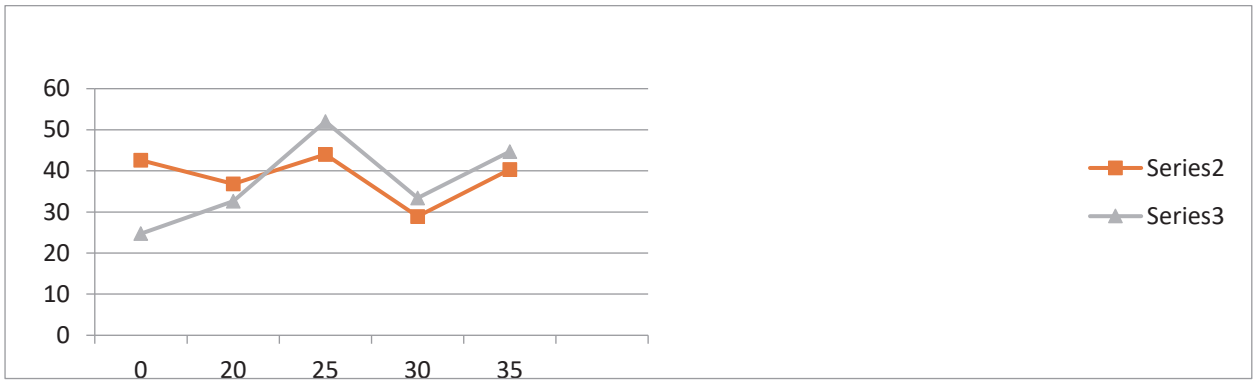

Graph 2 **Compressive Strength After 14 Days In Mpa**

SPLIT TENSILE STRENGTH AFTER 3 DAYS IN MPA

	Percentage of POLYPROPYLENE replaced				
Percentage of fiber	0	0.6	1.6	2.2	3.3
0	2.10	2.27	2.41	1.65	1.93
1	2.46	2.0	2.19	1.72	2.18

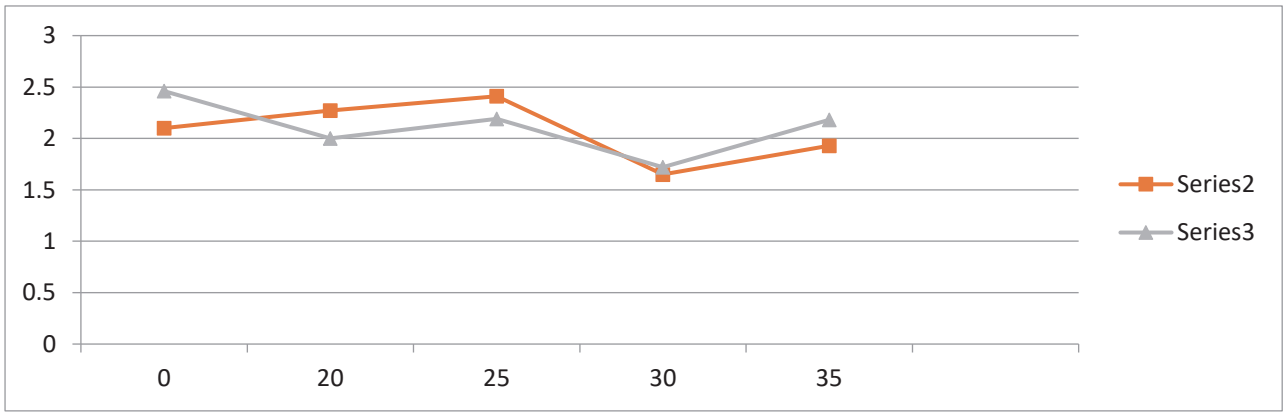

Graph 3

SPLIT TENSILE STRENGTH AFTER 14 DAYS IN MPA

	Percentage of POLYPROPYLENE replaced				
Percentage of fiber	0	0.6	1.6	2.2	3.3
0	2.12	3.46	2.92	2.91	2.09
1	1.51	3.03	2.85	1.88	3.04

CONCLUSIONS

The steel fibre reinforced concrete yield higher compressive strength with addition of 0.6% steel fibre by volume of concrete. Fibre reinforced concrete with crimped steel fibre of 25mm length with aspect ratio 50 yields better compressive strength than hooked end steel fibre of 30mm length with aspect ratio 50. The steel fibre reinforced concrete yield higher splitting tensile strength with addition of 0.6% steel fibre by volume of concrete. The polypropylene fibre reinforced concrete yield higher splitting tensile strength with addition of 1.6% polypropylene fibre by volume of concrete. Fibre reinforced concrete with crimped steel fibre of 25mm length with aspect ratio 50 yields better splitting tensile strength than hooked end steel fibre of 30mm length with aspect ratio 50. The steel fibre reinforced concrete yield higher flexural strength with addition of 2.2% steel fibre by volume of concrete. The polypropylene fibre reinforced concrete yield higher flexural strength with addition of 0.5% polypropylene fibre by volume of concrete. Fibre reinforced concrete with crimped steel fibre of 25mm length with aspect ratio 50 yields better flexural strength than hooked end steel fibre of 30mm length with aspect ratio 50.

REFERENCES

1. MR. Mehul J Patel, MRS. S. M Kulkarni, *"Effect of polypropylene fiber on the High Strength Concrete", Journal of Information, Knowledge and Reserch in Civil Engineering,* Volume 2, Issue 3, Nov-12-Oct-13.

2. Roohollah Bagherzadeh Ph.D, Hamid Reza Pakravan, Adol-Hossein Sadeghi, Mazoud Latifi, Ali Akbar Merati, *"An Investigation on Adding Polypropylene Fibers to Reinforce Lightweight Cement Composites", Journal of Engineered Fibers and Fabrics,* Volume7. Issue 4, 2012

3. Eray Baran, Tolga Akis, Seda Yesimen, *"Pull-out behavior of Prestressing strands in steel fiber reinforced concrete", Construction and Building Materials* 28(2012) 362-371

4. Budia Aulia. (2002), *"Effects of polypropylene fibers on the properties of high strength concrete", Lacer journal no*. 7, pp. 21-26.

5. Shetty M. S., *"Concrete Technology",* Chand S. and Company Limited, New Delhi, 6th Edition, 2005.

6. IS: 456- 2000, *"Plain and reinforced concrete- code of practice (fourth revision)"*, Bureau of Indian Standards, New Delhi, India.

7. Marco Orgrass and Yvette Klug. (2004), *"Steel Fiber Reinforced Ultra High Strength Concretes", Lacer journal no* -9, pp. 31-36.

8. Balasubramanian. K, Bharatkumar. B. H, and Gopalkrishnan S. (1996), *"Impact resistance of steel fiber reinforced concrete using drop weight impact method"*, The Indian Concrete Journal, mar, pp. 257-262.

9. Amir A. Mirsayah and Nemkumar Banthia. (2002), *"Shear Strength of Steel Fiber Reinforced Concrete"*, ACI Materials Journal, Vol. 99, No. 5, pp. 473-479.

10. Talukdar S. and Baruah P. (2007), *"A Comparative Study of Compressive, Flexural, Tensile and Shear Strength of Concrete with Fibers of Different Origins",* Indian Concrete Journal, Oct, pp 17-24.

AN EXPERIMENTAL STUDY ON STRENGTH PARAMETERS OF SELF HEALING CONCRETE USING BACILLUS SUBTILIS BACTERIA AND SELF COMPACTION BY (12MM AGGREGATE SIZE)

ASST PROF. MOHD ZAKER

Department of Civil Engineering

NSAKCET, India

SAHARISH FATIMA

Department of Civil Engineering

NSAKCET, India

ABSTRACT Concrete is a commonly used building medium in the world. To increase the consistency of concrete, modifications are required. A special form of concrete is self-healing bacterial concrete. Crack healing takes place in this concrete as it comes into contact with air and water, which begins creating lime stone (calcium carbonate) and begins covering cracks. The precipitation of calcium carbonate takes place through the microbial activity of bacteria. BACILLUS SUBTILIS bacteria are used in this work to repair the fractures as a curing agent. Concrete is applied to Bacillus subtilis bacteria with varying dosage amounts such as 6ml, 12ml, 18ml, and 24ml. This analysis uses 53 grade ordinary Portland cement and gravel sand. M50 grade concrete cubes are casted in this current job with the mixture of self-healing and self-compacting concrete and the strength parameters are tested on the 3rd, 7th, 14th, 28th day of curing for various dose, strength parameters such as compressive strength, tensile strength and flexural strength.
.

1. INTRODUCTION

Concrete forms significant components in the construction industry since casting is cheap, easy to access, and convenient. But the disadvantage of these materials is that they are weak in tension, so they crack under sustained loading and aggressive environmental agents that ultimately reduce the life of the structure built using these materials. This damaging process occurs in the building structure's early life and also during its lifetime. The present work aims to study the strength, durability, and crack healing characteristics of bio concrete compared to the standard Concrete. To achieve this aim, the following objectives have been framed: - a) To isolate the most efficient bacteria for crack remediation. 16 b) To study durability properties with various dosages like 6 ml, 12ml, 18ml and 24ml. c) To compare the compressive strength, split tensile strength, and flexural strength of bacterial Concrete. d) To check the efficiency of potential bacterial strain towards crack remediation of the concrete structure.

2 Literature Review

SakinaNajmuddinSaifee et.al 1 (Released a Critical Assessment Paper on Bacterial Concrete) In this Document, they discussed the various types of bacteria and their uses. Bacterial Concrete is advantageous in enhancing cement materials' durability, repairing calcareous monuments, sealing concrete highly durable cracks, etc. It is also useful for low-cost, long-lasting road construction, high-strength buildings with higher bearing capacity, loose sand erosion prevention, and low-cost, durable housing. They have also briefed on the working principle of bacterial Concrete as a material for repair. The study also observed that the microorganisms' metabolic activities occur within the concrete results to increase concrete performance, including its compressive force. This study also explains the chemical process required to remedy cracks.

Meera C M and Dr. Subha V2: In this paper, they discussed the effect of Bacillus subtilis JC3 on concrete strength and durability. They used 150 mm x 150 mm x 150 mm x 150 mm cubes and M20-grade concrete cylinders with a 100 mm diameter and a height of 200 mm with and without microorganisms. Cubes were tested for various bacterial concentrations at 7 days and 18 28 days for strength assessments, and cylinders were tested at 28 days for split tensile strength. It was observed that the concrete compressive strength showed a significant increase of 42 percent for the cell concentration of 105 mixturesWater.And there is also a substantial increase in tensile strength by 63 percent with the addition of bacteria for a concentration of 105cells / ml at 28 days. Acid durability test, chloride test, for durability assessment.

Rabindranath, N. Kannan, Likhit M. 3 (Have published a paper about Bacterial Self-healing Material Specific.) In this paper, a comparison study was carried out with concrete cubes and beams subjected to compressive and flexural strength tests with and without the Bacillus pasteurii bacterium. The concrete dumplings and beams were prepared by adding a calculated quantity of bacterial solution, and compressive and flexural strengths were tested for 7 and 28 days. It was found that strength and healing increased sharply of the cracks that are loaded onto concrete specimens. The microbe has proved

efficient in enhancing the Concrete's properties by increasing its initial strength. Carbonate Calcium some percentage of the bacteria's void volume has been filled, making the texture more compact and resistive to infiltration.

3. BACTERIAL CONCRETE

Therefore, bacterial-induced Calcium Carbonate (Calcite) precipitation was proposed as an alternative and environmentally friendly crack remediation and improved building material strength. A novel technique is adopted to remediate cracks and fissures in calcium concrete using Microbiologically Induced Calcite or Carbonate (CaCO3). Precipitation (MICP) is a technique that falls within a broader scientific category called biomineralization. MICP is highly desirable because the Calcite precipitation caused by microbial activity is pollution-free and natural. The method can be used to improve the compressive strength and rigidity of cracked concrete specimens.

The research leading to microbial precipitation of Calcium Carbonate and its ability to heal cracks of building materials has resulted in many applications such as crack remediation of Concrete, consolidation of sand, restoration of historical monuments, and such applications. Thus it can be defined as "The process can occur within or outside the microbial cell or even some distance within the Concrete. Often bacterial activities simply trigger a change in solution chemistry that leads to over-saturation and mineral precipitation. Using these bio-mineralogy concepts in Concrete leads to the potential invention of new material called bacterial Concrete.

4. SELF HEALING BACTERIAL CONCRETE

The autogenous crack-healing capacity of Concrete has been recognized in several recent studies. Mainly micro cracks with widths typically between 0.05 and 0.1 mm have been observed to be completely sealed, especially under repetitive dry/wet cycles. This autogenous healing mechanism is primarily due to secondary hydration of non- or partially reacted cement particles present in the Concrete. Due to capillary forces, water under changing wet and dry cycles is repeatedly drawn into the micro cracks, resulting in the expansion of hydrated cement particles due to the formation of calcium silicate hydrates and calcium hydroxide. These reaction products are capable of sealing cracks completely provided crack widths are small. Because of the limited amount of non-reacted cement particles present, larger-sized gaps can only be partially filled, resulting in only a thin layer of hydration products on the crack surface. Hence, an alternative and more sustainable self-healing mechanism are needed for these reasons.

The bacteria to be used in Concrete as a self-healing agent should be fit for the job, i.e., they should perform long-term efficient crack sealing, preferably during the lifetime of the total constructions. Bacterial crack healing's primary mechanism is that the bacteria act primarily as a catalyst, transforming a precursor compound into an appropriate filler material. The newly manufactured compounds, such as mineral precipitates based on calcium carbonate, should act as a type of bio-cement which effectively seals freshly formed cracks. Therefore, both bacteria and a bio-cement precursor compound should be integrated into the material matrix for effective self-healing.

5. DETERMINATION OF FINENESS OF CEMENT BY SIEVING

Sl. No.	Weight of sample taken (W) (in g.)	Weight of residue (R) (in g.)	%age of residue $=\frac{R}{W}\times 100$	Average % of the residue
1	100	90	90/100*100	9%
2	110	100	100/110*100	10%
3	120	110	110/120*100	11%

Table 1 : finess of cement

6. CONSISTENCY TEST ON CEMENT

Sl. No.	Wt of cement in gram	Wt of water in gram	Height not penetrated (in mm)	Consistency Of cement in % b/a*100

1	200	52 ml	33mm	26
2	200	60ml	28mm	30
3	200	64 ml	28mm	32
4	200	66ml	14.5mm	33
5	200	70 ml	7 mm	35

Table 2 consistency test on cement

7.DETERMINATION OF SETTING TIMES OF CEMENT

Time in minutes:	0 10 20 30 40 50 60
Height in mm fails to penetrate	40 40 40 40 40 39 37

Table 3: setting time of cement

8.DETERMINATION OF COMPRESSIVE STRENGTH OF CEMENT

For 3 days' strength:

Sl. No	Length (L) in mm	Breadth (B) in mm	Load (F) in N	compressive strength in N/mm2
1	150 mm	150 mm	300 kn	24.5
2	150 mm	150 mm	300 kn	25.6
3	150 mm	150 mm	300 kn	26

For 7 days' strength:

Sl. No	Length (L) in mm	Breadth (B) in mm	Load (F) in N	compressive strength in N/mm2
1	150 mm	150 mm	300 kn	25.6
2	150 mm	150 mm	300 kn	26.1
3	150 mm	150 mm	300 kn	26.68

For 28 days of strength

Sl. No	Length (L) in mm	Breadth (B) in mm	Load (F) in N	compressive strength in N/mm2
1	150 mm	150 mm	300 kn	38.1
2	150 mm	150 mm	300 kn	39.56
3	150 mm	150 mm	300 kn	40.2

Compressive test: using a universal testing machine

Days	6ml	12 ml	18ml	24ml
3	367.0	298.0	236.5	149.5
7	25.6	26.1	26.68	26.02
14	35.8	36.14	36.44	35.88
28	39.38	39.56	40.2	40.06

Table 4 compressive strength of SCC with bacteria in different dosage at different ages of concrete

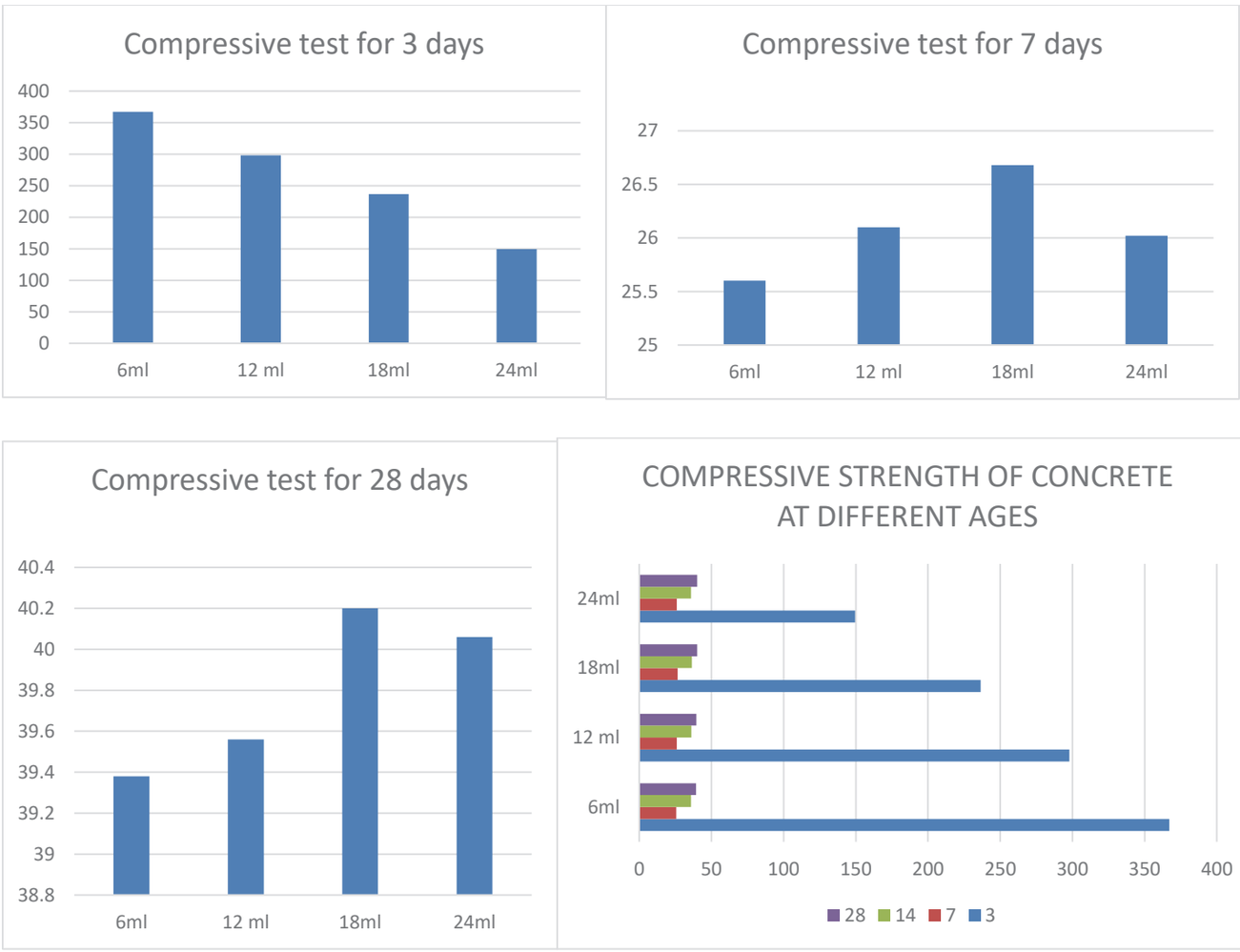

Figure 1: compressive strength of SCC with bacteria in different dosage and 3,7,14 and 28 days curing of concrete

TENSILE TEST: USING UNIVERSAL TESTING MACHINE

Days	6ml	12 ml	18ml	24ml
3	4.5	4.8	5.0	5.1
7	4.8	4.92	5.00	5.26
14	5.68	5.72	5.86	5.76
28	6.24	6.46	6.74	6.52

Table 5: Tensile strength of SCC with bacteria in different dosage at different ages of concrete

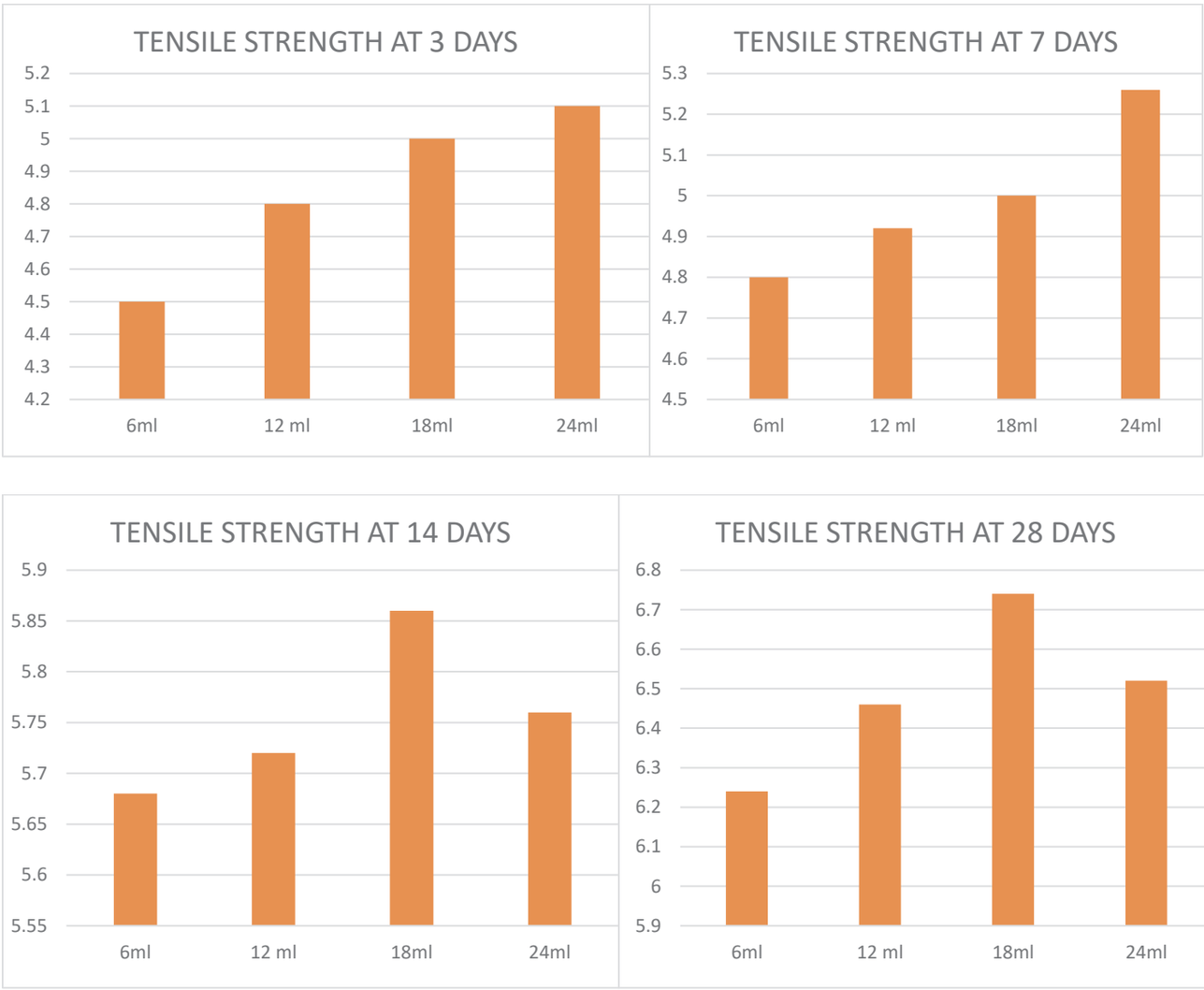

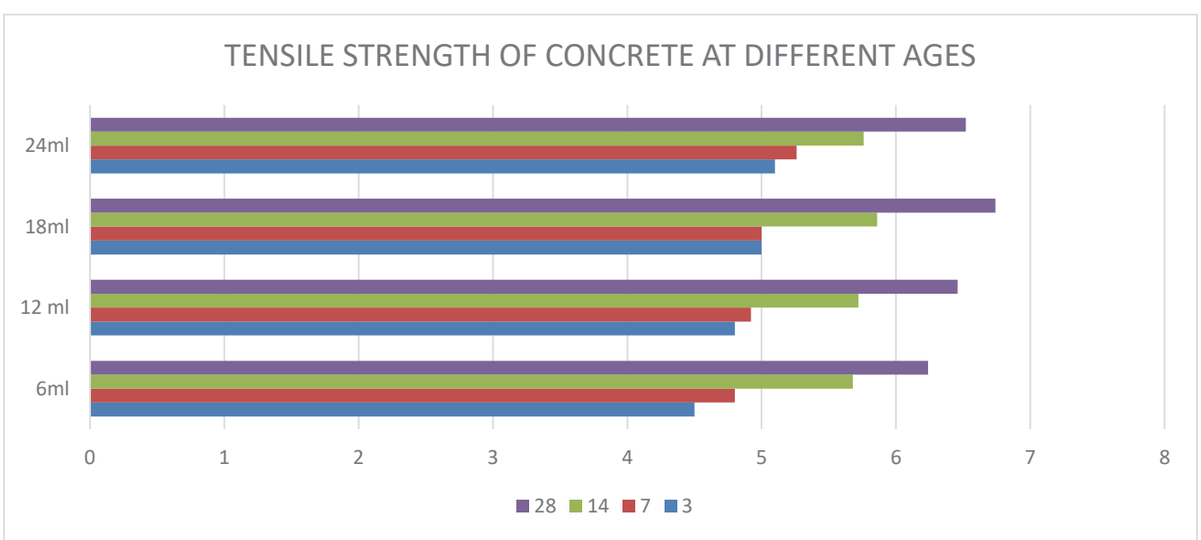

Figure 2: Tensile strength of SCC with bacteria in different dosage at 3,7,14 and 28 days of concrete curing.

FLEXURAL TEST: USING UNIVERSAL TESTING MACHINE

Days	6ml	12 ml	18ml	24ml
3	3.5	3.8	3.0	3.1
7	3.8	3.92	3.00	3.26
14	4.46	4.62	4.84	4.74
28	5.12	5.2	5.36	5.22

Table 6: Flexural strength of SCC with bacteria in different dosage at different ages of concrete

Figure 3: Flexural strength of SCC with bacteria in different dosage at 3, 7, 14, and 28 days of concrete curing

9 CONCLUSIONS

The goal of this study was to enhance the engineering properties of concrete, using a single species of bacteria. Many bacteria are reported in literature that can enhance the power, durability and other mechanical characteristics of Concrete. To study the variation of compressive strength, flexural strength and split tensile strength of concrete cube with various dosage of bacteria, a concrete of water cement ratio of 0.40 are considered to prepare the cubes. Accordingly, different cubes with bacterial concentration of 6ml, 12ml, 18ml and 24ml are prepared.

- The required bacteria should be carefully chosen to enhance the properties of the cement mortar or concrete. In the given environment, for example, Bacillus cereus could not survive, while another Bacillus sphaericus species survived.
- With an increase in bacterial dosage of up to 24ml, the compressive strength at 18 ml (at 7 days and at 28 days) of the cube was observed to be growing. Further changes in bacteria concentration, however, have been shown to decrease the compressive strength of concrete cube.
- With an increase in bacterial dosage of up to 24ml, the split tensile strength for 18 ml (at 7 days and at 28 days) of the cube was observed to be growing. Further changes in bacteria concentration, however, have been shown to decrease the tensile strength of concrete cube.
- With an increase in bacterial dosage of up to 24ml, the flexural strength for 18 ml (at 7 days and at 28 days) of the cube was observed to be growing. Further changes in 79 bacteria concentration, however, have been shown to decrease the flexural strength of concrete cube.
- The optimum doses of bacteria found to increase the average compressive strength, flexural strength and split tensile strength by 4% (at 7-day) and 2% (at 28-day) over the control specimen. The more increase in strength after 7-day curing may be due to the presence of nutrient medium and it getting depleted as it reaches 28 days and causing death of bacteria.

10. SCOPE OF FURTHER STUDY

- In this study only durability properties of SSC concrete has been studied like compressive strength, split tensile strength and flexural strength.
- The morphology of the bacterial can be studied by FESEM and XRD methods.

REFERENCES

[1] Siddique, R and Chahal, N. K. (2011). Effect of ureolytic bacteria on concrete properties. Construction and Building Materials, 25, 3791–3801

[2] Pacheco-Torgal, F., and Labrincha, J.A. (2013) Biotech cementitious materials: Some aspects of an innovative approach for Concrete with enhanced durability, Construction and Building Materials, 40, 1136–1141

[3] Wiktor, V., and Jonkers, H. M. (2011) Quantification of crack-healing in novel bacteria

based self-healing concrete, Cement & Concrete Composites, 33 ,763–770.

[4] Chahal, N., Siddique, R. and Rajor, A. (2012). Influence of bacteria on the compressive strength, water absorption and rapid chloride permeability of Concrete incorporating silica fume, Construction and Building Materials, 37, 645–651

[5] Achal, V., Mukerjee, A., Basu, P. C. and Reddy, M. S (2009). Strain improvement of Sporosarcina pasteurii for enhanced urease and calcite production, Journal of Industrial Microbiology Biotechnology, 36, 981–988

[6.] Is 3812-1981, Indian standards specification for fly ash for use of pozzolana and admixture. Bureau of Indian Standards. New Delhi.

[7]. Hajime Okamura, "Self-Compacting High Performance Concrete Ferguson Lecture for 1996", Concrete International, Vol.19, No.7, pp. 50-54.

[8]. Ozawa K., Kunishama M, Makala K, "Development of High Performance Concrete Based on the Durability Design of Concrete Structures" Proceeding of the second East-Asia and Pacific Conference on Structural Engineering and construction (EASEC2), Vol.1, pp. 445-450, January 1989.

[9]. K C Panda, P K Bal, "Properties of self-compacting concrete using recycled coarse aggregate", procedia engineering 51(2013) 159- 164.

[10] IS 456-2000. Design Specifications of Plain & Reinforced Concrete, Bureau of Indian Standards. New Delhi

[11].IS 10262-2009. Recommended guidelines for Concrete Mix Design, Bureau of Indian Standards. New Delhi.

[12] Achal, V., Mukerjee, A., and. and Reddy, M. S, (2011) Effect of calcifying bacteria on permeation properties of concrete structures, Journal of Industrial Microbiology Biotechnology, 38, 1229–1234

[13] Majumdar., Sarkar, M., Chowdhury, T., Chattopadhyay, B., and Mandal's. (2012) Use of bacterial protein powder in commercial fly ash pozzolana cements for high performance construction materials, Open Journal of Civil Engineering, 2, 218-228

AN EXPERIMENTAL STUDY ON STRENGTH PARAMETERS OF SELF HEALING CONCRETE USING BACILLUS SUBTILIS BACTERIA AND SELF COMPACTION BY (12MM AGGREGATE SIZE)

ASST PROF. MOHD ZAKER

Department of Civil Engineering

NSAKCET, India

SAHARISH FATIMA

Department of Civil Engineering

NSAKCET, India

ABSTRACT Concrete is a commonly used building medium in the world. To increase the consistency of concrete, modifications are required. A special form of concrete is self-healing bacterial concrete. Crack healing takes place in this concrete as it comes into contact with air and water, which begins creating lime stone (calcium carbonate) and begins covering cracks. The precipitation of calcium carbonate takes place through the microbial activity of bacteria. BACILLUS SUBTILIS bacteria are used in this work to repair the fractures as a curing agent. Concrete is applied to Bacillus subtilis bacteria with varying dosage amounts such as 6ml, 12ml, 18ml, and 24ml. This analysis uses 53 grade ordinary Portland cement and gravel sand. M50 grade concrete cubes are casted in this current job with the mixture of self-healing and self-compacting concrete and the strength parameters are tested on the 3rd, 7th, 14th, 28th day of curing for various dose, strength parameters such as compressive strength, tensile strength and flexural strength.
.

1. INTRODUCTION

Concrete forms significant components in the construction industry since casting is cheap, easy to access, and convenient. But the disadvantage of these materials is that they are weak in tension, so they crack under sustained loading and aggressive environmental agents that ultimately reduce the life of the structure built using these materials. This damaging process occurs in the building structure's early life and also during its lifetime. The present work aims to study the strength, durability, and crack healing characteristics of bio concrete compared to the standard Concrete. To achieve this aim, the following objectives have been framed: - a) To isolate the most efficient bacteria for crack remediation. 16 b) To study durability properties with various dosages like 6 ml, 12ml, 18ml and 24ml. c) To compare the compressive strength, split tensile strength, and flexural strength of bacterial Concrete. d) To check the efficiency of potential bacterial strain towards crack remediation of the concrete structure.

2 Literature Review

SakinaNajmuddinSaifee et.al 1 (Released a Critical Assessment Paper on Bacterial Concrete) In this Document, they discussed the various types of bacteria and their uses. Bacterial Concrete is advantageous in enhancing cement materials' durability, repairing calcareous monuments, sealing concrete highly durable cracks, etc. It is also useful for low-cost, long-lasting road construction, high-strength buildings with higher bearing capacity, loose sand erosion prevention, and low-cost, durable housing. They have also briefed on the working principle of bacterial Concrete as a material for repair. The study also observed that the microorganisms' metabolic activities occur within the concrete results to increase concrete performance, including its compressive force. This study also explains the chemical process required to remedy cracks.

Meera C M and Dr. Subha V2: In this paper, they discussed the effect of Bacillus subtilis JC3 on concrete strength and durability. They used 150 mm x 150 mm x 150 mm x 150 mm cubes and M20-grade concrete cylinders with a 100 mm diameter and a height of 200 mm with and without microorganisms. Cubes were tested for various bacterial concentrations at 7 days and 18 28 days for strength assessments, and cylinders were tested at 28 days for split tensile strength. It was observed that the concrete compressive strength showed a significant increase of 42 percent for the cell concentration of 105 mixturesWater.And there is also a substantial increase in tensile strength by 63 percent with the addition of bacteria for a concentration of 105cells / ml at 28 days. Acid durability test, chloride test, for durability assessment.

Rabindranath, N. Kannan, Likhit M. 3 (Have published a paper about Bacterial Self-healing Material Specific.) In this paper, a comparison study was carried out with concrete cubes and beams subjected to compressive and flexural strength tests with and without the Bacillus pasteurii bacterium. The concrete dumplings and beams were prepared by adding a calculated quantity of bacterial solution, and compressive and flexural strengths were tested for 7 and 28 days. It was found that strength and healing increased sharply of the cracks that are loaded onto concrete specimens. The microbe has proved

efficient in enhancing the Concrete's properties by increasing its initial strength. Carbonate Calcium some percentage of the bacteria's void volume has been filled, making the texture more compact and resistive to infiltration.

3. BACTERIAL CONCRETE

Therefore, bacterial-induced Calcium Carbonate (Calcite) precipitation was proposed as an alternative and environmentally friendly crack remediation and improved building material strength. A novel technique is adopted to remediate cracks and fissures in calcium concrete using Microbiologically Induced Calcite or Carbonate (CaCO3). Precipitation (MICP) is a technique that falls within a broader scientific category called biomineralization. MICP is highly desirable because the Calcite precipitation caused by microbial activity is pollution-free and natural. The method can be used to improve the compressive strength and rigidity of cracked concrete specimens.

The research leading to microbial precipitation of Calcium Carbonate and its ability to heal cracks of building materials has resulted in many applications such as crack remediation of Concrete, consolidation of sand, restoration of historical monuments, and such applications. Thus it can be defined as "The process can occur within or outside the microbial cell or even some distance within the Concrete. Often bacterial activities simply trigger a change in solution chemistry that leads to over-saturation and mineral precipitation. Using these bio-mineralogy concepts in Concrete leads to the potential invention of new material called bacterial Concrete.

4. SELF HEALING BACTERIAL CONCRETE

The autogenous crack-healing capacity of Concrete has been recognized in several recent studies. Mainly micro cracks with widths typically between 0.05 and 0.1 mm have been observed to be completely sealed, especially under repetitive dry/wet cycles. This autogenous healing mechanism is primarily due to secondary hydration of non- or partially reacted cement particles present in the Concrete. Due to capillary forces, water under changing wet and dry cycles is repeatedly drawn into the micro cracks, resulting in the expansion of hydrated cement particles due to the formation of calcium silicate hydrates and calcium hydroxide. These reaction products are capable of sealing cracks completely provided crack widths are small. Because of the limited amount of non-reacted cement particles present, larger-sized gaps can only be partially filled, resulting in only a thin layer of hydration products on the crack surface. Hence, an alternative and more sustainable self-healing mechanism are needed for these reasons.

The bacteria to be used in Concrete as a self-healing agent should be fit for the job, i.e., they should perform long-term efficient crack sealing, preferably during the lifetime of the total constructions. Bacterial crack healing's primary mechanism is that the bacteria act primarily as a catalyst, transforming a precursor compound into an appropriate filler material. The newly manufactured compounds, such as mineral precipitates based on calcium carbonate, should act as a type of bio-cement which effectively seals freshly formed cracks. Therefore, both bacteria and a bio-cement precursor compound should be integrated into the material matrix for effective self-healing.

5. DETERMINATION OF FINENESS OF CEMENT BY SIEVING

Sl. No.	Weight of sample taken (W) (in g.)	Weight of residue (R) (in g.)	%age of residue $=\frac{R}{W}\times 100$	Average % of the residue
1	100	90	90/100*100	9%
2	110	100	100/110*100	10%
3	120	110	110/120*100	11%

Table 1 : finess of cement

6. CONSISTENCY TEST ON CEMENT

Sl. No.	Wt of cement in gram	Wt of water in gram	Height not penetrated (in mm)	Consistency Of cement in % b/a*100

1	200	52 ml	33mm	26
2	200	60ml	28mm	30
3	200	64 ml	28mm	32
4	200	66ml	14.5mm	33
5	200	70 ml	7 mm	35

Table 2 consistency test on cement

7.DETERMINATION OF SETTING TIMES OF CEMENT

Time in minutes:	0 10 20 30 40 50 60
Height in mm fails to penetrate	40 40 40 40 40 39 37

Table 3: setting time of cement

8.DETERMINATION OF COMPRESSIVE STRENGTH OF CEMENT

For 3 days' strength:

Sl. No	Length (L) in mm	Breadth (B) in mm	Load (F) in N	compressive strength in N/mm2
1	150 mm	150 mm	300 kn	24.5
2	150 mm	150 mm	300 kn	25.6
3	150 mm	150 mm	300 kn	26

For 7 days' strength:

Sl. No	Length (L) in mm	Breadth (B) in mm	Load (F) in N	compressive strength in N/mm2
1	150 mm	150 mm	300 kn	25.6
2	150 mm	150 mm	300 kn	26.1
3	150 mm	150 mm	300 kn	26.68

For 28 days of strength

Sl. No	Length (L) in mm	Breadth (B) in mm	Load (F) in N	compressive strength in N/mm2
1	150 mm	150 mm	300 kn	38.1
2	150 mm	150 mm	300 kn	39.56
3	150 mm	150 mm	300 kn	40.2

Compressive test: using a universal testing machine

Days	6ml	12 ml	18ml	24ml
3	367.0	298.0	236.5	149.5
7	25.6	26.1	26.68	26.02
14	35.8	36.14	36.44	35.88
28	39.38	39.56	40.2	40.06

Table 4 compressive strength of SCC with bacteria in different dosage at different ages of concrete

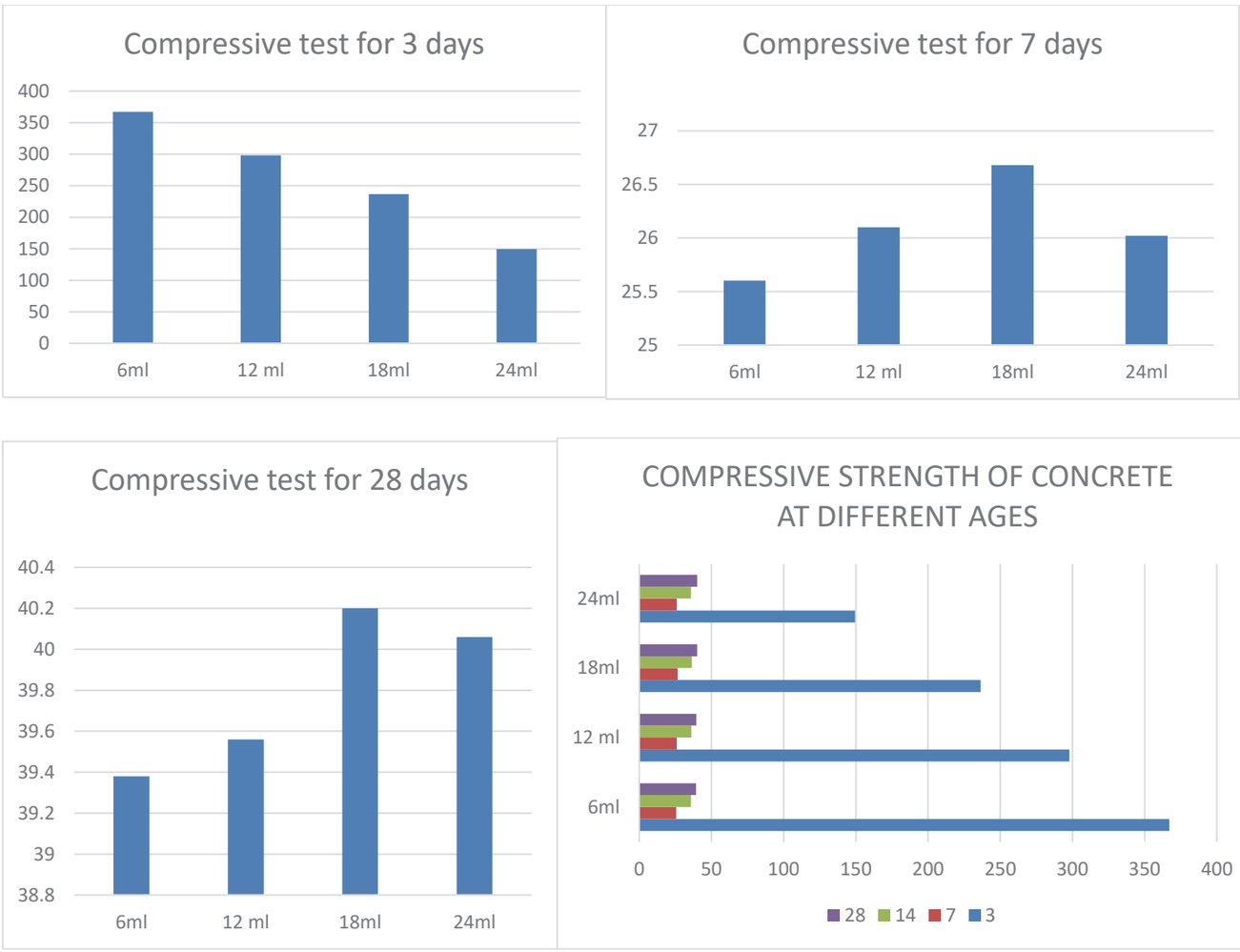

Figure 1: compressive strength of SCC with bacteria in different dosage and 3,7,14 and 28 days curing of concrete

TENSILE TEST: USING UNIVERSAL TESTING MACHINE

Days	6ml	12 ml	18ml	24ml
3	4.5	4.8	5.0	5.1
7	4.8	4.92	5.00	5.26
14	5.68	5.72	5.86	5.76
28	6.24	6.46	6.74	6.52

Table 5: Tensile strength of SCC with bacteria in different dosage at different ages of concrete

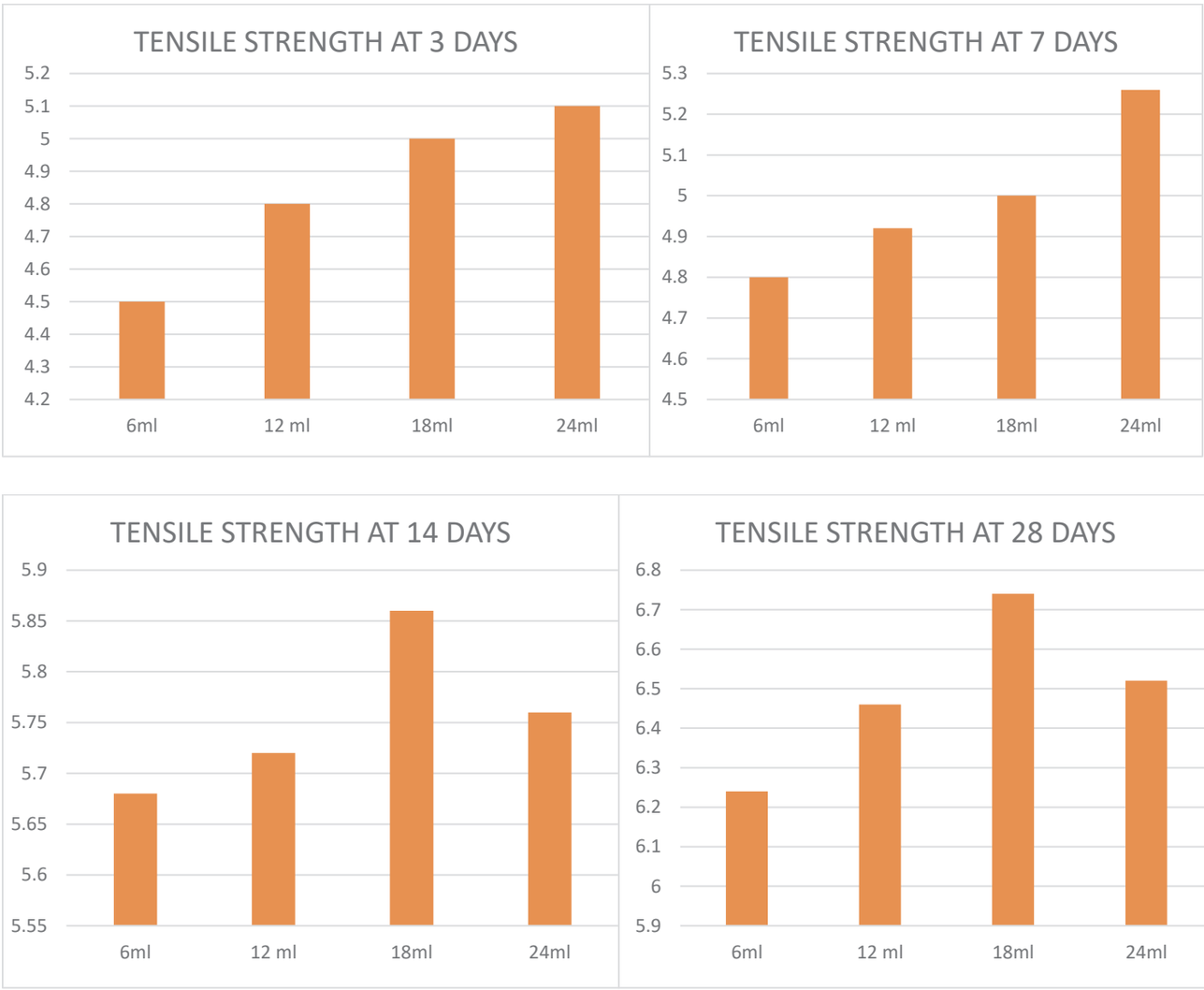

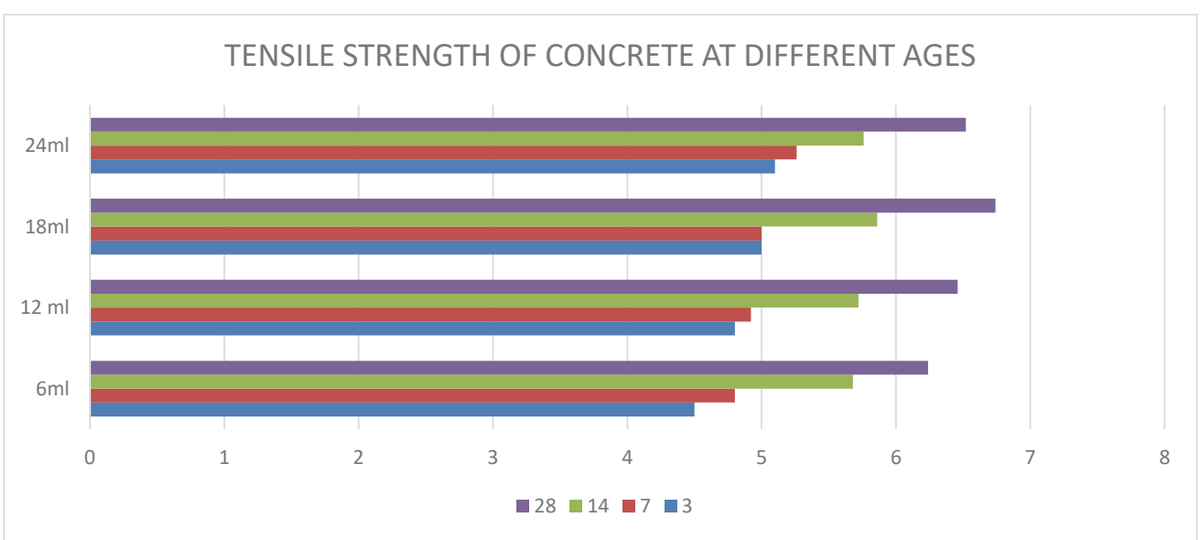

Figure 2: Tensile strength of SCC with bacteria in different dosage at 3,7,14 and 28 days of concrete curing.

FLEXURAL TEST: USING UNIVERSAL TESTING MACHINE

Days	6ml	12 ml	18ml	24ml
3	3.5	3.8	3.0	3.1
7	3.8	3.92	3.00	3.26
14	4.46	4.62	4.84	4.74
28	5.12	5.2	5.36	5.22

Table 6: Flexural strength of SCC with bacteria in different dosage at different ages of concrete

Figure 3: Flexural strength of SCC with bacteria in different dosage at 3, 7, 14, and 28 days of concrete curing

9 CONCLUSIONS

The goal of this study was to enhance the engineering properties of concrete, using a single species of bacteria. Many bacteria are reported in literature that can enhance the power, durability and other mechanical characteristics of Concrete. To study the variation of compressive strength, flexural strength and split tensile strength of concrete cube with various dosage of bacteria, a concrete of water cement ratio of 0.40 are considered to prepare the cubes. Accordingly, different cubes with bacterial concentration of 6ml, 12ml, 18ml and 24ml are prepared.

- The required bacteria should be carefully chosen to enhance the properties of the cement mortar or concrete. In the given environment, for example, Bacillus cereus could not survive, while another Bacillus sphaericus species survived.
- With an increase in bacterial dosage of up to 24ml, the compressive strength at 18 ml (at 7 days and at 28 days) of the cube was observed to be growing. Further changes in bacteria concentration, however, have been shown to decrease the compressive strength of concrete cube.
- With an increase in bacterial dosage of up to 24ml, the split tensile strength for 18 ml (at 7 days and at 28 days) of the cube was observed to be growing. Further changes in bacteria concentration, however, have been shown to decrease the tensile strength of concrete cube.
- With an increase in bacterial dosage of up to 24ml, the flexural strength for 18 ml (at 7 days and at 28 days) of the cube was observed to be growing. Further changes in 79 bacteria concentration, however, have been shown to decrease the flexural strength of concrete cube.
- The optimum doses of bacteria found to increase the average compressive strength, flexural strength and split tensile strength by 4% (at 7-day) and 2% (at 28-day) over the control specimen. The more increase in strength after 7-day curing may be due to the presence of nutrient medium and it getting depleted as it reaches 28 days and causing death of bacteria.

10. SCOPE OF FURTHER STUDY

- In this study only durability properties of SSC concrete has been studied like compressive strength, split tensile strength and flexural strength.
- The morphology of the bacterial can be studied by FESEM and XRD methods.

REFERENCES

[1] Siddique, R and Chahal, N. K. (2011). Effect of ureolytic bacteria on concrete properties. Construction and Building Materials, 25, 3791–3801

[2] Pacheco-Torgal, F., and Labrincha, J.A. (2013) Biotech cementitious materials: Some aspects of an innovative approach for Concrete with enhanced durability, Construction and Building Materials, 40, 1136–1141

[3] Wiktor, V., and Jonkers, H. M. (2011) Quantification of crack-healing in novel bacteria

based self-healing concrete, Cement & Concrete Composites, 33 ,763–770.

[4] Chahal, N., Siddique, R. and Rajor, A. (2012). Influence of bacteria on the compressive strength, water absorption and rapid chloride permeability of Concrete incorporating silica fume, Construction and Building Materials, 37, 645–651

[5] Achal, V., Mukerjee, A., Basu, P. C. and Reddy, M. S (2009). Strain improvement of Sporosarcina pasteurii for enhanced urease and calcite production, Journal of Industrial Microbiology Biotechnology, 36, 981–988

[6.] Is 3812-1981, Indian standards specification for fly ash for use of pozzolana and admixture. Bureau of Indian Standards. New Delhi.

[7]. Hajime Okamura, "Self-Compacting High Performance Concrete Ferguson Lecture for 1996", Concrete International, Vol.19, No.7, pp. 50-54.

[8]. Ozawa K., Kunishama M, Makala K, "Development of High Performance Concrete Based on the Durability Design of Concrete Structures" Proceeding of the second East-Asia and Pacific Conference on Structural Engineering and construction (EASEC2), Vol.1, pp. 445-450, January 1989.

[9]. K C Panda, P K Bal, "Properties of self-compacting concrete using recycled coarse aggregate", procedia engineering 51(2013) 159- 164.

[10] IS 456-2000. Design Specifications of Plain & Reinforced Concrete, Bureau of Indian Standards. New Delhi

[11].IS 10262-2009. Recommended guidelines for Concrete Mix Design, Bureau of Indian Standards. New Delhi.

[12] Achal, V., Mukerjee, A., and. and Reddy, M. S, (2011) Effect of calcifying bacteria on permeation properties of concrete structures, Journal of Industrial Microbiology Biotechnology, 38, 1229–1234

[13] Majumdar., Sarkar, M., Chowdhury, T., Chattopadhyay, B., and Mandal's. (2012) Use of bacterial protein powder in commercial fly ash pozzolana cements for high performance construction materials, Open Journal of Civil Engineering, 2, 218-228

STUDY ON MECHANICAL PROPERTIES OF HYBRID FIBRE REINFORCED TERNARY BLENDED CONCRETE WITH RECYCLE AGGREGATE

DR. AMARESH BABU (2)

Department of Civil Engineering

NSAKCET, India

SYED SULEMAN JALAL (1)

Department of Civil Engineering

NSAKCET, India

ABSTRACT Extensive research work is in progress throughout the world in concrete technology to find alternative materials which can be partially or fully replace of Ordinary Portland Cement and coarse aggregate, which can also meet the required strength and durability, mainly aims at reducing cost and environmental effects due to cement manufacturing processes. In the present study, Ordinary Portland Cement (OPC) of 43 grade is partially replaced by up to 20% of mineral admixtures by Fly Ash (FA) 10%, and Silica Fume (SF) 10% by weight of cement used and coarse aggregate by 30% with Recycle aggregate in making Hydrid Fibre Reinforced Concrete. Hybrid Fibre Reinforced Concrete with 1.0% of steel fibres and 0.5% polypropylene Fibre content by volume fraction are considered for study M30 grade of concrete with a constant Water- Cement ratio of 0.4 has been used in the work.

Keywords: Ordinary Portland Cement, coarse aggregate, Fly Ash, Silica Fume, steel fibres, polypropylene Fibre

.

1. Introduction

The use of recycled aggregate concrete (RAC) is acquiring a particular interest in civil construction regarding sustainable development. Many studies demonstrate the feasibility of the use of crushed concrete as a coarse aggregate. The urbanization growth rate in India is very high due to industrialization. Rapid infrastructure development requires a large number of construction materials, land requirements, and the site. For large construction, concrete is preferred as it has a longer life, low maintenance cost & better performance.

- The experimental study is carried out to investigate the behavior of Ternary blended concrete of grade M30 blended with fly ash, silica fume, and steel fiber, polypropylene fibers by varying the percentage of steel fibers by 0.25%, 0.5%, 0.75% and 1.0%.and percentage of polypropylene fibers are kept as 0.5%.

- The present study is carried out to obtain the optimum percentage of steel fiber and polypropylene fibers required to enhance the flexural, compressive and split tensile strength

2 Literature Review

Nguyen Van CHANH [5] (2005) has submitted a paper on influence of steel fiber reinforced concrete. It is now well established that one of the important properties of steel fiber reinforced concrete (SFRC) is its superior resistance to cracking and crack propagation. As a result of this ability to arrest cracks, fiber composites possess increased extensibility and tensile strength, both at first crack and at ultimate, particular under flexural loading; and the fiber are able to hold the matrix together even after extensive cracking. The net result of all these is to impart to the fiber composite pronounced post – cracking ductility which is unheard of in ordinary concrete. The transformation from a brittle to a ductile type of material would increase substantially the energy absorption characteristics of the fiber composite and its ability to withstand repeatedly applied, shock or impact loading.

The fibers themselves are, unfortunately, relatively expensive; a 1% steel fiber addition will approximately double the material costs of the concrete, and this has tended to limit the use of SFRC to special applications.

T.D. Gunneswara Rao [4] (2003) has carried out an investigation consisted of short-term tests on plain steel fiber reinforced concrete members of same cross sectional area varying the volume fraction of fibers and strength of concrete. The volume fraction of the fiber varied from 0% to 1.2% at an equal interval of 0.3%. The grades of concrete considered for the study are 20, 30, 40 and 50MPa). Thus, 20 beams of size 100_200_2000 mm were cast for testing under pure torsion. During the casting of each beam three companion cube specimens and three cylindrical specimens for assessing the compressive strength and split tensile strength of the matrix were cast and cured along with the corresponding beams under same conditions of environment. He concluded that a minimum volume fraction of fiber content of 0.9% is required to impart noticeable ductility to the SFRC beams under torsion.

Saravanan et al (2002) has submitted a paper on Fiber Reinforced Polymer (FRP) as an external

reinforcement is used extensively to address the strength requirements related to flexure and shear in structural systems. But the strengthening of members subjected to torsion is yet to be explored. In this paper, the behavior and performance of reinforced concrete members strengthened with externally bonded Glass FRP (GFRP) sheets subjected to pure torsion is presented. The variables considered in the experimental study include the fiber orientation, the number of beam faces strengthened (three or four), the effect of number of FRP plies used, and the influence of anchors in U-wrapped test beams. Experimental results reveal that externally bonded GFRP sheets can significantly increase both the cracking and the ultimate torsional capacity. Predicted strengths of the test beams using the proposed theoretical models were found to be in good agreement with the experimental results.

3.Steel Fiber Reinforced Concrete (SFRC)

Concrete is the most widely used structural material in the world with an annual production of over seven billion tons. For a variety of reasons, much of this concrete is cracked. The reason for concrete to suffer cracking may be attributed to structural, environmental, or economic factors, but most of the cracks are formed due to the inherent weakness of the material to resist tensile forces. Again, concrete shrinks and will crack, when it is restrained. It is now well established that steel fiber reinforcement offers a solution to the problem of cracking by making concrete tougher and more ductile**.** Steel-fiber volumes used in concrete typically range from 0.25% to 2%. Volumes of more than 2% generally reduce workability and fiber dispersion and require special mix design or concrete placement techniques. The compressive strength of concrete is only slightly affected by the presence of fibers. The addition of 1.5% by volume of steel fibers can increase the direct tensile strength by up to 40% and the flexural strength up to 150%. As per ASTM A820.

4. Polypropylene fibers

Polypropylene fibers were first suggested as an admixture to concrete in 1965 for the construction of blast resistant buildings for the US Corps of Engineers. The fiber has subsequently been improved further and at present, it is used either as short discontinuous fibrillated material for the production of fiber-reinforced concrete or a continuous mat for the production of thin sheet components. Since then the use of these fibers has increased tremendously in the construction of structures because the addition of fibers in concrete improves the toughness, flexural strength, tensile strength, and impact strength as well as failure mode of concrete. Polypropylene twine is cheap, abundantly available, and like all manmade fibers of consistent quality.

5. finess of Cement:

DESCRIPTION	SAMPLE		
	I	II	III
a) Weight of cement (W) g	10	10	10
b) I.S. sieve size μ	90	90	90
c) Sieving time min.	15	15	15
d) Weight retained on sieve(W_1) g	0.71	0.80	0.86
e) Percent weight retained on sieve =(W_1/W)x100	7.1	8.0	8.6

Table 1: finess of cement

6. SOUNDNESS OF CEMENT

DESCRIPTION	SAMPLE		
	I	II	III
Weight of sample (C)	100	100	100
Water added to the sample(0.78xPxC)	25.74	25.74	25.74
Time at which the sample is kept in water at 27°C to 32 °C	12.15pm	12.15pm	12.15pm
Distance between the pointer ends before heating (D_1) mm	38	37	32
Time when the water is brought to boiling point	1.00pm	1.00pm	1.00pm
Time of heating, hr	3	3	3
Distance between the pointer ends after heating (D_2) mm	34	35	33
Difference (D_2-D_1) mm	4	2	1

Table 2 soundness of cement

7.DETERMINATION OF SETTING TIMES OF CEMENT

S.No.	Time in minutes after water added	Penetration reading
1.	5	16
2.	10	25
3.	15	15
4.	20	23
5.	25	24
6.	30	24
7.	35	24
8.	40	28
9.	45	30
10.	50	31
11.	55	36

Initial setting time of cement was found to be 55 minutes.

Table 3: setting time of cement

8.DETERMINATION OF COMPRESSIVE STRENGTH OF CEMENT

28 DAYS COMPRESSIVE STRENGTH

S.NO	SAMPLE	LOAD (KN)	AREA mm^2 (150 X 150)	COMPRESSIVE STRENGTH	AVG COMPRESSIVE STRENGTH N/mm^2
1	M_0	620	22500	27.57	29.01
		650	22500	28.88	
		690	22500	30.6	
2	M_1	800	22500	35.5	33.43
		740	22500	32	
		720	22500	32.8	
3	M_2	820	22500	36.4	36.42
		780	22500	34.66	
		860	22500	38.22	
4	M_3	890	22500	39.55	39.50
		850	22500	37.77	
		930	22500	41.33	
5	M_4	1050	22500	46.66	46.22
		970	22500	44	
		1080	22500	48	
6	M_5	970	22500	43.11	41.33
		930	22500	41.33	
		890	22500	39.55	

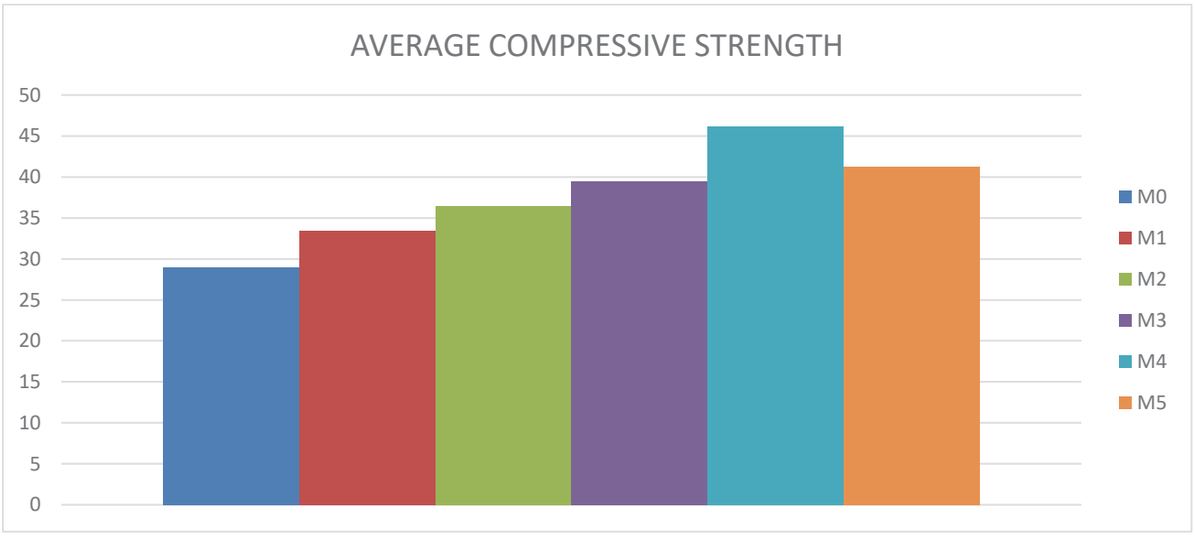

Figure 1: average compressive strength of concrete with different ratio of steel and: Polypropylene fibers

M_0: TBC (cement 80% + silica flume 10% + fly ash 10%)

M_1: TBC + PPF (0.5 %)

M_2: TBC + PPF (0.5 %) + SF (0.25%) M_3: TBC +

PPF (0.5 %) + SF (0.5%) M_4: TBC + PPF (0.5 %)

+ SF (0.75%) M_5: TBC + PPF (0.5 %) + SF (1%)

TBC: Ternary blended concrete (cement 80% + silica flume 10% + fly ash 10%) PPF:

Polypropylene fibers

SF: Steel fibers.

SIZE OF CUBE: 150 x 150 x 150.

9.TENSILE TEST: USING UNIVERSAL TESTING MACHINE

28 DAYS SPLIT TENSILE STRENGTH

S.No	SAMPLE	LOAD (KN)	π X l X d	SPLIT TENSILE STRENGTH N/mm^2	AVG SPLIT TENSILE STRENGTH N/mm2
1	M_0	180	141371.67	2.54	2.28
		230		3.25	
		190		2.68	
2	M_1	220	141371.67	3.11	3.03
		200		2.82	
		225		3.18	
3	M_2	240	141371.67	3.39	3.39
		220		3.11	
		160		3.67	
4	M_3	270	141371.67	3.81	3.76
		250		3.53	
		280		3.96	
5	M_4	290	141371.67	4.1	4.19
		280		3.96	
		320		4.52	
6	M_5	280	141371.67	3.96	3.87
		240		3.39	
		300		4.24	

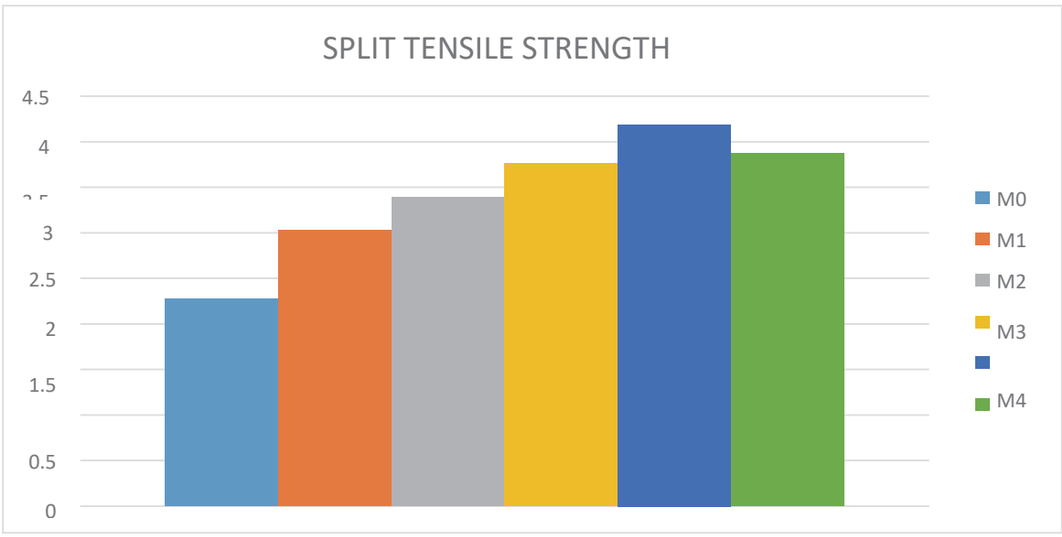

Figure 2 split tensile strength of concrete with different ratio of steel and: Polypropylene fibers

M_0: TBC (cement 80% + silica flume 10% + fly ash 10%)

M_1: TBC + PPF (0.5 %)

M_2: TBC + PPF (0.5 %) + SF (0.25%) M_3: TBC +

PPF (0.5 %) + SF (0.5%) M_4: TBC + PPF (0.5 %)

+ SF (0.75%) M_5: TBC + PPF (0.5 %) + SF (1%)

TBC: Ternary blended concrete (cement 80% + silica flume 10% + fly ash 10%) PPF:

Polypropylene fibers

SF: Steel fibers.

SIZE OF CUBE: 150 x 150 x 150.

FLEXURAL TEST: USING UNIVERSAL TESTING MACHINE

S.No	SAMPLE	LOAD (KN) (P)	Flexural strength $f=Pl/bd^2$	f_{Avg} (N/mm^2)
1	M_0	20	3.55	
		21.5	3.82	
		18	3.2	3.52
2	M_1	20.5	3.64	
		19	3.37	
		24.5	4.35	3.78
3	M_2	22.5	4	
		25	4.44	
		20.5	3.64	4.02
4	M_3	23.5	4.17	
		26	4.62	
		21	3.73	4.17
5	M_4	25.5	4.53	
		27	4.8	
		24	4.26	4.53
6	M_5	22.5	4	
		24	4.26	
		21	3.73	3.99

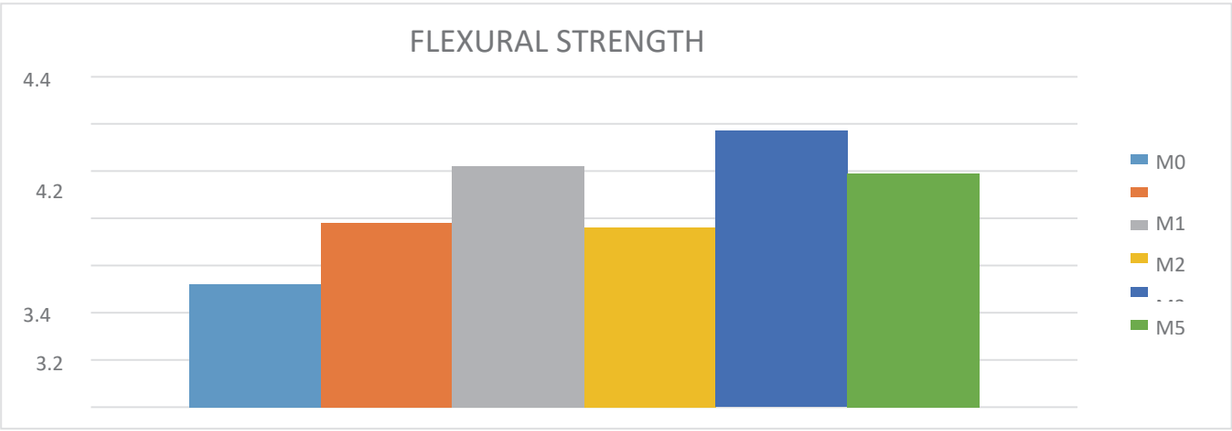

M_0: TBC (cement 80% + silica flume 10% + fly ash 10%)

M_1: TBC + PPF (0.5 %)

M_2: TBC + PPF (0.5 %) + SF (0.25%) M_3: TBC +

PPF (0.5 %) + SF (0.5%) M_4: TBC + PPF (0.5 %)

+ SF (0.75%) M_5: TBC + PPF (0.5 %) + SF (1%)

TBC: Ternary blended concrete (cement 80% + silica flume 10% + fly ash 10%) PPF:

Polypropylene fibers

SF: Steel fibers.

SIZE OF CUBE: 150 x 150 x 150

Figure 3: flexural strength of concrete with different ratio of steel and: Polypropylene fibers

9 CONCLUSIONS

From the limited research work conducted the following conclusions are drawn

- The 28-days flexural strength in M4 with TBC + PPF (0.5 %) + SF (0.75%) RCA mix has higher target strength compared to other samples.
- The 28-days compressive strength in M4 with TBC + PPF (0.5 %) + SF (0.75%) RCA mix has the required target strength higher than other samples.
- The 28-days split tensile strength in M4 with TBC + PPF (0.5 %) + SF (0.75%) RCA mix has achieved the required target strength.

10. SCOPE OF FURTHER STUDY

- Due to large elastic modulus and shrinkage deformations, RAC is not recommended to structural members. So Monitoring of long term performance and volume change (elastic modulus and shrinkage) must be assessed in the concrete produced with 100% RCA.
- Micro structural analysis using SEM and XRD to study the effect of porous layers between old mortar and aggregates in 100% RCA concrete. Micro filling of ITZ zone must be studied
- Study of crack initiation and propagation in 100% RAC concrete: The weakness of old attached mortar will lead to reduced bond between old and new mortar in RAC.

REFERENCES

1. Larbi Belagraa1, Miloud Beddar, Study of the Mechanical Performance of a Recycled Aggregate Concrete with Admixture Addition, Open Journal of Civil Engineering, 2013, Vol 3, pp.99-103)

2. Mr. Tushar R Sonawane, Prof. Sunil S. Pimplikar, Use of Recycled Aggregate Concrete, IOSR Journal of Mechanical and Civil Engineering, pp.52-59)

3. Suryakantam Rao, Lakshmi, Recycled aggregate concrete for Transportation Infrastructure, Science Direct, Vol.104,2013, pp.1158–1167)

4. Ryan Morgan. Umed Aziz, Simon Herfellner and Kenneth Ho., Performance and Implementation of Low-Quality Recycled Concrete Aggregate the Journal of Sustainable Development Vol.10, 2013,

Pp.72-84)

5. Vivian W.Y. Tam, X.F. Gao and C.M. Tam., Microstructural analysis of recycled aggregate concrete produced from two-stage mixing

approach, Journal of Cement and Concrete Research, Vol.35,2005, pp.1195–1203.11)

6. Vivian W.Y. Tam, X.F. Gao and C.M. Tam., Microstructural analysis of recycled aggregate concrete produced from two-stage mixing approach, Journal of Cement and Concrete Research, Vol.35,2005, pp.1195–1203.11)101

7. Zhang, J., Shi, Li, Y Pan, X., Poon, C, Xin, Z, Performance Enhancement of Recycled Concrete Aggregates through Carbonation, "American Society of Civil Engineers2015", Volume 27, (2015), pp.04015029 – (1-6)

8. Ahmed Shaban Abdel-Hay, Properties of recycled concrete aggregate under different curing conditions "Housing and Building National Research Center", 2015, Volume 11, pp.1-6

9. Mmasetlhomo Tommy Gumede1, Shodolapo Oluyemi Franklin, Studies on Strength and Related Properties of Concrete Incorporating Aggregates from Demolished Wastes "Open Journal of Civil.

10. Prachi Sohoni and Vaishali Sahu, Comparative Strength Studies of Recycled Aggregate Concrete and Fresh Concrete, "An International Journal, 2015, Vol.2, No.3, pp.9-13

11. Sherif Yehia, Kareem Helal, Anaam Abusharkh, Amani Zaher, and Hiba Istaitiyeh, Strength and Durability Evaluation of Recycled Aggregate Concrete, "International Journal of Concrete Structures.

12. K. C. Chew, Singapore's strategies towards sustainable construction, "The IES Journal Part A: Civil & Structural Engineering, 2015 pp.196-202.102

RECOGNIZING HANDWRITTEN CHARACTERS USING MULTI-LAYER PERCEPTRON – A COMPARATIVE STUDY

[1]Syeda Maherunnisa, [2]Mohammad Sanaullah Qaseem
[1]PG scholar, Department of CSE, Nawab Shah Alam Khan College of Engineering and Technology, Hyderabad.
[2]Professor and Head, Department of CSE, NSAKCET, Hyderabad

ABSTRACT

Handwritten Character Recognition (HCR) is an intriguing area for applying artificial intelligence. It is a popular belief that the doctor's handwriting is not so legible. But when it comes to the other languages especially the regional languages it becomes more difficult to interpret the scribbled nature of various types of handwritten letters, scriptures, postcards, diary entries, paper post it messages to name a few. Its not a difficult job for a literate human to recognize the characters or '*lipi*' of a language, but when it comes to using Artificial intelligence as a cutting-edge technology, interpretation becomes easy. The handwritten text is partitioned based on its understanding, into three levels viz, directly understandable, moderately understandable and troublesome. A Handwritten Character Recognition method is proposed which is totally dependent on Artificial Intelligence, using the Multi-Layer Perceptron (MLP) calculations. The manually written textual styles utilized here are multi-content, which comprises of pictorial datasets of Bangla Textual Style, Latin Style and MNIST Style. Different pictures utilized in this trial are preprocessed using the OCR. The originally image set was the MNIST, Latin and Bangla text style set in a test to quantify the adequacy of this exploration. The trial and the outcomes show more precise consequences of this framework contrasted with the other methodologies.

Keywords: Handwritten Character Recognition, Multi-Layer Perceptron, OCR, Bangla data, Latin data, MNIST

1. INTRODUCTION

Manually Written Character Recognition is a difficult subject in the field of artificial intelligence. This technique encourages the interpretation of various types of scribbled texts of various types of handwritten letters, scriptures, postcards, diary entries, paper post it messages etc. The complexity based in understanding it is isolated into three levels, basic (Fig 1), moderate (Fig 2) and troublesome (Fig 3) as appeared in the figure's underneath.

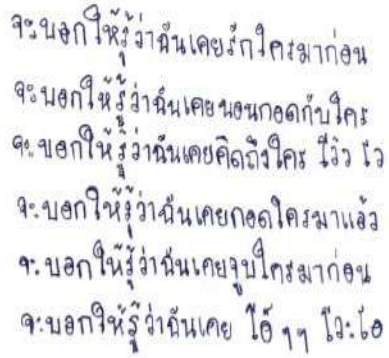

Fig. 1. A Basic Handwriting

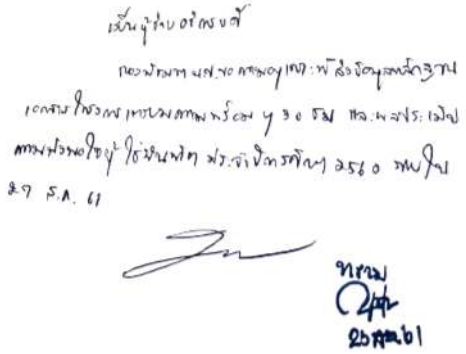

Fig. 2. A Moderate Handwriting

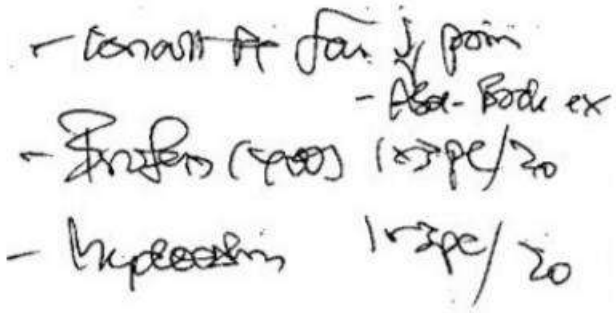

Fig. 3. A Troublesome Handwriting

In this paper, we examine a proper technique to build up another calculation for penmanship recognition using artificial insight dependent on the applied structure of research. The test and the outcomes show better results of

this framework contrasted with the Support Vector Machine (SVM) calculation.

The Data Set models viz Bangla, Latin and MNIST is given in the Fig. 4, Fig.5, and Fig.6 separately. Bangla is the second most mainstream language in India. It consists of 50 basic alphabets which includes 11 vowels and 39 consonants. Even though its a widely used language, there has not been much research conducted on the handwriting recognition of this language, compared to English. Latin is utilized for Identifying measurable names and utilizing the firemaker informational index as manually written notes. MNIST informational index is a digitized picture that is scaled to the norm and fixated on a manually written static size. The MNIST database (Modified National Institute of Standards and Technology database) is an enormous database of handwritten digits which are used usually for training various image processing systems. The database is also widely used for training and testing in the field of machine learning.

Fig. 4. Bangla Data Set

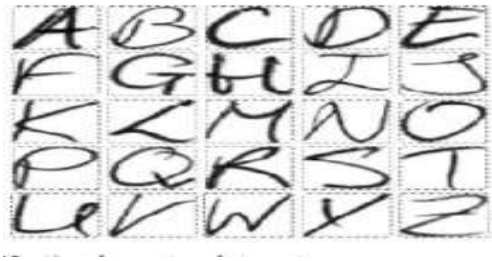

Fig. 5 Latin Data Set

Fig. 6. MNIST Data Set

2. LITERATURE REVIEW

Earlier works by researchers [1] is delivers a group of character fragments (fraglets). Utilizing a codebook of fraglets from a free set, the likelihood appropriation of fraglet shapes was figured for an autonomous set. Another study [2] discusses the various informational collections utilizing the field of archive examination, to show that new techniques can possibly outflank conventional strategies applied to diagram portrayals. In [3] the dissemination of samples is seen by the closest neighbor investigation and network examination, the two of which don't make any estimate and subsequently don't degenerate the subtleties of the circulation. Vapnik Etal in their study suggest that the Support Vector Machine (SVM) calculation was applied to numerous sorts of acknowledgment issues. Straight SVM valuable for arrangement issues and will locate the best hyperplanning, with the greatest separation at the preparation guide close toward the hyperplane. Non-Linear SVM issues are for various gatherings which it does by making and joining numerous parallel identifiers.

3. PROPOSED METHODOLOGY

The proposed handwritten character recognition methodology has been implemented using Optical Character Recognition (OCR)**.** The change of pictures of printed, transcribed or composed content is finished by Optical Character Reader (OCR). The Conversion of pictures is done from a checked archive, a photograph of the record.

Broadly utilized as a type of data whether it is identification information, it is a typical technique for digitalizing printed messages so they can be electronically altered, looked, put away more minimally, showed on-line, and utilized in machine interpretation, (extricated) text-to-discourse, key information and text mining. OCR is a tremendous field of examination in design acknowledgment, artificial knowledge and PC vision. It is a process of classifying optical patterns with respect to alphanumeric or other characters.

Optical character recognition process includes segmentation, feature extraction and classification. Text capture converts Analog text-based resources to digital text resources. And then these converted resources can be used in several ways like searchable text in indexes so as to identify documents or images.

1. Preprocessing
2. Segmentation
3. Feature Extraction
4. Class Prediction

As the first stage of text capture a scanned image of a page is taken. And this scanned copy will form basis for all other

stages. The very next stage involves implementation of technology Optical Character Recognition for converting text content into machine understandable or readable format. OCR analysis takes the input as digital image which is printed or handwritten and converts it to machine readable digital text format using the Multilayer Perceptron Learning Algorithm developed is pertaining to the stages as described below:
Step 1: Initializes the Network, with all the weights and set to random numbers between -1 to +1.
Step 2: Presents the First Training Patter and Obtain the Output.
Step 3: Compares the Network Output with the Target Output.
Step 4: Propagates the error backwards. We need to correct the weights of the output layer and then Correct the input weights.
Step 5: Takes the average difference between the target and the output vector to calculate the error.
Step 6: Repeats Step 2 to 5 for each pattern in the training set. (one complete epoch).
Step 7: Shuffle the training set randomly.
Step 8: Repeat Step 2 for a set number of epochs, or until the error ceases to change.

The OCR then processes this digital image after performing the MLP algorithm into small components for analysis of finding text or word or character blocks. And again, the character blocks are further broken into components and are compared with dictionary of characters.

Preprocessing

Information Preprocessing alludes to the means which are applied to make information more appropriate for information mining. The means utilized in Data Preprocessing are generally of two classifications:
• Selecting information objects and characteristics for the examination.
• Creating/changing the traits.

Segmentation

Picture division is the way toward separating advanced picture into various sections. The point of division is to rearrange, change the picture into something more significant and simpler to examine. Picture division is commonly used to find articles and limits which are typically lines, bends and so on in pictures.

Feature Extraction

Feature Extraction in Image handling for handwriting recognition begins with estimated information and manufactures inferred values, which are expected to be educational, which encourages the ensuing learning and speculation steps, prompting better human understandings.

Highlight Extraction is the most basic aspect of this theory, consequently expounding some more subtleties. The eight-neighbor contiguous philosophy is utilized for extraction data on the limit of a manually written character. Limit of the character is examined and identified by checking it in the parallel picture design. Clockwise bearing inquiry is completed. The Two pixels are associated on the off chance that they are neighbors and their grayscale levels are in accordance with the predefined exactness of closeness. The informational collection of the apparent multitude of pixels associated P is called part containing P. This is appeared in Fig.7.

P1	P2	P3
P8	P	P4
P7	P6	P5

Fig. 7. Pixel P with 8-Neighbors

At the point when a white pixel is identified, it checks another new white pixel and afterward that pixel again checks another white pixel, etc the way toward finding the white pixels proceed. The following follows on persistently till the limit is naturally got. The limit is reserved as appeared in Fig. 8.

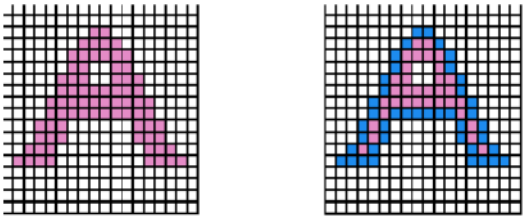

Fig. 8. Images showing the boundary

The Inner Boundary Tracing is finished utilizing the Inner Boundary Tracing Algorithm. Right off the bat the picture from upper left until a pixel of another area is found is looked, this pixel P1, at that point has least section estimation of the apparent multitude of pixels of that locale having a column esteem. At that point search the 3x3 neighborhood of the flow pixel in hostile to clockwise bearing. The if the flow limit component P1 is same to the second limit component P2, and if the past fringe component Pn-1 is same as P1, stop, else then keep on looking through the 3x3 neighborhood of the current pixel. The internal limit is distinguished and spoken to by pixels P1 … .. Pn-2.

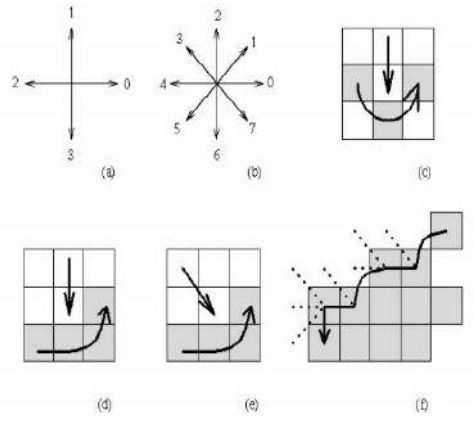

Fig. 9 Inner Boundary Tracing:

9(a) Direction Notation, 4-connectivity;
9(b) It depicts the 8-boundary;
9(c) This is the Pixel Neighborhood search sequence in 4-connectivity;
9(d) and 9(e) These are the search sequences in 8-connectivity;
9(f) Boundary Tracing in 8-connectivity with the dashed lines showing pixels tested during the border tracing.

The Outer Boundary Tracing is finished by utilizing the Outer Boundary Tracing Algorithm. Here right off the bat the internal district of the limit in 4-availability is done work it is obviously got. At that point all the non-locale pixels from the external limit which are pertinent that were tried during the inquiry cycle is done; on the off chance that a few pixels were tried more than once, at that point they are recorded more than once in the external limit list which is appeared in Fig. 10.

Once the boundaries are earmarked and found. The Fourier Descriptors are involved in finding the Discrete Fourier coefficients through equations (1) and (2) as given below.

$$a[k] = 1/L \, \Sigma \, x[m] e^{-jk(2\pi/L)m} \qquad (1)$$

$$b[k] = 1/L \, \Sigma \, y[m] e^{-jk(2\pi/L)m} \qquad (2)$$

Once the Discrete Fourier Coefficients are derived, they are computed by eliminating the size of the character and thus the Feature is extracted.

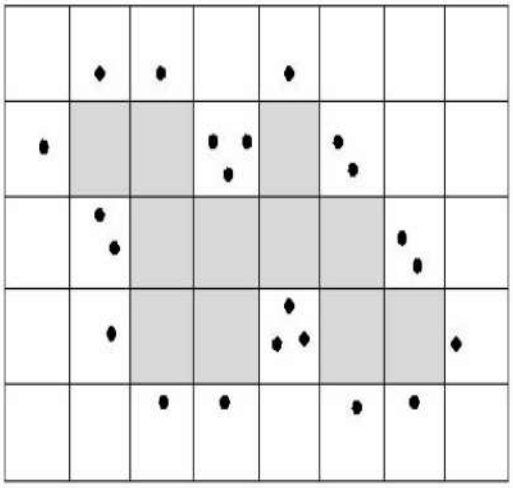

Fig. 10. Outer Boundary Tracing. The Dots denoted the out-boundary elements.

Class Prediction

Yield of the Algorithm is alluded as "Expectation", after it has been prepared on verifiable dataset and applied to new information when attempting to estimate the probability of a specific result. The calculation creates plausible qualities for an obscure variable in the new information for each record, permitting the model developer to recognize what that worth will in all likelihood.

4. EXPERIMENTAL INVESTIGATIONS

In view of the different examination measures depicted the productivity of the calculation and strategies introduced were tried and the exactness of the proposed calculation is determined. This paper manages perceiving transcribed characters from 3 informational indexes of characters from different analyst's dependent on artificial knowledge. The difficulties of these characters are comparative. Bangla is second most famous language in India and comprises of 45 classes and 4,627 classes for the preparation set and 900 models in the test suite. Latin transcribed characters were in Dutch with 251 journalists who had 37,616 characters ie., 26,329 practice models and 11,287 examples. MNIST informational index was a bigger information bases of numbers which is frequently utilized for preparing picture handling frameworks. The underneath Table 1. sums up the Handwritten Data Series.

Data set	Class	Training set	Testing set
Bangla	45	4,627	900
Latin	25	26,329	11,287
MNIST	10	60,000	10,000

Table 1: Summary of the Handwritten Data Series for Bangla, Latin and MNIST

The Handwritten Character Recognition system to recognize or show measured values close to actual values was Evaluated. To Calculate the accuracy or precision the following equation was used. This paper compares the methodology used by Support Vector Machine; k Nearest Neighbor and Multi Layered Perceptron (MLP) on the above Data., Bangla, Latin and MNIST. The results of the classification accuracy is shown in the Table 2.

Data Set	Accuracy Rate		
	MLP	kNN	SVM
Bangla	91.05	85.60	90.5
Latin	94.58	93.31	93.8
MNIST	94.8	94.11	94.6

Table 2. Accuracy Rates using 3 Handwritten Character Sets from the Comparison (%) of SVM, kNN and MLP

The accuracy of the handwriting recognition on MNIST data set with MLP was Bangla set up to 91.05 %, Latin set up to 94.58 %, and MNIST set up to 94.8 %. Therefore, the MLP Character Recognition can be recognized as the better alternative.

5. IMPLEMENTATION & RESULTS

Python programming language was used to develop an application, the Server process is maintained by using the TensorFlow. It has a huge library we can import the library for performing OCR task. A use of python includes analysis, algorithm development, computation and much more. The following screen shots Screenshots 1 to 5, showcase the implementation of the recognition of handwritten language characters successfully.

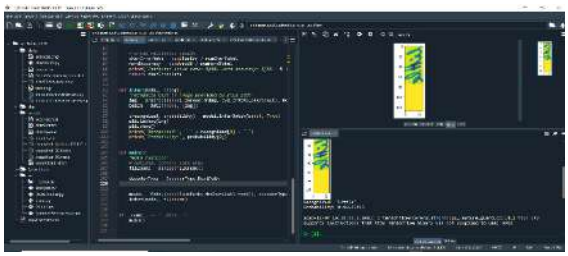

Screenshot 1

Screenshot 2

Screenshot 3

Screenshot 4

Screenshot 5

6. CONCLUSION

This study aims to devise a new progressed calculation for manually handwritten frameworks. This examination utilizes a lot of in sequential order pictures in Bangla, Latin and MNIST textual styles, which are regularly utilized in the current case for character acknowledgment. During the various stages the pictures utilized in this analysis are separated into arrangement of pictures sets. The originally set was the Bangla, Latin and MNIST textual style set in a test to check the exactness of this examination. The test picture is a very much shaped textual style between the content and the foundation where the foundation of the image is white.

This analysis and the outcomes show improved outputs of this framework compared with the Multi-Layer Perceptron (MLP) algorithm performance. The comparative analysis shows that the accuracy of the Bangla set up to 91.05 %, Latin set up to 94.58 %, and MNIST set up to 94.8 % which indicates that the performance of Multi-Layer Perceptron (MLP) is better than is counterparts.

7. FUTURE ENHANCEMENTS

In future there is extent of expanding the quantity of the shrouded layers as much as we need i.e., the Input Layer and the Output Layer will be normal. Also, the model can be made more unpredictable by utilizing different number of centers concealed layers for numerous preparing of the picture information type for exact outcomes.

REFERENCES

[1] Schomaker, L. R. B., Franke, K., and Bulacu, M. (2007). Using codebooks of fragmented connected-component contours in forensic and historic writer identification. Pattern Recognition the Letters, 28(6):719–727. Pattern Recognition in Cultural Heritage and Medical Applications.

[2] Bunke, H. and Riesen, K. (2011). Recent the advances in graph-based pattern self-recognition with applications in document analysis. Pattern Recognition, 44(5):1057–1067.

[3] Liwicki, M., Bunke, H., Pittman, J., and Knerr, S. (2011). Combining the diverse systems for handwritten text lineself recognition. Machine Vision and Applications, 22(1):39–51.

[4] Uchida, S., Ishida, R., Yoshida, A., Cai, W., and Feng, Y. (2012). Character of the image patterns as big data. In Frontiers in Handwriting Self Recognition (ICFHR), The 13th International Conference on, pages 479–484.

[5] Khakham, P., Chumuang, N., and Ketcham, M., "Isan Dhamma Handwritten Characters Recognition Self System by Using the Functional Trees Classifier," 2015 11th International Conference on SignalImage Technology & Internet-Based Systems (SITIS), Bangkok, 2015, pp. 606-612. doi: 10.1109/SITIS.2015.68

[6] Chumuang, N. and Mahasak, K., "The Most Intelligence algorithm for self-character recognition on palm leaf manuscript" Far East Journal of Mathematical Sciences (FJMS) volume 98, Issue 3, pp. 333-345, October 2015.

[7] Chamchong, R., Fung, C., and Wong, K. W. (2010). Comparing total binarisation techniques for the processing of self-ancient manuscripts. In Nakatsu, R., Tosa, N., Naghdy, F., Wong, K. W., and Codognet, P., editors, The Cultural Computing, volume 312 of IFIP Advances in Future Information and Communication Technology, pages 55–64. Springer Berlin Heidelberg.

[8] Van der Zant, T., Schomaker, L. R. B., and Haak, K. (2008). Handwritten word spotting using most recent biologically inspired features. Pattern Self Analysis and Machine Intelligence, IEEE Transactions on, 30(11):1945–1957.

[9] N. Chumuang and M. Ketcham, "Model for Handwritten Recognition Based on Artificial Intelligence," 2018 International Joint Symposium on Artificial Intelligence and Natural Language Processing (iSAI-NLP), Pattaya, Thailand, 2018, pp. 1-5, doi: 10.1109/iSAI-NLP.2018.8692958.

SMART WASTE COLLECTION MONITORING AND ALERT SYSTEM VIA IOT

[1]Nazeera Parveen, [2]Ayesha Fatima
[1]PG Scholar, Department of Electronics and Communication Engineering,
[2]Assistant Professor, Department of Electronics and Communication Engineering,
Nawab Shah Alam Khan College of Engineering & Technology, Hyderabad

ABSTRACT: The uncollected waste material when the waste bin is full is a common problem nowadays. Thus, an efficient waste management for the waste material is essential in ensuring a clean and green surrounding environment. This paper presents an Internet of Things (IoT) based Smart Waste Collection Monitoring and Alert System to monitor the waste material at the selected site of garbage collection area. The system is implemented using an ultrasonic sensor which is connected to Arduino UNO as to monitor waste bin garbage level. In this system, waste bin depth level will be sent via Arduino Ethernet Shield with an Internet connection to the Ubidots IoT Cloud. The Ubidots store the collected waste bin level data into IoT database and display the waste bin depth level on online dashboard for real-time visualization. The Ubidots Event manager invoke a notification alert to garbage collector mobile phone via a SMS when the waste bin is nearly filled for immediate waste collection. Therefore, the waste collection became more effective and systematic.

Keywords— Ultrasonic Sensor, Arduino UNO, Smart Waste Collection Monitoring and Alert System, Ubidots.

INTRODUCTION

At present, more than 23,000 tons of waste is delivered each day in Malaysia. Nonetheless, this sum is required to ascend to 30,000 tons constantly 2020. The measure of waste produced keeps on expanding because of the expanding populace and improvement, and just under 5% of the squander is being reused. Notwithstanding the enormous sum and intricacy of waste created, the principles of waste the executives in Malaysia are as yet poor. Subsequently, the nation will confront an issue when there is no legitimate administration for this waste assortment. As Malaysia is a non-industrial country and besides has relative issues, for instance, authentic advancements, work, show up deficiency and various workplaces which are insufficient to adjust to the routinely growing rate of waste age [1].

A productive waste material assortment is basic to keep the loss from influencing human wellbeing and dirtying climate. Enormous amounts of uncollected waste material are one of what can influence society wellbeing and environmental framework on the off chance that it isn't appropriately overseen. The nation will confront an issue when there is no legitimate administration for this waste assortment office. As the nation develop, squander material additionally develops as well. Consequently, one of the issues to fathom the uncollected waste issue by knowing when the waste container is full and prepared for squander assortment. This data can help the city committee to appropriately plan their trash truck for squander assortment inside their over saw territory.

This will improve the development of waste assortment armada assets while upgrade the proficiency of waste assortment framework. Strong waste administration is one of significant angle which must be considered as far as making metropolitan zone climate more advantageous. It is gotten fundamental and testing to deal with the strong waste with quick urbanization and expanded populace development. A climate will be dirtied and messy if the waste material isn't been oversee and gathered as expected. A superior waste the executives' arrangement can helps improving the general prosperity of a network and developed a superior neighborhood. These days, various IoT based answer for squander the board are actualized to improve the assortment of trash which would guarantee sound climate for life on this green planet, with more prominent effectiveness [2],[3],[4],[5]. Regions needing to accomplish cleaner metropolitan conditions can actualize an IoT based arrangement [6], [7]. A portion of the IoT based arrangements [8],[9],[10] for squander the board give a notice ready when the trash receptacle arrives at its full limit with respect to prompt waste assortment. An IoT based savvy framework that can screen the ordinary trash IoT based strong waste the executive's framework which empowers trash container observing, dynamic booking and steering of city worker trucks in a keen city [11],[12]. An audit of existing IoT-empowered arrangements in keen refers to's waste administration is done here to unite the cutting-edge answer for instance in term of self-fueled solution. [13], [14].

IoT which is another stage that is helpful for individuals in this world. IoT is the center of such progressive of developing motors. IoT is conceivable because of adequate force flexibly and web connectivity [15]. The term of IoT is normally used to portray a system where sensors are associated with articles and help these items to share their 'computerized voice' with the outer world over web association. In the ongoing time, IoT has become an arrangement of direction fabricated organizations. There were numerous IoT stages for example, Blink, Ubidots, IBM Blue mix and Device pilots as bidots is picked as a foundation of IoT for this task. Ubidots is a cloud administration that offers an amicable and instinctive interface where the clients

can associate with an assortment of gadgets, going from a phone or a PC, to an implanted framework, for example, a microcontroller framework. Basically, Ubidots is a stage that permits to interface various kinds of gadgets to a cloud information base and spare factors that can speak to them in a basic and quick manner and secure way.

This paper presents a Smart Waste Collection Monitoring what's more, Alert System (SWCMAS) utilizing IoT innovation on Ubidots Cloud. This task proposed a framework to control a waste material from flood from the waste container and alarm is ship off cleaner for squander assortment. Utilizing the foreseen framework, checking of the waste assortment status could be observed adequately.

This undertaking assigns a method where could screen the trash level at customary stretches as flood of the container can be forestalled. The filling level of the trash in the dustbin and its unique level tallness could be detected/checked by the ultrasonic sensor. Programming in the Arduino UNO is done so that once a specific degree of filling is detected, data as a message is shipped off the client, mentioning for cleaning of the residue container. Alluding to the square outline in underneath, the created framework comprises of a

1) Sensor hub that actualized utilizing an Arduino Uno board associated with Arduino Ethernet Shield, HCRS-04 ultrasonic sensor and signal;
2) Wired switch that interconnected the sensor hub to Ubidots IoT Cloud stage and
3) Ubidots Cloud stage that comprise made sure about IoT gadgets association.

Ubidots Dashboard to show and imagine the waste container profundity level information and Ubidots Event trough to advise an alarm to purchaser by means of message/SMS on cell phone when the squander container is almost filled. The framework advancement comprises of equipment and programming advancement stage. In equipment advancement stage, the Arduino Uno is use as a microcontroller for the sensor hub. The sensor hub is interface with Ultrasonic sensor for recognition of the waste container profundity.

SYSTEM DEVELOPMENT

A Framework Hardware Development shows the schematic chart for association of Arduino Uno and Ultrasonic sensor. The pin that is utilized is all advanced pins, thus no use of simple pins. The ground pin of ultrasonic sensor must be associated with ground pin of Arduino Uno to dodge cut off. The trig pin and reverberation pin is associated with (computerized) separately. When the squander is begun to be filled, the Ultrasonic sensor begins transmitting sound waves. At one side is the transmitter and other is the beneficiary, which estimates separation by sending out a sound wave at a particular recurrence and tuning in for that sound wave to bob back. By recording the slipped by time between the sound wave being created and the sound wave bobbing back, it is conceivable to figure the separation between the ultrasonic sensor and the item. After numerous means of microcontroller coding utilizing Arduino, Node design, Arduino Ethernet Shield design, and the information is at long last gathered and shipped off Ubidots IoT Cloud.

BLOCK DIAGRAM

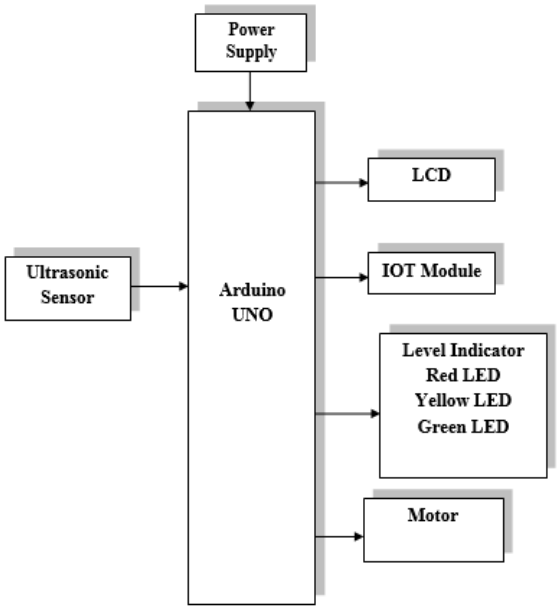

Fig.1. Block diagram

POWER SUPPLY

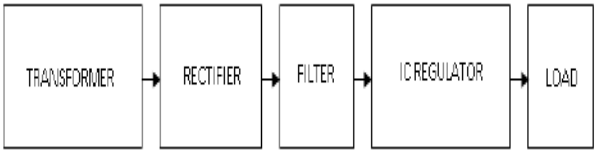

Fig.2. Block diagram of power supply

- Step down Transformer converts 230 AC to 12 AC
- Bridge rectifier converts AC to pulsating DC
- Filter will remove the AC component
- Regulator will provide required constant DC 5v/9v/12v. Voltage.

ARDUINO UNO

Arduino/genuino uno is a microcontroller board based on the atmega328p (datasheet). It has 14 digital input/output pins (of which 6 can be used as PWM outputs), 6 analog inputs, a 16 MHz quartz crystal, a USB connection, a power jack, an ICSP header and a reset

button. It contains everything needed to support the microcontroller; simply connect it to a computer with a USB cable or power it with a ac-to-dc adapter or battery to get started. You can tinker with your uno without worrying too much about doing something wrong, worst case scenario you can replace the chip for a few dollars and start over again.

"Uno" means one in Italian and was chosen to mark the release of Arduino software (ide) 1.0. The uno board and version 1.0 of Arduino software (ide) were the reference versions of Arduino, now evolved to newer releases. The uno board is the first in a series of USB Arduino boards, and the reference model for the Arduino platform; for an extensive list of current, past or outdated boards see the Arduino index of boards.

PRODUCT SPECIFICATIONS

Microcontroller	ATmega328P
Operating Voltage	5V
Input Voltage (recommended)	7-12V
Input Voltage (limit)	6-20V
Digital I/O Pins	14 (of which 6 provide PWM output)
PWM Digital I/O Pins	6
Analog Input Pins	6
DC Current per I/O Pin	20 mA
DC Current for 3.3V Pin	50 mA
Flash Memory	32 KB (ATmega328P) of which 0.5 KB used by bootloader
SRAM	2 KB (ATmega328P)
EEPROM	1 KB (ATmega328P)
Clock Speed	16 MHz
LED_BUILTIN	13
Length	68.6 mm
Width	53.4 mm
Weight	25 g

MAX232 IC:

Max 232 is an IC which changes over TTLrationale level sign in to its identical RS-232c level sign and Rs-232c level to its comparable TTL level signal. This IC is significant in the event that when we have to make association and move information between gadgets that deals with various sign level wave forms (TTL, Rs232c and so on)

For instance, the vast majority of the microcontrollers 8051(89c51, 89c52), PIC (16f877), AVR takes a shot at TTL rationale wave structure. These microcontrollers have a form in UART (Universal Synchronous-Asynchronous Receiver and Transmitter) which can send and get sequential information. Since they deal with TTL level so they send and get information included TTL wave from. Whereas Standard PC (Personal Computers) takes a shot at RS-232 level wave structure. Presently on the off chance that we have to move information from microcontroller to PC (Personal PC) we have to change information from TTL over to RS-232 level and in the event that we need to send information from PC to microcontroller we need to change over information from Rs-232 to TTL. Max-232 is answer for this issue. There is wide reach where we use max232 yet its principle object is clarified previously.

Voltage Level

RS232 line type and logic level	RS232 voltage	TTL voltage to/from MAX232
Data transmission (Rx/Tx) logic 0	+3 V to +15 V	0 V
Data transmission (Rx/Tx) logic 1	-3 V to -15 V	5 V
Control signals (RTS/CTS/DTR/DSR) logic 0	-3 V to -15 V	5 V
Control signals kjnic 1	+3 V to +15 V	0 V

Table showing voltage of RS232 & MAX232

LIQUID CRYSTAL DISPLAY

LCD (Liquid Crystal Display) screen is an electronic display module and find a wide range of applications. A 16x2 LCD display is very basic module and is very commonly used in various devices and circuits. These modules are preferred over seven segments and other multi segment LEDs. The reasons being: LCDs are economical; easily programmable; have no limitation of displaying special & even custom characters (unlike in seven segments), animations and so on.

A 16x2 LCD means it can display 16 characters per line and there are 2 such lines. In this LCD each character is displayed in 5x7 pixel matrix. This LCD has two registers, namely, Command and Data.

The command register stores the command instructions given to the LCD. A command is an instruction given to LCD to do a predefined task like initializing it, clearing its screen, setting the cursor position, controlling display etc. The data register stores the data to be displayed on the LCD. The data is the ASCII value of the character to be displayed on the LCD.

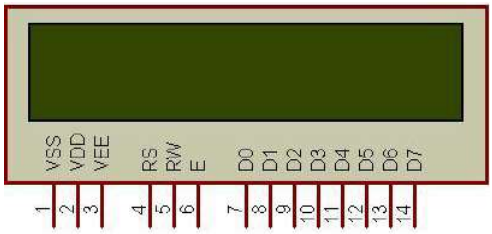

Fig 3: 16x2 LCD

ULTRASONIC SENSOR

HC-SR04 separation sensor is ordinarily utilized with both microcontroller and chip stages like Arduino, ARM, PIC, Raspberry Pie and so forth The accompanying aide is generally since it must be followed independent of the sort of computational gadget utilized.

Force the Sensor utilizing a managed +5V through the Vcc promotion Ground pins of the sensor. The current devoured by the sensor is under 15mA and henceforth can be straightforwardly controlled by the on board 5V pins (If accessible). The Trigger and the Echo pins are both I/O pins and subsequently they can be associated with I/O pins of the microcontroller. To begin the estimation, the trigger pin must be made high for 10uS and afterward killed. This activity will trigger a ultrasonic wave at recurrence of 40Hz from the transmitter and the beneficiary will trust that the wave will return. When the wave is returned after it getting reflected by any item the Echo pin goes high for a specific measure of time which will be equivalent to the time taken for the wave to return back to the sensor.

INTERNET OF THINGS MODULE

IOT Module esp8266 is used by applying 3.3 volts as operating voltage. It's useful to upload the status of the sensors to a network in the form of webpage or IP address. It will provide a secured platform in terms of user id and IP address sword along with serial port number.

Fig 4. ESP8266 IOT Module

By utilizing this stage, you can make a function or cautioning messages, send them to a cell phone and arrange the gadget to execute a control activity. The framework will alarm the client and will make an impression on client through phone through Wi-Fi. The gadget must be worked in the Ubidots stage to accept the gadgets API ID as to synchronize with Arduino IDE coding. Inside Ubidots, the information can be recovered in a moment. The entirety of the information and data subtleties were gathered to assess the framework execution. The outcome comprises of two sections. The initial segment is an Ultrasonic sensor separation result that demonstrate the profundity level of waste receptacle information show in the chronic screen on Arduino IDE. The subsequent part is acquired from profundity level of waste canister information assortment through IoT Cloud on Ubidots Dashboard which is an online presentation. By making a gadget in Dashboard, we can gather and store the waste canister profundity level information on the predefined gadget. The notice alarm can be summoned when certain estimation of gadget information changes more or less from the predetermined worth. The exhibitions of this waste assortment checking framework can be observed through Ubidots Dashboard. The information or data of the separation worth can be see in crude, normal or generally. The information and data that is gathered is from squander receptacle from the chose site. The information will be sends from Sensor hub through Arduino Ethernet Shield to Ubidots gadgets that had been made.

As the trash level increment, the separation between the squander canister top with ultrasonic sensor will diminish Once the level of separation not exactly the decided worth (4 cm), Ubidots will alarm and send message to approved individual in type of SMS we propose another answer for upgrade squander assortment productively utilizing the Arduino Uno with Arduino Ethernet Shield innovation and ultrasonic sensor frameworks. In this proposed framework, the trash flood of trash bin be stayed away from and oversaw effectively. This will suggest or send SMS or email to the approved individual through Ubidots stage. The trash overseeing framework and he office of gathering the trash by and by doesn't fit to the current necessity. Consequently, better office of gathering trash and transportation ought to be given. Since, this framework gives the data when the canister gets totally loaded up with trash, it decreases the quantity of times the appearance of vehicle which gathers the trash. This strategy at last aides in keeping the climate

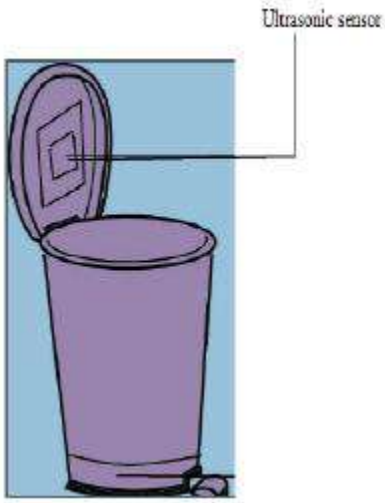

RESULTS & DISCUSSIONS

This section shown the results of data gathered during this project implementation. All of the data and information details were collected to evaluate the system performance. The result consists of two parts. The first part is an Ultrasonic sensor distance result that indicate the depth level of waste bin data display in the serial monitor on Arduino IDE. The second part is obtained from depth level of waste bin data collection through IoT Cloud on Ubidots Dashboard which is an online display. By creating a device in Dashboard, we can collect and store the waste bin depth level data on the specified device. The notification alert can be invoked when certain value of device data changes more or less from the specified value.

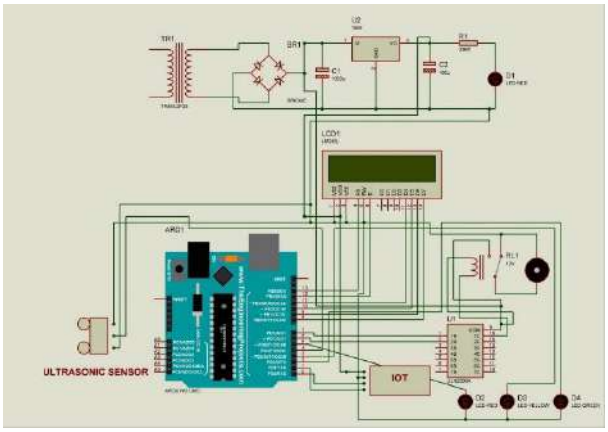

Figure 5. Schematic Diagram

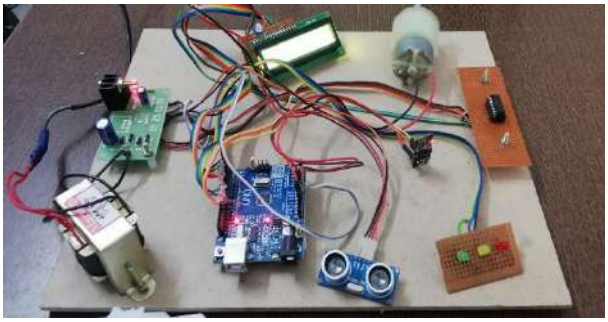

Figure 6: Complete Setup

Figure 7 Screenshot of App

Figure 8 Display showing output

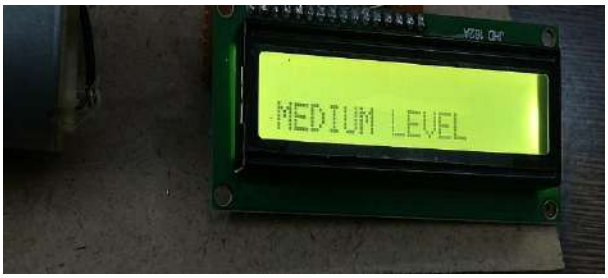

Figure 9 Display showing output

Figure 10 Display showing output

IV. CONCLUSION

In this paper, we propose a new solution to enhance waste collection efficiently using the Arduino Uno with Arduino Ethernet Shield technology and ultrasonic sensor systems. In this proposed system, the garbage overflow of garbage can be avoided and managed efficiently. This will intimate or send SMS or email to the authorized person through Ubidots platform. The garbage managing system and the facility of collecting the garbage presently doesn't fit to the current requirement. Hence better facility of collecting garbage and transportation should be provided. Since, this system provides the information when the bin gets completely filled with garbage, it reduces the number of times the arrival of vehicle which collects the garbage. This method finally helps in keeping the environment clean. Thus, the waste collection is made more efficient.

REFERENCES

[1] J. Sreenivasan, M. Govindan, M. Chinnasami, and I. Kadiresu, "Solid Waste Management in Malaysia – A Move Towards Sustainability," *Waste Manag. An Integr. Visions*, vol. 2005, no. April 2005, pp. 55–70, 2012.

[2] M. Adam, M. E. Okasha, O. M. Tawfeeq, M. A. Margan and B. Nasreldeen, "Waste Management System Using IoT," 2018 International Conference on Computer, Control, Electrical, and Electronics Engineering (ICCCEEE), Khartoum, 2018, pp. 1-4

[3] S. Aleyadeh and A. M. Taha, "An IoT-Based Architecture for Waste Management," 2018 IEEE International Conference on Communications Workshops (ICC Workshops), Kansas City, MO, 2018, pp. 1-4.

[4] G. K. Shyam, S. S. Manvi and P. Bharti, "Smart waste management using Internet-of-Things (IoT)," 2017 2nd International Conference on Computing and Communications Technologies (ICCCT), Chennai, India, 2017, pp. 199-203.

[5] W. Chen, Y. Wang, P. Huang, Y. Huang and M. Tsai, "A Smart IoT System for Waste Management," *2018 1st International Cognitive Cities Conference (IC3)*, Okinawa, 2018, pp. 202-203.

[6] S. S. Chaudhari and V. Y. Bhole, "Solid Waste Collection as a Service using IoT-Solution for Smart Cities," 2018 International Conference on Smart City and Emerging Technology (ICSCET), Mumbai, 2018, pp. 1-5.

[7] E. Al-Masri, I. Diabate, R. Jain, M. H. Lam and S. Reddy Nathala, "Recycle.io: An IoT-Enabled Framework for Urban Waste Management," 2018 IEEE International Conference on Big Data (Big Data), Seattle, WA, USA, 2018, pp. 5285-5287

[8] S. Paul, S. Banerjee and S. Biswas, "Smart Garbage Monitoring Using IoT," 2018 IEEE 9th Annual Information Technology, Electronics and Mobile Communication Conference (IEMCON), Vancouver, BC, 2018, pp. 1181-1185.

[9] H. N. Saha, S. Gon, A. Nayak, S. kundu and S. Moitra, "Iot Based Garbage Monitoring and Clearance Alert System," 2018 IEEE 9th Annual Information Technology, Electronics and Mobile Communication Conference (IEMCON), Vancouver, BC, 2018, pp. 204-208.

[10] S. K. Memon, F. Karim Shaikh, N. A. Mahoto and A. Aziz Memon, "IoT based smart garbage monitoring & collection system using WeMos & Ultrasonic sensors," 2019 2nd International Conference on Computing, Mathematics and Engineering Technologies (iCoMET), Sukkur, Pakistan, 2019, pp. 1-6.

[11] R. N. Subrahmanian, S. K. S, T. Suvidharbabu, and B. Manikandan, "Smart Bin using IoT with Fog Computing," International Journal of Emerging

Technology in Computer Science & Electronics vol. 24, no. 6, pp. 13–16, 2017.

[12] S. Murugaanandam, V. Ganapathy and R. Balaji, "Efficient IOT Based Smart Bin for Clean Environment," 2018 International Conference on Communication and Signal Processing (ICCSP), Chennai, 2018, pp. 0715-0720.

[13] N. Alsbou, M. A. Samad, M. Alhashem and A. S. A. Abuabed, "Developing a Self-Powered Enlarging Smart Waste Bin," 2018 14th International Wireless Communications & Mobile Computing Conference (IWCMC), Limassol, 2018, pp. 683-689.

[14] S. Mdukaza, B. Isong, N. Dladlu and A. M. Abu-Mahfouz, "Analysis of IoT-Enabled Solutions in Smart Waste Management," IECON 2018 - 44th Annual Conference of the IEEE Industrial Electronics Society, Washington, DC, 2018, pp. 4639-4644.

[15] D. Evans, “The Internet of Things How the Next Evolution of the Internet” Cisco Internet Business Solutions Group (IBSG) no. April, 2011.

SMART SWITCHING SYSTEM USING BLUETOOTH TECHNOLOGY

[1]Mohammed Mustafa Ali, [2]Shaik Mohammed Saifullah
[1]PG Scholar, Department of Electronics and Communication Engineering,
[2]Assistant Professor, Department of Electronics and Communication Engineering,
Nawab Shah Alam Khan College of Engineering & Technology, Hyderabad

ABSTRACT:

While being "SMART" is profoundly in pattern these days, why stop just to cell phones or PCs? So here the home apparatuses are made conceivable to control utilizing a basic advanced mobile phone. An Android application is utilized to control the devices that are employed in day by day life. The other significant gadgets that are utilized in this task are Bluetooth module, microcontroller, transfer board, and bulb. The apparatus and programming design of the entire framework are portrayed in this paper. It has been ensured that this endeavor can be refined under outrageous low cost so it can undoubtedly be executed in natural air. This framework was remotely controlled the changes from a separation of roughly 30 m range. It is perhaps utilized in wellbeing focus, nursing home, and home machines for older.

Keywords: Bluetooth module HC-05; Home automation; Microcontroller Atmega328; Relay board; Smartphone.

INTRODUCTION

Home computerization framework utilizing Bluetooth innovation is chiefly worked utilizing data innovation which can assist with limiting human effort. Due to quickly developing advancements, these days' individuals utilize diverse PDAs and controller savvy devices. As mechanized gadget is invaluable as it is adaptable, simple to apply and introduce. After it has found the situation, there are numerous ways used to make our home more brilliant. As sparing energy and above all time are our essential worry in our repetitive rushed life, there isn't anything better than home mechanization. It will be changed from extravagance to need when utilized for the truly tested or matured individuals. There are numerous Advancements used to make our home Smarter; such as ZigBee, Z – product, GSM, GPRS, infrared, Wi-Fi, Bluetooth and so forth [1, 2]. Bluetooth innovation can be introduced in extremely ease

These days PDAs are accessible to everybody, it a unique the simplest to utilize technologies. Bluetooth framework is quicker than the larger part of different advances. It tends to be powerful for sequential information correspondence where information can be communicated up to3 mbps speed a way off of 10–100m.This composition has organized as follows; segment 2 presents the condition of the art. Segment 3 examines the nitty gritty depiction of proposed framework furthermore; the calculation is introduced in segment 4. Area 5 finishes up with future examination.

SYSTEM DESIGN

Constant chip KIT and Arduino based home observing framework has been introduced in though, it was a decent and ease framework yet was not as low as the Bluetooth innovation. It was a touch more expensive than the Bluetooth innovation. A short time later, scientists were planned an ease and remote-controlled computerization framework. For the most part, Bluetooth innovation was successfully worked from far off adverts with high accuracy and the objective is to help to the impeded or matured individuals. In creator examined about Arduino and android application-based conservative, quick, dependable, and keen home robotization system. Their proposed framework was tried on various shrewd gadgets, for example, DC Servomotors and lights. It was seen fit for performing different activities, for example, controlling rate of D.C engine, exchanging functionalities, light power control and position control of Servomotor and so forth S. Kumar proposed a modest shrewd home framework, which was worked utilizing miniature web worker. Their proposed framework was effectively test and performed different home applications for example, interruption identification, natural control, and different programmed exchanging functionalities. In creator examined about the versatile climate station dependent on WI-FI innovation. Their proposed framework can remotely screen pressure, temperature, relative stickiness, downpour, wind speed, and direction. Home mechanization utilizing PDA and Bluetooth remote innovation has been introduced, which can permit to the client for working different contraptions associated into the organization. Along these lines, our proposed savvy exchanging framework worked through Bluetooth remote organization. The equipment and programming prerequisite of our proposed framework has portrayed in area beneath. In proposed system Arduino and Bluetooth modules used. Android application used to control all appliances via Bluetooth.

COMPONENT SELECTION

The selection of components should be such that the size of the device should be compact and the response

time taken by each and every module should be very less for quick output.

BLOCK DIAGRAM

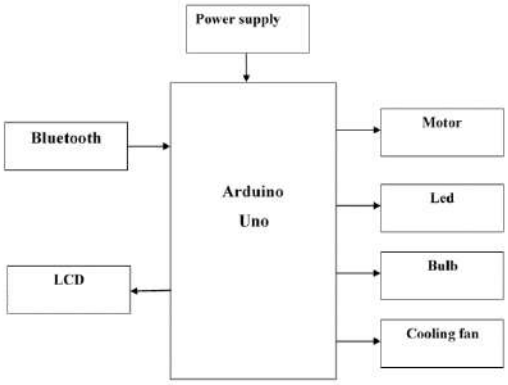

Power supply

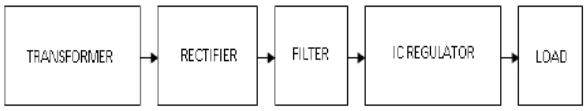

Fig.1. Block diagram of power supply

- Step down Transformer converts 230 AC to 12 AC
- Bridge rectifier converts AC to pulsating DC
- Filter will remove the AC component
- Regulator will provide required constant DC 5v/9v/12v. Voltage.

ARDUINO UNO

The Arduino UNO is the best board to begin with hardware and coding. This is your first experience dabbling with the stage, the UNO is the heartiest board you can begin playing with the UNO is the most utilized and recorded leading group of whole Arduino family. Arduino/genuine Uno is a MCU board based totally at the atmega328p (datasheet). It has 14 virtual input/output pins (of which 6 may be used as PWM outputs), 6 analog inputs, a sixteen MHz quartz crystal, A USB connection, a energy jack, an ICSP header and a reset button. It incorporates everything needed to assist the microcontroller; absolutely connect it to a computer with a USB cable or electricity it with a ac-to-dc adapter or battery to get started. You may tinker together with your UNO without demanding too much about doing something wrong, worst case scenario you can replace the chip for some bucks and begin yet again. "Uno" means one in Italian and become selected to mark the release of Arduino software program (IDE) 1.0. The UNO board and version 1.0 of Arduino software (IDE).

TECHNICAL SPECIFICATIONS

Microcontroller	ATmega328P
Operating Voltage	5V
Input Voltage (recommended)	7-12V
Input Voltage (limit)	6-20V
Digital I/O Pins	14 (of which 6 provide PWM output)
PWM Digital I/O Pins	6
Analog Input Pins	6
DC Current per I/O Pin	20 mA
DC Current for 3.3V Pin	50 mA
Flash Memory	32 KB (ATmega328P) of which 0.5 KB used by bootloader
SRAM	2 KB (ATmega328P)
EEPROM	1 KB (ATmega328P)
Clock Speed	16 MHz
LED_BUILTIN	13
Length	68.6 mm
Width	53.4 mm
Weight	25 g

LIQUID CRYSTAL DISPLAY

LCD (Liquid Crystal Display) screen is an electronic display module and find a wide range of applications. A 16x2 LCD display is very basic module and is very commonly used in various devices and circuits. These modules are preferred over seven segments and other multi segment LEDs. The reasons being: LCDs are economical; easily programmable; have no limitation of displaying special & even custom characters (unlike in seven segments), animations and so on.

A **16x2 LCD** means it can display 16 characters per line and there are 2 such lines. In this LCD each character is displayed in 5x7 pixel matrix. This LCD has two registers, namely, Command and Data.

The command register stores the command instructions given to the LCD. A command is an instruction given to LCD to do a predefined task like initializing it, clearing its screen, setting the cursor position, controlling display etc. The data register stores the data to be displayed on the LCD. The data is the ASCII value of the character to be displayed on the LCD.

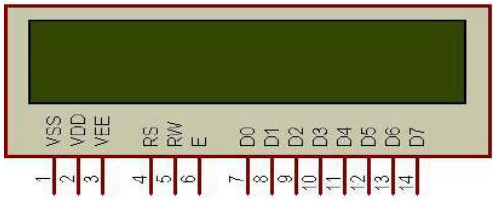

The most commonly used Character based LCDs are based on Hitachi's HD44780 controller or other which are compatible with HD44580.

RELAY

The transfer module acts like a switch of mains voltage. It is helpful for controlling apparatuses utilizing microcontrollers. Fig. 3 shows the 2 transfer modules. The working voltage is 5 V and driver ebb and flow is 15 – 20 mA. The hand-off module has 4 pins which are VCC, GND, IN1, and IN2 separately.

ULN2003: -

The ULN2003 is a IC comprises of 7 NPN Darlington semiconductor sets with HIGH voltage & current capacity. It is ordinarily utilized for applications, hand-off drivers, show drivers, driven light drivers, engine, logic cradles, line drivers, knock drivers and other high voltage momentum applications. It comprises of basic cathode brace diodes NPN Darlington pair which makes this driver IC helpful for exchanging inductive burdens.

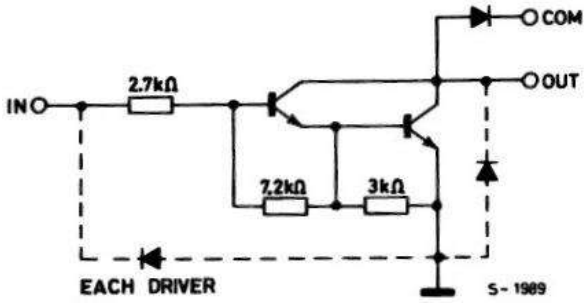

BLUETOOTH

Bluetooth HC-05 has six pins that follows:

a) Key/Enable: By default, this pin works in information mode with baud rates is 9600 bps. At the point when the baud rate is 34800 bps and works in order mode.

b) VCC: This pin interfaces with 5 V or 3.3 V of the module.

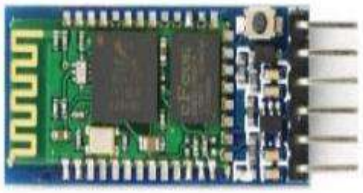

c) GND: This pin associates with ground pin.

d) State: The pin checks whether the module is associated or not.

e) TXD/RXD: The TXD & RXD pins associate with RXD and TXD pins of microcontroller individually. The TXD pin communicates sequential information which will be remotely gotten by the Bluetooth. Essentially, RXD pin is remotely communicated the got data by Bluetooth module

IV. RESULTS

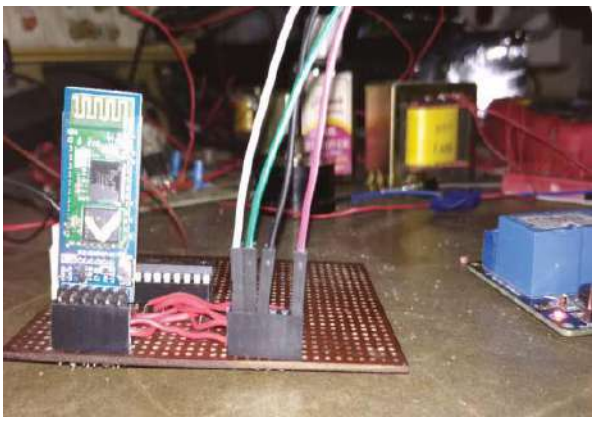

Figure: Circuit of smart switching system

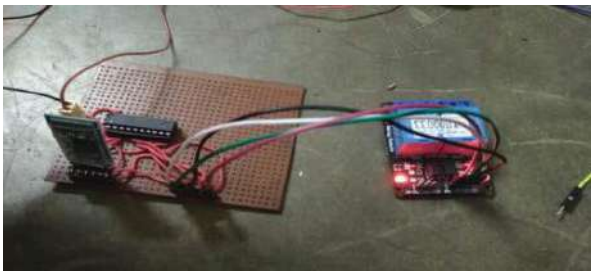

Figure: Smart switching system

V. CONCLUSION

Here an ease brilliant exchanging framework is proposed which is easy to work from cell phone gadgets. This automation system isn't just worthy for matured, disabled people, and Parkinson's patient, yet it is additionally helpful for limiting the human work.

The machines (like fan, light, or other helpful gadgets) where240V power gracefully is required can be associated and installed with this exchanging framework. As Bluetooth is utilized so the range of this framework will be significantly more than the different home automations frameworks.

REFERENCES:

[1] M. B. Yassein, W. Mardini, and A. Khalil, “Smart homes automation using Z-wave protocol,” 2016 International Conference on Engineering & MIS (ICEMIS), Morocco, 2016.

[2] Y. Zhao and Z. Ye, “A low cost GSM/GPRS based wireless home security system,” IEEE Transaction on Consumer Electronics, vol. 54, no. 2, 2008, pp. 567 – 572.

[3] R. Piyare and M. Tazil, "Bluetooth based home automation system using cell phone," 2011 IEEE 15th International Symposium on Consumer Electronics (ISCE), Singapore, 2011, pp. 192-195.

[4] R. A. Ramlee, M. H. Leong, R. S. S. Singh, M. M. Ismail, M. A. Othman, H. A. Sulaiman, M. H. Misran, and M. A. Meor Said, "Bluetooth Remote Home Automation System Using Android Application", The International Journal of Engineering and Science (IJES), vol. 2, no. 1, pp. 149- 153, 2013.

[5] B. Ghazal and K. AI-Khatib, "Smart Home Automation System for Elderly, and Handicapped people using XBee," International Journal of SmartHome, vol. 9, no. 4, pp. 203- 210, 2015.

[6] S. Raghavan and G. S. Tewolde, "Cloud based low-cost Home Monitoring and Automation System," Proc. of the 2015 ASEE North Central Section Conference, pp. 1 – 10, 2015.

[7] R. A. Ramlee, M. A. Othman, M. H. Leong, M. M. Ismail, and S. S. S.Ranjit, "Smart home system using android application,"2013International Conference of Information and Communication Technology (ICoICT), Indonesia, 2013.

[8] R. A. Ramlee, D. H. Z. Tang, and M. M. Ismail, “Smart home system for Disabled People via Wireless Bluetooth,” 2012 International Conference on System Engineering and Technology (ICSET), Indonesia, 2012.

[9] S. Das, S. Ganguly, S. Ghosh, R. Sarker, and D. Sengupta, “A bluetooth based sophisticated home automation system using smartphone,” 2016 International Conference on Intelligent Control Power and Instrumentation (ICICPI), India, 2016.

[10] S. Kumar, “Ubiquitous Smart Home System Using Android Application," International Journal of Computer Networks & Communications (IJCNC), vol. 6, no. 1, pp. 33-43, 2014.

[11] I. Sarkar, B. Pal, A. Dutta, and S. Roy, “Wi-Fi Based Portable Weather Station for Monitoring Temperature, Relative Humidity, Pressure, Precipitation, Wind Speed and Direction,” International Conference on ICT for Sustanable Development (ICT4SD), India, 2018.

[12] B. M. O. AI-thobaiti, I. M. A. Abosolaiman,H. M. Alzahrani, S.H. A. Almalki, and M. S. Soliman, "Design and Implementation of a Reliable Wireless Real-Time Home Automation System Based on Arduino Uno Single-Board Microcontroller", International Journal of Control, Automation and Systems, vol. 3, no. 3, pp. 11-15, 2014.

[13] ATMEL, “8-bit AVR Microcontroller with 2K Bytes In-System Programmable Flash, ATtiny2313/V,” 2543M–AVR–10/16, pp. 1 – 224, 2016.

[14] J. Jessen, M. Venzke, and V. Turau, “ Design considerations for a universal smart energy module for energy harvesting in wireless sensor networks,” 2011 Proc. of the Ninth International Workshop on Intelligent Solutions in Embedded Systems,” Germany, 2011.

[15] ITead Studio, “HC-05 Bluetooth module,” 1 – 13, 2010.

[16] SUNFOUNDER, “2 Channel 5V Relay Module,” 1, 2017.

[17] Handson Technology, “4 Channel 5V Optical Isolated Relay Module,” 1 – 6, 2018.

[18] S. Jayapradha, P. M. D. R. Vincent, “An IOT based human healthcare system using Arduino uno board,” 2017 International Conference on Intelligent Computing, Instrumentation and Control Technologies (ICICICT), India, 2017

SELF DEFENSE DEVICE WITH GSM ALERT AND GPS TRACKING WITH FINGERPRINT VERIFICATION FOR WOMEN SAFETY

[1]Mohd Yousuf, [2]Sharea Takreem
[1]PG Scholar, Department of Electronics and Communication Engineering,
[2]Assistant Professor, Department of Electronics and Communication Engineering,
Nawab Shah Alam Khan College of Engineering & Technology, Hyderabad

ABSTRACT

Another methodology is given towards the security of ladies as a gadget. The goal of the gadget is to give ladies an apparatus that can give them security and guarantee their wellbeing in the event of any disaster. The paper proposes a superior methodology which utilizes a high voltage current creating circuit which will be utilized to stagger the resistance for few moments. The unique mark module for initiation of gadget, electric stun creating circuit, GSM/GPS module for cautioning and area following all interfaced with a microcontroller to plan a little mallet formed gadget which will be helpful and effectively compact.

Security of ladies is a significant subject of worry in India. A large portion of the ladies in India have encountered some type of viciousness or provocation out in the open. There is a development in wrongdoings identified with ladies badgering and the fundamental explanation that a lady is being a casualty is absence of public security and powerlessness of a lady to safeguard her. So as to have the option to ensure herself, she should prepare herself through different self-preservation courses, which isn't workable for each lady to enlist into these courses. As to issue there are different applications accessible on portable stage that are implied uniquely for ladies wellbeing, yet these applications doesn't ensure security at the hour of the episode on the grounds that these applications just take care of the work of advising individuals worried about ladies' wellbeing and couldn't help her to guard herself neither the accessibility of the concerned individuals is ensured at the hour of the occurrence.

In certain nations the utilization of self-preservation gear is real. These supplies like immobilizer and pepper splash are produced for a lady to protect herself by assaulting the resistance utilizing these types of gear, however in the event that the casualty needs help or she is in detached territory with nobody to help then these types of gear can be named as impermanent wellbeing supplies. Additionally, these gadgets can be abused whenever fallen in wrong hands.

Keywords- security, GSM, GPS, FPR

I. INTRODUCTION

Security of women is a major topic of concern in India. Most of the women in India have experienced some form of violence or harassment in public. There is a growth in crimes related to women harassment and the main reason that a woman is being a victim is lack of public security and inability of a woman to defend her. In order to be able to protect herself, she must train herself through various self-defense courses, which is not possible for every woman to enroll into these courses. Regarding this issue there are various applications available on mobile platform that are meant specially for women safety, but these applications doesn't guarantee security at the time of the incident because these applications only do the job of informing people concerned about women's safety and could not assist her to defend herself neither the availability of the concerned people is guaranteed at the time of the incident. In some countries the use of self-defense equipment is legitimate. These equipment like stun gun and pepper spray are developed for a woman to defend herself by attacking the opposition using this equipment, but if the victim needs assist or she is in secluded area with no one to help then this equipment can be termed as temporary safety equipment's. Also, these devices can be misused if fallen in wrong hands

COMMON OVERVIEW TO EMBEDDED SYSTEM

An embedded system can be defined as a computing device that does a specific focused job. Appliances such as the air-conditioner, VCD player, DVD player, printer, fax machine, mobile phone etc. are examples of embedded systems. Each of these appliances will have a processor and special hardware to meet the specific requirement of the application along with the embedded software that is executed by the processor for meeting that specific requirement. The embedded software is also called "firm ware". The desktop/laptop computer is a general-purpose computer. You can use it for a variety of applications such as playing games, *word* processing, accounting, software development and so on. In contrast, the software in the embedded systems is always fixed listed below.

Embedded systems do a very specific task, they cannot be programmed to do different things. . Embedded systems have very limited resources, particularly the memory. Generally, they do not have secondary storage devices such as the CDROM or the floppy disk. Embedded systems have to work against some deadlines. A specific job has to be completed within a specific time. In some embedded systems, called real-time systems, the deadlines are stringent. Missing a deadline may cause a catastrophe-loss of life or damage to property. Embedded systems are constrained for power. As many embedded systems operate

through a battery, the power consumption has to be very low.

· Some embedded systems have to operate in extreme environmental conditions such as very high temperatures and humidity.

II. BLOCK DIAGRAM

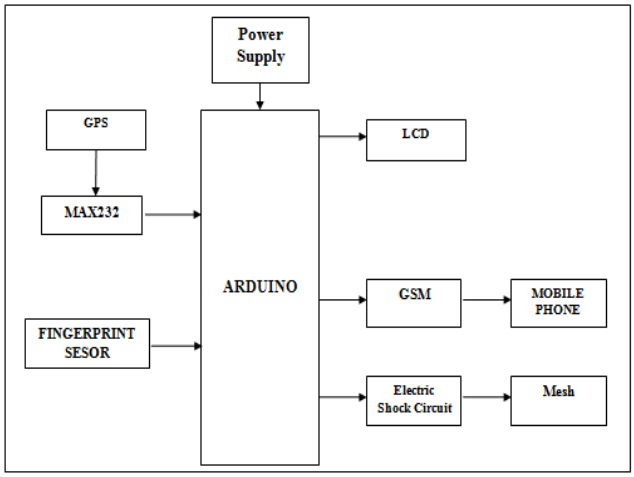

POWER SUPPLY

The force flexibly area is the part framework power flexibly is more mind boggling, with up to eight diverse gracefully voltage esteems, with 5 V and 3.3 V gave by the CPCI body. 5 V supplies the DC/DC gadget with buck to create other flexibly voltages, and supplies capacity to the 1553 transport's transformer. 3.3 V is the primary framework power gracefully, including the USB PHY, clock gadgets, FPGA and CPU and PCI connect gadgets (PLX6466) I/O parts. Other gracefully voltages are gotten from a 5V or 3.3 V flexibly voltage venture down.

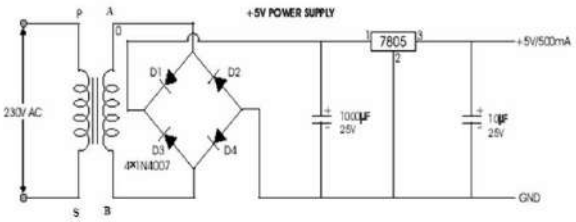

ARDUINO UNO

The Arduino UNO is the best board to begin with hardware and coding. This is your first experience dabbling with the stage, the UNO is the heartiest board you can begin playing with the UNO is the most utilized and recorded leading group of whole Arduino family.

Arduino/genuine Uno is a MCU board based totally at the atmega328p (datasheet).

It has 14 virtual input/output pins (of which 6 may be used as PWM outputs), 6 analog inputs, a sixteen MHz quartz crystal, A USB connection, a energy jack, an ICSP header and a reset button. It incorporates everything needed to assist the microcontroller; absolutely connect it to a computer with a USB cable or electricity it with a ac-to-dc adapter or battery to get started. You may tinker together with your UNO without demanding too much about doing something wrong, worst case scenario you can replace the chip for some bucks and begin yet again. "Uno" means one in Italian and become selected to mark the release of Arduino software program (IDE) 1.zero. The UNO board and version 1.zero of Arduino software (IDE) had been the reference variations of Arduino, now evolved to newer releases. The UNO board is the first in a chain of USB Arduino boards, and the reference model for the Arduino platform; for an intensive list of contemporary, past or outdated boards see the Arduino index of forums

TECHNICAL SPECIFICATIONS

Microcontroller	ATmega328P
Operating Voltage	5V
Input Voltage (recommended)	7-12V
Input Voltage (limit)	6-20V
Digital I/O Pins	14 (of which 6 provide PWM output)
PWM Digital I/O Pins	6
Analog Input Pins	6
DC Current per I/O Pin	20 mA
DC Current for 3.3V Pin	50 mA
Flash Memory	32 KB (ATmega328P) of which 0.5 KB used by bootloader
SRAM	2 KB (ATmega328P)
EEPROM	1 KB (ATmega328P)
Clock Speed	16 MHz
LED_BUILTIN	13
Length	68.6 mm
Width	53.4 mm
Weight	25 g

LIQUID CRYSTAL DISPLAY

The most regularly utilized Character put together LCDs are based with respect to Hitachi's HD44780 regulator or other which are viable with HD44580.we will examine about character based LCDs, their interfacing with different microcontrollers, different interfaces (8-cycle/4-bit), programming, unique stuff and deceives you can do with these straightforward looking LCDs which can give another look to your application.

The most regularly utilized LCDs found in the market today are 1 Line, 2 Line or 4 Line LCDs which have just 1 regulator and backing all things considered of 80 charachers, while LCDs supporting in excess of 80 characters utilize 2 HD44780 regulators.

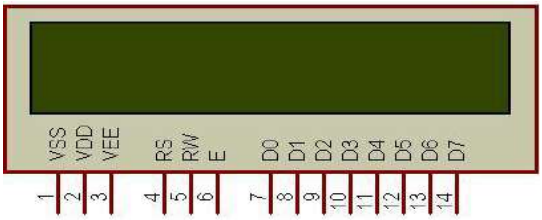

FINGER PRINT

This is a unique mark sensor module with TTL UART interface for direct associations with microcontroller UART or to PC through MAX232/USB-Serial connector. The client can store the unique mark information in the module and can arrange it in 1:1 or 1: N mode for distinguishing the individual. The FP module can legitimately interface with 3v3 or 5v Microcontroller. A level converter (like MAX232) is needed for interfacing with PC sequential port. Optical biometric unique mark per user with incredible highlights and can be installed into an assortment of final results, for example, access control, participation, wellbeing store box, vehicle entryway locks.

GLOBAL SYSTEM FOR MOBILE

Global System for Mobile Communications (GSM) modems are specific sorts of modems that work over membership based remote organizations, like a cell phone. A GSM modem acknowledges a Subscriber Identity Module (SIM) card, and fundamentally acts like a cell phone for a PC. Such a modem can even be a devoted cell phone that the PC utilizes for GSM network capacities.

GSM Modem Application

GLOBAL POSITIONING SYSTEM

The Global Positioning System (GPS) is a U.S.- claimed utility that gives clients situating, route, and timing (PNT) administrations.

The Global Positioning System (GPS) is a route framework utilizing satellites, a beneficiary and calculations to synchronize area, speed and time information for air, ocean and land travel.

The satellite framework comprises of a heavenly body of 24 satellites in six Earth-focused orbital planes, each with four satellites, circling at 13,000 miles (20,000 km) above Earth and going at a speed of 8,700 mph (14,000 km/h).

While we just need three satellites to deliver an area on earth's surface, a fourth satellite is frequently used to approve the data from the other three. The fourth satellite likewise moves us into the third-measurement and permits us to compute the height of a gadget.

ULN2003: -

The ULN2003 is a IC comprises of 7 NPN Darlington semiconductor sets with high voltage and current capacity. It is ordinarily utilized for applications, for example, hand-off drivers, engine, show drivers, driven

light drivers, rationale cradles, line drivers, hammer drivers and other high voltage momentum applications. It comprises of basic cathode brace diodes for each NPN Darlington pair which makes this driver IC helpful for exchanging inductive burdens.

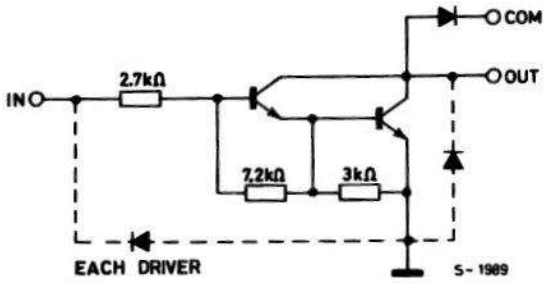

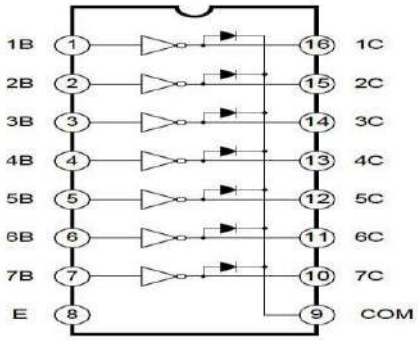

Logic Diagram of ULN2003

FEATURES

* High-voltage yields: 50V
* Inputs viable with different kinds of logic.
* Relay driver application

500mA appraised gatherer current (Single yield)

RELAY

The transfer module acts like a switch of mains voltage [16, 17]. It is helpful for controlling apparatuses utilizing microcontrollers. Fig. 3 shows the 2 transfer modules. The working voltage is 5 V and driver ebb and flow is 15 – 20 mA. The hand-off module has 4 pins which are VCC, GND, IN1, and IN2 separately.

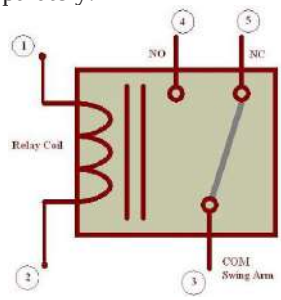

Representation of Relay

III. RESULTS

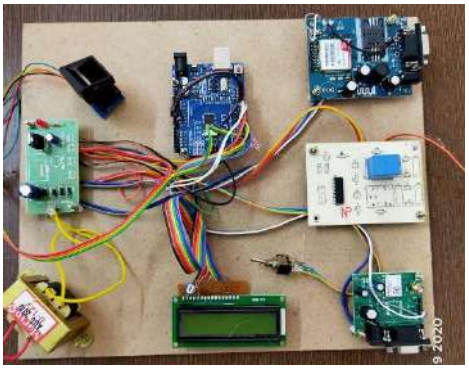

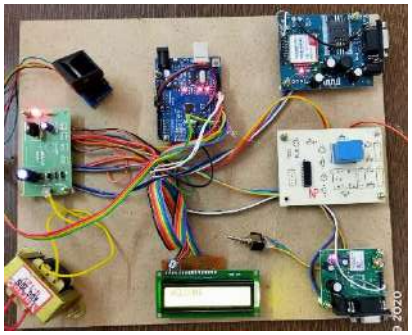

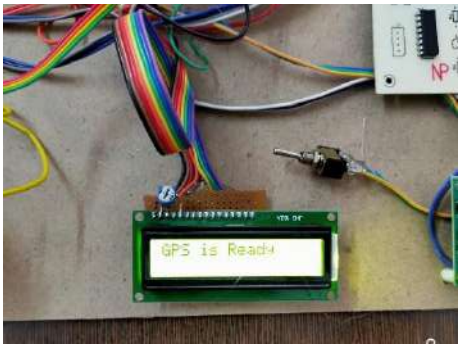

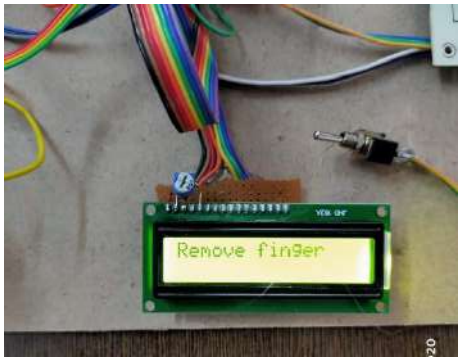
Remove finger

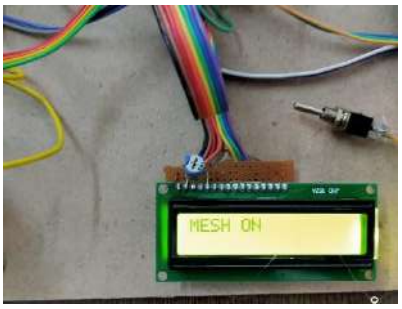
MESH ON

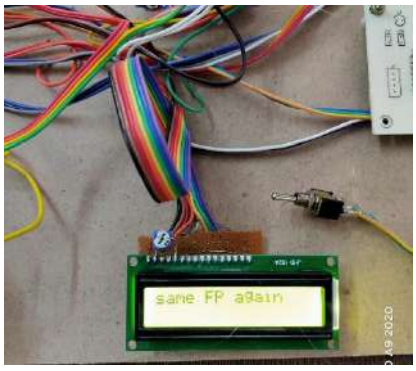
same FP again

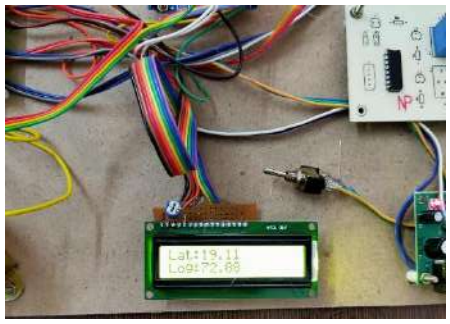
Lat:19.11
Log:72.88

Found ID:1

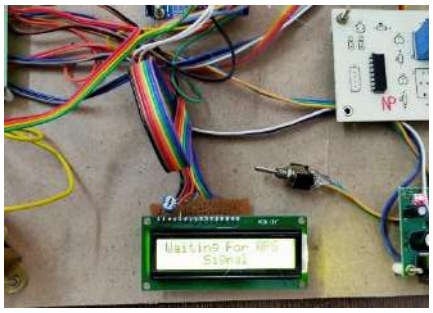
Waiting For FPS
Scan...

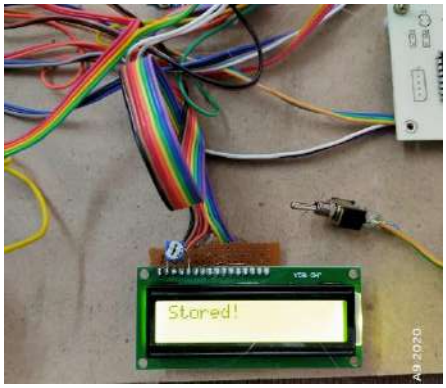

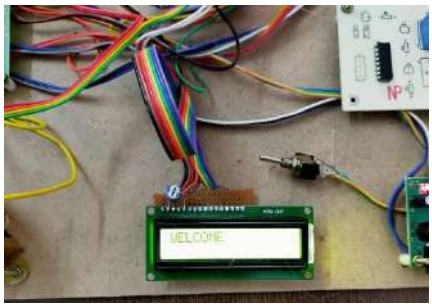

IV. CONCLUSION

There are numerous gadgets which are produced for women's safety however none of the gadget incorporates GSM/GPS cautioning and area following alongside hostile abilities. The applications which are as of now utilized for the ladies security don't have any arrangement for protecting herself and does no tenure wellbeing till the messages are shipped off the casualty's closed ones and they show up at a position of episode and spare her from the disaster. The proposed plan for Biometric Self Defense Device with GSM Alert and GPS Tracking is the best possible tool for a lady to safeguard herself. This paper gives an algorithm to build up a gear which a casualty can utilize to defend herself by staggering the resistance with a high electric current and simultaneously she can send a caution message with her flow area to her shut ones. For abrupt assaults, outside catch can be given for activation of gadget. Spotlight can be incorporated as an additional security.

REFERENCES

[1] Mrinmoy Dey, Md. Akteruzzaman Arif and Md. Asif Mahmud, „ Antitheft Protection of Vehicle by GSM & GPS with Fingerprint Verification", International Conference on Electrical, Computer and Communication Engineering (ECCE), February 16-18, 2017, Cox's Bazar, Bangladesh.

[2] Bharati M Nelligani, Dr. N V Uma Reddy, Mr. Nithin Awasti Smart, "ATM Security System using FPR, GSM, GPS", Incentive Computation Technologies (ICICT), International Conference in the year 2016.

[3] http://www.financialexpress.com/industry/technology/-indianscientistmanisha-mohan-at-mit-creates-wearable-sensor-to-stop-rape/781836/

[4] http://cdn.sparkfun.com/datasheets/Sensors/Biometric/-GT511C3_datash eet_V2.1_2016 1025.pdf

[5] https://store.arduino.cc/usa/arduino-nano

[6] https://cdnshop.adafruit.com/datasheets/SIM808_Hard-ware+Design_V1. 00.pdf

[7] https://www.homemade-circuits.com/mosquito-swatter-bat-circuit/

[8] B. Chougula, "Smart girls security system," International Journal of Application or Innovation in Engineering & Management, Volume 3, Issue 4, April 2014.

[9] http://www.technodiscoveries.com/technology/society-harnessing equipment-she-anti-rape undergarments-by-indian-students.html

[10] Tiwalade O. Majekodunmi, Francis E. Idachaba "A Review of the Fingerprint, Speaker Recognition, Face Recognition and Iris Recognition Based Biometric Identification Technologies" World Congress on Engineering 2011 Vol II WCE 2011, July 6 - 8, 2011, London, U.K.

SELF DEFENSE DEVICE WITH GSM ALERT AND GPS TRACKING WITH FINGERPRINT VERIFICATION FOR WOMEN SAFETY

[1]Mohd Yousuf, [2]Sharea Takreem
[1]PG Scholar, Department of Electronics and Communication Engineering,
[2]Assistant Professor, Department of Electronics and Communication Engineering,
Nawab Shah Alam Khan College of Engineering & Technology, Hyderabad

ABSTRACT

Another methodology is given towards the security of ladies as a gadget. The goal of the gadget is to give ladies an apparatus that can give them security and guarantee their wellbeing in the event of any disaster. The paper proposes a superior methodology which utilizes a high voltage current creating circuit which will be utilized to stagger the resistance for few moments. The unique mark module for initiation of gadget, electric stun creating circuit, GSM/GPS module for cautioning and area following all interfaced with a microcontroller to plan a little mallet formed gadget which will be helpful and effectively compact.

Security of ladies is a significant subject of worry in India. A large portion of the ladies in India have encountered some type of viciousness or provocation out in the open. There is a development in wrongdoings identified with ladies badgering and the fundamental explanation that a lady is being a casualty is absence of public security and powerlessness of a lady to safeguard her. So as to have the option to ensure herself, she should prepare herself through different self-preservation courses, which isn't workable for each lady to enlist into these courses. As to issue there are different applications accessible on portable stage that are implied uniquely for ladies wellbeing, yet these applications doesn't ensure security at the hour of the episode on the grounds that these applications just take care of the work of advising individuals worried about ladies' wellbeing and couldn't help her to guard herself neither the accessibility of the concerned individuals is ensured at the hour of the occurrence.

In certain nations the utilization of self-preservation gear is real. These supplies like immobilizer and pepper splash are produced for a lady to protect herself by assaulting the resistance utilizing these types of gear, however in the event that the casualty needs help or she is in detached territory with nobody to help then these types of gear can be named as impermanent wellbeing supplies. Additionally, these gadgets can be abused whenever fallen in wrong hands.

Keywords- security, GSM, GPS, FPR

I. INTRODUCTION

Security of women is a major topic of concern in India. Most of the women in India have experienced some form of violence or harassment in public. There is a growth in crimes related to women harassment and the main reason that a woman is being a victim is lack of public security and inability of a woman to defend her. In order to be able to protect herself, she must train herself through various self-defense courses, which is not possible for every woman to enroll into these courses. Regarding this issue there are various applications available on mobile platform that are meant specially for women safety, but these applications doesn't guarantee security at the time of the incident because these applications only do the job of informing people concerned about women's safety and could not assist her to defend herself neither the availability of the concerned people is guaranteed at the time of the incident. In some countries the use of self-defense equipment is legitimate. These equipment like stun gun and pepper spray are developed for a woman to defend herself by attacking the opposition using this equipment, but if the victim needs assist or she is in secluded area with no one to help then this equipment can be termed as temporary safety equipment's. Also, these devices can be misused if fallen in wrong hands

COMMON OVERVIEW TO EMBEDDED SYSTEM

An embedded system can be defined as a computing device that does a specific focused job. Appliances such as the air-conditioner, VCD player, DVD player, printer, fax machine, mobile phone etc. are examples of embedded systems. Each of these appliances will have a processor and special hardware to meet the specific requirement of the application along with the embedded software that is executed by the processor for meeting that specific requirement. The embedded software is also called "firm ware". The desktop/laptop computer is a general-purpose computer. You can use it for a variety of applications such as playing games, *word* processing, accounting, software development and so on. In contrast, the software in the embedded systems is always fixed listed below.

Embedded systems do a very specific task, they cannot be programmed to do different things. . Embedded systems have very limited resources, particularly the memory. Generally, they do not have secondary storage devices such as the CDROM or the floppy disk. Embedded systems have to work against some deadlines. A specific job has to be completed within a specific time. In some embedded systems, called real-time systems, the deadlines are stringent. Missing a deadline may cause a catastrophe-loss of life or damage to property. Embedded systems are constrained for power. As many embedded systems operate

through a battery, the power consumption has to be very low.

· Some embedded systems have to operate in extreme environmental conditions such as very high temperatures and humidity.

II. BLOCK DIAGRAM

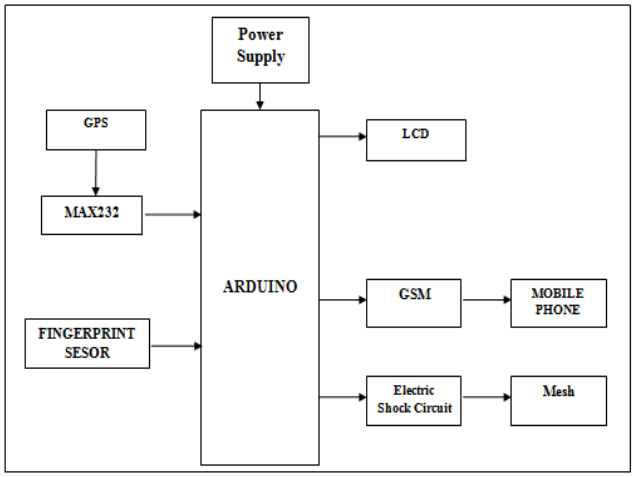

POWER SUPPLY

The force flexibly area is the part framework power flexibly is more mind boggling, with up to eight diverse gracefully voltage esteems, with 5 V and 3.3 V gave by the CPCI body. 5 V supplies the DC/DC gadget with buck to create other flexibly voltages, and supplies capacity to the 1553 transport's transformer. 3.3 V is the primary framework power gracefully, including the USB PHY, clock gadgets, FPGA and CPU and PCI connect gadgets (PLX6466) I/O parts. Other gracefully voltages are gotten from a 5V or 3.3 V flexibly voltage venture down.

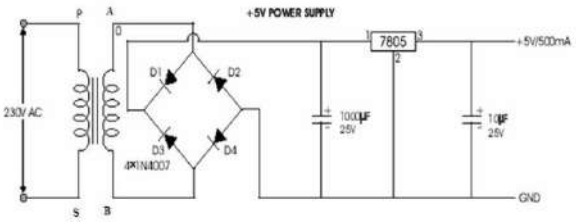

ARDUINO UNO

The Arduino UNO is the best board to begin with hardware and coding. This is your first experience dabbling with the stage, the UNO is the heartiest board you can begin playing with the UNO is the most utilized and recorded leading group of whole Arduino family.

Arduino/genuine Uno is a MCU board based totally at the atmega328p (datasheet).

It has 14 virtual input/output pins (of which 6 may be used as PWM outputs), 6 analog inputs, a sixteen MHz quartz crystal, A USB connection, a energy jack, an ICSP header and a reset button. It incorporates everything needed to assist the microcontroller; absolutely connect it to a computer with a USB cable or electricity it with a ac-to-dc adapter or battery to get started. You may tinker together with your UNO without demanding too much about doing something wrong, worst case scenario you can replace the chip for some bucks and begin yet again. "Uno" means one in Italian and become selected to mark the release of Arduino software program (IDE) 1.zero. The UNO board and version 1.zero of Arduino software (IDE) had been the reference variations of Arduino, now evolved to newer releases. The UNO board is the first in a chain of USB Arduino boards, and the reference model for the Arduino platform; for an intensive list of contemporary, past or outdated boards see the Arduino index of forums

TECHNICAL SPECIFICATIONS

Microcontroller	ATmega328P
Operating Voltage	5V
Input Voltage (recommended)	7-12V
Input Voltage (limit)	6-20V
Digital I/O Pins	14 (of which 6 provide PWM output)
PWM Digital I/O Pins	6
Analog Input Pins	6
DC Current per I/O Pin	20 mA
DC Current for 3.3V Pin	50 mA
Flash Memory	32 KB (ATmega328P) of which 0.5 KB used by bootloader
SRAM	2 KB (ATmega328P)
EEPROM	1 KB (ATmega328P)
Clock Speed	16 MHz
LED_BUILTIN	13
Length	68.6 mm
Width	53.4 mm
Weight	25 g

LIQUID CRYSTAL DISPLAY

The most regularly utilized Character put together LCDs are based with respect to Hitachi's HD44780 regulator or other which are viable with HD44580.we will examine about character based LCDs, their interfacing with different microcontrollers, different interfaces (8-cycle/4-bit), programming, unique stuff and deceives you can do with these straightforward looking LCDs which can give another look to your application.

The most regularly utilized LCDs found in the market today are 1 Line, 2 Line or 4 Line LCDs which have just 1 regulator and backing all things considered of 80 charachers, while LCDs supporting in excess of 80 characters utilize 2 HD44780 regulators.

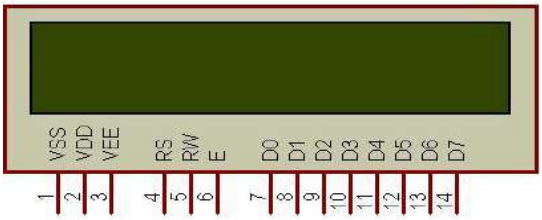

FINGER PRINT

This is a unique mark sensor module with TTL UART interface for direct associations with microcontroller UART or to PC through MAX232/USB-Serial connector. The client can store the unique mark information in the module and can arrange it in 1:1 or 1: N mode for distinguishing the individual. The FP module can legitimately interface with 3v3 or 5v Microcontroller. A level converter (like MAX232) is needed for interfacing with PC sequential port. Optical biometric unique mark per user with incredible highlights and can be installed into an assortment of final results, for example, access control, participation, wellbeing store box, vehicle entryway locks.

GLOBAL SYSTEM FOR MOBILE

Global System for Mobile Communications (GSM) modems are specific sorts of modems that work over membership based remote organizations, like a cell phone. A GSM modem acknowledges a Subscriber Identity Module (SIM) card, and fundamentally acts like a cell phone for a PC. Such a modem can even be a devoted cell phone that the PC utilizes for GSM network capacities.

GSM Modem Application

GLOBAL POSITIONING SYSTEM

The Global Positioning System (GPS) is a U.S.- claimed utility that gives clients situating, route, and timing (PNT) administrations.

The Global Positioning System (GPS) is a route framework utilizing satellites, a beneficiary and calculations to synchronize area, speed and time information for air, ocean and land travel.

The satellite framework comprises of a heavenly body of 24 satellites in six Earth-focused orbital planes, each with four satellites, circling at 13,000 miles (20,000 km) above Earth and going at a speed of 8,700 mph (14,000 km/h).

While we just need three satellites to deliver an area on earth's surface, a fourth satellite is frequently used to approve the data from the other three. The fourth satellite likewise moves us into the third-measurement and permits us to compute the height of a gadget.

ULN2003: -

The ULN2003 is a IC comprises of 7 NPN Darlington semiconductor sets with high voltage and current capacity. It is ordinarily utilized for applications, for example, hand-off drivers, engine, show drivers, driven

light drivers, rationale cradles, line drivers, hammer drivers and other high voltage momentum applications. It comprises of basic cathode brace diodes for each NPN Darlington pair which makes this driver IC helpful for exchanging inductive burdens.

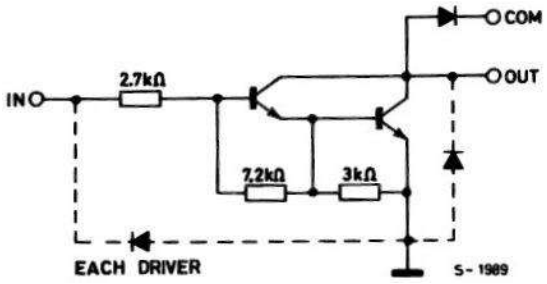

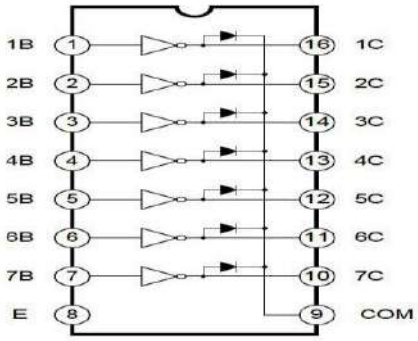

Logic Diagram of ULN2003

FEATURES

* High-voltage yields: 50V
* Inputs viable with different kinds of logic.
* Relay driver application

500mA appraised gatherer current (Single yield)

RELAY

The transfer module acts like a switch of mains voltage [16, 17]. It is helpful for controlling apparatuses utilizing microcontrollers. Fig. 3 shows the 2 transfer modules. The working voltage is 5 V and driver ebb and flow is 15 – 20 mA. The hand-off module has 4 pins which are VCC, GND, IN1, and IN2 separately.

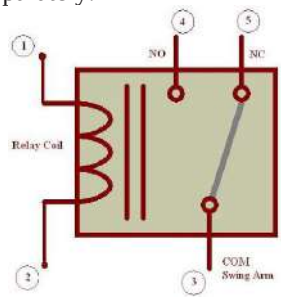

Representation of Relay

III. RESULTS

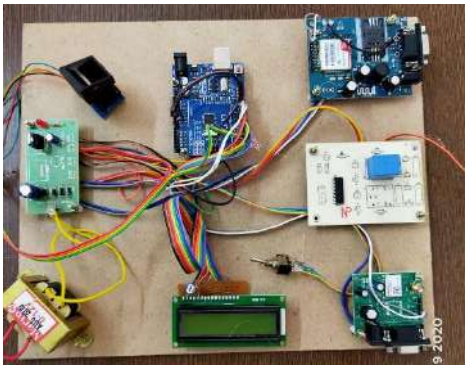

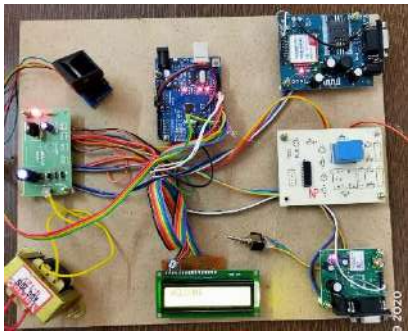

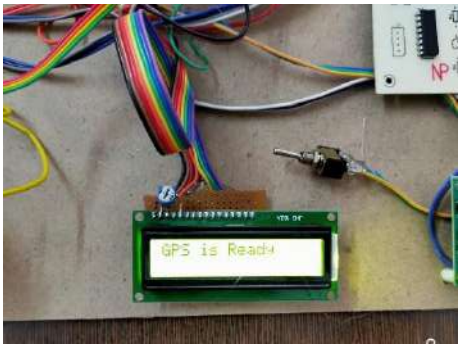

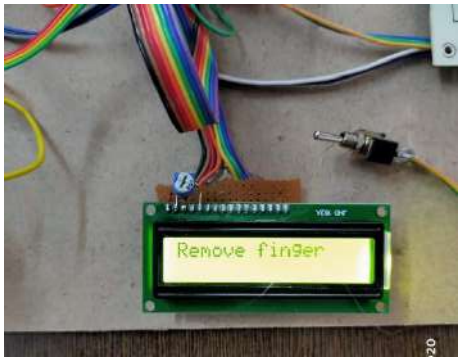
Remove finger

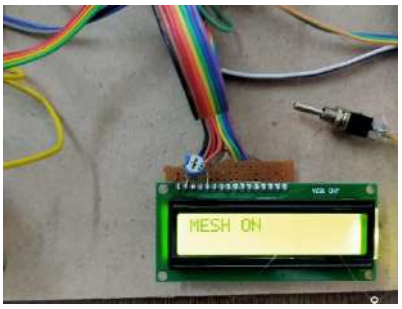
MESH ON

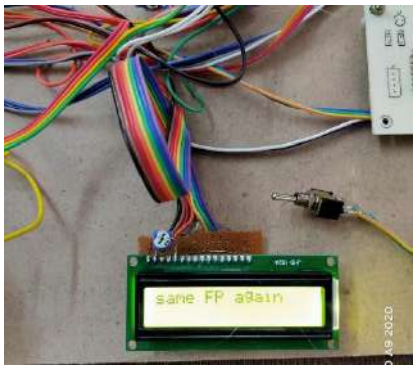
same FP again

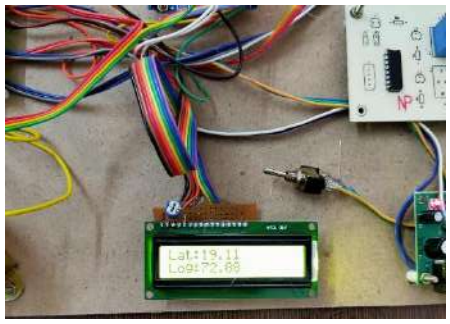
Lat:19.11
Log:72.88

Found ID:1

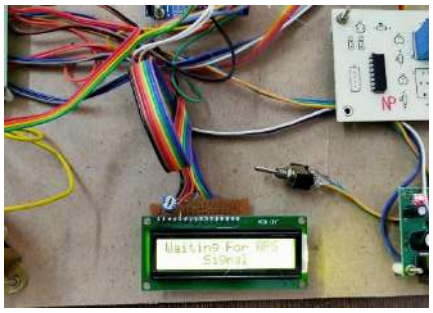
Waiting For FPS
Scan...

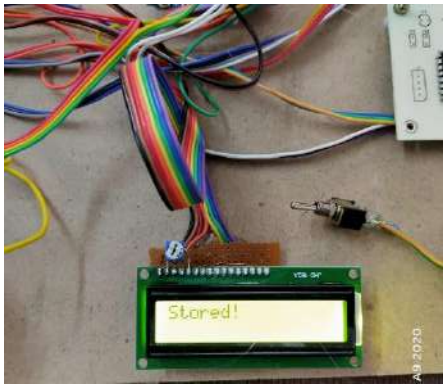

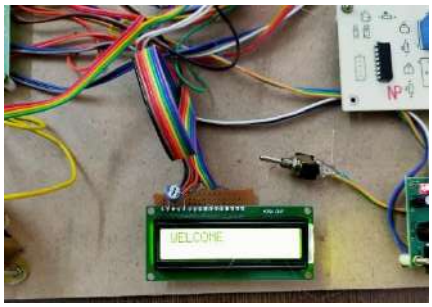

IV. CONCLUSION

There are numerous gadgets which are produced for women's safety however none of the gadget incorporates GSM/GPS cautioning and area following alongside hostile abilities. The applications which are as of now utilized for the ladies security don't have any arrangement for protecting herself and does no tenure wellbeing till the messages are shipped off the casualty's closed ones and they show up at a position of episode and spare her from the disaster. The proposed plan for Biometric Self Defense Device with GSM Alert and GPS Tracking is the best possible tool for a lady to safeguard herself. This paper gives an algorithm to build up a gear which a casualty can utilize to defend herself by staggering the resistance with a high electric current and simultaneously she can send a caution message with her flow area to her shut ones. For abrupt assaults, outside catch can be given for activation of gadget. Spotlight can be incorporated as an additional security.

REFERENCES

[1] Mrinmoy Dey, Md. Akteruzzaman Arif and Md. Asif Mahmud, „ Antitheft Protection of Vehicle by GSM & GPS with Fingerprint Verification", International Conference on Electrical, Computer and Communication Engineering (ECCE), February 16-18, 2017, Cox's Bazar, Bangladesh.

[2] Bharati M Nelligani, Dr. N V Uma Reddy, Mr. Nithin Awasti Smart, "ATM Security System using FPR, GSM, GPS", Incentive Computation Technologies (ICICT), International Conference in the year 2016.

[3] http://www.financialexpress.com/industry/technology/-indianscientistmanisha-mohan-at-mit-creates-wearable-sensor-to-stop-rape/781836/

[4] http://cdn.sparkfun.com/datasheets/Sensors/Biometric/-GT511C3_datash eet_V2.1_2016 1025.pdf

[5] https://store.arduino.cc/usa/arduino-nano

[6] https://cdnshop.adafruit.com/datasheets/SIM808_Hard-ware+Design_V1. 00.pdf

[7] https://www.homemade-circuits.com/mosquito-swatter-bat-circuit/

[8] B. Chougula, "Smart girls security system," International Journal of Application or Innovation in Engineering & Management, Volume 3, Issue 4, April 2014.

[9] http://www.technodiscoveries.com/technology/society-harnessing equipment-she-anti-rape undergarments-by-indian-students.html

[10] Tiwalade O. Majekodunmi, Francis E. Idachaba "A Review of the Fingerprint, Speaker Recognition, Face Recognition and Iris Recognition Based Biometric Identification Technologies" World Congress on Engineering 2011 Vol II WCE 2011, July 6 - 8, 2011, London, U.K.

MAINTAINING CONFIDENTIALITY AND SECURITY BY REVOKING MALICIOUS USER BY USING 3DRMAKA PROTOCOL

[1]Amtul Noor, [2]Mohammed Khaleel Ahmed, [3]mohammad Sanaullah Qaseem
M.Tech Scholar, Department of Computer Science Engineering and Technology,
Associate Professor & Project Coordinator, Department of Computer Science and Engineering,
Professor and Head, Department of CSE, VICE PRINCIPAL (Academics) IQAC Coordinator,
Nawab Shah Alam Khan College of Engineering & Technology, Hyderabad

ABSTRACT: With the development of distributed computing innovation as far as unwavering quality and proficiency, countless administrations have moved to the cloud stage. To advantageous admittance to the administrations and secure the protection of correspondence in the public organization, three-factor Mutual Authentication and Key Agreement (MAKA) conventions for multi-worker structures increase wide consideration. Not with standing, the vast majority of the current three-factor MAKA conventions don't give a proper security confirmation bringing about different assaults on the related conventions, or they have high calculation and correspondence costs. Furthermore, a large portion of the three-factor MAKA conventions haven't a dynamic renouncement system, which prompts pernicious clients cannot be quickly repudiated. To address these downsides, we propose a provable unique revocable three-factor MAKA convention that accomplishes the client dynamic administration utilizing Schnorr marks and gives a conventional security verification in the arbitrary prophet. Security examination shows that our convention can satisfy different needs in the multi-worker conditions. Execution investigation shows that the proposed plot is appropriate for processing asset compelled brilliant gadgets. The full form of the reenactment usage demonstrates the achievability of the convention.

Index Terms: Protocols, Cloud computing, Smart cards, Authentication, Bio ceramics.

I. INTRODUCTION

In the continuous decade, circulated figuring development has been completely showcased. It can't simply improve organization profitability yet also decline costs. An ever-expanding number of associations are putting their organizations on the cloud stage for development and support. This not simply brings down the close by upkeep inconvenience for these endeavors, yet furthermore gives bound together security and movement the board for all organizations on the untouchable cloud stage, as showed up in Fig.1. Yet untouchable cloud stages have even more prevailing advancements and progressively standard specific points of interest to ensure that the workers run in a decently secure condition, customers and workers pass on in everyone organize. Thusly, check and key comprehension are fundamental for the correspondence security.

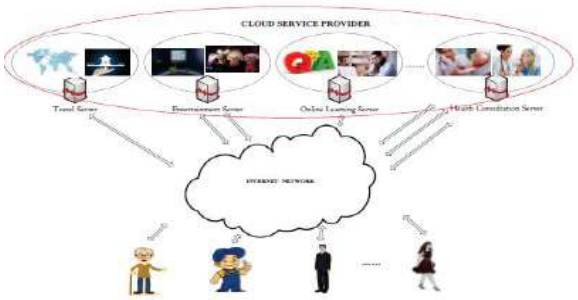

Fig 1: Cloud service environment

The usage of basic confirmation and key comprehension (MAKA) shows not simply shield aggressors from mauling worker resources, yet furthermore dodge pernicious attackers acting like the worker to secure the customer's information. Along these lines, the MAKA shows have been generally examined since Lamport proposed a mystery word-based approval show [1]. Earlier

MAKA shows [2], [3], [4] are planned for single-worker plan.

As Internet customers grow exponentially, the amount of cloud workers delivering unprecedented organizations has moreover grown inside and out. For the single-worker plan, it is difficult for customers to keep up an assortment of passwords for each worker. To improve customer experience, various analysts propose progressively versatile MAKA shows [5], [6], [7], [8], [9], [10] for multi-worker conditions. The shows for multi-worker plans model as showed up in Fig.2, customers and cloud workers simply need to select the enlistment center (RC) to shared check and key comprehension. In the multi-worker conditions, the MAKA shows can be also separated into two classes, two-factor MAKA shows, to be explicit character, mystery word, and three-factor MAKA shows, to be explicit character, mystery word, and biometrics. The works in [11], [12] have shown that the mystery expression estimating mystery state attack.

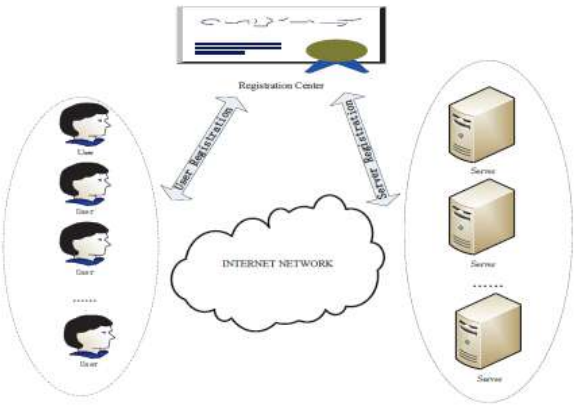

Fig 2: Multi-service architectures of the protocol model

The cost of the mystery key estimating attack on mystery word-based show becomes lower and lower as the quick headway of PCs. Then again, customers generally speaking utilize direct letters or numbers as their passwords, and even a tremendous number of customers honestly utilize the default mystery key if the splendid contraptions don't need the customer to modify the mystery word mandatory. To clarify this issue, a couple of biometrics-based MAKA shows [13], [14], [15], [16], [17], [18], [19], [20], [21], [22], [23] have been proposed. As a result of the uniqueness, openness and non-adaptability of biometrics keys (palm print, iris, unique mark, etc.), the three-factor MAKA shows for multi-worker conditions give more security than the two-factor shows. In context on the straightforwardness of far off frameworks, a rival can hinder, change, delete and replay any correspondence messages. Indefinite quality and un-obviousness are moreover urgent bit of the MAKA shows [24], [25], [26], [27], [28] to restrict the recently referenced attacks. In any case, the current three-factor MAKA shows actually have the going with blemishes.

1) Security weaknesses: Most of the current MAKA shows subject to the three factors haven't formal proof, yet some easygoing security examination. Additionally, a couple of shows were embed problematic parts for instance, key approval factors successfully eliminated. We will separate such inadequacies in the security assessments and sepulcher examination segment.

2) Incomplete principal limits: Some huge fundamental limits, for instance, dynamic customer food, affirmation stage without RC, are not considered in most MAKA shows.

3) High cost: Some three-factor MAKA shows didn't survey their genuine application condition, which results these shows are unquestionably not proper for the confined resource of the contraptions. Along these lines, it still a test to design a fruitful three factor MAKA show for achieving secure correspondence among customer and worker.

II. RELATED WORKS

In 2001, Li et al. [5] introduced the possibility of check show for multi-worker circumstances and proposed the primary mystery word based MAKA show using the neural framework. In view of the befuddled neural framework, Li et al's. show isn't proper for splendid contraptions with limited enrolling control. To improve viability, Juang [6] proposed a MAKA show for multi-worker plans by using hash limits and symmetric key cryptosystems. In the comparable year, Chang et al. [7] raised that Juang's show is faulty to the extent capability. They proposed an inexorably capable MAKA plot for multi-worker circumstances. Regardless, in their show RC shares structure private key with all workers. This will doubtlessly achieve various security weaknesses. To improve security, some new MAKA shows [8], [9] using hash limits and symmetric-key cryptosystems had furthermore been proposed. In 2013, Liao et al. [10] proposed a multi-worker far off customer check show using self-ensured open keys for adaptable clients. Nevertheless, their plot doesn't set up a typical meeting key and the correspondence cost is forbidden. Given how distant frameworks are open condition, the security affirmation is moreover considered in such shows. To give customer mystery, Das et al. [24] proposed the key powerful two-factor affirmation plan which uses dynamic pseudo-characters as opposed to a customer's veritable character. Unfortunately, in 2009 Wang et al. [25] brought up that Das et al's. Show fails to give shared check, customer mystery and they proposed an improved variation. Nevertheless, Yeh et al. [26] and Wen et al. [27] found that Wang et al. improved transformation is powerless against emulate attack and is unequipped for giving customer haziness, independently. In 2016, taking into account self-guaranteed open key cryptography, He et al. [28] proposed a provable security obscure MAKA show for multi-worker structures. The shows analyzed above are mystery key based, yet such shows are inconsistent under separated theorizing mystery key attack. We will inspect the show [28] that has such security inadequacy in the security assessments and cryptanalysis subsection. To address this inadequacy, taking into account remarkable imprint, Lee et al. [13] proposed an approval show using sharp card. Regardless, Lin et al. [14] and Chang et al. [15] found that Lee et al's. Show encounters the mask attack and the conspiring attack, independently. To improve security, Kim et al. [16] proposed another biometrics-based approval show using keen card. Tragically, Scott [17] called attention to that Kim et al's. Show can be completely subverted by an idle enemy. Thereafter, Khan et al. [18] found that Lin et al's. plot similarly encounters the worker disparaging attack and proposed an improved version. For multi-worker models, Yoon et al. [19] proposed a biometrics-based affirmation show using roundabout twist cryptosystem (ECC) and adroit card. Appallingly, Kim et al. [20] and He [29] pointed out that Yoon et al.'scheme is

questionable under the separated mystery express hypothesizing attack, the uncommon insider attack and the emulate attack. A short time later, He et al. [21] proposed a healthy biometrics-based approval plot for multi-worker models. Regardless, Odelu et al. [22] bring up that He et al's. show encounters the known meeting unequivocal momentary information attack, the emulate attack, and so forth. Regardless, every approval and key comprehension in Odelu et al.'protocol requires the commitment of RC. In 2017, Reedy et al. [23] similarly proposed biometrics based MAKA show for multi-worker conditions. Lamentably, after our examination in the security assessments besides, cryptanalysis subsection of this paper, their show is vulnerable the worker emulate attack and the man-in the-middle attack. On the other hand, the MAKA show is moreover commonly used in various conditions, for instance, Passive Web of Things [30], Vehicles in Smart City [31], and Cell telephones [32], [33].

III. OUR CONTRIBUTIONS

In this paper, we propose a unique revocable three-factor shared confirmation and key understanding (3DRMAKA) convention which has progressively sweeping limits, dependable security and moderately higher execution capability. Our responsibility can be summed up as follows:

1) We plan a three-factor MAKA convention which executes three-factor security. Furthermore, we show that the proposed convention can satisfy the requirements of multi-worker designs, for instance, obscurity, no recognizability, obstruction secret key hypothesizing assault and keen card extraction assault, etc.

2) Our arrangement accomplishes the customer's dynamic administration. In our convention, customers can be powerfully dismissed to quickly keep assaults from pernicious customers. Without a powerful renouncement instrument, RC can't repel malevolent customers in a promising way. This may achieve such malignant customers still dynamic in the framework to speak with various workers.

3) In the irregular prophet, we give a conventional proof of the proposed convention dependent on BDH, CDH and Schnorr marks un produce capacity suspicions. We show that the proposed convention is shared validation secure and confirmed key understanding secure.

4) Our convention has a good execution adequacy. Particularly on the client side, the calculation cost of our arrangement is the most minimal in the related existing conventions. This shows that our convention is dynamically reasonable for contraption mobiles with compelled enlisting resource. What's more, to exhibit that the convention is in fact stable, we automatically reproduce the proposed convention.

IV. PROPOSAL

We describe the proposed 3DRMAKA protocol. The proposed protocol can be divided into eight phases:

i) Initialization Phase: The RC initializes the system private key and the system parameters in this phase.

1) According the definition of bilinear pairing, RC selects two groups G1, G2 of the same prime order q and a bilinear paring e:G1 G1 ! G2.

ii) Server Registration Phase: In this phase, the server Sj registers with the RC in order to be an authorized server of the network. The processes of communication between Sj and RC are performed as follows.

1) Sj transmits registration request with his/her identity IDsj to RC securely.

2) RC computers dsj = s1 H00(IDsj), H1(ASK) and delivers them back to Sj under a secure channel.

3) Upon receiving (dsj ;H1(ASK)), the Sj can validate the private key by checking whether the equation e(dsj ; P)? = e(H00(IDsj); Ppub) holds. If the equation holds, the private key is valid and vice versa.

4) RC maintains a table database Tsj ,which stores the status of the corresponding registration servers.

iii) Users Registration Phase: Under multi-server environments, a new user Ui who wants to access the services provided by Sj must register with the RC. As shown in Fig.4, the steps of communication between Ui and RC are carried out as follows.

1) Ui inputs his/her identity IDui, password PWui and biometrics BIOui. Then Ui generates a random number rui 2 Z_ q and computers Gen(BIOui)= (_ui; @ui), PIDui = H2(IDui; rui), PWDui = H3(PWui; PIDui; rui), and PBIOui = H2(@ui; rui). Finally Ui transmits (IDui, PIDui, PWDui, PBIOui) to RC through an out of band (secure) channel.

2) RC calculates dui = s1 _ H01(PIDui), Gui = dui _ PWDui, Vui = H4(PWDui;Gui) for corresponding user. To reduce the user's computational burden, RC computes e(dui;H00(IDsj)) for the user based on valid server entries in the Tsj table database. And then generates a Tui table whose data is Rsj = e(dui;H00(IDsj)) _PWDui _ PBIOui. RC inserts (Tui;Gui; Vui;H1(ASK)) into smartcard(SC) for corresponding user and sends SC to the user under a secure channel. Finally, RC creates a form database Tsui with hash of user identity information in which also stores the status of the corresponding registration users to dynamically manage users.

3) Upon receiving SC, Ui computes Wui = rui _ H1(@ui), h1 = H1(ASK) _ rui _ PBIOui and then replaces H1(ASK) with _ui, Wui, Hi(i =00; 01; 1; : : : ; 7), h1, gpub.

iv) Time Key Update Phase: In order to manage users dynamically, RC periodically updates. The time key to legitimate users in the Tsui. The steps below are run between RC and Ui.

1) Before updating the time key for a user, RC checks the status of the corresponding anonymous user PIDui in Tsui. Then, RC chooses a random number bui 2 Z q , valid time period t and computes Bui = gbui , dtui = bui+H5(Bui; PIDui; t) s2modq for the legitimate user. RC transmits (Bui; dtui; t) to the corresponding user through a public channel.
2) Upon receiving (Bui; dtui; t), the user first enters IDui, BIOui and then computes @ui = Rep(BIOui, ui), rui = Wui H1(@ui), PIDui = H2(IDui; rui). Ui checks gdtui? = BuigH5(Bui;P IDui;t) pub to verify the validity of the time key. If the equation holds, the user inserts (Bui; dtui; t)to SC. The elements contained in the SC are fTui;Gui; Vui; h1; ui;Wui;Hi(i = 00; 01; 1; : : : ; 7); gpub;Bui; dtui; tg.

v) Login and Mutual Authentication Phase: The user must first complete the smart card login. Then, Ui and Sj can authenticate each other and negotiate a session key. This phase is described as follows.
1) Ui inputs his/her IDui, PWui and BIOui into SC. SC uses its stored information to calculate @ui = Rep(BIOui; ui), rui = Wui H1(@ui), PIDui = H2(IDui; rui), PWDui = H3(PWui; PIDui; rui), PBIOui = H2(@ui; rui). SC validates whether the equation Vui? = H4(PWDui;Gui) holds. If the equation holds, the user logins successfully, otherwise, rejects the request.
2) Using the information in table Tui, the user chooses a target server IDsj . SC generates a random number N1 2 Z q and calculates H1(ASK) = h1 rui PBIOui, kui = gN1 , Fui = PIDui H6(kui; IDsj ;H1(ASK)). Then, SC sends (Fui, kui, Bui, dtui, t) to the corresponding server Sj .
3) Upon receiving the messages, Sj first verifies the time key correctness by checking gdtui? = Bui gH5(Bui;P IDui;t) pub , where PIDui = Fui H6(kui; IDsj ;H1(ASK)). If the equation holds, Sj continues next steps; otherwise, rejects the request.
4) Sj chooses a random number N2 2 Z_ q and computes k1t = e(dsj ;H01(PIDui)), ksj = gN2 and Dsj = H7(k1t; ksj ; kui; gpub; PIDui; IDsj). Then, Sj transmits (Dsj ; ksj) to the corresponding Ui.
5) Upon receiving (Dsj ; ksj), Ui computes k1 = Rsj _ PWDui _ PBIOui and then checks whether the Dsj? = H7(k1; ksj ; kui; gpub; PIDui; IDsj) holds. If the equation holds, Ui computes ku = kN1 sj , Dui = H7(gpub; kui; ksj ; k1; PIDui; IDsj), the session key sk = H7(ku; gpub; ksj ; kui; PIDui; IDsj). Then, Ui sends Dui to Sj .
6) When Sj receives the message Dui, he/she checks whether the Dui? = H7 (gpub; kui; ksj ; k1t; PIDui; IDsj) holds. If the equation holds, Sj computes ks = kN2 ui and the session key sk = H7(ks; gpub; ksj ; kui; PIDui; IDsj).

vi) Password and Biometrics Change Phase: In order to reduce the burden of RC, the user can change the password and biometrics without RC in our scheme.The detailed steps are as follows.

1) Ui enters his/her IDui, PWui, BIOui and new PWnui, BIOnui into SC. The SC computes @ui = Rep(BIOui; ui), rui = Wui H1(@ui), PIDui = H2(IDui; rui), PWDui = H3(PWui; PIDui; rui), PBIOui = H2(@ui; rui). The SC validates whether the equation Vui? = H4(PWDui;Gui) holds. If not, SC terminates the follow-up operations.
2) SC computes PWDnui = H3(PWnui; PIDui; rui), Gen(BIOnui) = (nui; @nui), PBIOnui = H2(@nui ; rui) and then uses them to update other relevant informations in SC, namely Rnsj = Rsj PWDui PBIOui PBIOnui PWDnui ! Tnui, Gnui = Gui PWDui PWDnui, Vnui = H4 (PWDnui,Gnui), hn1 = h1 PBIOui PBIOnui, Wnui = Wui H1(@ui) H1(@nui). Finally, SC replaces (Tui,Gui; Vui,h1,Wui; ui) with (Tnui,Gnui,Vnui, hn1,Wnui, nui).

vii) New Server Update Phase:
When a new server wants to join the network, the proposed protocol can insert the new server information without RC . The detailed processes are as follows.
1) When a new server Snj has finished registration, the RC updates the Tsj and broadcasts IDnsj all valid users in the Tsui.
2) Upon receiving IDnsj, users input IDui, PWui; BIOui and IDnsj into SC. The SC computes @ui = Rep(BIOui; ui), rui = Wui H1(@ui), PIDui = H2(IDui; rui), PWDui = H3(PWui; PIDui; rui), PBIOui = H2(@ui; rui), dui = Gui PWDui, Rnsj = e(dui; H00(IDnsj)) PWDui PBIOui. Then, the SC inserts Rnsj into Tui.

viii) Dynamic Revocation Phase: In practice, the importance of an efficient revocation mechanism is self-evident. It has positive meaning both in preventing malicious users and improving the efficiency of RC management. In this phase, we introduce two kinds of dynamic revocation supported by this scheme, namely, the revocation of malicious users and the user initiative to apply for revocation.
1. Malicious User Revocation: During the session, if servers find that a user is visiting illegally, the server reports the RC. RC will verify the authenticity. If the situation is true, he/she immediately stop updating the user time key. Otherwise, RC will punish the service to a certain degree of downgrade.
2. User Apply For Revocation: The user sends the revocation request with identity ID through the secure channel. After receiving the message, RC checks the identity ID and then stops updating the corresponding user time key.

V. PROPOSED ALGORITHM

3DRMAKA Protocol:

We propose a provable unique revocable three-factor MAKA convention that accomplishes the client dynamic administration. In our convention, clients can be powerfully renounced to immediately keep assaults from malignant clients. In this part, we portray the proposed

3DRMAKA convention. The proposed convention can be separated into eight stages: Initialization Phase, Server Registration Phase, Users Registration Phase, Time Key Update Phase, Login and Mutual Authentication Phase, Password and Biometrics Change Phase, New Server Update Phase and Dynamic Revocation Phase.

ADVANTAGES

i) More efficient and accurate
ii) Confidentiality is maintained.

V. RESULT

1) This is for new user registration. After successfully registering then user need to go through one authentication to get access to his/her account.

2) After going through successful registration these would be his login screen and here user need to provide name and valid email id for authentication, If the provided credentials are true then he will get OTP to his/her valid emailed then he would get access to his/her account.

VI. CONCLUSION

To contradict the exhaustion of mystery word attack on the two-factor MAKA shows, a tremendous number of three-factor MAKA shows have been proposed. Nevertheless, essentially each of the three factor MAKA shows don't give formal confirmations. In order to achieve logically versatile customer the board and higher security, this paper proposes another three-factor MAKA show that upholds dynamic disavowal and gives formal affirmation. The security shows that our show achieves the security properties of necessities from multi-worker conditions. On the other hand, through the exhaustive assessment of execution, our show doesn't relinquish efficiency while improving the limit. All things considered, the proposed show has remarkable ideal conditions the extent that the total figuring time.

REFERENCES

[1] L. Lamport, "Password authentication with insecure communication," Communications of the ACM, vol. 24, no. 11, pp. 770–772, 1981.

[2] X. Huang, Y. Xiang, A. Chonka, J. Zhou, and R. H. Deng, "A generic framework for three-factor authentication: Preserving security and privacy in distributed systems," IEEE Transactions on Parallel and Distributed Systems, vol. 22, no. 8, pp. 1390–1397, 2011.

[3] X. Huang, Y. Xiang, E. Bertino, J. Zhou, and L. Xu, "Robust multifactor authentication for fragile communications," IEEE Transactions on Dependable and Secure Computing, vol. 11, no. 6, pp. 568– 581, 2014.

[4] D. He, S. Zeadally, N. Kumar, and J. Lee, "Anonymous authentication for wireless body area networks with provable security," IEEE Systems Journal, pp. 1–12, 2016.

[5] L. Li, L. Lin, and M. Hwang, "A remote password authentication scheme for multi-server architecture using neural networks," IEEE Transactions on Neural Networks, vol. 12, no. 6, pp. 1498–1504, 2001.

[6] W. Juang, "Efficient multi-server password authenticated key agreement using smart cards," IEEE Transactions on Consumer Electronics, vol. 50, no. 1, pp. 251–255, 2004.

[7] C. C. Chang and J. S. Lee, "An efficient and secure multi-server password authentication scheme using smart cards," in International Conference on Cyber worlds, 2004, pp. 417–422.

[8] J.-L. Tsai, "Efficient multi-server authentication scheme based on one-way hash function without verification table," Computers & Security, vol. 27, no. 3C4, pp. 115–121, 2008.

[9] W. Tsaur, J. Li, and W. Lee, "An efficient and secure multi-server authentication scheme with key agreement," Journal of Systems and Software, vol. 85, no. 4, pp. 876–882, 2012.

[10] Y. Liao and C. Hsiao, "A novel multi-server remote user authentication scheme using self-certified public keys for mobile clients," Future Generation Computer Systems, vol. 29, no. 3, pp. 886–900, 2013.

LIVER CANCER DETECTION AND CLASSIFICATION USING NEURAL NETWORKS ON MRI IMAGES

[1]Minha, [2]Mohammed Khaleel Ahmed, [3]Mohammad Sanaullah Qaseem
M.Tech Scholar, Department of Computer Science Engineering and Technology,
Associate Professor & Project Coordinator, Department of Computer Science and Engineering,
Professor and Head, Department of CSE, VICE PRINCIPAL (Academics) IQAC Coordinator,
Nawab Shah Alam Khan College of Engineering & Technology, Hyderabad

ABSTRACT

Image processing is a processing method with the assistance of numerical tasks. It utilizes any of the type of sign processing. Here the information is an image or video and the yield is likewise an image or a lot of image. This procedure is additionally utilized in clinical applications for different discovery and treatment. In this paper, it has been utilized to distinguish malignant growth cell of the liver. Here OSTU's strategy is utilized for upgrading the MRI image and watershed technique is utilized to section the malignant growth cell from the image.

INTRODUCTION

Disease is the unusual development of the tissue in an organ. Liver malignant growth is a kind of disease which influences the biggest organ of the midsection, liver. It is of two sorts specifically Primary Liver Cancer and Secondary Liver Cancer. Essential Liver Cancer starts in the liver itself and is known as Hepatocellular Carcinoma (HCC) or Hepatoma. Auxiliary Liver Cancer is a sort development of malignant growth cell where the disease cell begins from various organ and spreadto liver. The initial step is to discover an image to do the further processing. X-ray is an excellent imaging procedure which delivers the structure of human organ in more characterized way and helpful for analysis of ailments and Biological Research

OBJECTIVE

In this paper, it has been utilized to distinguish malignant growth cell of the liver. Here ostu's technique is utilized for improving the MRI image and watershed strategy is utilized to section the malignancy cell from the image.

Existing System:

MRI is a great imaging procedure which creates the structure of human organ in more characterized way and valuable for determination of maladies and Biological Research. The consequences of an MRI image are significantly improved via car and exact characterization of image.

LITERATURE SURVEY:

1. Magnetic Resonance Brain Image Classification by an Improved Artificial Bee Colony Algorithm

Robotized and exact arrangement of magnetic resonance (MR) brain images is a hotly debated issue in the field of neuroimaging. As of late a wide range of and inventive techniques have been proposed to develop this innovation. In this investigation, we introduced a cross breed technique dependent on forward neural network (FNN) to arrange a MR brain image as typical or unusual. The strategy first utilized a discrete wavelet change to remove highlights from images, and afterward applied the procedure of principle component analysis (PCA) to lessen the size of the highlights. The diminished highlights were shipped off a FNN, of which the boundaries were enhanced through an improved artificial bee colony (ABC) calculation dependent on both wellness scaling and chaotic hypothesis. We alluded to the improved calculation as scaled chaotic artificial bee colony (SCABC). Additionally, the K-overlap delineated cross approval was utilized to abstain from overfitting. In the examination, we applied the proposed technique on the informational collection of T2-weighted MRI images comprising of 66 brain images (18 ordinary and 48 anomalous). The proposed SCABC was contrasted and customary preparing strategies, for example, BP, force BP, hereditary calculation, world class hereditary calculation with relocation, reenacted strengthening, and ABC. Every calculation was run 20times to lessen haphazardness. The outcomes show that our SCABC can get the most un-mean MSE and 100% grouping exactness.

2. MRI induced heating of deep brain stimulation leads: effect of the air-tissue interface

We have examined the dissipating of the Magnetic Resonance Imaging (MRI) radiofrequency (RF) field by inserts for Deep Brain Stimulation (DBS) and the resultant warming of the tissue encompassing the DBS anodes. The limited component strategy has been utilized to perform full 3-D reasonable recreations. The close to field has been figured for differing separations of the associating segment of the lead from the air-tissue interface. Disseminated controls and initiated temperature rise conveyances have been acquired in the area encompassing the terminals. It is indicated that the

close to closeness of the air-tissue interface brings about a decrease in the initiated temperature rise.

3. Effect of realistic modeling of deep brain stimulation on the prediction of volume of activated tissue

Deep brain stimulation (DBS) is a settled treatment for Parkinson's malady, basic quake and dystonia. It has likewise been effectively applied to treat different other neurological and mental conditions including wretchedness and over the top enthusiastic issue. Various computational models, generally dependent on the Finite Element Method (FEM) approach have been proposed to examine the biophysical instruments of electromagnetic wave-tissue association during DBS. These models, in spite of the fact that stressing the significance of different electrical and mathematical boundaries, generally have utilized streamlined calculations over a firmly limited tissue volume on account of monopolar stimulation. In the current work we show that topological game plans and mathematical properties of the model significantly affect the dissemination of voltages in the concerned tissues. The outcomes uphold reexamining the current methodology for demonstrating monopolar DBS which utilizes a limited cubic region broadened a couple of centimeters around the dynamic cathode to foresee the volume of actuated tissue. We propose another strategy called multi-goal FEM displaying, which may improve the exactness of the expectation of volume of initiated tissue but be computationally manageable on PCs.

4. Concentration of the Specific Absorption Rate Around Deep Brain Stimulation Electrodes During MRI

During Magnetic Resonance Imaging (MRI), the presence of an embed, for example, a Deep Brain Stimulation (DBS) lead in a patient's body can represent a noteworthy danger. This is because of the way that the MR radiofrequency (RF) field can accomplish an extremely high quality around the DBS terminals. Consequently, the particular assimilation rate (SAR), which is relative to the square of the greatness of the RF electric field, can have an exceptionally high focus in the close field area of the terminals. The subsequent tissue warming can arrive at hazardous levels. The level of warming relies upon the degree of SAR focus. The impacts can be extreme, prompting tissue removal and brain harm, and critical security concerns emerge at whatever point a patient with an embedded DBS lead is presented to MR filtering. In this paper, SAR, electric field, and temperature rise conveyances have been found around real DBS cathodes. The greatness and spatial dissemination of the incited temperature rises are discovered to be a component of the length and structure of the lead gadget, tissue properties and the MR stimulation boundaries.

5. Phased-array near field radiometry for brain intracranial applications

During the previous a long time there has been a huge increment all through established researchers for creating strategies for understanding human brain usefulness, as determination and treatment of sicknesses and glitches, could be successfully evolved through comprehension of how the brain functions. In equal, research exertion is driven on limiting disadvantages of existing imaging strategies including possible dangers from radiation and intrusive ascribes of the imaging procedures. Towards that bearing another close to field radiometry imaging framework has been hypothetically considered, created and tentatively tried and the entirety of the previously mentioned research stages are thus introduced. The framework activity principle depends on the way that human tissues discharge chaotic warm sort radiation at temperatures over without a doubt the zero. Utilizing stage moved receiving wire exhibit framework, spatial goal, identification profundity and affectability are expanded. Joining past exploration results, just as new discoveries, the abilities of the developed framework, just as the chance of utilizing it as a correlative strategy for brain imaging are examined in this paper.

Proposed System

The image enhancement strategy is partitioned into two sections which are spatial space method and recurrence area procedure. In spatial space procedure the estimation of the pixel is changed concerning the necessity while the recurrence area strategy manages the pace of progress of pixels which are changing because of spatial space. It can't be resolved that what kind of procedure is useful for image upgrade. There are numerous procedures for image upgrade strategy out of which we have utilize ostu's technique.

PROJECT DESCRIPTION

The image enhancement procedure is partitioned into two sections which are spatial space method and recurrence area strategy. In spatial space strategy the estimation of the pixel is changed as for the prerequisite while the recurrence area method manages the pace of progress of pixels which are changing because of spatial space.

MODULES:

INPUT IMAGE:

The first step is to find an image to do the further processing. MRI is a high-quality imaging technique which produces the structure of human organ in more defined manner and useful for diagnosis of diseases and Biological Research.

PRE-PROCESSING:

Image enhancement is image pre-processing stage. The motivation behind the cycle of image upgrade is to improve the image quality for the natural eye. This cycle is likewise need to give a superior information image to additional processing, so the aftereffect of the image in the wake of processing all the stages contains less blunders.

SEGMENTATION:

We can separation or parcel the image into different parts called segmentation. It is anything but an extraordinary thought to handle the whole image simultaneously as there will be districts in the image which don't contain any data. By isolating the image into portions, we can utilize the significant fragments for processing the image. That, basically, is the means by which image division works.

FEATURE EXTRACTION:

Image feature extraction is one of the most important technique of image processing Watershed ridge and boundaries images. It uses different techniques and algorithm to isolate and detect various shapes and portions of the image. The watershed label matrix and Superimposed image. There are numerous techniques to apply this to the image. Wavelet transform is one of the tool for feature extraction. The wavelet transform has a characteristic of analyzing the image with varying unit of resolution and has multiresolution analytic property.

CLASSIFICATION:

Image processing is implemented to classify the liver cancer by training on these examples. Different network configurations are experimented with to optimize the results of cancer in the human body.

TECHNIQUE USED OR ALGORITHM USED

Otsu's method

It convert grey scale image into binary image. It assumes that the image contain two level of pixel which are foreground pixel and background pixel (bi-modal histogram). It calculates the optimum threshold by separating two classes. The result gives minimum combined-spread and maximum inter-class variance.

SNAPSHOTS:

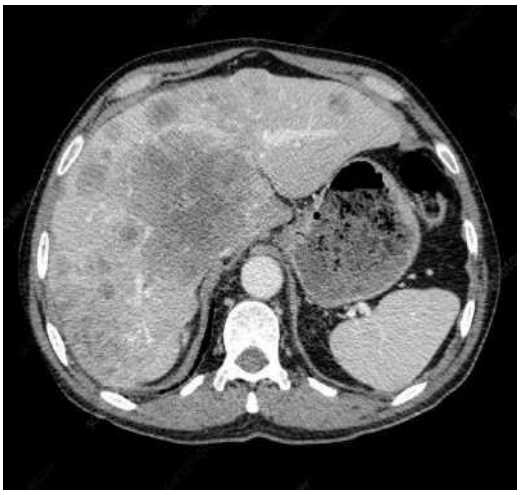

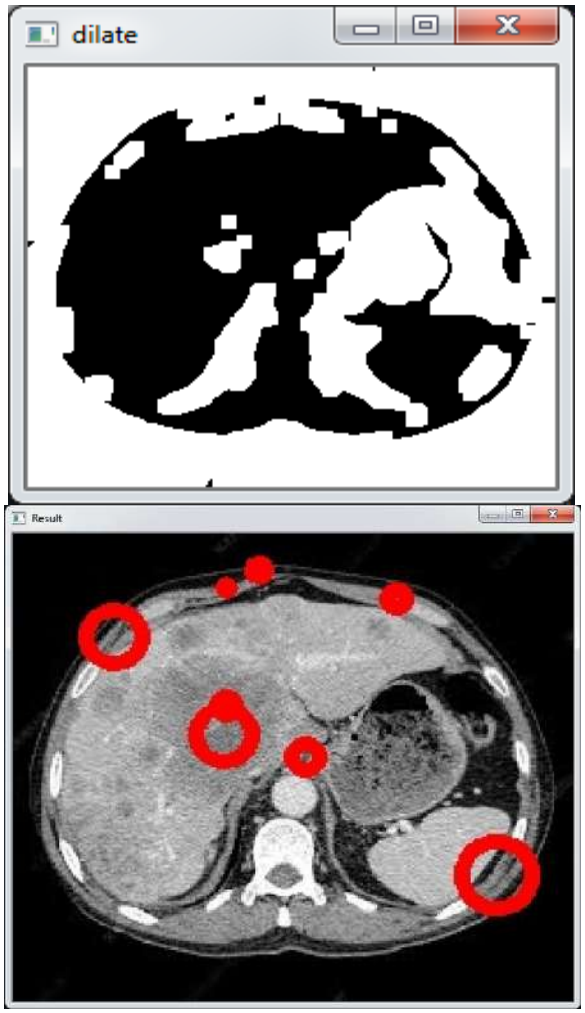

CONCLUSION

Diverse MRI Images where obtained from the web, fundamental Ostu preprocessing strategy was utilized, for division Marker-Controlled Watershed Segmentation was utilized and it was seen that for a couple of images' divisions was done accurately, so our future works incorporates making a GUI and empowering a solitary snap highlight extraction utilizing wavelet change, with the precision.

REFERENCES

[1] Zhang, Y., L. Wu, and S. Wang, "Magnetic resonance brain image classification by an improved artificial bee colony algorithm," Progress In Electromagnetics Research, Vol. 116, 65–79, 2011.

[2] Mohsin, S. A., N. M. Sheikh, and U. Saeed, "MRI induced heating of deep brain stimulation leads: Effect of the air-tissue interface," Progress In Electromagnetics Research, Vol. 83, 81–91, 2008.

[3] Golestanirad, L., A. P. Izquierdo, S. J. Graham, J. R. Mosig, and C.Pollo, "Effect of realistic modeling of deep brain stimulation on the prediction of volume of activated tissue," Progress In Electromagnetics Research, Vol. 126, 1–16, 2012.

[4] Mohsin, S. A., "Concentration of the specific absorption rate around deep brain stimulation electrodes during MRI," Progress In Electromagnetics Research, Vol. 121, 469–484, 2011.

[5] Oikonomou, A., I. S. Karanasiou, and N. K. Uzunoglu,"Phasedarray near field radiometry for brain intracranial applications," Progress In Electromagnetics Research, Vol. 109, 345–360, 2010.

[6] Scapaticci, R., L. Di Donato, I. Catapano, and L. Crocco, "A feasibility study on microwave imaging for brain stroke monitoring," Progress In Electromagnetics Research B, Vol. 40, 305–324, 2012.

[7] Asimakis, N. P., I. S. Karanasiou, P. K. Gkonis, and N. K. Uzunoglu, "Theoretical analysis of a passive acoustic brain monitoring system," Progress In Electromagnetics Research B, Vol. 23, 165–180, 2010.

[8] Chaturvedi, C. M., V. P. Singh, P. Singh, P. Basu, M. Singaravel, R. K. Shukla, A. Dhawan, A. K. Pati, R. K. Gangwar, and S. P. Singh."2.45GHz (CW) microwave irradiation alters circadian organization, spatial memory, DNA structure in the brain cells and blood cell counts of male mice, mus musculus," Progress In Electromagnetics Research B, Vol. 29, 23–42, 2011.

[9] Emin Tagluk, M., M. Akin, and N. Sezgin, "Classification of sleep apnea by using wavelet transform and artificial neural networks," Expert Systems with Applications, Vol. 37, No. 2, 1600–1607, 2010.

AN EFFECTIVE MOISTURE CONTROL BASED MODERNIRRIGATION SYSTEM (MIS) WITH ARDUINO

[1]Mohammed Ismail Sharief, [2]MdFurkhanuddin
[1]PG Scholar, Department of Electronics and Communication Engineering,
[2]Assistant Professor, Department of Electronics and Communication Engineering,
Nawab Shah Alam Khan College of Engineering & Technology, Hyderabad

ABSTRACT
Agriculture plays a cardinal role in India, which established during the times of Indus valley civilization. There was a GDP of 15.4% accounted in 2016 for agriculture and its associated sectors. India stands first in the agricultural sectors followed to the US and China. Agriculture needs an irrigation infrastructure, which includes major and minor canals from river bodies, groundwater stored in wells, tank storages and rainwater harvesting systems. The irrigation infrastructure improvements have helped India to improve food security, increase agricultural output and decreased dependency on rainwater. This project focused on proposing an effective moisture control based Modern Irrigation System (MIS) using Arduino Nano with various adjustments to the plantation. The main purpose of this project is to reduce the excess water usage, thereby saving crops from damage. There were numerous projects and prototypes for automatic irrigation using Arduino, but these projects are effective only for only one crop. The proposed system can be applied to various crops, as those crops have different moisture conditions for its growth.
Keywords—Automated, Variable, Arduino, Nano, Effective, Irrigation.

I. INTRODUCTION

An automated irrigation system is defined as the operation of the system with no human intervention or just monitoring of the system. Almost all the agricultural systems can be made automatic with the help of sensors, timers, relays, and tiny controller chip. The automated process makes the irrigation more effective and efficient, thus helping the farmers to focus on other farming activities. The advantages of these automated irrigation systems are manual operation of water operation such as opening and closing values, easy to change the frequency of irrigation process, increased and efficient use of water from various sources, water evaporation can be minimized by
Operating at night and operation can be done only when needed, thus saving energy. On the other hand, setting up these systems can be more expensive and tedious.

II. RELATED WORK

This section briefly discusses the related works carried on the automated irrigation system, its advantages, and disadvantages. J. Galindo [2] proposed an optimal use of energy and water in the modern irrigation system, the project proposed a twolayer approach, where each layer focuses on strategies to deliver water to the irrigation system. The proposed system only focuses on the water delivery to the plantation but doesn't focus on the moisture controlled irrigation system. Earl Vories[3] investigated the various irrigation scheduling for rice paddy, where a variable rate based system is used to determine the total irrigation of rice for an area. A. Pawlowski [4] evaluated an event based irrigation system using tomato crop, where an event-based technique is used to reduce the usage of water with improved efficiency. Jonathan M et al [5] developed an iterative-integrated model with coupled water planning and crop irrigation model to test the sensitivity of crops such as corn, wheat, and rice. Won-Ho Nam et al [6] used a wireless sensor network to create an application for irrigation management, which uses RFID tags for monitoring the irrigation parameters and carrying out decisions according to it. Daniele Masseroni et al [7] evaluated the performance of an automated irrigation system in Europe for paddy irrigation for the parameters such as hydraulics, control, and economics with its sustainable investment for the farmers. Hongjun Li [8] proposed a web-based irrigation system with decision support, which identifies a suitable area for irrigation with its water necessity. The proposed system can be deployed in internet and farmers can take decisions according to the area of plantation. AmarendraGoap [9] proposed an IoT based automated irrigation system with a machine learning approach to providean appropriate irrigation plan by soil moisture prediction. The approaches discussed are applicable only for a single type of crop, but it is not adapted to the variable type such as rice, corn, and raisins on a common plantation region.

III. DESIGN AND IMPLEMENTATION

There are numerous ways for establishing an automated irrigation system using microcontrollers, which includes a solar powered irrigation system, GSM-based irrigation system, and soil moisture-based irrigation system, but the main problem of these irrigation systems is that they focus on only one crop at a time, but when the farmer needs to plant another crop in the same region, the irrigation system will not be effective.

This project focuses on modifying the moisture content parameters according to the crop they plant.

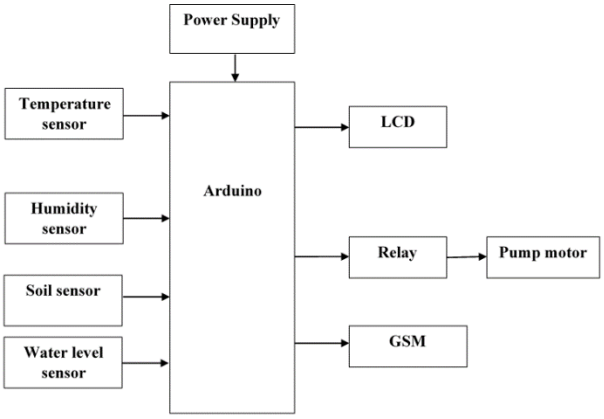

POWER SUPPLY

The power supply section is the section which provide +5V for the components to work. IC LM7805 is used for providing a constant power of +5V.The ac voltage, typically 220V, is connected to a transformer, which steps down that ac voltage down to the level of the desired dc output. A diode rectifier then provides a full-wave rectified voltage that is initially filtered by a simple capacitor filter to produce a dc voltage. This resulting dc voltage usually has some ripple or ac voltage variation.A regulator circuit removes the ripples and also retains the same dc value even if the input dc voltage varies, or the load connected to the output dc voltage changes. This voltage regulation is usually obtained using one of the popular voltage regulator IC units.

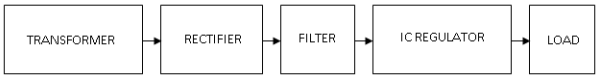

Block Diagram of Power Supply

ARDUINO UNO

Arduino/genuino Uno is a microcontroller board based on the atmega328p (datasheet). It has 14 digital input/output pins (of which 6 can be used as pwm outputs), 6 analog inputs, a 16 MHz quartz crystal, a usb connection, a power jack, an icsp header and a reset button. It contains everything needed to support the microcontroller; simply connect it to a computer with a usb cable or power it with a ac-to-dc adapter or battery to get started.. You can tinker with your uno without worrying too much about doing something wrong, worst case scenario you can replace the chip for a few dollars and start over again.

"Uno" means one in Italian and was chosen to mark the release of Arduino software (ide) 1.0. The uno board and version 1.0 of Arduino software (ide) were the reference versions of Arduino, now evolved to newer releases. The uno board is the first in a series of usb Arduino boards, and the reference model for the Arduino platform; for an extensive list of current, past or outdated boards see the Arduino index of boards.

TECHNICAL SPECIFICATIONS

Microcontroller	ATmega328P
Operating Voltage	5V
Input Voltage (recommended)	7-12V
Input Voltage (limit)	6-20V
Digital I/O Pins	14 (of which 6 provide PWM output)
PWM Digital I/O Pins	6
Analog Input Pins	6
DC Current per I/O Pin	20 mA
DC Current for 3.3V Pin	50 mA
Flash Memory	32 KB (ATmega328P) of which 0.5 KB used by bootloader
SRAM	2 KB (ATmega328P)
EEPROM	1 KB (ATmega328P)
Clock Speed	16 MHz
LED_BUILTIN	13
Length	68.6 mm
Width	53.4 mm
Weight	25 g

LIQUID CRYSTAL DISPLAY (LCD)

- LCD (Liquid Crystal Display) screen is an electronic display module and find a wide range of applications. A 16x2 LCD display is very basic module and is very commonly used in various devices and circuits. These modules are preferred over seven segments and other multi segment LEDs. The reasons being: LCDs are economical; easily programmable; have no limitation of displaying special & even custom characters (unlike in seven segments), animations and so on.
- A **16x2 LCD** means it can display 16 characters per line and there are 2 such lines. In this LCD each character is displayed in 5x7 pixel matrix. This LCD has two registers, namely, Command and Data.
- The command register stores the command instructions given to the LCD. A command is an instruction given to LCD to do a predefined task like

initializing it, clearing its screen, setting the cursor position, controlling display etc. The data register stores the data to be displayed on the LCD. The data is the ASCII value of the character to be displayed on the LCD.

Fig. 16x2 LCD

HUMIDITY SENSOR

HR202 humidity Sensor resistance use the organic polymer materials, is a new type of humidity sensor, a sense of the wet range, long-term performance and stability, can be applied to warehousing, car, indoor air quality control, building automation, medical, industrial control systems and research fields a wide range of applications.

Technical parameters:

- Parameters: (at 1kHz) Unit: Ohm
- Operating range: 20 ... 95% RH 0 ... 60
- Supply voltage: 1.5V AC (Max sine wave)
- Frequency: 500Hz ... 2kHz
- Rated power: 0.2mW (Max sine wave)
- Central value: (at25 1kHz 1V AC 60% RH sine wave) 31.0kΩ
- Resistance range: (at25 1kHz 1V AC 60% RH sine wave) 19.8 ... 50.2kΩ
- Humidity detection accuracy : ± 5% RH

Application:

- Account for temperature and humidity display, temperature and humidity gift table, atmospheric environmental monitoring, industrial process control, agriculture, instrumentation and other applications

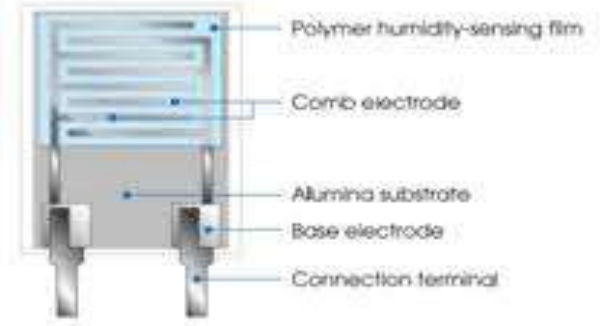

Temperature sensor

Temperature is the most-measured process variable in industrial automation.Most commonly, a temperature sensor is used to convert temperature value to an electrical value. Temperature Sensors are the key to read temperatures correctly and to control temperature in industrials applications.

A large distinction can be made between temperature sensor types. Sensors differ a lot in properties such as contact-way, temperature range, calibrating method and sensing element. The temperature sensors contain a sensing element enclosed in housings of plastic or metal. With the help of conditioning circuits, the sensor will reflect the change of environmental temperature.

Pin Definition

The definition of gray-scale sensor pin is

1. Signal Output
2. GND
3. Power

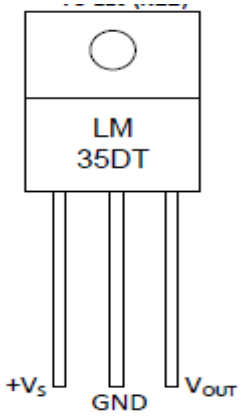

Features Of Temperature Sensor

- Calibrated directly in Celsius (centigrade)
- 0.5^0 C Ensured accuracy (at $+25^0$ C)
- Suitable for remote applications
- Operate from 4 to 30 V
- Low cost due to wafer-level trimming

Specifications

- Type: Analog
- Sensitivity: 10mV per degree Celsius
- Functional range: 0 degree Celsius to 100 degree Celsius.

GLOBAL SYSTEM FOR MOBILE

Global System for Mobile Communications (GSM) modems are specialized types of modems that operate over subscription based wireless networks, similar to a mobile phone. A GSM modem accepts a Subscriber Identity Module (SIM) card, and basically acts like a mobile phone for a computer. Such a modem can even be a dedicated mobile phone that the computer uses for GSM network capabilities.

Traditional modems are attached to computers to allow dial-up connections to other computer systems. A GSM modem operates in a similar fashion, except that it sends and receives data through radio waves rather than a telephone line. This type of modem may be an external device connected via a Universal Serial Bus (USB) cable or a serial cable. More commonly, however, it is a small device that plugs directly into the USB port or card slot on a computer or laptop.

It is widely used mobile communication system in the world. GSM is an open and digital cellular technology used for transmitting mobile voice and data services operates at the 850MHz, 900MHz, 1800MHz and 1900MHz frequency bands.

Features

- Improved spectrum efficiency
- International roaming
- Compatibility with integrated services digital network (ISDN)
- Support for new services.
- SIM phonebook management
- Fixed dialing number (FDN)
- Real time clock with alarm management
- High-quality speech
- Uses encryption to make phone calls more secure
- Short message service (SMS)

RELAY

A relay is an electromechanical switch, which perform ON and OFF operations without any human interaction. General representation of double contact relay is shown in fig. Relays are used where it is necessary to control a circuit by a low-power signal (with complete electrical isolation between control and controlled circuits), or where several circuits must be controlled by one signal.

Generally, the relay consists a inductor coil, a spring (not shown in the figure), Swing terminal, and two high power contacts named as normally closed (NC) and normally opened (NO). Relay uses an Electromagnet to move swing terminal between two contacts (NO and NC). When there is no power applied to the inductor coil (Relay is OFF), the spring holds the swing terminal is attached to NC contact.

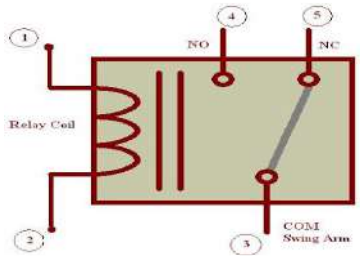

Fig. Representation of Relay

Whenever required power is applied to the inductor coil, the current flowing through the coil generates a magnetic field which is helpful to move the swing terminal and attached it to the normally open (NO) contact. Again when power is OFF, the spring restores the swing terminal position to NC.

SOIL MOISTURE SENSOR

This can be used to monitor the moisture level in the crop. It is based on Ohm's law and uses resistance between the poles in order to calculate the moisture of the soil.

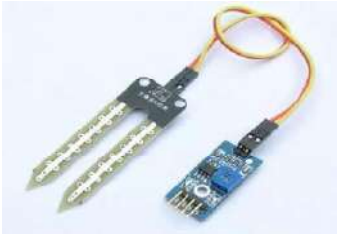

SOIL MOISTURE SENSOR

ULN2003: -

The ULN2003 is a monolithic IC consists of seven NPN Darlington transistor pairs with high voltage and current capability. It is commonly used for applications such as relay drivers, motor, display drivers, led lamp drivers, logic buffers, line drivers, hammer drivers and other high voltage current applications. It consists of common cathode clamp diodes for each NPN Darlington pair which makes this driver IC useful for switching inductive loads.

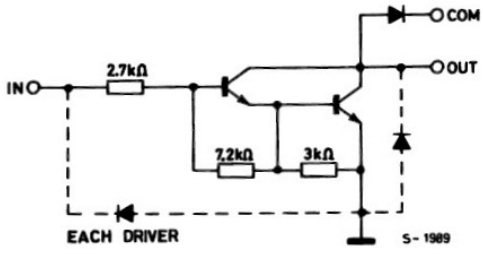

The output of the driver is open collector and the collector current rating of each Darlington pair is 500mA. Darlington pairs may be paralleled if higher current is required. The driver IC also consists of a 2.7KΩ base resistor for each Darlington pair. Thus each

Darlington pair can be operated directly with TTL or 5V CMOS devices. This driver IC can be used for high voltage applications up to 50V.

SUBMERSIBLE WATER PUMP

Description:

This submersible pump is designed for reliability and ultra-quiet operation to provide years of service. The small profile size makes the pump easy to hide or disguise. Has adjustable flow and is easy to clean. This submersible water pump is great for aquarium, fountains, spout and hydroponic systems.

Working Principle:

It is often used as a booster pump for home water pressure. It can be completely submerged into the fluid and the motor is hermetically sealed. The motor is close-coupled to the body of the water booster pump. It pumps the water to the surface by energy conversion that works in a cycle. The rotary energy is converted into kinetic energy that is further converted into pressure energy.

The submersible pump works by pulling the fluid towards itself. During the intake, the rotating impeller pushes the fluid through the diffuser. From there, the fluid goes to the surface. The submersible pumps are self-priming as they are already submerged in the fluid. Cavitation is never an issue and they are also quiet because they work underwater.

FEATURES:

- Adjustable water flow rate
- Suction cup mounting feet for either vertical or horizontal mounting
- Contains no seals or messy oils
- Good for both fresh water and salt water

SPECIFICATION:

- Max Flow Rate: 20L/H
- H-Max (Lift height): 1.6 feet
- Power: 6-18 Watt
- Voltage: 110 – 120/230 V @ 50 Hz
- Outlet: Fits 0.315" ID (inside diameter) tubing

IV. RESULTS

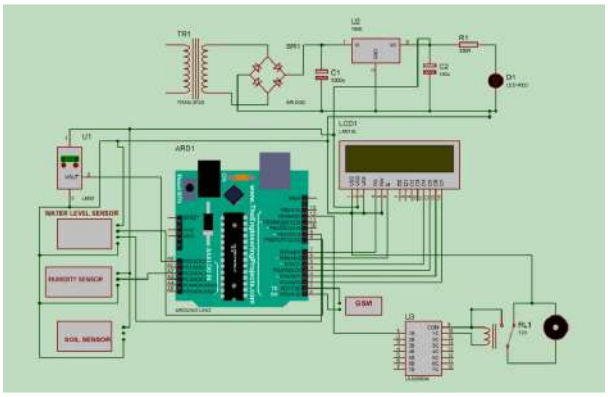

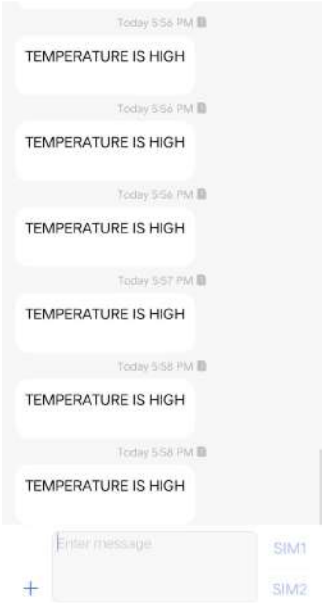

V. CONCLUSION

A Modern Irrigation System (MIS) is proposed in this paper, which supports multiple operations of crops, which is not supported by the existing automated irrigation systems, this also helps the farmers to save the energy wasted unnecessarily. Since it is an automated process, it doesn't require any intervention of the farmers other than monitoring the automated system.

REFERENCES

[1] "India outranks US, China with world's highest net cropland area". Retrieved 17 November 2018

[2] J. Galindo, S. Torok, F. Salguero, S. de Campos, J. Romera, V. Puig, Optimal Management of Water and Energy in Irrigation Systems: Application to the Bardenas Canal, IFAC-PapersOnLine, Volume 50, Issue 1, 2017, Pages 6613-6618.

[3] Earl Vories, William (Gene) Stevens, Matthew Rhine, Zachary Straatmann, Investigating irrigation scheduling for rice using variable rate irrigation, Agricultural Water Management, Volume 179, 2017, Pages 314- 323.

[4] A. Pawlowski, J.A. Sanchez-Molina, J.L. Guzman, F. Rodraguez, S. Dormido, Evaluation of event-based irrigation system control scheme for tomato crops in greenhouses, Agricultural Water Management, Volume 183, 2017, Pages 16-25.

[5] Jonathan M. Winter, Charles A. Young, Vishal K. Mehta, Alex C. Ruane, MarziehAzarderakhsh, Aaron Davitt, Kyle McDonald, Van R. Haden, Cynthia Rosenzweig, Integrating water supply constraints into irrigated agricultural simulations of California, Environmental Modelling & Software, Volume 96, 2017, Pages 335-346.

[6] Won-Ho Nam, Taegon Kim, Eun-Mi Hong, Jin-Yong Choi, Jin-Taek Kim, A Wireless Sensor Network (WSN) application for irrigation facilities management based on Information and Communication Technologies (ICTs), Computers and Electronics in Agriculture, Volume 143, 2017, Pages 185-192.

[7] Daniele Masseroni, Peter Moller, Reece Tyrell, Marco Romani, Alberto Lasagna, Guido Sali, Arianna Facchi, Claudio Gandolfi, Evaluating performances of the first automatic system for paddy irrigation in Europe, Agricultural Water Management, Volume 201, 2018, Pages 58-69.

[8] Hongjun Li, Jiazhen Li, YanjunShen, Xiying Zhang, Yuping Lei, Webbased irrigation decision support system with limited inputs for farmers, Agricultural Water Management, Volume 210, 2018, Pages 279-285.

[9] AmarendraGoap, Deepak Sharma, A.K. Shukla, C. Rama Krishna, An IoT based smart irrigation management system using Machine learning and open source technologies, Computers and Electronics in Agriculture, Volume 155, 2018, Pages 41-49.

[10] https://www.arduino.cc

[11] WojciechSkierucha, AndrzeWilczek, A FDR Sensor for Measuring Complex Soil Dielectric Permittivity in the 10–500 MHz Frequency Range, Sensors, 10, 3314-3329, 2010.

[12] Will, Bianca. "Time domain transmission sensors for soil moisture measurements." In Telecommunications Forum (TELFOR), 2011 19th, pp. 16-19. IEEE, 2011.

[13] Visvalingam, M.; Tandy, J. D, The Neutron Method For Measuring Soil Moisture Content-A Review, Journal of Soil Science. 23 (4): 499–511, 1972.

[14] Precision Farming Tools: Soil Electrical Conductivity" (PDF). Retrieved Jun 12, 2016.

AUTHOR'S PROFILE

Mr. MOHAMMED ISMAIL SHARIEF has completed his B.Tech (ECE) fromDR. Y.S.R. Anu College Of Engineering&TechnologyAcharya Nagarjuna University, Guntur. Presently, he is pursuing his Masters inEmbedded System from Nawab Shah Alam khan College of Engineering & Technology,Malakpet Hyderabad TS India

Mr. MD FURKHANUDDIN has completed B.E. (ECE) from Guru Nanak DevEngineering College Bidar Karnataka Visvesvaraya Technological University,Belgaum, M.Tech (EC) from SirVisvesvaraya TechnologicalUniversity, Belgaum currently he is working as an Assistant Professor of ECE Department inNawab Shah Alam khan College of Engineering & Technology, Malakpet Hyderabad TSIndia

DEEP LEARNING BASED ATTACK ON SOCIAL AUTHENTICATION SYSTEM

[1]Syed Abid Hasan,[2]Mohammed Abdul Rawoof, [3]Mohammed Khaleel Ahmed
[1]PG scholar, Department of CSE, NSAKCET, Hyderabad.
[2,3]Assoc Professor, Department of CSE,NSAKCET, Hyderabad

ABSTRACT

As the fast advancement of the Internet, informal communities' destinations, for example, Twitter and Facebook, are gotten increasingly mainstream. These destinations expect clients to give different sorts of individual information to customize their administrations. Be that as it may, accidentally revealed individual information used by programmers may present numerous security issues. In this paper, we present a deep learning put together assault with respect to the social validation in the Facebook site. Social verification, known as the fourth factor confirmation, uses social connection information to accomplish the distinguishing proof of clients. During the time spent record recuperation and distant login, the social validation which expects clients to recognize names of companions showed in photographs is utilized as a piece of the confirmation module. Subsequent to gathering public information of companions' photographs through web crawler, the connect framework utilizes deep learning networks dependent on face recognition library and convolutional neural network (CNN for short) to prepare the model. The assault is accomplished through the fruitful ID of companions' names utilizing the prepared deep learning model.

INTRODUCTION

There are two kinds of social affirmation: trustee based social check and information based social approval. In the trustee based social approval, customers show social accreditations given by trustees to exhibit the social development happened among them and to be affirmed.

OBJECTIVE

The principal objective this venture to give security to the informal communities from the assailants. By that giving security to the client.

EXISTING SYSTEM:

The informal organization is dispersed across different PC organizations. The informal communities are naturally PC organizations, connecting individuals, association, and information.A long-range relational correspondence organization (in like manner informal correspondence site or electronic media) is an online stage which people use to amass informal associations or social relationship with other people who share equivalent individual or calling interests, activities, establishments or real affiliations.

Disadvantages:

- LessSecure
- Easy to accessinformation

PROPOSEDSYSTEM

A convolutional neural organization (CNN, or ConvNet) is a class of profound neural organizations, most by and large applied to inspecting visual imagery.

Multilayer perceptron's generally speaking imply totally related organizations, that is, each neuron in one layer is related with all neurons in the accompanying layer.

However, CNNs receive a substitute system towards regularization: they abuse the different leveled plan in data and gather more unpredictable models using more humble and less perplexing models

Advantages

- Security using face recognition
- Local spatialcoherence

LITERATURE SURVEY:

With a ultimate objective to agitate aggressors from dealing customer accounts, Facebook dispatched a kind of two-factor check called social approval (SA), where customers are expected to recognize photos of their allies to complete a sign in undertaking. Late assessment, in any case, demonstrated that attackers can evade the framework by using face affirmation programming. Here we show an elective attack that uses picture assessment methodologies to recognize the SA photos inside a detached arrangement of the customers' photos. In this paper, we re-visitation of the possibility of SA and plan a system with a novel photo assurance and change measure, which makes troubles that are generous against these attacks. The impulse behind our photo assurance is to use photos that bomb programming-based face affirmation, while remaining undeniable to individuals who think about the depicted people. The photo change measure makes challenges as photo courses of action, where faces are changed to convey picture planning procedures incapable. We probably certify the strength of our strategy against three format planning counts that tackle 0.4% of the challenges, while requiring four critical degrees moreover getting ready effort. Additionally, when the progressions are applied, face revelation programming fails to recognize even a lone face.

Two-factor check is for the most part used by high-regard organizations to shield adversaries from dealing accounts using taken confirmations. Facebook has actually conveyed a two-factor affirmation framework, suggested as Social Authentication, which anticipates that customers should recognize a bit of their associates in indiscriminately picked photos. Another report has given an appropriate assessment of social

check shortcomings against aggressors inside the loss' gatherings of companions. In this paper, we expand the risk model and study the attack surface of social approval eventually, and show how any aggressor can get the information expected to handle the troubles presented by Facebook. We execute a proof-of-thought system that utilizes commonly open face affirmation programming and cloud benefits, and evaluate it using real open information assembled from Facebook. Under the doubts of Facebook's threat model, our results show that an aggressor can get induction to (sensitive) information for in any occasion 42% of a customer's buddies that Facebook uses to make social approval challenges. By depending entirely on openly open data, an easygoing aggressor can settle 22% of the social verification tests in a computerized style, and gain a huge preferred position for an extra 56% of the tests, instead of simply speculating. Also, we mimic the situation of a decided assailant putting himself inside the casualty's group of friends by utilizing sham records. For this situation, the exactness of our assault significantly increments and arrives at 100% when 120 countenances for each companion are available by the aggressor, despite the fact that it is exceptionally precise with as meager as 10 appearances.

Pieces of tattle and defamation are by and by transforming into a key risk to Online Social Networks (OSNs). To forestall them, Real Name System (RNS) was proposed, anyway has been exhibited exposed by the information spillage in South Korea. In this paper, we propose another character model, Social Authentication Identity (SAI), to follow tattle makers. In SAI, only couple of customers (called roots) are should have been approved by RNS. Additionally, the others are approved by vouching of partners, called social confirmation. We evaluate factors that impact the profitability of SAI. Results show that picking sets up in networks are the best methodology, differentiating and subjective and most outrageous degree strategies. We furthermore give a social after framework to follow down tattle makes. Examination shows our social after is satisfactorily ground-breaking to shield Sybil attacks.

Affirmation is a critical strategy to guarantee security. Many web applications, for instance, adaptable banking, messages, electronic shopping anticipate that customers should give their affirmations to affirm themselves before they can use the organizations. Four parts, including mystery state, token, biometrics, relational associations, have been proposed for confirmation. Regardless, the proposed check plans of the four factors all experience the evil impacts of different shortcomings. In this paper, we propose an amazed social approval structure. Our examination shows that the design is impressively more remarkable than the current approaches. Even more fundamentally, we limit the potential security disclosure of customers during the confirmation strategy. We present our framework, lead execution assessment and diverse security attack examination.

We propose a significant convolutional neural association plan codenamed "Commencement", which was at risk for setting the new forefront for request and revelation in the ImageNet Large-Scale Visual Recognition Challenge 2014 (ILSVRC 2014). The standard indication of this designing is the improved utilization of the figuring resources inside the association. This was cultivated by a meticulously made arrangement that considers extending the significance and width of the association while keeping the computational spending consistent. To propel quality, the primary decisions relied upon the Hebbian standard and the intuition of multi-scale getting ready. One explicit appearance used in our convenience for ILSVRC 2014 is called Google Net, a 22 layers significant association, the idea of which is assessed with respect to request and revelation.

MODULES NAME:

1. User InterfaceDesign
2. User
3. Make aFriend
4. Authentication
5. PostData

User InterfaceDesign

In this module we plan the windows for the endeavor. These windows are used for secure login for all customers. To connect with specialist customer should give their username and secret phrase then nobody yet they can prepare to interface the laborer. If the customer as of now exits straightforwardly can login into the laborer else customer should enroll their nuances, for instance, username, secret word and Email id, into the specialist. Specialist will make the record for the entire customer to keep up exchange and download rate. Name will be set as customer id. Marking in is by and large used to enter a specific page.

User

In this module customer will enroll and login. By then customer needs to find the person who is open in the image then customer will go to point of arrival. Later customer can post the records and customer will see the nuances of associates. Customer can see the posts of various customers.

Make aFriend

In this module customer will login and a short time later search for partners. By then customer will make requesting to those customers. Besides, customer can see the buddy requests which are went to his/her. By then customer can may insist or excuse the requesting. Later customer can visit with those customers who are as of now allies to that customer.

Authentication

In this module customer affirmation will done after customer login to the application. From the outset system will take all the records that customer shared. By then structure will require short the photos which have the person in the image. The image will cloud the face and customer needs to find the person who is available in the image. By then the approval will complete if customer find the right name of the person.

PostData

In this module customer login first, by then customer can post the reports like pictures, records and doc archives. By then customer can see the friend's posts. Likewise, customer can download the records. Customer can send the messages to the colleagues

TECHNIQUE USED OR ALGORITHMUSED

CNN model

- A convolutional neural organization (CNN, or ConvNet) is a class of profound neural organizations, most by and large applied to inspecting visual imagery.
- Multilayer perceptron's generally speaking imply totally related organizations, that is, each neuron in one layer is related with all neurons in the accompanying layer.
- However, CNNs receive a substitute system towards regularization: they abuse the different leveled plan in data and gather more unpredictable models using more humble and less perplexing models.

SYSTEM ARCHITECTURE

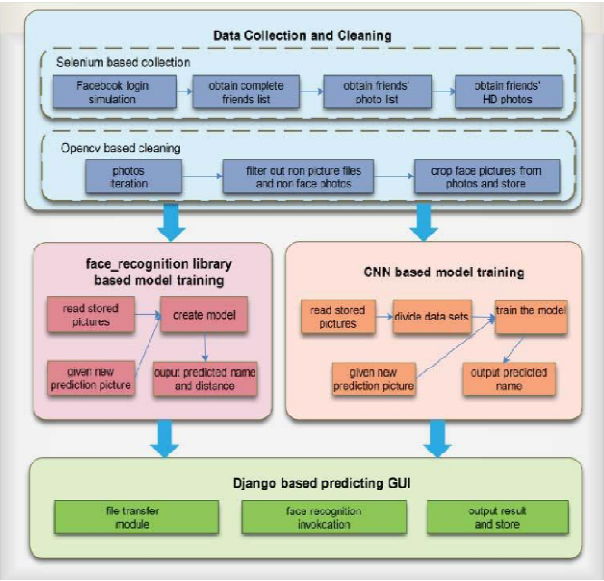

Fig 4.12: System Architecture

SNAPSHOTS

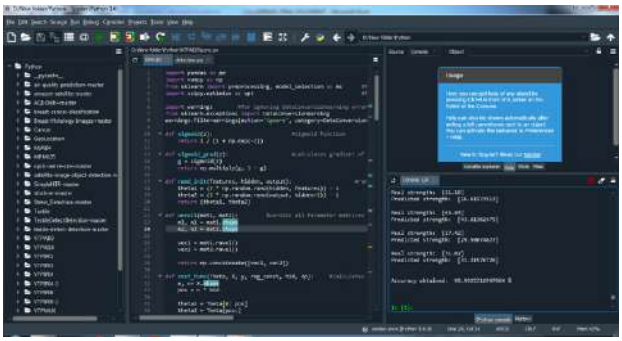

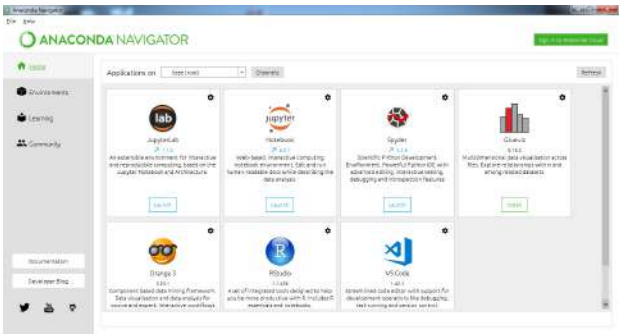

CONCLUSION

Social validation is considered as the new fourth sort of confirmation way. Information based social confirmation is utilized in the biggest interpersonal organization site, Facebook, during the time spent password recuperation and far off login. A profound learning innovation-based assault framework is developed to pass the Facebook's social confirmation. Using selenium library, the framework initially recreates human client's activity to acquire top notch photographs of client's companions. Target face photographs at that point was sifted through and stored by utilizing OpenCV library

FUTURE ENHANCEMENT

Face affirmation library and R-CNN headways are both used to plan show and envision target name freely. Finally, evaluation results show that foreseen results subject to both arranged model can complete the social affirmation appraisal of Facebook.

REFERENCES

[1] Facebook's Trusted Contacts. goo.gl/xHmVHA, 2013.

[2] Facebook's Trusted Friends. goo.gl/KdyYXJ, 2011.

[3] Brainard, J., Juels, A., Rivest, R.L., Szydlo, M. and Yung, M., Fourthfactor authentication: somebody you know. in ACM conference on computer and communications security, (2006), 168-178.

[4] Cooperband, J. Two-factor Authentication, 2015.

[5] Frankel, A.D. and Maheswaran, M., Feasibility of a socially aware authentication scheme. in Consumer Communications and Networking Conference, 2009. CCNC 2009. 6th IEEE, (2009), IEEE, 1-6.

[6] Polakis, I., Ilia, P., Maggi, F., Lancini, M., Kontaxis, G., Zanero, S., Ioannidis, S. and Keromytis, A.D. Faces in the Distorting Mirror: Revisiting Photo-based Social Authentication 21st ACM Conference on Computer and Communications Security (CCS), Arizona, USA, 2014.

[7] Polakis, I., Lancini, M., Kontaxis, G., Maggi, F., Ioannidis, S., Keromytis, A.D. and Zanero, S., All your face are belong to us: breaking Facebook's social authentication. in Proceedings of the 28th Annual Computer Security Applications Conference, (2012), ACM, 399-408.

[8]Rice, A. A Continued Commitment to Security. https://m.facebook.com/notes/facebook/a-continued-commitment-tosecurity/486790652130/ https://www.facebook.com/notes/facebook/acontinued-commitment-to-security/486790652130, 2011.

[9] Schechter, S., Egelman, S. and Reeder, R.W., It's Not What You Know, But Who You Know. in Proceedings of the 27th ACM SIGCHI Conference on Human Factors in Computing Systems (CHI), (2009), 172.

COMPARATIVE STUDY OF R.C.C AND COMPOSITE MULTI STOREYED BUILDING WITH AND WITHOUT TUNED MASS DAMPER

[1]Dr S.Amaresh Babu, [2]Mohd Huzaifa Yaman, [3]Mohammed Mohiuddin Umair,
[1]Professor and Head, Department of Civil Engineering,
[2]Associate Professor, Department of Structural Engineering,
[3]M.Tech Scholar, Department of Structural Engineering,
Nawab Shah Alam Khan College of Engineering & Technology, Hyderabad

ABSTRACT:

In India reinforced concrete structures are mostly used since this is the most convenient and economic system for low-rise buildings. However, for medium to high-rise buildings this type of structure is no longer efficient. Use of composite material is of particular interest, due to its significant potential in improving the overall performance by making modest changes in manufacturing and constructional technologies. Steel-concrete composite columns are extensively used in modern buildings. Extensive researches on composite columns in which structural steel section are encased in concrete have been carried out. In-filled composite columns, however have received limited attention compared to encased columns. The recent development in the computer applications has helped the structural engineering field significantly. The Non-Linear Time History Analysis (NL-THA) of seismic evaluation of a structure is precise, exact and highly accurate when compared to the other non-linear static and dynamic procedures.

Research has also been undergone to develop techniques that control the seismic response of the structures. Such techniques include use of energy dissipation devices like dampers and base isolation techniques. The present study is on the Non-linear time history analysis comparing the effects of energy dissipation device, tuned mass damper at mid storey for high-rise symmetric building. The frame considered was loaded with gravity loads (dead load & live load) and Bhuj earth quake loading and is modelled and then Non-Linear Time History Analysis (NLTHA) was performed. The analysis engine used for the analysis and design is SAP 2000 version 19. In the study, displacement and base shear of the structure was studied without tuned mass damper and the results obtained were compared with those obtained from the structure with seismic control device. So, it is also necessary to enhance the seismic performance of composite buildings by using seismic control techniques. So, in the present study an attempt will be made to control the seismic response of the structure using Tuned mass damper. Since non-linear modal time history analysis (non–linearity only when link elements are used) was fast and sufficiently accurate analysis when compared to non-linear direct integration, the former method was adopted for structures with tuned mass dampers.

The results illustrated the significant reduction of 18% inthe base shear and decrement in displacement by 35%in Composite structure compared to RCC and reduction in base shear as well as displacement was observed when Tuned mass damper was used. It was also seen that there was a reduction in weight of the structure by 45% when composite structure was replaced with RCC.

Key Words: Tuned Mass Damper, Dynamic analysis and Non-linear time history analysis

1. INTRODUCTION

An earthquake is an involuntary movement of the Crust of the earth, the origin of which usually is on the surface or below it. Here, the term 'natural' is adopted as it removes shock waves generated by nuclear tests, human-made blasts, etc. The Crust is made of plates. The junction between the two plates is known as a fault. In the Indian context, the primary border fault is this fault, stretching from the west through Uttaranchal, Bihar, Assam to Burma through the terrain region and Himachal Pradesh. Through the Andaman-Nicobar Islands and the Bay of Bengal, this plate descends and enters Indonesia. When plates move, the rocks feel stress. Through this process, a crack happens, and this is finally called an earthquake. Earthquakes are a natural hazard that is sometimes unforeseeable, like many other natural hazards, rendering it impossible to preserve property and life through engineering. The seismic reliability of the building environment must be developed by designing numerous analytical methods to solve these problems triggered by an earthquake, which will ensure that buildings survive occasional small earthquakes and provide sufficient caution if significant earthquake events are experienced. This will significantly add to savings of life and land. Specific seismic architecture codes are usable and are being updated over time in nearly all countries. Depending on the importance and cost, the framework of the framework ranges from linear to nonlinear to measure the earthquake powers and their demand. A building's behavior depends on several factors during an earthquake, such as stiffness, sufficient lateral strength, and ductility, comfortable and natural configurations. The quake did not kill

humans, but the structures did. Therefore, it is the primary responsibility of a structural (design) engineer to build on the criteria of previous practice and consider all possible dangers to which the framework may be exposed in the future to create the structure successfully. Through the finite portion of computer technology/software, structural engineers have built techniques to boost the efficiency of systems subjected to earthquakes that model, interpret and display the results efficiently in a careful manner. Study in civil engineering has reached much broader horizons than one might have anticipated. Due to the rise in computer systems and technologies, structural engineers can save a lot of time and effort. Each seismic code emphasizes such a design that can help a framework survive a certain amount of ground acceleration and motion based on the seismic threat. When an earthquake exerts intense pressure on the structure, itis usually built to have some yield. Earthquake Engineering's motto is to reduce the loss of life and property arising from the generating systems' collapse. Several applications are available on the market that can aid with structural simulation, research, and design. The production of a network intended for a specific load and a degree of safety is critical for practicing structural/design engineers.

It may simply be concluded that the seismic architecture is a two-step operation. First, it is essential to configure all critical seismic efficiency objectives, such as serviceability considerations for life protection and collapse prevention, and an appropriate structural framework. This stage consists of the engineer's creative capacity to construct a structure that satisfies seismic efficiency objectives and considers the functional and economic limitations set by the owner, the architect, and other practitioners involved in constructing and designing a home. This development method is genuinely based on the engineer's experience, judgment, and interpretation of seismic activity instead of particular statistical formulations. To configure an effective structural system based on rudimentary awareness of ground motion and elastic and inelastic dynamic reaction characteristics, thumb rules for rigidity and strength goals should be sufficient. For the study of the structures and determining their performance under the loading offered, a range of techniques is readily accessible. The most precise of them is the nonlinear time history review. Using conventional methods known as nonlinear static methods (N.S.P.s) and linear dynamic methods, often referred to as response spectrum methods, which have been established, frameworks deemed less critical are studied. Such techniques do not produce conclusions as valid as those derived through the analysis of time history.

Today, urbanization consists of two materials that are undeniably used as a construction material for buildings ranging from skyscrapers to pavements, steel, and concrete, while both products have distinct characteristics from each other. Steel significantly resists tensile loading, but it has a lower weight ratio. Slender pieces that might be vulnerable to buckling phenomena are therefore adopted. Concrete, on the other side, is excellent at resisting compression. Steel is adopted for high-rise construction to affect ductility; on the other side, concrete can resist corrosion and serve thermal insulation.

Similarly, concrete will even regulate the buckling of steel. It is necessary to consider composite design to derive the least benefits from both materials. In composite buildings' structure, two columns, namely encased columns and concrete-filled steel tube columns, are introduced.

1.2 Reinforced Concrete

Both steel and concrete are used in tandem in reinforced cement concrete building to serve as a hybrid medium in which steel absorbs both stress and strain, while concrete can only endure compression. R.C.C. is a structural material commonly used and is used in several forms of structures.

The objective of the study has also been discussed. Chapter 2 explains the literature review, Chapter 3 explains the methodology, Chapter 4 explains the description. Chapter 5discusses the results obtained by the analysis of framed buildings using the SAP package. Finally, chapter 6 gives the summary, conclusions, and scope for future work.

2 RELATED WORK

Panchal and Marathe (2011), in their analysis, steel and concrete were contrasted with composite steel and concrete for a commercial building in an earthquake environment. An analogous static methodology is being used. For modeling of Composite, Steel, and R.C.C structures, ETABS program is used, and the findings are contrasted, and it is found that axial force in the column is decreased by 7 percent in composite structure and 46 percent in steel structure compared to R.C.C. structure, and it is also found that overall savings are around 10 percent for composite and 6-7 percent for steel structure compared to R.C.C.

Ashish Mohite and Patil (2015) evaluated buildings' seismic activity by calculating structural dampers' volume. The seismic behavior– 10, 12, 14, 16, 18, and 21 stories – with and without a tuned mass damper was tested. TMD is a type of load-bearing that reduces displacement and acceleration and can be used for seismic stabilization of structures. This research aims to reduce the drift, displacement, and shear of

buildings in the top eleven, twelve, fourteen, sixteen, eighteen, and twenty floors. It has been noticed that ambient vibration can be regulated using the structure of the TMD. For the standard building frame, 5% of TMD lowers the top story displacement by roughly 5%. The reduction in the 10 and 12 story buildings is 38 and 36, the reduction in the 14 and 16 story buildings is 35 and 33, the reduction in the 18 and 21 story buildings is 31 and 30. And ratios of binding lipids by around 2 percent.

Renavikar Aniket and Suryawanshi Yogesh's (2015) proposal would evaluate a steel-concrete structure and R.C.C. residential house. The planned layout is four buildings, each covering three floors of G+9, G+12, G+15, and G+18, at 3.0m in height. The overall construction plan dimension of the building is 15 feet by 9 feet. The material is collected, processed, and is then modeled using STAAD-Pro software. A load mixture has been analyzed according to the Indian Norm Code of Procedure. The dissertation includes the study of an analogous R.C.C. structure such that contrast of expense may be produced between an R.C.C. structure and a steel-concrete composite structure. The paper stated that, relative to the steel composite structures and composite structures, the axial force, B.M., and deflections in R.C.C. are much more considerable.

Sandipetal.(2016),Seismic waves have been studied on the earth and are transformed into dynamic loads causing the ground and the attachments to vibrate and affect structures and other structural components in a complicated way. Civil engineering continually improves ways to counter this underlying tendency. Conventional device enhancement techniques use more materials and electricity. Also, increased masses contribute to increased seismic powers. Alternative solutions, including passive control systems, successfully reduce seismic and alternative dynamic impacts on civil engineering. A tuned mass damper (TMD) is a mass system with a spring connected to the structure to minimize its dynamic reaction. It has been shown that Tuned Mass Damper (TMD), for harmonic and wind excitation structural response control, is most efficient. Base isolation is also commonly recognized as an essential technique to defend seismic excitement-prone systems. The efficiency and calibrated mass damper of the linear base isolation device to minimize seismic reaction is studied. TMD and B.I. are used effectively to manage structural vibration and are compelling instruments in defending structures from different lateral forces as wind loads and seismic impacts. At the same time, TMD decreases the movement reactions of structures with low damping ratios more effectively.

Sattainathan Sharma et al. (2016) this paper aims to compare a reinforced concrete frame and a composite material frame located in an earthquake zone of IV (20 floors + basement). Using E-TABS tools, the templates of both systems were compared. The research investigated the deflection, shear power, moment, tale drift, stiffness, and displacement of the system. To measure the seismic load, the seismic architecture criterion of the Indian norm of code for quake tolerant design of frameworks IS 1893 (PART-1): 2002 and IS-875 (PART-3) have been used. It is observed that the dead weight of composite construction ranges from 20% to 25%, less than R.C.C. structure, which tends to mitigate seismic forces from 15% to 20% greatly. The tests show that the bending moment of structures utilizing composite materials was decreased from 12% to 24%, and the stability of the composite structures was more excellent as contrasted with R.C.C. structures.

3. METHODOLOGY

3.1 Degrees of Freedom

The cumulative amount of shifts in the displacement of all masses is named the number of degrees of freedom. A small number of free-body coordinates defines Multi-degree free-body structures. A complex system's correct answer can be calculated only by measuring the inertia effects at each system particle since the system's configuration is constant for infinite degrees-of-freedom. Methods to explain such systems' configuration are restricted to operating structures with uniform material properties and regular geometry. The techniques involve a large amount of computational calculation. However, the measurement is significantly simplified by replacing the structure's total displacement with a small number of displacements and assuming the structure's entire mass is contained in some distinct points, as seen in fig. 3.1.

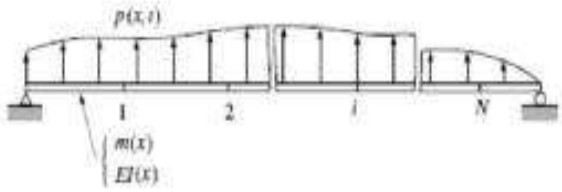

Fig 3.1: Discretization of General Beam Type Problem

By expressing the balance of the productive forces aligned with each of its degrees of freedom, the system's equation of motion can be formulated. In general, at every level I four kinds of forces would be involved: the externally imposed load pi(t) and the forces arising from the motion, i.e., inertia fIi, damping fDi, elastic fSi. The dynamic balance can

then be expressed as a dynamic equilibrium for each of the many degrees of freedom.

$$f_{D1} + f_{S1} + f_{I1} = p_1(t)$$

$$f_{D2} + f_{S2} + f_{I2} = p_2(t)$$

$$f_{D3} + f_{S3} + f_{I3} = p_3(t)$$

$$\ldots\ldots\ldots\ldots\ldots\ldots\ldots$$

$$f_{Di} + f_{Si} + f_{Ii} = p_i(t)$$

where,

$f_{Ii} = [m][\ddot{y}]$

$f_{Si} = [k][y]$

or when the force vectors are written in matrix form,

$f_{Ii} + f_{Di} + f_{Si} = p_i(t)$

$$[m][\ddot{y}] + [c][\dot{y}] + [k][y] = [p(t)] \quad (3.1)$$

3.2 SDOF Harmonic Vibration with Viscous Damping

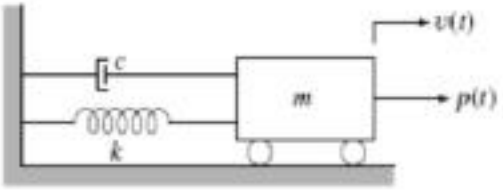

Fig 3.2: Idealised SDOF System: Basic Components

Consider a system consisting of mass (m), stiffness (k) and damping (c) as shown in fig 3.2. The single displacement coordinate $v(t)$ completely defines its position. The system is subjected to a harmonically varying load $p(t)$ of sine wave form having an amplitude p_0 and circular frequency $\bar{\omega}$ as shown by the system of equation

$$m\,\ddot{v}(t) + c\,\dot{v}(t) + k\,v(t) = p_0 \sin\bar{\omega}t$$

Dividing the above equation by m, and noting that $c/m = 2\xi\omega$ leads to

$$\ddot{v}(t) + 2\xi\omega\dot{v}(t) + \omega^2 v(t) = \frac{p_0}{m}\sin\bar{\omega}t$$

The complimentary solution of the equation is the damped free vibration response given by

$$v_c(t) = [A\cos\omega_D t + B\sin\omega_D t]e^{-\xi\omega t}$$

The particular solution is of the form

$$v_p(t) = G_1\cos\bar{\omega}t + G_2\sin\bar{\omega}t$$

Substituting the particular solution into the equation of motion and separating the multiples of $\cos\bar{\omega}t$ from the multiples of $\sin\bar{\omega}t$ leads to

$$[-G_1\bar{\omega}^2 + G_2\bar{\omega}(2\xi\omega) + G_1\omega^2]\cos\bar{\omega}t + \left[-G_2\bar{\omega}^2 - G_2\bar{\omega}(2\xi\omega) + G_2\omega^2 - \frac{p_0}{m}\right]\sin\bar{\omega}t = 0$$

In order to satisfy this equation for all the values of t, it is necessary that each of the two square bracket quantities equal zero; thus one obtains

$$G_1(1-\beta^2) + G_2(2\xi\beta) = 0$$

$$G_2(1-\beta^2) - G_1(2\xi\beta) = (p_0/k)$$

Solving these two equations simultaneously, we get

$$G_1 = \frac{p_0}{k}\left[\frac{-2\xi\beta}{(1-\beta^2)^2 + (2\xi\beta)^2}\right]$$

$$G_2 = \frac{p_0}{k}\left[\frac{1-\beta^2}{(1-\beta^2)^2 + (2\xi\beta)^2}\right]$$

β is defined as the ratio of the applied loading frequency to the natural free vibration frequency i.e., $\beta = \bar{\omega}/\omega$. Substituting the values of G_1 and G_2 in the particular solution and combining the result with the complimentary solution, the total response is obtained in the form of

$$v(t) = [A\cos\omega_d t + B\sin\omega_d t]e^{-\xi\omega t} + \frac{p_0}{k}\left[\frac{1}{(1-\beta^2)^2 + (2\xi\beta)^2}\right][(1-\beta^2)\sin\bar{\omega}t - 2\xi\beta\cos\bar{\omega}t]$$

The first term on the right-hand side of this equation represents the transient response, which damps out following $e^{-\xi\omega t}$, while the second term represents the steady-state harmonic response, which will continue indefinitely.

3.3 Tuned Mass Damper Theory for SDOF Systems

Figure 3.3 depicts an SDOF device subject to outward forced and ground motion with mass m, stiffness k, and viscous damping c. A tuned weight damper is mounted to the primary mass with mass md and rigidity kd and viscous damping CD. The separate mobility measurements are ug, absolute land movement; u, relative movement from the primary mass to the ground; and ud, relative movement from damper to central mass. Given the reality that the device is subject to external forcing and excitement, movement equations are

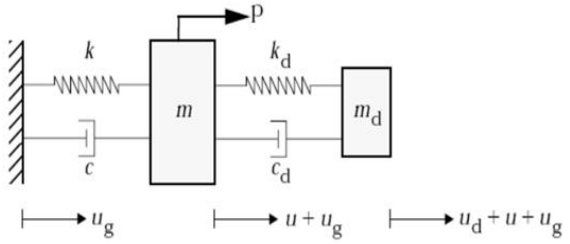

Fig 3.3: SDOF – TMD system

$$m_d \ddot{u}_d + c_d \dot{u}_d + k_d u_d + m_d \ddot{u} = -m_d a_g \qquad (3.2)$$

$$m\ddot{u} + c\dot{u} + k u - c_d \dot{u}_d - k_d u_d = -m a_g + p \qquad (3.3)$$

$$u = \bar{u} e^{i\bar{\omega}t}$$

$$u_d = \bar{u}_d e^{i\bar{\omega}t}$$

The solution due to periodic excitation(both p and u_g) is expressed in polar form:

$$\bar{u} = \frac{\hat{p}}{k} H_1 e^{i\delta_1} - \frac{\hat{a}_g m}{k} H_2 e^{i\delta_2} \qquad (3.4)$$

$$\bar{u}_d = \frac{\hat{p}}{k} H_3 e^{-i\delta_3} - \frac{\hat{a}_g m}{k} H_4 e^{i\delta_4} \qquad (3.5)$$

$$G_2 = \frac{p_0}{k}\left[\frac{1-\beta^2}{(1-\beta^2)^2 + (2\xi\beta)^2}\right]$$

β is defined as the ratio of the applied loading frequency to the natural free vibration frequency i.e., $\beta = \bar{\omega}/\omega$. Substituting the values of $G_1$and G_2in the particular solution and combining the result with the complimentary solution, the total response is obtained in the form of

$$v(t) = [A\cos\omega_d t + B\sin\omega_d t]e^{-\xi\omega t} + \frac{p_0}{k}\left[\frac{1}{(1-\beta^2)^2 + (2\xi\beta)^2}\right][(1-\beta^2)\sin\bar{\omega}t - 2\xi\beta\cos\bar{\omega}t]$$

Where age is the absolute ground acceleration and p is the force loading applied to the primary mass.

It is convenient to work initially with the solution expressed in terms of complex quantities. The excitation is considered to be periodic of frequency $\bar{\omega}$. One expresses the excitation as

$$a_g = \hat{a}_g e^{i\bar{\omega}t}$$
$$p = \hat{p} e^{i\bar{\omega}t}$$

where $\hat{a}_g$and $\hat{p}$ are real quantities. The response is taken as

$$u = \bar{u} e^{i\bar{\omega}t}$$

The *H* factors define the amplitude of the pseudo-static response, and the δ's are the phase angle between the response and the excitation. The various H and δ terms are defined below

$$H_1 = \frac{\sqrt{[f^2 - \rho^2]^2 + [2\xi_d \rho f]^2}}{|D_1|}$$

$$H_2 = \frac{\sqrt{[(1+\bar{m})f^2 - \rho^2]^2 + [2\xi_d \rho f\,(1+\bar{m})]^2}}{|D_1|}$$

$$H_3 = \frac{\rho^2}{|D_1|}$$

$$H_4 = \frac{\sqrt{1 + [2\xi_d \rho]^2}}{|D_1|}$$

$$|D_1| = \left\{[-f^2\rho^2\bar{m} + (1-\rho^2)(f^2-\rho^2) - 4\xi\xi_d f\rho^2]^2 + 4\left[\xi\rho(f^2-\rho^2) + \xi_d f\rho\left(1-\rho^2(1+\bar{m})\right)^2\right]\right\}$$

$$\rho = \frac{\bar{\omega}}{\omega} = \frac{\bar{\omega}}{\sqrt{\frac{k}{m}}}$$

$$f = \frac{\omega_d}{\omega}$$

$$\delta_1 = \alpha_1 - \delta_3$$

$$\delta_2 = \alpha_2 - \delta_3$$

$$\delta_4 = \alpha_3 - \delta_3$$

$$\tan\delta_3 = 2\,\frac{\xi\rho(f^2-\rho^2) + \xi_d f\rho(1-\rho^2(1+\bar{m}))}{-f^2\rho^2\bar{m} + (1-\rho^2)(f^2-\rho^2) - 4\xi\xi_d f\rho^2}$$

$$\tan\alpha_3 = 2\xi\rho$$

$$\tan\alpha_1 = \frac{2\xi_d\rho f}{f^2-\rho^2}$$

$$\tan\alpha_2 = \frac{2\xi_d\rho f(1+\bar{m})}{(1+\bar{m})f^2-\rho^2}$$

3.5 Tuned Mass Damper Theory for MDOF Systems

A 2-DOF system having a damper attached to mass 2 is demonstrated here. The governing equations for the system shown in fig 3.4 are:

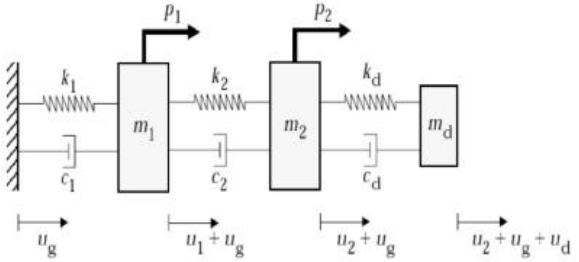

Fig 3.4 2-DOF System with TMD

$$m_1\ddot{u}_1 + c_1\dot{u}_1 + k_1u_1 - k_2(u_2 - u_1) - c_2(\dot{u}_2 - \dot{u}_1) = p_1 - m_1\ddot{u}_g \quad (3.9)$$

$$m_2\ddot{u}_2 + c_2(\dot{u}_2 - \dot{u}_1) + k_2(u_2 - u_1) - k_du_d - c_d\dot{u}_d = p_2 - m_2\ddot{u}_g \quad (3.10)$$

$$m_d\ddot{u}_d + k_du_d + c_d\dot{u}_d = -m_d(\ddot{u}_2 + \ddot{u}_g) \quad (3.11)$$

We combine the equations 3.9 and 3.10 and express the resulting equation in a form similar to the SDOF case. This operation reduces the problem to an equivalent SDOF system. Introducing matrix notation, equations 3.9 and 3.10 are written as

$$\mathbf{M}\ddot{\mathbf{U}} + \mathbf{C}\dot{\mathbf{U}} + \mathbf{K}\mathbf{U} = \begin{bmatrix} p_1 - m_1a_g \\ p_2 - m_2a_g \end{bmatrix} + \begin{bmatrix} 0 \\ k_du_d + c_d\dot{u}_d \end{bmatrix}$$

$$\mathbf{U} = \begin{bmatrix} u_1 \\ u_2 \end{bmatrix}$$

$$\mathbf{M} = \begin{bmatrix} m_1 & 0 \\ 0 & m_2 \end{bmatrix}$$

$$\mathbf{K} = \begin{bmatrix} k_1 + k_2 & -k_2 \\ -k_2 & k_2 \end{bmatrix}$$

$$\mathbf{C} = \begin{bmatrix} c_1 + c_2 & -c_2 \\ -c_2 & c_2 \end{bmatrix}$$

Expressing **U** in terms of modal vectors and coordinates

$$\mathbf{U} = \Phi_1q_1 + \Phi_2q_2$$

The modal vectors satisfy the following orthogonality relations

$$\Phi_j^T\mathbf{K}\Phi_i = \delta_{ij}\omega_j^2\Phi_j^T\mathbf{M}\Phi_i$$

Defining modal mass, stiffness and damping terms,

$$\tilde{m}_j = \Phi_j^T\mathbf{M}\Phi_j$$

$$\tilde{k}_j = \Phi_j^T\mathbf{K}\Phi_j = \omega_j^2\tilde{m}_j$$

$$\tilde{c}_j = \Phi_j^T\mathbf{C}\Phi_j$$

Expressing the elements of Φ_j as

$$\Phi_j = \begin{bmatrix} \Phi_{j1} \\ \Phi_{j2} \end{bmatrix}$$

Assuming damping is proportional to stiffness

$$\mathbf{C} = a\mathbf{K} \quad (3.12)$$

One obtains a set of uncoupled equations for q_1 and q_2, j = 1,2

$$\tilde{m}_j\ddot{q}_j + \tilde{c}_j\dot{q}_j + \tilde{k}_jq_j = \Phi_{j1}(p_1 - m_1a_g) + \Phi_{j2}(p_2 - m_2a_g + k_du_d + c_d\dot{u}_d) \quad (3.13)$$

With this assumption the modal damping ratio is given by

$$\xi_j = \frac{\tilde{c}_j}{2\omega_j\tilde{m}_j} = \frac{a\omega_j}{2}$$

$$\tilde{m}_1\ddot{q}_1 + \tilde{c}_1\dot{q}_1 + \tilde{k}_1q_1 = \Phi_{11}p_1 + \Phi_{12}p_2 - [m_1\Phi_{11} + m_2\Phi_{12}]a_g + \Phi_{12}[k_du_d + c_d\dot{u}_d]$$

In general, u_2 is obtained by superimposing the modal contributions

$$u_2 = \Phi_{12}q_1 + \Phi_{22}q_2$$

However when the external forcing frequency is close to ω_1, the first mode response will dominate, and it is reasonable to assume

$$u_2 \approx \Phi_{12}q_1$$

Solving for q_1

$$q_1 = \left[\frac{1}{\Phi_{12}}\right]u_2$$

And then substituting in eqn 3.13, one obtains

$$\tilde{m}_{1e}\ddot{u}_2 + \tilde{c}_{1e}\dot{u}_2 + \tilde{k}_{1e}u_2 = k_du_d + c_d\dot{u}_d + \tilde{p}_{1e} - \Gamma_{1e}\tilde{m}_{1e}a_g \quad (3.14)$$

Where $\tilde{m}_{1e}, \tilde{k}_{1e}, \tilde{c}_{1e}, \tilde{p}_{1e}$ and Γ_{1e} represent the equivalent SDOF parameters for the combination of mode 1 and node 2, the node at which the TMD is attached. Their definition equations are

$$\tilde{m}_{1e} = \left[\frac{1}{\Phi_{12}^2}\right]\tilde{m}_1$$

$$\tilde{k}_{1e} = \left[\frac{1}{\Phi_{12}^2}\right]\tilde{k}_1$$

$$\tilde{c}_{1e} = a\tilde{k}_{1e}$$

$$\tilde{p}_{1e} = \frac{\Phi_{11}p_1 + \Phi_{12}p_2}{\Phi_{12}}$$

$$\Gamma_{1e} = \frac{\Phi_{12}}{\tilde{m}_1}(m_1\Phi_{11} + m_2\Phi_{12})$$

Equations 3.11 and 3.14 are similar in form to the SDOF equations treated in the previous section. Both set of equations are compared below.

TMD equation

$$m_d\ddot{u}_d + c_d\dot{u}_d + k_du_d = -m_d(\ddot{u} - a_g)$$

vs

$$m_d\ddot{u}_d + c_d\dot{u}_d + k_du_d = -m_d(\ddot{u}_2 - a_g)$$

Primary mass equation

$$m\ddot{u} + c\dot{u} + ku = c_d\dot{u}_d + k_du_d + p - ma_g$$

vs

$$\tilde{m}_{1e}\ddot{u}_2 + \tilde{c}_{1e}\dot{u}_2 + \tilde{k}_{1e}u_2 = k_du_d + c_d\dot{u}_d + \tilde{p}_{1e} - \Gamma_{1e}\tilde{m}_{1e}a_g$$

Taking

$$u_2 \equiv u, \quad \tilde{m}_{1e} \equiv m, \quad \tilde{c}_{1e} \equiv c, \quad \tilde{k}_{1e} \equiv k, \quad \tilde{p}_{1e} \equiv p, \quad \Gamma_{1e} \equiv \Gamma$$

$$u_2 \equiv u, \quad \tilde{m}_{1e} \equiv m, \quad \tilde{c}_{1e} \equiv c, \quad \tilde{k}_{1e} \equiv k, \quad \tilde{p}_{1e} \equiv p, \quad \Gamma_{1e} \equiv \Gamma$$

Transforms the primary mass equation for the MDOF case to

$$m\ddot{u} + c\dot{u} + ku = c_d\dot{u}_d + k_du_d + p - \Gamma ma_g$$

$$H_6 = \frac{\sqrt{[(\Gamma + \bar{m})f^2 - \Gamma\rho^2]^2 + [2\xi_d\rho f\,(\Gamma + \bar{m})]^2}}{|D_3|}$$

$$H_8 = \frac{\sqrt{[1 + \rho^2(\Gamma - 1)]^2 + [2\xi_d\rho]^2}}{|D_3|}$$

$$\tan\alpha_2 = \frac{2\xi_d\rho f(\Gamma + \bar{m})}{(\Gamma + \bar{m})f^2 - \Gamma\rho^2}$$

$$\tan\alpha_3 = \frac{2\xi\rho}{1 + (\Gamma - 1)\rho^2}$$

$$\delta_6 = \alpha_2 - \delta_7$$

$$\delta_6 = \alpha_3 - \delta_7$$

$$|D_3| = \left\{[-f^2\rho^2\bar{m} + (1-\rho^2)(f^2-\rho^2) - 4\xi\xi_d f\rho^2]^2 + 4\left[\xi\rho\,(f^2-\rho^2) + \xi_d f\rho\,(1-\rho^2(1+\bar{m}))^2\right]\right\}$$

$$\tan\delta_7 = 2\,\frac{\xi\rho\,(f^2-\rho^2) + \xi_d f\rho(1-\rho^2(1+\bar{m}))}{-f^2\rho^2\bar{m} + (1-\rho^2)(f^2-\rho^2) - 4\xi\xi_d f\rho^2}$$

From this point on, one proceeds as described in SDOF case. The mass ratio is defined in terms of equivalent SDOF mass.

$$\bar{m} = \frac{m_d}{\bar{m}_{1e}}$$

Den Hertzog's equation is as follows:

$$\alpha\ \text{opt} = \frac{1}{1+\mu}$$

Where μ is mass ratio.

The effect of TMD damping on peak response of the structure is examined under optimal frequency ratio. The damping of the structure is assumed to be negligibly small.In this case,the optimal damping, ξ opt, becomes

$$\xi\ \text{opt} = \sqrt{\frac{3\mu}{8(1+\mu)}}$$

Using the values of α opt and ξ opt, optimum values of damping cd and stiffness kd of thedamper can be calculated as:

$$c_d = 4\pi\mu\alpha\xi_{opt}m_s/Ts \quad (3.15)$$

$$k_d = 4\pi^2\mu\alpha^2 m_s/Ts^2 \quad (3.16)$$

3.5 Analysis procedure

The methods for determining the vulnerability of buildings are complicated and may take considerably longer to complete. More advanced approaches, suggesting a more comprehensive analysis process and more refined models, require much more periods and function, therefore assessing specific buildings only, probably as a further stage after the rapid screening of possible dangerous buildings in the multi-phase procedure. They are not ideal for earthquake scenario programs where structures need to be tested. Nonetheless, the idea behind the approaches in question may be useful for creating a new technique, and thus, the core research framework shall be illustrated. The research method may be broken down into linear procedures (static and dynamic analysis), as well as nonlinear procedures (differential and integral) (nonlinear static and nonlinear dynamic).

3.5.1 Linear Static Analysis

In a linear static analysis technique, the building is called a structure with just one degree of independence, defined by linear elasticity and viscous damping. The seismic is modeled by the influence of an equal lateral force on the earthquake's stress and strain to generate the same earthquake. Using observational associations or Rayleigh's rule, the spectral acceleration is estimated from the response distribution. After multiplying the effect by the mass of the house, the result provides the lateral power. The coefficient considers the decrease in expected stiffness due to plasticity anddecreased force due to the expected inelastic actions. The height of the building measures the lateral force, and the sum of exterior force added.

Typical linear static structures are only used for construction purposes and are implemented in most building codes. Their budget is limited. Even, they only refer to traditional buildings with the dominant first mode of vibration.

3.5.2 Nonlinear Static Analysis

A nonlinear, static analysis is used for the construction model. The inelastic material reaction of the specific components and elements was accounted for directly. Several method escapes (e.g., A.T.C. 40 and FEMA 273).They both have in common that the building model's nonlinear force-deformation feature is defined by subjecting the building model to monotonically rising lateral forces or increasing displacement, spread over the building's height in correspondence to the first mode of vibration, before the building collapse. The upper limit of earthquake displacement is calculated using either strongly damped or inelastic feedback spectra. The protocols concerning the linear material reaction and the measured internal force and deformation would be more precise approximations to those predicted during an earthquake. However, only the first mode of vibration is considered, and thus the above modes can't be used on unusual surfaces, and more are not appropriate.

3.5.4 Nonlinear Dynamic Analysis

In a nonlinear dynamic analysis process, the structure is modeled like the one used in nonlinear static analysis. The construction model is identical to the one used in the nonlinear static analysis by utilizing general finite elements. The seismic feedback is modeled using a time history analysis focused on measuring building reaction over time. The most reliable method for estimating values of force and displacement is included in this report.

However, the measured response is very responsive to the ground motion used as an input, so many time-

history studies are needed utilizing different ground motions data. The nonlinear dynamic technique serves as a testing instrument to model a building system's actions in-depth and measure fractures' progression, the distribution of vertical and shear pressures, the forms of hysteresis curves, etc.

3.5.4.1 Nonlinear System

The deformation of a substance after a nonlinear force has been applied. This point is named yieldpoint since it is the point at which the substance is starting to yield. The device is linearly elastic on initial loading as long as the applied force is less than the yield power (i.e., the stiffness is zero). Generally, force is referred to as yield power. The system turns into a plastic region that is made up of elastic content. As the deformation rises, the tension stays unchanged. The overload and unload method proceeds until the substance enters a state of equilibrium. It means that force Fs do not have a single value and rely on the deformations and whether the deformation is increasing or declining (negative velocity).

Fs=Fs (u, u')

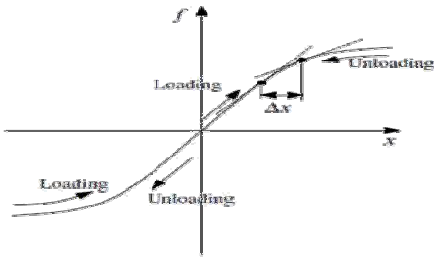

Fig 3.7 Non-Linear Force-Deformation Relationship

3.6 Nonlinear Modal Time History Analysis in SAP 2000

Following are the general sequence of steps involved in performing NLTHA using

SAP2000 in the present study:

- A two or three-dimensional model that represents the overall structural behavior created.
- For reinforced concrete elements, the appropriate reinforcement is provided for the cross-sections.
- Gravity loads are composed of dead loads, and a specified proportion of live load is assigned as a seismic weight to the structure.
- Free vibration un-damped modal analysis is performed to note the frequencies and periods of the structure.
- The time history function from a file is selected, and the time history function is defined.
- Nonlinear link elements are included in the structure.
- The nonlinear modal time-history load cases are defined by assigning the ground acceleration time history function as loading in X, Y, and X.Y. directions and by assigning proportional damping
- NLTHA is set to run.

After the completion of the analysis, the displacement pattern of the structure is studied.

The other responses, such as base shear, time period, are noted.

4. **SPECIMEN CALCULATIONS**

Total weight calculations for R.C.C structure

Weight of Beams = c/s Area of Beam x Total Length x unit wt. of concrete
= 0.60 x 0.30 x (24x5+24x5) x 25 = 1080 KN

Weight of Columns = c/s Area of Column x Height x No of columns x unit wt. of concrete
= 0.65 x 0.65 x (16 x 3 x 25) x 25 = 12675 KN

Imposed load = 10 x 24 x 24 = 92160 KN

Total weight of R.C.C building frame = 105915 KN

Total weight calculations for Composite structure

Weight of Beams= c/s Area of Beam x Total Length x unit wt. of concrete
= 0.012 x (24x5+24x5) x 76.97
= 221.67 KN

Weight of Columns = c/s area of column x Height x No. of columns x unit wt. of Concrete
= (0.35 x 0.35 x 25 + 1.6 x 0.025 x 76.97) x (16 x 3 x 25)
= 7369.56 KN

Imposed load = 10 x 24 x 24
= 92160 KN

Total weight of R.C.C building frame = 99751.23 KN

Tuned mass damper parameter calculations for R.C.C structure:

Weight of TMD = 5% of total weight

= 5% x 105915

= 5295.75 KN

Mass of TMD = $\frac{5295.75}{9.8}$ = 540.38 KN s^2 /m

Stiffness of TMD (Kd) = $4 \times \pi^2 \times \mu \times \alpha opt^2 \times \frac{Ms}{Ts^2}$

=39.47 x 0.05 x 0.906 x 2295.15

=4077.41 KN/m

Damping of TMD (Cd) = $4 \times \pi \times \mu \times \alpha opt \times \xi opt \times \frac{Ms}{Ts}$

= 12.56 x 0.05 x 0.95 x 0.13 x 4980.49

=386.47 KN s/m

Tune mass damper parameter calculations for Composite structure:

Weight of TMD = 5% of total weight

= 5% x 99751.23

= 4987.56 KN

Mass of TMD = $\frac{4987.56}{9.8}$ = 508.93 KN s^2 /m

Stiffness of TMD (Kd) = $4 \times \pi^2 \times \mu \times \alpha opt^2 \times \frac{Ms}{Ts^2}$

=39.47 x 0.05 x 0.906 x 1449.44

=2574.97 KN/m

Damping of TMD (Cd) = $4 \times \pi \times \mu \times \alpha opt \times \xi opt \times \frac{Ms}{Ts}$

= 12.56 x 0.05 x 0.95 x 0.13 x 3841.02

=298.05 KN s/m

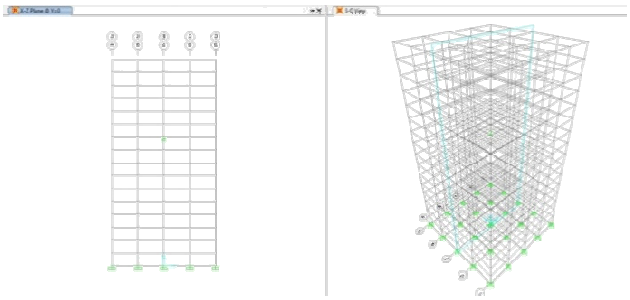

Fig 4.1 Plan and 3D View of Model without TMD

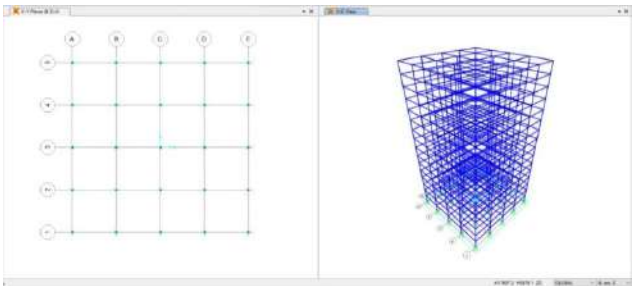

Fig 4.2 Elevation and 3D View of Model with 5% TMD at Mid Storey

4.3Analysis methods

Research approaches are graded according to their origin in static and dynamic analysis. When undergoing earthquake impact, the structural loads exceed their full potential, and the material stresses are beyond their capacity. The study can integrate the substance nonlinearity and geometric nonlinearity to achieve better performance. These numerical methods often allow the determination of the power, deformation, and ductility of structures and the distribution of strength demands throughout the system.

4.3.1 Equivalent static method

The equivalent static architecture analysis technique is linear, which assumes the system's reaction is linearly elastic. The study is carried out as defined by IS 1893. (Part 1).

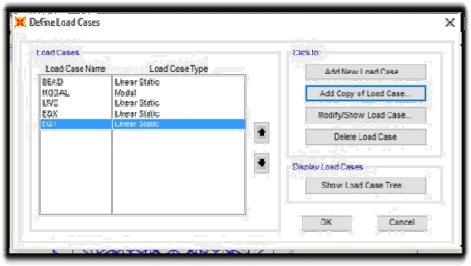

Fig 4.4 Modal Load Case Set to Calculate the Mode Shapes

Fig 4.5 Load Cases Set to Perform the Linear Static Analysis

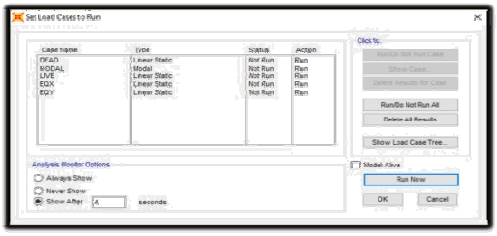

4.3.2 Nonlinear Time History Analysis

NLTHA is an applied physics tool used to explain the actions of structures that undergo seismic motions. As the name suggests, it is the method of figuring out the background of responses over the life cycle of the dynamic loading like an earthquake ground acceleration record before the structure hits a limit state.

The dynamic loading consists of applying the earthquake ground acceleration record of vertical loads to a structure and incrementally raising those loads that differ in time to evaluate the structure's response.

For this analysis, earthquake ground acceleration records that include the different N-W BHUJ components have been used. BHUJ is an institute situated in Gujarat in the high-intensity earthquake region of zone factor 0.36 and falls under the zone-v according to the classification of areas by the IS 1893-2002 part-1.

The data's acceleration points are described in terms of time (i.e., within 0.005 seconds). The acceleration record has units of m/2, has a total number of 27,000 acceleration data coordinates, and the most critical data are the first 13,000, which are of the maximum strength.

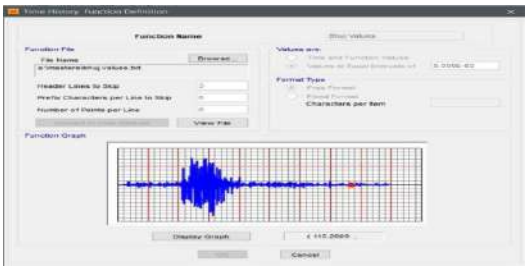

Fig 4.6 BHUJ Component Earthquake Ground Acceleration Record

4.4 Nonlinear Modal Time History Load Cases

Modal fast nonlinear analysis is used to extract the nonlinear time history modal loads for a structure. The data points are transformed into the mass matrix compounded with the structure's mass matrix to generate loading. Trajectory details in a time history load case can be taken from a nonlinear static load case. The correct additional parameters are regarded, such as damping matrix, algorithm collection, and some time measures.

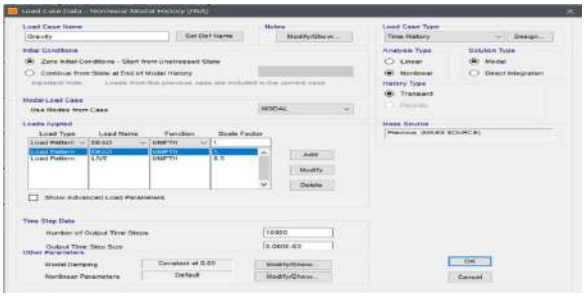

Fig4.7 Illustrates theLoad Cases Applied on the Structure

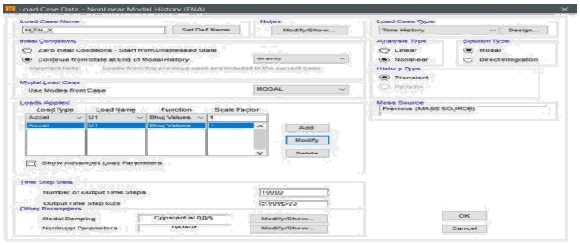

Fig4.8 Illustrates the Gravity Load Case Applied on the Structure

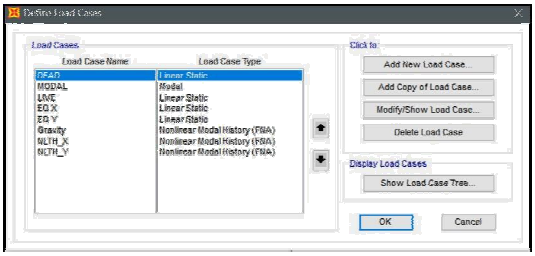

Fig4.9 Illustrates the Non-Linear Modal Time History Load Case in X Direction Using BHUJTime History Function.

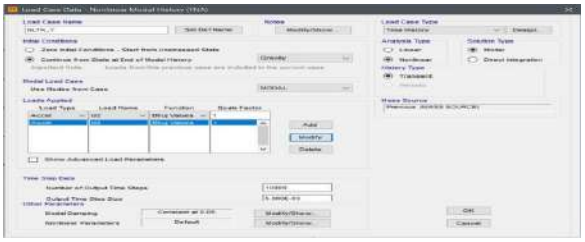

Fig4.10 Illustrates the Non-Linear Modal Time History Load Case in Y Direction Using BHUJTime History Function.

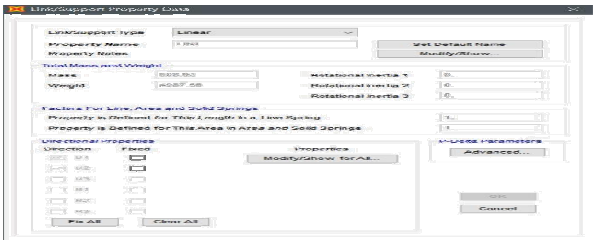

Fig4.11 Illustrates Tuned Mass Damper Parameters for R.C.C Structure

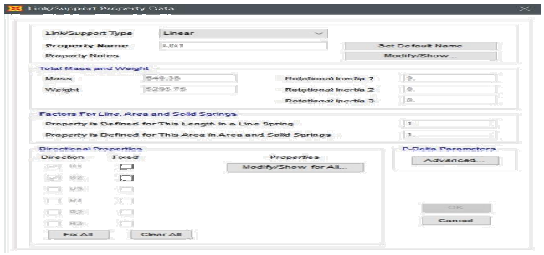

Fig4.12 Illustrates Tuned Mass Damper Directional Properties for R.C.CStructure

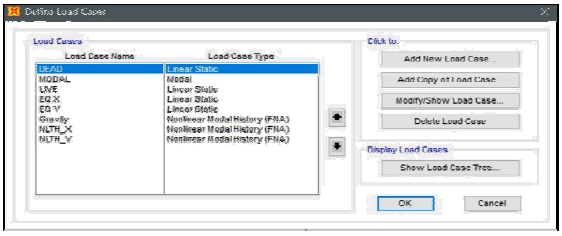

Fig4.13 Illustrates Tuned Mass Damper Parameters for Composite Structure

Fig4.14 Illustrates Tuned Mass Damper Directional Properties for Composite Structure

5.5 Comparison of Base shear X&Y due to NLTH-X & NLTH- Y without and with TMD

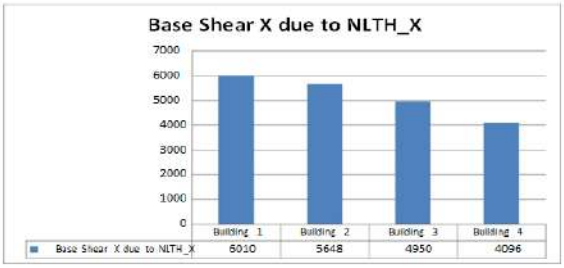

Fig 5.21 Base Shear(kN)XDue to NLTH_X Without and With Tuned Mass Damper

Fig 5.21 illustrates the base shear X in the X direction where it can be seen that there was a reduction in the base shear value of 1060kN without TMD in Composite structure when compared to R.C.C. and 1552kN with TMD in Composite structure when compared to R.C.C. structure. It can also be seen that there was a reduction in the base shear value of 362kN in the R.C.C. structure using TMD and 854kN in the Composite structure using TMD.

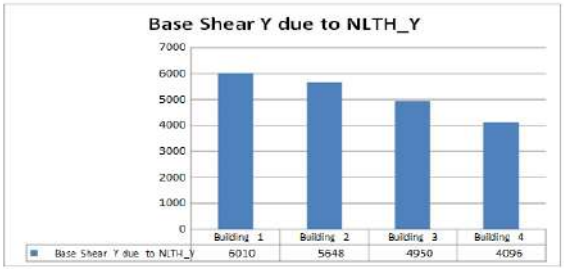

Fig 5.22 Base Shear(kN)YDue to NLTH_Y Without and With Tuned Mass Damper

Fig 5.22 illustrates the base shear Y in the Y direction where it can be seen that there was a reduction in the base shear value of 1060kN without TMD in Composite structure when compared to R.C.C. and 1552kN with TMD in Composite structure when compared to R.C.C. structure. It can also be seen that there was a reduction in the base shear value of 362kN in the R.C.C. structure using TMD and 854kN in the Composite structure using TMD.

5.6 Comparison of Displacement x & y due to NLTH- X & NLTH- Y without and with TMD

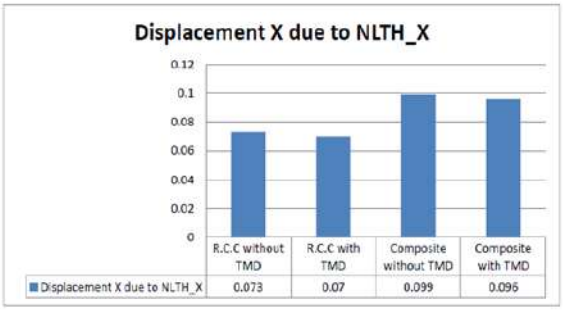

Fig.5.23 Displacement(m) xDue to NLTH_X Without and With Tune Mass Damper

Fig 5.23 illustrates the displacement X in the X direction where it can be seen that there was an increment in displacement value of 26mm with and without TMD in Composite structure when compared to R.C.C. due to ductility. It can also be seen that there was a reduction in displacement value of 3mm in R.C.C. structure and Composite structure using TMD.

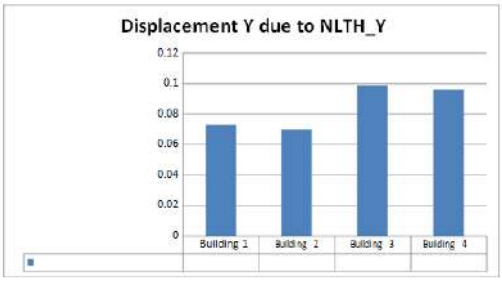

Fig 5.24 Displacement(m) due to NLTH_YWithout and With Tuned Mass Damper

Fig 5.24 illustrates the displacement Y in the Y direction where it can be seen that there was an increment in displacement value of 26mm with and without TMD in Composite structure when compared to R.C.C. due to ductility. It can also be seen that there was a reduction in displacement value of 3mm in R.C.C. structure and Composite structure using TMD.

6. CONCLUSIONS

Based on Non-Linear Time History Analysis carried out, the following lists of conclusions are drawn:

- The composite building frame base shear was reduced by 18% compared to the R.C.C building frame without TMD and 28% with TMD.
- The structure's combined building frame weight was found to reduce by 45% compared to the R.C.C building frame.
- The composite building frame displacement was found to increase by 35% compared to the R.C.C building frame with and without TMD.
- In the R.C.C building, frame displacement in X direction due to NLTH_X at a joint was found to reduce by4% by introducinga tuned mass damper at the building's mid-story.
- In the R.C.C building, frame displacement in the Y direction due to NLTH_Y at a joint was found to reduce by 4% by introducinga tuned mass damper at the building's mid-story.
- In the R.C.C building, frame base shear in X direction due to NLTH_X was found to reduce by 7% by introducinga tuned mass damper at the building's mid-story.
- In the R.C.C building, frame base shear in the Y direction due to NLTH_Y was found to reduce by 7% by introducinga tuned mass damper at the building's mid-story.
- In the Composite building, frame displacement in the X direction due to NLTH_X at a joint was reduced by 3% by introducinga tuned mass damper at the building's mid-story.
- In the Composite building, frame displacement in the Y direction due to NLTH_Y at a joint was reduced by 3% by introducinga tuned mass damper at the building's mid-story.
- In the Composite building frame base, shear in X direction due to NLTH_X was found to reduce by 18% by introducing tuned mass damper at the building's mid-story.
- In the Composite building frame base, shear in the Y direction due to NLTH_Y was found to reduce by 18% by introducinga tuned mass damper at the building's mid-story.

FUTURE WORK

As the various researchers are getting attracted to the composite structures, the studies' scope under the particular topic can be stretched to wide horizons where the building plan can be more realistic by considering different dimensions of beams/columns with wall openings and slabs. Asymmetry of the composite structure can be considered, finding out the best suitable location for TMD placement.

REFERENCES

1. AshishMohite, A. and Patel, G.R., (2015). "Earthquake Analysis of Tall Building with Tuned Mass Damper". IOSR Journal of Mechanical and Civil Engineering, 113-122.
2. Bandivadekar, T.P. and Jangid, R.S., (2012). "Mass distribution of multiple tuned mass dampers for vibration control of structures". International Journal of Civil and Structural Engineering, Vol-3(1), 70-84.
3. Chen, G. and Wu, J., (2001). "Optimal placement of multiple tune mass dampers for seismic structures".Journal of Structural Engineering, ASCE, Vol. 127(9), 1054–1062.
4. Chen, G. and Wu, J., (2003). "Experimental study on multiple tuned mass dampers to reduce seismic responses of a three-storey building structure". Earthquake Eng. Struct. Dyn., Vol. 32, 793–810.
5. Computers and structures Inc., 2003, "SAP 2000 version 19 ".
6. DeepakJirage, Sayagavi, V.G. and Gore, N.G., (2015). "Comparative Study of R.C.C. and Composite Multi-Storeyed Building". International Journal of Scientific Engineering and Applied Science, Vol-1(6), 236-240.
7. Earthquake Resistant Design of Structures by Pankaj Agarwal and Manish Shrikhande.
8. IS:1893-2002 (Part 1), Criteria for Earthquake Resistant Design of Structures – Part1: General Provisions and Buildings (Fifth revision); Bureau of Indian standards, New Delhi.
9. IS:11384-1985, Code of Practice for Composite Construction in Structural Steel and Concrete, Bureau of Indian standards, New Delhi.
10. IS:456-2000, Plain and Reinforced Concrete, Bureau of Indian standards, New Delhi.

11. Jaiswal, O.R., (2004). "Simple tuned mass damper to control seismic response of Elevated tanks" .13th World Conference on Earthquake Engineering, Paper No. 2923.
12. Jonathan SALVI, Egidio RIZZI and Michele GAVAZZE, (2014). "Analysis on optimum performance of tuned mass damper devices in the context of earthquake engineering" .Proceedings of the 9th International Conference on Structural Dynamics, EURODYN, 1729-1736.
13. Ormondroyd, J. and Den Hartog, J.P., (1920). "The theory of the dynamic vibration absorber". Journal of Applied Mechanics, ASME, Vol-50(7), 9–22.
14. Panchal, D.R. and Mara the, P.M., (2011). "Comparative Study of R.C.C., Steel and Composite Building". International Conference on Current Trends in Technology, 1-6.
15. Renavikar Aniket, V. and Suryawanshi Yogesh, (2016). "Comparative Study on Analysis and Cost of R.C.C. and Steel-Composite Structure". International Journal of Science and Research, Vol-5(7), 1421-1425.
16. Sandip Shevale, S.,Kadam, S.S., Pise, C.P., Pawar,Y.P., Deshmukh, C.M. and Mohite, D.D., (2016). "Seismic Behavior of Multi-Storied Building by Using Tuned Mass Damper and Base Isolation- A Review". International Journal of Engineering Research and Applications, Vol-6(10), Part-5, 1-6.
17. Sattainathan Sharma, A., Anjughap Priya, R., Thirugnanam, R. and Rathna Priya P., (2016). "Comparative Study on Multi-Storey Structure of R.C.C. and Composite Material". Indian Journal of Science and Technology, Vol-9(2), 1-5.
18. Shilpa Chandran, P. and Prasad Varma Thampan, CK., (2013). "Seismic Effectiveness of Tuned Mass Damper-A Review". International Research Journal of Engineering &Technology(IRJET), Vol-4(3), 1997-2000.
19. Thakur, V.M. and Pachpor, P.D., (2012). "Seismic Analysis of Multistoried Building with TMD (Tuned Mass Damper)".International Journal of Engineering Research and Applications (IJERA), ISSN: 2248-9622;Vol- 2(1),319-326.
20. Villaverde,R., (1985). "Reduction in seismic response with heavily-damped vibration absorbers". Earthquake Engineering and Structural Dynamics,Vol-13(1),33–42.

CONTROLLING APPLICATIONS WITH HAND GESTURES USING SIXTH SENSEPROTOTYPE / WEAR YOUR WORLD USINGSIXTH SENSE TECHNOLOGY

[1]Uzma Nikhat, [2]Shanila Mahreen
[1]PG Scholar, Department of Electronics and Communication Engineering,
[2]Assistant Professor, Department of Electronics and Communication Engineering,
Nawab Shah Alam Khan College of Engineering & Technology, Hyderabad

ABSTRACT

We grew up interacting with the physical objects around us. And there are large numbers of them that we use every day. These objects are more fun to use than our computing devices. Taking about objects, another thing that gets attached with objects is gestures, how we manipulate these objects & how we use them in everyday life. These gestures are used to interact with objects as well as to interact with each other. So using Sixth Sense Technology we get to know about everyday objects and gestures and how using these objects can leverage (power to influence situation) our interaction with digital world. This technology helps us to build bridge between physical world and the digital world. It brings part of digital world to physical world. Some part of digital information in brought into physical world which can be manipulated in physical world.Anybody that is equipped with sixth sense device can use its applications at any place and any time. Working of Sixth sense technology, its applications, advantages, future scope and different implementation approaches are presented in this paper.

In this paper we worked on a new type of technology which is going to be soon launched in the market. Its name is the sixth sense technology. It's a wearable interface that augments the physical world around us with the digital information. It's just born concept which allows user to connect with the internet seamlessly. Without use of keyboard, mouse we can see videos access, change, move data simply.

I. INTRODUCTION

This technology is a revolutionary way to interface the physical world with digital information. Modern technologies include the touch screen techniques which is used widely and it makes ease of operation and saves utilization time. Sixth sense is a wearable gestural interface that augments the physical world around us with digital information and lets us use natural hand gestures to interact with that information. But the bottle necks of this method such as position of camera, for capturing gestures interprets the accuracy in the projected output, lead to use of commands instead of hand gestures. The position of camera is a major constraint in the image capturing and projected output efficiency and accuracy. Therefore, the actions which we regularly perform in our daily life, are converted to commands and are trained to a speech IC. They are stored as a database in the integrated circuit and corresponding actions are performed when the speech is recognized from the user.

It's a hi-tech device seamlessly integrate Analog information with our everyday physical world. The voice is directly performed into operation within fractions of seconds, and the action is projected on the surface. It's a portable device and eases the operation which we regularly perform. Basically, the sixth sense technology concept involves the use of hand gestures. thefingertip will contain colored markers and hence gestures performed will be captured by the camera. Then it's given to the mobile device for the corresponding action to be performed. The action is projected on the surface through the projector. Software algorithms and computer vision technologies will be used to enable the action from the mobile device for the corresponding gesture captured in the camera. This gesture-based technology is used for variety of applications like performing basic actions, locating points in the map, watching video in newspaper, dialing number in hand etc. The slight modification of this method leads to the use of commands that is analog information into real world. The analog data is converted into digital and performed as action, as all times the hand gestures cannot be used.

This was how the wearable device is fit to the human body. Herecolor markers are used in the finger tips. In our technology we use commands for performing the same operations. Many high technology speech integrated circuits evolved which makes our operation enhanced with more advanced features.

To ensure accurate gesture recognition and an intuitive interface a number of constraints are applied. A region in the front of the projection screen is defined as the active zone and the gestures are ignored, if the gestures are performed out of this area. Gestures are also defined by a set start posture, end posture and dynamic motion between the start and end postures. Perhaps the use of gestures is most powerful when combined with other input modalities, especially voice. Allowing combined voice and gestural input has several tangible advantages. The first is purely practical-ease of expression. Ease corresponds to the efficiency with which commands can be remembered and expressiveness, size of command vocabulary.

SIXTH SENSE

Intuition depends on the ideas of increased reality and has all around executed its impression. Intuition innovation has coordinated this present reality objects with computerized world. The remarkable Sixth Sense innovation is a mix of numerous wonderful advances.

The thing which makes it great is the heavenly reconciliation of every one of those innovations and presents it into a single versatile and prudent item. It partners advancements like hand motion acknowledgment, picture catching, preparing, and control, and so forth It superimposes the computerized world on this present reality. Like faculties empower us to see data about the climate in various manners it additionally targets seeing data. Intuition is truth be told, about appreciating data more than our accessible faculties.

Furthermore, today there isn't only this physical world from where we get data yet additionally the computerized world which has gotten a part of our life. This advanced world is presently as essential to us as this physical world. What's more, with the web the computerized world can be extended commonly the physical world. God hasn't given us sense to connect with the computerized world so we have made them like advanced cells, tablets, PCs, PCs, net books, PDAs, music players, and others contraptions.

These devices empower us to convey with the computerized world around us. In any case, we're people and our physical body isn't intended for computerized world so we can't collaborate legitimately to the advanced world. For example, we press keys to dial a number; we type text to look through it, etc. This implies for an individual to speak with the advanced world he/she must learn it.

We don't convey legitimately and proficiently to the computerized world as we do with this present reality. The Sixth Sense innovation is tied in with cooperating to the computerized world in generally productive and direct manner. Subsequently, it wouldn't not be right to close Sixth Sense innovation as passage among computerized and genuine world.

Prior to Wear Ur World (WuW) came, there were other strategies like speech recognition programming, contact acknowledgment and so on, which engaged us with direct interfacing. This WuW or Sixth Sense gadget is a model of next degree of advanced to genuine world interfacing. This innovation empowers individuals to connect in the advanced world as though they are connecting in reality.

COMMON OVERVIEW TO EMBEDDED SYSTEM

An embedded system can be defined as a computing device that does a specific focused job. Appliances such as the air-conditioner, VCD player, DVD player, printer, fax machine, mobile phone etc. are examples of embedded systems. Each of these appliances will have a processor and special hardware to meet the specific requirement of the application along with the embedded software that is executed by the processor for meeting that specific requirement. The embedded software is also called “firm ware”. The desktop/laptop computer is a general-purpose computer. You can use it for a variety of applications such as playing games, word processing, accounting, software development and so on. In contrast, the software in the embedded systems is always fixed listed below.

Embedded systems do a very specific task, they cannot be programmed to do different things. Embedded systems have very limited resources, particularly the memory. Generally, they do not have secondary storage devices such as the CDROM or the floppy disk. Embedded systems have to work against some deadlines. A specific job has to be completed within a specific time. In some embedded systems, called real-time systems, the deadlines are stringent. Missing a deadline may cause a catastrophe-loss of life or damage to property. Embedded systems are constrained for power. As many embedded systems operate through a battery, the power consumption has to be very low.

• Some embedded systems have to operate in extreme environmental conditions such as very high temperatures and humidity.

II. BLOCK DIAGRAM

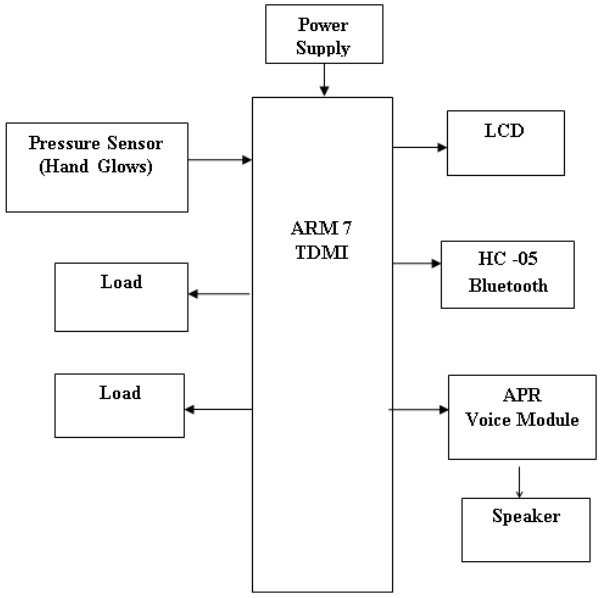

POWER SUPPLY

- Step-down transformer is used for voltages from 230v-12vAC.
- Bridge rectifier is used for conversion of AC-DC.
- IC7805 is used for constant 5V
- Load is for indication purpose of required 5V.

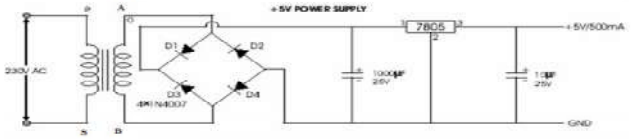

ADVANCED RISC MACHINE 7(ARM7)

The LPC2148 is based on a 16/32 bit ARM7TDMI-SCPU with real-time emulation and embedded trace

support, together with 128/256 kilobytes (kb) of embedded high speed flash memory. A 128-bit wide memory interface and unique accelerator architecture enable 32-bit code execution at maximum clock rate. For critical code size applications, the alternative 16-bit Thumb.

Mode reduces code by more than 30 % with minimal performance penalty. With their compact 64 pin package, low power consumption, various 32-bit timers, 4-channel 10-bit ADC, 2 advanced CAN channels, PWM channels and 46 GPIO lines with up to 9 external interrupt pins these microcontrollers are particularly suitable for automotive and industrial control applications as well as medical systems and fault-tolerant maintenance buses. With a wide range of additional serial communications interfaces, they are also suited for communication gateways and protocol converters as well as many other general-purpose applications.

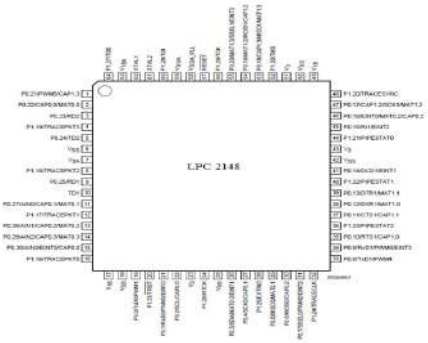

Key Features

- 16/32-bit ARM7TDMI-S microcontroller in a tiny LQFP64 package.
- 16 kb on-chip Static RAM.
- 128/256 kb on-chip Flash Program Memory. 128-bit wide interface/accelerator enables high speed 60 MHz operation.
- In-System Programming (ISP) and In-Application Programming (IAP) via on-chip boot-loader software. Flash programming takes 1 ms per 512 byte line. Single sector or full chip erase takes 400 ms.
- Embedded ICE-RT interface enables breakpoints and watch points. Interrupt service routines can continue to execute while the foreground task is debugged with the on-chip RealMonitor“ software.
- Embedded Trace Macrocell enables non-intrusive high speed real-time tracing of instruction execution.
- Two interconnected CAN interfaces with advanced acceptance Filters.
- Four channel 10-bit A/D converter with conversion time as low as 2.44 ms.
- Multiple serial interfaces including two UARTs (16C550), Fast I2C (400 kbits/s)and two SPIs
- 60 MHz maximum CPU clock available from programmable on-chip Phase-Locked Loop with settling time of 100 □s.
- Vectored Interrupt Controller with configurable priorities and vector addresses.
- Two 32-bit timers (with four capture and four compare channels), PWM unit (six outputs), Real Time Clock and Watchdog.
- Up to forty-five 5 V tolerant general purpose I/O pins. Up to nine edge or level sensitive external interrupt pins available.
- On-chip crystal oscillator with an operating range of 1 MHz to 30 MHz.
- Two low power modes Idle and Power-down.
- Processor wake-up from Power-down mode via external interrupt.
- Individual enable/disable of peripheral functions for power optimization.
- Dual power supply:
    - CPU operating voltage range of 1.65 V to 1.95 V (1.8 V ±0.15 V).
    - I/O power supply range of 3.0 V to 3.6 V (3.3 V ± 10 %) with 5 V tolerant I/O pads.

LIQUID CRYSTAL DISPLAY

LCD (Liquid Crystal Display) screen is an electronic display module and find a wide range of applications. A 16x2 LCD display is very basic module and is very commonly used in various devices and circuits. These modules are preferred over seven segments and other multi segment LEDs. The reasons being: LCDs are economical; easily programmable; have no limitation of displaying special & even custom characters (unlike in seven segments), animations and so on.

A 16x2 LCD means it can display 16 characters per line and there are 2 such lines. In this LCD each character is displayed in 5x7 pixel matrix. This LCD has two registers, namely, Command and Data.

The command register stores the command instructions given to the LCD. A command is an instruction given to LCD to do a predefined task like initializing it, clearing its screen, setting the cursor position, controlling display etc. The data register stores the data to be displayed on the LCD. The data is the ASCII value of the character to be displayed on the LCD.

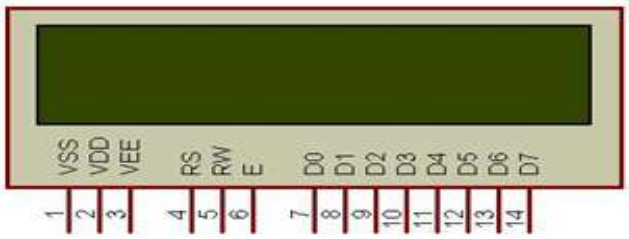

FLEX SENSOR

A flex sensor or bend sensor is a sensor that measures the amount of deflection or bending. Usually the sensor is stuck to the surface, and resistance of sensor element is varied by bending the surface. Since the resistance is directly proportional to amount of bend it is used as goniometer, and often called flexible potentiometer.

Features

- Angle Displacement Measurement
- Bends and Flexes physically with motion device
- Possible Uses
 - Robotics
 - Gaming (Virtual Motion)
 - Medical Devices
 - Computer Peripherals
 - Musical Instruments
 - Physical Therapy
- Simple Construction

APPLICATIONS

- automotive applications
- industrial applications, e.g. safety switches, shipping, machine control
- medical applications (e.g. “SmartBed”)
- gaming devices
- measuring devices
- assistive technology
- robotics (e.g. floor mapping, collision detection)

Fiber-optic bend sensors (also called optical goniometers) consist of a light source, a plastic optical fibre (POF) with an abraded section and a photosensitive detector4). Light is emitted into the POF at one end and sensed at the other end. Bending the optical fibre results in a loss of light (intensity). The loss of light is often enhanced by cutting, polishing or abrasing a part of the POF5). Due to the sensing principle single fiber-optical bend sensors are uni-polar devices.

BLUETOOTH

Bluetooth is a wireless technology standard for exchanging data over short distances (using short-wavelength UHF radio waves in the ISM band from 2.4 to 2.485 GHz) from fixed and mobile devices and building personal area networks (PANs). In 1994 a group of engineers at Ericsson, a Swedish company, invented a wireless communication technology, later called Bluetooth. In 1998, the original group of Promoter companies—Ericsson, Intel, Nokia, Toshiba and IBM—came together to form the Bluetooth Special Interest Group (SIG).

Bluetooth networking transmits data via low-power radio waves. It communicates on a frequency of 2.45 gigahertz (actually between 2.402 GHz and 2.480 GHz, to be exact). This frequency band has been set aside by international agreement for the use of industrial, scientific and medical devices (ISM). By comparison, the most powerful cell phones can transmit a signal of 3 watts. The low power limits the range of a Bluetooth device to about 10 meters (32 feet), cutting the chances of interference between your computer system and your portable telephone or television.

Some specification of Bluetooth

- Operates in the 2.4 GHZ band which is globally available
- It has 79 channels
- Uses FHSS, GFSK modulation
- 1600 hops per second
- Can support up to 8 devices in a piconet
- Omni-directional, non-line of sight transmission through walls
- 10m to 100m range
- Low cost, $20
- 1mW power
- Extended range with external power amplifier (100 meters)

APR 9600 VOICE IC:

The APR9600 device offers true single-chip voice recording, non-volatile storage, and playback capability for 40 to 60 seconds. The IC is 28 pin devices used to record & playback of maximum of 8 messages. The device supports both random and sequential access of multiple messages. Sample rates are user-selectable, allowing designers to customize their design for unique quality and storage time needs. the device is ideal for use in portable voice recorders, toys, and many other consumer and industrial applications.

The replayed sound exhibits high quality with a low noise level. Sampling rate for a 60 second recording period I s 4.2 kHz that gives a sound record/replay bandwidth of 20Hz to 2.1 kHz. However, by changing an oscillation resistor, a sampling rate as high as 8.0 kHz can be achieved. This shortens the total length of sound recording to 32 seconds.

This APR9600 voice IC has 28 pin DIP package works in supply voltage between 4.5V & 6.5V. During recording and replaying, current consumption is 25 mA. In idle mode, the current drops to 1 mA. The APR9600 experimental board is an assembled PCB board consisting of an APR9600 IC, an electrets microphone, support components and necessary switches to allow users to explore all functions of the APR9600 chip. The oscillation resistor is chosen so that the total recording period is 60 seconds with a sampling rate of 4.2 kHz. The board measures 80mm by 55mm.

PIN DIAGRAM

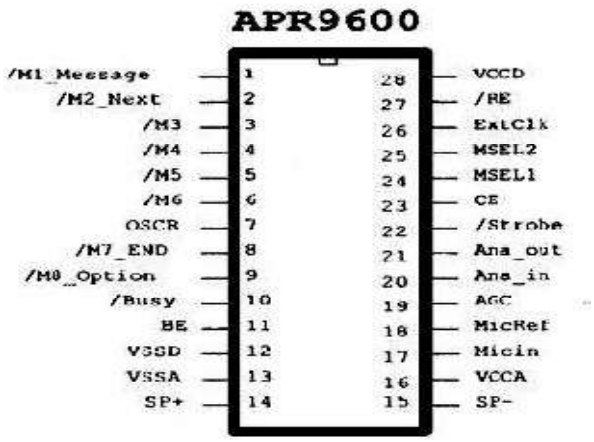

Fig: Pin-out of APR9600

RESULTS

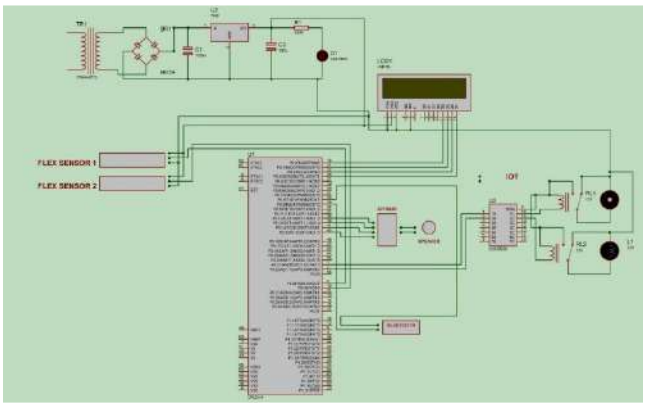

CONCLUSION

The sixth sense technology using gesture movement and speech integrated circuits are emerging innovative ideas. We have a seamless access to data or information that may exist to help us make decisions. This provides access to relevant information about the things in the environment and enables the new interactions between the real world and the world of data. Although the miniaturization of computing devices allows us to carry computers in our pockets, there had been no link between the digital devices we carry and our interactions with the physical world, and our speech in a efficient level. Sixth sense is developed to seamlessly integrate information into reality. The future may depend upon this sixth sense. May be within this 2020, the proliferation and the use of this technology is immense. Sufficient awareness of the sixth sense will lead to further development of any technology which aids for getting information and performing any type of action practically at any time, using simply the gestures and commands given. The advantage of this technology is portable, its connectedness between the world and the information as speech. Its cost effectiveness and data can access from the machine directly in real time. It can also be said as an open-source technology. Within twenty years this technology will bring a drastic change in field of science and will create a revolutionary change among the mass. The device will soon be up for sale and will be available to the common public the device will cost around 350$ without the custom-made PC. which aids for getting information and performing any type of action practically at any time, using simply the gestures and commands given.

The advantage of this technology is portable, its connectedness between the world and the information as speech. Its cost effectiveness and data can access from the machine directly in real time. It can also be said as an open-source technology. Within twenty years this technology will bring a drastic change in field of science and will create a revolutionary change among the mass.

REFERENCES

[1] Alon,J.Athitsos,V.Quan,YuanSclaroff,S. Computer Science Dept., Boston Univ., Boston, MA, USA, A Unified Framework for Gesture Recognition and Spatiotemporal Gesture Segmentation, IEEE transactions on Pattern Analysis and Machine Intelligence, Volume: 31, Issue:9 pp 1685 - 1699, Sept. 2009

[2] Mu-Chun SuInst. of Computer Science & Inf. Eng., Nat. Central Univ., Chung-Li A fuzzy rule-based approach to spatio-temporal hand gesture recognition,Systems, Man, and Cybernetics, Part C: Applications and Reviews, IEEE Transactions on Volume: 30, Issue:2 pp276 – 281., May 2000

[3] Kirishima, T. Sato, K. Chihara, K.Dept. of Electr. Eng., Nara Nat. Coll.

of Technol., Japan Robotics, Gesture Spotting and Recognition for Human–Robot Interaction, IEEE Transactions on Volume: 23, Issue:2 pp256 – 270., April 2007

[4] Real-time gesture recognition by learning and selective control of visual interest points: Pattern Analysis and Machine Intelligence, IEEE Transactions on, Volume: 27 , Issue:3, pp351 – 364., March 2005

[5] Ozer, I.B. Tiehan Lu Wolf, W. Princeton Univ., NJ, USA Design of a real-time gesture recognition system: high performance through algorithms and software Signal Processing, IEEE Volume: 22, Issue:3, pp 57 – 64., May 2005

[6] Evans, J.R. Tjoland, W.A. Allred, L.G.Ogden Air Logistics Center, Hill AFB, UT Achieving a hands-free computer interface using voice recognition and speech synthesis [for Windows-based ATE] Aerospace and Electronic Systems, IEEE Volume: 15, Issue:1, pp 14-16., Jan 2000

[7] Kaynak, M.N. Qi Zhi Cheok, A.D. Sengupta, K. Zhang Jian Ko Chi Chung Dept. of Electr. Eng., Arizona State Univ., Tempe, AZ, USA Analysis of lipgeometric features for audio-visual speech recognition Systems, Man and Cybernetics, Part A: Systems and Humans, IEEE Transactions on Volume: 34, Issue: 4, pp-564 – 570., July 2004

[8] Gomez, A.M. Peinado, A.M. Sanchez, V. Rubio, A.J.dept. eoria de la Senal, Granada Univ Recognition of coded speech transmitted over wireless channels Wireless Communications, IEEE Transactions on Volume: 5, Issue: 9, pp-2555 – 2562., September 2006

[9] Pelaez-Moreno, C. Gallardo-Antolin, A. Diaz-de-Maria, F. Dept. de Tecnologias de las Comunicaciones, Univ. Carlos III de Madrid, Recognizing voice over IP: a robust front -end for speech recognition on the world wide webMultimedia, IEEE Transactions on Volume: 3, Issue:2, pp-209 – 218., Jun 2001

[10] http://boingboing.net/2009/11/12/sixthsense-technology.html

[11] http://theviewspaper.net/sixth-sense-technology-will-revolutionise-the world

FOREST FIRE ALERTING SYSTEM WITH GPS CO-ORDINATES USING IOT

[1]Kolluru Vinay Raja, [2]Ayesha Fatima
[1]PG Scholar, Department of Electronics and Communication Engineering,
[2]Assistant Professor, Department of Electronics and Communication Engineering,
Nawab Shah Alam Khan College of Engineering & Technology, Hyderabad

ABSTRACT

In the advancing world, it is very crucial to protect our environment. Many incidents of man-made and natural disasters were happening around the world. Forest fires are one such catastrophe for environment. Once the fire inside deep forest starts, it burns and destroys everything and spreads everywhere within the forest. Fire spreads on hot days destroys trees and grasses due to drought conditions peaks in a forest region. Such forest fires disasters should be curbed in order to protect fauna and flora habitats in the forest. The objective of this work is to design and implement an IoT based system which is self-sustaining and would predict and detect the forest fires and sends the exact location to concerned officials which would help firefighting personnel to extinguish the fire in the location where it starts slowly. This would prevent the fire to spread over a huge area and also able to take precautionary measures in order to prevent the fire which may occur in near future.

Keywords— Fire Detection, Arduino, Sensors, GPS-Module Authentication, Notification.

I INTRODUCTION

Forest is a large area where it is dominated by trees and animals. Forest covers an area of around four billion hectares or approximately around 30% of world's land area. Forest is one of the huge supports for a country economic. Forest normally contains various species of trees and animals.Even human beings receive a huge profit from the forest.Some medical materials, house-hold requirements and other human requirements are got from the forest. Forest also has a huge impact on the environment which prevents the earth from over heatings.The pollution made by the humans are reduced in a greater extent by the forest. So the fire in the forest causes a great impact in the world. Forest fires are unnoticed and spread very quickly, causing millions of acres in damage and claiming many human lives every year in many countries. These forest fire can lead to a huge disaster in the environment. The losses in the forest fire are huge which affects both animals and trees. Forest fire in the world is increasing in recent times.This fire in the forest is due to natural or man-made disasters.

Lightning is one of the reason for natural forest fire.It occurs due to combustion of dry fuel in the forest like leaves.Fire caused due to man-made are more like smoking , due to any miscellaneous activities. The fire caused due to man-made are more than natural forest fire.But large area damage is caused by natural forest fire because it cannot be predicted.

The damage cause due to forest fires are more in recent years. The survey taken by National Interagency Center says that in 2016, there more than 65,575 wildlife are affected due to forest fire.In 2017, the damage has increased to around 71,499 and around 10 million acres were burned in the fire. By taking a awareness schemes,the damage has reduced to 55,911 wildlife's and about 8.6 million acres of were burned which is less compared to the year 2017. The survey also suggests that the forest fire are more in northern countries. USA has a huge number of forest fires.Early detection of hot spots and the initiation of appropriate measures can prevent, or, at least minimize damage and casualties.

So from this we can find that the damage in the forest are more and an immediate precautions has to be taken to reduce the forest fires. A possible action has to be taken by the government and also by the forest department to reduce the fire. Some of the actions taken by the government is restricting the people to enter the forest areas without any permission from the forest officers. Usage of fire causing materials are prohibited inside the forest areas,in any wild life sanctuaries and also in local forest areas. A regular monitoring activity are taken by the forest department by using cameras in the forest areas.

To avoid huge damage of forest from the natural fire an precautions are taken by the government and forest departments by having some emergency equipment's to reduce the fire like fire extinguisher and some rangers are appointed in the forest areas to give immediate information about the fire in the forest so that immediate necessary actions can be taken.

So to reduce the damages in the forest area due to forest fires a device can be used were the device is built with some modern technologies. In the modern world immediate information are send and received in a quick time. Even normal activities are informed through these technologies, it is possible and important to inform this kind of information in a quicker time. This information helps the government to reduce the damage in the forest by fire.

II. PROPOSED SYSTEM

In this system we have given an idea to detect the fire in the forest by using modern equipment's. The system is proposed to detect the fire in the forest and also to alert the forest officer about the fire in the forest. Here a micro- controller is used to control the system activities, some sensors are used to detect the fire in the forest, with detecting the fire the exact location of the fire is detected and located to the nearby forest officer. So the system is a complete IoT based system were the activities of the system is continuously monitored and the monitoring details are stored in online pages which is viewed by the officer regularly. The details are stored as a data and this data can be viewed at any time.

The figure shows the block diagram of the proposed system. Here solar panel with a battery is used to supply the source to the system. Since the system is designed to implement in the forest it not possible to provide power supply through transmission line hence a solar panel is used which can be charged and stored in a battery. It is given as source to the system.

BLOCK DIAGRAM:

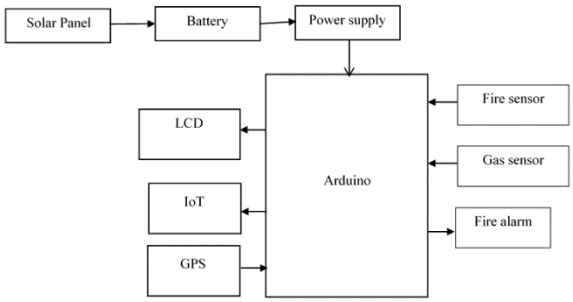

POWER SUPPLY

The power supply section is the section which provide +5V for the components to work. IC LM7805 is used for providing a constant power of +5V.

The ac voltage, typically 220V, is connected to a transformer, which steps down that ac voltage down to the level of the desired dc output. A diode rectifier then provides a full-wave rectified voltage that is initially filtered by a simple capacitor filter to produce a dc voltage. This resulting dc voltage usually has some ripple or ac voltage variation.

A regulator circuit removes the ripples and also retains the same dc value even if the input dc voltage varies, or the load connected to the output dc voltage changes. This voltage regulation is usually obtained using one of the popular voltage regulator IC units.

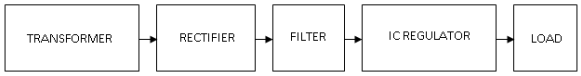

Block Diagram of Power Supply

ARDUINO UNO

Arduino/genuino Uno is a microcontroller board based on the atmega328p (datasheet). It has 14 digital input/output pins (of which 6 can be used as pwm outputs), 6 analog inputs, a 16 MHz quartz crystal, a usb connection, a power jack, an icsp header and a reset button. It contains everything needed to support the microcontroller; simply connect it to a computer with a usb cable or power it with a ac-to-dc adapter or battery to get started.. You can tinker with your uno without worrying too much about doing something wrong, worst case scenario you can replace the chip for a few dollars and start over again.

"Uno" means one in Italian and was chosen to mark the release of Arduino software (ide) 1.0. The uno board and version 1.0 of Arduino software (ide) were the reference versions of Arduino, now evolved to newer releases. The uno board is the first in a series of usb Arduino boards, and the reference model for the Arduino platform; for an extensive list of current, past or outdated boards see the Arduino index of boards.

TECHNICAL SPECIFICATIONS

Microcontroller	ATmega328P
Operating Voltage	5V
Input Voltage (recommended)	7-12V
Input Voltage (limit)	6-20V
Digital I/O Pins	14 (of which 6 provide PWM output)
PWM Digital I/O Pins	6
Analog Input Pins	6
DC Current per I/O Pin	20 mA
DC Current for 3.3V Pin	50 mA
Flash Memory	32 KB (ATmega328P) of which 0.5 KB used by bootloader
SRAM	2 KB (ATmega328P)
EEPROM	1 KB (ATmega328P)
Clock Speed	16 MHz
LED_BUILTIN	13
Length	68.6 mm
Width	53.4 mm
Weight	25 g

LIQUID CRYSTAL DISPLAY (LCD)

- LCD (Liquid Crystal Display) screen is an electronic display module and find a wide range of applications. A 16x2 LCD display is very basic module and is very commonly used in various devices and circuits. These modules are preferred over seven segments and other multi segment LEDs. The reasons being: LCDs are economical; easily programmable; have no limitation of displaying special & even custom characters (unlike in seven segments), animations and so on.
- A **16x2 LCD** means it can display 16 characters per line and there are 2 such lines. In this LCD each character is displayed in 5x7 pixel matrix. This LCD has two registers, namely, Command and Data.
- The command register stores the command instructions given to the LCD. A command is an instruction given to LCD to do a predefined task like initializing it, clearing its screen, setting the cursor position, controlling display etc. The data register stores the data to be displayed on the LCD. The data is the ASCII value of the character to be displayed on the LCD.

Fig. 16x2 LCD

ESP8266 WIFI IOT MODULE

Description:

- These modules include 1MB (8Mbit) of flash memory, twice the size of the older blue colored ESP-01 module
- The ESP8266 Serial/UART to Wi-Fi module is a great way to connect your Arduino or other microcontroller projects to a Wi-Fi network
- Create your next internet of things (IOT) project with affordable network connectivity by implementing this module into your design
- The module has the ability to run independent of a host controller
- The eight-pin header includes two GPIO pins that allow for direct connection of the module to sensors, peripherals, or host controller
    - Check out our ESP8266 breadboard adapter to use your ESP8266 module with a breadboard
- The ESP8266 has 3.6V tolerant I/Os so you will need a logic level converter to connect it with higher voltage devices such as Arduino
- The ESP8266 requires 3.3V power so you may need a 3.3V voltage regulator to provide the correct voltage, depending on your setup

Product Contents:

- 1 — ESP8266 ESP-01 Wi-Fi Transceiver Module with baud rate set at 115200 bps
- 1 (per order) — Addicore ESP8266 info card (includes pinout diagram)

Specifications:

- 802.11 b/g/n
- Serial/UART baud rate: 115200 bps
- Integrated TCP/IP protocol stack
- Input power: 3.3V (see "Recommended Accessories" below for 3.3V power options)
- I/O voltage tolerance: 3.6V Max (see "Recommended Accessories" below for level converters to connect to higher voltage devices (i.e. Arduino))
- Regular operation current draw: ~70mA
- Peak operating current draw: ~300mA

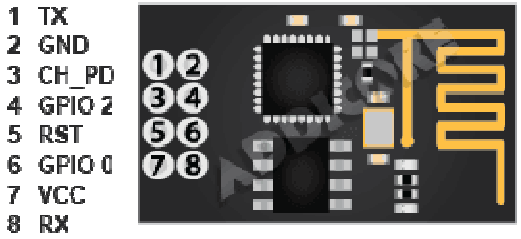

GLOBAL POSITIONING SYSTEM

- The Global Positioning System (GPS) is a satellite-based navigation system that can be used to locate positions anywhere on earth. Designed and operated by the U.S. Department of Defense, it consists of satellites, control and monitor stations, and receivers. GPS receivers take information transmitted from the satellites and uses triangulation to calculate a user's exact location. GPS is used on incidents in a variety of ways, such as:

- GPS is made up of three parts: between 24 and 32 satellites orbiting the Earth, four control and monitoring stations on Earth, and the GPS receivers owned by users. GPS satellites broadcast signals from space that are used by GPS receivers to provide three-dimensional location (latitude, longitude, and altitude) plus the time.

BUZZER

- A buzzer or beeper is a signaling device, usually electronic, typically used in automobiles, house hold appliances such as a microwave oven, or game shows.
- It most commonly consists of a number of switches or sensors connected to a control unit that determines if and which button was pushed or a preset time has lapsed, and usually illuminates a light on the appropriate button or control panel, and sounds a warning in the form of a continuous or intermittent buzzing or beeping sound.
- Initially this device was based on an electromechanical system which was identical to an electric bell without the metal gong (which makes the ringing noise). Often these units were anchored to a wall or ceiling and used the ceiling or wall as a sounding board. Another implementation with some AC-connected devices was to implement a circuit to make the AC current into a noise loud enough to drive a loudspeaker and hook this circuit up to a cheap 8-ohm speaker. Nowadays, it is more popular to use a ceramic-based piezoelectric sounder like a Son alert which makes a high-pitched tone. Usually these were hooked up to "driver" circuits which varied the pitch of the sound or pulsed the sound on and off.

GAS SENSOR

A gas detector is a device which detects the presence of various gases within an area, usually as part of a safety system. This type of equipment is used to detect a gas leak and interface with a control system so a process can be automatically shut down. A gas detector can also sound an alarm to operators in the area where the leak is occurring, giving them the opportunity to leave the area. This type of device is important because there are many gases that can be harmful to organic life, such as humans or animals.

In current technology scenario, monitoring of gases produced is very important. From home appliances such as air conditioners to electric chimneys and safety systems at industries monitoring of gases is very crucial. Gas sensors are very important part of such systems. Small like a nose, gas sensors spontaneously react to the gas present, thus keeping the system updated about any alterations that occur in the concentration of molecules at gaseous state.

Gas sensors are available in wide specifications depending on the sensitivity levels, type of gas to be sensed, physical dimensions and numerous other factors. This Insight covers a methane gas sensor that can sense gases such as ammonia which might get produced from methane. When a gas interacts with this sensor, it is first ionized into its constituents and is then adsorbed by the sensing element. This adsorption creates a potential difference on the element which is conveyed to the processor unit through output pins in form of current.

FIRE SENSOR

The Fire sensor, as the name suggests, is used as a simple and compact device for protection against fire. The module makes use of IR sensor and comparator to detect fire up to a range of 1-2 meters. The device, weighing about 5 grams, can be easily mounted on the device body. It gives a high output on detecting fire. This output can then be used to take the requisite action. An on-board LED is also provided for visual indication.

Feature

- Typical Maximum Range :2 m .
- Indicator LED with 3 pin easy interface connector.
- Operating Voltage 5v

An automatic fire sensor sense the unwanted presence of fire by monitoring environmental changes associated with combustion. In general, a fire alert system is classified as either automatically actuated, manually actuated, or both. Fire sensor are intended to notify the fire in the building occupants to evacuate in the event of a fire or other emergency, report the event to an off-premises location in order to summon emergency services, and to prepare the structure and

associated systems to control the spread of fire and smoke.

BATTERY

A battery is a device consisting of one or more electrochemical cells that convert stored chemical energy into electrical energy. Batteries are another way to produce electricity. They are smaller and more safe. Batteries have one end that is positive and one end that is negative. For batteries to work, you need to make sure you put them in the right way. Batteries have become a common power source for many household and industrial applications.

There are two types of batteries: primary batteries (disposable batteries), which are designed to be used once and discarded, and secondary batteries (rechargeable batteries), which are designed to be recharged and used multiple times. Batteries come in many sizes, from miniature cells used to power hearing aids and wristwatches to battery banks the size of rooms that provide standby power for telephone exchanges and computer data centers.

A battery is a device that converts chemical energy directly to electrical energy. It consists of a number of voltaic cells; each voltaic cell consists of two half-cells connected in series by a conductive electrolyte containing anions and cations. One half-cell includes electrolyte and the electrode to which anions (negatively charged ions) migrate, i.e., the anode or negative electrode; the other half-cell includes electrolyte and the electrode to which cations (positively charged ions) migrate, i.e., the cathode or positive electrode. In the redox reaction that powers the battery, cations are reduced (electrons are added) at the cathode, while anions are oxidized (electrons are removed) at the anode. The electrodes do not touch each other but are electrically connected by the electrolyte. Some cells use two half-cells with different electrolytes. A separator between half-cells allows ions to flow, but prevents mixing of the electrolytes

SOLAR PANEL

Solar panels are devices that convert light into electricity. They are called "solar" panels because most of the time, the most powerful source of light available is the Sun, called Sol by astronomers. Some scientists call them *photovoltaic* which means, basically, "light-electricity."

Fig. Solar Panel

Solar panel consists of solar power cells convert sunlight into electricity, using the energy of speeding photons to create an electrical current within a solar panel.

Photons are created in the center of the sun by the fusion of atoms. It takes a photon about a million years to work its way to the surface of the sun, but once free it is hurled through space so fast that it reaches earth in just eight minutes - after traveling 93 million miles.

This tremendous energy from the sun is abundant, and has been powering the earth for billions of years - feeding plants, redistributing and refreshing water supplies and ultimately creating other forms of energy (such as fossil fuels) that largely power our civilization today.

Over the past several decades, scientists have been learning to harness this ancient energy source with more efficiency to do the work of non-renewable fuels - without pollution, noise or radiation, and not subject to economic whims that drive costs higher each year.

IV. RESULTS

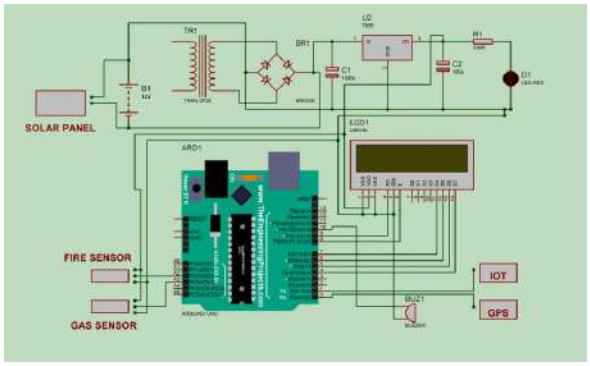

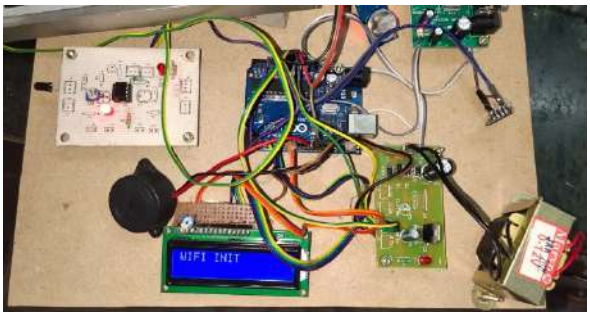
WIFI INIT

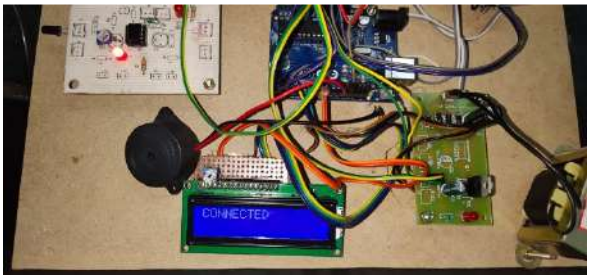
CONNECTED

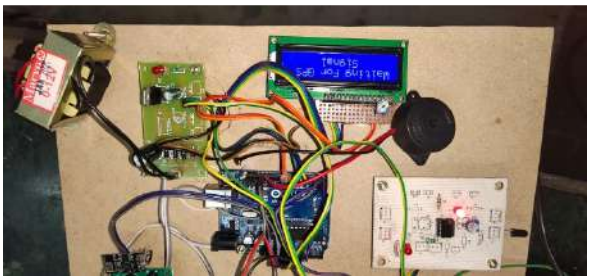

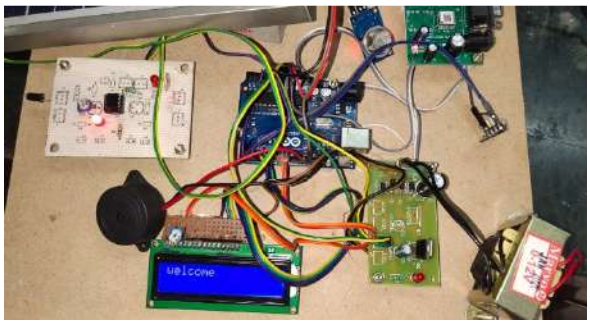
welcome

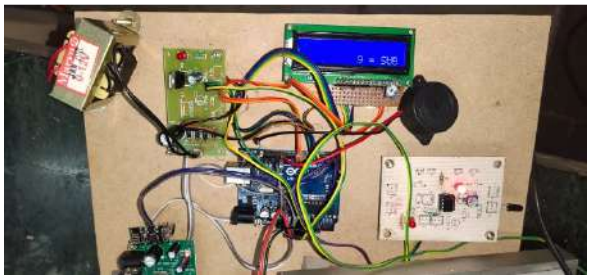

V. CONCLUSION

Science and technology is panacea for all our growing problems. Predicting the natural processes are highly complex and our system needs to be tested against real time conditions. Though our system is self- sustaining and standalone, other factors which would affect the hardware were tested against time. It shall be implemented in small forest areas where chances of occurrence of forest fires were high. The system needs to be robust to withstand all the climate changes which may affect its functioning. However, our system will play a crucial role in curbing the forest fires which would prevent loss of huge resources and financial losses. We have tested in forest like conditions, but real hardship which we may face is during implementation in large area in real time.

REFERENCES

[1] Imteaj, Rahman, Husain, M. K., Alam, M. S., & Rahat, S. A.(2017, February) „An IoT based fire alarming and authentication system for workhouse using Raspberry Pi 3"In Electrical, Computer and Communication Engineering (ECCE), International Conference on (pp. 899-904). IEEE.

[2] Sharma, Abhinav Kumar, M d Faiz Raza Ansari, M d Firoz Siddiqui, and Mirza Ataullah Baig. Iot Enabled Forest Fire Detection and Online Monitoring System. "

[3] Owayjan, Freiha, Achkar, Abdo & M allah, (2014, April)Firoxio: Forest fire detection and alerting system"In Mediterranean Electro technical Conference(M ELECON), 2014 17th IEEE (pp. 177-181). IEEE.

[4] H. Anandakumar and K. Umamaheswari, "Supervised machine learning techniques in cognitive radio networks during cooperative spectrum handovers," Cluster Computing, vol. 20, no. 2, pp. 1505– 1515, Mar. 2017.

[5] A. Roshini and H. Anandakumar, "Hierarchical cost-effective leach for heterogeneous wireless sensor networks," 2015 International Conference on Advanced Computing and Communication Systems, Jan. 2015.

[6] H. Anandakumar and K. Umamaheswari, "An Efficient Optimized Handover in Cognitive Radio Networks using Cooperative Spectrum Sensing," Intelligent Automation & Soft Computing, pp. 1–8, Sep. 2017.

[7] M. Suganya and H. Anandakumar, "Handover based spectrum allocation in cognitive radio networks," 2013 International Conference on Green Computing, Communication and Conservation of Energy (ICGCE), Dec. 2013.

[8] H. Anandakumar and K. Umamaheswari, "A bio-inspired swarm intelligence technique for social aware cognitive radio handovers," Computers & Electrical Engineering, vol. 71, pp. 925–937, Oct. 2018.

[9] Anandakumar, "Energy Efficient Network Selection Using 802.16g Based Gsm Technology," Journal of Computer Science, vol. 10, no. 5, pp. 745–754, May 2014.

[10] Kirubaharan, Sunder, Ramesh, & Dhinakar, (2014). „Intruder Detection and Forest Fire Alert System with Using Wireless Sensor Network" International Advanced Research Journal in Science, Engineering and Technology.

[11] Akash V. Bhatkule1 Ganesh, Anand, Arun, Dinesh,Gunaseelan, & Karthik, R. (2013) „ Forest fire detection using optimized solar–powered ZigBee wireless sensor networks "International journal of scientific and engineering research, 4, 586-596.

[12] Sathishkumar, R., Vinothkumar, M., Devaraj Varatharaj, S., & Gowthaman, S. M. (2016) „Design and Development of Automatic Fire Detection Using Sms And Voice Alert System" International Journal of Scientific & Engineering Research, 7(5), 114-117.

AUTHOR'S PROFILE

Mr. KOLLURU VINAY RAJA has completed his B.Tech (ECE) from Mahaveer Institute of Science and Technology, Bandlaguda, Hyderabad District, JNTUH. Presently, he is pursuing his Masters in Embedded system from Nawab Shah Alam khan College of Engineering and Technology, Hyderabad, TS. India.

Ms. AYESHA FATIMA has completed B.Tech (ECE) from Vignan Institute of technology and Science, JNTUH, M.Tech (VLSI) from Royal Institute of Technology, JNTUH, Currently she is working as an Assistant Professor of ECE Department in Nawab Shah Alam khan College of Engineering and Technology, Hyderabad, TS. India.

RESEARCH AND DESIGN OF CRYPTOGRAPHY CLOUD FRAMEWORK

[1]Sidra Mahveen Farha, [2]Mohammed Abdul Rawoof, [3]Mohammad SanaullahQaseem
[1]M.Tech Scholar, Department of Computer Science Engineering and Technology,
[2]Associate Professor & Project Coordinator, Department of Computer Science and Engineering,
[3]Professor and Head, Department of CSE, Vice Principal (Academics) IQAC Coordinator,
Nawab Shah Alam Khan College of Engineering & Technology, Hyderabad

ABSTRACT: Since the application method of cryptography innovation presently has various sorts in the cloud climate, a novel cryptography cloud system was proposed, because of the non-expandability of cryptography assets. Through investigating on the application models of the current encryption innovation, the cryptography administration interest under the haze climate and the virtual construction of the cloud cryptography machine, this paper planned the system of the cryptography cloud structure that furnishes cryptography administrations with the distributed computing mode. The plan thought of the structure is elucidated from two viewpoints incorporate the capacity of modules and administration stream of cryptography cloud, which brought about the improvement of the adaptability of the use of cryptography innovation in the cloud climate. Through the investigation of framework capacity and the board mode, it outlined the accessibility and security of cryptography cloud system. It was demonstrated that cryptography cloud has the qualities of high-accessibility in the execution and analysis, and it can fulfill cryptography administration interest in the cloud climate.

1. INTRODUCTION

As of now, data innovation with the quick advancement advances the beat and speed of society. With the help of attributes of distributed computing that incorporate high versatility, high dependability and adaptability, increasingly more application frameworks relocate to the cloud to conveyed, for accomplishing the objective of brought together administration of information and productive utilization of assets. Distributed computing innovation has been broadly utilized in the data arrangement of industry, account and government, which incredibly encourages the work and life of individuals; simultaneously, network data has become a significant vital asset, whose security can't be thought little of. To ensure security of data information in the organization climate, cryptography application mode under the haze registering climate turns out to be especially significant. While the conventional cryptography innovation is restricted to fixed transporter and non-adaptable cryptography figuring asset, so it can't fulfill the encryption prerequisites of enormous cloud information [1]. The origination of Crypto as a Service (CaaS) [2] [3] built up the idea of distributed computing from the part of data security, it finds another path for the utilization of the cryptography innovation in the cloud climate, likewise assists with advancing the new strategy. As indicated by the report of distributed computing standard [4] distributed by the NIST in 2011, the security of distributed computing can be partitioned into 3 sections, which are the security of cloud application, the security of cloud information and the security of cloud equipment with the virtualization. There into, the security of cloud application is mostly about the examination on terminal gear and organization gear upheld by confided in innovation, additionally on the unwavering quality and security of rethinking estimations; the exploration on cloud information security incorporates privacy, honesty, consistency and dependability of distributed storage information; the significant examination on the security of cloud equipment with the virtualization are weaknesses of equipment offices regarding virtualization, security conventions and procedure of virtualized organization and security innovation of cloud asset pool just as the upper virtual machine [5]. Cloud cryptography specialist organizations that incorporate Amazon Web Services (AWS), Alibaba Cloud, JN TASS and Sansec have advanced highavailable security arrangements of the cloud, for example, AWS CloudHSM administration that is the first to be accomplished commercialization. Notwithstanding that, CloudHSM administration primarily gives key administration capacities to the AWS cloud, and equipment security module (HSM) in which has the capacity of capacity and the board of clients' private key, and has the attributes of fast figuring and significant level security necessities [6]. Alibaba Cloud dispatched cloud information encryption administration [7] jointed JN TASS, which is to give believable information security answers for clients that dependent on equipment figure machine affirmed by State Cryptography Administration (SCA). Sansec set forward a progression of cloud security arrangements from the point of view of framework security, application stage security and organization transmission security, all of which have the duty of an assurance to ensure security of keys and the believability of cloud cryptography administration. At the current stage, the vast majority of cryptography applications have given security of business application data by the cloud figure machine and other equipment gadgets. So that, research on cloud cryptography administration that depends on offices with virtualization work is getting continuously develop, however it actually comes up short on the cryptography

administration framework with distributed computing model to give cryptography administrations.

2. RELATED APPLICATIONS

At present, the acknowledgment of cloud cryptography administration mostly relied upon the arrangement of cryptography gear in cloud climate, for example, the cloud worker with HSM worked in that AWS and HUAWEI had dispatched, the confided in worker that was the advancement of INSPUR and the cloud security arrangement dependent on crypto card that was created by Sansec. Zeroed in on the security of cloud server farm, it is the primary answer for "three-in-one" cloud security chain of command incorporate equipment security, framework wellbeing and programming security, and which depends on security and dependability of the basic confided in equipment hardware. Also, utilizing the key with privacy and controllability, it could fortify security assurance of the framework to give high security-level equipment encryption administration for application information. Plan of cryptography administration framework has bunches of types, which is principally founded on the customary code machine, additionally it has been not able to meet the prerequisites of information security under the current distributed computing climate. KOU [8] introduced a superior cryptography administration model, through the plan of a brought together help interface and the relating cryptography sources booking calculation, intending to accomplish bound together administration for cryptography administration assets of various code machines. However, it is as yet lacking in the parts of security the board of keys and execution of cryptography administration, for example, key security issues and execution disengagement issues. Focusing on the security of keys, WANG [9] introduced a cryptography administration system dependent on the outsider that key administration community. Keys are put away in the outsider that is respectable, and access control strategy and validation innovation are utilized to keep classified data of clients from malevolent altering or pilferage. The unlawful client gets to their own vital data as indicated by their necessities, however trust of the outsider can't be estimated equitably, so there are as yet existing security dangers partly. The influx of believed worker of INSPUR dispatched a major answer for the trust issue of key administration community. From the BIOS to the equipment arrangement of worker, and afterward to the working framework and utilizations of framework, believed estimation innovation makes the essential equipment offices of key administration community dependable in a general sense. In any case, it actually couldn't dispose of misappropriation of the inner chief, and to address which, it needs to reinforce the imperatives and the board from the point of approaches and guidelines [10]. Ciphergraph in cloud climate is applied in the entire cloud administration chain of importance that incorporate three layers, IaaS, PaaS and SaaS[11] individually. What's more, which gives cryptography assets and administrations to safety efforts utilized in the assistance order, including a wide range of cryptography calculations, cryptography application interfaces and cryptography administration conventions? AWS CloudHSM administrations, encryption administrations of Alibaba Cloud [19] and key administration administrations of HUAWEI all upheld by HSM, additionally, which is utilized as a key store transporter conveyed in distributed computing climate as shown in Figure 1, cryptography service mode.

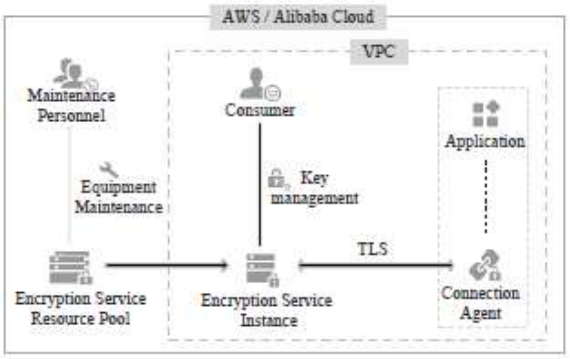

Figure 1. Cryptography service mode

Public cloud is made out of a majority of virtual private cloud (VPC). The cloud encryption administration asset pools are shaped by cloud figure machine group that upheld virtualization capacities. What's more, upkeep staffs are answerable for the upkeep of cloud figure machine and specialized help. Plus, cloud encryption administration asset pools associate with VPC through actual organization, and give whom cryptography administration occurrences. Correspondences channel between business cloud and cryptography administration occurrences are scrambled by security attachment layer (SSL) convention to fulfill cryptography administration need of business application. Figure 2 is the key administration design that is standard at present. Purchasers can encode information by DEK that given by key administration (KMS) to guarantee that basic business information is secure. There into, business information is encoded by DEK, and DEK is scrambled by CMK that put away in key administration community (KMC), in addition, CMK is encoded by root key dependent on HSM that as the foundation of trust to guarantee that root key can't be taken from outside of the framework, in this way, a total chain of trust can be organized. What's more, data channel is encoded by transport layer security (TLS1.2) convention among HSM and KMS, and which among KMS and business to guarantee the dependability of the chain of trust.

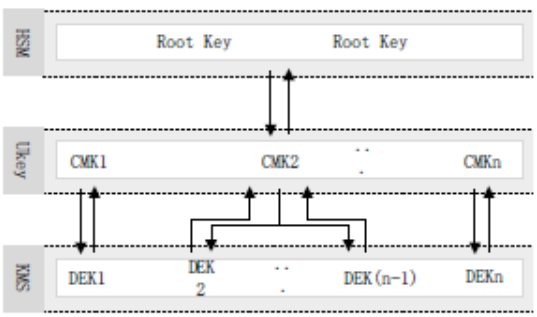

Figure 2. Key management service architecture

The turn of events and utilization of cloud cryptographs administrations improved on the plan and execution of cryptography administration framework, with the goal that the utilization of code chart in the cloud climate become standardized, and purchasers regularly need encryption and unscrambling activities to hold information [3] [16]. Furthermore, the administration and dispersion of keys and certifications can exist as fundamental security administrations. Drawing on the attributes of the current cloud cryptography administrations, and for that the cryptography administration framework become more adjusted to distributed computing climate, it is basic to contemplate the cryptography administration framework, which should be considered a further plan with key administration work, adaptable augmentation, simple to utilize, and meeting administrative consistence prerequisites.

3. PROPOSED CONSTRUCTION

A. Requirement Analysis of Cloud Cryptography Services

As increasingly more business frameworks are conveyed or relocated to the cloud, the application issue of customary ciphergraph in the cloud climate is turning out to be increasingly more featured [17]. Nonetheless, there are predominantly four angles to expound. To start with, limitation of the applicable cryptography standard and strategy; Second, cryptography registering assets could be squandered halfway, and support the executives is troublesome; Third, the board and utilization of the key are portrayed by decentralization and intricacy, and there is the danger of security and the board; Fourth, the way that cloud gives keys and cryptography administrations to customers is dangerous and untrusted. Distributed computing has the qualities of versatility figuring and dynamic extension, and it has incredible adaptability on the stockpile side of processing assets. The cryptography administration framework embracing distributed computing mode is not difficult to meet the necessities about encryption capacity focusing on the huge information that is progressively moving. In view of the possibility of programming characterize cryptography, the cryptography assets are virtualized into a cryptography assets pool by virtualization innovation (VT), and which furnishes purchasers with cloud cryptography administration dependent on organization as per their requirements. Additionally, registering capacity of the framework is versatility extendible, to give cryptography benefits that can be progressively planned and to oversee keys that is brought together and productive. Additionally, it can maintain a strategic distance from cryptography assets being inactive or inadequate.

B. Virtualization Structure of Cloud Encrypt Machine

Cryptography cloud gives customers secure and dependable cryptography administrations. The client situated cryptography specialist organization is Virtual Cipher Machine (VCM). VCM is a finished code machine framework that is a product reproduced framework with capacities same as equipment encode framework, and which runs in a totally segregated climate. Figure 3 shows virtualization design of cloud figure machine. Cloud figure machine upholds equipment virtualization innovation, and which changes the conventional crypto gadget into a cloud crypto gadget that underpins sending in cloud. The gadgets in the basic equipment framework, like CPU, memory, network gadget and crypto card, are coherently partitioned into different virtual Units, like vCPU, virtual memory, virtual crypto card (vCC, etc. KVM oversees and arranges cloud cryptography capacities utilizing VCM as administration transporter. Thereinto, crypto card gives shareable cryptography assets dependent on single-root I/O virtualization (SR-IOV), and the SR-IOV standard permits effective sharing of PCIe gadgets among VCMs, and it can have I/O execution equivalent to that of host machine [11][10]. VCMs are detached from one another and have totally segregated key frameworks and spaces. To guarantee the total security of customer scratches, all cryptography tasks are eventually finished by crypto cards, moreover, plaintext enters just show up in equipment.

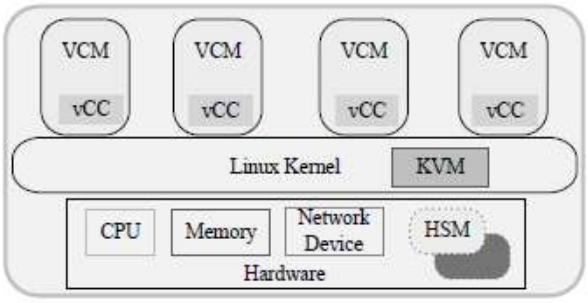

Figure 3. Virtualization structure of cloud cipher machine

4. IMPLEMENTATION AND EXPERIMENT

A. Plan of Deployment

CC depends on OpenStack [14] that is a sort of cloud stage has a place with open source. Which is like a cloud administration foundation of Amazon, and there are correspondence and relationship between work modules of framework and useful segments of OpenStack. OpenStack incorporates four significant useful segments, who are Keystone that is confirmation administration, Glance that is picture administration, Neutron that is network the board administration, and Nova that is virtual machine the executive's administration. Also, OpenStack was grown furthermore to turn into an administration foundation of CC [15]. Thereinto, Keystone relates with validation module, Neutron compares with network supervisor, Glance and Nova was coordinated into a natural entire that relates with screen of cloud figure machine and VCM the board scheduler.

B. Environment of System

Cloud figure machine is made by Inspur worker and Intel quickening agent. There are 4 arrangements of Inspur worker, whose model number is NF5270M4, and the motherboard is Intel C610, there are six arrangements of PCI-E 3.0 extension, a few 6-center processers, whose model number is Intel(R) Xeon(R) CPU E5-2620 v3 @ 2.40GHz. In addition, there are memory that is a sum of, several Gigabit Ethernet, and quadruplicate SSD plates that is an aggregate of 4TB. Per worker is embedded with six quickening agents, whose model number is Intel Corporation DH895XCC Series QAT. KMC is made out several confirmation workers, whose model number is Net Attest EPS ST 01. Cloud figure machine is sent with Linux working framework, whose rendition is CentOS7-x86_64-1511, portion form in which is Linux 3.10.0; OpenStack variant is the steadiest Newton. Confirmation worker upholds confided in figuring innovation, with proficient CA capacities.

C. Implementation of VCM

The center component of the redeveloped OpenStack is foundation the executives of cryptography administrations, there are essentially creation, relocation and erasure of VCM. Figure 4 is the administration cycle of VCM. Thereinto, the relocation of VCM as the concentration in the underlying phase of examination. the essential examination is the execution of fundamental elements of framework, which is the creation and erasure of VCM.The process of creating VCM by users is described as following pseudo code:

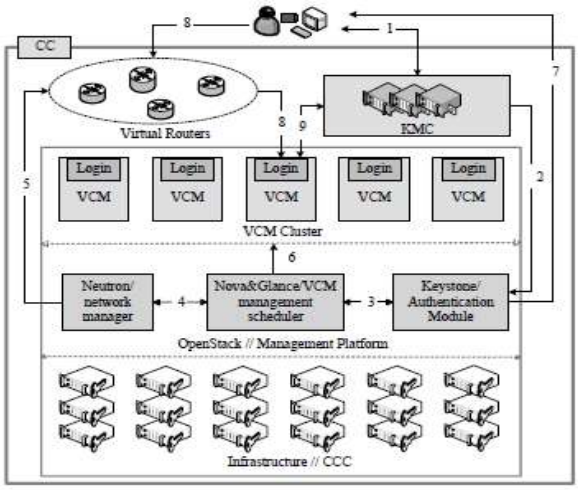

Figure 4. The management process of VCM

i) Process of VCM Creation:
INPUT USER ID //*from USBkey*//
build_vcm_request() //*from business VM*//

Step one
If **USBkey**TRUE
ID→Terminal
Then
Terminal responding
auth_identity_request()→KMC
build_vcm_request()→KMC
//*A→B is interpreted as that A is delivered into B*//

Step Two
KMC responding
If **ID** TURE
user_vcm_token is generated
user_vcm_token→Keystone

Step Three
Keystone responding
user_vcm_tokenis writed into **Keystone_Database**
user_vcm_token→Nova

Step Four
Nova responding
user_vcm_IDis generated
secure-region_deploy_request()→Neutron
instance_build_order()→Glance

Step Five
Neutron responding
secure-region_info() defines **vcm_virtual-net**

Step Six
Glance responding
VCM-Image is generated
return build_successful→Keystone

Step Seven
Keystone responding
login_permit() is generated
login_permit()→Terminal

Step Eight
Terminal responding
Login()→VCM_instance

Step Nine
VCM_instanceresponding
Terminal responding
KMC responding
CRYPTOGRAPHY SERVICE OF THE USER (ON)

The process of deleting VCM by users is described as Following pseudo-code:
ii) Process of Deletion of VCM:
INPUT USER ID //*from USBkey*//
deleted_vcm_request() //*from business VM*//

Step one
If USBkey TRUE
ID→Terminal
Then
Terminal responding
auth_identity_request()→KMC
delete_vcm_request()→KMC
//*A→B is interpreted as that A is delivered into B*//

Step Two
KMC responding
If ID TURE
user_vcm_token is deleted
token_delete()→Keystone

Step Three
Keystone responding
user_vcm_token is deleted from Keystone_Database
instance_delete()→Nova&&Glance

Step Four
Nova responding
secure-region_delete_request()→Neutron
instance_delete_order()→Glance
user_vcm_ID is deleted

Step Five
Neutron responding
Secure_delete_info is generated as Deletion Plan
then
vcm_virtual-net is deleted

Step Six
Glance responding
VCM-Image is deleted

return delete_successful→Keystone

Step Seven
Keystone responding
delete_permit() is generated
delete_permit()→Terminal

Step Eight
Terminal responding
PRINT "NO CRYPTO-SERVICE OFFER"
CRYPTOGRAPHY SERVICE OF THE USER (OFF)

5. RESULT

Figure: New User Registration

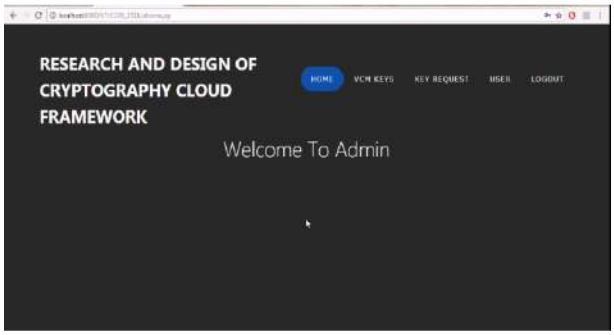

Figure: Admin Homepage

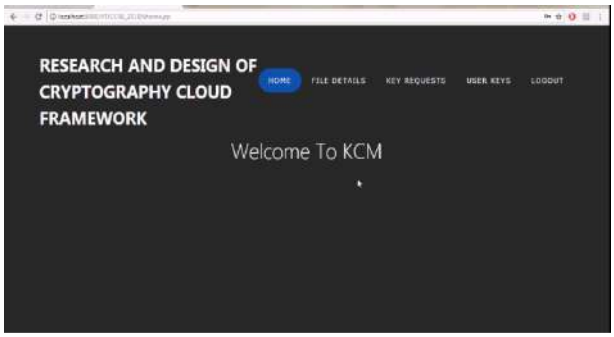

Figure: KCM Homepage

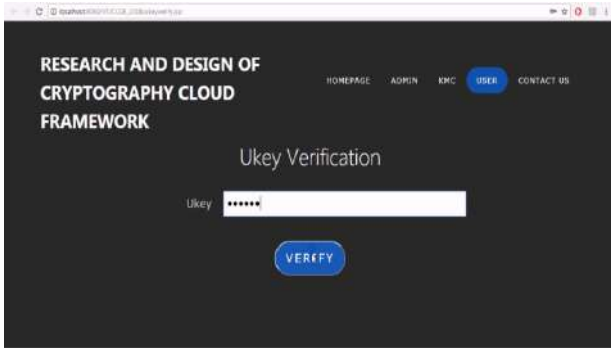

Figure: User UKeys Verification

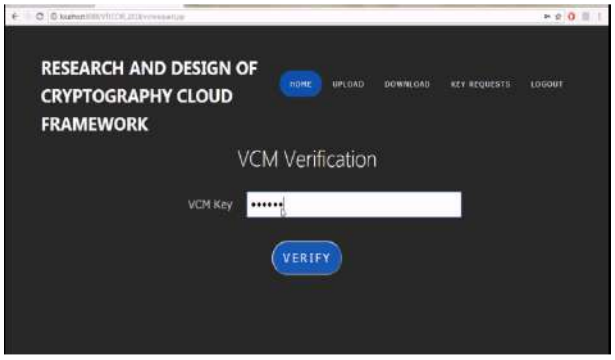

Figure: Providing UKeys For Verification

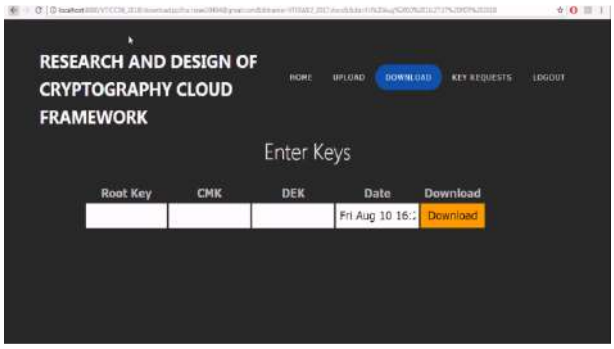

Figure: Decrypting Files Key

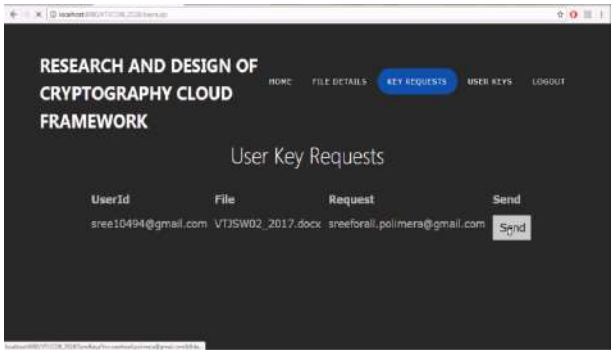

Figure: User Key Requests

6. CONCLUSION

The persistent advancement of code chart has gone to the phase of cloud cryptography administration. Cryptography administration is moving toward normalization, systematism and industrialization. The plan of CC system is proposed in this paper, which gives that offering cryptography administration with distributed computing model to the shoppers. It takes care of the issue of the contradiction of conventional code diagram in the cloud climate and beats the constraints of transporter of customary cryptography administration framework to extend and share cryptography asset. Notwithstanding, there are as yet numerous logical issues should be concentrated critically, for example, key exchange issue in the planning interaction of cryptograph assets and key stockpiling issue in the sharing cycle of cryptography asset, etc.

REFERENCES

[1] ZHANG Y, CEN R, SHEN Y, et.al. The Application of Cryptography Resource System in Cloud Computing [J]. Journal of Information Security Research, 2016, 2(6):558-561.

[2] SUN L, DAI Z. Research on Framework of Security Service Cloud Computing [J]. Journal of Computer Applications, 2012, 32(1):13-15.

[3] Wang M, Liu L. CRYPTO AS A SERVICE[C]//THE 2th International Workshop on Cloud Computing and Information Security. Atlantis Press. shanghai: CCIS, 2013:152-155.

[4] National Institute of Standards and Technology. The NIST definition of cloud computing. Technical Report, No.800-145, 2011.

[5] ZHANG Y, WANG X, LIU X, et.al. Survey on Cloud Computing Security [J]. Journal of Software, 2016, 27(6):1328-1348.

[6] AWS Support Center. AWS CloudHSM User Guide [EB/OL]. Seattle: Amazon Web Services, Inc. or its affiliates.2017[2017-12-02].

[7] QI K. The first Cloud Data Encryption Service released by Alibaba Cloud and JN TASS [J]. Information Security and Communications Privacy, 2016(1):87-87.

[8] KOU W, CHEN L. General High-Performance Cryptographic Service System Model [J]. MICROELECTRONICS & COMPUTER, 2016, 33(10):87-90.

[9] WANG Z, SUN L, GUO S. Real-time Task Threshold Scheduling Method for Cryptography Cloud based on Rolling Optimization [J]. Journal of Computer Applications, 2017, 37(10):2780-2786.

[10] LIU G, WU B, ZHANG Y. Research on Key Techniques of Trusted Server Platform in Cloud Environment [J]. Journal of Information Security Research, 2017, 3(4):323-331.

[11] Dong Y, Yang X, Li J, et al. High-performance network virtualization with SR-IOV[C]// IEEE, International Symposium on High PERFORMANCE Computer Architecture. IEEE, 2010:1471-1480.

[12] LIU W, QIU X, WANG X. Software Defined Security -SDN/NFV Disclosure of New Network Security [M]. Beijing: China Machine Press, 2017.

[13] LU W, CAI X, WANG H. Discussion on Availability Analysis of Cloud Computing System [J]. Information and Communication technologies, 2015(2):16-21.

[14] YI Y. OpenStack: Open-Source Cloud[M]. Beijing: Tsinghua University press, 2014.

[15] YANG S G, ZHANG Y Y. A cloud computing resource pool system and its implementation: CN, CN103581324A[P]. 2014-02-12.

[16] FENG D G, ZHANG M, ZHANG Y, et al. Study on cloud computing security[J], Journal of Software, 2011, 22(1):71-83.

[17] ZHANG Y, QIN R W, SHEN Y C, et al. The application of cryptography resource system in cloud computing[J]. Journal of Information Security Research, 2016, 2(6): 558-561.

[18] WANG B F, SU J S, CHEN L. Review of the design of data center network for cloud computing[J]. Journal of Computer Research and Development, 2016, 53(9):2085-2106.

Strength and Permeability Properties of concrete using fly Ash, rice husk Ash, and Ground Granulated Blast Furnace Slag

Salem Ahmed Ali[1],Salahuddin Shakeeb S.M[2] Mohd Farrukh Anwar[3]

[1] Pg Student, M.Tech in Structural engineering, Department of Civil Engineering, Nawab Shah Alam Khan College of Engineering and Technology, 6-4-1, New Malakpet, Near Railway Station, Hyderabad, Telangana 500024

[2] Assistant Professor, M.Tech in Structural engineering, Department of Civil Engineering, Nawab Shah Alam Khan College of Engineering and Technology, 6-4-1, New Malakpet, Near Railway Station, Hyderabad, Telangana 500024

[3]Head of the Department (PHD) , Vice Principal ,M.Tech in Structural engineering, Department of Civil Engineering, Nawab Shah Alam Khan College of Engineering and Technology, 6-4-1, New Malakpet, Near Railway Station, Hyderabad, Telangana 500024

Abstract: ***cement industry may be one amongst the key sources of environmental pollution so the reduction of cement demand should be improved. Fly ash(FA), Rice husk ash(RHA) and Ground granulated blast furnace slag (GGBS) are the by-products of industries and it ought to be reused to scale back the waste pollution. Therefore the present study is directed towards developing a better understanding on the combined performance of FA,RHA and GGBS on the strength properties of Ternary concrete over an Ordinary concrete. This work primarily deals with the strength characteristics such as Compressive, Split Tensile and Flexural Strength. Total 5 Different concrete mixtures were cast and tested with different cement replacement levels (5%, 10%,15%,20%,25%) of combination of three byproducts .Compressive ,Split Tensile and Flexural Strength of Ternary Blended Concrete At the ages of 7, 28, 60 and 90 days for various combinations FA,RHA, and GGBS..All Mixes were studied at water cement ratio of 0.50 and 0.40. The cement has been replaced by rice husk ash, accordingly in the range of 0%, 5 %, 10 %, 15 %, and 20 % by weight. Concrete mixture of M 30 and M40with RHA, were produced, tested and compared in terms of compressive strengths with the Conventional concrete. These tests were carried out to evaluate the mechanical properties for the test results of 7, 28, 56, 90 days for compressive strengths in normal water and in MgSO4 solution of 1% and 5%. Also the durability aspect for rice husk ash concrete for sulphate attack was tested. Similarly the above tests were also performed for FA and SCBA The experimental results shows that, the strength properties of ternary blended concrete increase with increase in cement replacement levels of FA,RHA, and GGBS.. (20%),the addition of FA,RHA, and GGBS does not improve the strength properties of compressive, Split Tensile and Flexural, durability tests are also performed.***

Key words: ***Fly Ash, Rice Husk Ash, GGBS, Concrete, M30 grade concrete M40 grade concrete, cubes, cylinders, MgSO4, durability.***

I.INTRODUCTION

These days researchers are studying different agro-based waste materials. The major quantities of waste generated from agricultural sources include sugarcane bagasse, rice husk, and coconut husk. Reusing such waste as a sustainable construction material seems to be a suitable solution for the problem of land filling and the high cost of building materials (Rabi et al 2009). These days, agricultural solid waste materials are being reused in manufacturing blended mortars and concrete for better performance and price. The use of waste materials in concrete has been a continuous procedure in different industries. These waste agricultural materials are used to heighten the mechanical properties of a building material while they are not useful in agriculture fields. Rice husk ash (RHA), sugarcane bagasse ash (SCBA), sawdust and cork granules have been used as pozzolanic materials for reactivity in concrete. They are added to concrete to partially replace cement in concrete mixtures so that the concrete will have sufficient engineering physical and chemical properties. RHA has been used as a suitable raw material to make hydraulic cement and as a good corrective admixture to reduce expansion that occurs as a result of an alkali-silicate reaction, and also to reduce the temperature in high-strength concrete SCBA is a valuable cement-replacing material for cement and concrete production because of its high content of silicon and aluminium oxides. Also, the effect of elevated temperature on strength of normal and high strength concrete with and without different ashes is investigated by different researchers.

FLY ASH

Fly ash is a fine powder which is a byproduct from burning pulverized coal in electric generation power plants. Fly ash is a pozzolana, a substance containing aluminous and siliceous material that forms cement in the presence of water. When mixed with lime and water it forms a compound similar to Portland cement. The fly ash produced by coal-fired power plants provide an excellent prime material used in blended cement, mosaic tiles, and hollow blocks among others. Fly ash can be an expensive replacement for Portland cement in concrete although using it improves strength, segregation, and ease of pumping concrete. The rate of substitution typically specified is 1 to 1 ½ pounds of fly ash to 1 pound of cement. Nonetheless, the amount of fine aggregate should be reduced to accommodate fly ash additional volume.

RICE HUSK ASH

Rice husk is an agricultural residue which accounts for 20% of the 649.7 million tons of rice produced annually worldwide[1]. The produced partially burnt husk from the milling plants when used as a fuel also contributes to pollution and efforts are being made to overcome this environmental issue by utilizing this material as a supplementary cementing material[2]. The chemical composition of rice husk is found to vary from one sample to another due to the differences in the type of paddy, crop year, climate and geographical conditions

GROUND GRANULATED BLAST FURNACE SLAG

Ground Granulated Blast furnace Slag (GGBS) is a byproduct from the blast furnaces used to make iron. These operate at a temperature of about 1500 degrees centigrade and are fed with a carefully controlled mixture of iron ore, coke and limestone. The iron ore is reduced to iron and the remaining materials from a slag that floats on top of the iron. This slag is periodically tapped off as a molten liquid. and if it

is to be used for the manufacture of GGBS it has to be rapidly quenched in large volumes of water. The quenching optimizes the cementations properties and produces granules similar to coarse sand. This „granulated" slag is then dried and ground to a fine powder. Although normally designated as "GGBS" in the UK, it can also be referred to as "GGBS" or "Slag cement" Concrete is basically a mix of fine aggregate, coarse aggregate and cement. The main problem is the original conventional materials are depleting and we are in hunt for alternate building materials which lands us here on the purpose of GGBS. Being a by product and waste using it effectively up to some extent serves as a step for a greener environment and at the same time keeping in mind that the strength of the concrete doesn't degrade by the usage GGBS.

OBJECTIVE OF THE STUDY

Depending on the suitability of Bagasse ash, it can be used as resource material in the following applications:

- Silica source as it contains high amount of silica in it.
- Brick production as BA used as additive in making bricks that have high compressive strength and low water absorption bricks.
- Farm fertilizer as it contains traces of potassium and phosphorus compounds etc.
- To compare the tests results of fly ash, rice husk ash, and sugarcane Bagasse ash with the normal concrete.
- To find the optimum usage of the percentage replacement of the fly ash , rice husk ash, baggage ash to the concrete.

SCOPE OF THE STUDY

The primary aim of experimental work is to study the properties of sugar cane bagasse ash. Preparation of mix design Replacement of cement with SCBA as different proportions with cement.

- Effect of a GGBS on workability.
- Effect of fly ash and rice husk ash on the strength of the concrete.
- Effect on compressive strength of concrete.
- Effect on split tensile strength of concrete.
- To determine the optimum dosage of the GGBS, Fly ash, Rice husk ash to be added to the concrete mix.
- Comparison of result of different tests with varying proportion of FA, RHA and GGBS.

II.LITERATURE REVIEW

Sagar Dhengare [1], Sourabh Amrodiya[2] and Mohanish Shelote[3] et all,. In developing countries, accumulation of unmanaged agricultural waste has resulted in an increased environmental concern. Recycling of such agricultural wastes is the viable solution not only to pollution problem, but also the problem of land filling. In view of utilization of agricultural waste in concrete and mortar, the present paper reviews, utilization of sugarcane Bagasse ash (SCBA) in different compositions that were added to the raw material at different levels to develop sustainable concrete and mortar. Various physic-mechanical properties of the concrete and mortar incorporating sugarcane Bagasse ash are reviewed and recommendations are suggested as the outcome of the study. The study in turn is useful for various resource SCBA material to develop sustainable construction material.

Mangesh V Madurwar, Sachin A Mandavgane, Ph.D. et al (2014) SBA-QD-L bricks are up to40%

lighter than the conventional locally available bricks and hence support in lightweight construction projects with larger design loads. Observations during the tests showed that SBA-QD-L brick composition with SBA (50% by weight), quarry dust (30% by weight), and lime (20% by weight) exhibits the water absorption of 19.70% (less than 20%) and the compressive strength of 6.59 MPa, which is almost double the conventional commercially available clay bricks (3.5 MPa) and satisfies the requirements in IS: 2185 (Part-I) (BIS 1979) and SP: 21 (BIS 1983) for a building material.

Cbatveera, P. NtmJtyonglkul. et al (1994) This research is conducted to develop new kinds of pozzolana from other agricultural wastes apart from rice husk and rice straw. The study investigated the use of coconut husk, Corn cob and peanut shell ash as pozzolana. The properties of CHA, CCA and PSA namely specific gravity, fineness, chemical composition and the strength activity index with Portland cement were determined. For properties of paste, only ordinary Portland cement and 30% PSA were investigated for normal consistency and initial and final setting time. CCA mortars have lower compressive strength than the controlled mortar (0% CCA) while PSA mortars showed higher compressive strength than the controlled mortar (0% PSA).Among the four mortars tested for chemical attack, PSA mortars showed higher resistance against sulphate attach and RHA against acidic attack.

III.METHODOLOGY

CEMENT

Cement is a binder, a substance used in construction that sets and hardens and can bind other materials together. The most important types of cement are used as a component in the production of mortar in masonry, and of concrete which is a combination of cement and an aggregate to form a strong building material.

OPC 53 GRADE CEMENT

COARSE AGGREGATE

Crushed stone aggregate of 20mm size is brought from nearby quarry. Aggregates of size more than 20mm size are separated by sieving. Tests are carried in order to find out the

• Specific gravity = 2.98

• Fineness modulus = 7.5

Coarse aggregate

FINE AGGREGATE:

Locally available fresh sand, free from organic matter is used. The result of sieve analysis confirms it to Zone-II (according to IS: 383-1970).The tests conducted and results plotted below.

- Specific gravity = 2.3
- Fineness modulus = 3.06

Fine aggregates

Super plastizers (perma super plast 220)

Perma Plast Super- 220 is a high range, low dosage, super plasticising admixture for slump retention. It is a product based on refined naphthalene formaldehyde and ligno sulfonate blends. To produce self-compacting flowing concrete. To produce high early strength concrete for delayed slump retention and for long overhauls. Ideally suited for commercial RMC plants and concrete made with crushed sand.For the production of high workability concrete where heavily congested reinforcement exist or poor access is available. To produce flowing self Compacting concrete which requires minimal labour to place. For the production of high strength, high workability concrete. Particularly beneficial in hot climatic conditions and in ready mix concrete. It is based on naphthalene formaldehyde blends.

MIX DESIGN

Final trial mix for M30 grade concrete is 1:1.64:2.55 at w/c of 0.45

GRADE OF CONCRETE	CEMENT KGS	Granulated ground blast furncace slag (GGBS)	Fly Ash	Rice husk Ash	Fine aggregates	coarse aggregates	water content	Admixture
M30	183.82	7.32	7.32	7.32	502	780	88	4
Addition of extra 10%	202.20	8.052	8.052	8.052	552.2	858	96.8	4.818

Final trial mix for M40 grade concrete is 1:2.29:3.56 at w/c of 0.40

GRADE OF CONCRETE	CEMENT KGS	Granulated ground blast furnace slag (GGBS)	Fly Ash	Rice husk Ash	Fine aggregates	coarse aggregates	water content	Admixture
M40	194	7.32 Kgs	7.32 kgs	7.32 kgs	502	780	87.2	4.38
Addition of extra 10%	213.4	8.05	8.05	8.05	552.2	858	8.72	0.44

IV.RESULTS

MATERIAL PROPERTIES

Test results on the cement

Sl.no	Test	Results	IS code used	Acceptable limit
1	Specific gravity of cement	3.10	IS:2386:1963	3 to 3.2
2	Standard consistency of cement	6mm at 32% w/c	IS:4031:1996	w/c ratio 28%-35%
3	Initial and final setting time	45 mins and 10 hours	IS:4031:1988	Minimum 30mins and should not more than 10 hours
4	Fineness of cement	4.00%	IS:4031:1988	<10%

Test results on coarse aggregates

Sl.no	Test	Results	Is code used	Acceptable limit
1	Fineness modulus	6.8	IS:2386:1963	6.0 to 8.0mm
2	Specific gravity	2.95	IS:2386:1963	2 to 3.1mm
3	Porosity	46.83%	IS:2386:1963	Not greater than 100%
4	Voids ratio	0.8855	IS:2386:1963	Any value
5	Bulk density	1.50g/cc	IS:2386:1963	-
6	Aggregate impact value	35.5	IS:2386:1963	Less than 45%
7	Aggregate crushing value	27.5%	IS:2386:1963	Less than 45%

Test results on the fine aggregates

Sl.no	Test	Result	Is code used	Acceptable limits
1	Fineness modulus	4.5	IS:2386:1963	Not more than 3.2 mm
2	Specific gravity	2.43	IS:2386:1963	2.0 to 3.1
3	Porosity	36.6%	IS:2386:1963	Not greater than 100%
4	Voids ratio	0.577	IS:2386:1963	Any value
5	Bulk density	1.5424	IS:2386:1963	-
6	Bulking of sand	4.0%	IS:2386:1963	Less than 10%

slump values for concrete

S.NO	% Replacement	Slump for M30grade	Slump for M40 grade
1	0%	55	52
2	1.67% FA+1.67% RHA+1.67% GGBS	67	68
3	3.33% FA+3.33% RHA+3.33% GGBS	72	79
4	5% FA+5% RHA+5% GGBS	78	80
5	6.67% FA+6.67% RHA+6.67% GGBS	85	92

Compaction factor Test

S.NO	% Replacement	Compaction factor for M30 grade concrete	Compaction factor for M40 grade concrete
1	0%	0.98	0.94
2	1.67% FA+1.67% RHA+1.67% GGBS	0.95	0.9
3	3.33% FA+3.33% RHA+3.33% GGBS	0.88	0.88
4	5% FA+5% RHA+5% GGBS	0.88	0.84
5	6.67% FA+6.67% RHA+6.67% GGBS	0.86	0.86

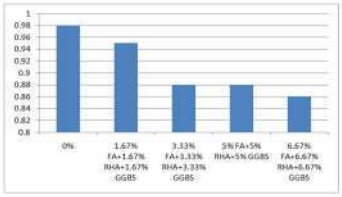

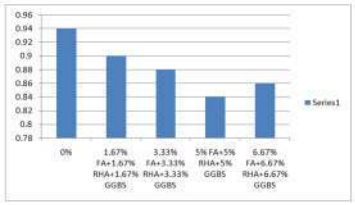

Compressive strength:

s.no	% Replacement	Compressive strength of concrete			
		M30 grade concrete		M40 grade concrete	
		7 days	28 days	7 days	28 days
1	0%	28.84	29.6	38.6	39.86
2	1.67% FA+1.67% RHA+1.67% GGBS	28.6	29.2	37.24	37.44
3	3.33% FA+3.33% RHA+3.33% GGBS	27.4	29.8	36.6	37.9
4	5% FA+5% RHA+5% GGBS	26.4	27	35.4	36.2
5	6.67% FA+6.67% RHA+6.67% GGBS	25.6	26.4	32.8	34.22

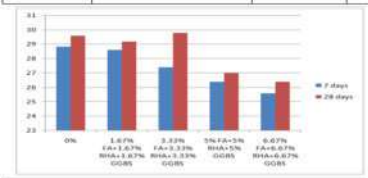

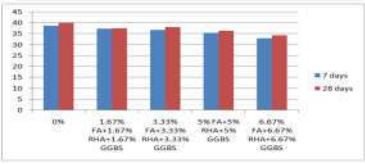

Split tensile strength of concrete

S.no	% Replacement	28 days split tensile strength for M30 grade	28 days split tensile strength for M40 grade
1	0%	4.82	5.28
2	1.67% FA+1.67% RHA+1.67% GGBS	5.21	5.16
3	3.33% FA+3.33% RHA+3.33% GGBS	5.53	5.2
4	5% FA+5% RHA+5% GGBS	5.45	5.46
5	6.67% FA+6.67% RHA+6.67% GGBS	5.8	4.8

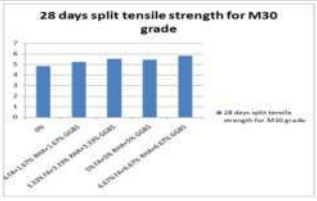

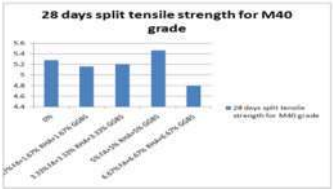

Flexural strength of concrete:

S.no	% Replacement	28 days flexural strength for M30 grade concrete	28 days flexural strength for M40 grade concrete
1	0%	5.54	5.8
2	1.67% FA+1.67% RHA+1.67% GGBS	5.71	5.6
3	3.33% FA+3.33% RHA+3.33% GGBS	5.74	5.74
4	5% FA+5% RHA+5% GGBS	5.92	6.1
5	6.67% FA+6.67% RHA+6.67% GGBS	6.36	6.4

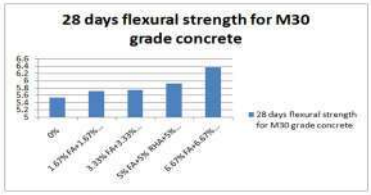

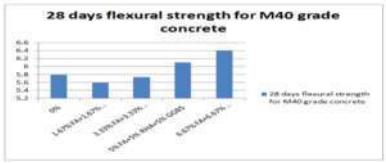

Durability

For M30 grade concrete for acid attack

Sl.no	% replacement	Initial weight of cube after 28days curing in grams	Final weight of cubes after 90days curing in grams	% loss of weight due to acid attack	Compressive strength of cube after 28days curing	Compressive strength of cubes after 90days curing	% loss of compressive strength due to acid attack
1	0%	2261	2242	0.82	29.6	26.95	8.96
2	1.67% FA+1.67% RHA+1.67% GGBS	2340	2318	0.94	29.2	26.51	9.2
3	3.33% FA+3.33% RHA+3.33% GGBS	2351	2323	1.2	29.8	26.94	9.6
4	5% FA+5% RHA+5% GGBS	2234	2202	1.44	27	24.5	9.2
5	6.67% FA+6.67% RHA+6.67% GGBS	2394	2356	1.6	26.4	23.6	10.6

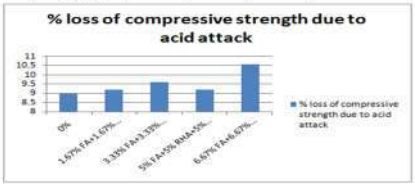

Alkaline attack

Sl. No	% replacement	Initial weight of cube after 28days curing in grams	Final weight of cubes after 90days curing in grams	% loss of weight due to alkaline attack	Compressive strength of cube after 28days curing	Compressive strength of cubes after 90days curing	% loss of compressive strength due to alkaline attack
1	0%	2266	2239	1.2	29.6	25.98	12.26
2	1.67% FA+1.67% RHA+1.67% GGBS	2340	2306	1.44	29.2	25.3	13.34
3	3.33% FA+3.33% RHA+3.33% GGBS	2280	2244	1.6	29.8	25.86	13.2
4	5% FA+5% RHA+5% GGBS	2310	2268	1.84	27	23.32	13.62
5	6.67% FA+6.67% RHA+6.67% GGBS	2296	2251	1.96	26.4	22.67	14.1

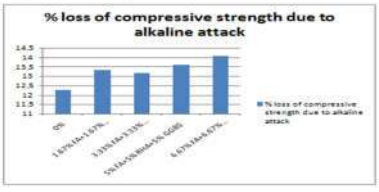

Sulphate attack test

Sl.no	% replacement	Compressive strength of cube after 28days curing	Compressive strength of cubes after 90days curing	% loss of compressive strength due to sulphate attack
1	0%	29.6	24.07	18.66
2	1.67% FA+1.67% RHA+1.67% GGBS	29.2	23.65	18.98
3	3.33% FA+3.33% RHA+3.33% GGBS	29.8	24.07	19.2
4	5% FA+5% RHA+5% GGBS	27	21.87	18.98
5	6.67% FA+6.67% RHA+6.67% GGBS	26.4	21.27	19.4

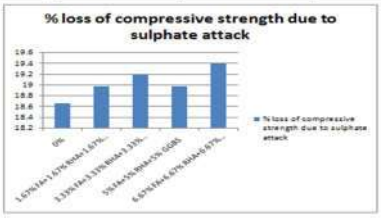

For M40 grade concrete:

Sl.no	% replacement	Initial weight of cube after 28days curing in grams	Final weight of cubes after 90days curing in grams	% loss of weight due to acid attack	Compressive strength of cube after 28days curing	Compressive strength of cubes after 90days curing	% loss of compressive strength due to acid attack
1	0%	2351	2349	0.09	39.86	35.4	11.24
2	1.67% FA+1.67% RHA+1.67% GGBS	2340	2312	1.2	37.44	33	11.84
3	3.33% FA+3.33% RHA+3.33% GGBS	2351	2318	1.4	37.9	33.5	11.6
4	5% FA+5% RHA+5% GGBS	2234	2194	1.8	36.2	31.81	12.12
5	6.67% FA+6.67% RHA+6.67% GGBS	2394	2341	2.2	34.22	29.98	12.4

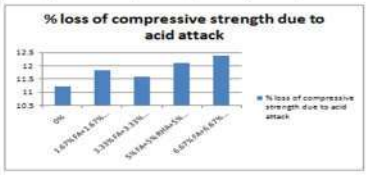

Alkaline attack

Sl. No	% replacement	Initial weight of cube after 28days curing in grams	Final weight of cubes after 90days curing in grams	% loss of weight due to alkaline attack	Compressive strength of cube after 28days curing	Compressive strength of cubes after 90days curing	% loss of compressive strength due to alkaline attack
1	0%	2351	2320	1.3	39.86	34.12	14.4
2	1.67% FA+1.67% RHA+1.67% GGBS	2340	2302	1.6	37.44	31.9	14.8
3	3.33% FA+3.33% RHA+3.33% GGBS	2260	2228	1.4	37.9	32	15.6
4	5% FA+5% RHA+5% GGBS	2245	2205	1.8	36.2	30.33	16.2
5	6.67% FA+6.67% RHA+6.67% GGBS	2260	2210	2.2	34.22	28.52	16.66

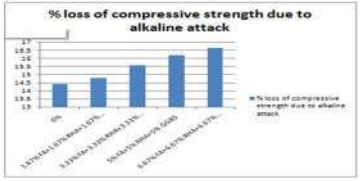

Sulphate attack test

Sl.no	% replacement	Compressive strength of cube after 28days curing	Compressive strength of cubes after 90days curing	% loss of compressive strength due to sulphate attack
1	0%	39.86	33.4	16.22
2	1.67% FA+1.67% RHA+1.67% GGBS	37.44	31.13	16.84
3	3.33% FA+3.33% RHA+3.33% GGBS	37.9	31.37	17.22
4	5% FA+5% RHA+5% GGBS	36.2	29.82	17.6
5	6.67% FA+6.67% RHA+6.67% GGBS	34.22	28	18.2

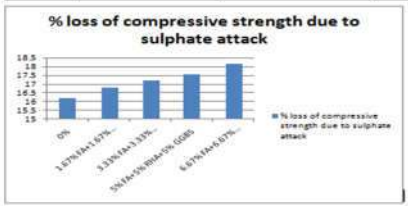

V.CONCLUSIONS

From the above experimental program the following conclusions were made

1. The material properties of the cement, fine aggregates and coarse aggregates are within the acceptable limits as per IS code recommendations so we will use the materials for research.
2. Slump cone value for the RHA, FA, GGBS concrete increases with increasing in the percentage of RHA, FA, GGBS so the concrete was not workable.
3.Compaction factor value of RHA, FA, GGBS concrete decreases with increase in the percentage of RHA, FA, GGBS
4. The compressive strength of concrete is maximum at 20% replacement of RHA, FA, GGBS and is the optimum value for 7days curing and 28days curing
5. Split tensile strength for the cylindrical specimens is maximum at 40% of replacement of copper slag for 28days curing.
6. The flexural strength of copper slag concrete is also maximum at 20% replacement of copper slag for 28 days of curing.
7. So the replacement of 5% to 20% of RHA, FA, GGBS is generally useful for better strength values in M30 And M40 grade of concrete.

FUTURE RECOMMENDATIONS:

- Using RHA, FA, GGBS with cement checking out whether the minimum strength

required for M50 and M60 grades of concrete can be achieved.

- Checking out the feasibility of utilization of HA, FA, GGBS finding the Strength characteristics of Concrete.

REFERENCES

1. Brindha, D and Nagan, S (2010). "Utilization of copper slag as a partial replacement of fine aggregate". International Journal of Earth Sciences and Engineering, Vol.3, No.4, pp.579-585

2. Wei Wu, Weide Zhang, Guowei Ma "Optimum content of copper slag as a fine aggregate in high strength concrete" Materials and Design, Elsevier science Ltd, Vol. 31, 2010, pp. 2878–2883.

3. Pazhani K, Jeyaraj R, "Study on durability of high performance concrete with industrial wastes", Peer-reviewed & Open access journal, ATI- Applied Technologies & Innovations, Vol. 2, Issue 2, August 2010, pp. 19-28.

4.Khalifa S Al-Jabri, Abdullah H Al-Saidy, Ramzi Taha, "Effect of copper slag as a fine aggregate on the properties of cement mortars and concrete", Construction and Building Materials, Vol. 25, 2011, pp. 933 – 938

5.Mostafa Khanzadi, Ali Beholds(2009), " Mechanical properties of high strength concrete incorporating copper slag as coarse aggregate" , Construction and Building Materials 23 pp 2183–2189.

6. Meenakshi Sudarvizhi, S. and Ilangovan, R. "Performance of copper slag and ferrous slag as partial replacement of sand in concrete", International Journal of Civil and Structural Engineering, Vol.1, No.4, 2011.

7. Chavan, R.R. and Kulkarni, D.B. "Performance of copper slag on strength properties as partial replacement of fine aggregate in concrete mix design", International Journal of Advanced Research and Studies, Vol.2, No.4, pp.95-98, 2013.

8. IS: 10262 – 2009, Concrete Mix Proportioning, Bureau of Indian Standards, New Delhi.

9. IS 516 (1959): Method of Tests for Strength of Concrete [CED 2: Cement and Concrete]

10.IS 2386-1 (1963): Methods of Test for Aggregates for Concrete, Part I: Particle Size and Shape [CED 2: Cement and Concrete]